# NUCLEAR PHYSICS

MONTHLY JOURNAL DEVOTED TO THE EXPERIMENTAL AND THEORETICAL STUDY OF ATOMIC NUCLEI, NUCLEAR FIELDS AND THE FUNDAMENTAL ASPECTS OF COSMIC RADIATION

EDITOR: L. ROSENFELD - COPENHAGEN

VOLUME VIII

SEPTEMBER 1958—NOVEMBER 1958

NORTH - HOLLAND PUBLISHING COMPANY - AMSTERDAM

PRINTED IN THE NETHERLANDS BY
DRUKKERIJ VOORHEEN GEBROEDERS HOITSEMA, GRONINGEN

1.D.3:
2.F

*Nuclear Physics* **8** (1958) 1—12; © *North-Holland Publishing Co., Amsterdam*
Not to be reproduced by photoprint or microfilm without written permission from the publisher

# PROTON-ALPHA REACTIONS IN LIGHT AND HEAVY NUCLEI

P. E. HODGSON
*Department of Physics, University of Reading*

Received 8 June 1958

**Abstract:** Nuclear emulsion has been irradiated with 45 MeV protons, and measurements made on the tracks of alpha-particles emitted from disintegrations of the light and heavy nuclei within it. There is a forward excess of energetic alpha-particles in each case, and this can be accounted for by direct interaction processes, for which several possible models are discussed. Conclusions are drawn on the probability of finding alpha-particles in nuclear matter, and on their momentum distribution.

## 1. Introduction

At low energies, proton-alpha reactions proceed through one or more excited states of the compound nucleus, and may be satisfactorily analysed using the resonance theory of nuclear reactions. Experiments at higher energies, however, provide evidence that this interpretation is insufficient, and that some form of direct interaction processs must be postulated.

For the lighter elements, this is indicated by the work of Marion, Weber and Mozer [1]) on $Li^6$(p, α) $He^3$ at 2.91 MeV, of Likely and Brady [2]) on $F^{19}$ (p, α) $O^{16}$ at 16 and 18.5 MeV, of Muirhead and Rosser [3]) on CNO (p, α) at 140 MeV, and of Combe, Cüer and Samman [4–8]) on CNO (p, α) at 180 and 340 MeV.

For heavier elements, evidence of direct interaction processes has been found by Sörensen [9]) and Crussard [10]) for very energetic cosmic-ray disintegrations, by Fulmer and Cohen [11]) for an incident proton energy of 23 MeV, by Hodgson [12]) (referred to below as I) and Grilli, Vitale, Hodgson and Ladu [13]) at 45 to 450 MeV and by Deutsch [14]) at 332 MeV. It was found in each case that more high energy alpha-particles were emitted in the forward direction with respect to the incident protons than could be accounted for by the compound nucleus theory.

This evidence concerning the (p, α) reaction is supplemented by that drawn from similar studies of the (α, p) reaction. These have been made by Eisberg, Igo and Wegner [15]) with 40 MeV alpha-particles on copper, silver and gold, by Hunting and Wall [16]) with 30.5 MeV alpha-particles on $Al^{27}$ and $P^{31}$, and by von Herrmann and Pieper [17]) with 7.0 and 8.1 MeV alpha-particles on $P^{31}$. In each case evidence for a direct interaction process was found.

Similar results have been found for (n, α) reactions by Ribe and Davis [18]) for Zr at 14 MeV.

In this paper additional experimental data on (p, α) reactions in light and heavy nuclei are presented, and some possible explanations discussed.

## 2. Experimental Procedure

Ilford C2 nuclear emulsions were exposed to the proton beam of the Harwell cyclotron. Allowing for their energy loss in absorbers and emulsion, the average energy of the incident protons was [19]) $45 \pm 6$ MeV. Nuclear disintegrations ('stars') in the light (carbon, nitrogen and oxygen) and heavy (silver and bromine) nuclei of the emulsion from which one or more alpha-particles were emitted were identified by the criteria described in I. The validity of these criteria, which depend on the alpha particles from the heavy nuclei having energies in excess of 9 MeV, has recently received additional support from the work of Deutsch [14]) and Fulmer and Cohen [11]).

Measurements were made on the tracks of 618 alpha-particles coming to rest in the emulsion, and the energies of the alpha-particles and their angles of emission found. The usual corrections were made to allow for those alpha-particles that did not come to rest in the emulsion.

The tracks of singly-charged particles could be distinguished by inspection from those of doubly charged particles. However, the tracks of deuterons and tritons could not usually be distinguished from those of protons, nor those of helium three from those of alpha-particles. All singly-charged particles were therefore grouped together and will be referred to as protons, and doubly charged particles as alpha-particles. The errors introduced by this procedure are likely to be small.

## 3. Alpha-Particles from Light Nuclei

### 3.1 EXPERIMENTAL RESULTS

The disintegration of a light nucleus by an energetic proton proceeds initially by a cascade stage that results in the ejection of a number of fast particles in the forward direction, and this is followed by the breakup of the residue into two or more relatively slow fragments. Thus the fast forward particles are the ones most likely to be associated with a direct interaction process.

Accordingly, measurements were made only on alpha-particles of more than 9 MeV emitted in the forward direction with respect to the incident protons. The limit was chosen to correspond to that used for the alpha particles from the heavy nuclei. The energy-angle correlation for these alpha-particles is shown in fig. 1.

The numbers of stars of different types having an alpha particle satisfying the acceptance criteria are given in table 1, together with the mean energies of the fast alpha-particles associated with them. These show no significant variation with star type.

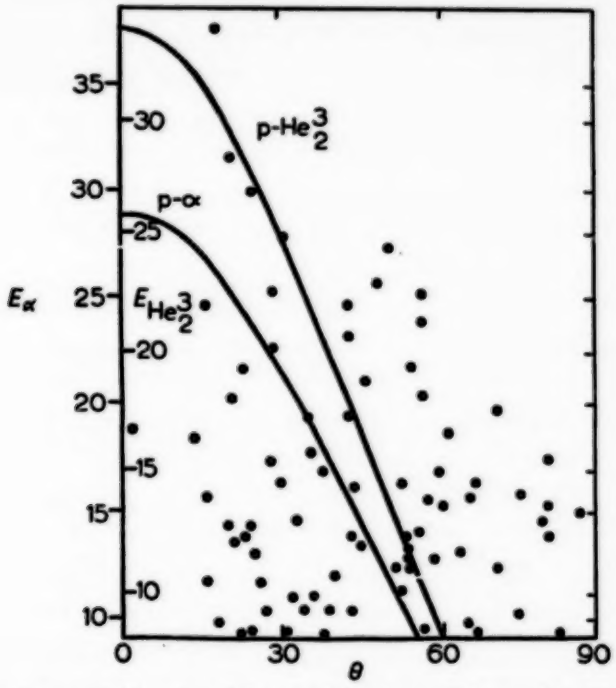


Fig. 1. Energy-angle correlation for alpha-particles from light nuclei. The curves show the relation to be expected from free proton-alpha and proton-He$^3$ collisions. $\theta$ is the angle with the forward direction.

TABLE 1

| Star type | Number | Mean Alpha Energy (MeV) | |
|---|---|---|---|
| 4α | 14 | 21.4±2.0 | 19.0±1.8 |
| 4α1p | 7 | 13.1±3.5 | |
| 3α | 6 | 20.3±2.2 | 18.0±1.0 |
| 3α1p | 38 | 17.6±1.1 | |
| 3α2p | 1 | 12.9 | |
| 2α | 3 | 13.2±4.5 | 14.8±2.0 |
| 2α1p | 6 | 15.7±2.2 | |
| 2α2p | 3 | 14.4±4.5 | |

### 3.2. THE DIRECT INTERACTION PROCESS

Energetic protons and alpha-particles emitted in the forward direction from light nuclei bombarded with energetic protons have been interpreted by Sörensen [1]) Muirhead and Rosser [3]) and Combe, Cüer and Samman [4–8]), as the result of quasi-free proton-alpha collisions in the target nucleus. The latter authors made a particular study of the fast alpha-particles and protons emitted in the reaction $C^{12}$ (p, p′) 3α, and were able to determine the relative

proportions of different possible nuclear sub-structures, the energy distribution of the nuclear-alpha particles, and the distribution in excitation energy of the residual nuclei of $Be^8$.

An alternative explanation of the forward alpha-particles is that they result from a triton pickup process. Both this and the quasi-elastic proton-alpha process can be treated by quantum mechanics [2]), but, as they give similar angular distributions for the alpha-particles, it is not easy to distinguish between them. However, if the triton pickup process takes place, it implies a corresponding probability of finding a triton near the surface of the nucleus. If such tritons are present, many more alpha-particles will be present also, because of their higher binding energy. Thus the proton-alpha knockout process is likely to predominate over the triton pickup process.

If the former interpretation is provisionally adopted, it is interesting to compare the experimental results with the energy-angle relation $E_\alpha = (16/25)E_p \cos^2 \theta$ that follows from the dynamics of a free proton-alpha collision. This is done in fig. 1 for both proton-alpha and proton-$He^3$ collisions. The experimental points lie in a rather broad band in the general direction of the curves. This spread may be readily interpreted as due to the momentum distribution of the nuclear alpha-particles.

If the theory of the direct interaction process were well understood, it could be used to derive the form of the momentum distribution from the experimental results, as Cladis, Hess and Moyer [20]) found the momentum distribution of nucleons in carbon from their measurements of the inelastic scattering of 340 MeV protons, using the theory of Wolff [21]). This theory uses the Born approximation, which is hardly likely to be very accurate at the energies of the present experiment. However, it can be estimated qualitatively that the nuclear alpha particles have energies up to some five or ten MeV, and this is in agreement with the results of Samman.

The absolute cross-section for fast alpha-particle emission may be used to estimate the mean number of alpha-particles in the nucleus. From the conditions of the experiment, the cross-section for emission of alpha-particles of more than 9 MeV from light nuclei was found to be $23 \pm 8$ mb. This may be compared with the total cross-section for producing an alpha-particle of these energies by a free proton-alpha collision, which may be estimated from the measurements of many authors [22]) to be about 27 mb. Combining this with the maximum number (3.3) of alpha-particles that could be formed in the light nuclei, averaged over their proportions in emulsion, it is found that a nucleon in a light nucleus spends about a quarter of its time as part of an alpha-particle. This is on the assumption that a struck alpha-particle always escapes, whatever its direction of emission with respect to the rest of the nucleus. If allowance is made for the possibility that a second collision will sometimes prevent its escape, the above estimate is raised to one-third to

one-half. This rather high value is in qualitative accord with recent calculations on the Brueckner nuclear model [23]).

If the proton-alpha knockout interpretation is correct, fast secondary protons might be expected in many cases, while they would not result from the triton pickup process. Secondary protons were often observed, but their energies and directions of emission could not be correlated with those expected from quasi-free collisions because of the unknown energies and initial directions of motion of the alpha-particles in the nucleus. Samman and Cüer [8]) were only able to do this because they selected $C^{12}$ (p, p') $3\alpha$ events and assumed that no neutrons were emitted.

One event was found which may be interpreted as due to this latter reaction. The fast alpha-particle was emitted in the forward direction in a way nearly consistent with a free proton-alpha collision ($E_\alpha = 14$ MeV, $\theta = 37°$), while the remaining alpha-particles from the breakup of the residual nucleus were emitted backwards with energies of 0.9 and 1.4 MeV. The incident proton was scattered so as to conserve momentum for the whole event, within experimental error.

## 4. Alpha-Particles from Heavy Nuclei

### 4.1 EXPERIMENTAL RESULTS

The energy distribution of the alpha-particles from heavy nuclei is given in fig. 2. It may be compared with that given by the expression [24])

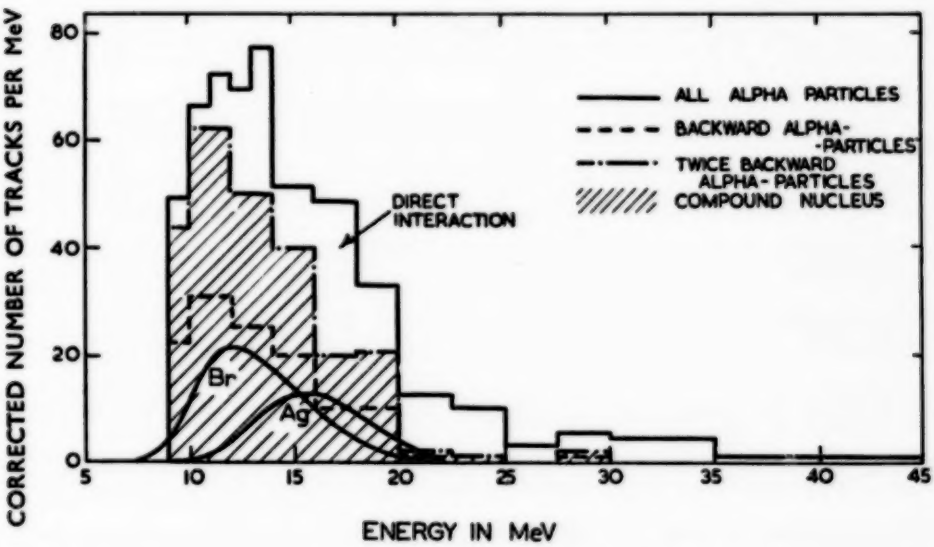


Fig. 2. Energy distribution of alpha-particles from heavy nuclei. The curves show the calculated distributions for emission from silver and bromine. The mean cross-sections for the emission of an alpha-particle of any energy is $(8.9 \pm 3.0) \times 10^{-26}$ cm$^2$.

$$P(E)\mathrm{d}E \propto E\sigma_c(E)w(E^*-E)\mathrm{d}E \qquad (1)$$

where $\sigma_c(E)$ is the cross-section for the capture of the emitted particle by the compound nucleus C at an energy $E$ and $w(E^*-E)$ is the level density of the residual nucleus at an excitation energy $(E^*-E)$. The cross-section $\sigma_c(E)$ was found for silver and bromine by interpolation between the values given by Blatt and Weisskopf (p. 353), and the level density computed from the expression [25])

$$w(E) \propto \exp\,[2(aE)^{\frac{1}{2}}] \qquad (2)$$

in which $a = A/10.5$. The resulting energy distributions, which are relative only, because of the uncertainties due to neutron emission, are shown in fig. 2. They are quite similar to the experimental distributions in the backward direction, but there is an observed excess of energetic alpha-particles in the forward direction.

The angular distribution of the alpha-particles is given in fig. 3, and shows a considerable forward excess, the fraction of alpha-particles emitted

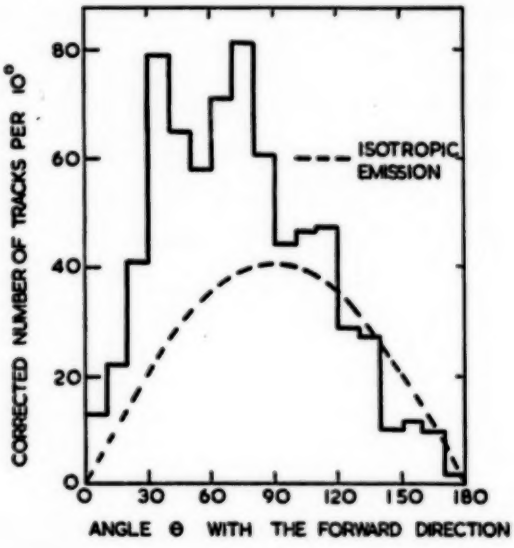


Fig. 3. Angular distribution of alpha-particles from heavy nuclei with respect to the direction of the incident protons.

in the forward direction being $0.67\pm0.04$. It was shown in I that such a forward excess cannot be due to the forward motion of the nucleus due to the impact of the incident particle; this effect, even making somewhat extreme assumptions, cannot give a forward fraction of more than 0.51 or 0.52.

Thus both the energy and the angular distributions of the alpha-particles differ from what would be expected from the statistical theory of nuclear disintegration. However, if only those alpha-particles emitted in the backward direction with respect to the incident protons are considered, it is found that they have energy and angular distributions in good accord with

the statistical theory. The energy distribution may be fitted by an evaporation formula of the usual form [26]) with a nuclear temperature of 2.4 MeV.

This suggests that all the backward alpha-particles, together with an equal number of forward ones, be interpreted as due to a compound nucleus process. The remainder, the excess of the forward over the backward, may then be ascribed to direct interaction; they amount to $34 \pm 8$ % of all the alpha-particles. The energy and angular distributions of these direct interaction alpha-particles may then be found, as shown in figs. 2 and 3, by subtraction. The subtracted angular distribution, divided by $\sin\theta$ to convert it to relative differential cross-section, is shown separately in fig. 4, in order

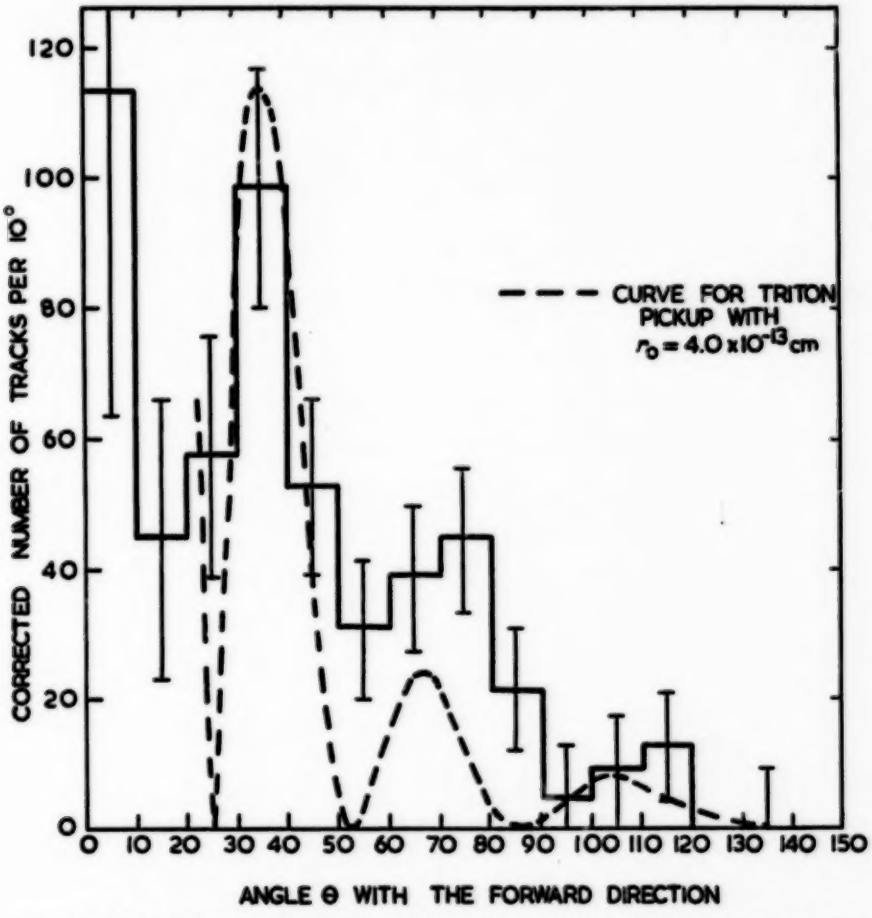


Fig. 4. Angular distribution of direct interaction alpha-particles from heavy nuclei, compared with the theoretical distribution for triton pickup.

that it may be compared with theories of the direct interaction process (cf. § 4.2). The correlation between the energies of the alpha-particles and their angles of emission is shown in fig. 5.

A search was made for protons emitted together with alpha-particles in a way appropriate to the dynamics of a free proton-alpha collision like the

event reported by Muirhead and Rosser [3]). None was found, but this does not exclude the knock out process, as the proton may well be deflected or captured by the target nucleus.

Most of the alpha-particles from the heavy nuclei were not accompanied by any other charged particles. Occasionally, however, disintegrations were found in which another alpha particle, or perhaps one or two protons, were emitted as well. The frequencies of the different types of event are given in table 2.

TABLE 2

| p \ α | 1 | 2 | 3 |
|---|---|---|---|
| 0 | 357 | 12 | 1 |
| 1 | 127 | 8 | 0 |
| 2 | 10 | 2 | 0 |
| 3 | 1 | 0 | 0 |

The frequencies of multiple emission are much lower than those given by the Bernoulli distribution corresponding to random emission [19]). This

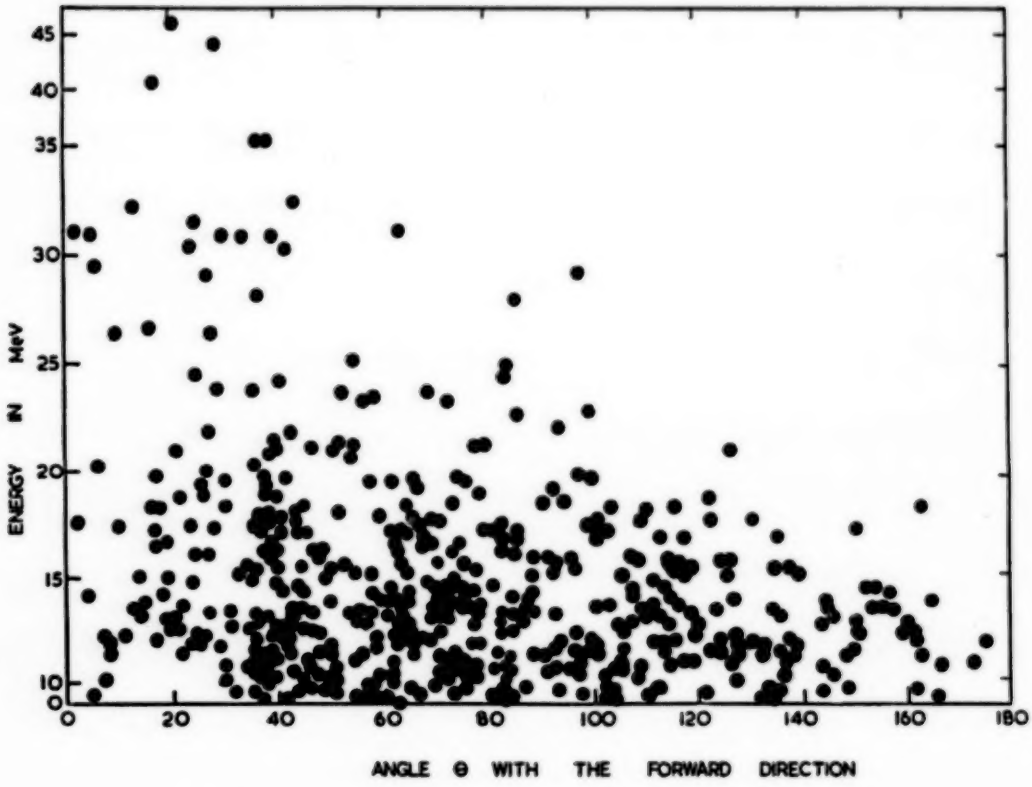


Fig. 5. Energy-angle correlation for alpha-particles from heavy nuclei.

implies that the emission of one particle sharply reduces the probability of emission of another particle, due to the lowering of the excitation energy of the residual nucleus.

The average energies of the alpha-particles emitted in stars of different types are given in table 3.

The statistical uncertainty is quite large in all cases except for the 1α and 1α1p stars, but there is good evidence that the average energy of the alpha-particles is less for the larger stars than for the smaller.

TABLE 3

| p \ α | 1 | 2 | 3 |
|---|---|---|---|
| 0 | 16.5±0.2 | 12.3±1.2 | 12.7 |
| 1 | 14.9±0.4 | 11.2±1.5 | — |
| 2 | 13.9±1.9 | 16.4 | — |
| 3 | 12.2 | — | — |

## 4.2 THE DIRECT INTERACTION PROCESS

The same processes, alpha-particle knock out and triton pickup, may be used to interpret the direct interaction alpha-particles from the heavy nuclei. Now, however, the process must be assumed to take place only at the nuclear surface, instead of throughout the nuclear volume, because of the small mean free path of alpha-particles in nuclear matter [27]).

The alpha-particle angular distributions calculated by quantum mechanics for either of these processes have maxima and minima characteristic of pickup and stripping angular distributions, and Likely and Brady were able to fit their results for the reaction $F^{19}$ (p, α) $O^{16}$ to them, assuming that only waves of zero angular momentum contribute. In the present case, however, the energy is sufficient for higher $l$-values to contribute, and the sum of all the individual curves might be expected to be a monotonically decreasing function of angle like the classical expression. Such a curve is consistent with the experimental angular distribution shown in fig. 4.

The experimental results do, however, show some indications of structure, though the statistics are insufficient to establish this beyond doubt. If this is subsequently confirmed, it would show that the major contribution to the interaction comes from the $l = 0$ wave. This implies, in the case of the knock out process, that the alpha-particle in the target and the proton in the final state are both in S-orbits. For the triton pickup process it implies that the triton is in an S-orbit.

The theoretical curves for both direct interaction processes can be fitted to the observed angular distribution. For illustration, this was done for the triton pickup process, using the formula derived by Thomas (ref.[2]), eq. (1)).

The best fit was obtained with an interaction radius $r_0 = 4 \times 10^{-13}$ cm and a triton reduced width $\theta^2 = 4.7$ (see fig. 4). These are of the right order of magnitude.

Discrimination between the two postulated direct interaction processes could be obtained in theory from the data of table 3. If the effect of nuclear cooling is neglected, the mean energies of the alpha-particles from 1$\alpha$ and from 1$\alpha$ 1p stars should be the same in the case of the pickup process. But in the case of the alpha knockout process the incident proton may be directly emitted as a secondary particle, with the result that alpha-particles from 1$\alpha$ 1p stars are on the whole more energetic than those from 1$\alpha$ stars. In fact the opposite is observed, and this is due to nuclear cooling reducing the mean energy of the alpha-particles from 1$\alpha$ 1p stars. So nuclear cooling cannot be neglected, and until it is evaluated by detailed consideration of the de-excitation process this method cannot be used to distinguish between the two processes.

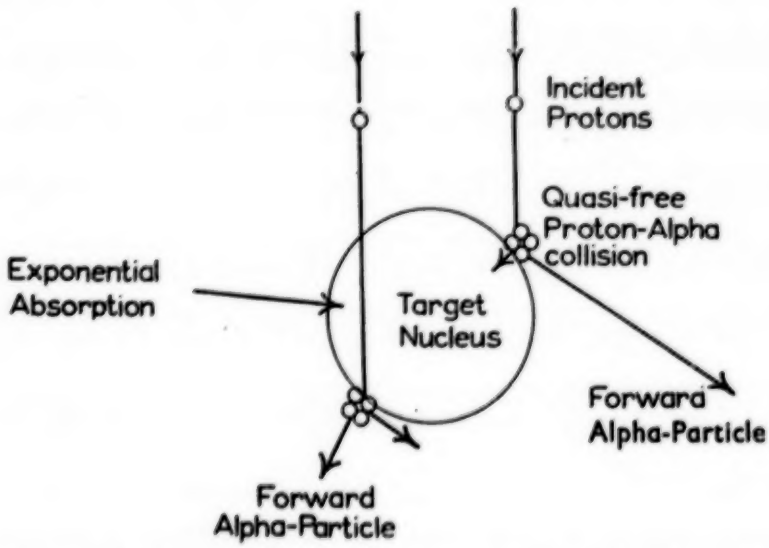


Fig. 6. Illustration of semi-classical calculation of the probabilty of surface alpha-particles being knocked out of the target nucleus by the incident protons.

The experimental cross-section for the direct alpha-particle emission process was found to be $30 \pm 10$ mb. Assuming, for the reasons discussed above, the predominance of the alpha-particle knock out process, the fraction of its time that a surface nucleon spends as part of an alpha-particle may be estimated by dividing this figure by the total number of alpha-particles that could exist on the nuclear surface, the cross-section for knocking on an alpha-particle of more than 9 MeV in a free proton-alpha collison (27 mb.), and the mean probability that such an alpha-particle will escape from the target nucleus.

If the nuclear surface is defined as the region in which the nuclear density is decreasing, the maximum number of surface alpha-particles comes to about fifteen (mean of silver and bromine).

The mean probability of escape may be calculated geometrically, assuming that nuclear matter is opaque to the knocked-on alpha-particles, so that they can emerge only if their direction of motion is away from the target nucleus, and that the incident protons, while on their way to the alpha-particles waiting on the underside of the target nucleus, are exponentially absorbed by the nuclear matter through which they pass. Finally, it is assumed that the free proton-alpha elastic scattering cross-section may be used to find the frequency of this knock-on process. These assumptions are illustrated in fig. 6.

The value used for the attenuation mean free path of protons in nuclear matter was taken from the work of Morrison, Muirhead and Rosser [28]) to be $4\times10^{-13}$ cm. The differential cross-section for proton-alpha scattering was taken from the results of Brussel and Williams [29]) at a proton energy of 40 MeV multiplied by a factor of 0.9 to give, approximately, the cross-section at 45 MeV.

The mean probability of escape was found in this way to be 0.2. This leads to the conclusion that a surface nucleon of a heavy nucleus spends about 0.4 of its time as part of an alpha-particle, a result in good accord with that found above for the nucleons in light nuclei.

It should be pointed out once more that many of the tracks attributed to alpha-particles could be due to $He^3$ nuclei. If so, the direct interaction process would be $He^3$ knock-on or deuteron pickup. Discrimination between these possibilities could be made with electronic counters more easily than with nuclear emulsions.

I would like to thank Professor P. M. S. Blackett, F. R. S. and Mr. N. C. Barford for permitting and enabling me to use the facilities of Imperial College, the Director of the Atomic Energy Research Establishment, Harwell, for permission to work there, Dr. D. M. Skyrme, Professor J. M. Cassels and the Harwell cyclotron operators for assistance during the exposures, Dr. A. J. Herz for developing the plates, Professor R. E. Peierls, F. R. S. and Dr. A. Herzenberg for some useful comments and Dr. A. M. Lane for many valuable and stimulating discussions.

## References

1) J. B. Marion, G. Weber and F. S. Mozer, Phys. Rev. **104** (1956) 1402
2) J. G. Likely and F. P. Brady, Phys. Rev. **104** (1956) 118
3) H. Muirhead and W. G. V. Rosser, Phil. Mag. **46** (1955) 652
4) J. Combe and P. Cüer, Glasgow Conference on Nuclear and Meson Physics (Pergamon Press, 1955) p. 89

5) P. Cüer, J. Combe and A. Samman, Compt. Rend. **240** (1955) 75
6) P. Cüer, A. Samman and J. Combe, Compt. Rend. **240** (1955) 1527
7) A. Samman, Compt. Rend. **242** (1956) 3062; **242** (1956) 2232; J. Phys. Rad. **18** (1957) S. 77
8) A. Samman and P. Cüer, J. Phys. Rad. **19** (1958) 13
9) S. O. C. Sörensen, Phil. Mag. **42** (1951) 188
10) J. Cussard, Compt. Rend. **233** (1951) 611
11) C. B. Fulmer and B. L. Cohen, Bull. Am. Phys. Soc., Ser. II, **3** (1958) 56
12) P. E. Hodgson, Phil. Mag. **44** (1953) 1113
13) M. Grilli, B. Vitale, P. E. Hodgson and M. Ladu, Nuovo Cimento **1** (1955) 314
14) R. W. Deutsch, Phys. Rev. **97** (1955) 1110
15) R. M. Eisberg, G. Igo and H. E. Wegner, Phys. Rev. **100** (1955) 961; **100** (1955) 1309
16) C. E. Hunting and N. S. Wall, Phys. Rev. **108** (1957) 901
17) P. von Herrmann and G. F. Pieper, Phys. Rev. **105** (1957) 1556
18) F. L. Ribe and R. W. Davis, Phys. Rev. **99** (1955) 331
19) P. E. Hodgson, Phil. Mag. **43** (1952) 190
20) J. B. Cladis, W. N. Hess and B. J. Moyer, Phys. Rev. **87** (1952) 425
21) P. A. Wolff, Phys. Rev. **87** (1952) 434
22) P. E. Hodgson, Phil. Mag. Supp. **7** (1958) 1
23) R. E. Peierls, Private communication (1958)
24) J. M. Blatt and V. F. Weisskopf, Theoretical Nuclear Physics (Wiley, 1952)
25) J. M. B. Lang and K. J. Le Couteur, Proc. Phys. Soc. A **67** (1954) 586
26) K. J. Le Couteur, Proc. Phys. Soc. A **63** (1950) 259
27) W. B. Cheston and A. E. Glassgold, Phys. Rev. **106** (1957) 1215
28) G. C. Morrison, H. Muirhead and W. G. V. Rosser, Phil. Mag. **44** (1953) 1326
29) M. K. Brussel and J. H. Williams, Phys. Rev. **106** (1957) 286

8.B *Nuclear Physics* 8 (1958) 13—18; © *North-Holland Publishing Co., Amsterdam*
Not to be reproduced by photoprint or microfilm without written permission from the publisher

# APPLICATION OF THE SERBER POTENTIAL TO LOW ENERGY HYPERON-NUCLEON SCATTERING

D. B. LICHTENBERG
*Physikalisches Staatsinstitut, Universität Hamburg* †

Received 26 June 1958

**Abstract:** Theoretical expressions for the hyperon-nucleon scattering cross sections at low energy are derived which give these cross sections as simple linear combinations of the nucleon-nucleon cross sections. The assumptions necessary for this derivation are: a) there exists a universal coupling between pions and baryons, and b) the nucleon-nucleon interaction can be described by a Serber potential. In addition, the approximations must be made of neglecting effects of K mesons and baryon mass differences. The restriction to low energy is necessary because the assumption is needed that the scattering be appreciable only when the hyperon and nucleon are in a state of zero orbital angular momentum.

## 1. Introduction

The idea of Wigner [1]), Gell-Mann [2]) and Schwinger [3]) that there may exist a universal coupling between pions and baryons is useful to obtain predictions about the potentials between hyperons and nucleons. In particular, the YN potentials (Y means a $\Lambda$, $\Sigma$ or $\Xi$ hyperon; N means a nucleon) can be obtained quite easily if effects of baryon mass differences and effects due to K mesons are neglected ††. The YN potentials can then be given [5]) in terms of linear combinations of the *experimentally determined* NN potentials in the states of isobaric spin $T = 0$ and $T = 1$. One difficulty in applying this result to obtain information about scattering cross sections is that the NN potentials are not well known in states of odd orbital angular momentum $l$ of the two nucleons. Thus, the resulting YN potentials are not well determined either.

The YN scattering cross sections at low energy have been previously calculated [5]) using one particular NN potential — the Brueckner-Watson potential [6]). In this paper, we use another potential which fits the low energy NN scattering information — the Serber potential [7]).

The advantage of applying the Serber potential to the YN problem is one of simplicity. For with the approximations mentioned previously (neglect of

† Address after September, 1958: Physics Department, Michigan State University, East Lansing, Michigan.

†† Some effects of K mesons and baryon mass differences are given by D. Lichtenberg and M. Ross [4]).

K mesons and baryon mass differences), the YN low energy scattering cross sections can be given quite simply in terms of the NN cross sections. This will be shown in the next section.

## 2. Hyperon-Nucleon Cross Sections

Throughout this paper, we assume that the idea of a universal coupling between pions and baryons is valid. To obtain the YN scattering cross sections, it is convenient to follow Gell-Mann [2]) and introduce the "particles" $Y^0$ and $Z^0$ defined as $Y^0 = 2^{-\frac{1}{2}}(\Lambda - \Sigma^0)$ and $Z^0 = 2^{-\frac{1}{2}}(\Lambda + \Sigma^0)$.

Then the pairs of particles (p, n) $(\Sigma^+, Y^0)$, $(Z^0, \Sigma^-)$ and $(\Xi^0, \Xi^-)$ all have the same interaction with the pion field. Each pair of particles can be considered as an isobaric spin doublet, the first member of each pair having $T_z = \frac{1}{2}$ and the second member having $T_z = -\frac{1}{2}$.

Let us denote by $a_{TS}$ the amplitude for scattering any two non-identical particles in a state of total isobaric spin $T$ and ordinary spin $S$. Both $T$ and $S$ may take on the values 0 and 1. We can write the cross sections for the scattering of two real baryons in terms of the amplitudes $a_{TS}$. As an illustration, consider the elastic scattering process $p+\Lambda \to p+\Lambda$. Letting the symbol for a particle denote its isobaric spin wave function, we can write the $p\Lambda$ wave function as follows:

$$p\Lambda = 2^{-\frac{1}{2}}p(Z^0+Y^0) = 2^{-\frac{1}{2}}(pZ^0)+\tfrac{1}{2}[2^{-\frac{1}{2}}(pY^0+n\Sigma^+)]+\tfrac{1}{2}[2^{-\frac{1}{2}}(pY^0-n\Sigma^+)]$$

where $pZ^0$ and $2^{-\frac{1}{2}}(pY^0+n\Sigma^+)$ are $T=1$ wave functions and $2^{-\frac{1}{2}}(pY^0-n\Sigma^+)$ is a $T=0$ wave function. It follows that the amplitude $a_S(p\Lambda, p\Lambda)$ for the scattering process $p+\Lambda \to p+\Lambda$ in a spin state $S$ is

$$a_S(p\Lambda, p\Lambda) = [(2^{-\frac{1}{2}})^2+(\tfrac{1}{2})^2]a_{1S}+(\tfrac{1}{2})^2 a_{0S} = \tfrac{3}{4}a_{1S}+\tfrac{1}{4}a_{0S}.$$

The other YN scattering amplitudes are obtained similarly. The cross sections are

$$\begin{aligned}
&\sigma_S(\Sigma^+p, \Sigma^+p) = \sigma_S(\Xi^0p, \Xi^0p) = |a_{1S}|^2 \\
&\sigma_S(\Sigma^+n, \Sigma^+n) = \sigma_S(\Xi^-p, \Xi^-p) = \tfrac{1}{4}|a_{1S}+a_{0S}|^2 \\
&\sigma_S(\Sigma^+n, \Sigma^0p) = \sigma_S(\Sigma^+n, \Lambda p) = \tfrac{1}{8}|a_{0S}-a_{1S}|^2 \\
&\sigma_S(\Xi^-p, \Xi^0n) = \tfrac{1}{4}|a_{0S}-a_{1S}|^2 \\
&\sigma_S(\Sigma^0p, \Sigma^0p) = \sigma_S(\Lambda p, \Lambda p) = \tfrac{1}{16}|3a_{1S}+a_{0S}|^2 \\
&\sigma_S(\Sigma^0p, \Lambda p) = \tfrac{1}{16}|a_{1S}-a_{0S}|^2
\end{aligned} \tag{1}$$

where $\sigma_S(B_1B_2, B_3B_4)$ is the differential cross section for the scattering of the baryons $B_1$ and $B_2$ into the baryons $B_3$ and $B_4$ in a spin state $S$. Coulomb forces are neglected in these expressions for the cross sections. The remaining YN cross sections are given by the condition of charge symmetry, i.e. the cross sections are unchanged under the simultaneous replacements

$$p \longleftrightarrow n, \qquad \Sigma^+ \longleftrightarrow \Sigma^-, \qquad \text{and} \qquad \Xi^0 \longleftrightarrow \Xi^-. \tag{2}$$

To write down the NN cross sections we must take into account the Pauli principle. It is convenient to split the amplitudes into contributions from states of even and odd angular momentum $l$:

$$a_{TS} = a_{TS+} + a_{TS-}$$

where $a_{TS+}$ and $a_{TS-}$ are the contributions from $l$ even and odd respectively. Then the NN cross sections can be written

$$\begin{aligned} \sigma_{pp} &= 3|a_{11-}|^2 + |a_{10+}|^2 \\ \sigma_{np} &= \tfrac{3}{4}|a_{11-} + a_{01+}|^2 + \tfrac{1}{4}|a_{10+} + a_{00-}|^2 \end{aligned} \tag{3}$$

where $\sigma_{pp}$ and $\sigma_{np}$ denote the proton-proton and neutron-proton cross sections averaged over spin. The extra factor 4 in $\sigma_{pp}$ arises from the fact the 2 protons are identical particles.

We now specialize to the case of the Serber potential. By a Serber potential we mean an NN potential which is zero for odd angular momentum. According to the Pauli principle, $l$ is odd when $T$ and $S$ are both unity or both zero. Therefore, the Serber potential must depend on spin and isobaric spin in such a way as to be zero when $T = S = 1$ or when $T = S = 0$.

It should be emphasized that exchange forces are absent in the YN system † and that therefore the YN potentials are not zero for odd $l$, but are the same as in even states of $l$. The requirement that the potential vanish for $T = S = 1$ or $T = S = 0$ means that the amplitudes $a_{11}$ and $a_{00}$ are identically zero. The YN cross sections of eqs. (1) when averaged over spin then become

$$\begin{aligned} \sigma(\Sigma^+ p, \Sigma^+ p) &= \sigma(\Xi^0 p, \Xi^0 p) = \tfrac{1}{4}|a_{10}|^2 \\ \sigma(\Sigma^+ n, \Sigma^+ n) &= \sigma(\Xi^- p, \Xi^0 n) = \sigma(\Xi^- p, \Xi^- p) \\ &= \tfrac{3}{16}|a_{01}|^2 + \tfrac{1}{16}|a_{10}|^2 \\ \sigma(\Sigma^+ n, \Sigma^0 p) &= \sigma(\Sigma^+ n, \Lambda p) = \tfrac{3}{32}|a_{01}|^2 + \tfrac{1}{32}|a_{10}|^2 \\ \sigma(\Sigma^0 p, \Sigma^0 p) &= \sigma(\Lambda p, \Lambda p) = \tfrac{3}{64}|a_{01}|^2 + \tfrac{9}{64}|a_{10}|^2 \\ \sigma(\Sigma^0 p, \Lambda p) &= \tfrac{3}{64}|a_{01}|^2 + \tfrac{1}{64}|a_{10}|^2. \end{aligned} \tag{4}$$

Similarly, the NN cross sections become

$$\begin{aligned} \sigma_{pp} &= |a_{10+}|^2 \\ \sigma_{np} &= \tfrac{3}{4}|a_{01+}|^2 + \tfrac{1}{4}|a_{10+}|^2. \end{aligned} \tag{5}$$

If we restrict ourselves to scattering at an energy which is low enough so that scattering is important only for $l = 0$, we note that

$$a_{TS} = a_{TS+}. \tag{6}$$

Therefore, using eqs. (4), (5), and (6) we can write the spin-averaged YN cross sections in terms of $\sigma_{pp}$ and $\sigma_{np}$ as follows:

† K mesons, which we are neglecting, can lead to YN forces with exchange properties.

$$\begin{aligned}
&\sigma(\Sigma^+\mathrm{p}, \Sigma^+\mathrm{p}) = \sigma(\Xi^0\mathrm{p}, \Xi^0\mathrm{p}) = \tfrac{1}{4}\sigma_{\mathrm{pp}} \\
&\sigma(\Sigma^+\mathrm{n}, \Sigma^+\mathrm{n}) = \sigma(\Xi^-\mathrm{p}, \Xi^-\mathrm{p}) = \sigma(\Xi^-\mathrm{p}, \Xi^0\mathrm{n}) = \tfrac{1}{4}\sigma_{\mathrm{np}} \\
&\sigma(\Sigma^+\mathrm{n}, \Sigma^0\mathrm{p}) = \tfrac{1}{8}\sigma_{\mathrm{np}} \\
&\sigma(\Sigma^0\mathrm{p}, \Sigma^0\mathrm{p}) = \sigma(\Lambda\mathrm{p}, \Lambda\mathrm{p}) = \tfrac{1}{16}\sigma_{\mathrm{np}} + \tfrac{1}{8}\sigma_{\mathrm{pp}} \\
&\sigma(\Sigma^+\mathrm{n}, \Lambda\mathrm{p}) = \tfrac{1}{8}(k_f/k_i)\sigma_{\mathrm{np}} \\
&\sigma(\Sigma^0\mathrm{p}, \Lambda\mathrm{p}) = \tfrac{1}{16}(k_f/k_i)\sigma_{\mathrm{np}}.
\end{aligned} \tag{7}$$

We have included a simple phase space correction to the cross sections $\sigma(\Sigma\mathrm{N}, \Lambda\mathrm{N})$ by multiplying by the ratio of the relative momentum of the outgoing particles $k_f$ to that of the incoming particles $k_i$. This factor is important at low energy where, for example, $k_f/k_i \approx 4$ if the $\Sigma$N system has a centre of mass energy of 5 MeV. The formulas (7) hold for the differential cross sections. Since the total pp cross section is defined by integrating the differential cross section over only half the sphere, the coefficients of $\sigma_{\mathrm{pp}}$ in (7) must be multiplied by 2 to make the formulas apply to the total cross sections. The remaining YN cross sections are given by the charge symmetry condition (2).

Thus we have succeeded in reducing the low energy YN cross sections to simple linear combinations of the NN cross sections.

## 3. Discussion

We here briefly consider the validity of some of the approximations made in deriving eqs. (7) for the YN cross sections.

Two approximations are the neglect of K mesons and baryon mass differences in obtaining the YN potentials. The error involved is difficult to estimate, but it may be of the order of 20 % [4]. Unfortunately, a given percentage error in the depth of a potential leads to twice that percentage error in the resulting cross section (in Born approximation). If the potential is large, the error in the cross section may become even larger.

A third approximation is the neglect of baryon mass differences in obtaining the YN cross sections from the potentials, except for phase space factors. Even if the YN potentials were correct, the YN cross sections would be in error due to this approximation. To obtain the cross sections exactly, one must solve a two-body Schrödinger equation using the correct masses. Although it is not necessary to neglect baryon mass differences in obtaining the cross sections from the potentials, it is consistent to do so because it was necessary to ignore mass differences in obtaining the potentials themselves.

A fourth approximation is the neglect of Coulomb forces, which become important in the very low energy region ($\lesssim$ 1 MeV) †. Even at higher

† Procedures in treating mixed Coulomb and nuclear forces are of course known; e.g. N. Mott and H. Massey [6]).

energies, measurements of the cross sections for charged particles should be restricted to large angle scattering for the purpose of comparing with (7).

A fifth approximation is the assumption that the Serber potential can be used to represent the interaction between two nucleons. High energy ($\approx$ 150 MeV laboratory energy) NN scattering experiments show that the NN potential cannot be zero in odd angular momentum states. However, one of the principal corrections which is needed is an additional spin-orbit potential [9]). Since a spin-orbit potential vanishes for $l = 0$, it does not affect the low energy cross sections of eqs. (7). It is not yet established how big the remaining corrections to the Serber potential must be.

In view of our approximations, the formulas (7) are certainly not quantitatively accurate. But they may be useful to predict the order of magnitudes of the YN scattering cross sections.

In this connection, note that the cross sections of eq. (7) are different from those predicted in ref.[5]). In particular, the cross sections $\sigma(\Sigma N, \Lambda N)$ obtained here are much larger than those of ref.[5]). There are two reasons why the calculations do not give identical results. The first is simply that the Serber potential is not the same as the Brueckner-Watson potential †. The second reason is that baryon mass differences were not treated alike in the two papers. The $\Sigma$-$\Lambda$ mass difference, although small compared to other baryon mass differences which we have neglected, can have a large effect on $\sigma(\Sigma N, \Lambda N)$ because the YN potentials couple the $\Lambda$ and $\Sigma$. We cannot take the $\Sigma-\Lambda$ mass difference into account in our present work without writing the YN potentials explicitly. Here we had to assume only that the NN potentials vanish for odd $l$.

There are at present almost no experimental data with which to compare the calculated YN cross sections ††. Furthermore, when more experimental information becomes available, much of it is likely to be at energies above those for which our formulas are valid. (If the energy is sufficiently high so that scattering is important in states with $l \neq 0$, eqs. (7) break down completely.) In a subsequent paper we shall apply the Serber potential to YN scattering at higher energies.

The author would like to thank Professor A. Bohr and Professor B. Mottelson for the hospitality shown him during a month's stay at the Institute for Theoretical Physics in Copenhagen, during which time this work was begun. He also acknowledges the receipt of a Fulbright travel grant.

† Note also that tensor forces were neglected in the calculation of ref. [5]). No such approximation is made in the present treatment.

†† For a very preliminary result, see ref. [10]). Some evidence about the YN cross sections can also be obtained from analyses of more complicated processes such as Y + nucleus → Y + nucleus.

## References

1) E. Wigner, Proc. Nat. Acad. Sci. U.S. **38** (1952) 449
2) M. Gell-Mann, Phys. Rev. **106** (1957) 1296
3) J. Schwinger, Annals of Physics **2** (1957) 407
4) D. Lichtenberg and M. Ross, Padua-Venice Conference on Mesons and Recently Discovered Particles (1957) and Phys. Rev. **109** (1958) 2163
5) D. Lichtenberg and M. Ross, Phys. Rev. **107** (1957) 1714
6) K. Brueckner and K. Watson, Phys. Rev. **92** (1953) 1023
7) J. Blatt and V. Weisskopf, Theoretical Nuclear Physics (John Wiley, New York, 1952) p. 170
8) N. Mott and H. Massey, Theory of Atomic Collisions (Oxford, 1949)
9) J. Gammel and R. Thaler, Phys. Rev. **107** (1957) 291;
P. Signell and R. Marshak, Phys. Rev. **109** (1958) 1229
10) Alvarez, Bradner, Falk-Vairant, Gow, Rosenfeld, Solmitz and Tripp, Nuovo Cimento **5** (1957) 1026

1.D.1:
6.D

*Nuclear Physics* 8 (1958) 19—40; © *North-Holland Publishing Co., Amsterdam*
Not to be reproduced by photoprint or microfilm without written permission from the publisher

# SHORT RANGE FORCES AND NUCLEAR SHELL THEORY

MARCOS MOSHINSKY

*Instituto de Física, Universidad de México, e Instituto Nacional de la Investigación Científica, México, D.F.* †

Received 29 April 1958

**Abstract:** We develop a procedure for obtaining, in nuclear shell theory, the matrix elements associated with short range interactions between nucleons. We show that potentials of arbitrary range, both central and spin dependent, can be developed in terms of a series of velocity dependent potentials in increasing powers of the momentum, but all of zero range. The coefficients of the terms in this series are the successive moments of the potential; thus, for short range forces, only the first few terms of the series will be relevant. We obtain all the matrix elements for two nucleons in the same shell and in *LS* coupling, up to terms containing the first moment of the potential. We compare the matrix elements for central, spin-orbit coupling and tensor forces, taking for the interaction potential between nucleons, a value that has been proposed recently.

## 1. Introduction

The development of nuclear shell theory as means of coordinating information on ground and low excited states of nuclei, has been very significant in the last decade [1]). It seems that in the future more refined calculations will be necessary, using the different types of nuclear forces acting in nuclear matter [2]). It is well known that all matrix elements [3]) for the interaction forces, can be reduced to two particle interaction matrix elements. These two particle interaction matrix elements, have been evaluated [3]) by the standard methods of atomic spectroscopy in terms of the Slater coefficients. But the procedure of development in terms of Slater coefficients has one definite disadvantage in nuclear shell theory. If the forces between the nucleons were of long range compared with the size of the wave function, i.e. with the nuclear radius, then only the Slater coefficient $F^0$ would be of importance, and the calculations would be very simple. But if the forces are of short range, as compared with the nuclear radius, then all the Slater coefficients are of the same order of magnitude, and the calculations are complex.

It would be convenient to develop a method of evaluating two particle interaction matrix elements, by a procedure that would give simple and compact results for short range rather than for long range forces. This is

† An abstract of this paper appeared in the Proceedings of the International Conference on Nuclear Structure, Rehovoth, Israel [18]).

done in the present paper by showing that forces of arbitrary range, both central and spin dependent, could be developed in terms of a series of velocity dependent forces, in increasing powers of the momentum, but all of zero range. The coefficients of the terms in this series are the successive moments of the potential, so that for short range forces, only the first, or the first few terms of the series, will contribute significantly to the two particle interaction matrix elements. These matrix elements will also be easy to evaluate, as the velocity dependent forces, being of zero range, i.e. containing a $\delta(\mathbf{r}_1-\mathbf{r}_2)$ function, will reduce the double integrals in the matrix elements to single integrals.

We shall first illustrate the development of the potential by a one dimensional example, and later apply similar developments to central, spin orbit coupling and tensor two particle interactions.

If we consider a one dimensional potential $V(x)$ of non-zero range, then in a momentum space representation [4]) it will be given by the operator

$$v(p'-p'') = (2\pi\hbar)^{-1}\int_{-\infty}^{\infty} \exp(-ip'x/\hbar)V(x)\exp(ip''x/\hbar)\mathrm{d}x. \tag{1.1}$$

Developing the exponentials in a series, we obtain

$$v(p'-p'') = (2\pi\hbar)^{-1}\sum_{n'=0}^{\infty}\sum_{n''=0}^{\infty} i^{n''-n'}[n'!\,n''!\,\hbar^{n'+n''}]^{-1} I_{n'+n''}(p')^{n'}(p'')^{n''}, \tag{1.2}$$

where

$$I_{n'+n''} = \int_{-\infty}^{\infty} V(x)x^{n'+n''}\,\mathrm{d}x. \tag{1.3}$$

We assume of course, that the potential is of short range, in such a way that all the $I$'s are bounded.

Let us now construct in configuration space the zero range velocity dependent potential

$$\sum_{n'=0}^{\infty}\sum_{n''=0}^{\infty} i^{n''-n'}[n'!\,n''!\,\hbar^{n'+n''}]^{-1} I_{n'+n''}p^{n'}\,\delta(x)p^{n''}, \tag{1.4}$$

where $p$ is the operator

$$p = (\hbar/i)(\partial/\partial x). \tag{1.5}$$

It is obvious that the operator (1.4) has in momentum space the representation (1.2). Therefore $V(x)$ and (1.4) have the same representation in momentum space, which means that they are also identical in any other representation. This indicates that a short range potential could, in principle, be developed in a series of velocity dependent potentials in increasing powers of the momentum, but of zero range.

The development (1.4) is not a very useful one if we were interested in using it to obtain exact solutions of the Schroedinger equation, such as for example in scattering problems. It is a very useful one though, if we are

interested only in matrix elements. In fact, if we would like to have the matrix element of $V(x)$ between the states $\psi_q(x)$, $\psi_r(x)$ then applying the equivalent representation (1.4) we would have, integrating by parts,

$$\int_{-\infty}^{\infty} \psi_q^*(x) V(x) \psi_r(x) \mathrm{d}x$$

$$= \sum_{n'=0}^{\infty} \sum_{n''=0}^{\infty} [n'!\, n''!]^{-1} I_{n'+n''} (\mathrm{d}^{n'} \psi_q^*/\mathrm{d}x^{n'})_{x=0} (\mathrm{d}^{n''} \psi_r/\mathrm{d}x^{n''})_{x=0} \tag{1.6}$$

$$\equiv \int_{-\infty}^{\infty} [\sum_{n'=0}^{\infty} (n'!)^{-1} (\mathrm{d}^{n'} \psi_q/\mathrm{d}x^{n'})_{x=0} x^{n'}]^* V(x) [\sum_{n''=0}^{\infty} (n''!)^{-1} (\mathrm{d}^{n''} \psi_r/\mathrm{d}x^{n''})_{x=0} x^{n''}] \mathrm{d}x.$$

From (1.6) we see that taking the representation (1.4) of the potential in a matrix element, amounts to taking a Taylor expansion of the wave functions around the origin $x = 0$. It is clear that this type of expansion is useful if $V(x)$ is of short range, as in this case we could limit the expansion to the first or at most the first few terms, permitting a quick and simple determination of the matrix element.

In the following sections we shall make expansions similar to (1.4) for the different types of nuclear forces, and we shall keep in these expansions the first or at most the first few relevant terms. We shall then evaluate the two particle interaction matrix elements for these terms, and give tabulations for the case that the two particles are in the same shell. In previous [5,6]) and following publications, we apply this technique to problems of relevance in nuclear shell theory, and in the theory of nuclear forces.

## 2. Short Range Central Forces

Let us take a short range central force $V(r)$ and consider its representation in momentum space

$$v(\mathbf{p}'-\mathbf{p}'') = (2\pi\hbar)^{-3} \int \exp[-i(\mathbf{p}' \cdot \mathbf{r})/\hbar] V(r) \exp[i(\mathbf{p}'' \cdot \mathbf{r})/\hbar] \mathrm{d}\tau. \tag{2.1}$$

Integrating over the angular variables and expanding the sine function, we obtain

$$\begin{aligned} v(\mathbf{p}'-\mathbf{p}'') &= (2\pi\hbar)^{-3} \int_0^{\infty} [4\pi r^2 V(r)][\hbar^{-1}|\mathbf{p}'-\mathbf{p}''|r]^{-1} \sin[\hbar^{-1}|\mathbf{p}'-\mathbf{p}''|r] \mathrm{d}r \\ &= (2\pi\hbar)^{-3} 4\pi [I_0 - (I_1/3!)\hbar^{-2}(p'^2 + p''^2 - 2\mathbf{p}' \cdot \mathbf{p}'') + \ldots], \end{aligned} \tag{2.2}$$

where the $I$'s are the moments of the potential given by

$$I_0 = \int_0^{\infty} V(r) r^2 \mathrm{d}r, \qquad I_1 = \int_0^{\infty} V(r) r^4 \mathrm{d}r, \text{ etc.} \tag{2.3}$$

From (2.2) and the reasoning of the previous section, $V(r)$ can be represented as

$$V(r) = I_0 4\pi\delta(\mathbf{r}) - (I_1/3!) 4\pi\hbar^{-2} [p^2 \delta(\mathbf{r}) + \delta(\mathbf{r}) p^2 - 2\mathbf{p} \cdot \delta(\mathbf{r}) \mathbf{p}] + \ldots, \tag{2.4}$$

where $\mathbf{p}$ is the operator

$$\mathbf{p} = (\hbar/i)\nabla. \tag{2.5}$$

If $V(r)$ is taken now as an interaction potential between two nucleons whose coordinates are $\mathbf{r}_1$, $\mathbf{r}_2$ and whose corresponding momenta are $\mathbf{p}_1$, $\mathbf{p}_2$, we have to replace $\mathbf{r}$, $\mathbf{p}$ in (2.4) by

$$\mathbf{r} = \mathbf{r}_1 - \mathbf{r}_2, \qquad \mathbf{p} = \tfrac{1}{2}(\mathbf{p}_1 - \mathbf{p}_2). \tag{2.6}$$

We shall give the matrix elements of $V(|\mathbf{r}_1 - \mathbf{r}_2|)$ up to the first moment $I_1$. The matrix elements will be obtained for $LS$ coupling as the passage to $jj$ coupling can be done directly with the tables [7]) of $9j$ coefficients. Furthermore, we shall restrict ourselves to matrix elements in which the two particles are in the same shell.

We designate the configuration space part of the wave function of a single nucleon as

$$|nlm\rangle = \Re_{nl}(r) Y_{lm}(\theta, \varphi), \tag{2.7}$$

where $Y_{lm}$ is a spherical harmonic. The wave function for a system of two nucleons with total orbital angular momentum $L$ is then given by

$$|(nl)^2 LM\rangle = \Re_{nl}(r_1)\Re_{nl}(r_2) \sum_{m_1 m_2} \langle ll m_1 m_2 | LM\rangle Y_{lm_1}(\theta_1, \varphi_1) Y_{lm_2}(\theta_2, \varphi_2), \tag{2.8}$$

where $\langle ll m_1 m_2 | LM\rangle$ is a Clebsch-Gordan coefficient. The operation of the $\delta$ function potential $\delta(\mathbf{r}_1 - \mathbf{r}_2)$ on the ket $|(nl)^2 LM\rangle$ will give zero unless $L$ is even, as

$$\sum_{m_1 m_2} \langle ll m_1 m_2 | LM\rangle Y_{lm_1}(\theta, \varphi) Y_{lm_2}(\theta, \varphi) = [(2l+1)^2/4\pi(2L+1)]^{\frac{1}{2}} \langle ll00|L0\rangle Y_{LM}(\theta, \varphi), \tag{2.9}$$

and $\langle ll00|L0\rangle \neq 0$ only if $l+l+L$ is even [8]). On the other hand,

$$[\tfrac{1}{2}(\mathbf{p}_1 - \mathbf{p}_2)|(nl)^2 LM\rangle]_{\mathbf{r}_1 = \mathbf{r}_2} \tag{2.10}$$

is zero unless $L$ is odd, as shown in the appendix of ref. [5]). We conclude therefore, that two different parts of (2.4) contribute to the matrix elements, according as $L$ is even or odd. For $L$ even, we have

$$\langle (nl)^2 L|V(r)|(nl)^2 L\rangle = I_0 \langle (nl)^2 L|4\pi\delta(\mathbf{r})|(nl)^2 L\rangle - \tfrac{1}{3} I_1 \langle (nl)^2 L|4\pi\hbar^{-2}\delta(\mathbf{r})p^2|(nl)^2 L\rangle, \tag{2.11}$$

while for $L$ odd, we have

$$\langle (nl)^2 L|V(r)|(nl)^2 L\rangle = \tfrac{1}{3} I_1 \langle (nl)^2 L|4\pi\hbar^{-2}\mathbf{p}\cdot\delta(\mathbf{r})\mathbf{p}|(nl)^2 L\rangle, \tag{2.12}$$

where in both cases, $\mathbf{r}$, $\mathbf{p}$ are given by (2.6).

The matrix elements of $\delta(\mathbf{r})$ and $\mathbf{p}\cdot\delta(\mathbf{r})\mathbf{p}$ have been obtained previously [5]), and that for $\delta(\mathbf{r})p^2$ is given in appendix 1. We quote the results for the matrix elements. For $4\pi\delta(\mathbf{r})$ we have

$$\langle (nl)^2 L|4\pi\delta(\mathbf{r})|(nl)^2 L\rangle = B_{nl} G(l, L), \tag{2.13}$$

where

$$B_{nl} = \int_0^\infty r^2 [\Re_{nl}(r)]^4 \, dr, \tag{2.14}$$

and

$$G(l, L) = (2l+1)^2(2L+1)^{-1}[\langle ll00|L0\rangle]^2. \tag{2.15}$$

For $4\pi\hbar^{-2}\delta(\mathbf{r})p^2$ we have

$$\langle (nl)^2 L|4\pi\hbar^{-2}\delta(\mathbf{r})p^2|(nl)^2 L\rangle = G(l, L)\{-\tfrac{2}{3}D_{nl}+[\tfrac{1}{3}l(l+1)-\tfrac{1}{4}L(L+1)]A_{nl}\}, \tag{2.16}$$

where $G(l, L)$ is given in (2.15) and

$$A_{nl} = \int_0^\infty [\Re_{nl}(r)]^4 \, dr, \tag{2.17}$$

$$D_{nl} = \int_0^\infty \Re_{nl}^3 \left[\frac{1}{r^2}\frac{d}{dr}r^2\frac{d}{dr} - \frac{l(l+1)}{r^2}\right]\Re_{nl} r^2 \, dr. \tag{2.18}$$

Finally, for $4\pi\hbar^{-2}\,\mathbf{p}\cdot\delta(\mathbf{r})\mathbf{p}$ we have [5])

$$\langle (nl)^2 L|4\pi\hbar^{-2}\,\mathbf{p}\cdot\delta(\mathbf{r})\mathbf{p}|(nl)^2 L\rangle = A_{nl}H(l, L), \tag{2.19}$$

where $A_{nl}$ is given by (2.17) and $H(l, L)$ by [5,6])

$$H(l, L) = (l+1)(2l+3)(2l+1)^3[\langle l+1l00|L0\rangle]^2[W(ll+1LL;\,1l)]^2, \tag{2.20}$$

where $W$ is a Racah coefficient [8]).

In section 5 we discuss and tabulate the radial integrals $A_{nl}$, $B_{nl}$, $D_{nl}$ and the coefficients $G(l, L)$ and $H(l, L)$.

## 3. Short Range Spin-Orbit Coupling Forces

We now take the two particle spin-orbit coupling potential

$$V_{ls} = V(r)\hbar^{-1}\mathbf{l}\cdot\mathbf{S}, \tag{3.1}$$

where

$$\mathbf{l} = \mathbf{r}\times\mathbf{p}, \qquad \mathbf{S} = \tfrac{1}{2}(\boldsymbol{\sigma}_1+\boldsymbol{\sigma}_2), \tag{3.2}$$

with $\mathbf{r}$, $\mathbf{p}$ being the relative coordinate and momentum as in (2.6), and $\boldsymbol{\sigma}_1$, $\boldsymbol{\sigma}_2$ the spin operators for the two particles.

The representation of $V_{ls}$ in momentum space has the form

$$v_{ls}(\mathbf{p}', \mathbf{p}'') = (2\pi\hbar)^{-3}\int \exp[-i(\mathbf{p}'\cdot\mathbf{r})/\hbar][-V(r)\hbar^{-1}][\mathbf{r}\cdot(\mathbf{S}\times\mathbf{p})]\exp[i(\mathbf{p}''\cdot\mathbf{r})/\hbar]d\tau. \tag{3.3}$$

As the momentum $\mathbf{p}$ operates only on the exponential to the right, it gives the constant $\mathbf{p}''$, and taking the vector product outside of the integral, we obtain

$$v_{ls}(\mathbf{p}', \mathbf{p}'') = (2\pi\hbar)^{-3}\sum_{m=-1}^{1}(-1)^m(\mathbf{S}\times\mathbf{p}'')_{-m}\int[-V(r)\hbar^{-1}]\chi_m\exp[i(\mathbf{p}''-\mathbf{p}')\cdot\mathbf{r}/\hbar]d\tau, \tag{3.4}$$

where the indices $m = -1, 0, 1$ stand for the spherical component of the vectors, so that for example

$$\chi_m = (\tfrac{4}{3}\pi)^{\frac{1}{2}} r Y_{1m}(\theta, \varphi). \tag{3.5}$$

Integrating over the angular part in (3.4), we obtain [9])

$$v_{ls}(\mathbf{p}', \mathbf{p}'') = (2\pi\hbar)^{-3} \sum_{m=-1}^{1} [(-1)^m (\mathbf{S}\times\mathbf{p}'')_{-m} Y_{1m}(\alpha, \beta)] \cdot (\tfrac{4}{3}\pi)^{\frac{1}{2}} \{4\pi i \int_0^\infty r^3 [-\hbar^{-1} V(r)] j_1(Pr/\hbar) \mathrm{d}r\}, \tag{3.6}$$

where $j_1$ is the spherical Bessel function of order 1. In (3.6) the vector $\mathbf{P}$ stands for $\mathbf{P} = \mathbf{p}''-\mathbf{p}'$, and the spherical coordinates for the point it designates in momentum space, are denoted by $P, \alpha, \beta$.

If the potential $V(r)$ is of short range, we can expand $j_1(Pr/\hbar)$ in a power series, and keeping only the first term $\frac{1}{3}(Pr/\hbar)$, we see that (3.6) becomes

$$v_{ls}(\mathbf{p}', \mathbf{p}'') \simeq (2\pi\hbar)^{-3}(-4\pi i/3\hbar^2) I_1 (\mathbf{S}\times\mathbf{p}'') \cdot (\mathbf{p}''-\mathbf{p}'), \tag{3.7}$$

where $I_1$ is the first moment of the potential $V(r)$ as in (2.3), and the vectors are denoted in the usual notation, rather than in spherical components.

From (3.7) and the reasoning of section 1, $V_{ls}$ can be represented as

$$V_{ls} = \tfrac{1}{3} I_1 4\pi i \hbar^{-2} \mathbf{p} \cdot \delta(\mathbf{r}) (\mathbf{S}\times\mathbf{p}). \tag{3.8}$$

We shall give the matrix elements of (3.8) in $LS$ coupling. The wave function for two particles in the same shell becomes now

$$|(nl)^2 L, S, JM\rangle = \sum_{M_L M_S} |(nl)^2 LM_L\rangle |SM_S\rangle \langle LSM_L M_S | JM\rangle, \tag{3.9}$$

where $|(nl)^2 LM\rangle$ is given by (2.8). The matrix element of (3.8) will be different from zero only in the triplet state, so that we have [8])

$$\langle (nl)^2 L', 1, J | V_{ls} | (nl)^2 L, 1, J\rangle = \tfrac{1}{3} I_1 (-1)^{L'+1-J} \langle (nl)^2 L' \| -4\pi i \hbar^{-2} \mathbf{p}\times\delta(\mathbf{r})\mathbf{p} \| (nl)^2 L\rangle \cdot \langle 1\|S\|1\rangle W(L' L 1 1; 1 J). \tag{3.10}$$

From (2.10) we see that the matrix element of $\mathbf{p}\times\delta(\mathbf{r})\mathbf{p}$ will be zero, unless both $L'$, $L$ are odd. Furthermore, from the Racah coefficient in (3.10), we have $L' = L\pm 1, L$, so that we conclude that $L' = L$ and $L$ is odd.

The matrix element of $\mathbf{p}\times\delta(\mathbf{r})\mathbf{p}$ was essentially derived in ref. [6]) in terms of the matrix element of $\mathbf{p}\cdot\delta(\mathbf{r})\mathbf{p}$. A more direct derivation is given in the appendix 2 of this paper. We quote the result

$$\langle (nl)^2 L \| -4\pi i \hbar^{-2} \mathbf{p}\times\delta(\mathbf{r})\mathbf{p} \| (nl)^2 L\rangle = [(2L+1)/L(L+1)]^{\frac{1}{2}} A_{nl} H(l, L), \tag{3.11}$$

where $A_{nl}$ is given by (2.17), and $H(l, L)$ by (2.20). For $\langle 1\|S\|1\rangle$ we have of course [8]),

$$\langle 1\|S\|1\rangle = (6)^{\frac{1}{2}}. \tag{3.12}$$

In section 5 we shall discuss and tabulate the matrix element (3.10).

## 4. Short Range Tensor Forces

We discuss in this section the tensor potential

$$V_T = V(r)r^{-2}[3(\sigma_1\cdot\mathbf{r})(\sigma_2\cdot\mathbf{r})-(\sigma_1\cdot\sigma_2)r^2] = 2V(r)r^{-2}[3(\mathbf{S}\cdot\mathbf{r})^2-S^2r^2], \quad (4.1)$$

where $\mathbf{S}$ is given by (3.2). Using the procedure developed in refs. [5,6]), we could write the tensor potential as the scalar product [8])

$$V_T = V(r)(\tfrac{32}{5}\pi)^{\frac{1}{2}}\,\mathbf{Y}_2\cdot\mathbf{X}_2 \quad (4.2)$$

where $\mathbf{Y}_2$ represents the Racah tensor [8]) whose components are the spherical harmonics $Y_{2m}(\theta,\varphi)$, and the $m=0$ component of the Racah tensor $\mathbf{X}_2$ is given by

$$X_{20} = \frac{1}{\sqrt{2}}(3S_z^2-S^2). \quad (4.3)$$

The representation of $V_T$ in momentum space has the form

$$v_T(\mathbf{p}'-\mathbf{p}'') = (2\pi\hbar)^{-3}(\tfrac{32}{5}\pi)^{\frac{1}{2}}\sum_{m=-2}^{2}\{(-1)^m X_{2-m} \int V(r)Y_{2m}(\theta,\varphi)\exp[i(\mathbf{p}''-\mathbf{p}')\cdot\mathbf{r}/\hbar]\mathrm{d}\tau\}. \quad (4.4)$$

Integrating over the angular part in (4.4), we obtain [9])

$$v_T(\mathbf{p}'-\mathbf{p}'') = (2\pi\hbar)^{-3}(\tfrac{32}{5}\pi)^{\frac{1}{2}}\sum_{m=-2}^{2}[(-1)^m X_{2-m}\,Y_{2m}(\alpha,\beta)] \cdot[-4\pi\int_0^\infty V(r)j_2(Pr/\hbar)r^2\,\mathrm{d}r], \quad (4.5)$$

where $j_2$ is the spherical Bessel function of order 2, and $P$, $\alpha$, $\beta$ have the same meaning as in the previous section.

If the potential $V(r)$ is of short range, we can expand $j_2(Pr/\hbar)$ in a power series, and keeping only the first term $\frac{1}{15}(Pr/\hbar)^2$, we see that (4.5) becomes

$$v_T(\mathbf{p}'-\mathbf{p}'') = (2\pi\hbar)^{-3}(-\tfrac{2}{15}I_1)\,\mathfrak{T}_2\cdot\mathbf{X}_2, \quad (4.6)$$

where $I_1$ is the first moment of the potential given in (2.3), and $\mathfrak{T}_2$ is a second order Racah tensor whose $m=0$ component is

$$\mathfrak{T}_{20} = \frac{4\pi}{\sqrt{2}}\hbar^{-2}[3(p_z''-p_z')^2-(\mathbf{p}''-\mathbf{p}')^2]. \quad (4.7)$$

From (4.6) and the reasoning of section 1, $V_T$ can be represented as

$$V_T = -\tfrac{2}{15}I_1\,\mathbf{T}_2\cdot\mathbf{X}_2, \quad (4.8)$$

where the Racah tensor $\mathbf{T}_2$ is now an operator whose $m=0$ component has the form

$$T_{20} = \frac{4\pi}{\sqrt{2}}\hbar^{-2}\{\delta(\mathbf{r})(3p_z^2-p^2)+(3p_z^2-p^2)\delta(\mathbf{r}) - 2[3p_z\delta(\mathbf{r})p_z-\mathbf{p}\cdot\delta(\mathbf{r})\mathbf{p}]\}. \quad (4.9)$$

We now discuss the matrix elements of $V_T$ in $LS$ coupling. For nucleons in the same shell, the wave function is given by (3.9) and as the tensor force acts only on the triplet state, the general matrix element is [8])

$$\langle (nl)^2 L', 1, J|V_T|(nl)^2 L, 1, J\rangle = -\tfrac{2}{15} I_1 (-1)^{L'+1-J} \langle (nl)^2 L'||T_2||(nl)^2 L\rangle \cdot (15)^{\frac{1}{2}} W(L'L11; 2J), \quad (4.10)$$

where we have replaced the matrix element for $\mathbf{X}_2$ by the value [6])

$$\langle 1||X_2||1\rangle = (15)^{\frac{1}{2}}. \quad (4.11)$$

To evaluate the matrix element of $\mathbf{T}_2$, we notice first that because of (2.9), (2.10), two different parts of (4.9) contribute to the matrix element, according to whether $L'$, $L$ are odd of even. For $L'$, $L$ odd, we have that

$$\langle (nl)^2 L' M|T_{20}|(nl)^2 LM\rangle = -\sqrt{2}\langle (nl)^2 L' M|4\pi\hbar^{-2}[3p_z \delta(\mathbf{r}) p_z - \mathbf{p}\cdot\delta(\mathbf{r})\mathbf{p}]|(nl)^2 LM\rangle, \quad (4.12)$$

while for $L', L$ even we have

$$\langle (nl)^2 L' M|T_{20}|(nl)^2 LM\rangle = \frac{1}{\sqrt{2}} \langle (nl)^2 L' M|4\pi\hbar^{-2}[\delta(\mathbf{r})(3p_z^2 - p^2) + (3p_z^2 - p^2)\delta(\mathbf{r})]|(nl)^2 LM\rangle, \quad (4.13)$$

where in both cases $\mathbf{r}$, $\mathbf{p}$ are given by (2.6).

The matrix element of $\mathbf{T}_2$ for $L'$, $L$ odd was evaluated in ref. [6]), where it was shown to be zero unless $L' = L$. A more direct derivation is given in the appendix 3 of this paper. We quote the result

$$\langle (nl)^2 L||T_2||(nl)^2 L\rangle = -\sqrt{2} A_{nl} H(l, L) \cdot [(2L-1)(2L+1)(2L+3)]^{\frac{1}{2}} [L(L+1)]^{-\frac{1}{2}}, \quad (4.14)$$

where $A_{nl}$ is given by (2.17) and $H(l, L)$ by (2.20).

The tensor operator appearing in the matrix element (4.13) for $L', L$ even, could be expressed as the sum of two operators

$$\mathbf{T}_2 = \frac{1}{\sqrt{2}} (\mathbf{T}'_2 + \mathbf{T}''_2), \quad (4.15)$$

where the $m = 0$ components for $\mathbf{T}'_2$ and $\mathbf{T}''_2$ are given by

$$T'_{20} = 4\pi\hbar^{-2}(3p_z^2 - p^2)\delta(\mathbf{r}), \qquad T''_{20} = 4\pi\hbar^{-2}\delta(\mathbf{r})(3p_z^2 - p^2). \quad (4.16)$$

A matrix element of the type (4.13) for the tensor operator $\mathbf{T}'_2$, is clearly the transposed conjugate of the same matrix element for $\mathbf{T}''_2$. We need therefore only to derive the matrix element for $\mathbf{T}''_2$ which is done in appendix 3 of this paper. We quote the result

$$\langle (nl)^2 L'||T''_2||(nl)^2 L\rangle = -\tfrac{4}{3} D_{nl} K(l; L', L) - A_{nl}\{K(l; L', L)\chi(l; L', L) + G(l, L')[(2l-1)l(l+1)(2l+3)(2l+1)(2L+1)(2L'+1)]^{\frac{1}{2}} W(llLL'; 2l)\}, \quad (4.17)$$

where $L'$, $L$ are even. In (4.17) $A_{nl}$, $D_{nl}$ are the radial integrals given by (2.17) and (2.18) respectively, and $G(l, L')$ is defined by (2.15). The $W$ in (4.17) is a Racah coefficient, and $K(l; L', L)$ is given by

$$K(l; L', L) = (2l+1)^2(2L'+1)^{-\frac{1}{2}}\langle ll00|L0\rangle\langle ll00|L'0\rangle\langle L200|L'0\rangle. \quad (4.18)$$

Finally $\chi(l; L', L)$ has the explicit form

$$\begin{aligned} \chi(l; L+2, L) &= \tfrac{10}{3}l(l+1)+\tfrac{3}{4}-\tfrac{1}{2}L^2, \\ \chi(l; L, L) &= \tfrac{10}{3}l(l+1)-\tfrac{3}{4}+\tfrac{1}{2}L(L+1), \\ \chi(l; L-2, L) &= \tfrac{10}{3}l(l+1)+\tfrac{3}{4}-\tfrac{1}{2}(L+1)^2. \end{aligned} \quad (4.19)$$

In the next section we discuss and tabulate the matrix elements for tensor forces, for both $L$ even and odd.

## 5. Discussion and Tabulation of the Matrix Elements

In the previous section we obtained the matrix elements for short range central, spin-orbit coupling and tensor forces, in terms of the coefficients $G(l, L)$ defined by (2.15), $H(l, L)$ defined by (2.20) and the radial integrals $A_{nl}$, $B_{nl}$ and $D_{nl}$ given by (2.17), (2.14) and (2.18) respectively.

From the explicit form of the Clebsch-Gordan coefficients given by Racah [8]), we obtain for $G(l, L)$ the recurrence relation

$$G(l, 0) = (2l+1), \quad (5.1)$$

$$\frac{G(l, L+2)}{G(l, L)} = \frac{(L+1)^2}{(L+2)^2}\,\frac{(2l+1)^2-(L+1)^2}{(2l+1)^2-(L+2)^2}; \; L \text{ even}. \quad (5.2)$$

Using this relation, $G(l, L)$ is tabulated for all the shells of interest in terms of simple fractions (table 1) and of decimal fractions (table 2). Note that from (2.15), $G(l, L)$ is defined only for even $L$ in the range $0 \leqq L \leqq 2l$.

From (2.20) and using again the explicit form of the Clebsch-Gordan and Racah coefficients [8, 10]), we obtain for $H(l, L)$ the recurrence relation [6])

$$H(l, 1) = \tfrac{1}{2}l(l+1)(2l+1), \quad (5.3)$$

$$\frac{H(l, L+2)}{H(l, L)} = \frac{L(L+2)}{(L+1)(L+3)}\,\frac{4l(l+1)-(L+1)(L+3)}{4l(l+1)-L(L+2)}; \; L \text{ odd}. \quad (5.4)$$

Using this relation, $H(l, L)$ is tabulated for all the shells of interest in terms of simple fractions, (table 3), and of decimal fractions (table 4). Note that from (2.20) $H(l, L)$ is defined only for odd $L$ in the range $0 < L < 2l$.

To evaluate the radial integrals $A_{nl}$, $B_{nl}$, $D_{nl}$ it is necessary to specify the common potential for the nucleons. It is useful to assume [11]) that the common potential has the harmonic oscillator form. In this case, the equation satisfied by the radial wave function $\mathfrak{R}_{nl}(r)$ is [11])

$$\left\{-\frac{\hbar^2}{2m}\left[\frac{1}{r^2}\frac{\mathrm{d}}{\mathrm{d}r}r^2\frac{\mathrm{d}}{\mathrm{d}r}-\frac{l(l+1)}{r^2}\right]+\tfrac{1}{2}m\omega^2r^2\right\}\mathfrak{R}_{nl}=\hbar\omega(2n+l+\tfrac{3}{2})\mathfrak{R}_{nl}, \qquad (5.5)$$

where $\omega$ is the frequency of the harmonic oscillator and $m$ the mass of the nucleon. Using (5.5) we see that the radial integral $D_{nl}$ given by (2.18), can be expressed as

$$D_{nl}=\nu^2C_{nl}-(4n+2l+3)\nu B_{nl}, \qquad (5.6)$$

where $B_{nl}$ is given by (2.14), $C_{nl}$ is the radial integral

$$C_{nl}=\int_0^\infty r^4[\mathfrak{R}_{nl}(r)]^4\,\mathrm{d}r, \qquad (5.7)$$

and

$$\nu=m\omega/\hbar. \qquad (5.8)$$

It is convenient to introduce the radial integrals $A'_{nl}$, $B'_{nl}$, $C'_{nl}$ and $D'_{nl}$, that are nondimensional and independent of $\nu$ by the relations

$$A_{nl}=\left(\frac{\nu^5}{2\pi}\right)^{\frac{1}{2}}A'_{nl},\quad B_{nl}=\left(\frac{\nu^3}{2\pi}\right)^{\frac{1}{2}}B'_{nl},\quad C_{nl}=\left(\frac{\nu}{2\pi}\right)^{\frac{1}{2}}C'_{nl},\quad D_{nl}=\left(\frac{\nu^5}{2\pi}\right)^{\frac{1}{2}}D'_{nl}. \qquad (5.9)$$

Defining the integral $M^k_{nl}$ as

$$M^k_{nl}=(2\pi)^{\frac{1}{2}}N^4_{nl}\int_0^\infty x^{2k+4l}\exp(-2x^2)v^4_{nl}(x^2)\mathrm{d}x, \qquad (5.10)$$

where $v_{nl}(x^2)$ are the associate Laguerre polynomials, and $N_{nl}$ the normalization constants for $\nu=1$, as given by Talmi [11]), we see from (5.9), (5.6) and (2.14), (2.17) that

$$A'_{nl}=M^0_{nl},\quad B'_{nl}=M^1_{nl},\quad C'_{nl}=M^2_{nl},\quad D'_{nl}=C'_{nl}-(4n+2l+3)B'_{nl}. \qquad (5.11)$$

From the explicit form [11]) of the polynomials $v_{nl}(x^2)$ we see that the radial integrals are rational numbers, and we tabulate these integrals as simple fractions in table 5, and as decimal fraction in table 6. The radial integral $B'_{nl}$ is, except for a factor of two, the same as the one tabulated by Zeldes [12]) (diagonal terms in tables 2a, 2b of his paper), but is reproduced here for the sake of completeness. The radial integral $D'_{nl}$ is always negative, so $-D'_{nl}$ is given in tables 5 and 6.

With the help of tables 1 to 6, we easily determine, up to first moment of the potentials, the matrix elements in $LS$ coupling for the different types of short range forces. It is convenient to express these matrix elements in units of the moments of the potentials $I_k$, $k=0,1,\ldots$, as in this way we do not need to specify in advance the parameters for the potentials. As the moments of the potentials, the first of which are given by (2.3), do not have the same units, we may define the reduced moments $I'_k$ as

$$I'_k\equiv(2k+1)^{-1}I_k\left(\frac{\nu^{2k+3}}{2\pi}\right)^{\frac{1}{2}}, \qquad (5.12)$$

and the $I'_k$ have the units of energy. In terms of the $I'_k$, the matrix elements for the short range central forces of section 2, take the form

$$\langle (nl)^2 L|V(r)|(nl)^2 L\rangle = I'_0 B'_{nl} G(l, L) - I'_1 U(nl, L), \tag{5.13}$$

where

$$U(nl, L) \equiv G(l, L)\{-\tfrac{2}{3}D'_{nl} + [\tfrac{1}{3}l(l+1) - \tfrac{1}{4}L(L+1)]A'_{nl}\}, \tag{5.14}$$

when $L$ is even, and the form

$$\langle (nl)^2 L|V(r)|(nl)^2 L\rangle = I'_1 A'_{nl} H(l, L), \tag{5.15}$$

when $L$ is odd.

For convenient use, we give the values of $B'_{nl}G(l, L)$ in table 7, and of $U(nl, L)$ in table 8, for all the relevant shells and for all even values of $L$ in the range $0 \leqq L \leqq 2l$. In table 9 we give the values of $A'_{nl}H(l, L)$ for all odd $L$ in the relevant range $0 < L < 2l$. To compare the contribution to the matrix elements of the different moments of the potentials, we need to estimate $I'_0$, $I'_1$ for the forces under discussion. We shall do this in the next section.

For the spin-orbit coupling force of section 3, the matrix element up to first moment of the potential is given by (3.10) and (3.11), so it becomes

$$\begin{aligned}
&\langle (nl)^2 L, 1, J|V_{LS}|(nl)^2 L, 1, J\rangle \\
&= [I'_1 A'_{nl} H(l, L)]\left\{(-1)^{L+1-J}(6)^{\frac{1}{2}}\left[\frac{2L+1}{L(L+1)}\right]^{\frac{1}{2}} W(LL11; 1J)\right\} \\
&= I'_1 A'_{nl} H(l, L)\begin{cases} (L+1)^{-1} & \text{if } J = L+1 \\ -[L(L+1)]^{-1} & \text{if } J = L \\ (-L)^{-1} & \text{if } J = L-1, \end{cases}
\end{aligned} \tag{5.16}$$

where $L$ is restricted to odd values. From table 9, we can immediately obtain the matrix elements for a short range spin-orbit coupling force in units of the reduced moment $I'_1$. We note that the $I'_1$ in this case, is in general, different from the one that appears in (5.13) and (5.15), as the parameters of the radial part of the spin-orbit potential are, in general, different from those of the central force.

For the tensor force, we first consider the matrix elements in which $L$ is odd, and from (4.10) and (4.14) we have

$$\begin{aligned}
&\langle (nl)^2 L, 1, J|V_T|(nl)^2 L, 1, J\rangle \\
&= I'_1 A'_{nl} H(l,L)\begin{cases} \dfrac{2}{5}\dfrac{(2L-1)}{(L+1)} & \text{if } J = L+1 \\ -\dfrac{2}{5}\dfrac{(2L-1)(2L+3)}{L(L+1)} & \text{if } J = L \\ \dfrac{2}{5}\dfrac{(2L+3)}{L} & \text{if } J = L-1. \end{cases}
\end{aligned} \tag{5.17}$$

The matrix elements for the tensor force with $L$ odd, can also be obtained from table 9, in units of the reduced moment $I'_1$.

For $L$ even, the matrix elements for the tensor forces are given by (4.10) and (4.17). Using the explicit forms for the Clebsch-Gordan and Racah coefficients [8,10]) we can reduce (4.17) to simple expressions containing $G(l, L)$ as well as the radial integrals $A_{nl}$, $D_{nl}$. We shall limit ourselves to considering the diagonal matrix elements for the tensor forces, i.e. those for which $L' = L$, as they give the interaction energy in $LS$ coupling. From (4.10), (4.17) and the definition (2.15) of $G(l, L)$, we obtain

$$\langle (nl)^2 L, 1, J|V_T|(nl)^2 L, 1, J\rangle = I'_1 Z(nl, L) \begin{cases} -[L/(2L+3)] & \text{if } J = L+1 \\ 1 & \text{if } J = L \\ -[(L+1)/(2L-1)] & \text{if } J = L-1, \end{cases} \tag{5.18}$$

where $Z(nl, L)$ is defined by

$$Z(nl, L) = \tfrac{4}{5} G(l, L)\{\tfrac{2}{3} D'_{nl} + [\tfrac{8}{3} l(l+1) + \tfrac{3}{8} - \tfrac{1}{2} L(L+1)] A'_{nl}\}. \tag{5.19}$$

In table 10, we give the values of $Z(nl, L)$ for all relevant shells, and for even values of $L$ in the range $0 \leqq L \leqq 2l$. These values correspond to the interaction energy for tensor forces in $LS$ coupling, when $L$ is even and $J = L$, given in units of the reduced moment.

The matrix elements obtained in this paper are for two nucleons in the same shell and in $LS$ coupling. We can pass to $jj$ coupling with the help of the $9j$ coefficients [7]). For nucleons in different shells, the methods discussed in this paper are still applicable, though the matrix elements will be more complex. A general tabulation is in progress.

TABLE 1

Table of the coefficient $G(l, L)$ defined by (5.2). Simple fractions

| $l$ \ $L$ | 0 | 2 | 4 | 6 | 8 | 10 | 12 |
|---|---|---|---|---|---|---|---|
| 0 | 1 | | | | | | |
| 1 | 3 | 6/5 | | | | | |
| 2 | 5 | 10/7 | 10/7 | | | | |
| 3 | 7 | 28/15 | 14/11 | 700/429 | | | |
| 4 | 9 | 180/77 | 1458/1001 | 180/143 | 4410/2431 | | |
| 5 | 11 | 110/39 | 22/13 | 880/663 | 5390/4199 | 8316/4199 | |
| 6 | 13 | 182/55 | 364/187 | 5200/3553 | 4550/3553 | 9828/7429 | 396396/185725 |

TABLE 2

Table of the coefficient $G(l, L)$ defined by (5.2). Decimal fractions

| $l$ \ $L$ | 0 | 2 | 4 | 6 | 8 | 10 | 12 |
|---|---|---|---|---|---|---|---|
| 0 | 1 | | | | | | |
| 1 | 3 | 1.200 | | | | | |
| 2 | 5 | 1.429 | 1.429 | | | | |
| 3 | 7 | 1.867 | 1.273 | 1.632 | | | |
| 4 | 9 | 2.338 | 1.457 | 1.259 | 1.814 | | |
| 5 | 11 | 2.821 | 1.692 | 1.327 | 1.284 | 1.980 | |
| 6 | 13 | 3.309 | 1.947 | 1.464 | 1.281 | 1.323 | 2.134 |

TABLE 3

Table of the coefficient $H(l, L)$ defined by (5.4). Simple fractions

| $l$ \ $L$ | 1 | 3 | 5 | 7 | 9 | 11 |
|---|---|---|---|---|---|---|
| 1 | 3 | | | | | |
| 2 | 15 | 30/7 | | | | |
| 3 | 42 | 14 | 70/11 | | | |
| 4 | 90 | 2430/77 | 2430/143 | 1260/143 | | |
| 5 | 165 | 770/13 | 440/13 | 4620/221 | 48510/4199 | |
| 6 | 273 | 1092/11 | 10920/187 | 136500/3553 | 8190/323 | 108108/7429 |

TABLE 4

Table of the coefficient $H(l, L)$ defined by (5.4). Decimal fractions

| $l$ \ $L$ | 1 | 3 | 5 | 7 | 9 | 11 |
|---|---|---|---|---|---|---|
| 1 | 3 | | | | | |
| 2 | 15 | 4.286 | | | | |
| 3 | 42 | 14.000 | 6.364 | | | |
| 4 | 90 | 31.558 | 16.993 | 8.811 | | |
| 5 | 165 | 59.231 | 33.846 | 20.905 | 11.553 | |
| 6 | 273 | 99.273 | 58.396 | 38.418 | 25.356 | 14.552 |

TABLE 5

Table of the radial integrals $A'_{nl}$, $B'_{nl}$, $C'_{nl}$, $-D'_{nl}$ defined by (5.11) and (5.10) Simple fractions

| $(n+1)l$ | $A'_{nl}$ | $B'_{nl}$ | $C'_{nl}$ | $-D'_{nl}$ |
|---|---|---|---|---|
| 1s | 8 | 2 | 3/2 | 9/2 |
| 1p | 2/3 | 5/6 | 35/24 | 65/24 |
| 1d | 7/30 | 21/40 | 231/160 | 357/160 |
| 1f | 33/280 | 429/1120 | 6435/4480 | 9009/4480 |
| 1g | 143/2016 | 2431/8064 | 46189/32256 | 60775/32256 |
| 1h | 4199/88704 | 4199/16896 | 96577/67584 | 121771/67584 |
| 1i | 7429/219648 | 185725/878592 | 5014575/3514368 | 6128925/3514368 |
| 2s | 275/24 | 41/32 | 147/128 | 1001/128 |
| 2p | 373/480 | 363/640 | 8575/7680 | 30629/7680 |
| 2d | 26312/107520 | 6579/17920 | 78969/71680 | 210507/71680 |
| 2f | 130823/1128960 | 58487/215040 | 188045/172032 | 2101099/860160 |
| 2g | 94757/1419264 | 136357/630784 | 24694319/22708224 | 48938461/22708224 |
| 3s | 87347/6144 | 8257/8192 | 32307/32768 | 331001/32768 |
| 3p | 777083/860160 | 224081/491520 | 378491/393216 | 9759757/1966080 |
| 3d | 186797/688128 | 4113433/13762560 | 3486285/3670016 | 12967447/3670016 |

TABLE 6

Table of the radial integrals $A'_{nl}$, $B'_{nl}$, $C'_{nl}$, $-D'_{nl}$ defined by (5.11) and (5.10). Decimal fractions

| $(n+1)l$ | $A'_{nl}$ | $B'_{nl}$ | $C'_{nl}$ | $-D'_{nl}$ |
|---|---|---|---|---|
| 1s | 8 | 2 | 1.5 | 4.5 |
| 1p | 0.667 | 0.833 | 1.458 | 2.708 |
| 1d | 0.233 | 0.525 | 1.444 | 2.231 |
| 1f | 0.118 | 0.383 | 1.436 | 2.011 |
| 1g | 0.071 | 0.301 | 1.432 | 1.884 |
| 1h | 0.047 | 0.249 | 1.429 | 1.802 |
| 1i | 0.034 | 0.211 | 1.427 | 1.744 |
| 2s | 11.458 | 1.281 | 1.148 | 7.820 |
| 2p | 0.777 | 0.567 | 1.117 | 3.988 |
| 2d | 0.245 | 0.367 | 1.102 | 2.937 |
| 2f | 0.116 | 0.272 | 1.093 | 2.443 |
| 2g | 0.067 | 0.216 | 1.087 | 2.155 |
| 3s | 14.217 | 1.008 | 0.986 | 10.101 |
| 3p | 0.903 | 0.456 | 0.963 | 4.964 |
| 3d | 0.271 | 0.299 | 0.950 | 3.533 |

TABLE 7

Table of $B'_{nl}G(l, L)$

| $(n+1)l$ \ $L$ | 0 | 2 | 4 | 6 | 8 | 10 | 12 |
|---|---|---|---|---|---|---|---|
| 1s | 2 | | | | | | |
| 1p | 2.5 | 1 | | | | | |
| 1d | 2.625 | 0.75 | 0.75 | | | | |
| 1f | 2.681 | 0.715 | 0.488 | 0.625 | | | |
| 1g | 2.713 | 0.705 | 0.439 | 0.379 | 0.547 | | |
| 1h | 2.734 | 0.701 | 0.421 | 0.330 | 0.319 | 0.492 | |
| 1i | 2.748 | 0.700 | 0.411 | 0.309 | 0.271 | 0.280 | 0.451 |
| 2s | 1.281 | | | | | | |
| 2p | 1.702 | 0.681 | | | | | |
| 2d | 1.836 | 0.524 | 0.524 | | | | |
| 2f | 1.904 | 0.508 | 0.346 | 0.444 | | | |
| 2g | 1.946 | 0.505 | 0.315 | 0.272 | 0.392 | | |
| 3s | 1.008 | | | | | | |
| 3p | 1.368 | 0.547 | | | | | |
| 3d | 1.494 | 0.427 | 0.427 | | | | |

TABLE 8

Table of $U(nl, L)$ defined by (5.14)

| $(n+1)l$ \ $L$ | 0 | 2 | 4 | 6 | 8 | 10 | 12 |
|---|---|---|---|---|---|---|---|
| 1s | 3 | | | | | | |
| 1p | 6.750 | 1.500 | | | | | |
| 1d | 9.771 | 2.292 | 1.125 | | | | |
| 1f | 12.684 | 3.052 | 1.556 | 0.938 | | | |
| 1g | 15.561 | 3.793 | 2.002 | 1.239 | 0.820 | | |
| 1h | 18.420 | 4.523 | 2.433 | 1.563 | 1.056 | 0.738 | |
| 1i | 21.270 | 5.246 | 2.856 | 1.875 | 1.316 | 0.934 | 0.677 |
| 2s | 5.214 | | | | | | |
| 2p | 9.530 | 2.413 | | | | | |
| 2d | 12.236 | 2.972 | 1.748 | | | | |
| 2f | 14.644 | 3.581 | 1.925 | 1.428 | | | |
| 2g | 16.936 | 4.165 | 2.255 | 1.486 | 1.234 | | |
| 3s | 6.734 | | | | | | |
| 3p | 11.735 | 3.068 | | | | | |
| 3d | 14.492 | 3.559 | 2.202 | | | | |

TABLE 9

Table of $A'_{nl}H(l, L)$

| $(n+1)l$ \ $L$ | 1 | 3 | 5 | 7 | 9 | 11 |
|---|---|---|---|---|---|---|
| 1p | 2 | | | | | |
| 1d | 3.5 | 1 | | | | |
| 1f | 4.950 | 1.650 | 0.750 | | | |
| 1g | 6.384 | 2.239 | 1.205 | 0.625 | | |
| 1h | 7.811 | 2.804 | 1.602 | 0.990 | 0.547 | |
| 1i | 9.233 | 3.358 | 1.975 | 1.299 | 0.858 | 0.492 |
| 2p | 2.331 | | | | | |
| 2d | 3.671 | 1.049 | | | | |
| 2f | 4.867 | 1.622 | 0.737 | | | |
| 2g | 6.009 | 2.107 | 1.135 | 0.588 | | |
| 3p | 2.710 | | | | | |
| 3d | 4.072 | 1.163 | | | | |

TABLE 10

Table of $Z(nl, L)$ defined by (5.19)

| $(n+1)l$ \ $L$ | 0 | 2 | 4 | 6 | 8 | 10 | 12 |
|---|---|---|---|---|---|---|---|
| 1s | 0 | | | | | | |
| 1p | 4.800 | 0 | | | | | |
| 1d | 9.333 | 1.867 | 0 | | | | |
| 1f | 13.860 | 3.168 | 1.320 | 0 | | | |
| 1g | 18.386 | 4.378 | 2.149 | 1.071 | 0 | | |
| 1h | 22.911 | 5.554 | 2.884 | 1.709 | 0.924 | 0 | |
| 1i | 27.436 | 6.715 | 3.581 | 2.257 | 1.455 | 0.823 | 0 |
| 2s | −0.733 | | | | | | |
| 2p | 4.265 | −0.532 | | | | | |
| 2d | 8.198 | 1.503 | −0.455 | | | | |
| 2f | 11.890 | 2.651 | 0.982 | −0.405 | | | |
| 2g | 15.474 | 3.645 | 1.726 | 0.752 | −0.369 | | |
| 3s | −1.122 | | | | | | |
| 3p | 4.434 | −0.828 | | | | | |
| 3d | 8.358 | 1.457 | −0.714 | | | | |

## 6. The Moments of the Potentials

In the previous section we obtained the matrix elements for short range forces, in units of the moments $I'_0$, $I'_1$ of these forces. To be able to compare the matrix elements due to different types of potentials, as well as the contribution to a given matrix element of the terms due to different moments of

the same potential, we have to make an estimate of these moments. We would like to use the potentials acting between nucleons in nuclear matter [2]), but as these are not yet well defined, we shall use for the purpose of discussion, the interaction potentials between free nucleons as given by Gammel and Thaler [13]).

The radial part of the potentials of Gammel and Thaler [13]) is always of the form of a Yukawa potential with a repulsive core

$$V(r) = \begin{cases} +\infty & \text{if } r < a \\ -V_0(b/r)\exp(-r/b) & \text{if } r > a. \end{cases} \tag{6.1}$$

It was shown by Bauer and Moshinsky [14]) that the repulsive core can be taken into consideration if we replace the potential $V(r)$, by a potential translated by the length $a$ of the repulsive core, plus a $\delta$ function potential of strength $4\pi(\hbar^2 a/m)$, so the equivalent potential $V_{eq}$ becomes

$$V_{eq} = -V_0[b/(r+a)]\exp[-(r+a)/b] + 4\pi(\hbar^2 a/m)\delta(\mathbf{r}). \tag{6.2}$$

Taking into account that $4\pi\delta(\mathbf{r})$ can also be expressed as $r^{-2}\delta(r)$, the moments $I_0$, $I_1$ of (2.3), for the equivalent potential $V_{eq}(r)$ take the form

$$I_0 = -V_0 b^3\{(1-c)\exp(-c) + c^2[-Ei(-c)]\} + (\hbar^2 a/m), \tag{6.3}$$

$$I_1 = -V_0 b^5\{(6-2c+c^2-c^3)\exp(-c) + c^4[-Ei(-c)]\}, \tag{6.4}$$

where

$$-Ei(-c) = \int_c^\infty x^{-1}\exp(-x)\mathrm{d}x, \qquad c = (a/b). \tag{6.5}$$

The potentials of Gammel and Thaler [13]) for the forces between nucleons, are classified as even-triplet, even-singlet, odd-triplet, odd-singlet, to indicate the even or odd character of the relative orbital angular momentum of the two nucleons, and the state of total spin of the two nucleons. The matrix elements discussed in the previous sections were obtained for the wave function $|(nl)^2LM\rangle$ defined by (2.8). From the symmetry properties of the Clebsch-Gordan coefficient in (2.8), we see that under interchange of the two nucleons $|(nl)^2LM\rangle$ will be symmetric if $L$ is even and antisymmetric if $L$ is odd. If we expand [6]) the $|(nl)^2LM\rangle$ in terms of the wave functions of the relative coordinates $\mathbf{r}' = \mathbf{r}_1 - \mathbf{r}_2$, and centre of mass coordinates $\mathbf{r}'' = \frac{1}{2}(\mathbf{r}_1 + \mathbf{r}_2)$, then, as shown by Talmi [11]), symmetric $|(nl)^2LM\rangle$ would contain only even wave functions of the relative coordinates, and antisymmetric $|(nl)^2LM\rangle$ would contain only odd wave functions of the relative coordinates. We conclude therefore, that the matrix elements with even $L$ have to be evaluated with the even parity potentials of Gammel and Thaler, while the matrix elements with odd $L$ correspond to the odd parity potentials of Gammel and Thaler.

In table 11 we specify the parameters of the potentials of Gammel and Thaler [13]), and their moments $I_0$, $I_1$ given by (6.3), (6.4) respectively. The

central odd-triplet potential does not appear in the tables, as it vanishes [13]). The spin-orbit coupling even-triplet potential is not included in the table, as up to the moment $I_1$, the spin-orbit coupling force has only matrix elements with odd $L$. The values of $I_0$ are only given for the central even-triplet and even-singlet potentials, as other matrix elements do not contain $I_0$.

TABLE 11

The moments of the potentials †

| Potentials | $V_0$ (MeV) | $b$ ($f$) | $a$ ($f$) | $c$ | $I_0$ ($f^3$ MeV) | $I_1$ ($f^5$ MeV) | $I'_0$ (MeV) | $I'_1$ (MeV) |
|---|---|---|---|---|---|---|---|---|
| Central even-triplet | 100.7 | 0.813 | 0.4 | 0.49 | −7.74 | −114 | −0.21 | −0.171 |
| Central even-singlet | 425.5 | 0.69 | 0.4 | 0.58 | −38.5 | −189 | −1.04 | −0.283 |
| Central odd-singlet | −100 | 1 | 0.5 | 0.50 | | 314 | | 0.471 |
| Spin-orbit odd-triplet | 7317.5 | 0.27 | 0.4125 | 1.53 | | −9.44 | | −0.014 |
| Tensor odd-triplet | −22 | 1.25 | 0.4125 | 0.33 | | 262 | | 0.393 |
| Tensor even-triplet | 257 | 0.831 | 0.4 | 0.48 | | −328 | | −0.493 |

† We denote by $f$ the length $10^{-13}$ cm.

To obtain the reduced moments $I'_k$ of (5.12) we have to determine $\nu^{\frac{1}{2}} = (m\omega/\hbar)^{\frac{1}{2}}$, which implies specifying $\hbar\omega$. We use the estimate of Moszkowski [15])

$$\hbar\omega \approx 41 A^{-\frac{1}{3}} \text{ MeV}, \tag{6.6}$$

where $A$ is the mass number of the nucleus. In units † of $f^{-1}$, $\nu^{\frac{1}{2}}$ becomes then

$$\nu^{\frac{1}{2}} \approx A^{-\frac{1}{3}} f^{-1}. \tag{6.7}$$

The analysis carried out in the previous sections applies to short range forces, i.e. those whose range is small compared with the radius of the nucleus. It is convenient therefore to estimate $I'_0$, $I'_1$ for a large nucleus, so we take $A = 216$. For the corresponding value $\nu = \frac{1}{6} f^{-2}$, we give the reduced moments $I'_0$, $I'_1$ in the last two columns of table 11.

Using the reduced moments of table 11, we first compare the contributions of the zero moment $I'_0$ and the first moment $I'_1$ to the matrix elements for even parity central forces. For the even-triplet central forces, $I'_0$, $I'_1$ are given in the first line of table 11, and multiplying their value by table 7 and 8

respectively, we see that the contribution of the first moment is larger than the contribution of the zero moment for all shells, but particularly for shells of large $l$. For the central even-triplet forces of Gammel and Thaler, it would not be correct therefore to idealize them as $\delta$ function potentials, even for large nuclei. For the central even-singlet forces, $I'_0$, $I'_1$ are given in the second line of table 11, and multiplying their values by tables 7 and 8 respectively, we see that only for the first shells would the contribution of the zero moment be larger than the contribution of the first moment, which again shows the limitation of the $\delta$ function potentials frequently employed in nuclear shell theory.

For $L$ odd, the matrix elements for central odd-singlet, spin-orbit coupling odd-triplet, and tensor odd-triplet forces, are very similar as indicated in (5.15), (5.16) and (5.17) respectively. Their relative importance is determined by the corresponding $I_1$ or $I'_1$. From table 11 we see that the spin orbit coupling force gives a much smaller matrix element, that either the central odd-singlet or the tensor odd-triplet potential.

For $L$ even, we can have matrix elements with either $S = 0$ or 1. For the singlet case, only the central even-singlet potential discussed above, gives a contribution. For the triplet case, we have contributions of both the central even-triplet force and the tensor even-triplet force. Comparing the values of $I_1$ and $I'_1$ for these two forces, and the tables 8 and 10, we see that the contribution of the tensor even-triplet forces is, in general (the exceptions are the matrix elements for which $L = 2l$), larger than that of the central even-triplet force, if we are dealing with a large nucleus for which we could limit ourselves to the first moment contributions to the matrix elements.

## Appendix 1

In this appendix we evaluate the matrix element (2.16) of $\delta(\mathbf{r})\hat{p}^2$. We start by considering the effect of $\hat{p}^2 = \frac{1}{4}(\mathbf{p}_1 - \mathbf{p}_2)^2$ on $|(nl)^2LM\rangle$, when $\mathbf{r}_1 = \mathbf{r}_2 = \mathbf{r}$. As $L$ is even, we have from the symmetry properties [8]) of the Clebsch-Gordan coefficients, that

$$\begin{aligned}\{\hat{p}^2|(nl)^2LM\rangle\}_{\mathbf{r}_1=\mathbf{r}_2=\mathbf{r}} &= \sum_{m_1 m_2} \langle ll m_1 m_2|LM\rangle [\hat{p}^2 \mathfrak{R}_{nl}(r) Y_{lm_1}(\theta,\varphi)][\mathfrak{R}_{nl}(r) Y_{lm_2}(\theta,\varphi)] \\ &\quad -\tfrac{1}{4}\hat{p}^2 \sum_{m_1 m_2} \langle ll m_1 m_2|LM\rangle [\mathfrak{R}_{nl}(r) Y_{lm_1}(\theta,\varphi)][\mathfrak{R}_{nl}(r) Y_{lm_2}(\theta,\varphi)],\end{aligned} \tag{A.1}$$

where $\hat{p}^2 = -\hbar^2\nabla^2$.

From (2.9) we see that (A.1) reduces to

$$\begin{aligned}&\{\hat{p}^2|(nl)^2LM\rangle\}_{\mathbf{r}_1=\mathbf{r}_2=\mathbf{r}} \\ &= -\hbar^2\left\{\mathfrak{R}_{nl}\left[\frac{1}{r^2}\frac{\mathrm{d}}{\mathrm{d}r}r^2\frac{\mathrm{d}}{\mathrm{d}r} - \frac{l(l+1)}{r^2}\right]\mathfrak{R}_{nl} - \frac{1}{4}\left[\frac{1}{r^2}\frac{\mathrm{d}}{\mathrm{d}r}r^2\frac{\mathrm{d}}{\mathrm{d}r} - \frac{L(L+1)}{r^2}\right]\mathfrak{R}_{nl}^2\right\} \\ &\cdot [4\pi(2L+1)]^{-\frac{1}{2}}(2l+1)\langle ll00|L0\rangle Y_{LM}(\theta,\varphi).\end{aligned} \tag{A.2}$$

As $\{|(nl)^2LM\rangle\}_{\mathbf{r}_1=\mathbf{r}_2=\mathbf{r}}$ can also be reduced with the help of (2.9), the matrix element of $\delta(\mathbf{r})\hat{p}^2$ can be given in terms of radial integrals. Taking into account that

$$\int_0^\infty \mathfrak{R}_{nl}^2 \left(\frac{\mathrm{d}}{\mathrm{d}r} r^2 \frac{\mathrm{d}\mathfrak{R}_{nl}^2}{\mathrm{d}r}\right) \mathrm{d}r = \tfrac{4}{3}\int_0^\infty \mathfrak{R}_{nl}^3 \left(\frac{\mathrm{d}}{\mathrm{d}r} r^2 \frac{\mathrm{d}\mathfrak{R}_{nl}}{\mathrm{d}r}\right) \mathrm{d}r, \tag{A.3}$$

which can be proved by integration by parts, we rearrange terms to obtain (2.16) for the matrix element of $\delta(\mathbf{r})\hat{p}^2$.

## Appendix 2

The matrix element (3.11) could be obtained from the expectation value of the $z$ component of the operator $\mathbf{p}\times\delta(\mathbf{r})\mathbf{p}$ (designated in the spherical notation by the index 0), since

$$\begin{aligned}\langle (nl)^2LM|[\mathbf{p}\times\delta(\mathbf{r})\mathbf{p}]_0|(nl)^2LM\rangle \\ \equiv \langle (nl)^2L||\mathbf{p}\times\delta(\mathbf{r})\mathbf{p}||(nl)^2L\rangle (2L+1)^{-\frac{1}{2}}\langle L1M0|LM\rangle \\ = \int [(\mathbf{p}\psi)^*_{1-2}\times(\mathbf{p}\psi)_{1-2}]_0\,\mathrm{d}\tau,\end{aligned} \tag{A.4}$$

where $(\mathbf{p}\psi)_{1-2}$ is given, as in the appendix of ref. [5]), by

$$(\mathbf{p}\psi)_{1-2} = \sum_{m_1 m_2} \langle ll m_1 m_2|LM\rangle [\mathbf{p}\mathfrak{R}_{nl}(r)Y_{lm_1}(\theta,\varphi)][\mathfrak{R}_{nl}(r)Y_{lm_2}(\theta,\varphi)]. \tag{A.5}$$

We can express the vector $\mathbf{p}$ in the form

$$\mathbf{p} = r^{-2}\mathbf{r}(\mathbf{r}\cdot\mathbf{p}) - r^{-2}(\mathbf{r}\times\mathbf{l}), \tag{A.6}$$

where $\mathbf{l} = \mathbf{r}\times\mathbf{p}$. As $L$ in (A.5) is odd, we see from the relation (2.9) that only the second part of (A.6) contributes to (A.5). The vector product in (A.6) can be put in terms of spherical components under the form

$$(\mathbf{r}\times\mathbf{l})_m = -i\sqrt{2}\sum_{\mu\nu}\langle 1 1\mu\nu|1m\rangle \chi_\mu l_\nu, \tag{A.7}$$

and using the standard methods of Racah [8, 5]) we obtain

$$\begin{aligned}-r^{-2}(\mathbf{r}\times\mathbf{l})_m Y_{lm_1}(\theta,\varphi) = (i\hbar/r)[6l(l+1)]^{\frac{1}{2}}(2l+1) \\ \sum_{l' q_1}[(2l'+1)^{-\frac{1}{2}}\langle l100|l'0\rangle W(11ll;1l')\langle l1m_1 m|l' q_1\rangle Y_{l'q_1}(\theta,\varphi)],\end{aligned} \tag{A.8}$$

where $l'$ is limited to $l' = l\pm 1$.

Substituting (A.8) into (A.5), and again using Racah methods [8, 5]), we have

$$\begin{aligned}(\hat{p}_m\psi)_{1-2} = (4\pi)^{-\frac{1}{2}}(i\hbar/r)[\mathfrak{R}_{nl}(r)]^2 \\ [(2l+1)^3(l+1)(2l+3)]^{\frac{1}{2}}\langle l+1l00|L0\rangle W(l+1lLL;1l) \\ \cdot\langle 1LmM|LM'\rangle Y_{LM'}(\theta,\varphi),\end{aligned} \tag{A.9}$$

where $M' = m+M$. We introduce this result into (A.4), writing the vector product in a spherical form similar to (A.7) and keeping in mind that

$(p_m\psi^*)_{1-2} = -(-1)^m(p_{-m}\psi)^*_{1-2}$, we obtain finally

$$\langle(nl)^2LM|[\mathbf{p}\times\delta(\mathbf{r})\mathbf{p}]_0|(nl)^2LM\rangle$$
$$= \{(\hbar^2/4\pi)\int_0^\infty [\Re_{nl}(r)]^4\,dr(2l+1)^3(l+1)(2l+3)[\langle l+1l00|L0\rangle]^2 \quad (A.10)$$
$$[W(l+1lLL;\,1l)]^2\}i[6(2L+1)]^{\frac{1}{2}}W(11LL;\,1L)\langle L1M0|LM\rangle.$$

Introducing the explicit value [10]) of the Racah coefficient $W(11LL;\,1L)$ in (A.9), we obtain, using (A.4), the matrix element (3.11).

## Appendix 3

For $L' = L$ and $L$ odd, the matrix element (4.12) which we designate by $-(4\pi\hbar^{-2})Q$ could be written as

$$Q = \sqrt{2}\int[3(p_z\psi)^*_{1-2}(p_z\psi)_{1-2} - (\mathbf{p}\psi)^*_{1-2}\cdot(\mathbf{p}\psi)_{1-2}]d\tau$$
$$= -(12)^{\frac{1}{2}}\sum_{mm'}\left\{\langle 11mm'|20\rangle\,(-1)^m\int[(p_{-m}\psi)^*_{1-2}(p_{m'}\psi)_{1-2}]\,d\tau\right\}. \quad (A.11)$$

Using the expression (A.9) for $(p_m\psi)_{1-2}$ and the standard procedure of Racah [8]), we obtain

$$Q = \{(\hbar^2/4\pi)A_{nl}H(l,L)(60)^{\frac{1}{2}}(2L+1)W(11LL;\,2L)\}(2L+1)^{-\frac{1}{2}}\langle L2M0|LM\rangle, \quad (A.12)$$

where $A_{nl}$ is given by (2.17) and $H(l,L)$ by (2.20). Taking the explicit expression for the Racah coefficient, we see that the term contained inside the curly bracket of (A.11) gives us (4.14).

To evaluate the matrix element of the operator $T''_{20}$ defined by (4.16), when $L'$, $L$ are even, we start by considering the effect of

$$(3p_z^2-p^2) = \tfrac{1}{4}[3(p_{1z}-p_{2z})^2-(\mathbf{p}_1-\mathbf{p}_2)^2], \quad (A.13)$$

on the $|(nl)^2LM\rangle$ of (2.8), when $\mathbf{r}_1 = \mathbf{r}_2 = \mathbf{r}$. As $L$ is even, we have from the symmetry properties of Clebsch-Gordan coefficients that

$$\{(3p_z^2-p^2)|(nl)^2LM\rangle\}_{\mathbf{r}_1-\mathbf{r}_2=\mathbf{r}}$$
$$= \sum_{m_1m_2}\langle ll m_1m_2|LM\rangle[(3p_z^2-p^2)\Re_{nl}(r)Y_{lm_1}(\theta,\varphi)][\Re_{nl}(r)Y_{lm_2}(\theta,\varphi)] \quad (A.14)$$
$$-\tfrac{1}{4}(3p_z^2-p^2)\sum_{m_1m_2}\langle ll m_1m_2|LM\rangle[\Re_{nl}(r)Y_{lm_1}(\theta,\varphi)][\Re_{nl}(r)Y_{lm_2}(\theta,\varphi)].$$

From the explicit form of the operators [6]) $p_z$, $p^2$, we have that the operator $(3p_z^2-p^2)$ appearing in the right hand side of (A.14) is given by

$$3p_z^2-p^2 = -\hbar^2\left[(3\cos^2\theta-1)\left(\frac{1}{r^2}\frac{\partial}{\partial r}r^2\frac{\partial}{\partial r}-\frac{3}{r}\frac{\partial}{\partial r}+\frac{1}{r^2}l^2\right)\right.$$
$$\left.+3\cos\theta\sin\theta\frac{\partial}{\partial\theta}\left(\frac{1}{r^2}-\frac{2}{r}\frac{\partial}{\partial r}\right)+\frac{1}{r^2}(3l_z^2-l^2)\right], \quad (A.15)$$

where $l^2$, $l_z$ are the usual angular momentum operators

$$l^2 = -\left[\frac{1}{\sin\theta}\frac{\partial}{\partial\theta}\sin\theta\frac{\partial}{\partial\theta}+\frac{1}{\sin^2\theta}\frac{\partial^2}{\partial\varphi^2}\right], \qquad l_z = \frac{1}{i}\frac{\partial}{\partial\varphi}. \tag{A.16}$$

Taking into account the well known effect [8]) of the operators $(3\cos^2\theta-1)$, $3\cos\theta\sin\theta\partial/\partial\theta$ and of $l^2$, $l_z$ on the spherical harmonics, and reducing the radial integrals with the help of (A.3), and of the relation

$$\int_0^\infty [\Re_{nl}^3 r^{-1}(\partial\Re_{nl}/\partial r)]r^2\,dr = -\tfrac{1}{4}\int_0^\infty \Re_{nl}^4\,dr, \tag{A.17}$$

we obtain straightforwardly the value (4.17) for the matrix element of $\mathbf{T}_2''$.

## References


1) J. P. Elliot and A. M. Lane, The nuclear shell model, in Handbuch der Physik, Vol. XXXIX (Springer-Verlag, Berlin-Göttingen-Heidelberg, 1957) pp. 241–410
2) Brueckner, Eden and Francis, Phys. Rev. **99** (1955) 76
3) J. P. Elliot and A. M. Lane, ref. [1]), pp. 333, 401
4) N. F. Mott and I. N. Sneddon, Wave mechanics and its applications (Clarendon Press, Oxford, 1948) p. 69
5) M. Moshinsky, Phys. Rev. **106** (1957) 117
6) M. Moshinsky, Phys. Rev. **109** (1958) 933
7) H. Matsunobu and H. Takebe, Progr. Theoret. Phys. **14** (1955) 589
8) G. Racah, Phys. Rev. **62** (1942) 438
9) J. A. Stratton, Electromagnetic theory (McGraw-Hill Book Co., New York, 1941) pp. 405, 410
10) Biedenharn, Blatt and Rose, Revs. Mod. Phys. **24** (1952) 249
11) I. Talmi, Helv. Phys. Acta **25** (1952) 185
12) N. Zeldes, Nuclear Physics **2** (1956/57) 1
13) J. L. Gammel and R. M. Thaler, Phys. Rev. **107** (1957) 1338
14) M. Bauer and M. Moshinsky, Nuclear Physics **4** (1957) 615
15) S. A. Moszkowski, Models of nuclear structure, in Handbuch der Physik, Vol. XXXIX (Springer-Verlag, Berlin-Göttingen-Heidelberg, 1957) p. 469
16) Proceedings of the Rehovoth Conference on Nuclear Structure (North-Holland Publishing Co., Amsterdam, 1958)

1.C *Nuclear Physics* 8 (1958) 41—50; © *North-Holland Publishing Co., Amsterdam*
Not to be reproduced by photoprint or microfilm without written permission from the publisher

# THE USE OF AN EFFECTIVE THREE-BODY POTENTIAL IN THE NUCLEUS

E. J. SQUIRES
*U.K.A.E.A. Research Group, Atomic Energy Research Establishment, Harwell, Didcot, Berks.*

Received 23 May 1958

**Abstract:** A discussion is given of the possibility of taking into account the state dependence of the Brueckner $t$-matrix by using an effective potential containing a three-body force. It is shown that this can be chosen so that the binding energy and its density dependence and also the single particle energies are given correctly. The contribution of the three-body force to the binding energy per particle is shown to be about 17 MeV if the Brueckner and Gammel calculations of the $t$-matrix are used.

## 1. Introduction

Recent work on the many body problem initiated by Watson [1]) and Brueckner [2]) has thrown some light on the validity of shell-model considerations of atomic nuclei. It has been made plausible that, provided the inter-nucleon potential (assumed 2-body) is replaced by a certain operator known as the reaction matrix, then good results will be obtained when purely shell-model wave-functions are used. This statement depends upon certain remaining terms of the original perturbation series being small and this has been made plausible by several authors. It will not be discussed here.

The reaction matrix, which we shall denote by $t$, is a two body operator in that, acting on a shell-model state it can only change the state of two particles. However, its form depends upon the states occupied by the other particles in the nucleus, and, in this sense, it differs from the "effective potentials" usually used in shell-model theory. The fact that one aspect of this dependence of $t$ on the occupied states is a density dependence has led to the suggestion by Skyrme [3]) that one can reproduce its effect by having an effective potential which contains a three-body part. It is the purpose of this work to see how far one can, in fact, simulate the occupied state dependence of $t$ by a three-body potential.

We shall first consider the binding energy of nuclei and shall equate the value of the binding energy and its density dependence calculated with the $t$-matrix and with an effective potential containing a three-body part. A difficulty arises when this is applied to the evaluation of single particle energies since a different factor must now be associated with the three-body potential. One can use this, however, to take account of the so called re-

arrangement energy which must be included in the Brueckner theory [4]). In fact the condition that the density dependence of the binding energy should be correctly given by the three-body potential already ensures that the rearrangement energy for the removal of a particle at the top of the Fermi sea is also given correctly. The momentum dependence and magnitude of the three-body potential are discussed in sections 4 and 5 and section 6 contains a discussion of the effective mass.

## 2. Binding Energies

We introduce an effective potential defined by

$$V = \tfrac{1}{2}\sum_{ij} v^{(2)}(\mathbf{r}_i, \mathbf{r}_j) + \tfrac{1}{6}\sum_{ijk} v^{(3)}(\mathbf{r}_i, \mathbf{r}_j, \mathbf{r}_k) \tag{1}$$

and shall endeavour to equate the nuclear properties obtained with this potential with those obtained from the reaction matrix. The notation

$$v(\mathbf{k}_1, \mathbf{k}_2) = \langle \mathbf{k}_1\mathbf{k}_2|v|\mathbf{k}_1\mathbf{k}_2\rangle - \langle \mathbf{k}_1\mathbf{k}_2|v|\mathbf{k}_2\mathbf{k}_1\rangle \tag{2}$$

etc. will be used. Momentum states $|k\rangle$ are normalized to $\delta$ functions and spin variables are not indicated explicitly.

In order to obtain the correct binding energy and density for nuclear matter we require

$$\tfrac{1}{2}\sum_{ij}^{\rho} t_\rho(\mathbf{k}_i\mathbf{k}_j) = \tfrac{1}{2}\sum_{ij}^{\rho} v^{(2)}(\mathbf{k}_i\mathbf{k}_j) + \tfrac{1}{6}\sum_{ijk}^{\rho} v^{(3)}(\mathbf{k}_i, \mathbf{k}_j, \mathbf{k}_k) \tag{3}$$

for all densities in the neighbourhood of $\rho_0$, the density of nuclear matter. In this equation $t_\rho$ is the reaction matrix for nuclear matter at density $\rho$ in its ground state, and the summations are over all momenta and spins occupied in the ground state at the density indicated.

Two modifications arise when finite nuclei are considered. First, different densities are involved and, secondly, since the nuclear states are no longer plane waves, the sums over momenta are weighted by distribution functions different from the simple Fermi distribution used in eq. (2). Thus the only simple way of obtaining agreement for the binding energies is to choose the effective potential so that an equation of the form of eq. (3) but without the sums over the momenta $\mathbf{k}_i\mathbf{k}_j$ is satisfied. Two (essentially similar) approximations are involved here; it is assumed that the $t$-matrix corresponding to nuclear matter at the local density can be used and that the momentum distribution of the third particle in the three-body potential can be taken to be the Fermi distribution at the local density. This gives

$$\tfrac{1}{2}t_\rho(\mathbf{k}_i, \mathbf{k}_j) = \tfrac{1}{2}v^{(2)}(\mathbf{k}_i, \mathbf{k}_j) + \tfrac{1}{6}\sum_{k}^{\rho} v^{(3)}(\mathbf{k}_i, \mathbf{k}_j, \mathbf{k}_k). \tag{4}$$

In general it will not be possible with any simple form for the potentials to satisfy eq. (4) exactly for all $\rho$, a fact which corresponds to the limitation

we have made by only including two and three-body potentials in the effective potential. We shall therefore choose the effective potential so that the first two terms of the Taylor expansion about $\rho = \rho_0$ are satisfied, i.e.

$$t_{\rho_0}(\mathbf{k}_i, \mathbf{k}_j) = v^{(2)}(\mathbf{k}_i, \mathbf{k}_j) + \tfrac{1}{3} \sum_k^{\rho_0} v^{(3)}(\mathbf{k}_i, \mathbf{k}_j, \mathbf{k}_k) \tag{5}$$

and

$$\left[\frac{\partial t_\rho}{\partial \rho}(\mathbf{k}_i, \mathbf{k}_j)\right]_{\rho_0} = \tfrac{1}{3}\left[\frac{\partial}{\partial \rho} \sum_k^{\rho} v^{(3)}(\mathbf{k}_i, \mathbf{k}_j, \mathbf{k}_k)\right]_{\rho_0}. \tag{6}$$

Using the well known relation

$$\rho = \frac{2}{3\pi^2} k_f^3 \tag{7}$$

where $k_f$ is the Fermi momentum at the density $\rho$, we can write eq. (6) in the form

$$\left[\frac{\partial t_\rho}{\partial \rho}(\mathbf{k}_i, \mathbf{k}_j)\right]_{\rho_0} = \frac{(2\pi)^3}{3} v^{(3)}(\mathbf{k}_i, \mathbf{k}_j, \mathbf{k}_f) \tag{8}$$

where here, and subsequently, $k_f$ refers to the density $\rho_0$.

We shall see later that there may be difficulties in choosing the momentum dependence of $v^{(3)}$ so as to satisfy eq. (8) and it is therefore of interest to consider the equation obtained by substituting eq. (5) into the first derivative with respect to $\rho$ of eq. (3). This is

$$\sum_{ij}^{\rho_0} \left[\frac{\partial t_\rho}{\partial \rho}(\mathbf{k}_i, \mathbf{k}_j)\right]_{\rho_0} = \frac{(2\pi)^3}{3} \sum_{ij}^{\rho_0} v^{(3)}(\mathbf{k}_f, \mathbf{k}_i, \mathbf{k}_j), \tag{9}$$

i.e. the averaged form of eq. (8).

If the three-body potential is assumed to be independent of momentum then it can be eliminated between eqs. (5) and (8). Then, using eq. (7), we have

$$v^{(2)}(\mathbf{k}_i, \mathbf{k}_j) = t_{\rho_0}(\mathbf{k}_i, \mathbf{k}_j) - \left[\frac{\partial t_\rho}{\partial \rho}(\mathbf{k}_i, \mathbf{k}_j)\right]_{\rho_0} \rho. \tag{10}$$

Thus, if the linear approximation to $t_\rho$ is reasonable for all $\rho$ less than $\rho_0$, it follows that $v^{(2)}$ is equal to the free space (zero density) $t$-matrix.

## 3. Single Particle Energies

Let $-E(k)$ be the energy required to remove a particle of momentum $k$ from the nucleus for $k < k_f$, and let $E(k)$ be the energy required to add a particle of momentum $k$ to the nucleus for $k > k_f$. Then

$$E(k) = M(k) + R(k) \tag{11}$$

where

$$M(k) = \frac{\hbar^2 k^2}{2M} + \frac{(2\pi)^3}{\Omega} \sum_i^{\rho_0} t_{\rho_0}(\mathbf{k}_i, \mathbf{k}) \tag{12}$$

and

$$R(k) = \tfrac{1}{2} \sum_{ij}^{\rho_0} \frac{\delta_k t_{\rho_0}(\mathbf{k}_i, \mathbf{k}_j)}{\delta_k A}. \tag{13}$$

In eq. (13) $\delta_k t$, for $k < k_f$, is the change in the $t$-matrix due to the removal of all particles with momenta between $k$ and $k+\delta k$ and $\delta_k A$ is the corresponding change in the total number of particles in the nucleus. For $k < k_f$, minus $\delta_k t$ and minus $\delta_k A$ are the changes caused by adding particles with momenta in the neighbourhood of $k$. Note that the limit of a very large nucleus is being considered and suitable averages over spins and momentum directions are being carried out to remove minor irregularities. The volume of the nucleus is denoted by $\Omega$.

The quantities $M(k)$ and $R(k)$ have been called by Thouless [4]) the "model energies" and the "rearrangement energies" respectively.

An interesting special case is for $k = k_f$ when $E(k_f)$ is the energy of the top particle and must therefore be equal to the average binding energy per particle in the nucleus. Thus $R(k_f)$ is the difference between the average binding energy and the model energy of the top particle. The calculations of Brueckner and Gammel [5]) using the Gammel and Thaler [6]) potential yield for this quantity a value of 17 MeV, i.e.

$$R(k_f) = 17 \text{ MeV}. \tag{14}$$

Using eq. (13) we have

$$R(k_f) = \frac{1}{2\Omega} \sum_{ij}^{\rho_0} \frac{\partial t_\rho(\mathbf{k}_i, \mathbf{k}_j)}{\partial \rho}.$$

Substituting from eq. (9) gives

$$R(k_f) = \frac{(2\pi)^3}{\Omega} \cdot \tfrac{1}{6} \sum_{ij}^{\rho_0} v^{(3)}(\mathbf{k}_i, \mathbf{k}_j, \mathbf{k}_f). \tag{15}$$

This equation, combined with eq. (14) gives immediately a particular average of the three body potential.

We now consider the single particle energies obtained from the effective potential. These are given by

$$E(k) = \frac{\hbar^2 k^2}{2M} + \frac{(2\pi)^3}{\Omega} [\sum_{i}^{\rho_0} v^{(2)}(\mathbf{k}_i, \mathbf{k}_j) + \tfrac{1}{2} \sum_{i,j}^{\rho_0} v^{(3)}(\mathbf{k}_i, \mathbf{k}_j, \mathbf{k})] \tag{16}$$

$$= M(k) + \tfrac{1}{6} \frac{(2\pi)^3}{\Omega} \sum_{ij}^{\rho_0} v^{(3)}(\mathbf{k}, \mathbf{k}_i, \mathbf{k}_j), \tag{17}$$

on using eqs. (9) and (12). Note that, as pointed out in section 1 the presence of the term corresponding to the rearrangement energy in eq. (17) is due to the different factor associated with the three body potential according to whether total or single particle energies are considered.

In order that the single particle energies should be correctly given by the effective potential we require that the second term on the right hand side of eq. (17) should be equal to $R(k)$, i.e.

$$\tfrac{1}{6}\frac{(2\pi)^3}{\Omega}\sum_{ij}^{\rho_0} v^{(3)}(\mathbf{k}_i, \mathbf{k}_j, \mathbf{k}) = \tfrac{1}{2}\sum_{ij}^{\rho_0}\frac{\delta_k t_{\rho_0}(\mathbf{k}_i, \mathbf{k}_j)}{\delta_k A}. \tag{18}$$

For $k = k_f$ this is already satisfied provided that eq. (9) is satisfied. For $k \neq k_f$ eq. (18) can be satisfied by choosing a suitable momentum dependence for the three-body potential. Note that it is in principle possible to choose the momentum dependence so that both eq. (8) and (18) are satisfied. With a simple quadratic form however this will not in general be possible (section 4).

## 4. The Momentum Dependence of the Three-Body Potential

To study the momentum dependence of the three-body potential we must consider the way the $t$-matrix depends on the occupied states. The Brueckner expression for $t$ in terms of the fundamental two body interaction is

$$t = v + v\frac{Q}{e}t \tag{19}$$

where $Q$ is an operator designed to exclude states which violate the exclusion principle, and where $e$ is the excitation energy in the intermediate states. Thus

$$\Delta t = t\left[\Delta\left(\frac{Q}{e}\right)\right]t. \tag{20}$$

It is reasonable to assume that the main change in $t$, when the occupied states are altered, arises from a change in $Q$ and that changes in $e$ give rise to only small effects. This has been made quantitative by Thouless [4]). We shall therefore ignore $\Delta e$ and put

$$\Delta t = t\frac{\Delta Q}{e}t. \tag{21}$$

To evaluate this quantity we must make some assumptions about $t$. For the present we take the simplest possible form, i.e. a $t$ which is local in co-ordinate space and has zero range. Such a $t$-matrix is very unrealistic and chosen only for simplicity. For the exchange character we take a Serber mixture with singlet and triplet parts equal. This seems a reasonable approximation to the results obtained by Brueckner and Gammel [5]) and there is also some phenomenological evidence that the space exchange character is approximately Serber. Thus we take

$$\langle \mathbf{k}_1, \mathbf{k}_2|t|\mathbf{k}'_1, \mathbf{k}'_2\rangle = (2\pi)^{-3}\,\delta(\mathbf{k}_1+\mathbf{k}_2-\mathbf{k}'_1-\mathbf{k}'_2)T_0 \tag{22}$$

where $T_0$ represents here a suitable operator in spin space.

For the energy denominators in eq. (21) the effective mass approximation is used. We obtain

$$\left[\frac{\partial t_\rho(\mathbf{k}_i, \mathbf{k}_j)}{\partial \rho}\right]_{\rho_0} = \frac{3|T_0|^2}{(2\pi)^6 E_f^*}\,\Omega\,\frac{k_f}{K}\log\frac{2K^2+2k_f^2+4K\,k_f-\frac{1}{2}l^2}{2k_f^2-2K^2-\frac{1}{2}l^2} \tag{23}$$

where the notation

$$\mathbf{l} = \mathbf{k}_i - \mathbf{k}_j \tag{24}$$

$$\mathbf{K} = \tfrac{1}{2}(\mathbf{k}_i + \mathbf{k}_j) \tag{25}$$

$$E_f = \frac{\hbar^2 k_f^2}{2M^*} \tag{26}$$

has been used and where $k_f$ is the Fermi momentum corresponding to the density $\rho_0$. A difficulty arises here in that the derivative does not exist for $|\mathbf{k}_i| = |\mathbf{k}_j| = k_f$. For our purposes this difficulty can be ignored by only considering states which are separated from the Fermi surface by a small energy gap — which may be taken to be equal to the mean energy difference between states of a finite nucleus. Note that the divergence in the R.H.S. of eq. (23) is logarithmic so that the integrals required for $R(k)$ are finite.

By integrating eq. (23), and similar expressions for $\delta_k t/\delta_k A$, over $\mathbf{l}$ and $\mathbf{K}$ one can obtain values for $R(k)$. The integral over $K$ has to be done numerically. The result is given by

$$R(k) = \frac{3|T_0|^2 k_f^6}{(2\pi)^4 E_f^*}\,A(k) \tag{27}$$

where $A(k) = 0.19,\ 0.31,\ 0.34$ for $k = k_f,\ 0.7\ k_f$ and 0 respectively. The ratio $R(k_f)/R(0)$ given by these values agrees with that calculated by Thouless [4]) with the same assumptions about $t$.

We shall consider the possibility of fitting $\partial t/\partial\rho$ and $R(k)$ with a three-body potential which is quadratic in momenta. Such a form is consistent with the effective mass approximation and has been used in the phenomenological calculations of Skyrme [7]). Thus we take

$$v^{(3)}(\mathbf{k}_1, \mathbf{k}_2, \mathbf{k}_3) = v^{(3)}[1+\alpha\sum_{i=1}^{3} k_i^2+\beta\sum_{i>j=1}^{3}\mathbf{k}_i\cdot\mathbf{k}_j]\,\frac{\Omega}{(2\pi)^9}. \tag{28}$$

Then, from eq. (17),

$$R(k) = \frac{v^{(3)} k_f^6}{36\pi^4}\,(1+\tfrac{6}{5}\alpha k_f^2+\alpha k^2). \tag{29}$$

One can obtain a value of $\alpha$ by comparing eq. (29) with eq. (27). To fit the extremes $k = k_f$ and $k = 0$ requires

$$k_f^2\alpha = -0.29 \tag{30}$$

whilst to fit the $k = k_f$ and $k = 0.7\ k_f$ values would require a value of about one-third for this quantity.

In order to satisfy the density dependence of the $t$-matrix for all momenta we must satisfy eq. (8) which becomes, with the form of eq. (28),

$$\tfrac{1}{2}\left[\frac{\partial t_\rho}{\partial \rho}(\mathbf{k}_i, \mathbf{k}_j)\right]_{\rho_0} = \frac{\Omega}{(2\pi)^6} v^{(3)}\{1+\alpha k_f^2+(2\alpha+\beta)K^2+(\tfrac{1}{2}\alpha-\tfrac{1}{4}\beta)l^2\}. \quad (31)$$

It is of course impossible to fit such a simple expression to eq. (23) but the general trend is given by the values

$$k_f^2\alpha \approx \tfrac{1}{3}, \qquad k_f^2\beta \approx -\tfrac{2}{3}, \quad (32)$$

which make the R.H.S. of eq. (31) independent of $K$.

It follows from eq. (32) and eq. (30) that, with the assumptions made about $t$, and the form chosen for $v^{(3)}$, the two types of momentum dependence are incompatible †. However, in both cases, the momentum dependence can be considered to be quite small. To see this we calculate the contribution of the three-body force to the binding energy per particle of an infinite nucleus. This is given by

$$B^{(3)} = \frac{k_f^6 v^{(3)}}{36\pi^4}[1+\tfrac{9}{5}\alpha k_f^2]. \quad (33)$$

If the three-body force is chosen to give the correct density dependence of nuclear matter then, as we saw in section 3, it must give $R(k_f)$ correctly. So, from eq. (29)

$$R(k_f) = \frac{v^{(3)} k_f^6}{36\pi^4}[1+\tfrac{11}{5}\alpha k_f^2]. \quad (34)$$

Thus

$$B^{(3)} = \frac{1+\frac{9}{5}\alpha k_f^2}{1+\frac{11}{5}\alpha k_f^2} R(k_f). \quad (35)$$

This ranges from about 0.9 $R(k_f)$ to 1.3 $R(k_f)$ according to whether $\alpha$ is given by eq. (32) or eq. (30) respectively. The contribution of the three-body force to the binding energy is thus already determined to within 20 %.

It is doubtful whether much meaning can be attached to this type of calculation of the momentum dependence of the three-body force unless a more realistic $t$-matrix is used. Qualitatively it appears likely that the use of a more realistic $t$-matrix would tend to give momentum dependent contributions to the three-body potential which vary with momentum in the opposite directions to those found above. To see this for the evaluation of $R(k)$ we note that, as $k$ is decreased below $k_f$, the lowest possible relative momentum in the intermediate state on the right hand side of eq. (20) increases (one particle must have momentum $k$ and the other momentum greater than $k_f$), and this will result in a decrease in the $t$-matrix and hence in $R(k)$. On the other hand, a reduction of the relative momentum of the

† If we allow a more general momentum dependence then there is no incompatibility.

two particles considered in $(\partial t/\partial \rho)(\mathbf{k}_i, \mathbf{k}_j)$ will give rise to an increase in the magnitude of this term due to the momentum dependence of $t$. Thus, in both cases, the momentum dependence of the $t$-matrix tends to reduce in magnitude the value of $\alpha$ from that calculated above — it may even, indeed, alter the sign. These considerations could be made quantitative by carrying out the calculations with a more realistic $t$-matrix, taken, for example, from the work of Brueckner and Gammel [5]). In view of the fact that, as indicated above, there is some cancellation between the various effects, it seems reasonable to assume that a momentum independent three-body potential will not be seriously in error.

## 5. The Magnitude of the Three Body Potential

This can be obtained directly from an assumed nuclear potential using calculations of the type performed by Brueckner and Gammel [5]). In their calculations they use the fundamental two body interaction of Gammel and Thaler [6]) which, with certain approximations, leads to the value given by eq. (14). Thus, from eq. (29)

$$v^{(3)} = \frac{36\pi^4}{k_f^6} 17 \text{ MeV} \tag{36}$$

where $v^{(3)}$ is defined by eq. (28) with $\alpha = \beta = 0$. This leads, by (35), to a three-body contribution to the binding energy per particle given by

$$B^{(3)} = 17 \text{ MeV}. \tag{37}$$

As discussed in § 4 this quantity is not very sensitive to the momentum dependence of the three body potential. The value of 17 MeV agrees well with that obtained, phenomenologically, by Skyrme [3]).

It is interesting to see how far the approximate calculation leading to eq. (27) reproduces this value. The contribution of the reaction matrix of eq. (22) to the binding energy per particle is given by

$$B^{(t)} = -\frac{T_0 k_f^3}{(2\pi)^2}. \tag{38}$$

Hence the total binding energy per particle is given by

$$B = -\frac{T_0 k_f^3}{(2\pi)^2} - \tfrac{3}{5} E_f \tag{39}$$

where $E_f$ is the maximum Fermi energy, given by $\hbar^2 k_f^2/2M$. This leads to

$$\frac{T_0 k_f^3}{(2\pi)^2} \approx -37 \text{ MeV} \tag{40}$$

which gives, using (27a)

$$R(k_f) \approx 25 \frac{M^*}{M} \tag{41}$$

for a reasonable value of $M^*/M$ this is of the right order of magnitude.

## 6. The Effective Mass

The assumption that we can approximate the dependence of $E(k)$ upon $k$ by a quadratic term has often been made. This leads to the idea of an effective mass, $M^*$, defined by the equation

$$E(k) = \frac{\hbar k^2}{2M^*} + \text{const.} \tag{42}$$

Assuming that this is reasonably accurate for all $k$ less than $k_f$ we shall consider how far the effective mass can be determined from the properties of nuclear matter. The argument used here is identical to that of Weisskopf [8]) except that we include the three body potential.

We first write the two body effective potential in a quadratic form since this is necessary in order to obtain eq. (42). Thus we put

$$v^{(2)}(\mathbf{k}_i, \mathbf{k}_j) = v^{(2)}[1+\gamma(k_i^2+k_j^2)]. \tag{43}$$

A possible term depending on $\mathbf{k}_i \cdot \mathbf{k}_j$ has not been included since it will not contribute below. For convenience of writing a Serber potential will be assumed although this does not affect the result.

Using eqs. (28) and (43) we obtain for the binding energy and single particle energies the following expressions

$$B = \tfrac{3}{5}E_f + \frac{k_f^3 v^{(2)}}{(2\pi)^2}(1+\tfrac{6}{5}\gamma k_f^2) + \frac{k_f^6 v^{(3)}}{36\pi^4}(1+\tfrac{9}{5}\alpha k_f^2) \tag{44}$$

$$E(k) = \frac{\hbar^2 k^2}{2M} + \frac{k_f^2 v^{(2)}}{(2\pi)^2}(1+\tfrac{3}{5}\gamma k_f^2+\gamma k^2) + \frac{3k_f^6 v^{(3)}}{36\pi^4}(1+\tfrac{6}{5}\alpha k_f^2+\alpha k^2). \tag{45}$$

Comparing eq. (45) with eq. (42) we have

$$\frac{1}{M^*} = \frac{1}{M} + \frac{4k_f^3 v^{(2)}\gamma}{\hbar^2(2\pi)^2} + \frac{6k_f^6 v^{(3)}\alpha}{36\pi^4\hbar^2}. \tag{46}$$

We now use the fact that $B = E(k_f)$ and subtract eq. (45) with $k = k_f$ from twice eq. (44). On substituting for $\gamma$ from eq. (46) we find

$$B = \tfrac{3}{5}E_f\left(1-\tfrac{2}{3}\frac{M}{M^*}\right) - B^{(3)}. \tag{47}$$

Thus the value of $M^*$ can only be found in this way if the contribution of the three body potential to the binding energy is known. With $B^{(3)}$ equal to $R(k_f)$, and $R(k_f)$ given by the work of Brueckner and Gammel we obtain

$$M^* \approx \tfrac{2}{3}M \tag{48}$$

which agrees with the value of $M^*$ quoted by Brueckner and Gammel, and also with that obtained by Skyrme [3]). Note that the case of $B^{(3)}$ equal to $R(k_f)$ corresponds to no momentum dependence in the three body potential in which case the value of $M^*$ which fits $M(k)$, which is the value quoted by Brueckner and Gammel, is the same as that which fits $E(k)$. This is of course not true in general. One can show (Brueckner [9])) that the $M^*$ which fits $M(k)$ is given by an equation like eq. (47) but with $B^{(3)}$ replaced by $R(k)$.

The value of $M^*$ deduced from eq. (47) is quite sensitive to $B^{(3)}$ so that, even assuming that the quadratic form, eq. (42), is satisfactory, it is not possible at this stage to give, for example, the variation of the nuclear potential depth with momentum for momenta near the Fermi surface, which is required for the optical potential of the nucleus.

## 7. Conclusions

It is shown that much of the occupied state dependence of the $t$-matrix can be taken into account in shell-model type calculations by using a three-body effective potential in addition to the usual two-body one. A discussion of the momentum dependence of the three-body potential shows that it is reasonable at this stage to assume it to be independent of momentum. Its contribution to the binding energy per particle is around 17 MeV if the calculations of Brueckner and Gammel [5]) are realistic. The two-body effective potential, under certain approximations, is equal to the free space $t$-matrix.

I am grateful to Dr. J. S. Bell and to T. H. R. Skyrme for discussions on the contents of this paper.

## References

1) K. M. Watson, Phys. Rev. **89** (1953) 575
2) An extensive list of references on the Brueckner theory is given in ref. [5])
3) T. H. R. Skyrme, Proc. of the Rehovoth Conference (North Holland Publishing Co., Amsterdam, 1958)
4) D. J. Thouless, to be published (1958)
5) K. A. Brueckner and J. L. Gammel, Phys. Rev. **109** (1958) 1023
6) J. L. Gammel and R. M. Thaler, Phys. Rev. **107** (1957) 291, 1337
7) T. H. R. Skyrme, unpublished
8) V. F. Weisskopf, Nuclear Physics **3** (1957) 423
9) K. A. Brueckner, to be published (1958)

1.B:2.G *Nuclear Physics* **8** (1958) 51—54; © *North-Holland Publishing Co., Amsterdam*
Not to be reproduced by photoprint or microfilm without written permission from the publisher

# THE (d, t) REACTIONS AND THE INTERNAL STRUCTURE OF THE TRITON

M. EL NADI and L. ABOU HADID
*Faculty of Science, Cairo University, U.A.R.*

Received 11 June 1958

**Abstract:** From the experimental values of the differential cross sections for $Li^7$(d, t) $Li^8$ and $Li^7$(p, d)$Li^8$; $F^{18}$(d, t) $F^{19}$ and $F^{19}$ (p, d) $F^{18}$, the probability for the existence of the triton in the configuration of a deuteron ground state plus a second neutron was calculated and found to be very small.

It was pointed out by Butler and Salpeter [1]) that for cases when contributions to the (d, t)-reactions arise mainly form direct pick up reactions, Butler's stripping theory [2]) can be used to provide valuable information concerning the internal structure of the triton. If the experimental cross-sections for both a (d, t) and a (p, d) reaction between the same two nuclear levels are known, then it would be possible to calculate the probability for the triton to have the configuration of deuteron ground state plus a second neutron [3]).

Let the triton wave function $\psi_T(\mathbf{r}, \mathbf{R})$ be expanded in terms of the states $\chi_{ti}(\mathbf{r})$ of the deuteron, where $i$ refers to its spin state:

$$\psi_T(\mathbf{r}, \mathbf{R}) = \sum_{ti} A_{ti}\, \chi_{ti}(\mathbf{r}) f_{ti}(\mathbf{R}); \qquad (1)$$

where $\mathbf{r}$ is the difference between the coordinates of the proton and one of the neutrons, and $\mathbf{R}$ is the position vector of the second neutron with respect to the midpoint of the vector $\mathbf{r}$; the wave functions $\psi_T$, $\chi_{ti}$ and $f_{ti}$ are normalized to unity. If the Fourier transform of $f_{0i}(\mathbf{R})$, denoted by $\Phi_T$, is known, the experimental ratio $\sigma$(d, t)/$\sigma$(d, p) enables us to calculate the quantity $A_0^2 \equiv \sum_i |A_{0i}|^2$ which is the probability of finding the triton in the configuration of a deuteron and a neutron. When the energies used in the (d, t) reactions are not high enough to make possible the determination of the function $\Phi_T$ completely, the experimental ratio $\sigma$(d, t)/$\sigma$(d, p) between the same two nuclear states gives $C_T^2|A_0|^2$, where $C_T$ is the normalization factor of the wave function of the second neutron $f(\mathbf{R})$. A lower limit to $C_T^2$ was obtained theoretically by A. Werner [3]), by assuming the triton to consist of an unpolarized deuteron plus a second neutron: she showed that $C_T^2 > 16.4$. Thus an upper limit to $A_0^2$ can be determined. Using the experimental data

on the angular distributions of protons in $C^{12}$ (d, p) $C^{13}$ by Rotblat [4]) and of tritons in $C^{13}$ (d, t) $C^{12}$ by Holmgren *et al.*[5]), A. Werner obtained an upper limit of 0.11 for $A_0^2$ i.e. for the probability of finding the triton in the configuration of deuteron ground state plus second neutron. This is to be compared with the maximum possible value of $A_0^2$, viz. 0.75 (which is the probability of obtaining a triplet neutron-proton spin factor from the triton spin function).

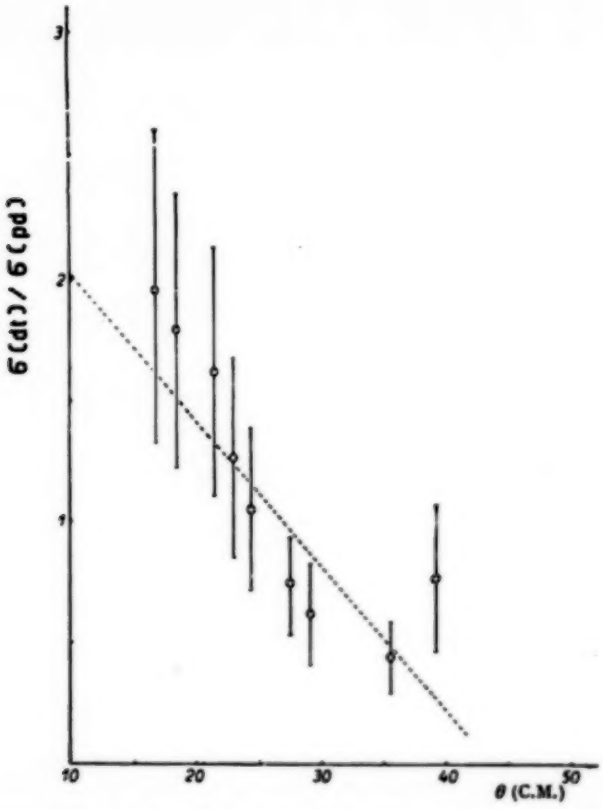


Fig. 1. Values of ratio $\sigma$(d, t)/$\sigma$ (p, d) at different angles in the C.M.S. for the reactions $Li^7$(d, t) $Li^8$ and $Li^7$(p, d)$Li^8$. Experimental values · · · Theoretical curve with $C_T^2|A_0|^2 = 1.08$.

In view of the importance of the internal structure of the triton in theoretical considerations similar calculations were carried out for the following two sets of reactions:

a) The experimental results of Levine, Bender and McGruer [6]) for $Li^7$(d, t)$Li^6$ and of Reynolds and Standing [7]) for $Li^7$(p, d) $Li^6$, with the momentum transfer $l = 1$ for the ground level. A fit of the experimental results with Butler's formula was obtained for the values of the nuclear radius parameter $r_0 = 6.0\times10^{-13}$ cm and $5.5\times10^{-13}$ cm, respectively, $\Phi_T$ being taken to be proportional to [3]) $1/(k^2+\lambda^2)$. The ratio of the experi-

mental cross sections as a function of the angle is shown in fig. 1. The ratio of the two theoretical curves shows the same angle dependence and agrees with the experimental values if one chooses $C_T^2|A_0|^2 = 1.08$. Therefore, $A_0^2 < 0.06$.

b) The experimental results of El-Bedewi and Hussein [8]), for $F^{19}$(d, t)$F^{18}$ and of Reynolds and Standing for $F^{19}$(p, d) $F^{18}$ with the momentum transfer $l = 0$ for the ground level. The fit of the first experimental data with

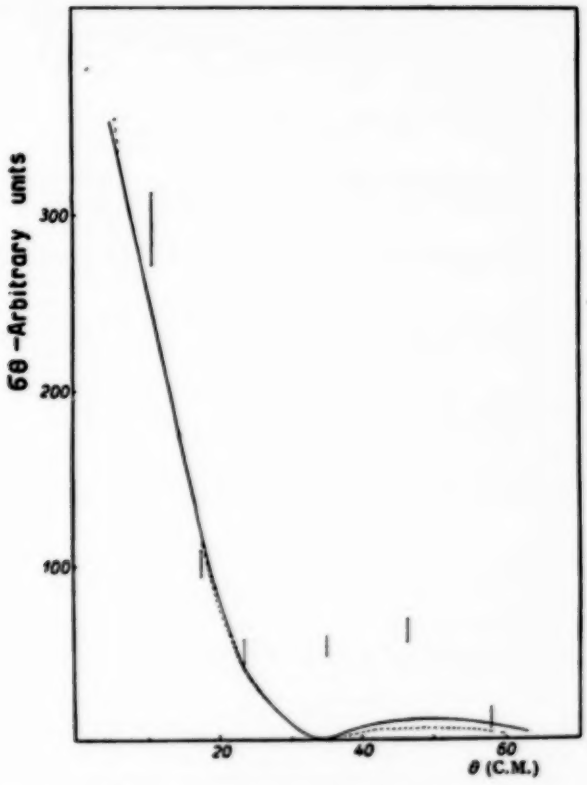


Fig. 2. Values of $\sigma$(d, t) at different angles in the C.M.S. for the reaction $F^{19}$(d, t)$F^{18}$. Experimental points by El Bedewi *et al.*[8]), fitted by both Butler's formula (heavy line) with $r_0 = 5.0 \times 10^{-13}$ cm and Bhatia's *et al.*[9]) formula (dashed line) with $R = 6.9 \times 10^{-13}$ cm and $l = 0$ in the ground level.

Butler's formula is shown in fig. 2 and was achieved with $r_0 = 5.0 \times 10^{-13}$ cm; the fit of the second data was also achieved with the same value of $r_0$ [7]). The same form of $\Phi_T$ as in (a) above was used also in this case.
The ratio of the experimental cross-sections as a function of the angle is shown in fig. 3, together with the theoretical curve. Agreement is obtained between the two curves when we take $C_T^2|A_0|^2 = 0.27$, whence $A_0^2 < 0.02$.

It may be noticed that in these cases, unlike the example chosen by Werner, the experimental and theoretical ratios of the cross sections are not angle independent. These two examples, in addition to that given by A.

Werner, show that the probability of finding the triton in the configuration of deuteron ground state plus second neutron is very small.

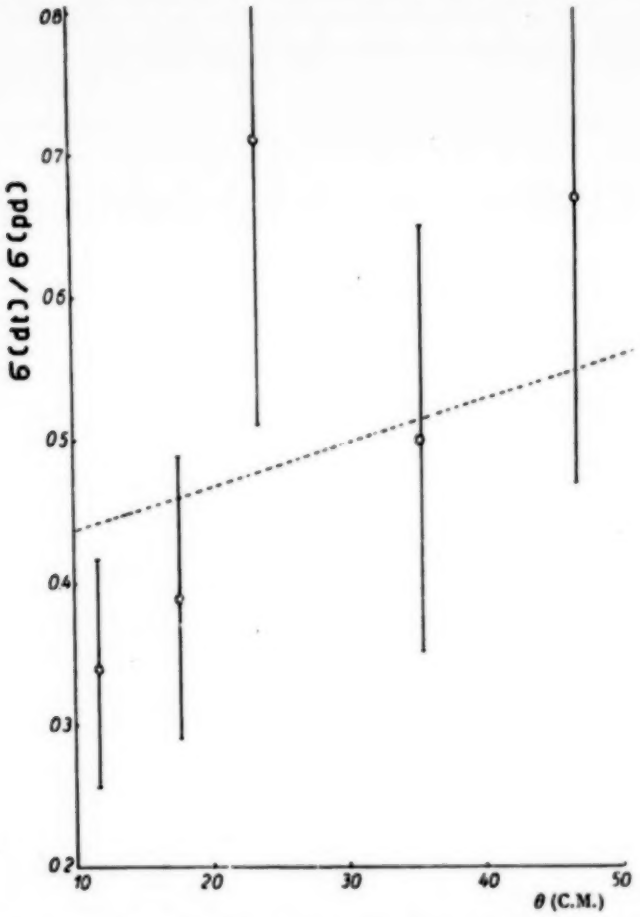


Fig. 3. Values of ratio $\sigma$(d, t)/$\sigma$(p, d) at different angles in the C.M.S. for the reactions $F^{19}$(d, t)$F^{18}$ and $F^{19}$(p, d)$F^{18}$. ⧓ Experimental values · · · Theoretical curve normalized with $C_T^2|A_0|^2 = 0.27$.

## References

1) S. T. Butler and E. E. Salpeter, Phys. Rev. **88** (1952) 133
2) S. T. Butler, Proc. Roy. Soc. A **208** (1951) 559
3) A. Werner, Nuclear Physics **1** (1956) 9
4) J. Rotblat, Nature **167** (1951) 1027
5) A. D. Holmgren *et al.*, Phys. Rev. **95** (1954) 1544
6) S. H. Levine, R. S. Bender and J. N. McGruer Phys. Rev. **97** (1955) 1249
7) J. B. Reynolds and K. G. Standing, Phys. Rev. **101** (1956) 158
8) F. A. El Bedewi and I. Hussein, Proc. Phys; Soc. A **70** (1957) 233
9) A. B. Bhatia, K. Huang, R. Huby and H. C. Newns, Phil. Mag. **43** (1952) 485

2.L

*Nuclear Physics* **8** (1958) 55—60; © *North-Holland Publishing Co., Amsterdam*

Not to be reproduced by photoprint or microfilm without written permission from the publisher

# PROTON-PROTON SCATTERING WITH UNPOLARIZED BEAM AND TARGET

KRISTIAN SKARSVÅG

*Joint Establishment for Nuclear Energy Research, Kjeller per Lillestrøm, Norway*†

Received 4 May 1958

**Abstract:** The general form of the scattering matrix in the singlet-triplet representation is found, and the formulae for the differential cross section, the polarization and the correlation coefficients are derived.

## 1. Introduction

The general theory is given by R. H. Dalitz [1]), L. Wolfenstein and J. Ashkin [2]) and by R. Oehme [3]). We can characterize a beam of protons of uniform momentum by the density matrix of the beam, $\rho$, which is a Hermitian 2-by-2 matrix in spin space. The expectation value of any operator for the beam is given as the trace of a matrix

$$\langle \omega \rangle_{\text{beam}} = \text{Tr}\ (\rho\omega) \tag{1}$$

where $\text{Tr}\ \rho = 1$. We may [4]) take eq. (1) as the definition of the density matrix $\rho$. The density matrix can be expanded in terms of a complete set of $2^2 = 4$ basic Hermitian matrices $\omega^\mu$ in spin space, which obey the relations

$$\text{Tr}\ (\omega^\mu \omega^\nu) = 2\delta_{\mu\nu}.$$

In the scattering p+p → p+p we will describe the system by the density matrix in the combined spin space of the two-proton system. The expectation value of any operator $\Omega$ before scattering is

$$\langle \Omega \rangle_{\text{in}} = \text{Tr}(\rho_{\text{in}} \Omega) \tag{2}$$

where $\text{Tr}\ \rho_{\text{in}} = 1$. Let $\Omega^\mu$ be a complete set of $2^2 \cdot 2^2 = 16$ basic Hermitian matrices in this combined spin space with the property

$$\text{Tr}(\Omega^\mu \Omega^\nu) = 2 \cdot 2\delta_{\nu\mu}. \tag{3}$$

We can expand $\rho_{\text{in}}$ in terms of these operators and find with eqs. (2) and (3)

$$\rho_{\text{in}} = \tfrac{1}{4} \sum_{\mu=1}^{16} \langle \Omega^\mu \rangle_{\text{in}} \Omega^\mu. \tag{4}$$

The system after scattering consists of two proton beams. If the scattering

† Most of this work was done while the author was at Nuclear Physics Research Laboratory, University of Liverpool, England.

matrix is $M$, we find for the density matrix of the two outgoing proton beams

$$\rho_{\text{out}} = M\rho_{\text{in}}M\dagger; \tag{5}$$

$\rho_{\text{out}}$ is a Hermitian matrix. The expectation value of any operator $\Omega'$ in the combined spin space of the scattered protons and the recoil protons is then

$$\langle\Omega'\rangle_{\text{out}} = \text{Tr}(\rho_{\text{out}}\Omega')/\text{Tr}\,\rho_{\text{out}} \tag{6}$$

and the differential cross section is

$$Q = \text{Tr}\,\rho_{\text{out}}. \tag{7}$$

In the case of an unpolarized target and an unpolarized incident proton beam only the unit matrix has non-zero expectation value before scattering, and we get from eq. (4)

$$\rho_{\text{in}} = \tfrac{1}{4}I. \tag{4a}$$

We find for the density matrix $\rho_{\text{out}}$, the differential cross section $Q$ and for any operator $\Omega'$

$$\rho_{\text{out}} = \tfrac{1}{4}MM\dagger, \tag{5a}$$

$$Q = \tfrac{1}{4}\text{Tr}\,MM\dagger, \tag{7a}$$

$$\langle\Omega'\rangle_{\text{out}} = \text{Tr}\,MM\dagger\Omega'/\text{Tr}\,MM\dagger. \tag{6a}$$

The general form of $M$ is given in ref. [2]). The expectation value of any operator can be expressed [5,3,6,7]), from eq. (6), in terms of the coefficients occurring in $M$; these coefficients are given in terms of phase-shifts by Wright[8]). Stapp [6]) uses the singlet-triplet representation and gives the matrix elements in terms of phase-shifts [6,9]); in the present paper this representation will be used.

## 2. General Form of the Scattering Matrix $M$ in the Singlet-Triplet Representation

In the single particle representation the basic Hermitian matrices $\Omega^\mu$ are the direct products $\Omega^\mu = \omega_1{}^\alpha \times \omega_2{}^\beta$ of the corresponding basic matrices $\omega_1{}^\alpha$ and $\omega_2{}^\beta$ in the spin spaces of the scattered proton and the recoil proton. For convenience we arrange the corresponding basic vectors in a column matrix

$$\phi = \begin{Bmatrix} \alpha(1)\alpha(2) \\ \alpha(1)\beta(2) \\ \beta(1)\alpha(2) \\ \beta(1)\beta(2) \end{Bmatrix} = \begin{Bmatrix} \phi_1(\tfrac{1}{2},\tfrac{1}{2}) \\ \phi_2(\tfrac{1}{2},-\tfrac{1}{2}) \\ \phi_3(-\tfrac{1}{2},\tfrac{1}{2}) \\ \phi_4(-\tfrac{1}{2},-\tfrac{1}{2}) \end{Bmatrix} \tag{8}$$

where $\alpha$ and $\beta$ are the two spin eigenfunctions, and 1 and 2 stand for the scattered and the recoil proton.

In the singlet-triplet representation we have

$$\chi = \begin{Bmatrix} \chi_1 \\ \chi_0 \\ \chi_{-1} \\ \chi_s \end{Bmatrix} = U\phi, \tag{9}$$

$$S^\mu = U\Omega^\mu U^{-1}, \tag{10}$$

where $\chi_1$, $\chi_0$, $\chi_{-1}$ are the triplet and $\chi_s$ the singlet eigenfunctions, $S^\mu$ are the new basic Hermitian matrices, and $U$ is a unitary matrix

$$U = \begin{Bmatrix} 1 & 0 & 0 & 0 \\ 0 & 1/\sqrt{2} & 1/\sqrt{2} & 0 \\ 0 & 0 & 0 & 1 \\ 0 & 1/\sqrt{2} & -1/\sqrt{2} & 0 \end{Bmatrix}; \tag{11}$$

$$U^{-1} = U\dagger \quad \text{or} \quad UU\dagger = 1. \tag{12}$$

Let $\mathbf{k}_i$ and $\mathbf{k}_f$ be unit vectors in the direction of the momenta in the centre of mass system of the incoming proton before and after scattering. We define the three orthogonal unit vectors

$$\mathbf{n} = \frac{\mathbf{k}_i \times \mathbf{k}_f}{\sin\vartheta}; \qquad \mathbf{m} = \frac{\mathbf{k}_i - \mathbf{k}_f}{2\sin(\vartheta/2)}; \qquad \mathbf{l} = \frac{\mathbf{k}_i + \mathbf{k}_f}{2\cos(\vartheta/2)}. \tag{13}$$

We choose the $z$-axis in the direction of $\mathbf{k}_i$, and the $y$-axis in the direction of $\mathbf{n}$. We measure the polar angle $\vartheta$ from the $z$-axis and the azimuthal angle $\varphi$ from the $x$-axis.

The basic Hermitian matrices $\omega^\alpha$ are the unit matrix and the three Pauli matrices

$$I = \begin{Bmatrix} 1 & 0 \\ 0 & 1 \end{Bmatrix}; \quad \sigma_x = \begin{Bmatrix} 0 & e^{-i\varphi} \\ e^{i\varphi} & 0 \end{Bmatrix}; \quad \sigma_y = \begin{Bmatrix} 0 & -ie^{-i\varphi} \\ ie^{i\varphi} & 0 \end{Bmatrix}; \quad \sigma_z = \begin{Bmatrix} 1 & 0 \\ 0 & -1 \end{Bmatrix}.$$

The $z$-axis is the axis of quantization, and $\sigma_x$ and $\sigma_y$ are therefore $\varphi$-dependent. The scattering matrix may be written in the form

$$M = \begin{Bmatrix} M_{11} & M_{10}e^{-i\varphi} & M_{1-1}e^{-2i\varphi} & M_{1s}e^{-i\varphi} \\ M_{01}e^{i\varphi} & M_{00} & M_{0-1}e^{-i\varphi} & M_{0s} \\ M_{-11}e^{2i\varphi} & M_{-10}e^{i\varphi} & M_{-1-1} & M_{-1s}e^{i\varphi} \\ M_{s1}e^{i\varphi} & M_{s0} & M_{s-1}e^{-i\varphi} & M_{ss} \end{Bmatrix} \tag{14}$$

where the $M_{\mu\nu}$ are functions only of the polar angle $\vartheta$. The indices $\mu, \nu = 1, 0, -1, s$ refer to the basic vectors $\chi_1$, $\chi_0$, $\chi_{-1}$ and $\chi_s$.

The scattering matrix $M$ is invariant under space rotations and reflections and time reversal. $\mathbf{m}$ and $\mathbf{l}$ are polar vectors and change sign under space reflections, and $\boldsymbol{\sigma}$ and $\mathbf{n}$ are axial vectors and do not change sign. The forms

$\boldsymbol{\sigma}_1 \cdot \mathbf{m}$, $\boldsymbol{\sigma}_2 \cdot \mathbf{m}$, $\boldsymbol{\sigma}_1 \cdot \mathbf{l}$, $\boldsymbol{\sigma}_2 \cdot \mathbf{l}$, $(\boldsymbol{\sigma}_1 \cdot \mathbf{m})(\boldsymbol{\sigma}_2 \cdot \mathbf{n})$, $(\boldsymbol{\sigma}_1 \cdot \mathbf{l})(\boldsymbol{\sigma}_2 \cdot \mathbf{n})$, $(\boldsymbol{\sigma}_2 \cdot \mathbf{m})(\boldsymbol{\sigma}_1 \cdot \mathbf{n})$, $(\boldsymbol{\sigma}_2 \cdot \mathbf{l}^k)(\boldsymbol{\sigma}_1 \cdot \mathbf{n})$ are invariant under space rotations. They change signunder space reflections, however, and therefore cannot enter into the expression for $M$. From eq. (3) it then follows that the traces of the products of $M$ and any linear combinations of these matrices must vanish:

$$\begin{aligned} \operatorname{Tr} M(\sigma_x \times 1) &= \operatorname{Tr} M(1 \times \sigma_x) = 0, \\ \operatorname{Tr} M(\sigma_z \times 1) &= \operatorname{Tr} M(1 \times \sigma_z) = 0, \\ \operatorname{Tr} M(\sigma_x \times \sigma_y) &= \operatorname{Tr} M(\sigma_y \times \sigma_x) = 0, \\ \operatorname{Tr} M(\sigma_y \times \sigma_z) &= \operatorname{Tr} M(\sigma_z \times \sigma_y) = 0. \end{aligned} \tag{15}$$

Since the two particles are identical we have spin symmetry [1,3]:

$$\operatorname{Tr} M(1 \times \sigma_y) = \operatorname{Tr} M(\sigma_y \times 1), \quad \operatorname{Tr} M(\sigma_x \times \sigma_z) = \operatorname{Tr} M(\sigma_z \times \sigma_x). \tag{16}$$

From eqs. (15) and (16) we get

$$\begin{gathered} M_{11} = M_{-1-1}; \quad M_{1-1} = M_{-11}; \quad M_{10} = -M_{-10}; \quad M_{01} = -M_{0-1}; \\ M_{08} = M_{80} = M_{18} = M_{-18} = M_{81} = M_{8-1} = 0 \end{gathered} \tag{17}$$

and the scattering matrix is then

$$M = \begin{Bmatrix} M_{11} & M_{10}e^{-i\varphi} & M_{1-1}e^{-2i\varphi} & 0 \\ M_{01}e^{i\varphi} & M_{00} & -M_{01}e^{-i\varphi} & 0 \\ M_{1-1}e^{2i\varphi} & -M_{10}e^{i\varphi} & M_{11} & 0 \\ 0 & 0 & 0 & M_{88} \end{Bmatrix}. \tag{18}$$

From the invariance of $M$ under space rotations and reflections and from spin symmetry it thus follows that there are no transitions between singlet and triplet states, which also follows from the conservation of parity. The total spin of the two protons is thus a constant of motion.

Now, $\boldsymbol{\sigma}$, $\mathbf{l}$ and $\mathbf{n}$ change sign under time reversal, and $\mathbf{m}$ does not change sign. The form

$$\begin{aligned} &(\boldsymbol{\sigma}_1 \cdot \mathbf{m})(\boldsymbol{\sigma}_2 \cdot \mathbf{l}) + (\boldsymbol{\sigma}_1 \cdot \mathbf{l})(\boldsymbol{\sigma}_2 \cdot \mathbf{m}) \\ &\qquad = \sin\vartheta(\sigma_z \times \sigma_z - \sigma_x \times \sigma_x) - \cos\vartheta(\sigma_x \times \sigma_z + \sigma_z \times \sigma_x) \end{aligned} \tag{19}$$

therefore changes sign under time reversal, and cannot be contained in $M$. The trace of the product of $M$ and (19) must vanish, i.e. [2]

$$M_{11} - M_{00} - M_{1-1} = \sqrt{2}\cot\vartheta \cdot (M_{10} + M_{01}). \tag{20}$$

The scattering matrix thus depends upon five distinct complex functions i.e., excluding the absolute phase factor, on nine real parameters [3]. The parity of the two proton system is odd. The singlet spin eigenfunction is antisymmetric, and the triplet spin eigenfunctions are symmetric. The singlet matrix element is therefore symmetrical, and the triplet matrix elements (functions of $\vartheta$ and $\varphi$) are antisymmetrical: $M_{11}$ and $M_{00}$ are

proportional to $\cos\vartheta$, $M_{1-1}$ to $\sin^2\vartheta\cos\vartheta$ and $M_{10}$ and $M_{01}$ to $\sin\vartheta$ [3]). At an angle $\vartheta = \frac{1}{2}\pi$ we have

$$M_{11}(\tfrac{1}{2}\pi) = M_{1-1}(\tfrac{1}{2}\pi) = M_{00}(\tfrac{1}{2}\pi) = 0. \tag{21}$$

## 3. Formulae for the Differential Cross Section, the Polarization and the Correlation Coefficients

It may be derived from eqs. (6a) and (18), and it also follows from spin symmetry, that the polarization $\mathbf{P}_1$ and correlation coefficients $C_{xy}, \ldots$ satisfy the relations

$$\begin{aligned} \mathbf{P}_1 &= \langle \boldsymbol{\sigma} \times 1 \rangle = \langle 1 \times \boldsymbol{\sigma} \rangle = \mathbf{P}_2 = \mathbf{P}, \\ C_{zz} &= \langle \sigma_z \times \sigma_z \rangle = \langle \sigma_x \times \sigma_z \rangle = C_{xz}. \end{aligned} \tag{22}$$

It may be derived from eqs. (6a) and (18), and it follows from the invariance of the scattering matrix under space rotations and reflections, that there is no polarization in the scattering plane, and no correlation between spin components in the scattering plane and components normal to the scattering plane:

$$\begin{aligned} P_{x1} = P_{x2} = P_{z1} = P_{z2} = 0, \\ C_{xy} = C_{yx} = C_{yz} = C_{zy} = 0. \end{aligned} \tag{23}$$

We find the expectation values of the operator $S_\mu$, the polarization and the correlation coefficients, from eqs. (6a) and (18):

$$\begin{aligned} QP &= QP_y = \frac{2\sqrt{2}}{4} \operatorname{Im} \{M_{01} M_{11}^* + M_{00} M_{10}^* - M_{01} M_{1-1}^*\} \\ QC_{xx} &= \tfrac{1}{4}\{4 \operatorname{Re} M_{11} M_{1-1}^* - 2|M_{10}|^2 + 2|M_{01}|^2 + |M_{00}|^2 - |M_{ss}|^2\} \\ QC_{yy} &= \tfrac{1}{4}\{-4 \operatorname{Re} M_{11} M_{1-1}^* + 2|M_{10}|^2 + 2|M_{01}|^2 + |M_{00}|^2 - |M_{ss}|^2\} \\ QC_{zz} &= \tfrac{1}{4}\{2|M_{11}|^2 + 2|M_{10}|^2 + 2|M_{1-1}|^2 - 2|M_{01}|^2 - |M_{00}|^2 - |M_{ss}|^2\} \\ QC_{xz} &= \frac{2\sqrt{2}}{4} \operatorname{Re} \{M_{01} M_{11}^* + M_{00} M_{10}^* - M_{01} M_{1-1}^*\}. \end{aligned} \tag{24}$$

The corresponding quantities in the $\mathbf{m}$, $\mathbf{l}$, $\mathbf{n}$ co-ordinate system may be calculated from the geometry:

$$\begin{aligned} P_{\mathbf{n}} &= P_y = P; \\ C_{\mathbf{nn}} &= C_{yy}, \\ C_{\mathbf{mm}} &= \tfrac{1}{2}(C_{xx} + C_{zz}) - \tfrac{1}{2}\cos\vartheta (C_{zz} - C_{xx}) - \sin\vartheta\, C_{xz}, \\ C_{\mathbf{ll}} &= \tfrac{1}{2}(C_{xx} + C_{zz}) + \tfrac{1}{2}\cos\vartheta (C_{zz} - C_{xx}) + \sin\vartheta\, C_{xz}, \\ C_{\mathbf{ml}} &= C_{\mathbf{lm}} = \tfrac{1}{2}\sin\vartheta (C_{zz} - C_{xx}) - \cos\vartheta\, C_{xz}. \end{aligned} \tag{25}$$

We get the differential cross section from eqs. (7a) and (18) and we have finally for the polarization and the correlation coefficients

$$
\begin{aligned}
Q &= \tfrac{1}{4}\{2|M_{11}|^2+2|M_{10}|^2+2|M_{1-1}|^2+2|M_{01}|^2+|M_{00}|^2+|M_{ss}|^2\} \\
QC_{nn} &= \tfrac{1}{4}\{-4\ \mathrm{Re}\ M_{11}M_{1-1}^*+2|M_{10}|^2+2|M_{01}|^2+|M_{00}|^2-|M_{ss}|^2\} \\
Q(1-C_{nn}) &= \tfrac{1}{2}\{|M_{11}+M_{1-1}|^2+|M_{ss}|^2\} \\
Q(C_{mm}+C_{ll}) &= \tfrac{1}{2}\{|M_{11}+M_{1-1}|^2-|M_{ss}|^2\} \\
QP &= \frac{\sqrt{2}}{4}\,\mathrm{Im}\,\{(M_{10}^*-M_{01}^*)(M_{11}-M_{1-1}+M_{00})\} \\
QC_{mm} &= \tfrac{1}{4}\{|M_{11}+M_{1-1}|^2-|M_{ss}|^2-\frac{1}{\cos\vartheta}\,(|M_{11}-M_{1-1}|^2-|M_{00}|^2)\} \\
QC_{ll} &= \tfrac{1}{4}\{|M_{11}+M_{1-1}|^2-|M_{ss}|^2+\frac{1}{\cos\vartheta}\,(|M_{11}-M_{1-1}|^2-|M_{00}|^2)\} \\
QC_{ml} &= \frac{1}{2\sin\vartheta}\{|M_{10}|^2-|M_{01}|^2\}.
\end{aligned}
\tag{26}
$$

The last four formulae are derived by means of eq. (20). It will be seen that $C_{ml}$ has the opposite sign of Stapp's $C_{KP}$ because $\mathbf{m} = -\mathbf{K}$ and $\mathbf{l} = \mathbf{P}$. From eq. (21) it follows that the formulae are very simple at an angle of $\vartheta = 90°$. $C_{nn} = -1$ for scattering in singlet states, and $C_{nn} = 1$ for scattering at 90° in triplet states, and a measurement of $C_{nn}$ at 90° will therefore give the ratio between the singlet and triplet scattering cross sections.

When scattered in a second target (the analyser) the component of polarization normal to the scattering plane gives an asymmetry in the differential cross section. It follows that polarization parallel to the direction of motion is not detected [5]). This difficulty can be overcome by introducing a magnetic field between the first and second target (7). The correlation coefficients $C_{nn}$ and $C_{ml}$ (and also $C_{mm}$ and $C_{ll}$ with a magnetic field) can be measured with two analysers in coincidence [6]). $C_{nn}$ has been measured at 90° (in the centre of mass system) at 382 MeV [10]).

The author is indebted to the Royal Norwegian Council for Scientific and Industrial Research for a fellowship.

## References

1) R. H. Dalitz, Proc. Phys. Soc. A **65** (1952) 175
2) L. Wolfenstein and J. Ashkin, Phys. Rev. **85** (1952) 947
3) R. Oehme, Phys. Rev. **98** (1955) 147
4) U. Fano, Revs. Mod. Phys. **29** (1957) 74
5) L. Wolfenstein, Phys. Rev. **96** (1954) 1654 and Ann. Rev. Nuclear Science **6** (1956) 43
6) H. P. Stapp, U.C.R.L.–3098 (1955)
7) T. V. Kanellopoulos and G. E. Brown, Proc. Phys. Soc. A **70** (1957) 690
8) S. C. Wright, Phys. Rev. **99** (1955) 996
9) H. P. Stapp, T. J. Ypsilantis and N. Metropolis, Phys. Rev. **105** (1957) 302
10) A. Ashmore, A. N. Diddens, G. Huxtable and K. Skarsvåg (to be published in Proc. Phys. Soc.)

1.D.2 *Nuclear Physics* **8** (1958) 61—64; © *North-Holland Publishing Co., Amsterdam*
Not to be reproduced by photoprint or microfilm without written permission from the publisher

# THE LEVELS OF $Na^{23}$ ON THE UNIFIED MODEL

E. B. PAUL and J. H. MONTAGUE
*Atomic Energy Research Establishment, Harwell, Didcot, Berks.*

Received 23 May 1958

In connection with experimental work in this laboratory on the levels of $Na^{23}$ [1]) an attempt has been made to describe this nucleus in terms of the rotational model in a way similar to $F^{19}$ [2]). In this latter case the model was unexpectedly successful. However in the case of $Na^{23}$ the spins and parities of only two states are known with any certainty at present and the predictions cannot be checked. For this reason only a first trial using reasonable parameters is reported.

The ground state quadrupole moment has been measured as $0.10\times10^{-24}$ $cm^2$ [3]). Assuming that the ground state is fairly pure $K=\frac{3}{2}$ (we shall see later that this is approximately so) and computing the strong coupling projection factor we obtain a value of $\beta\approx+0.4$. The Coulomb excitation cross section [4]) for transitions to the first excited state yields $\beta=0.3$. Examination of the Nilsson [5]) level diagram in this region shows that the next excited particle configurations above the $K=\frac{3}{2}$ ground state consist of two configurations nearly degenerate having $K=\frac{1}{2}$ and $K=\frac{5}{2}$. Both of these may be expected to mix with the ground state configurations through the rotation-particle coupling [6]) in contrast to $F^{19}$ where only one excited configuration is expected to mix strongly. The appropriate moment of inertia can be derived from the position of the first excited 2+ states in the neighbouring even-even nuclei $Ne^{20}$ and $Mg^{24}$. This yields a value of $\hbar^2/2\mathscr{I}=0.25$ MeV. From the assumption of $\beta=+0.4$, we derive values for the decoupling parameter (which fixes the level order in the $K=\frac{1}{2}$ band) of $-0.25$ and for the matrix elements for the interaction of the mixing bands $A_{\frac{1}{2}\frac{1}{2}}=-1.1\hbar^2/2\mathscr{I}$ and $A_{\frac{1}{2}\frac{3}{2}}=+2.1\hbar^2/2\mathscr{I}$ [6]).

One excited state will be expected to be pure and therefore not subject to shift due to the interaction of different bands. This is the $I=\frac{1}{2}, K=\frac{1}{2}$ state. This is therefore used as the starting point and is identified with the observed state at 2.39 MeV. If other states in this region are chosen the agreement is rather poorer. The $K=\frac{1}{2}$ rotational set is then based on this state as shown on the left hand side of fig. 1.

The $I=\frac{3}{2}$ states occur in only two bands, $K=\frac{1}{2}$ and $K=\frac{3}{2}$. The perturbed position of the $K=\frac{3}{2}$ member must coincide with the ground state. The

unperturbed position of this state is then at 0.08 MeV and the rotational set based on it is shown in the second diagram from the left in fig. 1. The small shift in the $I = \frac{3}{2}$ member indicates that it is fairly pure $K = \frac{3}{2}$.

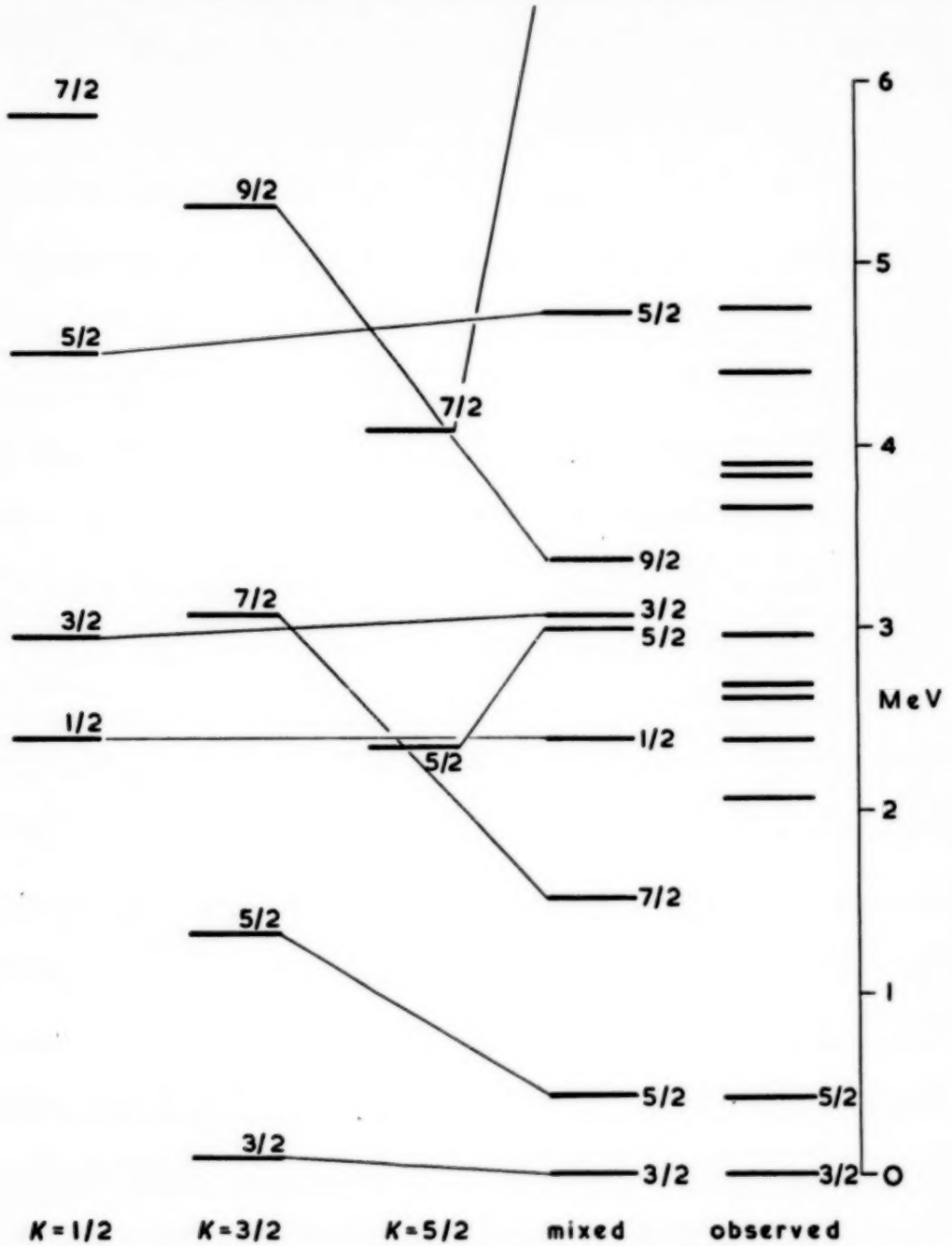


Fig. 1. Comparison between the known levels of $Na^{23}$ and the levels predicted by the present calculations. The first three columns show the unperturbed positions of the levels in the rotational bands of $K = \frac{1}{2}, \frac{3}{2}$ and $\frac{5}{2}$ respectively; each level is labelled with its total angular momentum, $I$. The fourth column shows the resulting level spectrum after considering mixing between levels of the same $I$ but different $K$.

For the $I = \frac{5}{2}$ states all three bands will mix. The ground state of the unperturbed $K = \frac{5}{2}$ band was fixed at 2.35 MeV so that the lowest $I = \frac{5}{2}$ state coincided with the observed 0.439 MeV first excited state of $Na^{23}$. The $K = \frac{5}{2}$ band based on this unperturbed ground state is shown in the third diagram from the left in fig. 1.

The final positions of the $I = \frac{7}{2}$ and $\frac{9}{2}$ states are now determined and are as shown in the fourth diagram of fig. 1. The observed states of $Na^{23}$ are shown on the right hand diagram in fig. 1 for comparison. The set of five states predicted between 1.5 and 3.5 MeV bear some resemblance to the states observed between 2 and 3 MeV. The spacing of the predicted states is however too great and this may well reflect the fact that too small a moment of inertia was used.

The group of states near 4 MeV are not accounted for by this model. It may be that these are states produced by many-particle excitations. The first state in $Al^{25}$ unaccounted for by this model occurs at 4 MeV [7]).

On this model the ground state of $Ne^{23}$ should be $I = \frac{5}{2} K = \frac{5}{2}$. Allowed $\beta$-transitions are observed [8]) to the ground, 0.44 and 2.08 MeV states which is consistent with the spin of $\frac{7}{2}+$ assigned by this model to the 2.08 MeV state. The spin of $Ne^{23}$ is not definitely established but stripping measurements by Burrows *et al.*[9]) strongly suggest that its level structure is similar to that of $Mg^{25}$.

TABLE 1

Gamma ray transitions

| Transitions from Level at | Quantity | Predicted | | Observed | |
|---|---|---|---|---|---|
| | | This Model | Weisskopf [10]) | | Ref. |
| 0.44 MeV assumed $I = \frac{5}{2}$ | $\tau_{M1}$ (sec) | $4 \times 10^{-13}$ | $1.5 \times 10^{-13}$ | $10^{-12} - 10^{-13}$ | [14]) |
| | $\tau_{E2}$ (sec) | $6 \times 10^{-10}$ | $1.5 \times 10^{-8}$ | $3 \times 10^{-10}$ | [4]) |
| | $\frac{T_{M1}(0.44)}{T_{E2}(0.44)}$ | 2400 | $10^5$ | $\geqq 20$ | [15]) |
| | | | | $300 - 3000$ | † |
| 2.08 MeV assumed $I = \frac{7}{2}$ | $\frac{T_{M1}(1.64)}{T_{E2}(2.08)}$ | 55 | 3000 | 6 | [1]) |
| 2.39 MeV assumed $I = \frac{1}{2}$ | $\frac{T_{M1}(2.39)}{T_{E2}(1.95)}$ | 90 | 8000 | 3 | [1]) |

† Derived from the measured lifetimes.

The ground state magnetic moment is predicted on this model to be 2.39 n.m. which may be compared with the measured value of 2.22 n.m.[10]).

Models for $Na^{23}$ along similar lines have been suggested by Rakavy [11]) and by Litherland *et al.*[12]). Rakavy considered only the interaction of $K = \frac{1}{2}$ and $K = \frac{3}{2}$ bands. States of $\frac{1}{2}$, $\frac{7}{2}$ and $\frac{9}{2}$ are predicted for the 2nd, 3rd and 4th excited states. Litherland considered only the interaction of $K = \frac{5}{2}$

and $K = \frac{3}{2}$ bands. States of $\frac{7}{2}$ and $\frac{5}{2}$ are predicted for the 2nd and 3rd excited states.

The excitation functions and cascading of gamma rays resulting from inelastic neutron scattering in $Na^{23}$ [1]) are not inconsistent with the proposed spin assignments for the 2nd and 3rd excited states. Angular distributions of deuterons inelastically scattered by $Na^{23}$ [13]) indicate that the parities of the 2.08, 2.71 and 3.85 MeV states are even.

If we identify the 2nd and 3rd excited states observed with the corresponding $\frac{7}{2}$ and $\frac{1}{2}+$ states in the predicted spectrum and assume that these along with the ground and 0.44 MeV states have the amounts of $K$ admixture predicted by this model, the $\gamma$-ray decay properties of these states can then be calculated. The results are shown in table 1 along with the usual Weisskopf estimate and the observed values for comparison. The agreement is as satisfactory as can be expected from this first trial.

When the spins of a few more states are established with certainty it will be interesting to make a more detailed fit using similar considerations.

## References

1) J. M. Freeman and J. H. Montague (to be published)
2) E. B. Paul, Phil. Mag. **2** (1957) 311
3) M. L. Perl, I. I. Rabi and B. Senitzky, Phys. Rev. **98** (1955) 611
4) G. M. Temmer and N. P. Heydenberg, Phys. Rev. **96** (1954) 426
5) S. G. Nillson, Mat. Fys. Medd. Dan. Vid. Selsk. (1955) no. 16
6) A. K. Kerman, Mat. Fys. Medd. Dan. Vid. Selsk. **30** (1956) no. 15
7) A. E. Litherland, H. E. Gove and A. J. Ferguson, Bull. Am. Phys. Soc. **3** (1958) 37
8) J. R. Penning and F. H. Schmidt, Phys. Rev. **79** (1957) 647
9) H. B. Burrows, T. S. Green, S. Hinds and R. Middleton, Proc. Phys. Soc. A **69** (1956) 310
10) J. E. Mack, Revs. Mod. Phys. **22** (1950) 64
11) G. Rakavy, Nuclear Physics **4** (1957) 375
12) A. E. Litherland, H. McManus, E. B. Paul, D. A. Bromley and H. E. Gove, Can. J. Phys. **36** (1958) 378
13) P. M. Endt and C. M. Braams, Revs. Mod. Phys. **29** (1957) 687
14) R. W. Krone, A. Everett and S. S. Hanna, Bull. Am. Phys. Soc. **1** (1956) 329
15) R. Berenbaum, J. H. Towle and J. H. Matthews, Proc. Phys. Soc. A **69** (1956) 858
16) D. H. Wilkinson, A.E.R.E. Report T/R 2492 (1958)

2.B *Nuclear Physics* **8** (1958) 65—68; © *North-Holland Publishing Co., Amsterdam*
Not to be reproduced by photoprint or microfilm without written permission from the publisher

# TIME REVERSAL AND POLARIZED NUCLEAR REACTIONS

G. R. SATCHLER
*Clarendon Laboratory, Oxford*

Received 1 June 1958

**Abstract:** Providing the interactions responsible are invariant under time reversal, it is shown there is a simple general relation between the spin polarization moments produced in a collision process, and the angular distribution induced by these moments in the time inverse collision.

There is a well-known relation between the angular distribution of products from a nuclear reaction induced by polarized spin $\frac{1}{2}$ particles, and the polarization of the particles produced in the inverse reaction [1]). This has been called the polarization — asymmetry equality [2]) and is valid provided the interactions responsible are invariant under time reversal. However, it does not seem to have been noticed that this is a special case of a very general relation between a collision process and its time inverse when spin polarization moments of any order are involved, provided time reversal invariance is satisfied.

The theorem can be deduced from the general formulae for polarized nuclear reactions [3]), but probably is most transparent if we start from first principles with the collision or scattering matrix $S$. Consider the reaction A+B → C+D, in which A † is incident along the direction of the unit vector $\mathbf{k}_1$ and C emerges along $\mathbf{k}_2$. This we call I. The time inverse of I, C+D → A+B, in which spin directions are reversed and C is incident along $-\mathbf{k}_2$, A emerging along $-\mathbf{k}_1$, we call II. To avoid a multiplicity of indices we denote the corresponding spins by $a$, $b$, $c$ and $d$ respectively, and their $z$-components by $\alpha$, $\beta$, $\gamma$ and $\delta$.

The transition amplitude for reaction I between states with definite magnetic quantum numbers is then given by the $S$ matrix element

$$\langle c\gamma d\delta; \mathbf{k}_2|S|a\alpha b\beta; \mathbf{k}_1\rangle. \tag{1}$$

The corresponding differential cross-section for the unpolarized case is then

$$\frac{\mathrm{d}\sigma(\mathbf{k}_1,\mathbf{k}_2)}{\mathrm{d}\omega} = \frac{\pi\lambda_1^{\,2}}{(2a+1)(2b+1)} \sum|\langle c\gamma d\delta; \mathbf{k}_2|S|a\alpha b\beta; \mathbf{k}_1\rangle|^2, \tag{2}$$

summed over all magnetic quantum numbers.

† A may be a particle or a photon. For the interpretation of photon 'spin', see for example refs.[3]).

We adopt a widely used representation for the angular momentum functions [4,5]) so that their behaviour under time reversal is

$$K\psi_{a\alpha} = (-)^{a+\alpha}\psi_{a,-\alpha}.$$

With this representation the collision matrix elements for I and II are related by [6])

$$\langle c\gamma d\delta; \mathbf{k}_2|S|a\alpha b\beta; \mathbf{k}_1\rangle = (-)^{a+\alpha+b+\beta+c+\gamma+d+\delta} \times \langle a, -\alpha, b, -\beta; -\mathbf{k}_1|S|c, -\gamma, d, -\delta; -\mathbf{k}_2\rangle, \quad (3)$$

provided the interactions are time reversal invariant.

We use the term polarization to denote any ordering of spins. A detailed description is given by the usual multipole or tensor moments $T_{kq}$ [3]). If the relative amplitude for a spin **a** to have a $z$-component $\alpha$ is $A_\alpha$, the component $q$ of the spin tensor of rank $k$ is defined here as

$$T_{kq}(a) = \sum_\alpha \sqrt{2a+1}(-)^{k+a+\alpha}\langle a, -\alpha, a, \alpha+q|kq\rangle A_\alpha A^*_{\alpha+q}. \quad (4)$$

$\langle a\alpha b\beta|c\gamma\rangle$ is the usual Clebsch-Gordan vector addition coefficient. Then $T_{00}$ is unity provided $\sum_\alpha |A_\alpha|^2 = 1$, while, for example, the dipolarization tensor ($k = 1$) has components

$$\begin{aligned} T_{10}(a) &= \sqrt{3/a(a+1)}\sum_\alpha \alpha|A_\alpha|^2 \\ &= \sqrt{3a/(a+1)}\, P_z, \quad (5) \\ T_{1\pm1}(a) &= \sqrt{3a/2(a+1)}(P_x \pm iP_y), \end{aligned}$$

if **P** is the usual 'polarization' vector, $\mathbf{P} = \langle \mathbf{a}/a\rangle$. Of course, moments up to $k = 2a$ can be defined in this way.

Consider now the reaction I when the incident particle A is polarized in some way. The differential cross-section $d\sigma(\mathbf{k}_1, \mathbf{k}_2)/\mathrm{d}\omega$, which apart from irrelevant factors we write as $I(\theta)$, now becomes

$$I(\theta) = \sum A_\alpha A^*_{\alpha'}\langle c\gamma d\delta; \mathbf{k}_2|S|a\alpha b\beta; \mathbf{k}_1\rangle\langle c\gamma d\delta; \mathbf{k}_2|S|a\alpha' b\beta; \mathbf{k}_1\rangle^*, \quad (6)$$

summed over all magnetic quantum numbers. Inverting (4) and introducing into (6),

$$I(\theta) = \sum_{kq} T^{\mathrm{I}}_{kq}(a)\sum \sqrt{2a+1}(-)^{k+a+\alpha}\langle a, -\alpha, a, \alpha+q|kq\rangle \times \langle c\gamma d\delta; \mathbf{k}_2|S|a\alpha b\beta; \mathbf{k}_1\rangle\langle c\gamma d\delta; \mathbf{k}_2|S|a, \alpha+q, b\beta; \mathbf{k}_1\rangle^*. \quad (7)$$

Of course, the $k = q = 0$ term, $I_{\mathrm{un}}(\theta)$ say, corresponds to the unpolarized distribution (2); the additional terms are introduced by the incident polarization.

Now in the inverse reaction II the expectation value of the spin tensor $T^{\mathrm{II}}_{k,-q}$ for the emergent particle A is, summing over all magnetic quantum numbers,

$$\frac{T^{\mathrm{II}}_{k,-q}(a)}{\sqrt{2a+1}} = \frac{\begin{array}{l}\sum(-)^{k+a-\alpha}\langle a\alpha a, -\alpha-q|k, -q\rangle \\ \langle a, -\alpha, b, -\beta; -\mathbf{k}_1|S|c, -\gamma, \mathrm{d}-\delta; -\mathbf{k}_2\rangle \\ \times\langle a,-\alpha-q, b, -\beta; -\mathbf{k}_1|S|c, -\gamma, d, -\delta; -\mathbf{k}_2\rangle^*\end{array}}{\sum|\langle a, -\alpha, b-\beta; -\mathbf{k}_1|S|c, -\gamma, d, -\delta; -\mathbf{k}_2\rangle|^2}, \tag{8}$$

again normalized so that $T^{\mathrm{II}}_{00} = 1$. Using (3) and the symmetry properties of the Clebsch-Gordan coefficients [5]) this becomes

$$\frac{T^{\mathrm{II}}_{k,-q}(a)}{\sqrt{2a+1}} = \frac{\begin{array}{l}(-)^{k+q}\sum(-)^{k+a+\alpha}\langle a, -\alpha, a, \alpha+q|kq\rangle \\ \langle c\gamma d\delta; \mathbf{k}_2|S|a\alpha b\beta; \mathbf{k}_1\rangle \\ \times\langle c\gamma d\delta; \mathbf{k}_2|S|a, \alpha+q, b\beta; \mathbf{k}_1\rangle^*\end{array}}{\sum|\langle c\gamma d\delta; \mathbf{k}_2|S|a\alpha b\beta; \mathbf{k}_1\rangle|^2}. \tag{9}$$

The denominator of (9) is just the unpolarized intensity $I_{\mathrm{un}}(\theta)$, while the numerator is just the factor occurring in the $k$, $q$ term of (7), the angular distribution $I(\theta)$ for the inverse reaction I. Hence this latter can be written

$$I(\theta) = I_{\mathrm{un}}(\theta)\sum_{kq}(-)^{k+q}T^{\mathrm{I}}_{kq}(a)T^{\mathrm{II}}_{k,-q}(a). \tag{10}$$

This is the generalization of the dipolarization-asymmetry equality for spin $\frac{1}{2}$ particles. We note that the spin tensors occur in the form of a scalar product [5]), as they should since the angular distribution cannot depend on our choice of axes. It should be remembered when using (10) that while $T^{\mathrm{I}}_{kq}$ describes the polarization of particles incident along $\mathbf{k}_1$, $T^{\mathrm{II}}_{kq}$ refers to the polarization of particles emerging along $-\mathbf{k}_1$ in the inverse reaction (with incident beam along $-\mathbf{k}_2$), but referred to the *same* coordinate axes. For example, the dipolarization $\mathbf{P}^{\mathrm{I}}$ in I would conventionally be regarded positive if directed along $\mathbf{n} = \mathbf{k}_1\times\mathbf{k}_2$. This must be retained for $\mathbf{P}^{\mathrm{II}}$ for II in (10), rather than the conventional $(-\mathbf{k}_2)\times(-\mathbf{k}_1) = -\mathbf{n}$.

Since in the centre of mass system the reaction I is quite symmetrical in 'incident' particle and 'target' particle the result (10) applies equally to reactions with unpolarized incident beam but oriented target nuclei B. Then $T^{\mathrm{II}}_{kd}$ refers to the polarization of the recoiling residual nuclei B in the inverse reaction II. Further, we may include polarization of both particles; that is, have a polarized beam incident on oriented target nuclei in reaction I. The angular distribution is then related by (10) to the inverse II in which the polarization of both emergent and recoil particles is measured. The tensors appearing in (10) would then be composites of the tensors for each particle

$$T_{kq}(a, b) = \sum_{k_1 k_2 q_1 q_2} T_{k_1 q_1}(a)T_{k_2 q_2}(b)\langle k_1 q_1 k_2 q_2|kq\rangle. \tag{11}$$

Unfortunately these further considerations are somewhat academic at the present stage of experimental techniques.

Finally we should remark that although the above discussion has been in terms of nuclear reactions it is equally true, of course, of mesonic and other

collision or reaction processes, provided only that the interactions responsible are invariant under time reversal.

*Note added in proof:* It should have been stressed in the above that the result, eq. (10), is dependent only upon the time reversal invariance expressed in eq. (3), but does not depend upon invariance under parity inversion. The latter can be used, for example, to require that the dipolarization vector be perpendicular to the reaction plane, and it is in this form that the dipolarization-asymmetry equality is usually expressed [1]) (but see ref. [2]) however). Eq. (10) reduces for $k = 1$ to the more general form which is valid even without invariance under parity inversion [2]). That is,

$$I(\theta) = I_{\mathrm{un}}(\theta)\left[1 - \mathbf{P}^{\mathrm{I}} \cdot \mathbf{P}^{\mathrm{II}}\left(\frac{3a}{a+1}\right)\right]$$

in the notation used above, where now $\mathbf{P}^{\mathrm{II}}$ is not necessarily perpendicular to the reaction plane.

## References

1) R. J. Blin-Stoyle, Proc. Phys. Soc. A **65** (1952) 452; R. H. Dalitz, Proc. Phys. Soc. A **65** (1952) 175; L. Wolfenstein and J. Ashkin, Phys. Rev. **85** (1952) 947
2) J. S. Bell and F. Mandl, Proc. Phys. Soc. A **71** (1958) 272 and 867
3) A. Simon and T. A. Welton, Phys. Rev. **90** (1953) 1036; A. Simon, Phys. Rev. **92** (1953) 1050; S. Devons and L. J. B. Goldfarb, Handbuch der Physik **42** (1957) 362
4) E. P. Wigner and L. Eisenbud, Phys. Rev. **72** (1947) 29; R. G. Sachs, Nuclear Theory (Addison-Wesley, Cambridge, Mass., 1953) Appendix 3; R. Huby, Proc. Phys. Soc. A **67** (1954) 1103
5) A. R. Edmonds, Angular Momentum in Quantum Mechanics (Princeton, 1957)
6) F. Coester, Phys. Rev. **84** (1951) 1259; **89** (1953) 619

1.D.2 *Nuclear Physics* 8 (1958) 69—70; © *North-Holland Publishing Co., Amsterdam*
Not to be reproduced by photoprint or microfilm without written permission from the publisher

# $F^{19}$ IN THE UNIFIED MODEL

G. ABRAHAM
*Atomic Energy Establishment, Trombay, Bombay, India*
and
C. S. WARKE
*Tata Institute of Fundamental Research, Bombay, India*

Received 22 May 1958

**Abstract:** The energies of the $F^{19}$ levels $I = \frac{1}{2}, \frac{5}{2}, \frac{3}{2}$ of positive parity and the magnetic moments of the $\frac{1}{2}$ and $\frac{5}{2}$ levels are calculated with the unified model, assuming weak coupling.

## 1. Introduction

Recent work has focussed interest on radically different approaches to the structure of $F^{19}$. Elliot and Flowers [1]) use the shell model of the nucleus, and construct the wave-functions from the three particles outside the inert doubly-closed shell. Paul [2]) and Rakavy [3]) assume strong coupling between the last odd particle and the collective oscillations. This note is based on weak coupling between particle and surface oscillations of the core.

## 2. The Weak Coupling Model

The unified model with weak coupling has been discussed by many authors [4]), and the procedure will not be given here. In the case of $F^{19}$, the odd proton is coupled to the surface oscillations of the core of 8 protons and 10 neutrons ($O^{18}$). The special assumptions made in this calculation are the following:

1) For the surface oscillations, spherical harmonics of order greater than the second are neglected.

2) In the absence of coupling, the odd proton can be in the single particle shell model states $1d_{\frac{5}{2}}$, $2s_{\frac{1}{2}}$, $1d_{\frac{3}{2}}$ with excitation energies as in $O^{17}$. With coupling, these particle states combine with surface quanta to form nuclear states of positive parity having angular momentum $I = \frac{1}{2}, \frac{3}{2}, \frac{5}{2} \ldots$, the single particle parameters being no longer good quantum numbers.

3) The effect of three and more quanta is neglected.

4) The energy of one surface quantum, $\hbar\omega$, is taken as 2 MeV, which is approximately the excitation energy of the $2^+$ level in $O^{18}$.

## 3. Results

The coupling parameter $P$ is taken as defined by Feenberg [4]):

$$P = \frac{5}{32\pi} k^2 \hbar (BC)^{-\frac{1}{2}} (\hbar\omega)^2.$$

It is found that for $P = 0.78$, the calculated energy levels approximately fit the observed levels. These are given in table 1, together with the calculated

TABLE 1

| | $E_{\frac{3}{2}} - E_{\frac{1}{2}}$ | $E_{\frac{5}{2}} - E_{\frac{1}{2}}$ | $\mu_{\frac{3}{2}}$ | $\mu_{\frac{5}{2}}$ |
|---|---|---|---|---|
| Experimental | 0.2 | 1.59 | 2.6 | $3.5 \pm 0.45$ |
| Calculated | 0.25 | 1.66 | 2.76 | 4.3 |

and experimental magnetic moments. The core gyromagnetic ratio $g_c$ is taken to be $Z/A$. The magnetic moments are somewhat better than the Schmidt values $\mu_{\frac{3}{2}} = 2.8$ and $\mu_{\frac{5}{2}} = 4.8$. However, the fair agreement with experiment is not a true indication of the success of the model because of the large two quanta amplitudes in the nuclear wave-functions. These are given in table 2. Here the symbol $(n, K, j)$ indicates the amplitude of the normalized

TABLE 2

| $I$ | $(00I)$ | $(12\frac{1}{2})$ | $(12\frac{3}{2})$ | $(12\frac{5}{2})$ | $(20I)$ | $(22\frac{1}{2})$ | $(22\frac{3}{2})$ | $(22\frac{5}{2})$ | $(24\frac{3}{2})$ | $(24\frac{5}{2})$ |
|---|---|---|---|---|---|---|---|---|---|---|
| $\frac{1}{2}$ | 0.659 | 0.646 | 0 | 0.226 | 0.197 | −0.239 | 0 | −0.074 | 0 | 0 |
| $\frac{3}{2}$ | 0.713 | −0.449 | 0.424 | −0.082 | 0.155 | 0.088 | −0.140 | 0.044 | 0.194 | 115 |
| $\frac{5}{2}$ | 0.282 | −0.286 | 0.701 | 0.130 | 0.105 | −0.205 | 0.106 | 0.110 | 0.505 | 0 |

wave-function composed of $n$ quanta of total angular momentum $K$ and the particle of angular momentum $j$ to give the normalized nuclear wave-function of the state of spin $I$. Table 2 shows that, particularly for $I = \frac{3}{2}$, the two quanta amplitudes are so large that the effect of more quanta may radically change the results.

We are grateful to Mr. Ivar Espe, who has worked on the same problem at Copenhagen, for helpful comments on preliminary calculations made by us, and to Professor L. Rosenfeld for his advice.

## References

1) J. P. Elliot and B. H. Flowers, Proc. Roy. Soc. A **229** (1955) 536
2) E. B. Paul, Phil. Mag **2** (1957) 311
3) G. Rakavy, Nuclear Physics **4** (1957) 375
4) E. Feenberg, Shell Theory of the Nucleus (Princeton University Press, 1955) Ch. IX

1.E.1:
2.G

*Nuclear Physics* **8** (1958) 71—78; © *North-Holland Publishing Co., Amsterdam*
Not to be reproduced by photoprint or microfilm without written permission from the publisher

# MAGNETIC ANALYSIS OF THE REACTION $V^{51}$ (d, p) $V^{52}$

F. A. EL BEDEWI and S. TADROS
*Faculty of Science, University of Alexandria, U. A. R.*

Received 22 April 1958

**Abstract:** The protons emitted from the bombardment of a thin vanadium target by 8.67 MeV deuterons have been analysed with a magnetic spectrograph and detected by nuclear photographic emulsions. Seven new excited levels in $V^{52}$ have been observed at 3.74, 4.27, 4.46, 4.72, 4.92, 5.23 and 5.48 MeV with errors varying between $\pm$ 0.02 and $\pm$ 0.03 MeV.

The angular distributions of some proton groups corresponding to a number of low lying levels are measured and compared with theoretical curves based on stripping mechanism. For the ground level in $V^{52}$, the neutron is captured in the $2p_{\frac{3}{2}}$ state. This suggests that in the shell model the $1f_{\frac{7}{2}}$ state lies above the $2p_{\frac{3}{2}}$ state. A spin of $3^+$ is proposed for this ground level.

## 1. Introduction

Bethe and Butler [1]) have suggested certain deuteron induced reactions to test the accuracy of the shell model in ascribing definite angular momentum states to nucleons in a nucleus. One of these proposed reactions is $V^{51}$(d, p)$V^{52}$ which should yield, for the ground level, protons characterized by $l_n = 3$ if the $1f_{\frac{7}{2}}$ state lies in the shell model below the $2p_{\frac{3}{2}}$ state. However, in this region, the energy corresponding to each of these states is nearly the same, and accordingly they may cross over in a way similar to that observed by El Bedewi [2]) for the $1d_{\frac{5}{2}}$ and $2s_{\frac{1}{2}}$ states. Thus, investigation of such reaction cannot only be considered as a test for the shell model, but rather a means for yielding information regarding the structure of the model itself. Moreover, the target nucleus is known to have a closed neutron subshell and it will be of interest to study the orbital angular momentum carried by the captured $29^{th}$ neutron in various excited levels.

The only experimental angular distributions for the two long range proton groups were reported by King and Parkinson [3]). Although these authors have found both distributions to be characterized by $l_n = 1$, yet they did not rule out the possibility of a considerable admixture of $l_n = 3$. Reliable interpretation of these results seems difficult in view of the present known level structure of $V^{52}$ which indicates that a number of different groups have been involved in their measurement. For this reason it is necessary to reinvestigate this reaction with high resolution apparatus.

Up to the present time, the most accurate determination of the energy levels in $V^{52}$ has been reported by Schwagner and Cox [4]) who used a magnetic spectrometer to analyse the protons emitted from vanadium targets bombarded with 6 MeV deuterons from an electrostatic generator. Although these workers have measured 23 proton groups corresponding to different levels in $V^{52}$ reaching an excitation energy of 3.30 MeV, yet no angular distributions have been reported. In the present experiment, we have employed deuterons of higher energy in the hope to observe some higher excited levels in $V^{52}$. The outgoing particles were analysed by a magnetic spectrograph which allows to study the angular distributions of a number of resolved proton groups.

## 2. Procedure

A self supported vanadium target of 0.5 mg/cm² areal density, prepared by evaporation onto stainless steel and then pealed off, was bombarded with

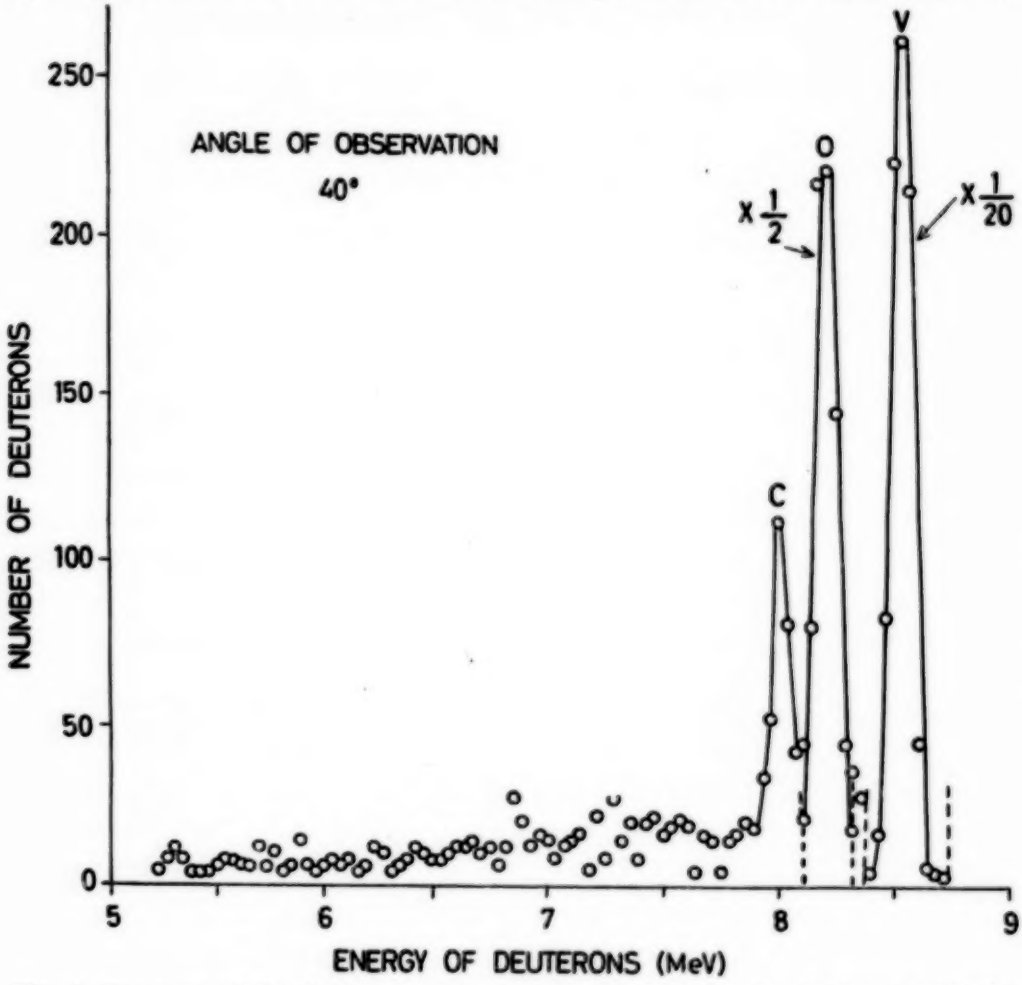


Fig. 1. Spectrum of the deuterons scattered from the deuteron bombardment with the vanadium target.

a beam of deuterons of $8.67 \pm 0.02$ MeV mean energy provided by the Liverpool 37-inch cyclotron. The charged particles emitted from this target were analysed by a magnetic spectrograph and detected in Ilford $C_2$ emulsion 100 $\mu$ thick. This equipment and its use in similar studies have been reported in detail by Green and Middleton [5]) and El Bedewi [2]).

In order to find out the composition of this target, mass analysis was carried out from elastic deuteron scattering. The distribution of these scattered deuterons, shown in fig. 1, at an angle of observation of 40°, indicates that oxygen and carbon are present as main contamination. Deuterons elastically scattered from vanadium isotopes, which naturally exist as $V^{50}$ and $V^{51}$, are not resolved. The abundance of the latter isotope is known to be 99.76 % and should be responsible for most of the observed proton groups. However, weak groups are ignored in this investigation. It should be mentioned, as shown from this spectrum, that no definite deuteron group which could be scattered inelastically is identified above the general back ground.

## 3. Results and Discussion

### 3.1. ENERGY SPECTRUM

A typical proton spectrum observed at an angle of observation 20° is shown in fig. 2A. Groups due to vanadium are easily sorted out from those due to oxygen and carbon on account of the variation of energy shift with angle. However, each group is identified by assuming a certain reaction and calculating the corresponding $Q$-value. The agreement of the results obtained at all angles of observation favours that assumption. Moreover, the groups denoted by $C_0$, $C_1$, $O_0$ and $O_1$ are identified, from known $Q$-values, to belong to $C^{12}$ and $O^{16}$ leaving the residual nuclei in the ground and first excited levels respectively. Groups labelled by $V_0$, $V_1$, ... $V_{21}$ are assigned to the reaction $V^{51}$(d, p)$V^{52}$. As shown in the presented spectrum, the groups corresponding to $V_9$, $V_{10}$, $V_{13}$ and $V_{14}$ are obscured by the two contamination groups $C_0$ and $O_0$, but they are observed at other angles and their positions at an angle of observation of 50° are shown in fig. 2B.

The $Q$-values corresponding to these various groups are calculated at all angles of observation. The ground level reaction energy is found to have a mean value of $5.08 \pm 0.02$ MeV, in agreement with the value $5.079 \pm 0.008$ MeV determined from neutron capture gamma rays from vanadium which was reported by Barthlomew and Kinsey [6]) or the value $5.072 \pm 0.008$ MeV obtained from $V^{51}$(d, p)$V^{52}$ reaction by Schwagner and Cox [4]). The values of the energy levels in $V^{52}$ deduced from the present work are compared with those obtained by Schwagner and Cox [4]) as shown in table 1. With exceptions of some complex levels, good agreement is generally achieved. In case of these low-spacing levels, which are difficult to resolve by the present

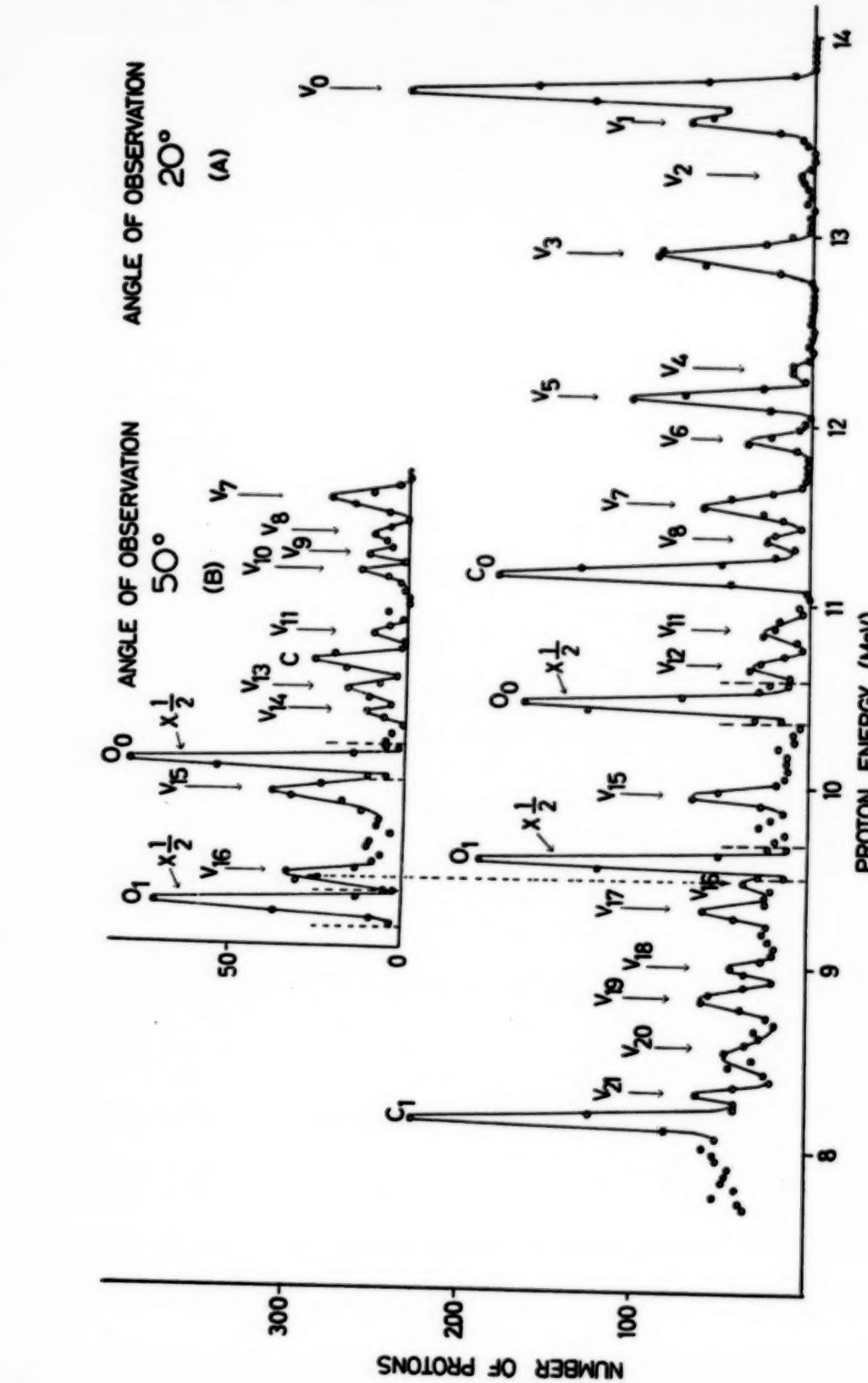


Fig. 2. Proton spectrum from the reaction $V^{51}(d, p)V^{52}$ at angles of observation 20(A) and 50(B).

arrangement, our results may correspond to the mean value of these levels, or refer to the most intense component. Outside the region investigated by Schwagner and Cox, seven groups denoted by $V_{15}$, $V_{16}$, ... $V_{21}$ are observed.

TABLE 1

Energy levels in $V^{52}$

| Group | Present | Schwagner and Cox (1953) | Group | Present | Schwagner and Cox (1953) |
|---|---|---|---|---|---|
| $V_1$ | 0.14±0.02 | 0.131±0.011 | $V_9$ | 2.40±0.02 | 2.415±0.011 |
| $V_2$ | 0.43±0.02 | 0.418±0.011 | | | 2.458±0.011 |
| $V_3$ | 0.81±0.02 | 0.780±0.011 | $V_{10}$ | 2.51±0.03 | 2.525±0.011 |
| | | 0.834±0.011 | $V_{11}$ | 2.84±0.02 | 2.848±0.011 |
| $V_4$ | 1.40±0.02 | 1.402±0.011 | $V_{12}$ | 3.03±0.02 | 3.002±0.011 |
| | | 1.475±0.011 | | | 3.051±0.011 |
| $V_5$ | 1.55±0.02 | 1.545±0.011 | $V_{13}$ | 3.16±0.03 | 3.189±0.011 |
| | | 1.753±0.011 | $V_{14}$ | 3.28±0.03 | 3.306±0.011 |
| $V_6$ | 1.76±0.02 | 1.785±0.011 | $V_{15}$ | 3.74±0.02 | – |
| | | 1.841±0.017 | $V_{16}$ | 4.27±0.02 | – |
| | | 2.088±0.011 | $V_{17}$ | 4.46±0.02 | – |
| $V_7$ | 2.11±0.02 | 2.131±0.015 | $V_{18}$ | 4.72±0.03 | – |
| | | 2.150±0.015 | $V_{19}$ | 4.92±0.02 | – |
| $V_8$ | 2.29±0.02 | 2.307±0.011 | $V_{20}$ | 5.23±0.02 | – |
| | | | $V_{21}$ | 5.48±0.03 | – |

The corresponding excited levels in $V^{52}$ are 3.74±0.02, 4.27±0.02, 4.46±0.02, 4.46±0.02, 4.72±0.03, 4.92±0.02, 5.23±0.02 and 5.48±0.03 MeV. From an investigation on the $V^{51}(n, \gamma)V^{52}$ reaction, Barthlomew and Kinsey [6]) have suggested that two gamma ray groups of energies 3.73 MeV and 3.59 MeV are in cascade between the capturing level at 7.305 MeV and the ground state. These authors have thus suspected a level to occur at 3.575 MeV or 3.715 MeV. The existence of the latter level is supported in view of a level obtained at 3.74 MeV from the present investigation.

### 3.2. ANGULAR DISTRIBUTIONS

The angular distributions for protons associated with the transition to the ground state and various levels up to an excitation energy of 2.29 MeV ($V_8$) are plotted in the centre-of-mass system as shown in fig. 3. The theoretical curves are calculated from Butler's formula [7]), using for the interaction the Gamow radius $6.25 \times 10^{-13}$ cm and choosing a value for the angular momentum $l_n$ transferred by the captured neutron to give the best fit. The results are consistent with those derived from the formula of Bhatia, Huang, Huby and Newns [8]) using a larger radius of interaction $7.35 \times 10^{-13}$ cm.

In case of the angular distribution for the resolved proton group $V_0$, corresponding to the transition to the ground state, a reasonable fit is observed between the experimental points and the theoretical curve for $l_n = 1$. It follows that the 29th neutron carries in the ground state of $V^{52}$

one unit of orbital angular momentum, and accordingly is captured in the $2p_{\frac{3}{2}}$ state. Thus, this state lies in the shell model lower than the $1f_{\frac{7}{2}}$ state, and thus the ambiguity mentioned by Bethe and Butler [1]) is removed.

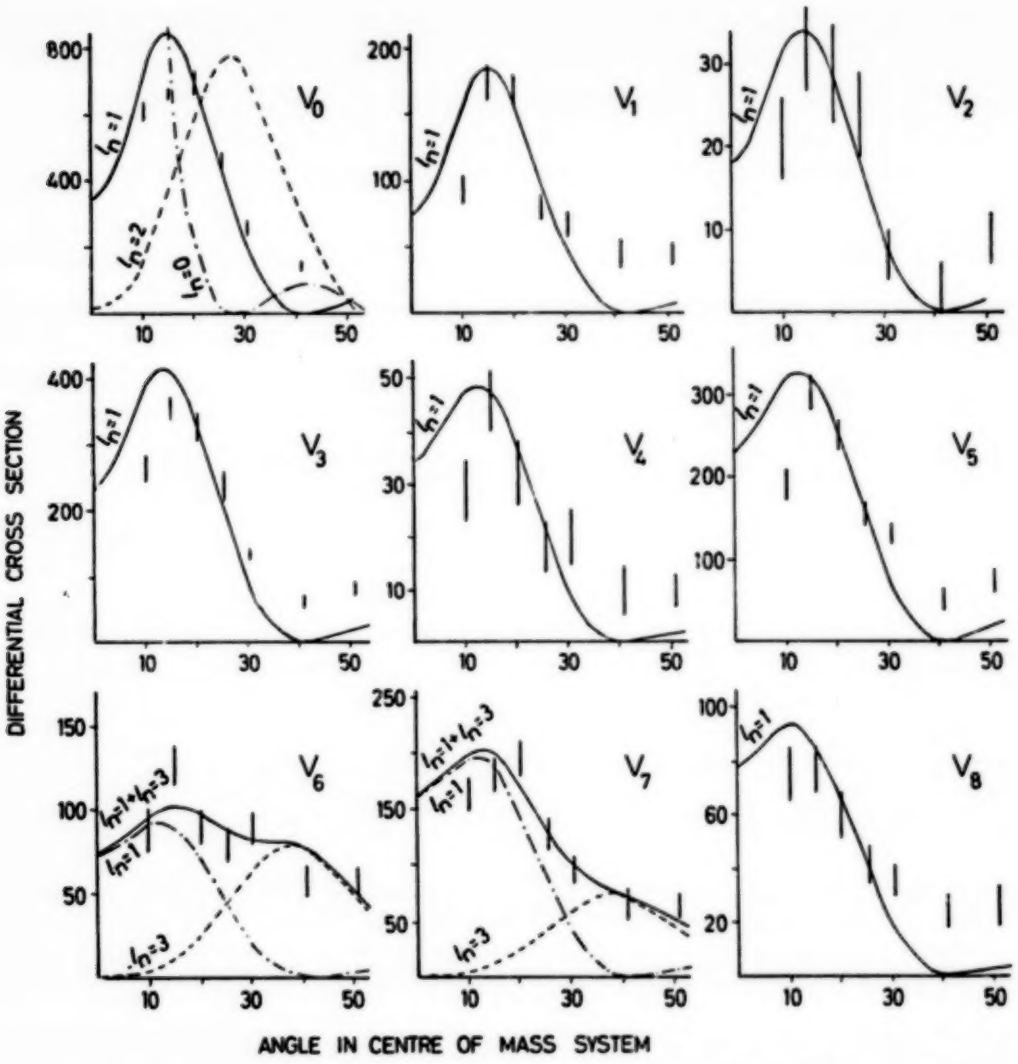


Fig. 3. Angular distribution of proton groups emitted from the reaction $V^{51}$(d, p)$V^{52}$. The curves are calculated from Butler theory using $r = 6.25 \times 10^{-13}$ cm.

Since the ground state of $V^{51}$ has an odd parity and spin $\frac{7}{2}$ (Bleaney *et al.* [9])), then, according to the selection rules, the ground level of $V^{52}$ must have even parity and spin 2, 3, 4 or 5 which satisfies the combination between the $2p_{\frac{3}{2}}$ state of the odd neutron with the $1f_{\frac{7}{2}}$ state of the odd proton. Leblanc *et al.* [10]) have reported a $\beta^-$-activity between this ground level and a level at 1.44 MeV in $Cr^{52}$ which is found by El Bedewi and Tadros [11]) to have spin $2^+$. According to the Gamow-Teller selection rules one can thus exclude

spins $4^+$ and $5^+$ for the ground level of $V^{52}$. In view of Nordheim's rule [12]) spin $2^+$ is omitted and accordingly we can suggest for this ground level an even parity and spin 3.

TABLE 2

| Group | $l_n$-value | Parity | Suggested spin of the final nucleus $J_B$ | Relative neutron capture probability $A$ | Relative reduced width $\gamma^2(2J_B+1)$ |
|---|---|---|---|---|---|
| $V_0$ | 1 | even | 3 | 100 | 100 |
| $V_1$ | 1 | even | $2 \rightarrow 5$ | 24 | 24 |
| $V_2$ | 1 | even | $2 \rightarrow 5$ | 3.9 | 4.0 |
| $V_3$ | 1 | even | $2 \rightarrow 5$ | 41 | 43 |
| $V_4$ | 1 | even | $2 \rightarrow 5$ | 3.7 | 4.0 |
| $V_5$ | 1 | even | $2 \rightarrow 5$ | 28.8 | 30 |
| $V_6$ | 1<br>3 | even<br>even | $2 \rightarrow 5$<br>$0 \rightarrow 7$ | 7.9<br>1.9 | 8.6<br>2.1 |
| $V_7$ | 1<br>3 | even<br>even | $2 \rightarrow 5$<br>$0 \rightarrow 7$ | 15.6<br>1.7 | 16.9<br>1.8 |
| $V_8$ | 1 | even | $2 \rightarrow 5$ | 6.1 | 6.7 |

With regard to the other investigated groups $V_1, V_2, \ldots V_8$, the angular momentum $l_n$ is found to be either unity or a mixture of $l_n = 1$ and $l_n = 3$. The results on the spins and parities of the various levels in $V^{52}$ are listed in table 2 together with the relative capture probabilities and relative reduced widths calculated from both stripping theories. It should be noted that, in general, the experimental points at small angles are below the theoretical curves. This discrepancy, which may be due to the approximations involved in the stripping theories, has been observed by other authors as Middleton, El Bedewi and Tai [13]) and Holt and Marsham [14]).

One of the authors (F.B.) is grateful to Professor H. W. B. Skinner for his encouragement and advice during the performance of this experiment at the Nuclear Physics Research Laboratory, Liverpool.

The authors would also like to express their gratitude to Professor M. A. El Sherbini for his interest and discussion.

## References

1) H. A. Bethe and S. T. Butler, Phys. Rev. **85** (1952) 1045
2) F. A. El Bedewi, Proc. Phys. Soc. A **69** (1956) 221
3) T. S. King and W. C. Parkinson, Phys. Rev. **89** (1953) 1080
4) J. E. Schwagner and L. A. Cox, Phys. Rev. **92** (1953) 102
5) T. Green and R. Middleton, Proc. Phys. Soc. A **69** (1956) 16

6) G. A. Barthlomew and B. B. Kinsey, Phys. Rev. **89** (1953) 386
7) S. T. Butler, Proc. Roy Soc. A **208** (1951) 559
8) A. B. Bhatia, K. Huang, R. Huby and H. C. Newns, Phil. Mag. **43** (1952) 485
9) B. Bleaney, D. J. E. Ingram and H. E. D. Scovil, Proc. Phys. Soc. A **64** (1951) 601
10) J. M. Leblanc, J. M. Cork, S. B. Burson and W. C. Jordan, Phys. Rev. **93** (1954) 1124
11) F. A. El Bedewi and S. Tadros, Nuclear Physics **6** (1958) 434
12) L. A. Nordheim, Revs. Mod. Phys. **23** (1951) 322
13) R. Middleton, F. A. El Bedewi and C. T. Tai, Proc. Phys. Soc. A **66** (1953) 95
14) J. R. Holt and T. N. Marsham, Proc. Phys. Soc. A **66** (1953) 249

1.E.1: 2.G

*Nuclear Physics* **8** (1958) 79—84; © *North-Holland Publishing Co., Amsterdam*
Not to be reproduced by photoprint or microfilm without written permission from the publisher

# LOW ENERGY LEVELS IN COBALT 60

F. A. EL BEDEWI and S. TADROS

*Faculty of Science, University of Alexandria, U. A. R.*

Received 20 April 1958

**Abstract:** The angular distributions of a number of proton groups emitted from the deuteron bombardment with a cobalt target are compared with theoretical curves based on nuclear stripping mechanism. The spins of the ground and first excited levels of $Co^{60}$ are found to be $5^+$ and $2^+$ respectively.

In a recent report [1]), we have given some evidence, by investigating the $V^{51}(d, p)V^{52}$ reaction, that the $2p_{\frac{3}{2}}$ state in the shell model lies lower than the $1f_{\frac{7}{2}}$ state. This arrangement has been achieved since $V^{51}$ isotope contains 28 neutrons filling the $1f_{\frac{7}{2}}$ subshell, and the captured neutron is found to carry in one unit of orbital angular momentum. It will thus be of interest to carry on similar experiments on nuclei containing 32 neutrons to find out whether they fill the subshell $2p_{\frac{3}{2}}$ of Mayer's model. For this reason, cobalt $_{27}Co^{59}$, which naturally exists as a single isotope, has been chosen.

Foglesong and Foxwell [2]) have carefully analysed magnetically the proton groups emitted from the $Co^{59}(d, p)Co^{60}$ reaction. As expected for an odd-odd nucleus, the proton spectrum is so complicated and many levels are found to have close spacing as low as 14 keV. These authors have observed 35 levels up to an excitation energy of 4.6 MeV. However, no angular distribution of any of these proton groups has yet been reported.

In the present work, a deuteron beam of mean energy 8.70 MeV from the Liverpool 37-inch cyclotron is used to bombard a self supported cobalt target of 1.5 mg/cm$^2$ surface density prepared by electrolysis. The outgoing protons have been analysed by a magnetic spectrograph with photographic detection [3]). The experimental procedure is similar to that previously described by El Bedewi [4]). A typical proton spectrum observed at an angle 15° is shown in fig. 1. At the high energy region, five groups of considerable intensity are assigned to the $Co^{59}(d, p)Co^{60}$ reaction, since the corresponding $Q$-values calculated at different angles of observation are in agreement with those reported by Foglesong and Foxwell [2]). These authors have determined the reaction energy $Q_0$ as $5.283 \pm 0.008$ MeV and gave energy levels in $Co^{60}$ which correspond to the present investigated proton groups as shown in the table. Group A is found to represent a doublet corresponding to the transition to the ground and the first excited levels (0.06 MeV). Groups labelled by

B, D, and E correspond to transitions to excited levels at 0.286 MeV, 0.792 MeV and 1.012 MeV respectively. The group C is of complex structure,

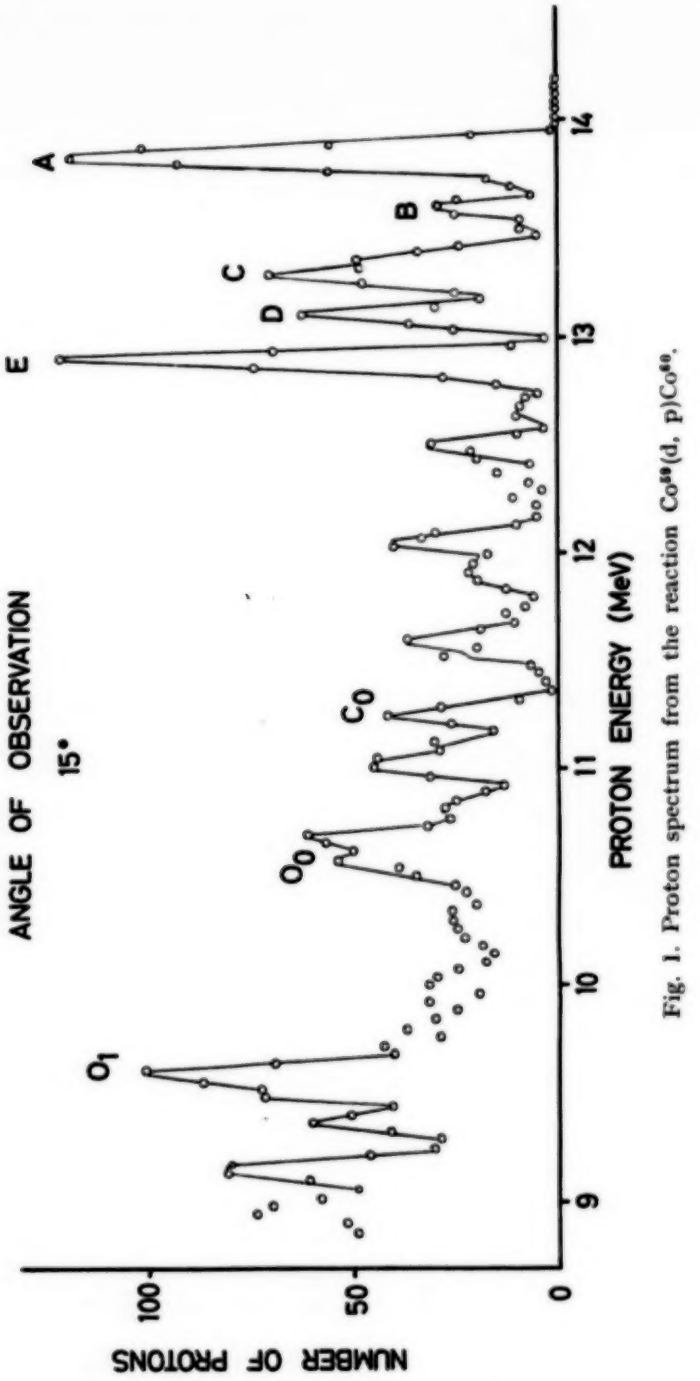


Fig. 1. Proton spectrum from the reaction $Co^{59}(d, p)Co^{60}$.

and correspond to transitions to four closely spaced levels at 0.445, 0.513, 0.557 and 0.622 MeV.

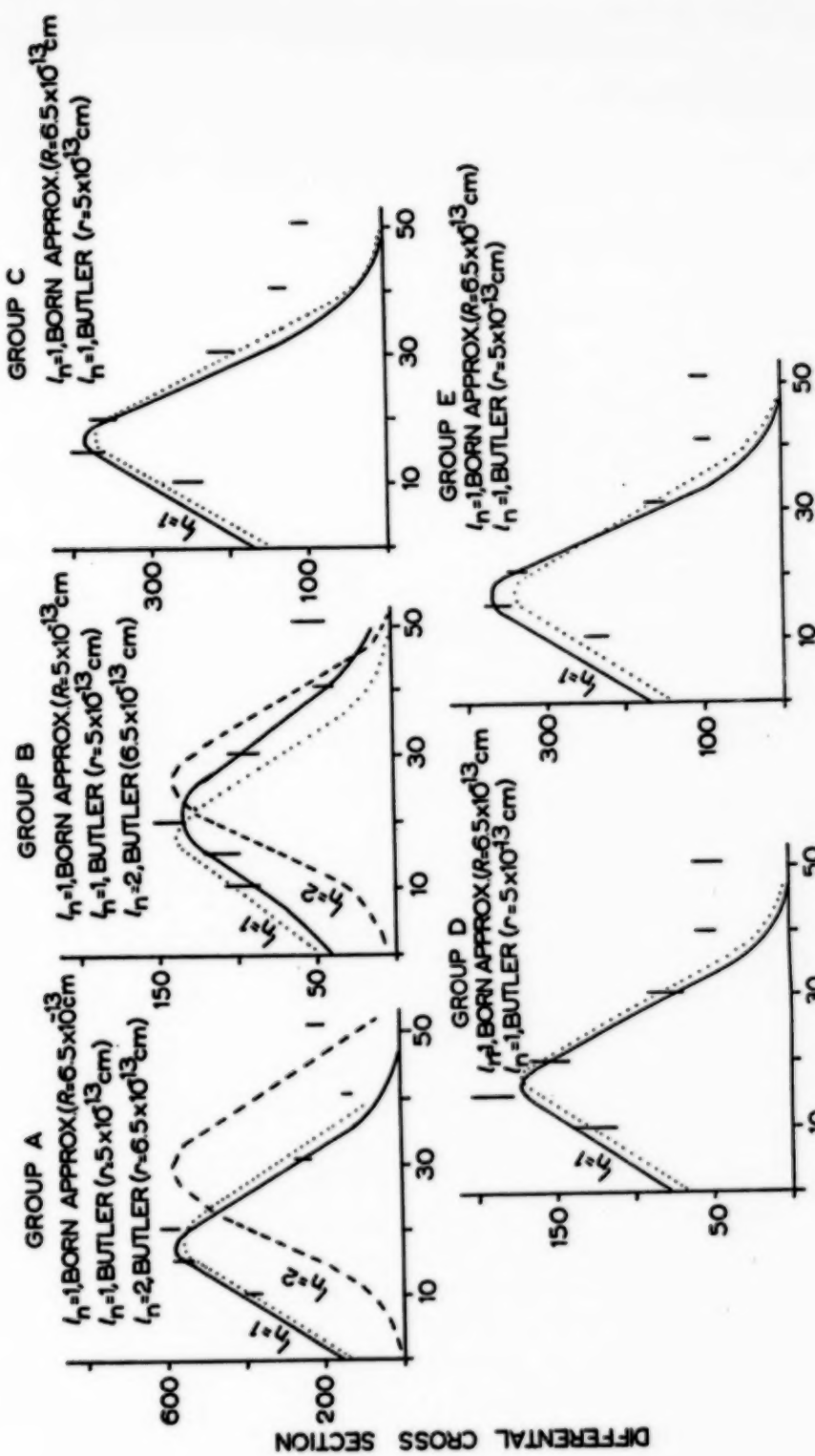


Fig. 2. Angular distribution of proton groups emitted from the reaction $Co^{59}(d, p)Co^{60}$.

The angular distributions of each of these groups are represented in the centre-of-mass system as shown in fig. 2. Attempts have been made to fit the distributions by theoretical curves calculated from the nuclear stripping

TABLE 1

| Group | Energy level [2]) | $l_n$-value | Parity | Suggested spin of the final nucleus $J_B$ | Relative neutron capture probability $A$ | Relative reduced width $\gamma^2(2J_B+1)$ |
|---|---|---|---|---|---|---|
| A | 0<br>0.060±0.003 | 1 | even | 5<br>2 | 100 | 100 |
| B | 0.286±0.003 | 1 | even | 2 → 5 | 27 | 27 |
| C | 0.445±0.003<br>0.513±0.003<br>0.557±0.005<br>0.622±0.004 | 1 | even | 2 → 5 | 55 | 56 |
| D | 0.792±0.003 | 1 | even | 2 → 5 | 22 | 23 |
| E | 1.012±0.003 | 1 | even | 2 → 5 | 47 | 49 |

theories of Butler [5]) and Bhatia, Huang, Huby and Newns [6]). The value of $l_n$ chosen to give the best fit in each case is found to be unity. It is surprising to point out that a rather small radius of interaction has to be used in these calculations. The most satisfactory value required for all the Born approximation curves is found to be the Gamow radius $6.5\times10^{-13}$ cm, with an exception to group B where a much smaller radius $5.0\times10^{-13}$ cm is necessary for better agreement. In case of the Butler curves, best fitting was achieved when the radius of interaction is $5.0\times10^{-13}$ cm. It should be mentioned that no theoretical curve characterized by an angular momentum greater than unity can give satisfactory agreement with the experimental results unless the radius of interaction is highly increased beyond a reasonable value.

As shown from the table, groups B, D and E represent transitions to single levels where the neutron is captured with a unit orbital angular momentum. Group C is of complex structure since it corresponds to the transition to four excited levels. Proton groups associated with the formation of $Co^{60}$ in one or more of these excited levels may be then responsible for the shape of the total angular distribution characterized by $l_n = 1$. In case of group A, the symmetry of its shape, as seen from various spectra at different angles of observations, suggests that its two components are of nearly the same intensity, i.e. having similar angular distributions and accordingly, the neutron carries into either the ground or the first excited levels a unit angular momentum. As predicted by the shell model, the spin of the target nucleus $Co^{59}$ is $\frac{7}{2}^-$. Thus, according to the selection rules, each of the investigated levels in $Co^{60}$ must have even parity and spin 2, 3, 4 or 5.

Some of these possible assignments for the spin of the ground and first excited levels could be ruled out on account of the beta spectrum measured by Deutsch and Goldhaber [7]) and by Chang Yun Fan [8]) as shown in fig. 3.

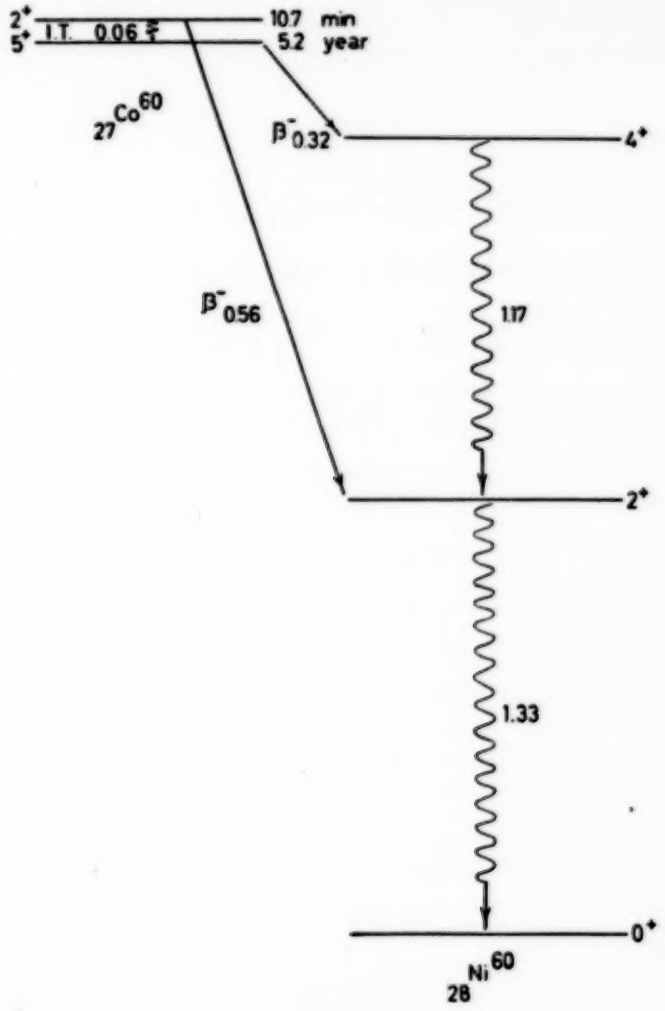


Fig. 3

These authors have detected $\beta^-$ transition from the ground level of $Co^{60}$ to the second excited level in $Ni^{60}$ (at 2.25 MeV) of spin $4^+$, but there is no evidence for such transition to lower levels. Thus according to the Gamow-Teller selection rule, the assignment of $2^+$ or $3^+$ for this ground level is omitted, leaving it with a spin $4^+$ or $5^+$. On the other hand, the reported $\beta$ decay transition between the first excited level in $Co^{60}$ and the first excited level in $Ni^{60}$ of spin $2^+$, and the absence of such transition between that level and the second excited level in $Ni^{60}$ exclude all the possible spins for that level except the value of $2^+$. But, on account of the life-time of the isomeric transition between the first and ground levels in $Co^{60}$, a spin change

of 3 is required [9]). It follows that the spin of this ground level has to be only $5^+$.

If the spin assignment of this ground level is correct, then the 33rd captured neutron is not a $2p_{\frac{1}{2}}$ nucleon, but ought to be a $2p_{\frac{3}{2}}$ one and accordingly, the subshell $2p_{\frac{1}{2}}$, in Mayer's model, is not filled in the $Co^{59}$ structure. The configuration of this nucleus can be thus suggested as $(\pi 1f_{\frac{7}{2}})_{\frac{7}{2}}^{-1}(\nu 2p_{\frac{3}{2}})_0^2(\nu 1f_{\frac{7}{2}})_0^2$, coupled together to give spin $\frac{7}{2}$. On capturing a neutron, the configuration of the resulting ground level of $Co^{60}$ becomes $(\pi 1f_{\frac{7}{2}})_{\frac{7}{2}}^{-1}(\nu 2p_{\frac{3}{2}})_{\frac{3}{2}}^3(\nu 1f_{\frac{7}{2}})_0^2$, coupled together to give spin 5. This configuration can also represent the first excited level since it can couple to give spin 2 which has been assigned to that level.

One of the authors (F.B.) is grateful to Professor H. W. B. Skinner for his encouragement and advice during the performance of this experiment at the Nuclear Physics Research Laboratory, Liverpool.

The authors would also like to express their gratitude to Professor M. A. El Sherbini for his interest and discussions.

## References

1) F. A. El Bedewi and S. Tadros, Nuclear Physics **8** (1958) 71
2) G. M. Foglesong and D. G. Foxwell, Phys. Rev. **96** (1954) 1001
3) T. Green and R. Middleton, Proc. Phys. Soc. A **69** (1956) 16
4) F. A. El Bedewi, Proc. Phys. Soc. A **69** (1956) 221
5) S. T. Butler, Proc. Roy. Soc. A **208** (1951) 559
6) A. B. Bhatia, K. Huang, R. Huby and H. C. Newns, Phil. Mag. **43** (1952) 485
7) M. Deutsch and G. Scharff-Goldhaber, Phys. Rev. **83** (1951) 1059
8) Chang Yun Fan, Phys. Rev. **87** (1952) 252
9) M. Goldhaber and A. W. Sunyar, Phys. Rev. **83** (1951) 906

8.B *Nuclear Physics* 8 (1958) 85—90; © *North-Holland Publishing Co., Amsterdam*
Not to be reproduced by photoprint or microfilm without written permission from the publisher

# ON THE INTERACTION OF STRANGE PARTICLES

NING HU
*Joint Institute of Nuclear Research,*
*Laboratory of Theoretical Physics, Dubna, USSR*

Received 19 March 1958

**Abstract:** The similarity between $\pi$-interaction and K-interaction is stressed in the present investigation. It is found that both interactions can be reduced to the universal form

$$H = \bar{\psi} i\gamma_5 \varphi \psi.$$

It is also shown that after all symmetry requirements have been imposed, the number of independent coupling constants is six, which is less by two than that in the theory of Prentki and d'Espagnat.

One of the complications of meson theory compared to quantum electrodynamics is the necessity of introducing isobaric spin space. The interaction Hamiltonian between nucleons and mesons is given by

$$H_{\text{in}} = g\bar{\psi} i\gamma_5 \varphi \psi \tag{1}$$

where $\psi$ is the field operator for nucleons and $\varphi$ is a $2\times 2$ matrix in isobaric spin space whose elements are proportional to the field operators of mesons. Eq. (1) possesses essentially the same form as the interaction Hamiltonian in quantum electrodynamics. This general form of the interaction Hamiltonian seems to have been rejected in the recent formulation of Prentki and d'Espagnat [1]) devised to express the Gell-Mann-Nishijima scheme [2,3]) for strong interactions. However, Gell-Mann has been able to restore form (1) for interactions involving $\pi$-mesons by expressing $\Sigma$ and $\Lambda$ particles in terms of spinor operators $\psi$. In the present note we shall show that if we demand the interactions involving K-mesons to be also of the form (1), the resulting interaction Hamiltonian will be slightly different from that obtained by Prentki and d'Espagnat but reduces to a special case of it when further symmetry requirements are imposed. Our new interaction Hamiltonian also leads to the Gell-Mann-Nishijima scheme in the general case.

We shall begin by writing down the following four matrices of the field operators:

$$\begin{aligned}
\psi^{(1)} &= \begin{pmatrix} \Xi^0 & \mathrm{N}^+ \\ \Xi^- & \mathrm{N}^0 \end{pmatrix}, \quad \psi^{(2)} = \begin{pmatrix} \mathrm{Z}^0 & \Sigma^+ \\ \Sigma^- & \mathrm{Y}^0 \end{pmatrix} = \begin{pmatrix} \frac{1}{\sqrt{2}}(\Lambda+\Sigma^0) & \Sigma^+ \\ \Sigma^- & \frac{1}{\sqrt{2}}(\Lambda-\Sigma^0) \end{pmatrix} \\
\varphi^{(1)} &= \boldsymbol{\tau}\cdot\boldsymbol{\pi} = \begin{pmatrix} \frac{1}{\sqrt{2}}\pi^0 & \pi^+ \\ \pi^- & -\frac{1}{\sqrt{2}}\pi^0 \end{pmatrix}, \quad \varphi^{(2)} = \begin{pmatrix} \mathrm{K}^0 & \mathrm{K}^+ \\ \mathrm{K}^- & -\tilde{\mathrm{K}}^0 \end{pmatrix}
\end{aligned} \tag{2}$$

where $\Xi^0$, $N^+$, $\Lambda$, $\pi^+$, $K^0$, etc., represent field operators for the corresponding particles. We shall temporarily ignore the differences in mass among various baryons.

To make $\varphi^{(1)}$ still more similar to $\varphi^{(2)}$, we shall use the following modified expression:

$$\varphi^{(1)} = \begin{pmatrix} \eta^0 & \pi^+ \\ \pi^- & -\eta^0 \end{pmatrix} = \begin{pmatrix} \frac{1}{\sqrt{2}}(\pi^0+i\pi^{0\prime}) & \pi^+ \\ \pi^- & -\frac{1}{\sqrt{2}}(\pi^0-i\pi^{0\prime}) \end{pmatrix}$$

where $\pi^{0\prime}$ represents a fictitious particle which, as we shall see below, does not actually participate in the interaction. $\pi^0$ and $\pi^{0\prime}$ now correspond exactly to $\theta_1$ and $\theta_2$ defined by

$$K^0 = \frac{1}{\sqrt{2}}(\theta_1+i\theta_2), \quad \tilde{K}^0 = \frac{1}{\sqrt{2}}(\theta_1-i\theta_2).$$

It should also be pointed out that there is no reason whatsoever for preferring $\Lambda$ to $-\Lambda$ when we write down $\Psi^{(2)}$ in (2). Thus in the following considerations, we shall have to consider also $\Psi^{(2)\prime}$ obtained from $\Psi^{(2)}$ by reversing the sign of $\Lambda$:

$$\Psi^{(2)\prime} = \begin{pmatrix} -Y^0 & \Sigma^+ \\ \Sigma^- & -Z^0 \end{pmatrix}.$$

To express the interaction Hamiltonian in form (1), Gell-Mann broke $\Psi^{(1)}$ and $\Psi^{(2)}$ into the following four spinors:

$$\psi^{(1)} = \begin{pmatrix} N^+ \\ N^0 \end{pmatrix}, \quad \psi^{(2)} = \begin{pmatrix} \Xi^0 \\ \Xi^- \end{pmatrix}, \quad \psi^{(3)} = \begin{pmatrix} \Sigma^+ \\ Y^0 \end{pmatrix}, \quad \psi^{(4)} = \begin{pmatrix} Z^0 \\ \Sigma^- \end{pmatrix}. \tag{3}$$

He found that the Hamiltonian for $\pi$-interaction can be put in the following form:

$$H_1 = \tfrac{1}{2}\sum_{j=1}^{4} f_j\{\bar{\psi}^{(j)}\, i\gamma_5\, \varphi^{(1)}\, \psi^{(j)} + \bar{\psi}^{(j)}\, i\gamma_5\, \varphi^{(1)*T}\, \psi^{(j)}\} \tag{4}$$

where the second term in the brackets is simply the Hermitian conjugate of the first term, and $\varphi^{(1)*T}$ represents the transposed and complex conjugate of $\varphi^{(1)}$. It can easily be seen that terms containing $\pi^{0\prime}$ in the above expression cancel out and the result may simply be written as

$$H_1 = \sum_{j=1}^{4} f_j\, \bar{\psi}^{(j)}\, i\gamma_5\, \boldsymbol{\tau}\cdot\boldsymbol{\pi}\psi^{(j)}. \tag{4a}$$

For reasons mentioned above, the terms obtained from those of (4a) with $j = 3$ and $j = 4$ by reversing the sign of $\Lambda$ but with different coupling constants must be added to (4a). Thus the modified interaction Hamiltonian becomes

$$H_1 = \tfrac{1}{2}\sum_{j=1}^{4} f_j\, \bar{\psi}^{(j)}\, i\gamma_5\, \varphi^{(1)}\, \psi^{(j)} + \tfrac{1}{2}\sum_{j=3}^{4} f'_j\, \bar{\psi}^{(j)\prime}\, i\gamma_5\, \psi^{(j)\prime} + \text{h.c.} \tag{5}$$

where

$$\psi^{(3)\prime} = \begin{pmatrix} \Sigma^+ \\ -\mathrm{Z}^0 \end{pmatrix}, \quad \psi^{(4)\prime} = \begin{pmatrix} -\mathrm{Y}^0 \\ \Sigma^- \end{pmatrix}. \tag{6}$$

If we further require that $\Sigma_3 = \Sigma^0$, $\Sigma_1 = (1/\sqrt{2})(\Sigma^+ + \Sigma^-)$ and $\Sigma_2 = (1/\sqrt{2}i)(\Sigma^+ - \Sigma^-)$ should appear in the result as components of a vector, then we must have

$$f_3 = f_4, \qquad f'_3 = f'_4. \tag{7}$$

Writing down the result explicitly, we obtain

$$\begin{aligned} H_1 = {} & f_1 \bar{\psi}^{(1)} i\gamma_5 \boldsymbol{\tau} \cdot \boldsymbol{\pi} \psi^{(1)} + f_2 \bar{\psi}^{(2)} i\gamma_5 (\boldsymbol{\tau} \cdot \boldsymbol{\pi}) \psi^{(2)} \\ & + (f_3 - f'_3)[\bar{\Lambda} i\gamma_5 \boldsymbol{\pi} \cdot \boldsymbol{\Sigma} + \text{h.c.}] \\ & + (f_3 + f'_3)[i\boldsymbol{\Sigma} i\gamma_5 \times \boldsymbol{\Sigma}] \cdot \boldsymbol{\pi} \end{aligned} \tag{8}$$

which is just the first part of the interaction Hamiltonian obtained by Prentki and d'Espagnat.

To obtain the interaction Hamiltonian involving K-mesons, we shall divide $\Psi^{(1)}$ and $\Psi^{(2)}$ in another way:

$$\phi^{(1)} = \begin{pmatrix} \mathrm{N}^+ \\ \Xi^0 \end{pmatrix}, \quad \phi^{(2)} = \begin{pmatrix} \mathrm{N}^0 \\ \Xi^- \end{pmatrix}, \quad \phi^{(3)} = \begin{pmatrix} \Sigma^+ \\ \mathrm{Z}^0 \end{pmatrix}, \quad \phi^{(4)} = \begin{pmatrix} \mathrm{Y}^0 \\ \Sigma^- \end{pmatrix}. \tag{9}$$

In contrast with the case of $\pi$-interaction, we shall now require that $\bar{\phi}^{(i)}$ and $\phi^{(j)}$, which appear in the same term, should have different values of $i$ and $j$. For instance, when $i = 1$, $j = 3$ we must put

$$H_{13} = f_{13}\{\bar{\phi}^{(1)} i\gamma_5 \varphi^{(2)} \phi^{(3)} + \bar{\phi}^{(3)} i\gamma_5 \varphi^{(2)*\mathrm{T}} \phi^{(1)}\} \tag{10}$$

where the second term in the brackets is the Hermitian conjugate of the first term. Similarly, for $i = 2$, $j = 4$, we have

$$H_{24} = f_{24}\{\bar{\phi}^{(2)} i\gamma_5 \varphi^{(2)} \phi^{(4)} + \bar{\phi}^{(4)} i\gamma_5 \varphi^{(2)*\mathrm{T}} \phi^{(2)}\}. \tag{11}$$

We see easily that for $i = 1, j = 4$ and $i = 2, j = 3$, the resulting expressions cannot conserve the electric charge of the system and therefore these terms must be dropped from the interaction Hamiltonian. Furthermore, we shall require that whenever $i$ and $j$ are interchanged, $\varphi^{(2)}$ must be at the same time replaced by $\varphi^{(2)*\mathrm{T}}$; thus no new terms are obtained by interchanging $i$ and $j$. As before, terms obtained by reversing the sign of $\Lambda$ must also be added to the result. We finally obtain

$$\begin{aligned} H_2 = {} & f_{13} \bar{\phi}^{(1)} i\gamma_5 \varphi^{(2)} \phi^{(3)} + f_{24} \bar{\phi}^{(2)} i\gamma_5 \varphi^{(2)} \phi^{(4)} \\ & + f'_{13} \bar{\phi}^{(1)} i\gamma_5 \varphi^{(2)} \phi^{(3)\prime} + f'_{24} \bar{\phi}^{(2)} i\gamma_5 \varphi^{(2)} \phi^{(4)\prime} + \text{ h.c.} \end{aligned} \tag{12}$$

where

$$\phi^{(3)\prime} = \begin{pmatrix} \Sigma^+ \\ -\mathrm{Y}^0 \end{pmatrix}, \quad \phi^{(4)\prime} = \begin{pmatrix} -\mathrm{Z}^0 \\ \Sigma^- \end{pmatrix}. \tag{13}$$

An interaction Hamiltonian of the same type has been recently proposed by

the present author [5]) for weak $\pi$-interaction. This Hamiltonian may be obtained from (12) by the substitution

$$f_{ij} \to g_{ij}, \qquad f'_{ij} \to g'_{ij}, \qquad \phi^{(j)} \to \psi^{(j)} \quad \text{and} \quad \varphi^{(2)} \to \varphi^{(1)}.$$

Eq. (12) can also be written explicitly as

$$\begin{aligned} H_2 &= \frac{1}{\sqrt{2}}(f_{13}-f'_{13})(\bar{\mathrm{N}}^+\mathrm{K}^+ - \bar{\Xi}^0\tilde{\mathrm{K}}^0)i\gamma_5\Lambda \\ &+ \frac{1}{\sqrt{2}}(f_{24}-f'_{24})(\bar{\mathrm{N}}^0\mathrm{K}^0+\bar{\Xi}^-\mathrm{K}^-)i\gamma_5\Lambda \\ &+ \frac{1}{\sqrt{2}}(f_{13}+f'_{13})[(\bar{\mathrm{N}}^+\mathrm{K}^+-\bar{\Xi}^0\tilde{\mathrm{K}}^0)i\gamma_5\Sigma^0+\sqrt{2}(\bar{\mathrm{N}}^+\mathrm{K}^0+\bar{\Xi}^0\mathrm{K}^-)i\gamma_5\Sigma^+] \\ &+ \frac{1}{\sqrt{2}}(f_{24}+f'_{24})[(-\bar{\mathrm{N}}^0\mathrm{K}^0-\bar{\Xi}^-\mathrm{K}^-)i\gamma_5\Sigma^0+\sqrt{2}(\bar{\mathrm{N}}^0\mathrm{K}^+-\bar{\Xi}^-\tilde{\mathrm{K}})i\gamma_5\Sigma^-]+\text{h.c.} \end{aligned} \tag{14}$$

This should be compared with the second part of the interaction Hamiltonian obtained by Prentki and d'Espagnat which may be written down explicitly as follows:

$$\begin{aligned} H' &= g_5(\bar{\mathrm{N}}^+\mathrm{K}^+ + \bar{\mathrm{N}}^0\mathrm{K}^0)i\gamma_5\Lambda + g_6(-\bar{\Xi}^0\tilde{\mathrm{K}}^0+\bar{\Xi}^-\mathrm{K}^-)i\gamma_5\Lambda \\ &+ g_7[(\bar{\mathrm{N}}^+\mathrm{K}^+-\mathrm{N}^0\mathrm{K}^0)i\gamma_5\Sigma^0+\sqrt{2}\,\bar{\mathrm{N}}^+\mathrm{K}^0 i\gamma_5\Sigma^+ + \sqrt{2}\,\bar{\mathrm{N}}^0\mathrm{K}^+ i\gamma_5\Sigma^-] \\ &+ g_8[(-\bar{\Xi}^0\tilde{\mathrm{K}}^0-\bar{\Xi}^-\mathrm{K}^-)i\gamma_5\Sigma^0+\sqrt{2}\,\bar{\Xi}^0\mathrm{K}^- i\gamma_5\Sigma^+ - \sqrt{2}\,\bar{\Xi}^-\tilde{\mathrm{K}}^0 i\gamma_5\Sigma^-]+\text{h.c.} \end{aligned} \tag{15}$$

Comparing (14) and (15) we see that these two expressions will be the same if

$$\frac{1}{\sqrt{2}}(f_{13}-f'_{13}) = \frac{1}{\sqrt{2}}(f_{24}-f'_{24}) = g_5 = g_6 \tag{16}$$

$$\frac{1}{\sqrt{2}}(f_{13}+f'_{13}) = \frac{1}{\sqrt{2}}(f_{24}+f'_{24}) = g_7 = g_8. \tag{17}$$

The assumption that the interaction Hamiltonian should be of the form (1) means physically that the interaction is charge independent in the original sense of Kemmer [6]). This means, in particular, that the interaction is independent of the charge states of $\psi^{(j)}$ or $\phi^{(j)}$. This charge independence should not be confused with charge symmetry or charge invariance which imply invariance under reflection or rotation in isobaric space. For instance, Hamiltonian (15) will not represent a charge independent K-interaction if $g_5 \neq g_6$, $g_7 \neq g_8$. On the other hand, charge independence does not imply any symmetry between the pairs $(\Sigma^+, \Sigma^-)$, $(\mathrm{N}^+, \mathrm{N}^0)$ and $(\Xi^0, \Xi^-)$; to ensure these symmetries, conditions (7), (16) and (17) have to be introduced.

Besides the assumption that the interaction Hamiltonian should be of the form (1), the following two rules have also been introduced in the present theory: (i) the rule which prescribes how two-component spinors can be chosen from $\Psi^{(1)}$ and $\Psi^{(2)}$ for various interactions, and (ii) the rule which imposes the condition that for $\pi$-interactions, $\bar{\psi}^{(i)}$ and $\psi^{(j)}$ appearing in the same term should have the same values of $i$ and $j$, whereas for K-interactions,

$\tilde{\phi}^{(i)}$ and $\phi^{(j)}$ should have different values of $i$ and $j$. Rule (ii) is directly responsible for the selection rule $\Delta S = 0$.

We shall now discuss in more detail the consequence of rule (i). We first consider $\psi^{(1)}$ given by (3). When the interaction is charge independent, the interaction with $\pi$-mesons will not produce any mass difference between $N^+$ and $N^0$. The observed mass difference between $N^+$ and $N^0$ is usually ascribed to electromagnetic interaction as the electromagnetic field interacts differently with $N^+$ and $N^0$. From our foregoing result we see that a mass difference can also be produced by interaction with K-mesons if (16) and (17) are not strictly satisfied. The approximate equality of masses of $N^+$ and $N^0$ shows that conditions (16) and (17) are indeed correct to a very good approximation. On the other hand, if now we consider the spinor $\phi^{(2)}$ defined in (9), we find that the difference in mass between $N^0$ and $\Xi^-$ must be due to the fact that $\pi$-mesons interact differently with $N^0$ and $\Xi^-$. Therefore the strength of interaction of $\pi$-mesons with various baryons cannot be the same. If we assume that the large mass differences among baryons are all due to $\pi$-interactions, then we find that in order to reproduce the observed mass spectrum the following relation must be satisfied:

$$f_1 < f_3 - f'_3 < f_3 + f'_3 < f_2 \tag{18}$$

and

$$f_{13} = f_{24}, \quad f'_{13} = f'_{24} = 0 \qquad (\text{i.e. } g_5 = g_6 = g_7 = g_8)$$

or

$$f'_{13} = f'_{24}, \quad f_{13} = f_{24} = 0 \qquad (\text{i.e. } g_5 = g_6 = -g_7 = -g_8).$$

This is just opposite to the recent suggestion of Gell-Mann which requires that the interaction with $\pi$-mesons should be universal and that the interaction with K-mesons should be responsible for the mass differences of various baryons. In the present theory the suggestion of Gell-Mann cannot be made to agree with the experimental results.

An alternative possibility is to put $f'_3 = 0$. Then neither $\pi$-interaction nor K-interaction is universal. The $\pi$-interaction will be responsible for the mass differences of N, $\Sigma$ and $\Xi$ particles, while K-interaction will be responsible for the mass difference between $\Lambda$ and $\Sigma$ particles. In other words, $\pi$-interaction will be responsible for the splitting of two doublet states of $\Psi^{(1)}$ and K-interaction will be responsible for splitting of the triplet and singlet states of $\Psi^{(2)}$.

The above investigation reflects the viewpoint that the matrix operators given in (2) will perhaps play a very profound and fundamental role in the future theory of elementary particles. The dimension $2 \times 2$ of these matrices is directly connected with the fundamental fact that no multiply charged elementary particles have ever been found in nature.

## References

1) Prentki and d'Espagnat, Nuclear Physics **1** (1956) 33
2) M. Gell-Mann, Phys. Rev. **92** (1953) 833
3) Nishijima, Proc. Theor. Phys. **10** (1953) 581
4) M. Gell-Mann, Phys. Rev. **106** (1957) 1296
5) N. Hu, JETP **34** (1958) 646; Padua-Venice Conference (1957)
6) N. Kemmer, Proc. Cambridge Phil. Soc. **34** (1938) 354

1.C *Nuclear Physics* **8** (1958) 91—105; © *North-Holland Publishing Co., Amsterdam*
Not to be reproduced by photoprint or microfilm without written permission from the publisher

# SUR LA DÉTERMINATION DES PREMIERS ÉTATS D'UN SYSTÈME DE FERMIONS DANS LE CAS DÉGÉNÉRÉ

CLAUDE BLOCH et JULES HOROWITZ
*Centre d'Études Nucléaires de Saclay, Gif-sur-Yvette (S. & O.)*

Reçu le 1$^{r}$ mai 1958

**Abstract:** The linked diagram expansion of the ground state energy and wave function of a system of fermions are extended to the case where the ground state of the unperturbed system is degenerate, as, for instance, in a nucleus with an incomplete shell. The state where all the complete shells are filled is taken as vacuum state. It is then shown, to all orders in the perturbation expansion, that the energy of the first levels is given by the sum of two terms. The first term, is the energy of the core alone and is given by a linked diagram expansion of the usual form. The second term is the energy of the particles outside the core. It is obtained by solving an eigenvalue problem in the space of the degenerate unperturbed wave functions. The corresponding eigen-functions are given by linked diagram expansions very similar with the usual ones. A few generalizations of the method, and its relation to the Brillouin-Wigner perturbation method are discussed.

## 1. Introduction

Le développement de l'énergie de l'état fondamental d'un système de particules en une somme de termes relatifs à l'ensemble des diagrammes connexes n'est pas sous sa forme habituelle [1–4]), applicable lorsque l'état fondamental du système sans interaction est dégénéré. Cet état joue en effet dans la théorie le rôle d'état de référence (ou état du vide) et tous les raisonnements présentés dans les articles cités plus haut ne peuvent pas s'étendre lorsque celui-ci n'est pas défini d'une manière unique. On peut le voir en remarquant, par exemple, que la notion essentielle de diagramme connexe ou non-connexe n'est définie que par rapport à un état de référence donné, et change lorsqu'on change celui-ci.

Si la dégénérescence de l'état fondamental du système non- perturbé ne joue pas un rôle important dans l'étude de la matière nucléaire infinie, il n'en est pas de même dans le cas des noyaux réels finis. Le système non-perturbé est alors constitué par le modèle des couches et son état fondamental sera dégénéré chaque fois que le noyau comportera une couche incomplète. L'un des problèmes essentiels de la théorie est dans ce cas la détermination de la manière dont les interactions lèvent la dégénérescence. La résolution de ce problème donne les énergies, spins et parités de l'état fondamental et généralement aussi des premiers états excités du noyau.

La méthode proposée ici repose sur un traitement différent des états des couches complètes et des états de la couche incomplète. Le traitement des états des couches complètes est le même que dans le cas non-dégénéré. Il conduit pour la contribution correspondante à l'énergie de l'état, à une expression explicite sous la forme d'un développement dont les dénominateurs ne contiennent que les énergies non-perturbées. Pour les états de la couche incomplète, on utilise, au contraire, une méthode du type de Brillouin-Wigner [5]) (l'analogie sera précisée au paragraphe 5). La contribution correspondante à l'énergie de l'état est alors donnée implicitement par la résolution d'une équation se présentant sous la forme d'un développement où les dénominateurs contiennent l'énergie vraie de l'état.

Nous allons montrer qu'on peut, tout au moins formellement, séparer rigoureusement à tous les ordres les contributions des deux sortes d'états.

Dans le cas d'un système très grand, la méthode de Brillouin-Wigner présente le défaut de ne pas conduire à une mise en évidence simple de la dépendance de l'énergie de liaison par rapport au volume [1]). Cet inconvénient n'apparaît pas dans la méthode proposée ici, car la méthode de Brillouin-Wigner n'est appliquée qu'à un petit nombre d'états au voisinage de la surface de Fermi. La plus grande partie de l'énergie de liaison fournie par le cœur est donnée par une expression explicite qui est bien proportionnelle au volume du système.

## 2. Formalisme Général

Nous utiliserons le formalisme de la seconde quantification. Les indices $m, n, \ldots$ serviront à énumérer un ensemble complet d'états des nucléons se déplaçant indépendamment dans un certain potentiel moyen. Les énergies de ces états seront désignées par $\varepsilon_m, \ldots$, et nous appellerons $\eta_m^+, \eta_m, \ldots$ les opérateurs de création et d'annihilation dans les états de particules indépendantes.

Soit $E_0$ la valeur propre la plus basse de l'Hamiltonien $H_0$ du système de $A$ particules indépendantes. Lorsque cette valeur propre n'est pas dégénérée, on fait jouer à l'état correspondant le rôle d'*état du vide*. Dans le cas où elle est dégénérée, nous ferons jouer ce rôle à *l'état non-dégénéré obtenu en remplissant complètement tous les niveaux de particules indépendantes dont l'énergie est inférieure à une énergie donnée* $\varepsilon^c$. On prendra en principe une énergie $\varepsilon^c$ tout juste inférieure ou tout juste supérieure à l'énergie $\varepsilon^F$ de la couche incomplète (nous indiquerons toutefois au paragraphe 5 une généralisation possible de ce choix). Le „*cœur*" ainsi défini sera alors constitué par les nucléons remplissant entièrement soit les couches complètes du noyau, soit l'ensemble des couches complètes et de la couche incomplète. Le nombre $A^c$ des nucléons du cœur n'étant pas égal à $A$, il faut pour former les états d'énergie $E_0$ du noyau soit ajouter $A^P = A - A^c$ particules au cœur,

soit créer dans celui-ci $A^T = A^c - A$ trous, suivant qu'on a choisi $\varepsilon^c < \varepsilon^F$ ou $\varepsilon^c > \varepsilon^F$. Les deux cas se traitant d'une manière tout à fait parallèle, nous raisonnerons, pour fixer les idées, sur le système cœur plus couche incomplète ($\varepsilon^c < \varepsilon^F$).

Nous désignerons par $|0\rangle$ la fonction d'onde normalisée du cœur et par $E_0^c$ son énergie:

$$(H_0 - E_0^c)|0\rangle = 0. \tag{1}$$

Nous utiliserons dans l'espace $\Omega_0$ des fonctions d'énergie $E_0$:

$$E_0 = E_0^c + E_0^P, \quad E_0^P = A^P \varepsilon^F, \tag{2}$$

du noyau de masse $A$, la base constituée par les fonctions d'onde

$$|\gamma\rangle_0 = \eta_m^+ \eta_n^+ \ldots |0\rangle, \quad (\varepsilon_m = \varepsilon_n = \ldots = \varepsilon^F), \tag{3}$$

*obtenues en faisant agir sur la fonction d'onde du cœur tous les produits de $A^P = A - A^c$ opérateurs de création de nucléons dans des états de la couche incomplète.* Nous désignerons par $|\gamma\rangle_0, |\gamma'\rangle_0, \ldots$ les $g$ fonctions orthonormales ainsi définies †.

Nous nous appuierons, comme dans le cas non-dégénéré [4]) sur les propriétés des opérateurs

$$G(\varepsilon) = \frac{1}{\varepsilon - H}, \qquad U(\beta) = e^{\beta H_0} e^{-\beta H}, \tag{4}$$

où

$$H = H_0 + V \tag{5}$$

est l'Hamiltonien du système. Ces deux opérateurs sont liés par la transformation

$$U(\beta) = \frac{1}{2\pi i} \int_C e^{\beta(H_0 - \varepsilon)} G(\varepsilon) d\varepsilon, \tag{6}$$

où le contour C se compose d'une parallèle à l'axe réel au-dessous de l'axe réel, parcourue dans le sens croissant et d'une parallèle au-dessus de l'axe réel, parcourue dans le sens décroissant.

Nous indiquerons au paragraphe suivant la manière de construire les développements des éléments de matrice de $U(\beta)$ pris entre les fonctions de la base $|\gamma\rangle_0$ définie par (3). Par combinaison linéaire de ceux-ci, on peut déterminer les éléments de matrice de $U(\beta)$ pris entre n'importe quelles fonctions de $\Omega_0$. Nous allons maintenant montrer comment l'étude du comportement asymptotique pour $\beta \to +\infty$ des éléments de matrice de $U(\beta)$ pris entre certaines fonctions de $\Omega_0$ permet, tout au moins en principe, de déterminer $g$ valeurs propres du noyau considéré.

† Cette représentation des fonctions de base dans le cas dégénéré a aussi été utilisée par J. Goldstone [4]).

Nous partirons pour cela du développement formel de $U(\beta)$

$$U(\beta) = e^{\beta H_0} \sum_n |n\rangle e^{-\beta E_n} \langle n|, \tag{7}$$

où les $|n\rangle$ et $E_n$ désignent l'ensemble complet des fonctions et des valeurs propres de $H$. De cet ensemble, nous allons extraire $g$ fonctions et valeurs propres $|\alpha\rangle$ et $E_\alpha$ de $H$, de la manière suivante:

$|1\rangle$ sera la fonction d'onde de l'état fondamental du noyau. Nous désignerons par $|1\rangle_0$ sa projection sur l'espace $\Omega_0$;

$|2\rangle$ sera la fonction d'onde d'énergie la plus basse possible dont la projection $|2\rangle_0$ sur $\Omega_0$ soit *linéairement indépendante de* $|1\rangle_0$;

$|3\rangle$ sera la fonction d'onde d'énergie la plus basse possible dont la projection $|3\rangle_0$ sur $\Omega_0$ soit *linéairement indépendante de* $|1\rangle_0$ et $|2\rangle_0$, et ainsi de suite.

Nous obtiendrons bien ainsi $g$ fonctions $|\alpha\rangle$ en général. Nous désignerons par $|\alpha\rangle_0$ leurs projections sur $\Omega_0$. Ces projections étant linéairement indépendantes on peut leur associer $g$ vecteurs $|\tilde{\alpha}\rangle_0$ de manière à former un *système biorthogonal* [7]), c'est à dire tel que

$${}_0\langle\alpha|\tilde{\alpha}'\rangle_0 = \delta_{\alpha\alpha'}. \tag{8}$$

Si on forme maintenant l'élément diagonal ${}_0\langle\tilde{\alpha}|U(\beta)|\tilde{\alpha}\rangle_0$ de l'expression (7), on voit que dans la somme qui figure au second membre, le terme dont l'énergie est la plus basse est celui qui correspond à la valeur propre $E_\alpha$. On a par conséquent

$$\lim_{\beta \to +\infty} {}_0\langle\tilde{\alpha}|U(\beta)|\tilde{\alpha}\rangle_0 = e^{-\beta \Delta E_\alpha}, \tag{9}$$

où nous avons posé

$$\Delta E_\alpha = E_\alpha - E_0. \tag{10}$$

Inversement, si nous pouvons trouver un certain nombre (qui ne pourra pas dépasser $g$) de fonctions de $\Omega_0$, $|\tilde{\alpha}\rangle_0$ telles que la relation (9) soit vérifiée avec des $\Delta E_\alpha$ *différents*, nous aurons déterminé autant de valeurs propres du noyau considéré.

## 3. Développement de $U(\beta)$ et Calcul des Valeurs Propres

Les développements en puissances de l'interaction des opérateurs (4) s'écrivent:

$$\begin{aligned} G(\varepsilon) &= \frac{1}{\varepsilon - H_0} \sum_{p=0}^{\infty} \left( V \frac{1}{\varepsilon - H_0} \right)^p, \\ U(\beta) &= \sum_{p=0}^{\infty} (-)^p \int_{\beta > u_1 > \cdots > u_p > 0} du_1 du_2 \ldots du_p V(u_1) V(u_2) \ldots V(u_p), \end{aligned} \tag{11}$$

où

$$V(u) = e^{uH_0} V e^{-uH_0}. \tag{12}$$

En remplaçant dans ces développements $V$ par son expression en fonction des opérateurs $\eta$ et $\eta^+$:

$$V = \tfrac{1}{2} \sum_{rsmn} \langle rs|v|mn\rangle \eta_r^+ \eta_s^+ \eta_n \eta_m + \ldots, \tag{13}$$

on est conduit après application du théorème de Wick [8]) à représenter chacun des termes obtenus par un diagramme.

Précisons que dans l'application du théorème de Wick sur les opérateurs ordonnés, il faut, conformément à la définition du vide introduite au paragraphe précédent considérer les opérateurs $\eta_n$ et $\eta_n^+$ *relatifs à des états du „cœur" comme créant et annihilant des trous, respectivement.* Les opérateurs $\eta_n$ et $\eta_n^+$ *relatifs aux autres états, au contraire, annihilent et créent des particules, respectivement.* Sur les diagrammes, les lignes ayant des flèches dirigées dans le sens des temps décroissants seront donc relatives toujours à des états du cœur, alors que les lignes dirigées vers les temps croissants se rapporteront aux autres états.

Nous allons d'abord considérer les éléments de matrice de $U(\beta)$ pris entre les fonctions $|\gamma\rangle_0$ définies par (3). Les diagrammes intervenant dans le calcul de ${}_0\langle\gamma|U(\beta)|\gamma'\rangle_0$ sont ceux qui *se terminent du côté des temps croissants par les lignes ouvertes relatives aux états m, n, ... de la couche incomplète intervenant dans l'expression* (4) *de* $|\gamma\rangle_0$ *et du côté des temps décroissants par les lignes m', n' ... relatives à l'état* $|\gamma'\rangle_0$ (fig. 1).

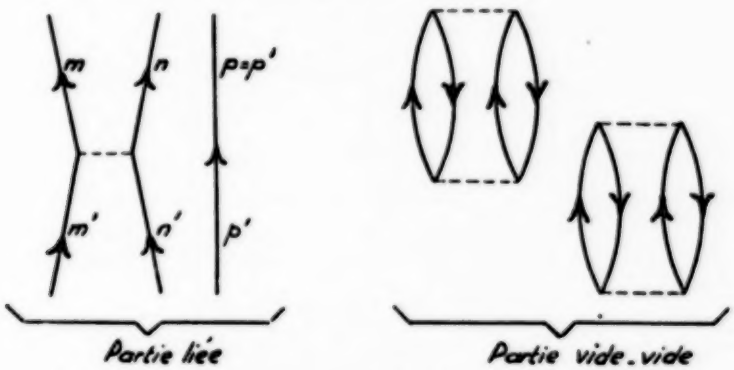


Fig. 1. Un diagramme pour le calcul de ${}_0\langle\gamma|U(\beta)|\gamma'\rangle_0$.

Le diagramme le plus général se compose d'une *partie liée* (la partie qu'on peut atteindre en suivant les lignes du diagramme lorsqu'on entre dans celui-ci par toutes les lignes ouvertes) et d'une *partie vide-vide.* Ces deux parties peuvent être elles-mêmes formées de plusieurs parties connexes. La sommation des parties vide-vide non-connexes se fait comme dans le cas non-dégénéré grâce à la formule exponentielle [4]), et on peut écrire

$${}_0\langle\gamma|U(\beta)|\gamma'\rangle_0 = {}_0\langle\gamma|U(\beta)|\gamma'\rangle_{0L}\, e^{\langle 0|U(\beta)|0\rangle_c}, \tag{14}$$

où le premier facteur du second membre désigne *la somme de tous les diagram-*

*mes liées* (c'est-à-dire sans partie vide-vide) et où l'argument de la fonction exponentielle consiste en la *somme de tous les diagrammes vide-vide connexes.*

Pour calculer la limite pour $\beta \to +\infty$ de (14), il suffit de calculer séparément la limite de chaque facteur. La limite de $\langle 0|U(\beta)|0\rangle_c$ se calcule exactement comme dans le cas non-dégénéré, et on trouve

$$\lim_{\beta \to +\infty} \langle 0|U(\beta)|0\rangle_c = F'(E_0^c) - \beta \Delta E^c, \tag{15}$$

où

$$F(\varepsilon) = \langle 0|V \sum_{p=0}^{\infty} \left(\frac{1}{\varepsilon - H_0} V\right)^p |0\rangle_c, \tag{16}$$

et où

$$\Delta E^c = F(E_0^c) \tag{17}$$

est la *différence entre l'énergie vraie et l'énergie non-perturbée $E_0^c$ du cœur.* La présence des particules de la couche incomplète n'intervient pas, en effet, dans le calcul de $\Delta E^c$, sauf, éventuellement dans le choix du potentiel moyen servant à définir les fonctions de base des particules indépendantes.

Pour calculer la limite du premier facteur de (14), nous partirons de la relation (6) écrite sous la forme

$${}_0\langle \gamma|U(\beta)|\gamma'\rangle_{0L} = \frac{1}{2\pi i} \int_C e^{\beta(E_0 - \varepsilon)} {}_0\langle \gamma|G(\varepsilon)|\gamma'\rangle_{0L} \, d\varepsilon, \tag{18}$$

et nous chercherons parmi les singularités de la fonction à intégrer celle qui a l'énergie la plus faible.

Considérons un terme d'ordre donné dans le développement de ${}_0\langle \gamma|G(\varepsilon)|\gamma'\rangle_{0L}$. Ses singularités possibles sont les énergies des états non-perturbés du noyau étudié. La singularité ayant l'énergie la plus faible est le pôle $\varepsilon = E_0$. Mais ici, contrairement au cas non-dégénéré, ce pôle peut être d'un ordre quelconque supérieur à deux, car des états intermédiaires d'énergie $E_0$ peuvent apparaître à n'importe quel endroit d'un diagramme lié. Par exemple, il suffira que sur le diagramme de la fig. 2, les états $m'$, $n', \ldots m'', n'', \ldots$ appartiennent à la couche incomplète, pour qu'on ait deux états intermédiaires d'énergie $E_0$.

Nous définirons alors une matrice $\Phi(\varepsilon)$ de l'espace $\Omega_0$ par la relation

$${}_0\langle \gamma|\Phi(\varepsilon)|\gamma'\rangle_0 = {}_0\langle \gamma|V \sum_{p=0}^{\infty} \left(\frac{Q_0}{\varepsilon - H_0} V\right)^p |\gamma'\rangle_{0L}, \tag{19}$$

où $Q_0$ est *l'opérateur de projection en dehors de l'espace $\Omega_0$.* Cet opérateur assure qu'aucun état d'énergie $E_0$ n'interviendra dans le développement (19). La matrice $\Phi(\varepsilon)$ n'a donc pas de singularité pour $\varepsilon = E_0$.

Le diagramme lié le plus général peut être décomposé (fig. 2) en un certain nombre de parties comprises entre des états intermédiaires d'énergie $E_0$, mais à l'intérieur desquelles aucun de ceux-ci n'intervient. On peut alors

écrire

$$
\begin{aligned}
{}_0\langle\gamma|G(\varepsilon)|\gamma'\rangle_{0L} &= \sum_{p=0}^{\infty} \frac{1}{(\varepsilon-E_0)^{p+1}}\, {}_0\langle\gamma|\Phi(\varepsilon)^p|\gamma'\rangle_0 \\
&= {}_0\langle\gamma|\, \frac{1}{\varepsilon-E_0-\Phi(\varepsilon)}\, |\gamma'\rangle_0 .
\end{aligned}
\tag{20}
$$

Ceci nous conduit à considérer le problème de valeurs propres à $g$ dimensions dans $\Omega_0$

$$
[\varepsilon-E_0-\Phi(\varepsilon)]|\rangle_0 = 0. \tag{21}
$$

Nous montrerons en appendice que les valeurs propres de (21) sont toutes réelles.

Désignons par

$$
\varepsilon = E_\alpha{}^{\mathrm{P}} = E_0+\Delta E_\alpha{}^{\mathrm{P}} \quad \text{et} \quad |\alpha\rangle_0
$$

*un ensemble de solutions de* (21) *ayant la propriété suivante*:

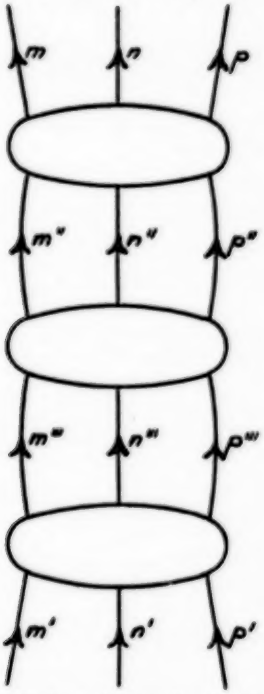


Fig. 2. Les états intermédiaires d'énergie $E_0$ dans un diagramme lié.

*$E_1{}^{\mathrm{P}}$ est la valeur propre la plus petite;*

*$E_2{}^{\mathrm{P}}$ est la valeur propre la plus petite dont la fonction propre $|2\rangle_0$ est linéairement indépendante de $|1\rangle_0$;*

*$E_3{}^{\mathrm{P}}$ est la valeur propre la plus petite dont la fonction propre $|3\rangle_0$ est linéairement indépendante de $|1\rangle_0$ et $|2\rangle_0$; . . . et ainsi de suite.*

Nous montrerons en appendice qu'on peut toujours en principe (sous réserve de convergence) trouver $g$ solutions de (21) ayant cette propriété.

Les fonctions $|\alpha\rangle_0$ étant linéairement indépendantes, on peut trouver $g$

fonctions $|\bar{\alpha}\rangle_0$ de $\Omega_0$ formant avec elles un *système biorthogonal*, c'est-à-dire satisfaisant aux relations (8).

Cette manière de définir les $|\bar{\alpha}\rangle_0$ n'est pas la seule. Les raisonnements qui suivent s'appliquent aussi bien à des fonctions $|\bar{\alpha}\rangle_0$ définies ainsi:

$|\bar{1}\rangle_0$ est n'importe quelle fonction de $\Omega_0$ telle que ${}_0\langle 1|\bar{1}\rangle_0 = 1$;

$|\bar{2}\rangle_0$ est n'importe quelle fonction de $\Omega_0$ orthogonale à $|1\rangle_0$ telle que ${}_0\langle 2|\bar{2}\rangle_0 = 1$;

$|\bar{3}\rangle_0$ est n'importe quelle fonction de $\Omega_0$ orthogonale à $|1\rangle_0$ et $|2\rangle_0$ telle que ${}_0\langle 3|\bar{3}\rangle_0 = 1$ etc. . . .

Ceci permet, en particulier d'étendre les raisonnements au cas où pour une raison quelconque on ne pourrait déterminer *qu'un nombre de solutions de* (21) *inférieur à* $g$.

On remarquera que les fonctions $|\bar{\alpha}\rangle_0$ ne servent qu'aux besoins de la démonstration. Elles ne figurent pas dans les résultats finaux qui ne font intervenir que les fonctions $|\alpha\rangle_0$ (voir les équations (21), (29) et (33)).

Nous allons maintenant étudier les singularités des fonctions analytiques de $\varepsilon$ constituées par les éléments de matrice

$$ {}_0\langle\bar{\alpha}'|\frac{1}{\varepsilon - E_0 - \Phi(\varepsilon)}|\bar{\alpha}\rangle_0 \tag{22}$$

pris entre deux des fonctions $|\bar{\alpha}\rangle_0$ et $|\bar{\alpha}'\rangle_0$ qui viennent d'être définies. Nous allons montrer que:

a) *les éléments de matrices* (22) *n'ont pas de singularité en dehors de l'axe réel;*

b) *les éléments non-diagonaux n'ont aucune singularité pour des énergies inférieures ou égales à la plus grande des valeurs propres* $E_\alpha^{\,P}$ *et* $E_{\alpha'}^{\,P}$.

c) *les éléments diagonaux* ($\alpha = \alpha'$) *n'ont pas de singularité pour des énergies inférieures à* $E_\alpha^{\,P}$. *Ils ont un pôle simple pour* $\varepsilon = E_\alpha^{\,P}$.

Pour une valeur donnée de $\varepsilon$ où $\Phi(\varepsilon)$ est régulière, $\varepsilon - E_0 - \Phi(\varepsilon)$ est une matrice de dimension finie $g$. Une telle matrice possède toujours un inverse bien défini lorsque l'équation (21) n'a pas de solution autre que la solution triviale $|\rangle_0 = 0$. Les seules singularités possibles des éléments de matrice (22) sont donc les valeurs réelles de $\varepsilon$ pour lesquelles, ou bien $\Phi(\varepsilon)$ aura une singularité, ou bien l'équation (21) aura une solution non-triviale.

Pour une valeur réelle de $\varepsilon$, la matrice $\varepsilon - E_0 - \Phi(\varepsilon)$ est hermitique et on peut, en désignant par $|k, \varepsilon\rangle_0$ et $\lambda_k(\varepsilon)$ ses fonctions et valeurs propres l'écrire sous la forme

$$ \varepsilon - E_0 - \Phi(\varepsilon) = \sum_{k=1}^{g} |k, \varepsilon\rangle_0 \lambda_k(\varepsilon) {}_0\langle k, \varepsilon| . \tag{23}$$

Cette diagonalisation permet d'écrire (22) sous la forme

$$ {}_0\langle\bar{\alpha}'|\frac{1}{\varepsilon - E_0 - \Phi(\varepsilon)}|\bar{\alpha}\rangle_0 = \sum_{k=1}^{g} {}_0\langle\bar{\alpha}'|k, \varepsilon\rangle_0 \frac{1}{\lambda_k(\varepsilon)} {}_0\langle k, \varepsilon|\bar{\alpha}\rangle_0 . \tag{24}$$

Si le système étudié comprend un nombre fini de particules, $\Phi(\varepsilon)$ et par conséquent les fonctions $\lambda_k(\varepsilon)$ n'ont pas de singularités autres que des pôles. Ces points ne sont pas des singularités pour (24).

Il nous reste à étudier le comportement des éléments de matrice (22) au voisinage des valeurs propres de (21). Pour ces valeurs de $\varepsilon$, l'un des $\lambda_k(\varepsilon)$ s'annulle. Nous montrerons dans l'appendice que les $\lambda_k(\varepsilon)$ *n'ont que des zéros simples.* Le développement (24) montre alors *qu'une valeur propre de l'équation* (21) *ne sera un pôle de l'élément de matrice* (22) *que si la fonction propre correspondante n'est orthogonale ni à* $|\tilde{\alpha}\rangle_0$ *ni à* $|\tilde{\alpha}'\rangle_0$. Sinon, en effet, l'un des produits scalaires ${}_0\langle k, \varepsilon|\tilde{\alpha}\rangle_0$ ou ${}_0\langle k, \varepsilon|\tilde{\alpha}'\rangle_0$ au moins présenterait un zéro pour la valeur considérée de $\varepsilon$, ce qui ferait disparaître le pôle simple introduit par le zéro de $\lambda_k(\varepsilon)$.

Cette propriété, et la manière dont les vecteurs $|\tilde{\alpha}\rangle_0$ ont été choisis entraînent immédiatement pour conséquences les propriétés a) et b). Tout vecteur $|\tilde{\alpha}\rangle_0$ est en effet orthogonal aux vecteurs propres de (21) correspondant à des valeurs propres plus petites que $E_\alpha^{\mathrm{P}}$.

Calculons enfin le résidu de l'élément diagonal (22) pour $\varepsilon = E_\alpha^{\mathrm{P}}$. En désignant par l'indice 1 la valeur propre $\lambda(\varepsilon)$ qui est nulle au point $E_\alpha^{\mathrm{P}}$ on a au voisinage de cette valeur

$$\begin{aligned} \lambda_1(\varepsilon) &= (\varepsilon - E_\alpha^{\mathrm{P}})\lambda'_1(E_\alpha^{\mathrm{P}}) + \ldots, \\ |\mu, \varepsilon\rangle_0 &= a|\alpha\rangle_0 + \ldots; \end{aligned} \tag{25}$$

où $a$ est une constante de normalisation.

En reportant dans (24) on obtient

$${}_0\langle\tilde{\alpha}|\frac{1}{\varepsilon - E_0 - \Phi(\varepsilon)}|\tilde{\alpha}\rangle_0 = \frac{|a|^2}{(\varepsilon - E_\alpha^{\mathrm{P}})\lambda'_1(E_\alpha^{\mathrm{P}})} + \ldots,$$

où les termes omis sont finis. En dérivant la relation (23) pour $\varepsilon = E_\alpha^{\mathrm{P}}$ et en prenant l'élément de matrice diagonal pour la fonction $|\alpha\rangle_0$ on obtient

$${}_0\langle\alpha|1 - \Phi'(E_\alpha^{\mathrm{P}})|\alpha\rangle_0 = \frac{\lambda'_1(E_\alpha^{\mathrm{P}})}{|a|^2}.$$

Les deux dernières relations conduisent à l'expression

$${}_0\langle\tilde{\alpha}|\frac{1}{\varepsilon - E_0 - \Phi(\varepsilon)}|\tilde{\alpha}\rangle_0 = \frac{1}{(\varepsilon - E_\alpha^{\mathrm{P}})\,{}_0\langle\alpha|1 - \Phi'(E_\alpha^{\mathrm{P}})|\alpha\rangle_0} + \ldots. \tag{26}$$

valable pour $\varepsilon$ voisin de $E_\alpha^{\mathrm{P}}$.

Les considérations qui précèdent permettent maintenant de trouver la valeur asymptotique pour $\beta \to +\infty$ des éléments diagonaux de l'opérateur (18) calculés pour les fonctions $|\tilde{\alpha}\rangle_0$. D'après (18), (20) et (26) on a

$$\lim_{\beta \to +\infty} {}_0\langle\tilde{\alpha}|U(\beta)|\tilde{\alpha}\rangle_{0\mathrm{L}} = \frac{e^{-\beta \Delta E_\alpha^{\mathrm{P}}}}{{}_0\langle\alpha|1 - \Phi'(E_\alpha^{\mathrm{P}})|\alpha\rangle_0}. \tag{27}$$

En rapprochant enfin (9) des relations (14), (15) et (27) on voit que les quantités $E_0+\Delta E_\alpha$ où

$$\Delta E_\alpha = \Delta E^c + \Delta E_\alpha{}^P \tag{28}$$

sont des valeurs propres. Nous obtenons également la relation

$${}_0\langle\alpha|1-\Phi'(E_\alpha{}^P)|\alpha\rangle_0 = e^{F'(E_0{}^c)} \tag{29}$$

qui fixe le coefficient de normalisation des fonctions $|\alpha\rangle_0$. Celles-ci sont en effet définies à la normalisation près par le problème de valeurs propres (21). La normalisation déterminée par la relation (29) correspond à la condition que les $|\alpha\rangle_0$ soient les projections sur $\Omega_0$ des fonctions propres $|\alpha\rangle$ de $H$ normalisées à l'unité.

En résumé, une valeur propre de $H$ est la somme de $E_0$ et de deux contributions: *la contribution du „cœur"* $\Delta E^c$ donnée explicitement par les formules (16) et (17), et la *contribution des particules de la couche incomplète* $\Delta E_\alpha{}^P$ qui s'obtient en résolvant le problème de valeurs propres (21).

## 4. Le Calcul des Fonctions Propres

Pour construire les fonctions propres relatives aux valeurs propres déterminées au paragraphe précédent, nous partirons de la relation

$$|\alpha\rangle = \lim_{\beta\to+\infty} e^{\beta(E_\alpha-H_0)}U(\beta)|\tilde{\alpha}\rangle_0 \tag{30}$$

qui résulte du développement (7) et de la définition des fonctions non-perturbées $|\tilde{\alpha}\rangle_0$ et des valeurs propres $E_\alpha$ qui leur correspondent.

Le calcul de $U(\beta)|\tilde{\alpha}\rangle_0$ fait intervenir les diagrammes qui se terminent vers les temps décroissants par $A^P$ lignes relatives à des états de la couche incomplète, et vers les temps croissants d'une manière quelconque. Le diagramme le plus général de ce type comprend une partie vide-vide composée de plusieurs parties connexes. La sommation de ces parties vide-vide se fait comme dans le calcul des valeurs propres et conduit au même facteur exponentiel que dans la relation (14). En tenant compte de (15), l'expression (30) prend alors la forme

$$|\alpha\rangle = \lim_{\beta\to+\infty} e^{\beta(E_\alpha-\Delta E^c-H_0)+F'(E_0{}^c)}U(\beta)|\tilde{\alpha}\rangle_{0L},$$

où le dernier facteur résulte maintenant de la sommation des *diagrammes liés* exclusivement. En utilisant la transformation (6), et en remplaçant $E_\alpha$ par $\Delta E^c+E_\alpha{}^P$, l'expression de $|\alpha\rangle$ devient

$$|\alpha\rangle = \lim_{\beta\to+\infty}\frac{1}{2\pi i}\int_C e^{\beta(E_\alpha{}^P-\varepsilon)+F'(E_0{}^c)}G(\varepsilon)|\tilde{\alpha}\rangle_{0L}\,d\varepsilon. \tag{31}$$

Dans chaque terme du développement de $G(\varepsilon)|\tilde{\alpha}\rangle_{0L}$, un certain nombre d'états intermédiaires d'énergie $E_0$ peuvent apparaître. La sommation des

éléments de matrice de $G(\varepsilon)$ pris entre des états d'énergie $E_0$ se fait comme au paragraphe précédent, et conduit à la relation

$$G(\varepsilon)|\bar{\alpha}\rangle_{0L} = \sum_{\alpha'} \sum_{p=0}^{\infty} \left(\frac{Q_0}{\varepsilon - H_0} V\right)^p |\alpha'\rangle_{0L\,0}\langle\bar{\alpha}'| \frac{1}{\varepsilon - E_0 - \Phi(\varepsilon)} |\bar{\alpha}\rangle_0. \quad (32)$$

Nous avons utilisé ici la relation, valable pour tout système biorthogonal,

$$P_0 = \sum_{\alpha'} |\alpha'\rangle_{0\,0}\langle\bar{\alpha}'|,$$

où $P_0$ est l'opérateur de projection sur $\Omega_0$.

La relation (31) implique que le second membre a pour $\beta \to +\infty$ une limite finie. Pour cela il faut que la fonction $G(\varepsilon)|\bar{\alpha}\rangle_{0L}$ ait un pôle simple pour $\varepsilon = E_\alpha{}^P$ et aucune singularité aux énergies plus petites. Dans l'expression (32) le second facteur possède précisément ces propriétés ainsi qu'on l'a vu au paragraphe précédent. Il en résulte que le premier facteur est régulier pour toutes les valeurs de $\varepsilon$ inférieures ou égales à $E_\alpha{}^P$. En calculant alors le résidu de l'intégrale (31) pour $\varepsilon = E_\alpha{}^P$, on obtient, en tenant compte de (26) et (29),

$$|\alpha\rangle = \sum_{p=0}^{\infty} \left(\frac{Q_0}{E_\alpha{}^P - H_0} V\right)^p |\alpha\rangle_{0L}, \quad (33)$$

où, rappelons le, la sommation doit être étendue aux *diagrammes liés* seulement. Les fonctions $|\alpha\rangle_0$ et les énergies $E_\alpha{}^P$ qui doivent être introduites dans cette expression sont obtenues par résolution du problème de valeurs propres (21).

## 5. Généralisations

Le formalisme qui vient d'être décrit se prête à plusieurs généralisations immédiates.

Ainsi, on peut prendre un *cœur plus petit* (ou plus grand, dans le cas où le cœur comprend un nombre de particules supérieur à $A$) que nous l'avons indiqué. Les diagrammes liés se termineront alors par un nombre de lignes ouvertes plus grand. La contribution du cœur à l'énergie de liaison sera plus faible, alors que la contribution des particules extérieures au cœur sera augmentée.

Il est intéressant de considérer alors le cas extrême où on prend un *cœur inexistant*. Les trous disparaissent, et les diagrammes se composent tous de $A$ lignes dirigées dans le sens des temps croissants. Ils sont tous liés. Considérons pour simplifier un cas où l'état fondamental de $H_0$ est non-dégénéré et désignons par $|\rangle_0$ la fonction d'onde normalisée correspondante. La matrice $\Phi(\varepsilon)$ se réduit à un nombre pur,

$$\Phi(\varepsilon) = {}_0\langle| V \sum_{p=0}^{\infty} \left(\frac{Q_0}{\varepsilon - H_0} V\right)^p |\rangle_0.$$

La sommation est ici étendue à tous les diagrammes, et on a donc affaire à l'élément de matrice de l'opérateur complet. L'équation (21) s'écrit ici

$$\varepsilon - E_0 - \Phi(\varepsilon) = 0.$$

Cette équation est exactement celle à laquelle aboutit la *méthode de perturbation de Brillouin-Wigner* [5]) caractérisée par la présence de l'énergie véritable $\varepsilon$ dans les dénominateurs de la fonction $\Phi(\varepsilon)$.

On peut enfin envisager une autre généralisation lorsque le système non-perturbé comprend en plus des $g$ états d'énergie $E_0$, $g'$ états *quasi-dégénérés*, c'est-à-dire ayant une énergie voisine de $E_0$. Dans le but d'améliorer la convergence des développements, on peut alors inclure les $g'$ états quasi-dégénérés dans l'espace $\Omega_0$. La matrice $\Phi(\varepsilon)$ aura alors $g+g'$ dimensions, et l'équation aux valeurs propres (21) devra être écrite

$$[\varepsilon - H_0 - \Phi(\varepsilon)]|\rangle_0 = 0,$$

car les états de $\Omega_0$ n'ayant plus la même énergie on ne peut plus remplacer $H_0$ agissant sur ces états par $E_0$. A cette modification près, les raisonnements des paragraphes précédents s'étendent immédiatement.

## Appendice

Nous allons ici indiquer ou rappeler quelques propriétés de la matrice $\Phi(\varepsilon)$ et des matrices qui s'y rattachent. Ces propriétés généralisent certaines de celles que Wigner [9]) a établies pour les „fonctions $R$".

Nous considérerons ici des *matrices de dimension finie dont les éléments sont des fonctions méromorphes dans tout le plan complexe de la variable $\varepsilon$.*

La matrice $\Phi(\varepsilon)$, dans le cas d'un système de dimension finie satisfait à ces conditions, sous réserve, toutefois, que le développement qui la définit soit convergent, ce que nous admettrons.

Toute matrice finie $A(\varepsilon)$ peut être écrite sous la forme

$$A(\varepsilon) = a(\varepsilon) + i\alpha(\varepsilon), \tag{A.1}$$

où $a(\varepsilon)$ et $\alpha(\varepsilon)$ sont des matrices hermitiques. Nous nous intéresserons ici à des matrices $A(\varepsilon)$ telles que

$$\alpha(\varepsilon) = \operatorname{Im} A(\varepsilon) > 0^{\dagger} \quad \text{si} \quad \operatorname{Im}\varepsilon > 0,$$
$$\alpha(\varepsilon) = \operatorname{Im} A(\varepsilon) < 0 \quad \text{si} \quad \operatorname{Im}\varepsilon < 0.$$

Montrons d'abord que

*Th. I: La matrice $\Phi(\varepsilon)$ définie par* (19) *possède la propriété suivante:*

$$\operatorname{Im}\Phi(\varepsilon) \leqq 0, \quad \text{si} \quad \operatorname{Im}\varepsilon > 0,$$
$$\operatorname{Im}\Phi(\varepsilon) \geqq 0, \quad \text{si} \quad \operatorname{Im}\varepsilon < 0.$$

† Cette inégalité signifie que $\operatorname{Im} A(\varepsilon)$ est positive définie.

Le raisonnement qui suit est tout à fait semblable à celui que Van Hove [10]) a appliqué aux parties diagonales de la fonction de Green.

Pour deux valeurs $\varepsilon$ et $\varepsilon'$ quelconques on a

$$G(\varepsilon)-G(\varepsilon') = (\varepsilon'-\varepsilon)G(\varepsilon)G(\varepsilon'),$$

d'où

$$_0\langle\gamma|G(\varepsilon)-G(\varepsilon')|\gamma'\rangle_{0L} = (\varepsilon'-\varepsilon)\,{}_0\langle\gamma|G(\varepsilon)G(\varepsilon')|\gamma'\rangle_{0L}. \qquad (A.2)$$

Posons

$$A(\varepsilon) = \varepsilon-E_0-\Phi(\varepsilon),$$
$$B(\varepsilon) = \frac{1}{A(\varepsilon)}. \qquad (A.3)$$

Compte tenu de (20), nous pouvons alors écrire (A.2) sous la forme

$$B(\varepsilon)-B(\varepsilon') = B(\varepsilon)[\varepsilon'-\varepsilon+\Phi(\varepsilon)-\Phi(\varepsilon')]B(\varepsilon')$$
$$= (\varepsilon'-\varepsilon)_0\langle\gamma|G(\varepsilon)G(\varepsilon')|\gamma'\rangle_{0L}.$$

En multipliant cette relation à droite par $A(\varepsilon')$ et à gauche par $A(\varepsilon)$, on obtient

$$\Phi(\varepsilon)-\Phi(\varepsilon') = (\varepsilon-\varepsilon')[1-\sum_{\gamma\gamma'}A(\varepsilon)|\gamma\rangle_{00}\langle\gamma|G(\varepsilon)G(\varepsilon')|\gamma'\rangle_{0L\,0}\langle\gamma'|A(\varepsilon')].$$

En désignant par $P_0$ le projecteur sur l'espace $\Omega_0$ et par $Q_0$ le projecteur sur l'espace orthogonal à $\Omega_0$, nous pouvons écrire

$$_0\langle\gamma|G(\varepsilon)G(\varepsilon')|\gamma'\rangle_{0L} = {}_0\langle\gamma|G(\varepsilon)P_0G(\varepsilon')|\gamma'\rangle_{0L}+{}_0\langle\gamma|G(\varepsilon)Q_0G(\varepsilon')|\gamma'\rangle_{0L}.$$

Les diagrammes intervenant dans le calcul du premier terme se composent de deux parties liées relatives à $G(\varepsilon)$ et à $G(\varepsilon')$, respectivement. On a donc

$$_0\langle\gamma|G(\varepsilon)P_0G(\varepsilon')|\gamma'\rangle_{0L} = \sum_{\gamma''}{}_0\langle\gamma|G(\varepsilon)|\gamma''\rangle_{0L\,0}\langle\gamma''|G(\varepsilon')|\gamma'\rangle_{0L}$$
$$= {}_0\langle\gamma|B(\varepsilon)B(\varepsilon')|\gamma'\rangle_0.$$

D'où

$$\Phi(\varepsilon)-\Phi(\varepsilon') = -(\varepsilon-\varepsilon')[\sum_{\gamma\gamma'}A(\varepsilon)|\gamma\rangle_{00}\langle\gamma|G(\varepsilon)Q_0G(\varepsilon')|\gamma'\rangle_{0L\,0}\langle\gamma'|A(\varepsilon')].$$

En posant $\varepsilon' = \varepsilon^*$, le crochet devient visiblement une matrice hermitique positive semi-définie, ce qui entraîne le théorème I.

*Th. II*: *Les matrices* $A(\varepsilon)$ *et* $-B(\varepsilon)$ *définies par* (A.3) *satisfont à la condition* (A).

La propriété relative à $A(\varepsilon)$ est évidente. Elle entraîne immédiatement que l'équation (21) qui s'écrit avec les notations présentes

$$A(\varepsilon)|\rangle_0 = 0, \qquad (A.4)$$

où $\varepsilon$ n'est pas réel, n'a pas de solution autre que $|\rangle_0 = 0$. Il en résulte que $A(\varepsilon)$ a bien un inverse lorsque $\varepsilon$ n'est pas réel.

Posons

$$A = a+i\alpha, \quad B = b+i\beta.$$

En exprimant que

$$AB = BA = 1,$$

on obtient (entre autres) les relations

$$a\beta+\alpha b = 0, \quad ba-\beta\alpha = 1. \tag{A.5}$$

En multipliant la seconde relation à droite par $\beta$, la première à gauche par $b$, et en retranchant, on obtient

$$\beta = -b\alpha b-\beta\alpha\beta.$$

Il en résulte que $\beta \leqq 0$ puisque $\alpha > 0$ et que $b$ et $\beta$ sont hermitiques. Mais s'il existait un vecteur $|\rangle_0$ tel que $\beta|\rangle_0 = 0$, on aurait d'après (A.5) $\alpha b|\rangle_0 = 0$, c'est-à-dire $b|\rangle_0 = 0$ puisque $\alpha\rangle 0$. On aurait donc $B|\rangle_0 = 0$ ce qui contredit le fait que $B$ est l'inverse de $A$. On a donc bien $\beta\langle 0$, ce qu'il fallait établir.

Nous avons noté en passant que (A.4) n'avait pas de solution non- triviale pour $\varepsilon$ complexe. Autrement dit:

*Th. III*: *Les valeurs propres de l'équation* (21) *sont toutes réelles.*

La valeur moyenne ${}_0\langle|A(\varepsilon)|\rangle_0$ de la matrice $A(\varepsilon)$ pour tout vecteur $|\rangle_0$ est une fonction $R$. Nous avons alors les résultats suivants qu'il suffira de rappeler:

*Th. IV*: *Pour $\varepsilon$ réel, ${}_0\langle|A(\varepsilon)|\rangle_0$ est pour tout vecteur $|\rangle_0$ une fonction monotone croissante, ayant des poles simples à résidus négatifs situés sur l'axe réel.*

Soient $\lambda_k(\varepsilon)$ et $|k, \varepsilon\rangle_0$ une valeur propre et une fonction propre normalisée de $A(\varepsilon)$ pour $\varepsilon$ réel. On a

$$\frac{\mathrm{d}}{\mathrm{d}\varepsilon}\lambda_k(\varepsilon) = \frac{\mathrm{d}}{\mathrm{d}\varepsilon}{}_0\langle k, \varepsilon|A(\varepsilon)|k, \varepsilon\rangle_0 = {}_0\langle k, \varepsilon|\frac{\mathrm{d}}{\mathrm{d}\varepsilon}A(\varepsilon)|k, \varepsilon\rangle_0 > 0$$

d'après le théorème IV. D'où:

*Th. V*: *Pour $\varepsilon$ réel, les valeurs propres de $A(\varepsilon)$ sont des fonctions monotones croissantes.*

En particulier, les fonctions $\lambda_k(\varepsilon)$ n'ont que des *zéros simples*, car leurs dérivées sont partout positives et jamais nulles.

Ce théorème permet de démontrer le théorème suivant:

*Th. VI*: *Les fonctions propres de l'équation* (21) $A(\varepsilon)|\rangle_0 = 0$, *correspondant à des valeurs propres situées dans un intervalle réel $\varepsilon_1$, $\varepsilon_2$ à l'intérieur duquel $A(\varepsilon)$ est bornée, sont linéairement indépendantes.*

S'il n'en était pas ainsi, il existerait dans $\Omega_0$ un sous-espace $\Omega'_0$ de dimension $g'\langle g$ contenant $k(k\rangle g')$ vecteurs propres de $A(\varepsilon)|\rangle_0 = 0$. Soit alors $A^1(\varepsilon)$ la restriction de $A(\varepsilon)$ à l'espace $\Omega'_0$. C'est visiblement une matrice $R$ à $g'$ dimensions. Ses $g'$ fonctions propres sont donc des fonctions monotones croissantes, continues dans l'intervalle $\varepsilon_1$, $\varepsilon_2$ puisque $A(\varepsilon)$ y est bornée.

Elles ne peuvent pas avoir plus de $g'$ zéros. Ceci contredit le fait que l'équation $A^1(\varepsilon)|\rangle_0 = 0$ a évidemment les mêmes $k$ valeurs propres que l'équation de départ.

Ce théorème a pour conséquence immédiate la propriété suivante: *les fonctions propres de l'équation* (21) *correspondant à des valeurs propres inférieures au pôle de* $\Phi(\varepsilon)$ *ayant l'énergie la plus faible sont linéairement indépendantes.*

Cette propriété permet de repérer certaines des fonctions $|\alpha\rangle_0$ définies dans le texte, mais elle ne permet pas forcément de les repérer toutes. Nous n'avons pas trouvé de règle générale permettant de dire à l'avance quelles sont les valeurs propres de (21) qui donneront des fonctions propres linéairement indépendantes † mais on peut cependant affirmer que:

*Th. VII: L'équation* $A(\varepsilon)|\rangle_0$ *a toujours g fonctions propres linéairement indépendantes.*

Supposons qu'il n'en soit pas ainsi, et appelons $\Omega'_0$ l'espace sous-tendu par les fonctions propres de (21). Soit $\Omega''_0$ le sous-espace de $\Omega_0$ orthogonal à $\Omega'_0$. La restriction à $\Omega''_0$ de la matrice $B(\varepsilon)$ inverse de $A(\varepsilon)$ n'aurait aucune singularité. Les éléments de matrice de $B(\varepsilon)$ étant par hypothèse des fonctions méromorphes de $\varepsilon$ devraient alors se réduire à des constantes. Pour $\varepsilon \to -\infty$, $B(\varepsilon) \to 0$. La restriction à $\Omega''_0$ de $B(\varepsilon)$ devrait donc être nulle quel que soit $\varepsilon$, ce qui est contraire avec le fait que $B(\varepsilon)$ est l'inverse d'une matrice finie partout sauf en des pôles isolés.

† En particulier, il n'est pas exact que les zéros ayant l'énergie la plus faible pour chacune des fonctions $\lambda_\alpha(\varepsilon)$ correspondent toujours à des fonctions propres linéairement indépendantes.

## Références


1) K. A. Brueckner, Phys. Rev. **100** (1955) 36
2) J. Goldstone, Proc. Roy. Soc. A **239** (1957) 267
3) N. M. Hugenholtz, Physica **23** (1957) 481
4) C. Bloch, Nuclear Physics **7** (1958) 451
5) Voir, par exemple, P. M. Morse et H. Feshbach, Methods of Theoretical Physics (Mc Graw-Hill Book Company, New-York, 1953) Ch. 9
6) J. Goldstone, Communication privée
7) C. Bloch, Nuclear Physics **6** (1958) 329
8) G. Wick, Phys. Rev. **80** (1950) 268
9) E. P. Wigner, Ann. of Math. **53** (1951) 36
10) L. van Hove, Physica **21** (1955) 901

8.B *Nuclear Physics* 8 (1958) 106—112: © *North-Holland Publishing Co., Amsterdam*
Not to be reproduced by photoprint or microfilm without written permission from the publisher

# DETERMINATION OF THE RELATIVE $\Sigma-\Lambda$ PARITY

GORDON FELDMAN and THOMAS FULTON
*The Johns Hopkins University, Baltimore, Maryland*†

Received 7 May 1958

**Abstract:** An investigation has been undertaken to determine whether there are definitive experiments which can determine, at least in principle, the relative $\Sigma-\Lambda$ parity. Two such methods are discussed. They are both based upon the parity-conserving electromagnetic decays of the $\Sigma^0$. The first involves the process $\Sigma^0 \to \Lambda^0+\gamma$. It is necessary to measure the decay asymmetries of the $\Lambda^0$ together with the direction of the photon polarization. The second method (also calculated recently by Feinberg) involves an accurate measurement of the branching ratio for the reactions $\Sigma^0 \to \Lambda^0+e^+ +e^-$ and $\Sigma^0 \to \Lambda^0+\gamma$. The appendix is concerned with some properties of a general vertex part.

## 1. Introduction

Since we may expect that larger numbers of strange particles will become available in the near future, it is of some interest to examine the possibility of determining various properties, such as the parities, of these particles. Since parity is not conserved in weak interactions, we cannot expect to determine the parities of all of the strange particles relative to the nucleon [1]). There are still certain relative parities which can be determined since the particles involved take part in strong or electromagnetic interactions. An example is the parity of the $\Sigma$ relative to the $\Lambda$ [2]). Pais and Treiman [2]) have recently suggested that the reaction $\Sigma^- + p \to \Lambda^0 + n$ (with the $\Sigma^-$ being captured from an S or P state) could be used to determine this relative parity. The experiment involves measuring the direction of the $\Lambda$ polarization through its decay asymmetry. In order that the $\Lambda$ be polarized, it is necessary that the incoming $\Sigma$ be produced polarized and retain its polarization in the process of slowing down. The determination of the relative parity, in the above experiment, also requires knowing whether the $\Sigma$ is captured from an S or P state.

It is the purpose of this note to examine other experiments which could, at least in principle, serve as a more definitive determination of the $\Sigma-\Lambda$ relative parity. The reactions which we discuss below involve the decay of the $\Sigma^0$ into the $\Lambda^0$. Although this is a decay process, only strong and electromagnetic interactions are involved, and parity is therefore conserved. Specifically we consider the reactions

† Supported in part by the U.S. Air Force through the OSR.

$$\Sigma^0 \to \Lambda^0 + \gamma, \tag{1}$$

and

$$\Sigma^0 \to \Lambda^0 + e^+ + e^-. \tag{2}$$

## 2. Polarization of the $\Lambda^0$ in $\Sigma^0$ Decay

First, let us examine the process (1). Let $\hat{\mathbf{q}}$ be a unit vector in the direction of the $\Lambda^0$ momentum in the $\Sigma^0$ rest system, $\boldsymbol{\varepsilon}^{(\alpha)}$ be the polarization of the $\gamma$-ray ($\boldsymbol{\varepsilon}^{(\alpha)} \cdot \hat{\mathbf{q}} = 0$) and $\mathbf{P}_\Sigma$ the polarization of the incoming $\Sigma^0$. The general expression, $S$, for the transition amplitudes in this process must be linear in $\boldsymbol{\varepsilon}^{(\alpha)}$. Expressed as a matrix in spin space, $S$ has the forms

$$S \text{ (even)} = A\boldsymbol{\sigma} \cdot (\boldsymbol{\varepsilon}^{(\alpha)} \times \hat{\mathbf{q}}), \tag{3}$$

$$S \text{ (odd)} = A'\boldsymbol{\sigma} \cdot \boldsymbol{\varepsilon}^{(\alpha)}, \tag{4}$$

where the components of $\boldsymbol{\sigma}$ are the Pauli spin matrices. $A$ and $A'$ are constants. Eq. (3) is the invariant form of the matrix element for an even $\Sigma$—$\Lambda$ relative parity and eq. (4) the form for an odd relative parity.

The expression for the $j$-th component of the polarization, $(\mathbf{P}_\Lambda)_j$, of the outgoing $\Lambda^0$ is given by [3])

$$(\mathbf{P}_\Lambda)_j = \frac{\mathrm{Tr}(\sigma_j S S^\dagger) + (\mathbf{P}_\Sigma)_i \mathrm{Tr}(\sigma_j S \sigma_i S^\dagger)}{\mathrm{Tr}(SS^\dagger) + (\mathbf{P}_\Sigma)_i \mathrm{Tr}(S\sigma_i S^\dagger)}. \tag{5}$$

This leads to

$$\mathbf{P}_\Lambda^{(\alpha)}(\text{even}) = -\mathbf{P}_\Sigma + 2\boldsymbol{\varepsilon}^{(\alpha)} \times \hat{\mathbf{q}}\{\mathbf{P}_\Sigma \cdot (\boldsymbol{\varepsilon}^{(\alpha)} \times \hat{\mathbf{q}})\}; \tag{6}$$

$$\mathbf{P}_\Lambda^{(\alpha)}(\text{odd}) = -\mathbf{P}_\Sigma + 2\boldsymbol{\varepsilon}^{(\alpha)}(\mathbf{P}_\Sigma \cdot \boldsymbol{\varepsilon}^{(\alpha)}). \tag{7}$$

For either alternative, the $\Lambda^0$ has a component of polarization in the direction of the $\Sigma^0$ polarization. The feature which distinguishes between (6) and (7) is the existence of a component parallel [(7)] or perpendicular [(6)] to the photon polarization. If this experiment were feasible, it could serve as an unambiguous determination of the relative $\Sigma$—$\Lambda$ parity. It is only required that the incoming $\Sigma^0$ be polarized.

If we sum over the two photon polarizations $\boldsymbol{\varepsilon}^{(\alpha)}$ in expressions (6) and (7), we obtain for a given $\Lambda$ direction $\hat{\mathbf{q}}$,

$$\mathbf{P}_\Lambda = -\hat{\mathbf{q}}(\mathbf{P}_\Sigma \cdot \hat{\mathbf{q}}) \tag{8}$$

for either relative parity. This may be a means of determining whether $\Sigma^0$—s are produced polarized, since directly produced $\Lambda^0$-s are polarized perpendicular to their direction of motion. If we do not select $\Lambda^0$-s in any specific direction,

$$\mathbf{P}_\Lambda = -\tfrac{1}{3}\mathbf{P}_\Sigma. \tag{9}$$

The $\Lambda$-polarization in process (2) is almost equivalent to the results obtained for process (1) after summing over the photon polarizations (see eq. (8)).

## 3. The Internal Conversion - $\gamma$ Emission Branching Ratio †

In order to make use of the process considered in section 2, it is required that the $\Sigma^0$ be polarized. We would now like to consider possible measurements which do not depend on this polarization, namely, those connected with the relative probabilities of reactions (1) and (2).

The general covariant form for the matrix element in $\Sigma^0$ decay is

$$M = \Gamma_\mu \Omega_\mu, \tag{10}$$

where

$$\Omega_\mu = \varepsilon_\mu^{(\alpha)}/\sqrt{2|\mathbf{k}|} \tag{11}$$

in process (1), and

$$\Omega_\mu = e\sqrt{\frac{m^2}{r_0 s_0}}\,\frac{\bar{u}(\mathbf{r})\gamma_\mu v(\mathbf{s})}{k^2} \tag{12}$$

in process (2). The functions $u$ and $v$ are negaton and positon spinors of momentum $\mathbf{r}$ and $\mathbf{s}$ respectively, $e$, $m$ are the electronic charge and mass, and $k$ is the four-momentum of the photon. $\Gamma_\mu$ is the vertex part which describes the decay of a $\Sigma^0$ into a $\Lambda^0$ and a photon (real or virtual). The general covariant form for $\Gamma_\mu$ is derived in the appendix. It is

$\Gamma_\mu$ (even)

$$= \sqrt{\frac{M_\Sigma M_\Lambda}{p_0 q_0}}\,\bar{\Lambda}(\mathbf{q})\left\{f_1(k^2)\left[i\gamma_\mu\frac{k^2}{M^2}+\frac{\Delta k_\mu}{M^2}\right]+f_2(k^2)\sigma_{\mu\nu}\frac{k_\nu}{M}\right\}\Sigma(\mathbf{p}); \tag{13}$$

$\Gamma_\mu$ (odd)

$$= \sqrt{\frac{M_\Sigma M_\Lambda}{p_0 q_0}}\bar{\Lambda}(\mathbf{q})\left\{f'_1(k^2)\left[i\gamma_5\gamma_\mu\frac{k^2}{M^2}+\frac{2k_\mu}{M}\gamma_5\right]+f'_2(k^2)\gamma_5\sigma_{\mu\nu}\frac{k_\nu}{M}\right\}\Sigma(\mathbf{p}). \tag{14}$$

The spinors $\bar{\Lambda}(\mathbf{q})$ and $\Sigma(\mathrm{p})$ satisfy the equations

$$\bar{\Lambda}(\mathbf{q})(i\gamma q+M_\Lambda)=0,$$

and $\tag{15}$

$$(i\gamma p+M_\Sigma)\Sigma(\mathbf{p})=0.$$

Other symbols used above are defined as follows:

$$M = \tfrac{1}{2}(M_\Sigma+M_\Lambda), \tag{16}$$

$$\Delta = M_\Sigma - M_\Lambda, \tag{17}$$

and

$$k = p - q. \tag{18}$$

For the case of the emission of a real $\gamma$, the $f_1$ terms do not contribute since $k^2=0$ and $\varepsilon_\mu k_\mu = 0$. The result for the transition probability $w_\gamma$ is

† G. Feinberg [4]) has recently calculated this branching ratio, assuming that only the terms $f_2$ and $f'_2$, defined in eqs. (13) and (14) below, contribute. These terms indeed provide the major contribution and our numerical results are in agreement with his.

$$w_\gamma(\text{even}) = \frac{|f_2(0)|^2}{\pi}\frac{\Delta^3}{M^2}, \tag{19}$$

$$w_\gamma(\text{odd}) = \frac{|f'_2(0)|^2}{\pi}\frac{\Delta^3}{M^2}. \tag{20}$$

(A perturbation calculation involving exchanges of virtual $\pi$-mesons leads to $w_\gamma \approx 10^{19}\,\text{sec}^{-1}$.)

Calculation of the internal conversion yields for the momentum distribution, $w_{2e}(|\mathbf{q}|)$, of the $\Lambda^0$ in the $\Sigma^0$ rest system

$$w_{2e}(|\mathbf{q}|, \text{even}) = \frac{2}{3}\frac{\alpha}{\pi^2}\frac{|f_2(0)|^2}{M^2}\left\{\frac{\mathbf{q}^4}{\delta^2-\mathbf{q}^2} + \frac{M_\Lambda}{M_\Sigma}\frac{2m^2\mathbf{q}^4}{(\delta^2-\mathbf{q}^2)^2}\right\}; \tag{21}$$

$$w_{2e}(|\mathbf{q}|, \text{odd}) = \frac{2}{3}\frac{\alpha}{\pi^2}\frac{|f'_2(0)|^2}{M^2}\left\{\frac{\mathbf{q}^4}{\delta^2-\mathbf{q}^2} + \frac{M_\Lambda}{M_\Sigma}\frac{2m^2\mathbf{q}^4}{(\delta^2-\mathbf{q}^2)^2} + 3\left[\tfrac{1}{2} + \frac{\Delta}{M_\Sigma}\frac{\text{Re}\, f'_1(0) f'^*_2(0)}{|f'_2(0)|^2}\right]\mathbf{q}^2\right\}, \tag{22}$$

where

$$\delta = \left(\frac{M_\Lambda}{M_\Sigma}\right)^{\frac{1}{2}}\Delta. \tag{23}$$

The above results are accurate if we neglect corrections of order $(\Delta/M)^2$ to the dominant terms. $\alpha$ is the fine structure constant $(e^2/4\pi)$.

The transition probability, $w_{2e}$, is

$$w_{2e} = \int_0^{q_{\max}} w_{2e}(|\mathbf{q}|)\,dq; \qquad q_{\max} = \left(\frac{M_\Lambda}{M_\Sigma}\right)^{\frac{1}{2}}\sqrt{\Delta^2-4m^2}. \tag{24}$$

Finally, the branching ratio $R = w_{2e}/w_\gamma$ is given by

$$R(\text{even}) = \frac{2}{3}\frac{\alpha}{\pi}\left(\frac{M_\Lambda}{M_\Sigma}\right)^{\frac{1}{2}}\left[\ln\frac{\Delta}{m} - \frac{13}{12}\right], \tag{25}$$

and

$$R(\text{odd}) = \frac{2}{3}\frac{\alpha}{\pi}\left(\frac{M_\Lambda}{M_\Sigma}\right)^{\frac{1}{2}}\left[\ln\frac{\Delta}{m} - \frac{7}{12} + \frac{\Delta}{M_\Sigma}\frac{\text{Re}\, f'_1(0) f'^*_2(0)}{|f'_2(0)|^2}\right]. \tag{26}$$

Although the momentum distributions (21) and (22) differ significantly for low momenta, the number of events involving low momentum $\Lambda$'s is small. For example, restricting ourselves to events for which $q \leqq 0.95\, q_{\max}$, we accept only about 20 % of the total number of internal conversions. Integrating (21) and (22) up to $0.95\, q_{\max}$, we obtain

$$\left[\int_0^{0.95\,q_{\max}} \frac{w_{2e}(q, \text{odd})}{w_\gamma(\text{odd})}\,dq\right] \Big/ \left[\int_0^{0.95\,q_{\max}} \frac{w_{2e}(q, \text{even})}{w_\gamma(\text{even})}\,dq\right] \approx 1.7. \tag{27}$$

The above ratio is very sensitive to the upper limit of the integration.

The branching ratios (25) and (26), themselves, differ by approximately 13 %. Their values are

$$R(\text{even}) = \tfrac{1}{182}, \tag{28}$$

$$R(\text{odd}) = \tfrac{1}{161}. \tag{29}$$

In making the above estimates we have neglected the interference term

$$\frac{\Delta}{M_\Sigma} \frac{\operatorname{Re} f'_1(0) f'^*_2(0)}{|f'_2(0)|^2}. \tag{30}$$

The ratio of this correction term to the leading term is probably not greater than

$$\frac{\Delta}{M_\Sigma} \Big/ \ln \frac{\Delta}{m} \approx 0.01.$$

Indeed, a perturbation calculation indicates that

$$\frac{\operatorname{Re} f'_1(0) f'^*_2(0)}{|f'_2(0)|^2} \approx \frac{1}{4}.$$

The other terms we have neglected (see discussion following equations (21) and (22)) involved assuming $(\Delta/M)^2 \ll 1$, which is certainly reasonable. Thus the error of $R$(odd) is about 1 %, and the error in the difference between $R$(odd) and $R$(even) is about 10 %.

## 4. Conclusions

The analysis in sections 2 and 3 has demonstrated that there are, at least in principle, two methods by which we may determine the relative $\Sigma-\Lambda$ parity. They are both based upon the parity-conserving electromagnetic decays of the $\Sigma^0$. The method discussed in section 2 depends upon the fact that the $\Sigma^0$ is polarized. No other assumptions are made. It is necessary to measure the decay asymmetries of the $\Lambda^0$ together with the direction of the photon polarization. The analysis of section 3 is independent of the $\Sigma^0$ polarization. However, it is necessary to make a very accurate measurement (better than 10 %) of the branching ratio in the $\Sigma^0$ decay. Corrections of order 1 % to the branching ratio were neglected.

The authors would like to thank Dr. L. Madansky for helpful discussions.

## Appendix

We derive below the covariant form for the vertex part $\Gamma_\mu$ used in eqs. (13) and (14):

$$\Gamma_\mu(p, q) = \int e^{-ikx} \langle \Lambda(q) | j_\mu(x) | \Sigma(p) \rangle d^4x, \tag{A.1}$$

where $|\Sigma(p)\rangle$, $|\Lambda(q)\rangle$ are states of real $\Sigma$ and $\Lambda$ particles, and $k = p-q$. $j_\mu(x)$ is the current operator. It satisfies the conservation equation

$$\frac{\partial j_\mu(x)}{\partial x_\mu} = 0. \tag{A.2}$$

This conservation equation leads to the following condition on $\Gamma_\mu$:

$$k_\mu \Gamma_\mu = 0. \tag{A.3}$$

The most general forms for $\Gamma_\mu$ are

$$\Gamma_\mu(\text{even}) = \bar{\Lambda}(q)\left[ig_1(k^2)\gamma_\mu + g_2(k^2)\sigma_{\mu\nu}\frac{k_\nu}{M} + g_3(k^2)\frac{k_\mu}{M}\right]\Sigma(p), \tag{A.4}$$

and

$$\Gamma_\mu(\text{odd}) = \bar{\Lambda}(q)\left[ig'_1(k^2)\gamma_5\gamma_\mu + g'_2(k^2)\gamma_5\sigma_{\mu\nu}\frac{k_\nu}{M} + g'_3(k^2)\gamma_5\frac{k_\mu}{M}\right]\Sigma(p). \tag{A.5}$$

The $g$'s are scalar functions of $k^2$ and $\Sigma(p)$, $\Lambda(q)$ are defined by equation (15). All other terms such as $(p_\mu+q_\mu)$, $\gamma k$ etc. reduce to the terms in (A.4) and (A.5) when one makes use of eq. (15). Application of the condition (A.3) and eq. (15) leads to the relations

$$\left[(M_\Sigma - M_\Lambda)g_1(k^2) - \frac{k^2}{M}g_3(k^2)\right]\bar{\Lambda}(q)\Sigma(p) = 0, \tag{A.6}$$

and

$$\left[(M_\Sigma + M_\Lambda)g'_1(k^2) - \frac{k^2}{M}g'_3(k^2)\right]\bar{\Lambda}(q)\gamma_5\Sigma(p) = 0. \tag{A.7}$$

Note that $g_3(k^2)$ would vanish if $M_\Sigma$ were to equal $M_\Lambda$ and $g_1(k^2)$ and $g'_1(k^2)$ vanish for real photon emission ($k^2 = 0$). Accordingly, we define a new function $f_1(k^2)$, where

$$g_1(k^2) = \frac{k^2}{M^2}f_1(k^2); \tag{A.8}$$

therefore

$$g_3(k^2) = \frac{M_\Sigma - M_\Lambda}{M}f_1(k^2). \tag{A.9}$$

Also

$$g_2(k^2) = f_2(k^2). \tag{A.10}$$

Similarly, we have

$$g'_1(k^2) = \frac{k^2}{M^2}f'_1(k^2); \tag{A.11}$$

therefore

$$g'_3(k^2) = \frac{M_\Sigma + M_\Lambda}{M}f'_1(k^2). \tag{A.12}$$

Also

$$g'_2(k^2) = f'_2(k^2). \tag{A.13}$$

It may be noted that if the vertex part involves particles of equal mass which are coupled indentically in the interaction, the application of time reversal invariance excludes the $g_3$ and $g'_2$ terms [5]).

Further, for either process considered here, $\Gamma_\mu$ is multiplied by $\Omega_\mu$. The expression $k_\mu \Omega_\mu$ vanishes, since for real photon emission $k_\mu \varepsilon_\mu = 0$, and for internal conversion $\Omega_\mu$ is simply the electronic vertex part, which also satisfies a current conservation condition. Thus, the $g_3$ and $g'_3$ terms will not contribute to either process.

It is interesting to observe that the current conservation condition (A.3) provides a simple means for the renormalization of vertex parts in perturbation theory. It is the $g_1$ term which is divergent in perturbation theory. In place of the usual prescription for renormalization, one can evaluate the convergent $g_3$ for $M_\Sigma \neq M_\Lambda$ and then perform

$$\lim_{M_\Sigma \to M_\Lambda} \left( \frac{g_3(k^2)}{M_\Sigma - M_\Lambda} \right).$$

## References

1) P. T. Matthews, Nuovo Cimento **6** (1957) 642
2) A. Pais and S. Treiman, Phys. Rev. **109** (1958) 1759
3) R. H. Dalitz, Proc. Phys. Soc. A **65** (1952) 175; L. Wolfenstein and J. Ashkin, Phys. Rev. **85** (1952) 947
4) G. Feinberg, Phys. Rev. **109** (1958) 1019
5) M. Goldberger and S. Treiman (to be published)

7.A:8.C *Nuclear Physics* **8** (1958) 113—123; © *North-Holland Publishing Co., Amsterdam*
Not to be reproduced by photoprint or microfilm without written permission from the publisher

# ON THE SELF-STRESS OF COMPOSITE PARTICLES

J. STRATHDEE and Y. TAKAHASHI
*Dublin Institute for Advanced Studies, Dublin, Ireland*

Received 23 May 1958

**Abstract:** It is proved that the Pais-Epstein formula which shows the close relation between self-stress and self-energy holds true even for bound states. This formula is used to show that the self-stress of the composite particle vanishes in the rest frame, i.e. that the binding energy transforms like a mass. This makes it possible for the composite particle models proposed by many authors in connection with strange particles to join company with the relativistic particles.

## 1. Introduction

The interesting question has been raised whether the particles so far observed are of an elementary or composite nature. The words elementary and composite, however, have not been given unambiguous meaning by the present quantum field theory and are used in a casual sense only. It was, as far as we know, Taketani who first suggested a possible experimental distinction between the two kinds of particles [1]).

The mass of a composite particle, calculated on field theory, should be given as the algebraic sum of the binding energy and the constituent elementary masses. It is therefore important to ensure that the binding energy so calculated behaves like a mass under Lorentz transformations. In other words it must be shown that the self-stress of the composite particle vanishes in the rest frame [2]). This consideration, which was raised by Sakata a few years ago [3]) becomes quite important in view of the number of composite models proposed in connection with the strange particles [4]).

In this paper we shall discuss the self-stress of composite particles. In order to treat this problem we must, of course, assume the existence of a bound state solution to the eigenvalue problem. In section 2 we shall prove, in a formal manner, that the self-stress indeed vanishes. This proof employs a generalized Pais-Epstein formula which is derived in section 3. Further, it is shown that the formal proof is contradicted by an actual calculation using the Fermi-Yang model (made covariant by Maki [5])).

Previous derivations of the Pais-Epstein formula are open to certain objections. On one hand, a number of these derivations make use of perturbation methods and so leave unanswered the question as to the formula's exact validity [6]). The others neglect the *implicit* dependence of the observ-

ables on the parameters of the system — a procedure which, though unjustified, leads to the correct result in this case [7]). This point will be clarified in section 3. We emphasize that for the treatment of bound states these considerations are of essential importance because the state vector cannot be expressed either independently of the coupling constant or by means of a perturbation expansion. This formula must be proved without any recourse to approximation.

In the last section we shall discuss briefly the physical significance of the Pais-Epstein formula. Here also we indicate, formally, how a theory which lacks divergences would also be free of the self-stress difficulty.

## 2. The Self-Stress of a Composite Particle

For this discussion we make use of the Pais-Epstein formula for the case of two particles bound together by some interaction. (This formula will be derived in section 3.) If $S(0)$ and $E(0)$ are the self-stress and energy respectively (measured in the rest frame) and $\kappa$, $m$ are the component particle masses and $g$ the coupling constant (of dimension $\mathrm{L}^n$ in natural units), then

$$S(0) = \tfrac{1}{3}\left(\kappa\frac{\partial}{\partial\kappa} + m\frac{\partial}{\partial m} - ng\frac{\partial}{\partial g} - 1\right)E(0). \tag{2.1}$$

It follows from dimensional considerations that $E(0)$ is of the form

$$E(0) = \sum_{i,j,k} a_{ijk}\kappa^i m^j g^k, \tag{2.2}$$

where the $a_{ijk}$ are dimensionless numbers and the sum is restricted by

$$1 = i+j-nk. \tag{2.3}$$

The substitution of (2.2) into (2.1), on the other hand, yields

$$S(0) = \tfrac{1}{3}\sum_{i,j,k}(i+j-nk-1)a_{ijk}\kappa^i m^j g^k$$

so that, by (2.3),

$$S(0) = 0. \tag{2.4}$$

It can be seen, however, that just as for elementary particles, the relation (2.2) does not always hold true. This effect is an immediate consequence of the divergences inherent in the present field theory. To illustrate this we cite the example of the composite nucleon-antinucleon model of the pion. The The pion mass $E(0)$, as calculated by Maki [5]), is given by

$$E(0)^2 = (J'_0)^{-1}\{(4I_2^0 + I_0)\kappa^2 - (4g)^{-1}\}, \tag{2.5}$$

where $I_0$, $I_2^0$ and $J'_0$ are diverging quantities which, on introducing a cut-off momentum $\lambda$ and putting $\alpha = \lambda/\kappa$, can be written in the form

$$\begin{aligned} I_0 &= \ln \alpha - 2, \\ I_2^0 &= \tfrac{1}{4}(1+\alpha-2\ln\alpha), \\ J'_0 &= \tfrac{1}{108}(97-54\ln\alpha). \end{aligned} \tag{2.6}$$

In (2.6) the terms $\leqq O(1/\alpha)$ have been omitted.

It is evident now that the dimensional justification of (2.2) is no longer valid: the new parameter $\lambda$ has dimension $L^{-1}$ and should be entered also. In fact a straightforward substitution of (2.5) into (2.1) yields

$$S(0) = \tfrac{1}{6}\frac{\kappa^2}{E(0)}(J'_0)^{-2}\left[-\frac{1}{4\kappa^2 g} - \tfrac{11}{102}\alpha + \frac{\alpha}{2}\ln\alpha + \tfrac{3}{2}\ln\alpha - \tfrac{43}{54}\right]. \tag{2.7}$$

Thus the self-stress of the composite particle fails to vanish because the energy diverges. This situation is exactly the same as for the elementary particle. In other words, *the self-stress difficulty is again absorbed in the self-energy difficulty and would not arise in a divergence-free theory.*

## 3. The Generalized Pais-Epstein Formula

The primary task in this section is the derivation of an expression for the derivative of an energy eigenvalue with respect to one of the parameters contained in the Lagrangian density, viz.

$$\frac{\partial E_\alpha}{\partial \lambda_\kappa} = -\int \mathrm{d}\sigma(x)\left(\Phi_\alpha, \left(\frac{\partial \mathscr{L}}{\partial \lambda_\kappa}\right)_{\phi\phi_\mu}\Phi_\alpha\right),$$

where $\mathscr{L}(x)$ is the Lagrangian density, $\Phi_\alpha$ is an eigenstate of the Hamiltonian, and $\lambda_\kappa$ is some parameter appearing in the Lagrangian. It must be born in mind that the field operators also depend on the $\lambda_\kappa$'s; hence the suffices $\phi$, $\phi_\mu$, on $(\partial\mathscr{L}/\partial\lambda_\kappa)_{\phi\phi_\mu}$ which mean that the derivative is explicit.

Our purpose might be clarified by a short digression on the matter of derivatives. Consider a system with one degree of freedom characterized by a Hamiltonian $H$ and suppose that only one parameter appears in $H$ (e.g. the harmonic oscillator: $H = \frac{1}{2}(p^2+\omega^2 q^2)$, $\omega$ is the parameter). Evidently $\partial H/\partial\omega$ is not well-defined whereas $(\partial H/\partial\omega)_{qp}$ is. And, in general $(\partial H/\partial\omega)_{qp} \neq (\partial H/\partial\omega)_{q'p'}$ where $qp$ and $q'p'$ are two different sets of canonical variables. It is possible, however, to define a total derivative

$$\frac{\mathrm{d}H}{\mathrm{d}\omega} = \left(\frac{\partial H}{\partial\omega}\right)_{qp} - i[H, \Gamma_{qp}],$$

which is independent of the chosen set $qp$. The diagonal elements of $(\partial H/\partial\omega)_{qp}$ in the energy representation are then seen to be independent of the set $qp$. In fact

$$\langle E'|\mathrm{d}H/\mathrm{d}\omega|E'\rangle = \langle E'|\partial H/\partial\omega|E'\rangle.$$

(For the simple harmonic oscillator $\Gamma_{qp} = (i/2\omega)qp$.)

It can then be shown that

$$\mathrm{d}E'/\mathrm{d}\omega = \langle E'|\partial H/\partial\omega|E'\rangle$$

and

$$\langle E'|(\mathrm{d}/\mathrm{d}\omega|E''\rangle) = \langle E'|(\mathrm{d}H/\mathrm{d}\omega)|E''\rangle/(E'-E'')$$
$$= \langle E'|(\partial H/\partial\omega)|E''\rangle/(E'-E'')-i\langle E'|\Gamma|E''\rangle \qquad (E' \neq E'').$$

This last term, $\langle E'|\Gamma|E''\rangle$, seems to have been overlooked in the past [8]). It will concern us no more in this paper as we are interested only in diagonal elements.

For the remainder of this section the Heisenberg picture is used and the states are specified on space-like hyperplanes $\sigma(\tau)$ defined by

$$n_\mu x^\mu = -\tau$$

where $n^\mu$ is a time-like future directed ($n^0 > 0$) unit vector. The metric $(-1, +1, +1, +1)$ is used ($x^0 = t$). Natural units ($\hbar = c = 1$) are used. The abbreviations

$$\frac{\partial}{\partial x^\mu}\phi^r(x) = \partial_\mu \phi^r(x) = \phi_\mu{}^r(x)$$

and

$$n^\mu \partial_\mu \phi^r(x) = \frac{\partial}{\partial\tau}\phi^r(x) = \partial_\tau \phi^r(x) = \phi_\tau{}^r(x)$$

will prove convenient.

The system to be considered comprises a number of interacting boson and fermion fields $\phi^r(x)$ characterized by the Lagrangian density

$$\mathscr{L}(x) = \mathscr{L}^{(0)}(x) + \sum_i g_i \mathscr{L}^{(i)}(x), \tag{3.1}$$

where $\mathscr{L}^{(0)}$ is the sum of the free field densities and the $\mathscr{L}^{(i)}$ are interaction terms. The latter need not be specified in detail except for restrictions on terms of the type $(\phi_\mu)^2$, $\phi_{\mu\nu}$, etc. which must not appear. The particle masses are assumed to appear in $\mathscr{L}^{(0)}$ only.

The canonical momentum and Hamiltonian density operators are

$$\begin{aligned} \pi^r(x) &= -n_\mu(\partial\mathscr{L}/\partial\phi_\mu{}^r) = \partial\mathscr{L}/\partial\phi_\tau{}^r \\ \mathscr{H}(x) &= \sum_r \pi^r(x)\phi_\tau{}^r(x) - \mathscr{L} \end{aligned} \tag{3.2}$$

and the total Hamiltonian is

$$\mathbf{H}(\tau) = \int_{\sigma(\tau)} \mathrm{d}\sigma(x)\mathscr{H}(x) \tag{3.3}$$

which must satisfy

$$\partial_\tau \mathbf{H}(\tau) = 0. \tag{3.4}$$

(The eigenvalues of $\mathbf{H}$ are energies in a coordinate system with

$n^\mu = (1, 0, 0, 0).$)

The commutation rules are

$$\int_{\sigma(\tau)} d\sigma(x')[\phi^r(x),\ \phi^s(x')]_\pm = \int_{\sigma(\tau)} d\sigma(x')[\pi^r(x),\ \pi^s(x')]_\pm = 0, \qquad x\epsilon\sigma(\tau)$$

$$\int_{\sigma(\tau)} d\sigma(x')[\phi^r(x),\ \pi^s(x')]_\pm = i\delta_{rs}, \qquad x\epsilon\sigma(\tau). \tag{3.5}$$

The equations of motion are

$$\begin{aligned} i\partial_\tau \phi^r(x) &= [\phi^r(x),\ \mathbf{H}] \\ i\partial_\tau \pi^r(x) &= [\pi^r(x),\ \mathbf{H}] \end{aligned} \tag{3.6}$$

together with $\partial_\tau \Psi = 0$

where $\Psi$ is the state vector.

Let $\lambda$ represent one of the parameters in the Lagrangian so that $\mathbf{H} = \mathbf{H}(\lambda)$ and $\phi^r = \phi^r(\lambda; x)$, $\pi^r = \pi^r(\lambda; x)$. If $\lambda$ were replaced by $\lambda+\delta\lambda$ the Hamiltonian would change and the evolution in time of the system would be altered. The commutation rules (3.5), however, would be unchanged. The latter fact implies the existence of a unitary operator $\Lambda(\tau)$ such that

$$\phi^r(\lambda+\delta\lambda; x) = \Lambda^{-1}(\tau)\phi^r(\lambda; x)\Lambda(\tau), \qquad x\epsilon\sigma(\tau) \tag{3.7}$$

and similarly for $\pi^r$, where $\Lambda(\tau)$ satisfies

$$i\partial_\tau \Lambda(\tau) = \mathbf{K}(\delta\lambda, \lambda, \tau)\Lambda(\tau) \tag{3.8}$$

with $\mathbf{K}$ a functional of the $\phi^r(\lambda; x)$, $\pi^r(\lambda; x)$ to be determined.

We cannot in general find a $\tau_0$ such that $\Lambda(\tau_0) = 1$ (as evidenced by the discussion at the beginning of the section) so we put

$$\Lambda(\tau_0) = 1 - i\delta\lambda\Gamma + O(\delta\lambda^2). \tag{3.9}$$

The equations of motion for the $\phi^r(\lambda+\delta\lambda; x)$ must be examined now. From (3.6), (3.7) and (3.8)

$$\begin{aligned} i\partial_\tau \phi^r(\lambda+\delta\lambda; x) &= \Lambda^{-1}(\tau) i\partial_\tau \phi^r(\lambda; x) \cdot \Lambda(\tau) \\ &\quad + \Lambda^{-1}(\tau)[\phi^r(\lambda; x),\ \mathbf{K}(\delta\lambda, \lambda, \tau)]\Lambda(\tau) = [\phi^r(\lambda+\delta\lambda; x), \mathbf{M}(\tau)] \end{aligned} \tag{3.10}$$

where

$$\mathbf{M}(\tau) \equiv \Lambda^{-1}(\tau)(\mathbf{H}(\lambda)+\mathbf{K}(\delta\lambda, \lambda, \tau))\Lambda(\tau) \tag{3.11}$$

and, similarly,

$$i\partial_\tau \pi^r(\lambda+\delta\lambda; x) = [\pi^r(\lambda+\delta\lambda; x),\ \mathbf{M}(\tau)]. \tag{3.12}$$

It follows also from (3.8) that

$$\partial_\tau \mathbf{M}(\tau) = 0. \tag{3.13}$$

From (3.10), (3.12), (3.13) we deduce that $\mathbf{M}(\tau)$ can differ by no more than a $c$-number from $\mathbf{H}(\lambda+\delta\lambda)$. Thus we put

$$\mathbf{H}(\lambda+\delta\lambda) = \Lambda^{-1}(\tau)(\mathbf{H}(\lambda)+\mathbf{K}(\delta\lambda, \lambda, \tau))\Lambda(\tau). \tag{3.14}$$

If we write $\mathbf{K}(\delta\lambda, \lambda, \tau) = \delta\lambda\mathbf{K}(\lambda, \tau)+\mathrm{O}(\delta\lambda^2)$, it is a simple matter to deduce that

$$\mathbf{K}(\lambda, \tau) = \int_{\sigma(\tau)} \mathrm{d}\sigma(x) \left(\frac{\partial \mathscr{H}(\lambda; x)}{\partial\lambda}\right)_{\phi,\pi}. \tag{3.15}$$

In general, if $\mathbf{F} = \mathbf{F}(\boldsymbol{\phi}(\lambda; x), \boldsymbol{\pi}(\lambda; x), \lambda)$, then

$$\begin{aligned}\frac{\mathrm{d}F}{\mathrm{d}\lambda} &= \lim_{\delta\lambda\to 0} \frac{1}{\delta\lambda} [\mathbf{F}(\boldsymbol{\phi}(\lambda+\delta\lambda; x), \boldsymbol{\pi}(\lambda+\delta\lambda; x), \lambda+\delta\lambda)-\mathbf{F}(\boldsymbol{\phi}(\lambda; x), \boldsymbol{\pi}(\lambda; x), \lambda)] \\ &= \lim_{\delta\lambda\to 0} \frac{1}{\delta\lambda} [\Lambda^{-1}(\tau)\mathbf{F}(\boldsymbol{\phi}(\lambda; x), \boldsymbol{\pi}(\lambda; x), \lambda+\delta\lambda)\Lambda(\tau)-\mathbf{F}(\boldsymbol{\phi}(\lambda; x), \boldsymbol{\pi}(\lambda; x), \lambda)] \\ &= \lim_{\delta\lambda\to 0} \frac{1}{\delta\lambda} [\Lambda^{-1}(\tau)\mathbf{F}(\lambda; x)\Lambda(\tau)-\mathbf{F}(\lambda; x)+\delta\lambda\Lambda^{-1}(\tau)(\partial\mathbf{F}/\partial\lambda)_{\phi\pi}\cdot\Lambda(\tau)]\end{aligned}$$

i.e.

$$\frac{\mathrm{d}}{\mathrm{d}\lambda}\mathbf{F}(\lambda; x) = \left(\frac{\partial\mathbf{F}}{\partial\lambda}\right)_{\phi\pi} - i[\mathbf{F}(\lambda; x), \boldsymbol{\Gamma}+\int_{\tau_0}^{\tau(x)} \mathrm{d}\tau'\,\mathbf{K}(\lambda, \tau')] \tag{3.16}$$

where we have used

$$\Lambda(\tau) = 1-i\delta\lambda\left(\boldsymbol{\Gamma}+\int_{\tau_0}^{\tau} \mathrm{d}\tau'\mathbf{K}(\lambda, \tau')\right)+\ldots \tag{3.17}$$

which follows from (3.8) and (3.9).

An immediate consequence of (3.16) is

$$(\boldsymbol{\Phi}_\alpha, \mathrm{d}\mathbf{H}/\mathrm{d}\lambda\boldsymbol{\Phi}_\alpha) = \int \mathrm{d}\sigma(x)(\boldsymbol{\Phi}_\alpha, (\partial\mathbf{H}/\partial\lambda)_{\phi\pi}\boldsymbol{\Phi}_\alpha), \tag{3.18}$$

where $\boldsymbol{\Phi}_\alpha$ is an eigenstate of $\mathbf{H}$. (We have used the symbol $\mathrm{d}/\mathrm{d}\lambda$ somewhat unconventionally in the above work. It implies that the dependence on $\lambda$ of observables through the $\boldsymbol{\phi}^r, \boldsymbol{\pi}^r$ is taken into account. If $\lambda$ is one of several parameters then these are regarded, together with $x$, as fixed in the evaluation of $\mathrm{d}\mathbf{F}/\mathrm{d}\lambda$.)

We are now in a position to calculate the derivatives of the energy eigenvalues. Since the Hamiltonians $\mathbf{H}(\lambda)$ and $\mathbf{H}(\lambda+\delta\lambda)$ are $\tau$-independent we can introduce the two sets (complete) of their respective eigenvectors $\{\boldsymbol{\Phi}_\alpha(\lambda)\}$ and $\{\boldsymbol{\Phi}_\alpha(\lambda+\delta\lambda)\}$. The index $\alpha$, standing for the eigenvalues of a complete commuting set of observables, runs over both the discrete and the continuous spectra. These vectors are chosen such that

$$\boldsymbol{\Phi}_\alpha(\lambda+\delta\lambda) = \Omega\boldsymbol{\Phi}_\alpha(\lambda) = (1+\delta\lambda\Omega_1+(\delta\lambda)^2\Omega_2+\ldots)\boldsymbol{\Phi}_\alpha(\lambda). \tag{3.19}$$

Consider now

$$\begin{aligned}&(\boldsymbol{\Phi}_\alpha(\lambda), (\mathbf{H}(\lambda+\delta\lambda)-\mathbf{H}(\lambda))\boldsymbol{\Phi}_\beta(\lambda+\delta\lambda)) = (E_\beta(\lambda+\delta\lambda)-E_\alpha(\lambda))(\boldsymbol{\Phi}_\alpha(\lambda), \Omega\boldsymbol{\Phi}_\beta(\lambda)) \\ &=\delta\lambda\frac{\mathrm{d}E_\beta(\lambda)}{\mathrm{d}\lambda}(\boldsymbol{\Phi}_\alpha(\lambda), \boldsymbol{\Phi}_\beta(\lambda))+\delta\lambda(E_\beta(\lambda)-E_\alpha(\lambda))(\boldsymbol{\Phi}_\alpha(\lambda), \Omega_1\boldsymbol{\Phi}_\beta(\lambda))+\mathrm{O}(\delta\lambda^2),\end{aligned} \tag{3.20}$$

so that

$$(\Phi_\alpha(\lambda), \mathrm{d}\mathbf{H}(\lambda)/\mathrm{d}\lambda\Phi_\beta(\lambda))$$
$$= \frac{\mathrm{d}E_\beta(\lambda)}{\mathrm{d}\lambda}(\Phi_\alpha(\lambda), \Phi_\beta(\lambda)) + (E_\beta(\lambda) - E_\alpha(\lambda))(\Phi_\alpha(\lambda), \Omega_1\Phi_\beta(\lambda)) + \mathrm{O}(\delta\lambda^2).$$

It is easily shown that an appropriate choice of phases for the $\Phi_\alpha(\lambda)$ will make the diagonal elements of $\Omega_1$ vanish. Thus, using (3.18),

$$\frac{\mathrm{d}E_\alpha(\lambda)}{\mathrm{d}\lambda} = (\Phi_\alpha(\lambda), \mathrm{d}\mathbf{H}(\lambda)/\mathrm{d}\lambda\Phi_\alpha(\lambda))$$
$$= \int \mathrm{d}\sigma(x)(\Phi_\alpha(\lambda), (\partial\mathscr{H}(\lambda)/\partial\lambda)_{\phi\pi}\Phi_\alpha(\lambda)), \tag{3.21}$$

where it is understood that the normalizing factor $(\Phi_\alpha, \Phi_\alpha)$ has been removed from the right hand side.

We shall next make use of the following two formulae which are derived in the appendix:

$$(\partial\mathscr{H}(\lambda; x)/\partial\lambda)_{\phi\pi} = -(\partial\mathscr{L}(\lambda; x)/\partial\lambda)_{\phi\phi_\mu}, \tag{3.22}$$

and

$$\mathbf{T}_\mu{}^\mu = \sum_l n_l g_l(\partial\mathscr{L}/\partial g_l)_{\phi\phi_\mu} - \sum_s m_s(\partial\mathscr{L}/\partial m_s)_{\phi\phi_\mu}, \tag{3.23}$$

where $\mathbf{T}_{\mu\nu}$ is the energy-momentum tensor, the $m_s$ are the different particle masses and the $g_l$ are coupling constants. The dimension of $g_l$ is given by $n_l$ (In natural units if $[x] = \mathrm{L}$, then $[g_l] = \mathrm{L}^{n_l}$.)
Assuming that the $m_s$ and $g_l$ are the only parameters appearing in $\mathscr{L}$, then $E_\alpha$ will be a function of just these variables and (reverting to the usage $\partial/\partial\lambda$ for $\mathrm{d}/\mathrm{d}\lambda$) we have

$$[\sum_s m_s\partial/\partial m_s - \sum_l n_l g_l\partial/\partial g_l]E_\alpha(m, g) = \int \mathrm{d}\sigma(x)(\Phi_\alpha, \mathbf{T}_\mu{}^\mu(x)\Phi_\alpha), \tag{3.24}$$

where we have used (3.21), (3.22) and (3.23). Choosing a coordinate system in which $n^\mu = (1, 0, 0, 0)$, so that $E_\alpha$ becomes an energy then, for a state $\Phi_\alpha$ with zero momentum in this system,

$$[\sum_s m_s\partial/\partial m_s - \sum_l n_l g_l\partial/\partial g_l - 1]E_\alpha = 3\int \mathrm{d}^3x(\Phi_\alpha, \mathbf{T}_{11}(x)\Phi_\alpha)_{\mathrm{rest}}, \tag{3.25}$$

which is the generalized Pais-Epstein formula used in section 2.

## 4. Discussion

This section is devoted to a few remarks which, it is hoped, may help to clarify the present theoretical situation with regard to self-stress.

It was pointed out in the introduction that the use of a cut-off parameter in evaluating ambiguous integrals lies at the root of the difficulty. This can

now be illustrated very simply. Suppose that the self-energy $E(0)$ is made finite by the use of some sort of cut-off radius $a$ (with the dimensions of length) so that $E(0)$ can be regarded as a function of the $m_s$ and $g_l$ and of $a$. Then, from dimensional considerations,

$$-E(0) = [a\partial/\partial a - \sum_s m_s \partial/\partial m_s + \sum_l n_l g_l \partial/\partial g_l] E(0). \tag{4.1}$$

All of these parameters except $a$ appear in the Hamiltonian so that equations (3.21), (3.22) and (3.23) can be applied, i.e.,

$$\begin{aligned} -E(0) &= a\partial E(0)/\partial a + (\Phi, [-\sum_s m_s \partial/\partial m_s + \sum_l n_l g_l \partial/\partial g_l]\mathbf{H}\Phi)_{\text{rest}} \\ &= a\partial E(0)/\partial a - \Big(\Phi, \int \mathrm{d}^3x [-\sum_s m_s \partial/\partial m_s + \sum_l n_l g_l \partial/\partial g_l]\mathscr{L}(x)\Phi\Big)_{\text{rest}} \\ &= a\partial E(0)/\partial a + \Big(\Phi, \int \mathrm{d}^3x \mathbf{T}_\mu{}^\mu(x)\Phi\Big)_{\text{rest}}, \end{aligned} \tag{4.2}$$

where $\Phi$ is a state of zero momentum. Thus

$$S(0) = -\tfrac{1}{3} a\partial E(0)/\partial a. \tag{4.3}$$

It might be thought that $a$ could be regarded as a function of the other parameters (e.g. $a = \alpha/m_1$, with $\alpha$ dimensionless). Then the term $a\partial E(0)/\partial a$ would not appear in (4.1) and we should conclude that $S(0) = 0$. This conclusion, however, would be incorrect simply because

$$\partial E(0)/\partial m_1 \neq (\Phi, \partial H/\partial m_1 \Phi)_{\text{rest}}$$

if $a = \alpha/m_1$. So the difficulty remains †.

The physical meaning of self-stress can be made more clear by qualitative considerations. Let us regard $a$ as the radius of a particle and $V = \frac{4}{3}\pi a^3$ as its volume. Then (4.3) reads

$$S(0) = -V(\partial E(0)/\partial V). \tag{4.3'}$$

We can picture $V(\partial E/\partial V)$ as the work done in compressing the energy into a volume $V$ so that $-\partial E/\partial V$ corresponds to the outward pressure at the surface of the particle. A non-vanishing self-stress then implies that the particle is unstable.

One should not conclude from this that a particle of finite size cannot be stable. Eq. (4.3') was arrived at under the assumption that $E(0)$ contained $a$ while the Hamiltonian did not. If the theory is constructed from the start with a view to obtaining a finite self- energy, i.e. if $a$ is built into the Lagrangian then the argument must be altered. Proceeding again from (4.1) we have

$$-E(0) = (\Phi, [a\partial/\partial a - \sum_s m_s \partial/\partial m_s + \sum_l n_l g_l \partial/\partial g_l]\mathbf{H}\Phi)_{\text{rest}},$$

† See, for instance, S. Borowitz and W. Kohn, ref. [6]); E. Arnous and W. Heitler, ref. [7])

i.e.

$$-E(0) = \left(\Phi, \int \mathrm{d}^3x[a\partial/\partial a - \sum_s m_s\partial/\partial m_s + \sum_l n_l g_l \partial/\partial g_l]\mathscr{L}(x)\Phi\right)_{\text{rest}}$$

$$= \left(\Phi, \int \mathrm{d}^3x \mathbf{T}_\mu{}^\mu(x)\Phi\right)_{\text{rest}} = -E(0)+3S(0)$$

whence

$$S(0) = 0. \tag{4.4}$$

This argument shows that the self-stress problem would disappear if the cut-off could be introduced consistently from the beginning in the Lagrangian †. It also explains the success of the mixed field and regulator theories in giving a zero self-stress.

## Appendix

In order to verify equation (3.22) we need to know the operations $(\partial\phi_\mu/\partial\lambda)_{\phi\pi}$. These are easily discovered by introducing the derivatives normal and parallel to $\sigma(\tau)$, respectively,

$$\partial_\tau = n^\mu\partial_\mu \quad \text{and} \quad \partial_{\nu\mu} = \partial_\mu - n_\mu\partial_\tau. \tag{A.1}$$

Then any function of $\phi_\mu$ can be considered a function of $\phi_{\nu\mu}+n_\mu\phi_\tau$ and the problem becomes one of examining $(\partial\phi_{\nu\mu}/\partial\lambda)_{\phi\pi}$ and $(\partial\phi_\tau/\partial\lambda)_{\phi\pi}$. Now

$$\begin{aligned}(\partial\phi^r{}_{\nu\mu}/\partial\lambda)_{\phi\pi} &= \lim_{\delta\lambda\to 0}(\delta\lambda)^{-1}[\Lambda(\tau)\partial_{\nu\mu}\phi^r(\lambda+\delta\lambda;x)\cdot\Lambda^{-1}(\tau) - \partial_{\nu\mu}\phi^r(\lambda;x)] \\ &= \partial_{\nu\mu}\lim_{\delta\lambda\to 0}(\delta\lambda)^{-1}[\Lambda(\tau)\phi^r(\lambda+\delta\lambda;x)\Lambda^{-1}(\tau) - \phi^r(\lambda;x)] \qquad \text{(A.2)} \\ &= \partial_{\nu\mu}(\partial\phi^r(\lambda;x)/\partial\lambda)_{\phi\pi} = 0.\end{aligned}$$

But because $[\Lambda, \partial_\tau] \neq 0$ it is seen that, in general,

$$(\partial\phi_\tau{}^r(\lambda;x)/\partial\lambda)_{\phi\pi} \neq 0. \tag{A.3}$$

Using the definition (3.2) of $\mathscr{H}(\lambda;x)$.

$$\mathscr{H}(\lambda;x) = \sum_r \pi^r(\lambda;x)\phi_\tau{}^r(\lambda;x) - \mathscr{L}(\lambda;x)$$

we have

$$\begin{aligned}\left(\frac{\partial\mathscr{H}}{\partial\lambda}\right)_{\phi\pi} &= \sum_r \pi^r\left(\frac{\partial\phi_\tau{}^r}{\partial\lambda}\right)_{\phi\pi} - \left(\frac{\partial\mathscr{L}}{\partial\lambda}\right)_{\text{explicit}} - \sum_r \frac{\partial\mathscr{L}}{\partial\phi_\tau{}^r}\left(\frac{\partial\phi_\tau{}^r}{\partial\lambda}\right)_{\phi\pi} \\ &= -\left(\frac{\partial\mathscr{L}}{\partial\lambda}\right)_{\text{explicit}} = -\left(\frac{\partial\mathscr{L}}{\partial\lambda}\right)_{\phi',\mu}.\end{aligned} \tag{A.4}$$

Formula (3.23) can be arrived at by simple dimensional considerations. In natural units the dimensions are

† This point was emphasized by F. Rohrlich in his application of the regulator method to the electron self-stress. See Jauch and Rohrlich (ref. [2]), section 16–4.

$$\begin{aligned} &[x^\mu] = \mathrm{L}, \qquad [\hbar] = [c] = \mathrm{L}^0 \\ &[m_s] = \mathrm{L}^{-1}, \qquad [g_l] = \mathrm{L}^{n_l} \\ &[\mathscr{L}] = \mathrm{L}^{-4}, \qquad [\phi^r] = \mathrm{L}^{f_r}, \quad \text{and} \quad [\phi_\mu{}^r] = \mathrm{L}^{f_r-1}. \end{aligned} \tag{A.5}$$

We regard $\mathscr{L}$ as a function of $\phi^r$, $\phi_\mu{}^r$, $m_s$ and $g_l$. Applying Euler's formula we get

$$\begin{aligned} -4\mathscr{L} = &- \sum_s m_s \left(\frac{\partial \mathscr{L}}{\partial m_s}\right)_{\phi\phi_\mu} + \sum_l n_l g_l \left(\frac{\partial \mathscr{L}}{\partial g_l}\right)_{\phi\phi_\mu} \\ &+ \sum_r \left[ f_r \frac{\partial \mathscr{L}}{\partial \phi^r} \phi^r + (f_r - 1) \frac{\partial \mathscr{L}}{\partial \phi_\mu{}^r} \phi_\mu{}^r + \text{H.C.} \right]. \end{aligned} \tag{A.6}$$

The equations of motion can be used to write

$$\frac{\partial \mathscr{L}}{\partial \phi^r} \phi^r = \partial_\mu \left( \frac{\partial \mathscr{L}}{\partial \phi_\mu{}^r} \right) \phi^r = \partial_\mu \left( \frac{\partial \mathscr{L}}{\partial \phi_\mu{}^r} \phi^r \right) - \frac{\partial \mathscr{L}}{\partial \phi_\mu{}^r} \phi_\mu{}^r. \tag{A.7}$$

Substituting (A.7) into (A.6) we get

$$\begin{aligned} -4\mathscr{L} = &- \sum_s m_s \left(\frac{\partial \mathscr{L}}{\partial m_s}\right)_{\phi\phi_\mu} + \sum_l n_l g_l \left(\frac{\partial \mathscr{L}}{\partial g_l}\right)_{\phi\phi_\mu} \\ &- \sum_r \frac{\partial \mathscr{L}}{\partial \phi_\mu{}^r} \phi_\mu{}^r - \text{H.C.} - \partial_\mu \mathbf{F}^\mu, \end{aligned} \tag{A.8}$$

where $\mathbf{F}^\mu$ is some function of the $\phi^r$ which can be dropped by a suitable choice of Lagrangian. The canonical energy-momentum tensor $\mathbf{T}^\mu{}_\nu$ is defined

$$\mathbf{T}^\mu{}_\nu = \frac{\partial \mathscr{L}}{\partial \phi_\mu{}^r} \phi_\nu{}^r + \text{H.C.} - \delta^\mu{}_\nu \mathscr{L}(x)$$

so that

$$\mathbf{T}^\mu{}_\mu(x) = \frac{\partial \mathscr{L}}{\partial \phi_\mu{}^r} \phi_\mu{}^r(x) + \text{H.C.} - 4\mathscr{L}(x). \tag{A.9}$$

Combining (A.8) and (A.9)

$$\mathbf{T}^\mu{}_\mu(x) = - \sum_s m_s \left(\frac{\partial \mathscr{L}}{\partial m_s}\right)_{\phi\phi_\mu} + \sum_l n_l g_l \left(\frac{\partial \mathscr{L}}{\partial g_l}\right)_{\phi\phi_\mu}. \tag{A.10}$$

## References


1) M. Taketani, Sorûshiron no Kenkyu **2** (1950) 188
2) A. Pais, Developments in the Theory of Electrons (Institute for Advanced Study and Princeton University, 1948); W. Heitler, The Quantum Theory of Radiation, 3rd ed. (Oxford, 1954); J. M. Jauch and F. Rohrlich, Theory of Photons and Electrons (Addison-Wesley Publishing Co., Cambridge, Mass., 1955); G. Källén, Handbuch der Physik **5/1** (Springer, Berlin, 1958); H. Umezawa, Quantum Field Theory (North-Holland Publishing Co., Amsterdam, 1956)
3) S. Sakata, Private communication
4) S. Sakata, Prog. Theor. Phys. **16** (1956) 686; M. G. Goldhaber, Phys. Rev. **101** (1956) 433

5) C. N. Yang and E. Fermi, Phys. Rev. **76** (1949) 1739; Z. Maki, Prog. Theor. Phys. **16** (1956) 667
6) J. Yukawa and H. Umezawa, Prog. Theor. Phys. **4** (1949) 468; Y. Takahashi and H. Umezawa, Prog. Theor. Phys. **8** (1952) 193; S. Borowitz and W. Kohn, Phys. Rev. **86** (1952) 985
7) A. Pais and S. T. Epstein, Revs. Mod. Phys. **21** (1949) 445; F. Rohrlich, Phys. Rev. **77** (1950) 357; F. Villars, Phys. Rev. **79** (1950) 122; E. Arnous and W. Heitler, Nuovo Cimento **2** (1955) 1282
8) For instance, W. Pauli, Handbuch der Physik **5/1** (Springer, Berlin, 1958); R. C. Tolman, The Principles of Statistical Mechanics (Oxford, 1938)
9) J. Yukawa and H. Umezawa, Prog. Theor. Phys. **4** (1949) 468; F. Villars, Phys. Rev. **79** (1950) 122; F. Rohrlich, Phys. Rev. **77** (1950) 357

*Nuclear Physics* **8** (1958) 124; © *North-Holland Publishing Co., Amsterdam*

# BOOK REVIEWS

A. D. GALANIN, *The Theory of Thermal-Neutron Nuclear Reactors* (Consultants Bureau Inc. 1958. 291 pages, in two parts. 60 $).

The publication of a new source book on Reactor Theory is an event of some importance and the fact this one is also the first to come out of the U.S.S.R. makes it of even greater interest.

It is divided into two parts of which the first contains an account of the more elementary aspects of the subject. Such basic topics as Diffusion theory, Fermi-age theory, Criticality of heterogeneous reactors, Perturbation theory, Poisoning and Reactor kinetics are all discussed in detail. The second part deals with Transport theory, Thermal spectra and the more refined calculations of neutron behaviour in lattices. No striking advances in theory or technique are made but the general presentation is very thorough and the notation is sufficiently close to that used in the West to give no difficulties of interpretation. Careful attention has been paid to the limits of validity of the various approximations which are introduced and many useful hints on the best choice of methods are given. In fact it is pleasing to find that the general emphasis throughout is placed on practical application without any sacrifice of rigorous analysis when required.

Main criticisms are the absence of mention of modern developments in the use of high speed digital computers and a tendency to restrict consideration to conventional reactors with rod type fuel elements and $D_2O$ or graphite moderators. Minor drawbacks include the lack of an index and the use of the term 'flux' instead of the more conventional 'current'. The latter fault is presumably due to the translators who must otherwise be congratulated on getting out the English version so quickly, although not without such absurdities as referring to several Western publications by their corresponding translations in the U.S.S.R.

This book will be of the very greatest value to all those engaged in reactor calculations and should become a standard text book on the subject in spite of the ridiculously high price which is asked for it.

K. T. Spinney

D. MASSIGNON, *Mécanique statistique des fluides*. (Dunod, Paris. 1958. XIV-264 pages. 3900 fr.)

This book is devoted to setting up the general machinery of statistical hydrodynamics both for the classical case and also, in the last chapter of 60 pages, for the quantal case. It is very much a research book in that the author generalizes earlier expositions, and makes some use of the distribution theory associated with the name of Laurent Schwartz. It is not the author's aim to exhibit in detailed applications the power of the methods he has developed — a matter much regretted by the present reviewer. For these reasons it is likely that the book will be read really carefully only by a small group of specialists, but these should find a great deal to interest them.

P. T. Landsberg

I. D. 2 *Nuclear Physics* 8 (1958) 125—138; © *North-Holland Publishing Co., Amsterdam*
Not to be reproduced by photoprint or microfilm without written permission from the publisher

# NUCLEAR MOMENTS OF INERTIA AND EFFECTIVE NUCLEON MASS

D. R. INGLIS
CERN, *Geneva* †

Received 22 June 1958

**Abstract:** The nuclear moment of inertia may be calculated as the sum of individual-nucleon contributions by treating the dynamics of one sample nucleon in the ellipsoidal harmonic-oscillator potential representing its interaction with the others, on the plausible assumption that the moment of inertia due to all the other nucleons is simply associated with the orientation of the axes of the distortion ellipsoid. The ellipsoid is allowed to rotate freely (in two dimensions) with conservation of angular momentum, but the treatment is rather similar to that given earlier on the basis of a constant angular velocity of the ellipsoid ("cranked model"), and the result is the same. The moment of inertia has the rigid value when the magnitude of the distortion of an open-shell nucleus is obtained in the most simple manner, by minimizing the sum of the oscillator energies with constant nuclear volume. The analogous problem of linear translation may be similarly treated.

The moments of inertia of highly distorted nuclei are observed to be about half of the rigid value. One might hope to understand this discrepancy in terms of the nucleonic "effective mass" $M_e \approx \frac{1}{2}M$ which appears in some problems involving nucleons passing through nuclear matter, and is required in the shell model to reconcile excitation with binding energies. The shell-model-type assumption considered most plausible is that the effective mass arises from simple dependence of the potential not on the canonical momentum but on the nucleon velocity relative to the axes of the rotating ellipsoid, and this is the assumption whose analogue gives a sensible result in the linear problem. The velocity dependence is taken to be a quadratic one, giving a simple expression for $M_e$. It is shown that, with these assumptions, $M_e$ is not effective for the moment-of-inertia problem and one still obtains the rigid value.

## 1. Introduction

The phenomenon of collective nuclear rotation manifested by the well-known sequences of rotational states raises the question why the magnitude of the spacings of these states should be what they are, that is, why the observed nuclear moment of inertia should be something like five times larger than the irrotational-hydrodynamic value of the droplet model and about two to five times smaller than the rigid rotation value [1,2]). Of the many interesting attempts to solve this challenging problem [3]), one of the simplest [4]) employs the "cranked model", the zero-order wave functions of a perturbation theory being given by an ellipsoidal harmonic fictitious potential cranked at constant angular speed about a fixed axis. The single-

† Permanent address, Argonne National Laboratory, Lemont, Illinois.

nucleon behaviour in such a potential is described by normal coordinates corresponding to elliptical orbits, and the lower-energy states of each shell have orbits circulating in such a direction as to add appreciably to the angular momentum of the system. In this model, this is the source of the moment of inertia, and if the magnitude of the distortion from spherical shape is given by minimizing the zeroth-order harmonic-oscillator energies of the nucleons in a nucleus of constant volume, the moment of inertia thus calculated is the rigid-body value, considerably too large. Judged by a simple example [3a]), pairwise interactions of nucleons tend to suppress these individual-nucleon contributions and thus act in a direction to improve the agreement with experiment.

The cranked model is made to seem rather plausible by the success of the shell model in explaining many detailed nuclear features, including large ellipsoidal distortions, and by the thought that the rotational levels prove that the distorted nuclei rotate in a fairly regular manner, making it reasonable to assume a steadily rotating, collectively distorted, shell within which to work out the details of individual-nucleon behaviour, just as it is reasonable to assume a non-rotating shell within which to work out the shell-model stability of the ellipsoidal distortion as Nilsson and others have done.

Some of the more ambitious calculations, which are concerned mainly with the separation into collective and internal coordinates and do not make use of the shell model until perhaps the very end, have the advantage that they do not require the introduction of external machinery to turn the crank steadily. As soon as one eliminates this constraint, the rotational coordinate becomes a degree of freedom and we cannot consistently retain all the internal degrees of freedom as independent. The need to resolve this situation complicates some of the calculations. It is very similar to a difficulty concerning translation that is usually ignored in practical applications of the shell model, which treat the centre of the fictitious potential rather than the centre of mass as fixed in space. When it is treated properly, with the correct number of coordinates, a very few of the (fairly high) states of the shell model disappear [5]), a modification not seriously affecting the usual applications to the few lowest states. Failure to eliminate an extra coordinate in the rotation problem may similarly be expected to give little trouble.

## 2. The Freely Rotating Model

We here treat the problem in such a way as not to need an external "crank", and at the same time to take advantage of the simplicity of shell-model methods from the beginning. In the spheroidal shell model it is usually assumed not only that the fictitious oscillator potential has its centre fixed in space, but also that the direction of the major axis is fixed,

which implies fixing two superfluous angle coordinates in addition to the translation coordinates. In order to study rotations in a simple manner, we relax this condition by permitting the azimuthal coordinate $\Phi$ to vary freely, still keeping the polar angle fixed at $\theta = \frac{1}{2}\pi$ because it seems clear that the determination of the moment of inertia must be essentially a two-dimensional phenomenon. That is, we permit the major axis of the spheroid to rotate freely in the plane normal to a fixed axis.

As usual in the shell model, we let each nucleon interact with the others only through its individual potential energy in the common average potential ("strong coupling" approximation)

$$V(y, z) = \tfrac{1}{2}(K_2 y^2 + K_3 z^2) = \tfrac{1}{2}M(\omega_2^2 y^2 + \omega_3^2 z^2). \qquad (1)$$

We concentrate our attention † on one nucleon in a state $a = l, m, n$ (oscillator quantum numbers in the three dimensions $x, y, z$). The $x$-axis is fixed in space, so this component is unaffected by the rotation and the corresponding potential term, $\frac{1}{2}K_2 x^2$, is omitted from eq. (1). The $z$-axis is the major axis of the spheroid with orientation given by the angle $\Phi$. The total moment of inertia $\mathcal{I}_T$ is taken to be the sum of the contribution $\mathcal{I}_a$ of this nucleon and the combined contribution $\mathcal{I}$ of all the other nucleons, and we assume that $\mathcal{I}$ may be treated as constant and associated with the orientation of the spheroidal average potential. Here we neglect fluctuations, there being many other nucleons ††. This assumption has some similarity to

† The Hamiltonian must of course be symmetric and the wave function antisymmetric in permutation of particles and our concentration on the nucleon in one state must be understood in this context. With the wave equation $(H - E_a)\psi_a = 0$, our model consists in assuming separability, that is, assuming that each term of the antisymmetric wave function is separable into a rotational and internal part, thus:

$$\chi_a(1, \cdots, A) = \sum_Q (-)^Q Q \psi_{\text{rot}}(1, \cdots A-1)\psi_a(A),$$

and that the Hamiltonian operating on any one such term is well approximated by

$$\mathcal{H}(1, \cdots, A)\psi_{\text{rot}}(1, \cdots, A-1)\psi_a(A) = \{F(1, \cdots, A-1) + H(A)\}\psi_{\text{rot}}(1, \cdots, A-1)\psi_a(A),$$

where $F = P^2/2\mathcal{I} = F(\Phi)$ with $\Phi = \Phi(1, \cdots, A-1)$ and we proceed to evaluate $H(A) = h(A) + h^{(1)}(A)$. As usual in the shell model, $h(A)$ contains the effective potential $V(A)$ and we assume that this is also effective for the other nucleons, leading to orthogonality between terms differing by a permutation $Q$ exchanging the nucleon in $\psi_a$ with one of the others. The internal antisymmetry of $\psi_{\text{rot}}$ is not visible in this collective treatment.

†† The sudden appearance of stable spheroidal nuclei and distinct rotational spectra on passing neutron number $N = 88$, for example, is associated with populating the nucleon states of distorted nuclei in such a way as to open the "closed shell" of the next lower magic-number group. Although the closed shells contribute very little to the moment of inertia, there are thus two open shells and many open-shell nucleons contributing to the moment of inertia in just those nuclei in which the rotation is clearly evident. The number of nucleons contributing to $\mathcal{I}$ is particularly large in the nuclei in which we are most directly interested those having the largest distortions and with $\mathcal{I}_{\text{obs}} \approx \frac{1}{2}\mathcal{I}_{\text{rigid}}$ (which one might hope to associate with $M_{\text{eff}} \approx \frac{1}{2}M$).

the assumption of constant angular velocity which it replaces, but it is not the same and has the conceptual advantage that it is an internal assumption within the self-contained system and does not require external machinery.

The kinetic energy is then

$$T = \tfrac{1}{2}\mathscr{I}\dot{\Phi}^2+\tfrac{1}{2}M[\dot{r}^2+r^2(\dot{\Phi}+\dot{\varphi})^2]$$
$$= \tfrac{1}{2}(\mathscr{I}+Mr^2)\dot{\Phi}^2+M(y\dot{z}-z\dot{y})\Phi+\tfrac{1}{2}M(\dot{y}^2+\dot{z}^2). \quad (2)$$

The three momenta conjugate to the coordinates $\Phi$, $y$, $z$ obtained as derivatives of the Lagrangian, are

$$\begin{aligned} p_y &= \partial\mathscr{L}/\partial\dot{y} = \partial T/\partial\dot{y} = M(\dot{y}-z\dot{\Phi}) \\ p_z &= M(\dot{z}+y\dot{\Phi}) \\ P &= \partial\mathscr{L}/\partial\dot{\Phi} = \mathscr{I}\dot{\Phi}+p \end{aligned} \quad (3)$$

with $p = yp_z-zp_y = p_\varphi$. The Hamiltonian, expressed as a function of coordinates and momenta, is thus

$$\mathscr{H} = T+U = P^2/2\mathscr{I}-(P/\mathscr{I})p+h,$$
$$h = (p_y^2+p_z^2)/2M+U(y,z)+p^2/2\mathscr{I}. \quad (4)$$

The term in $p^2$ may either be neglected on the grounds that it does not depend on $P$ and that we have made a rough approximation to the average potential, or we may more explicitly include it in the oscillator potential by putting $U(y,z)+p^2/2\mathscr{I} = V(y,z)$. It is then convenient to use the usual oscillator coordinates $\eta = (M\omega_2/\hbar)^{\frac{1}{2}}y$, $p_\eta = (\hbar/i)\partial/\partial\eta = (\hbar/M\omega_2)^{\frac{1}{2}}p_y$ in

$$h = \tfrac{1}{2}\hbar[\omega_2(\eta^2-\partial/\partial\eta^2)+\omega_3(\zeta^2-\partial^2/\partial\eta^2)],$$
$$p = (\hbar/i)[(\omega_2/\omega_3)^{\frac{1}{2}}\eta\partial/\partial\zeta-(\omega_3/\omega_2)^{\frac{1}{2}}\zeta\partial/\partial\eta]. \quad (5)$$

The wave equation put directly in a form for separation and a perturbation treatment is then

$$[-(\hbar^2/2\mathscr{I})\partial^2/\partial\Phi^2+h+h^{(1)}-E_{\rm rot}^{(0)}-E_a-e_a-\varepsilon_a]\psi_{\rm rot}\psi_a = 0. \quad (6)$$

Here $\psi_{\rm rot} = \exp(i\mathscr{M}\Phi)$ and thus $P = \mathscr{M}\hbar$ and

$$E_{\rm rot}^{(0)} = (\mathscr{M}\hbar)^2/2\mathscr{I} \quad (7)$$

because $\Phi$ does not appear explicitly; $h^{(1)} = -(\mathscr{M}\hbar/\mathscr{I})p$ is the perturbation term and the energies $E_a$, $e_a$ and $E_a$ are of successively smaller orders in the perturbation, with $(h-E_a)u_a = 0$ for the oscillator part. We expand $\psi_a = \psi_a(\eta,\zeta) = u_a+\sum_\beta c_{\beta a}u_\beta$ and obtain, just as in the previous treatment [4]) $e_a = 0$, $c_{\beta a} = -(\mathscr{M}\hbar/\mathscr{I})\langle\beta|p|a\rangle/(E_\beta-E_a)$, and

$$\varepsilon_a = \sum_\beta |\langle a|h^{(1)}|\beta\rangle|^2/(E_a-E_\beta) = -(\mathscr{M}\hbar/\mathscr{I})^2 f_a,$$
$$f_a = \sum_\beta |\langle a|p|\beta\rangle|^2/(E_\beta-E_a). \quad (8)$$

Thus both the rotational energy $E_{\rm rot}(0)$ of $\mathscr{I}$ and the additional energy of the

nucleon due to rotation, $\varepsilon_a$, are proportional to the square of the angular momentum, $(\mathscr{M}\hbar)^2$, and the total moment of inertia $\mathscr{I}_T$ is defined by the total rotational energy

$$E_{\text{rot}} = (\mathscr{M}\hbar)^2/2\mathscr{I}_T = E_{\text{rot}}^{(0)}+\varepsilon_a = [(\mathscr{M}\hbar^2/2\mathscr{I}](1-2f_a/\mathscr{I}). \tag{9}$$

As long as the moment of inertia $\mathscr{I}_a$ contributed by the nucleon in state $a$ is small compared with the sum of all the others, $\mathscr{I}_a \ll \mathscr{I}$, we may expand the reciprocal

$$\mathscr{I}+\mathscr{I}_a = \mathscr{I}_T = \mathscr{I}/(1-2f_a/\mathscr{I}) \approx \mathscr{I}+2f_a \tag{10}$$

and obtain

$$\mathscr{I}_a = 2f_a = 2\sum_\beta |\langle a|p|\beta\rangle|^2/(E_\beta-E_a). \tag{11}$$

This is the same formula that has been derived [4]) from the "cranked model", most simply by putting the calculated angular momentum equal to $(\mathscr{I}+\mathscr{I}_a)\dot{\Phi}$, and has been shown [3a, 4b]) to give the rigid-rotation result when summed over $a$.

## 3. The Linear Analogue

Let us compare this derivation in detail with the corresponding problem of linear translation, for which one knows that the mass of the system must be the sum of the masses of its parts. In one dimension, we have a mass $M$ (the rest of the nucleus) at position $X$ to which another mass $m$ (the selected nucleon) at position $X+x$ is attached by a spring represented by the potential $V(x)$. Thus we have

$$\begin{aligned} T &= \tfrac{1}{2}M\dot{X}^2+\tfrac{1}{2}m(\dot{X}+\dot{x})^2, \\ p &= \partial T/\partial\dot{x} = m(\dot{X}+\dot{x}), \qquad P = \partial T/\partial\dot{X} = M\dot{X}+p; \end{aligned} \tag{12}$$

$$\begin{aligned} \mathscr{H} &= T+V = (P-p)^2/2M+p^2/2m+V \\ &= P^2/2M-(P/M)p+h, \\ h &= p^2/2\mu+V, \qquad \mu = mM/(m+M), \qquad (h-E_a)u_a = 0. \end{aligned} \tag{13}$$

The coordinate $X$ does not appear in the potential and $P$ is a constant of the motion. Of course we know a better way to solve this problem by use of the coordinate of the centre of mass, as is discussed below, but here we preserve the strict analogy with the preceding rotational treatment, and obtain

$$\begin{aligned} \varepsilon_a &= -(P/M)^2 f, \qquad f = \sum_\beta p_{a\beta}p_{\beta a}/(E_\beta-E_a), \\ E_{\text{trans}} &= P^2/2M+E_a = P^2/2M_T, \qquad M_T = M^2/(M-2f). \end{aligned} \tag{14}$$

The evaluation of $f$ may be carried out by a method used in connection with intensity sum rules in atomic spectroscopy †, so long as the potential $V(x)$

† As was pointed out by Professor V. F. Weisskopf (personal communication).

is independent of the momentum. From the commutation relation

$$xp-px = i\hbar$$

one has by multiplying by $p$ first from the left, then from the right, and adding,

$$xp^2+p^2x = 2i\hbar p = 2\mu(xh-hx), \quad p_{ab} = (\mu/i\hbar)(E_b-E_a)x_{ab}. \tag{15}$$

We have here assumed that $V$ commutes with $x$, which implies that it does not contain $p$ or $\dot{x}$.

By using (15) first for one factor $p$ of (14), then for the other, and adding, one has

$$2f = (\mu/i\hbar)\sum_\beta (x_{a\beta}p_{\beta a}-p_{a\beta}x_{\beta a}) = (\mu/i\hbar)(xp-px)_{aa} = \mu,$$
$$M_T = M^2/(M-\mu) = M+\mu. \tag{16}$$

The procedure thus leads simply to the expected result with any momentum-independent potential $V(x)$.

The question immediately arises why one cannot obtain a similarly simple and universal result for the rotational case. The reason is that there is an additional coordinate, $r$, which does not commute with the angular momentum, $p$. This additional degree of freedom makes possible the elliptical orbits of the normal motions in the cranked model, for example, which have no analogue in the linear problem. If in the rotational problem one retains in (2) and (4) the coordinates $r$, $\varphi$ and their momenta $p_r = m\dot{r}$, $p = mr^2(\dot{\Phi}+\dot{\varphi})$, in place of $y$, $z$, $p_y$, $p_z$, one has in (4)

$$h = p_r^2/2m+p^2/2mr^2+U(r,\varphi)+p^2/2\mathcal{I} \tag{4'}$$

which differs from the corresponding part of (13) in that the simple constant factor $1/m$ of $p^2$ has been replaced by the variable factor $1/mr^2$. Thus in place of (15) one obtains

$$(p/r^2)_{ab} = (m/i\hbar)(E_b-E_a)\varphi_{ab} \tag{15'}$$

whereas we would need a simple expression for the matrix element $p_{ab}$ alone in terms of $\varphi_{ab}$ in order to obtain $p\varphi-\varphi p$ from $f$.

A similar difficulty prevents one from constructing a simple rotational analogue of the standard simple treatment of the linear problem involving the rest mass $\mu = mM/(M+m)$ and the coordinate of the centre of mass, $\mathcal{X} = X+(m/(M+m))x$. In terms of these the kinetic energy (12) is

$$T = \tfrac{1}{2}(M+m)\dot{\mathcal{X}}^2+\tfrac{1}{2}\mu\dot{x}^2 \tag{17}$$

and with an internal potential dependent only on $x$ the problem separates in $x$ and $\mathcal{X}$. The angular centre of inertia

$$\Theta = \Phi+[mr^2/(\mathcal{I}+mr^2)]\varphi \tag{18}$$

depends on $r$ as well as the angles and the separation cannot be made exactly †.

## 4. Velocity-Dependent Potential in the Linear Problem

The perturbation procedure in the linear problem thus leads to the expected mass if the potential commutes with the coordinate. A momentum-dependent or velocity-dependent potential with its associated effective nucleon mass is, however, expected on the basis of the theory of nuclear matter [6]) and it is needed to make the shell model consistent, in particular to give total energies corresponding to bound nuclei [7]). It is therefore of interest to study such potentials both in the linear and in the rotation problem. We consider first the linear problem.

In the Lagrangian

$$\mathscr{L} = \tfrac{1}{2}M\dot{X}^2+\tfrac{1}{2}m(\dot{X}+\dot{x})^2-V(x,\dot{x}) \tag{19}$$

and the subsequent Hamiltonian

$$\mathscr{H} = P^2/2M+[p^2-(\partial V/\partial\dot{x})^2]/2\mu-(P/M)p+V \tag{20}$$

it is important that the potential be a function of $\dot{x}$ rather than $p$ because the effective mass is associated with the motion of a nucleon relative to the nuclear matter surrounding it, whereas

$$p = \partial\mathscr{L}/\partial\dot{x} = m(\dot{X}+\dot{x})-\partial V/\partial\dot{x} \tag{21}$$

is the momentum relative to the laboratory. If simply $p$ and hence $\dot{X}$, the velocity of the nuclear matter, were to appear in the potential, this would couple the potential to the collective motion and one would of course get strange effects equivalent to an unfamiliar total mass. One needs also

$$P = \partial\mathscr{L}/\partial\dot{X} = M\dot{X}+p-\partial V/\partial\dot{x} \tag{22}$$

to eliminate the velocities and obtain (20) in terms of the momenta. The derivative $\partial V/\partial\dot{x}$ can also be expressed in terms of $p$ and $P$, though not always simply.

A simple choice of $V$, as an example, is

$$V(x,\dot{x}) = V(x)+\tfrac{1}{2}c\dot{x}^2 \tag{23}$$

and if we consider $c$ small, neglecting terms in $c^2$, in the interest of further simplicity, we have

$$\mathscr{H} = (1+c/M)P^2/2M-(1+c/\mu)(P/M)p+h,$$
$$h = (1+c/\mu)p/2\mu+V(x), \tag{24}$$

† The problem of optimizing the separability of the internal and collective coordinates along these lines is discussed in an interesting recent paper of A. Bohr and B. R. Mottelson (recent preprint). Their first steps parallel in other language those associated with our eqs. (2) to (4).

in place of (13), and again $(h-E_a)u_a = 0$ but with $E_a$ altered from its former values in keeping with a change of effective mass, for the internal motion, $1/\mu \to (1+c/\mu)/\mu$. In place of (15) we have

$$xp^2-p^2x = [2\mu/(1+c/\mu)](xh-hx), \quad p_{ab} = [\mu/i\hbar(1+c/\mu)](E_b-E_a)x_{ab}, \quad (25)$$

which leads immediately to

$$2f = \mu/(1+c/\mu). \quad (26)$$

Because the perturbation term also contains the factor $(1+c/\mu)$ we now have

$$\varepsilon_a = -(1+c/\mu)^2(P/M)^2 f \quad (27)$$

in place of (14), and thus

$$1/M_{\text{eff}} = (1+c/M)/M-(1+c/\mu)\mu/M^2 = 1/M-\mu/M^2 = 1/(M+m). \quad (28)$$

That a correct treatment must obtain this result is shown by the simple separability, eq. (17), with a potential dependent on $\dot{x}$ and not on $\dot{X}$, but it is of interest to see thus how it works out for a special case by a method quite similar to that used in the following discussion of rotation. The difference of method is that in the rotation problem we do not consider $c$ small but instead introduce the simplification of an oscillator potential.

## 5. Velocity-Dependent Potential in Rotation

Pending extension of a more fundamental treatment [6]) to include the effects not only of boundaries but of moving boundaries, we may reasonably investigate the question, whether the small "effective" nucleon mass is effective in the moment-of-inertia problem, by modifying the shell-model approach to include some sort of velocity-dependent potential. One might do this by assuming a simple momentum dependence in the Hamiltonian, but, as we have seen in the linear problem, to be consistent one should instead introduce a velocity dependence in the Lagrangian, since this affects the definition of the momenta entering the Hamiltonian.

In the rotating problem we have the nucleon coordinates $x$, $y$, $z$, in the rotating coordinate system of the collective distortion. Among possible simple assumptions it seems most plausible to take this coordinate system as representative of the nuclear matter through which any one nucleon must "swim". This seems particularly reasonable if the calculated nuclear moment of inertia turns out to have nearly the rigid-body value, as it does, indicating that nuclear matter rotates approximately as rapidly as the coordinate axes *on the average* (the closed-shell nucleons less and the open-shell nucleons more), as is discussed further below. Let us therefore see the consequences of assuming that the effective potential in which one nucleon moves is dependent on its velocity relative to this coordinate system.

We start with the Lagrangian $\mathscr{L} = T-V$ with $T$ as in eq. (2) and

$$V = V(y, z, \dot{y}, \dot{z}) = U(y, z)+\tfrac{1}{2}c(\dot{y}^2+\dot{z}^2). \tag{29}$$

Thus, with the "effective mass" $M_e = M-c$, we have

$$\mathscr{L} = \tfrac{1}{2}(\mathscr{I}+Mr^2)\dot{\Phi}^2+\tfrac{1}{2}M_e(\dot{y}^2+\dot{z}^2)+M(y\dot{z}-z\dot{y})\dot{\Phi} -U, \tag{30}$$

$$\begin{aligned} p_y &= M_e\dot{y}-Mz\dot{\Phi}, \qquad \dot{y} = (p_y+M_z\dot{\Phi})/M_e, \\ p_z &= M_e\dot{z}+My\dot{\Phi}, \qquad \dot{z} = (p_z-M_y\dot{\Phi}/M_e, \\ P &= \partial\mathscr{L}/\partial\dot{\Phi} = \mathscr{I}_0\dot{\Phi}+(M/M_e)p, \qquad \dot{\Phi} = [P-(M/M_e)p]/\mathscr{I}_0. \end{aligned} \tag{31}$$

Here we have defined

$$\mathscr{I}_0 = \mathscr{I}-(Mc/M_e)r^2, \qquad p = yp_z-zp_y = \partial\mathscr{L}/\partial\dot{\varphi} \tag{32}$$

and have used

$$y\dot{z}-z\dot{y} = p/M_e-(M/M_e)r^2\dot{\Phi}. \tag{33}$$

We need further

$$\tfrac{1}{2}M_e(\dot{y}^2+\dot{z}^2) = (p_y^2+p_z^2+M^2r^2\dot{\Phi}^2-2Mp\dot{\Phi})/2M_e \tag{34}$$

to put the Lagrangian in a form preparatory to forming the Hamiltonian, but still retaining $\dot{\Phi}$ for brevity:

$$\mathscr{L} = \tfrac{1}{2}\mathscr{I}_0\dot{\Phi}^2+(p_y^2+p_z^2)/2M_e-U. \tag{35}$$

Similarly, and again with cancellation of two terms $(M/M_e)p\dot{\Phi}$,

$$\sum p_i\dot{q}_i = P\dot{\Phi}+p_y\dot{y}+p_z\dot{z} = \mathscr{I}_0\dot{\Phi}^2+(p_y^2+p_z^2)/M_e. \tag{36}$$

Taking the difference of these two, with $\dot{\Phi}$ from eq. (31), we obtain the Hamiltonian

$$\mathscr{H} = [P-(M/M_e)p]^2/2\mathscr{I}_0+(p_y^2+p_z^2)/2M_e+U. \tag{37}$$

Thus, the effective mass appears with the internal momenta and, in spite of the factor $(\mathscr{I}+Mr^2)$ in the first term of eq. (30), the only moment of inertia appearing directly in the Hamiltonian is $\mathscr{I}_0$. This is not strictly a constant; it depends on $r$, eq. (32), but the term in $r$ is small compared to the leading term $\mathscr{I}$ (arising from many nucleons) and the reciprocal may be expanded, giving us a new perturbation term $h_1^{(1)}$ in the Hamiltonian:

$$\begin{aligned} h^{(1)} &= h_0^{(1)}+h_1^{(1)}, \\ h_0^{(1)} &= -(M/M_e\mathscr{I})Pp, \\ h_1^{(1)} &= (\hbar c/2\mathscr{I}^2M_e)Mr^2\partial^2/\partial\Phi^2. \end{aligned} \tag{38}$$

The distinction between $\mathscr{I}$ and $\mathscr{I}_0$ is immaterial in $h_0^{(1)}$ because this term is itself small. With $V(y, z)$ again representing a distorted harmonic-oscillator potential, as above, we then have

$$\begin{aligned} \mathscr{H} &= P^2/2\mathscr{I}+h+h^{(1)}, \\ h &= (p_y^2+p_z^2)/2M_e+\tfrac{1}{2}(K_2y^2+K_3z^2) \\ &= \tfrac{1}{2}\hbar[\omega_2(\eta^2-\partial^2/\partial\eta^2)+\omega_3(\zeta^2-\partial^2/\partial\zeta^2)], \end{aligned} \tag{39}$$

as in eq. (5), but now with $M_e$ playing the role of $M$ in determining the relation between the strength of the potential (hence the energy denominators) and the size of the nucleus:

$$y = (\hbar/M_e\omega_2)^{\frac{1}{2}}\eta, \qquad \omega_2^2 = K_2/M_e. \tag{40}$$

With $h^{(1)}$ thus modified, eq. (6) still applies, the separation proceeds as before and $E_{\text{rot}}^{(0)}$ is again given by eq. (7). The new term $h_1^{(1)}$ has a diagonal matrix element and contributes to the energy the first-order term

$$e_a = (\mathscr{M}^2\hbar^2\, c/2\mathscr{I}^2\, M_e)\langle a|Mr^2|a\rangle.$$

The second-order contribution of this term is smaller by a factor of the order $(P/\mathscr{I}\omega_i)^2(c/M)^2$ and the only change in the second-order energy, eq. (8), is that $f_a$ becomes

$$\begin{aligned} f_a &= (M/M_e)^2 \sum_\beta |\langle a|p|\beta\rangle|^2/(E_\beta - E_a) \\ &= (M/M_e)^2(\hbar/4\omega_2\omega_3)\{(m+n+1)(\omega_2-\omega_3)^2/(\omega_2+\omega_3) \\ &\quad +(n-m)(\omega_2+\omega_3)^2/(\omega_2-\omega_3)\}, \end{aligned} \tag{41}$$

the latter according to the development of eq. (8) of ref. [4b]), wherein the only modification required is in the definition of the $\omega$'s.

As in eq. (10), we assume the moments of inertia $\mathscr{I}$ and $\mathscr{I}_a$ to be additive, and have

$$\begin{aligned} E_{\text{rot}} &= (\mathscr{M}\hbar)^2/2(\mathscr{I}+\mathscr{I}_a) = E_{\text{rot}}^{(0)} + e_a + \varepsilon_a \\ &= [(\mathscr{M}\hbar)^2/2\mathscr{I}][1+(c/\mathscr{I}M_e)\langle a|Mr^2|a\rangle - 2f_a/\mathscr{I}] \\ &\approx (\mathscr{M}\hbar)^2/2[\mathscr{I}-(c/M_e)\langle a|Mr^2|a\rangle + 2f_a]. \end{aligned} \tag{42}$$

Thus the contribution of the nucleon in state $a$ to the moment of inertia is

$$\mathscr{I}_a = 2f_a - (c/M_e)\langle a|Mr^2|a\rangle. \tag{43}$$

The quantity $\mathscr{I}$ which was used in the calculation and attributed to the other nucleons does not appear in this result, and the total nuclear moment of inertia $\mathscr{I}_T$ may now be obtained by summing the contributions of all the individual nucleons:

$$\mathscr{I}_T = \sum_a \mathscr{I}_a = \sum_a 2f_a - (c/M_e)\sum_a \langle a|Mr^2|a\rangle = \sum_a 2f_a - (c/M_e)\mathscr{I}_{\text{rigid}}. \tag{44}$$

The determination of the magnitude of the deformation is not affected by the consideration of effective mass. As long as we retain the simplification of calculating the nuclear energy as the sum of the oscillator energies of the nucleons in the three dimensions, the equilibrium deformation is the result of a competition between oscillator energies in different directions. In this competition such considerations as the reduced mass, the virial theorem, and the question of counting interactions twice (the famous factor $\frac{3}{4}$) introduce factors common to both sides of the competition and do not affect

the outcome. (Future more general consideration of the effect of boundaries on nuclear matter may of course give a different result.) The oscillator frequencies or stiffness constants in the two directions thus differ because of the different degree to which the populated states involve their oscillator excitations, according to eq. (11) of ref. [4b]):

$$\sum(n+\tfrac{1}{2}) = (\omega_2/\omega_3)\sum(n+\tfrac{1}{2}), \tag{45}$$

and with this, as in eq. (13) of ref. [4b]), one obtains from (41)

$$2\sum_a f_a = \hbar(M/M_e)^2[\sum(n+\tfrac{1}{2})/\omega_2+\sum(n+\tfrac{1}{2})/\omega_3]. \tag{46}$$

In these calculations we use as a convenient unit, for comparison, the rigid moment of inertia

$$\begin{aligned}\mathscr{I}_{\text{rigid}} &= M\sum(y^2+z^2)_{\text{Av}} = (M/M_e)\hbar[\sum(\eta^2)_{\text{Av}}/\omega_2+\sum(\zeta^2)_{\text{Av}}/\omega_3] \\ &= (M/M_e)\hbar[\sum(n+\tfrac{1}{2})/\omega_2+\sum(n+\tfrac{1}{2})/\omega_3] = (M_e/M)\sum_a 2f_a.\end{aligned} \tag{47}$$

This in eq. (44) now gives the rigid-rotation result

$$\mathscr{I}_{\text{T}} = (M/M_e)\mathscr{I}_{\text{rigid}}-(c/M_e)\mathscr{I}_{\text{rigid}} = \mathscr{I}_{\text{rigid}} \tag{48}$$

just as without any velocity-dependence of the potential. With $c$ set equal to zero, the derivation of course reduces to the previous one.

## 6. Discussion of the Assumed Velocity Dependence

In selecting a velocity dependence of the shell-model potential to simulate what one might expect from a treatment of the scattering of one nucleon on others, as inhibited by the Pauli principle, a dependence on the *relative* velocities of the nucleons seems most reasonable. Thus one might assume a term in the potential proportional to

$$\tfrac{1}{2}\sum_{i,j}[(\dot{y}_i-\dot{y}_j)^2+(\dot{z}_i-\dot{z}_j)^2] \approx \sum_i(\dot{y}_i^2+\dot{z}_i^2)-\sum_i\dot{y}_i\sum_j\dot{y}_j-\sum_i\dot{z}_i\sum_j\dot{z}_j \tag{49}$$

and in order to have the simple quadratic form we have used, that coordinate system should be selected in which

$$\sum_j\dot{y}_j = 0, \tag{50}$$

etc., the sum extending over all $j$. More properly, the summations over $i$ and $j$ should not be independent but related by the condition that the two nucleons should not be further apart than the range of nuclear interactions. Still, a condition similar to (50) but complicated by a weighting factor that must be averaged, should provide a selection of the proper coordinate system, and we have assumed that this is the system of the rotating distortion.

Because the result of the calculation is $\mathscr{I} = \mathscr{I}_{\text{rigid}}$, the average velocity of nucleons passing a representative point is zero in just this coordinate

system and the assumption seems from the simplest considerations to have been the most reasonable one. The assumption is thus compatible with the result but it is of interest to see how sensitive the result is to changes in the assumption.

Let us modify the above calculation by assuming that the velocity-dependent term in the potential is quadratic in a slightly different coordinate system $y'$, $z'$ whose $z'$-axis makes an angle $(1+\gamma)\Phi$ with the laboratory axis and whose angular speed thus differs from that of the $y$, $z$ system by $\gamma\dot{\Phi}$, $\gamma$ being a (fairly small) constant. Thus in place of eq. (29) we start with

$$\begin{aligned} V &= U(y,z)+\tfrac{1}{2}c[(\dot{y}')^2+(\dot{z}')^2] \\ y' &= y\cos\gamma\Phi+z\sin\gamma\Phi, \qquad z' = -y\sin\gamma\Phi+z\cos\gamma\Phi \end{aligned} \tag{51}$$

and follow through the subsequent analysis exactly as before. In place of eq. (48), we arrive at the modified result

$$\mathscr{I}_T = \mathscr{I}_{\text{rigid}}\{1+(c/M_e)[\gamma/2-(1-3c/4M)\gamma^2]\}. \tag{52}$$

Thus, if the average angular velocity of the nucleons encountered by a representative nucleon is increased by a factor $(1+\gamma)$ the moment of inertia is increased by a factor differing from unity somewhat less than half as much. That is, the result is not very sensitive to the altered assumption.

In a more detailed consideration one might study separately different sorts of representative nucleons, those in open shells near the top of the Fermi sea (which classically move preponderantly in forward-rotating orbits [4b,c]) as do the most easily scattered nucleons they encounter), and those in closed shells, both those moving forward and those in retrogressive orbits. Even without trying to go into detail about how the weighting factor entering a formula like eq. (50) should depend on such quantities as the ease of scattering of the nucleons encountered, it seems inevitable that there will be a great deal of cancellation between the effects of opposite sign in the various categories of representative nucleons. The result should then tend to satisfy, but only approximately, a consistency criterion which may be stated as follows: The relevant average velocity of the other nucleons encountered by one nucleon is that of a rigid rotation with an angular velocity such that when multiplied by $\mathscr{I}_{\text{rigid}}$ it gives the angular momentum which is also obtained as the product of $\dot{\Phi}$ and the calculated moment of inertia $\mathscr{I}_T$. We have seen that this criterion is satisfied exactly by our calculated result for $\gamma = 0$. For it to be satisfied approximately requires that the bracket of eq. (52) be approximately equal to $(1+\gamma)$, that is, that $\gamma$ be small.

Though this argument is far from rigorous, it does depict some of the effects that must come into play and suggests that the $\gamma = 0$ assumption of eq. (29) is the most plausible simple basis for trying to relate moment of inertia to effective nucleon mass. The resulting moment of inertia is thus

fairly insensitive both to this introduction of an effective mass and to the manner of introducing it.

This simple result and its derivation show, first, that it is not at all obvious that one can obtain [8]) the desired factor one-half in the moments of inertia of highly deformed nuclei from $M_e$, in fact, that one probably cannot, and second, that in more refined consideration of the problem one must be very careful about handling the canonical momenta which involve both collective and particle velocities.

Other possible sources of the discrepancy, not closely associated with $M_e$, are pairwise interactions [3a]) of nucleons and deviations [4b]) from the simple harmonic-oscillator potentials here assumed. Whatever the explanation it will be desirable to understand at the same time why the observed moments of inertia are so well-behaved in their dependence on deformation.

Relevant conversations have been enjoyed with F. Coester, V. F. Weisskopf, A. de Shalit, T. H. R. Skyrme, R. J. Blin-Stoyle and J. H. D. Jensen.

## Appendix

Our treatment has been based on defining the moment of inertia in terms of the energy, $E_{\text{rot}} = P^2/2\mathscr{I}_T$, as in eq. (9), because this is the definition most closely associated with the observation of nuclear rotational energy levels. If this is to be the consequence of a Hamiltonian of the form

$$\mathscr{H} = P^2/2\mathscr{I}_T + h, \tag{53}$$

then the relation

$$(\hbar/i)\dot{\Phi} = \mathscr{H}\Phi - \Phi\mathscr{H} \tag{54}$$

gives the other relation commonly used as a definition of moment of inertia, $P = \mathscr{I}_T\dot{\Phi}$. In the case we have discussed, in which $P$ is a constant of the motion but $\dot{\Phi}$ is not, this is, more explicitly,

$$P = \mathscr{M}\hbar = \langle a|\mathscr{I}_T|a\rangle\langle \mathscr{M}, a|\dot{\Phi}|\mathscr{M}, a\rangle \tag{55}$$

and we have used $\mathscr{I}_T = \langle a|\mathscr{I}_T|a\rangle$ as the expectation value common to the states of a rotational band. It is this alternative definition that justifies the assumption that nucleon contributions to the moment of inertia are additive, $P$ being a sum of single-particle operators.

The derivations given above, either with or without the velocity dependence of the potential, may be carried out consistently and as simply in this form. From eq. (54) with the Hamiltonian of eq. (39), we have

$$\begin{aligned}\langle \mathscr{M}, a|\dot{\Phi}|\mathscr{M}, a\rangle &= \langle \psi_a^* + \textstyle\sum c_{\beta a}\psi_\beta^*|[(P - Mp/M_e)/\mathscr{I}_0]|\psi_a + \sum c_{\beta a}\psi_\beta\rangle \\ &= \mathscr{M}\hbar\langle a|(\mathscr{I} - (c/M_e)Mr^2)^{-1}|a\rangle - (2/\mathscr{I})(M/M_e)\textstyle\sum c_{\beta a}\langle\beta|p|a\rangle \\ &= \mathscr{M}\hbar/[\mathscr{I} - (c/M_e)\langle a|Mr^2|a\rangle + 2f_a].\end{aligned} \tag{56}$$

We define $\mathscr{I}_a$ by equating this to $P/\mathscr{I}_T = P/(\mathscr{I} + \mathscr{I}_a)$ and thus obtain $\mathscr{I}_a$ as in eq. (43), whence we proceed as before to eq. (48).

## References

1) K. W. Ford, Phys. Rev. **95** (1954) 1250; A. W. Sunyar, Phys. Rev. **98** (1955) 656; N. P. Heydenberg and G. M. Temmer, Phys. Rev. **99** (1955) 1609; Ann. Rev. Nucl. Sci. **6** (1956) 77
2) A. Bohr, Rotational States of Atomic Nuclei (E. Munskgaards Forlag, Copenhagen, 1954); S. Moskowski, Handbuch der Physik **39** (1957) 411
3) a) A. Bohr and B. R. Mottelson, Mat. Fys. Medd. Dan. Vid. Selsk. **30** (1955) 1;
b) G. Lüders, Z. Naturforsch. **11a** (1956) 617;
c) F. Coester, Nuovo Cimento **4** (1956) 1307; Proc. U. of Pittsburgh Conf. (June 6–8, 1957) p. 543;
d) J. G. Valatin, Proc. Roy. Soc. **238** (1956) 132;
e) Lipkin, de Shalit and Talmi, Phys. Rev. **103** (1956) 1773;
f) S. Hayakawa and T. Marumori, Progr. Theor. Phys. **17** (1957) 43;
g) F. Villars, Nuclear Physics **3** (1957) 240;
h) R. E. Peierls and J. Yoccoz, Proc. Phys. Soc. **70** (1957) 381 and 388;
i) J. J. Griffin and J. A. Wheeler, Phys. Rev. **108** (1957) 311
4) D. R. Inglis, a) Phys. Rev. **96** (1954) 1059; b) Phys. Rev. **103** (1956) 1786; c) Am. Journ. Phys. **26** (1958) 82
5) J. P. Elliott and T. H. R. Skyrme, Proc. Roy. Soc. A **232** (1955) 561
6) K. Brueckner and C. Levinson, Phys. Rev. **97** (1955) 1344;
H. A. Bethe and J. Goldstone, Proc. Roy. Soc. A **238** (1957) 551
7) V. F. Weisskopf, Nuclear Physics **3** (1957) 423; J. H. van Vleck, Phys. Rev. **48** (1935) 367; Ross, Lawson and Mark, Phys. Rev. **107** (1956) 401
8) R. J. Blin-Stoyle, Nuclear Physics **2** (1956) 169

2.A,1 *Nuclear Physics* 8 (1958) 139—142; © *North-Holland Publishing Co., Amsterdam*
Not to be reproduced by photoprint or microfilm without written permission from the publisher

# CROSS-SECTIONS FOR (n, p) AND (n, α) REACTIONS OF MAGNESIUM WITH 14.8 MeV NEUTRONS; A NEW ISOTOPE $Na^{26}$

M. J. NURMIA † and R. W. FINK
*Departments of Physics and Chemistry, University of Arkansas, Fayetteville, Arkansas* ††

Received 16 June 1958

**Abstract:** Irradiation of natural magnesium metal or highly enriched $Mg^{26}O$ with 14.8 MeV neutrons gives rise to a new activity with a half-life of $1.04 \pm 0.03$ s which is assigned to $Na^{26}$ from the $Mg^{26}$(n, p) reaction. The decay appears to proceed mainly by high energy (> 5 MeV) $\beta$-particles. The reaction cross-section is $50 \pm 5$ mb, based on a value of 89 mb for the $O^{16}$(n, p)$N^{16}$ reaction at 14.8 MeV. Simultaneously, the $Mg^{26}$(n, α) reaction produces well-known $Ne^{23}$ with a cross-section of $89 \pm 5$ mb, based on the $O^{16}$(n, p) yield. A new measurement of the $Ne^{23}$ half-life gives a value of $38.0 \pm 0.3$ s. The cross-section for the $Mg^{25}$(n, p)$Na^{25}$ reaction is $60 \pm 10$ mb based on the $O^{16}$(n, p) reaction.

As part of a systematic investigation on the reactions in light nuclei caused by fast neutrons, natural magnesium metal was irradiated with approximately $10^{10}$ DT(14.8 MeV) neutrons/$cm^2 \cdot$ sec from the 400 kV Cockcroft-Walton accelerator at the University of Arkansas [1]) †††.

The samples were machined circular discs with a diameter of 1.6 cm and 2 to 3 mm thick, mounted in holes in polyethylene plate 2.8 cm square to facilitate the use of a rapid transfer and recording system *. As detector a $4 \times 4$ cm plastic scintillator mounted in a lead shield was used, a typical blank sample one second after a 7-second bombardment exhibiting 20 counts/sec (mostly due to $N^{16}$ arising from frost on the target) and decaying to about 2 counts/sec during the first 300 s.

In addition to 15.0-hour $Na^{24}$, a composite activity from a mixture of 38-second $Ne^{23}$ from the $Mg^{26}$ (n, α) reaction [3]) and 60-second $Na^{25}$ from the $Mg^{25}$(n, p) reaction [4]), and an activity with half-life of $1.04 \pm 0.03$ s were observed (see fig. 1). The last activity, consisting mainly of high energy (> 5 MeV) beta-particles, has not been reported previously, and it is assigned to a new isotope of sodium, $Na^{26}$.

To verify this assignment, samples of natural and enriched MgO (containing 99 % $Mg^{26}O$) were prepared by pressing the oxide with paraffin to

† Present address: University of Helsinki, Helsinki, Finland.
†† Supported in part by the U.S. Atomic Energy Commission.
††† For a detailed report on this accelerator see ref.[2]).
* To be described in detail elsewhere.

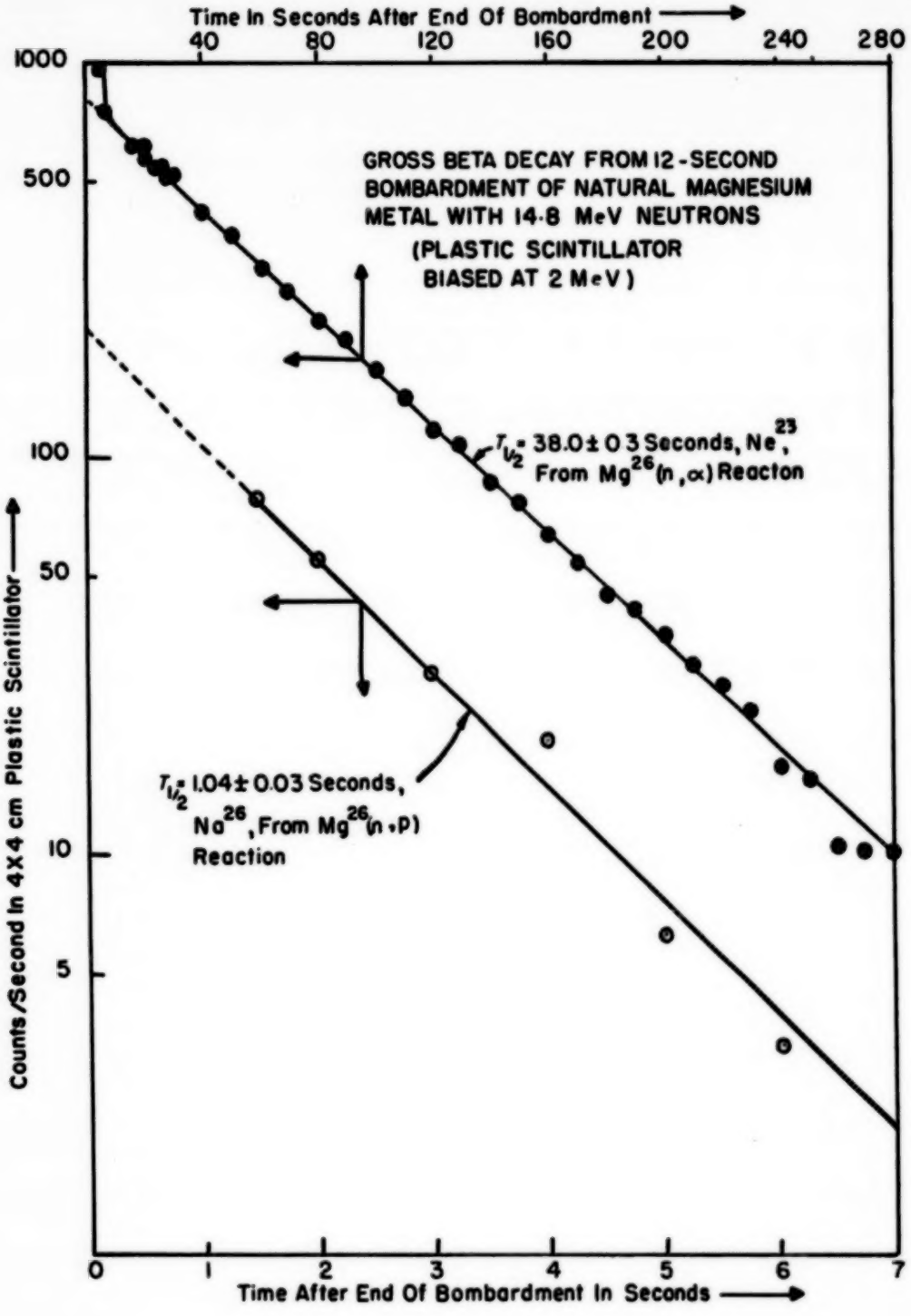


Fig. 1

form thin discs 1.6 cm in diameter for mounting in the polyethylene plates. Upon irradiation of these, the 1.04-second activity was found to be present

in the expected amount (see fig. 2). From results obtained with the enriched $Mg^{26}O$ sample, a new value of $38.0 \pm 0.3$ s was obtained for the half-life of $Ne^{23}$.

In determining the cross-sections of these reactions at 14.8 MeV, a series of bombardments was performed with the bias setting of the plastic scintillation counter being varied from 0.5 to 5 MeV. In the region from 1 to 2.5

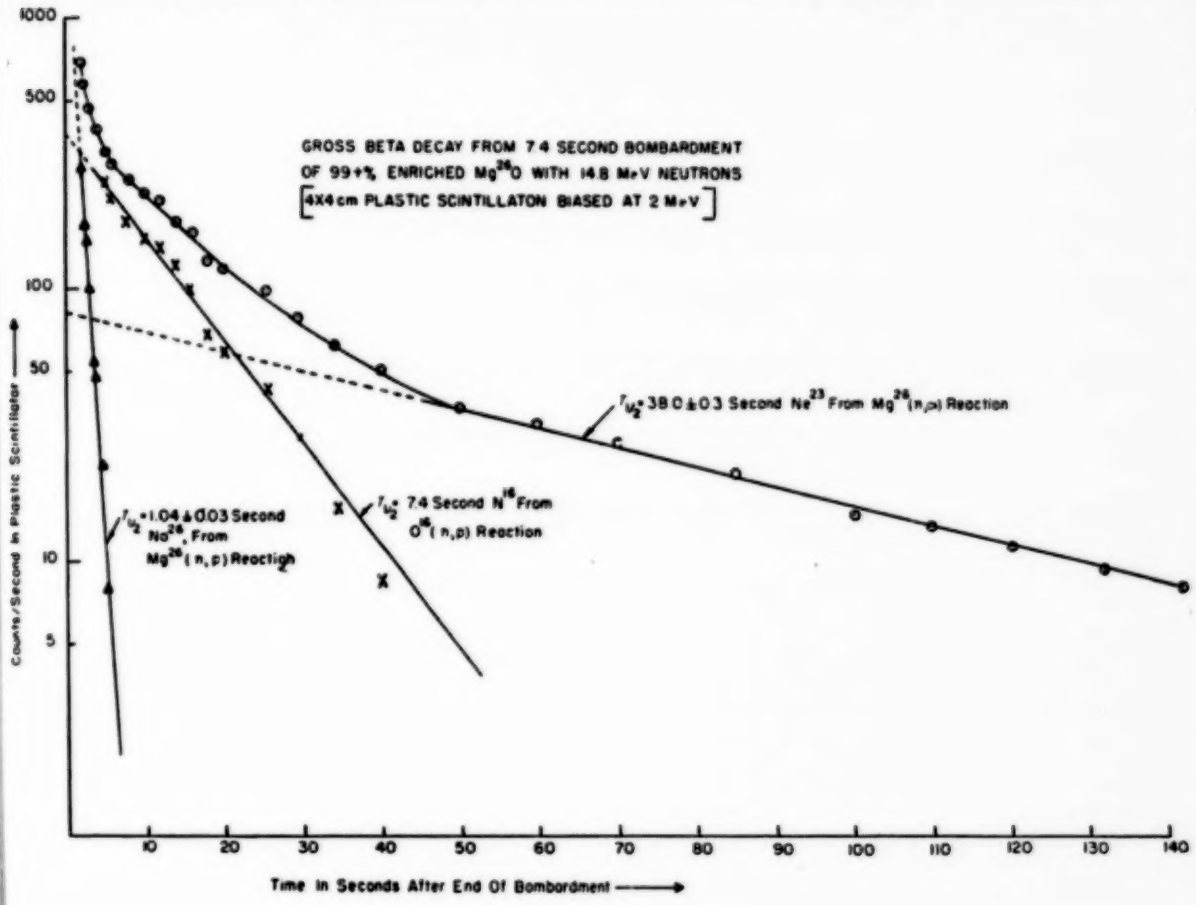


Fig. 2

MeV, the ratio of the observed activities changed very little, and by assuming equal detection efficiencies for all observed activities, the results shown in table 1 were obtained. From the results on natural MgO and natural Mg metal, we obtained an independent value for the yield of $Na^{26}$ relative to that of $N^{16}$:

$$\sigma[Mg^{26}(n, p)]/\sigma[O^{16}(n, p)] = 0.60$$

leading to a mean value of $0.56 \pm 0.05$ for this ratio (table 2). Similarly, from the ratio $S(C)/S(O)$, upon subtracting the known contribution of $Ne^{23}$, we obtain $\sigma[Mg^{25}(n, p)]/\sigma[O^{16}(n, p)] = 0.65$. Also, the ratio of 60 second $Na^{25}$ to 38 second $Ne^{23}$ required to produce the observed composite

TABLE 1

Relative yields at saturation for irradiations with 14.8 MeV neutrons

| Substance irradiated | Radioactive product | Cross-section ratio † |
|---|---|---|
| $Mg^{26}O$ | $Na^{24}$ | $S/S(O) = 0.53$ |
| $Mg^{26}O$ | $Ne^{23}$ | $S/S(O) = 1.00$ |
| Natural MgO | $Ne^{23}+Na^{25}$ | $S(C)/S(O) = 0.175$ |
| Natural Mg | $Na^{24}$ | $S/S(C) = 0.382$ |

† $S(O)$ stands for the $O^{16}(n, p)N^{16}$ cross-section which is being used as a standard, and $S(C)$ signifies the apparent cross-section for the $Ne^{23}+Na^{25}$ composite activity, not corrected for isotopic abundances.

half-life was found to be 0.645, which gives an independent value of 0.70 for the above ratio. Because of the relatively large uncertainties in both methods, the final result is given as

$$\sigma[Mg^{25}(n, p)]/\sigma[O^{16}(n, p)] = 0.67 \pm 0.10.$$

By assuming a value of 89 mb for the $O^{16}(n, p)$ reaction [5]) at 14.8 MeV, our results can be expressed in terms of absolute cross-sections as summarized in table 2.

TABLE 2

Summary of experimental results

| Reaction | Product nucleide | Measured half-life (sec) | $S/S(O)$ | Reaction cross-section † (mb) |
|---|---|---|---|---|
| $Mg^{26}(n, p)$ | $Na^{24}$ | $1.04 \pm 0.03$ | $0.56 \pm 0.05$ | $50 \pm 5$ |
| $Mg^{25}(n, p)$ | $Na^{25}$ | 60 | $0.67 \pm 0.10$ | $60 \pm 10$ |
| $Mg^{26}(n, \alpha)$ | $Ne^{23}$ | $38.0 \pm 0.3$ | $1.00 \pm 0.05$ | $89 \pm 5$ |

† These do not include the uncertainty in the value of the $O^{16}(n, p)$ cross-section, $89 \pm 30$ mb (ref.[5]).

Of the cross-sections given in table 2, only the $Mg^{25}(n, p)$ value has been reported previously. Paul and Clarke [6]) obtained a value of $44.9 \pm 18$ mb for this cross-section but it is not clear whether they took into account the contribution of $Ne^{23}$, so a direct comparison with our result is not possible.

An investigation into the decay scheme of $Na^{24}$ is in progress.

We are indebted to Mr. J. E. Wray of the Accelerator Laboratory for assistance in carrying out the bombardments.

## References

1) Bronner, Ehlers, Eukel, Gordon, Marker, Voelker and Fink, High Current 400 kV Cockcroft-Walton Accelerator for Nuclear Chemistry Research (to be published)
2) Annual Progress Report, AEC Contract, University of Arkansas (March 1, 1958) pp. 1–32
3) Amaldi, D'Agostino, Fermi, Pontecorvo, Rasetti and Segrè, Proc. Roy. Soc. A **149** (1935) 522
4) Huber, Lienhard, Scherrer and Wäffler, Helv. Phys. Acta **17** (1944) 139
5) H. C. Martin, Phys. Rev. **93** (1954) 498
6) E. B. Paul and R. L. Clarke, Can. J. Phys. **31** (1953) 267

1.E.1 *Nuclear Physics* 8 (1958) 143—154: © *North-Holland Publishing Co., Amsterdam*
Not to be reproduced by photoprint or microfilm without written permission from the publisher

# NEUTRON-DEFICIENT IRIDIUM ISOTOPES

R. M. DIAMOND† and J. M. HOLLANDER
*Radiation Laboratory and Department of Chemistry, University of California, Berkeley, California* ††

Received 7 May 1958

**Abstract:** A study has been made of the isotopes of iridium which are produced from natural rhenium by irradiations with alpha particles in the energy range 25 to 45 MeV. The known iridium isotopes of masses 190, 189, and 188 were observed, and in addition $Ir^{187}$, $Ir^{186}$, and $Ir^{185}$ were identified by means of the threshold energy for their production. Analyses are based upon scintillation spectra and conversion electron spectra taken with high-resolution permanent-magnet spectrographs.

The interesting situation is encountered in which the three isotopes $Ir^{187}$, $Ir^{186}$, and $Ir^{185}$ all have very similar half-lives; that of $Ir^{187}$ is 13 hours, $Ir^{186}$ 16 hours and $Ir^{185}$ 15 hours. A preliminary study of the radiations from the odd mass isotopes has been made, and also some new transitions in $Ir^{186}$, $Ir^{188}$, and $Ir^{190}$ are reported.

## 1. Introduction

In the region of atomic number between 74 and 78 significant changes in the order and the nature of nuclear energy levels may be expected. The preceding elements, $64 < Z < 74$, have been characterized by their rotational structure [1]), and in elements as heavy as tungsten, $Z = 74$, well-defined rotational bands appear and have been extensively studied [2]). At $Z \geqq 78$ the behaviour of nuclear levels has been described best in terms of the single-particle shell model. It is of interest, therefore, to obtain experimental information about the levels of nuclei in the intermediate region, for which there is at present little theoretical description. The isotopes of osmium, $Z = 76$, would be good examples, and their levels can be populated by the electron-capture decay of light iridium nuclei or by the beta decay of heavy rhenium nuclei. We here report on the synthesis of two new neutron-deficient isotopes of iridium, $Ir^{185}$ and $Ir^{187}$, and on the results of our preliminary study of the radiations from these isotopes and from $Ir^{189}$. Some additional data are given concerning transitions in $Os^{186}$, $Os^{188}$, and $Os^{190}$ following electron capture decay of the corresponding iridium nuclei.

## 2. Experimental Procedure

The light iridium isotopes were produced by $(\alpha, xn)$ reactions from irradiation in the Crocker 60-inch cyclotron of "thick" targets of rhenium

† On leave from Cornell University, Department of Chemistry, Ithaca, N. Y.
†† Work done under the auspices of the U.S. Atomic Energy Commission.

metal foil of natural isotopic abundance (37 % $Re^{185}$, 63 % $Re^{187}$). Alpha particles of 25 to 27, 33 to 34, and 45 MeV energy were used. Targets were either 5-mil foils bombarded singly or 1-mil foils bombarded in stack form. In this way the relative yields of the various isotopes could be varied and, in particular, the production of $Ir^{185}$ by $Re^{185}$ ($\alpha$, 4n) and of $Ir^{186}$ by $Re^{185}$ ($\alpha$, 3n) could be selectively eliminated.

After irradiation, carrier-free iridium fractions were obtained from the target foils by one of the two following procedures:

1. The rhenium foils were dissolved in concentrated nitric acid and the solution boiled to near-dryness to volatilize osmium as $OsO_4$. The small volume of residue was made about 4 *M* in $HNO_3$ and 1 *M* in HCl and absorbed onto a Dowex-1 anion exchange column which had been pretreated with a solution 4 *M* in $HNO_3$ and 1 *M* in HCl. The column was then rinsed with more of this acid mixture in order to remove rhenium. Afterwards, the iridium was stripped from the column with a solution 4 *M* in HCl and 1 *M* in $NH_2OH$. Concentrated nitric acid was added and the mixture was boiled in order to destroy the hydroxylamine and to reduce the volume.

2. Same initial treatment to remove the osmium. After evaporation to a small volume, the solution was diluted to about 0.5 *N* $HNO_3$ and passed through a Dowex-50 cation exchange column; under these conditions iridium is absorbed on the resin but rhenium can be washed through with several column volumes of 0.15 *M* $HNO_3$. The iridium was then eluted from the column with 8 *M* $HNO_3$ and boiled down to a small volume.

The following techniques were used to observe the radiations of the iridium fractions. Gross decay curves of the samples were obtained with proportional counters. Gamma-ray spectra were studied with a scintillation spectrometer employing a sodium iodide crystal, $1\frac{1}{2}$ in. in diameter by 1 in. high, coupled to a Penco 100-channel pulse-height analyzer. With this crystal the energy resolution of the 662 keV gamma ray of $Cs^{137}$ was $\approx$ 10 %. Electron spectra, upon which much of the analysis is based, were obtained primarily with the high-resolution ($\approx$ 0.1 %) permanent-magnet spectrographs of the type described by Smith and Hollander [3]). Use was made of six different spectrographs, with field strengths 50, 100, 125, 150, 200, and 340 gauss, respectively. Spectrograph sources were prepared by electrolytic deposition of iridium from dilute $NH_4HSO_4$ solutions onto 10-mil platinum wires. Some electron spectra in the higher energy region were also obtained with a lower resolution ($\approx$ 1 %) lens spectrometer.

## 3. Experimental Results

### 3.1. IRIDIUM-190 AND IRIDIUM-189

Two isomers of $Ir^{190}$ are known, the 11 day ground state discovered by Goodman and Pool [4]), and the 3 hour isomer found by Chu [5]). On the basis of

studies of the gamma radiation, Aten, deFeyfer, Sterk and Wapstra [6]), have given a decay scheme for these isomers; that of $Ir^{190m}$, which decays to the 10 minute $Os^{190m}$ isomer, has been elaborated further by Scharff-Goldhaber, Alburger, Harbottle and McKeown [7,8]).

$Ir^{189}$, which has an 11-day half-life similar to that of $Ir^{190}$, was discovered by Smith and Hollander [9]) as the daughter of 11-hour $Pt^{189}$. They observed from scintillation spectroscopy that its principal electromagnetic radiation is a 245-keV photon; higher energy photons are less intense by at least a factor ten. Recently, Scharff-Goldhaber *et al.*[7]) have shown that a 5.7 hour isomer of $Os^{189}$ is produced by the decay of 11-day $Ir^{189}$.

In this work, we have attempted to distinguish the photons of 11-day $Ir^{190}$ from those of 11-day $Ir^{189}$ by comparisons of the relative photon intensities in the scintillation spectrum as a function of bombarding energy. At the lowest energy (25 to 27 MeV) the yield ratio $Ir^{190}/Ir^{189}$ is expected to be higher by a factor of six or seven than at 33 to 34 MeV although the total cross sections will be lower for both products. We find, in fact, that the intensity ratio of the prominent 187 keV photon of $Ir^{190}$ to that of the prominent 245 keV photon of $Ir^{189}$ does increase by a factor of $\approx 7$ in the above bombarding energy interval.

The low-energy transitions (30 to 90 keV) cannot be assigned in the above manner because they are not resolved in the scintillation spectrum. In the conversion electron spectrum the lines of the low energy transitions are much more intense than those of the 245-keV transition, hence they are assigned to $Ir^{189}$; the decay of $Ir^{190}$ is fairly well understood and it is not expected that intense low-energy transitions other than the 39 keV isomeric transition of $Os^{190m}$ will be found in its decay.

In table 1 we present a brief summary of the information we have obtained about the transitions of 11-day $Ir^{190}$ and 11-day $Ir^{189}$. Transition energies are given, and multipolarity assignments are made from K/L ratios and L and M subshell conversion ratios. Fig. 1 shows the levels of $Os^{190}$ presently known. The main level order is from the work of Aten *et al.*[6]) and the isomeric state is from that of Scharff-Goldhaber *et al.*[8]); the second 2+ state and the energies of the lower levels are from this work. The energy of the transition from the 4+ to the 2+ state in $Os^{190}$ has been given as 356 keV by Aten *et al.*[6]) and as 359 by Scharff-Goldhaber *et al.*[8]). We observe this transition at 361.2 keV, and in addition a transition of 371.4 keV is seen in the electron spectrum. We suggest that the latter transition be assigned as the $2+ \rightarrow 2+$ transition and that the 558 keV transition is the crossover to the ground state. The sum $371.4+186.7 = 558.1$ is in agreement with the energy of the crossover transition. Also, the energy of this second 2+ state agrees well with the value obtained by extrapolation from the $Os^{186}$ and $Os^{188}$ energies (see fig. 3) and with the value of 0.57 MeV found from the Coulomb excitation [10]) of $Os^{190}$.

Transitions of 407, ≈525, 568, and ≈610 keV are assigned to $Ir^{190}$ decay, but their positions in the level scheme remain unknown.

We have assigned most of the low-energy transitions to the decay of $Ir^{189}$.

TABLE 1

Transitions from decay of $Ir^{189}$ and $Ir^{190}$

| Transition energy (keV) | Electron lines seen † | Photon observed (scint spect) | Multipole order | Mass assignment |
|---|---|---|---|---|
| 30.8 | $L_{III}(22)$ $M_I$ $M_{III}(6)$ N | | M3 | 189 |
| 33.3? | $L_{II}$ $L_{III}$ M | | E2 | |
| 36.2 | $L_I(35)$ $L_{II}$ $M_I(13)$ $N_I$ | | M1 | 189 |
| 56.4 or 117.3 | $L_I$ $M_I$ or K $L_{II}$ $L_{III}$ | | | |
| 59.0 | $L_I(55)$ $L_{II}(5)$ $M_I$ | | M1 | 189 |
| 69.5 | $L_I(\geq 100)$ $L_{II}(\geq 100)$ $L_{III}(\geq 100)$ $M_I$ $M_{II}(35)$ $M_{III}(35)$ N(25) O | | M1-E2 | 189 |
| 95.2 | K $L_I(3)$ $L_{II}$ $L_{III}$ M N | | M1 | 189 |
| 135.8 | K $L_I(2)$ $L_{II}$ | | M1 | |
| 147.1 | K | | | |
| 149.9 | K | | | |
| 164.0 | K | | | |
| 185.9 | K | | | |
| 186.7 | K $L_{II}$ $L_{III}$ $M_{II}$ $M_{III}$ N | yes | E2 | 190 |
| 188.6 | K | | | |
| 206.2 | K | | | |
| 216.6 | K $L_I$ $L_{II}$ | | | |
| 219.3 | K $L_I$ | | | |
| 233.6 | K $L_I$ $L_{II}$ | | | |
| 245.0 | K(15) $L_I$ $L_{II}(6)$ $L_{III}(6)$ $M_{II}$ $M_{I,I}$ N | yes | E2 | 189 |
| 275.8 | K $L_I$ | | | |
| 361.2 | K | | | 190 |
| 371.4 | K | yes | | 190 |
| 407 | K | | | 190 |
| 520–530 | | | | 190 |
| 558 | K | yes | | 190 |
| 568 | K | | | 190 |
| 600–620 | | yes | | 190 |
| ≈ 700 | | yes | | |
| 760 | K | | | |
| ≈ 800 | | yes | | |
| ≈1000 | | yes | | |

† Approximate intensity values of the stronger electron lines, given in parentheses following the shell designations, are for identification only and not for purposes of analysis.

Because of the preliminary character of the data, we have not attempted to construct a level scheme for $Os^{189}$. However, certain sum relationships are suggestive and are given in table 2. The 30.8 keV transition seen here from $Ir^{189}$ decay is assigned on the basis of its high $L_{III}$ and $M_{III}$ conversion as an

M3; this is without doubt the same transition as that observed by Scharff-Goldhaber *et al.*[8]) in the decay of the 5.7 hour $Os^{189}$ isomer. The transition is relatively weak in the $Ir^{189}$ spectrum, so that it appears that the isomeric

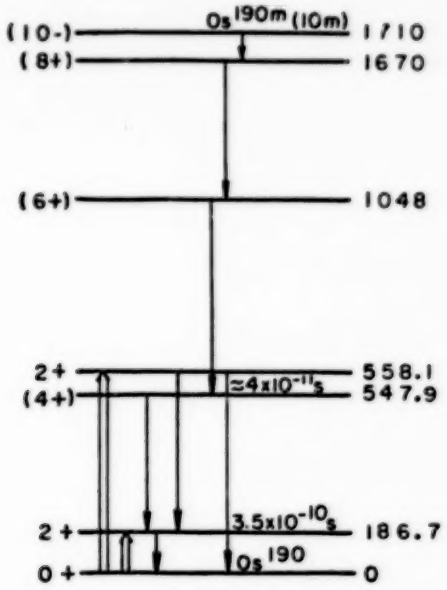


Fig. 1. $Os^{190}$ level scheme.

TABLE 2

$Ir^{189}$ transition sums

| | |
|---|---|
| (a) | 30.8+188.6 = 219.4 |
| | 69.5+149.9 = 219.4 |
| | Crossover = 219.3 |
| (b) | 95.2+149.9 = 245.1 |
| | 59.0+185.9 = 244.9 |
| | Crossover = 245.0 |
| (c) | 36.2+149.9 = 186.1 |
| | Crossover = 185.9 |
| (d) | 69.5+206.2 = 275.7 |
| | Crossover = 275.8 |
| (e) | 56.4+149.9 = 206.3 |
| | Crossover = 206.2 |
| (f) | 36.2+ 59.0 = 95.2 |
| | Crossover = 95.2 |
| (g) | 245.0+ 69.5 = 314.5 |
| | 219.3+ 95.2 = 314.5 |

state is not heavily populated in $Ir^{189}$ decay. The most intense transition is the one at 69.5 keV, assigned as a mixed M1-E2; this probably proceeds to the ground state and hence defines the second excited state of $Os^{189}$ to be 69.5 keV. From the sum relationships other states may be postulated to lie at 219.3, 255.5, 275.8, and 314.5 keV; however the transition orders must be

verified by intensity and coincidence studies before these states can be considered as definite.

### 3.2. IRIDIUM-188

A 41 hour activity in iridium was assigned to mass 188 by Chu [5]) on the basis of its production by an (α, 3n) reaction on enriched $Re^{187}$. Smith and Hollander confirmed this assignment [9]) and observed gamma rays from $Ir^{188}$ at approximately 150, 475, and 625 keV; these transitions appear to be the same as the lowest energy transitions found [11]) in the beta-decay of $Re^{188}$.

TABLE 3

| Transition energy (keV) | Electron lines seen† | Photon observed (scint spect) |
|---|---|---|
| 155.0 | K(≈ 350) $L_I$(70) $L_{II}$(320) $L_{III}$(250) $M_{II}$ $M_{III}$ N O | yes |
| 323.0 | K(≈ 12) L | yes |
| 478.5 | K(≈ 30) L M | yes |
| 633.5 | K L | yes |
| 825 | K | yes |
| 830 | K | |
| 1212 | K | yes |
| 1330 | | yes |
| 1450 | | yes (complex) |
| 1600 | | yes |
| 1710 | | yes( complex) |
| 1940 | | yes |
| 2050 | | yes |
| 2180 | | yes |

† See footnote of table 1.

The 41 hour half-life of $Ir^{188}$ is sufficiently different from that of the other iridium isotopes produced in this work to allow its prominent gamma transitions to be identified from spectra taken at timed intervals on the scintillation spectrometer and with the electron spectrographs. These are listed in table 3. The principal transitions observed at 155.0, 478.5, and 633.5 keV are those mentioned above. The 825- (or 830-) keV gamma ray is possibly the 828 keV transition observed from the $\beta$- decay of $Re^{188}$.

The 323.0 and 1212 keV transitions, observed here in both the scintillation and electron spectra, have not been reported from $Re^{188}$ decay. It is tempting to postulate that the 323.0 keV transition is the one between the 4+ and 2+ states of the ground-state rotational band because the energy so obtained for the 4+ state lies reasonably between the corresponding 4+ states of $Os^{186}$ and $Os^{190}$. The plausibility of this assignment seems to be marred by the fact that the postulated 478-keV level has not been seen from $Re^{188}$ decay. It is possible, however, that the spin of $Re^{188}$ is low while that of $Ir^{188}$ is high. Note

that the higher energy gamma rays observed in this study of $Ir^{188}$ do not correspond to those observed from $Re^{188}$ decay, which is an indication that

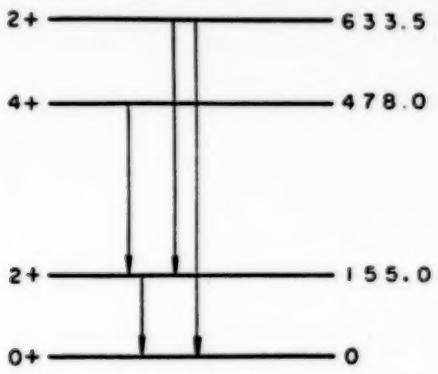


Fig. 2

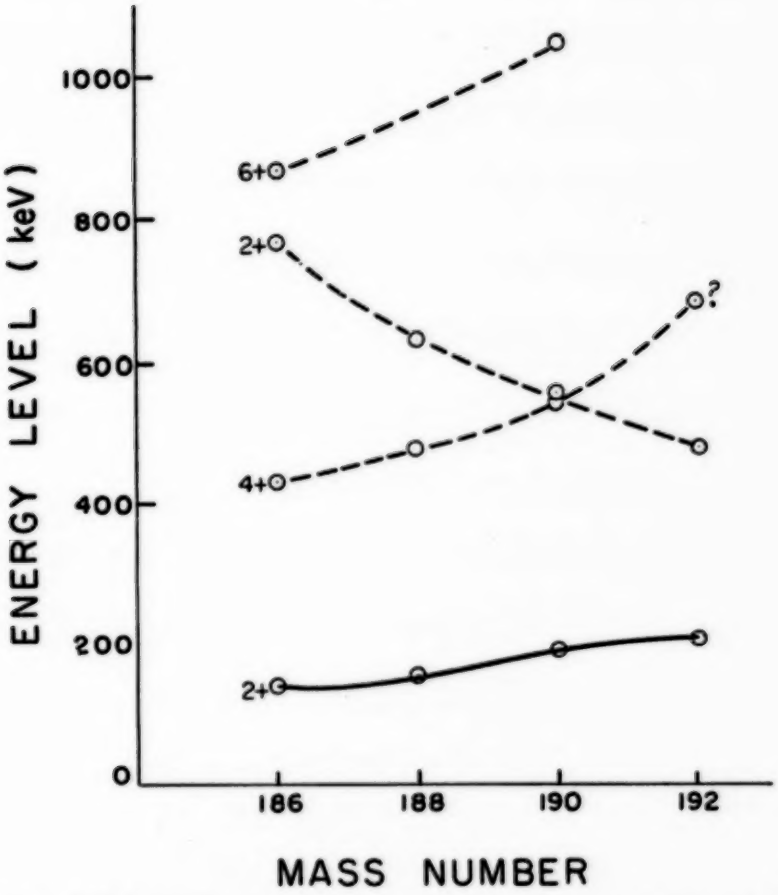


Fig. 3. Correlation diagram of energy levels of even-mass osmium nuclei.

there are other significant differences in the final states populated by the decay of these two nucleides.

Fig. 2 shows the lower levels of $Os^{188}$, and fig. 3 gives a correlation diagram of

the energies of the low-lying states in the even osmium isotopes. (We have listed the 691-keV state of $Os^{192}$ as 4+ even though there is some experimental evidence against this assignment [12]). As shown in the correlation diagram the energies of the rotational states (2+, 4+, and 6+) are increasing with mass number because these nuclei lie just beyond the "rotational" region and the moments of inertia are decreasing rapidly as the next closed shell is approached. But at the same time the energy of the vibrational (Goldhaber-Weneser) 2+ state is dropping as the nucleus becomes "softer" toward this type of excitation.

### 3.3. IRIDIUM-187

In irradiations of rhenium foils at an initial alpha particle energy of 25 to 27 MeV, i.e., below the threshold for the production of $Ir^{185}$ and $Ir^{186}$, several short-lived conversion electron lines and gamma rays were observed in the separated iridium fraction. By comparing the intensities of the more prominent of these electron lines in a series of timed exposures in the electron spectrographs with lines of known intensities in a group of standard plates, we obtained a value of $13 \pm 3$ hours for the half-life of this new activity. Actually, the magnitude of the half-life relative to those of $Ir^{185}$ and $Ir^{186}$ determined in the same manner can be measured more accurately than the absolute value, and the half-life is definitely shorter by 2 to 3 hours than those of $Ir^{185}$ and $Ir^{186}$.

The new activity might possibly be due to an isomer in $Ir^{188}$, $Ir^{189}$, $Ir^{190}$, or even in $Os^{188}$, $Os^{189}$, $Os^{190}$, but has been assigned to $Ir^{187}$ for the following reasons. It cannot be assigned to an osmium isomer because the half-life is shorter than that of the parent iridium isotope and yet no growth and subsequent decay with the parent half-life was observed. It is unlikely to be an isomer in $Ir^{188}$ or $Ir^{190}$ because the resulting even $Os^{188}$ or $Os^{190}$ nuclei formed would not be expected to have many low-lying levels (and no such levels have been seen in $Ir^{188}$ or $Ir^{190}$ decay, see above), whereas the most intense transitions of the decay under consideration are of low energy. Furthermore, no known transitions in $Os^{188}$ or $Os^{190}$ are observed as would be expected, and as are observed in the decay of the 3 hour $Ir^{190m}$. The number of intense low energy transitions strongly suggest an odd mass iridium isotope, but an isomer of $Ir^{189}$ is unlikely since its decay into excited levels in $Os^{189}$ would almost surely cascade into at least one of the several low-lying levels observed from the decay of 11-day $Ir^{189}$, and such transitions are not observed. Thus $Ir^{187}$ is the only remaining assignment for this 13-hour activity. Consistent also with this assignment were the variations in the relative yields of prominent transitions of $Ir^{186}$, $Ir^{188}$, and the 13-hour activity as a function of bombarding alpha-particle energy, as compared with the results obtained by John [13] on $(\alpha, x\text{n})$ cross-sections of lead ($Z = 82$).

TABLE 4

Transitions from decays of $Ir^{185}$, $Ir^{186}$, and $Ir^{187}$

| Transition energy (keV) | Electron lines seen | Photon observed | Multipole order | Mass assignment |
|---|---|---|---|---|
| 25.5 | $L_I$ $M_I$ N | | M1 | 187 |
| 37.4 | $L_I$ $L_{II}$ $L_{III}$ $M_I$ $N_I$ O | | M1-E2 | 185 |
| 59.9 | $L_I$ $L_{II}$ $M_I$ N | | M1 | 185 |
| (64.5) | $L_I$ | | | 187 |
| 65.2 | $L_{II}$ $L_{III}$ $M_{II}$ $M_{III}$ N O | | E2 | 187 |
| 70.8 | $L_I$ $L_{II}$ $M_{I,II}$ N | | | 186 or 187 |
| 74.2 | $L_I$ $L_{II}$ $M_I$ N | | M1 | 187 |
| 75.0 | $L_{II}$ $L_{III}$ $M_{II}$ $M_{III}$ N | | E2 | 187 |
| 90.5 | K $L_I$ $L_{II}$ | | | 187 |
| 97.3 | $L_I$ $L_{II}$ $L_{III}$ $M_{II}$ $M_{III}$ N O | | E2-(M1) | 185 |
| 100.8 | K $L_I$ $L_{II}$ $M_I$ | | M1 | 185 |
| 104.4 | K $L_I$ | | | 185 |
| 113.1 | K $L_I$ $L_{II}$ $L_{III}$ M | | M1-E2 | 187 |
| (115.6) | K | | | |
| 137.2 | K $L_I$ $L_{II}$ $L_{III}$ $M_{I,II}$ $M_{III}$ N O | yes | E2 | 186 |
| 149.9 or 89.0 | K or $L_I$ | | | possibly 185 |
| 153.6 or 92.7 | K or $L_I$ $M_I$ | | | 185 |
| (162.9) | K | | | 186 or 187 |
| (163.6) | K | | | 186 or 187 |
| 177.6 | K $L_I$ $L_{II}$ $L_{III}$ | yes | M1 | 187 |
| 187.5 | K $L_I$ $L_{II}$ $L_{III}$ M | yes | M1-E2 | 187 |
| 252.6 | K | | | |
| 254.4 | K $L_I$ | | | 185 |
| 296.9 | K $L_I$ $L_{II}$ $L_{III}$ $M_{II,III}$ N | yes | E2 | 186 |
| 299.9 | K | yes | | |
| 303.1 | K | yes | | probably |
| 306.1 | K | yes | | 185 or 186 |
| 309.7 | K | yes | | |
| 314.0 | K $L_{II,III}$ | yes | | 187 |
| 351.8 | K | | | probably 185 or 186 |
| 401.0 | K $L_{I,II}$ | | | 187 |
| 421.6 | K | | | 185—186 |
| 427.2 | K $L_I$ | yes | | 187 |
| 434.8 | K $L_{I,II}$ $L_{III}$ M N | yes | E2 | 186 |
| 442.2 | K | | | probably 187 |
| 493 | K $L_{I,II}$ | yes | | probably |
| 502 | K | yes | | 186 or 187 |
| 577 | K L | yes | | |
| 586 | K L | yes | | probably |
| 612 | K L M | yes | | 186 or 187 |
| 623 | K | yes | | |
| 631 | K | | | probably 186 |
| 768 | K | yes | | probably |
| 775 | K | yes | | 186 |
| 842 | K | | | |
| 914 | K L | yes | | probably 187 |
| 923 | K | yes | | 186 or 187 |
| 979 | K | yes | | probably |
| 990 | K | yes | | 187 |
| 1099 | K | | | |

The transitions assigned to $Ir^{187}$ decay, as well as those of $Ir^{186}$ and $Ir^{185}$, are listed in table 4, as are also some weak and some higher energy transitions which it was not possible to assign any more definitely than to these shorter lived isotopes.

### 3.4. IRIDIUM-186

Chu [5]), in 1950, synthesized an 11.8 hour iridium activity which he assigned to $Ir^{187}$ on the basis of excitation function experiments. A 14-hour iridium activity, obtained by Smith and Hollander [9]) as the daughter of a 2.5 hour platinum activity, was assigned to either mass 186 or 187, with 187 preferred. The principal radiations were reported to be transitions of 135, 300, and 435 keV. Scharff-Goldhaber *et al.*[8]) have made a definite assignment of this 14-hour iridium activity to mass 186 on the basis of the systematics of levels of the even-mass osmium isotopes and have observed transitions at 137, 297, 434, 625, and 773 keV, as well as several at higher energies. From K to L conversion ratios the multipolarities of the three lowest energy transitions were assigned as E2 and were interpreted as the cascade from the third rotational level ($6+ \rightarrow 4+ \rightarrow 2+ \rightarrow 0+$); the energy ratios are close to those calculated from the rotational formula,

$$E_i = \frac{\hbar^2}{2\mathscr{I}} I(I+1).$$

In this work we have established the transitions that belong to mass 186 by an observation of the particular electron lines and photons that disappear from the complex spectrum when the alpha particle bombarding energy is

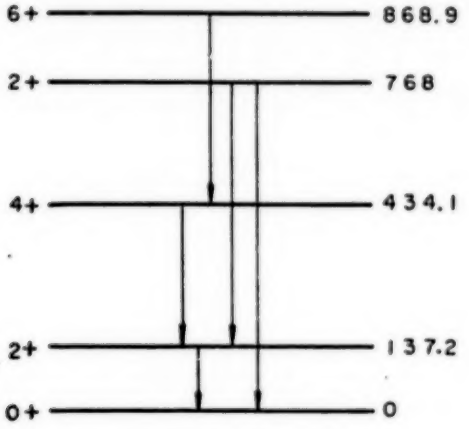


Fig. 4. $Os^{186}$ level scheme.

lowered from 33-34 MeV (threshold for production of $Ir^{185}$) to 25–27 MeV (threshold for production of $Ir^{186}$); such transitions are assigned to $Ir^{186}$. The assignment in this manner of the 137.2, 296.9, and 434.8 keV gamma rays to $Ir^{186}$ is in agreement with the work of Scharff-Goldhaber *et al.* These,

together with the 631 and 769 keV transitions in $Os^{186}$ previously known [14]) from the $\beta^-$ decay of $Re^{186}$ and also observed in this work, allow the scheme shown in fig. 4 to be constructed for the lower levels of $Os^{186}$. Again, by comparing the intensities of the most prominent of these conversion lines in a series of timed spectrograph exposures with lines of known intensity on standard plates, we have obtained a value for the half-life of $Ir^{186}$ of $16\pm3$ hours. The conversion lines and gamma rays definitely assigned to $Ir^{186}$ are listed in table 4. Some of the higher-energy unassigned transitions given there may also belong to $Ir^{186}$.

### 3.5. IRIDIUM-185

With alpha particles of 45 MeV initial energy $Ir^{185}$ is produced from rhenium by the reaction $Re^{185}(\alpha, 4n)\ Ir^{185}$; there are simultaneously produced the heavier isotopes of iridium from lower order reactions. The $Ir^{185}$ radiations can be distinguished, and the mass assignment made, by repeating the bombardment with alpha particles of initial energy lower than the threshold for the $(\alpha, 4n)$ reaction, i.e., 33—34 MeV, and observing which conversion lines and photons are eliminated at the lower energy irradiations. The conversion lines and photons so found and assigned to $Ir^{185}$ are listed in table 4.

As for $Ir^{186}$ and $Ir^{187}$ we have determined the half-life of $Ir^{185}$ by visual comparisons of electron line intensities with those on standard plates; the value of the half-life so obtained is $15\pm3$ hours, about 1 hour less than that of $Ir^{186}$ and 2 hours greater than that of $Ir^{187}$. All the lines assigned to $Ir^{185}$ show a half-life of this magnitude.

Confirmation of the production of $Ir^{185}$ in the 45 MeV alpha particle bombardments was obtained by volatilizing the 95 day $Os^{185}$ daughter at timed intervals from a target foil dissolved in concentrated nitric acid. The value of the parent half-life obtained in this way, 14 to 20 hours, is quite rough but is consistent with the value obtained directly from decay of the conversion lines. The "milked" osmium fractions were examined with the scintillation spectrometer and it was verified that they had the characteristic half-life and gamma ray spectrum of $Os^{185}$. The prominent gamma rays of $Os^{185}$ also appeared in the iridium fractions from all the 45 MeV bombardments but were not in evidence in the bombardments done at 33 MeV or lower energy.

We are indebted to Mr. Keith McNab, Mr. Henry Cline, and Mrs. Virginia Shirley for their extensive help during these experiments, and to Mr. W. B. Jones and the crew of the 60-inch cyclotron for their cooperation in providing the irradiations. One of the authors (RMD) would like to express his gratitude to Professor G. T. Seaborg for the opportunity of spending the summer (1957) with the Chemistry Division of the Radiation Laboratory, and to all the members of the group who made his stay so enjoyable.

## References

1) A. Bohr and B. R. Mottelson, Mat. Fys. Medd. Dan. Vid. Selsk. **27** (1953) no. 16; Beta and Gamma Ray Spectroscopy, edited by K. Siegbahn (North-Holland Publishing Co., Amsterdam) Ch. 17, p. 468
2) J. J. Murray, F. Boehm, P. Marmier and J. W. M. DuMond, Phys. Rev. **97** (1955) 1006; S. Thulin, J. O. Rasmussen, C. J. Gallagher, W. G. Smith and J. M. Hollander, Phys. Rev. **104** (1956) 471
3) W. G. Smith and J. M. Hollander, Phys. Rev. **101** (1956) 746
4) L. J. Goodman and M. L. Pool, Phys. Rev. **71** (1947) 288
5) T. C. Chu, Phys. Rev. **79** (1950) 582
6) A. W. H. Aten, G. D. deFeyfer, M. J. Sterk and A. H. Wapstra, Physica **21** (1955) 740, 990
7) G. Scharff-Goldhaber, D. E. Alburger, G. Harbottle and M. McKeown, Bull. Am. Phys. Soc. **2** (1957) 25
8) G. Scharff-Goldhaber, D. E. Alburger, G. Harbottle and M. McKeown, private communication (November 1957)
9) W. G. Smith and J. M. Hollander, Phys. Rev. **98** (1955) 1258
10) R. Barhout, P. Lehmann and A. Leveque, Compt. rend. **245** (1957) 523
11) M. W. Johns, C. C. McMullen, I. R. Williams and S. V. Nablo, Proc. Roy. Soc. Canada **44** (1956) 194A
12) V. Shiel, L. D. Wyly and C. H. Braden, Phys. Rev. **105** (1957) 1521
13) W. John Jr., Phys. Rev. **103** (1956) 704
14) M. W. Johns, C. C. McMullen, I. R. Williams and S. V. Nablo, Can. J. Phys. **34** (1956) 69

7.B *Nuclear Physics* **8** (1958) 155—156; © *North-Holland Publishing Co., Amsterdam*
Not to be reproduced by photoprint or microfilm without written permission from the publisher

# POLARIZATION OF ELASTICALLY SCATTERED GAMMA-RAYS

I. LOVAS

*Central Research Institute for Physics, Department of Neutron Physics, Budapest*

Received 12 June 1958

Disregarding resonance scattering, three different processes are responsible for the elastic scattering of gamma rays. These are the Thomson, the Rayleigh and the Delbrück scattering. Unfortunately, it is not possible to determine accurately the angular distributions of the last two processes [1,2]). Many experiments were performed to the elastic scattering but the results obtained were fairly ambiguous [3,4,5]). The existence of the Delbrück scattering is an unsolved problem. In the following we should like to suggest a possible way to obtain some definite information about the Delbrück scattering. There is a difference between the angular dependence of the polarization of the Delbrück scattering and that of the two other processes. Thus by measuring the polarization of elastically scattered gamma rays it is very probable that a conclusive knowledge as to the existence of Delbrück scattering may be obtained.

The amplitudes of Thomson, Rayleigh and Delbrück scattering are of the form [6,7,8]) $a_T(\vartheta)\mathbf{e}_1\cdot\mathbf{e}_2$, $a_R(\vartheta)\mathbf{e}_1\cdot\mathbf{e}_2$, and $a_D(\vartheta)\mathbf{e}_1\cdot\mathbf{e}_2+b(\vartheta)(\mathbf{e}_1\cdot\mathbf{n})(\mathbf{e}_2\cdot\mathbf{n},)$ respectively, where $\vartheta$ is the angle of scattering, $\mathbf{e}_1$ and $\mathbf{e}_2$ unit vectors of polarization for the incident and for the scattered gamma rays, and $\mathbf{n}$ a unit vector in the direction of the change in momentum. The differential cross section is therefore

$$\frac{\mathrm{d}\sigma}{\mathrm{d}\Omega}\propto|a(\vartheta)|^2(\mathbf{e}_1\cdot\mathbf{e}_2)^2+[a^*(\vartheta)b(\vartheta)+a(\vartheta)b^*(\vartheta)](\mathbf{e}_1\cdot\mathbf{e}_2)(\mathbf{e}_1\cdot\mathbf{n})(\mathbf{e}_2\cdot\mathbf{n})$$
$$+|b(\vartheta)|^2[(\mathbf{e}_1\cdot\mathbf{n})(\mathbf{e}_2\cdot\mathbf{n})]^2,$$
$$a(\vartheta)=a_T(\vartheta)+a_R(\vartheta)+a_D(\vartheta).$$

The coefficients $a_R(\vartheta)$, $a_D(\vartheta)$ and $b(\vartheta)$ are not yet exactly known; it is certain [9]), however, that $b(\vartheta)$ is a real function and appreciably smaller than $a_R(\vartheta)$. Therefore, the term $|b(\vartheta)|^2[(\mathbf{e}_1\cdot\mathbf{n})(\mathbf{e}_2\cdot\mathbf{n})]^2$ can be neglected and one may write

$$\frac{\mathrm{d}\sigma}{\mathrm{d}\Omega}\propto(\mathbf{e}_1\cdot\mathbf{e}_2)^2+\frac{2b(\vartheta)\ \mathrm{Re}\ [a(\vartheta)]}{|a(\vartheta)|^2}(\mathbf{e}_1\cdot\mathbf{e}_2)(\mathbf{e}_1\cdot\mathbf{n})(\mathbf{e}_2\cdot\mathbf{n}).$$

Since at present no high intensity sources emitting polarized gamma rays are available, our considerations will be restricted to the case of unpolarized gamma rays. Consequently, it is necessary to average over the incident polarization:

$$\frac{\mathrm{d}\sigma}{\mathrm{d}\Omega} \propto 1-\cos^2\eta[\sin^2\vartheta+f(\vartheta)(\cos\vartheta+\cos^2\vartheta)], \quad f(\vartheta)=\frac{b(\vartheta)\ \mathrm{Re}\ [a(\vartheta)]}{|a(\vartheta)|^2},$$

where $\eta$ is the azimuthal angle of the vector $\mathbf{e}_2$ measured from the plane of scattering.

The degree of polarization for a beam scattered at an angle $\vartheta$ is given by

$$P=\frac{N_\perp-N_\parallel}{N_\perp+N_\parallel}=\frac{\sin^2\vartheta+f(\vartheta)(\cos\vartheta+\cos^2\vartheta)}{2-[\sin^2\vartheta+f(\vartheta)(\cos\vartheta+\cos^2\vartheta)]},$$

where $N_\parallel$ and $N_\perp$ represent the number of gamma quanta polarized parallel and perpendicular to the plane of scattering. The measurement of the polarization of an elastically scattered beam by a detector which is sensitive to linear polarization may therefore lead to a definite proof of the existence of Delbrück scattering.

## References

1) I. S. Levinger, Phys. Rev. **87** (1952) 656
2) H. A. Bethe and F. Rohrlich, Phys. Rev. **86** (1952) 10
3) P. B. Moon, Proc. Phys. Soc. **63** (1950) 1189
4) R. R. Wilson, Phys. Rev. **82** (1951) 295
5) N. Cindro and K. Ilakovac, Nuclear Physics **5** (1958) 647
6) W. Heitler, The Quantum Theory of Radiation (Oxford, 1944) Ch. I, p. 37
7) W. Franz, Zeit. Physik **95** (1935) 652; **98** (1936) 314
8) A. Achieser and I. Pomerantschuk, Physik. Z. Sovjetunion **11** (1937) 478
9) F. Rohrlich and R. L. Gluckstern, Phys. Rev. **86** (1952) 1

9.A *Nuclear Physics* 8 (1958) 157—170; © *North-Holland Publishing Co., Amsterdam*

Not to be reproduced by photoprint or microfilm without written permission from the publisher

# THE ABSOLUTE DENSITY DISTRIBUTION OF COSMIC-RAY AIR SHOWERS AT LOW DENSITIES

H. S. MURDOCH

*The F.B.S. Falkiner Nuclear Research and Adolph Basser Computing Laboratories, School of Physics, The University of Sydney* †

Received 20 May 1958

**Abstract:** The integral density distribution of Cosmic Ray Air Showers has been found to be

$$N(>\rho) = 7.9\rho^{-(1.34+0.018\ln\rho)}\ \mathrm{min}^{-1}$$

at densities $\approx 1\mathrm{m}^{-2}$ in agreement with the results of most other workers at somewhat higher densities. It is shown that the hodoscope method is not valid for determination of the distribution over a range of density and that the deduction by Broadbent *et al.*[1]) of a constant exponent over a wide range of density is erroneous. Good agreement for the absolute rate is obtained from the results of many workers when these are suitably reduced to a common basis as regards range of density, altitude and counter tray separation, the rate quoted being for sea-level and 5 metres separation between trays.

## 1. Introduction

The density distribution of cosmic ray air showers has been studied by many workers. Experiments covering a limited range of particle density have been found to be consistent with a power law integral density distribution of the form

$$N(>\rho) = K\rho^{-\gamma} \tag{1}$$

where $K$ and $\gamma$ are constants. It may readily be shown [2]) that a density distribution of this form results from a power law shower size distribution with the same exponent (provided the lateral structure function is independent of shower size). Experiments conducted over a wide range of particle density by Cocconi and Tongiorgi [3]), Zatsepin *et al.*[4]) †† and Milone [6]) have shown a departure from the strict power law distribution. Greisen [5]) gives a useful summary of previous work and shows that the experiments of Cocconi and Zatsepin are consistent with an increase of $\gamma$ with density of the form

$$\gamma = 1.33+0.039\ln\rho \tag{2}$$

where $\gamma$ is now defined more precisely as $-\partial\log N/\partial\log\rho$. The data assembled by Greisen cover densities from 2 to 1000 particles per square metre. The results of Milone are also consistent with this expression. The

† Also supported by the Nuclear Research Foundation within the University of Sydney.

†† This work is known to the author only through reference to it by Greisen [5]).

results of other workers are consistent when interpreted as giving the value of $\gamma$ at the appropriate density. On the other hand, Broadbent *et al.*[1]) find that their results are better explained by a constant $\gamma$ in the range 5 to 500 $m^{-2}$.

Three methods have been used in Geiger counter experiments on density distribution. It is customary to assume in the analysis that for each shower recorded, the particle density is constant over the whole area covered by the counter trays. This ideal condition is never fulfilled in practice and it is important to consider whether the assumption of constant density introduces any bias into the results.

(1) *Variation of areas method.* In this method the rate of three-fold coincidences between counter trays is measured as a function of tray size. It is well known [2]) that for a power-law distribution and for a shower structure function which is independent of shower size, this method introduces no bias. Experimental evidence supports these assumptions to a fairly good approximation.

(2) *Multiple coincidence method.* In this method the rates of three-fold and four-fold coincidences between trays of a given size are compared. It is known to yield too high a value of $\gamma$ unless the fourth tray is placed symmetrically to the other three. Cocconi and Tongiorgi [3]) obtained consistent results by placing the fourth tray at the centre of an equilateral triangle with the other three trays at its apices.

(3) *Hodoscope method.* In this method the firing of individual counters in the trays is recorded. It has been used by Broadbent *et al.*[1]) and as it gives better density resolution, should in principle be more suitable for detecting any variation of $\gamma$ with $\rho$. They claim that their result is not significantly affected by differences in density between their two trays of counters 5 metres apart.

## 2. Experimental Arrangement

The present experiment was carried out in order to determine the density distribution at low densities and hence throw further light on the question whether $\gamma$ is a constant over a wide range of density or varies slowly with density. The experiment was carried out on the roof of the School of Physics at the University of Sydney at an altitude of 40 m above sea level. Three counter trays were arranged in an approximately equilateral triangle. Part of the experiment was performed with average distance between tray centres of 5.5 m and the remainder with a distance of 4.8 m. Each tray consisted of 24 counter-pairs of area 0.04 sq.m. giving a tray area of 0.96 sq. m. Each counter-pair consisted of two Geiger counters placed side by side and connected in parallel. The separation between counter-pairs was equal to the diameter of one single counter hence ensuring that only particles of

zenith angle greater than 60° could pass directly through two adjacent counter-pairs. Henceforth counter-pairs will be referred to simply as counters. Each counter tray together with quenching and storage circuits was protected from the weather by a light wooden framework covered on top by an aluminium roof of 0.2 $g \cdot cm^{-2}$.

The recording apparatus was triggered by a master pulse produced when one or more counters fired in each of the three trays. This master pulse was also used to gate the recording of individual counters. Each three-fold coincidence was recorded on a punched card, 12 positions in each of two adjacent columns corresponding to the 24 counters of a tray, and a hole being punched to indicate that the counter corresponding to the appropriate position on the card had fired. Hourly tests were made to detect any malfunction of the counters and recording equipment. Details of the system of recording and testing will be published separately [7]).

The counting rate was about 180/hour, being determined to a large extent by the dead-time of the punched card recording. The absolute rate of three-fold coincidences between the trays was determined by a separate run without the punched card recorder. The total number of events recorded n detail was 10051 with a tray separation of 5.5 m and 10026 with a separation of 4.8 m.

## 3. Analysis of Results

### Method I

#### 3.1. THEORY OF THE METHOD

Assuming a uniform density $\rho$ at all trays, the rate of events $C$ and the rate at which $k$ out of $n$ counters fire are given respectively by

$$C = \int_0^\infty (1-e^{-\rho A})^3 f(\rho) d\rho \tag{3a}$$

and

$$C_k = F_k \int_0^\infty (1-e^{-\rho a})^k e^{-(n-k)\rho a} f(\rho) d\rho \tag{3b}$$

where $f(\rho)d\rho$ is the differential density distribution, $a$ and $A$ represent respectively the areas of a counter and of a tray, and $F_k$ is the number of ways in which $k$ out of $n$ counters may fire subject to the condition that at least one must fire in each of the 3 sets of $\frac{1}{3}n$ counters.

The form of $f(\rho)d\rho$ adopted is

$$f(\rho)d\rho = -B_0 \rho^{-(\gamma_0+1+q \ln \rho)} d\rho. \tag{4}$$

The special case of a constant $\gamma$ is represented by $q = 0$. For any other case, it is necessary to relate the differential spectrum (4) to $\gamma$ as defined in (2). If the integral spectrum is written as

$$N(>\rho) = K_1 \rho^{-(\gamma_1 + p \ln \rho)} \tag{5}$$

then

$$\gamma = \gamma_1 + 2p \ln \rho \tag{6}$$

and the differential spectrum becomes

$$f(\rho)\mathrm{d}\rho = -B_1(\gamma_1 + 2p \ln \rho)\rho^{-(\gamma+1)}\,\mathrm{d}\rho.$$

For $(p/\gamma_1) \ln \rho \ll 1$, a condition which holds for values found in practice except at very high densities, the latter expression may be expressed in the form (4) with

$$\begin{aligned} B_0 &= \gamma_1 B_1, \\ \gamma_0 &= \gamma_1 - \frac{2p}{\gamma_1} \\ q &= p + \frac{2p^2}{\gamma_1^2}. \end{aligned} \tag{7}$$

and

These expressions allow ready conversion between the integral spectrum (5) and the differential spectrum (4), and expression (6) gives the value of $\gamma$ as defined in (2).

### 3.2. CORRECTIONS TO EXPERIMENTAL DATA

As only relative values of the various $C_k$ are significant and as these are determined simultaneously, no pressure correction of the results is necessary. Any second order effects such as possible variation of barometer coefficient with shower size should be negligible.

Certain small corrections to the experimental data are, however, necessary.

(i) Due to the large counting rates, chance coincidences are by no means negligible. The chance rate amounts to $3.7 \pm 0.5$ % of the total rate and includes a contribution from genuine two-fold coincidences accompanied by an accidental count in the third tray. The rate measured by introducing artificial delays is consistent with that calculated from an oscillograph measurement of the input pulses to the coincidence circuit. The error quoted includes an allowance for possible systematic errors. Most chance events contribute to $k = 3$ but some of those arising from genuine two-fold events will contribute to higher values of $k$. For technical reasons most chance events show at least one tray with no holes punched. Delay in the commencement of the master pulse reduces the effective resolving time for recording the firing of individual counters to less than that for coincidences between trays. It is assumed that all remaining chance events are $k = 3$.

(ii) A sample batch of events in which exactly two counters fire in one tray was analysed in order to ascertain any significant excess of cases in which two adjacent counters fire. Such an excess could be due to a genuine

close association of particles or to a single particle either entering at a zenith angle $> 60°$ or entering one counter and producing a secondary in the adjacent counter. It could also be due to associated pairs produced in the roof. A small excess was found which could be interpreted as due to a 1 % probability for a single particle to fire two adjacent counters, and a correction was applied on this basis.

(iii) There is a probability 0.7 % per event of one spurious counter firing due to a chance overlap with a master pulse. This is reduced somewhat for high $k$ values.

(iv) There is a probability of 0.6 % that any one counter will fail to record due to counter dead-time. If this is the only counter in a tray through which a particle passes, the event will not be recorded. Otherwise $k$ is reduced by one. This latter effect is most important for high $k$ values.

The various effects cancel to a large extent and a significant net correction is only necessary for very low and very high $k$ values.

### 3.3. TREATMENT OF RESULTS

No difference was detected between the experimental results for the two tray separations and the results have been combined. The $C_k$ were calculated for various values of $\gamma_0$ and $q$ by numerical integration on SILLIAC. $C$ was also calculated in each case and the necessary condition $C = \sum_3^n C_k$ was used as a check on the correctness of the calculations. Denoting the relative expected values by $k_i$ and the observed values by $l_i$ ($\sum k_i = \sum l_i = L$) then

$$\chi^2 = \sum_k \frac{(k_i - l_i)^2}{k_i},$$

and a minimum value of $\chi^2(\gamma_0, q)$ was sought. As there is some uncertainty in the corrections for $k = 3$ and to a lesser extent for $k = 4$, and as this is the region where $\gamma$ might be expected to vary most, separate fits to the experimetal data have been made (i) accepting all results (ii) rejecting $k = 3$ and (iii) rejecting $k = 3$ and 4.

The optimum parameters for the differential distribution for the case where $k = 3$ and 4 are rejected, are

$$\gamma_0 = 1.29 \text{ and } q = 0.039.$$

These values lead to

$$\gamma = 1.35 + 0.074 \ln \rho. \tag{8}$$

The value of $\chi^2$ is 55.9 with 38 degrees of freedom †. The probability of a value greater than this is 3 % and whilst this is not a particularly good fit, the best fit for constant $\gamma$ gives $\chi^2 = 80.1$, the probability of a value this large being 0.003 %. Table 1 shows the experimental results together with

† A certain amount of grouping of the data was necessary for high $k$ values.

the best fits for constant $\gamma$, and for $\gamma$ as given by (8). Greater grouping has been used in table 1 than was used in analysing the results. The result is much the same if the low density groups $k = 3$ and 4 are included but the fit is worse.

TABLE 1

| $k$ | Experimental | Constant $\gamma$ | Variable $\gamma$ |
|---|---|---|---|
| 5 | 2744 | 2799 | 2704 |
| 6 | 1927 | 2001 | 1988 |
| 7 | 1489 | 1456 | 1466 |
| 8 | 1069 | 1081 | 1104 |
| 9–10 | 1546 | 1459 | 1503 |
| 11–15 | 1826 | 1748 | 1812 |
| 16–25 | 1204 | 1144 | 1172 |
| 26–48 | 560 | 621 | 607 |
| 49–72 | 169 | 225 | 178 |
| | 12534 | 12534 | 12534 |

### 3.4 FACTORS AFFECTING THE VALIDITY OF THE RESULT

The significant feature of expression (8) is that the coefficient of the logarithmic term is almost twice as great as in the Greisen expression (2). Although the present experiment is sensitive to lower densities than previous work (approximately 0.3 to 30 $m^{-2}$), the overlap in density range is considerable and such a large discrepancy is not expected. In fact the probability of the present results being fitted by the Greisen expression is vanishingly small. Discarding further results from the low density end does not effect any improvement. This means that the discrepancy is not due to a sharp decrease in $\gamma$ at low density.

The uncorrected experimental results yield

$$\gamma = 1.34 + 0.080 \ln \rho.$$

This is not substantially different from (8) and the discrepancy cannot be attributed to inadequacy of the corrections made.

As the present result differs from that of Cocconi [3]) and as the latter was obtained by the "variation of areas" method which is not affected by density gradient, one is strongly suspicious that the variation of $\gamma$ found by the present experiment is excessive due to its sensitivity to the density gradient.

There is some evidence from the data for such a density gradient. In table 2, sample data for $k = 5$ and 6 are shown subdivided according to the number of counters which fire in each of the three trays.

In each case there are more events than expected in the asymmetric categories. This certainly could be caused by an average density gradient between

trays. The effect of such a density gradient is to reduce the number of observed events for both low and high $k$ values with a relative increase at intermediate values. This is just the effect required to simulate an increase in

TABLE 2

| $k$ | | observed | expected |
|---|---|---|---|
| 5 | 3−1−1 | 169 | 134 |
| 6 | 2−2−2 | 174 | 209 |
| | 4−1−1 | 51 | 38 |
| | 3−2−1 | 155 | 160 |
| | 2−2−2 | 35 | 43 |

$\gamma$ with $\rho$, and the conclusion seems inescapable that the present result is contaminated in this way. If this interpretation is correct, a similar effect should be present in the experiment of Broadbent *et al.*

### 3.5. RE-ANALYSIS OF BROADBENT RESULTS

The data of Broadbent *et al.*[1]) are shown in table 3 together with the expected values for $\gamma = 1.425$, which they find fits their results best.

TABLE 3

| $k$ | expected ($\gamma = 1.425$) | observed | new analysis |
|---|---|---|---|
| 3 | 896 | 885 | 866 |
| 4 | 691 | 682 | 727 |
| 5 | 471 | 511 | 504 |
| 6 | 317 | 340 | 335 |
| 7 | 218 | 235 | 224 |
| 8 | 157 | 164 | 154 |
| 9 | 124 | 112 | 112 |
| 10 | 165 | 110 | 117 |
| | 3039 | 3039 | 3039 |

Inspection shows at once that the fit is very poor at high densities. A $\chi^2$ test shows that the probability of a constant $\gamma$ is vanishingly small. Broadbent *et al.* fitted their data by minimising the quantity $\sum(k_i - l_i)^2$. This unweighted least squares fit biasses heavily towards the $k$ values with most events. This means that they determine $\gamma$ at $\rho \approx 10$ m$^{-2}$ but their conclusion that $\gamma$ is constant in the range 5—500 m$^{-2}$ is invalid. Their data have been re-analysed by the same method as the data of the present experiment and the best fit is obtained for

$$\gamma = 1.11 + 0.146 \ln \rho.$$

The expected frequencies have been entered in the final column of table 3.

The value of $\chi^2$ is 4.9 and for 5 degrees of freedom, the probability of this value being exceeded is about 40 %.

By contrast, $\chi^2$ for the Greisen expression is 14.6 with 1 % probability of being exceeded, and for the Broadbent value of $\gamma = 1.425$, $\chi^2 = 26.5$. The probability of this value of $\chi^2$ being exceeded is $< 0.001$ %.

Here too it must be assumed that there is a spurious effect due to the density gradient over the experimental array. Broadbent *et al.* find evidence for the existence of this density gradient but conclude that it does not significantly affect their determination of $\gamma$. This is no doubt approximately true as regards the best fit to a constant $\gamma$ but once a more realistic two-parameter fit is sought, density gradient can no longer be ignored.

## 4. Analysis of Results

### Method II

In an attempt to reduce the effect of density gradient, a modified method of analysis has been used which takes note of the number of counters which fire in one tray only, the other two trays merely ensuring a three-fold coincidence between trays †. This method should be less sensitive to the effects of density gradient particularly at high density. The rate at which $k$ counters fire out of $n$ in any one tray is given by

$$C_k = \binom{n}{k} \int_0^\infty (1-e^{-\rho a})^k e^{-(n-k)\rho a} (1-e^{-\rho A})^2 f(\rho) d\rho.$$

The data have been analysed for each tray separately and as they were self-consistent, they have been combined ††.

The maximum likelihood method of fitting has been used in this analysis. This method leads more directly to an estimation of error in the final result, on the assumption that the expression used for $\gamma$ is the correct one. A $\chi^2$ test is still necessary to test whether this is a good fit. Further details of the method are given in an appendix. The $k = 1$ events have been eliminated in fitting the data as this category is most likely to be affected by density gradient. In fact it was found impossible to obtain a good fit with $k = 1$ included, there being an excess of events in this category over that expected.

The values obtained for $\gamma_1$ and $p$ are

$$\gamma_1 = 1.341 \pm 0.010$$
$$2p = 0.055 \pm 0.010.$$

† This method has been used independently by Zawadzki [8]), but his method of evaluating $C_k$ does not adequately allow for the variation of $\gamma$ with $\rho$. A similar technique has been used by Norman [9]) in an experiment with proportional counters.

†† The data from the three trays have been treated as statistically independent. As this is not strictly true, the errors quoted may be slightly underestimated.

It is important to note that there is a strong negative correlation between these parameters when attempting to draw comparisons with other expressions. It may be shown, however, (see appendix) that the probability of the present results being fitted by the Greisen expression is effectively zero.

The value of $\gamma_1$ obtained by this method is essentially the same as that found by method I but the variation coefficient $2p$ is considerably reduced, thus confirming the expectation of a reduced effect of density gradient. Nevertheless $2p$ is still considerably in excess of that given by Greisen and the two results are incompatible. As in method I, removal of further low $k$ values does not effect any improvement and it must be assumed that this method also gives a result which is affected by density gradient. It is to be expected that both methods would give the same value for $\gamma_1$ as the experiment is most sensitive to densities of about 1 $m^{-2}$.

The data of Broadbent *et al.*[1]) have also been analysed by method II yielding the result

$$\gamma = 1.06+0.128 \ln \rho.$$

This is only a slight improvement on the result of method I and in fact is only significantly different at large $\rho$. Once again it was necessary to reject the $k = 1$ class of events, showing that this is a feature of the method of analysis and further indicating that it is in fact affected by density gradient. Some idea of the statistical accuracy of the above result can be obtained from the following:

$$\gamma(\text{at } \rho = 10\,m^{-2}) = 1.360\pm0.027$$
$$p = 0.64\pm0.23.$$

The probability of this result being fitted by either the Greisen expression or the result of the present experiment is very small. The discrepancy between the Broadbent data and those of the present experiment when both are analysed by the same method is further confirmation of the inadequacy of an analysis which neglects density gradient in this type of experiment.

## 5. The Value of $\gamma$

Although the hodoscope method is not suitable for obtaining an expression for $\gamma$ valid over a wide range of density, it seems reasonable to assume that the correct value of $\gamma$ should be obtained at the density to which the experiment is most sensitive, i.e. close to $1/A$ [5]). This value is approximately 1 $m^{-2}$ for the present experiment and 15 $m^{-2}$ for the Broadbent experiment. The present experiment gives $\gamma = 1.34\pm0.01$ at $\rho = 1$ $m^{-2}$ against 1.33 from the Greisen expression. The Broadbent experiment gives $\gamma = 1.41\pm0.03$ at $\rho = 15$ $m^{-2}$ against 1.43 for the Greisen expression. With this interpretation, both experiments are consistent with the Greisen expression.

This argument is reinforced by the value which has been obtained for $\gamma$ by comparing the respective counting rates for trays of area 0.96 m² and for half-size trays of area 0.48 m² (see table 4). This value is not affected by density gradient. A comparison of the rates for full and half-size trays gives a ratio of $2.55 \pm 0.04$ and from this the value of $\gamma$ at $\rho = 1$ m$^{-2}$ may be calculated as $1.34 \pm 0.02$ in excellent agreement with the Greisen value of 1.33 and the value of $1.34 \pm 0.01$ found in the two-parameter fit of method II for the present experiment. Combining this value with the data assembled by Greisen the best estimate of $\gamma$ seems to be

$$\gamma = 1.34 + 0.036 \ln \rho.$$

This expression should be valid at least down to $\rho = 0.5$ m$^{-2}$.

Zawadzki on the other hand finds [8])

$$\gamma = 1.323 + 0.06 \ln \left(1 + 0.065 \frac{1}{A}\right)$$

which gives too low a value of $\gamma$ at all densities to which his experiment is sensitive (3 to 200 m$^{-2}$). Although his result is based on large statistics and very precisely stated, he used an inadequate method of analysis which does not give a correct expression for $\gamma$ as a function of $\rho$, and further, his experiment is probably also subject to density gradient in the same manner as the present experiment.

## 6. The Absolute Rate of Showers

The three-fold coincidence rate has been measured without the punched card recorder for both tray separations used in the main experiment and also at a separation of 2.5 metres. At the larger tray separation, a separate rate has been determined for half-size trays. The results are summarised in table 4. The errors quoted include a contribution from the error in the chance rate. All readings have been corrected to the rate expected at 760 mm pressure assuming a barometric coefficient of $-10$ % per cm of Hg.

TABLE 4

| Tray Area (m²) | Tray Separation (m) | Number of counts | Rate (min$^{-1}$) |
|---|---|---|---|
| 0.96 | 5.5 | 28 761 | $6.89 \pm 0.06$ |
| 0.96 | 4.8 | 23 900 | $6.88 \pm 0.07$ |
| 0.96 | 2.5 | 47 656 | $7.59 \pm 0.04$ |
| 0.48 | 5.5 | 10 477 | $2.71 \pm 0.03$ |

By combining expressions (3) and (4), the coincidence rate may be written as

$$C = \gamma_1 B_1 A^{\gamma} I_{\gamma}$$

where (9)

$$I_{\gamma} = \int_0^{\infty} (1-e^{-x})^3 x^{-\left(\gamma_0 + q \ln \frac{x}{A}\right)} dx.$$

$I_{\gamma}$ is a slowly varying function of $\gamma_0$, $q$ and $A$. In calculating $B_1$ from expression (9) due allowance must be made for any uncertainty in the estimation of the sensitive area of the counters. The value obtained is $B_1 = 7.9 \pm 0.2$ min$^{-1}$.

In order to compare the absolute rate with values obtained by other workers it is necessary to reduce all results to a common basis as regards (i) density (ii) tray separation (iii) altitude. Various results have been assembled in table 5 and the reduction to a common basis has been dealt with as follows:

(i) The first order approximation to the density distribution in the vicinity of a density $\rho_0$ is given by

$$N(>\rho) = K\rho^{-\gamma(\rho_0)} = B_1 \rho_0^{\,p \ln \rho_0}\, \rho^{-\gamma(\rho_0)}. \quad (10)$$

In the case of a three-fold coincidence experiment, a suitable value of $\rho_0$ is $1/A$ [5]†. Expression (10) has been used in deducing $B_1$ for the experiment of Broadbent *et al.*[1]). Combining (3) and (1) and writing $\rho_0 = 1/A$ gives

$$C = \gamma B_1 A^{\left(\gamma_1 + p \ln \frac{1}{A}\right)} \int_0^{\infty} (1-e^{-x})^3 x^{-(\gamma+1)} dx. \quad (11)$$

This expression has been used to evaluate $B_1$ from $C$ in the remaining experiments considered.

TABLE 5

| Author | Altitude (m) | Tray separation (m) | $\rho_0$ (m$^{-2}$) | $C$ (min$^{-1}$) | $B_1$ (min$^{-1}$) |
|---|---|---|---|---|---|
| Babecki *et al.*[11]) | 230 | 3.4 | 2 | 3.51 ±0.03 | 7.9 |
| Broadbent *et al.*[1]) | 50 | 5 | 14 | | 8.0 |
| Greisen [6]) † | 260 | 4 | various | | 7.3 |
| Millar [12]) | — | 4 | 13 | 0.234±0.003 | 8.2 |
| Milone [4]) | 40 | 4 | 3 | 1.68 ±0.02 | 7.7 |
| Murdoch | 40 | 5 | 1 | 6.89 ±0.05 | 7.9±0.2 |
| Singer [13]) | — | 2 | 14 | 0.216±0.003 | 8.1 |

† Based on the results of Cocconi [3]).

(ii) The present data are insufficient to give a decoherence curve over a wide range of tray separation, and the decoherence curve of Cocconi *et al.*[10]) has been used to correct all results to the value expected at 5 metres separation. The rise in counting rate observed at 2.5 metres separation is 10 % in

† The mean value of $\rho$ is considerably greater than this but because of the asymmetric nature of the distribution is not a suitable value in this context.

comparison with about 8 % expected from the Cocconi curve. This difference is probably due, at least in part, to the size of a tray being comparable to the separation between tray centres in the present experiment.

(iii) All data have been reduced where necessary to the rate expected at sea level.

The agreement is remarkably good except for the Greisen value which appears to be slightly low.

The rate at negligible separation is somewhat uncertain. An extrapolation of the decoherence curve of Cocconi *et al.*[9]) indicates an increase of 35 % in the rate at negligible separation compared with that at 5 metres separation. This is in line with Singer's [13]) prediction of a rise of less than 50 %. The precise factor which should be allowed remains, however, uncertain.

## 7. Conclusion

It has been shown that the hodoscope method is not suitable for the precise evaluation of the density distribution over an appreciable range of density, and further that the conclusion of Broadbent *et al.* that $\gamma$ is constant over a wide range of density is erroneous. The diverse values given by various authors for the absolute rate of the density distribution have been shown to be consistent when density variation and other relevant factors are taken into account. The density distribution obtained with three trays of counters at 5 metres separation is given by

$$N(>\rho) = 7.9 \pm 0.2 \rho^{-(1.34 \pm 0.01 + 0.018 \ln \rho)} \text{ min}^{-1}.$$

The error in the logarithmic term is uncertain but is probably not greater than 0.003.

The author would like to acknowledge the encouragement and guidance at all times freely given by Drs. H. D. Rathgeber and K. W. Ogilvie. He would like to thank the C.S.I.R.O. for the grant of a studentship during part of the time spent on this work and the McMaster Laboratory, C.S.I.R.O. for access to their punched card analysing machines. Finally he would like to thank Professor H. Messel for the excellent facilities provided for carrying out this work.

## Appendix

Further details are given here of the analysis by method II.

Denoting $C_k/C$ by $p_i$, the probability of a given set of experimental results may be expressed as

$$P(\gamma_0, q) = C^L_{i_i} \prod p_i^{i_i}$$

where $C^L_{l_i}$ is the number of ways the experimental results may be arranged out of a total $L$ events. For a given set of experimental results, $C^L_{l_i}$ is constant and $\prod p_i^{l_i}$ which is a function of $\gamma_0$ and $q$, gives the relative likelihood of any associated pair of values of the parameters $\gamma_0$ and $q$.

As the time to calculate $\prod p_i^{l_i}$ and $\chi^2$ on SILLIAC is insignificant compared to the time to perform the integrations $C_k$, both expressions have been calculated for each set of parameters. The results are †

$$\gamma = 1.341 + 0.055 \ln \rho \text{ by maximum likelihood}$$

and

$$\gamma = 1.342 + 0.053 \ln \rho \text{ by } \chi^2 \text{ fit.} \tag{8}$$

The value of $\chi^2$ is 30.4 with an 8 % probability of being exceeded.

The maximum likelihood analysis gives the relative likelihood of any associated pair of values of the parameters $\gamma_0$ and $q$. These two parameters are strongly correlated. It is possible by treating the likelihood function (suitably normalised) as a probability distribution †† in the true value of $\gamma_0$ and $q$, to obtain a conditional probability distribution in say $\gamma_0$ at a specified value of $q$, or the marginal distribution by integrating over all possible values of $q$. These distributions are found to be approximately gaussian and we can therefore assign standard errors to $\gamma_0$ and $q$:

$\gamma_0 = 1.300 \pm 0.017$ when no restriction is placed on $q$,
$\gamma_0 = 1.300 \pm 0.008$ for the optimum value $q = 0.028$;
$q = 0.028 \pm 0.005$ when no restriction is placed on $\gamma_0$,
$q = 0.028 \pm 0.002$ for the optimum value of $\gamma_0$.

A similar treatment can be given for $\gamma_1$ and $p$ yielding the values given in section 4.

Alternately we may plot probability contours of $\gamma_0$ and $q$ for various values of the likelihood $l$. Denoting the area within the contours (a series of ellipses in the $\gamma_0 - q$ plane) by $\alpha(l)$, the probability (on an arbitrary scale) of a pair of parameters we wish to test by $l_0$, and the corresponding $\alpha$ by $\alpha_0$, then the probability $p'$ of obtaining a less likely parameter-pair than the one under test is

$$p' = \frac{\int_{\alpha_0}^{\infty} l \, d\alpha}{\int_0^{\infty} l \, d\alpha}.$$

In the one-parameter case, one would normally take $\frac{1}{2}p'$ as representing the

† Fisher [14]) has shown that as the sample size tends towards infinity, the parameter values giving a minimum of $\chi^2$ tend towards the maximum likelihood estimate, the latter being at all times the best estimate.

†† Fisher refers to this as a fiducial probability distribution. It may also be regarded as the posterior probability distribution in $\gamma_0$ and $q$ on the assumption that the prior distribution is constant [15]).

probability of a deviation from the optimum value by a greater amount than the value under test, and in the same direction. Denoting the results of the present experiment by MII and the analysis of the Broadbent results by BII the values of $p'$ obtained are as follows:

| Comparison | $p'$ |
|---|---|
| Greisen expression with MII | effectively zero |
| Greisen expression with BII | 3 % |
| MII with BII | effectively zero |

As the variances for MII are an order of magnitude smaller than for BII, statistical fluctuations in MII have been ignored in making comparison with BII.

## References

1) D. Broadbent, E. W. Kellerman and M. A. Hakeem, Proc. Phys. Soc. A **63** (1950) 864
2) J. Ise, Jr. and W. B. Fretter, Phys. Rev. **76** (1949) 933
3) G. Cocconi and V. C. Tongiorgi, Phys. Rev. **75** (1949) 1058
4) G. T. Zatsepin, V. V. Miller, I. L. Rosental and L. K. Eidus, J. Exp. Theor. Phys. **17** (1947) 1125
5) K. Greisen, Progress in Cosmic Ray Physics **3** (1956) 3
6) C. Milone, Nuovo Cimento **9** (1952) 549
7) H. S. Murdoch and H. D. Rathgeber, to be published
8) A. Zawadzki, Bull. Acad. Polon. Sci. Cl. **3**, **5** (1956) 147
9) R. J. Norman, Proc. Phys. Soc. A **69** (1956) 804
10) G. Cocconi, V. C. Tongiorgi and K. Greisen, Phys. Rev. **75** (1949) 1063
11) J. Babecki, L. Jurkiewicz, J. M. Massalski and M. Miesowicz, Acta Phys. Polon. **16** (1957) 121
12) D. D. Millar, Nuovo Cimento **8** (1951) 279
13) S. F. Singer, Phys. Rev. **81** (1951) 579
14) R. A. Fisher, Phil. Trans. Roy. Soc. A **222** (1922) 309
15) M. Annis, W. Cheston and H. Primakoff, Revs. Mod. Phys. **25** (1953) 818

1.C:
1.E.2

*Nuclear Physics* 8 (1958) 171—190; © *North-Holland Publishing Co., Amsterdam*
Not to be reproduced by photoprint or microfilm without written permission from the publisher

# ZUR PHÄNOMENOLOGISCHEN THEORIE DER KERNMATERIE

P. MITTELSTAEDT
CERN, *Geneva*

Eingegangen am 8. Juni 1958

**Abstract:** A semi-empirical formulation of the independent particle model for nuclear matter is given. Apart from the energy-dependence of the single-particle potential (effective mass), the rearrangement energy is also taken into account. An extension of this theory for real nuclei is shown to be related to the Weizsäcker-Bethe-formula and to the optical model for nuclear reactions. The undetermined parameters of the theory are adjusted to fit the corresponding experimental material. The single-particle potentials, the rearrangement energies and the optical potentials for protons and neutrons can then be calculated as functions of the neutron excess. The corresponding data for nuclear matter are obtained by taking equal numbers of protons and neutrons.

## 1. Einleitung

Die von Brueckner u.a.[1–6]) angegebene Begründung des independent particle Modells im Rahmen eines selbstkonsistenten Störungsverfahrens hat gezeigt, daß man die Energieabhängigkeit der Einteilchenpotentiale in guter Näherung durch eine effektive Masse beschreiben kann. Für den Grenzfall der Kernmaterie hat Weisskopf [7]) darauf hingewiesen, daß durch eine quadratische Impulsabhängigkeit des Einteilchenpotentials zwei wichtige experimentelle Daten, die mittlere Bindungsenergie eines Nukleons und die Abtrennarbeit miteinander in Einklang gebracht werden können. Eine Berechnung des Einteilchenpotentials ist dann, ohne Verwendung der Störungstheorie auf rein halbempirischem Wege möglich. Es wurde jedoch bereits von Weisskopf darauf hingewiesen, daß bei der Berechnung der Abtrennarbeit Vielkörpereffekte eine wesentliche Rolle spielen können, was durch die zusätzliche Berücksichtigung einer Rearrangementenergie in der erwähnten Theorie ausgedrückt werden kann. Weiterhin hat Brueckner bemerkt [8]), daß sich im Rahmen seines Störungsverfahrens eine Rearrangementenergie von etwa 16 MeV ergibt, also keinesfalls vernachlässigt werden darf.

Will man, wie es in der vorliegenden Arbeit geschieht, auch die Rearrangementenergie im Rahmen einer halbempirischen Theorie, also ohne Verwendung der Störungstheorie berücksichtigen, so ergibt sich zunächst die Schwierigkeit, daß aus Abtrennarbeit und Bindungsenergie allein nicht sowohl das Einteilchenpotential als auch die Rearrangementenergie bestimmt werden können. Dadurch, daß jetzt der Prozeß der Abtrennung eines

Nukleons aus dem Kern weitgehend richtig erfaßt wird, ergibt sich jedoch die Möglichkeit die optischen Potentiale für Kernreaktionen mit in die Theorie einzubeziehen. Hätte man eine direkte experimentelle Information über das optische Potential $\Phi_0$ der Kernmaterie (etwa bei der Energie $E = 0$), so ließe sich, wie in Kap. 2 gezeigt ist, eine halbempirische Theorie vollständig durchführen, in der neben dem energieabhängigen Einteilchenpotential auch die Rearrangementenergie berücksichtigt ist.

Da jedoch experimentelle Ergebnisse über optische Streupotentiale nur an wirklichen Kernen und nicht an Kernmaterie gewonnen werden können, soll das erwähnte halbempirische Verfahren in Kap. 3 in analoger Weise auf die wirklichen Kerne übertragen werden. Das bedeutet insbesondere, das Effekte, die vom Neutronenüberschuß $q = (N-Z)/(N+Z)$ [9]), sowie von der Coulombenergie herrühren, berücksichtigt werden müssen. Oberflächeneffekte, deren Berechnung verschiedene prinzipielle Schwierigkeiten bereitet, sollen in der vorliegenden Arbeit nicht diskuttiert werden [10, 11, 12]).

Eine solche halbempirische Behandlung macht es möglich, die in der Weizsäcker-Bethe Formel ausgedrückten experimentellen Fakten, sowie die experimentell bestimmten optischen Potentiale für Protonen und Neutronen einiger Kerne in die Theorie einzubeziehen. Damit lassen sich die Einteilchenpotentiale, die Rearrangementenergien und die optischen Potentiale für Protonen und Neutronen als Funktionen von $q$ berechnen.

Die entsprechenden Daten für Kernmaterie lassen sich dann ohne weitere Schwierigkeiten berechnen, da der Formalismus im Specialfall $q = 0$ in den der Kernmaterie übergeht.

## 2. Die Kernmaterie

### 2.1. ALLGEMEINES

Die Kernmaterie ist ein idealisierter Grenzfall der wirklichen Kerne, der dadurch entsteht, daß man sowohl von der Coulombenergie als auch von der Symmetrieenergie absieht, also gleiche Protonen- und Neutronenzahlen annimmt. Weiterhin sei die Zahl der Nukleonen genügend groß, sodaß auch die Oberflächeneffekte vernachlässigt werden dürfen. Der innere Teil der mittleren und schweren Kerne dürfte dann weitgehend die Eigenschaften der Kernmaterie besitzen. Im Rahmen einer halbempirischen Formulierung kommt der Kernmaterie insofern eine besondere Bedeutung zu, als bei der Entwicklung der verschiedenen Potentiale und Energien nach $A$ und $q$ jeweils die ersten, von diesen Variabeln unabhängigen Terme die entsprechenden Größen der Kernmaterie darstellen. (Vgl. Kap. 3).

Da die strukturellen Eigenschaften der einzelnen Kerne im Begriff der Kernmaterie nicht enthalten sind, lassen sich hier die Methoden der statistischen Theorie anwenden [13]). Ist $E = \int \varepsilon(\mathbf{r}) d\mathbf{r}$ die Gesamtenergie eines

Systems von $A$ Teilchen, mit der Teilchendichte $\rho$, die die Nebenbedingung $A = \int\rho(\mathbf{r})\mathrm{d}\mathbf{r}$ erfüllt, so muß die Variation der Gesamtenergie nach der Dichte unter dieser Nebenbedingung verschwinden. Daraus folgt, wenn das System, wie vorausgesetzt, genügend groß ist, sodaß man von der Ortsabhängigkeit von $\rho$ und $\varepsilon$ absehen kann,

$$S = -\frac{\mathrm{d}\varepsilon}{\mathrm{d}\rho}, \tag{2.1}$$

wobei $S = -\mathrm{d}E/\mathrm{d}A$ die Abtrennarbeit bedeutet, die notwendig ist, um ein Nukleon aus dem System herauszunehmen. Ist weiterhin $E/A$ die mittlere Energie pro Teilchen, so folgt aus der Minimalbedingung für die Gesamtenergie, daß $E/A = \mathrm{d}E/\mathrm{d}A$ gilt, und somit

$$S = -E/A \tag{2.2}$$

ist. Im Rahmen des statistischen Modells ist weiter $\varepsilon = \varepsilon_{\mathrm{kin}} + \varepsilon_{\mathrm{pot}}$ wobei

$$\varepsilon_{\mathrm{kin}} = \tfrac{3}{5}\left(\frac{3\pi^2}{2}\right)^{\frac{2}{3}}\frac{\rho^{5/3}}{2m} \quad \text{und} \quad \mathrm{d}\varepsilon_{\mathrm{kin}}/\mathrm{d}\rho = T$$

die kinetische Grenzenergie ist.

Aus (2.1) folgt damit

$$S = -T - \frac{\mathrm{d}\varepsilon_{\mathrm{pot}}}{\mathrm{d}\rho} \tag{2.3}$$

wobei über $\mathrm{d}\varepsilon_{\mathrm{pot}}/\mathrm{d}\rho$ allgemein nichts ausgesagt werden kann. Die Dichte der Kernmaterie entspricht weitgehend der Kerndichte im Mittelpunkt der schweren Kerne, und ist nach Messungen von Hofstadter [14]) $\rho = 1.72 \times 10^{38}$ $\mathrm{cm}^{-3}$ und somit $T = 38\mathrm{MeV}$.

## 2.2. EIGENSCHAFTEN DER KERNMATERIE †

Die dynamischen Eigenschaften der Kernmaterie lassen sich, in befriedigender Näherung mit einem Modell beschreiben, bei dem die Wirkung der Kernkräfte auf ein Nukleon durch ein mittleres Einteilchenpotential $V_0$ ausgedrückt wird, welches unabhängig von den Koordinaten der übrigen Nukleonen nur auf das eine Nukleon wirkt. Bei der unendlich ausgedehnten Kernmaterie ist das Potential $V_0$ nicht vom Ort abhängig, wird aber im Allgemeinen noch vom Impuls des betrachteten Teilchens abhängen.

Eine selbstkonsistente Berechnung des Potentials $V_0$ aus den Kernkräften ist in verschiedenen Arbeiten nach dem Brueckner'schen Störungsverfahren durchgeführt worden [1–6]). Dabei hat sich gezeigt, daß man die Impulsabhängigkeit des Einteilchenpotentials in guter Näherung durch eine quadratische Abhängigkeit

† Die Ergebnisse des folgenden Paragraphen wurden kürzlich auch von F. Beck gewonnen (private Mitteilung).

$$V_0(k) = V_{00} + V_{10}(k^2/k_F^2) \tag{2.4}$$

ausdrücken kann. Ein impulsabhängiges Potential, das in einem gewissen Energiebereich durch eine quadratische Abhängigkeit angenähert werden kann, ergibt sich bereits in der Hartree-Fock-Näherung. Die Impulsabhängigkeit rührt dann von den Austauschkräften und von der Antisymmetrisierung der Wellenfuncktion her †. Wir wollen daher im Folgenden für $V_0$ in dem betrachteten Energiebereich stets eine quadratische Impulsabhängigkeit annehmen ††.

Die Gesamtenergie eines Systems von $A$ Nukleonen berechnet sich dann im Einteilchenmodell zu

$$E = \sum_{i=1}^{A} \frac{k_i^2}{2m} + \tfrac{1}{2} V_0(k_i) = \left( \frac{3}{5} \frac{k_F^2}{2m} + \tfrac{1}{2} V_{00} + \tfrac{3}{10} V_{10} \right) A$$

Aus (2.2) folgt dann

$$S = -\tfrac{3}{5} T - \tfrac{1}{2} V_{00} - \tfrac{3}{10} V_{10}. \tag{2.5}$$

Die Glg. (2.3) nimmt im Einteilchenmodell eine besonders einfache Form an. Die Abtrennarbeit $S$ ist dort diejenige Energie, die man aufwenden muß, um ein Teilchen aus dem höchsten besetzten Niveau aus dem Kern zu entfernen, also $\mathrm{d}\varepsilon_{\mathrm{pot}}/\mathrm{d}\rho = V_0(k_F)$ und

$$S = -T - V_{00} - V_{10}. \tag{2.6}$$

Die Abtrennarbeit $S$ ist experimentell aus der Weizsäcker-Bethe-Formel bekannt. Daraus folgt [7]), daß man mit Hilfe der Glg. (2.5) und (2.6) die Größe der Potentiale $V_{00}$ und $V_{10}$ unabhängig von einem selbstkonsistenten Störungsverfahren allein aus den experimentellen Daten berechnen kann. Andererseits ersieht man aus (2.5) und (2.6), daß diese Glgn. nicht mit einem energieunabhängigen Potential, wie es früher oft verwendet wurde, befriedigt werden können. Die Glgn. (2.5) und (2.6) gelten jedoch nur in der strengen Einteilchennäherung. Berücksichtigt man in einer weiteren Näherung Mehrteilcheneffekte, so tritt, worauf Weisskopf [7]) und Brueckner [8]) hingewiesen haben, in Glg. (2.6) noch ein Zusatzterm auf †††. Leistet man am Kern nämlich die Arbeit $-(T+V(k_F))$, so wird einerseits ein Nukleon aus dem Kern abgetrennt, anderseits befindet sich der Restkern nach dieser Abtrennung in einem angeregten Zustand mit der Anregungsenergie $\Delta_0$.

†) Am speziellen Beispiel des Van-Vleck-Potentials ist diese Tatsache von Weisskopf [7]) genauer diskutiert worden.

†† Es ist von Weisskopf [7]) bereits bei der Diskussion des Van-Vleck-Potentials und weiterhin von Brueckner und Gammel [8]) darauf hingewiesen worden, dass eine quadratische Abhängigkeit von $V_0$ vermutlich nicht für alle Energien eine gute Näherung ist.

††† Im Rahmen des Einteilchenmodells tritt ein $\Delta_0$, wie Weisskopf gezeigt hat [7]), deshalb nicht auf, weil ein angeregter Zustand R′ sich vom Grundzustand nur in der Dichte unterscheiden könnte, die Gesamtenergie aber in bezug auf $\rho$ minimal ist, also im Gleichgewichtszustand in erster Ordnung nicht von $\rho$ abhängt.

Man muß daher diese Energie $\Delta_0$, die sogenannte Rearrangementenergie, noch zu $S$ hinzufügen und erhält an Stelle von (2.6) †

$$S = -T - V_{00} - V_{10} - \Delta_0. \tag{2.7}$$

Aus den Glgn. (2.5) und (2.7) ist es jedoch nicht mehr möglich, $V_{00}$, $V_{10}$ und $\Delta_0$ zu bestimmen. Es ist daher notwendig, weitere experimentelle Daten heranzuziehen, die im Zusammenhang mit $V_{00}$, $V_{10}$ und $\Delta_0$ stehen. Wir wollen hier als weitere Parameter das optische Potential $\Phi_0$ eines Teilchens einführen, das außerhalb des Kernes die Energie $E = 0$ besitzt. Dieses Potential ist aus Streumessungen experimentell bekannt ††; anderseits hängt es eng mit $V_{00}$, $V_{10}$ und $\Delta_0$ zusammen. Daß hier das optische Potential bei $E = 0$ gewählt wurde, hat den Grund, daß es vorteilhaft ist, die Energie so klein wie möglich zu wählen, da die quadratische Näherung für $V_0$ mit wachsender Energie schlechter wird [6,7]).

Um $\Phi_0$ zu bestimmen, gehen wir aus von der Abtrennarbeit $S(k)$, die notwendig ist, um ein Nukleon der Energie

$$E(k) = \frac{k^2}{2m} + V_0(k)$$

aus dem Kern zu entfernen. Ist $k = k_F$, so folgt aus (2.7)

$$S(k_F) = -\frac{k_F^2}{2m} - V_0(k_F) - \Delta_0.$$

Nehmen wir an, daß $\Delta_0$ nicht wesentlich davon abhängt, wie groß der Impuls des herausgegriffenen Teilchens ist, wenn $k_F \leqq k \leqq k_0$ ist†††, so ist

$$S(k) = -\frac{k^2}{2m} - V_0(k) - \Delta_0.$$

Ein Teilchen, das außerhalb des Kernes die Energie $E_A = 0$ hat, genügt im Kern der Beziehung

$$\frac{k_0^2}{2m} + W(k_0) = 0 \tag{2.8}$$

wobei $k_0$ der Impuls des Teilchens im Kern ist, und $W(k_0)$ das optische Potential bei dem Impuls $k_0$. Den Impuls $k_0$ erhält man aus der Bedingung, daß die Abtrennarbeit für ein Teilchen mit dem Impuls $k_0$ verschwinden muß, also $S(k_0) = 0$ ist. Daraus folgt

$$\frac{k_0^2}{2m} + V_0(k_0) + \Delta_0 = 0. \tag{2.9}$$

† Dies wird weiter unten bei Verwendung der $t$-Matrix zur Berechnung von $V_0$ besonders deutlich werden.

†† Das optische Potential $\Phi_0$ der Kernmaterie ist zwar nicht unmittelbar experimentell zugänglich, läßt sich jedoch durch geeignete Extrapolation der wirklichen Kerne gewinnen (Vgl. Kap. 3).

††† Wegen der Definition von $k_0$, vgl. (2.8).

Der Vergleich der Glgn. (2.8) und (2.9) zeigt, daß das gesuchte Potential $\Phi_0$ durch

$$\Phi_0 = W(k_0) = V_0(k_0)+\Delta_0$$

gegeben ist. Eine einfache Rechnung zeigt weiter, daß

$$\Phi_0 = \frac{T(V_{00}+\Delta_0)}{T+V_{10}} \tag{2.10}$$

ist. Die Tatsache, daß $\Phi_0$ das optische Potential bei $E = 0$ ist, kann man auch anhand des umgekehrten Prozesses deutlich machen, bei dem man ein

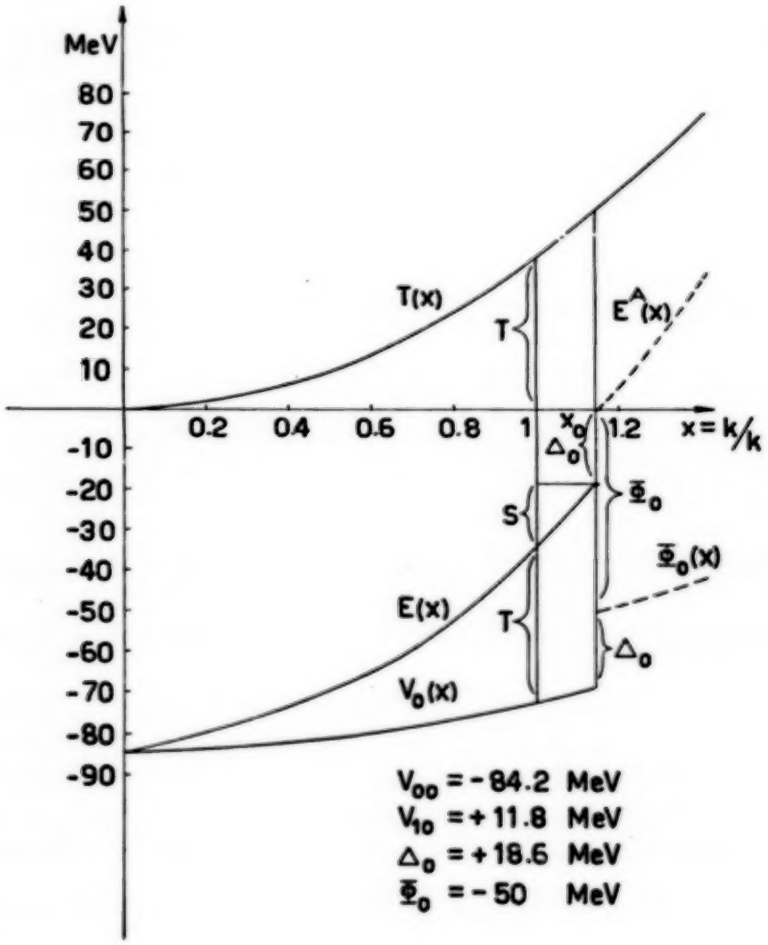


Abb. 1. Potentialbild.

Teilchen mit dem Impuls $k_0$ in den Kern hineinbringt. Die Gesamtenergie ist dann ($\Omega$ ist das Kernvolumen von $A$ Nukleonen) †

† Der Strich bei $E'$ soll andeuten, daß es sich nicht um die Energie des Grundzustandes handelt.

$$E'(A+1) = \tfrac{3}{5}TA + \frac{k_0^2}{2m} + [V_0(k_0) - V_0(k_F)] + \Omega_{A+1}(\varepsilon_{pot})_{A+1}$$

wobei $(V(k_0) - V(k_F))$ die Energie ist, die das Teilchen mehr hat als auf der Fermi-Oberfläche. Ist $\Omega_{A+1} \approx \Omega_A$, so ist

$$(\varepsilon_{pot})_{A+1} \simeq (\varepsilon_{pot})_A + \frac{1}{\Omega_A}\left(\frac{d\varepsilon_{pot}}{d\rho}\right) = (\varepsilon_{pot})_A + \frac{1}{\Omega}(V_0(k_F) + \Delta_0)$$

und damit

$$E'(A+1) = E(A) + \frac{k_0^2}{2m} + [V_0(k_0) + \Delta_0]; \qquad (2.11)$$

daraus folgt, daß $V_0(k_0) + \Delta_0 = W(k_0)$ das optische Potential an der Stelle $k_0$ ist. Der Wert von $k_0$ folgt dann aus der Tatsache, daß wegen $E^A = 0$ auch $k_0^2/2M + W(k_0) = 0$ sein muß.

Um die diskutierten Zusammenhänge zu erläutern, sind in Abb. 1 in Abhängigkeit von $x = k/k_F$ die Funktionen $V_0(x)$, $E(x)$ und $T(x)$ aufgetragen. Der Stelle $x_0$ entspricht dabei der Wert $k_0$, bei dem die Abtrennarbeit verschwindet. Für die Konstanten $V_{00}$, $V_{10}$, $\Delta_0$ und $\Phi_0$ wurden dabei diejenigen Werte gewählt, die nach den in Kap. 3 durchgeführten Rechnungen die beste Übereinstimmung mit dem Experiment ergeben.

### 2.3. BESTIMMUNG DER POTENTIALE

Da ohne eine genaue Untersuchung der wirklichen Kerne, wie sie in Kap. 3 durchgeführt werden soll, eine experimentelle Aussage über $\Phi_0$ nicht gemacht werden kann, soll hier zunächst untersucht werden, was über die Konstanten $V_{00}$, $V_{10}$ und $\Delta_0$ auch ohne genaue Kenntnis von $\Phi_0$ bereits bekannt ist. Mit Hilfe der Glgn. (2.5), (2.7) und (2.10) können die Konstanten $V_{00}$, $V_{10}$ und $\Delta_0$ in Abhängigkeit von $\Phi_0$ bestimmt werden. Aus physikalischen Gründen ist die Rearrangementenergie immer positiv, also $\Delta_0 \geqq 0$. Daraus folgt, wenn man nur den physikalisch sinnvollen Teil der Funktion $\Delta_0(\Phi_0)$ betrachtet, daß $\Phi_0 \leqq 44.2$ MeV sein muß †, wodurch auch die Werte von $V_{00}$ und $V_{10}$ stark eingeschränkt werden. Das Verhalten von $V_{00}(\Phi_0)$, $V_{10}(\Phi_0)$ und $\Delta_0(\Phi_0)$ ist in Abb. 2 dargestellt. Weiterhin nehmen die Größen $V_{00}$, $V_{10}$ und $\Delta_0$ für $\Phi_0 \to -\infty$ endliche Grenzwerte an, so daß der zur Verfügung stehende Wertebereich ziemlich klein ist. In Tab. 1 sind für einige Werte von $\Phi_0$ die entsprechenden Werte von $V_{00}$, $V_{10}$ und $\Delta_0$ angegeben. Ergänzend ist in einer weiteren Spalte die effektive Masse angegeben worden. In Tab. 1 ebenso wie in Abb. 2 ist der stark eingerahmte Bezirk der physikalisch wichtige Wertebereich der untersuchten Funktionen. Bei dieser Abgrenzung ist von der weiteren Einschränkung

† Für $S$ wurde dabei der aus der Weizsäcker-Bethe-Formel folgende Wert von $S = 15.74$ MeV gewählt [15]).

$$V_{10} \geqq 0 \qquad \frac{m^*}{m} \leqq 1 \tag{2.12}$$

Gebrauch gemacht worden, die im Folgenden noch genauer begründet werden soll.

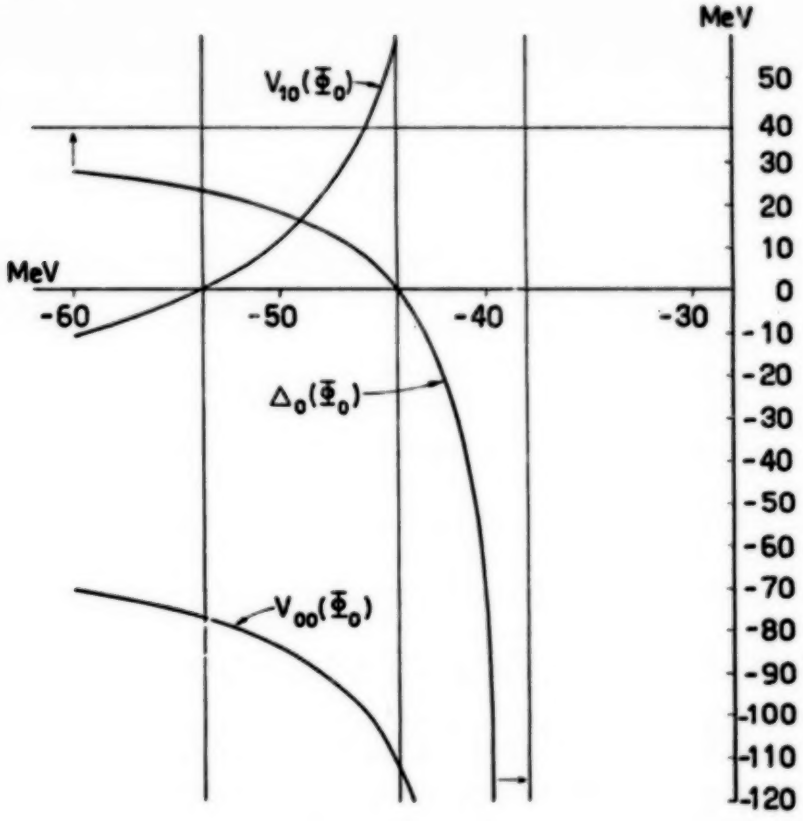


Abb. 2. Zusammenhang der Potentiale.

Aus der Untersuchung der wirklichen Kerne wird sich später (Kap. 4) ergeben, daß $\Phi_0 = -50$ MeV ist, (4.6) also innerhalb der angegebenen Schranken liegt. Der nach Tab. 1 daraus folgende Wert von $\Delta_0 = 18.6$ MeV stimmt angenähert mit dem von Brueckner [8]) berechneten Wert $\Delta_0 = 16$ MeV überein. Die entsprechenden Potentialwerte ($V_{00} = -84.185$ MeV, $V_{10} = +11.83$ MeV) weichen demgemäß von den früher [7]) mit $\Delta_0 = 0$ bestimmten Werten stark ab.

Verwendet man zur Berechnung von $V_0$ ein Hartree-Fock-Verfahren, so erhält man bei Verwendung von solchen Austauschkräften, die gleichzeitig Absättigung der Energie gewährleisten [7]), in erster Näherung einen positiven Wert für $V_{10}$. Da jedoch das Hartree-Fock-Verfahren in der Kernphysik durch die Anwesenheit von hard-core Kräften nicht anwendbar ist, soll hier die Glg. (2.12) etwas allgemeiner begründet werden. Im Rahmen der

TABELLE 1

| $-\Phi_0$ | $V_{00}$ | $\Delta_{10}$ | $V_0$ | $\frac{m^*}{m} = T/T+V_{10}$ |
|---|---|---|---|---|
| 38 | $-\infty$ | $+\infty$ | $-\infty$ | 0 |
| 40 | −233.61 | +261.0 | −81.08 | +0.127 |
| 42 | −144.0 | +111.5 | −21.27 | +0.254 |
| 44.207 | −112.1 | + 58.34 | 0 | +0.394 |
| 46 | − 99.03 | + 36.75 | + 8.62 | +0.508 |
| 48 | − 90.17 | + 21.8 | +14.54 | +0.635 |
| 50 | − 84.185 | + 11.83 | +18.6 | +0.762 |
| 52 | − 79.91 | + 4.71 | +21.5 | +0.889 |
| 53.74 | − 77.08 | + 0 | +23.33 | +1.0000 |
| 55 | − 75.36 | − 2.82 | +24.46 | +1.08 |
| 60 | − 70.55 | − 10.81 | +27.66 | +1.397 |
| $\infty$ | − 54.28 | − 38.0 | +38.54 | $+\infty$ |

Brueckner'schen Störungstheorie, bei der auch hard-core Kräfte berücksichtigt werden können, berechnet sich das Einteilchenpotential $V_0(\mathbf{k}_i)$ aus den Matrixelementen der $t$-Matrix [1–6])

$$V_0(\mathbf{k}_i) = \sum_j (t_{ij,ij} - t_{ij,ji}).$$

Nehmen wir an, daß die effektive Wechselwirkung eines Paares $(\mathbf{k}_i, \mathbf{k}_j)$ in der unendlich ausgedehnten Kernmaterie näherungsweise nur vom Relativimpuls abhängt, so gilt ($\Omega$ ist das Normierungsvolumen)

$$V_0(\mathbf{k}_i) = \Omega^{-1} \sum_j t(\mathbf{k}_i - \mathbf{k}_j). \tag{2.13}$$

Im Anschluß an Skyrme [11]) wollen wir annehmen, daß sich $t(\mathbf{k}_i - \mathbf{k}_j)$ in dem betrachteten Energiebereich durch einen quadratischen Ansatz

$$t = t_0 + t_1(\mathbf{k}_i - \mathbf{k}_j)^2 \tag{2.14}$$

approximieren läßt. Nimmt man weiter an, daß bei der Summation in (2.13) die gemischten Terme näherungsweise verschwinden, so folgt, wenn man die Summation durch Integration ersetzt,

$$V_0(k) = t_0\rho + t_1 \tfrac{3}{5} \left(\frac{3\pi^2}{2}\right)^{\frac{2}{3}} \rho^{5/3} + t_1 \rho k^2 \tag{2.15}$$

wobei $\rho = (2/3\pi^2)k_F^3$ die Dichte der Kernmaterie ist.

Die Energie pro Teilchen unter Einschluß der kinetischen Energie lautet

$$E/A = \frac{\rho^{\frac{2}{3}}}{2m} \frac{3}{5} \left(\frac{3\pi^2}{2}\right)^{\frac{2}{3}} + \tfrac{1}{2} t_0 \rho + \tfrac{3}{5} \left(\frac{3\pi^2}{2}\right)^{\frac{2}{3}} t_1 \rho^{5/3}. \tag{2.16}$$

Aus (2.2) und der Sättigungsbedingung $E/A = \mathrm{d}E/\mathrm{d}A$ folgt dann, daß $E/A$ in bezug auf $\rho$ ein Minimum haben muß. Im Rahmen eines selbstkonsistenten Verfahrens wird die $t$-Matrix stets von der Dichte abhängig

sein. Diese Abhängigkeit rührt in erster Näherung vom Normierungsvolumen her, da die Matrixelemente einen Faktor $\Omega^{-1}$ enthalten. In höheren Näherungen hängt $t$ noch über $k_F$ von der Dichte ab, und über Verschiebungen des Energiespektrums bei Veränderungen der Dichte. In der ersten Näherung sind also $t_0$ und $t_1$ nicht von der Dichte abhängig. Nimmt man an, daß die erste Näherung bereits eine gute Näherung ist, also $t_0$ und $t_1$ nicht stark von $\rho$ abhängen, so sieht man sofort aus (2.16), daß $E/A$ nur dann ein Minimum hat, wenn $t_0 \leqq 0$ und $t_1 \geqq 0$ ist. Wegen (2.5) und (2.15) heißt das, daß $V_{10} \geqq 0$ sein muß †.

Wir wollen hier noch (2.1) im Zusammenhang mit dem Ansatz (2.14) für die $t$-Matrix diskutieren. Aus (2.1) und (2.16) folgt, daß

$$-S = \frac{d\varepsilon}{d\rho} = T + V_0(k_F) + \left[\tfrac{1}{2}\rho^2 \frac{dt_0}{d\rho} + \frac{3}{5}\left(\frac{3\pi^2}{2}\right)^{\frac{2}{3}} \frac{dt_1}{d\rho}\right] \tag{2.17}$$

ist. Vergleicht man dies mit (2.7), so folgt, daß die Rearrangementenergie $\Delta_0$ durch

$$\Delta_0 = \tfrac{1}{2}\rho^2 \frac{dt_0}{d\rho} + \frac{3}{5}\left(\frac{3\pi^2}{2}\right)^{\frac{2}{3}} \frac{dt_1}{d\rho} \tag{2.18}$$

gegeben ist. Die Näherung (2.6), die dem Fall $\Delta_0 = 0$ entspricht, erhält man also, wenn man annimmt, daß $t_0$ und $t_1$ nicht von $\rho$ abhängen, die $t$-Matrixelemente also nur durch den Normierungsfaktor von $\rho$ abhängen. Um ein $\Delta_0 \neq 0$ zu erhalten, ist es daher notwendig, auch die höheren Näherungen des selbstkonsistenten Verfahrens zu berücksichtigen, in denen $t_0$ und $t_1$ nicht mehr von $\rho$ unabhängig sind.

## 3. Die wirklichen Kerne

### 3.1. ANSATZ UND RECHENMETHODE

In Kap. 2 hat sich gezeigt, daß zur Bestimmung von $V_{00}$, $V_{10}$ und $\Delta_0$ die Kenntnis des optischen Potentials $\Phi_0$ der Kernmatiere notwendig ist. Experimentell sind nur die optischen Potentiale $\Phi^P$ und $\Phi^N$ für Protonen und Neutronen an wirklichen Kernen bekannt. Um daraus $\Phi_0$ bestimmen zu können, soll im folgenden Kapitel die oben für Kernmaterie entwickelte Methode analog auf die wirklichen Kerne übertragen werden. Das bedeutet, daß insbesondere die Symmetrie- und Coulombenergien berücksichtigt werden müssen. Oberflächenenergien sollen wegen der großen rechnerischen Schwierigkeiten [11,12,13]) nicht behandelt werden, jedoch dürfte der dadurch entstehende Fehler sehr klein sein, weil auch in der Weizsäcker-Bethe-Formel die Oberflächenenergie von den übrigen Anteilen getrennt werden kann.

† Die Behauptung, daß aus der Absättigung $V_{10} \geqq 0$ folgt, gilt keineswegs allgemein, sondern nur, wenn $r_c \rho^{\frac{1}{3}}$ ($r_c$ ist der hard-core-Radius) so klein ist, dass höhere Näherungen nicht wesentlich sind, wie die Rechnungen von Brueckner und Gammel an $He^3$ zeigen.

Zur Berechnung der Einteilchenpotentiale verwenden wir als Ansatz für die Kernkräfte wegen der Ladungssymmetrie analog zu (2.14) zwei verschiedene effektive Wechselwirkungen:

$$\begin{aligned} &\text{zwischen gleichen Teilchen} && t_g = g_0+g_1k^2, \\ &\text{zwischen verschiedenen Teilchen} && t_v = v_0+v_1k^2. \end{aligned} \tag{3.1}$$

Ist $Z$ die Protonenzahl eines Kerns, $N$ die Neutronenzahl, so wollen wir annehmen, daß Protonen und Neutronen sich im gleichen Kernvolumen befinden, so daß die Dichte der Protonen bzw. Neutronen durch

$$\rho_P = \frac{Z}{\Omega}, \qquad \rho_N = \frac{N}{\Omega}, \qquad \rho = \frac{A}{\Omega} \tag{3.2}$$

gegeben ist †.

Für die Einteilchenpotentiale erhält man jetzt verschiedene Potentiale für Protonen und Neutronen. Im Unterschied zu (2.15) muß man jetzt nur Protonen und Neutronen bei der Summation unterscheiden. Es ist

$$V^P(k) = V_0{}^P+V_1{}^P k^2/k_F^{P2}, \qquad k_F{}^P = (3\pi^2)^{\frac{1}{3}}\rho_P{}^{\frac{1}{3}}; \tag{3.3}$$

$$V^N(k) = V_0{}^N+V_1{}^N k^2/k_F^{N2}, \qquad k_F{}^N = (3\pi^2)^{\frac{1}{3}}\rho_N{}^{\frac{1}{3}}; \tag{3.4}$$

wobei $V_i{}^P$ und $V_i{}^N$ analog zu (2.15) von $\rho_P$ und $\rho_N$ abhängen. Zur Berechnung der Rearrangementenergien $\Delta^P$ und $\Delta^N$ für Protonen und Neutronen gehen wir analog zu (2.4) on der potentiellen Energiedichte aus

$$\varepsilon_{pot} = \varepsilon_{pot}^P+\varepsilon_{pot}^N = \tfrac{1}{2}(V_0{}^P\rho_P+V_0{}^N\rho_N)+\tfrac{3}{10}(V_1{}^P\rho_P+V_1{}^N\rho_N). \tag{3.5}$$

Durch Differentiation nach $\rho_P$ bzw. $\rho_N$ erhält man nach einigen Umformungen zwei zu (2.17) analoge Beziehungen:

$$\frac{\partial\varepsilon}{\partial\rho_P} = V^P(k_F{}^P)+\Delta^P, \tag{3.6}$$

$$\frac{\partial\varepsilon}{\partial\rho_N} = V^N(k_F{}^N)+\Delta^N, \tag{3.7}$$

wobei $\Delta^P$ und $\Delta^N$ die Rearrangementenergien sind und analog zu (2.18) von $\rho_P$, $\rho_N$ sowie $\partial g_0/\partial\rho_P$ u.s.w. abhängen.

Um später einen Vergleich mit der Weizsäcker-Bethe-Formel durchführen zu können, entwickeln wir $V_0{}^P$, $V_1{}^P$, $V_0{}^N$, $V_1{}^N$, $\Delta^P$ und $\Delta^N$ nach Potenzen von $q = (N-Z)/(N+Z)$ (bis zu $q^2$), wobei wir annehmen wollen, daß $g_0$, $g_1$, $v_0$ und $v_1$ selbst nicht mehr von $q$ abhängen. Die Entwicklung der Potentiale ergibt

† Da die Tatsachen, daß sich die Protonen in einem kleineren Volumen als die Neutronen befinden, hauptsächlich auf einen Oberflächeneffekt zurückzuführen ist, ist est nicht sinnvoll diesen Effekt hier zu berucksichtigen. Vgl. dazu z. B. Ref.[16])

$$V_i^{\mathrm{P}} = V_{ik}(-q)^k, \qquad V_i^{\mathrm{N}} = V_{ik}q^k \qquad \begin{pmatrix} i = 0,1 \\ k = 0,1,2, \end{pmatrix}, \tag{3.8}$$

mit

$$\begin{aligned} V_{00} &= \alpha+\gamma+\tfrac{3}{5}(\beta+\delta) & V_{10} &= \beta+\delta \\ V_{01} &= \alpha-\gamma+\beta-\delta & V_{11} &= \tfrac{5}{3}\beta-\tfrac{1}{3}\delta \\ V_{02} &= \tfrac{1}{3}(\beta+\delta) & V_{12} &= \tfrac{5}{9}\beta-\tfrac{7}{9}\delta \end{aligned} \tag{3.9}$$

und

$$\begin{aligned} \alpha &= \tfrac{1}{2}g_0\rho & \gamma &= \tfrac{1}{2}v_0\rho \\ \beta &= g_1(3\pi^2)^{\frac{2}{3}}\left(\frac{\rho}{2}\right)^{5/3} & \delta &= v_1(3\pi^2)^{\frac{2}{3}}\left(\frac{\rho}{2}\right)^{5/3}. \end{aligned} \tag{3.10}$$

Bei der Entwicklung von $\Delta^{\mathrm{P}}$ und $\Delta^{\mathrm{N}}$ nach $q$ ergibt sich, wenn man hier auch die $q$-Abhängigkeit von $\partial g_0/\partial\rho^{\mathrm{P}}$, u.s.w. vernachlässigt,

$$\Delta^{\mathrm{N}} = \Delta^{\mathrm{P}} = \Delta_0+\Delta_2 q^2. \tag{3.11}$$

Damit lassen sich die Potentiale $V^{\mathrm{P}}$, $V^{\mathrm{N}}$ und die Rearrangementenergien $\Delta^{\mathrm{P}}$ und $\Delta^{\mathrm{N}}$ durch die sechs Größen $\alpha$, $\beta$, $\gamma$, $\delta$, $\Delta_0$ und $\Delta_2$ ausdrücken.

### 3.2. AUFSTELLUNG DES GLEICHUNGSSYSTEMS

Um die Koeffizienten $\alpha$, $\beta$, $\gamma$, $\delta$, $\Delta_0$ und $\Delta_2$ durch Vergleich mit den experimentell bekannten Koeffizienten der Weizsäcker-Bethe-Formel bestimmen zu können, berechnen wir zunächst die Gesamtenergie eines Kernes mit $Z$ Protonen und $N$ Neutronen. Ist $E_{\mathrm{c}}$ die Coulombenergie des Kernes, so folgt

$$E = \tfrac{3}{5}(ZT_{\mathrm{P}}+NT_{\mathrm{N}})+E_{\mathrm{c}}+(\tfrac{1}{2}V_0^{\mathrm{P}}+\tfrac{3}{10}V_1^{\mathrm{P}})Z+(\tfrac{1}{2}V_0^{\mathrm{N}}+\tfrac{3}{10}V_1^{\mathrm{N}})N \tag{3.12}$$

wobei $T_{\mathrm{P}}$ und $T_{\mathrm{N}}$ die kinetische Grenzenergie der Protonen bzw. Neutronen ist. Die Entwicklung dieser Größen nach $q$ lautet

$$\begin{aligned} T_{\mathrm{N}} &= T(1+\tfrac{2}{3}q-\tfrac{1}{9}q^2) \\ T_{\mathrm{P}} &= T(1-\tfrac{2}{3}q-\tfrac{1}{9}q^2). \end{aligned} \tag{3.13}$$

Weiterhin berechnen wir analog zu (2.1) die Abtrennarbeiten $S_{\mathrm{P}}$ und $S_{\mathrm{N}}$, die notwendig sind, um ein Proton bzw. Neutron aus dem Kern zu entfernen. Bezeichnet man mit $\bar{V}_{\mathrm{c}}$ das über das Kernvolumen gemittelte Coulombpotential einer homogenen Ladungsverteilung †, so ist, wenn $E$ die Gesamtenergie des Kerns ist,

† Bei der Berücksichtigung des Einflusses der Coulombenergie auf die Abtrennarbeit entsteht folgende Schwierigkeit; In der strengen Glg. (2.2) in der alle Großen ortsabhängig sind, wird dieser Einfluß durch das Coulombpotential der Ladungsverteilung ausgedrückt. Eine ortsunabhängige Dichte $\rho_{\mathrm{P}}$, wie sie hier stets angenommen wurde, ist insofern nicht verträglich mit (2.1), als dadurch zwar $T_{\mathrm{P}}$ und das Kernkraftpotential $V^{\mathrm{P}}$ weitgehend unabhängig vom Ort werden, das Coulombpotential jedoch weiterhin stark vom Ort abhängig ist. In einer ortsunabhängigen Formulierung hat man daher $V_{\mathrm{c}}(x)$ durch einen geeigneten Mittelwert zu ersetzen). Wir wählen hier das über das Kernvolumen gemittelte Coulombpotential einer homogenen Ladungsverteilung, $\bar{V}_{\mathrm{c}} = (6/5)\,Ze^2/R$, weil dieses mit der entsprechenden Coulombenergie durch die einfache Relation $E_{\mathrm{c}} = \frac{1}{2}\bar{V}_{\mathrm{c}}Z$ verbunden ist.

$$-S_P = \frac{\partial E}{\partial Z} = T_P + V^P(k_F{}^P) + \Delta + \bar{V}_c \tag{3.14}$$

$$-S_N = \frac{\partial E}{\partial N} = T_N + V^N(k_F{}^N) + \Delta. \tag{3.15}$$

Die Glgn. (3.12), (3.14) und (3.15) sollen nun mit dem entsprechenden Ausdruck der Weizsäcker-Bethe-Formel verglichen werden:

$$E = -aA + bAq^2 + cA^{\frac{2}{3}} + dZ^2/A^{\frac{1}{3}} \tag{3.16}$$

$$\frac{\partial E}{\partial Z} = -a - 2bq - bq^2 + \frac{2dZ}{A^{\frac{1}{3}}} + \frac{2}{3}cA^{-\frac{1}{3}} - \frac{1}{3}\frac{dZ^2}{A^{4/3}} \tag{3.17}$$

$$\frac{\partial E}{\partial N} = -a + 2bq - bq^2 + \tfrac{2}{3}cA^{-\frac{1}{3}} - \frac{1}{3}\frac{dZ^2}{A^{4/3}} \tag{3.18}$$

wobei die Koeffizienten $a$, $b$, $c$ und $d$ aus den Experimenten bestimmt werden können [15]) †.

Entwickeln wir nun die Glgn. (3.12), (3.14) und (3.15) mit Hilfe von (3.8) und (3.9) nach Potenzen von $q$, so können wir an den dabei entstehenden Ausdrücken einen Koeffizientenvergleich in bezug auf die Potenzen von $q$ mit den entsprechenden Ausdrücken der Glgn. (3.16), (3.17) und (3.18) durchführen.

Vergleicht man die Potenzen von $q^0$, $q^1$ und $q^2$ in den drei Gleichungen, so erhält man 9 Beziehungen für die 6 Unbekannten $\alpha$, $\beta$, $\gamma$, $\delta$, $\Delta_0$ und $\Delta_2$. Auf Grund der Ansätze (3.8), (3.9) und (3.11) sind jedoch nur 4 dieser Beziehungen voneinander unabhängig: die Glgn. I—IV in (3.23). Es müssen daher noch zwei weitere Gleichungen aufgestellt werden, um die 6 Unbekannten berechnen zu können.

Dazu bestimmen wir analog zu der in Kap. 2 angewandten Methode die optischen Potentiale $\Phi^P$ und $\Phi^N$ für Protonen bzw. Neutronen bei der Energie $E = 0$. Entsprechend zu (2.10) müssen dabei die Ausdrücke

$$\Phi^P = V^P(k_0{}^P) + \Delta$$
$$\Phi^N = V^N(k_0{}^N) + \Delta$$

berechnet werden, wobei $k_0{}^P$ bzw. $k_0{}^N$ durch die Glgn.

† Da in (3.12), (3.14) und (3.15) Oberflächenterme nicht berücksichtigt worden sind, so sollen auch die in den Glgn. (3.16), (3.17) und (3.18) auftretenden Oberflächenterme $cA^{\frac{2}{3}}$ und $\frac{2}{3}cA^{-\frac{1}{3}}$ bei dem nachfolgenden Vergleich nicht in Betracht gezogen werden. Der Vergleich der entsprechenden Coulombanteile in (3.14) und (3.17) macht insofern gewisse Schwierigkeiten als das in (3.14) verwendete mittlere Potential $\bar{V}_c$ nur mit $2dZA^{-\frac{1}{3}}$ in (3.17) verglichen werden kann, weshalb wir im Folgenden das Glied $-\frac{1}{3}dZ^2/A^{4/3}$ gegenüber $2dZ/A^{\frac{1}{3}}$ in (3.17) vernachlässigen wollen. Der Fehler der dadurch in $V_c$ entsteht, beträgt etwa 6 %, hebt sich jedoch in den folgenden Endresultaten weitgehend heraus. (Vgl. Seite 184.)

$$-S^{\mathrm{P}}(k_0^{\mathrm{P}}) = \frac{k_0^{\mathrm{P}2}}{2m} + V^{\mathrm{P}}(k_0^{\mathrm{P}}) + \Delta + \bar{V}_{\mathrm{c}} = 0$$
$$-S^{\mathrm{N}}(k_0^{\mathrm{N}}) = \frac{k_0^{\mathrm{N}2}}{2m} + V^{\mathrm{N}}(k_0^{\mathrm{N}}) + \Delta = 0 \tag{3.19}$$

gegeben sind †. Daraus erhält man ††

$$\Phi^{\mathrm{N}} = \frac{T_{\mathrm{N}}(V_0^{\mathrm{N}}+\Delta)}{T_{\mathrm{N}}+V_{1\mathrm{N}}} \approx \frac{T}{T+V_{10}}(V_0^{\mathrm{N}}+\Delta)$$
$$\Phi^{\mathrm{P}} = \frac{T_{\mathrm{P}}(V_0^{\mathrm{P}}+\Delta)}{T_{\mathrm{P}}+V_1^{\mathrm{P}}} - \frac{V_1^{\mathrm{P}}\bar{V}_{\mathrm{c}}}{T_{\mathrm{P}}+V_1^{\mathrm{P}}} \approx \frac{T(V_0^{\mathrm{P}}+\Delta)}{T+V_{10}} - \frac{V_{10}\bar{V}_{\mathrm{c}}}{T+V_{10}}. \tag{3.20}$$

Entwickelt man $\Phi^{\mathrm{N}}$ und $\Phi^{\mathrm{P}}$ nach $q$ bzw. $Z/A^{\frac{1}{3}}$, so folgt wegen (3.8) und (3.11)

$$\Phi^{\mathrm{N}} = \Phi_0 + \Phi_1 q + \Phi_2 q^2,$$
$$\Phi^{\mathrm{P}} = \Phi_0 - \Phi_1 q + \Phi_2 q^2 - \Phi_3 Z/A^{\frac{1}{3}}, \tag{3.21}$$

wobei

$$\Phi_0 = \frac{T}{T+V_{10}}(V_{00}+\Delta_0) \qquad \Phi_2 = \frac{T}{T+V_{10}}(V_{02}+\Delta_2)$$
$$\Phi_2 = \frac{T}{T+V_{10}}(V_{01}) \qquad \Phi_3 = \frac{2dV_{10}}{T+V_{10}} \tag{3.22}$$

ist und die $V_{ik}$ nach (3.9) von $\alpha$, $\beta$, $\gamma$, $\delta$ abhängen.

Die optischen Potentiale $\Phi^{\mathrm{N}}$ und $\Phi^{\mathrm{P}}$ sind für verschiedene Kerne K$(N, Z)$ experimentell bekannt (Kap. 4), so daß die theoretischen Ausdrücke (3.21) und (3.22) unmittelbar mit den Experimenten verglichen werden können. Zur Adjustierung von $\Phi^{\mathrm{P}}$ werden wir daher in Kap. 4 auch einen besonders gut untersuchten Kern heranziehen. Bei dem Vergleich von $\Phi^{\mathrm{N}}$ mit einem entsprechenden Experiment empfiehlt es sich jedoch aus praktischen Gründen, etwas anders vorzugehen. Wegen der Ungenauigkeit der Messungen von Neutronenpotentialen wollen wir nicht einen speziellen Kern zum Vergleich heranziehen, sondern stattdessen verschiedene Werte für $\Phi_0$ vorgeben, um dann erst anhand der jeweils berechneten gesamten Funktion $\Phi^{\mathrm{N}}(q)$ zu entscheiden, welches $\Phi_0$ bzw. welches $\Phi^{\mathrm{N}}(q)$ am besten mit den experimentellen Daten bei mehreren Kernen übereinstimmt.

Mit den oben diskutierten vier Gleichungen aus dem Koeffizienten-

† Es sei bemerkt, daß das Weglassen der Oberflächenenergie in (3.19) zur Bestimmung von $k_0^{\mathrm{P}}$ und $k_0^{\mathrm{N}}$ eine — allerdings nur unwesentlich ins Gewicht fallende — Näherung ist und nicht wie in (3.12), (3.14) und (3.15) durch die nachfolgend angewandte Methode des Koeffizientenvergleiches legitimiert werden kann.

†† Die Näherung $T_{\mathrm{N}}/(T+V_1^{\mathrm{N}}) \approx T/(T+V_{10})$ hat, wie sich aus den in Kap. 4 berechneten numerischen Werten zeigt, einen Fehler von 2 %, was im Rahmen dieser Theorie nicht wesentlich ist. Die Näherung $V_1^{\mathrm{P}}/(T_{\mathrm{P}}+V_1^{\mathrm{P}}) \approx V_{10}/(T+V_{10})$ liefert einen um 6 % zu kleinen Wert. Da dieser Ausdruck jedoch mit $V_{\mathrm{c}}$ multipliziert wird, was (nach Seite 183) um etwa 6 % zu groß ist, beträgt der Fehler des Produktes nur noch 0.4 %.

vergleich von (3.12, 14, 15) mit (3. 15, 17, 18) erhält man die sechs Gleichungen

$$
\begin{aligned}
&\text{(I)} && -a = \tfrac{3}{5}T+\tfrac{1}{2}V_{00}+\tfrac{3}{10}V_{10}\\
&\text{(II)} && +b = \tfrac{7}{15}T+\tfrac{1}{2}(V_{01}+V_{02})+\tfrac{3}{10}(V_{11}+V_{12})\\
&\text{(III)} && -a = T+V_{00}+V_{10}+\Delta_0\\
&\text{(IV)} && -b = -\tfrac{1}{9}T+V_{02}+V_{12}+\Delta_2 \qquad (3.23)\\
&\text{(V)} && \Phi_0 = \frac{T}{T+V_{10}}(V_{00}+\Delta_0)\\
&\text{(VI)} && \Phi^{\mathrm{P}} = \frac{T}{T+V_{10}}(V^{\mathrm{P}}+\Delta)-\frac{V_{10}\bar{V}_c}{T+V_{10}}
\end{aligned}
$$

für die 6 Unbekannten $\alpha, \beta, \gamma, \delta, \Delta_0, \Delta_2$ (Die Größen $V_{ik}$ können nach (3.9) durch $\alpha, \beta, \gamma, \delta$ ausgedrückt werden). Wie man unmittelbar sieht, sind die Glgn. (I), (III) und (V) identisch mit den Gleichungen (2.5), (2.7) und (2.10) so daß $V_{00}$, $V_{10}$ und $\Delta_0$ die in Kap. 2 gesuchten Größen der Kernmaterie sind †.

## 4. Vergleich mit dem Experiment

### 4.1 DIE EXPERIMENTELLEN DATEN

Zur Lösung von (3.23) werden verschiedene experimentelle Werte benötigt. Die Koeffizienten der Weizsäcker-Bethe-Formel (3.16) entnehmen wir einer Untersuchung von Green [15]). Danach ist

$$a = 15.74\ \mathrm{MeV}, \quad b = 23.685\ \mathrm{MeV}, \quad d = 0.709. \qquad (4.1)$$

In (3.23 VI) wird das optische Potential eines bestimmten Kernes für Protonenstreuung bei $E = 0$ benötigt. Experimentelle Streudaten für verschiedene Kerne liegen vor bei $E = 5.25$; 7.5; 17.5 und 31.5 MeV [17, 18, 19]). Eine Analyse dieser Experimente mit dem Ziel, die optischen Potentiale zu bestimmen, ist an einigen dieser Daten durchgeführt worden [20, 21, 22]). Für alle angegebenen Energiewerte liegt eine solche Analyse jedoch nur für den Kern Ni vor. Wir wollen daher im Folgenden bei der Lösung von (3.23) die Daten dieses Kernes verwenden. Um das optische Potential zu erhalten, extrapolieren wir die bei Saxon u.a.[20, 21, 22]) bestimmten Potentiale graphisch auf $E = 0$ (Abb. 3). Die Extrapolation ergibt

† Zur Vermeidung des Ansatzes (3.1) könnte man etwa auch von (3.8) und (3.11) ausgehen, hätte also 6 Unbekannte $V_{ik}$ sowie $\Delta_0$ und $\Delta_2$ zu bestimmen. Der Koeffizientenvergleich zwischen (3, 12, 14, 15) und (3.16, 17, 18) liefert dann 5 unabhängige Gleichungen, so daß man insgesamt mit (3.23 V) und (3.23 VI) 7 Bestimmungsgleichungen hat. Man muß daher noch einen weiteren experimentellen Wert hinzuziehen, z.B. das optische Potential $\Phi^{\mathrm{N}}(q_0)$ eines bestimmten Kernes mit $q = q_0$. Da die aus dem Ansatz (3.1) mit (3.23) berechnete Funktion $\Phi^{\mathrm{N}}(q)$ jedoch bereits mit allen gemessenen Werten $\Phi^{\mathrm{N}}(q)_{\mathrm{exp}}$ gut übereinstimmt, wie Abb. 4 zeigt, ändert ein solches Vorgehen an den Ergebnissen nichts.

$$\Phi^{p}_{exp}(\mathrm{Ni}) = -53.6\ \mathrm{MeV}. \tag{4.2}$$

Für die Lösung von (3.23) wird außerdem noch das Coulombpotential $\bar{V}_c$ benötigt. Mit (4.1) ist

$$\bar{V}_c(\mathrm{Ni}) = 10.128\ \mathrm{MeV}. \tag{4.3}$$

Experimentelle Daten für Neutronenstreuung sind für eine große Anzahl von Kernen bei verschiedenen Energien bis hinab zu 0.5 MeV bestimmt

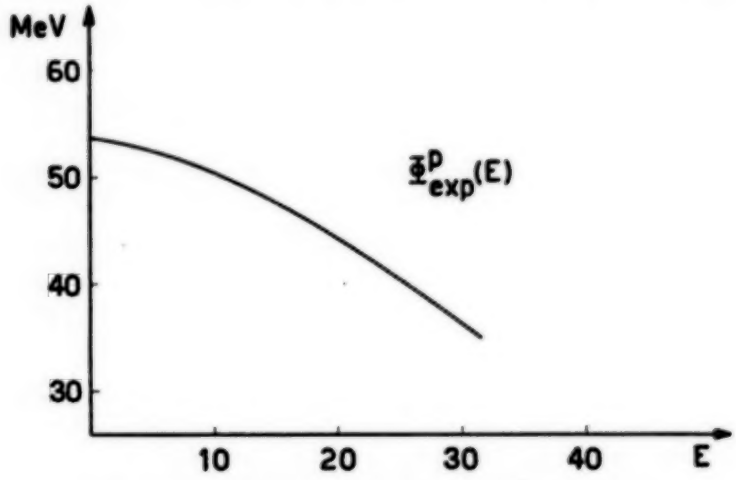


Abb. 3. Experimentelles optisches Potential für Ni.

worden [23]). Eine theoretische Analyse dieser Experimente zur Bestimmung der entsprechenden optischen Potentiale wurde bei den Kernen Fe, Zr, Sn und Bi durchgeführt. Da die Energieabhängigkeit der optischen Modell-Parameter dabei nur in wenigen Fällen berücksichtigt wurde, ist eine Extrapolation dieser Werte auf $E = 0$ nicht möglich. Wir wollen daher im Folgenden diejenigen Werte der optischen Potentiale verwenden, die durch Adjustierung an die experimentellen Daten bei $E = 0.5$ MeV gewonnen wurden. Im Hinblick auf die Ungenauigkeit der Experimente mit Neutronen dürfte dadurch kein wesentlicher Fehler verursacht werden. Die so bestimmten Werte der optischen Potentiale sind in Abb. 4 für die Kerne Zr, Sn und Bi in Abhängigkeit von $q$ eingezeichnet †.

### 4.2. LÖSUNG DES GLEICHUNGSSYSTEMS (3.23)

Das System (3.23) wurde unter Verwendung von (4.1), (4.2) und (4.3) für die drei Werte

$$\Phi_0 = -49\ \mathrm{MeV}, -50\ \mathrm{MeV}, -51\ \mathrm{MeV} \tag{4.4}$$

† Die experimentellen Daten für Fe sind – vermutlich durch einen systematischen Fehler der Messungen – bereits qualitativ mit den übrigen Messungen nicht zu vereinbaren und sollen daher in den folgenden Rechnungen nicht berücksichtigt werden.

gelöst. Mit (3.21) und (3.22) lassen sich dann aus den jeweils berechneten Werten $\alpha$, $\beta$, $\gamma$, $\delta$, $\Delta_0$ und $\Delta_2$ die drei Funktionen $\Phi^N_{49}(q)$, $\Phi^N_{50}(q)$, $\Phi^N_{51}(q)$ bestimmen.

In Abb. 4 sind diese Funktionen in Abhängigkeit von $q$ graphisch dargestellt. Der Vergleich der eingezeichneten Kurven mit den experimentellen Punkten zeigt eindeutig, daß man die beste Übereinstimmung mit den Experimenten bei $\Phi_0 = -50$ MeV erhält. Wir wollen daher $-50$ MeV als den experimentellen Wert von $\Phi_0$ ansehen.

Für die Unbekannten des Systems (3.23) erhält man dann die folgenden Werte:

$$\begin{aligned} \alpha &= -30.46 \text{ MeV} \qquad \gamma = -60.84 \text{ MeV} \\ \beta &= +\ 1.85 \text{ MeV} \qquad \delta = +\ 9.98 \text{ MeV} \end{aligned} \tag{4.5}$$

und für die Potentialparameter (in MeV)

$$\begin{aligned} V_{00} &= -84.2 & V_{01} &= +21.89 & V_{02} &= +3.943 \\ V_{10} &= +11.83 & V_{11} &= -0.245 & V_{12} &= -6.734 \\ \Phi_0 &= -50 & \Phi_1 &= +16.69 & \Phi_2 &= -9.689 \\ \Delta_0 &= +18.6 & \Delta_2 &= -16.65 \end{aligned} \tag{4.6}$$

wobei

$$\Phi_0 = -50;\quad V_{00} = -84.2;\quad V_{10} = 11.83;\quad \Delta_0 = 18.6 \quad \frac{m^*}{m} = 0.762 \tag{4.7}$$

die entsprechenden Daten für die in Kap. 2 behandelte Kernmaterie sind †. Diese Daten wurden bereits bei der Berechnung der Kurven in Abb. 1 verwendet (Vgl. auch Tab. 1).

### 4.3. DISKUSSION DER ERGEBNISSE

Aus (4.5) ersieht man, daß die effektive Wechselwirkung — wenn man von sehr hohen Relativimpulsen absieht — zwischen verschiedenen Teilchen wesentlich größer ist als zwischen gleichen. Dieses Ergebnis macht sich qualitativ sehr deutlich bemerkbar, wenn man die Potentiale $V^P$ und $V^N$ oder die optischen Potentiale $\Phi^P$ und $\Phi^N$ bei Kernen mit verschiedenen $q$-Werten betrachtet.

Bei dem optischen Potential eines Neutrons wird sich mit wachsendem $q$ der Beitrag der Wechselwirkungen zwischen gleichen Teilchen vermehren, der zwischen verschiedenen dagegen verringern. Es ist also zu erwarten, daß $-\Phi^N(q)$ eine mit $q$ abnehmende Funktion ist. Die in Abb. 4 dargestellte Funktion $\Phi^N(q)$ ($\Phi_0 = -50$ MeV) zeigt in der Tat ebenso wie die experimentellen Daten dieses Verhalten. Darüber hinaus sieht man am Vergleich mit

† Mit Hilfe der Störungstheorie wurde kürzlich von Medina [24]) für die effektive Masse des optischen Potentials bei $E = 0$ der Wert $m^*/m = 0.765$ gewonnen, was mit dem hier berechneten Wert sehr gut übereinstimmt.

den Experimenten, daß die Neigung der Kurve, also im wesentlichen $\Phi_1$ (das quadratische Glied spielt wegen der Kleinheit von $q$ keine merkliche Rolle) nicht nur qualitativ dem Verhalten der experimentellen Daten entspricht, sondern auch quantitativ den Verlauf der experimentellen Werte gut wiedergibt.

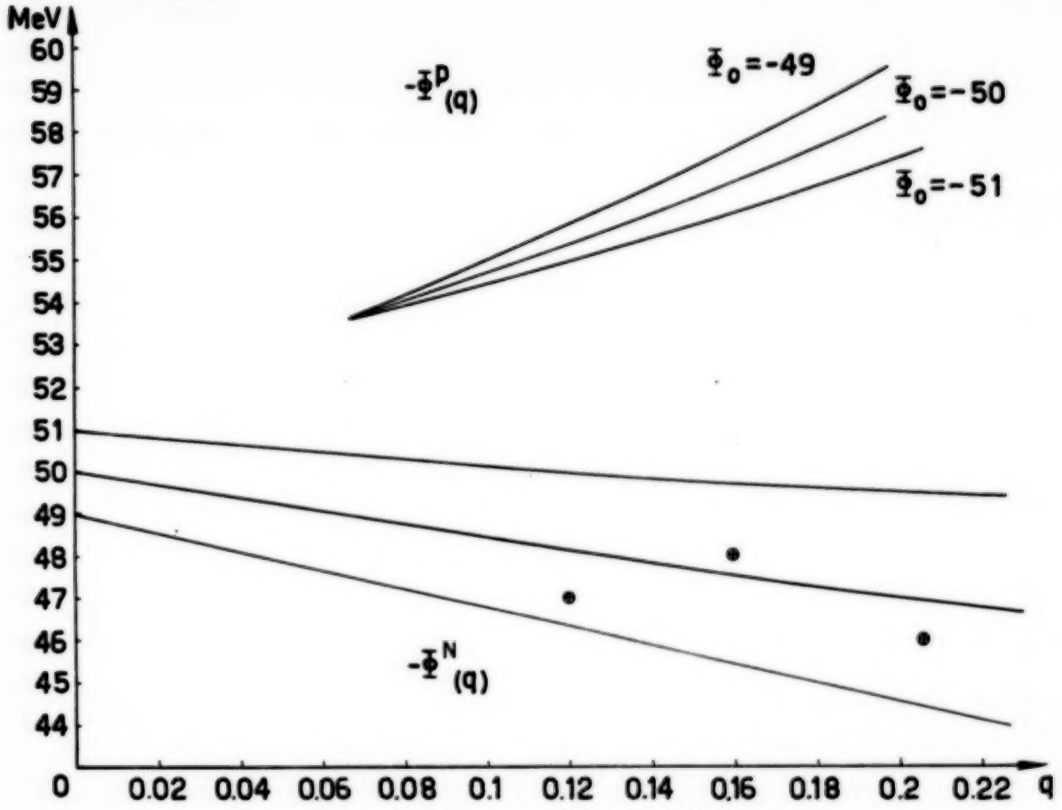


Abb. 4. Verlauf von $\Phi^N(q)$ und $\Phi^P(q)$.

Für das optische Potential eines Protons wird man das umgekehrte Verhalten erwarten, d.h., daß $\Phi^P(q)$ mit $q$ zunimmt. Die in Abb. 4 gezeichneten drei theoretischen Kurven zeigen zwar dieses Verhalten, jedoch ist ein Vergleich mit dem Verlauf der experimentellen Werte $\Phi^P_{exp}(q)$ dadurch erschwert, daß nur bei Ni Messungen bei so niedriger Energie vorliegen, daß eine sinnvolle Extrapolation auf $E = 0$ möglich ist. Der experimentelle Wert von $\Phi^P$ bei Ni (4.2) war deshalb auch zur Lösung von (3.23) verwendet worden.

Bei den Kernen Ag und Au liegen Experimente nur bei 17.5 und 31.5 MeV vor, weshalb eine Extrapolation von $\Phi^P_{exp}(E)$ auf $E = 0$ nicht sinnvoll ist.

Dagegen zeigt sich, daß eine Extrapolation der Differenz

$$f(E) = \Phi^P_{Ag} - \Phi^P_{Au} \tag{4.8}$$

auf $E = 0$ mit keiner besonders großen Willkür behaftet ist. Wählt man

für $f(0)$ versuchsweise die Werte, die sich theoretisch bei $\Phi_0 = -49$, $-50$, $-51$ MeV ergeben (das entspricht den drei Kurven in Abb. 4) und verbindet sie mit den experimentellen Werten bei 17.5 und 31.5 MeV, so ergeben sich die drei in Abb. 5 gezeichneten Kurven. Nimmt man nun an, daß $f(E)$ einen ähnlichen Verlauf hat wie der in Abb. 3 aufgezeichnete Absolutbetrag $\Phi^P(E)$ bei Ni, so entspricht von den drei Kurven in Abb. 5 am besten der Kurve in Abb. 3 diejenige, die mit dem Wert $\Phi_0 = 50$ MeV berechnet wurde.

Unabhängig von dieser vermutlich zufällig genauen Übereinstimmung geht jedoch aus Abb. 5 mit ziemlicher Sicherheit hervor, daß $f(0)$ positiv ist.

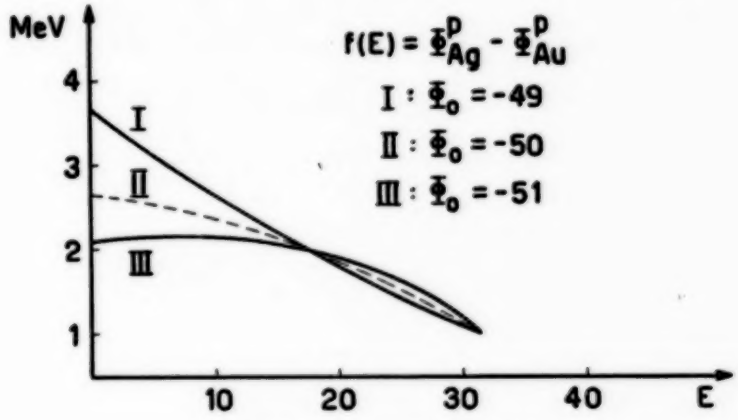


Abb. 5. Verlauf von $f(E)$.

Das bedeutet, daß $-\Phi^P_{exp}(q)$ mit wachsendem $q$ zunimmt, was genau dem oben diskutierten qualitativen Verhalten der berechneten Funktion (Abb. 4) entspricht.

Es zeigt sich somit, daß die theoretisch berechneten Werte von $\Phi^N$ und $\Phi^P$ mit allen zur Zeit vorliegenden Experimenten in guter Übereinstimmung stehen. Da jedoch bisher nur wenige Experimente vorliegen, die wirklich sinnvoll mit der Theorie verglichen werden können, kann die gefundene Übereinstimmung noch kein endgültiger Beweis für die Güte der Theorie sein.

## 5. Zusammenfassung

Mit Hilfe der in Kap. 3 entwickelten halbempirischen Formulierung des Einteilchenmodells der wirklichen Kerne, wurde unter Verwendung der Weizsäcker-Bethe-Formel sowie einiger experimenteller Daten aus Streumessungen mit Protonen und Neutronen die Einteilchenpotentiale $V^P(q)$ und $V^N(q)$ für Protonen bzw. Neutronen in Abhängigkeit vom Neutronenüberschuß $q$ berechnet. (cf. (3.8), (4.6)). Weiterhin wurden die entsprechenden optischen Potentiale $\Phi^P(q)$ und $\Phi^N(q)$ (bei der Streuenergie 0) (3.21), (4.6) und die Rearrangementenergie $\Delta(q)$ (3.11), (4.6) aus der Theorie bestimmt.

Soweit experimentelle Vergleichswerte vorliegen, ist die Übereinstimmung der berechneten optischen Potentiale mit den entsprechenden Meßresultaten gut (Kap. 4.3).

Geht man von $V^N(q)$, $\Delta(q)$ und $\Phi^N(q)$ aus, so entsprechen dem Spezialfall $q = 0$ die in Kap. 2 untersuchten Daten der Kernmaterie (Kap. 3.2). In der Bezeichnung von Kap. 2 ergibt sich für das Einteilchenpotential (4.7) $V_0 = -84.2+11.83\, k^2/k_F^2$ (MeV) für das „optische Potential" $\Phi_0 = -50$ MeV und für die Rearrangementenergie $\Delta_0 = +18.6$ MeV.

Herrn Professor V. F. Weisskopf möchte ich für wertvolle Diskussionen vielmals danken.

## Literatur

1) K. A. Brueckner, Phys. Rev. **96** (1954) 908
2) K. A. Brueckner, Phys. Rev. **97** (1954) 1353
3) H. A. Bethe, Phys. Rev. **103** (1956) 1353
4) H. A. Bethe und J. Goldstone, Proc. Roy Soc.
5) L. G. Gomes, J. D. Walecka und V. F. Weisskopf, Ann. of Phys. **3** (58) 241
6) K. A. Brueckner und J. Gammel, Phys. Rev. **109** (1958) 1023
7) V. F. Weisskopf, Nuclear Physics **3** (1957) 423
8) K. A. Brueckner, Phys. Rev. **110** (1958) 597
9) G. R. Sachler, Phys. Rev. **109** (1958) 429
10) W. J. Swiatecki, Proc. Roy. Soc. **64** (1951) 226; **68** (1955) 285; Phys. Rev. **98** (1955) 209
11) T. H. R. Skyrme, Phil. Mag. **1** (1956) 1043
12) R. B. Hall und R. J. Eden, Nuclear Physics **6** (1958) 157
13) P. Gombas, Die statistische Theorie des Atoms (Wien, 1949)
14) R. Hofstadter, Revs. Mod. Phys. **28** (1956) 214
15) A. E. S. Green, Phys. Rev. **95** (1954) 1006
16) P. Mittelstaedt, Z. Naturforschg. **10a** (1955) 379
17) R. M. Chase und F. Rohrlich, Phys. Rev. **94** (1954) 81
18) D. A. Bromley und N. S. Wall, Phys. Rev. **102** (1956) 1560
19) W. F. Waldorf und N. S. Wall, Phys. Rev. **107** (1957) 1602
20) R. D. Woods und D. S. Saxon, Phys. Rev. **95** (1954) 577
21) D. S. Saxon *et al.*, Phys. Rev. **101** (1956) 507
22) D. S. Saxon *et al.*, Phys. Rev. **106** (1957) 793
23) J. R. Beyster, M. Walt und E. M. Salmi, Phys. Rev. **104** (1956) 1319
24) F. Medina, Dissertation Göttingen (1958)

4. E *Nuclear Physics* 8 (1958) 191—198; © *North-Holland Publishing Co., Amsterdam*
Not to be reproduced by photoprint or microfilm without written permission from the publisher

# DIE FORMEN DER $\beta$-SPEKTREN VON $Na^{22}$, $Na^{24}$ und $P^{32}$

H. DANIEL
*Institut für Physik im Max-Planck-Institut für medizinische Forschung, Heidelberg*

Eingegangen am 30. Mai 1958

**Abstract:** The $\beta$-ray spectra of $Na^{22}$, $Na^{24}$ und $P^{32}$ have been investigated with an iron-free lens spectrometer. The $Na^{22}$ spectrum is found to follow the allowed distribution between 0.16 and 0.47 MeV. The $P^{32}$ spectrum shows a large deviation from the allowed shape. The deviation is proportional to the electron energy and amounts to $(-4.1 \pm 1.3) \times 10^{-2}/mc^2$. No clear cut result has been obtained for $Na^{24}$, but probably there is a small deviation from the allowed shape.

## 1. Ziel der Untersuchung

Unter gewissen Vernachlässigungen (vgl. Zif. 4) wird das Spektrum eines erlaubten $\beta$-Übergangs durch den folgenden Ausdruck gegeben:

$$N(W)\mathrm{d}W = \text{const}\, F(Z, W) pW (W_0 - W)^2 (1 \mp b/W)\mathrm{d}W. \qquad (1)$$

Die Symbole sind dabei in ihrer üblichen Bedeutung gebraucht [1]). Der Fierz-Koeffizient $b$ ist wahrscheinlich Null, auf jeden Fall aber klein (für eine neuere Zusammenstellung der Daten s. Ref.[2])). Im folgenden soll von einem erlaubten Spektrum gesprochen werden, wenn die Form genau durch Glchg. (1) mit $b = 0$ wiedergegeben wird.

Neben Abweichungen von der erlaubten Form proportional $1/W$ (Glchg. (1)) kann man an energieproportionale Abweichungen denken (vgl. Zif. 3):

$$N(W)\mathrm{d}W = \text{const}\, F(Z, W) pW (W_0 - W)^2 (1 + aE)\mathrm{d}W. \qquad (2)$$

Seit langem ist eine ganze Reihe verbotener Übergänge bekannt, deren Spektren nicht die erlaubte Form besitzen [1]). Dagegen wurden bei erlaubten Übergängen bis vor kurzem keine Abweichungen von der erlaubten Spektralform gefunden.

Im folgenden soll über eine Messung der Spektralformen von $Na^{22}$, $Na^{24}$ und $P^{32}$ berichtet werden. Abb. 1 zeigt die Zerfallsschemata [3]). Die verbotenen Übergänge bei $Na^{22}$ und $Na^{24}$ besitzen eine so geringe Intensität, daß sie die Messung an der Hauptgruppe nicht stören. Die untersuchten Übergänge aller drei Isotope haben folgendes gemeinsam: Sie sind nach den Auswahlregeln von Spin und Parität erlaubt, werden ausschließlich oder fast ausschließlich durch Gamow-Teller-Wechselwirkung vermittelt und besitzen *ft*-Werte, die ausgesprochen hoch für erlaubte Übergänge sind. Der $\beta$-Zerfall des $P^{32}$ ist „*l*-verboten".

Die Formen der genannten $\beta$-Spektren sind schon des öfteren Gegenstand von Untersuchungen gewesen [4–8]). Mit Ausnahme von Porter, Wagner und Freedman [6]) berichten alle Autoren, daß die Spektren eine erlaubte Form

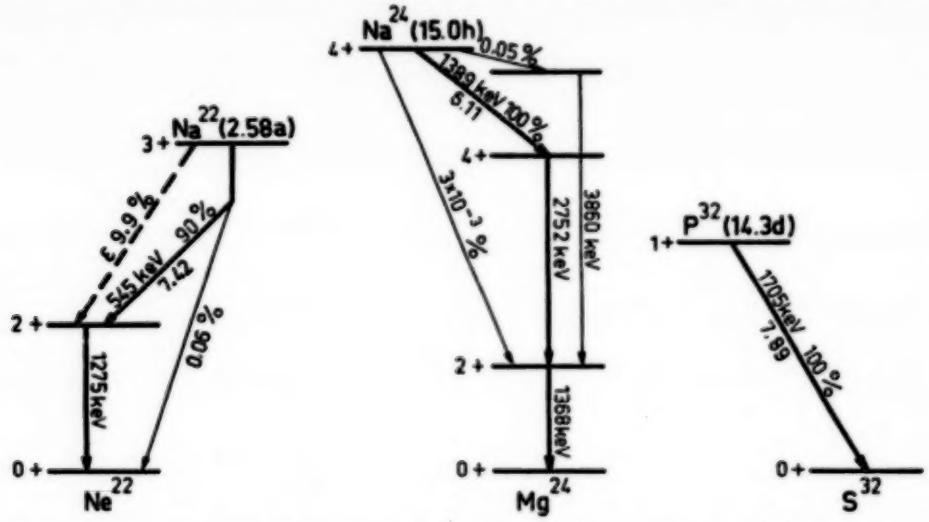


Abb. 1. Zerfallsschemata der untersuchten Isotope. Bei den ausgemessenen $\beta$-Gruppen sind die Werte des Log $ft$ mitangegeben.

besitzen. Porter *et al.*[6]) fanden einen kleinen Unterschied zwischen $Na^{24}$ und $P^{32}$, der wahrscheinlich auf einer nicht erlaubten Form bei $P^{32}$ beruht. Die Größe der Abweichung wird zu etwa 3 % entsprechend $a \approx -1 \times 10^{-2}/mc^2$ angegeben.

## 2. Meßverfahren und Quellenherstellung

Wenn ein $\beta$-Spektrum eine erlaubte Form besitzt, ist nach Glchg. (1) der sog. Formfaktor

$$\mathrm{Ff} = \frac{N(W)}{F(Z,W)pW(W_0-W)^2}$$

unabhängig von der Elektronenenergie. Von besonderer Bedeutung ist offensichtlich die genaue Kenntnis der Grenzenergie $W_0$. Ein etwaiger kleiner Eichfehler des Spektrometers ist dabei ohne wesentlichen Einfluß, weil Grenzenergie und Spektralform mit demselben Gerät bestimmt werden. Gemessen wurde mit dem eisenfreien Heidelberger Doppellinsen-Spektrometer. Als Detektor diente ein Anthracen-Szintillationszähler. Zur Aufnahme des gesamten Kontinuums wurde er in integraler Diskriminierung benutzt, zur separaten Bestimmung der Grenzenergie aus dem oberen Ende des Kontinuums in Einkanaldiskriminierung. Bei der Einkanaldiskriminierung ist der Untergrund praktisch Null.

Die Anordnung ist im Zusammenhang mit der Messung der Spektralform des Spiegelübergangs $N^{13} \rightarrow C^{13}$ ausführlich beschrieben worden[2]). Bei

diesem Spektrum war eine erlaubte Form beobachtet worden. Die jetzigen Messungen und ihre Auswertung wurden genauso ausgeführt. Insbesondere fanden die gleichen Präparathalter und die gleichen Korrekturen auf Zählverluste Verwendung.

Von $Na^{22}$ und $Na^{24}$ wurden je eine Quelle hergestellt und ausgemessen, von $P^{32}$ drei Quellen. Eine der $P^{32}$-Quellen wurde durch Eintrocknen aktiver Lösung auf 50 $\mu g/cm^2$ Celluloid bereitet, wobei die Bildung einzelner großer Kristalle nach Möglichkeit vermieden wurde. Die anderen Quellen wurden durch Aufdampfen hergestellt. Aufgedampft wurde auf 50 $\mu g/cm^2$ Celluloid ($Na^{22}$) oder 210 $\mu g/cm^2$ Al($Na^{24}$ und $P^{32}$). Alle aufgedampften Quellen waren praktisch unsichtbar und mit Sicherheit leichter als 200 $\mu g/cm^2$; diese obere Grenze wurde durch Wägungen ermittelt. Bei diesen Quellen- und Unterlagendicken ist keine Verfälschung des Spektrums zu befürchten [2]).

Jede Quelle wurde wiederholt ausgemessen, wobei zwischen Messungen von kleiner zu großer Elektronenenergie und solchen in umgekehrter Richtung abgewechselt wurde. Zur Kontrolle wurde ferner der zeitliche Abfall bei $Na^{24}$ und $P^{32}$ verfolgt. Die $P^{32}$-Quellen enthielten etwas $P^{33}$, das aber oberhalb seiner Grenzenergie von 0.25 MeV [3]) nicht störte.

## 3. Meßergebnisse

Abb. 2, 3 und 4 zeigen die Fermi-Kurven zur Grenzenergiebestimmung, Abb. 5, 6 und 7 die Formfaktoren als Funktion der Energie; eingezeichnet

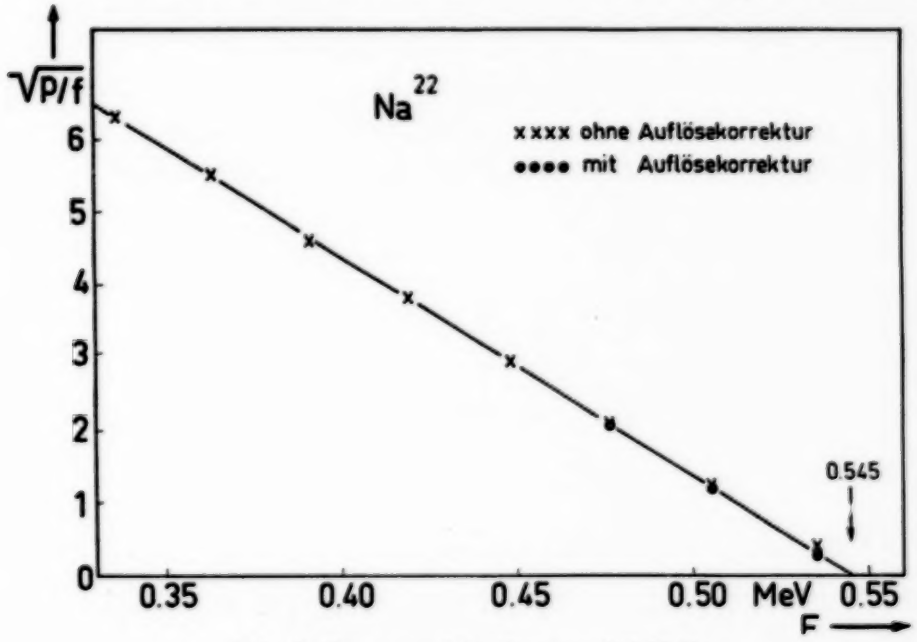


Abb. 2. Grenzenergiebestimmung bei $Na^{22}$.

sind die mittleren statistischen Fehler. Bei $P^{32}$ sind nur die Messungen an einer der beiden aufgedampften Quellen dargestellt. Offensichtlich ist der

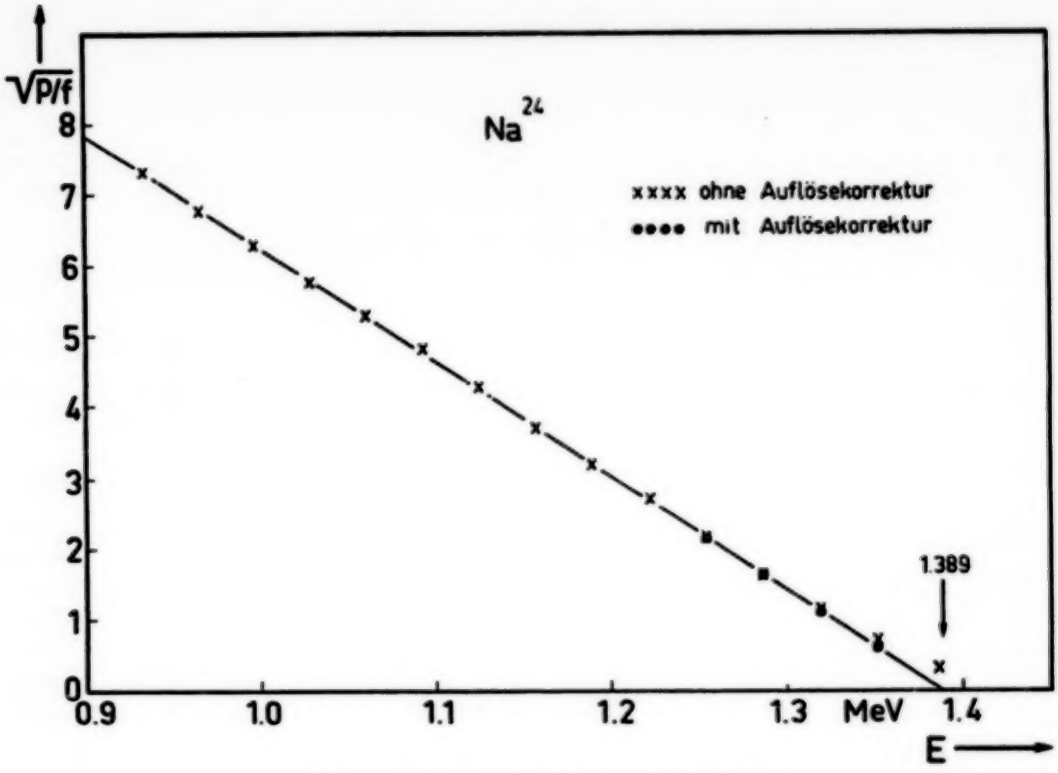


Abb. 3. Grenzenergiebestimmung bei $Na^{24}$.

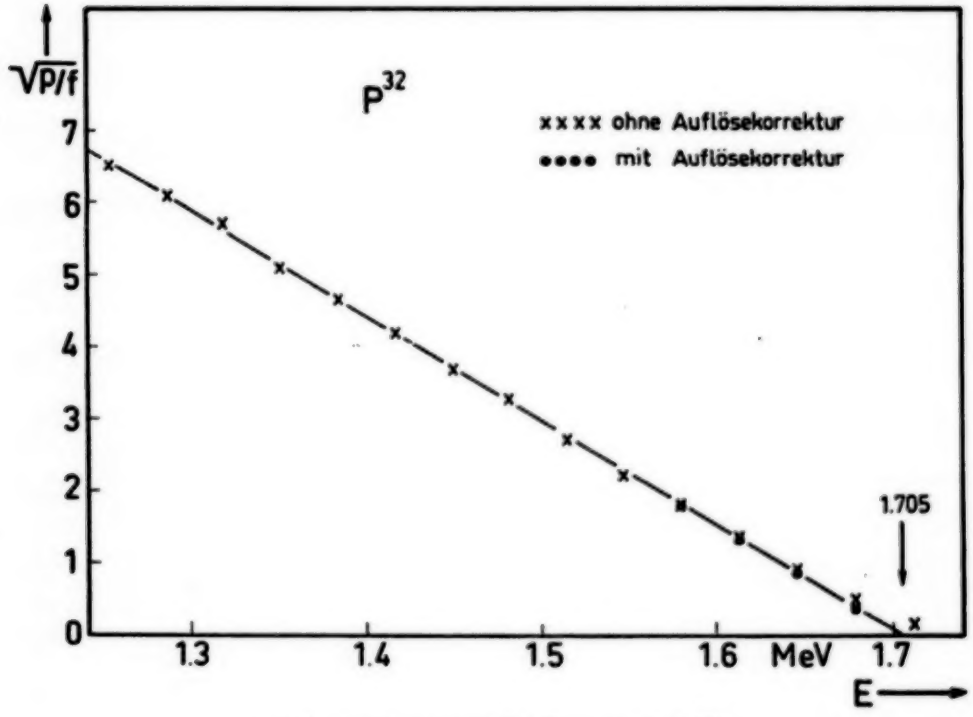


Abb. 4. Grenzenergiebestimmung bei $P^{32}$.

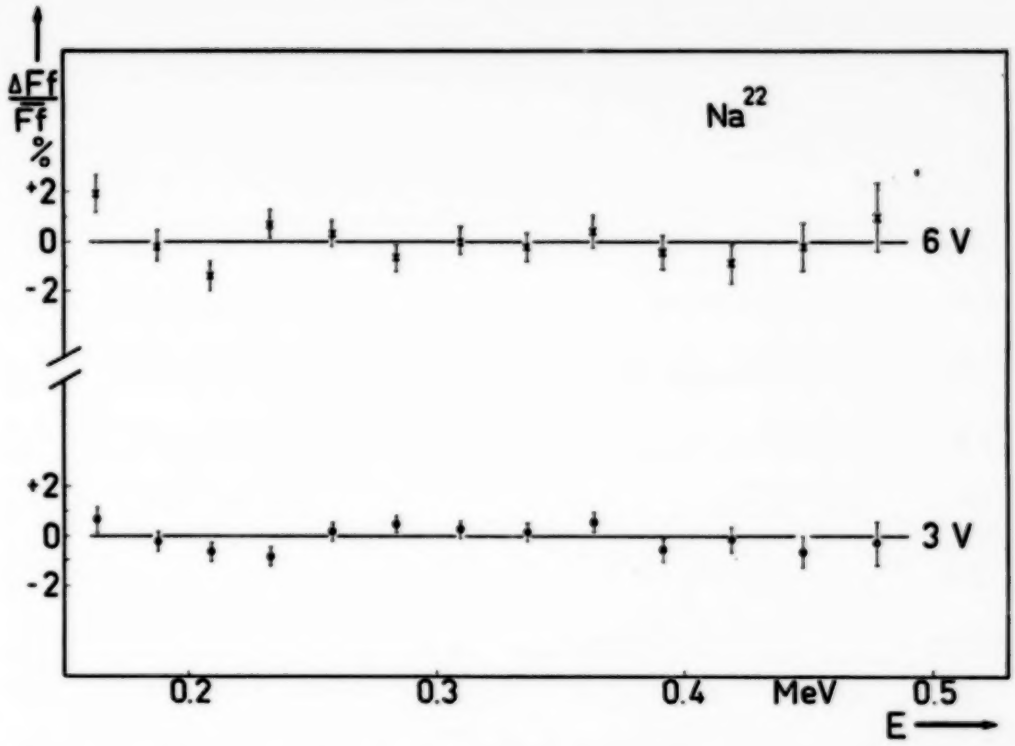


Abb. 5. Formfaktor von $Na^{22}$ als Funktion der Positonenenergie $E$. Obere Kurve: Diskriminierung bei 6 V, untere Kurve: Diskriminierung bei 3V. Die eingezeichneten Geraden parallel zur Abszissenachse stellen den Formfaktor bei erlaubter Spektralform dar.

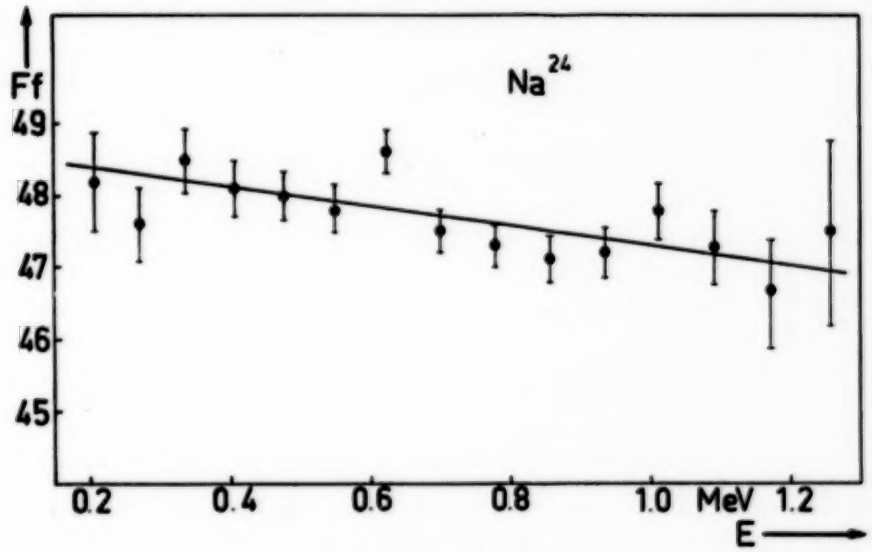


Abb. 6. Formfaktor von $Na^{24}$ als Funktion der Elektronenenergie $E$. Diskriminierung bei 3V. Die eingezeichnete Gerade ist den Meßpunkten durch Ausgleichsrechnung angepaßt.

Formfaktor von $Na^{22}$ im untersuchten Energiebereich konstant, während er bei $Na^{24}$ und $P^{32}$ mit wachsender Elektronenenergie abnimmt. Bei $P^{32}$ nimmt er innerhalb der Meßgenauigkeit linear mit der Energie ab, während die Art der Abnahme bei $Na^{24}$ aus Abb. 6 nicht unmittelbar zu entnehmen ist.

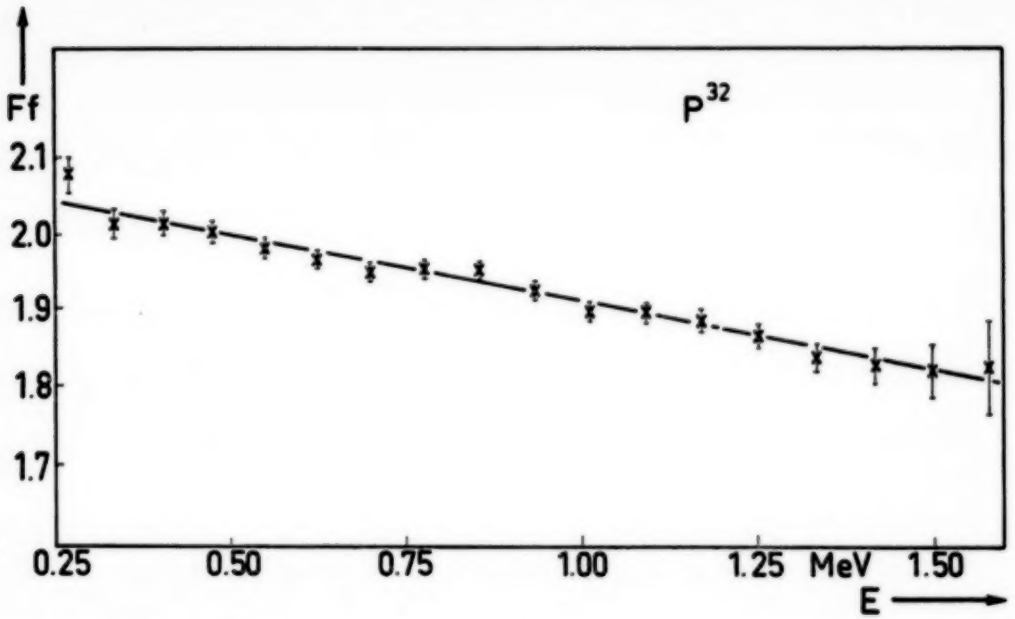


Abb. 7. Formfaktor von $P^{32}$ als Funktion der Elektronenenergie $E$. Diskriminierung bei 3V. Die eingezeichnete Gerade ist den Meßpunkten angepaßt.

Um ein klareres Bild zu gewinnen, wurden die folgenden Größen durch Ausgleichrechnung ermittelt: Koeffizient $b$ nach Glchg. (1) bei $Na^{22}$ und $Na^{24}$ und Koeffizient $a$ nach Glchg. (2) bei $Na^{24}$.

TABELLE 1

Zusammenstellung der Ergebnisse

Die Koeffizienten $b$ und $a$ sind durch Glchg. (1) bzw. Glchg. (2) definiert

| | $Na^{22}$ | $Na^{24}$ | $P^{32}$ |
|---|---|---|---|
| Halbwertzeit mit Fehlergrenze | – | $15.07 \pm 0.15$ h | $14.2 \pm 0.3$ d |
| Grenzenergie mit Fehlergrenze | $545 \pm 2$ keV | $1389 \pm 4$ keV | $1705 \pm 4$ keV |
| Koeffizient $b$ mit mittlerem Fehler | $(-1.6 \pm 2.0) \times 10^{-2}\, mc^2$ | $(+7.2 \pm 2.3) \times 10^{-2}\, mc^2$ | – |
| Koeffizient $b$ mit Fehlergrenze | $(-1.6 \pm 8.0) \times 10^{-2}\, mc^2$ | $(+7.2 \pm 7.2) \times 10^{-2}\, mc^2$ | – |
| Koeffizient $a$ mit mittlerem Fehler | – | $(-1.50 \pm 0.45) \times 10^{-2}/mc^2$ | – |
| Koeffizient $a$ mit Fehlergrenze | – | $(-1.50 \pm 1.50) \times 10^{-2}/mc^2$ | $(-4.1 \pm 1.3) \times 10^{-2}/mc^2$ |

Die Ergebnisse der Messungen und Rechnungen sind in Tab. 1 zusammengestellt. Die Werte für $b$ bei $Na^{22}$ sind aus den beiden in Abb. 5 dargestellten Meßkurven gewogen gemittelt. Der Wert für $a$ bei $P^{32}$ wurde aus den Messungen an den drei Quellen (Zif. 2) ebenfalls durch Mittelung erhalten.

Soweit Ausgleichrechnungen angestellt wurden, wurde als Beitrag der Statistik zu den Fehlergrenzen Tab. 1 der dreifache mittlere Fehler angesetzt.

## 4. Diskussion

Die Daten über Grenzenergie und Halbwertzeit Tab. 1 stimmen bis auf die Grenzenergie von $Na^{22}$ ausgezeichnet mit den Mittelwerten aus den älteren Messungen überein [3]). Auch bei $Na^{22}$ ist der Unterschied nicht außerhalb der Fehlergrenzen.

Innerhalb der Statistik hat das Spektrum des $Na^{22}$ im untersuchten Energiebereich genau die erlaubte Form, während die Abweichungen bei $P^{32}$ außerhalb aller statistischen Schwankungen liegen. Die Messung an $Na^{24}$ ist nicht vollständig unverträglich mit einer erlaubten Spektralform. Dennoch ist es viel wahrscheinlicher, daß eine geringe Abweichung vorhanden ist.

Die Größe der Abweichung bei $P^{32}$ legt es nahe, zunächst an einen systematischen Fehler zu denken, der in diesem Ausmaß jedoch nur bei $P^{32}$ aufgetreten sein dürfte. Ein solcher Fehler ist aber auszuschließen: Einmal wurde mit drei verschiedenen Quellen innerhalb der Statistik das gleiche Ergebnis erzielt, zum anderen ist früher durch ausgedehnte Versuche sichergestellt worden [2]), daß bei den jetzt verwendeten Quellen- und Unterlagendicken keine Verfälschungen auftreten konnten.

Bei $Na^{22}$ besteht Übereinstimmung nicht nur mit den früheren Messungen der Spektralform [4]), sondern auch mit einer Arbeit von Sherr und Miller [9]), die das Verhältnis Elektroneneinfang zu Positonenemission maßen und es gleich dem theoretischen für erlaubte Spektralform fanden.

Zwischen der hier gemessenen Spektralform des $Na^{24}$ und der von Porter *et al.*[6]) beobachteten besteht kein ausgesprochener Widerspruch, aber auch keine gute Übereinstimmung.

Obgleich die von Porter *et al.*[6]) angegebene Abweichung bei $P^{32}$ und die hier mitgeteilte das gleiche Vorzeichen haben, ist die Differenz in der Größe doch so beträchtlich, daß beide Messungen wohl nicht miteinander verträglich sind. Dagegen stimmt der von jenen Autoren gemessene Unterschied in den Spektralformen von $P^{32}$ und $Na^{24}$, der zuverlässiger als jede Spektralform für sich sein sollte [6]), mit dem bei dieser Arbeit zwischen $Na^{24}$ und $P^{32}$ gefundenen Unterschied befriedigend überein (Ref.[6]): $\Delta a \approx -1 \times 10^{-2}/mc^2$; diese Arbeit: $\Delta a = (-2.6 \pm 2.0) \times 10^{-2}/mc^2$).

Ein Teil der bei $Na^{24}$ beobachteten Abweichung von der erlaubten Spektralform könnte von Fierz-Interferenz herrühren; die obere Grenze des Fierz-Koeffizienten für Gamow-Teller-Wechselwirkung ist $4\times10^{-2}mc^2$. Die Messung an $Na^{22}$, dessen Spektrum dann entgegengesetzt gekrümmt sein müßte, schließt diese Möglichkeit nicht aus. Andererseits ist die starke Abweichung bei $P^{32}$ nicht durch Fierz-Interferenz zu erklären, und es erscheint vernünftiger, auch bei $Na^{24}$ eine andere Erklärung zu suchen.

Wie schon in Zif. 1 betont, besitzen alle drei untersuchten Übergänge anomal hohe *ft*-Werte. So ist bei $P^{32}$ die Übergangswahrscheinlichkeit drei Größenordnungen kleiner als bei normalen erlaubten Übergängen. Diese „zufällige" Reduzierung, die für das normalerweise ausschlaggebende Matrixelement gilt, braucht aber keineswegs für andere Matrixelemente zu gelten, mit denen Abweichungen von der erlaubten Spektralform verknüpft sein können.

Mit der Möglichkeit solcher Abweichungen befaßt sich eine Reihe theoretischer Arbeiten. Betrachtet wurden pseudoskalare Kopplung [10]), relativistische Korrekturen [11]) und mesonische Effekte [12]). Offensichtlich sind aber noch zu wenige experimentelle und theoretische Ergebnisse greifbar, um eine Entscheidung für oder gegen eine bestimmte Interpretation zu ermöglichen.

Für die Untersuchung wurden Apparate der Deutschen Forschungsgemeinschaft mitverwendet.

## Literatur

1) K. Siegbahn (Herausgeber), Beta- and Gamma-ray Spectroscopy (North-Holland Publishing Company, Amsterdam, 1955) Kap. IX, X und XI
2) H. Daniel und U. Schmidt-Rohr, Nuclear Physics (im Druck)
3) P. M. Endt und C. M. Braams, Revs. mod. Phys. **29** (1957) 683; B. S. Djelepov und L. K. Pecker, Zerfallsschemata radioaktiver Isotope (Akad. NAUK, Moskau, 1957)
4) P. A. Macklin, L. J. Lidofsky und C. S. Wu, Phys. Rev. **78** (1950) 318; D. E. Alburger, D. J. Hughes und C. Eggler, Phys. Rev. **78** (1950) 318; C. Wong, Phys. Rev. **95** (1954) 761
5) K. Siegbahn, Phys. Rev. **70** (1946) 127; E. F. De Haan und G. J. Sizoo, Physica **21** (1955) 818
6) F. T. Porter, F. Wagner jr. und M. S. Freedman, Phys. Rev. **107** (1957) 135
7) N. M. Anton'eva, A. A. Bashilov, B. S. Dzhelepov und V. I. Orlov, Izvest. Akad. Nauk Ser. Fiz. SSSR **18** (1954) 93 [zitiert nach Nucl. Cards, Nucl. Data Group, NBS, Washington]
8) A. V. Pohm, R. C. Waddell und E. N. Jensen, Phys. Rev. **101** (1956) 1315; dort auch ausführliches Verzeichnis der älteren Literatur über $P^{32}$
9) R. Sherr und R. H. Miller, Phys. Rev. **93** (1954) 1076
10) G. Alaga, O. Kofoed-Hansen und A. Winther, Mat. Fys. Medd. Dan. Vid. Selsk. **28** (1953) no. 3
11) G. Alaga, L. Šips und D. Tadić, Nuclear Physics **6** (1958) 303, und dort zitierte Literatur
12) M. Gell-Mann, Vorabdruck

9.A *Nuclear Physics* 8 (1958) 199—206; © *North-Holland Publishing Co., Amsterdam*
Not to be reproduced by photoprint or microfilm without written permission from the publisher

# ON THE ANGULAR DISTRIBUTION OF SHOWER PARTICLES GENERATED IN HIGH-ENERGY NUCLEAR INTERACTIONS

G. BOZÓKI, E. FENYVES and ÉVA GOMBOSI
*Central Research Institute of Physics Dept. of Cosmic Rays, Budapest*

Received 9 May 1958

**Abstract:** The differential and integral angular distributions of shower particles produced in high-energy nuclear interactions are calculated according to the multiple meson production theories of Fermi, Landau and Heisenberg [8-11]) for nucleon-nucleon interaction. Angular distributions calculated according to the theory of Landau are given for nucleon-nucleus interaction too. It is shown by summarizing the experimental data of jets of energies higher than $10^{13}$ eV that the angular distribution alone does not show unambiguously which of the multiple meson production theories, if any, is the correct one.

## 1. Introduction

Several authors have investigated the angular distribution of the secondaries of energetic jets and have reported that the angular distribution in the centre of mass system (CMS) is strongly anisotropic for primary energies higher than $10^{12}$ eV [1-5]). A significant deviation from isotropy was shown also for lower energies [6]). The angular distributions were compared generally with the distributions expected on the basis of current theories [8-11]) of multiple meson production. In some papers, however, comparison was not made with all theories, thus the conclusions drawn from their results concerning the agreement between the angular distribution as found experimentally and predicted theoretically cannot be accepted without reserve.

The aim of the present paper is to give the results of calculations of differential and integral angular distributions on the basis of the theories of Fermi [9]), Landau [10]) and Heisenberg [11]), respectively, and to compare them with the experimental data available.

## 2. Angular Distribution in Nucleon-Nucleon Collision

The differential and integral angular distribution of shower particles generated in nucleon-nucleon collisions were calculated †) according to the theories of Fermi, Landau and Heisenberg [9-11]). The distributions of the

† For the details of the calculation see ref. [7]), where the approximations used and the resulting expressions for the different angular distributions are given.

product $\gamma_c \operatorname{tg} \theta$† which is to a large extent independent of primary energy, are plotted in figs. 1 and 2.

The curves J in the figures correspond to an isotropic distribution and to the assumption that $m = \beta_0/\overline{\beta}_s$, the ratio of the velocities of the primary and secondary particles in the CMS, is equal to unity, this condition being approximately fulfilled at very high energies.

The angular distribution following from the first formulation of the Fermi theory [8]) is isotropic and at high energies it can be well approximated by the curve J. In the second paper of Fermi [9]) the conservation of angular momentum was also taken into account resulting in the modified differential angular distribution being anisotropic, the shape of the distribution curve depending on the impact parameter of the collision. Bearing in mind that the impact parameter of collision cannot be determined directly from the data obtained from a jet without some theoretical assumption, it becomes clear that the only way of comparing the angular distributions as found experimentally with those expected theoretically is to build on the one hand a

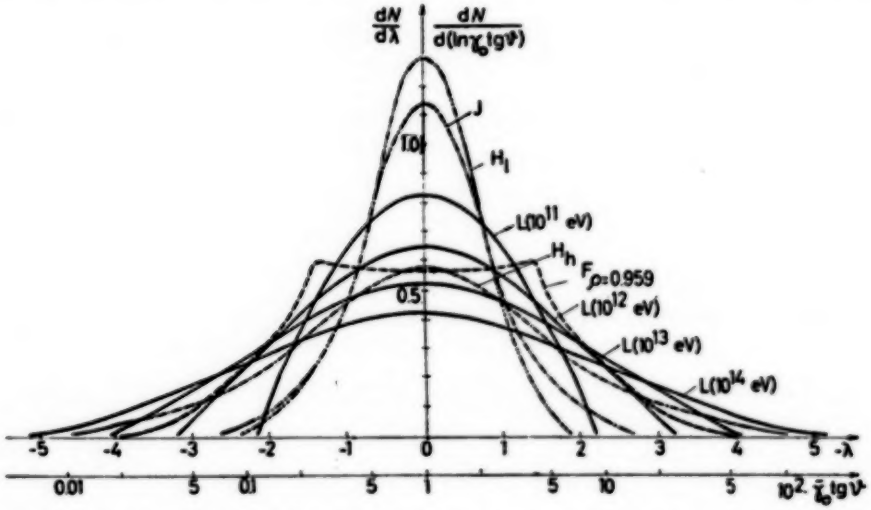


Fig. 1. Differential angular distribution of shower particles calculated according to 1) isotropic emission in the CMS and $m = 1$ (J), 2) Fermi theory using median impact parameter value ($F_{\rho=0.959}$), 3) Landau theory in the case of energies from $10^{11}$ to $10^{14}$ eV ($L(10^{11}$ eV) to $L(10^{14}$ eV)), 4) approximation of the Heisenberg theory at low energies ($H_l$) and 5) approximation of the Heisenberg theory at high energies ($H_h$).

composite jet from a great number of unbiased experimental events and to calculate on the other with the median impact parameter value $\rho = 0.959$ (see curve $F_{\rho=0.959}$ in the figures).

The angular distribution following from the theory of Landau is strongly anisotropic, the degree of anisotropy increasing with the primary energy. In

† $\gamma_c$ is the energy of the nucleon in the centre of mass system (CMS) in nucleon rest mass units, $\theta$ is the angle of emission in the laboratory system (LS) and $\ln \gamma_c \operatorname{tg} \theta = -\lambda$ the well-known parameter of the Landau theory [10]).

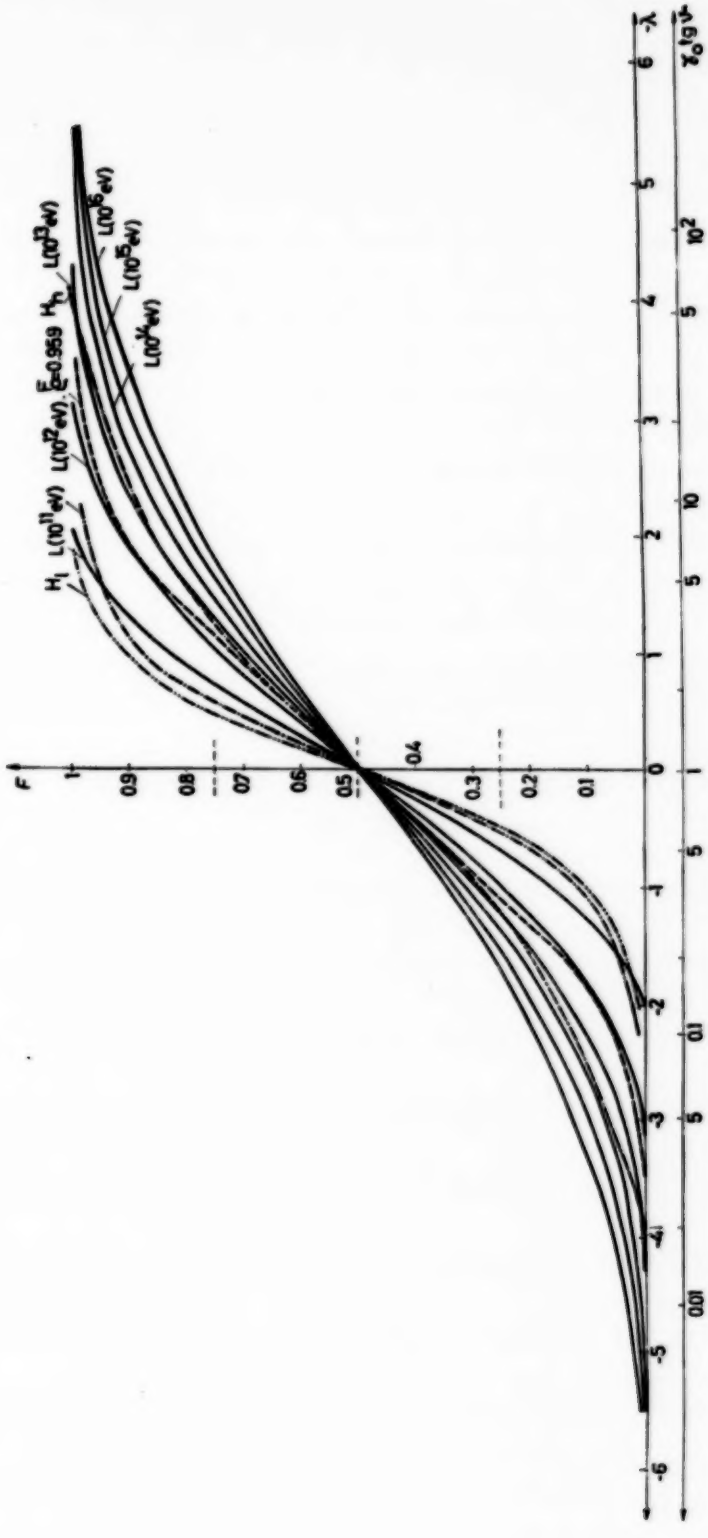


Fig. 2. Integral angular distribution of slower particles calculated according to various multiple meson production theories.

the figures the differential and integral Landau distributions are plotted for energies $10^{11}$, $10^{12}$, $10^{13}$ and $10^{14}$ eV, respectively.

The angular distribution of emitted particles in the Heisenberg theory is also anisotropic, here too the degree of anisotropy is strongly increasing with the primary energy. However, at relatively low energies it can be approximated by an isotropic distribution as was done by Symanzik [12]) (see curves $H_1$ in the figures). If the primary energy is very high, there is a strong collimation of emitted particles around the collision axis in the CMS. Consequently, the forward and backward cones of the CMS are separated in the LS to a large extent. The angular distribution in the case of maximum separation of the two cones was approximated by Symanzik [12]) and this approximation is valid for energies higher than $10^{12}$ eV (see curves $H_h$ in the figures).

In the case of a nucleon-nucleus collision the angular distribution of emitted particles depends not only on the particular theory applied but in addition on the model describing the event and therefore comparison between theory and experiment will be much more complex. This can be illustrated e.g. in the case of the Landau theory, where the angular distribution for a given primary energy is the less anisotropic the higher the mass number of the target nucleus (see app. 1).

## 3. Comparison of the Theoretical and Experimental Angular Distributions

It can be seen from the figures that the difference between the isotropic and anisotropic angular distributions increases with increasing primary energy of the colliding particles. So as to decide whether the theories resulting in isotropic (Fermi's first formulation) or those resulting in anisotropic angular distribution (Fermi's second formulation, Landau and Heisenberg) give better fit with the experimental data it is thus best to investigate jets with energies higher than $10^{12}$ or $10^{13}$ eV. Building up of a composite jet makes possible the comparison with the Fermi distribution calculated with the median impact parameter value, such a jet improving at the same time the statistical accuracy.

It must be emphasized, however, that the nuclear interactions found in emulsion plates seem to be rather nucleon-nucleus collisions than nucleon-nucleon ones and until now there exists no procedure by which it could be ascertained without any doubt whether the collision is a nucleon-nucleon interaction or not. The conventional selection of jets with a relatively small number of black and gray tracks ($N_h$) does not rule out with certainty the nucleon-nucleus interactions but provides a certain bias against them.

Following the above considerations we have selected jets of energies

higher than $10^{13}$ eV for which $N_h \leqq 3$ [1,3,4,5,14,15])† and built a composite jet containing thus 142 shower particles. The differential angular distribution of this composite jet is plotted in fig. 3 together with the theoretical distributions calculated respectively; assuming isotropic emission (J), on the basis of the second Fermi theory with median impact parameter ($F_{\rho=0.959}$), according to the Landau theory in the case of primary energies of $10^{13}$ and $10^{14}$ eV (L) and finally according to the Heisenberg theory at very high energies ($H_h$).

Assuming that the composite jet corresponds to an average nucleon-nucleon collision, it may be concluded that the experimental angular distribution agrees within the limits of errors with the Landau and Heisenberg distributions but deviates significantly from the isotropic and Fermi ($\rho = 0.959$) distributions, the Pearson probabilities for these using a $\chi^2$-test, being respectively

$$P_{\chi^2}(J) < 10^{-5} \quad \text{and} \quad P_{\chi^2}(F_{\rho=0.959}) < 10^{-3}.$$

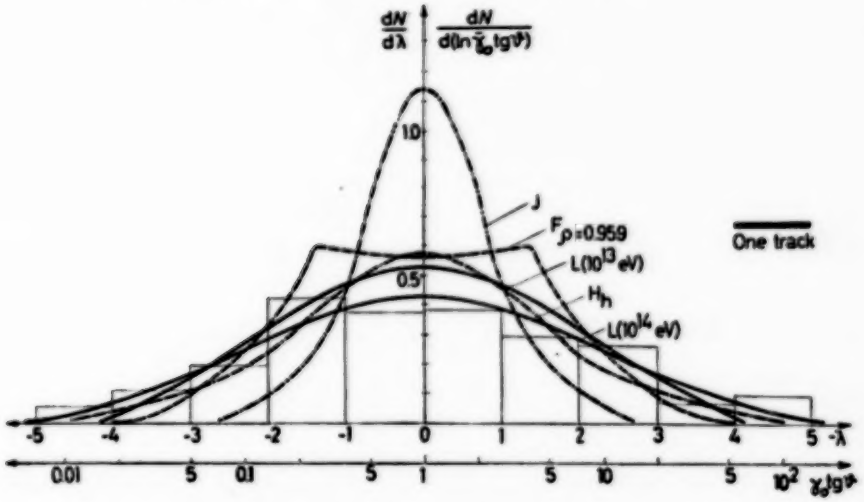


Fig. 3. Differential angular distribution of shower particles of jets with energies higher than $10^{13}$ eV: 1) sum of the experimental data published in ref. [1,3,4,5,13,15]) (histogram), 2) distribution calculated according to isotropic emission in the CMS and $m = 1$(J), 3) Fermi distribution using median impact parameter value ($F_{\rho=0.959}$), 4) Landau distribution in the case of $10^{13}$ and $10^{14}$ eV energies (L)$10^{13}$ eV), L($10^{14}$ eV)) and 5) approximation of the Heisenberg distribution at high energies ($H_h$).

From the above considerations it seems to be very probable that isotropic angular distribution can be ruled out as was pointed out also in several other papers (see e.g. ref.[5])). As regards, however, the comparison with the Fermi distribution calculated with the median impact parameter value caution is indicated. Three of the jets [3,4,5]) building up the composite jet

† From ref. [13]) we have selected the (0+4p) and (0+22p) showers, the $\gamma$ value of which had been determined unambiguously.

were produced as a matter of fact, by $\alpha$ particles and thus some of the very small-angle tracks in these jets may correspond to fragments of the primary particle. This effect will cause a more pronounced concentration of tracbs near the axis in the forward cone, i.e. for small $\theta$ values (see fig. 3). In addition, in cases where the incoming particle collides with a nucleus the emitted particles may be scattered in the nucleus before escaping, giving thus a broader distribution of angles in the LS. Some of these scattered particles may have sufficiently great angles to increase appreciably the tail of the differential distribution of $\gamma_c$ tg $\theta$ at high $\theta$ values. The strongest deviation between the experimental and $F_{\rho=0.959}$ curves is just in these regions. Neglecting terms corresponding to $|\ln \gamma_c \operatorname{tg} \theta| > 4$ in the $\chi^2$ test, the Pearson probability reduces to 0.005.

In the $\chi^2$-test we have taken into account only the statistical fluctuation of shower particles emitted in certain directions and neglected the systematic errors in the measurement of angles and the errors of the $\gamma_c$ values. The former source of error will be important at very small values increasing thus further the possible deviation at small angles, while the latter error simply decreases the significance of the $\chi^2$ test. A further source of error may be the relatively small number of jets ($n = 7$) used for building up the composite jet which may result in an average impact parameter significantly different from the median one.

Taking into account, moreover, the very rough basic assumption that the composite jet corresponds to a nucleon-nucleon collision, it becomes obvious that it is not possible to exclude with certainty the Fermi distribution following from the improved theory of Fermi [9]).

Furthermore it is quite clear from the figures that it is not possible to discriminate between the angular distributions calculated according to the Landau and Heisenberg theories.

By taking into account also jets having lower energies, the statistics may be increased, however, the difference between the various theoretical distributions becomes at the same time smaller and thus the problem of deciding which of the different theories gives a better fit becomes even more difficult.

## 4. Summary

From the above discussion it can be concluded that the angular distribution of high-energy jets is significantly anisotropic in the CMS. The angular distribution of a composite jet built up of jets of energies higher than $10^{13}$ eV and with $N_h \leqq 3$ is in good agreement with the Landau and Heisenberg distributions and even the Fermi distribution cannot be excluded with certainty. This result makes it very probable that from the angular distribution alone it is not possible to decide which of the multiple meson production theories above, if any, is the correct one.

## Appendix

### ANGULAR DISTRIBUTION OF SHOWER PARTICLES IN NUCLEON-NUCLEUS COLLISION CALCULATED ON THE BASIS OF THE LANDAU THEORY

We have calculated the distribution of $\gamma_c \operatorname{tg} \theta$ in high energy nucleon-nucleus collisions on the basis of the Landau theory. An energetic nucleon striking a nucleus interacts with all the nucleons in the nucleus lying on its track. Therefore, the collision between the nucleon and nucleus can be considered as a collision between the nucleon and a "tube" cut out of the nucleus: the cross section of this tube is equal to the cross section of the nucleon and the length of it is varying between the diameter of the nucleus and the diameter of one nucleon [10, 13]). The mean number of nucleons ($\bar{l}$) struck in this tube was estimated and the resulting angular distributions were calculated for C($A = 12$; $\bar{l} = 2.2$), Ag ($A = 107$; $\bar{l} = 3.9$) and the

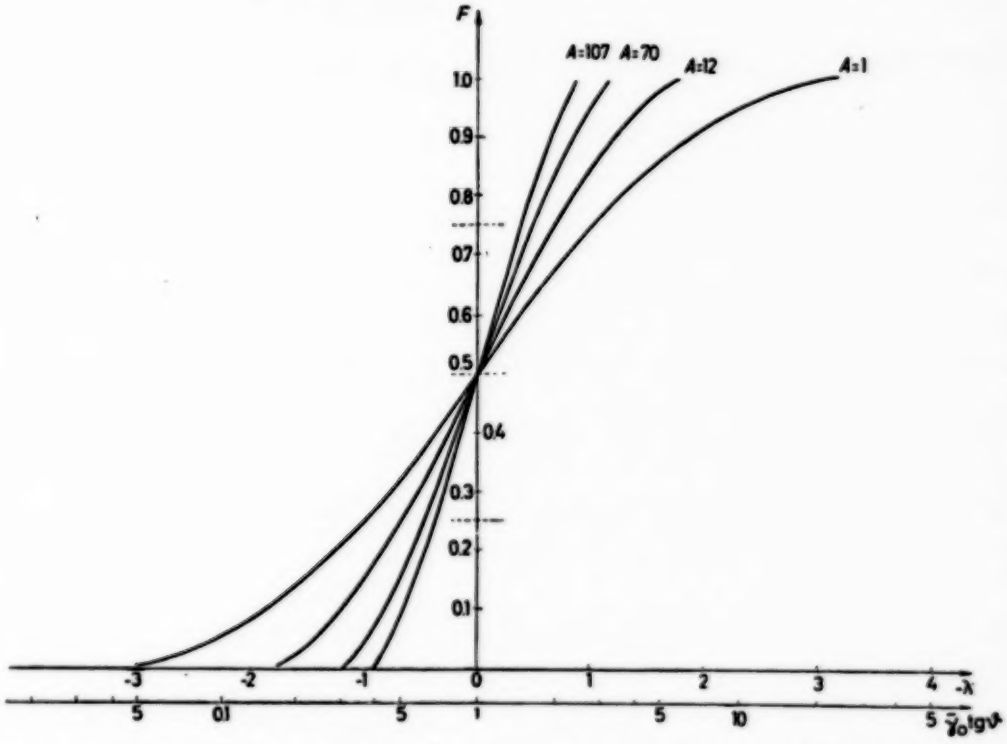


Fig. 4. Integral angular distribution of shower particles calculated on the basis of the Landau theory for nucleon-nucleus collision at $10^{12}$ eV energy and average "tube" lengths: 1) C($A = 12$; $\bar{l} = 2.2$), 2) Ag($A = 107$; $\bar{l} = 3.9$) and 3) average mass number of Ilford G5 emulsion ($A \approx 70$; $\bar{l} \approx 3.4$).

average mass number (weighted with the cross sections) of Ilford G5 emulsion ($A \approx 70$; $\bar{l} \approx 3.4$) at energies of $10^{12}$ eV (fig. 4).

It can be seen from fig. 4 that the anisotropy of the angular distribution decreases with increasing mass number of the target nucleus. This means,

comparing fig. 2 and fig. 4, that the angular distribution in nucleon-nucleus collisions is similar to the angular distribution in nucleon-nucleon collisions at lower energies. The fact that the shape of the angular distribution of shower particles is a function of both the primary energy and the number of nucleons struck in the target nucleus, makes the comparison of theoretical and experimental results far more complicated.

Similar difficulties arise if another multiple meson production theory is applied and the calculations are based on the above or some other of the usual models describing the processes occurring in nucleon-nucleus collision.

## References

1) M. Schein, R. G. Glasser and D. M. Haskin, Nuovo Cimento **2** (1955) 647
2) A. Debenedetti, C. M. Garelli, L. Tallone and M. Vigone, Nuovo Cimento **4** (1956) 1142
3) I. M. Gramenickii, G. B. Zdhanova, E. A. Zamacharova and M. N. Shcherbakova, JETP **32** (1957) 936
4) P. Ciok, M. Danysz, I. Gierula, A. Jurak, M. Miesowicz and W. Wolter, Nuovo Cimento **6** (1957) 1409
5) G. Bozóki, G. Domokos, E. Fenyves and E. Gombosi, K. Lanius and H. W. Meier, International Conference on Mesons and Recently Discovered Particles, Padova-Venice (Sept. 1957)
6) L. v. Lindern, Nuovo Cimento, **5** (1957) 491
7) G. Bozóki and E. Gombosi, KFKI Közl. (Reports of the Central Research Institute for Physics) **5** (1957)
8) E. Fermi, Progr. Theor. Phys. **5** (1950) 570
9) E. Fermi, Phys. Rev. **81** (1951) 683
10) L. D. Landau, Izv. Akad. Nauk. SSR (Ser. Fiz.) **17** (1953) 51;
S. Z. Belenkii and L. D. Landau, Usp. Fiz. Nauk **56** (1953) 309
11) W. Heisenberg, Zs. Phys. **133** (1952) 65;
see also Vorträge über kosmische Strahlung (Berlin-Göttingen-Heidelberg, 1953) p. 148
12) K. Symanzik, in W. Heisenberg, Vorträge über kosmische Strahlung (Berlin-Göttingen-Heidelberg, 1953) Anhang 7a, p. 563
13) M. Koshiba and M. P. Kaplon, Phys. Rev. **97** (1955) 193
14) S. Z. Belenkii and N. W. Gerasimova, JETP **32** (1955) 547
15) E. Edwards, J. Losty, D. A. Perkins, K. Pinkau and J. Reynolds, Phil. Mag. **3** (1958) 237

6.A *Nuclear Physics* 8 (1958) 207—209: © *North-Holland Publishing Co., Amsterdam*
Not to be reproduced by photoprint or microfilm without written permission from the publisher

# THE USE OF A SAMARIUM LOADED LIQUID SCINTILLATOR FOR THE DETERMINATION OF THE HALF-LIFE OF $Sm^{147}$

G. B. BEARD and W. H. KELLY
*Department of Physics and Astronomy, Michigan State University, East Lansing, Michigan* †

Received 12 June 1958

**Abstract:** An investigation of the use of metal loaded organic liquid scintillators for the study of long lived alpha emitters has been carried out. The method was checked using a samarium loaded scintillator. A specific activity corresponding to a half-life of $(1.28 \pm 0.04) \times 10^{11}$ years for the alpha decay of $Sm^{147}$ was found. This is in agreement with the published half-life measured using a different technique.

## 1. Introduction

The investigation of the alpha activities of radioactive isotopes with very long half-lives has been hindered by the very short ranges of the emitted alpha particles with the resulting large self absorption in all sources external to the particle detector. Because of this limitation and low specific activities, most such lifetime measurements have been made using nuclear emulsion techniques ††. Some work has also been done using geiger and proportional counters, especially for the case of $Sm^{147}$ which has a relatively high specific activity [2]). In both of these approaches only small amounts of source material could be utilized. However, with the advent of liquid scintillators that can be loaded with various elements, it should now be possible to work with considerably larger amounts of these isotopes. The improvement in counting rates would then allow more precise determinations of the specific activities.

Since a liquid scintillator solution loaded with samarium is now commercially available ††† an investigation of the specific activity of $Sm^{147}$ was carried out as a test of the method.

## 2. Experimental Procedure

A glass cell containing 80 $cm^3$ of the liquid scintillator loaded with $1.00 \pm 0.01$ % by weight of samarium was mounted on a Dumont 6363

† This research was supported in part by the United States Air Force under Contract No. AF49(638)—10 monitored by the AF Office of Scientific Research of the Air Research and Development Command.

†† See ref.[1]) and earlier papers cited there.

††† Obtained from Nuclear Enterprises Ltd.

photomultiplier and surrounded by several inches of lead and copper. The pulse height distribution was determined using a single channel analyzer. Fig. 1 is the differential spectrum showing the peak due to the $\alpha$ activity while the integral spectrum is shown in fig. 2. The background was estimated using an identical cell filled with an unloaded liquid scintillator. Since the responses of the two cells were somewhat different, the spectrum obtained with the unloaded scintillator was normalized to match that obtained with the loaded scintillator in the region above the alpha peak. This correction for background should be reliable down to the region where electronic noise becomes important. The estimated backgrounds are given by the lower

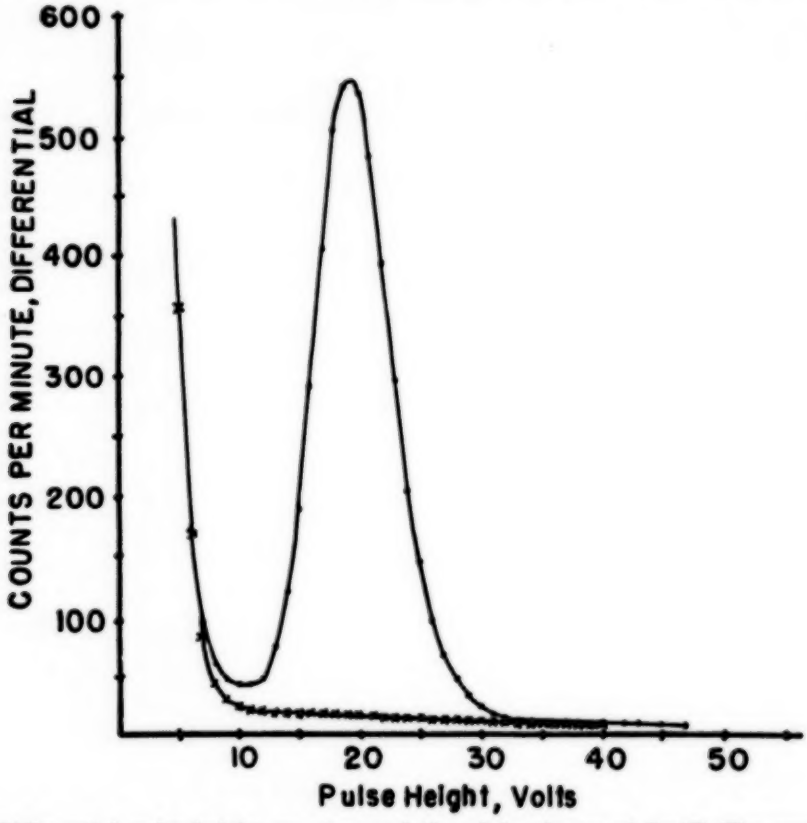


Fig. 1. Differential pulse-height spectrum of the alpha decay of $Sm^{147}$. The crosses refer to the background determined with an unloaded liquid scintillator of the same size.

curves in figs. 1 and 2. Fig. 2 also shows the net integral counts curve which represents the $Sm^{147}$ alpha activity.

Taking the value of the net integral counts curve extrapolated to zero energy and the known amount of $Sm^{147}$ in the source, one obtains a specific activity of $702 \pm 20$ counts per second per gram of $Sm^{147}$. This corresponds to a half-life of $(1.28 \pm 0.04) \times 10^{11}$ years. The estimate of the probable error includes the uncertainty in the extrapolated value of the integral counts curve and the uncertainty in the amount of samarium present. Because of

the very short range of the alpha particles, no correction was necessary for those few which struck the cell walls before losing all their energy. This value for the $Sm^{147}$ half-life agrees well with the result of previous work using a proportional counter with $4\pi$ geometry [2]).

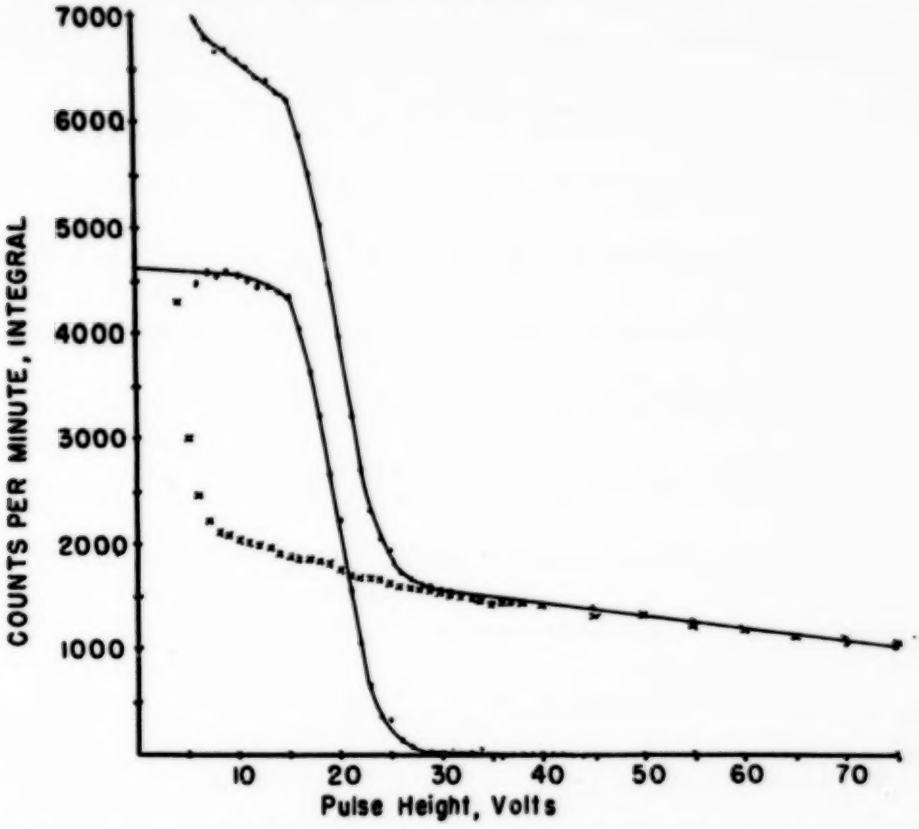


Fig. 2. Integral pulse height spectrum of the alpha decay of $Sm^{147}$. The crosses give the background spectrum. The middle curve is the spectrum with the background subtracted out (the net integral counts curve). The size of the dots indicate the statistical error.

## 3. Discussion

In view of the results using a samarium loaded liquid scintillator, the use of this method for the investigation of other long lived alpha emitters appears possible, particularly for the case of neodymium 144. It should also prove to be useful for some of the long lived beta emitters.

The authors wish to thank Dr. B. Lionel Funt who has been very helpful and cooperative in supplying the samarium loaded liquid scintillator and Mr. R. A. Hill who recorded some of the data.

## References

1) W. Porschen and W. Riezler, Z. Naturforsch. **11a** (1956) 143
2) George Beard and M. L. Wiedenbeck, Phys. Rev. **95** (1954) 1245

1. B *Nuclear Physics* 8 (1958) 210—212; © *North-Holland Publishing Co., Amsterdam*
Not to be reproduced by photoprint or microfilm without written permission from the publisher

# PHENOMENOLOGICAL TWO-NUCLEON POTENTIALS AND THE DEUTERON

K. V. LAURIKAINEN
NORDITA (*Nordisk Institut for Teoretisk Atomfysik*), *Copenhagen* †

Received 3 June 1958

On the basis of high energy neutron-proton and proton-proton scattering experiments one has recently proposed semiphenomenological two-nucleon potentials which contain a strong *LS*-term [1,2]). The properties of the bound states which these potentials determine for two-nucleon systems have as yet not been investigated, and different opinions have been expressed about the influence of the *LS*-term upon the ground state of the deuteron. Abraham [3]) gets the result that the *LS*-potential must change the deuteron binding energy by a very large amount while Biedenharn, Blatt and Kalos [4]) consider the spin-orbit-potential as negligible in low-energy interactions. Therefore some calculations have been made in order to test the potential proposed by Gammel and Thaler (in the following called GT-potential) from this point of view.

At first it was investigated, whether this potential yields other bound states of the two-nucleon system than the $^3S+^3D$ ground state of the deuteron. The most interesting case is the $^3P_2$-state, where in first approximation only the *LS*-term needs to be considered. Because of the very short range of the potential and a comparatively large cut off radius, the limit for the strength of the *LS*-potential, corresponding to zero binding energy, is as high as 21 000 MeV, and therefore the strength of the *LS*-term in the GT-potential, although it is as large as 7300 MeV, is not large enough to give a bound $^3P_2$-state. Then a bound state which would predominantly be a $^3D_3$-state is also obviously impossible, because the strength of the *LS*-term in the $^3V^+$-potential is only 5000 MeV, the range and the cut off radius being the same as in the $^3V^-$-potential. (An exact investigation has been postponed while waiting for the table of integrals mentioned below.) The singlet even states are also not bound (the $^1S_0$-state is nearly bound as it should be), and the singlet odd potential is repulsive ††. Thus the only bound state determined by the GT-potential is the $^3S+^3D$ state as it should be.

† On leave from University of Turku, Finland.

†† Meanwhile Signell and Marshak have found [5]) that the Gartenhaus' potential and, a fortiori, their own potential leads to a bound $^1P_1$-state, and they suggest a change of the cut off radius to avoid this difficulty.

An investigation of the properties of the deuteron ground state according to the GT-potential has also been started. All calculations have as yet been made without the use of electronic computers, employing a variational procedure proposed by Euranto and myself [6,7,8]). As a table of integrals needed for hard core potentials [9]) is under preparation, a preliminary calculation has been made by substituting in the *LS*-potential the infinite cut off (which corresponds to the hard core) by the zero cut off, and making no cut off in the central and the tensor potentials. The calculation has been carried out so as to fit exactly the binding energy and the quadrupole moment of the deuteron. At first the *LS*-term was dropped, whereby one obtains the strengths of the central and the tensor potential as the eigenvalue parameters. The calculation was then repeated for a potential including 1/10 of the *LS*-term of the GT-potential, modified in the above mentioned way. The results are as follows:

| | Strength of the | | D-state probability |
|---|---|---|---|
| | central potential (MeV) | tensor potential (MeV) | |
| Without *LS*-term | 24.5 | 44 | 0.042 |
| With 1/10 of the *LS*-term of the GT-potential, replacing infinite cut off by zero cut off | 6 | 53.5 | 0.064 |

We see that the *LS*-potential causes a repulsion which has an analogous effect as the hard core upon the strengths of the other terms: it diminishes the strength of the central potential and increases the strength of the tensor potential [4]). The numerical results obtained in this way can, of course, only be used for a qualitative estimation of the effect of the *LS*-potential upon the deuteron ground state. Because the *LS*-force predominantly acts on the D-function which is in every case small inside the hard core region, it seems obvious, however, that *the LS-term proposed by Gammel and Thaler causes difficulties in the theory of the deuteron.* The deuteron ground state which corresponds to the GT-potential seems to have rather incorrect values for the binding energy and the quadrupole moment. It has been pointed out earlier by Feshbach [10]) that this potential leads to difficulties with respect to the magnetic moment of the deuteron. (His result has been confirmed, using more exact wave functions.)

More exact calculations will be carried out as soon as two tables of integrals needed in our variational procedure have been calculated.

Numerical calculations in this work have been made by Miss Seija Lyytikäinen and by Mr. R. Hämäläinen. The financial support from NOR-

DITA which has made possible our stay in Copenhagen is gratefully acknowledged. I also like to thank Prof. L. Rosenfeld and Dr. Th. Maris for discussions concerning the two-nucleon interaction.

## References

1) J. L. Gammel and R. M. Thaler, Phys. Rev. **107** (1957) 291; and 1337
2) P. S. Signell and R. E. Marshak, Phys. Rev. **106** (1957) 832
3) G. Abraham, Nuclear Physics **1** (1956) 415
4) L. C. Biedenharn, J. M. Blatt and M. H. Kalos, Nuclear Physics **6** (1958) 359
5) P. S. Signell and R. E. Marshak, Phys. Rev. **109** (1958) 1229
6) K. V. Laurikainen and E. K. Euranto, Ann. Univ. Turku A **9** (1953) no. 3
7) K. V. Laurikainen and E. K. Euranto, Ann. Univ. Turku A **18** (1955) no. 2
8) K. V. Laurikainen, Ann. Sci. Fenn. A **1** (1955) 208
9) K. V. Laurikainen and Seija Lyytikäinen (to be published)
10) H. Feshbach, Phys. Rev. **107** (1957) 1626

1.D.2:
1.E.3

*Nuclear Physics* 8 (1958) 213—233; © *North-Holland Publishing Co., Amsterdam*
Not to be reproduced by photoprint or microfilm without written permission from the publisher

# MAGNETIC MOMENTS OF HIGHLY DEFORMED NUCLEI

J. N. L. GAUVIN

*The Clarendon Laboratory, Oxford, England*†

and

*Faculté des Sciences, Université Laval, Québec, Canada*

Received 31 March 1958

**Abstract:** It is shown that the values of magnetic moments of odd mass nuclei given by the model of independent particles moving in a spheroidal potential well, deviate from the measured values in a systematic way. The sense of this deviation is such that the calculated values lie between the measured values and strong coupling limits. This behaviour can be understood in terms of a polarization of the core of paired nucleons by virtue of their interaction with the odd nucleon; it is found that this mechanism gives a satisfactory account of the ground state moments of $Lu^{175}$ and of $Ta^{181}$.

## 1. Introduction and Summary

In this paper is presented an investigation of the magnetic moments of odd mass nuclei in the region $153 \leqq A \leqq 197$, where strong deformations occur and where the strong coupling model of Bohr and Mottelson [1,2]) has been highly successful. The object of the investigation is to determine to what extent these moments may be consistent with the general features of the strong coupling model and further to gain understanding of what perturbation effects may be responsible for the discrepancies between the actual moments and the values which the simple model would predict.

For this purpose, it is assumed that the wave functions for these nuclei may be written, to a good approximation, in the form proposed by Bohr and Mottelson

$$\psi(I,\ M,\ K,\ \Omega) = \sqrt{\frac{2I+1}{16\pi^2}}\,\{\chi_\Omega(\mathbf{r}_i)\mathscr{D}^I_{MK}(\theta_i) + (-1)^{I+K}\chi_{-\Omega}(\mathbf{r}_i)\mathscr{D}^I_{M-K}(\theta_i)\}, \quad (1)$$

with $\Omega = K$. The $\mathscr{D}^I_{MK}\ (\theta_i)$ are the eigenfunctions of a symmetric quantal rotator. The $\theta_i$ are considered to be the Euler angles of a frame of reference fixed with respect to the shape of the nuclear mass distribution and are to be treated as dynamic variables representing collective degrees of freedom. The $\chi_\Omega(\mathbf{r}_i)$ are the eigenfunctions for particle motion in the latter frame of reference, $\Omega$ being the projection of the angular momentum vector on the

† The major part of this work has been submitted in partial fulfilment of the requirements for the degree of D. Phil. in the University of Oxford.

nuclear axis of symmetry. It is further assumed that a good approximation of this function is obtained by considering the motion of independent nucleons in a fixed potential having a quadrupole deformation of suitably chosen magnitude. The wide success of this model in accounting for spins, parities and various features of nuclear spectra, as well as giving a reasonable account of nuclear moments and various transition probabilities, will be taken as justification for these assumptions.

Yet some discrepancies are to be expected for various reasons. First, there is a certain amount of interaction between collective rotation and particle motion. The mechanism of such interaction is to some extent understood [2,3]) and *a priori* estimates of its effect can be made. Secondly, some departures from independent particle behaviour must exist in the same way, and for the same reasons, that a breakdown of the independent particle shell model occurs. It is clear that our understanding of these effects will be enhanced according to our measure of success in accounting for the discrepancies which may be found between measured quantities such as magnetic moments and those calculated on the model.

In section 2 of this paper it is shown that between observed moments and values derived from the strong coupling model, using particle wave functions obtained by Nilsson [4]), the discrepancies are indeed both large and systematic. According to *a priori* estimates these cannot be reasonably attributed to the rotation-particle coupling as presently understood.

If the independence hypothesis is relaxed, however, it must be noticed that the odd particle introduces a preferred direction along the axis of symmetry of the nucleus. It is therefore able to induce a polarization in the states of the other nucleons, which states are, in zero order, pairwise symmetric along this axis. Arguing crudely for the present, it may be considered that when the odd nucleon interacts with like nucleons the exclusion principle favours states with intrinsic spin opposed. Consequently one is led to expect among paired nucleons of the odd group a predominance of intrinsic spin direction opposed to that of the unpaired nucleon. When it interacts with nucleons of the even group a rather similar polarization is produced by virtue of spin-exchange forces and the predominant spin direction for these nucleons is *along* that of the unpaired nucleon. The sign of the resulting contributions to the magnetic moment is thus the same for both groups and given the right order of magnitude it will satisfactorily account for the observed systematic discrepancies.

This argument is presented more rigorously in section 4 while in section 5 an account is given of a calculation of this effect to first order for the ground states of $Lu^{175}$ and $Ta^{181}$. An indication of the amplitudes of admixtures to the wave functions is given by the algebraic difference of these amplitudes for pairs of nucleon states: these are found to be 0.06 or less. When the

corresponding contributions to the magnetic moments are summed, the total corrections are found to be in quite reasonable agreement with the observed discrepancies.

It must therefore be considered that large contributions to magnetic moments arising from core polarization are possible and in fact do occur. It is then unfortunately not possible to detect with any certainty the effects of other perturbations on particle motion from measurements of magnetic moments since such effects will be obscured by the contributions from core polarization which cannot be accurately estimated.

Perturbations which depend on collective motion, however, will affect the states in a rotational band differentially and if appreciable will alter the relation between M1 transition matrix elements and ground state moments. It may be that this is the origin of some empirical values [8]) of collective gyromagnetic ratios which are judged to be somewhat unreasonable. Although it is not yet clear what should be considered reasonable in this regard there is hope of elucidating the point by a semi-empirical study of such possible perturbations.

## 2. Discrepancies

For cases (including all ground states) when $I = \Omega = K$ one obtains from eq. (1) the following expressions for the magnetic moment:

$$\mu = \frac{I}{I+1}(\chi_\Omega(\mathbf{r}_i),\ \mu_z\chi_\Omega(\mathbf{r}_i)), \quad \text{for} \quad I > \tfrac{1}{2}, \tag{2}$$

$$\mu = \tfrac{1}{3}(\chi_{\frac{1}{2}}(\mathbf{r}_i),\ \mu_z\chi_{\frac{1}{2}}(\mathbf{r}_i)) + \frac{\sqrt{2}}{3}(\chi_{\frac{1}{2}}(\mathbf{r}_i),\ \mu_{+1}\chi_{-\frac{1}{2}}(\mathbf{r}_i)), \quad \text{for} \quad I = \tfrac{1}{2}. \tag{3}$$

Here $\boldsymbol{\mu}$ is the magnetic moment operator with spherical components $\mu_z$, $\mu_{+1}$ and $\mu_{-1}$ referred to the nuclear fixed axes.

It is standard procedure, however, to relax the adiabatic hypothesis which is implied in writing eq. (1) by adding to the magnetic moment operator a correction term

$$g_R(\mathbf{I}-\mathbf{j}) \tag{4}$$

$\mathbf{j}$ being the angular momentum operator for the last odd nucleon. This is quite plausible since the expectation value of the angular momentum associated with the rotation, in this model, must be the expectation value of $\mathbf{I}-\mathbf{j}$, and further this rotation must induce a flow of charge in the same direction. Formally it can be regarded as taking into account the first order corrections to $\chi_\Omega(\mathbf{r}_i)$, this wave function being here derived from a stationary potential.

With this correction the expressions for the magnetic moment become

$$\mu = \frac{I}{I+1}\{(\chi_\Omega, \mu_z\chi_\Omega)+g_R\}, \quad \text{for} \quad I > \tfrac{1}{2}, \tag{5}$$

$$\mu = \tfrac{1}{3}\{g_R+(\chi_{\frac{1}{2}}, \mu_z\chi_{\frac{1}{2}})+\sqrt{2}\,(\chi_{\frac{1}{2}}, [\mu_{+1}+g_R j_{+1}]\chi_{-\frac{1}{2}})\}, \quad \text{for} \quad I = \tfrac{1}{2}, \tag{6}$$

where again (as in all that follows) the spherical components of $\mu$ and $\mathbf{j}$ are referred to the nuclear fixed axes.

It is immediately obvious that the second term of (6) depends only on the odd particle state. This is also true of $(\chi_\Omega, \mu_z\chi_\Omega)$ since the nucleons are taken to move independently and $\sum s_z = 0$, $\sum l_z = 0$ are then constants of the motion for each *pair* of nucleons as a consequence of the symmetry of the potential. In the present approximation nothing is changed, therefore, by writing $\chi_\Omega$ either as a single particle eigenstate or as an independent particle eigenstate of all $A$ particles. In the latter case, however, one is put in the awkward position of having explicitly introduced too many independent coordinates. This difficulty has attracted considerable attention recently [5]). Suffice it to say here that the problem has arisen in the discussion of other aspects of the model, in particular for the derivation of moments of inertia [6]), and further to point out that for the purposes of the present discussion it will only be necessary to write explicitly the wave function of more than the odd particle when a description of the states of the other particles will be required, in the subsequent sections, in order to assess the effects of residual internucleon forces.

The matrix elements occurring in (5) and (6) can be easily evaluated if an expansion of the odd particle state in terms of spherical components is known. Nilsson [4]) gives expressions for these matrix elements as well as expansions for the eigenstates of a spheroidal potential of harmonic oscillator type radial dependence. Using these one obtains the results which are shown in tables 1, 2, and 3. In tables 1 and 2 (for nuclei of spin greater than $\frac{1}{2}$) $\mu_0$ is defined by

$$\mu_0 = (\chi_\Omega, \mu_z\chi_\Omega). \tag{7}$$

In the notation of Bohr and Mottelson this would be written as $\Omega g_\Omega$.

It should be made clear, however, that $\mu_0$ depends only on the spin polarization (in the usual sense) of the odd particle state and not at all on its orbital angular momentum. This also applies to the first term of (6). For future arguments it will therefore be useful to expand the odd particle state (or any other single particle state) as

$$\chi_\Omega(\mathbf{r}) = \Phi_\Omega{}^+(\mathbf{r})\Sigma^+ + \Phi_\Omega{}^-(\mathbf{r})\Sigma^-, \tag{8}$$

where $\Sigma^+$ and $\Sigma^-$ are spin functions for 'spin up' and 'spin down' respectively. $\Phi_\Omega{}^+(\mathbf{r})$ and $\Phi_\Omega{}^-(\mathbf{r})$ are orbital functions having $z$-components of angular momentum $\Omega-\frac{1}{2}$ and $\Omega+\frac{1}{2}$ respectively (the $z$-axis being the nuclear axis of symmetry), and

TABLE 1

Magnetic moments of odd neutron nuclei ($\Omega > \frac{1}{2}$)

| Nucleus | level | $\delta$ | $\mu$(obs) | $\mu_0$(emp)+$g_R$ | $\eta$ | $\mu_0$(c) | $g_R$(emp) | $\mu$(c) | $\eta_\delta$ | $\Delta\mu$ |
|---|---|---|---|---|---|---|---|---|---|---|
| $_{64}Gd^{155}_{91}$ | $h_{9/2\,3/2}$ (52) | 0.31 | −0.31 | −0.52 | 4 | −0.81 | 0.3 | −0.25 | | |
| | | | | | 6 | −1.19 | 0.67 | −0.47 | 6.1 | +0.16 |
| $_{64}Gd^{157}_{93}$ | $h_{9/2\,3/2}$ (52) | 0.31 | −0.37(4) | −0.63(8) | 4 | −0.81 | 0.2(1) | −0.25 | | |
| | | | | | 6 | −1.19 | 0.56(8) | −0.47 | 6.1 | +0.10(4) |
| $_{66}Dy^{161}_{95}$ | $i_{13/2\,5/2}$(55) | 0.31 | −0.38(5) | −0.52(8) | 4 | −1.03 | 0.51(8) | −0.45 | | |
| | | | | | 6 | −1.19 | 0.63(8) | −0.56 | 6.1 | +0.19(5) |
| $_{66}Dy^{163}_{97}$ | $f_{7/2\,5/2}$ (44) | 0.27 | +0.53(5) | +0.71(7) | 4 | +0.871 | −0.17(7) | +0.91 | | |
| | | | | | 6 | +1.22 | −0.51(7) | +1.16 | 5.4 | −0.40(5) |
| $_{68}Er^{167}_{99}$ | $i_{13/2\,7/2}$ (54) | 0.29 | −0.5(1) | −0.64(15) | 4 | −1.31 | 0.67(15) | −0.63 | | |
| | | | | | 6 | −1.42 | 0.78(15) | −0.78 | 5.9 | +0.1(1) |
| $_{70}Yb^{173}_{103}$ | $h_{9/2\,5/2}$ (50) | 0.29 | −0.67(1) | −0.91(1) | 4 | −1.35 | 0.44(1) | −0.68 | | |
| | | | | | 6 | −1.55 | 0.64(1) | −0.82 | 5.9 | +0.15(1) |
| $_{72}Hf^{177}_{105}$ | $f_{7/2\,7/2}$ (41) | 0.26 | +0.61(3) | +0.77(3) | 4 | +1.35 | −0.58(3) | +1.35 | | |
| | | | | | 6 | +1.49 | −0.72(3) | +1.48 | 5.2 | −0.82(3) |
| $_{72}Hf^{179}_{107}$ | $i_{13/2\,9/2}$ (49) | 0.27 | −0.47(3) | −0.60(3) | 4 | −1.54 | 0.94(3) | −0.93 | | |
| | | | | | 6 | −1.6 | 1.00(3) | −0.98 | 5.4 | +0.50(3) |
| $_{76}Os^{189}_{118}$ | $p_{3/2\,3/2}$ (62) | 0.15 | +0.65 | +0.97 | 2 | +0.85 | +0.2 | +0.75 | | |
| | | | | | 4 | +1.32 | −0.35 | +1.27 | 3.0 | −0.35 |

The symbol $\delta$ indicates the deformation of the nucleus as deduced from quadrupole moments and excitation functions [4]). The actual values listed are taken mostly from the paper by Mottelson and Nilsson [15]). $\eta$ is another deformation parameter related [4]) to $\delta$, and $\eta_\delta$ is the value which corresponds to the particular value of $\delta$. $\mu_{(obs)}$ is the experimental value of the magnetic moment. $\mu_0$(c) is the quantity calculated by eq. (7), while $\mu_0$(emp) is that derived from $\mu$(obs) assuming $g_R = 0.4$. $g_R$(emp) is the value of $g_R$ required to fit the value of $\mu$(obs) with the calculated value of $\mu_0$. $\mu$(c) is the calculated value of the moment assuming $g_R = 0.4$ and $\Delta\mu$ is the discrepancy $\mu$(obs)−$\mu$(c) for the given value of $\delta$. The level assignments are identified by the label $l_{j\Omega}$ (No.) where $l$ and $j$ are the angular momenta of the state in the limit of zero deformation, and the number in parentheses corresponds to the Nilsson level scheme. The other numbers in parentheses in the table indicate the experimental error on the last digit.

TABLE 2

Magnetic moments of odd proton nuclei ($\Omega > \frac{1}{2}$)

| Nucleus | level | $\delta$ | $\mu$ (obs) | $\mu_o$(obs)+$g_R$ | $\eta$ | $\mu_o$(c) | $g_R$ (emp) | $\mu$(c) | $\eta_\delta$ | $\Delta\mu$ |
|---|---|---|---|---|---|---|---|---|---|---|
| $_{63}Eu^{153}_{90}$ | $g_{7/2\,5/2}$ (27) | 0.30 | 1.6 | 2.24 | 4 | +0.86 | +1.38 | +0.90 | | |
| | | | | | 6 | +.078 | +1.46 | +0.84 | 5.0 | +0.8 |
| $_{65}Tb^{159}_{94}$ | $d_{5/2\,3/2}$ (33) | 0.31 | 1.5(4) | 2.5(5) | 4 | +3.29 | −0.8(5) | +2.1 | | |
| | | | | | 6 | +3.43 | −0.9(5) | +2.3 | 5.2 | −0.5(4) |
| $_{67}Ho^{165}_{98}$ | $h_{11/2\,7/2}$(35) | 0.31 | 3.3(2) | 4.2(2) | 4 | +5.3 | −1.0(2) | +4.4 | | |
| | | | | | 6 | +5.4 | −1.2(2) | +4.5 | 5.2 | −1.2(2) |
| $_{71}Lu^{175}_{104}$ | $g_{7/2\,7/2}$ (25) | 0.26 | 2.9(5) | 3.7(6) | 4 | +1.46 | +2.2(6) | +1.45 | | |
| | | | | | 6 | +1.40 | +2.3(6) | +1.40 | 4.3 | +1.5(5) |
| $_{73}Ta^{181}_{108}$ | $g_{7/2\,7/2}$ (25) | 0.23 | 2.1 | 2.7 | 4 | +1.46 | +1.3 | +1.45 | | |
| | | | | | 6 | +1.40 | +1.2 | +1.40 | 4.0 | +0.7 |
| $Ta^{181*}$ (480 keV) | $d_{5/2\,5/2}$ (31) | 0.23 | 3.0(3) | 4.2(4) | 4 | +4.7 | −0.5(4) | +3.6 | | |
| | | | | | 6 | +4.7 | −0.5(4) | +3.6 | 4.0 | −0.6(4) |
| $_{75}Re^{185}_{110}$ | $d_{5/2\,5/2}$ (31) | 0.19 | 3.144 | 4.41 | 2 | +4.7 | −0.3 | +3.6 | | |
| | | | | | 4 | +4.7 | −0.3 | +3.6 | 3.2 | −0.50 |
| $_{75}Re^{187}_{112}$ | $d_{5/2\,5/2}$ (31) | 0.19 | 3.176 | 4.45 | 2 | +4.7 | −0.25 | +3.6 | | |
| | | | | | 4 | +4.7 | −0.25 | +3.6 | 3.2 | −0.46 |
| $_{77}Ir^{191}_{114}$ | $d_{3/2\,3/2}$ (42) | 0.14 | 0.16 | 0.27 | 2 | −0.37 | +0.64 | +0.04 | 2.5 | +0.15 |
| | | | | | 4 | −0.54 | +0.81 | −0.08 | | |
| $_{77}Ir^{193}_{116}$ | $d_{3/2\,3/2}$ (42) | 0.12 | 0.17(3) | 0.28(5) | 2 | −0.37 | +0.65(5) | +0.04 | 2 | +0.13(3) |
| | | | | | 4 | −0.54 | +0.82(5) | −0.08 | | |
| $_{79}Au^{197}_{118}$ | $d_{3/2\,3/2}$ (42) | | 0.16(2) | 0.27(3) | 2 | −0.37 | +0.64(3) | +0.04 | | +0.12(2) |
| | | | | | 4 | −0.54 | +0.81(3) | −0.08 | | +0.24(2) |

TABLE 3

Magnetic moments of spin $\frac{1}{2}$ nuclei ($\Omega = \frac{1}{2}$)

| Nucleus | level | $\delta$ | $\mu$ (obs) | $\eta$ | $\mu$(c) | $\mu$(c) | $g_R$ (emp) | $\eta_g$ | $\Delta\mu$ | $P$ |
|---|---|---|---|---|---|---|---|---|---|---|
| $_{69}Tm^{169}_{100}$ | $d_{3/2\,1/2}(31)$ | 0.28 | −0.20(5) | 5 | $-0.473+0.62g_R$ | −0.238 | +0.44(5) | 4.8 | +0.04(5) | −0.7 |
| | | | | 6 | $-0.463+0.56g_R$ | −0.225 | +0.47(5) | | | |
| $_{70}Yb^{171}_{101}$ | $p_{3/2\,1/2}(63)$ | 0.29 | +0.45 | 4 | $+0.637+0.023g_R$ | +0.65 | −8 | | | |
| | | | | 6 | $+0.637+0.039g_R$ | +0.65 | −4.8 | 4.9 | −0.2 | −0.4 |
| $_{74}W^{183}_{109}$ | $f_{5/2\,1/2}$ (71) | 0.21 | +0.11 | 2 | $+0.637+0.34g_R$ | +0.67 | −1.5 | | | |
| | | | | 4 | $+0.637+0.35g_R$ | +0.68 | −1.5 | 3.5 | −0.57 | +0.6 |
| $_{76}Os^{187}_{111}$ | $f_{5/2\,1/2}$ (71) | 0.18 | +0.12 | 2 | $+0.637+0.34g_R$ | +0.67 | −1.5 | | | |
| | | | | 4 | $+0.637+0.35g_R$ | +0.68 | −1.5 | 3.0 | −0.55 | +0.5 |

$P$ is the polarization $(\Phi^+, \Phi^+)-(\Phi^-, \Phi^-)$ for the given value of $\delta$.

$$(\Phi_\Omega^+(\mathbf{r}),\ \Phi_\Omega^+(\mathbf{r}))+(\Phi_\Omega^-(\mathbf{r}),\ \Phi_\Omega^-(\mathbf{r}))=1. \tag{9}$$

In this notation $\mu_0$ is simply

$$\mu_0=\tfrac{1}{2}(g_s-g_l)[(\Phi_\Omega^+,\ \Phi_\Omega^+)-(\Phi_\Omega^-,\ \Phi_\Omega^-)]+\Omega g_l, \tag{10}$$

where $g_s$ and $g_l$ are the usual spin and orbital $g$-factors.

In tables 1 and 2 the calculated values are compared with empirical values obtained from the measured values of $\mu$ taking $g_R$ to be 0.4. Both are also plotted against $\Omega$ in figures 1 and 2. The reference lines in these diagrams are the values of $\mu_0$ when $s_z$ is a good quantum number, $\mu^+$ corresponding to $\Phi_\Omega^-=0$ and $\mu^-$ corresponding to $\Phi_\Omega^+=0$. These will henceforth be referred to as strong coupling limits since they give the values

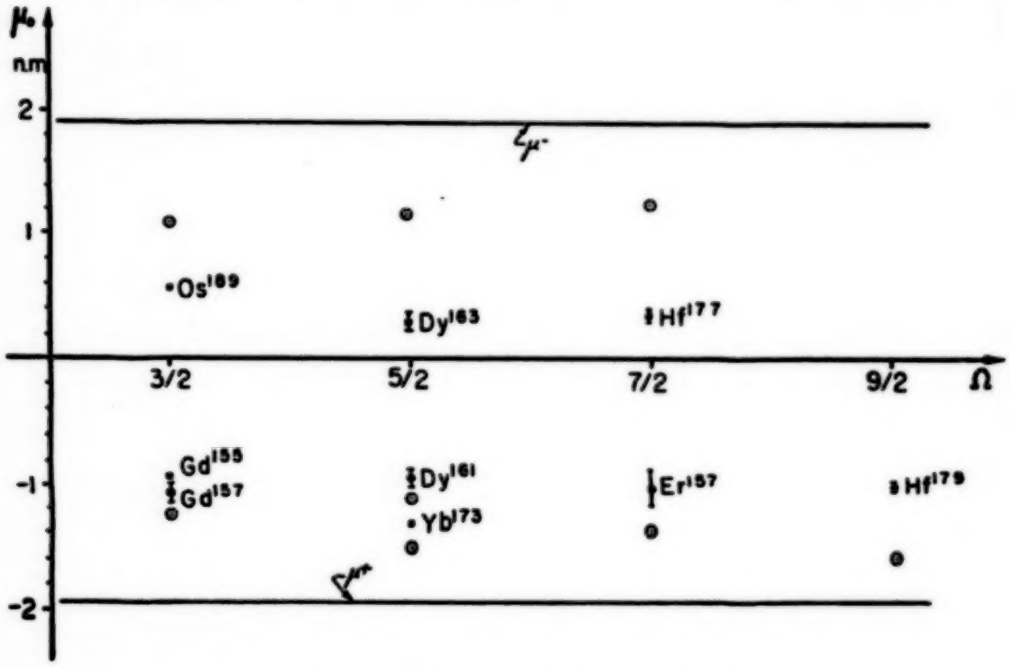


Fig. 1. Magnetic moments of odd neutron nuclei.

⊙ Calculated values.

Empirical values (assuming $g_R=0.4$) with experimental errors indicated.

of $\mu_0$ for single particle states when the coupling of orbital angular momentum to the symmetry axis, via the deformation of the potential, is much stronger than the spin-orbit coupling †.

The diagrams display the remarkable feature that all calculated values of $\mu_0$ lie between the empirical values and the nearest of the strong coupling limits. This means that in order to make the empirical points coincide with the calculated ones by alteration of the assumed values of $g_R$ one would have to decrease $g_R$ for moments lying near the upper strong coupling

† The author is indebted to Dr. D. M. Brink for suggesting these reference lines.

limit and to increase it for those lying near the lower limit. The required values are listed in tables 1, 2, and 3 under $g_R$ (emp).

*A priori*, the values of $g_R$ resulting from the effects of the rotation on the paired particle states is expected to be nearly the same for all nuclei

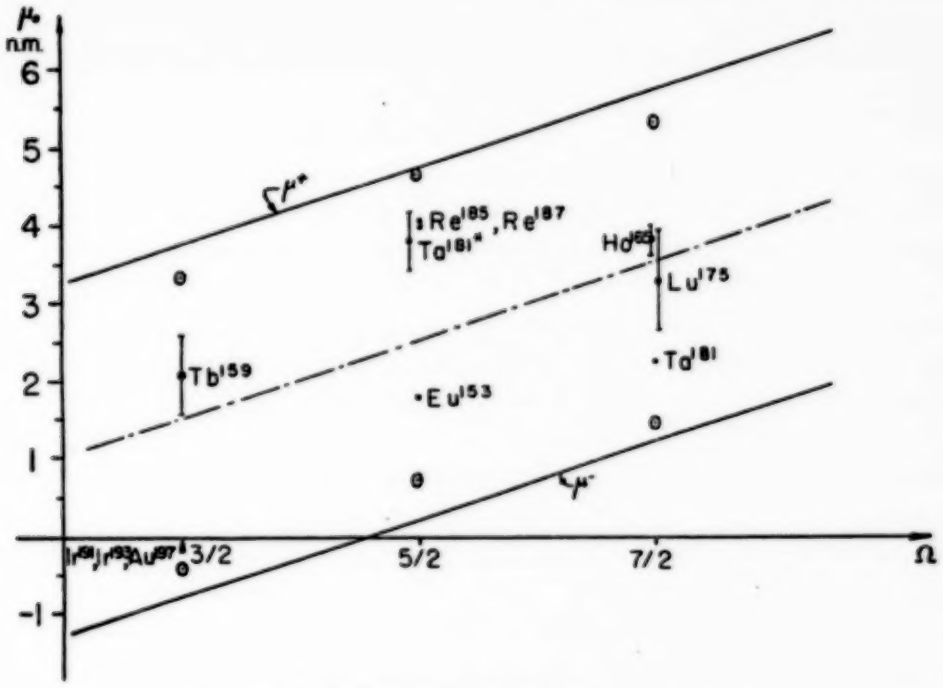


Fig. 2. Mafnetic moments of odd proton nuclei.
⊙ Calculated values.
Empirical values (with $g_R = 0.4$) with experimental errors indicated.

of the region $153 \leqq A \leqq 197$ and the expected value is about 0.4 in agreement with the simple picture of a rotating uniformly charged spheroid [2,7]).

There is, however, rather more ambiguity regarding the effect of the odd particle on the value which should be taken for $g_R$. On the one hand, estimates from the time dependent or so-called "cranking" model indicate that the effect might be appreciable. Moszkowski [7]) suggests the following formula:

$$g_R = \frac{Z}{A} + \left(\frac{\mu_0}{\Omega} - \frac{Z}{A}\right)\frac{\Delta\mathcal{I}}{\mathcal{I}} \tag{11}$$

where $\Delta\mathcal{I}$ is the effect of the odd particle on the moment of inertia and may be obtained empirically from a comparison of the actual moment of inertia of the nucleus with those of neighbouring even nuclei. Since this $\Delta\mathcal{I}$ is positive, however [7]), it is easily seen that improved agreement will not be obtained from this correction: for instance, the correction for a given value of $\Omega$ would make $g_R$ larger for the larger values of $\mu_0$ and vice versa, in contradiction to what is required.

On the other hand it would appear that the rotation-particle coupling (RPC) of Bohr and Mottelson represents a similar mechanism as that produced by "cranking" the potential well, so that the two effects are probably not independent and some care must be taken not to count things twice. But again, *a priori* estimates of the effect of the RPC indicate that corrections will be appreciable (up to say 0.3) only when the spectrum of the nucleus has a suitable interacting level within about 200 keV of the ground state. There is little likelihood that the case may be frequent and where it is suspected from the precent data, estimates obtained for the correction are less than 0.1.

Furthermore, in the approximation that the particle states in a rotational band are all identical there is a simple connection between the magnetic moments and the matrix elements for M1 transitions in this band [2]). From present data it is only possible to obtain the magnitude of the M1 matrix elements and not their phase. As a result one obtains pairs of consistent values of $\mu_0$ and $g_R$. When the most favourable of such pairs are chosen (for instance from those obtained by Heydenburg and Temmer [8])) an improved agreement is obtained in about half the cases; but in no case is the change found sufficient to remove the discrepancy. The general picture is therefore not altered significantly.

The effect of varying the well parameters is also indicated in the tables. $\eta$ is a parameter which depends on the deformation and is also related to the strength which is assumed for the phemenological spin-orbit coupling [4]). The values of $\mu_0$ are generally insensitive to this parameter (within reasonable limits for the latter).

The indications are, therefore, that the discrepancies in values of $\mu_0$ cannot reasonably be accounted for by effects corresponding either to uncertainties in potential well parameters or to rotation particle interactions (including $g_R$).

These considerations apply to all nuclei with spin greater than $\frac{1}{2}$ and in particular it is striking that no exception is found to the rule that the corrections required depend on the sign of the polarization of the odd nucleon, being negative for a positively polarized odd proton, positive for a similarly polarized odd neutron, and vice versa.

Spin $\frac{1}{2}$ nuclei will now bear closer inspection. For $Tm^{169}$ the calculated moment agrees with measurement within experimental accuracy. In $Yb^{171}$, according to our level assignment, the odd neutron is polarized negatively (−0.4) and the correction required is negative, in keeping with the behaviour of nuclei with $I > \frac{1}{2}$. Following Nilsson's level scheme we have assigned the odd neutron in $W^{183}$ and $Os^{187}$ to the same state, $f_{5/2\,1/2}(71)$, which has positive polarization ($\approx +0.5$). The corrections required for the magnetic moment, however, are negative, in violation of the above rule.

This may be serious in view of the explanations which are to be offered for the general behaviour; but it is not unlikely that it should be the level assignment which were at fault. There is another datum on the ground state of $W^{183}$ which does not fit the present assignment: the decoupling parameter is predicted to be negative throughout the range of positive deformations ($a = -0.05$ for $\delta = 0.14$) while Kerman [3]) finds empirically that a value of $+0.168$ is required to fit the level spectrum. Thus, in the absence of any obvious reason to the contrary, it may be considered likely that the levels $f_{5/2}$ and $p_{3/2}$ should be inverted from the relative positions which they occupy in the Nilsson scheme. Generally speaking, such an alteration in the level scheme does not effect appreciably the character of levels occurring in given positions at large deformations [4]), but in this case simple considerations indicate that it would.

The general behaviour can be understood by considering what happens to two close lying levels of the same spin under the influence of an increasing perturbation. The diagonal matrix elements of the perturbation will change the energy of each level directly, causing them either to approach each other or to move away from each other. In the first case, however, the levels will not cross because, as they approach, there will be an increasing repulsion effect arising from the off-diagonal matrix elements of the perturbation; but we may, nevertheless, speak of a virtual cross-over point, especially since there occurs, in the vicinity of this point, an exchange of the characters (i.e. wave functions) of the two levels. If, now, the order of the levels at zero perturbation is inverted, the virtual cross-over ceases to exist (or vice-versa). Consequently for large values of the perturbation the character of the upper and of the lower of the two levels, respectively, will not be greatly altered by this change.

In the present case, however, the two levels have no well defined cross-over point: for small deformations they are roughly parallel. Yet they "interact" sufficiently to effectively exchange their characters beyond $\eta \approx 0.2$. If the ordering is altered the levels may still be expected to exchange characters in the same way. Thus the one which lies the higher in energy, into which the odd neutron of $W^{183}$ and of $Os^{187}$ must go, would have a character more similar to that of the $p_{3/2\,1/2}(63)$ of the Nilsson level scheme.

### 3. Core Polarization

In taking the potential at the position $\mathbf{r}_i$ of nucleon $i$ to be of the form $V(\mathbf{r}_i)$, a residual term

$$\mathscr{H}'_i = \sum_j v_{ij} - V(\mathbf{r}_i) \tag{12}$$

has been neglected. Here $v_{ij}$ is the potential due to all the forces between

nucleons $i$ and $j$. The qualitative features of the changes which occur in the wave function when this residual Hamiltonian is taken into account are most easily found from the variation principle. For present purposes only changes which affect $\mu_0$ are of interest and, consequently, our attention may be confined to spin polarization effects (see eq. (10)). This applies also to spin $\frac{1}{2}$ nuclei apart from the changes in the odd particle state which alone contribute to the second term of (6). Such corrections to the odd particle state will not be considered further in this paper because they raise the whole complicated question of the self-consistency of the potential $V(\mathbf{r})$ for this (*odd*) particle, and it is very unlikely that such lack of self-consistency is responsible for more than a small part of the discrepancies.

The spin polarization of the core of paired particles, however, is relatively simple to predict. In zero order, spin and orbital angular momentum components along the axis of symmetry are separately constants of the motion, equal to zero, for each *pair* of particles, and so long as this situation remains unchanged the core will not contribute to $\mu_0$. Now, the single nucleon potential, $\sum_i V(\mathbf{r}_i)$, because of its symmetry, cannot, indeed, change such a situation. This is also true of $\sum'_{ij} v_{ij}$ with the sums over $i$ and $j$ extending over core particles only, since there can be no self-polarization by virtue of scalar forces (tensor forces are neglected). The core may be polarized, therefore, only by virtue of its interaction wich the unpaired nucleon.

To find the sign of this polarization we may appeal to the variation principle and assume that all terms of second order in the variation amplitude are negligible in comparison with first order ones. Then variations of each single particle wave function may be taken as independent within the limits imposed by the exclusion principle and each must be such as to decrease the expectation value of $\sum_{ij} v_{ij}$. The polarization for a pair of particle states will then go in the direction indicated by a decrease of the expectation value of $\sum_i v_{ij}$ with $i$ running over this pair of states and $j$ being the odd nucleon.

Considering, first, the case of paired nucleons of the odd group when the odd nucleon is in a strongly polarized state (corresponding to a zero order value of $\mu_0$ near to one of the strong coupling limits), it is at once obvious that for very short range Wigner or Majorana forces the magnitude of the interaction energy is increased if the spin of each paired nucleon becomes more predominantly polarized anti-parallel to that of the odd nucleon. The particles can approach to zero distance of each other only in this anti-parallel state. Thus the spins of pairs of nucleons are expected to be polarized (if at all) predominantly anti-parallel to that of the odd nucleon. This process of polarization will be adversely affected by the consequent changes in the orbital state but this will apply equally well to both types of polarization if the zero order wave functions are as good as one assumes. Bartlett and

Heisenberg forces, however, tend to polarize in the opposite direction since the formerly non-vanishing direct integral (for the interaction energy) now vanishes, and it is the exchange integral which now contributes, repulsively. In the limit of zero range, however, the two integrals can be subtracted directly and the difference is proportional to $w-b$ when the two-nucleon potential is written as

$$v_{ij} = -V_0\,\delta(\mathbf{r}_i-\mathbf{r}_j)(w+bP_\sigma), \tag{13}$$

$P_\sigma$ being the exchange operator for the nucleon spins, and $V_0$ a positive constant. The Rosenfeld mixture gives for the coefficients

$$w = 0.8, \quad b = 0.2, \tag{14}$$

so that the difference $w-b$ is positive and the spin polarization of core states should be in the direction predicted by attractive Wigner forces. Since nucleons of the odd group are under consideration it is now clear that the contribution to $\mu_0$ is such as to displace it away from the nearest strong coupling limit.

For the case of paired nucleons of the even group spin-independent forces will not produce any polarization. Bartlett and Heisenberg forces, however, are effective only when the spins of the interacting neutron and proton are parallel. Since these are also attractive in the zero range approximation, it is concluded that the polarization of the even group of nucleons will be parallel to the spin of the odd nucleon. Since, further, the factor $g_s-g_l$ for these nucleons has opposite sign from that of the odd nucleon the effect of this polarization is again to shift the value of $\mu_0$ away from the nearest strong coupling limit.

Thus, if it be established that the magnitude of this effect is appreciable, the principal feature of the discrepancies in values of $\mu_0$ will be qualitatively explained.

## 4. First-order Perturbation Corrections

In this section, perturbation theory will be applied to obtain expressions for the corrections discussed in the preceding section. In this formalism the polarization effect does not appear directly, but rather, the corrections to single particle states appear as the "excitations" schematized in fig. 3. Here the ground state is represented by dots on doubly degenerate single particle levels shown as solid lines. The arrows indicate the relative orientations of the total angular momenta. The dotted line represents a level which is vacant in the zero order state. The unpaired nucleon is shown on the singly occupied level labelled f, $\Omega$.

Admixtures to this state thus have the form of excited configurations in which one or more nucleons have gone to a formerly vacant level, con-

serving the quantum number $\Omega$. To first order, only those admixtures which differ from the original state by only one particle excitation will contribute to the magnetic moment. Since nuclear forces are taken to be

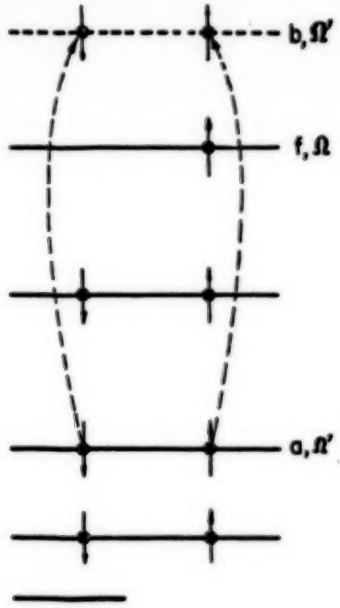


Fig. 3. Schematic representation of particle excitation.

scalar, such single particle excitation can go only to a state b' which has the same parity and the same value of the quantum number $\Omega$ as the state a which is left vacant. Now for each such possible excitation there is a corresponding one between the same levels but between the states having the opposite sign of $\Omega$ (dotted arrows in the figure). (The vacant state in the level occupied by the unpaired nucleon actually constitutes an exception, but to deal with it involves the self-consistency problem which was dismissed in the last section as too complicated.) If the admixture amplitudes for such a pair of excitations are designated by $\alpha$ and $\beta$, for that involving states with positive $\Omega$ (i.e. angular momentum alligned parallel to that of the odd nucleon) and that involving states with negative $\Omega$, respectively, the contribution to $\mu_0$ from this pair will be

$$\Delta\mu_0 = 2(\alpha-\beta)(\chi_{a,+\Omega},\ \mu_z\chi_{b,+\Omega}). \tag{15}$$

Thus the coefficients need not be calculated separately, since only $\alpha-\beta$ is relevant. The reason for this is that the magnetic moment matrix element between states with angular momenta oriented in the opposite direction is the same as that which is written here, but with the opposite sign. The latter is simply

$$(\chi_{a,+\Omega},\ \mu_z\chi_{b,+\Omega}) = (g_s-g_l)(\Phi^+_{a,+\Omega},\ \Phi^+_{b,+\Omega}). \tag{16}$$

By perturbation theory $\alpha-\beta$ is given by

$$\alpha-\beta = \frac{-1}{\Delta E}\{(\chi_{a,+\Omega'}(\mathbf{r}_1)\chi_{f,+\Omega}(\mathbf{r}_2),\ v_{12}\chi_{b,+\Omega'}(\mathbf{r}_1)\chi_{f,+\Omega}(\mathbf{r}_2))$$
$$-(\chi_{a,-\Omega'}(\mathbf{r}_1)\chi_{f,+\Omega}(\mathbf{r}_2),\ v_{12}\chi_{b,-\Omega'}(\mathbf{r}_1)\chi_{f,+\Omega}(\mathbf{r}_2))-\text{ exchange terms}\} \quad (17)$$

where $\Delta E$ is the positive energy difference between levels a and b, and where f labels the odd particle state. By expansion

$$(\chi_{a,-\Omega'}(\mathbf{r}_1)\ \chi_{f,+\Omega}(\mathbf{r}_2),\ v_{12}\chi_{b,-\Omega'}(\mathbf{r}_1)\chi_{f,+\Omega}(\mathbf{r}_2))$$
$$=\sum_{\substack{\sigma,\sigma'\\ \sigma'',\sigma'''}}(\Phi^{\sigma}_{a,-\Omega'}(\mathbf{r}_1)\Sigma^{\sigma}(1)\Phi^{\sigma''}_{f,+\Omega}(\mathbf{r}_2)\Sigma^{\sigma''}(2),\ v_{12}\Phi^{\sigma'}_{b,-\Omega'}(\mathbf{r}_1)\Sigma^{\sigma'}(1)\Phi^{\sigma'''}_{f,+\Omega}(\mathbf{r}_2)\Sigma^{\sigma'''}(2)), \quad (18)$$

where the $\Sigma^{\sigma}$ are spin functions and the $\sigma$ are the eigenvalues of the Pauli spin operator $\sigma_z$. Now the symmetry of paired states is such that

$$\Phi^{\sigma}_{a,-\Omega}(\mathbf{r}) = (-1)^{\lambda}i^{\sigma-1}(\Phi^{-\sigma}_{a,+\Omega}(\mathbf{r}))^*, \quad (19)$$

where the phase factor $i^{\sigma-1}$ is required in order that $\chi_{a,\Omega}$ (and also $\Phi^{\sigma}_{a,\Omega}$) have a positive definite norm, and the assumption has already been made in writing eq. (15) that the factor $(-)^{\lambda}$ depends only on parity. Thus if the interaction is taken to be of the form (13), so that no space exchange effects occur, (18) may be written as

$$(\chi_{a,-\Omega'}(\mathbf{r}_1)\chi_{f,\Omega}(\mathbf{r}_2),\ v_{12}\chi_{b,-\Omega'}(\mathbf{r}_1)\chi_{f,\Omega}(\mathbf{r}_2))$$
$$=-V_0\sum_{\substack{\sigma,\sigma'\\ \sigma'',\sigma'''}}(\Phi^{\sigma'}_{b,+\Omega'}(\mathbf{r}_1)\Phi^{\sigma''}_{f,\Omega}(\mathbf{r}_2),\ \delta(\mathbf{r}_1-\mathbf{r}_2)\Phi^{\sigma}_{a,+\Omega'}(\mathbf{r}_1)\Phi^{\sigma'''}_{f,\Omega}(\mathbf{r}_2))\cdot i^{\sigma'-\sigma}\langle-\sigma;\ \sigma''|w+bP_{\sigma}|-\sigma';\ \sigma'''\rangle, \quad (20)$$

where the spin matrix element is written in Dirac notation for simplicity. Further, since the $\Phi_{\Omega}{}^{\sigma}$ may be taken to be real apart from the factor $\exp i(\Omega-\sigma)\varphi$, it follows that

$$(\Phi^{\sigma'}_{b,\Omega'}(\mathbf{r}_1)\Phi^{\sigma''}_{f,\Omega}(\mathbf{r}_2),\ \delta(\mathbf{r}_1-\mathbf{r}_2)\Phi^{\sigma}_{a,\Omega'}(\mathbf{r}_1)\Phi^{\sigma'''}_{f,\Omega}(\mathbf{r}_2))$$
$$=(\Phi^{\sigma}_{a,\Omega'}(\mathbf{r}_1)\Phi^{\sigma''}_{f,\Omega}(\mathbf{r}_2),\ \delta(\mathbf{r}_1-\mathbf{r}_2)\Phi^{\sigma'}_{b,\Omega'}(\mathbf{r}_1)\Phi^{\sigma'''}_{f,\Omega}(\mathbf{r}_2)) \quad (21)$$

when both are non-vanishing. Otherwise the corresponding spin matrix element will vanish as well so that we may write

$$\alpha-\beta=\frac{V_0}{\Delta E}\sum_{\substack{\sigma,\sigma'\\ \sigma'',\sigma'''}}(\Phi^{\sigma}_{a,\Omega'}(\mathbf{r}_1)\Phi^{\sigma''}_{f,\Omega}(\mathbf{r}_2),\ \delta(\mathbf{r}_1-\mathbf{r}_2)\Phi^{\sigma'}_{b,\Omega'}(\mathbf{r}_1)\Phi^{\sigma'''}_{f,\Omega}(\mathbf{r}_2))$$
$$\{\langle\sigma;\ \sigma''|w+bP_{\sigma}|\sigma';\ \sigma'''\rangle-i^{\sigma'-\sigma}\langle-\sigma;\ \sigma''|w+bP_{\sigma}|-\sigma';\ \sigma'''\rangle$$
$$-\text{ exchange terms}\}. \quad (22)$$

The spin-dependent factor is easily evaluated to get

1) for non-identical particles (no exchange terms):

$bi^{\sigma''-\sigma}$ for $\sigma'=\sigma,\ \sigma'''=\sigma''$,

$2b$ for $\sigma''=-\sigma'''=\sigma'=-\sigma$,

$0$ otherwise;

2) for identical particles (including exchange terms):

$$\begin{aligned} &(b-w)i^{\sigma''-\sigma} && \text{for} \quad \sigma' = \sigma,\ \sigma''' = \sigma'', \\ &2(b-w) && \text{for} \quad \sigma'' = -\sigma''' = \sigma' = -\sigma, \\ &0 && \text{otherwise.} \end{aligned}$$

Therefore

$$\alpha-\beta = S(V_0/\Delta E) \sum_{\sigma,\sigma''} \{ i^{\sigma-\sigma''} (\Phi^{\sigma}_{a,\Omega'}(\mathbf{r}_1)\Phi^{\sigma''}_{l,\Omega}(\mathbf{r}_2),\ \delta(\mathbf{r}_1-\mathbf{r}_2)\Phi^{\sigma}_{b,\Omega'}(\mathbf{r}_1)\Phi^{\sigma''}_{l,\Omega}(\mathbf{r}_2)) + 2(\Phi^{\sigma}_{a,\Omega'}(\mathbf{r}_1)\Phi^{-\sigma}_{l,\Omega}(\mathbf{r}_2),\ \delta(\mathbf{r}_1-\mathbf{r}_2)\Phi^{-\sigma}_{a,\Omega'}(\mathbf{r}_1)\Phi^{\sigma}_{l,\Omega}(\mathbf{r}_2)) \}, \quad (23)$$

where

$$\begin{aligned} &S = b && \text{for particles of the even group,} \\ &S = b-w && \text{for particles of the odd group.} \end{aligned} \quad (24)$$

The expansions obtained by Nilsson [4]) for the functions $\Phi_{\Omega}{}^{\sigma}$ can be used to express the remaining integrals in terms of products of radial integrals over harmonic oscillator functions and angular integrals over four spherical harmonics. In the numerical work that follows the latter were evaluated using the method of Slater [9]) (used also by Condon and Shortley [10]))

$$\int_0^{2\pi}\int_0^{\pi} Y^*_{lm} Y^*_{l''m''} Y_{l'm'} Y_{l'''m'''} \sin\theta \, d\theta \, d\varphi = \frac{1}{4\pi} \sum_k (2k+1) c^k(l''', -m'''; l'', -m'') c^k(lm; l'm'), \quad (25)$$

where

$$c^k(lm; l'm') = (-1)^{m'} \frac{\sqrt{(2l+1)|2l'+1)}}{2k+1} \langle k0|l0; l0'\rangle \langle k, m'-m|l, -m; l'm'\rangle. \quad (26)$$

Here the $\langle k, m'+m|lm; l'm'\rangle$ are vector addition coefficients with phase as defined by Condon and Shortley. The coefficients $c^k(lm; l'm')$ for various $l$-values up to 4 are tabulated by these authors and by Shortley and Freed [11]). Further values for $l$ up to 6 are required and may be obtained from extended tables of the vector addition coefficients which will be published elsewhere.

The excitation energy $\Delta E$ in eq. (23) may also be obtained from the Nilsson level schemes. For $V_0$ the value

$$V_0 = (4\pi)105 \times 10^{-39} \text{ MeV} \cdot \text{cm}^3 \quad (27)$$

will be taken. This is derived from the strength of the nucleon-nucleon potential obtained from low energy scattering data. With $w = 0.8$ and $b = 0.2$, this value is equivalent to the triplet and singlet interaction strengths which have been used with considerable success to calculate configuration mixing effects on magnetic moments [12]), M1 transitions [13]), and $\beta$-decay [14]) in spherical nuclei.

## 5. Corrections to $Lu^{175}$ and $Ta^{181}$ Ground States

The foregoing formalism has been applied to the ground state configurations of $Lu^{175}$ and $Ta^{181}$, both of which have an unpaired proton in the level $g_{7/2\ 7/2}(25)$. These nuclei proved interesting on several accounts. First, the discrepancies to be accounted for are among the largest to be

TABLE 4

Neutron Polarization ($Lu^{175}$)

| \|a⟩ \|b⟩ | ⟨a\|μ\|b⟩ | α−β | $\Delta\mu_0$ |
|---|---|---|---|
| $p_{3/2\ 1/2} \leftarrow f_{5/2\ 1/2}$ | 1.04 | 0.0202 | 0.042 |
| $p_{1/2\ 1/2}$ | 0.30 | −0.0037 | −0.0022 |
| $h_{9/2\ 1/2} \leftarrow f_{5/2\ 1/2}$ | −0.481 | −0.00425 | 0.00341 |
| $p_{1/2\ 1/2}$ | −0.087 | −0.00156 | 0.0003 |
| $h_{9/2\ 3/2} \leftarrow f_{5/2\ 3/2}$ | −0.287 | 0.0023 | −0.0013 |
| $p_{3/2\ 3/2}$ | −1.04 | −0.0170 | 0.0354 |
| $h_{9/2\ 5/2} \rightarrow f_{5/2\ 5/2}$ | −0.855 | −0.0058 | 0.010 |
| $f_{7/2\ 1/2} \leftarrow p_{1/2\ 1/2}$ | 0.054 | −0.00055 | −0.00006 |
| $f_{5/2\ 1/2}$ | 0.323 | 0.0050 | 0.0031 |
| $f_{7/2\ 3/2} \leftarrow f_{5/2\ 3/2}$ | 0.128 | 0.0085 | 0.0022 |
| $p_{3/2\ 3/2}$ | 0.654 | 0.0074 | 0.0097 |
| $f_{7/2\ 5/2} \rightarrow f_{5/2\ 5/2}$ | 0.280 | 0.0015 | 0.0008 |
| $i_{13/2\ 1/2} \leftarrow g_{9/2\ 1/2}$ | −1.06 | −0.0107 | 0.0240 |
| $i_{11/2\ 1/2}$ | −1.52 | −0.0167 | 0.051 |
| $i_{13/2\ 3/2} \leftarrow g_{9/2\ 3/2}$ | −1.38 | −0.0142 | 0.039 |
| $i_{11/2\ 3/2}$ | −1.11 | −0.00106 | 0.0022 |
| $i_{13/2\ 5/2} \leftarrow g_{9/2\ 5/2}$ | −1.43 | −0.00645 | 0.0184 |
| $i_{11/2\ 1/2}$ | −0.74 | −0.00735 | 0.011 |
| $i_{13/2\ 7/2} \leftarrow g_{9/2\ 7/2}$ | −1.32 | −0.0191 | 0.050 |
| $i_{11/2\ 7/2}$ | −0.450 | −0.00356 | 0.0032 |

$\Delta\mu_0$ is the first order contribution to $\mu_0$ arising from the particular excitation symbolized in the left column. All these contributions will apply, also, to the $Ta^{181}$ ground state. ⟨a|μ|b⟩ is a shorthand Dirac notation for the matrix element given by eq. (16).

found (see table 2). Secondly, the difference in their magnetic moments which present measurements indicate is intriguing. Finally, the simplicity of the $g_{7/2\ 7/2}(25)$ state ($l = 4$ is a good quantum number apart from negligible. admixtures from the next higher positive parity group of states) reduces computational work considerably.

The complete configuration of $Lu^{175}$ can be assigned with little ambiguity since the odd particle state of this nucleus, as well as those of neighbouring odd neutron nuclei, agree well with the Nilsson level scheme for $\delta \approx 0.3$: $Hf^{175}$ is 5/2 − and $Yb^{175}$ is 7/2 −.

For $Ta^{181}$ it is most likely that the four extra neutrons are in the levels $f_{7/2\ 7/2}(41)$ and $i_{13/2\ 9/2}(49)$ as indicated by $Yb^{175}$ (above) and $Hf^{179}$ which has a spin of 9/2. The level occupied by the two extra protons is much less certain. It may be any of the following, in order of probability:

a) $f_{7/2\ 1/2}(47)$, a level which has not been identified in odd-mass nuclei,

b) $d_{5/2\ 5/2}(31)$, which, however, occurs for higher proton number as the ground states of $Re^{185}$ and $Re^{187}$,

c) $h_{11/2\ 9/2}(32)$, which has not been identified in the ground states of nuclei but would be expected, according to the level scheme of Nilsson, to lie above the $f_{7/2\ 1/2}(47)$ level.

TABLE 5

Proton Polarization ($Lu^{175}$)

| \|a⟩ | \|b⟩ | ⟨a\|μ\|b⟩ | $\alpha-\beta$ | $\Delta\mu_0$ |
|---|---|---|---|---|
| | $f_{7/2\ 1/2}$ [a] | 1.600 | 0.0487 | 0.157 |
| | $h_{9/2\ 1/2}$ | 1.500 | 0.0553 | 0.165 |
| $h_{11/2\ 1/2}$ → | $p_{3/2\ 1/2}$ | 0.374 | 0.0147 | 0.0110 |
| | $f_{5/2\ 1/2}$ | 0.105 | 0.00536 | 0.00113 |
| | $p_{1/2\ 1/2}$ | 0.015 | 0.00405 | 0.00012 |
| | $f_{7/2\ 3/2}$ | 1.880 | 0.0552 | 0.208 |
| $h_{11/2\ 3/2}$ < | $h_{9/2\ 3/2}$ | 0.990 | 0.0405 | 0.0803 |
| | $p_{3/2\ 3/2}$ | 0.158 | 0.0027 | 0.00086 |
| | $f_{5/2\ 3/2}$ | 0.028 | −0.00518 | −0.00029 |
| | $f_{7/2\ 5/2}$ | 1.660 | 0.0511 | 0.170 |
| $h_{11/2\ 5/2}$ → | $h_{9/2\ 5/2}$ | 0.590 | 0.0068 | 0.0080 |
| | $f_{5/2\ 5/2}$ | 0.057 | 0.002 | 0.00023 |
| $h_{11/2\ 7/2}$ < | $f_{7/2\ 7/2}$ | 1.400 | 0.0479 | 0.134 |
| | $h_{9/2\ 7/2}$ | 0.290 | 0.0103 | 0.0060 |
| $d_{3/2\ 1/2}$ → | $s_{1/2\ 1/2}$ | −0.860 | −0.020 | 0.0344 |
| $d_{5/2\ 1/2}$ → | $s_{1/2\ 1/2}$ | −0.310 | −0.0144 | 0.0089 |
| $g_{9/2\ 1/2}$ → | $s_{1/2\ 1/2}$ | 0.383 | 0.0037 | 0.00028 |
| $d_{5/2\ 3/2}$ → | $d_{3/2\ 3/2}$ | −1.040 | −0.014 | 0.029 |
| $g_{9/2\ 3/2}$ → | $d_{3/2\ 3/2}$ | 0.070 | 0.0187 | 0.0026 |
| $g_{7/2\ 5/2}$ → | $d_{5/2\ 5/2}$ [b] | −0.594 | −0.010 | 0.012 |
| $g_{9/2\ 5/2}$ → | $d_{5/2\ 5/2}$ [b] | −0.229 | −0.0194 | 0.0089 |

All these contributions apply, also, to the ground state of $Ta^{181}$ except that marked (a) (if the extra protons in $Ta^{181}$ are in the $f_{7/2\ 1/2}(47)$ level) or those marked (b) (if these protons are in the $d_{5/2\ 5/2}(31)$ level).

Each of these possibilities will be considered.

Since only those excitations which occur between levels of the same harmonic oscillator group of states will contribute in first order to $\mu_0$ (or to polarization) the possibilities are exhausted by the lists in tables 4, 5, and 6. The calculated coefficients $\alpha-\beta$ and the contributions to $\mu_0$ are found using wave functions with deformation parameter $\eta = 4$ throughout ($\eta$ defined by Nilsson). Slightly different values would be suggested for $Lu^{175}$ and for $Ta^{181}$, and also, according to Nilsson, for neutrons and for protons, respectively, but such refinements would not yield improvement commensurate with the added amount of computational work.

In table 5, (a) marks an excitation which cannot occur in $Ta^{181}$ if the extra protons are in the $f_{7/2\ 1/2}(47)$ level (see above), and likewise for those

marked (b) if these extra protons are in the $d_{5/2\,5/2}(31)$ level. In table 6 are given excitations which occur only in $Ta^{181}$; for the protons (a) and (c)

TABLE 6

Core Polarization in $Ta^{181}$

| \|a⟩ · \|b⟩ | ⟨a\|μ\|b⟩ | α−β | $\Delta\mu_0$ |
|---|---|---|---|
| *Protons* | | | |
| a) $f_{7/2\,1/2}$ level filled | | | |
| $f_{7/2\,1/2} \nearrow h_{9/2\,1/2}$ | −0.965 | −0.135 | 0.260 |
| $f_{7/2\,1/2} \rightarrow p_{3/2\,1/2}$ | −1.04 | −0.0306 | 0.064 |
| $f_{7/2\,1/2} \rightarrow f_{5/2\,1/2}$ | −0.388 | −0.0150 | 0.0116 |
| $f_{7/2\,1/2} \searrow p_{1/2\,1/2}$ | −0.064 | 0.0060 | −0.00076 |
| c) $h_{11/2\,9/2}$ level filled | | | |
| $h_{11/2\,9/2} \rightarrow h_{9/2\,9/2}$ | 1.00 | 0.00225 | 0.045 |
| *Neutrons* | | | |
| $f_{7/2\,7/2} \rightarrow h_{9/2\,7/2}$ | 0.383 | 0.0485 | 0.035 |
| $i_{13/2\,9/2} \nearrow g_{9/2\,9/2}$ | −1.12 | −0.019 | 0.041 |
| $i_{13/2\,9/2} \searrow i_{11/2\,9/2}$ | −0.224 | 0.00022 | −0.0001 |

The first group of excitation (a) will only occur if there are protons in the $f_{7/2\,1/2}(47)$ level, and similarly the second group (c), only if there are protons in the $h_{11/2\,9/2}(32)$ level.

are alternative possibilities depending on the level occupied by the extra protons.

The added corrections are as follows:

| | $Lu^{175}$ | $Ta^{181}$ | | |
|---|---|---|---|---|
| | | (a) | (b) | (c) |
| neutron polarization . . . . . | +0.30 | +0.38 | +0.38 | +0.38 |
| proton polarization. . . . . | +1.04 | +1.21 | +1.02 | +1.08 |
| total . . . . . | +1.34 | +1.59 | +1.40 | +1.46 |

The large difference between the contributions from proton polarization and from neutron polarization, respectively, is accounted for by the ratio of the factors $(g_s-g_l)S$ (see eq. (23)), which is 3.6 for an odd proton nucleus.

Thus the corrected values of $\mu_0$ are 2.80 for $Lu^{175}$, and (a) 3.05, (b) 2.86, or (c) 2.92 for $Ta^{181}$. Empirically one finds, assuming $g_R = 0.4$, the following values: for $Lu^{175}$, $3.3\pm0.6$, and for $Ta^{181}$, 2.3. Thus the corrected value is consistent with the measured value in the case of $Lu^{175}$ but is somewhat too large in the case of $Ta^{181}$. There is, of course, no pretention that

the calculated corrections should be accurate and the agreement which is obtained is considered quite satisfactory.

It is possible, also, that the difference in deformations of $Lu^{175}$ and $Ta^{181}$, which was not taken into account, might decrease the polarizability of the latter. Otherwise the difference in the moments of these nuclei would be difficult to resolve except by admitting different values of $g_R$. There is a case for this possibility, however, since the empirical values obtained by Heydenburg and Temmer [8]) include, in fact,

$$\text{for } Lu^{175}\text{: } \mu_0 = 2.56,\ g_R = 1.16;$$

$$\text{for } Ta^{181}\text{: } \mu_0 = 2.55,\ g_R = 0.15.$$

The common value of $\mu_0$ would be in good agreement with our corrected value; but it is now difficult to understand the widely different values of $g_R$. This situation still lacks clarification, but it does not impair the demonstration that large effects occur by virtue of core polarization by the unpaired nucleon.

It is a pleasure to thank Dr. R. J. Blin-Stoyle and Dr. G. R. Satchler for most helpful discussions and advice. The author is indebted, also, to the Rhodes Trustees for a Scholarship held during the course of elaboration of most of this work.

*Note added in proof:* A reinterpretation of the hyperfine structure measurement of the moment of $Ta^{181}$ taking account of perturbations on the atomic configurations has been proposed [16]). The new value is

$$\mu(Ta^{181}) = 2.4 \pm 0.2 \text{ n.m.}$$

This agrees with the value of $\mu(Lu^{175})$ within experimental accuracy. The corresponding value of

$$\mu_0(\text{emp}) = 2.7 \pm 0.3 \text{ n.m.}$$

is in excellent agreement with the corrected value obtained in this calculation.

The M1 transition rates deduced by Heydenberg and Temmer for $Ta^{181}$ are now consistent with

$$\mu_0 = 2.86 \pm 0.2, \quad g_R = 0.22 \pm 0.06$$

or

$$\mu_0 = 1.94 \pm 0.2, \quad g_R = 1.14 \pm 0.06.$$

Including the experimental uncertainty in the moment of $Lu^{175}$ the values for this nucleus are

$$\mu_0 = 3.2 \pm 0.5, \quad g_R = 0.51 \pm 0.14$$

or

$$\mu_0 = 2.56 \pm 0.5, \quad g_R = 1.16 \pm 0.14.$$

Values near the lower bound in the first set would agree quite well with the values of the first set for $Ta^{181}$ as well as with our corrected values of $\mu_0$; the values of $g_R$ are then reasonable and their difference is probably not very serious.

## References


1) A. Bohr, Mat. Fys. Medd. Dan. Vid. Selsk. **26** (1952) no. 14
2) A. Bohr and B. R. Mottelson, Mat Fys. Medd. Dan. Vid. Selsk. **27** (1953) no. 16; Mat. Fys. Medd. Dan. Vid. Selsk. **30** (1956) no. 1
3) A. K. Kerman, Mat. Fys. Medd. Dan. Vid. Selsk. **30** (1956) no. 15
4) S. G. Nilsson, Mat. Fys. Medd. Dan. Vid. Selsk. **29** (1955) no. 16
5) H. J. Lipkin, A. de Shalit and I. Talmi, Nuovo Cimento **10** (1955) 773; R. Skinner, Can. J. Phys. **34** (1956) 901
6) T. H. R. Skyrme, Proc. Roy. Soc. A **239** (1957) 399
7) S. A. Moszkowski, Phys. Rev. **103** (1956) 1328
8) N. P. Heydenburg and G. M. Temmer, Phys. Rev. **104** (1956) 981
9) Slater, Phys. Rev. **34** (1929) 1293
10) Condon and Shortley, The Theory of Atomic Spectra (Camb. Univ. Press, London)
11) G. H. Shortley and B. Freed, Phys. Rev. **54** (1938) 739
12) Arima, Horie and Sano, Progr. Theor. Phys. **17** (1957) 367
13) Arima and Horie, Progr. Theor. Phys. **11** (1954) 509
14) R. J. Blin-Stoyle and C. A. Caine, Phys. Rev. **105** (1957) 1810
15) B. R. Mottelson and S. G. Nilsson, Phys. Rev. **99** (1955) 1615
16) K. Murakawa, Phys. Rev. **110** (1958) 395

8.B *Nuclear Physics* **8** (1958) 234—236; © *North-Holland Publishing Co., Amsterdam*
Not to be reproduced by photoprint or microfilm without written permission from the publisher

# A MODEL OF THE UNIVERSAL FERMI INTERACTION

J. LEITE LOPES
*Faculdade Nacional de Filosofia and Centro*
*Brasileiro de Pesquisas Físicas, Rio de Janeiro, Brasil*

Received 30 May 1958

**Abstract:** It follows from the Feynman-Gell-Man theory that the Fermi interaction can be regarded as due to an exchange of charged vector mesons between fermions. An alternative model is possible: the weak couplings among fermions may be due to an exchange of charged and neutral vector mesons. An extra condition of conservation of the current which creates the neutral field is imposed to forbid unobserved reactions. The model differs from the Feynman-Gell-Mann picture in that it leads to an intrinsic electron-neutron interaction, the effective potential being of the order of 4 eV. If the coupling of this hypothetical vector meson with fermions has the same strength as the electric charge, the particle will have about 60 proton masses and will decay very fast into pairs of hyperons.

The hypothesis of a universal Fermi interaction must be formulated in such a way as to predict a sufficiently small or vanishing transition rate for fermion decays which have not been observed experimentally.

It is usual to say that the coupling acts between given pairs of fermions: $(e^+, \nu)$ with $(\mu^+, \nu)$ and with $(p, \bar{n})$, $(\Sigma^+, \bar{\Lambda})$, $(\Sigma^+, \bar{\Sigma}_0)$, $(\bar{\Xi}^-, \Xi_0)$ [1]. This association excludes couplings of $(\mu^+, e)$ with $(e^+, e)$ or $(\bar{p}, p)$ which would give rise to the non-observed reactions

$$\mu^+ \to e^+ + e + e^+, \qquad \mu^- + p \to p + e. \tag{1}$$

However, in the decay of muons,

$$\mu^+ \to e^+ + \nu + \tilde{\nu},$$

the experimental data are consistent with the vector-axial-vector coupling of $(\mu^+, \nu)$ with $(\tilde{\nu}, e)$ which is equivalent to the same coupling of $(\mu^+, e)$ with $(\tilde{\nu}, \nu)$. If the latter is regarded as physically possible one does not see any reason to forbid the couplings which would give rise to reactions (1) in first order.

Feynman and Gell-Mann [2] have proposed a vector-axial-vector coupling theory for the Fermi interaction which is in agreement with most of the data on the reactions involving fermions only. As they pointed out, this coupling may be regarded as due to a virtual exchange of charged heavy vector mesons between two fermions. The relation between the mass of this hypothetical meson $m_X$, the coupling constant $f_X$ of this meson X with the

Fermi field and the Fermi coupling constant $G$ is

$$4\pi \frac{f_X^2}{m_X^2} = \sqrt{8}G. \tag{2}$$

The ordering of the fermion pairs in the Fermi couplings will now be well defined if we take this model seriously and postulate that *the weak interaction between two fermions is due to the virtual exchange of charged vector mesons.* It then becomes clear that reactions where there can be no charge exchange will be forbidden in first order in $G$. Thus the reactions (1) † can only occur as a result of the successive exchange of two charged vector mesons and are therefore less probable than the first order processes $\mu^+ \to e^+ + \nu + \bar{\nu}$ and $\mu^- + p \to n + \nu$, respectively, by a factor of order $10^{12}$.

A consequence of this postulate is that the scattering of neutrinos by electrons is possible in first order as well as the neutron-proton scattering due to a weak, non-parity conserving interaction. *The Fermi scattering of neutrons by electrons is, however, forbidden in first order*: the electron can only emit negative vector mesons which the neutron cannot accept ††.

We wish to point out that there is an alternative picture which describes the observed reactions, forbids the undesirable fermion decays and leads to some consequences which are different from those mentioned above and can be tested in principle. The model is the following: *assume that any two fermions can exchange charged and neutral vector mesons.* Assume, further, that the neutral vector meson enters the coupling with the Fermi field in such a way that *the current which creates the neutral field is conserved* (the interaction is, then, not charge-independent). Reactions like those in (1), which have in a vertex one neutral vector meson line and two fermion lines corresponding to different fermion masses violate this condition and are therefore forbidden. This also excludes the coupling of $(\mu^+, e)$ with $(\bar{\nu}, \nu)$ and prescribes the unique interaction of $(\mu^+, \nu)$ with $(\bar{\nu}, e)$ for the $\mu$-e decay. In the scattering of neutrinos by electrons, the interaction is now of the form

$$G\{(\bar{e}\gamma_\mu a\nu)(\bar{\nu}\gamma_\mu ae) + (\bar{\nu}\gamma_\mu \nu)(\bar{e}\gamma_\mu e)\}, \quad a = \tfrac{1}{2}(1+i\gamma_5).$$

Conservation of the fermion current which emits neutral mesons imposes

† Direct radiative decays like $\mu \to e+\gamma$ and $\Sigma^+ \to p+\gamma$ cannot obviously occur by vector coupling with the electromagnetic field owing to gauge invariance with respect to the latter. An effective tensor interaction with $F_{\mu\nu}$ is possible and results from the muon changing into an intermediate neutrino with the creation of a proton-antineutron closed loop which emits the $\gamma$-ray and annihilates the neutrino into the final electron. The rate is, however, of order $G^2$ and thus undetectible. If the radiative decay of $\Sigma^+$ proceeds via an intermediate pion and proton the lifetime is of order $10^{-3}$ sec.

†† We assume the principle of baryon number conservation. In first order in $G$, the exchange of vector mesons between e and n may lead to the reaction $e+n \to \Sigma^- + \nu$ for which one needs neutrons with energy higher than about 260 MeV. In second order, one may have the e–n scattering $e+n \to \Sigma^- + \nu \to e+n$ which, however, gives no detectible contribution to the scattering cross section.

that the second term must conserve parity. Thus, if this model is true, *only the weak interaction which involves charge exchange violates parity conservation*; there exist weak interactions, those involving an exchange of neutral vector mesons, which conserve parity.

An essential difference between this model and that which assumes the existence of only charged vector mesons is in the intrinsic electron-neutron interaction: the former leads to a scattering of neutrons by electrons due to a weak, non-electromagnetic, parity conserving coupling. If the corresponding effective potential is represented by a well of depth $V$ and radius $e^2/(m_e c^2)$, the value of $V$ is of the order of 4 eV, if we take the value $1.4\times 10^{-49}$ erg · cm$^3$ for the Fermi coupling constant $G$. A Fermi-type coupling between electrons and neutrons has already been suggested by Foldy [3]). It follows from our model of the universal Fermi interaction whereas it is practically non-existent in the Feynman-Gell-Mann picture. The scheme suggested here depends crucially on the vector-axial-vector nature of the Fermi coupling. Only for neutral vector mesons can the extra condition be imposed to rule out the unobserved reactions.

The hypothetical vector meson would be a very heavy and unstable particle. Its lifetime is

$$\tau_X \approx \frac{16\pi}{f_X^2/\hbar c}\,\frac{\hbar}{m_X c^2}$$

for a decay into a nucleon (or hyperon) pair ($m_p/m_X \ll 1$). Taking (2) into account and $G \approx 10^{-5}\hbar^3/m_p{}^2 c$ we have, with $X \equiv m_X/m_p$,

$$\tau_X \approx \frac{10^{-17}}{X^3}\,\text{sec}, \quad \text{and} \quad f_X^2/\hbar c \approx 2.2\times 10^{-6} X^2.$$

If we set $f_X^2/\hbar c \approx e^2/\hbar c$, one obtains $m_X \approx 60\ m_p$ and $\tau_X \approx 10^{-22}$ sec.

The author had stimulating conversations with C. M. G. Lattes, J. Tiomno, L. Marquez and P. Srivastava.

## References

1) See for example, J. Leite Lopes, An. Acad. Brasil. Ci. **29** (1957) 521
2) R. P. Feynman and M. Gell-Mann, Phys. Rev. **109** (1958) 193; E. C. G. Sudarshan and R. E. Marshak, Padua-Venice International Conference (September 22-28, 1957)
3) L. L. Foldy, Phys. Rev. **87** (1952) 693

1.D.2. *Nuclear Physics* 8 (1958) 237—249; © *North-Holland Publishing Co., Amsterdam*
Not to be reproduced by photoprint or microfilm without written permission from the publisher

# ROTATIONAL STATES IN EVEN ATOMIC NUCLEI

A. S. DAVYDOV and G. F. FILIPPOV
*Moscow State University*

Received 29 March 1958

**Abstract:** A theory of the energy states and the electromagnetic transitions between them is developed for nuclei which do not possess axial symmetry. It is shown that violation of axial symmetry does not significantly change the rotational states of axial nuclei and leads to the appearance of new energy states. The reduced probabilities for E2 and M1 transitions between various rotational states are computed.

## 1. Introduction

In some previous papers of the authors [1–4]) energy levels of non-spherical nuclei corresponding to collective excitations not involving violation of axial symmetry of the nuclei were investigated on basis of the generalized nuclear model proposed by A. Bohr and B. Mottelson [5,6]). It was shown that the rotational-vibrational energy of collective nuclear excited states is a function of only two parameters, viz., of the frequency of nuclear surface vibrations and of the ratio of the equilibrium deformation to the zero vibration amplitude. It seems natural to inquire to what extent these results are applicable if one takes into account possible violation of axial symmetry of the nucleus.

The problem of violation of axial symmetry of nuclei has been qualitatively treated in a number of papers [5,7,8]). Recently it has even become usual to ascribe nuclear excited states to the so-called $\gamma$-vibrations [9,10]). This type of assignment is usually based on the spin values of these levels and on the large probability of electromagnetic transitions which confirms the collective nature of the levels. No quantitative theory of $\gamma$-vibrations has been proposed.

In the present paper we investigate energy levels corresponding to rotation of the nucleus which does not entail changes of its internal state. It will be shown that violation of axial symmetry of even nuclei only slightly affects the rotational spectrum of the axial nucleus although some new rotational states with total angular momenta of 2, 3, 4 ... do appear. If the deviations from axial symmetry are small these levels lie very high and are not excited. As the deviations from axial symmetry are increased some of the additional levels become much lower. Thus, for example, the



October (1) 1958

ratio of the second excited state with spin 2 to the first state (which also exists in axial nuclei), varies from infinity to two. The probabilities for electric transitions between rotational levels in non-axial nuclei are evaluated in sec. 3. The probabilities for magnetic transitions are computed in sec. 4. From comparison of the proposed theory with the experimental data (sec. 5) it can be concluded that the properties of the experimentally observed energy states of even nuclei can be satisfactorily explained by assuming that these nuclei do not possess axial symmetry.

## 2. Energy States in Non-Axial Nuclei

Proceeding from the generalized nuclear model, consider the energy states of an even nucleus corresponding to rotation of the latter as a whole with no change of its internal state. The operator corresponding to the rotation energy of the nucleus has the form

$$H = \sum_{\lambda=1}^{3} \frac{A J_\lambda^2}{2\sin^2\left(\gamma - \frac{2\pi}{3}\lambda\right)}, \tag{1.1}$$

where $A = \hbar^2/4B\beta^2$ is a quantity which has the dimension of energy; $\gamma$ varies between 0 and $\pi/3$ and determines the deviation of the shape of the nucleus from axial symmetry; the $\hat{J}_\lambda$ are operators of the projections of the nuclear angular momenta on the axes of a coordinate system connected with the nucleus. The commutation rules for these projections differ from the rules for the projections in a space-fixed coordinate system by the signs in the right hand side.

According to (1.1), for $\gamma \neq 0$ or $\pi/3$ the nucleus should be regarded as an asymmetric top. In stationary states of the asymmetric top not one of the projections of the total angular momentum on axes 1, 2, 3 of the body-fixed coordinate system has a definite value and hence the energy levels cannot be specified by the values of $K = J_3$. Each value of the total angular momentum in the asymmetric top corresponds to $2J+1$ different energy levels. These levels can be classified with respect to the irreducible representations of group $D_2$ with symmetry elements $C_2^1$, $C_2^2$, $C_2^3$ corresponding to rotation through $\pi$ about the coordinate axes 1,2, 3, because operator (1.1) and the commutation between the $J_\lambda$ are invariant with respect to this transformation group. Thus the energy levels of an asymmetric top split up into four types of levels which correspond to the four irreducible representations of group $D_2$ (see ref.[11]), § 101 and ref.[12])).

In virtue of the symmetry conditions imposed on the wave function [5]), in even nuclei of the $2J+1$ different levels only those energy levels with a given $J$ can exist which correspond to a completely symmetric

representation of group $D_2$. Rotation states of the required symmetry will not exist if $J = 1$. Two such states will exist for $J = 2$, one for $J = 3$, three for $J = 4$, two for $J = 5$, four for $J = 6$, etc.

If the energy is expressed in units of $A = \hbar^2/4B\beta^2$ the energy of two levels of the required symmetry are, for $J = 2$, defined by the expression

$$\varepsilon_1(2) = \frac{9\left(1-\sqrt{1-\frac{8}{9}\sin^2(3\gamma)}\right)}{\sin^2(3\gamma)}, \quad \varepsilon_2(2) = \frac{9\left(1+\sqrt{1-\frac{8}{9}\sin^2(3\gamma)}\right)}{\sin^2(3\gamma)}. \tag{1.2}$$

The energy of a level with angular momentum $J = 3$ is given by

$$\varepsilon(3) = \frac{18}{\sin^2(3\gamma)}. \tag{1.3}$$

The three spin 4 energy levels are the roots of the third degree equation

$$\varepsilon^3 - \frac{90}{\sin^2(3\gamma)}\varepsilon^2 + \frac{48}{\sin^4(3\gamma)}[27+26\sin^2(3\gamma)]\varepsilon - \frac{640}{\sin^4(3\gamma)}[27+7\sin^2(3\gamma)] = 0.$$

The two spin 5 energy levels are given by the formula

$$\varepsilon_\tau(5) = \frac{45 \pm 9\sqrt{9-8\sin^2(3\gamma)}}{\sin^2(3\gamma)}. \tag{1.4}$$

In (1.4) $\tau = 1$, if a minus sign is before the root and $\tau = 2$, if a plus is before it. The energy levels of states possessing an angular momentum equal to 6 are defined by a fourth degree equation which we shall not present here.

The following simple relation between the spin 2 and spin 3 energy levels follows from (1.2) and (1.3)

$$\varepsilon_1(2)+\varepsilon_2(2) = \varepsilon(3). \tag{1.5}$$

The energy levels of even nuclei computed on basis of the preceding formulas are plotted in fig. 1 as a function of $\gamma$. For $\gamma = 0$ the energy spectrum is identical to that of an axially-symmetric nucleus. For a fixed value of $\beta$ violation of axial symmetry of the nucleus leads to an increase of the energy of the levels belonging to the axial nucleus. This increase of the level energy corresponds to a decrease of the effective moment of inertia of the nucleus or of the effective deformation parameter $\beta_{ett}$. For the first excited state of spin 2 the effective deformation parameter can be determined from the formula

$$\beta_{ett} = \beta\left[\frac{4\sin^2(3\gamma)}{9-\sqrt{81-72\sin^2(3\gamma)}}\right]^{\frac{1}{2}}.$$

Besides the comparatively small change of the level energies of an axially symmetric nucleus, violation of axial symmetry of the nucleus leads to the appearance of some new energy levels $\varepsilon_2(2)$, $\varepsilon(3)$, $\varepsilon_2(4)$ etc. By using the

dependence of $\varepsilon_2(2)/\varepsilon_1(2)$ on $\gamma$, one can determine the corresponding value of $\gamma$ from the experimental value of the ratio. From fig. 1 the energy sequence of the spins and the energy values of the other nuclear levels can then be determined. Comparison of the theory with the experimental results will be performed in sec. 5.

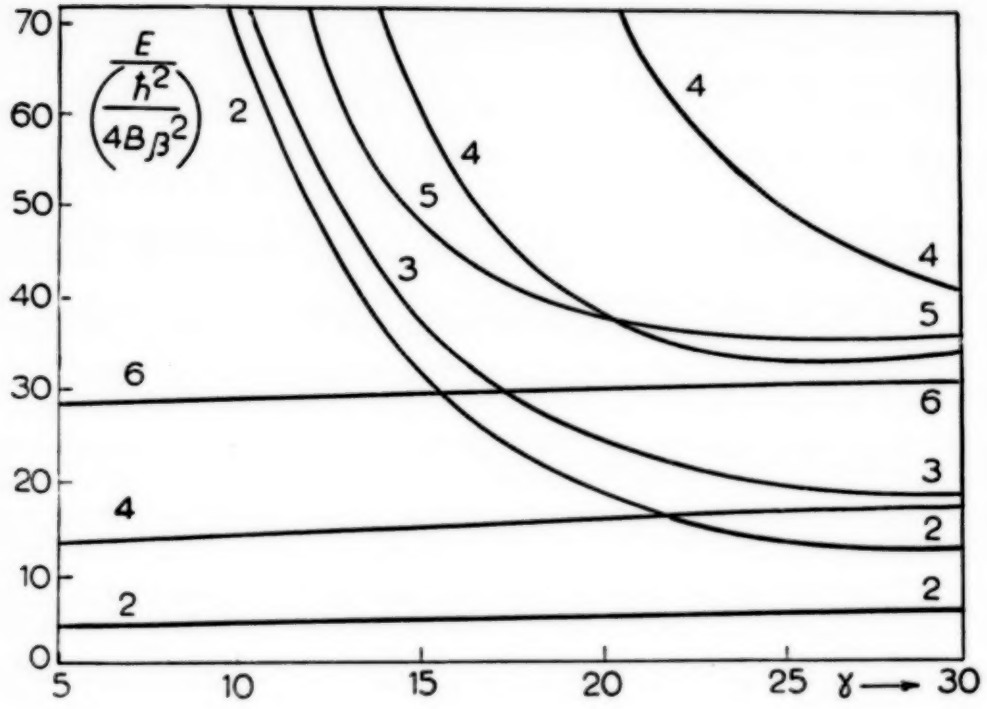


Fig. 1

## 3. Electric Transitions between Rotational Nuclear States

As is well known, measurements of the transition probabilities between electric states in a nucleus yield important information on the nature of the excited states. In particular, for elucidation of the nature of the second excited state of spin 2 in an even nucleus one may study the relative probability for transition from this level directly to the ground state or to the first excited state with a spin of 2. It has been assumed in a number of investigations that the first two spin 2 levels observed experimentally refer to one-phonon and two-phonon vibrations of the nuclear surface. In this case transition from the second state to the ground state can take place only as a result of violation of the oscillator approximation.

Assuming that both spin 2 levels can be assigned to rotational levels, we compute the ratio of the reduced transition probabilities for $\varepsilon_2(2) \to \varepsilon_1(2)$ and $\varepsilon_2(2) \to \varepsilon(0)$ as a function of the parameter $\gamma$ and hence as a function of the ratio $\varepsilon_2(2)/\varepsilon_1(2)$ since the latter depends on $\gamma$.

In order to calculate the probability for E2 type transitions between the rotational levels the operator of the nuclear quadrupole moment

$$\hat{Q}_{2\mu} = 2e\sqrt{\frac{4\pi}{5}}\sum_{i=1}^{Z} r_i^2 Y_{2\mu}(\vartheta_i \varphi_i)$$

should be expressed in terms of the Eulerian angles defining the orientation of the nucleus and in terms of the collective coordinates with respect to axes connected to the nucleus. Employing the transformation of the spherical functions

$$Y_{2\mu}(\vartheta\varphi) = \sum_{\nu} D^2_{\mu\nu} Y_{2\nu}(\vartheta' \varphi')$$

corresponding to transition to a coordinate system connected with the nucleus and expressing the proton coordinates $r_i \vartheta_i \varphi_i$ in this system (assuming the protons to be uniformly distributed within the nucleus) through the collective coordinates $a_\nu$ where $a_0 = \beta \cos\gamma$, $a_1 = a_{-1} = 0$, $a_2 = a_{-2} = \beta \sin\gamma/\sqrt{2}$ by aid of the formula

$$a_\nu = \frac{4\pi}{3Z}\sum_{i=1}^{Z}\left(\frac{r_i}{R}\right)^2 Y_{2\nu}(\vartheta'_i \varphi'_i)$$

we obtain the following expression for the $\mu^{\text{th}}$ component of the operator of the electric quadrupole moment

$$\hat{Q}_{2\mu} = eQ_0\left(D^2_{\mu 0}\cos\gamma + \frac{D^2_{\mu 2}+D^2_{\mu,-2}}{\sqrt{2}}\sin\gamma\right), \tag{2.1}$$

where

$$Q_0 = \frac{3ZR^2\beta}{\sqrt{5\pi}} \tag{2.2}$$

is the intrinsic electric quadrupole moment of an axial nucleus with a deformation parameter $\beta$; $D^2_{\mu\nu}$ are generalized spherical functions (which depend on the Eulerian angles) defining the unitary transformation from a coordinate system fixed in space to a coordinate system fixed to the nucleus.

The wave functions of the rotational states of a non-axial nucleus can be written in the form

$$\begin{aligned}
\psi_0 &= \frac{1}{\sqrt{8\pi^2}}\varphi(\beta,\gamma),\\
\psi_{21m} &= \left(\frac{5}{8\pi^2}\right)^{\frac{1}{2}}\varphi(\beta\gamma)\left[a_1 D^2_{m0} + b_1\frac{D^2_{m2}+D^2_{m,-2}}{\sqrt{2}}\right],\\
\psi_{22M} &= \left(\frac{5}{8\pi^2}\right)^{\frac{1}{2}}\varphi(\beta\gamma)\left[a_2 D^2_{M0} + b_2\frac{D^2_{M2}+D^2_{M,-2}}{\sqrt{2}}\right],
\end{aligned} \tag{2.3}$$

where $\varphi(\beta,\gamma)$ is a function corresponding to the internal state of a nucleus which is assumed to be the same in all three rotational states

$$
\begin{aligned}
a_1 N_1 &= -[\sin\gamma\sin(3\gamma)+3\cos\gamma\cos(3\gamma)+\sqrt{9-8\sin^2(3\gamma)}],\\
b_1 N_1 &= 3\sin\gamma\cos(3\gamma)-\cos\gamma\sin(3\gamma),\\
N_1^2 &= 2\sqrt{9-8\sin^2(3\gamma)}[\sqrt{9-8\sin(3\gamma)}+\sin\gamma\sin(3\gamma)+3\cos\gamma\cos(3\gamma)],\\
a_2 N_2 &= \sqrt{9-8\sin^2(3\gamma)}-\sin\gamma\sin(3\gamma)-3\cos\gamma\cos(3\gamma),\\
b_2 N_2 &= 3\sin\gamma\cos(3\gamma)-\cos\gamma\sin(3\gamma),\\
N_2^2 &= 2\sqrt{9-8\sin^2(3\gamma)}[\sqrt{9-8\sin^2(3\gamma)}-\sin\gamma\sin(3\gamma)-3\cos\gamma\cos(3\gamma)].
\end{aligned}
\tag{2.4}
$$

As was previously noted, $\gamma$ varies between 0 and $\pi/3$ and determines the deviation of the shape of the nucleus from axial symmetry. The axes of the ellipsoid employed to approximate the shape of the nucleus can be expressed through $\gamma$ and $\beta$ by the formula

$$R_\lambda = R\left[1+\beta\sqrt{\frac{5}{4\pi}}\cos\left(\gamma-\frac{2\pi}{3}\lambda\right)\right], \quad \lambda = 1, 2, 3.$$

If $\gamma = 0$ the nucleus is an elongated ellipsoid of revolution with a symmetry 3 axis. If $\gamma = \pi/3$ the nucleus is an oblate ellipsoid of revolution with a symmetry 2 axis. The rotational states of a nucleus defined by operator (1.1) and the probabilities for electromagnetic transitions between them are the same for $\gamma_1$ and $\pi/3-\gamma_1$. We therefore present the values of the various quantities in the interval between 0 and $\pi/6$.

In connection with the preceding it should be mentioned that one cannot decide on basis of measurements of the rotational energy of the nuclei or of the electromagnetic transitions between them whether the nucleus is an elongated or oblate ellipsoid. The only way to answer this question is to measure the mean values of the quadrupole electric moments in stationary states ($J, M = J$). In even nuclei the mean values of the quadrupole moments in the ground state are equal to zero. In the first excited state with spin 2 the mean value of the quadrupole moment is

$$Q_1 = -Q_0\frac{6\cos(3\gamma)}{7\sqrt{9-8\sin^2(3\gamma)}},$$

where $Q_0$ is defined in (2.2). In the second excited state of spin 2 the mean value of the quadrupole moment has a different sign

$$Q_2 = -Q_1.$$

The reduced probability for the electric quadrupole transition $J\tau \to J'\tau'$ averaged over the initial polarization states of the nucleus is

$$B(\mathrm{E2};\ J\tau \to J'\tau') = \frac{5}{16\pi(2J+1)}\sum_{Mm\mu}|(J'\tau' m|\hat{Q}_{2\mu}|J\tau M)|^2. \tag{2.5}$$

Since we assume that in this transition the internal state of the nucleus does not change, the reduced transition probability can be expressed through the

mean value of $\beta$ and $\gamma$ in the $\varphi(\beta, \gamma)$ state with help of (2.5). Inserting (2.3) into (2.5) and using (2.4) we find the following values for the reduced electric quadrupole transition probabilities expressed in $e^2Q_0^2/16\pi$ units. This unit corresponds to the reduced electric quadrupole transition probability in an axially symmetric nucleus between rotational levels of spin 2 and 0.

$$b(\mathrm{E2};\, 21 \to 0) = \frac{B(\mathrm{E2};\, 21 \to 0)}{\left(\frac{e^2Q_0^2}{16\pi}\right)} = \tfrac{1}{2}\left[1 + \frac{3 - 2\sin^2(3\gamma)}{\sqrt{9 - 8\sin^2(3\gamma)}}\right], \quad (2.6)$$

$$b(\mathrm{E2};\, 22 \to 0) = \tfrac{1}{2}\left[1 - \frac{3 - 2\sin^2(3\gamma)}{\sqrt{9 - 8\sin^2(3\gamma)}}\right], \quad (2.7)$$

$$b(\mathrm{E2};\, 22 \to 21) = \tfrac{10}{7}\frac{\sin^2(3\gamma)}{9 - 8\sin^2(3\gamma)}. \quad (2.8)$$

It is interesting to note that

$$b(\mathrm{E2};\, 21 \to 0) + b(\mathrm{E2};\, 22 \to 0) = 1.$$

The ratio $\varepsilon_2(2)/\varepsilon_1(1)$, the relative reduced transition probabilities (2.6) and (2.8) and the ratio of the reduced electric quadrupole transition probabilities $b(\mathrm{E2};\, 22 \to 21)/b(\mathrm{E2};\, 22 \to 0)$ are listed in table 1 for several

TABLE 1

| $\gamma$ | $\frac{\varepsilon_2(2)}{\varepsilon_1(2)}$ | $b(\mathrm{E2};\, 21 \to 0)$ | $b(\mathrm{E2};\, 22 \to 0)$ | $b(\mathrm{E2};\, 22 \to 21)$ | $\frac{b(\mathrm{E2};\, 22 \to 21)}{b(\mathrm{E2};\, 22 \to 0)}$ |
|---|---|---|---|---|---|
| 0 | $\infty$ | 1.000 | 0 | 0 | 1.43 |
| 5 | 64.2 | 0.993 | 0.0074 | 0.011 | 1.49 |
| 10 | 15.9 | 0.972 | 0.028 | 0.051 | 1.70 |
| 15 | 6.85 | 0.947 | 0.053 | 0.143 | 2.70 |
| 20 | 3.73 | 0.933 | 0.067 | 0.357 | 5.35 |
| 22.5 | 2.93 | 0.937 | 0.0625 | 0.563 | 19.02 |
| 24 | 2.59 | 0.948 | 0.052 | 0.782 | 15.1 |
| 25 | 2.41 | 0.955 | 0.0425 | 0.865 | 20.6 |
| 26 | 2.26 | 0.968 | 0.0324 | 1.01 | 31.2 |
| 28 | 2.07 | 0.99 | 0.010 | 1.28 | 126 |
| 29 | 2.01 | 0.996 | 0.004 | 1.41 | 363 |
| 30 | 2.00 | 1.000 | 0 | 1.43 | $\infty$ |

values of $\gamma$. From the data in table 1 it follows that the reduced probability (2.6) for transition from the first excited state to the ground state only slightly changes when axial symmetry of the nucleus is violated. The reduced probability (2.7) for transition from the second excited state of spin 2 directly to the ground state vanishes for $\gamma = 0°$ or $30°$ and comprises about 5—7 % of the corresponding reduced transition probability between the first excited and ground energy states when $\gamma = 15$—$24°$. The reduced E2 transition probability from the second excited spin 2 level to the first

excited level is very small for $\gamma \approx 0$ and subsequently rapidly increases and for $\gamma \approx 20°$ equals approximately 40 % of the reduced ground state transition probability in the axial nucleus and about 140 % for $\gamma \approx 30°$. Of special interest is the ratio of the reduced probabilities, $b(\mathrm{E2};\ 22 \to 21)/b(\mathrm{E2};\ 22 \to 0)$ as this quantity does not depend on the degree of population of level $\varepsilon_2(2)$ and can be directly measured.

With help of the explicit form of the wave function for energy level $\varepsilon(3)$

$$\psi_{31m} = \sqrt{\frac{7}{16\pi^2}}\,\varphi(\beta\gamma)\,[D^3_{m2} - D^3_{m,-2}],$$

the reduced electric quadrupole transition probabilities can be computed (in our units)

$$b(\mathrm{E2};\ 3 \to 22) = \tfrac{25}{28}\left(1 + \frac{3 - 2\sin^2(3\gamma)}{\sqrt{9 - 8\sin^2(3\gamma)}}\right);$$

$$b(\mathrm{E2};\ 3 \to 21) = \tfrac{25}{28}\left(1 - \frac{3 - 2\sin^2(3\gamma)}{\sqrt{9 - 8\sin^2(3\gamma)}}\right).$$

The values of these probabilities and their ratio are presented in table 2. These reduced probabilities satisfy the relation

$$b(\mathrm{E2};\ 3 \to 22) + b(\mathrm{E2};\ 3 \to 21) = \tfrac{25}{14}.$$

TABLE 2

| $\gamma$ | $b(\mathrm{E2};\ 3 \to 21)$ | $b(\mathrm{E2};\ 3 \to 22)$ | $\dfrac{b(\mathrm{E2};\ 3 \to 21)}{b(\mathrm{E2};\ 3 \to 22)}$ |
|---|---|---|---|
| 10 | 0.0132 | 1.77 | 0.0075 |
| 15 | 0.095 | 1.69 | 0.056 |
| 20 | 0.12 | 1.67 | 0.072 |
| 25 | 0.079 | 1.70 | 0.044 |
| 29 | 0.0696 | 1.72 | 0.039 |
| 30 | 0 | 1.78 | 0 |

## 4. Magnetic Dipole Transitions between Rotational States

According to Bohr and Mottelson [5]) the operator of the magnetic dipole moment corresponding to collective motions in an even nucleus is defined by the formula

$$\mathfrak{M}(1\mu) = \mu_0 g_R \int \mathbf{R}(\mathbf{r})\nabla(rY_{1\mu})\mathrm{d}\tau \qquad (3.1)$$

where $\mu_0 = e\hbar/2Mc$ is the nuclear magneton; $g_R$ is the gyromagnetic ratio corresponding to collective motion of the nucleons in the nucleus;

$$\mathbf{R}(\mathbf{r}) = BR_0^{-5} \sum_\lambda \dot{\alpha}_\lambda [\mathbf{r}\nabla(r^2 Y_{2\lambda})]$$

is the angular momentum density.

Introducing the operator $\mathbf{L} = -i[\mathbf{r}\nabla]$ we can write

$$[\mathbf{r}\nabla(r^2 Y_{2\lambda})] = ir^2 \mathbf{L} Y_{2\lambda} \text{ and } \nabla(r Y_{1\mu}) = (-1)^{\mu}\sqrt{\frac{3}{4\pi}}\mathbf{e}_{\mu}.$$

Inserting these values into (3.1) and employing the relation

$$(\mathbf{e}_{\mu}\mathbf{L})Y_{2\lambda} = (-1)^{\mu}\sqrt{6}\,(21, \lambda+\mu, -\mu|2\lambda)Y_{2,\lambda+\mu},$$

we reduce (3.1) to the form

$$\mathfrak{M}(1\mu) = \mathfrak{M}_0(1\mu)+\mathfrak{M}_1(1\mu)+\ldots \tag{3.2}$$

where

$$\mathfrak{M}_0(1\mu) = \frac{\mu_0 g_R}{2}\sqrt{\frac{3}{\pi}}J_{\mu}, \tag{3.3}$$

$$\mathfrak{M}_1(1\mu) = \mu_0 g_R \frac{5\sqrt{6}}{7\pi}\sum_{\nu}(21\mu-\nu, \nu|1\mu)\alpha^*_{\mu-\nu}J_{\nu}. \tag{3.4}$$

Here the $J_\nu$ are projections of the total angular momentum which in the classical theory are expressed through the coordinates $\alpha_\mu$ (in a space-fixed coordinate system these coordinates characterize the deviation of the shape of the nucleus from a spherical one) and through the corresponding velocities $\dot{\alpha}_\mu$ by the formula

$$J_\nu = i\sqrt{6}(-1)^{\nu} B \sum_{\mu}\dot{\alpha}_{\mu}\alpha_{\mu+\nu}(21, \mu+\nu, -\nu|2\mu),$$

where $B$ is the mass parameter of the theory; $(21, \mu+\nu, -\nu|2, \mu)$ is the vector addition coefficient. In quantum theory the $J_\nu$ are operators. The action of these operators on wave functions $D^J_{MK}$, in terms of which functions (2.3) of an asymmetric top are expressed, is defined by the equality

$$J_\nu D^J_{MK} = (-1)^{\nu}\sqrt{J(J+1)}(J1M+\nu, -\nu|J, M)D^J_{M+\nu,K}.$$

The reduced magnetic dipole radiation probability from the state 22 to state 21 defined by functions (2.3) is

$$B(M1; 22 \to 21) = \tfrac{1}{5}\sum_{m'\mu m}|(21m'|\mathfrak{M}(1\mu)|22m)|^2. \tag{3.5}$$

It is easy to verify that operator (3.3) does not contribute to this probability. Inserting (3.4) and (2.3) into (3.5) we get

$$B(\mathrm{M1}; 22 \to 21) = \frac{90}{49\pi^2}\mu_0^2 g_R^2 \beta^2 \frac{\sin^2(3\gamma)}{9-8\sin^2(3\gamma)}. \tag{3.6}$$

From (3.6) it follows that in an axial nucleus ($\gamma = 0$) the reduced magnetic dipole radiation probability is zero and increases with $\gamma$ reaching a maximal value at $\gamma = 30°$.

If the value of $\gamma$ is determined from the ratio $E_{22}/E_{21}$ of the energies of two spin levels, one can evaluate the value of the gyromagnetic ratio $g_R$ for

collective nucleon motion by using (3.6) and the results of measurement of the reduced magnetic dipole transition probabilities.

If one, furthermore, takes into account that according to (2.8) the reduced electric quadrupole radiation probability for transitions between the same levels is

$$B(\mathrm{E2};\ 22 \to 21) = \frac{10e^2 Q_0^2}{7\pi} \frac{\sin^2(3\gamma)}{[9-8\sin^2(3\gamma)]},$$

one may determine the ratio of the reduced probabilities

$$\frac{B(M1;\ 22 \to 21)}{B(\mathrm{E2};\ 22 \to 21)} = \frac{80}{7}\left(\frac{\mu_0 g_R}{eZR_0^2}\right)^2, \tag{3.7}$$

where $R_0$ is the nuclear radius. It is interesting to note that (3.7) is not dependent on $\gamma$ and $\beta$.

From (3.7) the ratio of the intensities of $\gamma$ quanta emitted in both types of radiation is

$$\frac{T(\mathrm{M1})}{T(\mathrm{E2})} = \frac{80}{0.21k^2}\left(\frac{\mu_0 g_R}{eZR_0^2}\right)^2, \tag{3.8}$$

where

$$k = \frac{E_{22}-E_{21}}{\hbar c}.$$

## 5. Comparison with Experiment

The results obtained in the preceding sections were based on the assumption that during rotation of a nucleus its internal state does not change. This assumption can be only approximately true and is the more accurate the farther the rotational energy levels are located from levels corresponding to excitation of the internal states of the nucleus and possessing the same $J$ values, parities, etc.

Experimental values of the ratio of the energy of the second spin 2 level to that of the first level are listed in table 3. The value of parameter $\gamma$ can be computed from this ratio with help of formulas (1.2). Employing (2.7) and (2.8) and making use of this value of $\gamma$ one can evaluate $\{b(\mathrm{E2};\ 22 \to 21)/b(\mathrm{E2};\ 22 \to 0)\}_{\mathrm{theor}}$. Comparison of these ratios with the experimental ones (column 7) indicates that the theory satisfactorily describes the experimentally observed rapid variation of the ratio of the reduced probabilities for transitions from a nucleus to one with a different $\gamma$ value.

As can be seen by comparing columns 4 and 5 of table 3 for many nuclei the sum of the energies of the two spin $2^+$ levels is equal to the energy of the spin 3 level, as required by equation (1.5), with an accuracy to 1 %. The deviation of 5 % observed in the $Cd^{114}$ nucleus can be explained by the effect of three other levels located near level 2 and possessing spins of 4, 0 and 2.

From fig. 1 it can be seen that for $\gamma < 21.5°$ the second excited $2^+$ level should lie above level $4^+$, whereas for $\gamma > 21.5°$ it should lie below this level. The level $3^+$ should always be higher than level $4^+$. These rules are valid for

TABLE 3

| Nucleus | $\frac{\varepsilon_2(2)}{\varepsilon_1(2)}$ | $\gamma^0$ | Experimental keV | | $\frac{b(E2;\ 22 \to 21)}{b(E2;\ 22 \to 0)}$ | | ref. |
|---|---|---|---|---|---|---|---|
| | | | $\varepsilon_1(2)+\varepsilon_2(2)$ | $\varepsilon(3)$ | theor. | exper. | |
| $Pt^{196}$ | 1.97 | 30 | 1040 | — | $\infty$ | >2500 | 9, 24 |
| $Pt^{192}$ | 1.94 | 30 | 929 | 920.9 | $\infty$ | 163 | 13 |
| $Xe^{128}$ | 2.0 | 30 | 1445 | — | $\infty$ | 197 | 14 |
| $Te^{126}$ | 2.14 | 27.5 | 2040 | — | 104 | 200 | 23 |
| $Cd^{114}$ | 2.17 | 26.75 | 1771 | 1860 | 78 | 77.9 | 15 |
| $Se^{76}$ | 2.2 | 26.6 | 1760 | — | 68 | 23.5 | 16 |
| $Te^{122}$ | 2.25 | 26.5 | 1760 | | 66 | 78.2 | 17 |
| $Hg^{198}$ | 2.66 | 23.2 | 1500 | | 13 | 25 | 23 |
| $Gd^{154}$ | 3.01 | 21.4 | 1133 | 1140 | 7.2 | — | 18 |
| $W^{186}$ | 8.08 | 13.9 | 1000 | 1000 | 2.0 | | 19 |
| $Sm^{152}$ | 8.9 | 13.48 | 1206 | 1226 | 1.9 | 1.7 | 18, 22 |
| $Dy^{160}$ | 11 | 12.2 | 1051 | 1047 | 1.9 | 2.38 | 10 |
| $W^{182}$ | 12.1 | 11.6 | 1322 | 1331 | 1.6 | 1.59 | 20 |
| $Pu^{238}$ | 23.4 | 8.13 | 1074 | 1076 | 1.2 | 1.3—1.5 | 25 |
| $Pu^{240}$ | 23.7 | 8.0 | 1063 | 1060 | 1.2 | — | 19 |

all the nuclei in table 3 for which the positions of levels with spins of 2, 4, 3 are known.

It is interesting to note that for $\gamma = 30°$ the theory predicts an equidistant spacing of energy levels $\varepsilon_1(2)$, $\varepsilon_2(2)$, $\varepsilon(3)$. A level spacing of this type can also be derived in the oscillator approximation for the energy of surface vibrations. However in this case the $\varepsilon_2(2)$ and $\varepsilon(3)$ levels should be degenerate with spin values of respectively 0, 2, 4 and 0, 2, 3, 4, 6.

Unfortunately, the experimental data which can be used to determine the ratio $b(E2; 3 \to 21)/b(E2; 3 \to 22)$ are quite sparse. We know this ratio only for $Kr^{81}$ [21]) for which it equals 0.016. This corresponds to a value of $\gamma$ which slightly exceeds 29. A value $\gamma > 29$ agrees with the observed value $\varepsilon_2(2)/\varepsilon_1(2) = 1.9$ if it be taken into accountt hat in this nucleus adiabatic conditions apparently are not rigorously fulfilled.

From formulas (2.6) and (2.7) one can compute the ratio of the reduced probabilities, $b(E2; 22 \to 0)/b(E2; 21 \to 0)$; it equals the ratio $b(E2; 0 \to 22)/b(E2; 0 \to 21)$ of the reduced probabilities for the inverse transitions which appear during Coulomb excitation of the nuclei. This ratio is maximal for $\gamma$ values lying between 15° and 25° (the variation of $\gamma$ in this interval corresponds to $6.28 > \varepsilon_2(2)/\varepsilon_1(2) > 2.4$) and is very small for $\gamma < 5°$ and $\gamma > 29°$. The values of the ratio $b(E2; 0 \to 22)/b(E2; 0 \to 21)$ presented in ref.[23]) and derived from Coulomb excitation data and also the theoretical

values of $\gamma$ computed from (2.6) and (2.7) for the corresponding energy ratio, $\varepsilon_2(2)/\varepsilon_1(2)$, are presented in table 4. It is apparent from the table that the theoretical values satisfactorily agree with the experimental ones.

TABLE 4

| Nucleus | $\frac{\varepsilon_2(2)}{\varepsilon_1(2)}$ | $\gamma$ | $\frac{b(\mathrm{E2};\ 0 \to 22)}{b(\mathrm{E2};\ 0 \to 21)}$ | |
|---|---|---|---|---|
| | | | exper. | theor. |
| $Os^{190}$ | 2.9 | 20 | $\approx 0.04$ | 0.072 |
| $Ru^{100}$ | 2.55 | 23.7 | 0.024 | 0.057 |
| $Ru^{104}$ | 2.56 | 24 | 0.013 | 0.055 |
| $Cd^{116}$ | 2.35 | 25.05 | 0.021 | 0.044 |
| $Ru^{102}$ | 2.24 | 25.07 | 0.015 | 0.043 |
| $Pd^{106}$ | 2.2 | 26.5 | 0.017 | 0.027 |
| $Pd^{108}$ | 2.18 | 27 | 0.01 | 0.02 |
| $Cd^{114}$ | 2.17 | 27 | 0.02 | 0.02 |

In order to compare the experimental ratio of the intensities of magnetic dipole and electric quadrupole radiations in the $2^+ \to 2^+$ transition with the values which formula (3.8) yields, we put $\mu_0 = 5.05 \times 10^{-24}$ erg · gauss$^{-1}$ $g_R = 0.4$; $R_0 = 1.2A^{\frac{1}{3}} \times 10^{-13}$ cm. The $T(\mathrm{M1})/T(\mathrm{E2})$ ratios computed in this way are given in table 5 (third column). The intensity of the E2 transition

TABLE 5

| Nucleus | $E_{22} - E_{21}$ keV | $\frac{T(\mathrm{M1})}{T(\mathrm{E2})}$ | exper. % of E2 transition |
|---|---|---|---|
| $Sc^{78}$ | 643 | $9.8 \times 10^{-2}$ | $98 \pm 1$ |
| $Te^{122}$ | 693 | $1.9 \times 10^{-2}$ | $92 \pm 4$ |
| $Os^{186}$ | 627 | $6.5 \times 10^{-3}$ | $99 \pm 1$ |
| $Os^{188}$ | 480 | $1.04 \times 10^{-2}$ | 99.6 |

relative to the total intensity of the $22 \to 21$ transition derived from the data of Lindvist and Marklund [25]) is given in the last column of the table.

Comparison of the predictions of the theory with the experimental data presently known to us thus confirms the assumption that some even nuclei do not possess axial symmetry.

## References

1) G. F. Filippov, Doklady AN SSSR **115** (1957) 4
2) A. S. Davydov and G. F. Filippov, JETP **33** (1957) 723
3) A. S. Davydov and A. A. Chaban, JETP **33** (1957) 547
4) A. S. Davydov and B. M. Murashkin, JETP **34** (1958) 1619
5) A. Bohr, Mat. Fys. Medd. Dan. Vid. Selsk., **28** (1952) no. 14
6) A. Bohr and B. Mottelson, Mat. Fys. Medd. Dan. Vid. Selsk. **27** (1953) no. 16
7) L. Wilets and M. Jean, Phys. Rev. **102** (1956) 788
8) C. Marty, Nuclear Physics **1** (1956) 85; **3** (1957) 193

9) K. Alder, A. Bohr, T. Huus, B. Mottelson and A. Winter, Revs. Mod. Phys. **28** (1956) 432
10) O. Nathan, Nuclear Physics **4** (1957) 125
11) L. Landau and E. Lifshitz, Quantum Mechanics (Moscow, 1948)
12) D. Dennison, Revs. Mod. Phys. **3** (1931) 280
13) L. Baggerly, P. Marmer, F. Boehm and J. Du Mond, Phys. Rev. **100** (1955) 1364
14) N. Benczer, B. Farrely, L. Koerts and C. S. Wu, Phys. Rev. **101** (1955) 1027
15) H. Motz, Phys. Rev. **104** (1956) 1353
16) J. Kurbatov, B. Murray and M. Sakai, Phys. Rev. **98** (1955) 674
17) M. Glaubman, Phys. Rev. **98** (1955) 645
18) O. Nathan and M. Waggoner, Nuclear Physics **2** (1956/57) 548
19) L. Peker, Conference on Nuclear Spectroscopy, (Leningrad, 1958)
20) F. Boehm, P. Marmier and J. Dumond, Phys. Rev. **95** (1954) 864
21) R. Waddell, and E. Jensen, Phys. Rev. **102** (1956) 816
22) S. K. Bhattcherjee, T. D. Nainan, S. Raman, Baldev and Sabal, Nuovo Cimento **7** (1958) 501
23) M. Jean and J. Touchard, Jour. Phys. Radium **19** (1958) 56
24) D. E. Alburger, Phys. Rev. **108** (1957) 812
25) T. Lindvist and I. Markland, Nuclear Physics **4** (1957) 189

3.A *Nuclear Physics* **8** (1958) 250—264; © *North-Holland Publishing Co., Amsterdam*
Not to be reproduced by photoprint or microfilm without written permission from the publisher

# GAMMA-RAY SPECTRUM OF RADIUM IN EQUILIBRIUM WITH ITS DECAY PRODUCTS

B. S. DŽELEPOW and N. N. ZHUKOVSKY
*V. G. Khlopin Radium Institute, USSR Academy of Sciences, Leningrad*
and
S. A. SHESTOPALOVA and I. F. UCHEVATKIN
*D. I. Mendeleyev Research Institute of Metrology, Leningrad*

Received 26 March 1958

**Abstract:** Results are described of an investigation of the radium gamma-spectrum in equilibrium with its decay products, based on recoil electron measurements in the energy range 150 – 2530 keV. Forty-four gamma-lines have been observed, and their relative intensities and the number of quanta per disintegration determined.

## 1. Introduction

Despite the large number of investigations of the $\beta$- and $\gamma$-spectra associated with the decay of radium there are as yet no firmly established decay schemes of RaB and RaC. This is due to the fact that the $\beta$- and $\gamma$-spectra of RaB and, especially, those of RaC are highly complex.

The $\gamma$-ray spectra of radium (B+C) have been repeatedly studied [1–7]). They are so complex that each improvement in the experimental technique brings out new details in them.

The energy of the $\gamma$-quanta are determined most accurately from the spectrum of conversion electrons.

The most complete data on the conversion electron spectrum were obtained in 1954 by Mladjenović and Slätis [5]) on a $\beta$-spectrometer with photographic recording. The authors assigned 16 $\gamma$-transitions in radium C′ ($Po^{214}$) and 5 $\gamma$-transitions in radium C ($Bi^{214}$). The relative intensities of the $\gamma$-lines are best determined from the recoil electron spectrum. Until recently there were no investigations of the $\gamma$-spectrum of radium B based on recoil electron measurements. Such investigations were carried out on the spectrum RaC in 1940 by Latyshev and co-workers [2]) and in 1954 by Mladjenović and Hedgran [3]). These authors firmly established the existence of 11 $\gamma$-lines. In 1956 a study of the $\gamma$-ray spectrum of radium C based on recoil electron measurements [8]) was carried out with a resolution approximately one and a half times greater than that claimed in ref.[3]). In addition to the previously known $\gamma$-line intensities, the authors gave

the intensities of 21 other lines. However, even these $\gamma$-lines did not account for the entire distribution of experimental points, leaving an excess of recoil electrons in some regions unexplained.

In order to elucidate the relative intensities in the $\gamma$-ray spectrum of RaB and RaC we undertook another investigation of this spectrum on the elotron of the Radium Institute [9]). The apparatus was operated under the conditions described in ref. [10]). In our experiments the width of the Compton line at one-half its height comprised 3.0 % in the vicinity of 400 keV and 1.5 % in the vicinity of 1500 keV and higher.

The $\gamma$-ray source was two grams of radium in the form of the salt $RaBr_2$. The form of the source is the same as described in ref. [8]).

## 2. Results

The experimental spectrum is shown in fig. 1. The black points represent the background, being the number of coincidences with the target out of the beam.

The experimental points of the background are so distributed that two lines can be drawn through them by the method of least squares; the background is then estimated from these lines. After subtraction of the background the curve was resolved into components of standard form. The form of the line was obtained from measurements of the single lines: 411.8 keV of $Au^{198}$, 661.6 keV of $Cs^{137}$, 1171.5 and 1331.6 keV of $Co^{60}$, 1367.9 and 2753.5 keV of $Na^{24}$ and 2614.3 keV of ThC''.

The strongest lines, such as 352.0, 609.3, 768.7, 934.8, 1120.4, 1378.2, 1509.3, 1764.4 and 2204.2 keV were used for the energy calibration. The values of the energy were taken from the paper by Mladjenović and Slätis [5]) based on conversion electron measurements. If the position of a weak line coincided with that indicated in ref. [5]), we took the value given in that paper as the most accurate one. If there was no such agreement, then we determined the energy from our calibration curve. The intensity of the components was selected to give the best explanation of the experimental points.

The results of the resolution are illustrated in figs. 2—5. Fig. 2 shows the spectral region from $\approx$ 150 to 630 keV. The spectral region up to the 609 keV line has been studied for the first time on the basis of recoil electron measurements. In addition to the well known lines of radium B: 241.9, 295.2 and 352.0 keV [5,6]), an excess of recoil electrons is clearly seen near 295 keV. The resolution shows that this excess is maximum near 285 keV. Among the unassigned lines in ref. [5]) are to be found lines No. 43—46, 59, 60, 62. If these are assigned to K- and L-conversion electrons of RaC, then for the gamma-line energies we obtain the values: 273.2, 273.9, 277.6 and 281.5 keV. All these lines taken together probably account for our excess of conversion electrons.

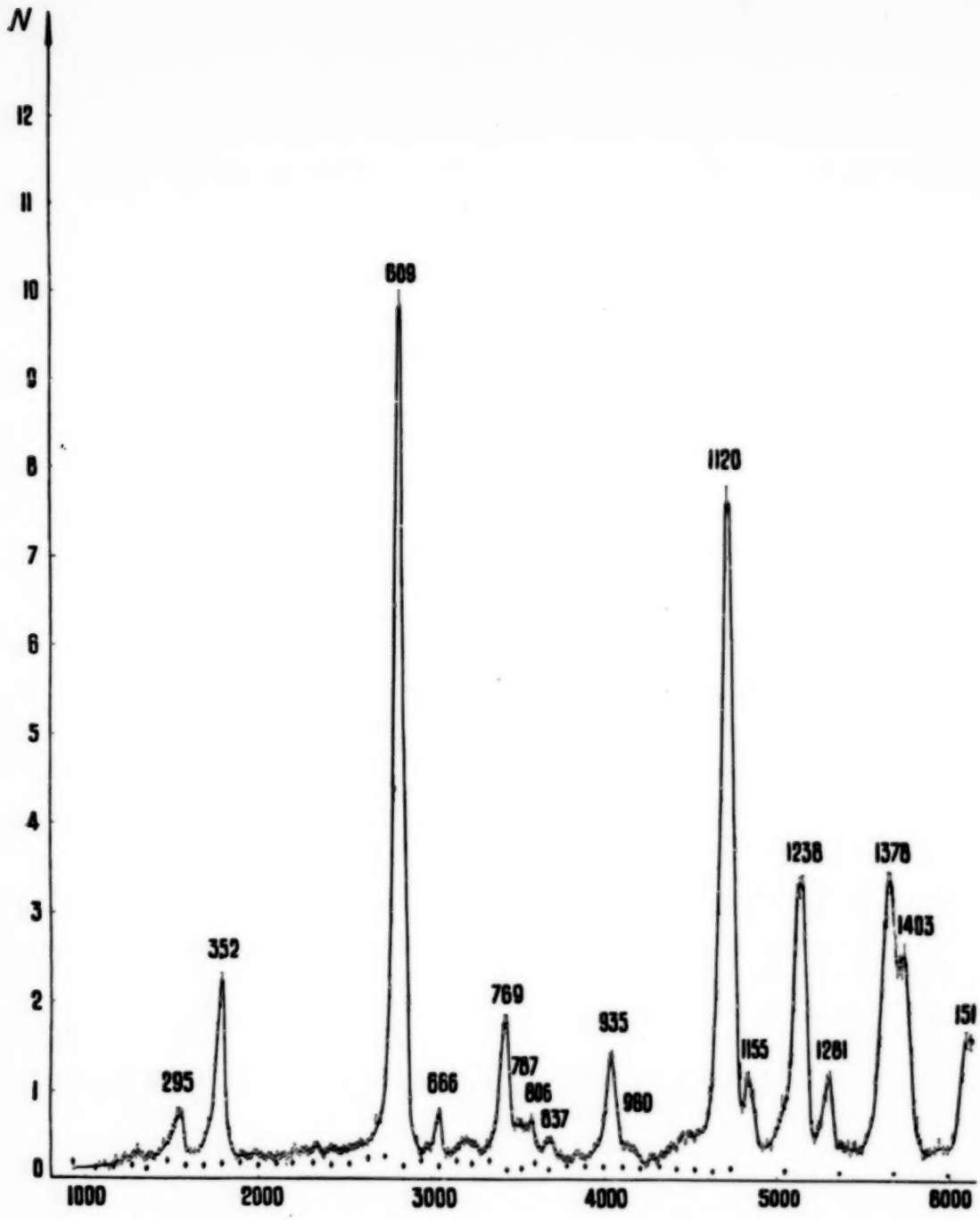


Fig. 1. Experimental gamma-ray spectrum of radium in equilibrium with its decay products. $\frac{\top}{\perp}$:coincidence with target in the gamma-ray beam. $\frac{\top}{\cdot}$:coincidence with target out of the beam (background).
*N* is number of coincidences per minute.

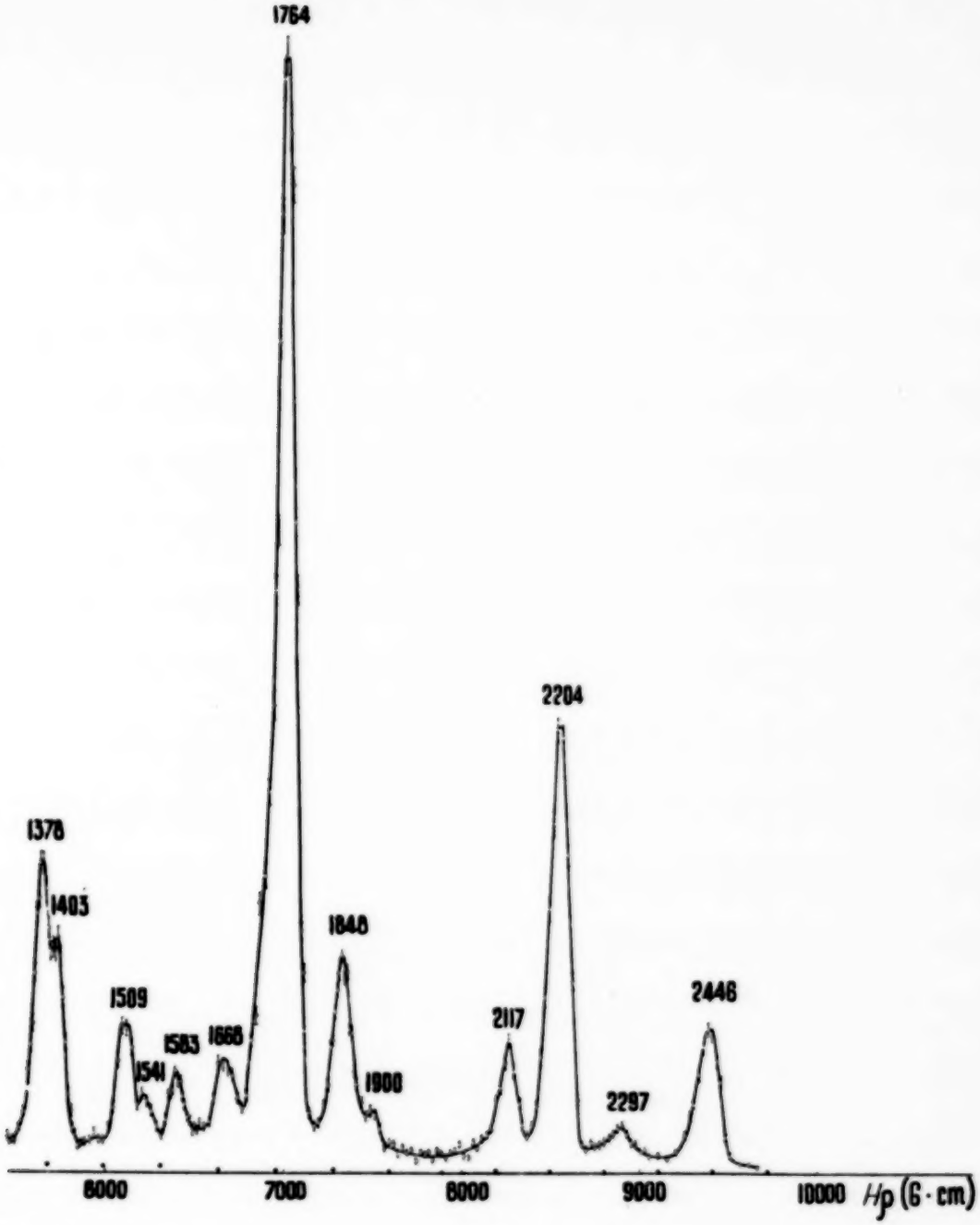


Fig. 1. (Continued.)

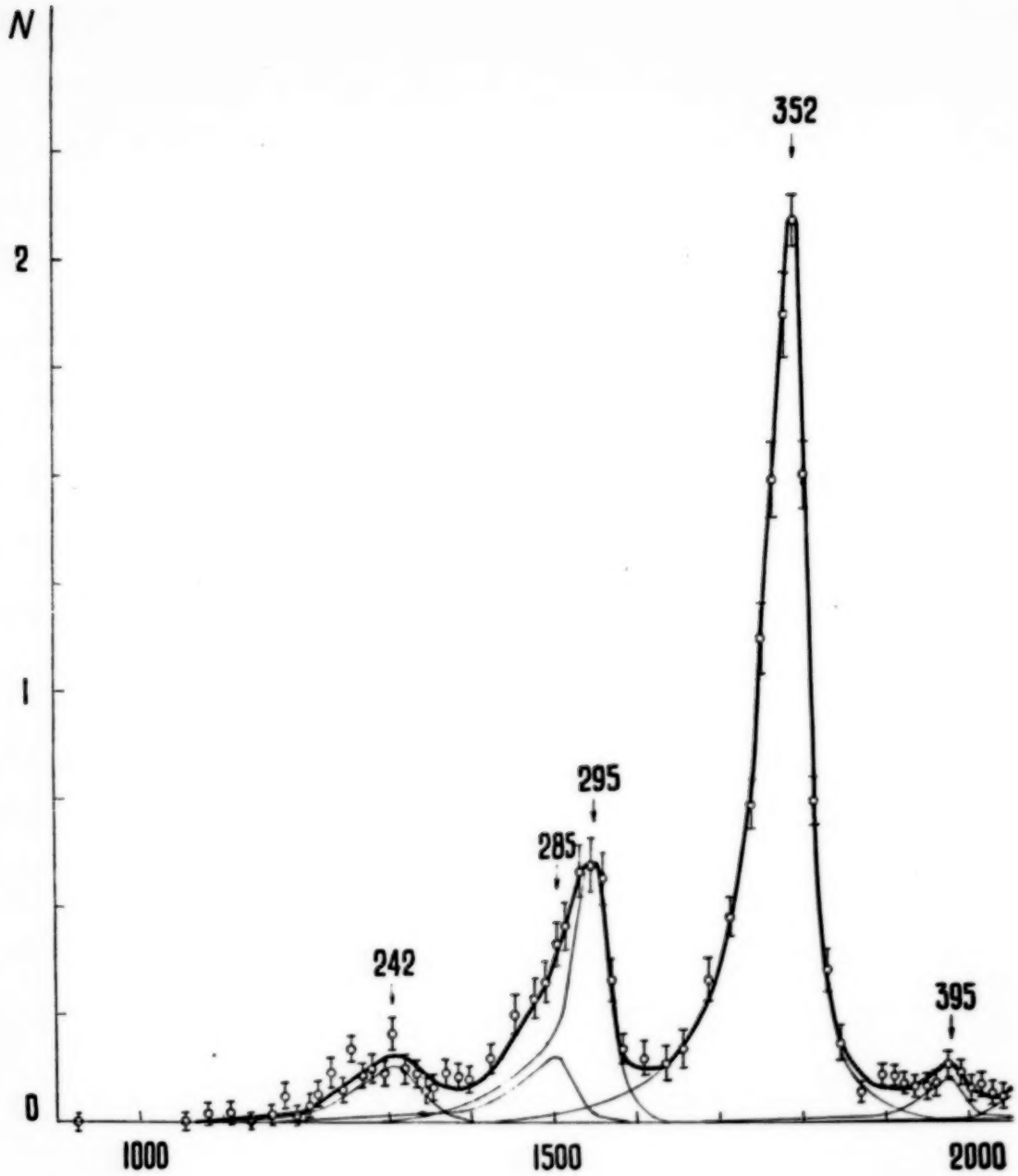


Fig. 2. Resolution of the gamma spectrum into components in the region ≈ 150–630 keV. $N$ is number of coincidences minus the background per/min.

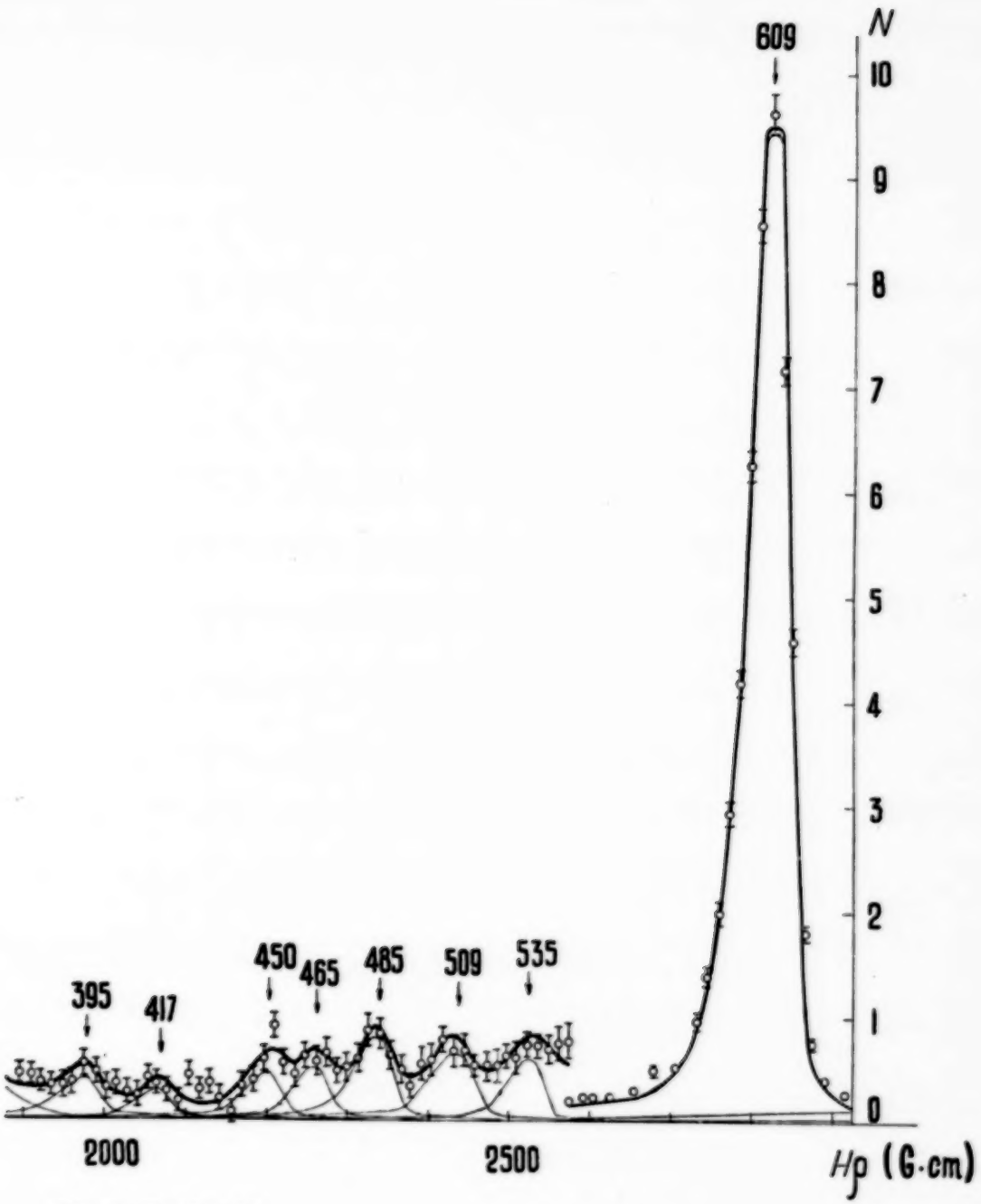


Fig. 2. (Continued.)

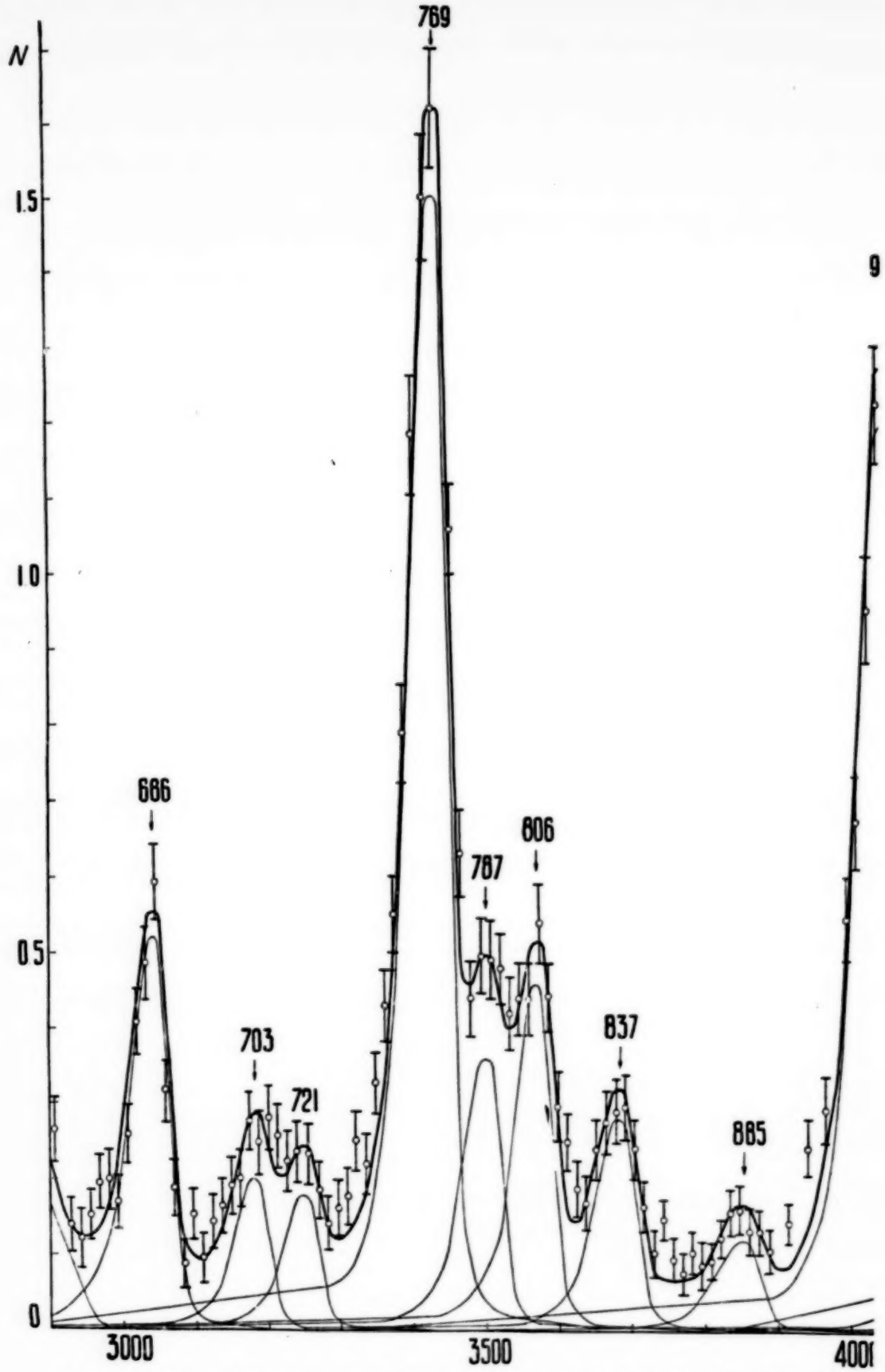


Fig. 3. Resolution of the gamma spectrum into components in the region 630—1170 keV. $N$ is number of coincidences minus the background per/min.

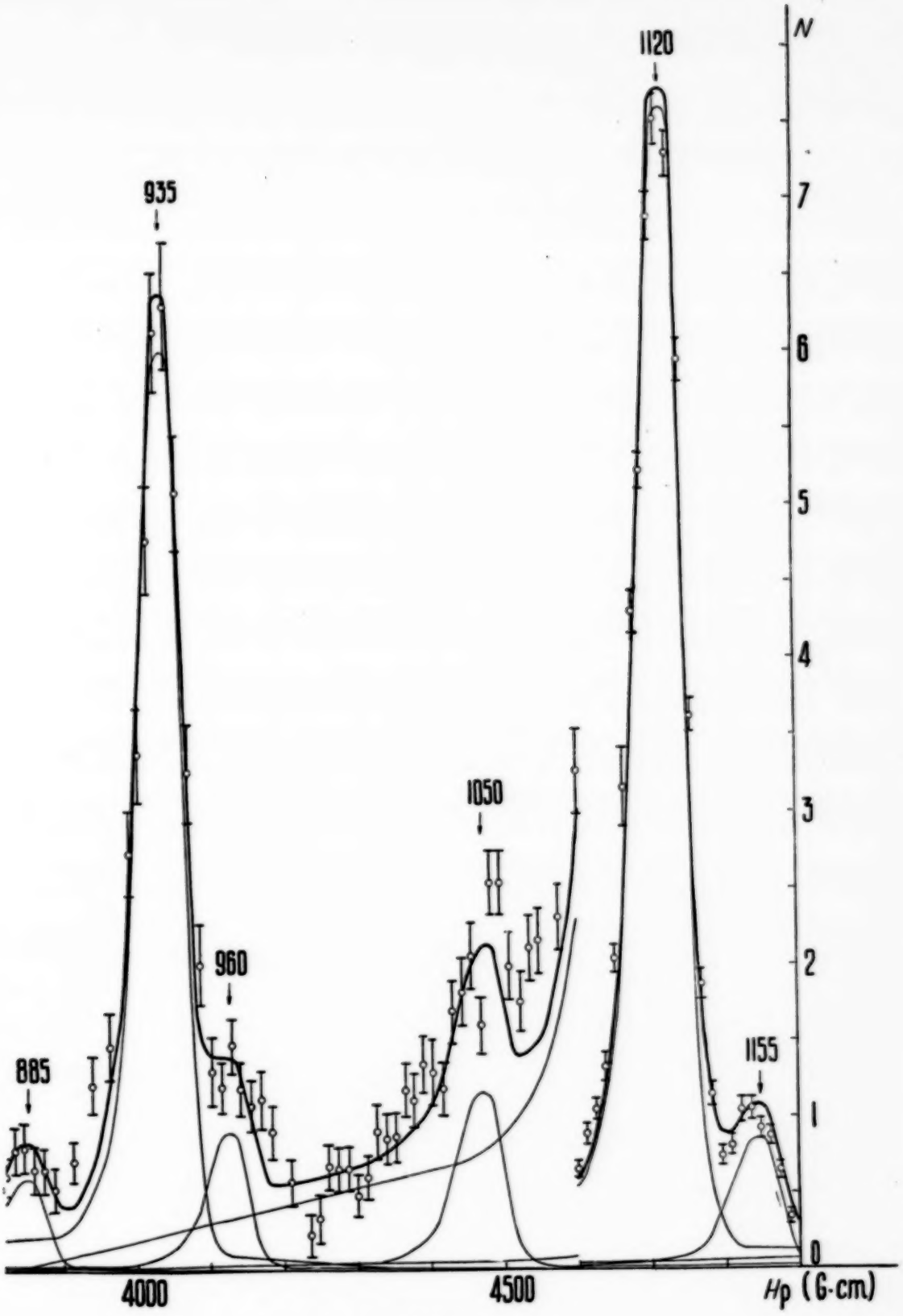


Fig. 3. (Continued.)

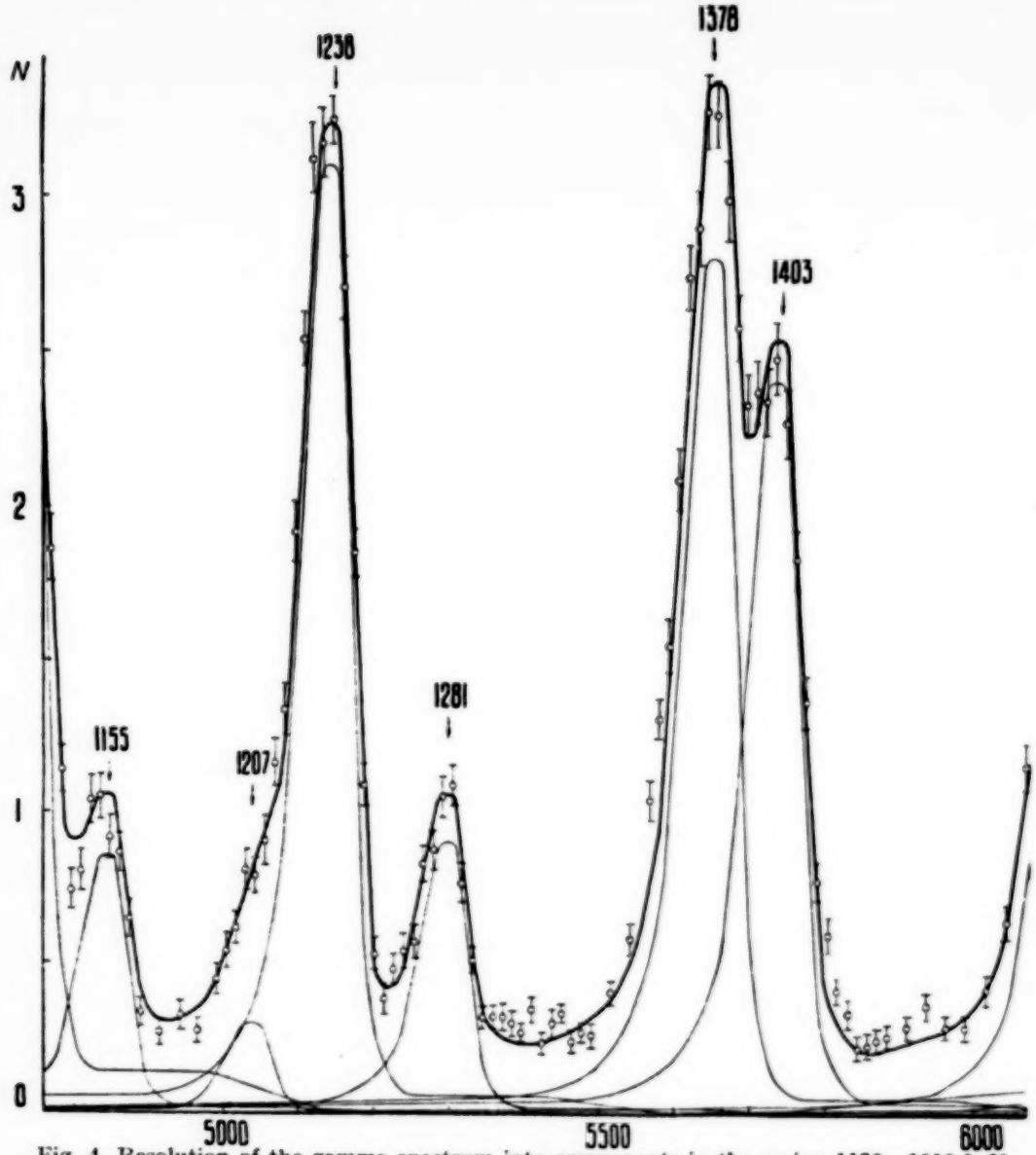


Fig. 4. Resolution of the gamma spectrum into components in the region 1130—1810 keV. *N* is number of coincidences minus the background per/min.

It can be seen in fig. 2 that between the strong 352.0 and 609.3 keV lines are situated a number of close-lying weaker gamma-lines. Several of them can probably be found among the assigned lines of ref. [5]): these are lines No. 68, 70, 77, 78, 79. If they are assigned to K-conversion electrons of radium C, then for the energy of the gamma-lines we obtain the values 386.8, 388.9, 466.7, 471.2 and 484.6 keV. Some of these lines coincide with those found by us and indicated in fig. 2.

Fig. 3 shows the spectral region from 630 to 1170 keV. In the region 630—769 keV the 666±7 keV line is clearly seen, and the 703.2 and 721±7

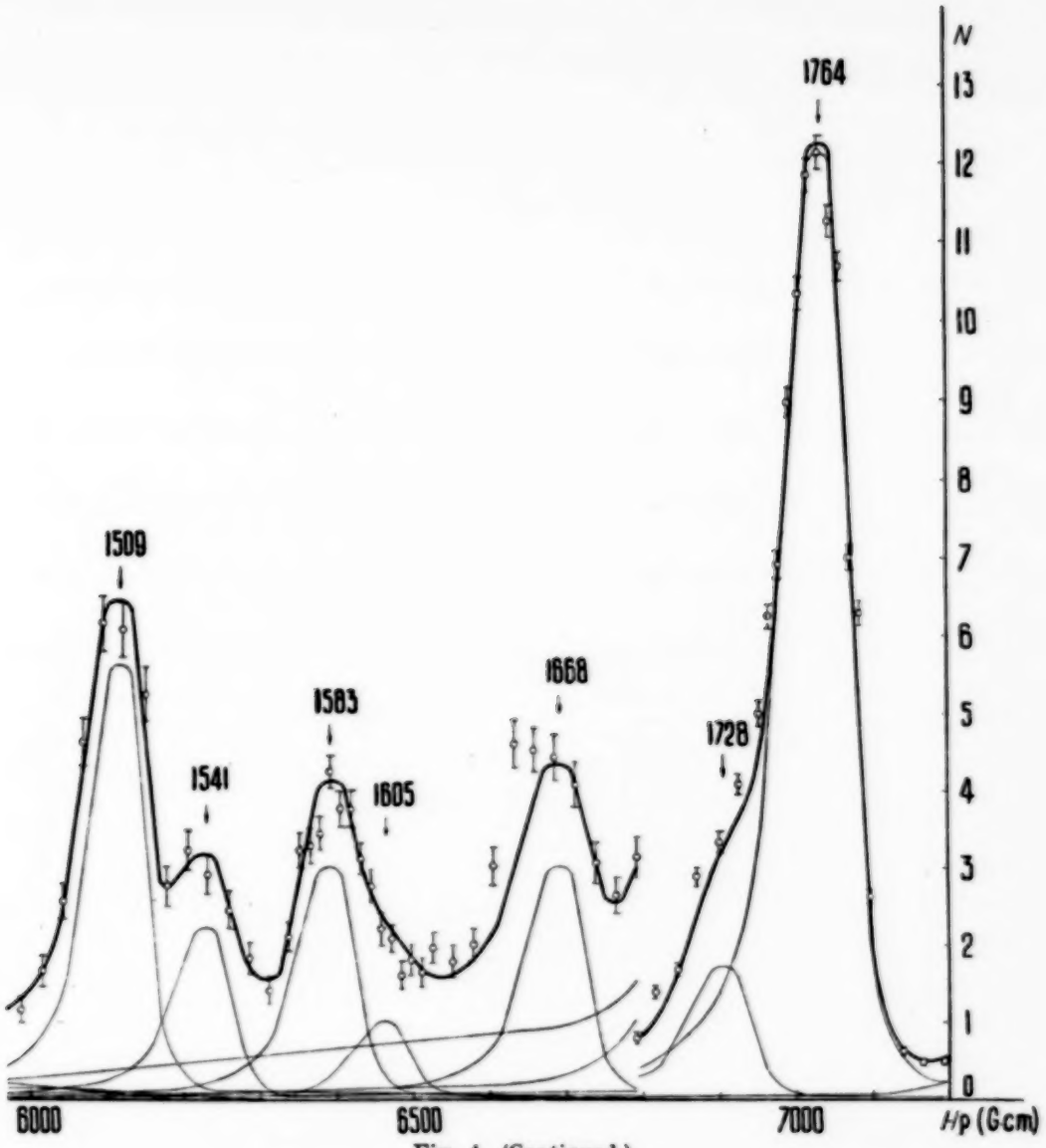


Fig. 4. (Continued.)

keV lines can be distinguished. In ref. [8]) the excess of recoil electrons between the 609.3 and 768.7 keV lines is attributed to the presence of the 652.4, 660.9 and 703.2 keV lines, and an excess is indicated in the vicinity of 720 keV. We did not discover the 652.4 keV line this time; had its intensity comprised $\frac{1}{7}$ the intensity of 666 keV line we would have observed it. After the lines indicated above have been drawn, a small excess of recoil electrons remains near 740 keV.

On the high energy side there are three lines near the 768.7 keV line: $h\nu = 787.1$, 806.3 and $837 \pm 8$ keV. In ref. [8]) an excess was observed in

this region which was attributed to the 787.1, 806.3 and 821.3 keV lines on the basis of the assignment of the lines found by Mladjenović and Slätis. Our curve confirms the existence of the first two lines, but the third clearly has greater energy.

In the region 840—900 and 950—1070 keV we discovered new gamma lines of energies 885±10, 960±5 and 1050±10 keV. In ref.[8]) an excess of recoil electrons was found approximately in these regions.

Fig. 4 shows the spectral region from 1130 to 1810 keV. The 1155.3 and 1281.3 keV lines found in ref.[5]) can be clearly seen. Near the 1238.3 keV line, on the low energy side, there is an excess of recoil electrons; these are due to the 1207.1 keV line which is among the unassigned lines in ref.[5]).

The trend of the curve in the spectral region of 1360—1440 keV confirms the existence in this region of no less than two transitions with close values of the energy. Formerly one wide maximum was observed here [3,8]); now it has faintly resolved into two. Judging by the spectrum of conversion electrons, there can be seven lines in this region. The resolution of our curve shows that the remainder left after separating out the 1378.2 keV line has the form of the line $h\nu = 1403\pm7$ keV.

Near the 1509.3 keV line clearly appears the 1541±5 keV line, which was hitherto not detected from conversion electron measurements[5]). The 1582.9 and 1668.4 keV lines are perfectly clear; the 1582.9 keV line falls off more slowly on the high energy side than the standard form of the line demands. This is probably due to the presence of the 1605.2 keV line [8]), which is to be found among the unassigned lines in ref. [5]).

Near the strong 1764.4 keV line, on the low energy side, appears the 1728.3 keV line, which was found from conversion electron measurements [5]).

We did not discover any noticeable broadening of the 1764.4 keV line on the high energy side.

Fig. 5 shows the spectral region from 1780 to 2530 keV. The peak near the well known 1848.5 keV line differs in form from that of the standard line: it is somewhat wider and falls off more slowly on the high energy side. After drawing the strongest possible 1848.5 keV line, we discovered an excess of electrons with a maximum in the vicinity of 1860 keV. We believe that this excess can be attributed to the presence of the 1862.3 keV line [8]). The existence of a 1900 keV gamma-line [8]) has been confirmed. There is an excess of recoil electrons in the vicinity of 2016.7 and 2090 keV; in intensity it is approximately three times less than indicated in ref. [8]).

The 2446±10 keV line proved to be slightly wider than should follow from the standard form. After the strongest possible 2446 keV line has been drawn, the excess on the low energy side has a maximum near 2410 keV of intensity approximately 10 times less than the area of the 2446 keV line.

The paper by Rutherford *et al.*[11]) reports an excitation level of 2513±5

keV in RaC'; one would have expected to find a $\gamma$-line $h\nu = 2513$ keV.

The position of the 2513 keV line is denoted by an arrow in fig. 5. If this line does exist, its intensity is less than $\frac{1}{40}$ the intensity of the 2446 keV line; i.e., comprises less than $4 \times 10^{-4}$ quanta per disintegration.

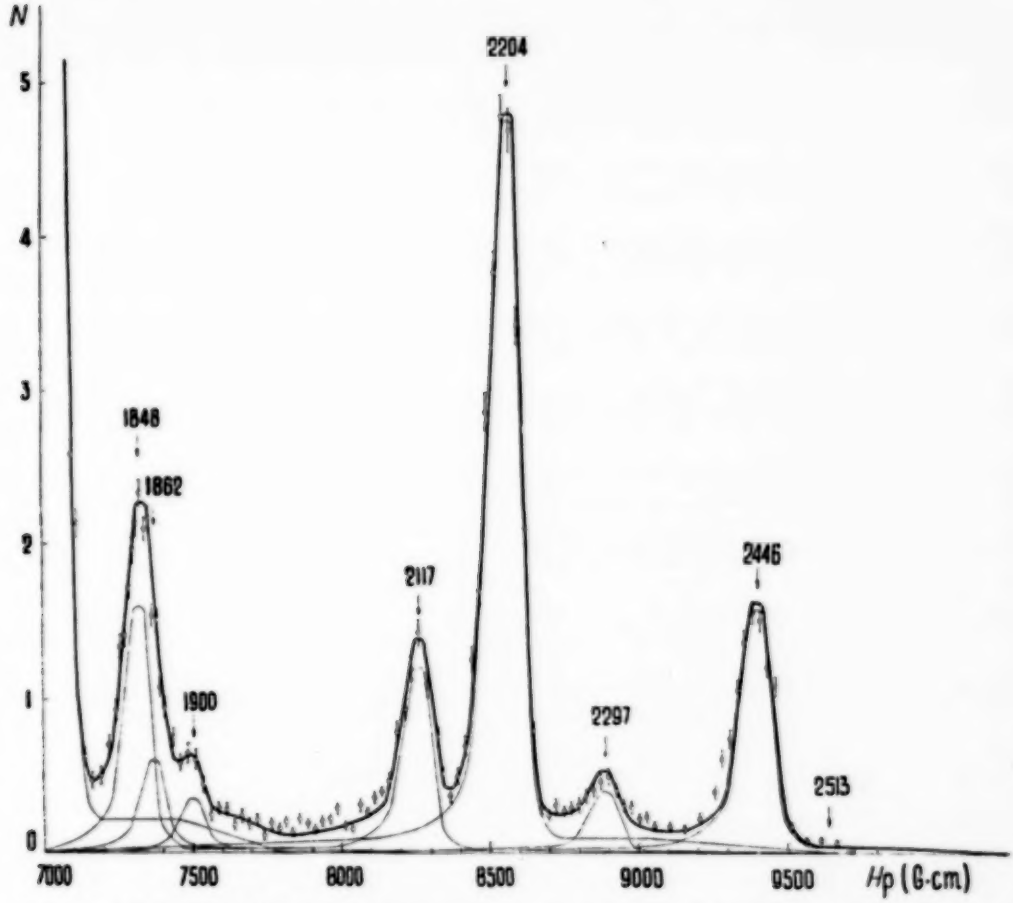


Fig. 5. Resolution of the gamma spectrum into components in the region 1780–2530 keV. $N$ is number of coincidences minus the background per/min.

To find the relative intensities we determined the area of each component, reduced to equal intervals of $H\rho$. We then corrected the values of the area for the sensitivity of the counters to electrons of different energy, for self-absorption in the source, for absorption in the walls of the apparatus and for the spectral sensitivity of the apparatus. It was assumed that the intensity of the lines is proportional to the areas thus determined.

The results are given in columns 4 and 5 of the table. Column 2 lists the energies of the lines found in ref. [5]). The lines denoted by an asterisk are among the unassigned conversion lines of ref. [5]) and have been assigned by us to K- and in some cases to L-conversion electrons of radium C. The energies of the lines denoted by two asterisks have been determined in ref. [8]).

TABLE 1

**Energies and relative intensities of gamma lines and number of quanta per disintegration in the spectrum of radium in equilibrium with its decay products**

| No. | $E_\gamma$(keV) Mladjenović and Slätis [3]) | Relative intensity | | $E_\gamma$(keV) | Number of quanta per disintegration |
|---|---|---|---|---|---|
| | | Dželepow and Shestopalova | Present paper | | |
| 1 | 2 | 3 | 4 | 5 | 6 |
| 1* | 239.6 | | | | |
| 2 | 241.9 | | 2.0 | 242 | 0.105 |
| 3 | 258.8 | | | | |
| 4* | 273.2 | | | | |
| 5* | 273.9 | | 1.0 | 285±10 | 0.052 |
| 6* | 277.6 | | | | |
| 7* | 281.5 | | | | |
| 8 | 295.2 | | 3.6 | 295 | 0.189 |
| 9* | 304.0 | | | | |
| 10* | 348.5 | | 7.18 | 352 | 0.377 |
| 11 | 352.0 | | | | |
| 12* | 386.8 | | ≈ 0.24 | ≈ 395 | ≈ 0.013 |
| 13* | 388.9 | | | | |
| 14 | — | | ≈ 0.15 | ≈ 417 | ≈ 0.008 |
| 15 | — | | ≈ 0.19 | 450±10 | ≈ 0.010 |
| 16* | 466.7 | | ≈ 0.19 | 465±10 | ≈ 0.010 |
| 17* | 471.2 | | | | |
| 18* | 484.6 | | 0.29 | 485±5 | 0.015 |
| 19 | — | | 0.24 | 509±5 | 0.013 |
| 20 | — | | 0.17 | 535±10 | 0.009 |
| 21 | 609.3 | 8.21 | 8.96 | 609 | 0.471 |
| 22* | 652.4 | 0.50 | < 0.06 | — | |
| 23* | 660.9 | | 0.43 | 666±7 | 0.023 |
| 24* | 703.2 | 0.28 | 0.15 | 703 | 0.008 |
| 25 | — | — | 0.13 | 721±7 | 0.007 |
| 26 | — | — | ≈ 0.07 | ≈ 740 (excess) | ≈ 0.004 |
| 27 | 768.7 | 1.05 | 1.01 | 769 | 0.053 |
| 28* | 787.1 | 0.25 | 0.23 | 787 | 0.012 |
| 29* | 806.3 | 0.34 | 0.29 | 806 | 0.015 |
| 30* | 821.3 | 0.15 | 0.17 | 837±8 | 0.009 |
| 31 | — | — | 0.07 | 885±10 | 0.004 |
| 32 | 934.8 | 0.74 | 0.62 | 935 | 0.033 |
| 33 | — | — | 0.09 | 960±5 | 0.005 |
| 34 | — | — | 0.10 | 1050±10 | 0.005 |
| 35 | 1120.4 | 2.95 | 3.16 | 1120 | 0.166 |
| 36 | 1155.3 | 0.45 | 0.34 | 1155 | 0.018 |
| 37* | 1207.1 | 0.33 | 0.11 | 1207 | 0.006 |
| 38 | 1238.3 | 1.14 | 1.15 | 1238 | 0.060 |
| 39 | 1281.3 | 0.33 | 0.32 | 1281 | 0.017 |
| 40 | 1378.2 | 0.89 | 0.91 | 1378 | 0.048 |

TABLE 1 (Continued)

| 1 | 2 | 3 | 4 | 5 | 6 |
|---|---|---|---|---|---|
| 41* | 1385.3 | | | | |
| 42* | 1391.1 | | | | |
| 43* | 1396.5 | 0.88 | 0.77 | 1403±7 | 0.040 |
| 44* | 1401.7 | | | | |
| 45* | 1408.0 | | | | |
| 46* | 1438.0 | | | | |
| 47 | 1509.3 | 0.54 | 0.42 | 1509 | 0.022 |
| 48 | — | — | 0.16 | 1541±5 | 0.008 |
| 49* | 1582.9 | 0.22 | 0.21 | 1583 | 0.011 |
| 50* | 1605.2 | 0.07 | 0.07 | 1605 | 0.004 |
| 51* | 1668.4 | 0.10 | 0.20 | 1668 | 0.010 |
| 52 | 1728.3 | 0.34 | 0.45 | 1728 | 0.024 |
| 53 | 1764.4 | 2.73 | 3.11 | 1764 | 0.163 |
| 54* | 1783.8 | 0.58 | — | — | — |
| 55* | 1790.7 | 0.16 | — | — | — |
| 56 | 1848.5 | 0.25 | 0.39 | 1848 | 0.020 |
| 57* | 1862.3 | 0.29 | 0.15 | 1862 | 0.008 |
| 58** | 1900 | 0.17 | 0.08 | 1900±10 | 0.004 |
| 59 | 2016.7 | 0.06 | ≈ 0.02 | 2017 (excess) | ≈ 0.001 |
| 60** | 2085 | 0.08 | ≈ 0.02 | 2090 (excess) | ≈ 0.001 |
| 61 | 2117.0 | 0.27 | 0.26 | 2117 | 0.014 |
| 62 | 2204.2 | 1 | 1 | 2204 | 0.052 |
| 63** | 2290 | 0.07 | 0.08 | 2297±10 | 0.004 |
| 64 | — | — | ≈ 0.03 | 2410 (excess) | ≈ 0.002 |
| 65** | 2450 | 0.36 | 0.30 | 2446±10 | 0.016 |

Column 3 gives the relative intensities of the lines as found in ref.[8]) with the following corrections:

1) the experimental curve for the 609.3 keV line now includes the standard line with the experimental half-width;

2) the relative intensities of lines No. 21—49 (No. 1—23 of table 1 in ref.[8])) have been corrected on the basis of new computations of the areas of the lines.

Column 6 gives the number of quanta per disintegration computed a) from the relative intensities of the $\gamma$-lines in column 4, and b) from the value of the total energy carried off by the $\gamma$-rays of one gram of radium in unit time, as determined by Zlotowski [12]) ($Q_0 = 9.1 \pm 0.15$ cal. per gram per hour. If $Q_0$ is expressed in MeV per disintegration, we obtain the value $Q = 1.81$ MeV [8])).

We take this opportunity to express our gratitude to the graduating students F. A. Predovsky (Leningrad Polytechnical Institute) and N. A. Voinova (Leningrad State University) for help with the measurements.

## References


1) Von O. Baeyer, O. Hahn and L. Meitner, Phys. Zs. **12** (1911) 1099; E. Rutherford and H. Robinson, Phil.Mag. **26** (1913) 717; C. Ellis and G. Aston, Proc. Roy. Soc. A **129** (1930) 180; K. Siegbahn, Arkiv. f. Mat. Astron. Fys. **30**A (1944) 20; S. Kageyama, J. Phys. Soc. Japan **7** (1952) 93; J. Itoh and Y. Watase, Phys. Math. Soc. Japan **20** (1938) 142; G. Latyshev, Revs. Mod. Phys. **19** (1947) 132; K. Mann and M. Ozeroff, Can. J. of Research **7** (1949) 164
2) G. Latyshev, A. Kompaneyets, N. Borisov and P. Gusak, Journ. Phys. USSR **3** (1940) 251; G. Latyshev, JETP **14** (1944) 65
3) M. Mladjenović and A. Hedgran, Arc. för Fys. **8** (1954) 49, Physica **18** (1952) 1242
4) C. Ellis, Proc. Roy. Soc. A **143** (1934) 350; Y. Cork, C. Branyan, A. Stoddard, H. Keller, J. Le Blanc and W. Childs, Phys. Rev. **83** (1951) 681
5) M. Mladjenović and H. Slätis, Arc. för Fys. **8** (1954) 65
6) D. Müller, H. Hoyt, D. Klein and J. Du Mond, Phys. Rev. **88** (1952) 775
7) K. Nielsen, O. Nielsen and M. Waggoner, Nuclear Physics **2** (1956) 476
8) B. Dželepow and S. Shestopalova, Izv. AN SSSR, ser. fyz. **21** (1957) 990; B. Dželepow and S. Shestopalova, Nuovo Cimento, **3** Suppl. **1** (1956) 54
9) B. Dželepow, N. Zhukovsky, V. Nedovesov, I. Uchevatkin and V. Chumin, Nuclear Physics **2** (1956) 408
10) B. Dželepow, N. Zhukovsky, V. Nedovesov, and G. Schukin, Izvestia AN SSSR, ser. fys. **21** (1957) 966
11) E. Rutherford, W. Lewis and B. Bonden, Proc. Roy. Soc. A **142** (1933) 347; E. Rutherford, C. Wynn-Williams, W. Lewis and B. Bonden, Proc. Roy. Soc. A **139** (1933) 617; G. Briggs, Revs. Mod. Phys. **26** (1954) 1
12) J. Zlotowski, J. Phys. Rad. **6** (1935) 242

1.C:1 E.1 :2.D *Nuclear Physics* **8** (1958) 265—283; © *North-Holland Publishing Co., Amsterdam*
Not to be reproduced by photoprint or microfilm without written permission from the publisher

# LEVEL DENSITY OF DEGENERATE FERMI SYSTEMS

TORLEIF ERICSON

NORDITA (*Nordisk Institut for Teoretisk Atomfysik*), *Copenhagen* †

Received 5 June 1958

**Abstract:** Model independent expressions for the level density of systems of non-interacting Fermions are given in a form that is suitable for treating degenerate systems. No formal distinction is made between discrete and continuous distribution of the single Fermion states. The explicit solution as well as approximate formulae in various limiting cases are given for the case when the single Fermion distribution can be analyzed in a power series or a Fourier series. As an application the effect of nuclear shell structure on the level density is estimated. Finally, the influence on the level density of an energy gap in the single Fermion spectrum is discussed. It is shown that the introduction of an energy gap can account for the observed difference in level densities of nuclei with odd and even number of nucleons.

## 1. Introduction

Systems which can be described as assemblies of independent Fermions are encountered in many branches of physics. The properties of such systems are especially simple when they are highly degenerate, i.e. when their excitation is so small that only Fermions near the Fermi level are affected and the finiteness of the system is irrelevant. The density of excited states at a certain excitation is determined only by the distribution of single Fermion states in the region around the Fermi level in which these Fermions are excited, and it is obtained as the solution of a combinatorial problem. If the distribution function is sufficiently regular and slowly varying in this interval, it can be replaced by its value at the Fermi level, leading to a very simple expression for the level density [1–3]). Some Fermi systems, however, exhibit anomalies in the distribution of single Fermion states near the Fermi level, associated e.g. with the existence of degenerate or nearly degenerate levels and energy gaps. An important case of such an anomalous system is the nucleus which can be considered as consisting of approximately independent Fermions. Though in the case of a heavy nucleus the degeneracies of the Fermion levels at the shells are expected to be removed, the distribution of the levels should still be significantly affected in certain regions. It is also possible that the nuclear system has a spectrum with an energy gap in analogy with a system of electrons in a superconductor [4–7]).

The effect of shell structure on the nuclear level density has been in-

† On leave from the Institute of Theoretical Physics, Lund, Sweden.

vestigated by an explicit counting of levels in specific nuclear models [8-11]) or by various approximations [12-13]). For light nuclei this problem has been treated in some generality by C. Bloch [14]). He takes the exact nucleon states in a central potential into account by an ingenious perturbation treatment and is able to treat remaining inter-nucleon forces of definite symmetry character. This line of approach is, however, difficult in the case of a heavy nucleus, not only owing to lack of knowledge about the forces, but also in view of the large number of levels involved. It is instead useful to consider the states as arising from 'elementary excitations' which take into account at least part of the interactions between the single particle states.

We will derive the expression for the level density in a form that is model independent and express it in such a way that it is particularly convenient for application to degenerate systems. For the evaluation of the partition function the saddle point method is used as the only approximation. We will write the expressions in such a form that there is no formal distinction between a discrete and a continuous distribution function, and so that the symmetries in the solution are clearly exhibited. Since, for the applications in this paper, we are interested essentially in ratios rather than absolute level densities, we have not taken into account the dependence of the level density on spin. This factor may be easily introduced by a technique similar to that employed below, but would be an unnecessary complication for our present purposes. The explicit solution for the level density will be given for the case of a continuous distribution function which can be analyzed in a power or a Fourier series. The former is best suited for treating slowly varying distribution functions, the latter for applications to more rapidly varying distributions of periodic character. The asymptotic expressions and approximations are given in detail for various cases, so as to facilitate estimates of shell effects, for example. Only the case of one system of identical Fermions is treated in all details, but as the nucleus consists of two such gases the trivial extension to this case is indicated.

The method which has been developed is then applied to a numerical estimate of the effect of shells in the case of a heavy nucleus. We also discuss the influence of an energy gap at the Fermi level on the level density, and it is shown that a model with such a gap, which reproduces the low energy values of the level density correctly, also correctly reproduces the difference in the level density of nuclei with odd and even number of nucleons [12, 15]).

## 2. General Derivation

Let us consider a non-degenerate system consisting of $N$ identical, non-interacting Fermions. These have one-Fermion levels $\varepsilon_i$, which are distributed according to a distribution function $g(\varepsilon)$ which can be written in terms

of $\delta$-functions as

$$g(\varepsilon) = \sum_i \delta(\varepsilon - \varepsilon_i). \tag{1.1}$$

If some of the levels are degenerate, we should think of the degeneracy as being removed by an infinitesimal amount, so that it is always possible to specify the level we are dealing with. In the ground state all levels $\varepsilon_1, \varepsilon_2, \ldots, \varepsilon_N$ are filled. Introducing the Fermi level $\varepsilon_0 = \frac{1}{2}(\varepsilon_N + \varepsilon_{N+1})$ † we can express the total number of particles $N$ and the total ground state energy $E_0$ as

$$N = \int_0^{\varepsilon_0} g(\varepsilon)\mathrm{d}\varepsilon \tag{1.2}$$

and

$$E_0 = \int_0^{\varepsilon_0} \varepsilon g(\varepsilon)\mathrm{d}\varepsilon. \tag{1.3}$$

The properties of a degenerate system of independent Fermions are completely specified by the excitation energy $U$ and by the distribution function $g(\varepsilon)$ in the region $\varepsilon_0 - U \leqq \varepsilon \leqq \varepsilon_0 + U$ (i.e. in a finite region around $\varepsilon_0$), and do not depend on the finiteness of the number of Fermions and the total ground state energy on the system. In order to obtain equations especially suited for the description of such a system we will, therefore, eliminate the explicit dependence on the non-relevant parameters $N$ and $E_0$.

The excited states are determined by the occupation numbers $n_i$ of the levels $\varepsilon_i$, where $n_i$ can take the values 0 and 1. The total energy, $E = E_0 + U$, and the total number of particles, $N$, of the system are related to the occupation numbers $n_i$ by

$$\begin{aligned} E &= \sum_i n_i \varepsilon_i \qquad \text{(a)} \\ N &= \sum_i n_i \qquad \text{(b).} \end{aligned} \tag{1.4}$$

We introduce a function $Z(\alpha, \beta)$, the 'sum over all states',

$$Z(\alpha, \beta) = \prod_i (1 + \mathrm{e}^{\alpha - \beta\varepsilon_i}) \tag{1.5}$$

with the property of counting each possible combination of $n_i$'s in eq. (1.4) exactly once. This can be written identically in terms of level densities as

$$Z(\alpha, \beta) = \sum \mathrm{e}^{\sum \alpha n_i - \beta n_i \varepsilon_i} = \sum_{N'} \int \mathrm{d}U' \, \rho(U', N') \mathrm{e}^{\alpha N' - \beta U' - \beta E'_0}, \tag{1.6}$$

where $\rho(U, N)$ is the density of states of a system of $N$ particles at excitation $U$. From eq. (1.6) the level density with the desired value of $U$ and with the correct number of particles can be determined by an inversion in terms of the Darwin-Fowler integral

† This definition of $\varepsilon_0$ is chosen in order to make $\mu$ in eq. (1.16′) go to $\varepsilon_0$ for $\beta \to \infty$, but is otherwise arbitrary, as any value between $\varepsilon_N$ and $\varepsilon_{N+1}$ would serve as well.

$$\rho(U,N)=\frac{1}{(2\pi i)^2}\iint_{-i\infty}^{i\infty} e^{f+\beta E-\alpha N}\,d\beta d\alpha, \tag{1.7}$$

where for shortness we denote $\log Z(\alpha,\beta)$ by $f$. This expression can be evaluated by the saddle point method. With denotations from thermodynamics the expression for $\rho(U,N)$ is given by

$$\rho(U,N)=\frac{1}{2\pi}\frac{e^S}{(\det A)^{\frac{1}{2}}}, \tag{1.8}$$

where $S$ is the entropy of the system,

$$S=f+\beta E-\alpha N, \tag{1.9}$$

and

$$A=\begin{pmatrix} \dfrac{\partial^2 f}{\partial\beta^2} & \dfrac{\partial^2 f}{\partial\alpha\partial\beta} \\ \dfrac{\partial^2 f}{\partial\beta\partial\alpha} & \dfrac{\partial^2 f}{\partial\alpha^2} \end{pmatrix}. \tag{1.10}$$

The saddle point is determined by

$$\frac{\partial S}{\partial\alpha}=0;\quad \frac{\partial S}{\partial\beta}=0. \tag{1.11}$$

By the introduction of the chemical potential of thermodynamics $\mu$ defined as $\mu=\alpha/\beta$, these equations transform into

$$\frac{\partial S}{\partial\mu}=0;\quad \frac{\partial S}{\partial\beta}=0. \tag{1.12}$$

The main dependence of $\rho(U,N)$ on $U$ is contained in $e^S$ and we will therefore only treat that factor here. For the expressions for det $A$ we refer to appendix 2.

We write $f$ of eq. (1.7) as

$$\begin{aligned} f=\log Z(\alpha,\beta)&=\int_0^\infty g(\varepsilon)\log(1+e^{\beta(\mu-\varepsilon)})d\varepsilon \\ &=\beta\int_0^\mu g(\varepsilon)(\mu-\varepsilon)d\varepsilon+\int_0^\infty\{g(\mu+\varepsilon)+g(\mu-\varepsilon)\}\log(1+e^{-\beta\varepsilon})d\varepsilon, \end{aligned} \tag{1.13}$$

defining $g(\varepsilon)$ to be 0 for $\varepsilon<0$. By the use of eqs. (1.2) and (1.3) we can further write $f$ in the form

$$\begin{aligned} f&=\beta\mu\int_0^{\varepsilon_0} g(\varepsilon)d\varepsilon-\beta\int_0^{\varepsilon_0}\varepsilon g(\varepsilon)d\varepsilon+\beta\int_{\varepsilon_0}^{\mu} g(\varepsilon)(\mu-\varepsilon)d\varepsilon \\ &\quad+\int_0^\infty\{g(\mu+\varepsilon)+g(\mu-\varepsilon)\}\log(1+e^{-\beta\varepsilon})d\varepsilon \\ &=\beta\mu N-\beta E_0+\beta\int_{\varepsilon_0}^{\mu} g(\varepsilon)(\mu-\varepsilon)d\varepsilon+\int_0^\infty\{g(\mu+\varepsilon)+g(\mu-\varepsilon)\}\log(1+e^{-\beta\varepsilon})d\varepsilon. \end{aligned} \tag{1.14}$$

Introducing this expression for $f$ in eq. (1.9) for the entropy, the terms

involving the quantities $N$ and $E_0$ drop out, and the entropy is given simply by

$$S = \beta U + \beta \int_{\varepsilon_0}^{\mu} g(\varepsilon)(\mu-\varepsilon)\mathrm{d}\varepsilon + \int_0^{\infty} \{g(\mu+\varepsilon)+g(\mu-\varepsilon)\} \log (1+\mathrm{e}^{-\beta\varepsilon})\mathrm{d}\varepsilon. \quad (1.15)$$

Substituting eq. (1.15) in the equations which determine the saddle point (1.12), these take the form

$$\frac{\partial S}{\partial \mu} = \beta \int_{\varepsilon_0}^{\mu} g(\varepsilon)\mathrm{d}\varepsilon + \int_0^{\infty} \{g'(\mu+\varepsilon)+g'(\mu-\varepsilon)\} \log (1+\mathrm{e}^{-\beta\varepsilon})\mathrm{d}\varepsilon \quad (1.16)$$

and

$$\frac{\partial S}{\partial \beta} = U + \int_{\varepsilon_0}^{\mu} g(\varepsilon)(\mu-\varepsilon)\mathrm{d}\varepsilon + \frac{\partial}{\partial \beta} \int_0^{\infty} \{g(\mu+\varepsilon)+g(\mu-\varepsilon)\} \log (1+\mathrm{e}^{-\beta\varepsilon})\mathrm{d}\varepsilon. \quad (1.17)$$

An alternative form of eq. (1.15), which is often very convenient, is obtained when the expression for $U$ from eq. (1.17) is introduced. Thus,

$$S = \left(1-\beta \frac{\partial}{\partial \beta}\right) \int_0^{\infty} \{g(\mu+\varepsilon)+g(\mu-\varepsilon)\} \log (1+\mathrm{e}^{-\beta\varepsilon})\mathrm{d}\varepsilon. \quad (1.15')$$

Eq. (1.16) can also be used in its partially integrated form

$$\int_{\varepsilon_0}^{\mu} g(\varepsilon)\mathrm{d}\varepsilon + \int_0^{\infty} \frac{g(\mu+\varepsilon)-g(\mu-\varepsilon)}{1+\mathrm{e}^{\beta\varepsilon}} \mathrm{d}\varepsilon = 0, \quad (1.16')$$

which is to be preferred especially when $g(\varepsilon)$ has discontinuities.
An alternative form of eq. (1.17) is

$$U = -\int_{\varepsilon_0}^{\mu} g(\varepsilon)(\mu-\varepsilon)\mathrm{d}\varepsilon + \int_0^{\infty} \frac{g(\mu+\varepsilon)+g(\mu-\varepsilon)}{1+\mathrm{e}^{\beta\varepsilon}} \varepsilon \mathrm{d}\varepsilon. \quad (1.17')$$

Eqs. (1.15)—(1.17') are still quite general. No specification has been made as to whether the distribution function is continuous or not, nor has any assumption been made about the finiteness of the system. However, these expressions have been obtained in a form which particularly stresses the importance of the form of the distribution function in the neighbourhood of the chemical potential. This potential usually does not deviate appreciably from the Fermi level, but the deviation sometimes implies a significant change in the level density formula. It is therefore obvious that this form is not very suitable for investigations of the limitations on the system due to the finiteness of the number of particles, but it is very well adapted for treating degenerate systems.

A system is completely degenerate as long as the maximum energy that can be concentrated on one particle is less than or equal to $\varepsilon_0$. The level density is clearly independent of what happens to $g(\varepsilon)$ outside the region $\varepsilon_0-U \leqq \varepsilon \leqq \varepsilon_0+U$. We are therefore at liberty to replace $g(\varepsilon)$ there by a mathematically more suitable function. The fact that at higher energy the

states formed by a concentration of the total excitation energy on one or a few of the particles are very few in comparison to all other possible configurations, gives an even greater freedom in this replacement. It is in fact sufficient to know the form of $g(\varepsilon)$ accurately in a region around $\mu$ of the order of a few times the temperature $t = \beta^{-1}$, as is easily seen from the equations above. In the case when $g(\varepsilon)$ is a continuous function, it is therefore possible to approximate $g(\varepsilon)$ by only a finite number of terms in a power or a Fourier expansion as well as desired. The Fourier expansion will be particularly suitable when $g(\varepsilon)$ has an oscillatory behaviour, as is the case for some types of shell structure. Although the equations are now independent of $N$, it is still necessary to make use of eq. (1.2) in some cases, e.g. when we want to compare level densities corresponding to systems with the Fermi level at different positions in a shell structure.

We now give the general expressions for eqs. (1.15)–(1.17) for the cases when $g(\varepsilon)$ can be expanded in a power † and a Fourier series, which will be taken to contain only a finite number of terms.

In order to exploit the fact that $g(\mu+\varepsilon)+g(\mu-\varepsilon)$ is an even function of $\varepsilon$, we make the power series expansion around $\mu$

$$g(\mu+\varepsilon) = \sum_k \frac{\varepsilon^k g^{(k)}(\mu)}{k!}. \tag{1.18}$$

A substitution of eq. (1.18) in eq. (1.15′) gives the entropy as

$$S = 2\sum_k g^{(2k)}(\mu)(2k+2)\beta^{-(2k+1)}(1-2^{-(2k+1)})\zeta(2k+2), \tag{1.19}$$

where we have introduced $\zeta(k) = \sum_{n=1}^{\infty} 1/n^k$. In terms of the temperature $t = \beta^{-1}$ and the Bernoulli numbers

$$B_k = \frac{(2k)!}{2^{2k-1}}\pi^{-2k}\zeta(2k)$$

this can be expressed as

$$S = 2\pi\sum_k \frac{g^{(2k)}(\mu)}{(2k+1)!}(2^{2k+1}-1)B_{k+1}(\pi t)^{2k+1}. \tag{1.20}$$

In the same way we get from eqs. (1.16) and (1.17)

$$-\sum_k g^{(k)}(\mu)\frac{(\varepsilon_0-\mu)^{k+1}}{(k+1)!} + 2\sum_k \frac{g^{(2k+1)}(\mu)}{(2k+2)!}(2^{2k+1}-1)B_{k+1}(\pi t)^{2k+2} = 0 \tag{1.21}$$

and

$$U = -\sum_k \frac{g^{(k)}(\mu)}{k!(k+2)}(\varepsilon_0-\mu)^{k+2} + 2\sum_k \frac{g^{(2k)}(\mu)}{(2k)!(2k+2)}(2^{2k+1}-1)B_{k+1}(\pi t)^{2k+2}. \tag{1.22}$$

† This is similar to the well-known Sommerfeld expansion [16]). It is given here for convenience and in a form suited for problems of this kind.

In particular, if the derivatives of $g(\varepsilon)$ at the Fermi level are rapidly decreasing with their order,

$$\mu - \varepsilon_0 \approx -\frac{g'(\varepsilon_0)}{g(\varepsilon_0)} \frac{\pi^2}{6} t^2, \tag{1.23}$$

and it is easily seen that the first surviving terms arising from $\mu - \varepsilon_0$ in eqs. (1.20) and (1.22) are of the order $g'(\varepsilon_0)^2$.

The preceding expansion is not very suitable for treating the problem when $g(\varepsilon)$ has an approximately periodic behaviour. In this case it is convenient to divide $g(\varepsilon)$ into two parts, the first consisting of a slowly varying function which can be treated by the preceding method, and the second containing the variations around this average function. This splitting is arbitrary, but should be made so as to get simple expressions for both parts. The natural way to treat the second part is to expand it in a Fourier series. We will for simplicity assume the first part to be a constant, but it is easy to generalize by exploiting the result of eqs. (1.20)–(1.22). We therefore express $g(\varepsilon)$ as

$$g(\varepsilon) = g_0 + \sum_k \{g_k \cos ak\varepsilon + h_k \sin ak\varepsilon\}, \tag{1.24}$$

where $2\pi a^{-1}$ is the periodicity length.

By substitution in eq. (1.15′), the entropy is found to be

$$S = \left(1 - \beta \frac{\partial}{\partial \beta}\right) \left[ 2g_0 \int_0^\infty \log (1 + e^{-\beta\varepsilon}) d\varepsilon + 2 \sum_k \{g_k \cos ak\mu + h_k \sin ak\mu\} \int_0^\infty \cos \varepsilon ak \log (1 + e^{-\beta\varepsilon}) d\varepsilon \right]. \tag{1.25}$$

The integrals of eq. (1.25) and those which appear in the following can all be expressed in terms of elementary functions. They are different combinations of

$$\Psi(\alpha) = \int_0^\infty \cos \alpha x \log (1 + e^{-x}) dx = \frac{\pi^2}{2} \left\{ \frac{1}{(\pi\alpha)^2} - \frac{1}{\pi\alpha \sinh \pi\alpha} \right\} \tag{1.26}$$

and its derivatives. $\Psi(\alpha)$ is derived in detail in appendix 1, where the functions introduced in the following are also given explicitly. The entropy can then be written in terms of $\Psi(\alpha)$ and $F(\alpha) = \Psi(\alpha) + \frac{1}{2}\alpha\Psi'(\alpha)$ † as

$$S = 4g_0 \Psi(0) t + 4t \sum_k \{g_k \cos ak\mu + h_k \sin ak\mu\} F(akt). \tag{1.27}$$

By the introduction of (see eq. (A4))

$$G(\alpha) = \Psi(\alpha) + \alpha\Psi'(\alpha) \tag{1.28}$$

the energy $U$ of eq. (1.17) may be written as

† See eq. (A3).

$$U = 2g_0\Psi(0)t^2+2t^2\sum_k\{g_k\cos ak\mu+h_k\sin ak\mu\}G(akt)$$

$$-\frac{g_0}{2}(\mu-\varepsilon_0)^2+(\mu-\varepsilon_0)\sum_k\frac{1}{ak}\{g_k\sin ak\varepsilon_0-h_k\cos ak\varepsilon_0\} \quad (1.29)$$

$$+\sum_k\frac{1}{(ak)^2}\{g_k(\cos ak\mu-\cos ak\varepsilon_0)+h_k(\sin ak\mu-\sin ak\varepsilon_0)\}.$$

The chemical potential $\mu$ in the preceding equations is obtained in the same way from eq. (1.16) as

$$g_0(\mu-\varepsilon_0)+\sum_k\frac{1}{ak}(g_k\sin ak\mu-h_k\cos ak\mu)H(akt)$$

$$-\sum_k\frac{1}{ak}\{g_k\sin ak\varepsilon_0-h_k\cos ak\varepsilon_0\}=0 \quad (1.30)$$

with

$$H(\alpha)=1-2\alpha^2\Psi(\alpha) \qquad \text{(see eq. (A5))}.$$

We have thus achieved an explicit solution of the problem for the case of a Fourier expansion. Though the expressions above are fairly complicated in the general case, they simplify considerably in special cases. Thus, when the product $at \gg 1$, i.e. when the mean excitation energy of the particles extends over the periodicity length, we obtain

$$S \approx 4g_0\Psi(0)t, \quad (1.31)$$

$$g(\mu-\varepsilon_0)\approx\sum_k\frac{1}{ak}\{g_k\sin ak\varepsilon_0-h_k\cos ak\varepsilon_0\} \quad (1.32)$$

and

$$U\approx 2g_0\Psi(0)t^2+\frac{g_0(\mu-\varepsilon_0)^2}{2}-\sum_k\frac{1}{(ak)^2}\{g_k\cos ak\varepsilon_0+h_k\sin ak\varepsilon_0\}. \quad (1.33)$$

In this limit the chemical potential takes a constant value. The density of states is the same as for a system with a distribution function equal to the mean of $g(\varepsilon)$, but taken at an excitation energy which is shifted by an amount $\Delta U$, where

$$\Delta U=-\frac{g_0(\mu-\varepsilon_0)^2}{2}+\sum_k\frac{1}{(ak)^2}\{g_k\cos ak\varepsilon_0+h_k\sin ak\varepsilon_0\}. \quad (1.34)$$

If the part of eq. (1.24) which is expanded in a Fourier series is small in comparison with the average value of $g(\varepsilon)$, quadratic and higher powers in the Fourier coefficients can be neglected to a first approximation in eqs. (1.27), (1.29), and (1.30). From eq. (1.30) we find that $\mu-\varepsilon_0$ is small, so that $\mu$ can be replaced by $\varepsilon_0$ in all terms multiplied by the Fourier coefficients. The expressions for $S$ and $U$ then simplify into

$$S = 4g_0\Psi(0)t+4t\sum_k \{g_k \cos ak\varepsilon_0+h_k \sin ak\varepsilon_0\}F(akt) \tag{1.35}$$

and

$$U = 2g_0\Psi(0)t^2+2t^2\sum_k \{g_k \cos ak\varepsilon_0+h_k \sin ak\varepsilon_0\}G(akt). \tag{1.36}$$

From eqs. (1.35) and (1.36) we can obtain a first order estimate of the change in the level density as a function of $\varepsilon_0$. This can be expressed as the change in the entropy, $\Delta S$, from its value for the constant distribution function $g(\varepsilon) = g_0$ for the same excitation energy $U$:

$$\Delta S \approx 2t_0\sum_k \{g_k \cos ak\varepsilon_0+h_k \sin ak\varepsilon_0\}\Psi(akt_0), \tag{1.37}$$

where $t_0$ is the temperature for the constant distribution at the same $U$, i.e.

$$U = 2g_0\Psi(0)t_0^2. \tag{1.38}$$

In this order the result is not influenced by the denominator (eqs. (1.8) and (1.10)). Eqs. (1.37) and (1.38) provide a useful form on which to base a first order estimate of the effect on the level density, when $g(\varepsilon)$ deviates from a constant.

For completeness we also indicate the trivial extension to two systems of independent Fermions, which is important for an application to nuclei. There are two different distribution functions, $g_1(\varepsilon)$ and $g_2(\varepsilon)$. Proceeding again by the saddle point method we obtain an expression for the level density which is very similar to that for one system (eq. (1.8)):

$$\rho(U) = \frac{e^S}{(2\pi)^{\frac{3}{2}}(\det A)^{\frac{1}{2}}}. \tag{1.39}$$

Here $S$ and $U$ are simply the sums of the corresponding quantities for each system separately:

$$\begin{aligned} S &= S_1(\beta)+S_2(\beta) \\ U &= U_1(\beta)+U_2(\beta). \end{aligned} \tag{1.40}$$

Similarly there are two equations of the type (1.16) (or (1.16')) determining $\mu_1$ and $\mu_2$ separately as functions of $\beta$. The expression for det $A$ will now contain derivatives with respect to all three variables, $\beta$, $\alpha_1$, and $\alpha_2$. The function $f$ of eq. (1.13) will be replaced by a sum $f_1+f_2$ in analogy with $S$ and $U$ above.

$$\det A = \begin{vmatrix} \dfrac{\partial^2(f_1+f_2)}{\partial\beta^2} & \dfrac{\partial^2 f_1}{\partial\beta\partial\alpha_1} & \dfrac{\partial^2 f_2}{\partial\beta\partial\alpha_2} \\ \dfrac{\partial^2 f_1}{\partial\alpha_1\partial\beta} & \dfrac{\partial^2 f_1}{\partial\alpha_1^2} & 0 \\ \dfrac{\partial^2 f_2}{\partial\alpha_2\partial\beta} & 0 & \dfrac{\partial^2 f_2}{\partial\alpha_2^2} \end{vmatrix}. \tag{1.41}$$

In appendix 2 this determinant is given in a more convenient form in terms of the chemical potentials $\mu_1$ and $\mu_2$.

## 3. Applications

We illustrate the general method developed in the preceding section by an application to a numerical estimate of the influence of shell structure on the level density of a heavy nucleus and by a discussion of the effect of an energy gap in the Fermion spectrum on the level density, particularly on the difference in level density between odd and even systems at the same excitation energy.

To investigate the influence of the shell structure we will assume the nucleons to move independently in a potential well. To a first approximation the single particle level density is the same for both neutrons and protons as a function of the Fermi level, and it can be described by only two terms in the Fourier expansion (eq. (1.24)):

$$g(\varepsilon) = g_0 + g_1 \cos a\varepsilon. \tag{2.1}$$

The constant, $a$, is determined by the distance between major shells, $\hbar\omega$, to be

$$a = 2\pi/\hbar\omega. \tag{2.2}$$

For simplicity we will assume in the following that the neutron and proton Fermi levels have the same relative position with respect to the nearest closed shell. This restriction can easily be removed. As two kinds of particles are involved, the additivity rules of eq. (1.40) have been applied. The change in the slowly varying factor, det $A$ of eq. (1.8), can be shown to be small and will be neglected. The influence of shell structure is experimentally most conveniently studied by comparing measured level densities for different nuclei referred to the same excitation energy. We will therefore use the theoretical level density for $g(\varepsilon) = g_0$ as a reference and study the ratio of the level densities determined from eq. (2.1) to this value for the same excitation energy as a function of the excitation. The logarithm of this ratio is the difference between the entropies. The variation of the temperature and the entropy differences for different positions in the shell are presented in figs. 1 and 2 for $g_1 = \frac{1}{2}g_0$. It should be particularly noticed that the entropy difference is very slowly disappearing with increasing energy.

In order to get a numerical estimate of the effect without attempting any detailed fit to the actual data, we have used

$$\hbar\omega = 9 \text{ MeV}, \qquad g_0 = 10 \text{ MeV}^{-1}, \qquad g_1 = 5 \text{ MeV}^{-1}$$

and taken $U = 6$ MeV, which is about the average neutron binding energy for a heavy nucleus. With these values we find that the ratio of level densities in nuclei with approximately closed neutron and proton shells ($a\varepsilon_0 = (2n+1)\pi$) and those with half-filled shells ($a\varepsilon_0 = 2n\pi$) is about $10^3$.

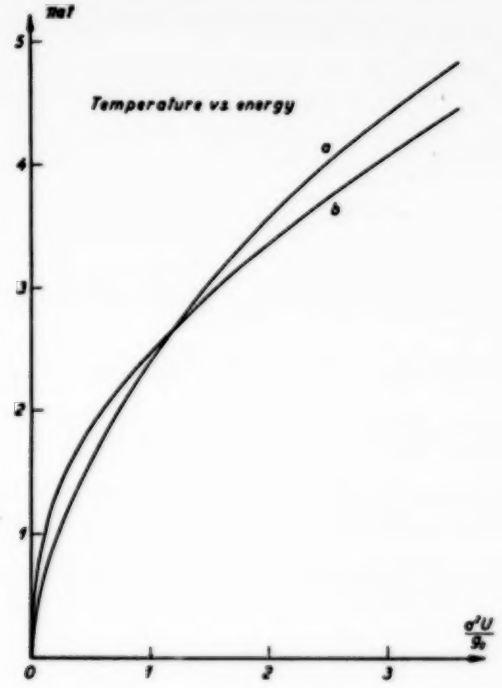


Fig. 1. Nuclear temperature vs. energy for distribution function (2.1) with $g_1 = \frac{1}{2}g_0$. The curves are for (a) doubly magic nucleus, (b) half-filled shell nucleus.

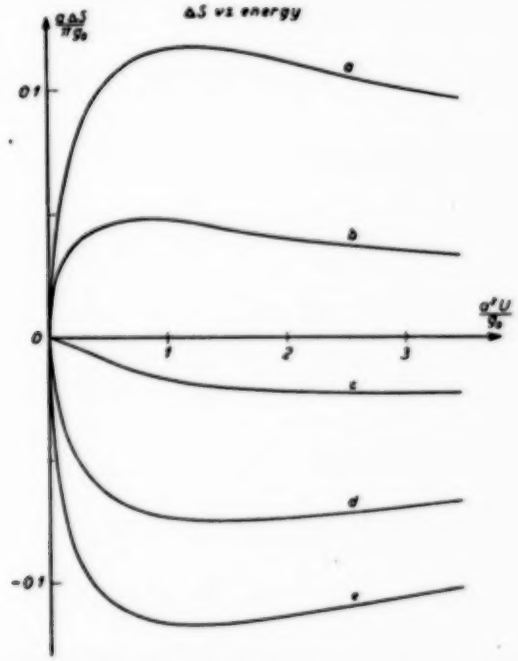


Fig. 2. Deviation of entropy for the distribution function (2.1) with $g_1 = \frac{1}{2}g_0$ from the entropy for $g(\varepsilon) = g_0$ vs. energy for differently filled shells. $\Delta S$ is essentially the logarithm of the ratio between the corresponding level densities. Neutrons and protons have the same relative position with respect to major shells. The curves are for
(a) $a\varepsilon_0 = 2n\pi$, (b) $a\varepsilon_0 = 2n\pi \pm \frac{1}{3}\pi$, (c) $a\varepsilon_0 = 2n\pi \pm \frac{1}{2}\pi$, (d) $a\varepsilon_0 = 2n\pi \pm \frac{2}{3}\pi$, (e) $a\varepsilon_0 = (2n+1)\pi$.

This ratio should be compared to the experimentally determined one obtained from the measurement of slow neutron resonances, which give level densities for the compound nucleus just above neutron binding energy. The level densities determined in this way depend, however, on spin, but this spin dependence can be eliminated by assuming it to follow a $(2I+1)$-law, which is known to be approximately valid for small spin values. An expression for the level density taking spin into account will also contain a factor associated with the moment of inertia of the excited nucleus. An estimate shows, however, that at 6 MeV excitation this will give rise to changes in the level density which are small in comparison to $10^3$. Odd-even effects and differences due to different neutron binding energies can be roughly eliminated by comparing nuclei of the same type and with approximately the same binding energy, whenever possible. For this comparison the compilation of Newton [12]) has been used. In the region around lead we find the experimentally measured ratio between nuclei with nearly closed and those with half-filled shells to be a few times $10^3$, in qualitative agreement with the rough estimate given above.

Though a number of nuclear properties can be described from a model with the nucleons moving independently in an average potential, the remaining interparticle correlations cause important deviations from the independent particle picture. This is particularly manifested in the excitation spectra of even nuclei. Thus, for a heavy, even nucleus the first excited 'intrinsic' state is at about 1 MeV excitation, which is considerably higher than the average independent particle spacing. In the case of spheroidal nuclei [17,18]) the particle levels remain doubly degenerate and the effect of the residual interactions is, to first order, to introduce a pairing effect between nucleons in the same orbits. It is then expected that states of excited pairs appear with an average spacing twice the independent particle spacing, which still is definitely lower than the actual energy of the first intrinsic state. It has therefore been pointed out [7]) that the nuclear excitation spectrum has the characteristics associated with the existence of an energy gap at the Fermi level. The fact that excited pairs are not found in the configurations for the first intrinsic states of odd mass nuclei supports this interpretation. Such a gap is found for a system of interacting electrons in a super-conducting metal [4–6]), and it should therefore not be surprising if the nuclear spectrum exhibits a similar anomaly †.

The energy gap is actually a generalization of the concept of a pairing energy. This is clearly seen if the pairing energy is taken to be the same for all pairs in a model with doubly degenerate levels [15]). In this case the pairing energy is equivalent to the introduction of an energy gap for the unpaired

† For a more complete discussion of the evidence for an energy gap in the nuclear spectrum, see ref.[7]).

excited particles, while the pairs remain unaffected. The effect of the energy gap is therefore to suppress the excitation of pairs at low energy.

The correlations between the particles beyond the average potential should be introduced in the calculations of nuclear level densities. They will be particularly important for the calculation of absolute level densities, but they will also affect the nuclear temperature and produce the observed odd-even effect. The description of the nuclear excitation spectrum in terms of an energy gap offers the possibility to introduce a major part of these correlations in a relatively simple way and has the further advantage that the calculations can be based on a model which reproduces the level density at low excitation correctly in contradistinction to the ordinary independent particle treatment.

To draw more definite conclusions about the effect of the energy gap at higher excitation, we have to make more specific assumptions about the nature of the spectrum, though it is not necessary to know its detailed structure. For simplicity we will treat the case of a spheroidal nucleus where the independent particle levels are doubly degenerate. The results of the theory of superconductivity [4–6]) indicate that the effect of the interactions is to produce an energy gap by repelling these levels symmetrically around the Fermi level of the even system without changing their relative order †. As the gap deforms the independent particle spectrum essentially it must be large in comparison with the average spacing of the independent particle levels. The influence of this change of the particle spectrum should, however, be small for levels far from the Fermi level. We can immediately draw a conclusion about the variation of the nuclear temperature with excitation for the even system. On account of the symmetry around the Fermi level $\varepsilon_0$ the chemical potential $\mu$ is constant and equal to $\varepsilon_0$. Eq. (1.17′) can then be written

$$U = \tfrac{1}{6}\pi^2 \bar{g}(t)t^2, \tag{2.3}$$

where $\bar{g}(t)$ is an average of $g(\varepsilon)$ in a region of the order of $t$ around $\varepsilon_0$. For low temperatures this average will be small owing to the lack of states within the gap. Therefore, if the temperature is compared to that of the non-interacting system at same $U$, the smallness of $\bar{g}(t)$ leads to a considerable compensating increase of $t$. With increasing $U$, $\bar{g}(t)$ increases, especially when the temperature reaches the order of the gap. The temperature will therefore vary more slowly with energy than in the case of independent particles, but will eventually reach the same value at high energies.

When an odd nucleon is added to the even system, a number of intrinsic states are found experimentally at low energy. The simplest way to picture

† The assumption of symmetry is equivalent to the neglect of shell effects. These can be included in the discussion, but if the shell structure is not strong in comparison to the gap the conclusions to be drawn remain essentially the same.

the odd system is, therefore, to add the odd nucleon to the even system with the Pauli principle taken into account. The odd nucleon is then already above the gap in the ground state. (The validity of this model will be discussed later.) This leads to an important difference in the level density of odd and even systems, which is conveniently expressed in terms of the chemical potential. Denoting the deviation of the chemical potential from the even Fermi level $\varepsilon'_0$ by $x$, eq. (1.16′) can be written in the form

$$(e^{\beta x}-e^{-\beta x})\int_0^\infty \frac{g(\varepsilon'_0+\varepsilon)d\varepsilon}{(1+e^{\beta(\varepsilon+x)})(1+e^{\beta(\varepsilon-x)})}=1, \tag{2.4}$$

where we have already exploited the fact that $x$ is smaller than the gap. For $\beta x$ small, we obtain

$$x = 1/\bar{g}_1(t), \tag{2.5}$$

where $\bar{g}_1(t)$ is again an average of $g(\varepsilon)$ in a region of the order of $t$ around the even Fermi level. The chemical potential will therefore move from the odd Fermi level towards the even Fermi level with increasing excitation. In practice $\beta x$ turns out to be small for rather low values of $U$. From eqs. (1.15′) and (1.17′) we can then immediately deduce the relation between the level density for the odd system, $\rho'_0(U)$, and the one for the even system, $\rho_e(U)$. Thus

$$\rho'_0(U) = \rho_e(U+\delta), \tag{2.6}$$

where $\delta$ is half the energy gap, and the relation is correct to order $\beta x$. This agrees closely with earlier results expressed in terms of pairing energies [12,15]. The same result is obtained for an odd system formed by making a hole in an even system.

The description of an odd system in terms of one particle added to an even system which remains unchanged is not entirely satisfactory. From this model the low energy excitations of the odd system are expected to be one-particle excitations, while it is found experimentally that one-particle and one-hole states occur with about equal frequency. This is not very surprising from the point of view of a gap model. The gap appears at the Fermi level of the even system. The odd nucleon can therefore equally well be regarded as a particle added to a system with a certain even number of nucleons and as one particle missing from a system with the same number of particles increased by two. As is easily realized in the limit when the energy gap goes to zero, the same configuration appears twice, once for each case. Half of the states are therefore spurious and must be eliminated. It might be argued that there is an equal probability for both situations and that it would therefore suffice to add the densities of the two configurations, each with a statistical weight of one half, leading again to eq. (2.6).

However, this would mean that at low energy in odd $A$ nuclei only one

half of the intrinsic one-particle or one-hole states would appear, while the analysis of the spectra of deformed nuclei [19]) indicates that all of these are populated. It is therefore tempting to use the configuration corresponding to the lowest energy. In this case we find after some calculations

$$\rho_o(U) = \frac{2e^{2\beta\delta}}{(1+e^{\beta\delta})^2}\{\rho'_o(U)+\rho_e(U)\}, \tag{2.7}$$

where a dash on $\rho_o(U)$ indicates that it is the level density for one nucleon above the gap in the ground state as in eq. (2.6). This model has the desired limit $2\rho'_o(U)$ at very low excitations. For very high excitations, when $\beta\delta$ is small, it goes over into $\rho_e(U+2\delta)$. For excitation energies of the order of neutron binding energies, the temperature is usually slightly above the expected value of $\delta$ (= half the pairing energy), and hence, the odd-even difference will be about 25 % larger than if this effect were only due to a displacement of the excitation energy according to eq. (2.6). Both expressions for this difference are within the uncertainty of the experimentally observed factor. In a similar way as above the effect for an odd-odd system can be found as

$$\rho'_{oo}(U) = \rho_e(U+2\delta) \tag{2.6'}$$

and

$$\rho_{oo}(U) = 4\left(\frac{e^{\beta\delta}}{1+e^{\beta\delta}}\right)^4\{\rho'_{oo}(U)+2\rho'_o(U)+\rho_e(U)\}, \tag{2.7'}$$

where $\rho'_{oo}(U)$ and $\rho_{oo}(U)$ are the respective analogues of $\rho'_o(U)$ and $\rho_o(U)$. At higher excitations eqs. (2.6') and (2.7') imply that the odd-even factor of eqs. (2.6) and (2.7) is squared.

It is thus possible to use for the calculation of nuclear level densities an energy gap model which reproduces the average level density correctly for low excitations, goes over into the expected independent particle limit at high excitations, and predicts an odd-even difference of the correct order of magnitude for excitations of the order of the neutron binding energies.

It is a great pleasure to thank Dr. B. R. Mottelson and Professor A. Bohr for many stimulating discussions and valuable suggestions, as well as Professor T. Gustafson for his kind interest and encouragement. Further thanks are due to many members of NORDITA, Copenhagen, and of the Institutes for Theoretical Physics in Copenhagen and Lund for discussions during the course of the work.

## Appendix 1

In this appendix we derive $\Psi(\alpha)$ in terms of elementary functions and give explicit expressions for a number of often occurring combinations of $\Psi(\alpha)$ with its derivatives.

We define $\Psi(\alpha)$ as (1.26),

$$\Psi(\alpha) = \int_0^\infty \cos \alpha x \log (1+e^{-x})dx = \mathrm{Re}\int_0^\infty e^{i\alpha x} \log (1+e^{-x})dx$$
$$= \mathrm{Re}\sum_{n=1}^{\infty} \frac{(-)^{n+1}}{n}\int_0^\infty e^{(i\alpha-n)x}dx = \sum_{n=1}^{\infty} \frac{(-)^{n+1}}{n^2+\alpha^2} = \frac{\pi^2}{2}\left\{\frac{1}{(\pi\alpha)^2} - \frac{1}{\pi\alpha}\cdot\frac{1}{\sinh \pi\alpha}\right\}. \tag{A1}$$

Thus

$$\Psi(\alpha) = \frac{\pi^2}{2}\left\{\frac{1}{(\pi\alpha)^2} - \frac{1}{\pi\alpha \sinh \pi\alpha}\right\} = \frac{\pi^2}{12} + O(\alpha^2) \tag{A2}$$

$$F(\alpha) = \Psi(\alpha) + \frac{\alpha}{2}\Psi'(\alpha) = \frac{\pi^2}{4}\left\{-\frac{1}{\pi\alpha} + \coth \pi\alpha\right\} \tag{A3}$$

$$G(\alpha) = \Psi(\alpha) + \alpha\Psi'(\alpha) = \frac{\pi^2}{2}\left\{-\frac{1}{(\pi\alpha)^2} + \frac{\coth \pi\alpha}{\sinh \pi\alpha}\right\} \tag{A4}$$

$$H(\alpha) = 1 - 2\alpha^2\Psi(\alpha) = \frac{\pi\alpha}{\sinh \pi\alpha} \tag{A5}$$

$$I(\alpha) = \frac{1}{2\alpha}\frac{d}{d\alpha}\{\alpha^2 G(\alpha)\} = -2\pi\alpha \coth \pi\alpha F(\alpha) + \frac{\pi^2}{4}H(\alpha). \tag{A6}$$

## Appendix 2

As the main part of the variation of the level density with energy and with irregularities in the distribution function is due to the change in the entropy $S$ which enters exponentially, the discussion of det $A$ of eqs. (1.10) and (1.41) has been postponed to this point. We will essentially limit ourselves to an elimination of the explicit dependence on $N$ and $E_0$ and to the transformation from derivatives in $\alpha$ to a convenient form in terms of derivatives in $\mu$.

By the substitution $\mu = \alpha/\beta$ in eq. (1.10) we get the transformation

$$\det A = \begin{vmatrix} \frac{\partial^2 f}{\partial\beta^2} & \frac{\partial^2 f}{\partial\beta\partial\alpha} \\ \frac{\partial^2 f}{\partial\alpha\partial\beta} & \frac{\partial^2 f}{\partial\alpha^2} \end{vmatrix} = \frac{1}{\beta^2}\begin{vmatrix} \frac{\partial^2 f}{\partial\beta^2} & \left(\frac{\partial}{\partial\beta} - \frac{1}{\beta}\right)\frac{\partial f}{\partial\mu} \\ \left(\frac{\partial}{\partial\beta} - \frac{1}{\beta}\right)\frac{\partial f}{\partial\mu} & \frac{\partial^2 f}{\partial\mu^2} \end{vmatrix}. \tag{A7}$$

Introducing for shortness the notation

$$B(\mu, \beta) = \int_0^\infty \{g(\mu+\varepsilon)+g(\mu-\varepsilon)\} \log (1+e^{-\beta\varepsilon})d\varepsilon, \tag{A8}$$

we obtain, using the expression for $f$ of eq. (1.13),

$$\det A = \beta^{-2}\begin{vmatrix} \dfrac{\partial^2 B}{\partial\beta^2} & \left(\dfrac{\partial}{\partial\beta}-\dfrac{1}{\beta}\right)\dfrac{\partial B}{\partial\mu} \\ \left(\dfrac{\partial}{\partial\beta}-\dfrac{1}{\beta}\right)\dfrac{\partial B}{\partial\mu} & \dfrac{\partial^2 B}{\partial\mu^2}+\beta g(\mu) \end{vmatrix}, \tag{A9}$$

which is independent of $N$ and $E_0$. This expression is convenient for further calculations, when $g(\varepsilon)$ is a continuous function of $\varepsilon$, as $B(\mu, \beta)$ can also be used for the derivation of $S$, $\mu$ and $U$. When $g(\varepsilon)$ consists e.g. of a sum of $\delta$-functions we transform it by partial integrations into the form

$$\det A = \begin{vmatrix} \displaystyle\int_0^\infty \frac{\{g(\mu+\varepsilon)+g(\mu-\varepsilon)\}e^{\beta\varepsilon}}{(1+e^{\beta\varepsilon})^2}\varepsilon^2 d\varepsilon & -\displaystyle\int_0^\infty \frac{\{g(\mu+\varepsilon)-g(\mu-\varepsilon)\}e^{\beta\varepsilon}}{(1+e^{\beta\varepsilon})^2}\varepsilon d\varepsilon \\ -\displaystyle\int_0^\infty \frac{\{g(\mu+\varepsilon)-g(\mu-\varepsilon)\}e^{\beta\varepsilon}}{(1+e^{\beta\varepsilon})^2}\varepsilon d\varepsilon & \displaystyle\int_0^\infty \frac{\{g(\mu+\varepsilon)+g(\mu-\varepsilon)\}e^{\beta\varepsilon}}{(1+e^{\beta\varepsilon})^2} d\varepsilon \end{vmatrix}. \tag{A10}$$

It should be noted that the off diagonal elements are proportional to the average asymmetry of the distribution in a region around $\mu$ of the order of the temperature. These terms can therefore often be neglected in comparison to the diagonal elements, especially as they always appear squared.

For the case of a distribution function expanded in a Fourier series (eq. (1.24))

$$g(\varepsilon) = g_0 + \sum_k (g_k \cos ak\varepsilon + h_k \sin ak\varepsilon) \tag{A11}$$

the determinant is given by the expression

$$\begin{aligned} \det A = {} & 4t^4[\{g_0 + \sum_k (g_k \cos ak\mu + h_k \sin ak\mu)H(akt)\} \\ & \times \{g_0\Psi(0) + \sum_k (g_k \cos ak\mu + h_k \sin ak\mu)I(akt)\} \\ & -4\{\sum_k (-g_k \sin ak\mu + h_k \cos ak\mu)aktG(akt)\}^2], \end{aligned} \tag{A12}$$

where †

$$I(\alpha) = \frac{1}{2\alpha}\frac{d}{d\alpha}\{\alpha^2 F(\alpha)\}. \tag{A13}$$

For the product $at \gg 1$ (cf. eqs. (1.31)–(1.33)) $\det A$ reduces to

$$\det A \approx 4t^4 g_0 \Psi(0). \tag{A14}$$

In the case of two systems $\det A$ is instead given by eq. (1.41):

$$\det A = \begin{vmatrix} \dfrac{\partial^2(f_1+f_2)}{\partial\beta^2} & \dfrac{\partial^2 f_1}{\partial\beta\partial\alpha_1} & \dfrac{\partial^2 f_2}{\partial\beta\partial\alpha_2} \\ \dfrac{\partial^2 f_1}{\partial\alpha_1\partial\beta} & \dfrac{\partial^2 f_1}{\partial\alpha_1^2} & 0 \\ \dfrac{\partial^2 f_2}{\partial\alpha_2\partial\beta} & 0 & \dfrac{\partial^2 f_2}{\partial\alpha_2^2} \end{vmatrix}. \tag{A15}$$

† See eq. (A6).

Similarly as for one system we obtain, with

$$\mu_i = \frac{\alpha_i}{\beta} \text{ and } B_i = \int_0^\infty \{g_i(\mu_i+\varepsilon)+g_i(\mu_i-\varepsilon)\} \log\,(1+\mathrm{e}^{-\beta\varepsilon})\mathrm{d}\varepsilon,$$

$$\det A = \begin{vmatrix} \dfrac{\partial^2(B_1+B_2)}{\partial\beta^2} & \left(\dfrac{\partial}{\partial\beta}-\dfrac{1}{\beta}\right)\dfrac{\partial B_1}{\partial\mu_1} & \left(\dfrac{\partial}{\partial\beta}-\dfrac{1}{\beta}\right)\dfrac{\partial B_2}{\partial\mu_2} \\ \left(\dfrac{\partial}{\partial\beta}-\dfrac{1}{\beta}\right)\dfrac{\partial B_1}{\partial\mu_1} & \dfrac{\partial^2 B_1}{\partial\mu_1{}^2}+\beta g_1(\mu_1) & 0 \\ \left(\dfrac{\partial}{\partial\beta}-\dfrac{1}{\beta}\right)\dfrac{\partial B_2}{\partial\mu_2} & 0 & \dfrac{\partial^2 B_2}{\partial\mu_2{}^2}+\beta g_2(\mu_2) \end{vmatrix}, \quad \text{(A16)}$$

which, analogously with eq. (A10), can be alternatively written as eq. (A17) on p. 283 where the off diagonal elements are still small in comparison to the diagonal ones.

## References


1) H. Bethe, Revs. Mod. Phys. **9** (1937) 69
2) C. v. Lier and G. E. Uhlenbeck, Physica **4** (1937) 531
3) J. M. Lang and K. J. LeCouteur, Proc. Phys. Soc. A **67** (1954) 585
4) J. Bardeen, L. N. Cooper and J. R. Schrieffer, Phys. Rev. **108** (1957) 1175
5) N. N. Bogolyubov, JETP **34** (1958) 58
6) J. G. Valatin, N. C. **7** (1958) 843
7) A. Bohr, B. R. Mottelson and D. Pines, Phys. Rev. **110** (1958) 936
8) J. Bardeen and E. Feenberg, Phys. Rev. **54** (1938) 809
9) H. Margenau, Phys. Rev. **59** (1941) 627
10) C. Critchfield and S. Oleksa, Phys. Rev. **82** (1951) 243
11) N. Rosenzweig, Phys. Rev. **108** (1957) 817
12) T. D. Newton, Can. J. Phys. **34** (1956) 804
13) A. A. Ross, Phys. Rev. **108** (1957) 720
14) C. Bloch, Phys. Rev. **93** (1954) 1094
15) T. Ericson, Nuclear Physics **6** (1958) 62
16) A. Sommerfeld, Z. Phys. **67** (1928) 1
17) A. Bohr, Mat. Fys. Medd. Dan. Vid. Selsk. **26** (1952) no. 14
18) A. Bohr and B. R. Mottelson, Mat. Fys. Medd. Dan. Vid. Selsk. **27** (1953) no. 16
19) B. R. Mottelson and S. G. Nilsson, Mat. Fys. Medd. Dan. Vid. Selsk. (in the press)

$$\det A = \begin{vmatrix} \sum_{i=1,2} \int_0^\infty \frac{\{g_i(\mu_i+\varepsilon)+g_i(\mu_i-\varepsilon)\}e^{\beta\varepsilon}}{(1+e^{\beta\varepsilon})^2}\varepsilon^2 d\varepsilon & -\int_0^\infty \frac{\{g_1(\mu_1+\varepsilon)-g_1(\mu_1-\varepsilon)\}e^{\beta\varepsilon}}{(1+e^{\beta\varepsilon})^2}\varepsilon d\varepsilon & -\int_0^\infty \frac{\{g_2(\mu_2+\varepsilon)-g_2(\mu_2-\varepsilon)\}e^{\beta\varepsilon}}{(1+e^{\beta\varepsilon})^2}\varepsilon d\varepsilon \\ -\int_0^\infty \frac{\{g_1(\mu_1+\varepsilon)-g_1(\mu_1-\varepsilon)\}e^{\beta\varepsilon}}{(1+e^{\beta\varepsilon})^2}\varepsilon d\varepsilon & \int_0^\infty \frac{g_1(\mu_1+\varepsilon)+g_1(\mu_1-\varepsilon)e^{\beta\varepsilon}}{(1+e^{\beta\varepsilon})^2} d\varepsilon & 0 \\ -\int_0^\infty \frac{\{g_2(\mu_2+\varepsilon)-g_2(\mu_2-\varepsilon)\}e^{\beta\varepsilon}}{(1+e^{\beta\varepsilon})^2}\varepsilon d\varepsilon & 0 & \int_0^\infty \frac{g_2(\mu_2+\varepsilon)+g_2(\mu_2-\varepsilon)e^{\beta\varepsilon}}{(1+e^{\beta\varepsilon})^2} d\varepsilon \end{vmatrix} \quad \text{(A17)}$$

2.B:2.E *Nuclear Physics* **8** (1958) 284—293; © *North-Holland Publishing Co., Amsterdam*
Not to be reproduced by photoprint or microfilm without written permission from the publisher

# ON ANGULAR DISTRIBUTIONS IN COMPOUND NUCLEUS PROCESSES

T. ERICSON

NORDITA (*Nordisk Institut for Teoretisk Atomfysik*), *Copenhagen* †

and

V. STRUTINSKI

*Universitetets Institut for Teoretisk Fysik, Copenhagen* ††

Received 7 July 1958

**Abstract:** The angular anisotropy of particles emitted in compound processes is due to restrictions on the directions of their angular momenta. These restrictions are imposed by the angular momentum distribution of the residual nucleus. The anisotropy is derived in a classical limit.

## 1. Introduction

The angular momentum of a compound nucleus formed by absorption of an incident particle prefers to be directed perpendicularly to the incident beam, as a result of the perpendicularity between the direction and orbital angular momenta of the incident particles. This can give rise to an anisotropic angular distribution of emitted particles [1]). If a large number of levels is involved, the statistical assumption becomes valid, i.e. the phase factors of the different channels are distributed at random, so that all interference terms become negligible. This is in a sense a classical approximation, as the interference terms arise from the wave properties of the system. The anisotropy is, in this limit, of classical origin and may be understood from simple physical considerations.

After the target nucleus has captured the projectile, the system rotates about an axis perpendicular to the incident beam so as to conserve angular momentum. The particles which evaporate from the rotating nucleus get an additional velocity if they are emitted at the equator, and the angular distribution has therefore a maximum in the equatorial plane. If one averages over the different possible directions of the rotational axis, there will be maxima in the forward and backward directions of the beam, as these directions are contained in all equatorial planes. The distribution will furthermore be symmetrical about 90°. In the classical limit, it is expected that the anisotropy will depend on the ratio of the two characteristic energies

† On leave from the Institute for Theoretical Physics, Lund, Sweden

†† On leave from the Institute of Atomic Energy of the Academy of Sciences, Moscow, USSR.

involved, namely the centrifugal energy of a particle due to the rotation, and the average kinetic energy of an evaporated particle at the nuclear surface. That is, it will be a function of $\mu_2\omega^2 R^2/2T$, where $T$ is the nuclear temperature, $\mu_2$ the mass of the emitted particle, $\omega$ the angular velocity, and $R$ the nuclear radius.

Alternatively, the origin of the anisotropy can be ascribed to the decrease of the number of available states in the residual nucleus with increasing spin, if trivial geometrical factors are neglected. This favours the emission of particles with orbital angular momentum parallel to the total angular momentum so as to leave the residual nucleus with a low spin. Taking into account the fact that the angular momentum of the outgoing particle is perpendicular to its direction, we are led to the same conclusion as before.

We will first derive an expression for the anisotropy using rather classical arguments, and we will then compare this to the corresponding quantal result. Details of the latter calculation are found in appendix B.

## 2. Classical Anisotropy

In the spirit of the classical approximation, we consider a spinless projectile incident on a spinless target which, after the formation of a compound nucleus, emits a spinless particle. The introduction of spins has the effect of smearing out the angular distribution, but the effect is small when the effective angular momenta involved are large. The differential cross-section for the emission of a particle of energy $E_2$ † in the direction $\mathbf{n}$ can be expressed as

$$\sigma(\mathbf{n}, E_2) = \int \mathrm{d}I\sigma_I^{(1)} \frac{1}{2\pi}\int_0^{2\pi} \mathrm{d}\varphi \int \mathrm{d}^3 l \frac{\Gamma_{\mathbf{I}}(\mathbf{l}, \mathbf{n}, E_2)}{\Gamma_I}, \tag{1}$$

where $\sigma_I^{(1)}$ is the cross-section for formation of the compound nucleus with angular momentum $I$, $\varphi$ the azimuthal angle of $\mathbf{I}$ with respect to the incident beam and $\mathbf{l}$ the angular momentum of the outgoing particle. $\hbar\Gamma_{\mathbf{I}}(\mathbf{l}, \mathbf{n}, E_2)$ is the probability per unit time for the emission of a particle with angular momentum $\mathbf{l}$ in the direction $\mathbf{n}$ from a compound state $\mathbf{I}$, and correspondingly $\hbar\Gamma_I$ is the total decay probability per unit time of the compound nucleus in a state $I$.

From the principle of detailed balancing $\Gamma_{\mathbf{I}}(\mathbf{l}, \mathbf{n}, E_2)$ of eq. (1) can be expressed in terms of the reversed process, namely, capture of a particle with angular momentum $-\mathbf{l}$ incident in the direction $-\mathbf{n}$. This cross-section can be written as

$$\mathrm{d}\sigma_{\mathbf{l}}(\mathbf{n}, E_2) = \lambda\!\!\!^{-}_2{}^2 T_2(l)\delta(\mathbf{n}\cdot\mathbf{l})\mathrm{d}^3 l, \tag{2}$$

† We denote quantities referring to the projectile and emitted particle by indices 1 and 2, respectively, those referring to initial and final states by indices i and f.

where $T_2(l)$ is a transmission coefficient and $\delta(x)$ is the one-dimensional $\delta$-function, which here takes into account the fact that $\mathbf{l}$ is perpendicular to the direction of the particles $\mathbf{n}$. Integration of (2) over the solid angle of $\mathbf{l}$ gives the usual expression for $\sigma_l \mathrm{d}l$. From detailed balancing we obtain

$$\Gamma_1(\mathbf{l}, \mathbf{n}, E_2)\mathrm{d}^3l = \frac{\mu_2 E_2}{\pi^2\hbar^3}\frac{\rho_f}{\rho_1}\mathrm{d}\sigma_1(\mathbf{n}, E_2) = \frac{1}{\hbar}\cdot\frac{1}{2\pi^2}\,\delta(\mathbf{n}\cdot\mathbf{l})\,T_2(l)\,\frac{\rho_f}{\rho_1}\mathrm{d}^3l, \quad (3)$$

where $\mu_2$ is the mass of the emitted particle and $\rho_1$ and $\rho_f$ are the densities of initial and final states. Here we can write $\rho_f$ more explicitly as

$$\rho_f = \int\rho(\mathbf{j})\delta^3(\mathbf{l}+\mathbf{j}-\mathbf{I})\mathrm{d}^3j, \quad (4)$$

where $\mathbf{j}$ is the spin of the residual nucleus. When there are many degrees of freedom in the residual nucleus, we can write very generally (see appendix A)

$$\rho(\mathbf{j}) = \rho_0\cdot\mathrm{e}^{-a\mathbf{j}^2}, \quad (5)$$

where $\rho_0$ does not depend on $\mathbf{j}$ †.

When eqs. (3), (4) and (5) are introduced into eq. (1), the angular distribution $W(\mathbf{n}, E_2)$ can be written as

$$W(\mathbf{n}, E_2) = \text{const}\times\int_0^\infty\frac{I T_1(I)}{\Gamma_I}\mathrm{d}I\cdot\frac{1}{2\pi}\int_0^{2\pi}\mathrm{d}\varphi\int T_2(l)\,\frac{\exp\{-\alpha_f(l^2+I^2\}}{\exp\{-\alpha_1 I^2\}} \quad (6)$$
$$\times\mathrm{e}^{2\alpha_f\mathbf{I}\cdot\mathbf{l}}\frac{1}{2\pi^2}\,\delta(\mathbf{n}\cdot\mathbf{l})\mathrm{d}^3l.$$

Eq. (6) contains the angular distribution of particles with a fixed projection $m$ of $\mathbf{l}$ on $\mathbf{I}$. With $\mathbf{I}$ as the polar axis, $\vartheta_l$ the angle between $\mathbf{l}$ and $\mathbf{I}$, $\vartheta$ the angle between $\mathbf{n}$ and $\mathbf{I}$, and $\varphi_l$ the azimuthal angle of $\mathbf{l}$, an application of the spherical cosine theorem and a subsequent integration over $\varphi_l$ yields

$$\int l\mathrm{d}\Omega_l\,\mathrm{e}^{2\alpha_f\mathbf{I}\cdot\mathbf{l}}\frac{1}{2\pi^2}\,\delta(\mathbf{n}\cdot\mathbf{l})$$
$$= \int_{-|\sin\vartheta|}^{|\sin\vartheta|}\mathrm{d}(\cos\vartheta_l)\mathrm{e}^{2\alpha_f Il\cos\vartheta_l}\frac{1}{2\pi^2\sqrt{\sin^2\vartheta-\cos^2\vartheta_l}}. \quad (7)$$

The factor $(2\pi^2\sqrt{\sin^2\vartheta-\cos^2\vartheta_l})^{-1}$ which results from the $\varphi_l$ integration is just the classical analogue of $|Y_{lm}|^2$ with $m = l\cos\vartheta_l$, where $Y_{lm}$ is a spherical harmonic. The angular distribution for arbitrary direction of $\mathbf{l}$, but fixed direction of $\mathbf{I}$, is obtained from eq. (7) by integration over $\vartheta_l$. This integration can be performed exactly:

† Eq. (5) is more familiar in its quantal form with a factor $(2j+1)^2$ (or $(2j+1)$ if we exclude the degeneracy of states with different projections along a fixed axis). This factor is, however, of geometrical origin and is represented by the volume element $\mathrm{d}^3j = j^2\mathrm{d}j\mathrm{d}\Omega_j$ of eq. (4).

$$\frac{1}{2\pi^2}\int_{-|\sin\vartheta|}^{|\sin\vartheta|} \mathrm{d}(\cos\vartheta_l)\,\frac{\mathrm{e}^{2\alpha_l Il\cos\vartheta_l}}{\sqrt{\sin^2\vartheta-\cos^2\vartheta_l}} = \frac{1}{2\pi}J_0(2i\alpha_l Il\sin\vartheta), \tag{8}$$

where $J_0(x)$ is the Bessel function of zeroth order. To obtain the angular distribution for fixed $I$ and $l$, we have still to average over the directions of **I**. For this it is convenient to exploit the expansion of $J_0(x\sin\vartheta)$ in Legendre-polynomials:

$$J_0(2i\alpha_l Il\sin\vartheta) = \sum_{k=0}^{\infty}(-)^k(4k+1)\,\frac{(2k)!}{(2^k k!)^2}\,j_{2k}(2i\alpha_l Il)P_{2k}(\cos\vartheta), \tag{9}$$

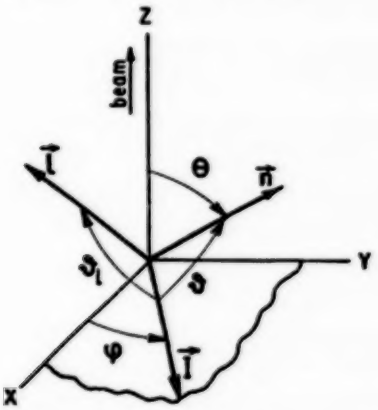


Fig. 1. Definition of angles $\vartheta$, $\varphi$, $\vartheta_l$ and $\Theta$.

where $j_{2k}(x)$ are spherical Bessel functions. If the angle $\Theta$ between **n** and the incident beam (see fig. 1) is introduced we can apply the addition theorem for $P_n(\cos\vartheta)$,

$$P_n(\cos\vartheta) = \frac{4\pi}{2l+1}\sum_m Y_{nm}(\tfrac{1}{2}\pi,\varphi)Y_{nm}(\Theta,0). \tag{10}$$

When eq. (10) is averaged over $\varphi$ we obtain

$$\overline{P_{2k}(\cos\vartheta)} = P_{2k}(0)P_{2k}(\cos\Theta) = \frac{(2k)!}{(2^k k!)^2}\,P_{2k}(\cos\Theta). \tag{11}$$

If we introduce the angular distribution associated with given $I$ and $l$, $W_{Il}(\Theta, E_2)$, normalized so that

$$\int W_{Il}(\Theta, E_2)\mathrm{d}\Omega = 1, \tag{12}$$

then eq. (11) together with eq. (9) gives

$$W_{Il}(\Theta, E_2) = \frac{1}{4\pi}\,\frac{\sum_{k=0}^{\infty}(-)^k(4k+1)\left[\frac{(2k)!}{(2^k k!)^2}\right]^2 j_{2k}(2i\alpha_l Il)P_{2k}(\cos\Theta)}{j_0(2i\alpha_l Il)}. \tag{13}$$

When this result is introduced into eq. (6), it can be expressed as

$$W(\mathbf{n}, E_2) = \text{const} \times \int I T_1(I)\mathrm{d}I \int l T_2(l) S(I, l) W_{II}(\Theta, E_2)\mathrm{d}l, \qquad (14)$$

where $S(I, l)$ is defined as

$$S(I, l) = \frac{\exp\{\alpha_1 I^2 - \alpha_f (I^2 + l^2)\}}{\Gamma_I}. \qquad (15)$$

The deviation of $S(I, l)$ from a constant has the same origin as the anisotropy. $\Gamma_I$ is a sum of widths due to different kinds of emitted particles. When neutron evaporation is predominant, $\Gamma_I$ depends only slightly on $I$. In this case, the variation of $S(I, l)$ with $I$ and $l$ is to a good approximation given by the numerator of eq. (15). Thus, the anisotropy given by eq. (15) is, to first order,

$$W(\mathbf{n}, E_2) \propto 1 + \frac{\alpha_f{}^2 \overline{I^2}\,\overline{l^2}}{2} \cos^2\Theta, \qquad (16)$$

where $\overline{I^2}$ and $\overline{l^2}$ are averages of $I^2$ and $l^2$ with the relative weighting factors $I T_1(I)$ and $l T_2(l)$ respectively.

In the sharp cut-off approximation for the transmission coefficients, $T_1(I)$ and $T_2(l)$ are 1 in the classically allowed region and 0 outside. Therefore in this case

$$\overline{I^2} = \tfrac{1}{2} I_{\max}^2 = \frac{\mu_1 (E_1 - B_1) R_1{}^2}{\hbar^2}, \qquad (17)$$

where $E_1$ is the energy of the projectile, $\mu_1$ its mass, $B_1$ the Coulomb barrier, and $R_1$ the interaction radius. Similarly

$$\overline{l^2} = \tfrac{1}{2} l_{\max}^2 = \frac{\mu_2 (E_2 - B_2) R_2{}^2}{\hbar^2} \qquad (18)$$

for outgoing particles of energy $E_2$. If all energies of the outgoing particles are considered simultaneously, $\overline{l^2}$ has to be averaged over all classically permitted energies, and we obtain

$$\overline{l^2} = \frac{2\mu_2 T R_2{}^2}{\hbar^2} \qquad (19)$$

in terms of the nuclear temperature $T$.

Therefore, if we express the $\alpha_f$ of eq. (16) in the form $\hbar^2/2\mathscr{I}T$ (appendix A eq. (4)), where $\mathscr{I}$ is the moment of inertia of the nucleus, we can write $W(\mathbf{n})$ as

$$W(\mathbf{n}) \propto 1 + \frac{\overline{\omega^2}\,\hbar^2 \overline{l^2}}{8T^2} \cos^2\Theta = 1 + \frac{\mu_2 \overline{\omega^2} R_2{}^2}{4T} \cos^2\Theta, \qquad (20)$$

where $\omega$ is the angular velocity of the compound nucleus. This expression for the anisotropy reflects the simple classical picture mentioned in the introduction.

The validity of the sharp cut-off approximation for the transmission coefficients should be checked in each case, as it tends to underestimate $\overline{l^2}$ and $\overline{I^2}$. This is obviously the case for particles emitted in the classically forbidden energy range, so that eq. (18) for $\overline{l^2}$ breaks down. The Coulomb barrier strongly enhances the relative transmission coefficients for higher $l$-values for energies near or below the barrier energy. In such cases it is necessary to use more exact expressions for these coefficients.

In appendix B we derive a non-classical expression for the anisotropy and use this to show the condition for exact isotropy. The result of the two approaches for the angular distribution is the same in the classical limit, with the exception that the sum over Legendre polynomials in eq. (13) contains all $k \geqq 0$ in spite of the well-known fact that only terms with $k \leqq \min(I, l)$ contribute. This is also correctly obtained in the appendix. However, the approximation for the Clebsch-Gordan coefficients becomes bad when $k$ is close to $l$. A condition for the validity of the classical expansion (13) is therefore that the contributions from terms with $k$ of the order of $l$ and larger should be small. This is so as long as

$$\alpha_t \min(I_{eff}, l_{eff}) \lesssim 1 \tag{21}$$

is valid for the effective angular momenta.

The classical replacement

$$\sum_m \exp\{2\alpha_t I m\}|Y_{lm}|^2 \to \int_{-|\sin\vartheta|}^{|\sin\vartheta|} e^{2\alpha_t I l \cos\vartheta_l} \cdot \frac{l}{2\pi^2\sqrt{\sin^2\vartheta - \cos^2\vartheta_l}} \mathrm{d}(\cos\vartheta_l) = (l/2\pi) J_0(2i\alpha_t I(\sin\vartheta), \tag{22}$$

which is closely related to our calculations (cf. eqs. (7) and (8)), is a very good approximation even for $l$ of the order of unity, providing that

$$2\alpha_t I \lesssim 1, \tag{23}$$

which is essentially the same as the condition (21) above. Actually, these conditions only express the uncertainty relation.

As an illustrative example to show the expected order of magnitude of the anisotropy, we consider the inelastic scattering of 18 MeV α-particles on Ni, the scattered particles having an energy equal to the Coulomb energy †. The inelastically scattered α-particles show in this case a typical evaporation spectrum with a maximum just below the Coulomb barrier energy (10.5 MeV) with a nuclear temperature of 1.1 MeV. The transmission coefficients are calculated using Coulomb wave functions with an interaction radius from elastic α-particle scattering [2]) and with a potential of 5 MeV for the α-particles within the nucleus [3]). From this we obtain $\overline{I^2} = 50$ (sharp cut-off approximation $\overline{I^2} = 42$) and $\overline{l^2} = 17$. For the cut-off factor $\alpha_t$ of the spin-

† We are much indebted to Dr. N. O. Lassen for the experimental data.

distribution we have used eq. (4) of appendix A with a nuclear radius $R = r_0 \times A^{\frac{1}{3}}$, $r_0 = 1.4 \times 10^{-13}$ cm. With these values for the parameters we obtain an estimated anisotropy $(W(135°)/W(190°)-1 = 0.15$. The corresponding experimental value averaged over all energies of the emitted particles is $\approx 0.33$ [4-5]). This difference from the estimated anisotropy seems to be only partly due to contributions from particles of higher energies. A possible explanation is the reduction of the moment of inertia caused by pairing correlations in the nucleus. This reduction is expected to be of the order of 20—30 % at this excitation (7.5 MeV), which is sufficient to explain the experimental value [6]). It should also be noticed that the estimated anisotropy is very sensitive to the value of $r_0$, which enters in the fourth power.

Preliminary results on the variation of the anisotropy with energy indicate that the anisotropy increases with increasing energy in qualitative agreement with eq. (16).

From the condition of isotropy given in appendix B, it is clear that the anisotropies are intimately connected with the cut-off factor $\alpha_t$ in the spin-distribution, that is with the finiteness of the moment of inertia. Therefore, the measurement of the anisotropy in acom pound nucleus reaction provides in principle a method to investigate the distribution of spins among the levels in the residual nucleus and more specifically to test if the moment of inertia of the nucleus deviates from the rigid body value at higher excitations.

From eq. (16) it is seen that the largest anisotropies are expected when the effective values of $I$ and $l$ are large. The anisotropies should therefore be expected to be of particular importance in reactions involving heavy particles, such as $\alpha$-particles, ions or fission fragments.

The authors are much indebted to Professor A. Bohr and Dr. B. R. Mottelson for stimulating and fruitful discussions, as well as to Dr. N. O. Lassen for making experimental material available to us in advance of publication. We are very grateful to Professor N. Bohr for the hospitality extended to us at his Institute. Finally, one of us (T.E.) has the great pleasure of thanking Professor T. Gustafson for his continued assistance and encouragement.

## Appendix A

### DISTRIBUTION OF SPINS AMONG THE LEVELS OF A HIGHLY EXCITED NUCLEUS

The spin distribution $\rho(\mathbf{j})\mathrm{d}^3j \propto \mathrm{e}^{-\alpha \mathbf{j}^2}\mathrm{d}^3j$ can be expected on very general grounds if $\mathbf{j}$ is the sum of a large number of component vectors oriented at random in space (central limit theorem). The coefficient $\alpha$ is given by

$$\alpha = \frac{1}{2\overline{M^2}}, \tag{A1}$$

where $\overline{M^2}$ is the average value of the square of the projection of the total spin along the same axis. The corresponding number of states between $j$ and $j+\mathrm{d}j$ is

$$\rho_j \mathrm{d}j \propto j^2 \mathrm{e}^{-\alpha j^2} \mathrm{d}j. \tag{A2}$$

Alternatively, as the excited nucleus can be pictured as a rotator with moment of inertia $\mathscr{I}$, only the part $U-\hbar^2\mathbf{j}^2/2\mathscr{I}$ of the total excitation energy $U$ is available for intrinsic excitations. If $\rho(U)$ is the density of intrinsic states of the non-rotating system at excitation $U$, we have

$$\rho(\mathbf{j}, U) = \rho(U-\hbar^2\mathbf{j}^2/2\mathscr{I}) \propto \mathrm{e}^{-\frac{\hbar^2}{2\mathscr{I}T}\mathbf{j}^2}, \tag{A3}$$

where $T$ is the nuclear temperature. In this case $\alpha$ is given by

$$\alpha = \frac{\hbar^2}{2\mathscr{I}T}. \tag{A4}$$

At high excitation, when the discreteness of the nuclear spectrum can be neglected, the moment of inertia will tend towards the rigid body value

$$\mathscr{I}_{\text{rigid}} = \tfrac{2}{5} m A R^2, \tag{A5}$$

where $m$ is the nucleon mass †.

For a quantal system we obtain similarly

$$\rho_j \propto (2j+1)^2 \mathrm{e}^{-\frac{\hbar^2}{2\mathscr{I}T}j(j+1)} \tag{A6}$$

or, when the trivial degeneracies due to the different values of $m_j$ along some axis are not included,

$$\rho_{0j} \propto (2j+1) \mathrm{e}^{-\frac{\hbar^2}{2\mathscr{I}T}j(j+1)}. \tag{A7}$$

## Appendix B

### QUANTAL ANGULAR DISTRIBUTION

The angular distribution which we have obtained in the classical approximation should also result from the corresponding quantal expression in the limit of high angular momenta. This derivation gives a somewhat better insight into the approximations involved when this limit is taken. We shall furthermore use the quantal distribution to prove that isotropy results if the distribution of spins of definite projection $m_j$ among the levels of the residual nucleus is proportional to $(2j+1)$ ††. As before, we shall use the statistical assumption of random phases, so that all interference terms cancel.

The angular distribution of emitted particles of angular momentum $l$ from

† Shown by Bethe for a square potential [7]) and somewhat more generally by C. Bloch [8]).
†† Cf. also the result of Hauser and Feshbach [9]).

a compound state $I$ with projection $M$ on the beam, is denoted by $W_{IIM}(\Theta,E_2)$. When $\mathbf{l}$ is coupled to the spin of the residual nucleus $\mathbf{j}$ to give the total spin $\mathbf{I}$, $W_{IIM}(\Theta, E_2)$ is given by

$$W_{IIM}(\Theta, E_2) \propto \sum_{m_l, j} C^2(ljI; m_l(M-m_l))|Y_{lm_l}(\Theta, \varphi)|^2 \rho_{0j} \dagger, \qquad \text{(B1)}$$

where $\rho_{0j}$ is the density of states with spin $j$ and definite $m_j$ (cf. appendix A eq. (7)), and $m_l$ is the projection of $\mathbf{l}$ along the beam. Eq. (B1) can be expanded by the coupling rule of spherical harmonics and summed over $m_l$ to give

$$W_{IIM}(\Theta, E_2)$$
$$\propto \sum_{\lambda} C(\lambda l; 00)C(\lambda II; 0M)P_\lambda(\cos\Theta) \sum_j \rho_{0j} \frac{(2\lambda+1)(-)^{-j}}{(2l+1)^{\frac{1}{2}}(2I+1)^{\frac{1}{2}}} W(llII; \lambda j). \qquad \text{(B2)}$$

The expression for $\rho_{0j}$ of appendix A shows that $\rho_{0j}$ is proportional to $(2j+1)$ in the limit of an infinite moment of inertia. It is easy to show that the resulting angular distribution is isotropic in this limit, if we observe that

$$W(llII; 0j) = \frac{(-)^{l+I-j}}{(2l+1)^{\frac{1}{2}}(2I+1)^{\frac{1}{2}}} \qquad \text{(B3)}$$

and if the orthonormality property of the Racah coefficients is used. Thus we have

$$\begin{aligned} W_{IIM}(\Theta, E_2) &\propto \sum_{\lambda} C(\lambda l; 00)C(\lambda II; 0M)P_\lambda(\cos\Theta) \\ &\quad \times \sum_j (2j+1)(2\lambda+1)W(llII; j0)W(llII; j\lambda) \qquad \text{(B4)} \\ &= \sum_{\lambda} C(\lambda l; 00)C(\lambda II; 0M)P_\lambda(\cos\Theta)\delta_{\lambda 0}. \end{aligned}$$

So we see that isotropy results irrespective of the angular momenta of the projectile and the target nucleus. This proof was carried out for a spinless emitted particle; when the spin $\neq 0$ the proof is very similar but somewhat more complicated. The distribution $\rho_{0j} \propto 2j+1$ implies that all $\mathbf{j}$ are equally probable, as are all directions of $\mathbf{l}$, since $\mathbf{j}+\mathbf{l} = \mathbf{I}$. Therefore we can get no anisotropy, since this arises only from restrictions on the direction of $\mathbf{l}$.

In the following we confine ourselves to the case treated earlier, namely spinless projectile and target, so that $M = 0$. We introduce the classical limits for the Racah and Clebsch-Gordan coefficients in eq. (B4). These are given by

$$C(\lambda l; 00) \approx (-)^\lambda P_\lambda(\tfrac{1}{2}\pi) \qquad (\lambda \ll 2l) \qquad \text{(B5)}$$

and

$$W(llII; \lambda j) \approx \frac{(-)^{l+I-j} P_\lambda(\cos\vartheta_l)}{(2l+1)^{\frac{1}{2}}(2I+1)^{\frac{1}{2}}}, \qquad \text{(B6)}$$

† The notation for the Clebsch-Gordan and Racah coefficients is that employed by Rose [10]).

valid for $I \gg 1$ and $l \gg 1$ with

$$2Il\cos\vartheta_l = I^2+l^2-j^2. \tag{B7}$$

In the classical approximation for $\rho_{0j}$,

$$\rho_{0j} \propto j\mathrm{e}^{-\alpha j^2}, \tag{B8}$$

the summation over $j$ can be changed into an integration and be performed exactly:

$$W_{I0}(\Theta, E_2) \propto \sum_{k=0}^{\min(I,l)} (4k+1)[P_{2k}(0)]^2 P_{2k}(\cos\Theta)\int_0^\infty P_{2k}(\cos\vartheta_l)\mathrm{e}^{-\alpha_l j^2} j\mathrm{d}j. \tag{B9}$$

By eq. (B7) for $j^2$ this transforms into

$$\begin{aligned} W_{I0}(\Theta, E_2) &\propto \sum_{k=0}^{\min(I,l)} (4k+1)[P_{2k}(0)]^2 P_{2k}(\cos\Theta)\int_0^\pi Il\mathrm{d}(\cos\vartheta_l)\mathrm{e}^{2\alpha_l Il\cos\vartheta_l}\cdot P_{2k}(\cos\vartheta_l) \\ &\propto \sum_{k=0}^{\min(I,l)} (4k+1)[P_{2k}(0)]^2 P_{2k}(\cos\Theta)(-)^k j_{2k}(2i\alpha_l Il). \end{aligned} \tag{B10}$$

Eq. (B10) is very similar to the expression derived earlier for $W_{Il}(\Theta, E_2)$ (eq. (13)).

## References


1) L. Wolfenstein, Phys. Rev. **82** (1951) 690
2) D. D. Kerlee, J. S. Blair and G. W. Farwell, Phys. Rev. **107** (1957) 1343
3) J. M. Blatt and V. Weisskopf, Theoretical Nuclear Physics (Wiley, 1952) p. 570
4) N. O. Lassen and N. O. Roy Poulsen, Congrès International de Physique Nucléaire, Paris (1958)
5) H. W. Fulbright, N. O. Lassen and N. O. Roy Poulsen (to be published in Mat. Fys. Medd. Dan. Vid. Selsk.)
6) I. Halpern and V. Strutinski, to be published; V. Strutinski, Congrès International de Physique Nucléaire, Paris (1958)
7) H. Bethe, Revs. Mod. Phys. **9** (1937) 69
8) C. Bloch, Phys. Rev. **93** (1954) 1094
9) W. Hauser and H. Feshbach, Phys. Rev. **87** (1952) 366
10) M. E. Rose, Elementary Theory of Angular Momentum (Wiley, 1957)

2.L:8.B *Nuclear Physics* **8** (1958) 294—302; © *North-Holland Publishing Co., Amsterdam*
Not to be reproduced by photoprint or microfilm without written permission from the publisher

# SCATTERING OF POLARIZED ELECTRONS BY A COULOMB FIELD

M. BERNARDINI, P. BROVETTO and S. FERRONI
*Istituto Nazionale di Fisica Nucleare, Sezione di Torino*

Received 11 June 1958

**Abstract:** In this work some equations, concerning the cross-section and polarization of a fermion beam scattered by a central field, are obtained by means of the density matrix formalism. These equations are applied to the case of electrons scattered in a Coulomb field. The precession of the polarization is given as a function of velocity for some values of the parameters. The double scattering experiment in orthogonal planes is discussed as a technique for evaluating the longitudinal component of the electron polarization.

## 1. Introduction

In the last few years, the phenomena concerning the polarization of electron beams assumed considerable interest in relation to parity effects. In this work, cross section anisotropy and particularly precession of polarization in the Coulomb scattering of relativistic electrons are investigated. The results obtained allow us to evaluate the longitudinal component of the polarization, by means of a double scattering experiment in orthogonal planes.

The polarization for the fermions is an axial vector that can be defined in different ways, viz. as expectation value of spin momentum, or magnetic moment or a linear combination of them. These definitions are equivalent in the centre of mass reference system of the fermion.

Following Mott [1]) and Tolhoek [2]) we define the polarization as the expectation value of the semi-difference of the spin momentum and magnetic moment operators, i.e., omitting some constant factors,

$$\tfrac{1}{2}(1-\gamma_4)\begin{vmatrix}\boldsymbol{\sigma} & 0\\ 0 & \boldsymbol{\sigma}\end{vmatrix}=\begin{vmatrix}0 & 0\\ 0 & \boldsymbol{\sigma}\end{vmatrix}, \qquad (1)$$

where $\boldsymbol{\sigma}$ is the Pauli spin operator. This definition of the polarization involves only the $\psi_3$, $\psi_4$ components of the spinor; on the other hand it is known that also the cross-section only depends on the $\psi_3$, $\psi_4$ components [3]). In this way, relativistically exact calculations can be performed by means of these two components as in the Pauli approximation.

## 2. Theory

### 2.1. EQUATIONS FOR THE CROSS-SECTION AND POLARIZATION OF A FERMION BEAM.

As it is well known, the polarization state of a fermion beam can be represented by means of a $2\times 2$ density matrix $\rho$. The equation expressing the polarization by means of the density matrix is

$$\mathbf{P} = \frac{\mathrm{Tr}\rho\boldsymbol{\sigma}}{\mathrm{Tr}\rho}. \tag{2}$$

It can be shown (see appendix) that the magnitude of $\mathbf{P}$ is related to the invariants Tr $\rho$ and Det $\rho$ by the equation

$$|\mathbf{P}| = \left[1-4\frac{\mathrm{Det}\rho}{(\mathrm{Tr}\rho)^2}\right]^{\frac{1}{2}}, \tag{3}$$

and that

$$\mathrm{Det}\ \rho \geqq 0; \tag{4}$$

Det $\rho$ vanishes only for a pure state. In this case, the polarization is unity; in general, it follows from eqs. (3) and (4) that

$$0 \leqq |\mathbf{P}| \leqq 1, \tag{5}$$

as it should be.

From eq. (2) we immediately obtain the density matrix as a function of $\mathbf{P}$:

$$\rho = \frac{\mathrm{Tr}\rho}{2}[\mathbf{1}+(\mathbf{P}\cdot\boldsymbol{\sigma})]. \tag{6}$$

In the case of a central field, cross-section and change of the polarization through the scattering are expressed by the matrix

$$M = \mathbf{1}f(\vartheta)-i(\mathbf{n}\cdot\boldsymbol{\sigma})g(\vartheta), \tag{7}$$

where $\mathbf{n}$ is the unit vector orthogonal to the scattering plane †, and $f(\vartheta)$, $g(\vartheta)$ are complex functions of the scattering angle. By means of the matrix $M$ and of the matrix $\rho_i$ of the incident wave, the density matrix $\rho_f$ of the scattered wave can be deduced:

$$\rho_f = M\rho_i M^+. \tag{8}$$

In this way, the polarization $\mathbf{P}_f$ of the scattered wave is expressed by means of the polarization $\mathbf{P}_i$ of the incident wave with the aid of eqs. (8), (6) and of the equation

$$\mathbf{P}_f = \frac{\mathrm{Tr}\rho_f\boldsymbol{\sigma}}{\mathrm{Tr}\rho_f}. \tag{9}$$

In the same way the cross-section depends on the polarization $\mathbf{P}_i$ through eqs. (8), (6) and the equation

† The sign of $\mathbf{n}$ is determined by the equation

$$\mathbf{n} = (\mathbf{K}_i\times\mathbf{K}_f)/|\mathbf{K}_i\times\mathbf{K}_f|,$$

where $\mathbf{K}_i$ and $\mathbf{K}_f$ are the unit vectors of the incoming and outgoing beam.

$$\sigma(\vartheta, \varphi) = \frac{\mathrm{Tr}\ \rho_f}{\mathrm{Tr}\ \rho_i}. \tag{10}$$

Eqs. (2), (6), (7), (8), (9), (10) are well known [4]).

Eq. (10) can be written by means of the $f$ and $g$ functions:

$$\sigma(\vartheta, \varphi) = \tfrac{1}{2}\mathrm{Tr}\{[1+(\mathbf{P}_i\cdot\boldsymbol{\sigma})]ff^*+[(\mathbf{n}\cdot\boldsymbol{\sigma})^2+(\mathbf{n}\cdot\boldsymbol{\sigma})(\mathbf{P}_i\cdot\boldsymbol{\sigma})(\mathbf{n}\cdot\boldsymbol{\sigma})]gg^* + i[(\mathbf{n}\cdot\boldsymbol{\sigma})+(\mathbf{P}_i\cdot\boldsymbol{\sigma})(\mathbf{n}\cdot\boldsymbol{\sigma})]fg^*-i[(\mathbf{n}\cdot\boldsymbol{\sigma})+(\mathbf{n}\cdot\boldsymbol{\sigma})(\mathbf{P}_i\cdot\boldsymbol{\sigma})]f^*g\}. \tag{11}$$

In this equation the incident beam is normalized assuming $\mathrm{Tr}\ \rho_i = 1$. By means of the following relations:

$$\begin{aligned}
&(\mathbf{n}\cdot\boldsymbol{\sigma})^2 = \mathbf{1},\\
&(\mathbf{n}\cdot\boldsymbol{\sigma})(\mathbf{P}_i\cdot\boldsymbol{\sigma}) = (\mathbf{n}\cdot\mathbf{P}_i)\mathbf{1}+i(\mathbf{n}\times\mathbf{P}_i)\cdot\boldsymbol{\sigma},\\
&(\mathbf{P}_i\cdot\boldsymbol{\sigma})(\mathbf{n}\cdot\boldsymbol{\sigma}) = (\mathbf{n}\cdot\mathbf{P}_i)\mathbf{1}-i(\mathbf{n}\times\mathbf{P}_i)\cdot\boldsymbol{\sigma},\\
&(\mathbf{n}\cdot\boldsymbol{\sigma})(\mathbf{P}_i\cdot\boldsymbol{\sigma})(\mathbf{n}\cdot\boldsymbol{\sigma}) = 2(\mathbf{n}\cdot\mathbf{P}_i)(\mathbf{n}\cdot\boldsymbol{\sigma})-(\mathbf{P}_i\cdot\boldsymbol{\sigma}),
\end{aligned} \tag{12}$$

eq. (11) becomes

$$\sigma(\vartheta, \varphi) = \tfrac{1}{2}\mathrm{Tr}\{[1+(\mathbf{P}_i\cdot\boldsymbol{\sigma})]ff^*+[1+2(\mathbf{n}\cdot\mathbf{P}_i)(\mathbf{n}\cdot\boldsymbol{\sigma})-(\mathbf{P}_i\cdot\boldsymbol{\sigma})]gg^* -2[(\mathbf{n}\cdot\boldsymbol{\sigma})+(\mathbf{n}\cdot\mathbf{P}_i)]\ \mathrm{Im}\ fg^*+2(\mathbf{n}\times\mathbf{P}_i)\cdot\boldsymbol{\sigma}\ \mathrm{Re}\ fg^*\}. \tag{13}$$

Taking into account that

$$\mathrm{Tr}\ \mathbf{1} = 2, \quad \mathrm{Tr}\ \boldsymbol{\sigma} = 0, \tag{14}$$

the cross-section is given by the equation

$$\sigma(\vartheta, \varphi) = ff^*+gg^*-2\ \mathrm{Im}\ fg^*(\mathbf{n}\cdot\mathbf{P}_i). \tag{15}$$

Comparing eq. (9) with eqs. (10) and (13) and remembering that

$$\mathrm{Tr}\{(\mathbf{A}\cdot\boldsymbol{\sigma})\boldsymbol{\sigma}\} = 2\mathbf{A}, \tag{16}$$

where $\mathbf{A}$ is any vector, the final polarization $\mathbf{P}_f$ becomes

$$\mathbf{P}_f = \frac{(ff^*-gg^*)\mathbf{P}_i+2\,\mathrm{Re}\,fg^*(\mathbf{n}\times\mathbf{P}_i)-2[\mathrm{Im}\,fg^*-(\mathbf{n}\cdot\mathbf{P}_i)gg^*]\mathbf{n}}{ff^*+gg^*-2\ \mathrm{Im}\ fg^*(\mathbf{n}\cdot\mathbf{P}_i)}. \tag{17}$$

### 2.2. THE CASE OF THE COULOMB FIELD

In the case of the Coulomb field it is convenient, according to Mott [1]), to express $f$ and $g$ in terms of two new functions $F, G$, of the scattering angle $\vartheta$, by means of the equations

$$\begin{aligned}
f &= \lambda\!\!\!^{-}[-iq\sqrt{1-\beta^2}\,F+G],\\
g &= \lambda\!\!\!^{-}[iq\sqrt{1-\beta^2}(1+\cos\vartheta)F+(1-\cos\vartheta)G]/\sin\vartheta,
\end{aligned} \tag{18}$$

where $\lambda\!\!\!^{-} = \hbar/p$ is the electron wave length, $\alpha$, for the nuclear charge $Ze$, is $= Ze^2/\hbar c$; $\beta = v/c$ is the electron velocity in units of $c$, and $q = \alpha/\beta$. The functions $F$ and $G$ can be expressed analytically by series involving $\Gamma$ functions and spherical polynomials [1]). They have been tabulated for mercury,

cadmium and aluminium, for some values of $\vartheta$ and $\beta$, by Sherman [5]) with the aid of a UNIVAC computer.

Bartlett, Watson and others [6]) showed that the correction due to the screening of the nuclear charge is very small.

Taking into account the eqs. (18) we get the following relations:

$$\begin{aligned}
ff^* &= \lambda\!\!\!^{-2}[q^2(1-\beta^2)FF^*+GG^*+2q\sqrt{1-\beta^2}\ \mathrm{Im}\ FG^*],\\
gg^* &= \lambda\!\!\!^{-2}[q^2(1-\beta^2)\cot\tfrac{1}{2}\vartheta FF^*+\tan\tfrac{1}{2}\vartheta GG^*-2q\sqrt{1-\beta^2}\ \mathrm{Im}\ FG^*],\\
\mathrm{Re}\ fg^* &= \lambda\!\!\!^{-2}[-q^2(1-\beta^2)\cot\tfrac{1}{2}\vartheta FF^*+\tan\tfrac{1}{2}\vartheta GG^*\\
&\qquad -q\sqrt{1-\beta^2}(\cot\tfrac{1}{2}\vartheta-\tan\tfrac{1}{2}\vartheta)\ \mathrm{Im}\ FG^*],\\
\mathrm{Im}\ fg^* &= -\lambda\!\!\!^{-2}q\sqrt{1-\beta^2}\sec\tfrac{1}{2}\vartheta\csc\tfrac{1}{2}\vartheta\ \mathrm{Re}\ FG^*.
\end{aligned} \tag{19}$$

By means of eqs. (19) and (15) the cross-section becomes

$$\begin{aligned}
\sigma(\vartheta,\varphi) = \lambda\!\!\!^{-2}[&q^2(1-\beta^2)\csc^2\tfrac{1}{2}\vartheta FF^*+\sec^2\tfrac{1}{2}\vartheta GG^*\\
&+2q\sqrt{1-\beta^2}\sec\tfrac{1}{2}\vartheta\csc\tfrac{1}{2}\vartheta\ \mathrm{Re}\ FG^*(\mathbf{P}_1\cdot\mathbf{n})].
\end{aligned} \tag{20}$$

The isotropic term of the cross-section, independent of $\mathbf{P}_1$, was tabulated in Sherman's work [5]).

The polarization, eq. (17), likewise becomes

$$\mathbf{P}_f = U(\vartheta,\varphi)\mathbf{P}_1+V(\vartheta,\varphi)\mathbf{n}\times\mathbf{P}_1+W(\vartheta,\varphi)\mathbf{n}, \tag{21}$$

where

$$\begin{aligned}
U(\vartheta,\varphi) &= k[q^2(1-\beta^2)(1-\cot^2\tfrac{1}{2}\vartheta)FF^*+(1-\tan^2\tfrac{1}{2}\vartheta)GG^*\\
&\quad +4q\sqrt{1-\beta^2}\ \mathrm{Im}\ FG^*],\\
V(\vartheta,\varphi) &= 2k[-q^2(1-\beta^2)\cot\tfrac{1}{2}\vartheta FF^*+\tan\tfrac{1}{2}\vartheta GG^*\\
&\quad +q\sqrt{1-\beta^2}(\tan\tfrac{1}{2}\vartheta-\cot\tfrac{1}{2}\vartheta)\ \mathrm{Im}\ FG^*],\\
W(\vartheta,\varphi) &= k\{2q\sqrt{1-\beta^2}\sec\tfrac{1}{2}\vartheta\csc\tfrac{1}{2}\vartheta\ \mathrm{Re}\ FG^*+[2q^2(1-\beta^2)\cot^2\tfrac{1}{2}\vartheta FF^*\\
&\quad +2\tan^2\tfrac{1}{2}\vartheta\, GG^*-4q\sqrt{1-\beta^2}\ \mathrm{Im}\ FG^*](\mathbf{n}\cdot\mathbf{P}_1)\},
\end{aligned} \tag{22}$$

and

$$k = \lambda\!\!\!^{-2}/\sigma(\vartheta,\varphi).$$

Eqs. (20), (21), (22) give the complete solution of the scattering problem for an electron beam of any initial polarization.

## 3. Numerical Results and Discussion

Let us consider, as application of the previous equations, a beam with longitudinal polarization, $\mathbf{P}_1\cdot\mathbf{n}=0$. In this case the cross section, eq. (20), is independent of the angle $\varphi$, and the final polarization, eq. (21), is decomposable into a component lying in the scattering plane, $\mathbf{P}_{f,\pi}$, and the

orthogonal component $\mathbf{P}_{f,n}$ by means of the equations

$$\mathbf{P}_{f,\pi} = U\mathbf{P}_1 + V(\mathbf{n}\times\mathbf{P}_1), \tag{23}$$

$$\mathbf{P}_{f,n} = W\mathbf{n}. \tag{24}$$

Since the component $\mathbf{P}_{f,n}$ is independent of the initial polarization, let us take as precession angle the angle $\xi$ between $\mathbf{P}_{f,\pi}$ and $\mathbf{P}_1$. One gets

$$\tan\xi = \frac{V}{U}. \tag{25}$$

It is interesting to observe that for extremely relativistic electrons we find from eq. (25)

$$\tan\xi = \tan\vartheta, \tag{26}$$

and the $\mathbf{P}_{f,n}$ component tends to zero. In other words, the polarization of the

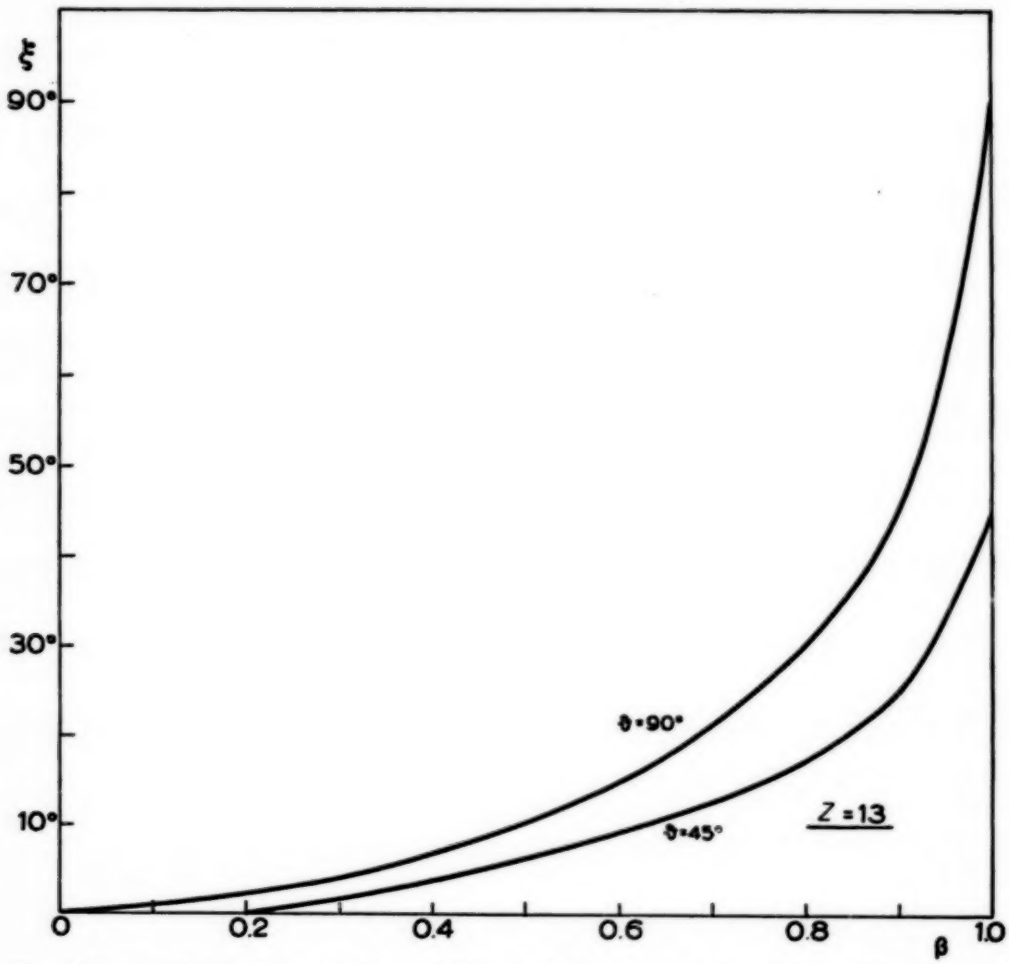


Fig. 1. Curves showing $\xi$ as a function of $\beta$ for electrons scattered at angles $\vartheta=45°$ and $\vartheta=90°$ by nuclei of charge $Z=13$.

scattered wave remains longitudinal. This result does not depend on the form of functions $F$, $G$ and therefore holds for any central field.

For the scattering of electrons against mercury and aluminium nuclei $\xi$ is plotted in fig. 1 and fig. 2 as a function of $\beta$, for $\vartheta = 45°$ and $\vartheta = 90°$.

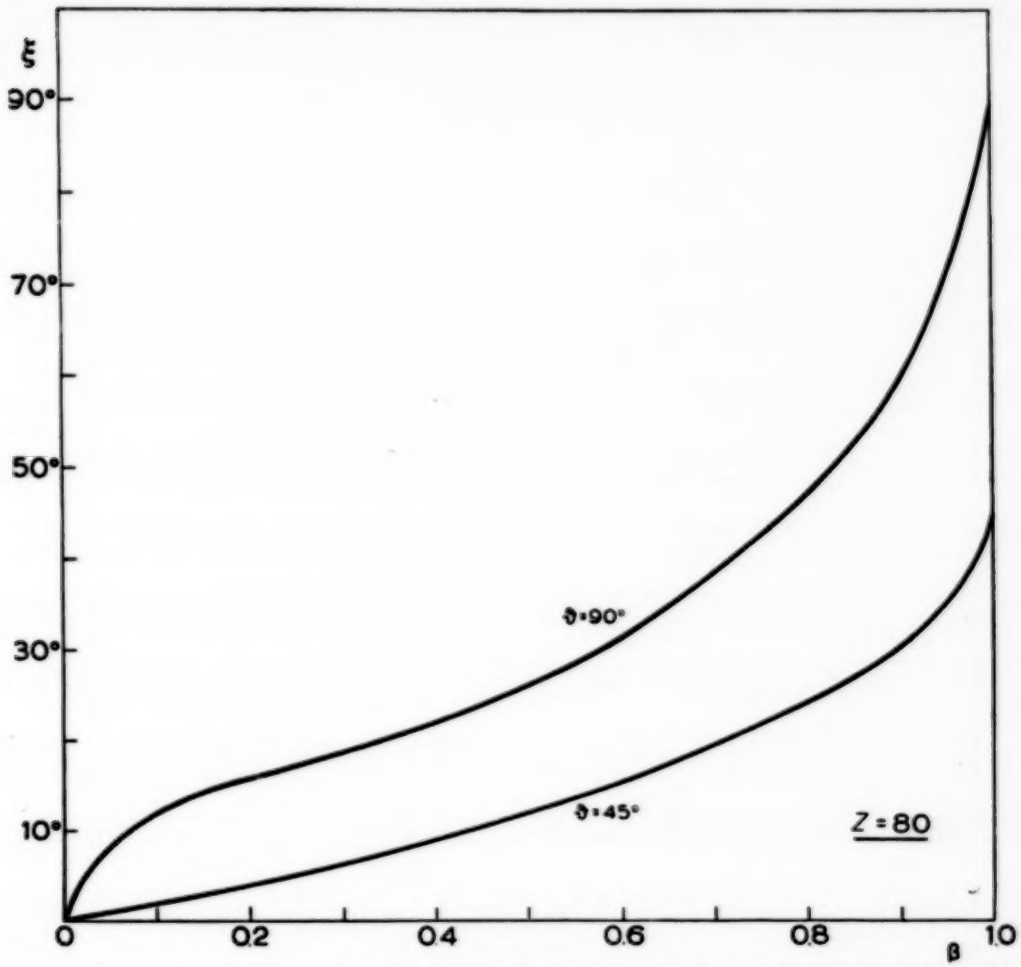


Fig. 2. Curves showing $\xi$ as a function of $\beta$ for electrons scattered at angles $\vartheta = 45°$ and $\vartheta = 90°$ by nuclei of charge $Z = 80$.

When the incident beam is not polarized, the outgoing wave, after a first scattering, presents a polarization $\mathbf{P}_f = \mathbf{P}_{f,n}$. In a second scattering, in a plane parallel to that of the first one, the cross section, given by eq. (20), presents an anisotropic term proportional to $\mathbf{P}_{f,n}$. Such a double scattering experiment is the classical one described by Mott.

The longitudinal polarization can be detected by means of a double scattering experiment in orthogonal planes. In this case the initial polarization $\mathbf{P}_i$ parallel or antiparallel to the unit vector $\mathbf{K}_i$ of the incoming direction gives rise, after the first scattering, to a component $\mathbf{P}_{f,p}$ in the scattering

plane, normal to the unit vector $\mathbf{K}_f$ of the direction of scattering, and of magnitude

$$|\mathbf{P}_{f,\nu}| = (U \sin\vartheta - V \cos\vartheta)|\mathbf{P}_1|. \tag{27}$$

In the second scattering such a component gives rise to an anisotropy

$$\begin{aligned} \Delta &= \frac{\sigma(\vartheta', \pi)-\sigma(\vartheta', 0)}{\frac{1}{2}[\sigma(\vartheta', \pi)+\sigma(\vartheta', 0)]} \\ &= \frac{4q\sqrt{1-\beta^2}\sec\frac{1}{2}\vartheta' \csc\frac{1}{2}\vartheta' \operatorname{Re} FG^*}{q^2(1-\beta^2)\csc^2\frac{1}{2}\vartheta' FF^*+\sec^2\frac{1}{2}\vartheta' GG^*}(U \sin\vartheta - V \cos\vartheta)|\mathbf{P}_1|, \end{aligned} \tag{28}$$

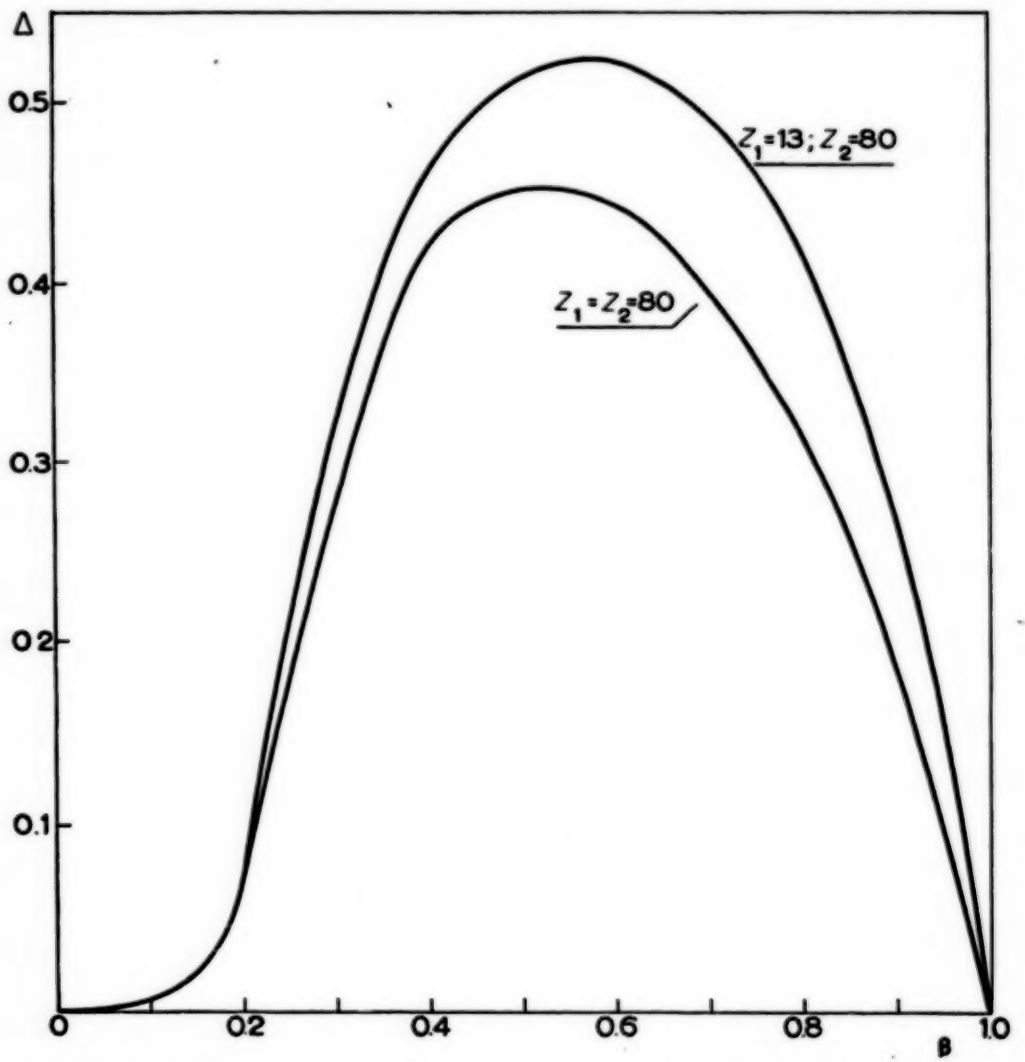


Fig. 3. Anisotropy $\Delta$ versus $\beta$ for the double scattering, in orthogonal planes, of longitudinally polarized electrons. Both scatterings are at right angle; the initial polarization is unity. Curves are computed in the case of $Z = 80$ for both targets and in the case of $Z = 13$ for the first target, $Z = 80$ for the second one.

where $\vartheta'$, $\varphi'$ are the angles of the second scattering; $\varphi' = 0$ corresponds to the electrons scattered in the direction in which the vector orthogonal to the plane of the second scattering is parallel to $\mathbf{P}_{t,p}$. In fig. 3 $\Delta$ is plotted as a function of $\beta$ for $\vartheta = \vartheta' = 90°$ in the case in which both targets have $Z = 80$, and also in the case of $Z = 13$ for the first target, $Z = 80$ for the second one.

The former results depend on the definition chosen for the polarization; it is possible, however, to pass from the polarization defined by eq. (1) to the polarization $\mathbf{P}^{(\sigma)}$ defined as the mean value of the spin momentum (in $\frac{1}{2}\hbar$ units) by means of the following equation:

$$\mathbf{P}^{(\sigma)} = \sqrt{1-\beta^2}(P_x\mathbf{I}+P_y\mathbf{J})+P_z\mathbf{K}. \tag{29}$$

The frame of reference for this equation is chosen with the $\mathbf{K}$ axis parallel to the momentum of the electrons. As stated above, in the reference system of the particle, i.e. for $\beta = 0$, $\mathbf{P}^{(\sigma)}$ is the same as $\mathbf{P}$. For $0 < \beta < 1$ if $\mathbf{P}(\mathbf{P}^{(\sigma)})$ is longitudinal, $\mathbf{P}^{(\sigma)}(\mathbf{P})$ is also longitudinal and of the same magnitude. For extremely relativistic electrons, i.e. $\beta = 1$, $\mathbf{P}^{(\sigma)}$ is always longitudinal and its magnitude is $P_z$. It follows in particular from eq. (29) that the anisotropy $\Delta$ remains unaltered of $\mathbf{P}^{(\sigma)}$ takes the place of $\mathbf{P}$ in eq. (28).

## Appendix

From eq. (2), with

$$\rho = \begin{vmatrix} \rho_{11} & \rho_{12} \\ \rho_{21} & \rho_{22} \end{vmatrix},$$

we obtain by direct computation

$$\mathbf{P} = [2\ \mathrm{Re}\ \rho_{12}\mathbf{I}+2\ \mathrm{Im}\ \rho_{12}\mathbf{J}+(\rho_{11}-\rho_{22})\mathbf{K}]/\mathrm{Tr}\ \rho.$$

From this it follows that

$$|\mathbf{P}| = [\rho_{11}^2+\rho_{22}^2+2\rho_{11}\rho_{22}-4(\rho_{11}\rho_{22}-|\rho_{12}|^2)]^{\frac{1}{2}}/\mathrm{Tr}\ \rho$$

which coincides with eq. (3) of the text.

Let us now give the proof of eq. (4). For this let us consider a spinor $a^{(\alpha)}$, where the index $\alpha$ means a component of the statistical ensemble. Choosing a system of orthonormal basis $\varphi_1$, $\varphi_2$, put

$$a^{(\alpha)} = c_1^{(\alpha)}\varphi_1+c_2^{(\alpha)}\varphi_2.$$

The density matrix depends upon $c_1^{(\alpha)}$, $c_2^{(\alpha)}$ through the equation

$$\rho_{ij} = \sum_{\alpha} c_j^{(\alpha)} c_i^{(\alpha)*} \qquad (i, j = 1, 2).$$

We then get

$$\begin{aligned}\mathrm{Det}\ \rho &= \sum_{\alpha}|c_1^{(\alpha)}|^2 \cdot \sum_{\beta}|c_2^{(\beta)}|^2-|\sum_{\alpha}c_1^{(\alpha)}c_2^{(\alpha)*}|^2 \geqq \sum_{\alpha\beta}|c_1^{(\alpha)}|^2|c_2^{(\beta)}|^2-(\sum_{\alpha}|c_1^{(\alpha)}c_2^{(\alpha)*}|)^2 \\ &= \sum_{\alpha\beta}\{|c_1^{(\alpha)}|^2|c_2^{(\beta)}|^2-|c_1^{(\alpha)}||c_2^{(\alpha)}||c_1^{(\beta)}||c_2^{(\beta)}|\} \\ &= \sum_{\alpha>\beta}\{|c_1^{(\alpha)}|^2|c_2^{(\beta)}|^2+|c_1^{(\beta)}|^2|c_2^{(\alpha)}|^2-2|c_1^{(\alpha)}||c_2^{(\beta)}||c_1^{(\beta)}||c_2^{(\alpha)}|\}.\end{aligned}$$

It follows that

$$\text{Det } \rho \geqq \sum_{\alpha > \beta} \{|c_1^{(\alpha)}||c_2^{(\beta)}| - |c_1^{(\beta)}||c_2^{(\alpha)}|\}^2 \geqq 0.$$

For a pure state the statistical ensemble has only one component; then

$$\text{Det } \rho = |c_1|^2 \, |c_2|^2 - |c_1 c_2^*|^2 \equiv 0,$$

which completes the proof.

## References

1) N. F. Mott, Proc. Roy. Soc. A **135** (1932) 429
2) H. A. Tolhoek and S. R. De Groot, Physica **17** (1951) 1
3) N. F. Mott and H. S. W. Massey, The theory of atomic collisions (Oxford, 1949) p. 74
4) H. A. Bethe and P. Morrison, Elementary nuclear theory (New York, 1956) Ch. XVII
5) N. Sherman, Phys. Rev. **103** (1956) 1601
6) J. H. Bartlett and R. E. Watson, Phys. Rev. **56** (1939) 612; see also ref.[3])

7.C *Nuclear Physics* 8 (1958) 303—309; © *North-Holland Publishing Co., Amsterdam*
Not to be reproduced by photoprint or microfilm without written permission from the publisher

# IMPULSE APPROXIMATION AND DISPERSION RELATIONS FOR PION-DEUTERON SCATTERING

FRANK KASCHLUHN

*Joint Institute of Nuclear Research, Laboratory of Theoretical Physics, Dubna, U.S.S.R.*

Received 24 February 1958

**Abstract:** The recently derived dispersion relation for elastic forward scattering of pions by unpolarized deuterons is compared with the experimental data in the Chew impulse approximation. It is shown that the dispersion relation is consistent with these data. However, for a more detailed test of the theory it is necessary to consider other $\pi-D$ processes for which the contribution from the non-observable part in the dispersion relations is not a small quantity. It is indicated that for this purpose consideration of the elastic forward scattering amplitude for spin-flip is sufficient.

## 1. Introduction

In a preceding paper [1]) we derived (under some definite assumptions) the following dispersion relation for elastic forward scattering of pions by unpolarized deuterons (ref.[1]), eq. (65)):

$$\bar{D}(E)-\bar{D}(m) = \frac{1}{2\pi^2}(E^2-m^2)\int_m^\infty \mathrm{d}E' \frac{E'\,\sigma_D(E')}{(E'^2-E^2)(E^2-m^2)} + \frac{f^2}{m^3}(E^2-m^2)[F(E)-\tfrac{1}{3}G(E)]; \tag{1}$$

$\bar{D}(E)$ is connected with the Hermitian part $D(E)$ of the scattering matrix by

$$\bar{D} = \tfrac{1}{3}\mathrm{tr}\, D \tag{2}$$

and the total cross section $\sigma_D(E)$ for pion scattering on unpolarized deuterons with the anti-Hermitian part $A(E)$ of the scattering matrix by the optical theorem

$$\sigma_D = \tfrac{1}{3}\mathrm{tr}\, A. \tag{3}$$

$E$ is the laboratory energy of the incoming pion with rest mass $m$ and $f = gm/2M$. The dimensionless quantities $F$ and $G$ are given by eqs. (60)–(63) of ref.[1]), but for our purposes it is sufficient to use the approximate eq. (64) of ref.[1]) accurate within 30 % (at any rate for a laboratory kinetic energy of 10 MeV or more) †

$$F = -0.5\frac{m^2}{E^2}, \quad \tfrac{1}{3}G = 0. \tag{4}$$

Comparison of relations (1)–(4) with the experimental scattering data is impaired by the following two difficulties:

† The connexion between $F$, $G$ and $X$, $Y$ is $F = 2.1\,X$ and $G = 2.1\,Y$, i.e. the connecting factor is 2.1 and not 0.45 as stated in ref.[1]) after eq. (65).

1) Whereas total cross section determinations for $\pi-D$ scattering have already been performed at a variety of energies (see ref.[3])), up to the present only two measurements of the cross sections and angular distributions for the individual processes have been performed, viz., the investigations of Nagle [2]) at 119 MeV and especially those of Rogers and Lederman [3]) at 85 MeV laboratory kinetic energy. However, these experiments are not sufficient for a test of the theory according to (1).

2) These measurements refer to scattering by unpolarized deuterons for which the theory of dispersion relations (without the aid of further relations) yields only an unequality as a test relation (see section 2).

However, in the case of $\pi-D$ scattering it should be sufficient to use Chew's impulse approximation [4]) which we adopt in the form of the pure-scattering model suggested by Fernbach, Green and Watson [5]). The accuracy of this approximation probably exceeds the present experimental possibilities † and we may thus assume that the errors connected with neglect of binding effects, multiple scattering and absorption phenomena are not much larger than 20 % ††. Moreover, in the special case of forward scattering we have a simple criterion of validity of the impulse approximation (see section 3) which is that the elastic $\pi-D$ scattering amplitude and the total cross section should be the direct sum of the total cross sections for scattering on free nucleons. This is fulfilled within the accuracy assumed above even in the resonance region [7]).

In section 2 the relations necessary for comparison with the experimental data will be derived and in section 3 it will be shown that the impulse approximation in fact permits one to check the dispersion relation (1).

## 2. Consequences from the Spin-Structure of the Scattering Matrix

Cheyshvili [8]) has recently determined the general spin-structure of the scattering matrix including the corresponding phase shift relations for elastic scattering of deuterons by zero spin nuclei. These formulas may be directly applied if we replace the initial and final deuteron momenta appearing in ref.[8]) by the corresponding pion momenta. The scattering matrix then has the following structure with respect to the deuteron spin $\mathbf{S}$:

$$T = a+b\mathbf{S}\cdot\mathbf{n}+c(\mathbf{S}\cdot\mathbf{n})^2+d\tfrac{1}{2}\{(\mathbf{S}\cdot\mathbf{q}_0)(\mathbf{S}\cdot\mathbf{q})+(\mathbf{S}\cdot\mathbf{q})(\mathbf{S}\cdot\mathbf{q}_0)\}; \qquad (5)$$

$a, \ldots, d$ are scalar amplitudes depending on the scattering angle and the energy of the incoming pion, the unit vectors $\mathbf{q}_0$ and $\mathbf{q}$ specify the directions of its initial and final momentum and $\mathbf{n}$ is the unit vector $(\mathbf{q}_0\times\mathbf{q})/|\mathbf{q}_0\times\mathbf{q}|$

† The measurements of Rogers and Lederman for the elastic scattering are only accurate to 40–50 % in the region of smaller angles so that the extrapolation to forward scattering is subjected to the corresponding uncertainties.

†† This is especially in accordance with the results of ref.[6]).

perpendicular to the scattering plane. In the case of forward scattering we get from the relations in ref.[8])

$$b = c = 0 \tag{6}$$

and with $\mathbf{q}_0 = \mathbf{q}$ eq. (5) becomes simply

$$T = a + d(\mathbf{S} \cdot \mathbf{q})^2. \tag{7}$$

(7) means that in contrast to pion-nucleon scattering the forward scattering amplitude for $\pi$—D scattering depends on the target spin $\mathbf{S}$. From this some complications follow for an experimental test of the dispersion relation (1) providing that one uses only experimental data pertaining to pion scattering by unpolarized deuterons.

The differential cross section for elastic scattering by unpolarized deuterons is given by

$$\frac{\mathrm{d}\sigma}{\mathrm{d}\Omega} = \tfrac{1}{3}\mathrm{tr}\, T^* T \tag{8}$$

whence we get for forward scattering, using (7),

$$\frac{\mathrm{d}\sigma}{\mathrm{d}\Omega_0} = a^* a + \tfrac{2}{3}(a^* d + a d^*) + \tfrac{2}{3} d^* d. \tag{9}$$

On the other hand the optical theorem (3) can be expressed in the form

$$\sigma_{\mathrm{D}} = \tfrac{1}{3}\mathrm{tr}\, A = \mathrm{Im}\, a + \tfrac{2}{3}\,\mathrm{Im}\, d. \tag{10}$$

Supposing the experimental quantities $\mathrm{d}\sigma/\mathrm{d}\Omega_0$ and $\sigma_{\mathrm{D}}$ to be known we may calculate another quantity from dispersion relation (1)

$$\bar{D} = \tfrac{1}{3}\mathrm{tr}\, D = \mathrm{Re}\, a + \tfrac{2}{3}\,\mathrm{Re}\, d. \tag{11}$$

From (9), (10) and (11) it then follows

$$\frac{\mathrm{d}\sigma}{\mathrm{d}\Omega_0} = |a + \tfrac{2}{3} d|^2 + \tfrac{2}{9}|d|^2 \geqq |a + \tfrac{2}{3} d|^2 \tag{12}$$

and according to (10) and (11) we can determine only the last expression in (12). We thus arrive at the result that a real test of the dispersion relation (without the aid of further relations) is in general impossible since the theory yields only an unequality as a necessary condition. Reliable answers can be given only if the quantity $(\frac{2}{9})|d|^2$ may be neglected in (12) (which, according to section 3, is true in the impulse approximation) or if the unequality (12) may be proved to be invalid (in which case the statement is clearly negative).

## 3. Comparison with the Impulse Approximation

The impulse approximation [4]) assumes that the amplitude $T$ for scattering of particles by a bound system can be written as the sum of the amplitudes $t_j$

for scattering by the corresponding free target particles, i.e., for the case of scattering by deuterons

$$T = t_{\mathrm{P}} + t_{\mathrm{N}}. \tag{13}$$

If one considers the matrix elements of $T$ between the initial state $\phi_{\mathrm{a}}$ and final state $\phi_{\mathrm{b}}$

$$\langle \phi_{\mathrm{b}} | T | \phi_{\mathrm{a}} \rangle = \langle \phi_{\mathrm{b}} | t_{\mathrm{P}} | \phi_{\mathrm{a}} \rangle + \langle \phi_{\mathrm{b}} | t_{\mathrm{N}} | \phi_{\mathrm{a}} \rangle \tag{14}$$

it may be seen [4]) that this approximation represents the scattering of the incoming particles by a wave packet of free target particles which has the same momentum distribution as the real bound state. In the pure-scattering model of Fernbach, Green and Watson [5]) for $\pi$—D scattering expression (14) may be further approximated in the form

$$\langle \phi_{\mathrm{b}} | T | \phi_{\mathrm{a}} \rangle = t^{\mathrm{P}}_{\mathrm{ab}} I^{\mathrm{P}}_{\mathrm{ab}} + t^{\mathrm{N}}_{\mathrm{ab}} I^{\mathrm{N}}_{\mathrm{ab}} \tag{15}$$

where $t^{\mathrm{P}}_{\mathrm{ab}}$ and $t^{\mathrm{N}}_{\mathrm{ab}}$ are the matrix elements for pion scattering on a free proton and neutron but whose spin states are related to the whole P—N system. $I^{\mathrm{P}}_{\mathrm{ab}}$ and $I^{\mathrm{N}}_{\mathrm{ab}}$ are some integrals depending on the special transition. The matrices $t^{\mathrm{P}}_{\mathrm{ab}}$ and $t^{\mathrm{N}}_{\mathrm{ab}}$ have the well-known spin-structure

$$t_j = u_j + i v_j \boldsymbol{\sigma}_j \cdot (\mathbf{q}' \times \mathbf{q}) \tag{16}$$

where $u_j$ and $v_j$ are scalar amplitudes, $\boldsymbol{\sigma}_j$ the proton and neutron spin vectors and $\mathbf{q}$ and $\mathbf{q}'$ the initial and final pion momenta.

In the case of elastic forward scattering the integrals $I^{\mathrm{P}}_{\mathrm{ab}}$ and $I^{\mathrm{N}}_{\mathrm{ab}}$ reduce to normalization integrals, i.e., simply to unity, whereas the spin dependence in the matrices $t^{\mathrm{P}}_{\mathrm{ab}}$ and $t^{\mathrm{N}}_{\mathrm{ab}}$ disappears owing to (16). Hence from (15)

$$\langle \phi_{\mathrm{b}} | T | \phi_{\mathrm{a}} \rangle = u^{\mathrm{P}}_{\mathrm{ab}} + u^{\mathrm{N}}_{\mathrm{ab}} \tag{17}$$

and in particular for the total cross section one obtains according to the optical theorem (3)

$$\sigma_{\mathrm{D}} = \sigma_{\mathrm{P}} + \sigma_{\mathrm{N}}, \tag{18}$$

the approximate nature of which has been discussed in the introduction. We note that the spin dependence of the scattering amplitude disappeared and consequently also the difficulties discussed in section 2.

Comparison of the dispersion relation with the results of the impulse approximation is now nearly trivial since in accord with (17) which contains only spin independent quantities it follows from (2) that

$$\bar{D} = D_{\mathrm{P}} + D_{\mathrm{N}}. \tag{19}$$

Taking into account the charge independence of the theory we may write (18) and (19) in the form

$$\bar{D} = D_+ + D_-, \qquad \sigma_{\mathrm{D}} = \sigma_+ + \sigma_- \tag{20}$$

where $D_+$, $D_-$ and $\sigma_+$, $\sigma_-$ are the Hermitian parts of the scattering matrix and the total cross section for scattering of $\pi^+$ or $\pi^-$ mesons on protons.

Now the amplitudes $D_+$ and $D_-$ satisfy the Goldberger relations [9])

$$D_+(E)+D_-(E)-[D_+(m)+D_-(m)] = \frac{1}{2\pi^2}(E^2-m^2)\int_m^\infty \mathrm{d}E' \frac{E'[\sigma_+(E')+\sigma_-(E')]}{(E'^2-E^2)(E'^2-m^2)} + 4f^2 \frac{E^2-m^2}{E^2-\left(\frac{m^2}{2M}\right)^2}\frac{1}{2M} \quad (21)$$

$$D_+(E)-D_-(E)-\frac{E}{m}[D_+(m)-D_-(m)] = \frac{1}{2\pi^2}(E^2-m^2)E\int_m^\infty \mathrm{d}E' \frac{\sigma_+(E')-\sigma_-(E')}{(E'^2-E^2)(E'^2-m^2)} + 4f^2 \frac{E^2-m^2}{E^2-\left(\frac{m^2}{2M}\right)^2}\frac{E}{m^2}. \quad (22)$$

According to (20), i.e., within the limits of the impulse approximation, the relation (21) is also the dispersion relation for $\pi^+$—D scattering and comparison with dispersion relation (1) requires that the contribution from the non-observable part be the same in both equations. We shall demonstrate that this is indeed the case within the limits of our approximation.

The contribution of the non-observable part in dispersion relation (1) becomes, using (4),

$$\frac{f^2}{m^3}(E^2-m^2)[F(E)-\tfrac{1}{3}G(E)] = -f^2\frac{E^2-m^2}{E^2}\frac{3.4}{M} \quad (23)$$

whereas the corresponding contribution in (21) may be written in the form

$$4f^2\frac{E^2-m^2}{E^2-\left(\frac{m^2}{2M}\right)^2}\frac{1}{2M} = f^2\frac{E^2-m^2}{E^2}\frac{2}{M} \quad (24)$$

where we have neglected the quantity $(m^2/2M)^2$ which is small compared to $E^2(E^2 \geqq m^2 \gg (m^2/2M)^2 = m^2/13.5^2)$. Furthermore we take into account the fact that (24) and consequently (23) are small quantities whose values are within the limits of the present experimental data or of the impulse approximation respectively. We notice that in the case of $\pi$—P scattering an experimental determination of the coupling constant $f$ is possible only because of the relatively large contribution of the non-observable part in (22): the ratio of the corresponding contributions in (22) and (21) is $E(2M/m^2) \geqq 13.5$ and the sum $D_+ + D_-$ and the difference $D_+ - D_-$ in (21) and (22) are in general of the same order of magnitude †.

## 4. Conclusion

In the last section it was shown that dispersion relation (1) for elastic forward scattering of pions by unpolarized deuterons is consistent with the results of the impulse approximation. However, a more detailed analysis revealed that the contribution to the dispersion relation resulting from inte-

† Compare for the details figs. 3, 4, and 5 in ref. [10]).

gration over the non-observable part is only a small quantity over the whole range of energy: this is by no means trivial for it is quite impossible to make a simple estimation of the order of magnitude of this quantity because of the divergences which appear and of the necessity of carrying out explicitly the analytic continuation [1]). Thus it is desirable to investigate other $\pi$—D processes for which a more detailed test of the theory would be possible, i.e., to perform a quantitative comparison of the contribution from the non-observable part. The inelastic and charge exchange $\pi$—D scattering, which also can be treated in the impulse approximation, are not very suitable since their forward scattering amplitudes vanish (it thus being necessary to consider non-forward scattering or the derivatives of the scattering matrix in the forward direction). However, it can be shown that the simpler consideration of the elastic forward scattering amplitude for spin-flip is sufficient. To this end we recall first of all that contrary to the case of no-spin-flip scattering the contribution from the non-observable part is large in the dispersion relation for the sum $D_+^{\mathrm{S}}+D_-^{\mathrm{S}}$ and small in that for the difference $D_+^{\mathrm{S}}-D_-^{\mathrm{S}}$ where $D_+^{\mathrm{S}}$ and $D_-^{\mathrm{S}}$ are the Hermitian parts of the spin-flip amplitudes for $\pi^+$—P and $\pi^-$—P scattering [11]). We now consider the general case of non-forward scattering and suppose the deuteron to be polarized perpendicular to the scattering plane. From (16) and (13) it follows for the spin-flip amplitudes using charge independence of the theory and again restricting ourselves to forward scattering

$$v_+ + v_- = \frac{1}{2i|\mathbf{q}'\times\mathbf{q}|}\{\langle\chi_{1,1}|T|\chi_{1,1}\rangle - \langle\chi_{1,-1}|T|\chi_{1,-1}\rangle\}|_{\mathbf{q}'=\mathbf{q}} \qquad (25)$$

where $\chi_{1,1}$ and $\chi_{1,-1}$ are the usual spin functions for the triplet-states. The corresponding dispersion relation for $D_+^{\mathrm{S}}+D_-^{\mathrm{S}}$ is given in ref.[11]) and [12]). (This last paper contains more general results, including non-forward scattering, but we can restrict ourselves, for practical purposes, to forward scattering.) On the other hand, we can derive for this case dispersion relations along the lines of ref.[1]), and it can be shown that now the resulting contribution from the non-observable part has the same sign as the corresponding contribution to the dispersion relation for $D_+^{\mathrm{S}}+D_-^{\mathrm{S}}$ (which should be the case if the theory is to be consistent since now the contribution from the non-observable part can be checked) †. A detailed evaluation of the integrals is in progress ††.

† Thus we may expect that it will be possible to determine the pion-nucleon coupling constant from the dispersion relation for the elastic spin-flip amplitude of pion-deuteron scattering (whereas from the dispersion relation for the corresponding no-spin-flip amplitude we can derive only an upper limit for the order of magnitude of the coupling constant corresponding to $f^2 = 0.1$).

†† *Note added in proof:* In the meantime the author has completed this work. The coupling constant was determined as $g^2/\hbar c = 18$, using Chew's impulse approximation, with an error which is, of course, a little larger than that affecting the determination by means of pion-nucleon dispersion relations. The details will be published in the near future in Nuclear Physics.

The author wishes to express his gratitude to Professor N. N. Bogolubov for his interest in this work and to the members of the Laboratory of Theoretical Physics for valuable discussions, especially to Dr. Lapidus. He would also like to thank Professor Pomeranchuk and Dr. Ioffe for interesting talks.

## References

1) F. Kaschluhn, Zs. f. Naturforsch. **13a** (1958) 183
2) D. E. Nagle, Phys. Rev. **97** (1955) 480
3) K. C. Rogers and L. M. Lederman, Phys. Rev. **105** (1957) 247
4) G. F. Chew, Phys. Rev. **80** (1950) 196;
G. F. Chew and G. C. Wick, Phys. Rev. **85** (1952) 636;
G. F. Chew and L. M. Goldberger, Phys. Rev. **87** (1952) 778
5) Fernbach, Green and Watson, Phys. Rev. **84** (1951) 1084
6) R. Rockmore, Phys. Rev. **105** (1957) 256
7) H. A. Bethe and F. de Hoffmann, Mesons and Fields (Row, Peterson and Co., Evanston, 1955) Vol. II, p. 405
8) O. D. Cheyshvili, JETP **30** (1956) 1147
9) M. L. Goldberger, Miyazawa and R. Oehme, Phys. Rev. **99** (1955) 986
10) G. Puppi and A. Stanghellini, Nuovo Cimento **5** (1957) 1305
11) R. Oehme, Phys. Rev. **100** (1955) 1503; see also W. C. Davidon and M. L. Goldberger, Phys. Rev. **104** (1956) 1119
12) N. N. Bogolubov, B. V. Medvedev and M. K. Polivanov, Problems of the Theory of Dispersion Relations (Gostekhizdat, Moscow) (in print) (abridged translation in German in Fortschr. d. Phys. **6** (1958) 169)

1.B

*Nuclear Physics* **8** (1958) 310—324; © *North-Holland Publishing Co., Amsterdam*
Not to be reproduced by photoprint or microfilm without written permission from the publisher

# CLASSIFICATION OF TRITON WAVE FUNCTIONS

G. DERRICK and J. M. BLATT

*The F.B.S. Falkiner Nuclear Research and Adolph Basser Computing Laboratories, School of Physics, The University of Sydney* †

Received 23 April 1958

**Abstract:** A classification of all angular momentum-isobaric spin functions which can be present in the ground state wave function of $H^3$ is carried out by methods of group theory. This classification, based on the behaviour of the functions under rotations of the co-ordinate axes and permutations of the three nucleons, yields three S-state functions, four P-state functions and three D-state functions. All ten states are present in $H^3$ if non-central forces exist between nucleons.

## 1. Introduction

The presence of non-central forces greatly complicates the wave function of the triton. Indeed, the only absolute quantum numbers left are

(1) the total angular momentum, $J = \frac{1}{2}$,
(2) the parity †† (even),
(3) the isobaric spin, $T = \frac{1}{2}$.

By contrast, with central forces only, we have as additional quantum numbers

(1′) the orbital angular momentum $L$,
(2′) the spin angular momentum $S$.

Furthermore, if the central forces involved are a mixture of ordinary (Wigner) and space-exchange (Majorana) forces, permutations of the positions in space of the particles (without permuting their spins or isobaric spins) are permitted, and give rise to an additional absolute quantum number, the 'partition' quantum number:

(3′) the partition of the space wave function.

In the three-body system, there are only three possible partitions (three irreducible representations of the permutation group on three things). These are: the completely symmetric representation, the completely anti-symmetric representation, and one 'mixed' representation. The matrices of

† Also supported by the Nuclear Research Foundation within the University of Sydney.
†† Recent evidence for non-conservation of parity in weak interactions is of no importance for this problem, in which the interactions are strong.

the three representations are given explicitly in appendix 3. We shall denote these three partitions by the symbols s, a and m, respectively.

The ground state of the triton under the action of central forces which are mixtures of Wigner and Majorana forces only is a symmetric $^2S_{\frac{1}{2}}$ state; that is, $L = 0$, $S = \frac{1}{2}$, and a fully symmetric space wave function.

Although the quantum numbers (1′), (2′) and (3′) fail with actual nuclear forces, they can still be used to simplify and systematize the construction of the most general wave function for the triton consistent with the absolute quantum numbers (1)—(3). This is quite analogous to, say, the construction of the deuteron wave function, as a superposition of $^3S_1$ and $^3D_1$ wave functions which are coupled to each other by the tensor force. The value of $L$ fails to be a constant of the motion, yet $L$ is useful in constructing the most general acceptable function. In the deuteron, we start out with six space coordinates for the two particles; centre-of-gravity symmetry reduces this to three coordinates (the three components of $\mathbf{r}_1 - \mathbf{r}_2$); by employing a classification according to a symmetry group (rotations of space coordinates only, quantum number $L$) which is not actually permitted by the problem, we reduce the problem from a partial differential equation in three independent variables to a set of two coupled total differential equations for the radial functions $u(r)$ and $w(r)$. This is a tremendous simplification.

This paper is devoted to making a similar simplification for the three-body problem. We start out with nine coordinates for the positions of the three particles. Centre-of-gravity symmetry reduces this to six coordinates. We can think of these six coordinates as three coordinates specifying the size and shape of the triangle formed by the three particles (for example, the three sides of the triangle: $r_{12}$, $r_{23}$ and $r_{31}$), and three Euler angles which are needed to specify the orientation in space of this triangle, relative to some standard orientation. The group classification carried out in this paper then serves to reduce the wave equation by eliminating the need to write down the Euler angle dependences explicitly. Instead of one partial differential equation in six independent variables, we arrive at a set of sixteen coupled partial differential equations with only three independent variables. Although there is clearly no hope of an exact solution of this reduced problem, the reduction is still most appreciable, and the reduced problem can and will be used as the basis of a variational calculation.

In previous work on this problem [1,2,3]) the classification has been less detailed, and the results of these authors are not easily comparable with ours. Gerjuoy and Schwinger, as well as Feshbach and Rarita, used as 'internal' coordinates (by this we mean coordinates specifying the shape and size of the triangle) the distance $r_{12}$ between two of the particles, the distance $\rho$ from the midpoint of $r_{12}$ to the third particle, and the angle $\theta$ between these two directions. This choice is unsuitable if one desires (as we do) to

make use of the permutation symmetry of the problem: whatever coordinates are chosen, they should be chosen so as to behave simply under permutations of the particles. Clapp [2]) does use more symmetrical coordinates, namely the sum of the squares of the sides of the triangle: $R^2 = r_{12}^2+r_{23}^2+r_{31}^2$, and two angular coordinates to specify the shape of the triangle. Apart from the fact that his two angles are necessarily somewhat unsymmetrically chosen, we prefer not to use Clapp's coordinates because we are envisaging calculations with repulsive core forces. A repulsive core in the nuclear force requires that the wave function vanishes whenever at least one side of the triangle is less than the core radius $r_0$. This condition is stated most simply by using the side-lengths $r_{12}$, $r_{23}$ and $r_{31}$ themselves as 'internal' coordinates, and that is what we have done here. Avery and Adams, and Pease and Feshbach [3]) used $r_{12}$, $r_{23}$ and $r_{31}$ as 'internal' coordinates, but their 'angular' functions are appreciably less symmetrically chosen than the ones we adopt here†.

## 2. Internal Wave Functions

We intend to write the final wave function as a sum of products, each product containing three factors:

(1) a factor depending on the three sides of the triangle: this is the 'internal' wave function;

2) a factor depending on the Euler angles which specify the orientation of the triangle in space: this is the 'Euler angle' wave function;

(3) a factor depending on the spin and isobaric spin indices of the three particles: this is the 'spin-isobaric-spin' wave function.

We shall construct these three types of wave functions separately, first; then we shall combine the factors (2) and (3) by the use of vector addition coefficients (Clebsch-Gordan coefficients) [4]) into 'total angular momentum' wave functions of definite symmetry type (symmetric, antisymmetric or mixed). Finally, the overall wave function of the system is obtained by combining the internal wave functions with the total angular momentum wave functions.

We shall use the following notation for the three sides of the triangle:

$$x_1 = r_{23}, \qquad x_2 = r_{31}, \qquad x_3 = r_{12}. \tag{1}$$

Permuting particles 1 and 2 interchanges $r_{13} = x_2$ and $r_{23} = x_1$, and leaves the distance $r_{12} = x_3$ invariant. Thus a permutation of the particles corresponds directly to the same permutation carried out on the internal coordinates $x_1$, $x_2$, $x_3$. An arbitrary function $f(x_1, x_2, x_3)$ may be symmetric, antisymmetric, or belong to one of the two rows of the mixed representation of the permutation group on three things. We can construct explicit examp-

† Prof. J. B. French has informed us that a classification somewhat similar to ours has been carried out by Y. Shimamoto (thesis, Rochester University).

les by considering functions of product type. Given one function $u(x)$, we can construct a symmetric function $f$:

$$f_s(x_1, x_2, x_3) = u(x_1)u(x_2)u(x_3). \tag{2}$$

If we introduce in addition a linearly independent function $v(x)$, we can construct three different functions $f$; one of them is symmetric:

$$f_s(x_1, x_2, x_3) = u(x_1)u(x_2)v(x_3)+u(x_1)v(x_2)u(x_3)+v(x_1)u(x_2)u(x_3) \tag{3}$$

and the two other functions span the mixed representation:

$$f_{m,1}(x_1, x_2, x_3) = 6^{-\frac{1}{2}}[v(x_1)u(x_2)+u(x_1)v(x_2)]u(x_3)-(\tfrac{2}{3})^{\frac{1}{2}}u(x_1)u(x_2)v(x_3), \tag{4}$$

$$f_{m,2}(x_1, x_2, x_3) = 2^{-\frac{1}{2}}[v(x_1)u(x_2)-u(x_1)v(x_2)]u(x_3). \tag{5}$$

The two functions $f_{m,k}$ transform into each other under permutations of the particles.

Finally, if we have three different functions to start with, say $u(x)$, $v(x)$, and $w(x)$, we can form six linearly independent functions each of which contains a sum of products, each product being of type $uvw$. These six linearly independent functions can be combined into one completely symmetric function, two sets of two functions, each pair belonging to the mixed representation in a way similar to (4) and (5), and finally one completely antisymmetric function, namely the determinant:

$$f_a(x_1, x_2, x_3) = \det \begin{vmatrix} u(x_1) & u(x_2) & u(x_3) \\ v(x_1) & v(x_2) & v(x_3) \\ w(x_1) & w(x_2) & w(x_3) \end{vmatrix}. \tag{6}$$

This last function is a counter-example to the statement † that "there is no anti-symmetric S-function" for the triton.

### 3. Choice of Normal Orientation of Triangle

Next, we must specify a 'normal' orientation for our triangle with sides $x_1$, $x_2$, $x_3$; thereafter the actual orientation of the triangle in space is obtained by rotating the triangle from its normal position to its actual position, and the rotation which achieves this is specified by three Euler angles $\alpha, \beta, \gamma$ in the usual way. For example, one could specify the 'normal' position of the triangle as one in which the triangle lies in the $xy$-plane, with its centre of gravity at the origin of coordinates and particle number 1 somewhere on the $x$-axis. Although such a specification appeals by its apparent simplicity, it fails to satisfy our criterion of simple behaviour under permutations of the particles: The first two statements (triangle in $xy$-plane, centre of gravity at origin) are indeed invariant under permutations of the

† R. G. Sachs, ref. [5]); as a result, Sachs gets two S-state functions, and three P-state functions, compared with our three S-state and four P-state functions.

particles, and we do retain them for our final specification of the 'normal' position. The third statement (particle number 1 on $x$-axis) is however blatantly dependent on which particle is called number 1, and is therefore unacceptable to us.

Accepting that the triangle is going to lie in the $xy$-plane in its 'normal' position, with its centre of gravity at the origin, it remains to find a permutation-invariant specification of an '$x$-axis' and a '$y$-axis' within the triangle. There are two specifications which have the virtue of simplicity:

1) We may compute the two principal axes of inertia of the triangle, and make the axis associated with the larger moment of inertia our $x$-axis.

2) The $x$-axis may be chosen as the invariant 'Euler line' within the triangle; this is the line through the following three points: the centre of gravity, the intersection of the normals drawn from the three vertices to the opposite sides (orthocentre), and the intersections of the normals through the midpoints of the three sides (circumcentre).

Possibility (1) has the disadvantage that the principal axes of inertia do not specify two directions in space, but rather two undirected lines; the $x$-axis is specified only up to a $\pm$ sign, and the same is true of the $y$-axis. Possibility (2) above has the advantage that the $x$-axis is defined uniquely as a directed line in space; however, the final expressions obtained with this choice are appreciably more complicated than with choice (1).

If one uses specification (1), some of the Euler-angle wave functions are double-valued; this is a nuisance, but it is less so than appears at first sight. It turns out that wave functions of even parity are necessarily single valued, and only these wave functions are of interest for the ground state of the triton.

Later on, when we shall extend the theory to include scattering states of odd parity, it will still be possible to overcome the sign ambiguity inherent in the choice (1) by coupling it with choice (2) in the following way: The wave functions are determined with choice (1), but their phases are normalized by comparison with (2). We have not worked out the details of this approach in our present investigation, but we are convinced it can be done without excessive effort, and indeed with much less effort than would be involved in the full use of specification (2).

We specify the $z$-axis of our triangle in its normal position as an axis perpendicular to the plane of the triangle (the $xy$-plane) and directed in such a way that traversing the triangle from particle 1 to 2, thence to particle 3, and then back again to 1, amounts to a counterclockwise walk around the $z$-axis. Hence the specification of the $z$-axis is invariant under even permutations of the three particles, and the $z$-axis reverses its direction if any two particles are exchanged.

The choice of the sense of the $x$-axis (the $\pm$ sign) is left open; once this

choice has been made, however, the $y$-axis must have its sense adjusted in such a way that $x$, $y$ and $z$ form a right-handed set of axes. We therefore have only one undetermined sign in our 'normal' position of the triangle, and it turns out that all even-parity wave functions are independent of the choice of this sign.

## 4. Euler Angle Wave Functions

Since the Euler angle wave function is by definition independent of the internal coordinates $x$ of the triangle, we may as well consider the triangle rigid for this part of the investigation. The Euler angle wave functions for a rigid molecule are well-known, however [4]). They are just the representation coefficients of the irreducible representations of the rotation group. The Euler angle function for orbital angular momentum $L$, $z$-component thereof $M_L$, and body-$z$-component $\mu$ is given by

$$D^L_{\mu M_L}(\alpha, \beta, \gamma) = \sum_\kappa i^{2\kappa+\mu+M_L} \frac{\sqrt{(L+\mu)!(L-\mu)!(L+M_L)!(L-M_L)!}}{\kappa!(L+M_L-\kappa)!(L-\mu-\kappa)!(\kappa+\mu-M_L)!} \quad (7)$$
$$\times e^{i\mu\alpha}(\cos\tfrac{1}{2}\beta)^{2L+M_L-\mu-2\kappa}(\sin\tfrac{1}{2}\beta)^{2\kappa+\mu-M_L}e^{iM_L\gamma};$$

the index $\kappa$ takes all integral values between the larger of 0 and $M_L-\mu$ and the smaller of $M_L+L$ and $L-\mu$. For each value of $L$, there are $2L+1$ values of $\mu$ and the same number of values of $M_L$. The $2L+1$ values of $M_L$ represent a necessary degeneracy; and these functions will later on be combined with spin functions with an index $M_S$, so as to give eigenfunctions of the total angular momentum $J$ and $z$-component $M_J$. On the other hand, the index $\mu$ labels different functions, which cannot be obtained from each other by rotations of the space axes (they can be obtained from each other by rotations of the 'normal' position of the triangle, but this is an 'internal' operation). Thus there are three essentially different P-states, five essentially different D-states, and so on.

However, not all these states have even parity. For example, consider the P-states. We can construct three linearly independent P-states by forming three linearly independent vectors out of the two basic vectors $\mathbf{r}_{12} = \mathbf{r}_1 - \mathbf{r}_2$ and $\mathbf{r}_{23} = \mathbf{r}_2 - \mathbf{r}_3$ (the third vector, $\mathbf{r}_{31}$, is the sum of $\mathbf{r}_{12}$ and $\mathbf{r}_{23}$ and thus linearly dependent). Three such vectors are, for example

$$\mathbf{r}_{12},\ \mathbf{r}_{23},\ \text{and}\ \ \mathbf{r}_{12}\times\mathbf{r}_{23}.$$

All three are P-state functions, but clearly the first two change sign under inversion of the space axes, whereas the third one is unchanged by this operation (i.e. the first two are vectors, the third one is a pseudovector). We conclude that, of the three linearly independent P-state functions, one has even parity, the other two have odd parity.

In general, it can be shown that the parity operation $\Pi$ applied to the Euler angle function (7) gives

$$\Pi D^L_{\mu M_L}(\alpha, \beta, \gamma) = (-1)^\mu D^L_{\mu M_L}(\alpha, \beta, \gamma). \tag{8}$$

Thus functions with even $\mu$ have even parity, functions with odd $\mu$ have odd parity. In the case of P-states, we have one function ($\mu = 0$) with even parity, and two functions ($\mu = 1$ and $\mu = -1$) with odd parity. The even parity function is proportional to $\mathbf{r}_{12} \times \mathbf{r}_{23}$, the odd parity functions are linear combinations of the vectors $\mathbf{r}_{12}$ and $\mathbf{r}_{23}$.

Taking states of even parity only, we therefore have one S-state, one P-state, and three D-state functions, the latter corresponding to $\mu = 0$, $\mu = 2$, and $\mu = -2$. Since the ground state $J$ of the triton is $\frac{1}{2}$, and the maximum spin $S$ is $\frac{3}{2}$, the orbital angular momentum $L$ cannot exceed two, and thus these five Euler angle functions suffice for the ground state of the triton.

It will be convenient to define our basic Euler angle functions in such a way that they are 'real' under the time reversal operation [6,7]. In addition we require that the functions be normalized so that the integral of their square over all orientations of the triangle is unity. The functions are automatically orthogonal to each other. This leads to the following five basic functions:

$$\text{S-state: } Y_0^0(\text{s}, 0) = 2^{\frac{1}{2}}/4\pi; \tag{9}$$

$$\text{P-state: } Y_M^1(\text{a}, 0) = \frac{i6^{\frac{1}{2}}}{4\pi} D^1_{0M}(\alpha, \beta, \gamma); \tag{10}$$

$$\text{D-state, } \mu = 0\text{: } Y_M^2(\text{s}, 0) = \frac{(10)^{\frac{1}{2}}}{4\pi} D^2_{0M}(\alpha, \beta, \gamma); \tag{11}$$

D-state, $|\mu| = 2$, symmetric:

$$Y_M^2(\text{s}, 2) = \frac{-5^{\frac{1}{2}}}{4\pi} [D^2_{2,M}(\alpha, \beta, \gamma) + D^2_{-2,M}(\alpha, \beta, \gamma)]; \tag{12}$$

D-state, $|\mu| = 2$, antisymmetric:

$$Y_M^2(a, 2) = \frac{-i5^{\frac{1}{2}}}{4\pi} [D^2_{2,M}(\alpha, \beta, \gamma) - D^2_{-2,M}(\alpha, \beta, \gamma)]. \tag{13}$$

We have used the notation $Y_M^L(\text{P}_e, |\mu|)$ for a state with permutation symmetry $\text{P}_e$(= s or a), and with body-$z$-component of angular momentum $\pm\mu$. ($|\mu| = 0, 2, \ldots, L$ or $L-1$).

All these functions have even parity; the P-state function and the last D-state function change sign under odd permutations of the particles (i.e., they belong to the antisymmetric irreducible representation of the permutation group); the other functions are invariant under permutations of the particles. With our highly symmetric choice of the 'normal' position of the triangle, the Euler angle functions must be either symmetric or antisymmetric under permutations; the mixed representation cannot occur.

## 5. Spin-Isobaric-Spin Wave Functions

The classification of the possible spin-isobaric-spin wave functions has been carried out in detail elsewhere †. The functions in question are called $V_{M_S \kappa}(P_t, T, S)$, where $P_t$ stands for the permutation symmetry (symmetric, antisymmetric, or mixed), $T$ is the total isobaric spin quantum number, which must equal $\frac{1}{2}$ or $\frac{3}{2}$, $M_S$ is the $z$-component of the spin, and $\kappa$ is the row index to distinguish the two different functions which appear in the case of mixed symmetry. The $\zeta$-component of the isobaric spin is fixed by the requirement that the function describes a triton (or, alternatively, a $He^3$ nucleus); we have therefore omitted this index.

These functions are given in detail in appendix 2. Here we merely list the possible values of $P_t$ and $S$ consistent with $T = \frac{1}{2}$:

Doublet functions $S = \frac{1}{2}$:

one symmetric function,
one antisymmetric function,
one set of two functions of mixed symmetry.

Quartet functions, $S = \frac{3}{2}$:

one set of two functions of mixed symmetry.

## 6. Total Angular Momentum Eigenfunctions

We now combine the Euler angle wave functions with the spin-isobaric-spin wave functions by the use of vector addition coefficients in the standard way [4]), so as to get eigenfunctions of the total angular momentum $J$ and its $z$-component $M_J$. We leave the details to appendix 3. Since the triton ground state has $J = \frac{1}{2}$, experimentally, this is the only value of $J$ of concern to us here. Furthermore, there is no loss of generality in restricting ourselves to $M_J = \frac{1}{2}$, since the state with $M_J = -\frac{1}{2}$ can be obtained from this by a rotation of the coordinate system.

Since there are three distinct possibilities for doublet state spin-isobaric spin functions, and only one possibility each for Euler angle functions with $L = 0$ and $L = 1$, we get three distinct $^2S_{\frac{1}{2}}$ states and three distinct $^2P_{\frac{1}{2}}$ states. The three $^2S$ states differ from each other by their behaviour under permutations of the particles, i.e., there is one symmetric $^2S_{\frac{1}{2}}$ wave function, one antisymmetric $^2S_{\frac{1}{2}}$ wave function, and a set of two $^2S_{\frac{1}{2}}$ wave functions which belong to the mixed symmetry representation.

We do *not* count the two functions belonging to the two rows of the mixed symmetry representation as two separate functions, since both functions must be combined linearly in a certain, predetermined way in order to get complete wave functions (including the dependence on the internal coordinates of the triangle) which are properly antisymmetric in accordance with the Pauli principle. Thus the two functions of the mixed symmetry rep-

† See J. M. Blatt ref. [8]); especially the appendix.

resentation finally give rise to only one acceptable overall wave function for the system.

On the other hand, there is just one spin-isobaric spin function for the quartet state (or rather, two functions which together span the representation of mixed symmetry). Hence there is only one kind of $^4P_{\frac{1}{2}}$ state, namely one of mixed symmetry. Since there are three distinct D-state Euler angle functions, there are also three distinct $^4D_{\frac{1}{2}}$ wave functions, all of them pairs of functions spanning the mixed symmetry representation.

## 7. Over-all Wave Functions

In order to get fully antisymmetric final wave functions, a symmetric internal wave function (e.g., (2) or (3)) must be combined with an anti-symmetric total angular momentum function (i.e. the anti-symmetric $^2S_{\frac{1}{2}}$ function, or the anti-symmetric $^2P_{\frac{1}{2}}$). Such an internal wave function *cannot* be combined with the $^4P_{\frac{1}{2}}$ wave function or with any one of the three $^4D_{\frac{1}{2}}$ wave functions, since all these functions belong to the mixed symmetry representation.

An anti-symmetric internal wave function, such as (6) for example, must be combined with a fully symmetric total angular momentum function, i.e., either the symmetric $^2S_{\frac{1}{2}}$ function, or the symmetric $^2P_{\frac{1}{2}}$ function.

Finally, a pair of internal wave functions of mixed symmetry type (e.g., the pair (4) and (5)) can be combined with a pair of total angular momentum wave functions of mixed symmetry type (e.g., the pair of wave functions for the $^4P_{\frac{1}{2}}$ state) in exactly one way so as to produce an over-all antisymmetric function.

Altogether we get ten different possibilities, which are listed in table 1 below, and given explicitly in appendix 4.

TABLE 1

Classification of Triton Wave Functions

| Spectroscopic Classification | $L$ | $S$ | Permutation Symmetry | | | $\lvert\mu\rvert$ |
|---|---|---|---|---|---|---|
| | | | Internal | Euler Angles | Spin-Iso-spin | |
| $^2S_{\frac{1}{2}}$ | 0 | $\frac{1}{2}$ | s | s | a | 0 |
| | 0 | $\frac{1}{2}$ | a | s | s | 0 |
| | 0 | $\frac{1}{2}$ | m | s | m | 0 |
| $^2P_{\frac{1}{2}}$ | 1 | $\frac{1}{2}$ | s | a | s | 0 |
| | 1 | $\frac{1}{2}$ | a | a | a | 0 |
| | 1 | $\frac{1}{2}$ | m | a | m | 0 |
| $^4P_{\frac{1}{2}}$ | 1 | $\frac{3}{2}$ | m | a | m | 0 |
| $^4D_{\frac{1}{2}}$ | 2 | $\frac{3}{2}$ | m | s | m | 0 |
| | 2 | $\frac{3}{2}$ | m | s | m | 2 |
| | 2 | $\frac{3}{2}$ | m | a | m | 2 |

## 8. Discussion

Table 1 and appendix 6 contain the essential results of this paper. All the functions listed in table 1 may, and presumably do, contribute to the total wave function of the triton in its ground state.

It is of interest, however, to estimate which of these ten functions are likely to be most important, i.e., which of them will give the main contribution to the total normalization integral. We have two clues for this:

(1) the symmetry character of the internal wave function,

(2) the symmetry character of the tensor force.

In the absence of any spin-orbit coupling, the ground state of the triton is a pure $^2S_{\frac{1}{2}}$ state. Furthermore, if the forces are not only central forces but also not explicitly dependent on spin (i.e., are mixtures of Wigner and Majorana forces) the symmetry of the internal wave function is a good quantum number, and the ground state of the system is one in which the internal wave function is fully symmetric. This point can be seen as follows: Other things being equal, a fully symmetric internal wave function need not be zero for any shape of the triangle. A pair of wave functions belonging to the mixed symmetry type (e.g., the functions (4) and (5)) is necessarily zero whenever the triangle formed by the three particles is equilateral, i.e., whenever $x_1 = x_2 = x_3$. Finally, a fully antisymmetric internal wave function such as (6) is necessarily zero whenever the triangle formed by the three particles is isosceles (for then two columns of the determinant (6) become identical). The more zeros a function possesses, the more it is forced to change, and hence the larger its derivatives and the larger the kinetic energy associated with such a function. Another way of saying the same thing is that we could form a fully symmetric internal wave function from just one function $u(x)$; we needed two independent functions, $u(x)$ and $v(x)$, to form functions of mixed symmetry type; and we needed three independent functions, $u$, $v$ and $w$, to form a fully anti-symmetric internal function. If these functions $u$, $v$, $w$, are chosen (for example) as eigenfunctions of some one-dimensional wave equation, then $u(x)$ has no nodes, $v(x)$ has one node, and $w(x)$ has two nodes.

Thus in the absence of any spin-orbit coupling, and with central forces of Wigner and Majorana types only, the entire wave function of the triton ground state is of the type described by the first line of table 1.

The main type of spin-orbit coupling in the triton is the tensor force †. The tensor operator is defined by

$$S_{12} = 3(\boldsymbol{\sigma}_1 \cdot \mathbf{e})(\boldsymbol{\sigma}_2 \cdot \mathbf{e}) - \boldsymbol{\sigma}_1 \cdot \boldsymbol{\sigma}_2 \qquad (14)$$

† A force proportional to $\mathbf{L} \cdot \mathbf{S}$ is generally believed to exist as well, but it is of very short range, and hence qualitatively of less importance. However, it is undoubtedly true that the presence of such a force will result in larger admixtures of P-states than can be expected with tensor forces only.

where $\boldsymbol{\sigma}_i$ is the Pauli spin vector for the $i$'th particle, and $\mathbf{e}$ is a unit vector in the direction from particle 1 to particle 2. This operator may be considered as the scalar product of two tensors of rank 2, one formed from the components of $\mathbf{e}$, and the other from bilinear combinations of the components of $\boldsymbol{\sigma}_1$ and $\boldsymbol{\sigma}_2$. A tensor of rank 2 formed from the components of one space vector corresponds to a reducible representation of the rotation group, with irreducible parts belonging to $L = 0$, 1 and 2 respectively. In the case of the tensor operator, the permutation symmetry of the tensor excludes the $L = 1$ part, and the construction is made in such a way that the average over all directions of $\mathbf{e}$ is zero, i.e., so that the $L = 0$ part drops out as well. We therefore have a pure $L = 2$ operator.

Since the ground state of the triton is pure $^2S_{\frac{1}{2}}$ in the absence of the tensor force, we expect that the $^2S_{\frac{1}{2}}$ state is also dominant when the tensor force is present. Since the tensor force behaves like $L = 2$, it couples D-states to this S-state, but does not couple in the P-states in first order; the P-states occur only in second order, as far as the tensor force is concerned.

This argument leads us to believe that the most important components of the full triton wave function are the first line of table 1 (the dominant S-state) and the last three lines of the table (the three D-states). It would be nice if one of these three D-states were much more important than the other two. Unfortunately, this is not the case. The internal wave functions all have the same symmetry (mixed), and thus allow no discrimination on that score; and the matrix elements of the tensor operator to all three $^4D_{\frac{1}{2}}$ states in table 1 are of the same general order of magnitude †. Furthermore, earlier calculations [2,3]) indicate very strongly that explicit inclusion of all three $^4D$ functions is necessary to get good results for the triton from a variational calculation ††.

Finally, the states which are likely to be *least* important in the triton are states with anti-symmetric internal wave functions, i.e., the second and

† The matrix elements of the kinetic energy operator and of all the standard types of potential energy operators, including the tensor force and the $\mathbf{L} \cdot \mathbf{S}$ force, have been worked out and will be published later.

†† Clapp [2]) does distinguish between the D-state functions through a quantum number $K$; $K = 2$ for one of the D-states, and $K = 4$ for the other two D-states which Clapp uses in his calculation. His method of classification differs from ours in that his 'internal' wave function depends on only one coordinate, namely $R^2 = x_1^2 + x_2^2 + x_3^2$. Thus Clapp has infinitely many D-states, fo which the three mentioned before are the ones associated with the lowest values of his quantum number $K$. The quantum number $K$ is associated with the 'angular' part of the kinetic energy, and a larger $K$ means more kinetic energy, hence less importance for the corresponding part of the wave function. However Clapp finds that the S-state alone gives a binding energy of the triton of 1.80 MeV, the $K = 2$ D-state raises this to 3.88 MeV, and inclusion of the two $K = 4$ D-states raises this to 5.79 MeV. Furthermore, the $K = 2$ D-state contributes 2.6 percent to the normalization integral, whereas the two $K = 4$ D-states together contribute 2.0 percent. We conclude that the value of the quantum number $K$ as a 'significance index' should not be overrated.

fifth entry in table 1. The kinetic energy associated with these states is likely to be so large that no serious error is made by omitting them altogether from a variational calculation, and this is what we intend to do. If desired, these states can be included at the end by a perturbation treatment applied to the variational function.

One of us (G.D.) would like to thank the Australian Atomic Energy Commission for the grant of a postgraduate research studentship, which has enabled him to carry out this work.

## Appendix 1.

### THE IRREDUCIBLE REPRESENTATIONS OF THE SYMMETRIC GROUP OF DEGREE 3.

The six elements of the group of permutations on three objects are (1), (123), (132), (12), (23) and (31), where we use the cycle notation. Of these the first three are even, and the remaining three odd.

There are three irreducible representations of this group, the 'symmetric', the 'antisymmetric' and the 'mixed' representations [4]). The first represents all permutations by 1. In the antisymmetric representation the even permutations are mapped on to 1, and the odd permutations on to $-1$. The mixed representation is two dimensional, the matrices for the elements in the above order being

$$\begin{pmatrix}1 & 0\\ 0 & 1\end{pmatrix}, \quad \begin{pmatrix}-\frac{1}{2} & -\frac{1}{2}\sqrt{3}\\ \frac{1}{2}\sqrt{3} & -\frac{1}{2}\end{pmatrix}, \quad \begin{pmatrix}-\frac{1}{2} & \frac{1}{2}\sqrt{3}\\ -\frac{1}{2}\sqrt{3} & -\frac{1}{2}\end{pmatrix},$$

$$\begin{pmatrix}1 & 0\\ 0 & -1\end{pmatrix}, \quad \begin{pmatrix}-\frac{1}{2} & \frac{1}{2}\sqrt{3}\\ \frac{1}{2}\sqrt{3} & \frac{1}{2}\end{pmatrix}, \quad \begin{pmatrix}-\frac{1}{2} & -\frac{1}{2}\sqrt{3}\\ -\frac{1}{2}\sqrt{3} & \frac{1}{2}\end{pmatrix}.$$

These are simply the two dimensional rotations and reflections which transform into itself an equilateral triangle with centroid at the origin and a vertex on one axis.

In complete analogy with the Clebsch-Gordan coefficients of the Rotation Group, there exist a set of addition coefficients for combining representation base functions which involve coordinates of different type. Let $\psi^{P_1}_{\kappa_1}(1', 2', 3')$ be a function which belongs to the row $\kappa_1$ of the representation with permutation symmetry $P_1$ when we make permutations of the variables $(1', 2', 3')$. Similarly let $\psi^{P_2}_{\kappa_2}(1'', 2'', 3'')$ belong to row $\kappa_2$ of the representation with symmetry $P_2$ for permutations of the coordinates $(1'', 2'', 3'')$. These two different sets of coordinates $(1', 2', 3')$ and $(1'', 2'', 3'')$ might be, for example, the spin variables and the isobaric-spin variables. Then we can form orthonormal linear combinations of products of the form

$$\psi^{P_1 P_2 P}_{\kappa} = \sum_{\kappa_1 \kappa_2} \left(\begin{matrix}P_1 & P_2 & P\\ \kappa_1 & \kappa_2 & \kappa\end{matrix}\right) \psi^{P_1}_{\kappa_1}(1', 2', 3')\psi^{P_2}_{\kappa_2}(1'', 2'', 3'')$$

which belong to row $\kappa$ of the representation with symmetry P for *joint* permutations of (1′, 2′, 3′) and (1″, 2″, 3″), i.e. where we carry out the same permutation on both sets of coordinates.

The coefficients $\binom{P_1\,P_2\,P}{\kappa_1\,\kappa_2\,\kappa}$ are unique † apart from arbitrary phase factors, which are here chosen to make all coefficients real. The non-zero values of $\binom{P_1\,P_2\,P}{\kappa_1\,\kappa_2\,\kappa}$ are then

$$\binom{s\ s\ s}{1\ 1\ 1} = \binom{s\ a\ a}{1\ 1\ 1} = \binom{a\ s\ a}{1\ 1\ 1} = \binom{a\ a\ s}{1\ 1\ 1} = 1,$$

$$\binom{s\ m\ m}{1\ \kappa\ \lambda} = \binom{m\ s\ m}{\kappa\ 1\ \lambda} = \sqrt{2}\binom{m\ m\ s}{\kappa\ \lambda\ 1} = \delta_{\kappa\lambda},$$

$$\binom{a\ m\ m}{1\ \kappa\ \lambda} = \binom{m\ a\ m}{\kappa\ 1\ \lambda} = -\sqrt{2}\binom{m\ m\ a}{\kappa\ \lambda\ 1} = \binom{0\ \ -1}{1\ \ \ 0}_{\kappa\lambda},$$

$$-\binom{m\ m\ m}{1\ 1\ 1} = \binom{m\ m\ m}{1\ 2\ 2} = \binom{m\ m\ m}{2\ 1\ 2} = \binom{m\ m\ m}{2\ 2\ 1} = \frac{1}{\sqrt{2}}.$$

The coefficients $\binom{P_1\,P_2\,P}{\kappa_1\,\kappa_2\,\kappa}$ satisfy the orthogonality relations

$$\sum_{\kappa_1\kappa_2}\binom{P_1\,P_2\,P}{\kappa_1\,\kappa_2\,\kappa}\binom{P_1\,P_2\,P'}{\kappa_1\,\kappa_2\,\kappa'} = \delta_{PP'}\,\delta_{\kappa\kappa'},$$

$$\sum_{P\kappa}\binom{P_1\,P_2\,P}{\kappa_1\,\kappa_2\,\kappa}\binom{P_1\,P_2\,P}{\kappa'_1\,\kappa'_2\,\kappa} = \delta_{\kappa_1\kappa'_1}\,\delta_{\kappa_2\kappa'_2}.$$

## Appendix 2

SPIN AND ISOBARIC-SPIN FUNCTIONS FOR THE TRITON [9])

Let $\alpha$ and $\beta$ denote the spin functions for a particle with spin up and spin down respectively. The spin functions of a three-particle system with $M_S = \frac{1}{2}$ may then be written

$$q_1 = 6^{-\frac{1}{2}}[\beta(1)\alpha(2)+\alpha(1)\beta(2)]\alpha(3)-(\tfrac{2}{3})^{\frac{1}{2}}\alpha(1)\alpha(2)\beta(3)$$
$$q_2 = 2^{-\frac{1}{2}}[\beta(1)\alpha(2)-\alpha(1)\beta(2)]\alpha(3)$$
$$q_3 = 3^{-\frac{1}{2}}[\alpha(1)\alpha(2)\beta(3)+\alpha(1)\beta(2)\alpha(3)+\beta(1)\alpha(2)\alpha(3)].$$

The pair of functions $(q_1, q_2)$ belongs to the mixed representation of the permutation group, and has total spin $S = \frac{1}{2}$. The function $q_3$ is completely symmetric in all spin variables and has total spin $S = \frac{3}{2}$.

In an analogous way we can construct three isobaric-spin functions with $T_\zeta = -\frac{1}{2}$: a mixed pair $(v_1, v_2)$ with total isobaric spin $T = \frac{1}{2}$, and a symmetric function $v_3$ with total isobaric spin $T = \frac{3}{2}$.

† The reduced form of the direct product of two irreducible representations of the Symmetric Group of degree 3 contains no representation more than once, at most. However with Permutation Groups of higher degree the direct product of two irreducible representations may contain the same representation more than once, in which case the corresponding addition coefficients would not be unique.

From the three spin functions $q_1$, $q_2$ and $q_3$, and the three isobaric-spin functions $v_1$, $v_2$ and $v_3$ we can form nine linearly independent combinations of products, each of which transforms under joint permutations of spin and isobaric-spin coordinates according to one of the three irreducible representations of the permutation group. Using the previously defined notation $V_{M_S\kappa}(\mathrm{P_t}, T, S)$ these nine spin-isobaric-spin functions are (omitting the index $\kappa$ for one dimensional representations)

$$
\begin{aligned}
V_{\frac{1}{2}}\,(\mathrm{s},\ \tfrac{1}{2},\tfrac{1}{2}) &= 2^{-\frac{1}{2}}(v_1q_1+v_2q_2)\\
V_{\frac{1}{2}}\,(\mathrm{s},\ \tfrac{3}{2},\tfrac{3}{2}) &= v_3q_3\\
V_{\frac{1}{2}}\,(\mathrm{a},\ \tfrac{1}{2},\tfrac{1}{2}) &= 2^{-\frac{1}{2}}(v_1q_2-v_2q_1)\\
V_{\frac{1}{2}1}(\mathrm{m},\tfrac{1}{2},\tfrac{1}{2}) &= -2^{-\frac{1}{2}}(v_1q_1-v_2q_2)\\
V_{\frac{1}{2}2}(\mathrm{m},\tfrac{1}{2},\tfrac{1}{2}) &= 2^{-\frac{1}{2}}(v_1q_2+v_2q_1)\\
V_{\frac{1}{2}1}(\mathrm{m},\tfrac{1}{2},\tfrac{3}{2}) &= v_1q_3\\
V_{\frac{1}{2}2}(\mathrm{m},\tfrac{1}{2},\tfrac{3}{2}) &= v_2q_3\\
V_{\frac{1}{2}1}(\mathrm{m},\tfrac{3}{2},\tfrac{1}{2}) &= v_3q_1\\
V_{\frac{1}{2}2}(\mathrm{m},\tfrac{3}{2},\tfrac{1}{2}) &= v_3q_2.
\end{aligned}
$$

Since we have assumed that the ground state of $H^3$ has the good quantum number $T=\frac{1}{2}$, the three $T=\frac{3}{2}$ functions formed from $v_3$ will not be needed.

## Appendix 3

### THE TOTAL ANGULAR MOMENTUM-ISOBARIC SPIN WAVE FUNCTIONS

We have to form linear combinations of products of the Euler angle functions $Y^L_{M_L}(\mathrm{P_e}, \mu)$ and spin-isobaric-spin functions $V_{M_S\kappa}(\mathrm{P_t}, T, S)$ which transform under 'complete' rotations and joint Euler angle-spin-isotopic-spin coordinate permutations according to a definite representation of the appropriate group. These total angular momentum-isobaric-spin functions will then be specified by the 'total' quantum numbers $J$, $T$ and permutation symmetry P, with corresponding row numbers $M_J$, $T_\zeta$ and $\kappa$, and the 'intermediate' quantum numbers $L$, $S$, $\mathrm{P_e}$, $\mathrm{P_t}$ and $\mu$. We denote these functions by $\mathscr{Y}_{M_J T_\zeta \kappa}(J, L, S, P, P_e, \mathrm{P_t}, \mu)$. Then, using the Permutation Group addition coefficients $\left(\begin{smallmatrix}\mathrm{P_1} & \mathrm{P_2} & \mathrm{P}\\ \kappa_1 & \kappa_2 & \kappa\end{smallmatrix}\right)$ defined in appendix 1,

$$
\begin{aligned}
&\mathscr{Y}_{M_J T_\zeta \kappa}(J, L, S, \mathrm{P}, \mathrm{P_e}, \mathrm{P_t}, \mu)\\
&\quad = \sum_{M_L M_S \kappa_t} \begin{pmatrix}\mathrm{P_e} & \mathrm{P_t} & \mathrm{P}\\ 1 & \kappa_t & \kappa\end{pmatrix} (LSM_LM_S|LSJM_J)Y^L_{M_L}(\mathrm{P_e}, \mu)\cdot V_{M_S\kappa_t}(\mathrm{P_t}, T, S).
\end{aligned}
$$

Taking $J=\frac{1}{2}$, $M_J=\frac{1}{2}$, $T=\frac{1}{2}$ and $T_\zeta=-\frac{1}{2}$ we obtain ten distinct states, where a pair of mixed representation functions is counted as one state.

## Appendix 4

THE OVERALL WAVE FUNCTIONS

Our ten overall wave functions for the triton are of the form

$$\sum_{\kappa' \kappa} \begin{pmatrix} P' & P & a \\ \kappa' & \kappa & 1 \end{pmatrix} f^{P'}_{\kappa'}(\chi, r_{23}, r_{31}, r_{12}) \mathscr{Y}_{\frac{1}{2}-\frac{1}{2}\kappa}(\chi)$$

where $\chi$ stands for any of the ten possible values of $(J, L, S, P, P_s, P_t, \mu)$ listed in table 1. In order that the Permutation Group addition coefficients $\begin{pmatrix} P' & P & a \\ \kappa' & \kappa & 1 \end{pmatrix}$ be non-zero, we must choose the permutation symmetry P' of the internal wave function $f^{P'}_{\kappa'}(\chi, r_{23}, r_{31}, r_{12})$ 'adjoint' to the symmetry P of the angular momentum-isobaric-spin function $\mathscr{Y}_{\frac{1}{2}-\frac{1}{2}\kappa}(\chi)$ i.e.

$$\begin{aligned} P' &= a \quad \text{if} \quad P = s \\ &= s \quad \text{if} \quad P = a \\ &= m \quad \text{if} \quad P = m. \end{aligned}$$

The wave function for the ground state of $H^3$ is a linear superposition of the above ten functions. We may choose both the probability amplitudes and the internal wave functions $f^{P'}_{\kappa'}$ real, since our functions $\mathscr{Y}_{M_J T_\zeta \kappa}(\chi)$ satisfy the reality condition

$$U \mathscr{Y}^{\dagger}_{M_J T_\zeta \kappa}(\chi) = (-1)^{J-M_J+T-T_\zeta} \mathscr{Y}_{-M_J -T_\zeta \kappa}(\chi),$$

where $U$ is the time and charge reversal operator [6,7] $\sigma_{1y}\sigma_{2y}\sigma_{3y}\tau_{1\eta}\tau_{2\eta}\tau_{3\eta}$.

## References


1) Gerjuoy and Schwinger, Phys. Rev. **61** (1942) 138;
Feshbach and Rarita, Phys. Rev. **75** (1949) 1384
2) Clapp, Phys. Rev. **76** (1949) 873 L
3) Avery and Adams, Phys. Rev. **75** (1949) 1106;
Pease and Feshbach, Phys. Rev. **81** (1951) 142
4) E. P. Wigner, Gruppentheorie (Vieweg, Braunschweig, 1931)
5) R. G. Sachs, Nuclear Theory (Addison-Wesley, Cambridge, 1953) p. 183
6) Wigner, Göttinger Nachrichten **31** (1932) 546
7) J. M. Blatt and V. F. Weisskopf, Theoretical Nuclear Physics (John Wiley and Sons, New York, 1952) Ch. X
8) J. M. Blatt, Phys. Rev. **89** (1953) 86

2.E *Nuclear Physics* 8 (1958) 325—337; © *North-Holland Publishing Co., Amsterdam*
Not to be reproduced by photoprint or microfilm without written permission from the publisher

# OPTICAL MODEL OF THE INTERACTION BETWEEN INTERMEDIATE ENERGY NEUTRONS AND NUCLEI

A. V. LUKYANOV, Yu. V. ORLOV
and
V. V. TUROVTSEV
*Moscow State University, U.S.S.R.*

Received 3 April 1958

**Abstract:** An optical model of the nucleus is investigated in which a complex potential with a tail expressed by a third degree polynomial is employed. Parameters of the model which give the best fit between the theoretical cross sections $\sigma_t$, $\sigma_r$ and $\sigma_s$ and the experimental values for 14 MeV neutrons have been determined. The agreement is quite satisfactory for nuclei heavier than the chromium nucleus. The elastic scattering neutron angular distributions computed with aid of these parameters also satisfactorily agree with experiment. A preliminary investigation at lower energies indicates that in a relatively broad range the parameters depend only weakly on the energy.

## 1. Introduction

At present the model which has met most success in explaining the interaction between nucleons and nuclei in an extensive energy range is the optical model of the nucleus in which the latter is represented by a complex potential. The square-well potential employed in ref.[1]) for the case of incident neutrons led to at least qualitative agreement between the theoretical results and the experimental data. However, it has not been possible to simultaneously obtain consistent results for the total neutron cross sections, reaction cross sections and elastic scattering cross sections (the reaction cross sections are much too low [2,3])). P. E. Nemirovsky and subsequently a number of other authors employed in this connection a model with a diffuse boundary which led to some definite progress. Nevertheless, even at present there still seems to be some uncertainty regarding the choice of the shape of the potential and the magnitude of its parameters as well as the limits of applicability of the optical model. In P. E. Nemirovsky's papers [4]) on the diffuse boundary optical model, low neutron energies were chiefly considered. The most recent paper devoted to this model [5]) refers to various energies up to 14 MeV. However, the parameters chosen by the authors were based on incomplete experimental data (obtained for four nuclei).

In the present paper we investigate the simplest possible diffuse boundary potential which satisfies the condition of smoothness; it differs from all

other previously considered potentials. The diffuse region of the potential is described by a third degree polynomial.

The aim of the present work was to determine those parameters which yield for 14 MeV neutrons the best agreement with the experimental data for the total cross sections $\sigma_t$, reaction cross sections $\sigma_r$ and ratios of the scattering cross sections $\sigma_s$ to the reaction cross sections [6,7,8,9]) and which are independent of the mass number as much as possible.

## 2. Solution of the Direct Problem

A nuclear potential of the following shape was investigated:

$$U(r) = V(r)+iW(r) = -U_0(1+i\zeta)f(r) \tag{1}$$

where

$$f(r) = \begin{cases} 1, & r \leqq R-d \quad \text{(I)} \\ 1+\dfrac{(r-R-2d)(r-R+d)^2}{4d^3}, & R-d \leqq r \leqq R+d \quad \text{(II)} \\ 0, & r \geqq R+d \,\text{(III)} \end{cases}$$

(see fig. 1).

In regions I and III the equation for the radial part $u(r)$ of the wave function can be solved analytically, whereas in region II only a numerical solution is feasible. In numerically solving the equation it is profitable to change to the dimensionless independent variable $x = k_0 r (k_0 = \sqrt{2MU_0/\hbar^2})$, lower the order of the equation by changing to the logarithmic derivative and then separate the real and imaginary parts in the equation. After these transformations are performed the following set of first order equations with real coefficients is obtained:

$$\begin{aligned} v'_1 &= v_2^2 - v_1^2 - a^2 + \frac{l(l+1)}{x^2} - f(x), \\ v'_2 &= -2v_1 v_2 - \zeta f(x), \end{aligned} \tag{2}$$

where

$$v_1 = \operatorname{Re}\frac{u'}{u}, \qquad v_2 = \operatorname{Im}\frac{u'}{u}, \qquad a^2 = E_n/U_0.$$

The amplitudes of the scattered waves $\eta_l$ † can be evaluated if a solution of system (2) at the point $x_2 = k_0(R+d)$ is known which satisfies at $x_1 = k_0(R-d)$ the initial conditions computed from the formulas in ref. [1]).

The following computation formulas for amplitudes $\eta_l$ can be deduced by using the recursion relations for half-integral order Hankel functions:

† The $\eta_l$ are related to the cross sections by the well known equations

$$\sigma_t = 2\pi\lambda^2 \sum_{l=0}^{\infty} (2l+1)(1-\operatorname{Re}\eta_l), \quad \sigma_r = \pi\lambda^2 \sum_{l=0}^{\infty} (2l+1)(1-|\eta_l|^2).$$

$$\mathrm{Re}\,\eta_l = \frac{D^2-A^2+B^2-C^2}{(A+D)^2+(B-C)^2}, \qquad \mathrm{Im}\,\eta_l = \frac{2(AB+CD)}{(A+D)^2+(B-C)^2}, \tag{3}$$

$$A = a\alpha_l - v_1(x_2)\gamma_l, \quad B = a\beta_l - v_1(x_2)\delta_l, \quad C = v_2(x_2)\gamma_l, \quad D = v_2(x_2)\delta_l.$$

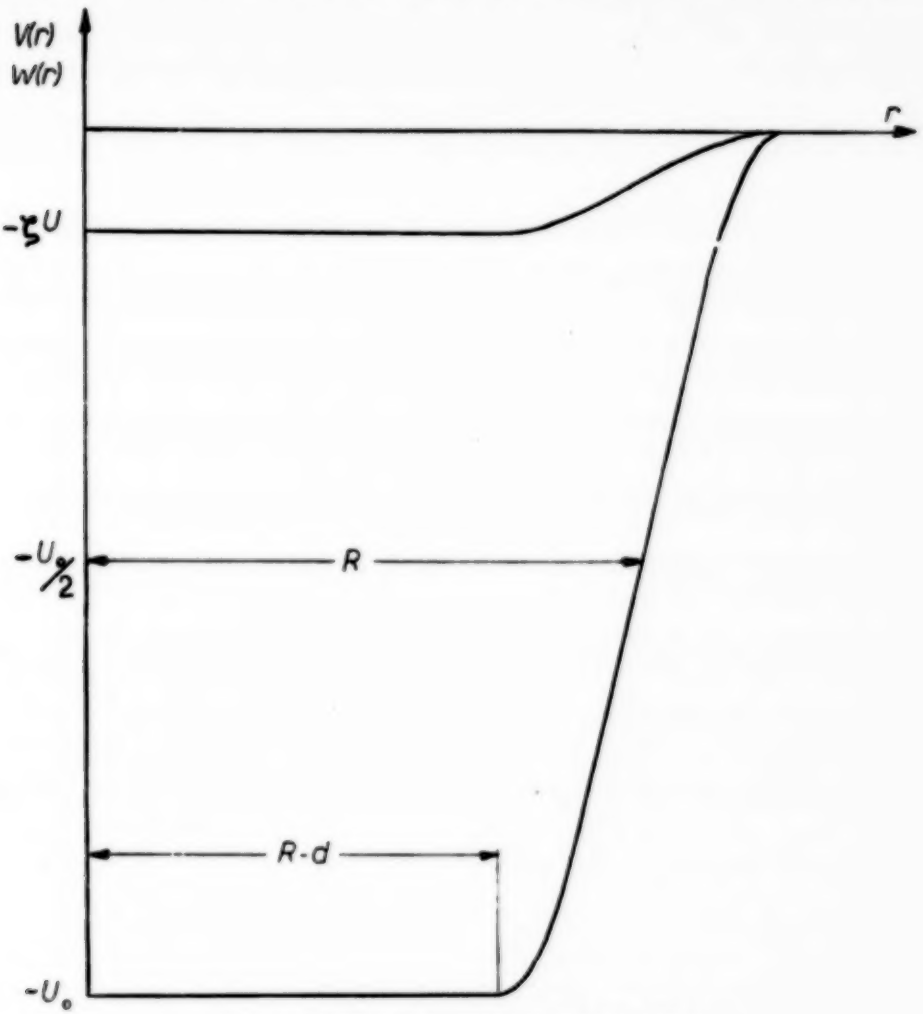


Fig. 1. Shape of investigated nuclear potential.

The quantities $\alpha_l$, $\beta_l$, $\gamma_l$, $\delta_l$ were computed here by using the recursion formulas

$$\gamma_{-1} = \cos y, \quad \gamma_0 = \sin y, \quad \gamma_i = \frac{2i-1}{y}\gamma_{i-1} - \gamma_{i-2} \quad (i = 1, 2, \ldots l)$$

$$\delta_{-1} = \sin y, \quad \delta_0 = -\cos y, \quad \delta_i = \frac{2i-1}{y}\delta_{i-1} - \delta_{i-2} \quad (i = 1, 2, \ldots l) \tag{4}$$

$$\alpha_l = \gamma_{l-1} - \frac{l}{y}\gamma_l, \quad \beta_l = \delta_{l-1} - \frac{l}{y}\delta_l,$$

where $y = ax_2$.

Solution of equation set (2) for a large number of values of the parameters in it is a very cumbersome task. The calculations can be successfully performed only with aid of a high speed computer. For this purpose the "Strela" computer of the Moscow University was employed. All computations, not only of the amplitudes $\eta_l$, but of the cross sections as well, were made automatically. Numerical solution of set (2) was performed by the Runge-Kutt method according to a programme with an automatic choice of the step. The constants on which the accuracy depend were chosen so as to ensure the amplitudes $\eta_l$ an accuracy to the fourth place after the decimal point. Summation over $l$ in the formulas for the cross sections was carried out from 0 to $l_0$, the number $l_0$ being automatically selected by the computer from the condition $\max\{(1-\operatorname{Re}\eta_{l_0}), |\operatorname{Im}\eta_{l_0}|\} \leqq 10^{-4}$. This number was found to vary from 4—5 to 12—13 depending on the nuclear radius and neutron energy. As was expected, $l_0$ increased with the radius of the nucleus and neutron energy. As a check all results were computed twice.

### 3. Method of Choosing the Parameters

The nuclear model under consideration involves four independent parameters $U_0$, $\zeta$, $d$ and $R$. Simultaneous variation of all parameters would be very difficult as then we would be dealing with four dimensional space. As a first step the well depth parameter was fixed at $U_0 = 42$ MeV. The main argument in favour of this choice is the existence of an ambiguity of the type $U_0 - R$ [1,5]) in the choice of the parameters which apparently is independent of the shape of the tail on the potential (within reasonable limits a change in $U_0$ can be compensated by a corresponding change in $R$ without any attendant appreciable change in the cross sections).

The nuclear radius was calculated from the formula

$$R = (r_0 A^{\frac{1}{3}} + \delta) \times 10^{-13} \text{ cm}. \tag{5}$$

The theoretical cross sections were determined for 8 values of $R$($R$ = 3.75; 4.05; 4.99; 5.39; 6.14; 6.63; 7.42 and 8.01 in units of $10^{-13}$ cm) and various values of $d$ and $\zeta$. The dependence of $\sigma_t^{\text{theor}}$ and $\sigma_r^{\text{theor}}$ on the parameter $d$ for various values of $\zeta$ could then be plotted for each value of $R$. The cross sections were found to strongly depend on $d$: $\sigma_t^{\text{theor}}$ and $\sigma_r^{\text{theor}}$ increase with $d$ and the rate of increase grows as one goes over to heavier nuclei. Similarly the dependence of the cross sections on $\zeta$ for fixed values of the diffuseness parameter $d$ were also determined. The reaction cross section naturally increases with $\zeta$, vanishes for $\zeta = 0$ and saturates at sufficiently large value of $\zeta$. A peculiar feature is the weak dependence of $\sigma_t^{\text{theor}}$ on $\zeta$ for a fixed $d$; with increase of $\zeta$ the total cross sections slowly increase for some values of $R$ and slightly decrease for other values of $R$.

The method of choosing the parameters consisted in the following. For

each given pair of values of $r_0$ and $\delta(1 \leqq r_0 \leqq 1.5)$ each of the values of $R$ was related to a definite value of $A$ by formula (5) and hence to definite experimental cross sections $\sigma_t \pm \Delta\sigma_t$ and $\sigma_r \pm \Delta\sigma_r$ ($\Delta\sigma$ is the experimental error). In those cases when no experimental data were available the cross sections were found by interpolation; a justification of this is that the cross sections vary smoothly from nucleus to nucleus and a comparatively large number of nuclei have been studied experimentally, especially in respect to their total cross sections (54 nuclei in the interval $2.8 \leqq A^{\frac{1}{3}} \leqq 6.2$). Figures (which we can conditionally call "quadrangles") were then plotted on the $\zeta d$ plane with aid of the graphs expressing the dependence of the cross sections on the parameters; these figures determine the region of values of parameters $d$ and $\zeta$ for which $\sigma_t^{\text{theor}}$ and $\sigma_r^{\text{theor}}$ agree within the experimental errors with the experimental values. In order to describe the experimental data for a possibly larger number of nuclei possessing the same parameters this procedure should be performed by varying $r_0$ and $\delta$ until the quadrangles approach each other as closely as possible (fig. 2). In this case

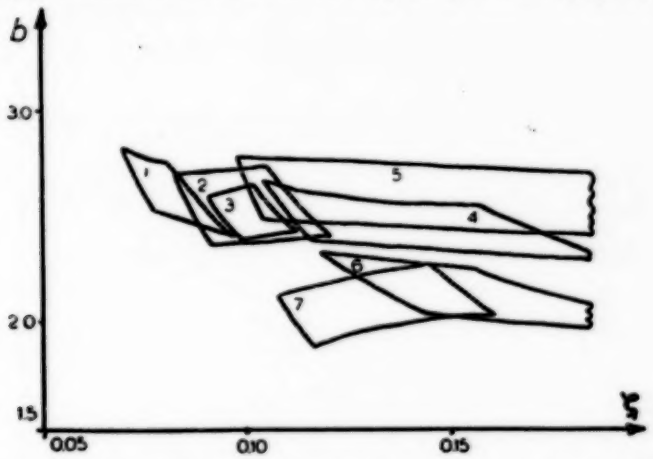


Fig. 2. Evaluation of parameters $b = k_0 d$ and $\zeta$ for given values of $U_0 = 42$ MeV, $r_0 = 1.25$, $\delta = 0.42$ (the figures 1, 2 . . . 7 refer respectively to $A = 220, 173, 121, 62, 19, 47, 24$).

the common "centre of gravity" of the "quadrangles" determines the unknown values of the parameters. A certain ambiguity was detected during this procedure, viz.: different sets of the parameters $r_0$, $\delta$, $d$ and $\zeta$ ($d$ and $\zeta$ lie in definite range) yielded satisfactory agreement between the calculated cross sections and the experimental values. In order to choose the most suitable set of parameters, another method was employed. The dependence of $R$ on $A^{\frac{1}{3}}$ was plotted for values of $d$ and $\zeta$ lying in the region defined above. In each given case $d$ and $\zeta$ were fixed, the unknown values being $r_0$ and $\delta$. The quantities $\sigma_t^{\text{theor}}$ and $\sigma_r^{\text{theor}}$ were defined if $R$, $d$ and $\zeta$ were given. The experimental curve (e.g., for the total cross section) was then used to determine from the condition $\sigma_t^{\text{theor}} = \sigma_t^{\text{exp}}$ the range of values of $A^{\frac{1}{3}}$ which within

the experimental errors corresponded to this value of the cross section. The corresponding graph is represented in fig. 3. The most suitable value of $d$ was first chosen by taking into account the weak dependence of $\sigma_t^{\text{theor}}$ on $\zeta$

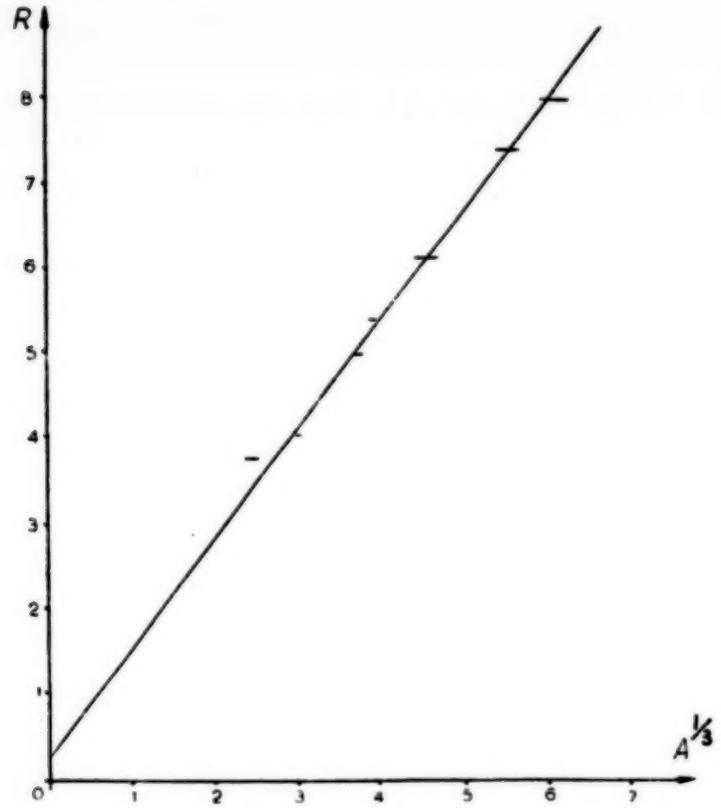


Fig. 3. Evaluation of parameters $r_0$ and $\delta$ for $U_0 = 42$ MeV, $b = 2.5$, $\zeta = 0.12$.

and proceeding from the requirement that agreement within the experimental errors between the theoretical and experimental cross sections hold for as many values of $R$ as possible, that is, that the segments on the plot $R = R(A^{\frac{1}{3}})$ lie on straight line. The characteristics of this straight line naturally determined parameters $r_0$ and $\delta$. The final choice of parameter $\zeta$ was made by comparing the theoretical results derived for the obtained values of parameters $d$, $r_0$ and $\delta$ and various values of $\zeta$ with the experimental values of $\sigma_r$ and $\sigma_0 = (\sigma_t/\sigma_r) - 1 = (\sigma_s/\sigma_r)$.

## 4. Results and Discussion

On the basis of the analysis the following values of the parameters were found to give the best fit:

$$b = k_0 d = 2.5; \quad \zeta = 0.12; \quad r_0 = 1.27; \quad \delta = 0.3. \qquad \text{(A)}$$

However, after the cross sections for a large number of nuclei were computed

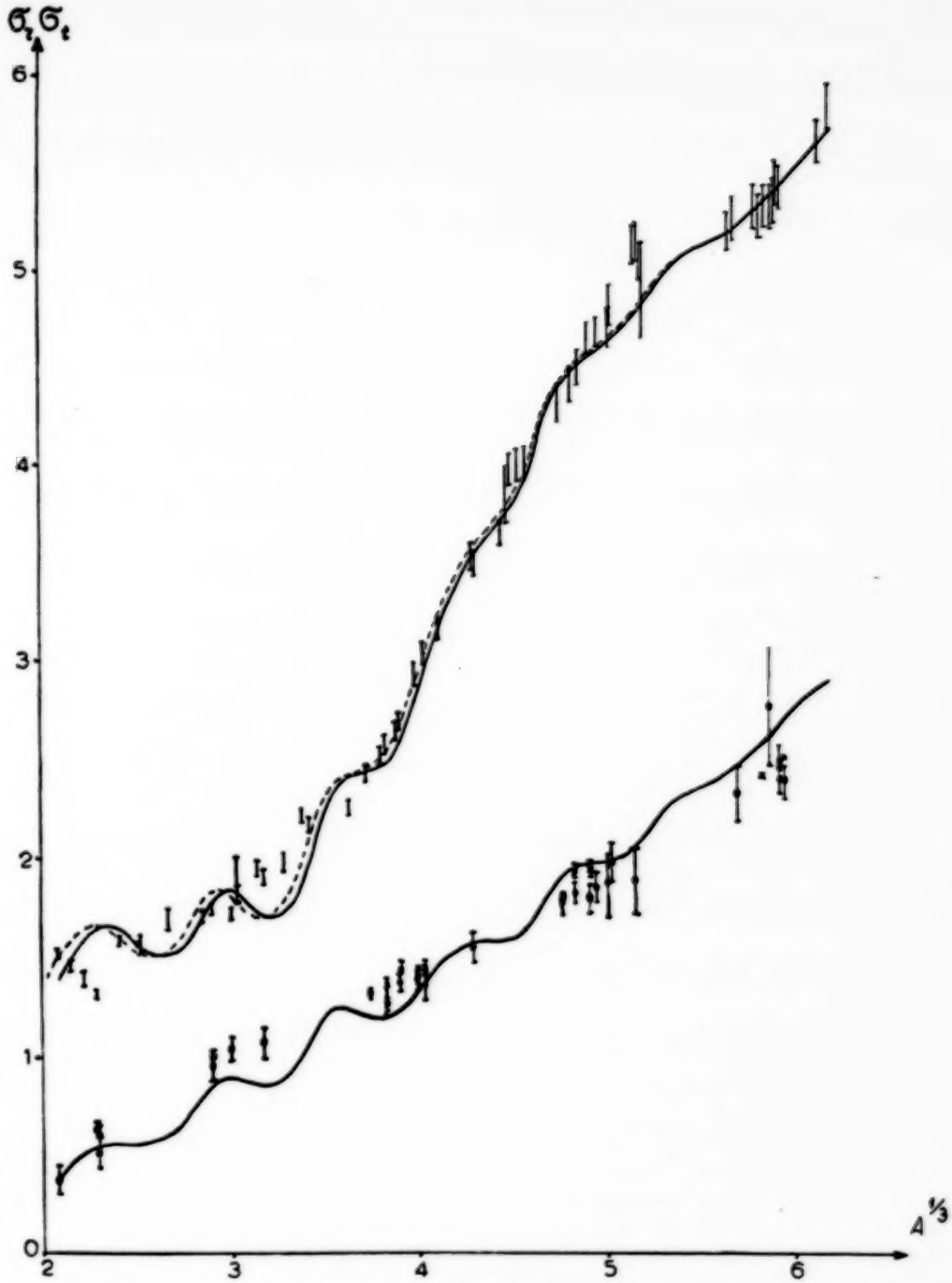


Fig. 4. Comparison of theoretical and experimental dependence of cross sections $\sigma_t$ and $\sigma_s$ (in barns) on mass number.

——— theoretical cross sections computed for parameter values $U_0 = 42$ MeV, $b = 2.5$, $\zeta = 0.12$, $r_0 = 1.27$, $\delta = 0.3$.

– – – – theoretical cross sections computed for parameter values $U_0 = 42$ MeV, $b = 2.5$, $\zeta = 0.12$, $r_0 = 1.25$, $\delta = 0.4$.

I—experimental data from ref.[6]); ⊢—data from ref.[7]); ⊢—data from ref.[8]); ⊢—data from ref.[9]).

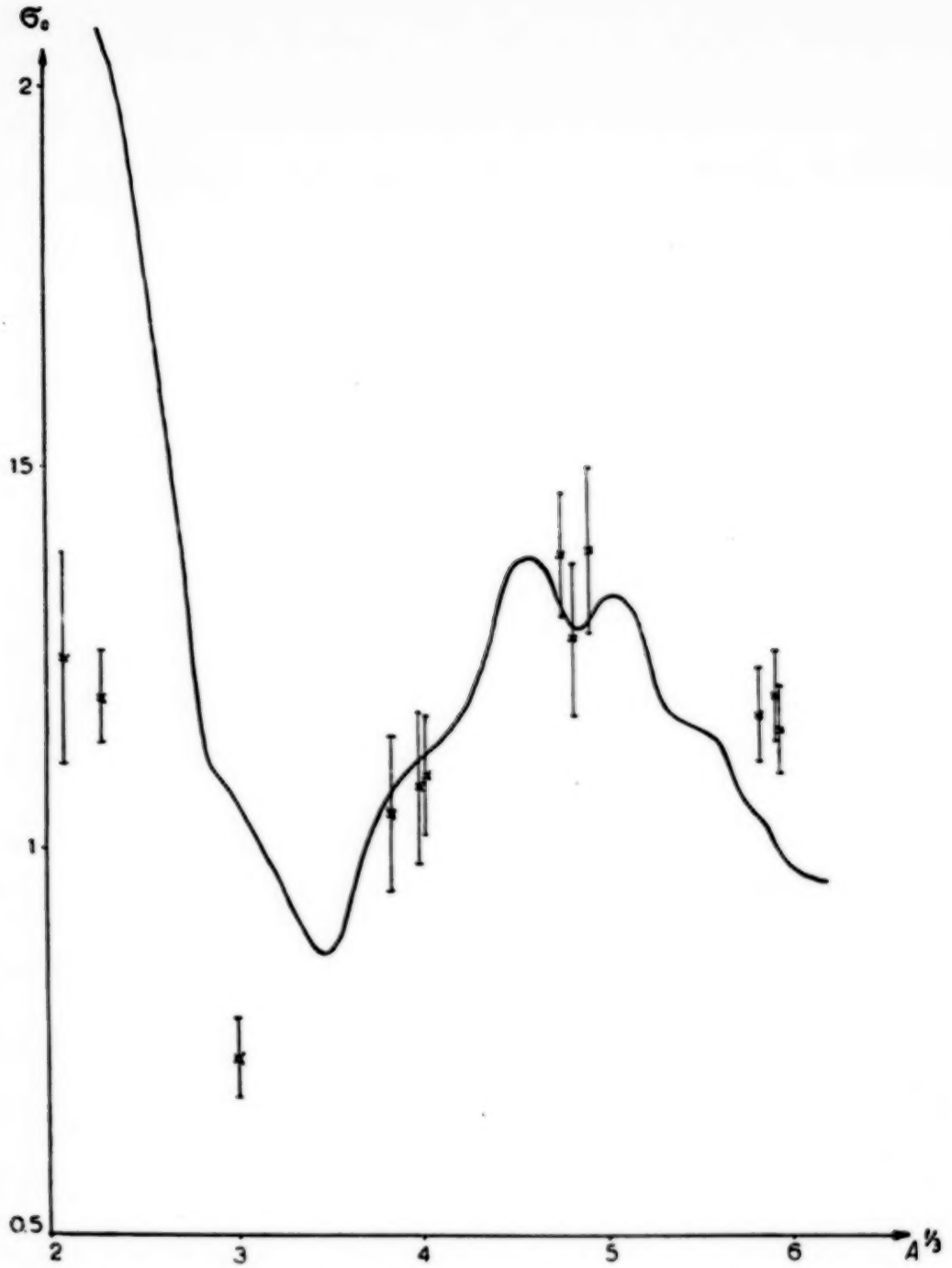


Fig. 5. Comparison of theoretical and experimental [9]) ratios of scattering cross sections to reaction cross sections as a function of mass number ($U_0 = 42$ MeV, $b = 2.5$; $\zeta = 0.12$; $r_0 = 1.27$; $\delta = 0.3$).

with aid of these parameter values it was found that better agreement with experiment could be attained if the values

$$r_0 = 1.25 \qquad \text{and} \qquad \delta = 0.4 \tag{B}$$

were accepted. Comparison of the theoretical cross sections $\sigma_t$, $\sigma_r$ and $\sigma_0$ with the experimental values is illustrated in figs. 4 and 5. Beginning from chromium the agreement is quite satisfactory for all intermediate and heavy nuclei. In the region of light nuclei the curve $\sigma_0(A^{\frac{1}{3}})$ lies above the experimental values. It can be lowered by accepting a larger value of $\zeta$ but then the agreement for heavy nuclei is less satisfactory. The discrepancy between theory and experiment for nuclei lighter than chromium may either be the result of dependence of the parameters on $A$ for these nuclei or to the fact that the model proposed here is invalid for light nuclei. This problem requires a special study.

The differential effective cross sections for neutrons elastically scattered on nuclei of Al, S, Fe, Cu, In, Sn, Ta, Pb, Bi ($E_n = 14.1$ MeV) and Mg, Ca, Cd, Bi ($E_n = 14.6$ MeV) were computed for parameter set (A) (fig. 6). For these nuclei experimental data are available (see refs.[10,11])). Although the parameters were chosen only on basis of the cross sections $\sigma_t$, $\sigma_r$ and $\sigma_0$ the angular distributions for elastically scattered neutrons were, as a whole, found to be in satisfactory agreement with the experimental values. The first maximum and the position of the maxima and minima are in good agreement. For not too very large angles the heights of the maxima comply satisfactorily with the experiment. The largest discrepancy between theory and experiment refers to the magnitude of the minima which are much deeper than the experimental ones; this fact is not connected with the shape of the tail on the potential as it also holds for other types of potentials (see, for example, ref.[5])).

It is possible that other values of the parameters exist which yield better agreement between the differential cross sections and experimental data without appreciably impairing the agreement with the values of $\sigma_t$, $\sigma_r$ and $\sigma_0$. To elucidate this problem an additional careful analysis of the dependence of the theoretical differential effective cross sections on the parameters of the model is desirable. Nevertheless, we do not believe that any radical improvement will be attained in this direction. In particular it does not seem that it will be possible to remove the deep minima in the theoretical angular distributions. A similar state of affairs is found to hold for a large variety of combinations of $d$ and $\zeta$. Variation of $r_0$ and $\delta$ also does not yield any significant improvement. For $b = 2.3$ and $\zeta = 0.125$ a $A^{\frac{1}{3}}$ dependence of the differential cross sections was found for all angles differing by 10° between 0° and 130°. The curves have deep and broad minima beginning at

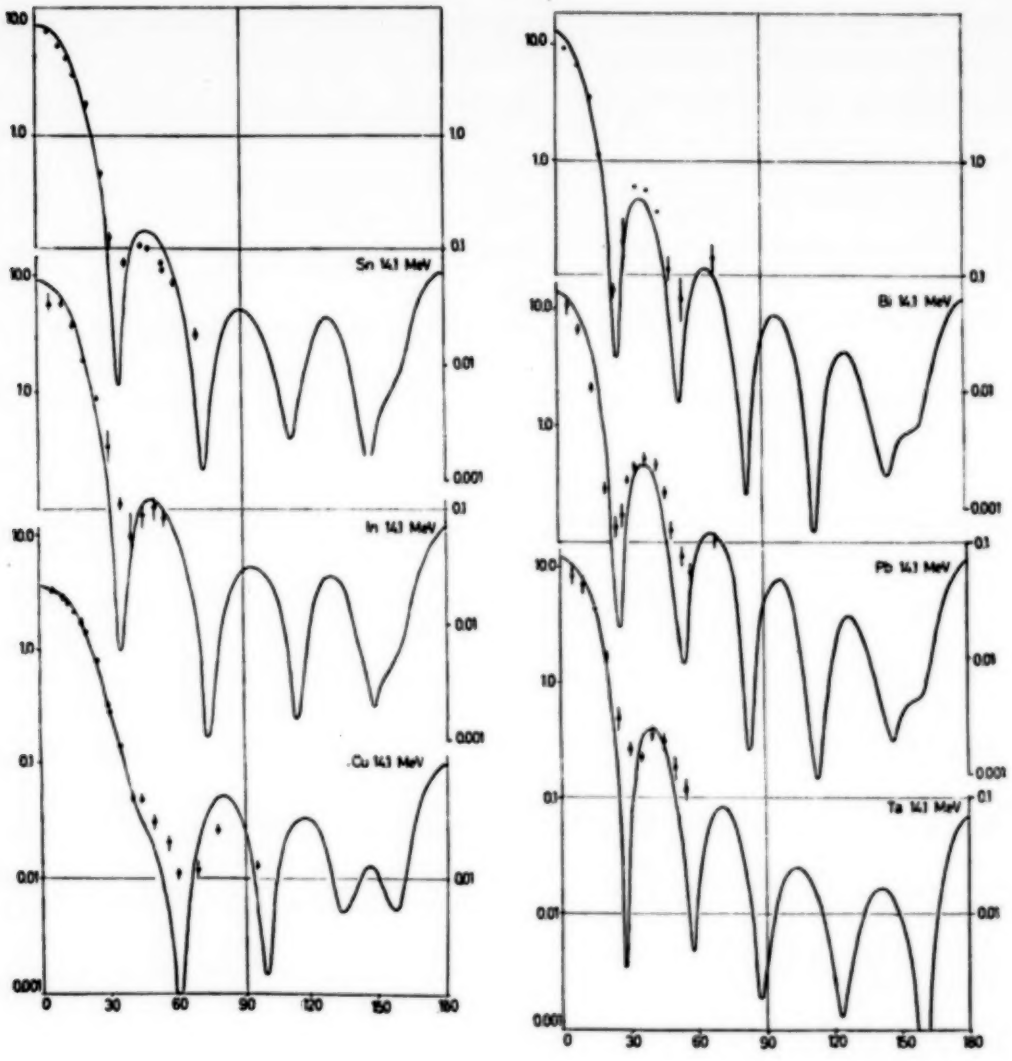


Fig. 6. Comparison of theoretical angular distributions of elastically scattered neutrons with experimental data [10, 11]). The angle (in degrees) is plotted along the abscissa axis and the differential cross section (in barn/sterad) is plotted along the ordinate axis in logarithmic scale.

30° so that variation of $r_0$ and $\delta$ decreases the depth of the minimum of certain nuclei and increases it for others.

## 5. Other Energies

The experimental cross sections for 14 MeV neutrons employed to determine the model parameters were chosen because a large amount of experi-

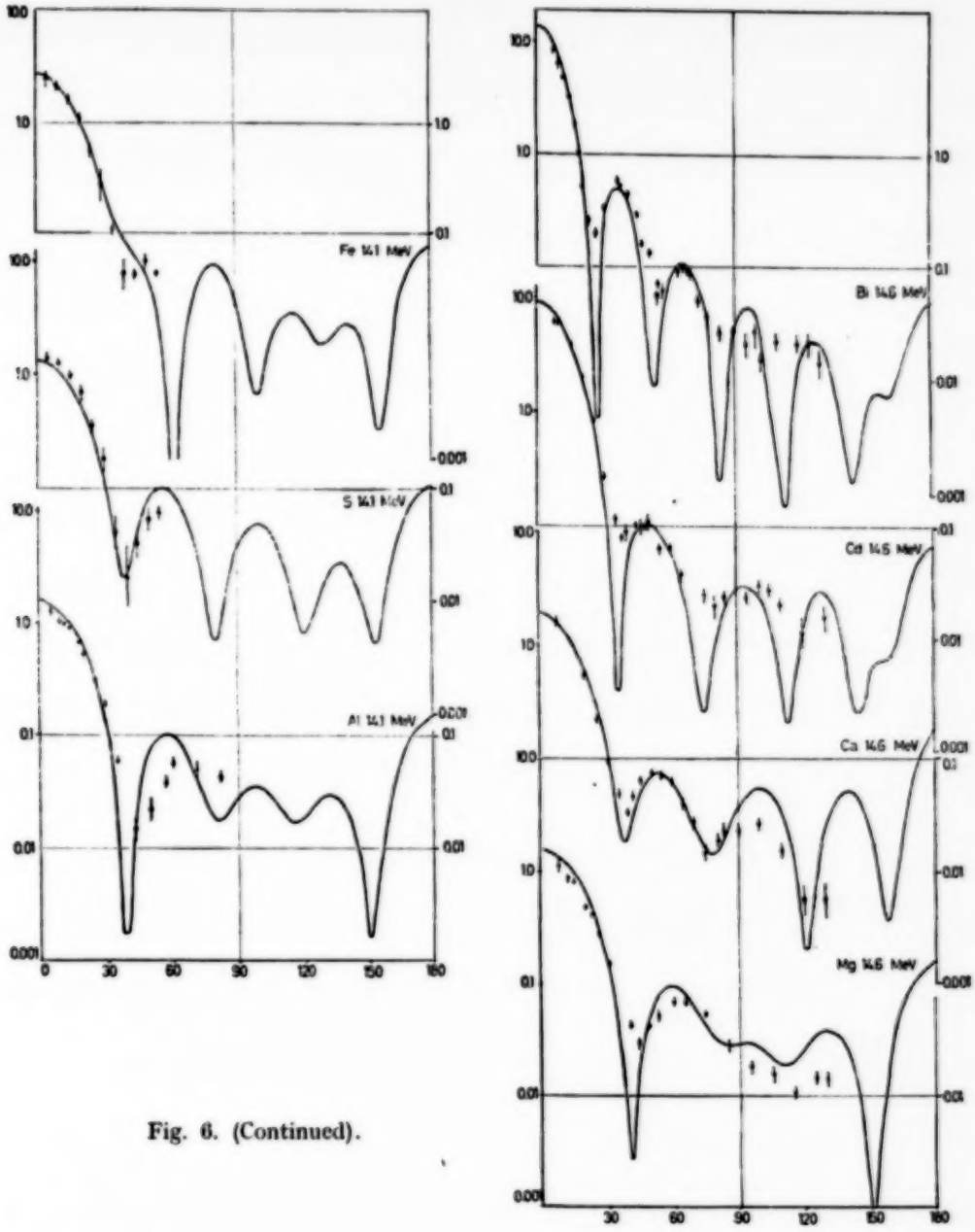


Fig. 6. (Continued).

mental data was available; in choosing the cross section values use was made of the fact that at the indicated energy the cross section for elastic scattering via a compound nucleus can be neglected [1]) and the experimental reaction and elastic scattering cross sections can thus be directly compared with the theoretical values. Some calculations for smaller energies were carried out by regarding $d$, $r_0$ and $\delta$ as energy independent parameters. The energy dependence of the parameters $U_0$ and $\zeta$ can be determined by comparing the

calculated cross sections with the experimental ones [5,8]). Some preliminary results were presented in fig. 7. As in ref.[5]) the model parameters $U_0$ and $\zeta$

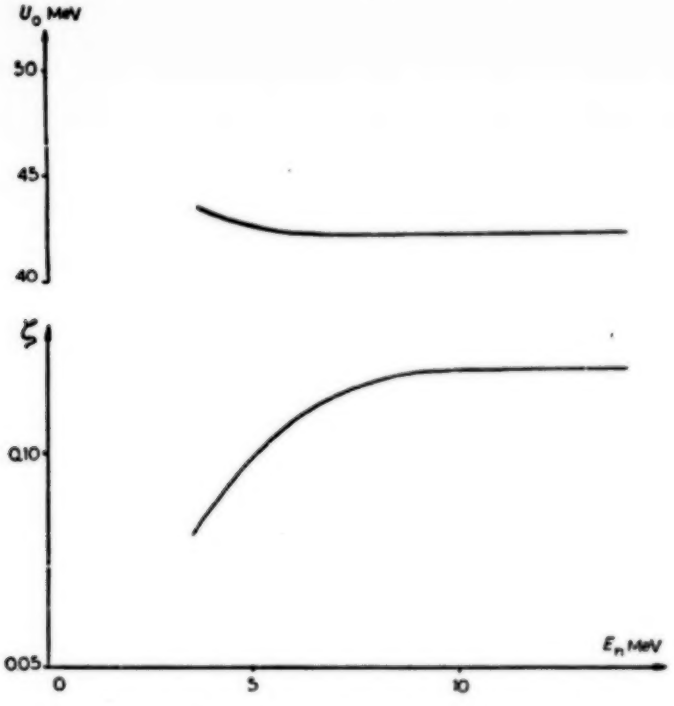


Fig. 7. Dependence of parameters $\zeta$ and $U_0$ on neutron energy.

were found to weakly depend on the energy in a relatively broad energy range.

The investigation of the optical model of the nucleus carried out by us indicates that a large amount of experimental data on scattering of neutrons by nuclei can be explained by employing a model with a complex potential possessing a tail described by a relatively simple function.

In conclusion the authors wish to thank Prof. I. S. Shapiro for suggesting the problem and interest in the present work and Prof. A. N. Tikhonov under whose guidance the computations were carried out. The authors are also thankful to G. A. Samoilova for help and the initiative displayed in coding the data and treatment of the results of the computations.

## References

1) H. Feshbach, C. E. Porter and V. F. Weisskopf, Phys. Rev. **96** (1954) 448
2) Mitsuji Kawai, Haruo Ui and Masayki Nagasaki, Progr. Theor. Phys. **14** (1955) 263
3) M. Walt and J. R. Beyster, Phys. Rev. **98** (1955) 677

4) P. E. Nemirovsky, Reports of Soviet Delegation at International Conference on Peaceful Uses of Atomic Energy, Geneva, 1955 (Moscow 1955) p. 287; JETP **32** (1957) 1143
5) J. R. Beyster, M. Walt and E. W. Salmi, Phys. Rev. **104** (1956) 1319
6) J. H. Coon, E. R. Graves and H. H. Barschall, Phys. Rev. **88** (1952) 562
7) V. I. Strizhak, Atomnaya Energia **2** (1957) 68
8) H. L. Taylor, O. Lönsjö and T. W. Bonner, Phys. Rev. **100** (1955) 174
9) E. R. Graves and R. W. Davis, Phys. Rev. **97** (1955) 1205
10) J. O. Elliot, Phys. Rev. **101** (1956) 684
11) G. Culler, S. Fernbach and N. Sherman, Phys. Rev. **101** (1956) 1047

1.C.1:
1.E.2

*Nuclear Physics* 8 (1958) 338—357; © *North-Holland Publishing Co., Amsterdam*
Not to be reproduced by photoprint or microfilm without written permission from the publisher

# NUCLEAR BINDING ENERGIES ON THE STATISTICAL MODEL

N. V. FINDLER

*The F.B.S. Falkiner Nuclear Research and Adolph Basser Computing Laboratories, School of Physics, The University of Sydney* †

Received 15 April 1958

**Abstract:** In this paper we have made an investigation of the binding energies of nuclei by means of the statistical theory. We have assumed a static, charge independent, scalar meson potential, and have used high energy nucleon-nucleon scattering results to limit the parameters occurring in the potential.

The weight factors obtained for the particular exchange forces are entirely different from the usual values. The mass of the meson used in the theory is close to that of the $\pi$-meson. Also the obtained mesonic charge is reasonable. The binding energies and the nuclear radii are in satisfactory agreement with the known values from $A = 10$ on. However, for the very light nuclei, the calculated binding energy is too high. The angular distribution of the differential cross section for n—p scattering also shows the shortcomings of our assumptions.

## 1. The Statistical Model and its Applications

The essence of the Thomas-Fermi method for the investigation of a system of particles can be summed up as follows: it handles the particles forming the system statistically, i.e. it neglects the individual properties of the particles and treats their ensemble as a so-called degenerate Fermi-gas which is at absolute zero. The procedure is justifiable when the number of particles is large.

Majorana [17]) was the first to apply the statistical theory to nuclei. He obtained valuable qualitative results by the rather arbitrary assumption that between protons there is only Coulomb-interaction, between neutrons none, and between neutrons and protons only those space-exchange forces which are necessary to produce the saturation of the binding energy. Later Heisenberg [10]) derived the expression for the potential energy using the other types of exchange forces.

The energy of surface tension qualitatively justified by Wick [25, 26]) was calculated by Weizsäcker [23, 24]) as a universal inhomogeneity correction and good results were obtained with an exchange potential depending on distance as

† In a generalised form the present work is part of a thesis completed at the Physical Institute of the Budapest University for Technical Science in 1956.

$$J(r) = ae^{-br}.$$

Similar calculations were carried out by Nakabayasi [18]), Wang [22]) and others. Their work is characterised by the assumption of a homogeneous density distribution and by the choice of the space-dependent part of the exchange potential once as

$$J(r) = ae^{-br} \text{ and then as } J(r) = ae^{-br^2}.$$

Flügge [3]) elaborated a theory for light nuclei which went beyond the above mentioned ones. He did not assume anything about the density *a priori* but determined it by the requirement of energy minimum.

We mention the papers of Ivanenko, Rodichev and Sokolov [12,13]) among the more recent work based on the statistical nuclear model. The authors mentioned carried out shell structure investigations with ordinary spin-independent nuclear forces of Yukawa-type.

Kompaneetz [16]) examined nuclei of saturated spin and charge with a self-consistent method. The potential used by him was the product of the Yukawa-function and the Serber-operator (ordinary and space-exchange forces with equal weights).

Román [20]) did his calculations with an exchange-free, ordinary Yukawa-interaction. Starting from a homogeneous and saturated density distribution he obtained good values for the binding energies in a semi-empirical way.

In several papers Gombás [7a,b,c]) applied all the three functions featured above, namely

$$J_1(r) = ae^{-br}, \quad J_2(r) = ae^{-br^2}, \text{ and } J_3(r) = a\frac{e^{-br}}{r}$$

for the space-dependent part of the interaction potential between nucleons. He assumed pure space-exchange, i.e. Majorana-type forces between protons and neutrons, and a Wigner cum Bartlett-type interaction between identical nucleons. The binding energies and the nuclear radii determined by the Ritz-method agree with the experimental values very well from the very light nuclei up to the heavy ones, though there was only one freely adjustable parameter in the theory. The results of the first approximation were refined further in the second one [7b]).

With the density so determined Gombás [8]) in another paper obtained results for the angular momentum distribution of nucleons in accordance with the magic numbers.

A similar method was used by Yang [27]) for the same purpose. The statistical model, of course, cannot supply the peaks in the binding energy curve, a fact pointed out by Paneth [19]).

Gombás [7d]) and Kisdi [14a]) using the results of ref. [7a]) determined the effective interaction potential between nuclei and nucleons; furthermore Kisdi [14b]) carried out valuable calculations on nuclear fission.

Inthoff [11]) worked out the binding energy of a single nucleus ($_{82}Pb^{206}$) with a combination of Wigner, Majorana, Bartlett, and Heisenberg forces of Yukawa space-dependence. The weight of each force has been chosen rather arbitrarily, corresponding only to the requirements of the above nucleus.

Kligman [15]) used a potential of the same type. By making some mathematical and physical simplifications he predicted binding energies and radii for heavy nuclei which were in qualitative agreement with the measured values.

It can be seen from this short résumé that while the earlier authors derived expressions valid only for either light or heavy nuclei, certain newer investigations yield the binding energies and radii of most of the stable nuclei by a single theory. The assumptions of force applied here, however, stand in sharp contrast with the results of the medium and high energy scattering. Every attempt to describe this latter phenomenon correctly has led to discrepancies for the binding energies.

## 2. The Investigation of Binding Energies on the Statistical Nuclear Model

The neutron and proton gas collectively possesses the Fermi-type kinetic energy

$$E_F = \kappa_F \int (\rho_p^{5/3} + \rho_n^{5/3})\, dv \tag{1}$$

where

$$\kappa_F = \frac{3\pi^2}{10}\left(\frac{3}{\pi}\right)^{2/3} \frac{\hbar^2}{M_0}, \tag{2}$$

$M_0$ is the (average) nucleon mass, $\rho_p$ the proton, $\rho_n$ the neutron density function. The integration has to be carried out over the whole volume of the nucleus.

Because of the non-homogeneous density distribution there is a certain correction to the Fermi-energy, the so-called Weizsäcker-energy

$$E_W = \kappa_W \int \left(\frac{\mathrm{grad}^2 \rho_p}{\rho_p} + \frac{\mathrm{grad}^2 \rho_n}{\rho_n}\right) dv \tag{3}$$

where

$$\kappa_W = \frac{\hbar^2}{8M_0}. \tag{4}$$

The total kinetic energy cannot be calculated simply as the sum of (1) and (3) because a certain part is taken into consideration twice †. By the method adopted by Hellmann, this deficiency can be approximately eliminated if we

† A consequence of the statistical treatment is that a single particle itself occupies a finite volume in phase space. A particular consideration of these correction terms can be found in ref. [6]) or [7]).

take for the total kinetic energy

$$E_K = kE_F + E_W \tag{5}$$

where

$$k = 1-(4/A). \tag{6}$$

The ordinary and exchange Coulomb energies of the protons are

$$E_C = \tfrac{1}{2}e^2 \int\int \frac{\rho_p(\mathbf{r}_1)\rho_p(\mathbf{r}_2)}{|\mathbf{r}_1-\mathbf{r}_2|}\,dv_1\,dv_2 = \tfrac{1}{2}e\int V_e(\mathbf{r}_1)\rho_p(\mathbf{r}_1)dv_1 \tag{7}$$

and

$$E_R = -\tfrac{1}{2}e^2 \int\int \frac{|\rho_p(\mathbf{r}_1, \mathbf{r}_2)|^2}{|\mathbf{r}_1-\mathbf{r}_2|}\,dv_1\,dv_2 \tag{8}$$

respectively. Here $V_e$ denotes the electrostatic potential caused by the protons

$$V_e(\mathbf{r}_1) = e\int \frac{\rho_p(\mathbf{r}_2)}{|\mathbf{r}_1-\mathbf{r}_2|}\,dv_2. \tag{9}$$

With the usual statistical method (8) can be transformed into

$$E_R = -\kappa_a \int \rho_p^{4/3}\,dv \tag{10}$$

where

$$\kappa_a = \tfrac{3}{4}\left(\frac{3}{\pi}\right)^{1/3} e^2. \tag{11}$$

The success or failure of the model depends entirely on the assumption about the nuclear interaction. In spite of the numerous physical and mathematical restrictions the scope of the possible assumptions is quite large †. In this paper we choose a two-body, static, and charge-independent potential as follows:

$$U_{ik} = V(\mathbf{r}_{ik})\,[W + M\mathscr{P}_r + B\mathscr{P}_\sigma + H\mathscr{P}_r\mathscr{P}_\sigma]. \tag{12}$$

Here $\mathscr{P}_r$ and $\mathscr{P}_\sigma$ are the well-known space- and spin-exchange operators respectively; $W$, $M$, $B$, $H$ are the weight factors to be determined later for the Wigner, Majorana, Bartlett and Heisenberg forces. We can assume that

$$W+M+B+H = 1. \tag{13}$$

We choose $V(\mathbf{r}_{ik})$, the common space-dependent part of the interaction potential, to be of Yukawa-type

$$V(\mathbf{r}_{ik}) = -g^2\,\frac{\exp\,(-r_{ik}/r_0)}{r_{ik}}; \tag{14}$$

$g$ is the so-called mesonic charge (the strength of the meson-nucleon cou-

† A detailed investigation of this can be found in ref. [2]).

pling). Its value is to be chosen to fit the experimental results. $r_0$ is the Compton-wavelength of the $\pi$-mesons †:

$$r_0 = \frac{\hbar}{m_\pi c}. \tag{15}$$

The energy of the nuclear interaction can be calculated in the Hartree-Fock approximation for a nucleon gas in a well-known way.

In the following we will restrict ourselves to nuclei with saturated spin. The physical reason for doing so is that the tensor forces responsible for non-central interaction are neglected; furthermore it seems meaningless on the statistical model to assign the resultant (and measurable) angular momentum of the nucleus to certain selected nucleons.

Let us introduce the potentials in an (exchange-free) nuclear field, analogously to the electrostatic potential (cf. eq. (9))

$$U_p(\mathbf{r}_1) = \int \rho_p(\mathbf{r}_2) V_{12}\, dv_2, \qquad U_n(\mathbf{r}_1) = \int \rho_n(\mathbf{r}_2) V_{12}\, dv_2. \tag{16}$$

These potentials satisfy the Klein-Gordon equations of the static fields with sources,

$$\Delta U_p - \frac{1}{r_0^2} U_p = -4\pi g^2 \rho_p, \qquad \Delta U_n - \frac{1}{r_0^2} U_n = -4\pi g^2 \rho_n. \tag{17}$$

Furthermore let us introduce the symbols

$$\begin{aligned} I_{pn} &= \iint \rho_p(\mathbf{r}_1, \mathbf{r}_2) \rho_n^*(\mathbf{r}_1, \mathbf{r}_2) V_{12}\, dv_1\, dv_2 \\ I_{pp} &= \iint |\rho_p(\mathbf{r}_1, \mathbf{r}_2)|^2 V_{12}\, dv_1\, dv_2 \\ I_{nn} &= \iint |\rho_n(\mathbf{r}_1, \mathbf{r}_2)|^2 V_{12}\, dv_1\, dv_2, \end{aligned} \tag{18}$$

where $\rho_{n,p}(\mathbf{r}_1, \mathbf{r}_2)$ denote the mixed densities. With these the whole nuclear interaction energy can be written as

$$\begin{aligned} E_u = &\left(\frac{W}{2} - \frac{M}{4} + \frac{B}{4} - \frac{H}{2}\right) \int [\rho_p(\mathbf{r}) U_p(\mathbf{r}) + \rho_n(\mathbf{r}) U_n(\mathbf{r})]\, dv \\ &+ \left(W + \frac{B}{2}\right) \int \rho_p(\mathbf{r}) U_n(\mathbf{r})\, dv - \left(\frac{W}{4} - \frac{M}{2} + \frac{B}{2} - \frac{H}{4}\right) (I_{pp} + I_{nn}) + \left(M + \frac{H}{2}\right) I_{pn}. \end{aligned} \tag{19}$$

If, as in statistical treatments, we assign a plane wave to the space-

† In order to simplify the calculations we will not distinguish between the masses of $\pi^0$-mesons (Wigner and Bartlett interactions) and $\pi^\pm$-mesons (Majorana and Heisenberg interactions). *Editor's note:* More accurately, $r_0$ is the range of the assumed interaction, which may be connected with a "meson" mass by eq. (15). The Editor does not regard the coincidence of this meson mass with that of the $\pi$-meson, found by the author (see p. 349), as significant.

dependent part of each nucleon wave function, after some rather lengthy calculations we obtain

$$I_{pn} = -\frac{g^2}{r_0^4}\int f(\omega_n, \omega_p)dv$$

$$I_{pp} = -\frac{g^2}{r_0^4}\int f(\omega_p, \omega_p)dv \qquad (20)$$

$$I_{nn} = -\frac{g^2}{r_0^4}\int f(\omega_n, \omega_n)dv$$

where

$$f(\omega_n, \omega_p) = \frac{1}{6\pi^3}\{3(\omega_n^3\omega_p + \omega_n\omega_p^3) - \omega_n\omega_p + \tfrac{1}{4}[1+6(\omega_n^2+\omega_p^2) - 3(\omega_n^2-\omega_p^2)^2]$$
$$\times\{\ln[1+(\omega_n+\omega_p)^2] - \ln[1+(\omega_n-\omega_p)^2]\} \qquad (21)$$
$$-4(\omega_n^3+\omega_p^3)\operatorname{arc\,tg}(\omega_n+\omega_p) + 4(\omega_n^3-\omega_p^3)\operatorname{arc\,tg}(\omega_n-\omega_p)\}$$

with the dimensionless variables

$$\omega_n = (3\pi^2)^{1/3} r_0 \rho_n^{1/3}, \quad \omega_p = (3\pi^2)^{1/3} r_0 \rho_p^{1/3}. \qquad (22)$$

## 3. The Choice of the Weight Factors

Our next task is to draw some conclusions from the high energy scattering experiments regarding the weight factors. As our approximation assumes a central, charge-independent, two-body internucleonic potential, it is reasonable to take the neutron-proton scattering into account.

In the energy range concerned, the Born-approximation seems to be able to supply the data with the necessary accuracy.

We have calculated the differential cross section of the proton-neutron scattering on the basis of the Born-approximation†:

† For the sake of completeness we mention the similar result for proton-proton scattering neglecting Coulomb and non-central interaction:

$$\frac{d\sigma_{pp}}{d\Omega} = \tfrac{1}{4}|{}^1f(\vartheta) + {}^1f(\pi-\vartheta)|^2 + \tfrac{3}{4}|{}^3f(\vartheta) - {}^3f(\pi-\vartheta)|^2$$
$$= c\left\{[W^2+M^2+B^2+H^2-2(WH+BM)-WM+WB+MH-BH]\right.$$
$$\cdot\left[\frac{1}{\left(1+4k^2r_0^2\sin^2\frac{\vartheta}{2}\right)^2} + \frac{1}{\left(1+4k^2r_0\cos^2\frac{\vartheta}{2}\right)^2}\right]$$
$$\left.-\frac{W^2+M^2+B^2+H^2-4(WM-WB-MH+BH)-2(WH+BM)}{\left(1+4k^2r_0^2\sin^2\frac{\vartheta}{2}\right)\left(1+4k^2r_0^2\cos^2\frac{\vartheta}{2}\right)}\right\}.$$

$$\frac{d\sigma_{np}}{d\Omega} = \tfrac{1}{4}|{}^1f(\vartheta)|^2+\tfrac{3}{4}|{}^3f(\vartheta)|^2$$

$$= c\left\{\frac{W^2+WB+B^2}{\left(1+4k^2r_0^2\sin^2\frac{\vartheta}{2}\right)^2}+\frac{M^2+MH+H^2}{\left(1+4k^2r_0^2\cos^2\frac{\vartheta}{2}\right)^2}\right. \tag{23}$$

$$\left.+\frac{2(WM+BH)+WH+BM}{\left(1+4k^2r_0^2\sin^2\frac{\vartheta}{2}\right)\left(1+4k^2r_0^2\cos^2\frac{\vartheta}{2}\right)}\right\},$$

where $\vartheta$ is the scattering angle in the c.m.s., $k$ is the absolute value of the wave vector, and $c$ is a certain constant. It must be pointed out that the similar calculations of Flügge [4]) contain an analytical mistake; our results are essentially different from his, which are not suitable for the explanation of the saturated binding energies.

Let us observe that the first term of the { } bracket in (23) expresses a predominantly forward scattering, the second term a predominantly backward scattering, while the third one is symmetrical about $\vartheta = \pi/2$.

The known symmetry of the differential cross section about $\vartheta = \pi/2$ (see e.g. ref. [8])) can therefore be expressed by the equation

$$W^2+WB+B^2 = M^2+MH+H^2. \tag{24}$$

This equation is indeed satisfied by the values $W = M$, $B = H$, but this assumption, which has usually been adopted, is but a special case and cannot yield saturation of binding energies.

With our assumption the space-dependent factor of the interaction potential is independent of the mutual states of nucleons; therefore, the ratio between the singlet and triplet potential for the deuteron is given by

$$q = \frac{{}^1U_{12}}{{}^3U_{12}} = \frac{W+M-B-H}{W+M+B+H} = W+M-B-H. \tag{25}$$

In a characteristic way the value $q$ is roughly independent of the different assumptions regarding the space-dependent factor of the potential and is equal to 0.6—0.7 for square well, exponential, Gaussian, etc. functions.

Rosenfeld (page 131 of ref. [21])) has published a semi-empirical relation for $q$ as a function of the mass of the meson associated with the nuclear field, in the sense that its Compton-wavelength appears in the exponent of the Yukawa-potential:

$$q = \frac{4.67\times10^{-4}\left(\frac{m_\pi}{m_e}\right)^2-0.965\times10^{-2}\frac{m_\pi}{m_e}}{4.67\times10^{-4}\left(\frac{m_\pi}{m_e}\right)^2+5.57\times10^{-2}\frac{m_\pi}{m_e}-0.535} \tag{26}$$

where $m_e$ is the mass of electron.

Eqs. (13), (24) and (26) imply

$$\begin{aligned} M &= -W+\frac{1+q}{2} \\ B &= -\frac{3+q}{3-q}W+\frac{3+q^2}{6-2q} \\ H &= \frac{3+q}{3-q}W-\frac{2q}{3-q}. \end{aligned} \tag{27}$$

Our task will be to find the value of $W$, $m_\pi$ and $g$ which yield binding energies closest to experience. A test of the theory would be that the values of $m_\pi$ and $g$ obtained are reasonable†.

## 4. The Determination of Binding Energies and Density Distributions

We look for the proton and neutron density functions which yield a minimum for the total energy

$$E = E_K+E_C+E_R+E_u. \tag{28}$$

The accessory conditions are that the total numbers of protons and neutrons are given by

$$\int \rho_p \, dv = Z, \qquad \int \rho_n \, dv = N. \tag{29}$$

With the Lagrangian multipliers $b_p$ and $b_n$ we obtain

$$\delta(E+b_p Z+b_n N) = 0 \tag{30}$$

where the variation is to be carried out with respect to $\rho_p$ and $\rho_n$. Besides the differential equation given by (30) we have to satisfy the Poisson equation for the electrostatic field of the protons

$$\Delta V_e = -4\pi e\rho_p \tag{31}$$

and the Klein-Gordon equations (17).

If we restrict ourselves to spherical symmetry, the gradients of the densities have to vanish at the centre of the nucleus, i.e.

$$\left(\frac{\partial \rho_p}{\partial r}\right)_{r=0} = 0, \qquad \left(\frac{\partial \rho_n}{\partial r}\right)_{r=0} = 0. \tag{32}$$

The densities themselves have to vanish at infinity.

† We mention that ref. [7]) uses the following weight factors:
force between nucleons of identical charge

$$W = \tfrac{1}{2}, \; M = 0, \qquad B = -\tfrac{1}{2}, \; H = 0;$$

force between nucleons of different charge

$$W = 0, \quad M = 1, \quad B = 0, \quad H = 0.$$

In the present calculations we restrict ourselves to trial density functions of the simple form

$$\rho_p = \rho_{p0}\, e^{-a^2(r/r_0)^2}, \qquad \rho_n = \rho_{n0}\, e^{-a^2(r/r_0)^2} \tag{33}$$

where from (29)

$$\rho_{p0} = \frac{Za^3}{\pi^{3/2} r_0{}^3}, \qquad \rho_{n0} = \frac{Na^3}{\pi^{3/2} r_0{}^3}. \tag{34}$$

After some lengthy calculations we obtain the following expressions †:

$$\begin{aligned} E_F &= \frac{\kappa_F}{\pi} \left(\tfrac{3}{5}\right)^{3/2} (a/r_0)^2 \frac{A^{5/3}}{2^{2/3}} \left(1+\tfrac{5}{9}n^2\right) \\ E_W &= 6\kappa_W (a/r_0)^2 A \\ E_C &= \frac{e^2}{4(2\pi)^{1/3}} \frac{a}{r_0} A^2 (1-2n+n^2) \\ E_R &= -\kappa_a (3/\pi)^{1/3} \left(\tfrac{3}{16}\right) (a/r_0) \frac{A^{4/3}}{2^{1/3}} \left(1-\tfrac{4}{3}n+\tfrac{2}{9}n^2\right), \end{aligned} \tag{35}$$

$$\begin{aligned} E_u = -\frac{g^2A^2}{r_0}\Bigg\{ & (1-n^2)\left\langle\left[\left(\frac{2}{\pi}\right)^{1/2} a^3 + e^{\frac{1}{2a^2}} \phi\left(\frac{1}{\sqrt{2}a}\right)\right]\left(\frac{W}{2}-\frac{M}{8}+\frac{B}{4}-\frac{H}{4}\right) - e^{\frac{1}{2a^2}}\left(\frac{W}{4}+\frac{B}{8}\right)\right\rangle \\ & - \left\langle e^{\frac{1}{2a^2}} + n^2\left\{\frac{4}{\pi}a^2 + 2e^{\frac{1}{2a^2}}\left[\tfrac{1}{2}\phi^2\left(\frac{1}{2a}\right) - \phi\left(\frac{1}{2a}\right)\right] + \frac{4}{\pi^{1/2}} a e^{\frac{1}{4a^2}}\left[\phi\left(\frac{1}{2a}\right)-1\right]\right\}\right\rangle \left(\frac{W}{4}-\frac{M}{8}+\frac{B}{8}-\frac{H}{4}\right)\Bigg\} \\ & + \frac{9g^2}{8}\left(\frac{3}{\pi}\right)^{1/2} \frac{a^3}{r_0} A^2 \Bigg\{\left(\frac{W}{2}-M+B-\frac{H}{2}\right)\left[\frac{a_0}{6^{2/3}}(1+n^2) + \frac{a_1 d}{7^{2/3}}\left(1+\tfrac{14}{9}n^2\right) + \frac{a_2 d^2}{8^{2/3}}\left(1+\tfrac{20}{9}n^2\right)\right. \\ & \left. + \frac{a_3 d^3}{27}(1+3n^2)\right] - \left(M+\frac{H}{2}\right)\left\langle \frac{4}{9\times 5^{2/3}} \frac{b_1}{d} n^2 + \frac{1}{6^{2/3}}\left[a_0\left(1-\tfrac{2}{3}n^2\right) + \tfrac{4}{9}b_2 n^2\right]\right. \\ & \left. + \frac{d}{7^{2/3}}\left[a_1\left(1-\tfrac{7}{9}n^2\right) + \tfrac{4}{9}b_3 n^2\right] + \frac{a_2 d^2}{8^{2/3}}\left(1-\tfrac{8}{9}n^2\right) + \frac{a_3 d^3}{27}(1-n^2)\right\rangle\Bigg\} \end{aligned} \tag{36}$$

where we have denoted the relative neutron excess by $n = (N-Z)/A$, the total number of nucleons by $A = N+Z$, and the error function by

$$\phi(x) = \frac{2}{\sqrt{\pi}} \int_0^x e^{-t^2} dt;$$

$a_0, a_1, a_2, a_3, b_1, b_2, b_3$ are certain constants required in the approximation to the function (21), and for the sake of brevity

$$d = \left(\tfrac{9}{4}\pi\right)^{1/6} a A^{1/3}. \tag{37}$$

With these we can rewrite (35)–(36) as follows ††:

† Some details about the calculation of $E_u$ can be found in the appendix.

†† The notation $0.\dot{5}$ means $0.555\ldots$

$$
\begin{aligned}
E &= kE_F+E_W+E_C+E_R+E_u \\
&= \left(\frac{a}{r_0}\right)^2 [1.10542\times 10^{-25}\, kA^{5/3}(1+0.\dot{5}n^2)+3.09834\times 10^{-25}\, A] \\
&+ \frac{a}{r_0}[1.43587\times 10^{-14}\, A^2(1-2n+n^2)-1.54629\times 10^{-14}\, A^{4/3}(1-1.\dot{3}n+0.\dot{2}n^2)] \\
&-6.24208\times 10^5 \frac{g^2}{r_0} A^2 \Big\{(1-n^2)\langle[0.797885a^3+e^{1/2a^2}\phi(1/\sqrt{2}\,a)]\gamma_1-e^{1/2a^2}\gamma_2\rangle \\
&-\Big\langle e^{1/2a^2}+n^2\left\{1.27324a^2+e^{1/2a^2}\left[\phi^2\left(\frac{1}{2a}\right)-2\phi\left(\frac{1}{2a}\right)\right]-2.25676ae^{1/4a^2}\left[1-\phi\left(\frac{1}{2a}\right)\right]\right\}\Big\rangle \gamma_3 \\
&-1.09936a^3\langle\gamma_4[0.197939-0.14777aA^{1/3}+0.0441592a^2A^{2/3}-0.0047617a^3A] \\
&+n^2[\gamma_5(0.197939-0.229864aA^{1/3}+0.0981315a^2A^{2/3}-0.0142851a^3A) \\
&-\gamma_6\left(0.0372117\frac{1}{aA^{1/3}}+0.138651-0.115091aA^{1/3}+0.0392526a^2A^{2/3}-0.0047617a^3A\right)]\rangle\Big\}
\end{aligned}
\tag{38}
$$

where we used the notations

$$
\begin{aligned}
\gamma_1 &= \tfrac{1}{2}W-\tfrac{1}{8}M+\tfrac{1}{4}B-\tfrac{1}{4}H \\
\gamma_2 &= \tfrac{1}{4}W+\tfrac{1}{8}B \\
\gamma_3 &= \tfrac{1}{4}W-\tfrac{1}{8}M+\tfrac{1}{8}B-\tfrac{1}{4}H \\
\gamma_4 &= \tfrac{1}{2}W-2M+B-H \\
\gamma_5 &= \tfrac{1}{2}W-M+B-\tfrac{1}{2}H \\
\gamma_6 &= M+\tfrac{1}{2}H.
\end{aligned}
\tag{39}
$$

To find the best values for the binding energies along the whole periodical system, we proceeded according to the following program executed on SILLIAC.

We made a routine for calculating the total energy of a certain nucleus ${}_zX^A$ as a function of the variational parameter $a$. This function also involves three independent parameters which are the weight factor of the Wigner force $W$, the ratio $\alpha$ between the mass of meson partaking in the nuclear interaction and that of the electron, and finally the square of the mesonic charge $g^2$. This routine supplied $E_{A,Z}^{(W,\alpha,g^2)}$ which was then minimised with respect to $a$ yielding $E_{\min} = E(a_{00})$ — the indices omitted for the moment. With the known binding energy $(E_{A,Z})_B$ we formed the relative deviation of the computed energy minimum from the experimental value $\varepsilon$. To obtain the best fit we minimised the sum of the values $\varepsilon^2$ over a certain number of nuclei. (We chose only 15 nuclei, shown in table 1, in order to save machine time.)

TABLE 1

$A$ mass number; $Z$ number of protons; $-E_B/A$ binding energy per nucleon in MeV

| $A$ | $Z$ | $-E_B/A$ |
|---|---|---|
| 10 | 5 | 6.443 |
| 14 | 5 | 7.477 |
| 20 | 10 | 7.999 |
| 30 | 14 | 8.497 |
| 40 | 18 | 8.556 |
| 50 | 22 | 8.695 |
| 60 | 28 | 8.752 |
| 78 | 36 | 8.633 |
| 99 | 44 | 8.594 |
| 119 | 50 | 8.497 |
| 139 | 57 | 8.336 |
| 160 | 64 | 8.202 |
| 198 | 78 | 7.879 |
| 220 | 86 | 7.669 |
| 242 | 96 | 7.488 |

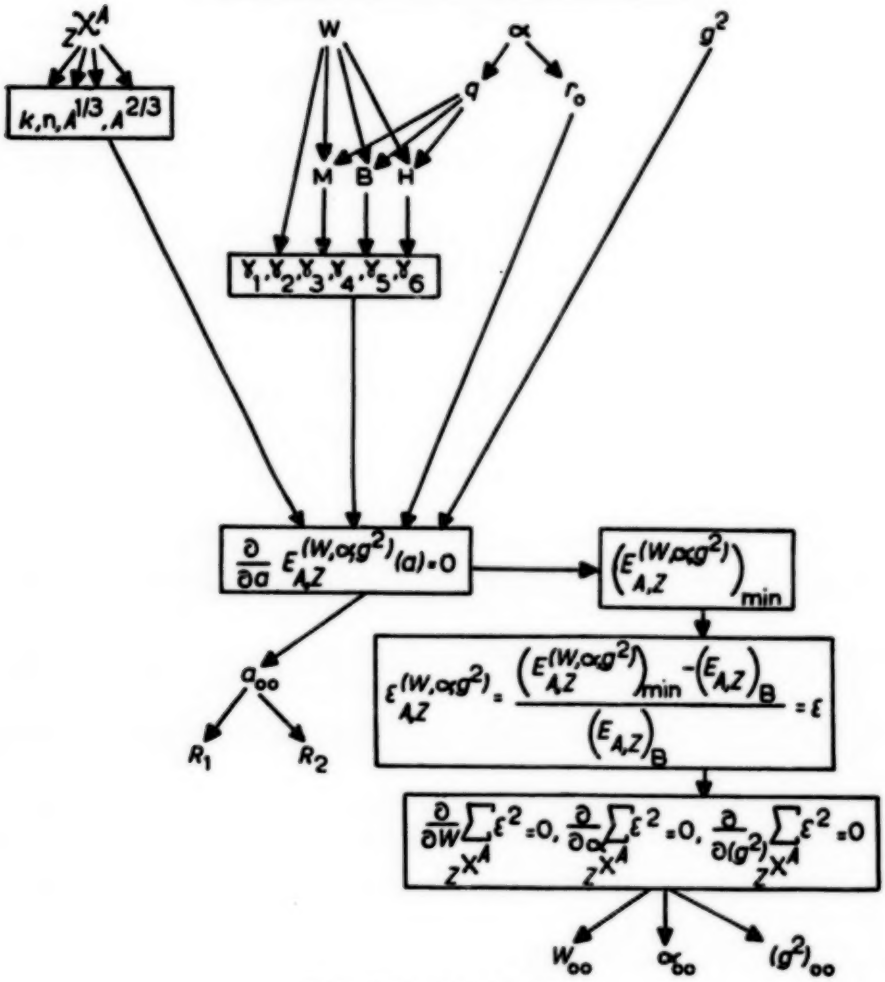


Flow chart (logical design).

This process yields

$$\begin{aligned} \alpha_{00} &= 273.23 \\ W_{00} &= 1.4311 \\ (g^2/r_0)_{00} &= 76.994 \text{ MeV}. \end{aligned} \tag{40}$$

We should note a few facts in connection with (40).

(a) The function $\sum_{Z^XA} \varepsilon^2$ is very flat in the range

$$\begin{aligned} 271 &\leqq \alpha \leqq 274 \\ 1.425 &\leqq W \leqq 1.445 \\ 76 &\leqq g^2/r_0 \leqq 77.5. \end{aligned} \tag{41}$$

Thus the fourth figures of the values (40) are affected by the way in which the "specimen" nuclei (table 1) are chosen (e.g. how many of them are of even or odd mass number, a property which cannot, of course, be reflected in the statistical theory).

(b) The weight factor of the Wigner force is not at all equal to that of Bartlett force. With (68)

$$\begin{aligned} W &= +1.4311 \\ M &= -0.6059 \\ B &= -1.4950 \\ H &= +1.6698. \end{aligned} \tag{42}$$

(c) $\alpha_{00}$ is remarkably close to the experimental value of the $\pi$-meson mass.

(d) For the nuclei with $A \geqq 7$ there is no bigger deviation than 20

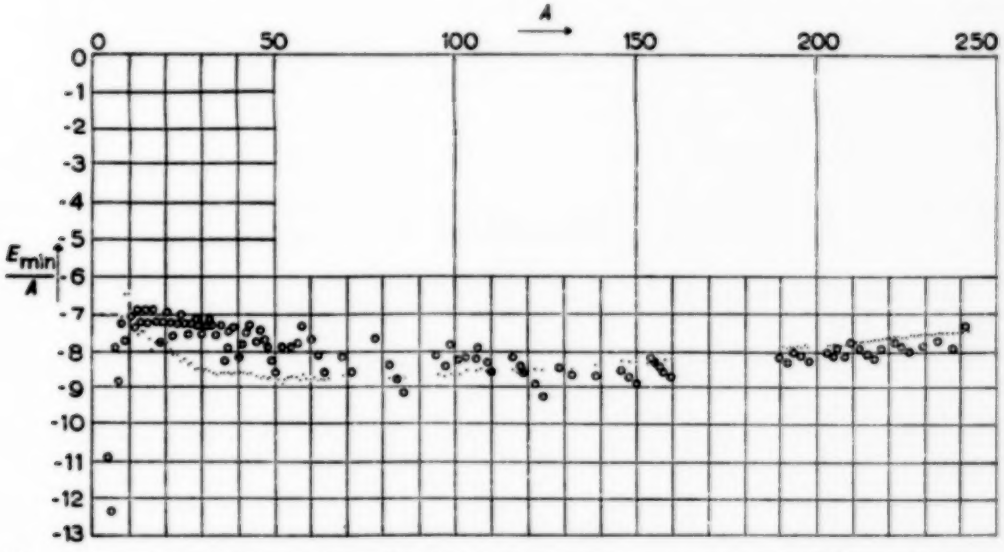


Fig. 1. Experimental (·) and theoretical (o) binding energies per nucleon in MeV as a function of the mass number.

TABLE 2

| $A$ | $Z$ | $-\frac{E_B}{A}$ | $-\frac{E_{min}}{A}$ | $\varepsilon$ | $R_1/A^{1/3}$ | $R_2/A^{1/3}$ | | $a_{00}$ |
|---|---|---|---|---|---|---|---|---|
| | | | | | | $\eta=0.5$ | $\eta=0.25$ | |
| 4 | 2 | 7.050 | 10.896 | −55 | 1.12 | 0.83 | 0.95 | 1.796 |
| 5 | 2 | 5.480 | 12.339 | −125 | 1.10 | 0.84 | 0.96 | 1.694 |
| 6 | 3 | 5.320 | 7.894 | −48 | 1.37 | 1.11 | 1.23 | 1.283 |
| 7 | 3 | 5.590 | 8.793 | −57 | 1.18 | 0.98 | 1.08 | 1.417 |
| 8 | 4 | 7.039 | 7.213 | −2 | 1.47 | 1.25 | 1.37 | 1.084 |
| 9 | 4 | 6.442 | 7.713 | −20 | 1.31 | 1.13 | 1.24 | 1.174 |
| 10 | 5 | 6.443 | 6.986 | −8 | 1.49 | 1.31 | 1.43 | 0.992 |
| 11 | 5 | 6.709 | 7.366 | −10 | 1.40 | 1.24 | 1.36 | 1.023 |
| 12 | 6 | 7.515 | 6.911 | +8 | 1.49 | 1.34 | 1.46 | 0.933 |
| 13 | 6 | 7.435 | 7.234 | +3 | 1.43 | 1.29 | 1.41 | 0.952 |
| 14 | 7 | 7.477 | 6.899 | +8 | 1.48 | 1.36 | 1.48 | 0.892 |
| 15 | 7 | 7.671 | 7.185 | +6 | 1.43 | 1.32 | 1.43 | 0.905 |
| 16 | 8 | 7.948 | 6.913 | +13 | 1.48 | 1.38 | 1.49 | 0.858 |
| 17 | 8 | 7.724 | 7.173 | +7 | 1.42 | 1.34 | 1.45 | 0.871 |
| 18 | 8 | 7.739 | 7.675 | +1 | 1.24 | 1.18 | 1.27 | 0.978 |
| 19 | 9 | 7.745 | 7.177 | +7 | 1.41 | 1.35 | 1.45 | 0.845 |
| 20 | 10 | 7.999 | 6.967 | +13 | 1.45 | 1.39 | 1.50 | 0.812 |
| 21 | 10 | 7.933 | 7.190 | +9 | 1.40 | 1.35 | 1.46 | 0.824 |
| 22 | 10 | 8.042 | 7.564 | +6 | 1.26 | 1.22 | 1.32 | 0.901 |
| 23 | 11 | 8.080 | 7.205 | +11 | 1.39 | 1.36 | 1.46 | 0.806 |
| 24 | 12 | 8.254 | 7.020 | +15 | 1.42 | 1.39 | 1.49 | 0.781 |
| 25 | 12 | 8.196 | 7.220 | +12 | 1.37 | 1.35 | 1.45 | 0.794 |
| 26 | 12 | 8.313 | 7.529 | +9 | 1.26 | 1.25 | 1.34 | 0.851 |
| 27 | 13 | 8.313 | 7.234 | +13 | 1.36 | 1.35 | 1.45 | 0.781 |
| 28 | 14 | 8.426 | 7.062 | +16 | 1.39 | 1.38 | 1.48 | 0.757 |
| 29 | 14 | 8.452 | 7.246 | +14 | 1.34 | 1.34 | 1.44 | 0.773 |
| 30 | 14 | 8.497 | 7.515 | +12 | 1.25 | 1.25 | 1.34 | 0.821 |
| 31 | 15 | 8.484 | 7.255 | +14 | 1.33 | 1.33 | 1.43 | 0.766 |
| 32 | 16 | 8.504 | 7.089 | +17 | 1.36 | 1.37 | 1.47 | 0.739 |

| $A$ | $Z$ | $-\frac{E_B}{A}$ | $-\frac{E_{min}}{A}$ | $\varepsilon$ | $R_1/A^{1/3}$ | $R_2/A^{1/3}$ | | $a_{00}$ |
|---|---|---|---|---|---|---|---|---|
| | | | | | | $\eta=0.5$ | $\eta=0.25$ | |
| 33 | 16 | 8.519 | 7.262 | +15 | 1.30 | 1.32 | 1.41 | 0.762 |
| 34 | 16 | 8.600 | 7.504 | +13 | 1.24 | 1.26 | 1.34 | 0.796 |
| 35 | 17 | 8.521 | 7.266 | +15 | 1.29 | 1.31 | 1.40 | 0.757 |
| 36 | 16 | 8.559 | 8.210 | +4 | 1.16 | 1.19 | 1.27 | 0.830 |
| 37 | 17 | 8.540 | 7.794 | +9 | 1.19 | 1.22 | 1.30 | 0.805 |
| 38 | 18 | 8.583 | 7.488 | +13 | 1.22 | 1.26 | 1.34 | 0.775 |
| 39 | 19 | 8.554 | 7.267 | +15 | 1.26 | 1.30 | 1.38 | 0.747 |
| 40 | 18 | 8.556 | 8.093 | +5 | 1.17 | 1.20 | 1.28 | 0.801 |
| 41 | 19 | 8.551 | 7.738 | +10 | 1.19 | 1.23 | 1.31 | 0.778 |
| 42 | 20 | 8.593 | 7.465 | +13 | 1.22 | 1.26 | 1.35 | 0.754 |
| 43 | 21 | 8.577 | 7.257 | +15 | 1.24 | 1.29 | 1.37 | 0.734 |
| 45 | 21 | 8.645 | 7.682 | +11 | 1.19 | 1.24 | 1.32 | 0.757 |
| 46 | 22 | 8.663 | 7.434 | +14 | 1.21 | 1.26 | 1.35 | 0.738 |
| 47 | 22 | 8.670 | 7.654 | +12 | 1.19 | 1.24 | 1.32 | 0.745 |
| 48 | 22 | 8.690 | 7.905 | +9 | 1.17 | 1.23 | 1.31 | 0.751 |
| 49 | 22 | 8.650 | 8.185 | +5 | 1.15 | 1.21 | 1.29 | 0.757 |
| 50 | 22 | 8.695 | 8.490 | +2 | 1.14 | 1.20 | 1.28 | 0.759 |
| 52 | 24 | 8.830 | 7.820 | +11 | 1.17 | 1.24 | 1.32 | 0.732 |
| 54 | 25 | 8.674 | 7.873 | +9 | 1.16 | 1.24 | 1.32 | 0.725 |
| 56 | 26 | 8.688 | 7.735 | +11 | 1.17 | 1.25 | 1.32 | 0.714 |
| 58 | 28 | 8.607 | 7.293 | +15 | 1.19 | 1.28 | 1.36 | 0.690 |
| 60 | 28 | 8.752 | 7.651 | +13 | 1.17 | 1.25 | 1.33 | 0.698 |
| 62 | 28 | 8.741 | 8.074 | +8 | 1.15 | 1.23 | 1.31 | 0.703 |
| 64 | 28 | 8.760 | 8.551 | +2 | 1.13 | 1.22 | 1.30 | 0.704 |
| 69 | 31 | 8.612 | 8.096 | +6 | 1.14 | 1.24 | 1.32 | 0.681 |
| 71 | 31 | 8.620 | 8.530 | +1 | 1.13 | 1.23 | 1.31 | 0.682 |
| 78 | 36 | 8.633 | 7.608 | +12 | 1.15 | 1.27 | 1.34 | 0.648 |
| 82 | 36 | 8.687 | 8.318 | +4 | 1.13 | 1.25 | 1.32 | 0.651 |
| 84 | 36 | 8.687 | 8.706 | — | 1.12 | 1.24 | 1.31 | 0.650 |
| 86 | 36 | 8.677 | 9.110 | −5 | 1.11 | 1.23 | 1.30 | 0.650 |
| 95 | 42 | 8.599 | 8.018 | +7 | 1.13 | 1.26 | 1.34 | 0.618 |

TABLE 2 (continued)

| $A$ | $Z$ | $-\frac{E_B}{A}$ | $-\frac{E_{min}}{A}$ | $\varepsilon$ | $R_1/A^{1/3}$ | $R_2/A^{1/3}$ | | $a_{00}$ |
|---|---|---|---|---|---|---|---|---|
| | | | | | | $\eta=0.5$ | $\eta=0.25$ | |
| 97 | 42 | 8.606 | 8.342 | +3 | 1.12 | 1.26 | 1.33 | 0.618 |
| 99 | 44 | 8.594 | 7.867 | +8 | 1.13 | 1.27 | 1.34 | 0.609 |
| 101 | 44 | 8.601 | 8.172 | +5 | 1.13 | 1.26 | 1.34 | 0.609 |
| 103 | 45 | 8.493 | 8.090 | +5 | 1.13 | 1.27 | 1.34 | 0.604 |
| 106 | 46 | 8.499 | 8.158 | +4 | 1.12 | 1.27 | 1.34 | 0.600 |
| 107 | 47 | 8.465 | 7.931 | +6 | 1.13 | 1.27 | 1.34 | 0.595 |
| 109 | 47 | 8.471 | 8.220 | +3 | 1.12 | 1.27 | 1.34 | 0.595 |
| 110 | 46 | 8.511 | 8.766 | −3 | 1.11 | 1.26 | 1.33 | 0.599 |
| 116 | 50 | 8.489 | 8.105 | +5 | 1.12 | 1.27 | 1.34 | 0.583 |
| 118 | 50 | 8.495 | 8.382 | +1 | 1.12 | 1.27 | 1.34 | 0.583 |
| 119 | 50 | 8.497 | 8.522 | — | 1.11 | 1.27 | 1.34 | 0.582 |
| 122 | 50 | 8.430 | 8.945 | −6 | 1.11 | 1.26 | 1.33 | 0.581 |
| 124 | 50 | 8.453 | 9.229 | −9 | 1.10 | 1.26 | 1.33 | 0.580 |
| 129 | 54 | 8.403 | 8.413 | — | 1.11 | 1.28 | 1.35 | 0.567 |
| 132 | 55 | 8.405 | 8.586 | −2 | 1.11 | 1.28 | 1.34 | 0.564 |
| 139 | 57 | 8.336 | 8.625 | −3 | 1.11 | 1.28 | 1.35 | 0.555 |
| 146 | 60 | 8.262 | 8.452 | −2 | 1.11 | 1.28 | 1.35 | 0.546 |
| 148 | 60 | 8.253 | 8.681 | −5 | 1.11 | 1.28 | 1.35 | 0.544 |
| 150 | 60 | 8.244 | 8.910 | −8 | 1.10 | 1.28 | 1.35 | 0.544 |
| 155 | 64 | 8.270 | 8.190 | +1 | 1.11 | 1.29 | 1.36 | 0.534 |
| 156 | 64 | 8.273 | 8.296 | — | 1.11 | 1.29 | 1.36 | 0.533 |
| 157 | 64 | 8.273 | 8.403 | −2 | 1.11 | 1.29 | 1.36 | 0.533 |
| 158 | 64 | 8.199 | 8.509 | −4 | 1.11 | 1.29 | 1.36 | 0.532 |
| 160 | 64 | 8.202 | 8.720 | −6 | 1.10 | 1.29 | 1.35 | 0.532 |
| 190 | 76 | 7.907 | 8.148 | −3 | 1.11 | 1.31 | 1.38 | 0.500 |
| 192 | 76 | 7.910 | 8.320 | −5 | 1.11 | 1.31 | 1.38 | 0.499 |
| 194 | 78 | 7.907 | 7.968 | −1 | 1.11 | 1.32 | 1.38 | 0.495 |
| 196 | 78 | 7.913 | 8.136 | −3 | 1.11 | 1.31 | 1.38 | 0.495 |
| 198 | 78 | 7.879 | 8.302 | −5 | 1.11 | 1.31 | 1.38 | 0.495 |

| $A$ | $Z$ | $-\frac{E_B}{A}$ | $-\frac{E_{min}}{A}$ | $\varepsilon$ | $R_1/A^{1/3}$ | $R_2/A^{1/3}$ | | $a_{00}$ |
|---|---|---|---|---|---|---|---|---|
| | | | | | | $\eta=0.5$ | $\eta=0.25$ | |
| 203 | 81 | 7.823 | 7.949 | −2 | 1.11 | 1.32 | 1.39 | 0.488 |
| 205 | 81 | 7.823 | 8.109 | −4 | 1.11 | 1.32 | 1.38 | 0.487 |
| 206 | 82 | 7.827 | 7.940 | −1 | 1.11 | 1.32 | 1.39 | 0.486 |
| 208 | 82 | 7.819 | 8.097 | −4 | 1.11 | 1.32 | 1.39 | 0.485 |
| 210 | 84 | 7.786 | 7.766 | — | 1.11 | 1.32 | 1.39 | 0.482 |
| 212 | 84 | 7.762 | 7.919 | −2 | 1.11 | 1.33 | 1.39 | 0.481 |
| 214 | 84 | 7.737 | 8.071 | −4 | 1.11 | 1.32 | 1.39 | 0.480 |
| 216 | 84 | 7.711 | 8.222 | −7 | 1.11 | 1.32 | 1.39 | 0.479 |
| 218 | 86 | 7.691 | 7.894 | −3 | 1.11 | 1.32 | 1.39 | 0.478 |
| 220 | 86 | 7.669 | 8.042 | −5 | 1.11 | 1.32 | 1.39 | 0.476 |
| 222 | 88 | 7.650 | 7.721 | −1 | 1.11 | 1.33 | 1.39 | 0.474 |
| 224 | 88 | 7.632 | 7.866 | −3 | 1.11 | 1.33 | 1.39 | 0.473 |
| 226 | 88 | 7.613 | 8.009 | −5 | 1.11 | 1.33 | 1.39 | 0.472 |
| 230 | 90 | 7.582 | 7.834 | −3 | 1.11 | 1.33 | 1.40 | 0.469 |
| 234 | 92 | 7.553 | 7.662 | −1 | 1.11 | 1.34 | 1.40 | 0.465 |
| 238 | 92 | 7.522 | 7.934 | −5 | 1.11 | 1.33 | 1.40 | 0.464 |
| 242 | 96 | 7.488 | 7.330 | +2 | 1.12 | 1.34 | 1.41 | 0.459 |

$A$ mass number; $Z$ number of protons; $-E_B/A$ and $-E_{min}/A$ the experimental and theoretical binding energy per nucleon in MeV; $\varepsilon$ relative deviation of the two latter quantities in percentages; $R_1/A^{1/3}$ and $R_2/A^{1/3}$ quantities related to nuclear radii in units of $10^{-13}$ cm; $a_{00}$ value of the variational parameter at energy minimum.

per cent between the experimental binding energy per nucleon $-E_B/A$ and the calculated value $-E_{min}/A$ (see table 2 and fig. 1). For smaller atomic numbers the statistical theory does not seem to be adequate; however, these extreme differences from the experimental values may be due to the overcompensating of the effect of the Weizsäcker correction (factor $k$ in (5)).

(e) In spite of the known deficiency of the Born approximation we compare the neutron-proton scattering formula (23) with experimental values. Fig. 2 contains the experimental data for 14.1 MeV and 17.9 MeV taken from ref. [5]). The full line represents the theoretical curve fitted at the angle

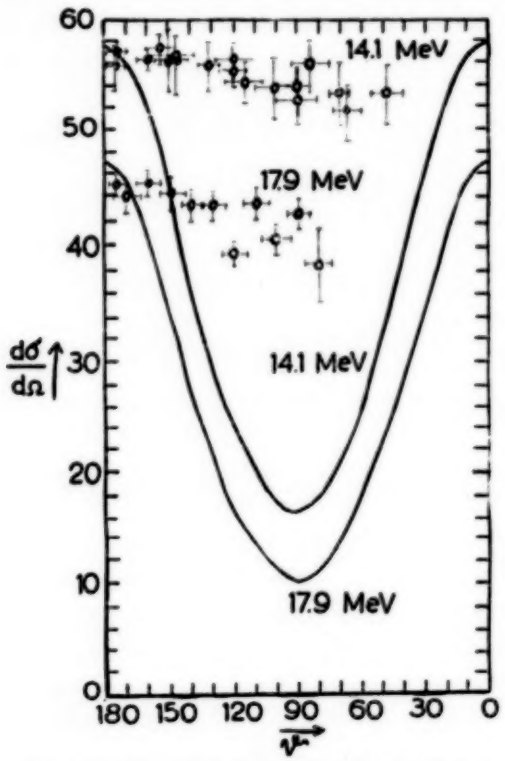


Fig. 2. Differential cross section for n−p scattering in mb/sterad as a function of scattering angle in c.m.s. at 14.1 MeV and 17.9 MeV. The experimental values are taken from [5]). The full line given by theory is fitted at $\vartheta = 0$.

$\vartheta = 0$. It can be seen that the agreement is rather poor and at higher energies it is still worse. The deviations cannot be due only to the inadequacy of the Born approximation but show the incompleteness of our force assumption.

(f) We have chosen a light ($_8O^{16}$), a medium ($_{36}Kr^{80}$) and a heavy nucleus ($_{80}Hg^{200}$) to illustrate in fig. 3 the density distribution

$$\rho = \rho_0 e^{-a^2 r^2/r_0^2}, \qquad \rho_0 = \rho_{p0} + \rho_{n0} = \frac{A a^3}{\pi^{3/2} r_0^3}. \tag{43}$$

We mention that $\rho_0$ is practically constant from $A = 40$ on.

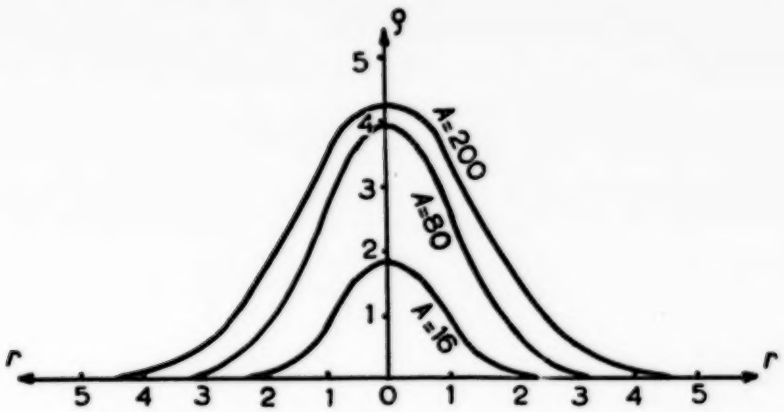


Fig. 3. Density distribution for the nuclei ${}_8O^{16}$, ${}_{36}Kr^{80}$, ${}_{80}Hg^{200}$; $r$ is given in units $r_0$ and $\rho$ in $r_0^{-3}$.

Following Gombás [7]) we may characterise such density distributions by two "radii" $R_1$, $R_2$ defined by

$$R_1 = \beta \cdot \langle r \rangle = \frac{4\beta\pi}{A} \int_0^\infty r^3 \rho(r) \mathrm{d}r = 2\beta/\sqrt{\pi}(r_0/a), \tag{44}$$

where we choose $\beta = 2$, which value is plausible from fig. 3, and

$$\eta = 4\pi \int_{R_2}^\infty r^2 \rho(r) \mathrm{d}r, \tag{45}$$

where $\eta$ is some small number ($\eta = 0.25-0.5$) representing the mean number of nucleons outside the radius $R_2$. The value of $R_2$ is not very sensitive to the choice of $\eta$. In the table 2, we have set out the values $R_1/A^{1/3}$ and $R_2/A^{1/3}$.

Finally, the author would like to express his thanks to Professor P. Gombás (Budapest) for his interest in a part of this work, to Professor H. Messel (Sydney) for his encouragement, and also to the staff of the Adolph Basser Computing Laboratory for the excellent computing facilities.

## Appendix

### ON THE NUCLEAR INTERACTION ENERGIES

Let us define the quantities

$$\begin{aligned} E_V^{pn} &= \int U_p(r) \rho_n(r) \mathrm{d}v \\ E_V^{pp} &= \int U_p(r) \rho_p(r) \mathrm{d}v \\ E_V^{nn} &= \int U_n(r) \rho_n(r) \mathrm{d}v \end{aligned} \tag{A.1}$$

where $\rho_p$ and $\rho_n$ are the proton and neutron density functions (33) and $U_p$ and $U_n$ the nuclear potentials caused by them in an exchange-free nuclear

interaction (31). In the case of spherical symmetry, $U_p$, for example, can be written as follows:

$$U_p(r_1) = -2\pi r_0 g^2 \left\{ \frac{e^{r_1/r_0} - e^{-r_1/r_0}}{r_1} \int_0^\infty e^{-r_2/r_0} \rho_p(r_2) r_2 \, dr_2 + \frac{e^{-r_1/r_0}}{r_1} \int_0^{r_1} e^{r_2/r_0} \rho_p(r_2) r_2 \, dr_2 - \frac{e^{r_1/r_0}}{r_1} \int_0^{r_1} e^{-r_1/r_0} \rho_p(r_2) r_2 \, dr_2 \right\}. \quad \text{(A.2)}$$

If we take into account the identity

$$\begin{aligned} \int_0^\infty e^{r_1/r_0} \rho_n(r_1) r_1 \int_0^{r_1} e^{-r_2/r_0} \rho_p(r_2) r_2 \, dr_2 \, dr_1 &= \int_0^\infty e^{r_1/r_0} \rho_n(r_1) r_1 \, dr_1 \int_0^\infty e^{-r_2/r_0} \rho_p(r_2) r_2 \, dr_2 \\ &- \int_0^\infty e^{-r_1/r_0} \rho_p(r_1) r_1 \int_0^{r_1} e^{r_2/r_0} \rho_n(r_2) r_2 \, dr_2 \, dr_1 \end{aligned} \quad \text{(A.3)}$$

and introduce the notations

$$\begin{aligned} P_p &= \int_0^\infty e^{r_1/r_0} \rho_p(r_1) r_1 \, dr_1, \qquad P_n = \int_0^\infty e^{r_1/r_0} \rho_n(r_1) r_1 \, dr_1, \\ S_p &= \int_0^\infty e^{-r_1/r_0} \rho_p(r_1) r_1 \, dr_1, \quad S_n = \int_0^\infty e^{-r_1/r_0} \rho_n(r_1) r_1 \, dr_1, \\ T_p &= \int_0^\infty e^{-r_1/r_0} \rho_n(r_1) r_1 \int_0^{r_1} e^{r_2/r_0} \rho_p(r_2) r_2 \, dr_2 \, dr_1, \\ T_n &= \int_0^\infty e^{-r_1/r_0} \rho_p(r_1) r_1 \int_0^{r_1} e^{r_2/r_0} \rho_n(r_2) r_2 \, dr_2 \, dr_1, \end{aligned} \quad \text{(A.4)}$$

we may write

$$\begin{aligned} E_V^{pn} &= -8\pi^2 r_0 g^2 [(P_n - S_n) S_p + T_p - P_n S_p + T_n] \\ &= -8\pi^2 r_0 g^2 (T_p + T_n - S_n S_p) \\ E_V^{pp} &= -8\pi^2 r_0 g^2 (2T_p - S_p^2) \\ E_V^{nn} &= -8\pi^2 r_0 g^2 (2T_n - S_n^2). \end{aligned} \quad \text{(A.5)}$$

The above integrals can be performed without any difficulty with the exception of one which is of the form

$$I = \int_{b/2}^\infty \phi(y) e^{-(y-b)^2} \, dy. \quad \text{(A.6)}$$

To evaluate $I$ we first differentiate the integral with respect to the parameter $b$ and then carry out the integral over $y$:

$$\begin{aligned} \frac{d}{db} I &= \int_{b/2}^\infty \phi(y) 2(y-b) e^{-(y-b)^2} \, dy - \tfrac{1}{2} \phi\left(\frac{b}{2}\right) e^{-b^2/4} \\ &= \tfrac{1}{2} \phi\left(\frac{b}{2}\right) e^{-b^2/4} + \frac{1}{\sqrt{2}} e^{-b^2/2}. \end{aligned} \quad \text{(A.7)}$$

Integrating this with respect to $b$ yields

$$I = \frac{\sqrt{\pi}}{4} \phi^2\left(\frac{b}{2}\right) + \frac{\sqrt{\pi}}{2} \phi\left(\frac{b}{\sqrt{2}}\right) + c. \quad \text{(A.8)}$$

The constant of integration can be determined by comparing (A.6) and (A.8) for the value $b = 0$. This gives

$$\int_0^\infty \phi(y)\mathrm{e}^{-y^2}\,\mathrm{d}y = \frac{\sqrt{\pi}}{4} = c. \tag{A.9}$$

## References


1) J. M. Blatt and V. F. Weisskopf, Theoretical Nuclear Physics (John Wiley & Sons. Inc., New York, 1947)
2) N. V. Findler, Thesis (Budapest, 1956) unpublished
3) S. Flügge, Z.f. Phys. **96** (1935) 459
4) S. Flügge, Erg. d. ex. Naturwiss. **26** (1952) 165
5) A. Galonsky and J. Judish, Phys. Rev. **98** (1955) 1168
6) P. Gombás, Die statistische Theorie des Atoms und ihre Anwendung (Springer; Wien, 1949)
7) P. Gombás, Acta Phys. Hung. a) **1** (1952) 329; b) **2** (1952) 223; c) **4** (1954) 267; d) **5** (1956) 511
8) P. Gombás, Acta Phys. Hung. **2** (1952) 247
9) J. Hadley, E. Kelly, C. Leith, E. Segrè, C. Wiegand and H. York, Phys. Rev. **75** (1949) 351
10) W. Heisenberg, Rapport du VIIe Congrès Solvay (Paris, 1934)
11) W. Inthoff, Ann. d. Phys. **15** (1955) 376
12) D. D. Ivanenko and D. Rodichev, Dokladi Akad. Nauk SSSR **70** (1950) 605
13) D. D. Ivanenko and A. A. Sokolov, Dokladi Akad. Nauk SSSR **74** (1950) 33
14) D. Kisdi, Acta Phys. Hung. a) **5** (1956) 519; b) **6** (1956) 251
15) F. I. Kligman, Zhurnal Exp. Teor. Fiz. **28** (1955) 297
16) A. S. Kompaneetz, Dokladi Akad. Nauk SSSR **85** (1952) 301
17) E. Majorana, Z.f. Phys. **82** (1933) 137
18) U. Nakabayasi, Z.f. Phys. **97** (1935) 211
19) H. R. Paneth, Proc. Phys. Soc. A **64** (1951) 937
20) P. Román, Acta Phys. Hung. **1** (1952) 107
21) L. Rosenfeld, Nuclear Forces (North Holland Publ. Co., Amsterdam, 1948)
22) F. S. Wang, Z.f. Phys. **100** (1936) 736
23) C. F. v. Weizsäcker, Z.f. Phys. **96** (1935) 431
24) C. F. v. Weizsäcker, Naturwiss. **26** (1938) 209, 225
25) G. C. Wick, Nuovo Cimento **11** (1934) no. 4
26) G. C. Wick, Rendi Accad. Lincei **19** (1934) 319
27) L. M. Yang, Proc. Phys. Soc. A **64** (1951) 632

2.C *Nuclear Physics* **8** (1958) 358—373; © *North-Holland Publishing Co., Amsterdam*
Not to be reproduced by photoprint or microfilm without written permission from the publisher

# EFFECTIVE RANGE EXPANSION OF THE SCATTERING MATRIX

L. M. DELVES
*Clarendon Laboratory, Oxford, England*

Received 22 May 1958

**Abstract:** The scattering matrix for the general $N$-channel reaction is diagonalized in the channel spin representation, and the eigen-phase-shifts and elements of the diagonalizing matrix are expanded in a power series about an arbitrary energy. Methods are given for calculating the coefficients in the series from numerical solutions of the wave equation, thus giving a complete generalization of the usual effective range theory to $N$-channel systems.

## 1. Introduction

The theoretical discussion of a binary collision $a+X \rightarrow Y+b$ becomes very involved when several closely coupled competing channels are present, so that the scattering matrix is not approximately diagonal, and the channels cannot be treated independently. Strictly this is always the case when reactions other than elastic scattering can occur; it may also be so for elastic scattering alone, if appreciable spin-orbit forces are present. It is just in these circumstances that numerical solutions become very laborious, so that a generalization of the usual single-channel effective range expansion of the scattering matrix [1–4]) to the $N$-channel case would be useful for minimizing the numerical work needed. Such an expansion has been given for neutral elastic scattering and $N = 2$ by Blatt and Biedenharn [5,6]). These results are extended here to the general case. All our formulae are applicable to any collision in which two particles (not necessarily elementary) enter and two particles emerge.

## 2. The Scattering Matrix near $E_0$

Consider a general two-body reaction $a+X \rightarrow Y+b$. We shall define the state of the system before or after the impact, i.e. in the external region, by the total angular momentum $J$ of the system and its $z$-component $M$, the channel spin $s$, the channel orbital angular momentum $l$, and an index $\rho$ to describe the internal states of the two nuclei. Thus the reaction may be represented by

$$J M \rho s l \rightarrow J' M' \rho' s' l'.$$

A given combination of $JM\rho sl$ is called a channel; and if there are $P$ of these we say the reaction is a $P$-channel reaction. $P$ is formally infinite, but we may usually neglect all but a very few possible $J$. If no external fields are present, $J$ and $M$ are conserved in the reaction, and the total scattering matrix is diagonal in $J, M$. This is usually the case; and then we will consider one value of $J, M$ and call the number of possible combinations of $\rho, s, l$ for this $J, M$ the number of channels $N$. Thus, when we refer to the scattering matrix it is understood that we refer only to a given value of $J, M$. We shall also usually replace the quantum numbers $\rho, s, l$ by a single quantum number $\alpha$ to denote a channel, and we shall distinguish quantities proper to that channel by a subscript $\alpha$. In the external region we can then write for the total wave-function of the system for total angular momentum $J$, $z$-component $M$

$$^{JM}\Psi^{\infty} = \sum_{\alpha=1}^{N} r_\alpha^{-1}\, \phi_\alpha U_\alpha(r_\alpha) \mathcal{Y}^M_{Jl_\alpha s_\alpha} \tag{1}$$

where $\phi_\alpha$ is the product of the intrinsic wavefunctions of the two nuclei in the channel $\alpha$, $r_\alpha$ is the distance between their centres of mass, and $\mathcal{Y}^M_{Jl_\alpha s_\alpha}$ is defined by

$$\mathcal{Y}^M_{Jls}(\theta\phi s) = \sum_{m_l m_s} (lsm_l m_s | lsJM)(i^l Y_l^{m_l}(\theta\phi))\chi_s^{m_s} \tag{2}$$

where $Y_l^m$ is as defined in Condon and Shortley [12]) and $\chi_s^{M_s}$ is the usual channel-spin function. This choice of phases is much the most convenient for scattering problems [7]). The wavefunction $U_\alpha(r_\alpha)$ describing the relative motion of the two nuclei will then have the usual form

$$U_\alpha(r_\alpha) = \left(\frac{m_\alpha}{k_\alpha}\right)^{\frac{1}{2}} \{A_\alpha F_{l_\alpha}(r_\alpha) - B_\alpha G_{l_\alpha}(r_\alpha)\} \tag{3}$$

where $m_\alpha$ is the reduced mass in the channel $\alpha$, and $k_\alpha$ is the channel wave-number, given by $k_\alpha^2 = 2m_\alpha(E - E_\alpha)/\hbar^2$, where $E_\alpha$ is the energy at which the channel opens. $F, G$ are the conventional regular and irregular solutions of the force-free or Coulomb wavefunctions, depending on whether $\alpha$ is neutral or charged, that is to say, depending on whether the product $(Z_1 Z_2)_\alpha$ of the charges of the nuclei in channel $\alpha$ is different from or equal to zero. $F$ and $G$ are defined to have unit amplitude at infinity. The wavefunction $\Psi$ will not, of course, be expressible in the form (1) in the internal region where the two product nuclei overlap.

Then we define the nuclear scattering or collision matrix $\mathbf{S}$ by the matrix equation

$$B = \mathbf{S}A; \tag{4}$$

$\mathbf{S}$ is unitary and symmetric, and can therefore be diagonalized by a real orthogonal matrix $\mathbf{T}$ in the form [8])

$$\mathbf{S} = \mathbf{T}^{\mathrm{T}} \mathrm{e}^{2i\delta} \mathbf{T} \tag{4a}$$

where $\boldsymbol{\delta}$ is a real diagonal matrix whose elements $\delta_\alpha$ are called the eigenphaseshifts of the reaction. The rows of **T** are the eigenvectors of **S** with eigenvalues $\exp 2i\boldsymbol{\delta}$; thus if we construct a linear combination of channels $\beta$ with amplitudes $A_\beta$ proportional to $T_{\alpha\beta}$, such a state is changed only in phase by the scattering, by an amount $2\delta_\alpha$. Such a state is called an eigenstate of the scattering matrix; there are $N$ such states corresponding to the $N$ rows of **T**, and each is associated with an eigenphaseshift $\delta_\alpha$. It is usually more convenient to work with **T** and $\boldsymbol{\delta}$ rather than **S**.

We should like an expansion for **S** and for **T** and $\boldsymbol{\delta}$, in powers of $(E-E_0)$ or some related parameter, about an arbitrary energy $E_0$. In particular it is often convenient to expand **S** about some energy $E_0$ at which new channels are just opening; for these channels $k_\alpha$ therefore tends to zero as $E \to E_0$. Having chosen an $E_0$ we shall call such channels "new"; channels which opened at an energy lower than $E_0$ and for which, therefore, $k_\alpha$ remains real and finite at $E_0$ are called "old."

Channels which are not open at $E_0$, i.e., which correspond to exponentially damped components of the wavefunction, have $k_\alpha$ imaginary at $E_0$. We shall ignore such channels; they do not interact appreciably with open channels except for energies close to that at which they will themselves open, after which, of course, they cannot be ignored. This means that our expansions will be valid up to an energy slightly less than that at which the next new channel with the same total angular momentum $J$ opens, although it may sometimes be a good approximation to ignore such further channels up to much higher energies.

Let us define a standard wave number $k$ by

$$k^2 = \frac{2m(E-E_0)}{\hbar^2} \tag{5a}$$

where $m$ is some arbitrary standard mass and $E$ is the total energy of the system. Then the variation of **S** with $k$ at $E_0$ has been discussed by Wigner and Eisenbud [9,10]). Note that the scattering matrix of these papers differs from ours in the case of charged channels in that they have included the Coulomb phase-shift in the scattering matrix instead of in the asymptotic form of the wavefunction.

We have from these papers the following form for **S** at $E_0$:

$$S_{\alpha\beta} = \exp(i\theta_\alpha)(\delta_{\alpha\beta}+ij_\alpha R_{\alpha\beta} j_\beta) \exp(i\theta_\beta)$$

where the matrix $R_{\alpha\beta}$ is real and symmetric and $\theta_\alpha$, $j_\alpha$ are real. $R_{\alpha\beta}$ is independent of $k$ at $E_0$, and $j$, $\theta$ vary with $k$ at $E_0$ in the way given in table 1. Note that $k_\alpha$ is independent of $k$ at $E_0$ if $\alpha$ is old, and is proportional to $k$ if $\alpha$ is new. Also

$$\eta_\alpha = m_\alpha(Z_1Z_2)_\alpha e^2/\hbar^2 k_\alpha \tag{5b}$$

TABLE 1

Variation of $j$, $\theta$ with $k$ at $E_0$

| | $j_\alpha$ | $\theta_\alpha$ |
|---|---|---|
| $\alpha$ old | 1 | 1 |
| $\alpha$ new, neutral | $k^{l_\alpha+\frac{1}{2}}$ | $k^{2l_\alpha+1}$ |
| $\alpha$ new, attractive | 1 | 1 |
| $\alpha$ new, repulsive | $e^{-\pi\eta_\alpha}$ | $e^{-2\pi\eta_\alpha}$ |

and near $k_\alpha = 0$

$$\begin{aligned} |e^{2\pi\eta_\alpha}-1| &= e^{2\pi\eta_\alpha} \quad \text{if} \quad (Z_1Z_2)_\alpha \text{ is positive, i.e. } \alpha \text{ repulsive.} \\ &= 1 \qquad \text{if} \quad (Z_1Z_2)_\alpha \text{ is negative, i.e. } \alpha \text{ attractive.} \end{aligned} \tag{5c}$$

These results can be used to find the variation of $\mathbf{T}$ and $\boldsymbol{\delta}$ with $k$ at $E_0$, but it is easier to start from a slightly different approach from that of Wigner and Eisenbud, which has been used by Guier and Hart [13]) in discussing thresholds of reactions involving more than two particles. The calculations are carried out in appendix A, with the results given in eqs. (6a) and (6b), and tables 2a and 2b; these may be verified by substituting into (4a) and carrying out the expansion, to regain table 1. $g_\alpha$ and $g_{\alpha\beta}$ are defined below in eq. (6); note that in all cases we have $g_\alpha = j_\alpha^2$.

From appendix A we then have the result that, near $E_0$,

$$\begin{aligned} g_\alpha \cot \delta_\alpha &= \text{const}, \\ g_{\alpha\beta} T_{\alpha\beta} &= \text{const} \end{aligned} \tag{6a}$$

and we can therefore expand $g_\alpha \cot \delta_\alpha$ and $g_{\alpha\beta}T_{\alpha\beta}$ in a power series in $k^2$ whose leading term is independent of $k$. We write

$$\begin{aligned} g_\alpha \cot \delta_\alpha &= \Delta_{\alpha 0}+\Delta_{\alpha 1}k^2+\Delta_{\alpha 2}k^4+ \ldots \\ g_{\alpha\beta}T_{\alpha\beta} &= {}_0T_{\alpha\beta}+{}_1T_{\alpha\beta}k^2+{}_2T_{\alpha\beta}k^4+ \ldots . \end{aligned} \tag{6b}$$

Comparing these results with the usual single-channel case, we see that the variation of the eigenphaseshifts with energy at $E_0$ is exactly the same as for the corresponding single-channel phaseshifts. The eigenphaseshift $\delta_\alpha$ is not however to be thought of as the phaseshift for channel $\alpha$; no such real phaseshift exists.

The question now arises as to how we can calculate the coefficients in the eqs. (6b) from numerical solutions of the wave equation.

TABLE 2a

A table of $g_\alpha$

| | $\alpha$ neutral | $\alpha$ charged attractive | $\alpha$ charged repulsive |
|---|---|---|---|
| $g_\alpha$, $\alpha$ new | $k^{2l_\alpha+1}$ | 1 | $e^{-2\pi\eta_\alpha}$ |
| $g_\alpha$, $\alpha$ old | 1 | 1 | 1 |

TABLE 2b

A table of $g_{\alpha\beta}$

| $\beta$ \ $\alpha$ | old | new, neutral | new, attractive | new, repulsive |
|---|---|---|---|---|
| old | 1 | $k^{-(l_\alpha+\frac{1}{2})}$ | 1 | $e^{\pi\eta_\alpha}$ |
| new, neutral | $k^{-(l_\beta+\frac{1}{2})}$ | $k^{-\lvert l_\alpha-l_\beta\rvert}$ | $k^{-(l_\beta+\frac{1}{2})}$ | $k^{l_\beta+\frac{1}{2}}e^{\pi\eta_\alpha}$ |
| new, attractive | 1 | $k^{-(l_\alpha+\frac{1}{2})}$ | 1 | $e^{\pi\eta_\alpha}$ |
| new, repulsive | $e^{\pi\eta_\beta}$ | $k^{l_\alpha+\frac{1}{2}}e^{\pi\eta_\beta}$ | $e^{\pi\eta_\beta}$ | $e^{\pi\lvert\eta_\alpha-\eta_\beta\rvert}$ |

## 3. The Leading Terms

Consider the form of the wavefunction near $E_0$ in the external region for eigenstates of the scattering matrix. That corresponding to the $\alpha$ eigenphase-shift is, from (1), (3) and the discussion following (4),

$$\Psi_\alpha^\infty = j_\alpha \sum_\gamma m_\gamma^{\frac{1}{2}} k_\gamma^{-\frac{1}{2}} T_{\alpha\gamma}\{\cot\delta_\alpha F_\gamma(r_\gamma)+G_\gamma(r_\gamma)\}r_\gamma^{-1}\phi_\gamma \mathscr{Y}_\gamma \qquad (7)$$

in which we can insert the leading terms for $T_{\alpha\gamma}$ and $\cot\delta_\alpha$ at $E_0$, and the asymptotic forms for $F_\gamma$ and $G_\gamma$ at $E_0$. These forms are listed for the various cases in appendix A. The $j_\alpha$ is a normalizing factor chosen to make $\Psi_\alpha$ finite at $E_0$. In general we will have, from numerical integration of the wave equation or by any other method, $N$ independent solutions $\xi_a$, say, of the wave equation at $E_0$, with the form in the external region

$$\xi_a^\infty = \sum_\gamma m_\gamma^{\frac{1}{2}} k_\gamma^{-\frac{1}{2}}\{A_{a\gamma}F_\gamma(r_\gamma)-B_{a\gamma}G_\gamma(r_\gamma)\}r_\gamma^{-1}\phi_\gamma \mathscr{Y}_\gamma \qquad (8)$$

and from these we wish to form linear combinations of the $\xi_a$ with the form (7).

We can do the following:

Substituting in (7) for the $F_\gamma$, $G_\gamma$, $T_{\alpha\gamma}$, and $\cot\delta_\alpha$ at $E_0$, the coefficients of $\phi_\gamma Y_\gamma/r_\gamma$ in $\Psi_\alpha$ are all of the same order. We can therefore take an arbitrary linear combination of the $\xi_a$ and equate coefficients of $\phi_\gamma Y_\gamma/r_\gamma$ with those in $\Psi_\alpha$. This gives us a set of quadratic equations, which, together with the

orthogonality relations

$$\sum_{\gamma} T_{\alpha\gamma} T_{\beta\gamma} = \delta_{\alpha\beta} \tag{9}$$

can always be solved, giving the leading terms in the series for $T_{\alpha\beta}$ and $\delta_{\alpha}$.

### 4. Relation between the Wavefunctions at Different Energies

To find the second and higher terms in the series it is necessary to know the form of the Schrödinger equation which the system satisfies. With this knowledge the coefficients of the second terms can be calculated from the solutions at $E_0$. Assume the forces between particles can be represented by a potential. Then the wave equation takes in the most general case the form

$$\left[\sum_j \frac{\hbar^2}{2m_j} \nabla_j^2 + E\right] \Psi = V\Psi \tag{10}$$

where the sums are over the various particles in the system and $V$ is the potential energy operator; if there are $p$ particles $\Psi$ is a function of $3(p-1)$ variables when the centre of mass motion has been removed, but we do not need to specify at this stage which particular set of variables we are using.

Using a subscript $x$ to denote quantities at an energy $E_x$, and considering the $\alpha$ and $\beta$ eigenstates, we have from (10)

$$\begin{aligned} \Psi_{2\beta}\left[\sum_j \frac{\hbar^2}{2m_j} \nabla_j^2 + E_1\right] \Psi_{1\alpha} &= \Psi_{2\beta} V_1 \Psi_{1\alpha} \\ \Psi_{1\alpha}\left[\sum_j \frac{\hbar^2}{2m_j} \nabla_j^2 + E_2\right] \Psi_{2\beta} &= \Psi_{1\alpha} V_2 \Psi_{2\beta}. \end{aligned} \tag{11a}$$

If the forces do not depend explicitly on energy, the right hand sides of these equations are equal. Note this is true for any system of forces representable by a potential; we are not restricted in any way to two body forces. We then have on subtracting the two equations

$$\Psi_{2\beta} \sum_j \frac{\hbar^2}{2m_j} \nabla_j^2 \Psi_{1\alpha} - \Psi_{1\alpha} \sum_j \frac{\hbar^2}{2m_j} \nabla_j^2 \Psi_{2\beta} = (E_2 - E_1) \Psi_{1\alpha} \Psi_{2\beta}. \tag{11b}$$

If the forces do depend explicitly on energy we must carry the extra term on the right hand side, but this does not introduce any complicating factor.

We can carry out the same process for the asymptotic wavefunctions given by (7), but these diverge when the relative coordinate $r_\gamma$ in any channel vanishes, unless $l_\gamma = 0$, and it is convenient following Blatt and Biedenharn first to define modified functions which do not. Returning to (1), define $\overline{\Psi}_\alpha$ by

$${}^{JM}\overline{\Psi}_\alpha = \sum_{\gamma=1}^{N} r_\gamma^{-1} \phi_\gamma \overline{U}_{\alpha\gamma}(r_\gamma) \mathcal{Y}^M_{Jl_\gamma s_\gamma} \tag{12a}$$

where

$$\overline{U}_{\alpha\gamma}(r_\gamma) = U_{\alpha\gamma}(r_\gamma) - [1-\delta_{l_\gamma,0}] j_\alpha \left(\frac{m_\gamma}{k_\gamma}\right)^{\frac{1}{2}} T_{\alpha\gamma} \frac{(2l_\gamma-1)!!}{(k_\gamma r_\gamma)^{l_\gamma}} \qquad (\gamma \text{ neutral})$$

$$= U_{\alpha\gamma}(r_\gamma) - [1-\delta_{l_\gamma,0}] j_\alpha \left(\frac{m_\gamma}{k_\gamma}\right)^{\frac{1}{2}} T_{\alpha\gamma} \frac{(2l_\gamma)!|e^{2\pi\eta_\gamma}-1|^{\frac{1}{2}}}{2^{l_\gamma+\frac{1}{2}}\pi^{\frac{1}{2}}|\eta_\gamma|^{l_\gamma+\frac{1}{2}}(k_\gamma r_\gamma)^{l_\gamma}} \quad (\gamma \text{ charged}) \quad (12b)$$

$$= U_{\alpha\gamma}(r_\gamma) - A_{\alpha\gamma} r_\gamma^{-l_\gamma}, \quad \text{say}$$

and

$$U_{\alpha\gamma}(r_\gamma) = j_\alpha m_\gamma^{\frac{1}{2}} k_\gamma^{-\frac{1}{2}} T_{\alpha\gamma}\{\cot\delta_\alpha F_\gamma(r_\gamma) + G_\gamma(r_\gamma)\}$$

on comparison with (1) and (7).

The $\overline{U}_{\alpha\gamma}$ obey the differential equations

$$\frac{\hbar^2}{2m_\gamma}\left[\frac{d^2}{dr_\gamma^2} - \frac{l_\gamma(l_\gamma+1)}{r_\gamma^2} + k_\gamma^2\right]\overline{U}_{\alpha\gamma} = \frac{(Z_1Z_2)_\gamma e^2}{r_\gamma}\overline{U}_{\alpha\gamma} - A_{\alpha\gamma} r_\gamma^{-l_\gamma}\left[\frac{\hbar^2 k_\gamma^2}{2m_\gamma} - \frac{(Z_1Z_2)_\gamma e^2}{r_\gamma}\right] \quad (13)$$

and are finite at $r_\gamma = 0$.

The $\phi_\gamma$ obey differential equations of the form

$$\left[\sum_j \frac{\hbar^2}{2m_j}\nabla_j^2 + E_{\text{int}\,\gamma}\right]\phi_\gamma = V'\phi_\gamma$$

where the number of dimensions is three less than for $\Psi$ and $V'$ on the right hand side refers only to sets of particles in the same nucleus.

We can carry out the same operations on (13) as on (10), to obtain

$$\frac{\hbar^2}{2m_\gamma}\left[\overline{U}_{2\beta\gamma}\frac{d^2}{dr_\gamma^2}\overline{U}_{1\alpha\gamma} - \overline{U}_{1\alpha\gamma}\frac{d^2}{dr_\gamma^2}\overline{U}_{2\beta\gamma}\right] + (E_1-E_2)\overline{U}_{1\alpha\gamma}\overline{U}_{2\beta\gamma}$$

$$= r_\gamma^{-l_\gamma}\left[\frac{k_{2\gamma}^2\hbar^2}{2m_\gamma}A_{2\beta\gamma}\overline{U}_{1\alpha\gamma} - \frac{k_{1\gamma}^2\hbar^2}{3m_\gamma}A_{1\alpha\gamma}\overline{U}_{2\beta\gamma}\right] \quad (13a)$$

$$- (Z_1Z_2)_\gamma e^2 r_\gamma^{-(l_\gamma+1)}[A_{1\alpha\gamma}\overline{U}_{2\beta\gamma} - A_{2\beta\gamma}\overline{U}_{1\alpha\gamma}].$$

Multiply (13a) by $r_\gamma^{-2}\phi_\gamma^2\mathscr{Y}_\gamma^2$, sum over $\gamma$ and add the resultant sum to (11b) and integrate over the whole of the configuration space. We have

$$\int\Big\{\Psi_{2\beta}\sum_j\frac{\hbar^2}{2m_j}\nabla_j^2\Psi_{1\alpha} - \Psi_{1\alpha}\sum\frac{\hbar^2}{2m_j}\nabla_j^2\Psi_{2\beta}$$

$$- \sum_\gamma\frac{\hbar^2}{2m_\gamma}\frac{\phi_\gamma^2\mathscr{Y}_\gamma^2}{r_\gamma^2}\left[\overline{U}_{2\beta\gamma}\frac{d^2}{dr_\gamma^2}\overline{U}_{1\alpha\gamma} - \overline{U}_{1\alpha\gamma}\frac{d^2}{dr_\gamma^2}\overline{U}_{2\beta\gamma}\right]\Big\}d\tau$$

$$= [E_2-E_1]\int(\Psi_{1\alpha}\Psi_{2\beta} - \overline{\Psi}_{1\alpha}\overline{\Psi}_{2\beta})d\tau \quad (14)$$

$$+ \sum_\gamma\int\frac{(Z_1Z_2)_\gamma e^2\phi_\gamma^2\mathscr{Y}_\gamma^2}{r_\gamma^{l_\gamma+3}}[A_{2\beta\gamma}\overline{U}_{1\alpha\gamma} - A_{1\alpha\gamma}\overline{U}_{2\beta\gamma}]d\tau$$

$$- \sum_\gamma\int\frac{\phi_\gamma^2\mathscr{Y}_\gamma^2}{r_\gamma^{l_\gamma+2}}\left[\frac{k_{2\gamma}^2\hbar^2}{2m_\gamma}A_{2\beta\gamma}\overline{U}_{1\alpha\gamma} - \frac{k_{1\gamma}^2\hbar^2}{2m_\gamma}A_{1\alpha\gamma}\overline{U}_{2\beta\gamma}\right]d\tau.$$

The first part of the lefthand side can be transformed by Green's theorem to a surface integral; the second part can also be put in this form, using

$$\overline{U}_2 \frac{\mathrm{d}^2}{\mathrm{d}r^2}\overline{U}_1 - \overline{U}_1 \frac{\mathrm{d}^2}{\mathrm{d}r^2}\overline{U}_2 = \frac{\mathrm{d}}{\mathrm{d}r}\left[\overline{U}_2 \frac{\mathrm{d}\overline{U}_1}{\mathrm{d}r} - \overline{U}_1 \frac{\mathrm{d}\overline{U}_2}{\mathrm{d}r}\right]. \tag{15}$$

The contributions from the hypersphere at infinity cancel, since here $\Psi = \overline{\Psi}$. At the origin that from $\Psi$ is zero, and the contribution from the barred functions is

$$\sum_\gamma j_{\alpha 1}\, j_{\beta 2} \frac{\hbar^2}{2(k_{\gamma 1}k_{\gamma 2})^{\frac{1}{2}}} T_{\alpha\gamma 1} T_{\beta\gamma 2}\left[\frac{k_{\gamma 1}B_{\gamma 2}}{B_{\gamma 1}}\cot\delta_{\alpha 1} - \frac{k_{\gamma 2}B_{\gamma 1}}{B_{\gamma 2}}\cot\delta_{\beta 2}\right]\delta_{l_\gamma, 0} \tag{16a}$$

where

$$\begin{aligned} B_\gamma &= 1, && \gamma \text{ neutral} \\ &= |\mathrm{e}^{2\pi\eta_\gamma} - 1|^{\frac{1}{2}}|\eta_\gamma|^{-\frac{1}{2}}, && \gamma \text{ charged.} \end{aligned} \tag{16b}$$

On the righthand side of (14) the second integrations can be carried out at once; together with (16a) the total result is

$$\begin{aligned} &\int (E_2 - E_1)[\Psi_{1\alpha}\Psi_{2\beta} - \overline{\Psi}_{1\alpha}\overline{\Psi}_{2\beta}]\mathrm{d}\tau \\ &= \sum_\gamma j_{\alpha 1} j_{\beta 2} \frac{\hbar^2}{2(k_{\gamma 1}k_{\gamma 2})^{\frac{1}{2}}} T_{\alpha\gamma 1} T_{\beta\gamma 2} k_{\gamma 1}^{(-l_\gamma+2)} k_{\gamma 2}^{(-l_\gamma+2)}\, {}_{12}P_\gamma [Q_{\gamma 1}\cot\delta_{\alpha 1} - Q_{\gamma 2}\cot\delta_{\beta 2}] \end{aligned} \tag{17a}$$

where

$$\begin{aligned} {}_{12}P_\gamma &= 1 && \gamma \text{ neutral}, \ l_\gamma \neq 0 \\ &= k_{\gamma 1}^{-2} k_{\gamma 2}^{-2} && \gamma \text{ neutral}, \ l_\gamma = 0 \\ &= B_{\gamma 1} B_{\gamma 2} && \gamma \text{ charged}, \ l_\gamma \neq 0 \\ &= k_{\gamma 1}^{-2} k_{\gamma 2}^{-2} B_{\gamma 1} B_{\gamma 2} && \gamma \text{ charged}, \ l_\gamma = 0 \end{aligned} \tag{17b}$$

$$\begin{aligned} \text{and } Q_{\gamma 1} &= k_{\gamma 1}^{2l_\gamma - 3} && \gamma \text{ neutral}, \ l_\gamma \neq 0 \\ &= k_{\gamma 1} && \gamma \text{ neutral}, \ l_\gamma = 0 \\ &= k_{\gamma 1}^{2l_\gamma - 3} B_{\gamma 1}^{-2} && \gamma \text{ charged}, \ l_\gamma \neq 0 \\ &= k_{\gamma 1} B_{\gamma 1}^{-2} && \gamma \text{ charged}, \ l_\gamma = 0. \end{aligned} \tag{17c}$$

Now consider (17a) for the case $\alpha = \beta$. Dividing each side by $E_2 - E_1$ and taking the limit as $E_2 \to E_1$, we have, dropping energy subscripts,

$$\int (\Psi_\alpha^2 - \overline{\Psi}_\alpha^2)\mathrm{d}\tau = \sum_\gamma j_\alpha^2 \frac{\hbar^2 T_{\alpha\gamma}^2}{2k_\gamma^{2l_\gamma - 3}} P_\gamma \frac{\mathrm{d}}{\mathrm{d}E}[Q_\gamma \cot\delta_\alpha]. \tag{18}$$

A glance at the expansion (6) for $\cot\delta_\alpha$ shows that what we are looking for is an expression for

$$\frac{\mathrm{d}}{\mathrm{d}k^2}[g_\alpha \cot\delta_\alpha]|_{E_0}.$$

Now $g_\alpha = j_\alpha^2$; and we have the identity

$$\frac{\mathrm{d}}{\mathrm{d}E}[Q_\gamma \cot \delta_\alpha] = \frac{2m_\gamma}{\hbar^2}\cot\delta_\alpha \frac{\mathrm{d}Q_\gamma}{\mathrm{d}k_\gamma^2} + \frac{2m_\alpha}{\hbar^2} g_\alpha Q_\gamma \cot\delta_\alpha \frac{\mathrm{d}}{\mathrm{d}k_\alpha^2}\left(\frac{1}{g_\alpha}\right) + \frac{2mQ_\gamma}{\hbar^2 g_\alpha}\frac{\mathrm{d}}{\mathrm{d}k^2}[g_\alpha \cot\delta_\alpha] \tag{19a}$$

obtained by writing $Q_\gamma \cot \delta_\alpha = g_\alpha Q_\gamma \cot\delta_\alpha / g_\alpha$ and differentiating by parts twice. On substitution into (18) this gives for the righthand side

$$\sum_\gamma g_\alpha T_{\alpha\gamma}^2 k_\gamma^{-2l_\gamma+3} P_\gamma \left\{ m_\gamma \cot\delta_\alpha \frac{\mathrm{d}Q_\gamma}{\mathrm{d}k_\gamma^2} + g_\alpha m_\alpha \cot\delta_\alpha Q_\gamma \frac{\mathrm{d}}{\mathrm{d}k_\alpha^2}\left(\frac{1}{g_\alpha}\right) + \frac{mQ_\gamma}{g_\alpha}\frac{\mathrm{d}}{\mathrm{d}k^2}[g_\alpha \cot\delta_\alpha]\right\}. \tag{19b}$$

Now we have for $E_2 = E_1$:

$$P_\gamma Q_\gamma k_\gamma^{-2l_\gamma+3} = 1 \text{ for all } \gamma,\ l_\gamma, \tag{19c}$$

so the second and third terms in (19b) contain $\gamma$ only as $\sum_\gamma T_{\alpha\gamma}^2 = 1$; so (18) can be rewritten

$$\int (\Psi_\alpha^2 - \overline{\Psi}_\alpha^2)\mathrm{d}\tau = \sum_\gamma \left( g_\alpha T_{\alpha\gamma}^2 k_\gamma^{-2l_\gamma+3} m_\gamma P_\gamma \cot\delta_\alpha \frac{\mathrm{d}Q_\gamma}{\mathrm{d}k_\gamma^2}\right) - m_\alpha \cot\delta_\alpha \frac{\mathrm{d}}{\mathrm{d}k_\alpha^2}(g_\alpha) + m\frac{\mathrm{d}}{\mathrm{d}k^2}(g_\alpha \cot\delta_\alpha). \tag{19d}$$

We want to take the limit of (19d) as $E \to E_0$, when, from (6),

$$\frac{\mathrm{d}}{\mathrm{d}k^2}(g_\alpha \cot\delta_\alpha)|_{E_0} = \Delta_{\alpha 1}.$$

But in this limit terms with $\gamma$ now diverge on both the left and right hand sides. The lefthand side contains the integral

$$\int \overline{U}_{\alpha\gamma}^2 \mathrm{d}r_\gamma = \int (U_{\alpha\gamma} - A_{\alpha\gamma} r_\gamma^{-l_\gamma})^2 \mathrm{d}r_\gamma$$

and if $\gamma$ is new, so that $k_\gamma \to 0$ as $E \to E_0$, the cross term in $r_\gamma^{-l_\gamma} F_{l\gamma}$ which occurs is $O(r_\gamma)$ and the integral of this diverges. We therefore subtract on both sides of 18)

$$\int \sum_\gamma 2j_\alpha \left(\frac{m_\gamma}{k_\gamma}\right)^{\frac{1}{2}} T_{\alpha\gamma} \cot\delta_\alpha A_{\alpha\gamma} F_\gamma(r_\gamma) r_\gamma^{-l_\gamma-2} \phi_\gamma^2 \mathscr{Y}_\gamma^2 \mathrm{d}\tau = \sum_\gamma 2j_\alpha \left(\frac{m_\gamma}{k_\gamma}\right)^{\frac{1}{2}} T_{\alpha\gamma} \cot\delta_\alpha A_{\alpha\gamma} R_\gamma \tag{20}$$

where

$$R_\gamma = \frac{{k_\gamma}^{l_\gamma-1}}{(2l_\gamma-1)!!} \qquad (\gamma \text{ neutral})$$

$$= \frac{2^{l_\gamma+\frac{1}{2}}\pi^{\frac{1}{2}}|\eta_\gamma|^{l_\gamma+\frac{1}{2}}{k_\gamma}^{l_\gamma-1}}{|e^{2\pi\eta_\gamma}-1|^{\frac{1}{2}}(2l_\gamma)!} \qquad (\gamma \text{ charged}).$$

Note this term is zero if $l_\gamma = 0$ due to the factor $(1-\delta_{l_\gamma,0})$ in $A_{\alpha\gamma}$. Adding this term to both sides of (18) then puts the lefthand side in a form regular at $E = E_0$, so that (18) can be rewritten, together with (19d)

$$\int(\Psi_\alpha^2-\overline{\Psi}_\alpha^2+\sum_\gamma 2j_\alpha T_{\alpha\gamma}A_{\alpha\gamma}\cot\delta_\alpha\left(\frac{m_\gamma}{k_\gamma}\right)^{\frac{1}{2}}F_\gamma(r_\gamma)r_\gamma^{-l_\gamma-2}\phi_\gamma^2\mathcal{Y}_\gamma^2)d\tau$$

$$= m\frac{d}{dk^2}[g_\alpha\cot\delta_\alpha]-m_\alpha\cot\delta_\alpha\frac{d}{dk_\alpha^2}(g_\alpha) \qquad (21)$$

$$+\sum_\gamma g_\alpha T_{\alpha\gamma}^2 m_\gamma\cot\delta_\alpha\left[\frac{2l_\gamma+1}{2k_\gamma^2}+B_\gamma^2\frac{d}{dk_\gamma^2}\left(\frac{1}{B_\gamma^2}\right)\right]$$

where we have used the identities

$$A_{\alpha\gamma}R_\gamma = j_\alpha\left(\frac{m_\gamma}{k_\gamma}\right)^{\frac{1}{2}}T_{\alpha\gamma}{k_\gamma}^{-1}(1-\delta_{l_\gamma,0}) \qquad (\text{all } \gamma, l_\gamma)$$

$$P_\gamma\frac{dQ_\gamma}{dk_\gamma^2} = {k_\gamma}^{2l_\gamma-3}B_\gamma^2\frac{d}{dk_\gamma^2}\left(\frac{1}{B_\gamma^2}\right)+\frac{2l_\gamma-3}{2}{k_\gamma}^{2l_\gamma-5} \qquad (l_\gamma \neq 0) \qquad (22)$$

$$= {k_\gamma}^{-3}B_\gamma^2\frac{d}{dk_\gamma^2}\left(\frac{1}{B_\gamma^2}\right)+\frac{{k_\gamma}^{-5}}{2} \qquad (l_\gamma = 0).$$

The required result then follows by taking the limit of (21) as $E \to E_0$. The righthand side becomes

$$m\Delta_{\alpha1}-m_\alpha\Delta_{\alpha0}\cdot\frac{1}{g_\alpha}\frac{d}{dk_\alpha^2}(g_\alpha)|_{E_0}$$

$$+\sum_\gamma{}_0 T_{\alpha\gamma}^2 m_\gamma\frac{\Delta_{\alpha0}}{g_{\alpha\gamma}^2}\left[\frac{2l_\gamma+1}{2k_\gamma^2}+B_\gamma^2\frac{d}{dk_\gamma^2}\left(\frac{1}{B_\gamma^2}\right)\right]_{E_0} \qquad (21a)$$

and all the quantities entering into this are known except $\Delta_{\alpha1}$. For $\alpha$ neutral the last term is always finite; the second and third terms are also if $\alpha$ is old, but if $\alpha$ is new both these diverge. However, in the third term only those members of the sum diverge for which $\gamma$ is new and $l_\gamma = l_\alpha$; thus we can subtract from the third term a part

$$\sum_\gamma{}_0\frac{T_{\alpha\gamma}^2 m_\alpha}{g_{\alpha\gamma}^2}\Delta_{\alpha0}\frac{(2l_\alpha+1)}{2k_\alpha^2} = \sum_\gamma T_{\alpha\gamma}^2 m_\alpha\Delta_{\alpha0}\frac{(2l_\alpha+1)}{2k_\alpha^2} = m_\alpha\Delta_{\alpha0}\frac{1}{g_\alpha}\frac{d}{dk_\alpha^2}(g_\alpha)$$

which includes all the divergent parts of the third term, leaving a finite sum, and cancels with the second term. Similarly the right hand side is in fact finite for $\alpha$ charged.

To get a similar result for the $T_{\alpha\beta}$, we return to equation (17a) for $\alpha \neq \beta$, and add to it the corresponding equation with $\alpha, \beta$ interchanged with respect to suffixes 1 and 2. We obtain on rearranging the result, dividing both sides by $E_2 - E_1$, and taking the limit as $E_2 \to E_1$,

$$\int 2(\overline{\Psi}_\alpha \overline{\Psi}_\beta - \Psi_\alpha \Psi_\beta)\,\mathrm{d}\tau = \sum_\gamma \left[ \frac{j_\beta^2 \hbar^2 T_{\beta\gamma}^2}{2k_\gamma^{2l_\gamma - 3}} P_\gamma \frac{\mathrm{d}}{\mathrm{d}E}\left\{ \frac{j_\alpha Q_\gamma \cot \delta_\alpha T_{\alpha\gamma}}{j_\beta T_{\beta\gamma}} \right\} + \frac{j_\alpha^2 \hbar^2 T_{\alpha\gamma}^2 P_\gamma}{2k_\gamma^{2l_\gamma - 3}} \frac{\mathrm{d}}{\mathrm{d}E}\left\{ \frac{j_\beta Q_\gamma \cot \delta_\beta T_{\beta\gamma}}{j_\alpha T_{\alpha\gamma}} \right\} \right]. \tag{23}$$

Now

$$\frac{\mathrm{d}}{\mathrm{d}E}\left\{ \frac{j_\alpha T_{\alpha\gamma} Q_\gamma \cot \delta_\alpha}{j_\beta T_{\beta\gamma}} \right\} = \frac{T_{\alpha\gamma} Q_\gamma}{T_{\beta\gamma}} \frac{\mathrm{d}}{\mathrm{d}E}\left\{ \frac{j_\alpha \cot \delta_\alpha}{j_\beta} \right\} + \frac{j_\alpha \cot \delta_\alpha}{j_\beta} \frac{\mathrm{d}}{\mathrm{d}E}\left\{ \frac{T_{\alpha\gamma} Q_\gamma}{T_{\beta\gamma}} \right\}. \tag{24a}$$

Substitute this in (23); then using (19c), the coefficient of $(\mathrm{d}/\mathrm{d}E)\{j_\alpha \cot \delta_\alpha / j_\beta\}$ has the form

$$X_{\alpha\beta} \sum_\gamma T_{\alpha\gamma} T_{\beta\gamma} = X_{\alpha\beta} \delta_{\alpha\beta} \tag{24b}$$

and we are considering the case $\alpha \neq \beta$. Moreover we may write identically

$$\begin{aligned} \frac{\mathrm{d}}{\mathrm{d}E}\left\{ \frac{T_{\alpha\gamma} Q_\gamma}{T_{\beta\gamma}} \right\} &= \frac{\mathrm{d}}{\mathrm{d}E}\left\{ \frac{g_{\alpha\gamma} T_{\alpha\gamma}}{g_{\beta\gamma} T_{\beta\gamma}} \cdot \frac{Q_\gamma g_{\beta\gamma}}{g_{\alpha\gamma}} \right\} \\ &= \frac{2mQ_\gamma}{\hbar^2 T_{\beta\gamma} g_{\alpha\gamma}} \frac{\mathrm{d}}{\mathrm{d}k^2}[g_{\alpha\gamma} T_{\alpha\gamma}] - \frac{2mQ_\gamma T_{\alpha\gamma}}{T_{\beta\gamma} g_{\beta\gamma} \hbar^2} \frac{\mathrm{d}}{\mathrm{d}k^2}[g_{\beta\gamma} T_{\beta\gamma}] \\ &\quad + \frac{2m g_{\alpha\gamma} T_{\alpha\gamma}}{\hbar^2 g_{\beta\gamma} T_{\beta\gamma}} \frac{\mathrm{d}}{\mathrm{d}k^2}\left\{ \frac{Q_\gamma g_{\beta\gamma}}{g_{\alpha\gamma}} \right\}. \end{aligned} \tag{24c}$$

Substituting (24b) and (24c) into (23) we find after some rearrangement

$$\begin{aligned} 2\int (\overline{\Psi}_\alpha \overline{\Psi}_\beta - \Psi_\alpha \Psi_\beta)\mathrm{d}\tau &= \sum_\gamma m j_\alpha j_\beta T_{\alpha\gamma} T_{\beta\gamma} \left\{ (\cot \delta_\alpha - \cot \delta_\beta) \left[ \frac{(g_{\alpha\gamma} T_{\alpha\gamma})'}{g_{\alpha\gamma} T_{\beta\gamma}} - \frac{(g_{\beta\gamma} T_{\beta\gamma})'}{g_{\beta\gamma} T_{\alpha\gamma}} \right.\right. \\ &\quad \left.\left. + \frac{g'_{\beta\gamma}}{g_{\beta\gamma}} - \frac{g'_{\alpha\gamma}}{g_{\alpha\gamma}} \right] + (\cot \delta_\alpha + \cot \delta_\beta) \frac{P_\gamma Q'_\gamma}{k_\gamma^{2l_\gamma - 3}} \right\} \end{aligned} \tag{25}$$

where a dash denotes differentiation with respect to $k^2$.

As before, the lefthand side may diverge at $E_0$ in this form; we therefore put it in a form regular at $E_0$ by subtracting on both sides of (25) the integral of

$$2\sum_\gamma \left[ j_\alpha \left(\frac{m_\gamma}{k_\gamma}\right)^{\frac{1}{2}} T_{\alpha\gamma} \cot \delta_\alpha A_{\beta\gamma} + j_\beta \left(\frac{m_\gamma}{k_\gamma}\right)^{\frac{1}{2}} T_{\beta\gamma} \cot \delta_\beta A_{\alpha\gamma} \right] \cdot [1 - \delta_{l_\gamma, 0}] r_\gamma^{-l_\gamma - 2} F_\gamma(r_\gamma) \phi_\gamma^2 \mathscr{Y}_\gamma^2 \tag{26a}$$

which is

$$2\sum_{\gamma} j_\alpha j_\beta T_{\alpha\gamma} T_{\beta\gamma} \frac{m_\gamma}{k^2{}_\gamma} (\cot \delta_\alpha + \cot \delta_\beta)(1-\delta_{l_{\gamma,0}}) \tag{26b}$$

so that (25) becomes

$$\begin{aligned} &2\int \Big\{ \overline{\Psi}_\alpha \overline{\Psi}_\beta - \Psi_\alpha \Psi_\beta + \sum_\gamma \Big[ j_\alpha \left(\frac{m_\gamma}{k_\gamma}\right)^{\frac{1}{2}} T_{\alpha\gamma} \cot \delta_\alpha A_{\beta\gamma} + j_\beta \left(\frac{m_\gamma}{k_\gamma}\right)^{\frac{1}{2}} T_{\beta\gamma} \cot \delta_\beta A_{\alpha\gamma} \Big] \\ &\times (1-\delta_{l_{\gamma,0}}) r_\gamma{}^{-l_\gamma - 2} F_\gamma(r_\gamma) \phi_\gamma{}^2 \mathscr{Y}_\gamma{}^2 \Big\} \, d\tau \\ &= \sum_\gamma m j_\alpha j_\beta T_{\alpha\gamma} T_{\beta\gamma} \Big\{ (\cot \delta_\alpha - \cot \delta_\beta) \left[ \frac{(g_{\alpha\gamma} T_{\alpha\gamma})'}{g_{\alpha\gamma} T_{\beta\gamma}} - \frac{(g_{\beta\gamma} T_{\beta\gamma})'}{g_{\beta\gamma} T_{\alpha\gamma}} + \frac{g'_{\beta\gamma}}{g_{\beta\gamma}} - \frac{g'_{\alpha\gamma}}{g_{\alpha\gamma}} \right] \\ &+ (\cot \delta_\alpha + \cot \delta_\beta) \left[ \frac{P_\gamma Q'_\gamma}{k_\gamma{}^{2l_\gamma - 3}} + \frac{2 m_\gamma k_\gamma{}^{-2}}{m} (1-\delta_{l_{\gamma,0}}) \right] \Big\}. \end{aligned} \tag{27}$$

As before, the right hand side of (27) is always finite at $E_0$; and we have

$$(g_{\alpha\gamma} T_{\alpha\gamma})'|_{E_0} = {}_1T_{\alpha\gamma}, \qquad (g_{\beta\gamma} T_{\beta\gamma})'|_{E_0} = {}_1T_{\beta\gamma}.$$

Thus taking the limit $E \to E_0$ gives $\frac{1}{2}N(N-1)$ equations for the different pairs of $\alpha$, $\beta$ involving only known quantities apart from the ${}_1T_{\alpha\beta}$ which we wish to calculate. This is sufficient together with the orthogonality condition on $\mathbf{T}$, which implies [11]) that ${}_1\mathbf{T}$ is skew-symmetric, i.e. ${}_1T_{\alpha\beta} = -{}_1T_{\beta\alpha}$. Note in particular that this means ${}_1T_{\alpha\alpha} = 0$ for all $\alpha$.

## 5. Third and higher Terms in the Series

We have from (6)

$$\begin{aligned} \Delta_{\alpha 2} &= \tfrac{1}{2} \frac{d^2}{d(k^2)^2} [g_\alpha \cot \delta_\alpha]|_{E_0} \\ {}_2T_{\alpha\beta} &= \tfrac{1}{2} \frac{d^2}{d(k^2)^2} [g_{\alpha\beta} T_{\alpha\beta}]|_{E_0} \end{aligned} \tag{28}$$

and thus expressions for ${}_2T_{\alpha\beta}$ and $\Delta_{\alpha 2}$ follow very simply from (27) and (21) by differentiating these with respect to $k^2$ before taking the limit as $E \to E_0$. To carry out the differentiation of the lefthand side of the equations we must know the second term in the expansion of the *wavefunctions* about $E_0$; if we write

$$\Psi_{\alpha E} = \Psi_{\alpha 0} + \Psi_{\alpha 1} k^2 + \ldots \tag{22}$$

where $\Psi_{\alpha 0}$ is the wavefunction at $E_0$, then $(d/dk^2)(\Psi_\alpha)|_{E_0} = \Psi_{\alpha 1}$.

Thus for a knowledge of the third terms in the series it is necessary to know $\Psi_{\alpha 1}$. This must be computed numerically in general, and the amount of work necessary to do so will be similar to that necessary to find $\Psi_{\alpha 0}$.

$\Psi_{\alpha 1}$ obeys the wave equation

$$\left[\sum_j \frac{\hbar^2}{2m_j}\nabla_j^2 + \frac{\hbar^2 k^2}{2m} - V\right]\Psi_{\alpha 1} = -\frac{\hbar^2}{2m}\Psi_{\alpha 0} \tag{29}$$

together with the boundary conditions $\Psi_1 = 0$ at the origin, and has the asymptotic form given by the expansion of (11) in powers of $k$.

## 6. Effects of Antisymmetrization

In the foregoing we have not made any explicit reference to the need to use antisymmetrized wavefunctions in accordance with the Pauli principle. We have only used an explicit form for the wavefunction however in the external region, and here the exclusion principle cannot change this form since the wavefunctions of the two nuclei by definition do not overlap in this region. The form of $\Psi$ in the internal region will of course be affected by the requirements of antisymmetry, but $\Psi$ appears in the formulae only as a parameter to be determined by numerical integration of the wave equation, or by other methods.

Thus none of the foregoing is changed by explicit consideration of the Pauli principle; the accuracy of results obtained using the theory will however depend on the accuracy of the wavefunctions inserted into the formula, and this of course includes the accuracy with which antisymmetrization of the numerical wavefunctions is carried out.

## 7. Summary

We have here generalized the usual effective range theory as applied to single channel nucleon-nucleon collisions to cover the case of the collision of complex particles reacting through an arbitrary number of channels. The expansions can be carried out about any energy of interest; it may often be of most interest to choose an energy at which new channels are just opening.

The advantages of the effective range expansion of the scattering matrix are slightly different in the many-channel case from the single-channel case. It is no longer true to call the use of the first two terms in the series the shape-independent approximation, since we now have more than two parameters to fit, and indeed we expect the manybody problem to be shape-dependent even at low energies. The use of the expansions given here is rather to extrapolate results obtained with great labour at one energy to a range of energies. The question is then important: for how large a range of energy are the first two terms likely to give a good approximation to the total series? For nucleon-nucleon scattering it is well-known that the

first two terms give a reasonable fit from 0 up to at least 10 MeV. Some numerical work on n–d scattering in the presence of tensor forces [14]) using a two-channel approximation and the effective range expansions of Blatt and Biedenharn [5,6]), indicates that for more complex systems the convergence is not as good as this. In this particular example the third terms were already important at 0.5 MeV neutron energy.

I should like to thank Dr. R. J. Blin-Stoyle and Dr. G. R. Satchler for many helpful discussions during this work, and the Shell Petroleum Company for the award of a Shell Scholarship.

## Appendix A

### THE ENERGY DEPENDENCE OF T AND $\delta$ AT THRESHOLDS

The energy dependence of **T** and $\boldsymbol{\delta}$ is determined solely by the asymptotic form of the wavefunctions, although of course the absolute magnitudes depend on the interaction at short distances. Consider an eigenstate $\Psi_\alpha$ of the scattering; in the external region this has the form (7), i.e.

$$\Psi_\alpha^{\infty} = \text{constant} \times \sum_\gamma \left(\frac{m_\gamma}{k_\gamma}\right)^{\frac{1}{2}} T_{\alpha\gamma}(\cot \delta_\alpha F_\gamma(r_\gamma)+G_\gamma(r_\gamma)) \frac{\phi_\gamma \mathcal{Y}_\gamma}{r_\gamma}. \quad \text{(A1)}$$

The forms of $F$ and $G$ are well-known. They are finite for finite $k_\gamma r_\gamma$; for large $k_\gamma r_\gamma \gg l_\gamma$ they have the forms

$$\begin{aligned} F_{l_\gamma}(r_\gamma) &= \sin\left(k_\gamma r_\gamma - \frac{l_\gamma \pi}{2}\right) && \gamma \text{ neutral} \\ &= \sin\left(k_\gamma r_\gamma - \frac{l_\gamma \pi}{2} - \eta_\gamma \log 2k_\gamma r_\gamma + \alpha_\gamma\right) && \gamma \text{ charged} \\ G_{l_\gamma}(r_\gamma) &= \cos\left(k_\gamma r_\gamma - \frac{l_\gamma \pi}{2}\right) && \gamma \text{ neutral} \\ &= \cos\left(k_\gamma r_\gamma - \frac{l_\gamma \pi}{2} - \eta_\gamma \log 2k_\gamma r_\gamma + \alpha_\gamma\right) && \gamma \text{ charged} \end{aligned} \quad \text{(A2)}$$

where

$$\eta_\gamma = \frac{m_\gamma (z_1 z_2)_\gamma e^2}{\hbar^2 k_\gamma}, \quad \alpha_\gamma = \arg \Gamma(l_\gamma + 1 + i\eta_\gamma).$$

We shall be concerned particularly with the form as $k_\gamma \to 0$; in this case the condition $kr \gg l$ is never fulfilled. $F$ and $G$ have the following forms for $k_\gamma r_\gamma \ll l_\gamma$:

$$\begin{aligned} F_{l_\gamma}(r_\gamma) &= \frac{(k_\gamma r_\gamma)^{l_\gamma+1}}{(2l_\gamma+1)!!} && \gamma \text{ neutral} \\ &= \frac{2^{l_\gamma+\frac{1}{2}}\pi^{\frac{1}{2}}|\eta_\gamma|^{l_\gamma+\frac{1}{2}}(k_\gamma r_\gamma)^{l_\gamma+1}}{|e^{2\pi\eta_\gamma}-1|^{\frac{1}{2}}(2l_\gamma+1)!} && \gamma \text{ charged} \\ G_{l_\gamma}(r_\gamma) &= \frac{(2l_\gamma-1)!!}{(k_\gamma r_\gamma)^{l_\gamma}} && \gamma \text{ neutral} \\ &= \frac{|e^{2\pi\eta_\gamma}-1|^{\frac{1}{2}}(2l_\gamma)!}{2^{l_\gamma+\frac{1}{2}}\pi^{\frac{1}{2}}|\eta_\gamma|^{l_\gamma+\frac{1}{2}}(k_\gamma r_\gamma)^{l_\gamma}} && \gamma \text{ charged.} \end{aligned} \tag{A3}$$

Now in the external region $\Psi$ must not become infinite nor vanish identically over a finite region of configuration space [13]). This condition must indeed be fulfilled everywhere if the potential energy is everywhere finite, but in the internal region it will not hold in the presence of infinite repulsive cores. In particular the condition is fulfilled in the external region for any $k_\gamma \to 0$, and this is sufficient, with (A3), to determine the behaviour of $\mathbf{T}$ and $\boldsymbol{\delta}$ at such a threshold.

There are several cases to be considered:

1) If $\alpha$ is old, cot $\delta_\alpha$ has a finite value at $E_0$, as does $k_\alpha$. Then (A1) together with (A3) show that $T_{\alpha\gamma}$ must have the following variation with $k$ at $E_0$:

$$\begin{aligned} T_{\alpha\gamma} &\to \text{const} && \gamma \text{ old} \\ &\to \text{const} \times k_\gamma^{\,l_\gamma+\frac{1}{2}} && \gamma \text{ new, neutral} \\ &\to \text{const} \times \frac{k_\gamma^{\,l_\gamma+\frac{1}{2}}|\eta_\gamma|^{l_\gamma+\frac{1}{2}}}{|e^{2\pi\eta_\gamma}-1|^{\frac{1}{2}}} && \gamma \text{ charged, new.} \end{aligned} \tag{A4a}$$

2) If $\alpha$ is new, we have firstly $T_{\alpha\alpha}$ is $\mathcal{O}(1)$, and therefore at $E_0$

$$\begin{aligned} \cot\delta_\alpha &\to \text{const} \times k_\alpha^{-(2l_\alpha+1)} && \alpha \text{ neutral} \\ &\to \text{const} \times k_\alpha^{-2l_\alpha+1}\frac{|e^{2\pi\eta_\alpha}-1|}{|\eta_\alpha|^{2l_\alpha+1}} && \alpha \text{ charged.} \end{aligned} \tag{A4b}$$

And moreover the constant in (A1) is seen to be

$$\begin{aligned} &\text{const} \times k_\alpha^{\,l_\alpha+\frac{1}{2}} && \alpha \text{ neutral} \\ &\text{const} \times \frac{k_\alpha^{\,l_\alpha+\frac{1}{2}}|\eta_\alpha|^{l_\alpha+\frac{1}{2}}}{|e^{2\pi\eta_\alpha}-1|^{\frac{1}{2}}} && \alpha \text{ charged} \end{aligned} \tag{A4b}$$

whence we see that at $E_0$

$$\begin{aligned} T_{\alpha\gamma} &\to \text{const} \times k_\alpha^{\,l_\alpha+\frac{1}{2}} && \gamma \text{ old, } \alpha \text{ neutral} \\ &\to \text{const} \times |e^{2\pi\eta_\alpha}-1|^{-\frac{1}{2}} && \gamma \text{ old, } \alpha \text{ charged} \\ &\to \text{const} \times k_\alpha^{|l_\alpha-l_\gamma|} && \alpha \text{ neutral, } \gamma \text{ new, neutral.} \end{aligned}$$

| | |
|---|---|
| $\to$ const $\times k_\alpha^{l_\alpha+\frac{1}{2}}\lvert e^{2\pi\eta_\gamma}-1\rvert^{\frac{1}{2}}$ | $\alpha$ neutral, $\gamma$ new, charged attractive |
| $\to$ const $\times k_\alpha^{-(l_\alpha+\frac{1}{2})}\lvert e^{2\pi\eta_\gamma}-1\rvert^{-\frac{1}{2}}$ | $\alpha$ neutral, $\gamma$ new, charged repulsive |
| $\to$ const $\times k_\gamma^{-(l_\gamma+\frac{1}{2})}\lvert e^{2\pi\eta_\alpha}-1\rvert^{-\frac{1}{2}}$ | $\alpha$ charged, repulsive, $\gamma$ neutral, new |
| $\to$ const $\times k_\gamma^{l_\gamma+\frac{1}{2}}\lvert e^{2\pi\eta_\alpha}-1\rvert^{\frac{1}{2}}$ | $\alpha$ charged, attractive $\gamma$ neutral, new |
| $\to$ const $\times e^{-\pi\lvert\eta_\alpha-\eta_\gamma\rvert}$ | $\alpha$ charged repulsive, $\gamma$ charged repulsive, new |
| $\to$ const | $\alpha$ charged attractive, $\gamma$ charged attractive, new |
| $\to$ const $\times e^{-\pi\eta_\alpha}$ | $\alpha$ charged repulsive, $\gamma$ charged attractive, new |
| $\to$ const $\times e^{-\pi\eta_\gamma}$ | $\alpha$ charged attractive, $\gamma$ charged repulsive, new. |

Here we have used the facts that $\eta \propto 1/k$, and that for $k_\gamma \to 0$,

| | | |
|---|---|---|
| $\lvert e^{2\pi\eta_\gamma}-1\rvert = 1$ | $\gamma$ attractive, i.e. $\eta_\gamma$ negative | (A4d) |
| $= e^{2\pi\eta_\gamma}$ | $\gamma$ repulsive. | |

Results (A4) are those given in table 2 in the text, together with the definition (6a) of $g_\alpha$ and $g_{\alpha\beta}$.

## References


1) H. A. Bethe, Phys. Rev. **76** (1949) 38
2) R. E. Peierls and M. A. Preston, Phys. Rev. **72** (1947) 250
3) Hatcher, Arfken and Breit, Phys. Rev. **75** (1949) 1389
4) G. F. Chew and M. L. Goldhaber, Phys. Rev. **75** (1947) 250
5) J. M. Blatt and L. C. Biedenharn, Phys. Rev. **86** (1952) 399
6) L. C. Biedenharn and J. M. Blatt, Phys. Rev. **93** (1954) 1387
7) R. Huby, Proc. Phys. Soc. **67** (1954) 1103
8) J. M. Blatt and L. C. Biedenharn, Revs. Mod. Phys. **24** (1952) 261
9) E. P. Wigner and L. Eisenbud, Phys. Rev. **72** (1947) 29
10) E. P. Wigner, Phys. Rev. **73** (1948) 1002
11) H. Weyl, The Classical Groups (Princeton, 1946) p. 68
12) E. U. Condon and G. H. Shortley, The Theory of Atomic Spectra (C.U.P. 1935)
13) W. H. Guier and R. W. Hart, Phys. Rev. **106** (1957) 296
14) L. M. Delves, Thesis, Auckland University, New Zealand, 1956 (unpublished)

7.A *Nuclear Physics* 8 (1958) 374—393; © *North-Holland Publishing Co., Amsterdam*
Not to be reproduced by photoprint or microfilm without written permission from the publisher

# SOME PROBLEMS ENCOUNTERED IN THE THEORY OF THE DISPERSION RELATIONS

A. A. LOGUNOV and A. N. TAVKHELIDZE
*Joint Institute of Nuclear Research, Laboratory of Theoretical Physics, Dubna, USSR*

Received 19 February 1958

**Abstract:** Dispersion relations are obtained for a reaction involving a variable number of particles (a fermion and boson prior to the reaction and a fermion and two identical bosons after the reaction). Cases are indicated for which an unobservable energy region is absent in the dispersion relations. A justification of the dispersion relations in the absence of an unobservable energy region is presented for the particular process $\gamma+p \to 2\gamma+p$.

## 1. Introduction

Much attention has recently been directed to further development of the theory of the dispersion equations. After the investigations of Bogolubov [1]) it has become apparent that the dispersion relations can be regarded as a corollary of some general principles of local field theory. Consequently an experimental test of the dispersion relations should cast light (assuming the relations to be violated) on the problem of localizability of elementary interactions. Apart from the conclusions of principle which can be drawn from an experimental test of the dispersion relations, their further study would also seem to be desirable, so as to include an investigation of the unobservable region in previously obtained dispersion relations as well as to extend the method to encompass reactions involving a variable number of particles.

An attempt to deduce the dispersion relations for reactions with a variable number of particles has been made in ref.[2]). However, the method applied in this work is not convincing and many serious objections can be raised. In the present paper we follow the general procedure employed in ref. [1,3]). We shall consider some aspects of the theory of dispersion relations for reactions with a variable number of particles of the following type: $\gamma+p \to 2\gamma+p$, $\gamma+p \to 2\pi+p$, $\pi+p \to 2\pi+p$, $\pi+p \to 2\gamma+p$. Electromagnetic corrections of higher order will not be considered and only the chief amplitude term will be taken into account.

## 2. Construction of Causality Amplitudes

In ref.[4]) N. N. Bogolubov proposed a general formulation of the causality principle which was expressed as an explicit condition on the scattering matrix †:

$$\frac{\delta j_\rho(x)}{\delta \varphi_{\rho'}(x')} = 0, \quad x' \lesssim x, \text{ where } j_\rho(x) = i\frac{\delta S}{\delta \varphi_\rho(x)} S\dagger = -iS\frac{\delta S\dagger}{\delta \varphi_\rho(x)}. \quad (2.1)$$

Formulation of the causality principle in this way is especially effective for construction of retarded amplitudes. However, in order to construct advanced amplitudes it is more convenient to write the causality principle in a somewhat different form:

$$\frac{\delta \Lambda_\rho(x)}{\delta \varphi_{\rho'}(x')} = 0, \quad x' \gtrsim x, \quad \Lambda_\rho(x) = i\frac{\delta S\dagger}{\delta \varphi_\rho(x)} S = -iS\dagger\frac{\delta S}{\delta \varphi_\rho(x)}. \quad (2.2)$$

It is easy to show that conditions (2.1) and (2.2) are related as follows:

$$\frac{\delta \Lambda_\rho(x)}{\delta \varphi_{\rho'}(x')} = -S\dagger\frac{\delta j_{\rho'}(x')}{\delta \varphi_\rho(x)} S. \quad (2.3)$$

In the future we shall study reactions of the type

$$\gamma+\mathrm{p} \to \mathrm{p}+2\gamma, \quad \pi+\mathrm{p} \to \mathrm{p}+2\gamma, \quad \pi+\mathrm{p} \to \mathrm{p}+2\pi, \quad \gamma+\mathrm{p} \to \mathrm{p}+2\pi$$

in which a nucleon and boson exist before the reaction and a nucleon and two bosons after the reaction.

We now proceed to construct the causality amplitudes for the indicated reactions. Let $p$ and $p'$ denote the momenta of the initial and final nucleons, $q$ and $q'$, $q''$ the momenta of the initial and final bosons. The matrix element of the process can then be written in the form

$$S_{\alpha,\omega}(q; q', q'') = (2\pi)^{\frac{3}{2}}\langle p' s'|\varphi_{\rho'}^{(-)}(q')\varphi_{\rho''}^{(-)}(q'')S\varphi_\rho{}^{(+)}(q)|ps\rangle. \quad (2.4)$$

Here $|ps\rangle$ denote the state amplitude of the scatterer and the indices $\alpha$ and $\omega$, which refer to the initial and final states respectively, include all quantum numbers characterizing the system except the momenta of the initial and final bosons. Transposing the creation operator $\varphi_\rho{}^{(+)}(q)$ to the extreme left position in (2.4) and taking into account the stability of state $|ps\rangle$,

$$S\dagger|ps\rangle = |ps\rangle,$$

we obtain

$$S_{\alpha,\omega}(q; q', q'') = \frac{-i(2\pi)^3}{\sqrt{2q^0}}\int e^{-iqx}\langle p' s'|\varphi_{\rho'}^{(-)}(q')\varphi_{\rho''}^{(-)}(q'')j_\rho(x)|ps\rangle dx$$

whence after transposing the absorption operators to the extreme right we get

† In the following by a field $\varphi_\rho(x)$ we shall understand real meson or electromagnetic fields.

$$S_{\alpha,\omega}(q;q',q'')$$
$$=-\frac{i}{\sqrt{8q'_0q''_0q_0}}\int e^{iq'x'+iq''x''-iqx}\langle p's'|\frac{\delta^2 j_\rho(x)}{\delta\varphi_{\rho'}(x')\delta\varphi_{\rho''}(x'')}|ps\rangle dx dx' dx''. \quad (2.5)$$

From translational invariance considerations

$$\langle p's'|\frac{\delta^2 j_\rho(x)}{\delta\varphi_{\rho'}(x')\delta\varphi_{\rho''}(x'')}|ps\rangle = e^{i(p'-p)x}\langle p's'|\frac{\delta^2 j_\rho(0)}{\delta\varphi_{\rho'}(x'-x)\delta\varphi_{\rho''}(x''-x)}|ps\rangle,$$

and expression (2.5) can be written as follows:

$$S_{\alpha,\omega}(q;q',q'')=\frac{i(2\pi)^4}{\sqrt{8q_0q'_0q''_0}}\delta(p+q-p'-q'-q'')T^{\rm ret}_{\alpha,\omega}(q;q',q'') \quad (2.6)$$

where

$$T^{\rm ret}_{\alpha,\omega}(q;q',q'')=-\int e^{i(q'x'+q''x'')}dx'dx''\langle p's'|\frac{\delta^2 j_\rho(0)}{\delta\varphi_{\rho'}(x')\delta\varphi_{\rho''}(x'')}|ps\rangle.$$

By taking into account the causality condition (2.1) it can readily be seen that integration in (2.5) is carried out in the region

$$x'>0, \quad x''>0. \quad (2.7)$$

The advanced amplitude is related to a matrix element of the following type:

$$S^\dagger_{\alpha,\omega}(q;q',q'')=(2\pi)^{\frac{3}{2}}\langle p's'|\varphi^{(-)}_{\rho'}(q')\varphi^{(-)}_{\rho''}(q'')S^\dagger\varphi_\rho{}^{(+)}(q)|ps\rangle. \quad (2.8)$$

Hence, taking into account (2.2) and employing the same technique as that used in deriving (2.6), we obtain

$$S^\dagger_{\alpha,\omega}(q;q',q'')=-i\frac{(2\pi)^4}{\sqrt{8q_0q'_0q''_0}}\delta(p+q-p'-q'-q'')T^{\rm adv}_{\alpha,\omega}(q;q',q'') \quad (2.9)$$

where

$$T^{\rm adv}_{\alpha,\omega}(q;q',q'')=\int e^{i(q'x'+q''x'')}dx'dx''\langle p's'|\frac{\delta^2 A_\rho(0)}{\delta\varphi_{\rho'}(x')\delta\varphi_{\rho''}(x'')}|ps\rangle.$$

Integration in (2.9) is carried out over the region

$$x'<0, \quad x''<0. \quad (2.10)$$

With the help of (2.6) and (2.9) the anti-Hermitian part of the process amplitude can be written in the form

$$A_{\alpha,\omega}(q;q',q'')=\frac{1}{2i}(T^{\rm ret}_{\alpha,\omega}(q;q',q'')-T^{\rm adv}_{\alpha,\omega}(q;q',q'')). \quad (2.11)$$

Before analysing in detail the anti-Hermitian part of the amplitude we shall first examine the kinematics of the process.

## 2.1 KINEMATICS OF PROCESS

According to the law of conservation of energy-momentum

$$p+q = p'+q'+q''. \tag{2.12}$$

In the future we choose a reference system in which

$$\mathbf{p}+\mathbf{p}' = 0. \tag{2.13}$$

Instead of vectors $q'$, $q''$ we introduce the vectors $Q$, $\Delta$ defined as follows:

$$\begin{aligned} Q &= \tfrac{1}{2}(q'+q'') \\ \Delta &= \tfrac{1}{2}(q'-q''). \end{aligned} \tag{2.14}$$

It is easy to see that $Q$ is a time-like vector. If the four dimensional square of vector $Q$ is fixed then

$$Q^2 = m_Q^2. \tag{2.15}$$

In the reference system chosen by us the law of conservation of energy-momentum (2.12) can be written as follows:

$$\begin{aligned} \mathbf{q}-2\mathbf{Q} &= -2\mathbf{p} \\ (\mathbf{q}-2\mathbf{Q})(\mathbf{q}+2\mathbf{Q}) &= 4m_Q^2-m^2 \end{aligned} \tag{2.16}$$

where $m$ is the mass of the initial boson. Hence after elementary calculations we obtain

$$\mathbf{q} = \lambda\mathbf{e}-(1+\varepsilon)\mathbf{p}, \quad 2\mathbf{Q} = \lambda\mathbf{e}+(1-\varepsilon)\mathbf{p} \tag{2.17}$$

where $\mathbf{e}$ is a unit vector orthogonal to vector $\mathbf{p}$,

$$\varepsilon = \frac{4m_Q^2-m^2}{4\mathbf{p}^2}, \quad \frac{\lambda^2}{4} = E^2-m_Q^2-\tfrac{1}{4}(1-\varepsilon)^2\mathbf{p}^2. \tag{2.18}$$

Here $E$ denotes the zero component of vector $\mathbf{Q}$. In the present paper we consider reactions in which bosons with equal masses are created:

$$q'^2 = q''^2 = m_1^2. \tag{2.19}$$

Taking into account (2.15) and (2.19) we get

$$\Delta^2 = -m_Q^2+m_1^2, \quad Q\Delta = 0. \tag{2.20}$$

In the following we shall consider the analyticity properties of the process amplitude with respect to the variable $E$. The dispersion relations are especially interesting in the absence of an unobservable region. In this case they relate only observable quantities.

If the dispersion relations contain a large unobservable region they are of less value not only because it becomes much more difficult to prove them rigorously, but also because it is much more difficult to derive from them any information on physical processes.

In the reactions considered by us one can, by suitably choosing vector $\Delta$, obtain dispersion relations in which the unobservable energy region is either totally absent or is not very significant.

Let the direction of vector $\Delta$ be chosen orthogonal to vectors $\mathbf{p}$ and $\mathbf{e}$. From conditions (2.20) it then follows that

$$\Delta_0 = 0, \quad \Delta^2 = m_Q^2 - m_1^2, \quad m_Q^2 \geqq m_1^2. \tag{2.21}$$

Thus, in the coordinate system chosen by us the process amplitude will be a function of the variables $E$, $\mathbf{e}$, $\mathbf{p}$, $\Delta$, vectors $\mathbf{e}$, $\mathbf{p}$, $\Delta$ being fixed when variable $E$ changes.

## 3. Analysis of Anti-Hermitian Process Amplitude

We now proceed to investigate the anti-Hermitian part of the process amplitude. Consider the expression

$$A_{q;q',q''} = -\frac{i}{\sqrt{8q_0 q'_0 q''_0}} \int e^{i(q'x'+q''x''-qx)} dx dx' dx'' \left\langle p' s' \left| \frac{\delta^2 j_\rho(x)}{\delta\varphi_{\rho'}(x')\delta\varphi_{\rho''}(x'')} + \frac{\delta^2 \Lambda_\rho(x)}{\delta\varphi_{\rho'}(x')\delta\varphi_{\rho''}(x'')} \right| ps \right\rangle. \tag{3.1}$$

By comparing (3.1) and (2.11) it will easily be seen that

$$A_{q;q'q''} = \frac{-2(2\pi)^4}{\sqrt{8q_0 q'_0 q''_0}} \delta(p+q-p'-q'-q'') A_{\alpha,\omega}(q; q', q''). \tag{3.2}$$

Taking into account the equation

$$\Lambda_\rho(x) = -S^\dagger j_\rho(x) S \tag{3.3}$$

and also the stability of states $|sp\rangle$, $|s'p'\rangle$ it is easy to obtain

$$\begin{aligned} &\langle p' s' | \frac{\delta^2 j_\rho(x)}{\delta\varphi_{\rho''}(x'')\delta\varphi_{\rho'}(x')} + \frac{\delta^2 \Lambda_\rho(x)}{\delta\varphi_{\rho''}(x'')\delta\varphi_{\rho'}(x')} |ps\rangle \\ &= i\langle p' s' | D_{\rho,\rho''}(x, x'') j_{\rho'}(x') + D_{\rho,\rho'}(x, x') j_{\rho''}(x'') \\ &+ j_\rho(x) D_{\rho',\rho''}(x', x'') - D_{\rho',\rho''}(x', x'') j_\rho(x) - j_{\rho'}(x') D_{\rho,\rho''}(x, x'') \\ &- j_{\rho''}(x'') D_{\rho,\rho'}(x, x') | ps\rangle \end{aligned} \tag{3.4}$$

where

$$D_{\rho,\rho'}(x, x') = \tfrac{1}{2}\left( \frac{\delta j_\rho(x)}{\delta\varphi_{\rho'}(x')} + \frac{\delta j_{\rho'}(x')}{\delta\varphi_\rho(x)} \right).$$

Inserting (3.4) in (3.1) and using (3.2), the anti-Hermitian part of the amplitude can be represented in the following form:

$$A_{\alpha,\omega}(q;q',q'')=\pi\sum_n\int d\mathbf{k}_n\{\delta(p'+q'-k_n)V_{q'}(n,p')D_{q;q''}(p,n)$$
$$-\delta(p-q'-k_n)D_{q;q''}(n,p')V_{q'}(p,n)+\delta(p'+q''-k_n)D_{q;q'}(p,n)V_{q''}(n,p')$$
$$-\delta(p-q''-k_n)D_{q;q'}(n,p')V_{q''}(p,n)$$
$$+\delta(p'+q'+q''-k_n)D_{-q';q''}(n,p')V_q(p,n)$$
$$-\delta(p-q'-q''-k_n)D_{-q';q''}(p,n)V_q(n,p')\} \tag{3.5}$$

where

$$(2\pi)^4\delta(p-q'-k_n)D_{q;q''}(n,p')$$
$$=\int e^{iq''x''-iqx}\langle p's'|D_{\rho,\rho''}(x,x'')|n\rangle dxdx'',\quad V_{q'}(n,p')=\langle p's'|j_{\rho'}(0)|n\rangle. \tag{3.6}$$

The translational invariance properties of the matrix elements and also the assumption that the energy-momentum operator possesses a complete system of state operators were employed in deriving (3.5). Performing the integration in (3.5) we obtain

$$A_{\alpha,\omega}(q;q',q'')=\pi\sum_n\{V_{q'}(n,p')D_{q;q''}(p,n)\delta(p'_0+q'_0-\sqrt{M_n^2+(\mathbf{p}'+\mathbf{q}')^2})$$
$$-\delta(p_0-q'_0-\sqrt{M_n^2+(\mathbf{p}-\mathbf{q}')^2})D_{q;q''}(n,p')V_{q'}(p,n)$$
$$+V_{q''}(n,p')D_{q;q'}(p,n)\delta(p'_0+q''_0-\sqrt{M_n^2+(\mathbf{p}'+\mathbf{q}'')^2})$$
$$-D_{q;q'}(n,p')V_{q''}(p,n)\delta(p_0-q''_0-\sqrt{M_n^2+(\mathbf{p}-\mathbf{q}'')^2})$$
$$+D_{-q';q''}(n,p')V_q(p,n)\delta(p'_0+q'_0+q''_0-\sqrt{M_n^2+(\mathbf{p}'+\mathbf{q}'+\mathbf{q}'')^2})$$
$$-V_q(n,p')D_{-q';q''}(p,n)\delta(p_0-q'_0-q''-\sqrt{M_n^2+(\mathbf{p}-\mathbf{q}'-\mathbf{q}'')^2})\}. \tag{3.7}$$

Consider the $\delta$ function of expression (3.7). It can easily be demonstrated that in a reference system in which the sum of the nucleon momenta before and after the reaction is zero, $\delta$ singularities of the functions under consideration will occur at the energies

$$E'=\pm\frac{M_n^2-M^2+m_Q^2-m_1^2-\frac{1}{4}m^2-\mathbf{p}^2}{2\sqrt{\mathbf{p}^2+M^2}}$$
$$E''=\pm\frac{M_n^2-M^2-2m_Q^2-2\mathbf{p}^2-\frac{1}{2}m^2}{4\sqrt{\mathbf{p}^2+M^2}}. \tag{3.8}$$

Taking into account (2.21), it can readily be seen that

$$|E''|<|E'|. \tag{3.9}$$

On the basis of (3.8) $\delta$ singularities of functions $M_n=M$ will occur respectively at the energies

$$E'_1=\pm\frac{m_Q^2-m_1^2-\frac{1}{4}m^2-\mathbf{p}^2}{2\sqrt{\mathbf{p}^2+M^2}}$$
$$E''_1=\pm\frac{m_Q^2+\mathbf{p}^2+\frac{1}{4}m^2}{2\sqrt{\mathbf{p}^2+M^2}}. \tag{3.10}$$

If no bound states of the meson-nucleon system are assumed to exist between $M$ and $M+\mu$ we obtain, assuming in (3.8) $M_n \geqq M+\mu$, that the continuous spectrum lies in a region for which

$$|E| \geqq \frac{2M\mu+\mu^2-2m_Q^2-2\mathbf{p}^2-\frac{1}{2}m^2}{4\sqrt{\mathbf{p}^2+M^2}}. \tag{3.11}$$

If

$$\begin{gathered}(m_Q^2+\mathbf{p}^2) < \tfrac{1}{2}(M\mu+\tfrac{1}{2}\mu^2-\tfrac{1}{4}m^2), \\ M\mu+\tfrac{1}{2}\mu^2 > \tfrac{1}{4}m^2\end{gathered} \tag{3.12}$$

the continuous spectrum will lie above the single-nucleon poles and the energy spectrum of the anti-Hermitian part of the process amplitude can then be diagrammatically represented as follows

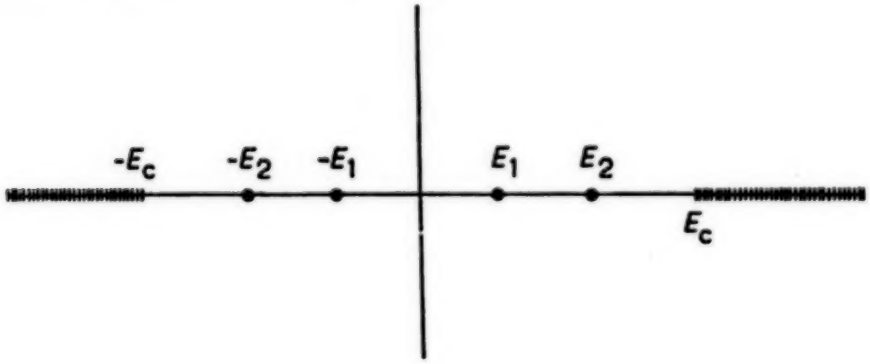


Fig. 1

$$E_1 = \frac{\mathbf{p}^2+m_1^2+\frac{1}{4}m^2-m_Q^2}{2\sqrt{\mathbf{p}^2+M^2}}, \quad E_2 = \frac{\mathbf{p}^2+\frac{1}{4}m^2+m_Q^2}{2\sqrt{\mathbf{p}^2+M^2}},$$

$$E_c = \frac{M\mu+\frac{1}{2}\mu^2-m_Q^2-\mathbf{p}^2-\frac{1}{4}m^2}{2\sqrt{\mathbf{p}^2+M^2}}. \tag{3.13}$$

It should be remarked that the observable energy region extends from $E_p$ (threshold energy value):

$$E_p^2 = m_Q^2+\tfrac{1}{4}(1-\varepsilon)^2\mathbf{p}^2, \qquad \varepsilon = \frac{m_Q^2}{\mathbf{p}^2}. \tag{3.14}$$

There will be no unobservable region in the dispersion relations if the continuous spectrum starts above the process threshold:

$$E_c \geqq E_p. \tag{3.15}$$

Condition (3.15) restricts the possible values of $m_Q^2$ and $\mathbf{p}^2$. In order to write these restrictions in an explicit form we shall consider some concrete examples.

### 3.1. DOUBLE COMPTON EFFECT ($\gamma+p \to 2\gamma+p$)

Assuming $m = m_1 = 0$ in formulae (3.13) and (3.14) we obtain in this particular case

$$E_1 = \frac{\mathbf{p}^2 - m_Q^2}{2\sqrt{\mathbf{p}^2+M^2}}, \quad E_2 = \frac{\mathbf{p}_2 + m_Q^2}{2\sqrt{\mathbf{p}^2+M^2}}, \quad E_c = \frac{M\mu + \frac{1}{2}\mu^2 - m_Q^2 - \mathbf{p}^2}{2\sqrt{\mathbf{p}^2+M^2}} \tag{3.16}$$

$$E_p = \tfrac{1}{2}(|\mathbf{p}| + m_Q^2/|\mathbf{p}|).$$

Hence the condition of absence of an unobservable region, (3.15), can be written as follows:

$$\frac{1}{2}\,\frac{\mathbf{p}^2+m_Q^2}{|\mathbf{p}|} \leqq \frac{M\mu+\frac{1}{2}\mu^2-m_Q^2-\mathbf{p}^2}{2\sqrt{\mathbf{p}^2+M^2}}; \tag{3.17}$$

or after some elementary transformations

$$\mathbf{p}^4(M+\mu)^2+\mathbf{p}^2[2m_Q^2(M+\tfrac{1}{2}\mu)^2-\mu^2(M+\tfrac{1}{2}\mu)^2+\tfrac{1}{2}\mu^2 m_Q^2]+m_Q^4 M^2 \leqq 0. \tag{3.18}$$

The condition which ensures that there will always be suitable values of $\mathbf{p}^2$, for which inequality (3.18) will be valid, can thus be written as follows:

$$m_Q^2 \leqq \tfrac{1}{4}\mu^2. \tag{3.19}$$

It should be noted that if $m_Q^2 = \frac{1}{4}\mu^2$, there will be only one value of the momentum,

$$\mathbf{p}_c^2 = \tfrac{1}{4}\mu^2\,\frac{M}{M+\mu}, \tag{3.20}$$

for which (3.18) will be true; if, however, $m_Q^2 < \frac{1}{4}\mu^2$ there will be an interval

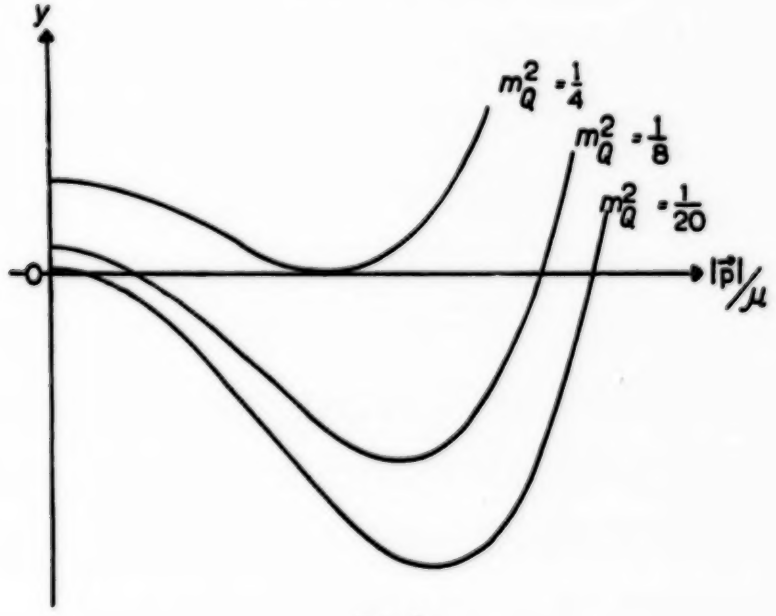


Fig. 2

of values of $\mathbf{p}^2$ which includes point $p_c$ and ensures validity of enequality (3.18) (fig. 2).

The following important fact should be noted. In ordinary scattering of mesons on nucleons the unobservable region is absent only if forward scattering is considered, and similarly the unobservable energy region will also be absent in the case under consideration only if some restrictions are imposed on the physical quantities determining the kinematics of the process $(\mathbf{p}^2, m_Q^2, \Delta^2)$. Consider the anti-Hermitian part of the process amplitude for the energy range $|E| < E_c$. It can readily be seen from (3.7) that in the region under consideration $A_{\alpha,\omega}(q; q', q'')$ can be written as follows:

$$A_{\alpha,\omega}(q; q', q'') = \pi \sum_{S''} \Big\{ \Big(1 - \frac{E_1}{p_0}\Big) [V_{q'}(p'', p') D_{q;q''}(p, p'') + V_{q''}(p'', p') D_{q;q'}(p, p'')] \delta(E+E_1) - \Big(1 - \frac{E_1}{p_0}\Big) [D_{q;q''}(p'', p') V_{q'}(p, p'') + D_{q;q'}(p'', p') V_{q''}(p, p'')] \delta(E-E_1) + \tfrac{1}{2} \Big(1 - \frac{2E_2}{p_0}\Big) [D_{-q';q''}(p'', p') \cdot V_q(p, p'') \delta(E+E_2) - V_q(p'', p') D_{-q';q''}(p, p'') \delta(E-E_2)] \Big\} \tag{3.21}$$

where summation is carried out over the spins of the intermediate single-nucleon state.

In the following the dispersion equations will be written in terms of the variable $E$. Employing the results obtained in this section, viz., (3.21), we can evaluate the contribution of the region $|E| < E_c$ to the dispersion integral

$$\frac{1}{\pi} \int_{-E_c}^{E_c} dE' \Big(\frac{E - E_0}{E' - E_0}\Big)^{n+1} \frac{S \pm A_{\alpha,\omega}(E')}{(E' - E)} = \sum_{i=1,2} \Big[ \Big(\frac{E_0 - E}{E_0 + E_i}\Big)^{n+1} \frac{S \pm R_i(\mathbf{p}, \Delta, \mathbf{e})}{E_i + E} + \Big(\frac{E_0 - E}{E_0 - E_i}\Big)^{n+1} \frac{S_\pm \Omega_i(\mathbf{p}, \Delta, \mathbf{e})}{E_i - E} \Big] \tag{3.22}$$

where

$$\begin{aligned} R_1(\mathbf{p}, \Delta, \mathbf{e}) &= -\Big(1 - \frac{E_1}{p_0}\Big) [V_{q'}(p'', p') D_{q;q''}(p, p'') + V_{q''}(p'', p') D_{q;q'}(p, p'')] \\ R_2(\mathbf{p}, \Delta, \mathbf{e}) &= -\tfrac{1}{2} \Big(1 - \frac{2E_2}{p_0}\Big) D_{-q';q''}(p'', p') V_q(p, p'') \\ \Omega_1(\mathbf{p}, \Delta, \mathbf{e}) &= -\Big(1 - \frac{E_1}{p_0}\Big) [D_{q;q''}(p'', p') V_{q'}(p, p'') + D_{q;q'}(p'', p') V_{q''}(p, p'')] \\ \Omega_2(\mathbf{p}, \Delta, \mathbf{e}) &= -\tfrac{1}{2} \Big(1 - \frac{2E_2}{p_0}\Big) V_q(p'', p') D_{-q';q''}(p, p''); \end{aligned} \tag{3.23}$$

$S_\pm$ is the symmetrization or antisymmetrization operator with respect to **e** (see section 4). Let us inquire as to the meaning of the operators $V$ and $D$ encountered in expression (3.23). From (3.6) we have

$$V_{\sigma'}(p'', p') = \langle p's'|j_{\rho'}(0)|p''s''\rangle. \tag{3.24}$$

From considerations of relativistic invariance and taking into account that $p'^2 = p^2 = M^2$, $q'^2 = 0$ we find that the matrix element of the electromagnetic current operator can be represented in the form [5])

$$\langle p's'|j_{\nu'}(0)|p''s''\rangle = \overline{U}_{s'}(p')\{e\tau_p\gamma_{\nu'} + \hat{\mu}\cdot\tfrac{1}{2}[(p'-p'')\cdot\gamma, \gamma_{\nu'}]\}U_{s''}(p''). \tag{3.25}$$

Here $e$ is the renormalized electric charge of the nucleon and $\hat{\mu} = \mu'_p\tau_p + \mu_n\tau_n$ where $\mu'_p$, $\mu_n$ are the anomalous proton and neutron magnetic moments and

$$\tau_p = \frac{1+\tau_3}{2}, \quad \tau_n = \frac{1-\tau_3}{2};$$

$U_{s'}(p')$ is the Dirac spinor.

We now turn to a study of operator $D$. As an example consider the operator $D_{q;q''}(p'', p')$ which, according to (3.2) and (3.6), is defined as follows:

$$\delta(p'+q''-q-p'')D_{q;q''}(p'', p') = \tfrac{1}{2}\int e^{iq''x''-iqx}\langle p's'|\frac{\delta j_\rho(x)}{\delta\varphi_{\rho''}(x'')} + \frac{\delta j_{\rho''}(x'')}{\delta\varphi_\rho(x)}|p''s''\rangle dx dx''. \tag{3.26}$$

It is evident from here that operator $D$ is identical with the Hermitian part of the scattering amplitude of photons on nucleons [6]). The vertex operator $V_{\sigma'}(p, p'')$ as well as operator $D_{qq''}(p'', p')$ possess a matrix structure in spin and isotopic space. The spin structure of operator $D$ consists of several independent combinations of vectors $q$, $q''$, $p''$, $\gamma$. The structural functions of the Hermitian part of amplitude $D^{\nu''\nu'}_{qq''}$ are invariant functions of two independent invariants:

$$\nu = \tfrac{1}{2}(p'+p'')q'', \quad \nu_1 = \tfrac{1}{2}(qq''). \tag{3.27}$$

On basis of relativistic invariance considerations operator $D$ can be represented as follows:

$$D_{q;q''}(p'', p') = \sum_s \Omega_s(\nu, \nu_1)\overline{U}(p')R^s_{\mu\nu}(\gamma, q, q'', p'')U(p'').$$

Dispersion relations in the variable $\nu$ [7]) can be written for the structural functions $\Omega_s(\nu, \nu_1)$. It should be noted that in a reference system in which $\mathbf{p}'+\mathbf{p}'' = 0$ the structural functions will depend on the variables $E_\lambda$ and $\mathbf{p}'^2_\lambda$, where

$$\nu_1 = \mathbf{p}'^2_\lambda, \quad \nu = E_\lambda\sqrt{\mathbf{p}'^2_\lambda + M^2}, \tag{3.29}$$

the index $\lambda$ indicating that the quantities refer to the system in which $\mathbf{p}'+\mathbf{p}''=0$. Comparing these expressions with the values of invariants $\nu_1$ and $\nu$ in the $(\mathbf{p}+\mathbf{p}'=0)$ system we find

$$\begin{gathered}\mathbf{p}_\lambda'^2=\tfrac{1}{2}(\mathbf{p}^2+m_Q^2)\\ \sqrt{\mathbf{p}_\lambda'^2+M^2}\cdot E'_\lambda=\sqrt{\mathbf{p}'^2+M^2}\cdot E_1-m_Q^2.\end{gathered}\tag{3.30}$$

Account has been taken here of the circumstance that the Hermitian part of $D_{q;q''}(p'', p')$ has been computed for energy values $E=E_1$. It can be seen from formula (3.30) that $\mathbf{p}'_\lambda$ and $E'_\lambda$ are real. This permits one to express the structural functions of the Hermitian part of $D_{q;q''}(p'', p')$ through the dispersion integral. It may be mentioned that if [8])

$$\mathbf{p}_\lambda'^2=\tfrac{1}{2}(\mathbf{p}^2+m_Q^2)\leqq\mu^2\frac{(M+\mu/2)^2}{(M+\mu)^2},\tag{3.31}$$

the dispersion integral will not contain an unobservable energy region and, generally, speaking, it can be used to compute the structural functions of $D_{q;q''}(p'', p')$. It should be noted that for energy values $\pm E_1$, $\pm E_2$ (lying below the threshold of the $\mathrm{p}+\gamma\to 2\gamma+\mathrm{p}$ reaction) the vectors $q$, $q''$, $p''$ entering $R^s_{\mu\nu}$ are complex, the imaginary part of these vectors being due to the vector component directed along $\mathbf{e}$. However, because of symmetrization or antisymmetrization with respect to $\mathbf{e}$, the inhomogeneous term in dispersion relations (3.22) will not contain these components.

The considerations applied above to $D_{q;q''}(p'', p')$ can also be repeated in the analysis of $D_{q;q''}(p, p'')$, $D_{q;q'}(p, p'')$, $D_{q;q'}(p'', p')$. In conclusion we consider operators $D_{-q';q''}(p, p'')$, $D_{-q';q''}(p'', p')$. It is easy to see, for example, that the operator $D_{-q';q''}(p, p'')$ is the Hermitian part of the amplitude of the fictitious process $\mathrm{p}\to\mathrm{p}+2\gamma$, involving the conservation law $p=q'+q''+p''$. It is quite obvious that the conservation law is valid only for complex momenta. Hence operator $D_{-q';q''}(p, p'')$ cannot be expressed in terms of observable quantities.

### 3.2. PHOTOPRODUCTION OF TWO $\pi$ MESONS $(\gamma+\mathrm{p}\to 2\pi+\mathrm{p})$.

On basis of (3.13) and taking into account that $m=0$, $m_1=\mu$ one can write the poles of the lower boundary of the continuous spectrum and the threshold of the process under consideration as follows:

$$\begin{gathered}E_1=\frac{\mathbf{p}^2+\mu^2-m_Q^2}{2\sqrt{\mathbf{p}^2+M^2}},\quad E_2=\frac{\mathbf{p}^2+m_Q^2}{2\sqrt{\mathbf{p}^2+M^2}},\\ E_c=\frac{M\mu+\frac{1}{2}\mu^2-m_Q^2-\mathbf{p}^2}{2\sqrt{\mathbf{p}^2+M^2}},\quad E_p=\tfrac{1}{2}\left(|\mathbf{p}|+\frac{m_Q^2}{|\mathbf{p}|}\right).\end{gathered}\tag{3.32}$$

Inasmuch as for the given process the reaction threshold and lower limit of the continuous spectrum are identical with the similar quantities for the

double Compton effect, the condition of absence of an unobservable region will have the form

$$m_Q^2 \leqq \tfrac{1}{4}\mu^2. \tag{3.33}$$

However, for mesons $m_Q^2$ will evidently always be greater than $\frac{1}{2}\mu^2$. Thus, the condition for absence of an unobservable region will not hold and therefore the dispersion relations will always contain some unobservable regions.

With regard to operators $V$ and $D$ which enter the inhomogeneous term in the dispersion relations, one can again apply considerations similar to those employed in the preceding section in the analysis of the corresponding operators.

It can readily be verified by performing the relevant analysis that in the problem under consideration along with matrix elements of the electromagnetic current operator, $V_q(\not p, \not p'')$, $V_q(\not p'', \not p')$, matrix elements of the meson current operator $V_{q'}(\not p'', \not p')$, $V_{q'}(\not p, \not p'')$, $V_{q''}(\not p'', \not p')$ and $V_{q''}(\not p, \not p'')$ will also be encountered.

From relativistic invariance considerations and by taking into account pseudoscalarity of the $\pi$ meson field and also that

$$p^2 = p'^2 = p''^2 = M^2, \quad q'^2 = q''^2 = \mu^2$$

one can write the matrix element of the meson current $j_\rho$ in the form [5])

$$\langle p's'|j_\rho(0)|ps\rangle = g\bar{U}_{s'}(p')\gamma_5\tau_\rho U_s(p)$$

where $g$ is the renormalized meson charge.

It is not difficult to verify that the operators

$$D_{q,q''}(\not p, \not p''), \quad D_{q,q''}(\not p'', \not p'), \quad D_{q,q'}(\not p, \not p''), \quad D_{q,q''}(\not p'', \not p')$$

can be considered as an analytic continuation in the unobservable energy region (with aid of the photoproduction dispersion relations) of the Hermitian part of the photoproduction amplitude of $\pi$ mesons on nucleons, and the operators $D_{-q',q''}(\not p'', \not p')$, $D_{-q',q''}(\not p, \not p'')$ can be considered as analytic extensions of the Hermitian part of the amplitude for fictitious decay of a free nucleon into a nucleon and two $\pi$ mesons.

### 3.3. CREATION OF MESONS IN THE SCATTERING OF MESONS ON NUCLEONS ($\pi$+p → 2$\pi$+p)

Putting $m = m_1 = \mu$ in formulas (3.13) we obtain the following expressions for the poles of the lower boundary of the continuous spectrum and for the reaction threshold:

$$E_1 = \frac{\mathbf{p}^2+\frac{5}{4}\mu^2-m_Q^2}{2\sqrt{\mathbf{p}^2+M^2}}, \quad E_2 = \frac{\mathbf{p}^2+\frac{1}{4}\mu^2+m_Q^2}{2\sqrt{\mathbf{p}^2+M^2}}, \quad E_c = \frac{M\mu+\frac{1}{4}\mu^2-m_Q^2-\mathbf{p}^2}{2\sqrt{\mathbf{p}^2+M^2}};$$

$$E_p^2 = m_Q^2+\tfrac{1}{4}(1-\varepsilon)^2\mathbf{p}^2, \quad \varepsilon = \frac{4m_Q^2-\mu^2}{4\mathbf{p}^2}. \tag{3.34}$$

The condition for absence of an unobservable region

$$E_c \geqq E_p \tag{3.35}$$

after elementary calculations can be written as follows:

$$\mathbf{p}^2 = (\tfrac{1}{4}\mu^2 - m_Q^2)\frac{M}{M+\mu}. \tag{3.36}$$

It can be seen from this formula that if there will always be a momentum value for which the unobservable region will be absent. However, recalling that for mesons $m_Q^2$ is always larger than $\frac{1}{2}\mu^2$, we see that condition (3.36) will not hold and hence an unobservable region will be present in the dispersion relations. The process $\pi+\mathrm{p} \to 2\gamma+\mathrm{p}$ should particularly be mentioned. For this process the lower boundary of the continuous spectrum and the reaction threshold coincide with the corresponding quantities for the process $(\pi+\mathrm{p} \to 2\pi+\mathrm{p})$. Thus in this case the condition of absence of an unobservable region can be written as

$$\mathbf{p}^2 = (\tfrac{1}{4}\mu^2 - m_Q^2)\frac{M}{M+\mu}. \tag{3.37}$$

Since the final particles are photons for which $m_Q^2$ can be larger or equal to zero one finds that for

$$m_Q^2 < \tfrac{1}{4}\mu^2 \tag{3.38}$$

there will always be a momentous value defined by formula (3.37) for which the unobservable region in the dispersion relations will be absent.

## 4. Analytic Properties of the Process Amplitude and the Dispersion Relations

In the present section we shall give a strict deduction of the dispersion relations (within the restrictions imposed in section 2) for the particular process $\gamma+\mathrm{p} \to 2\gamma+\mathrm{p}$.

The Fourier transforms of the retarded and advanced matrix elements of the reaction under consideration on basis of (2.6) and (2.9) can be written as follows:

$$\begin{aligned} T^{\mathrm{ret}}_{\alpha,\omega}(q; q', q'') &= -\int e^{i(q'x'+q''x'')}\,dx'\,dx''\langle p's'|\frac{\delta^2 j_\rho(0)}{\delta\varphi_{\rho'}(x')\delta\varphi_{\rho''}(x'')}|ps\rangle \\ T^{\mathrm{adv}}_{\alpha,\omega}(q; q', q'') &= \int e^{i(q'x'+q''x'')}\,dx'\,dx''\langle p's'|\frac{\delta^2 A_\rho(0)}{\delta\varphi_{\rho'}(x')\delta\varphi_{\rho''}(x'')}|ps\rangle. \end{aligned} \tag{4.1}$$

Integration in (4.1) is carried out in the region

$$x'_0 \geqq |\mathbf{x}'|, \quad x''_0 \geqq |\mathbf{x}''|, \qquad x'_0, x''_0 \geqq 0 \tag{4.2}$$

for the retarded amplitude, and in the region

$$|x'_0| \geqq |\mathbf{x}'|, \quad |x''_0| \geqq |\mathbf{x}''| \qquad x'_0, x''_0 \leqq 0 \tag{4.3}$$

for the advanced amplitude.

Changing the integration variables in expressions (4.1) in accord with the formulas

$$x' = \frac{x+y}{2}, \quad x'' = \frac{x-y}{2};$$

we obtain

$$\begin{aligned} T^{\mathrm{ret}}_{\alpha,\omega}(E, \mathbf{Q}, \Delta) &= -2^{-4}\int e^{iQx+i\Delta y} F^{\mathrm{ret}}_{\alpha,\omega}(x, y)\mathrm{d}x\mathrm{d}y \\ T^{\mathrm{adv}}_{\alpha,\omega}(E, \mathbf{Q}, \Delta) &= +2^{-4}\int e^{iQx+i\Delta y} F^{\mathrm{adv}}_{\alpha,\omega}(x, y)\mathrm{d}x\mathrm{d}y \end{aligned} \tag{4.4}$$

where

$$\begin{aligned} F^{\mathrm{ret}}_{\alpha,\omega}(x, y) &= \langle p's'| \frac{\delta^2 j_\rho(0)}{\delta\varphi_{\rho'}\left(\frac{x+y}{2}\right)\delta\varphi_{\rho''}\left(\frac{x-y}{2}\right)} |ps\rangle \\ F^{\mathrm{adv}}_{\alpha,\omega}(x, y) &= \langle p's'| \frac{\delta^2 \Lambda_\rho(0)}{\delta\varphi_{\rho'}\left(\frac{x+y}{2}\right)\delta\varphi_{\rho''}\left(\frac{x-y}{2}\right)} |ps\rangle. \end{aligned} \tag{4.5}$$

In accord with the causality condition, integration in (4.4) with respect to the variable $x$ should be carried out in the region

$$x_0 \geqq |\mathbf{x}|, \quad x_0 > 0 \tag{4.6}$$

for the retarded amplitude and in the region

$$|x_0| \geqq |\mathbf{x}|, \quad x_0 < 0 \tag{4.7}$$

for the advanced amplitude.

$E$ and $\mathbf{Q}$ are usually related by the condition

$$E^2 = \mathbf{Q}^2 + m_Q{}^2. \tag{4.8}$$

At present $E$ and $\mathbf{Q}$ will be considered as independent variables. Vectors $\Delta$ and $\mathbf{p}$ are then assumed to be fixed. Functions $T^{\mathrm{ret}}_{\alpha,\omega}$ and $T^{\mathrm{adv}}_{\alpha,\omega}$ are defined everywhere on the real axis for $|E| > E_s$ (process threshold). Consider the function

$$T(E, \mathbf{Q}, \Delta) = T^{\mathrm{ret}}(E, \mathbf{Q}, \Delta) - T^{\mathrm{adv}}(E, \mathbf{Q}, \Delta). \tag{4.9}$$

The energy spectrum of this function is given by fig. 3,

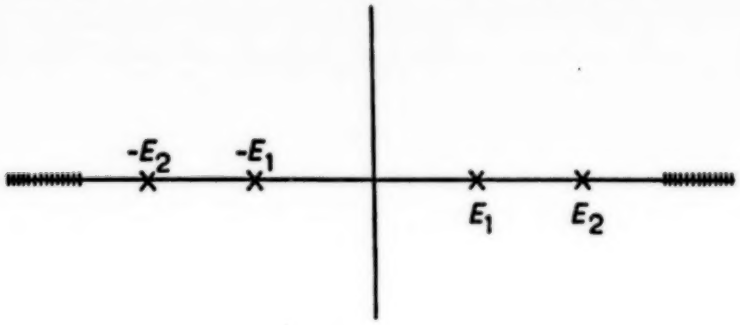


Fig. 3

where the poles $\pm E_1$ and $\pm E_2$ are defined by the equations

$$\begin{aligned} 4E^2(\mathbf{p}^2+M^2)-[Q^2+\Delta^2+2\mathbf{p}\cdot\mathbf{Q}]^2 &= 0 \\ E^2(\mathbf{p}^2+M^2)-[Q^2+\mathbf{p}\cdot\mathbf{Q}]^2 &= 0. \end{aligned} \tag{4.10}$$

An analysis of the $\delta$ singularities of the anti-Hermitian part of (4.9) indicates that the continuous spectrum of some terms of the anti-Hermitian part has the form of fig. 4,

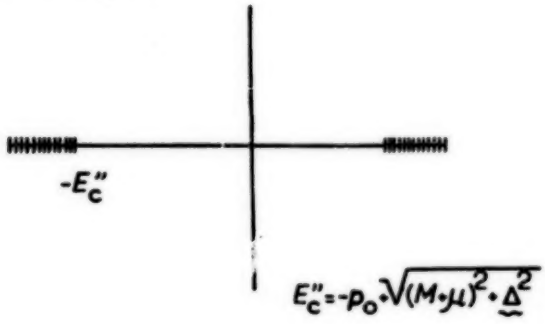


Fig. 4

whereas for other terms it is that of fig. 5.

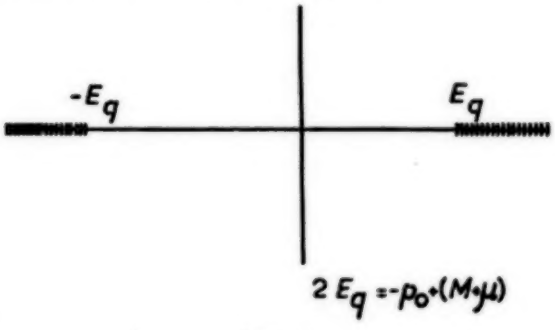


Fig. 5

It is easy to verify that

$$E''_c \geqq \tfrac{1}{2}(-p_0+M+\mu) = E_q, \quad \mathbf{p}^2 \leqq 2M\mu+\mu^2. \tag{4.11}$$

By using (4.11) and (4.10), the energy spectrum of the anti-Hermitian part can be represented as in fig. 6.

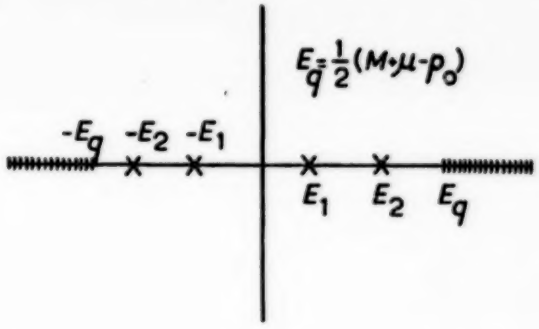


Fig. 6

We construct a function $\tilde{T}(E, \mathbf{Q}, \Delta)$ which vanishes for $|E| < E_q$. To do this we replace the functions $F^{\text{ret}}(x, y)$ and $F^{\text{adv}}(x, y)$ entering (4.4) by functions $\tilde{F}^{\text{ret}}(x, y)$ and $\tilde{F}^{\text{adv}}(x, y)$ as follows:

$$\overset{\text{ret}}{\tilde{F}^{\text{adv}}}(x, y) = \left\{4(\mathbf{p}^2+M^2)\frac{\partial^2}{\partial x_0^2}+\left[\Box_x^2+\Box_y^2+2i\left(p_j\frac{\partial}{\partial x_j}\right)\right]^2\right\}$$
$$\cdot\left\{\left[\Box_x^2+i\left(p_j\frac{\partial}{\partial x_j}\right)\right]^2+(\mathbf{p}^2+M^2)\frac{\partial^2}{\partial x_0^2}\right\}\overset{\text{ret}}{F^{\text{adv}}}(x, y) \quad (4.12)$$

or in the momentum representation

$$\overset{\text{ret}}{\tilde{T}^{\text{adv}}}(E, \mathbf{Q}, \Delta) = \{[Q^2+\Delta^2+2\mathbf{p}\cdot\mathbf{Q}]^2-4E^2(\mathbf{p}^2+M^2)\}$$
$$\cdot\{[Q^2+\mathbf{p}\cdot\mathbf{Q}]^2-E^2(\mathbf{p}^2+M^2)\}\overset{\text{ret}}{T^{\text{adv}}}(E, \mathbf{Q}\Delta). \quad (4.13)$$

The polynomial in (4.13) has been chosen so that the $\delta$ singularities of function $T(E, \mathbf{Q}, \Delta)$ at $\pm E_1$, $\pm E_2$ disappear. It is obvious that

$$\tilde{T}(E, \mathbf{Q}, \Delta) = \tilde{T}^{\text{ret}}(E, \mathbf{Q}, \Delta)-\tilde{T}^{\text{adv}}(E, \mathbf{Q}, \Delta) = 0 \quad (4.14)$$

if

$$|E| < E_q, \quad \text{Im } E = 0.$$

Recalling that

$$\tilde{T}(E, \mathbf{Q}, \Delta) = -\int e^{iQx+i\Delta y}\tilde{F}(x, y)\mathrm{d}x\mathrm{d}y \quad (4.15)$$

it is easy to deduce on basis of (4.14) and in virtue of independence of $E$ and $\mathbf{Q}$ the following important relation:

$$\int e^{iEx^0+i\Delta y}\tilde{F}(x_0, \mathbf{x}; y)\mathrm{d}x_0\mathrm{d}y = 0 \quad (4.16)$$

if

$$|E| < E_q, \quad \text{Im } E = 0.$$

We introduce the functions $\phi^{\text{r}}(E, \mathbf{e}, \mathbf{p}, \Delta, \rho)$ and $\phi^{\text{a}}(E, \mathbf{e}, \mathbf{p}, \Delta, \rho)$ in the following way:

$$\phi^{r}(E, \mathbf{e}, \mathbf{p}, \Delta, \rho)$$
$$= -S_{\pm}\int \tilde{F}^{\mathrm{ret}}(x, y)\exp\{iEx_0 - i\mathbf{e}\cdot\mathbf{x}\sqrt{E^2-E_p^2} - i\mathbf{x}\cdot\mathbf{p}\eta + i\Delta y - \rho\mathbf{x}^2\}dxdy$$
$$\phi^{a}(E, \mathbf{e}, \mathbf{p}, \Delta, \rho) \qquad (4.17)$$
$$= S_{\pm}\int \tilde{F}^{\mathrm{adv}}(x, y)\exp\{iEx_0 - i\mathbf{e}\cdot\mathbf{x}\sqrt{E^2-E_p^2} - i\mathbf{x}\cdot\mathbf{p}\eta + i\Delta y - \rho\mathbf{x}^2\}dxdy,$$

where $\rho > 0$, $\eta = \frac{1}{2}(1-m_Q^2/\mathbf{p}^2)$; $S_{\pm}$ is the symmetrization or antisymmetrization operation with respect to $\mathbf{e}$:

$$S_+ f(\mathbf{e}) = f(\mathbf{e}) + f(-\mathbf{e}), \quad S_- f(\mathbf{e}) = \frac{1}{\lambda}(f(\mathbf{e}) - f(-\mathbf{e}))$$

which is required to remove the double value of the square root $\sqrt{E^2-E_p^2}$. In writing (4.17) it was assumed that a relation of the type $E^2 = \mathbf{Q}^2 + m_Q^2$ exists between $\mathbf{Q}$ and $E$; $\mathbf{Q}$ has been replaced by the expression (see section 2)

$$\mathbf{Q} = \tfrac{1}{2}\lambda\mathbf{e} + \eta\mathbf{p}, \quad \frac{\lambda}{2} = \sqrt{E^2-E_p^2}.$$

Functions $\phi^r$, $\phi^a$ are analytic in the upper (lower) half-plane of energy $E$. On basis of (4.16) it follows that

$$\phi^{r}(E, \mathbf{e}, \mathbf{p}, \Delta, \rho) = \phi^{a}(E, \mathbf{e}, \mathbf{p}, \Delta, \rho) \qquad (4.18)$$

for

$$|E| < E_q, \ \mathrm{Im}\, E = 0.$$

Then there exists a function

$$\phi(E, \mathbf{e}, \mathbf{p}, \Delta, \rho) = \begin{cases} \phi^{r}(E, \mathbf{e}, \mathbf{p}, \Delta, \rho) & \mathrm{Im}\, E > 0 \\ \phi^{a}(E, \mathbf{e}, \mathbf{p}, \Delta, \rho) & \mathrm{Im}\, E < 0 \end{cases} \qquad (4.19)$$

which is analytic throughout the energy plane excepting the cuts

$$-\infty < \mathrm{Re}\, E < -E_q; \quad E_q < \mathrm{Re}\, E < \infty; \quad \mathrm{Im}\, E = 0. \qquad (4.20)$$

On the upper sides of the cuts the values of $\phi$ are equal to $\phi^r$ and on the lower ones they are equal to $\phi^a$.

If the degree of growth of function $\phi(E, \mathbf{e}, \mathbf{p}, \Delta, \rho)$ for $E \to \infty$ is not higher than $n+8$, one can apply Cauchy's integral theorem with the integration contour depicted in fig. 7 to the function

$$\frac{\phi(E, \mathbf{e}, \mathbf{p}, \Delta, \rho)}{(E-E_0)^{n+9}},$$

where $E_0$ is a real parameter, $|E_0| < E_q$.

If the radius of the large circle is made to approach infinity and the radii of the small semi-circles to approach zero, one obtains

$$\phi(E, \mathbf{e}, \mathbf{p}, \Delta, \rho)$$
$$= \frac{(E-E_0)^{n+9}}{2\pi i}\int_{-\infty}^{-E_q} \frac{\phi(E'+i0, \mathbf{e}, \mathbf{p}, \Delta, \rho)-\phi(E'-i0, \mathbf{e}, \mathbf{p}, \Delta, \rho)}{(E'-E)(E'-E_0)^{n+9}}\,dE' \qquad (4.21)$$
$$+ \frac{(E-E_0)^{n+9}}{2\pi i}\int_{E_q}^{\infty} \frac{\phi(E'+i0, \mathbf{e}, \mathbf{p}, \Delta, \rho)-\phi(E'-i0, \mathbf{e}, \mathbf{p}, \Delta, \rho)}{(E'-E)(E'-E_0)^{n+9}}\,dE' + P_{n+9}(E).$$

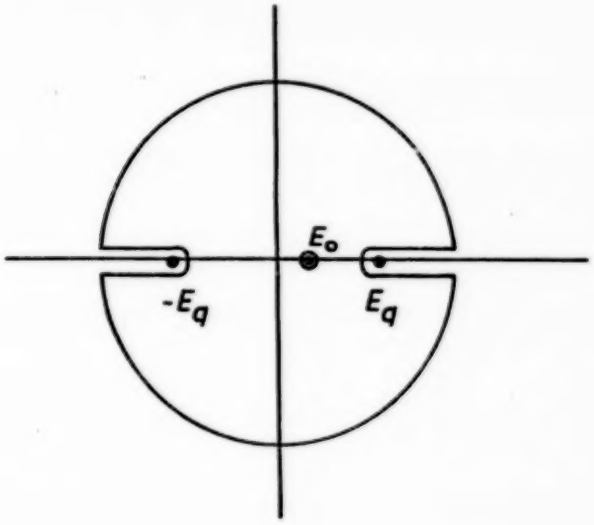


Fig. 7

It should be emphasized that in the case under consideration (absence of an unobservable region), $E_q > E_p$ and integration in (4.21) is performed over the observable region.

However, since the functions $\phi^r$ and $\phi^a$ are also defined in the observable region for $\rho = 0$, we may put $\rho = 0$ in the integrals. It is obvious that the right hand side of (4.21) will then be an analytic function over the entire plane of complex variable $E$, excluding the cuts (4.20). However, it follows from expression (4.21) that for $\rho = 0$ the right hand side defines a function $\phi(E, \mathbf{e}, \mathbf{p}, \Delta, 0)$ which is analytic throughout the entire $E$ plane, excluding the cuts (4.20). However function $\phi(E, \mathbf{e}, \mathbf{p}, \Delta, 0)$ differs from the function

$$S_\pm G(E, \mathbf{e}, \mathbf{p}, \Delta) = \begin{cases} S_\pm T^{\mathrm{ret}}(E, \mathbf{e}, \mathbf{p}, \Delta) & \mathrm{Im}\, E > 0 \\ S_\pm T^{\mathrm{adv}}(E, \mathbf{e}, \mathbf{p}, \Delta) & \mathrm{Im}\, E < 0 \end{cases}$$

only by factors which vanish at $E = \pm E_1$, $E = \pm E_2$. The function $S_\pm G(E, \mathbf{e}, \mathbf{p}, \Delta)$ will therefore be analytic over the entire plane of the complex variable $E$ with first degree poles at the points $E = \pm E_1$, $E = \pm E_2$ and cuts extending from $-\infty$ to $-E_q$ and from $E_q$ to $\infty$. The degree of increase of $S_\pm G(E, \mathbf{e}, \mathbf{p}, \Delta)$ is not higher than $n$. Thus Cauchy's theorem with the integration contour depicted in fig. 8 can be applied to the function

$$\frac{S_{\pm}G(E, \mathbf{e}, \mathbf{p}, \Delta)}{(E-E_0)^{n+1}}.$$

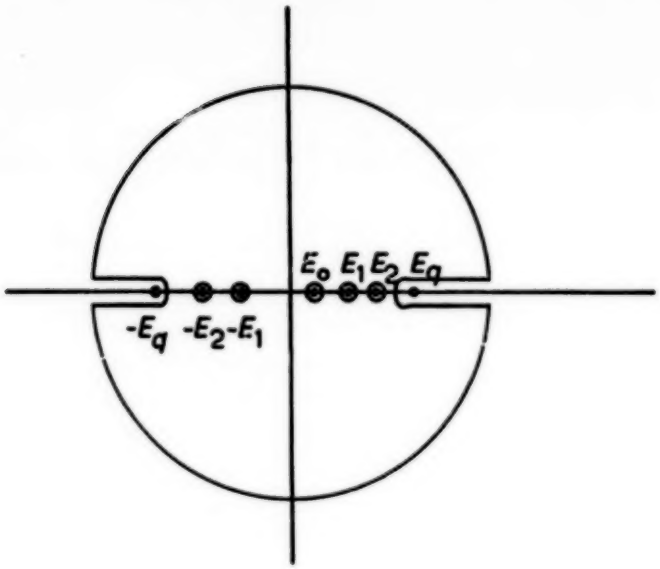


Fig. 8

If the radius of the large circle is made to approach infinity and the radius of the small semicircles are made to approach zero one obtains, taking into account (3.22) and (3.23),

$$S_{\pm}G(E, \mathbf{e}, \mathbf{p}, \Delta) = \frac{(E-E_0)^{n+1}}{2\pi i}\int_{|E'|\geq E_q}\frac{S_{\pm}T^{\mathrm{ret}}(E')-S_{\pm}T^{\mathrm{adv}}(E')}{(E'-E)(E'-E_0)^{n+1}}\,\mathrm{d}E' + \sum_{i=1,2}\left[\left(\frac{E_0-E}{E_0+E_i}\right)^{n+1}\frac{S_{\pm}R_i(\mathbf{p}, \Delta, \mathbf{e})}{E_i+E} + \left(\frac{E_0-E}{E_0-E_i}\right)^{n+1}\times\frac{S_{\pm}\Omega_i(\mathbf{p}, \Delta, \mathbf{e})}{E_i-E}\right]+P_n(E). \tag{4.22}$$

We now change to real values of $E$. Noting that

$$\lim_{\varepsilon\to 0} S_{\pm}G(E+i\varepsilon) = S_{\pm}T^{\mathrm{ret}}(E)$$
$$\lim_{\varepsilon\to 0} S_{\pm}G(E-i\varepsilon) = S_{\pm}T^{\mathrm{adv}}(E) \qquad \mathrm{Im}\,E = 0 \tag{4.23}$$

and taking into account the definition of the Hermitian and anti-Hermitian parts

$$D_{\alpha,\omega}(E) = \tfrac{1}{2}(T^{\mathrm{ret}}_{\alpha,\omega}(E)+T^{\mathrm{adv}}_{\alpha,\omega}(E)), \quad A_{\alpha,\omega}(E) = \frac{1}{2i}(T^{\mathrm{ret}}_{\alpha,\omega}(E)-T^{\mathrm{adv}}_{\alpha,\omega}(E)), \tag{4.24}$$

the following dispersion relations can easily be obtained:

$$S_{\pm}D_{\alpha,\omega}(E) = \frac{(E-E_0)^{n+1}}{\pi} \mathrm{P}\int_{|E'|>E_c} \mathrm{d}E' \frac{S_{\pm}A_{\alpha,\omega}(E')}{(E'-E)(E'-E_0)^{n+1}} \tag{4.25}$$

$$+\sum_{i=1,2}\left[\left(\frac{E_0-E}{E_0+E_i}\right)^{n+1}\frac{S_{\pm}R_i(\mathbf{p},\boldsymbol{\Delta},\mathbf{e})}{E_i+E}+\left(\frac{E_0-E}{E_0-E_i}\right)^{n+1}\frac{S_{\pm}\Omega_i(\mathbf{p},\boldsymbol{\Delta},\mathbf{e})}{E_i-E}\right]+P_n(E).$$

In the derivation of (4.25) account was taken of the fact that, in accord with (3.16), the anti-Hermitian part of amplitude $A_{\alpha,\omega}(E)$ vanishes in the energy region $E_q < E < E_c(E_p < E_q)$. The negative energy region in dispersion relations (4.25) can be excluded by using the symmetry properties of the anti-Hermitian part of the amplitude in the form

$$A_{\alpha,\omega}(E) = -P_{ss'}\, A^{*}_{\alpha,\omega}(-E); \tag{4.26}$$

$P_{ss'}$ is the transposition operator of the nucleon spin states. Symmetry property (4.26) can easily be deduced from (3.1).

In conclusion the authors express their deep appreciation to Academician N. N. Bogolubov for valuable discussions and to N. A. Chernikov for fruitful conversations.

## References

1) N. N. Bogolubov, B. V. Medvedyev and M. K. Polivanov, Some Problems Encountered in Dispersion Relations Theory (in print);
N. N. Bogolubov and D. V. Shirkov, Introduction to the theory of quantized fields (Gostekhizdat, 1957)
2) I. W. Polkinghorne, Nuovo Cimento **4** (1956) 216
3) A. A. Logunov, Doklady AN SSSR **117** (1957) 792
4) N. N. Bogolubov, Izvestia AN SSSR, ser. fiz. **19** (1955) 237
5) A. A. Logunov, A. N. Tavkhelidze and L. D. Solovyov, Nuclear Physics **4** (1957) 427
6) A. A. Logunov and P. S. Isayev, Nuovo Cimento (in print)
7) A. N. Tavkhelidze and V. K. Fedyanin, Doklady AN SSSR **119** (1958) 690
8) A. A. Logunov and A. R. Frenkin, Nuclear Physics (in print)

10.D *Nuclear Physics* 8 (1958) 394—395; © *North-Holland Publishing Co., Amsterdam*

# BOOK REVIEWS

S. FLÜGGE and E. CREUTZ (Editors), *Handbuch der Physik — Encyclopedia of Physics*, vol. 45 (Nuclear instrumentation II) (Springer, Berlin-Göttingen-Heidelberg 1958. vii—544 pages. 128 DM).

The present volume of the Encyclopedia deals with the various instruments used for the detection of nuclear particles and processes: ionization chambers, Geiger counters, scintillation and Čerenkov counters, proportional counters, coincidence methods, cloud chambers, bubble chambers, nuclear emulsions, devices for detection of neutrons of low or high energy. Each type of apparatus, as one would expect, is described very fully, with a wealth of practical detail and auxiliary tables and graphs. The theory of the processes involved is also adequately discussed to the extent necessary for the estimation of the qualities and limitations of the methods of measurement. On the whole, the treatment is rather dry, as befits the primarily practical aim of the volume; a welcome exception is afforded by the chapter on the bubble chamber, whose author (inspired by justified fatherly pride, perhaps) gives a very interesting account of the history and development of this wonderful apparatus.

L.R.

J. W. DUNGEY, *Cosmic electrodynamics* (Cambridge University Press, 1958. ix—183 pages. 32s. 6d.)

The peculiar phenomena exhibited by ionized media interacting with electromagnetic fields are coming more and more within the horizon of the nuclear physicist, although the scale at which they are hitherto mainly displayed is the cosmic one. The present monograph belongs to the Cambridge series 'on mechanics and applied mathematics': an old-fashioned label for such a modern development, but it may remind us that in this quantal age classical physics is still as powerful as ever in its proper domain of applicability.

The scope of cosmic electrodynamics is clearly defined by the author, who shows how the relative smallness of the displacement current provides a criterion for separating the processes which he discusses from those of radio-astronomy, which he excludes from consideration. The underlying theoretical conceptions are then those of magneto-hydrodynamics, and their basic simplicity, as well as the wide scope of their applications to cosmic phenomena, are perfectly brought out in this well-written treatise, which distinguishes itself by outstanding didactic qualities. The author's insistence on considerations of order of magnitude and on the peculiar causal sequence of electromagnetic and mechanical effects resulting from the dominant role of the magnetic field is quite helpful for the reader's orientation into an unfamiliar domain; some of the pitfalls into which he might stumble are also kindly pointed out to him. The exposition is sufficiently detailed to be easily accessible to students; and it wisely avoids unessential mathematical developments which would obscure the trend of the argument: for these, the reader is referred to the appropriate papers.

The emphasis is decidedly theoretical: the general theory is developed with great elegance in the first half of the book, and then successively applied to the origin of the cosmic radiation, solar phenomena (sunspots, corona, prominences, flares, *M* regions), magnetic storms and aurorae, and the ionosphere. Although the empirical data are only quoted to the extent required for the theoretical analysis, enough is said to convey a clear idea of the physical processes involved in these phenomena. In this way, we are not only presented with an account of cosmic problems of fascinating intrinsic interest, but also with a neat and concise exposition of the basic concepts and formulae which may be of great help in the treatment of related questions raised by well-known recent developments at the laboratory scale.

L.R.

J. I. FRENKEL, *Prinzipien der Theorie der Atomkerne* (translated into German by J. Bartels) (Akademie-Verlag, Berlin, 1957. xiii—201 pages. DM 26.00.)

This book reproduces in almost the original form a course of lectures given at the Leningrad Polytechnic in 1947. After the author's death, the Russian edition was edited by J. Smorodinski. The lectures were aimed at the "scientifically educated reader, the physicist or engineer". There are outlines of the constitution and structure of the extra-nuclear atom, a sketch of quantum mechanics, and an account of the properties of nuclei in the ground state. These sections prepare for the kernel of the book, a chapter each on fission and on the statistical theory of nuclear reactions, topics on which Frenkel himself had contributed. There are also short sections on the deuteron, the role of nuclear reactions in stars, and some technological applications of nuclear energy.

In spite of the book's being written before the great advances in the understanding of nuclear structure of the last ten years, the treatment seems fresh and interesting even now. The book will probably appeal most to an undergraduate near the end of his course, to whom it should serve as a good introduction to more recent works. He will find his interest maintained throughout, with everything within his range, and the large number of simple numerical estimates helping him to familiarity with the subject.

A. Herzenberg

W. J. PRICE, *Nuclear Radiation Detection* (McGraw-Hill Book Co., New York, 1958. vi—382 pages. 70 s.)

The book is intended for reactor engineers; many of its features, however, make it a good laboratory handbook not only for research workers in the nuclear field, but also for teachers and students of nuclear physics in laboratory courses. The author has collected a large body of practical data which are useful for the laboratory worker in the design and application of nuclear detectors. Furthermore, the book contains a comprehensive and nicely illustrated survey of up-to-date detectors which will be particularly interesting to the student.

Special emphasis is of course laid on the subjects which are important for reactor engineering. Thus, a large chapter is devoted to neutron detection methods, and the use of various detectors for dose measurements is described in some detail. Other detection methods, which are equally important for the research physicist, are treated more superficially. This is the case with cloud chambers, bubble chambers, and photographic emulsions which are discussed in a brief and poorly illustrated section. In conclusion, the book presents a chapter on electronics for nuclear detection systems, the treatment of which, however, appears to be so summary that it will be of limited use only. More recent developments are mentioned only in passing, and it is especially regrettable that no general account is given of the many available types of multichannel analysers which have become so important for almost all branches of experimental nuclear physics.

O. Nathan

T. F. MAGNER, *Manual of scientific Russian* (Burgess Publishing Co., Minneapolis, 1958. 102 pages. $ 4.60 spiral-bound, $ 4.00 unbound)

This elementary Russian primer aims only at providing a clue to the reading of Russian scientific texts, and accordingly leaves out many grammatical and phonetical complications and irregularities. Moreover, the author, working on the flattering assumption that his readers, being scientists, have no need of the "slow, shock-avoiding approach of the multi-purpose textbook", has presented his material with extreme concision. The result is quite satisfactory within the self-imposed limitations of this radically utilitarian approach. The most original feature of the book is a "finder" section, consisting of a series of lists of verbal forms, and tables of endings, intended to facilitate the identification of the words and their grammatical function.

L.R.

10.A

*Nuclear Physics* **8** (1958) 396; © *North-Holland Publishing Co., Amsterdam*

# NEWS ITEM

## SYMPOSIUM ON NUCLEAR FUEL CYCLES

The Institute of Physics, one of the constituent bodies of the British Nuclear Energy Conference, announces that it is arranging a Symposium in London on Nuclear fuel cycles on 22 and 23 January 1959.

The program is as follows:

Session 1: (a) Long term reactivity changes
(b) Theory of once-through fuel cycles
(c) Perturbations due to fuel cycles.

Session 2: Optimization of fuel cycles for nuclear power stations.

Session 3: Fuel cycle operational problems.

The papers which have been invited will cater mainly for persons working in the field, and will deal with the applied physics aspects of the fuel cycles which form the basis of the immediate nuclear power program. Abstracts (but not preprints) of the papers to be read or presented at the Symposium will be available early in January.

Application forms for tickets to attend the Symposium are obtainable from the Secretary of The Institute of Physics, 47 Belgrave Square, London S.W. 1, and should be returned as soon as possible.

The Symposium will be published in the Journal of the British Nuclear Energy Conference.

10.E

# ERRATUM

L. R. B. Elton, A Semi-empirical Formula for the Nuclear Radius, Nuclear Physics **5** (1958) 173.

In the last term of eq. (A4), *for* 6 *read* 3 and in the last term of eq. (7), *for* 8 *read* 24. This leads to changes in eqs. (9)—(12) as follows:

$$b = 1.115 \pm 0.005, \quad a = 0.540 \pm 0.015, \tag{9}$$

$$c = 1.115\, A^{\frac{1}{3}} - 0.860\, A^{-\frac{1}{3}}, \tag{10}$$

$$R = 1.115\, A^{\frac{1}{3}} + 2.151\, A^{-\frac{1}{3}} - 1.742\, A^{-1}, \tag{11}$$

$$t = 2.38 \pm 0.06. \tag{12}$$

The fit to the experimental results is as good as before except for $C^{12}$ where now $R_{\text{calc}} = 3.35$.

My thanks are due to Dr. L. J. Tassie for pointing out to me the error in eq. (A4).

8.B *Nuclear Physics* 8 (1958) 397—401; © *North-Holland Publishing Co., Amsterdam*
Not to be reproduced by photoprint or microfilm without written permission from the publisher

# ON SCHWINGER'S THEORY OF THE MUON

W. S. COWLAND
*Department of Mathematics, Imperial College, London*

Received 3 July 1958

**Abstract:** The muon self-mass and the contribution to the anomalous muon magnetic moment, arising from an interaction with a heavy Bose particle ($\sigma$) postulated by Schwinger, are calculated in lowest order perturbation theory. The parameters involved are then investigated to see whether a large muon self-mass is compatible with the observed magnetic moment of the muon. It is found that, with some reservations, they are compatible when the $\sigma$-particle has scalar space-time character.

## 1. Introduction

Schwinger [1]) has recently proposed a comprehensive scheme for the classification of elementary particles and their interactions. A striking feature of this scheme is the introduction of a hypothetical $\sigma$-particle, a massive spinless particle with the properties of a charge singlet in isotopic space — so far unknown among Bose-Einstein particles. Two of the main functions required of the $\sigma$-particle in Schwinger's scheme are:

(i) It should interact with both leptons and the strongly interacting particles, thereby establishing a dynamical relation between them;

(ii) It should serve to explain the very striking mass asymmetry between the charged leptons by attributing the large mass of the $\mu$-meson to a comparatively strong interaction with the $\sigma$-particle.

However, as Schwinger points out, any proposed interaction must be reconciled with the apparent absence of appreciable non-electromagnetic interactions of the $\mu$-meson. Specifically, perturbation calculations applied to the interaction of charged particles with an external electromagnetic field will give for the anomalous $\mu$-meson magnetic moment

$$\mu = \mu_0\left(1+\frac{\alpha}{2\pi}+\ldots\right)$$
$$= \mu_0(1.001),$$

where $\alpha = e^2/4\pi$ is the fine structure constant, and $\mu_0$ = Dirac magnetic moment. This theoretical result is to be compared with the latest experimental result [2]),

$$\mu = \mu_0(1.002\pm 0.001).$$



October (2) 1958

In the development of his scheme, Schwinger initially accepts the $\sigma$-particle as either scalar or pseudoscalar under space-reflection. Subsequently, however, he postulates scalar character of the $\sigma$-particle in order to develop other ideas. The position adopted here is to leave the question open and consider both cases (with non-derivative coupling).

## 2. Calculation

In order to test Schwinger's theory, the following investigations have been carried out using perturbation theory: (i) The second order $\mu$-meson self-mass $\delta m$ arising from the hypothetical $\sigma$-interaction is calculated in the form

$$\frac{\delta m}{m} = g^2 f\left(\kappa, \frac{\lambda}{m}\right),$$

where

$m$ = observed mass of the $\mu$-meson
$= 207\ m_e$,
$\kappa$ = mass of the $\sigma$-particle,
$g$ = coupling constant for the $\mu$-$\sigma$ interaction,
and $\lambda$ = momentum cut-off parameter.

(ii) The bare mass, $m_0$, of the $\mu$-meson is assumed to be approximately equal to the electron mass,

$$m_0 = m_e.$$

If the $\sigma$-interaction gives the $\mu$-meson its observed mass

$$m = m_0 + \delta m,$$

then the following condition is imposed on the parameters $g$, $\kappa$, $\lambda$:

$$\frac{\delta m}{m} \simeq 1 = g^2 f\left(\kappa, \frac{\lambda}{m}\right). \tag{1}$$

(iii) The contribution to the anomalous $\mu$-meson magnetic moment due to the $\sigma$-interaction is calculated in lowest order in the form

$$\delta\mu = \mu_0 \beta$$

with

$$\beta = g^2 h(\kappa)$$

and

$$\mu_0 = \frac{e}{2m}.$$

(iv) Finally, we investigate whether or not it is possible to choose values of $g$ and $\kappa$ such that

$$\mathrm{O}(\beta) \lesssim 0.001$$

while satisfying the condition (1) for some value of the cut-off $\lambda$.

The results of these investigations are given below for the two cases.

2.1. SCALAR $\sigma$-PARTICLE

In this case it is found that if $\lambda^2 \gg m^2$, then

$$\frac{\delta m}{m} = \frac{g^2}{16\pi^2}\left[-3\log\frac{\lambda}{m} + \phi(\eta)\right] \tag{2}$$

and

$$\beta = \frac{g^2}{8\pi^2}\int_0^1 \frac{x^3}{x^2+\eta(1-x)}\,dx \tag{3}$$

where

$$\phi(\eta) = \tfrac{5}{4} + \int_0^1 \frac{x(4-x)(\frac{1}{2}\eta-x)}{x^2+\eta(1-x)}\,dx \tag{4}$$

with

$$\eta = \frac{\kappa^2}{m^2}. \tag{5}$$

Now, $\delta m$ must be positive. The fact that the cut-off dependent term appears as $-\log(\lambda/m)$ is therefore a serious drawback to the attempt to give the $\mu$-meson a large mass by virtue of its interaction with a scalar $\sigma$-particle. However, $\delta m$ can be made positive in the following way. It is found that $\phi(\eta)$ increases monotonically with $\eta$, so that we can consider the asymptotic form of $\phi(\eta)$ when $\eta$ is large. The integral in (4) can be evaluated explicitly and we obtain

$$\phi(\eta) = \tfrac{3}{2}\log\eta + \frac{19}{12\eta} + O\left(\frac{1}{\eta^2}\right) = 3\log\frac{\kappa}{m} + \frac{19}{12\eta} + O\left(\frac{1}{\eta^2}\right).$$

Thus, if $\delta m$ is to be positive, $\eta$ (i.e., $\kappa$) must be large, in which case

$$\frac{\delta m}{m} = \frac{g^2}{16\pi^2}\left[3\log\frac{\kappa}{\lambda} + \frac{19}{12\eta}\right] = 1, \tag{6}$$

by (1).

When $\eta$ is large,

$$\beta = \frac{g^2}{8\pi^2}\cdot\frac{1}{\eta}\,(\log\eta - \tfrac{5}{3}). \tag{7}$$

It is found that the condition

$$O(\beta) \lesssim 0.001$$

will only be satisfied if we allow

$$\lambda < \kappa. \tag{8}$$

This is an undesirable feature, since we would like to have the momentum cut-off $\lambda$ greater than or equal to any physical mass occurring in the inter-

action. Suppose, however, we disregard this objection. Then, keeping in mind the assumption $\lambda^2 \gg m^2$, and making $\kappa/\lambda$ as low as possible, we find, for example, the following set of figures:

$$\frac{m^2}{\lambda^2} = \frac{1}{10} \qquad \frac{g^2}{4\pi} \approx 2$$

$$\frac{\kappa}{m} = 30 \qquad \kappa \approx 3 \text{ nucleon masses}$$

$$\eta = 900 \qquad \lambda \approx \tfrac{1}{3} \text{ nucleon mass}$$

$$\frac{\kappa}{\lambda} = \sqrt{90} \qquad \beta \approx 0.002.$$

$\beta$ can be made smaller by increasing $\kappa$; increasing $\lambda$ would require increasing $\kappa$ to maintain

$$O(\beta) \lesssim 0.001.$$

For a fixed value of $\lambda$, increasing $\kappa$ decreases $g^2$ and so enhances the validity of a perturbation expansion.

As regards a scalar $\sigma$-particle, the conclusion is the following. Within the framework of perturbation theory and accepting the condition (8), the existence of an interaction of the $\mu$-meson with an *extremely* massive scalar $\sigma$-particle would not be incompatible with the observed $\mu$-meson magnetic moment. The necessary $\sigma$-particle mass would be

$$\kappa \gtrsim 3 \text{ nucleon masses.}$$

### 2.2. PSEUDOSCALAR $\sigma$-PARTICLE

With again the assumption $\lambda^2 \gg m^2$, we obtain for this case

$$\frac{\delta m}{m} = \frac{g^2}{16\pi^2}\left[\log\frac{\lambda}{m} - \chi(\eta)\right] \tag{9}$$

and

$$\beta = -\frac{g^2}{8\pi^2}\int_0^1 \frac{x^2(2-x)}{x^2+\eta(1-x)}\,dx \tag{10}$$

where

$$\chi(\eta) = \tfrac{3}{4} + \int_0^1 \frac{x^2(\frac{1}{2}\eta - x)}{x^2+\eta(1-x)}\,dx. \tag{11}$$

It can be shown that

$$\beta = -\frac{g^2}{8\pi^2}\cdot\frac{1}{\eta}\left(\log\eta + \tfrac{11}{12}\right) + O\left(\frac{1}{\eta^2}\right)$$

and

$$\chi(\eta) = \tfrac{1}{2}\log\eta + \frac{1}{\eta}\left(\log\eta - \tfrac{11}{12}\right) + O\left(\frac{1}{\eta^2}\right).$$

Neglecting $O(1/\eta^2)$ compared to $1/\eta$ condition (1) becomes

$$\frac{g^2}{16\pi^2}\left[\log\frac{\lambda}{\kappa}-\frac{1}{\eta}\left(\log\eta-\tfrac{11}{12}\right)\right]=1, \tag{12}$$

and

$$|\beta|=\frac{g^2}{8\pi^2}\cdot\frac{1}{\eta}\left(\log\eta+\tfrac{11}{12}\right). \tag{13}$$

Consider the following values of $\kappa$ and $\lambda$ in *nucleon masses* for different orders of magnitude of $g^2$, given that

$$O(|\beta|)=0.001;$$

$$\frac{g^2}{4\pi}=10, \quad \eta\approx 10^4, \quad \kappa\approx 10, \quad \lambda\approx 35;$$

$$\frac{g^2}{4\pi}=1, \quad \eta\approx 10^3, \quad \kappa\approx 3, \quad \lambda\approx 3\times 10^6;$$

$$\frac{g^2}{4\pi}=\tfrac{1}{10}, \quad \eta\approx 10^2, \quad \kappa\approx 1, \quad \lambda\approx 10^{55}.$$

These figures indicate that a reasonable value of $\kappa$ and a value of $g^2$ compatible with perturbation calculations only vindicate the $\sigma$-$\mu$ theory when a totally unreasonable value is placed on the cut-off $\lambda$. It is concluded that an interaction of the $\mu$-meson with a pseudoscalar $\sigma$-particle is incompatible with the observed $\mu$-meson magnetic moment.

It is a pleasure to thank Professor Abdus Salam and Dr. P. T. Matthews for suggesting this problem and for helpful discussions.

## References

1) Julian Schwinger, Annals of Physics **2** (1957) No. 5
2) T. Coffin *et al.*, Phys. Rev. **109** (1958) 973

1.E.4 *Nuclear Physics* 8 (1958) 402—411; © *North-Holland Publishing Co., Amsterdam*
Not to be reproduced by photoprint or microfilm without written permission from the publisher

# LIFETIME MEASUREMENTS OF THE FIRST EXCITED STATES OF $Tl^{208}$ AND $Ra^{224}$

J. G. SIEKMAN and H. DE WAARD
*Natuurkundig Laboratorium der Rijks-Universiteit, Groningen*

Received 3 June 1958

**Abstract:** Half-lives $T_{\frac{1}{2}} = (2.6 \pm 1.0) \times 10^{-12}$ sec for the 40 keV state of $Tl^{208}$ and $T_{\frac{1}{2}} = (7.0 \pm 1.0) \times 10^{-10}$ sec for the 85 keV state of $Ra^{224}$ have been measured by the line shift method [1, 2]) using extremely thin sources especially prepared for these measurements. The method has been checked by determining the latter half-life also from a delayed coincidence measurement, which gave $T_{\frac{1}{2}} = (7.5 \pm 1.5) \times 10^{-10}$ sec in good agreement with the first value.

## 1. Introduction; the Line Shift Method

L-conversion electrons de-exciting the first excited states of $Tl^{208}$ and $Ra^{224}$ were focused in a magnetic lens spectrometer onto an anthracene detecting crystal; a thin (0.1 mm) plastic scintillator placed behind the source detected $\alpha$-particles feeding these states. Coincidences were recorded between these $\alpha$-particles and the conversion electrons. The conversion electrons selected in this way are emitted by recoiling nuclei shot out of the very thin sources within a certain solid angle. Their velocities are increased on the average by an amount

$$\bar{V} = f \cdot (M_\alpha / M_{\text{exc. nucl.}}) \cdot V_\alpha \qquad (1)$$

where $M$ refers to mass, $V$ to velocity and where $f$ is a factor determined by geometrical conditions and source thickness; $f$ would be unity in the ideal case of an "infinitely" thin source and if the coinciding $\alpha$-particles and conversion electrons would always move in exactly opposite directions. In this case Doppler shifts of the conversion lines of 0.36 % for $Tl^{208}$ and of 0.18 % for $Ra^{224}$ would be found.

In practice, $f$ is reduced by two effects which can be taken into account by writing $f$ as a product of two reduction factors $f_1$ and $f_2$:

$f_1$ is the geometrical reduction factor, calculated from the solid angle subtended by the $\alpha$-detecting scintillator (about 23 % of $4\pi$) and the average acceptance angle of the magnetic lens (27°). A value $f_1 = 0.69$ is found.

$f_2$ is the factor by which the recoil velocity is reduced as a result of the finite thickness of the source and its penetration into the source backing. Values for $f_2$ will be given in sections 2.1 ($Tl^{208*}$) and 3.1 ($Ra^{224*}$).

In our experiments the position of the centroid of the L-conversion line coincident with α's is compared with that of the L-conversion line anti-coincident with α's (obtained by subtracting the coincidence spectrum from the single count spectrum). Since some electrons with a small component of the recoil velocity contribute to the anti-coincidence line, this line will also have a small Doppler shift. It is calculated that as a result of this effect the distance between the centroids of the coincidence and the anti-coincidence line is smaller by 12.3 % than expected from (1). The Doppler shift of the conversion line may be reduced by placing a very thin foil at a small distance $d$ in front of the source. This foil does not affect the conversion electron velocity appreciably, but stops all recoiling nuclei. By measuring the reduction of the line shift as a function of source-to-foil distance, lifetimes down to $10^{-12}$ sec can in principle be estimated.

In this way Burde and Cohen [1]) found $T_{\frac{1}{2}} = (1 \pm 0.5) \times 10^{-12}$ sec for the 40 keV state of $Tl^{208}$, but as we have pointed out [3]) this value should be corrected considerably for penetration of source atoms into its backing, which occurs when the source is prepared by the usual recoil collection technique. It appeared to be worthwhile firstly to repeat the measurement with a source prepared in such a way that no penetration could occur, secondly to compare a result of the line shift method with one of the delayed coincidence method for a case within range of both methods. Such a case is met in the α-decay of $Th^{228}$ to the 85 keV state of $Ra^{224}$ ($T_{\frac{1}{2}} \approx 7.5 \times 10^{-10}$ sec) [4]). In the next sections details and results of the line shift method and the delayed coincidence measurement are given.

## 2. Half-life of the 40 keV Level of $Tl^{208}$

### 2 1. EXPERIMENTAL PROCEDURE

Fig. 1 shows the source assembly mounted in our spectrometer: The source-holder (S) is screwed into a rigid plate (1); the stopping foil-holder (T) is mounted on plate (2) which is tightly fixed to the backing-plate at one end. In this way the second plate forms a rather hard flat spring. On this a very much softer one (3) is screwed, that can be bent by turning the screw C (pitch 0.33 mm). By turning C over 10° the axis C′ is displaced by 9.2 $\mu$ and the stopping foil by about 0.2 $\mu$, the movement being quite linear for the range needed. The source foil consisted of 4 layers, the stopping foil of 1 layer of about 5 $\mu g/cm^2$ zapon lacquer. Both foils were covered with about 15 $\mu g/cm^2$ Al, the aluminized sides facing each other. According to measurements by Cohen *et al.*[2]), this thickness of the Al-layer is sufficient to stop all recoiling nuclei.

Our Th(B+C) sources were prepared in the following way: with a drop of very pure $HNO_3$, diluted in some drops conductance water, the activity was

extracted from a carefully cleaned Pt-electrode on which some Th(B+C) had been collected from an emanating RdTh source. The liquid took a fair part of the activity from the Pt-electrode. A droplet of this liquid was put on the source foil and evaporated just to dryness under an infrared heating

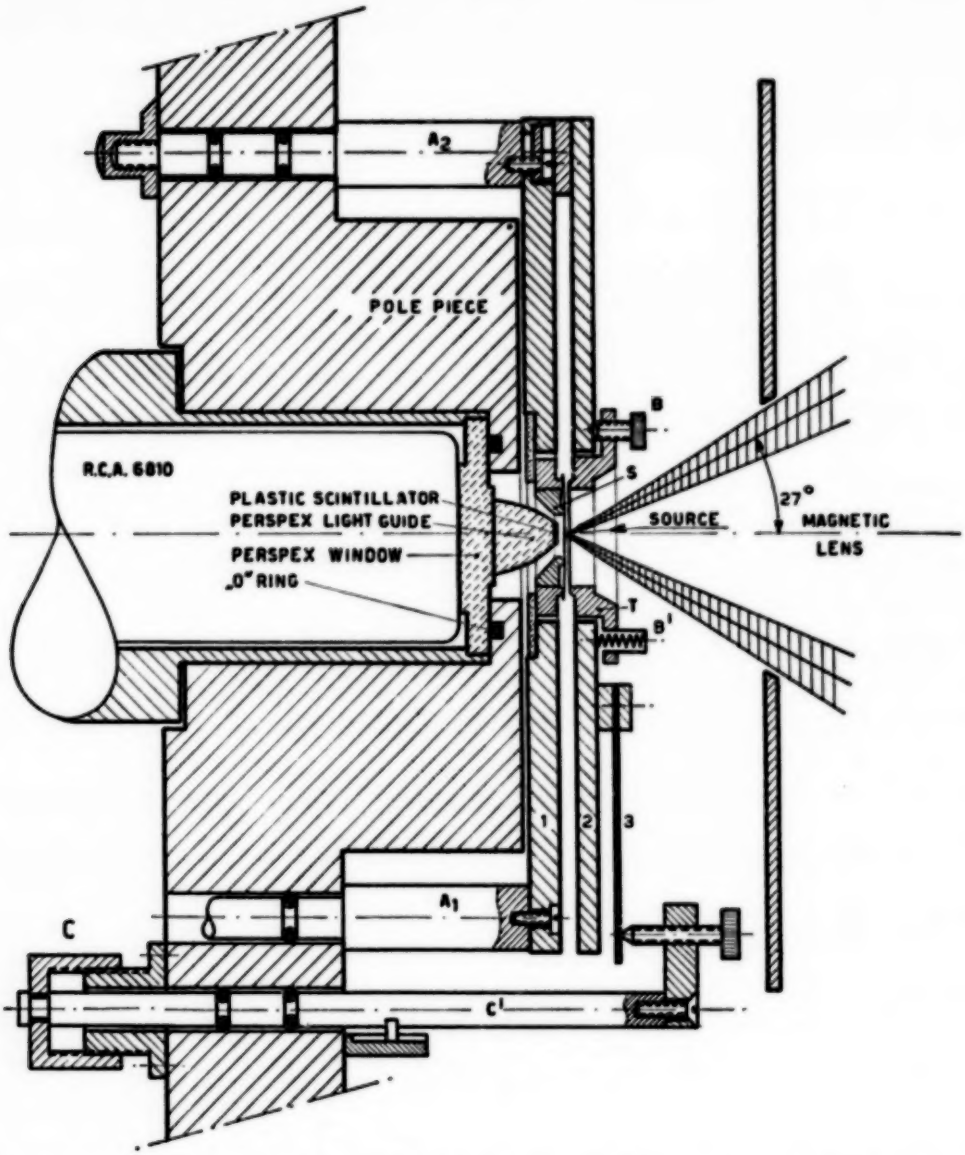


Fig. 1. Mounting of source and stopping foil and mechanism for varying the distance between these foils in the range of 1 $\mu$.

lamp. In order to avoid the forming of a ridge along the edge of the drop, this edge was shielded somewhat from the heating lamp. In this way we got sources of sufficient activity, invisible under a microscope. From the observed maximum line shift, a mean velocity loss of the recoil-nuclei of about

10 % of the initial velocity was deduced ($f_2 = 0.9$), showing that the sources were very thin.

After screwing the source-holder (S) into the backing-plate, plate (2) with stopping-foil holder (T) was fastened tightly to it. The stopping foil was adjusted parallel to the source foil with three screws B (one of them is drawn in fig. 1) looking at the interference pattern with a simple interferometer. Both foil-surfaces had to be absolutely dust-free, since dust particles would prevent us from bringing the foils in contact over the whole surface at the same time.

As the exact location of the source could not be seen, it proved to be very useful to be able to shift the source assembly perpendicular to the axis of the spectrometer. This movement was provided by excentric pins at the ends of the shafts $A_1$ and $A_2$. Thus the source could be adjusted from the outside to give a well-shaped conversion-line; the F-line of ThB was used for this purpose. The diaphragms were set to give a line-width of about 1 % (transmission about 2 %).

### 2.2. LINE SHIFT RESULTS

Fig. 2a summarizes the measurements with two sources. The horizontal errors include the inaccuracy in the zero foil distance setting. The line shift as a function of the stopping foil distance $d$ from the source is expressed by $f(d)$. ($f(\infty) = f$.) In a first approximation one expects a dependence $1 - (f(d)/f) = e^{-\Delta}$ with $\Delta = d \ln 2/\bar{V}T_{\frac{1}{2}}$ (broken line in fig. 2b). A more careful analysis, accounting for the contributions of the various directions of recoil nuclei to the Doppler shift yields a theoretical dependence of $f(d)/f$ on $\Delta$ represented by the solid lines in figs. 2a and 2b. Using the value $\bar{V}$ obtained from eq. (1) by putting $f = f_1 f_2 = 0.69 \times 0.90 = 0.62$ the best fit between the broken line of fig. 2b and the experimental points is obtained for $T_{\frac{1}{2}} = 2.6 \times 10^{-12}$ sec with an estimated standard deviation of $\pm 1.0 \times 10^{-12}$ sec.

## 3. Half-life of the 85 keV level of $Ra^{224}$

### 3.1. MEASUREMENT WITH THE LINE SHIFT METHOD

As this half-life is about 300 times longer than the former, the distance between source and stopping foil must be made larger by the same factor. Therefore we did not use the flat springs (2 and 3), but attached a holder carrying the stopping foil directly to axis C′.

Sources were prepared by adding some drops of conductance water to carrier-free RdTh (obtained from Harwell) and putting one droplet on an 0.8 mg/cm² mica foil. This was dried under an infra red heating lamp. Then the mica foil was pressed against a tungsten ribbon and heated in vacuum to a temperature of about 1000° C. In this way we managed to get

rid of impurities and of a part of the decay products which could give rise to a lower value of $\bar{V}$ and to a background of betas.

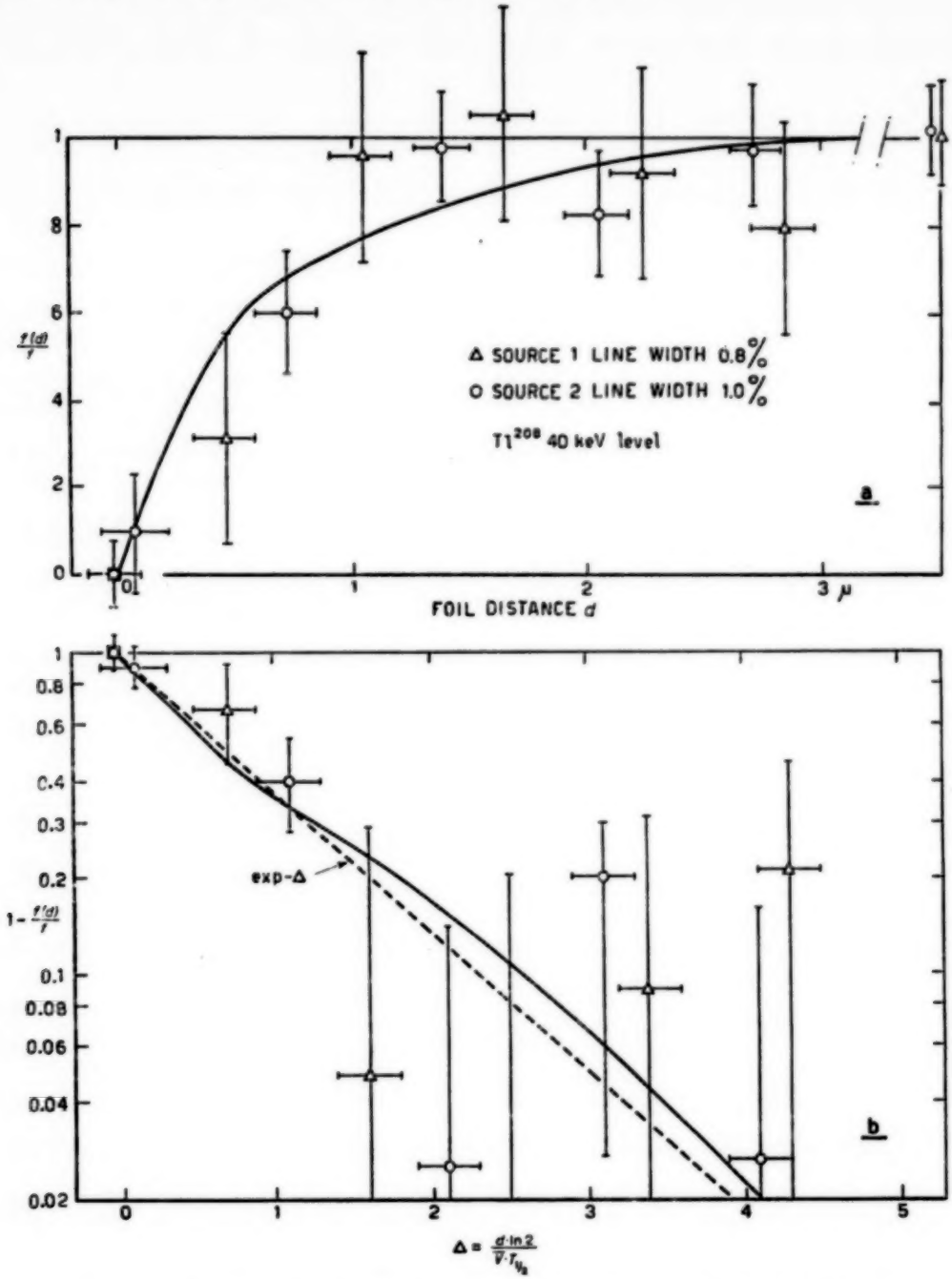


Fig. 2. Result of the line shift measurement of the 40 keV level of $Tl^{208}$.

a. observed line shift relative to the maximum shift plotted as a function of source-to-foil distance $d$.

b. line shift plotted on a logarithmic scale as a function of the source-to-foil distance expressed in $\Delta = d \ln 2/\bar{V}T_{\frac{1}{2}}$. The best fit is obtained for $T_{\frac{1}{2}} = 2.6\times10^{-12}$ sec. The solid lines give the theoretical dependence of $f(d)/f$ for this value of $T_{\frac{1}{2}}$.

As a figure of merit for the degree of purification of the source foil from decay products we used the ratio of the intensity of the well-known F-line and the measured 66 keV L-lines.

This ratio was somewhat smaller than $\frac{1}{6}$ of the value found for a source in which the decay products are in equilibrium. The activity of the sources was of the order of 1 $\mu$C. The diaphragms of the magnetic spectrometer were

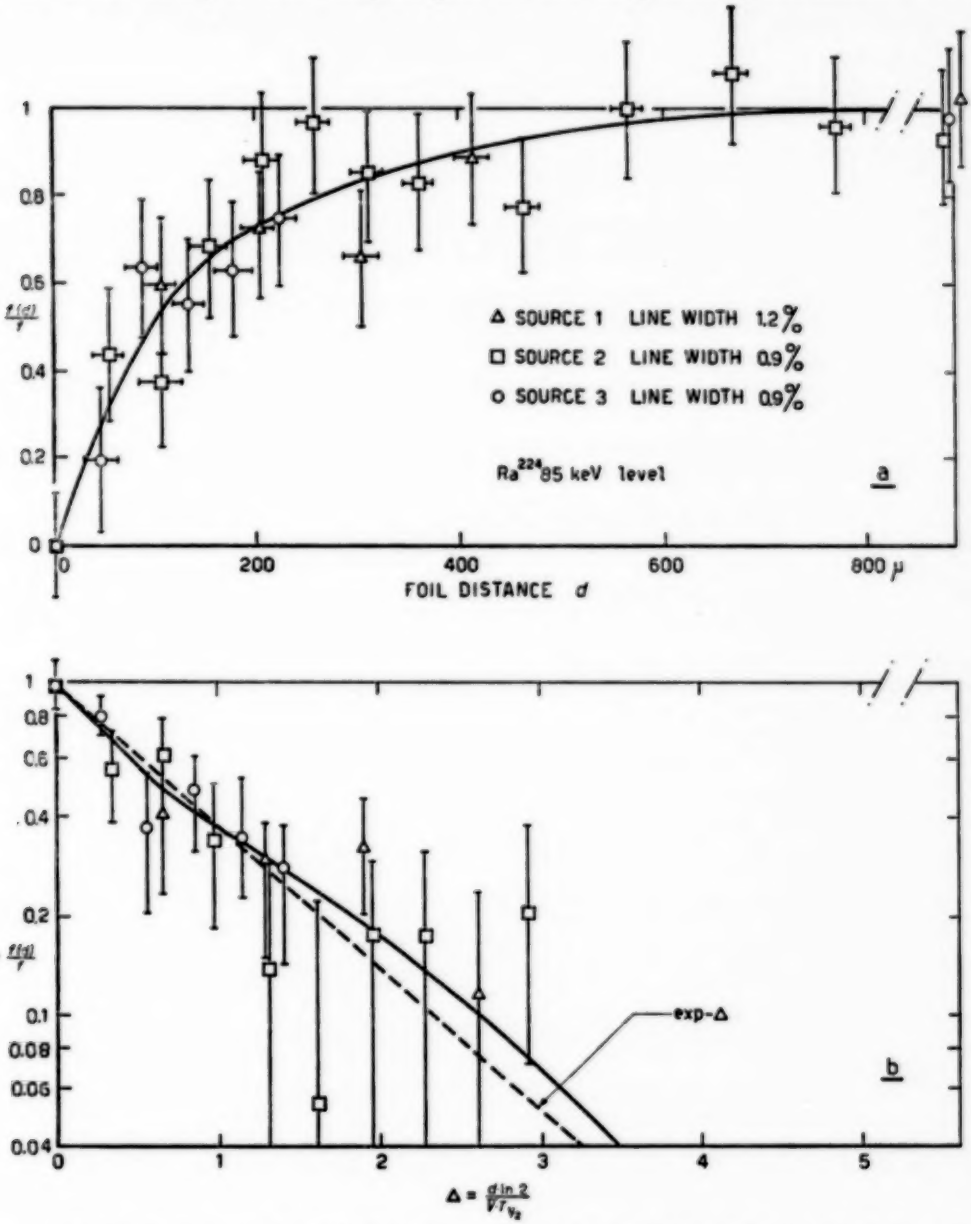


Fig. 3. Result of the line shift measurement of the 85 keV level of $Ra^{224}$.

a. observed line shift relative to the maximum shift plotted as a function of source-to-foil distance $d$.

b. line shift plotted on a logarithmic scale as a function of the source-to-foil distance expressed in $\Delta = d \ln 2/\bar{v} T_{\frac{1}{2}}$. The value $T_{\frac{1}{2}} = 7.0 \times 10^{-10}$ sec gives the best fit.

set to a linewidth of 1.2 % in the first measurement and of 0.9 % in the following two series of measurements.

$\bar{V}$ was derived again after each series of measurements by comparing the

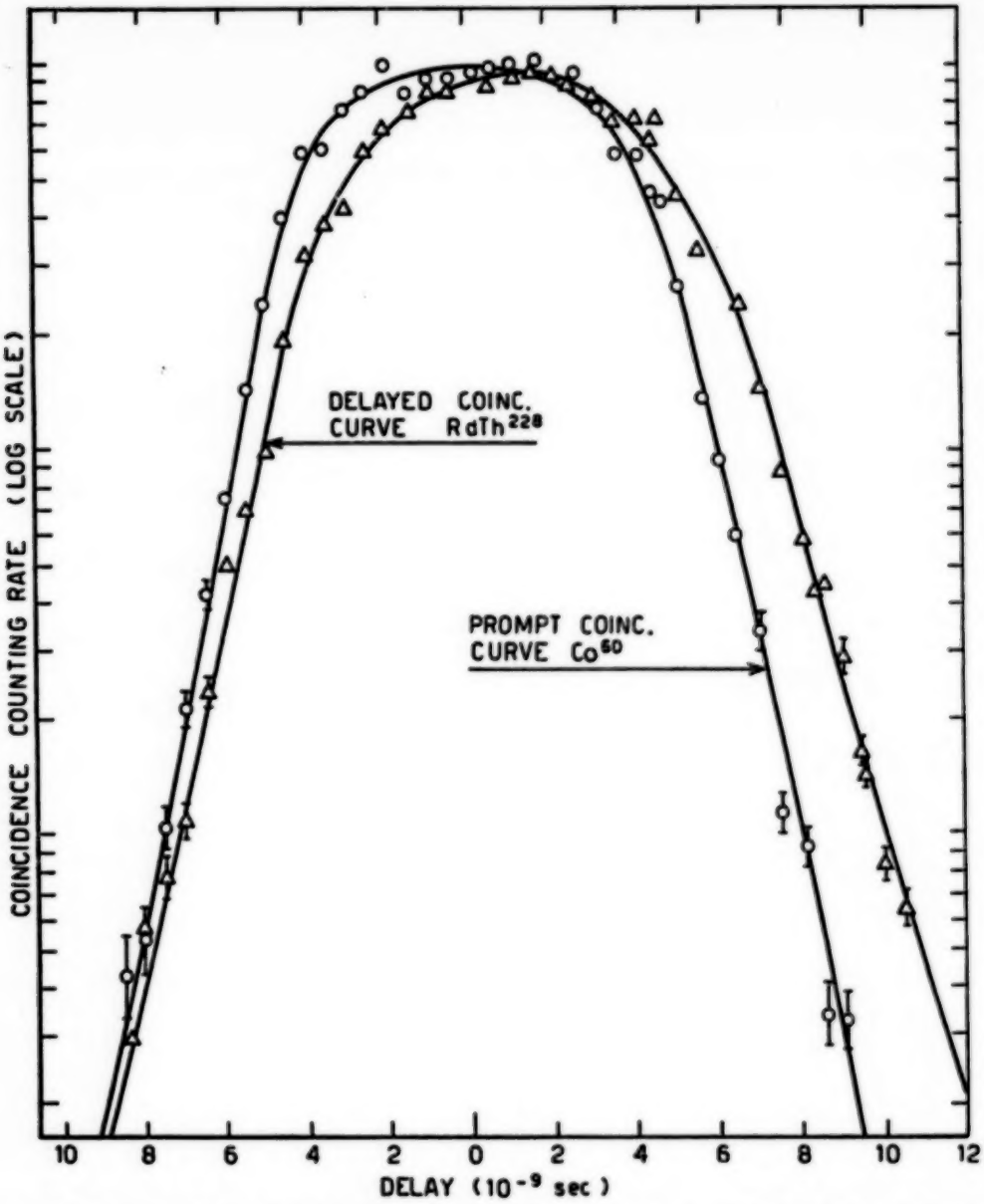
COINCIDENCE COUNTING RATE (LOG SCALE)
DELAYED COINC. CURVE RdTh228
PROMPT COINC. CURVE Co60
10 8 6 4 2 0 2 4 6 8 10 12
DELAY (10-9 sec)

Fig. 4. Prompt ($Co^{60}$) and delayed ($RdTh^{228}$) coincidence rate as a function of the inserted delay. Chance coincidences have been subtracted.

observed maximum shift with the calculated one. The average velocity loss was $(12\pm12)$ % for the three different sources used ($f_2 = 0.88\pm0.12$). This value was used in composing fig. 3 from the three series of measurements. From these $T_{\frac{1}{2}} = (7.0\pm1.0)\times10^{-10}$ sec was deduced in the same way as described in section 2.2.

### 3.2. MEASUREMENT WITH THE DELAYED FAST-SLOW COINCIDENCE METHOD

For this measurement a fast slow coincidence circuit similar to that introduced by Bell, Graham and Petch [5]) was used. The magnetic lens spectrometer, now adjusted to 6 % transmission, again selected the L-conversion electrons, and a plastic scintillator, now 2 mm thick, accepted the $\alpha$-particles within a solid angle close to 30 % of $4\pi$. Some details of this measurement have been given previously [4]).

The delayed coincidence curve of RdTh was carefully compared with one obtained from a $Co^{60}$ source by measuring coincidences between $\beta$-particles focused on the electron detector and Compton electrons accepted by the plastic scintillator. A 80 mg/cm$^2$ Al-absorber was placed between source and plastic to prevent any $\beta$-particle from reaching the scintillator. Exactly the same adjustment of the whole apparatus was used in both cases. The centroid shift of the RdTh-curve relative to the $Co^{60}$ curve (fig. 4) which equals the experimental lifetime [6]) was found to be

$$\tau_{exp} = (10.2 \pm 1.6) \times 10^{-10} \text{ sec}$$

while a Newton [7]) analysis yields

$$\tau_{exp} = (11.4 \pm 1.6) \times 10^{-10} \text{ sec.}$$

Averaging these two values we obtain

$$\tau_{exp} = (10.8 \pm 2.2) \times 10^{-10} \text{ sec}$$

or

$$T_{\frac{1}{2}} = (7.5 \pm 1.5) \times 10^{-10} \text{ sec.}$$

## 4. Discussion

We see that the measurements of the half-life of the 85 keV excited state of $Ra^{224}$ using two different methods are in good agreement, which adds to our confidence in the result for the half-life of the 40 keV state of $Tl^{208}$.

Asaro, Perlman and Stephens [8]) find an experimental total conversion coefficient $\alpha_{tot} = 16$ for the 85 keV transition in $Ra^{224}$. Using this value we propose a lifetime $\tau_\gamma = (17.7 \pm 2.5) \times 10^{-9}$ sec, as an average of both measurements. From this an intrinsic quadruple moment $|Q_0| = (7.2 \pm 0.7) \times 10^{-24}$ cm$^2$ is deduced for the nucleus $Ra^{224}$, fitting well in the $Q_0$ versus $A$ curve given by Alder *et al.*[9]).

From the experimental lifetime found for the 40 keV excited state of $Tl^{208}$ we deduce $\tau_\gamma = (1.2 \pm 0.5) \times 10^{-10}$ sec assuming a conversion coefficien- $\alpha_{tot} = 19.6$. De Shalit [10]) has calculated lifetimes for several possible cont figurations of the nucleus $Tl^{208}$ on the basis of the shell model. Our result

agrees best with the value $\tau_\gamma = 1.8 \times 10^{-10}$ sec which is found for a $(s_{\frac{1}{2}}, g_{\frac{9}{2}})$-configuration.

## 5. Final Remarks

### 5.1. RESIDUAL LINE SHIFT

A small line shift remains for $d = 0$. (The figs. 2 and 3 are corrected for this residual shift.) In our measurements this is about 5 % for $Tl^{208*}$ and for $Ra^{224*}$ about 10 % of the maximum shift observed. This residual shift can be explained by

a) different absorption of the conversion electrons emitted by "coincident" and "anti-coincident" nuclei respectively,

b) the additional velocity of the very small fraction of electrons emitted by excited nuclei in the source- and stopping-foil respectively before they have come to rest.

The latter effect becomes smaller as the lifetime of the excited state becomes larger and may be entirely neglected in the $Ra^{224*}$ measurement. Using for this case a figure of Paul and Steinwedel [11]), we find that this residual shift corresponds to an energy difference of $\approx$ 20 eV of the coincident and anti-coincident electrons. From this a mean recoil range $\approx 4$ $\mu g/cm^2$ for the $Ra^{224*}$ nuclei in mica and Al is deduced. This agrees reasonably with the value reported by Cohen *et al.*[2]).

### 5.2. DUST-FREE SOURCES

It is hard to make dust-free sources, therefore all foils and sources have to be prepared in a dust-free box. Yet, *only* 2 out of more than 20 Th(B+C) sources made for the Tl* lifetime measurement proved to be clean.

### 5.3. APPLICABILITY OF METHOD

The most important difficulties arising in this kind of experiments are that

1) the measurements consume a long time, and that

2) the sources must be *very thin*.

These circumstances limit the applicability to cases in which the parent nucleus has a lifetime not shorter than about one day nor longer than a few decades. The transition considered should be fed by a nice $\alpha$-branch and it should be appreciably converted.

In some cases the result may be affected by $\alpha$'s feeding a higher excited state that decays by $\gamma$ or $e^-$ emission to the excited state considered. In the RdTh-decay the 217 and 253 keV states are such, but here the correction for these "false" coincidences is negligible.

In table 1 cases are summarized where the line shift method as described above is applicable.

Using a double focusing electron spectrometer with extreme resolution as

TABLE 1

| Parent nucleus | Daughter nucleus | Energy (MeV) of α feeding the state | Multipole transition de-exciting the state | | Maximum shift in | | Half-life observed (sec) | Half-life expected (sec) | According to |
|---|---|---|---|---|---|---|---|---|---|
| | | | | (keV) | % | for | | | |
| $Bi^{211}$ | $Tl^{207}$ | 6.273 | M1(+E2) | 353 | 0.11 | $e_K$ | $\lesssim 3\times10^{-7}$ | $33\times10^{-12}$ | s.p. model |
| $Bi^{212}$ | $Tl^{208}$ | 6.04 | M1 | 40 | 0.36 | $e_L$ | $2.6\times10^{-12}$ | $4\times10^{-12}$ | de Shalit [10]) |
| $Ra^{223}$ | $Rn^{219}$ | 5.704 | M1(+E2) | 154 | 0.23 | $e_K$ | | $0.25\times10^{-12}$ | s.p. model |
| | | 5.569 | M1(+E2) | 268 | 0.18 | $e_K$ | | $0.55\times10^{-12}$ | s.p. model |
| $Ac^{225}$ | $Fr^{221}$ | 5.6 | – | 220 | 0.14 | $e_K$ | $< 10^{-9}$ | | |
| $Th^{226}$ | $Ra^{222}$ | 6.220 | E2 | 111.1 | 0.17 | $e_L$ | $< 1.5\times10^{-9}$ | | |
| $Th^{227}$ | $Ra^{223}$ | 5.972 | E2 | 61.6 | 0.24 | $e_L$ | | | |
| $Th^{228}$ | $Ra^{224}$ | 5.338 | E2 | 84.47 | 0.18 | $e_L$ | $7.2\times10^{-10}$ | | |
| $U^{230}$ | $Th^{226}$ | 5.813 | E2 | 72 | 0.21 | $e_L$ | | $\approx 10^{-9}$ | coll. model |
| $U^{232}$ | $Th^{228}$ | 5.261 | E2 | 57.9 | 0.23 | $e_L$ | $< 2\times10^{-8}$ | | |
| $Pu^{236}$ | $U^{232}$ | 5.75 | E2 | 45 | 0.31 | $e_L$ | | | |
| $Pu^{238}$ | $U^{234}$ | 5.452 | E2 | 42.6 | 0.29 | $e_L$ | $< 5\times10^{-10}$ | | |

described e.g. by Siegbahn and Edvarson [12]) to measure line shifts, lifetimes might be determined for some additional cases.

The authors owe Professor H. Brinkman a great debt of gratitude for having made it possible for them to perform these measurements and for reading the manuscript. Many thanks are also due to Mr. A. J. Wagner, Mr. K. G. Dik and Mr. G. T. Pott for their able and untiring assistance during various stages of the experiments and calculations.

## References

1) J. Burde and S. G. Cohen, Phys. Rev. **104** (1956) 1093
2) S. G. Cohen, Proc. Rehovoth Conf. on Nuclear Structure, Ed. H. J. Lipkin (North-Holl. Publ. Comp., Amsterdam, 1958) p. 571
3) J. G. Siekman and H. de Waard, Phys. Rev. **107** (1957) 1731
4) J. G. Siekman and H. de Waard, Proc. Rehovoth Conf. on Nuclear Structure, Ed. H. J. Lipkin (North-Holl. Publ. Comp., Amsterdam, 1958) p. 584
5) R. E. Bell and H. E. Petch, Phys. Rev. **76** (1949) 1409; R. E. Bell, R. L. Graham and H. E. Petch, Can. Journ. Phys. **30** (1952) 35
6) Z. Bay, Phys. Rev. **77** (1950) 419
7) T. D. Newton, Phys. Rev. **78** (1950) 490
8) F. Asaro, F. Stephens and I. Perlman, Phys. Rev. **92** (1953) 1495; F. Stephens, F. Asaro and I. Perlman, Phys. Rev. **96** (1954) 1568
9) K. Alder, A. Bohr, T. Huus, B. Mottelson and A. Winther, Revs. Mod. Phys. **28** (1956) 532, fig. V. 6
10) A. de Shalit, Phys. Rev. **105** (1957) 1531
11) W. Paul and H. Steinwedel, Beta- and Gamma-ray Spectroscopy, Ed. K. Siegbahn (North-Holl. Publ. Comp., Amsterdam, 1953) Ch. I, p. 10
12) K. Siegbahn and K. Edvarson, Nuclear Physics **1** (1955) 137

1.E.1:
3.B

*Nuclear Physics* 8 (1958) 412—415; © *North-Holland Publishing Co., Amsterdam*
Not to be reproduced by photoprint or microfilm without written permission from the publisher

# CORRELATION ANGULAIRE DES PAIRES DE CONVERSION INTERNE PROVENANT DES NIVEAUX 6.09 MeV DU CARBONE 14 ET 5.69 MeV DE L'AZOTE 14

S. GORODETZKY, P. CHEVALLIER, R. ARMBRUSTER, G. SUTTER
et A. GALLMANN

*Institut de Recherches Nucléaires, Strasbourg*

Reçu le 8 juin 1958

**Abstract:** The multipolarities of the 6.09 MeV transition in $C^{14}$ and of the 5.69 MeV transition in $N^{14}$, obtained by bombarding $C^{13}$ with 1.2 MeV deuterons, are determined by measuring the angular correlation of internal conversion pairs. As the resolution of the internal pair spectrometer utilised does not allow one to distinguish between these two transitions, the correlation is studied together for the two transitions, their relative intensities being measured with an external pair spectrometer.

The experimental results are compatible only with the spin $J = 1^-$ for the 6.09 MeV level of $C^{14}$ and agree with the value $J = 1^+$ for the 5.69 MeV level of $N^{14}$.

La mesure de la corrélation angulaire des paires de conversion interne a déjà été utilisée pour déterminer l'ordre de multipolarité des transitions électromagnétiques [1,2]). Nous avons mis au point un spectromètre beta à scintillation destiné à mesurer la corrélation angulaire des paires provenant d'une transition bien déterminée. La partie électronique de ce spectromètre est décrite dans une communication précédente [3]).

La boîte de corrélation est une grande cloche à vide (1 mètre de diamètre et de 1 mètre de hauteur) dans laquelle se trouvent les scintillateurs plastiques (50 % du rendement lumineux de l'Anthracène) destinés à détecter les négatons et les positons, les photomultiplicateurs et les „cathodes follower". Aucune matière n'est ainsi disposée entre la cible et les cristaux et en outre les bords de la cloche sont très éloignés de ces derniers; ceci a l'avantage de réduire au minimum toute diffusion possible des électrons et ainsi de perturber le moins possible la corrélation angulaire. La position angulaire des photomultiplicateurs est règlable de l'extérieur.

La résolution de ce spectromètre est de 12 % pour la raie monopolaire de $O^{16}$ (5.03 MeV). Cette résolution ne nous permet pas toujours de séparer des transitions trop voisines énergétiquement comme cela est souvent le cas dans les réactions induites par deutérons. Aussi employons-nous la méthode suivante: nous mesurons à la fois la corrélation angulaire des paires de conversion interne provenant des deux transitions, l'intensité relative des paires étant déduite auparavant de la mesure de l'intensité relative des rayonnements gamma provenant de ces deux mêmes transitions. Cette

dernière mesure est effectuée au moyen d'un spectromètre à paires externes à trois cristaux NaI. La résolution de ce spectromètre est de 5.5 % pour la raie 5.11 MeV provenant du rayonnement gamma 6.13 MeV de $O^{16}$. A cette énergie la proportion de „Bremstrahlung" des électrons dans le cristal NaI central est très importante, cette proportion a été mesurée expérimentalement et trouvée comparable à celle calculée d'une façon analogue à celle de H. I. West et G. Mann [4]).

Nous avons appliqué cette méthode aux niveaux 6.09 MeV et de $^{14}C$ et 5.69 MeV de $^{14}N$ (60 keV) obtenus en bombardant par des deutérons de 1.2 MeV. A cette énergie le niveau 5.83 MeV du $^{14}N$ n'apparaît pas encore [5]). La mesure au spectromètre à paires externes de l'intensité relative de ces deux transitions donne 65 % 6.09 MeV et 35 % 5.69 MeV (fig. 1).

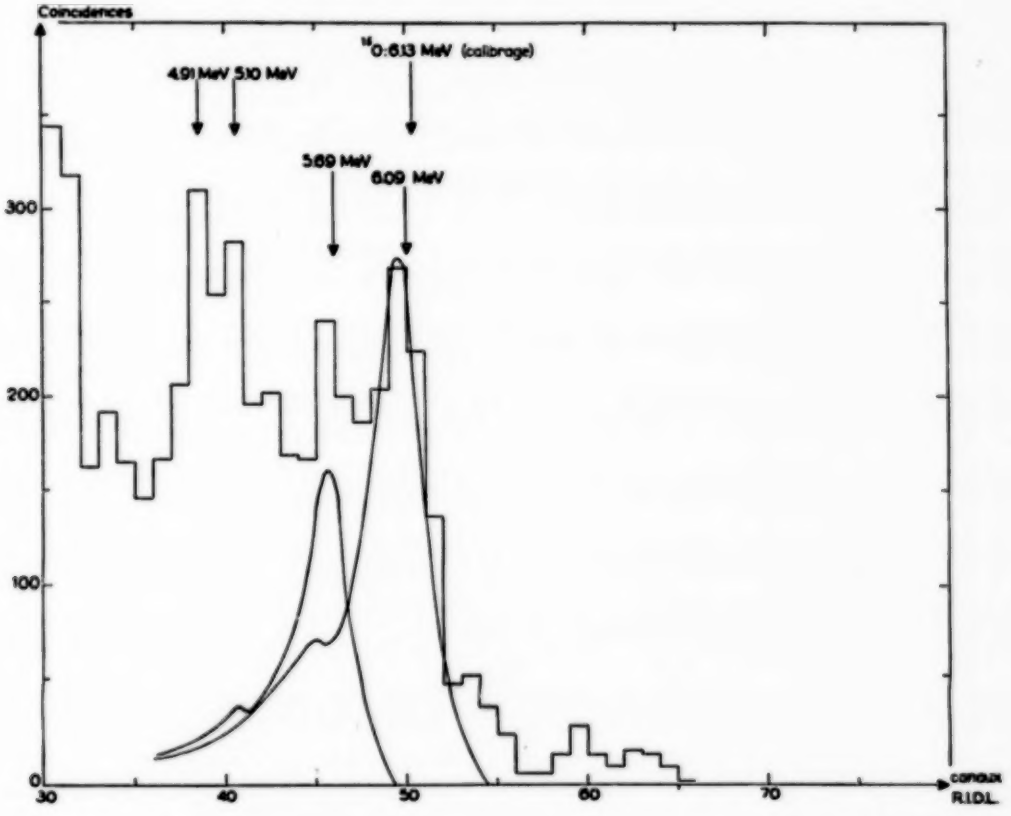


Fig. 1. Spectre des rayonnements gamma obtenus en bombardant une cible de $^{13}C$ de 60 keV d'épaisseur par des deutérons de 1.2 MeV. Ce spectre est obtenu au moyen d'un spectromètre à paires externes à 3 cristaux. Le forme des courbes pour les rayonnements gamma de 6.09 MeV et 5.69 MeV laisse apparaître une grande proportion de "Bremstrahlung". Cette proportion est déduite du spectre du rayonnement gamma de 6.13 MeV obtenu par la réaction $^{19}F(p, \alpha)\ ^{16}O$ à $E_p = 340$ keV.

Pour la mesure de la corrélation angulaire des paires de conversion interne une discrimination de 2 MeV a été utilisée afin d'éliminer toutes coïncidences

gamma — gamma et gamma — neutron provenant des niveaux 2.31 MeV, 3.95 MeV, 4.91 MeV, 5.10 MeV et 5.69 MeV de $^{14}N$.

La figure 2 montre les courbes théoriques qui sont calculées à partir de l'expression

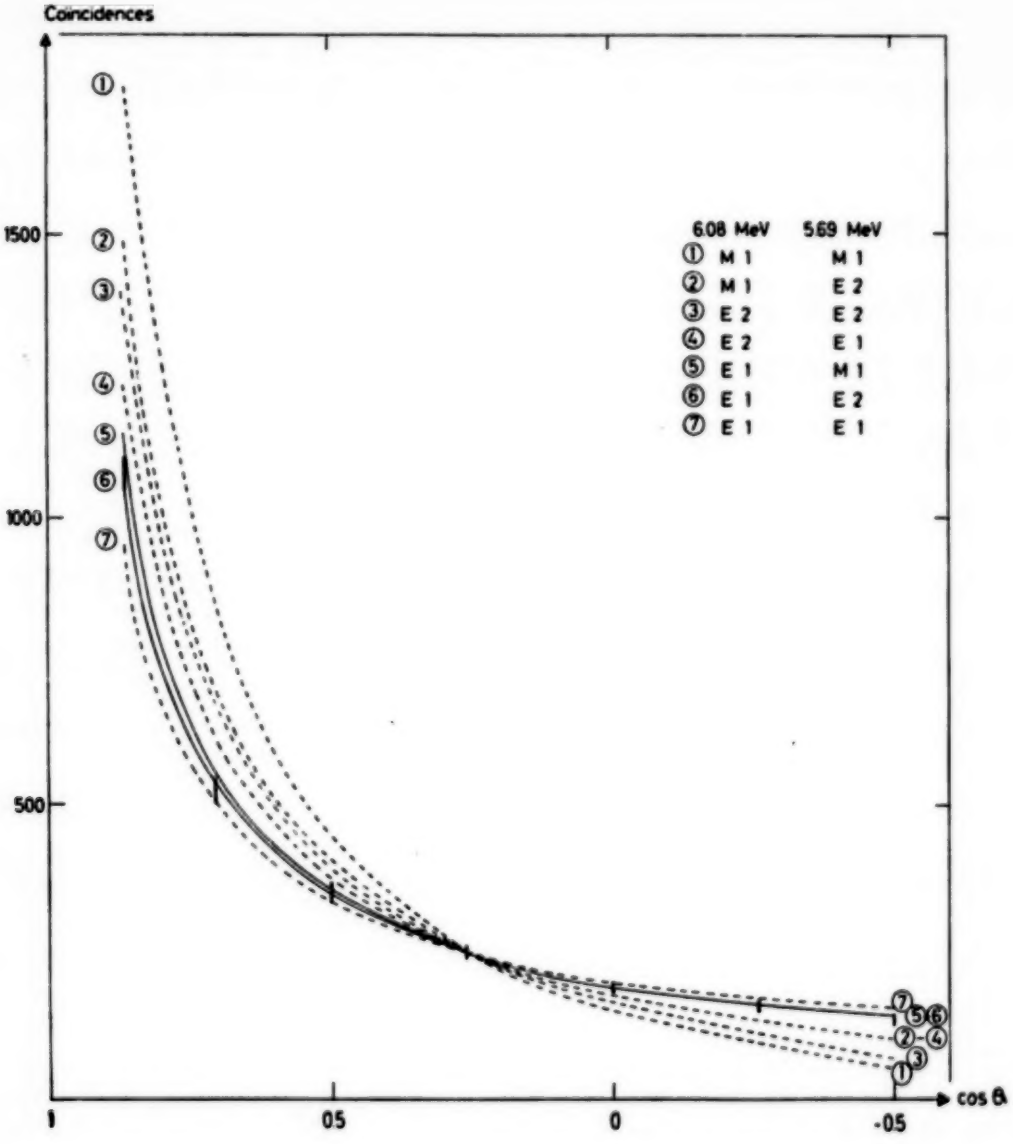


**Fig. 2. Corrélation angulaire des paires de conversion interne. Les courbes théoriques et les points expérimentaux sont normalisés a 75°.**

$$y(\theta) = 0.65 \int_{2\ \text{MeV}}^{3.045\ \text{MeV}} y_l(\theta;\ 6.09\ \text{MeV};\ E_{e^-}) \mathrm{d}E_{e^-} + 0.35 \int_{2\ \text{MeV}}^{2.845\ \text{MeV}} y_l(\theta;\ 5.69\ \text{MeV};\ E_{e^-}) \mathrm{d}E_{e^-}$$

où $y_i$ sont les fonctions de corrélation théoriques correspondant à une transition d'énergie et de multipolarité données et à une répartition d'énergie donnée entre le négaton et le positon.

Ainsi ces courbes théoriques tiennent compte de l'intensité relative des deux transitions, de l'influence de la différence d'énergie et de la multipolarité de ces transitions sur le coefficient de formation de paires internes et enfin de la discrimination relative différente pour les deux transitions.

Le résultat expérimental laisse apparaître que la transition la plus intense (6.09 MeV) est dipolaire électrique et que la transition la moins intense (5.69 MeV) n'est probablement pas dipolaire électrique mais plutôt quadrupolaire électrique ou dipolaire magnétique.

Ces résultats sont donc en accord avec l'attribution du spin $J = 1^-$ pour le niveau 6.09 MeV de $^{14}C$ et attribuent d'autre part au niveau 5.69 MeV de $^{14}N$ la parité + et un spin $J = 0$, 1 ou 2. Le spin $J = 0^+$ est éliminé automatiquement par la présence d'une transition gamma menant au niveau 2.31 MeV ($J = 0^+$) et de plus le niveau 5.69 MeV se désexcitant dans 65 % des cas par l'intermédiaire du niveau 2.31 MeV ($J = 0^+$) et seulement dans 35 % des cas directement au niveau fondamental ($J = 1^+$), le spin $J = 1^+$ pour le niveau 5.69 MeV est bien plus probable que $J = 2^+$ [6]).

## Bibliographie


1) S. Devons et G. Goldring, Proc. Phys. Soc. A **67** (1954) 413;
S. Devons, G. Goldring et G. R. Lindsay, Proc. Phys. Soc. A **67** (1954) 134
2) S. Gorodetzky, R. Armbruster, P. Chevallier et A. Gallmann, Comptes Rendus **239** (1954) 1623; **241** (1955) 482; **240** (1955) 698; **242** (1956) 898;
S. Gorodetzky, R. Armbruster et P. Chevallier, Physica **22** (1956)
3) S. Gorodetzky, P. Chevallier, R. Armbruster, A. Gallmann et G. Sutter, Nuclear Physics **7** (1958) 672
4) H. I. West et L. G. Mann, Rev. Sci. Instr. **25** (1954) 129
5) R. J. Martin Jr., W. B. Mims et W. R. Mills, Phys. Rev. **93** (1954) 950 A
6) F. Ajzenberg et T. Lauritsen, Revs. Mod. Phys. **27** (1955) 77

1.B:6.B *Nuclear Physics* 7 (1958) 416—420; © *North-Holland Publishing Co., Amsterdam*
Not to be reproduced by photoprint or microfilm without written permission from the publisher

# A VARIATIONAL PROCEDURE FOR HARD CORE POTENTIALS

K. V. LAURIKAINEN † and SEIJA LYYTIKÄINEN ††
NORDITA (*Nordisk Institut for Teoretisk Atomfysik*), *Copenhagen*

Received 27 May 1958

**Abstract:** A variational procedure proposed by Laurikainen and Euranto for the treatment of the deuteron problem has been generalized as to include hard core potentials. The procedure can, probably, also be applied, if tensor forces and *LS*-forces are introduced. Numerical results are presented for the case of pure central forces.

Euranto and one of us (K.V.L.) have proposed a variational procedure for the numerical treatment of the equation [1])

$$\frac{\mathrm{d}^2\phi}{\mathrm{d}x^2} - \left[k^2 + \frac{l(l+1)}{x^2} - b\,\frac{\mathrm{e}^{-\mu x}}{\mu x}\right]\phi = 0, \tag{1}$$

and also for the equation system [2,3])

$$\begin{aligned}
&\frac{\mathrm{d}^2\phi_0}{\mathrm{d}x^2} - \left(k^2 - b\frac{\mathrm{e}^{-\sigma x}}{\sigma x}\right)\phi_0 + 2\sqrt{2}\,\gamma b\,\frac{\mathrm{e}^{-\tau x}}{\tau x}\,f(x)\phi_2 = 0 \\
&\frac{\mathrm{d}^2\phi_2}{\mathrm{d}x^2} - \left(k^2 + \frac{6}{x^2} - b\frac{\mathrm{e}^{-\sigma x}}{\sigma x}\right)\phi_2 + \gamma b\,\frac{\mathrm{e}^{-\tau x}}{\tau x}\,f(x)(2\sqrt{2}\,\phi_0 - 2\phi_2) = 0,
\end{aligned} \tag{2}$$

which appears in the theory of the deuteron in the case of tensor forces. The procedure is a generalization of the method, which Hulthén has used for eq. (1) in the case $l = 0$ [4,5]). The main idea is as follows:

In the case of eq. (1) one has to search for a function $\phi(x)$ which gives an extremum for the integral

$$J = \int_0^\infty \left\{\phi'^2 + \left(k^2 + \frac{l(l+1)}{x^2}\right)\phi^2\right\}\mathrm{d}x \tag{3}$$

with the accessory condition

$$N = \int_0^\infty \frac{\mathrm{e}^{-\mu x}}{\mu x}\,\phi^2\,\mathrm{d}x = \text{const.}, \tag{4}$$

and, in addition, satisfies the usual boundary conditions, *viz.* $\phi(0) = \phi(\infty) = 0$. Analogously, the eigenvalue problem corresponding to the system (2) can be reduced to the following variational problem:

Search for the extremum of the integral

† On leave from University of Turku, Finland.
†† Permanent address: Turku, Finland.

$$J = \int_0^\infty \left\{\phi_0'^2+\phi_2'^2+k^2\phi_0^2+\left(k^2+\frac{6}{x^2}\right)\phi_2^2\right\} dx \tag{5}$$

with the two accessory conditions

$$N_1 = \int_0^\infty \frac{e^{-\sigma x}}{\sigma x}(\phi_0^2+\phi_2^2)dx = \text{const.}, \tag{6}$$

$$N_2 = 2\int_0^\infty \frac{e^{-\tau x}}{\tau x} f(x)(2\sqrt{2}\,\phi_0\phi_2-\phi_2^2)dx = \text{const.}, \tag{7}$$

besides which $\phi_0(x)$ and $\phi_2(x)$ have to satisfy the boundary conditions $\phi_i(0) = \phi_i(\infty) = 0 (i = 0, 2)$.

According to the method of Ritz, these variational principles can be employed to get approximate solutions for the eigenvalue problems connected with eq. (1) or the system (2), if one chooses an approximate trial function $\phi(x)$, or correspondingly trial functions $\phi_0(x)$ and $\phi_2(x)$, which contain some adjustable parameters. These parameters are then determined according to the variational principle. The usefulness of the method depends essentially on the more or less successful choice of the trial functions.

In the case of equation (1), the following trial functions have turned out to give very satisfactory results:

$$\text{for } l = 0\ ^{4,5}): \quad \phi = e^{-kx}(1-e^{-x})\sum_{i=0}^{n} h_i e^{-ix}$$

$$\text{for } l = 1\ ^{1}): \quad \phi = e^{-kx}(1-e^{-x})^2\left[k+\frac{1-e^{-x}}{x}\right]\sum_{i=0}^{n} h_i e^{-ix} \tag{8}$$

$$\text{for } l = 2\ ^{1}): \quad \phi = e^{-kx}(1-e^{-x})^3\left[k^2+3k\frac{1-e^{-x}}{x}+3\left(\frac{1-e^{-x}}{x}\right)^2\right]\sum_{i=0}^{n} h_i e^{-ix}.$$

$h_0, h_1, \ldots, h_n$ are the adjustable parameters. In the case of the system (2), the trial functions used in ref.[3]) are

$$\phi_0 = e^{-kx}(1-e^{-x})\sum_{i=0}^{m} h_i e^{-ix}$$

$$\phi_2 = e^{-kx}(1-e^{-x})^2\left[k^2+3k\frac{1-e^{-x}}{x}+3\left(\frac{1-e^{-x}}{x}\right)^2\right]\sum_{j=0}^{n} H_j e^{-jx}, \tag{9}$$

where again $h_0, \ldots, h_m$ and $H_0, \ldots, H_n$ are the adjustable parameters.

Some calculations have now been made in order to generalize these variational procedures to the case of the hard core model. Here we only discuss the single eq. (1). If $x = x_0$ corresponds to the hard core radius, we have to put $\phi = 0$ for $0 \leqq x \leqq x_0$ and to apply the boundary conditions in the form

$$\phi(x_0) = \phi(\infty) = 0. \tag{10}$$

The variational principle has now to be applied to functions which satisfy

these conditions, and thus the integrals $J$ and $N$ need only to be taken from $x_0$ to $\infty$. Hence the variational principle takes the form:

Search for the extremum of the integral

$$J = \int_{x_0}^{\infty} \left\{ \phi'^2 + \left( k^2 + \frac{l(l+1)}{x^2} \right) \phi^2 \right\} \mathrm{d}x \qquad (11)$$

with the accessory condition

$$N = \int_{x_0}^{\infty} \frac{\mathrm{e}^{-\mu x}}{\mu x} \phi^2 \, \mathrm{d}x, \qquad (12)$$

when the function $\phi$ has to satisfy the boundary conditions (10).

In the neighbourhood of the point $x = x_0$, the function $\phi$ has to behave like the first power of $(x-x_0)$. (If the derivative $\phi'$ also vanishes at the point $x = x_0$, the corresponding solution of eq. (1) vanishes identically.) We have, therefore, chosen the following trial functions (compare ref. [1]):

$$\begin{aligned}
&\text{for } l = 0: \quad \phi = \mathrm{e}^{-k\xi}(1-\mathrm{e}^{-\xi}) \sum_{i=0}^{n} h_i \mathrm{e}^{-i\xi}, \\
&\text{for } l = 1; \quad \phi = \mathrm{e}^{-k\xi}(1-\mathrm{e}^{-\xi}) \left[ k + \frac{1-\mathrm{e}^{-\xi}}{\xi} \right] \sum_{i=0}^{n} h_i \mathrm{e}^{-i\xi}, \qquad (13) \\
&\text{for } l = 2: \quad \phi = \mathrm{e}^{-k\xi}(1-\mathrm{e}^{-\xi}) \left[ k^2 + 3k \frac{1-\mathrm{e}^{-\xi}}{\xi} + 3 \left( \frac{1-\mathrm{e}^{-\xi}}{\xi} \right)^2 \right] \sum_{i=0}^{n} h_i \mathrm{e}^{-i\xi},
\end{aligned}$$

where

$$\xi = x - x_0. \qquad (14)$$

The integrals $J$ and $N$ are now of the form

$$J = \sum_{i,j=0}^{n} c_{ij} h_i h_j \qquad (15)$$

and

$$N = \sum_{i,j=0}^{n} d_{ij} h_i h_j. \qquad (16)$$

The coefficients $c_{ij}$ and $d_{ij}$ can all be expressed with the aid of the integrals

$$F_{x_0}(p, q; r; \alpha) = \int_0^{\infty} \frac{\mathrm{e}^{-\alpha\xi}(1-\mathrm{e}^{-\xi})^p}{\xi^{q+1}(\xi+x_0)^r} \mathrm{d}\xi, \qquad (17)$$

where $r$ can be 0, 1, or 2. Without cut off, only the case $r = 0$ appears. As an example, we give the expressions for the coefficients $c_{ij}$ and $d_{ij}$ in the case $l = 1$, $k = 0$, and $\mu = 1$:

$$\begin{aligned}
c_{ij} &= 2F_{x_0}(4, 1; 2; i+j) + ijF(4, 1; 0; i+j) \\
&\quad + F(4, 3; 0; i+j) + 4F(2, 1; 0; i+j+2) \qquad (18) \\
&\quad + (i+j)F(4, 2; 0; i+j) - 2(i+j)F(3, 1; 0; i+j+1) - 4F(3, 2; 0; i+j+1) \\
d_{ij} &= \mathrm{e}^{-x_0} F_{x_0}(4, 1; 1; i+j+1).
\end{aligned}$$

The variational principle leads now, if a Lagrange multiplier $\lambda$ is introduced, to the equation system

$$\frac{\partial J}{\partial h_i} - \lambda \frac{\partial N}{\partial h_i} = 0 (i = 0, 1, \ldots, n), \tag{19}$$

which is linear and homogeneous with respect to the parameters $h_i$. If $k$ is given, one gets the multiplier $\lambda$ from the determinant equation. This multiplier turns out to be identical with the eigenvalue parameter $b$. (The algebraically smallest root $\lambda_1$ gives the lowest eigenvalue $b_1$.) The ratios $h_i/h_0 (i = 1, \ldots, n)$ can then be calculated from the system (19), and $h_0$ is determined by the normalization condition

$$\int_{x_0}^{\infty} \phi^2 \, dx = \sum_{i,j=0}^{n} e_{ij} h_i h_j = 1, \tag{20}$$

where again the coefficients $e_{ij}$ can be expressed with the aid of the integrals (17).

We give here some numerical results which correspond to the case $k=0, \mu=1$. In order to give an idea of the convergence, we have, successively, chosen $n = 1$, 2, and 3 in the trial functions (13).

As the hard core radius we have taken the value 0.3 of the dimensionless quantity $x$.

TABLE 1

The case $k = 0$, $l = 0$

| $n$ | $b_1$ | $h_1/h_0$ | $h_2/h_0$ | $h_3/h_0$ |
|---|---|---|---|---|
| 1 | 3.255234 | 0.147 | — | — |
| 2 | 3.242175 | 0.489 | −0.420 | — |
| 3 | 3.242158 | 0.470 | −0.360 | −0.0456 |

TABLE 2

The case $k = 0$, $l = 1$

| $n$ | $b_1$ | $h_1/h_0$ | $h_2/h_0$ | $h_3/h_0$ |
|---|---|---|---|---|
| 1 | 10.47594 | −3.465 | — | — |
| 2 | 10.44979 | 0.182 | −0.501 | — |
| 3 | 10.449745 | 0.173 | −0.473 | −0.0197 |

TABLE 3

The case $k = 0$, $l = 2$

| $n$ | $b_1$ | $h_1/h_0$ | $h_2/h_0$ | $h_3/h_0$ |
|---|---|---|---|---|
| 1 | 22.92978 | −0.643 | — | — |
| 2 | 22.91305 | −0.332 | −0.320 | — |
| 3 | 22.90896 | −0.0570 | −1.184 | 0.5184 |

For the sake of comparison we give also results obtained in the case $k = 0$ without hard core [1]):

$$l = 0: \quad b_1 = 1.679812,$$
$$l = 1: \quad b_1 = 9.08197,$$
$$l = 2: \quad b_1 = 21.89500.$$

This variational procedure may also be applied if the hard core is introduced into the equation system (2). The numerical work can be reduced by more than one half if a table of integrals (17) is computed. Two such tables, one for the case $r = 0$, the other for the integrals needed for cut off potentials ($r = 1, 2$), will be published in the Annales Universitatis Turkuensis. In this connection we shall also investigate more closely the introduction of the hard core in the case of the coupled system (2).

Another method of generalizing the variational procedure of ref. [5]) to the case of hard core potentials has been proposed by Pluvinage and Proriol [6]).

We wish to thank the NORDITA for the financial support which has made possible our stay in Copenhagen. Preliminary work in Finland has been supported by the Eemil Aaltosen Säätiö and the State Commission for Natural Sciences.

## References

1) K. V. Laurikainen and E. K. Euranto, Ann. Univ. Turkuensis, A **9** (1953) no. 3
2) K. V. Laurikainen and E. K. Euranto, Ann. Univ. Turkuensis, A **18** (1955) no 2
3) K. V. Laurikainen, Ann. Acad. Sci. Fenn., A **1** (1955) 208
4) L. Hulthén, K. Fysiogr. Sällsk. Lund Förhandlingar **15** (1945) no. 22, p. 6
5) L. Hulthén and K. V. Laurikainen, Revs. Mod. Phys. **23** (1951) 1
6) P. Pluvinage and J. Proriol, C. R. Acad. Sci. **245** (1957) 2201

1.D.2. *Nuclear Physics* 8 (1958) 421—427; © *North-Holland Publishing Co., Amsterdam*
Not to be reproduced by photoprint or microfilm without written permission from the publisher

# ON THE CONNECTION BETWEEN DEGENERACY AND ROTATIONAL STATES IN THE NUCLEAR SHELL MODEL

H. J. LIPKIN
*Department of Physics, The Weizmann Institute of Science, Rehovoth, Israel*

Received 23 May 1958

**Abstract:** A method, applicable in systems where a degeneracy exists between states having different angular momenta, is presented for constructing the collective angle co-ordinate required for the description of rotational states. It is shown that the collective description can also lead to rotational bands having only a finite number of states.

## 1. Introduction

### 1.1 THE CONFIGURATION-MIXING MODEL

Elliott has recently shown [1]) that the characteristic features of rotational states can be obtained in a shell-model treatment of a system of particles moving in a harmonic oscillator well. By mixing configurations which happen to be degenerate in the harmonic oscillator case, one can obtain sets of states which have some of the properties of a rotational band. They are a series of states having the proper values of the total angular momentum. The expectation values of certain operators, such as the quadrupole moment, are related in a simple manner similar to that predicted by the collective model [2]) for all states of the band. These states were found using the invariance of the harmonic oscillator Hamiltonian under the transformations of the three-dimensional unitary group. Furthermore, a particular residual two-body interaction has been found which removes the degeneracy and results in rotational spectra proportional to $L(L+1)$, where $L$ is the total orbital angular momentum. However, the number of states in each band is finite; there is a maximum value of $L$ for each band, above which no states are found. This is not in accord with the usual interpretation of the collective model which predicts either an infinite number of states or a gradual breakdown of the model at high rotational excitation, but not a sharp cut-off in the spectrum.

### 1.2. THE BOHR-MOTTELSON CONDITIONS FOR ROTATIONAL SPECTRA

Bohr and Mottelson [3,4]) have shown that rotational states exist in systems where an angle variable † operator $\theta$ can be found which satisfies the following two conditions:

† The treatment presented here, using only a single angle and a single angular momentum operator, is applicable directly only to two dimensional rotations or to rotations in three dimensions about a single axis found in space. The generalization to the full three-dimensional case, however, is straightforward.

1. It should be canonically conjugate to the total angular momentum: i.e. it should satisfy the commutation relation

$$[J, \theta] = -i. \tag{1}$$

2. Its time derivative must be the angular momentum of the system $J$, divided by some constant; i.e. it should satisfy the commutation relation

$$[H, \theta] = i\hbar^2 J/\mathscr{I} \tag{2}$$

where $H$ is the Hamiltonian of the system.

A variable $\theta$ satisfying these conditions can be used to define a canonical transformation from the individual particle representation to a collective representation, in which $\mathscr{I}$ appears as the moment of inertia.

An equivalent statement of these conditions which is more suitable for our purposes † is the following: We require the existence of a *unitary* operator $\exp iM\theta$, where $M$ is any integer, satisfying the relations

$$[J, e^{iM\theta}] = Me^{iM\theta} \tag{1'}$$

$$[H, e^{iM\theta}] = \hbar^2 M(Je^{iM\theta} + e^{iM\theta} J)/2\mathscr{I}. \tag{2'}$$

The purpose of this work is to show how an angle variable satisfying the Bohr-Mottelson conditions can be defined in certain cases, like that of the harmonic oscillator shell model, where there is a degeneracy of states having different angular momenta. This might imply that states having properties of rotational bands can be constructed whenever the system possesses a degeneracy characterized by the existence of operators which commute with the Hamiltonian but not with the total angular momentum, or whenever the Hamiltonian is invariant under a group of transformations which does not commute with the three dimensional rotations.

The treatment presented here also shows how certain singularities in the angle variable can resolve the apparent contradiction between the infinite number of states appearing in the collective model and the finite number of actual states of the system which are obtained in certain cases, like that of the harmonic oscillator.

## 2. Construction of the Collective Angle Variable

In certain simple cases where degenerate states of different angular momenta occur, such as the hydrogen atom and the multi-dimensional harmonic oscillator, the degeneracy can be associated with the existence of an operator which is an integral of the motion (i.e. it commutes with the Hamiltonian) and which does not commute with the total angular momentum[5,6]). The existence of an operator $A$ satisfying the relations

† It has been pointed out that certain difficulties are encountered in the use of $\theta$ directly as an operator. These are avoided by the use of periodic functions of $\theta$, such as $\exp iM\theta$.

$$\begin{aligned}[A, H] &= 0 \\ [J, A] &\neq 0,\end{aligned} \tag{3}$$

requires degeneracy between states having different values of $J$. In the representation with $H$ and $J$ diagonal, $A$ cannot be diagonal and will have matrix elements connecting states having the same energy but different angular momentum. Operators satisfying the condition (3) always exist when there is a degeneracy between states of different angular momenta which is characterized by the invariance of $H$ under a group of transformations.

In a system where an operator $A$ exists satisfying the conditions (3), then the operators $JA$, $[J, A]$ etc. will also satisfy these conditions of the Hamiltonian is rotationally invariant. From these operators one can construct a series of operators $T_k$ which transform under rotation like an irreducible tensor of degree $k$, and all of which satisfy the conditions (3). From these tensor operators, one can construct the angle operators $\theta$ satisfying (2). One possible angle operator would be the function of the components $T_k$ specifying the orientation of certain principal axes of the tensor with respect to a set of axes fixed in space. Since $\theta$ is a function of the $T_k$'s which all commute with $H$, $\theta$ also commutes with $H$.

$$[H, \theta] = 0 \tag{4}$$

$\theta$ therefore satisfies the Bohr-Mottelson conditions (1) and (2) corresponding to an infinite moment of inertia implying the existence of sets of states having rotational properties which are all degenerate.

If the degeneracy is removed by adding an interaction, there is no guarantee that the rotational spacings proportional to $J(J+1)$ will be obtained. However, it is very tempting to look for such an interaction in addition to the trivial one $J^2$. This interaction should satisfy the relations

$$\begin{aligned}&[v, H] = 0 \\ &[v, \theta] = -i\hbar^2 J/\mathscr{I}; \quad \text{or} \quad [v, e^{iM\theta}] = \hbar^2 M(Je^{iM\theta} + e^{iM\theta}J)/2\mathscr{I}.\end{aligned} \tag{5}$$

One possible approach in looking for a suitable operator $v$ is to use functions of the components of the tensor used to define $\theta$. If the tensor is the sum of single particle operators, then quadratic functions of the tensor components will have the form of two-body forces (plus a self-energy term which can be added to the single particle potential). If these tensor components are infinitesimal transformation operators belonging to a group under which $H$ is invariant, then the Casimir operator of the group will commute with both $H$ and $\theta$. Thus any linear combination of this Casimir operator and $J^2$ will satisfy the relations (5).

In the simple example of the two-dimensional harmonic oscillator treated in the appendix, the operator $\theta$ and a possible interaction $v$ are constructed, using this method.

### 3. The Case of Spectra having only a Finite Number of States

The method described in the preceding section is apparently applicable to cases, like that treated by Elliott, where there are only a finite number of degenerate states having a given energy. There can therefore be only a finite number of independent linear combinations having collective properties. However, in the usual interpretation of the collective model, the existence of a collective degree of freedom which is *exactly* separable from the other degrees of freedom of the system implies the existence of an infinite number of rotational states. In fact, the existence of a unitary operator $\exp iM\theta$ satisfying relations (1′) and (2′) with $\mathcal{I} = \infty$ would itself seem to imply the possibility of constructing an infinite number of degenerate states. This can be shown as follows: Let $\psi_{M',E'}$ be an eigenfunction of the angular momentum $J$ and of the Hamiltonian $H$ with eigenvalues $M'$ and $E'$ respectively. Then

$$e^{iM\theta}\psi_{M',E'} = \psi_{(M+M'),E'} \tag{6}$$

is another eigenfunction having the same energy and having the angular momentum $M+M'$. By repeated application of this procedure, an infinite number of degenerate states can be constructed having angular momenta $M'$, $M'+M$, $M'+2M$, etc. Since the operator $\exp iM\theta$ is unitary, there is no possibility that any of these states can vanish.

To see what actually occurs when the method described above is used in a case where only a finite number of states exists, let us consider the simple example of the rotation of a spherically symmetric system about an axis fixed in space. Let this axis be the $z$-axis. Since the system is spherically symmetric, $J_z$ commutes with $H$; but also $J_x$ and $J_y$ commute with $H$ and they do not commute with $J_z$. $J_x$ and $J_y$ are thus operators of the type "A" in eq. (3) with respect to $J_z$ and indicate the existence of the well known degeneracy between states having different eigenvalues of $J_z$. However, we know very well that there are only a finite number of degenerate states having angular momenta from $-J$ to $+J$, where $J$ is the total angular momentum.

From the operators $J_x$, $J_y$, and $J_z$, an angle operator can be defined by the relation

$$e^{i\theta} = (J_x+iJ_y)(J_x^2+J_y^2-J_z)^{-\frac{1}{2}}. \tag{7}$$

This operator satisfies the conditions (1′) and (2′) with $\mathcal{I} = \infty$.

Thus we might expect to construct an infinite number of degenerate states by repeated application of eq. (6). However, we note that when operating on a state of maximum $J_z$ in a given band ($M = J$), the operator (7) is equal to 0/0 and is undefined. This singularity does not prevent the operator from being used to generate the entire band from a single state and to define a singular canonical transformation to a collective representation. However, it

does prevent the construction of more than the proper number of states. The details of the behaviour of wave functions under singular canonical transformations of the type defined by the operator (7) will be considered in a subsequent paper. The results show that although an infinite number of rotational states can be written formally in the collective representation, only a finite number correspond to real states and can be transformed back to the particle representation.

The same type of singularity is present in the case of the two-dimensional harmonic oscillator treated in the appendix.

## 4. Conclusions

We see, therefore, that in systems where there are sets of degenerate states having different angular momenta, one may be able to find a description in terms of rotational states. In particular, if there are several degenerate states for each value of the total angular momentum, one may expect to find linear combinations of these states having the properties of a rotational band. This may offer a possibility for finding a bridge between the shell model and the collective model which does not depend upon the incidental degeneracy of the harmonic oscillator potential. In any single particle model of the nucleus, there is a degeneracy of states having different values of the total angular momentum; namely those states in which the angular momenta of particles in the same shell are coupled in different ways. There may also be several degenerate states having the same angular momentum. If it is possible to treat this degeneracy by the method described here, one may be able to mix shell model states within a single configuration to obtain linear combinations having rotational properties. One may also gain insight into the specific forms of the residual interaction which lead to rotational energy spectra.

The author wishes to express his appreciation to I. Talmi for stimulating discussions and for his reading and criticism of the manuscript.

## Appendix

An example of a system having degenerate states which can be combined to form rotational bands is the system of particles moving in a harmonic oscillator well [1]). To illustrate the existence of the tensor operator satisfying the conditions (3), the angle variable satisfying the Bohr-Mottelson conditions (1) and (2) and a residual interaction satisfying the conditions (4), let us consider the two dimensional case, described by the Hamiltonian

$$H = \sum_i (p_{x_i}^2 + p_{y_i}^2 + x_i^2 + y_i^2), \tag{A.1}$$

where $x_i$, $y_i$, $p_{x_i}$, and $p_{y_i}$ are the co-ordinates and momenta of the $i$-th

particle and the constants of the oscillators have been chosen to make all the coefficients in (1) equal to unity. As has been pointed out [5,6]), the second rank tensor having components

$$\begin{aligned} C_1 &= \sum_i [(x_i^2-y_i^2)+(p_{x_i}^2-p_{y_i}^2)]/2\hbar \\ C_2 &= \sum_i (x_i y_i+p_{x_i}p_{y_i})/\hbar \end{aligned} \tag{A.2}$$

are integrals of the motion, commuting with $H$, but not with the total angular momentum $L$. In fact, they satisfy the relations

$$\begin{aligned} [L, C_1] &= 2iC_2 \\ [L, C_2] &= -2iC_1 \\ [C_1, C_2] &= 2iL. \end{aligned} \tag{A.3}$$

The angle variable $\theta$ defining the orientation of the principal axes of the tensor $C$ can be defined by the relation

$$e^{2i\theta} = (C_1+iC_2)(C_1^2+C_2^2-2L)^{-\frac{1}{2}}. \tag{A.4}$$

It is evident by direct substitution that (A.4) satisfies the Bohr-Mottelson conditions (1′) and (2′).

We note that the operator defined by (A.4) is singular in the same manner as that defined in the simple case of eq. (7). There will therefore be only a finite number of states in each rotational band. Furthermore, eq. (A.4) defines only $\exp 2i\theta$ and $\exp i\theta$ cannot be defined; thus the angular momenta within a band can jump only in steps of 2, and they must be either all even or all odd.

To remove the degeneracy and obtain a rotational spectrum, we note that an operator $v$ satisfying the conditions (5) can be constructed simply from the operators $C_1$ and $C_2$ by making use of the commutation relations (A.3):

$$v = C_1^2+C_2^2. \tag{A.5}$$

The operator $v$ is similar to the "two-body quadrupole interaction" introduced by Elliott and Mottelson [1]), but it depends upon momenta as well as upon the co-ordinates. The difference is necessary in order that $v$ commute with $H$. The quadrupole interaction depending only upon co-ordinates does not, and it has non-vanishing matrix elements between different shells. This has also been pointed out by Moszkowski [7]).

The operators $C_1$, $C_2$, and $L$ are the infinitesimal transformation operators of a group under which $H$ is invariant, and for which the Casimir operator is just $C_1^2+C_2^2+L^2$. Thus the interaction $v$ is a linear combination of the Casimir operator and $L^2$, as has been suggested above.

## References

1) J. P. Elliott to be published; See also B. H. Flowers, Proc. Rehovoth Conference (North Holland Publishing Co., 1958)
2) K. Alder, A. Bohr, T. Huus, B. Mottelson and A. Winther, Revs. Mod. Phys. **28** (1956) 530
3) A. Bohr and B. R. Mottelson, Proc. Rehovoth Conference (North Holland Publishing Company, 1958)
4) H. J. Lipkin, A. de-Shalit and I. Talmi, Phys. Rev. **103** (1958) 1773
5) G. Racah, Proc. Rehovoth Conference (North Holland Publishing Co., 1958)
6) J. M. Jauch and E. L. Hill, Phys. Rev. **57** (1940) 641
7) S. Moszkowski, A connection Between the Nuclear Shell Model and the Unified Model (preprint)

2.I *Nuclear Physics* 8 (1958) 428—443; © *North-Holland Publishing Co., Amsterdam*
Not to be reproduced by photoprint or microfilm without written permission from the publisher

# RELATIONS AMONG DIFFERENT MODELS OF THE NUCLEAR PHOTOEFFECT

J. S. LEVINGER
*Department of Mathematical Physics, University of Birmingham* †

Received 20 June 1958

**Abstract:** The collective and shell models of the photoeffect are each idealisations for the complicated behaviour of many overlapping compound states reached by photon absorption, and are not expected to agree in detail. We might, however, find agreement between the mean energies calculated from different models. This agreement in mean energy is found between the two-fluid collective model and the shell model (finite square well approximated as two Fermi gases). There is also agreement between collective and shell model calculations of the splitting of the giant resonance for deformed nuclei.

## 1. Introduction

A variety of models have been proposed for the nuclear photoeffect, each model having had appreciable success [1,2]) in the interpretation of certain experimental phenomena. In the next section we discuss each model briefly and also discuss relations already known to exist between certain models. We shall not concern ourselves with comparisons with experiment. From the approximate character of the various models we conclude that we should not expect to establish significant exact relations among the models. We investigate instead relations among the values of the mean energy for the photoeffect given by various models. In section 3 we show that the collective model of two oscillating fluids and the shell model of two Fermi gases give identical values for the nuclear polarizability and the corresponding mean energy $W_M$. We also discuss the splitting of the giant resonance for deformed nuclei. In the last section we summarise relations among the various nuclear models.

In this paper we are concerned with the "giant dipole resonance" for the curve $\sigma(W)$. Here $\sigma(W)$ is the cross section for absorption of a photon of energy $W$. The experimental $\sigma(W)$ curves have moderately narrow peaks, with resonance energy $E_m$ about 20 MeV for medium nuclei such as copper, decreasing slowly to about 15 MeV for heavy nuclei such as lead. The full width at half-maximum (hereafter denoted as the width $\Gamma$) is about 4 MeV for closed shell nuclei such as lead, and has an appreciably larger value for deformed nuclei such as tantalum. The peak in the $\sigma(W)$ curve is assigned as

† On sabbatical leave from Lousiana State University; Guggenheim Fellow.

a dipole resonance since the experimental cross sections are in rough agreement with calculations for electric-dipole transitions; and therefore the cross sections are orders of magnitude larger than those calculated for other multipoles.

The experimental data on $\sigma(W)$ are not very precise at present: there is an uncertainty of 15 % or more for any point on a $\sigma(W)$ curve, and an uncertainty of about 1 MeV in measurements of either $E_m$ or $\Gamma$.

Photon absorption in the giant dipole resonance produces excited states for which the levels of the compound nucleus lie very close together. The compound levels overlap appreciably for most nuclei; while for the lightest nuclei ($6 \leqq A \leqq 17$) they may just be resolved by present experimental techniques.

The giant dipole resonance has been interpreted in terms of the collective model, and in terms of the shell model. In the collective model interpretation, the collective model in which protons oscillate against neutrons has a natural frequency which can be calculated from the parameters of the model. This natural frequency is identified as the resonance frequency $E_m/\hbar$. In the shell model interpretation, each transition in which a particle jumps from an occupied to a vacant state has a characteristic energy $E_n$. If the energies $E_n$ of the principal electric dipole shell model transitions are nearly the same, then these shell model transitions are identified as forming the giant dipole resonance.

## 2. Nuclear Models for the Photoeffect

Goldhaber and Teller [3]) proposed two different classical collective models for the dipole oscillations of neutrons vs protons:

$C_1$ : the two-fluid model,

$C_2$ : the rigid-spheres model.

In the two-fluid model the neutrons and protons are represented as two fluids confined inside a sphere. The electric field excites waves in which one fluid vibrates against the other. The boundary condition at the edge of the sphere determines the wavelength of the fundamental two-fluid oscillation, and the corresponding photon energy, which is identified as the energy of the giant dipole resonance. This model was extended to give a theory without arbitrary parameters by using the nuclear symmetry energy [4]); by including the effects of the Coulomb energy of the protonic fluid [5]); by including the effect of changes of the sum of the densities of neutronic and protonic fluids [6]); and by using an ellipsoidal instead of a spherical nuclear surface [7, 8]).

In the rigid spheres model the protons form one rigid sphere and the neutrons another. The electric field excites harmonic oscillations of one sphere against the other.

The classical oscillations of the two-fluid model can be quantized, giving us a quantal collective model:

$C_3$ : plasma oscillations.

A preliminary investigation of this model was made by Ferentz, Gell-Mann and Pines [9]).

The shell model of a square well with spin-orbit coupling and a diffuse boundary has not been used for photoeffect calculations; though it has had significant success in calculations of nucleon scattering. Three drastically simplified shell models have been applied to the nuclear photoeffect problem:

$S_1$ : simple harmonic oscillator shell model,

$S_2$ : finite square well shell model,

$S_3$ : Fermi gases model.

The harmonic oscillator model was proposed by Wu [10]) and extended by Levinger [11]). The energy difference between levels in the harmonic oscillator well is determined from the nuclear mean square radius, and is identified with the energy of the giant dipole resonance.

The finite square well model was used by Burkhardt [12]) who found that it disagreed with the experimental value of the resonance energy. Wilkinson[13]) has used it with much success for calculations of the width of the giant dipole resonance and of the resonance-direct emission of fast nucleons. Soga and Fujita [14]) have made a preliminary study of the photoeffect in deformed nuclei.

The Fermi gas model was used by Levinger and Kent [15]) for calculation of the mean square nuclear dipole moment.

The sub-unit model has been used by Khokhlov [16]), Levinger [17]), Dedrick [18]) and Gottfried [19]) for calculations of the high energy photoeffect, but is not applicable for the giant dipole resonance.

Each of these different models represent a different drastic simplification of the dispersion theory formalism — e.g. Kapur-Peierls [20]) — which uses the properties of the very large number of compound nucleus levels reached by photon absorption in the giant resonance region.

While the dispersion theory formalism is rigorously true, it is not of practical direct use in the region of many overlapping resonances. One can, however, hope that the very many compound levels contributing to some given process (e.g. photon absorption, or photoemission of fast nucleons) will cluster closely around the energy given by one of the idealised models, in which case that particular idealised model would be of practical value in photoeffect calculations [3]).

While we see how the dispersion theory result might be approximated by one or another of the collective or shell models, we would like to understand

why the collective and shell models give reasonable agreement with each other for the properties of the giant dipole resonance. We would also like to see how any one of the models might be combined with the sub-unit model to give an idealised model for photon absorption applicable both for the giant dipole resonance and for the high energy photoeffect (100 to 300 MeV). Relations between certain pairs of models have already been pointed out; but before examining these relations let us first examine which features of the photoeffect are sensitive and which are insensitive to the idealised model assumed.

All the models find that photon absorption for a spherical nucleus occurs almost entirely in a small energy range, identified as the giant dipole resonance. Other multipoles than the electric dipole (E1) give only the order of ten percent of the integrated cross section. E1 absorption goes to a single excited state for the harmonic oscillator models (2 rigid spheres or harmonic oscillator shell model). In the other models there may be a spread in the transition energy due to two causes:

i) the high degeneracy of the isotropic harmonic oscillator is removed;

ii) the quantum number may change by more than unity (or classically, overtones of the fundamental dipole vibration may be excited).

The first does not occur in the two-fluid model and the second effect is small: the fundamental accounts for 85 % of the integrated cross section [5]). In the square well model the splitting due to the first effect spreads the resonance for spherical nuclei by several MeV [13]) or about 20 % of the resonance energy. There is only a very small absorption for large changes of the principal quantum number. The Fermi gas model shows similar effects to the square well model. Much of the observed width of the giant resonance is ascribed in each model to the spread of energies of the model-like compound levels around the idealised model energy. This spread is interpreted as a viscosity in the classical models, or as an opacity of the nuclear potential in the shell models (see Lane, Thomas and Wigner [21]) for the interpretation of the opacity of the cloudy crystal ball model in terms of the width of the distribution of strength functions).

These models each predict a giant dipole resonance which can be characterised by three numbers:

i) the integrated cross section $\sigma_{\mathrm{int}} = \int \sigma \mathrm{d}W$,

ii) the resonance energy $E_{\mathrm{m}}$,

iii) the resonance width $\Gamma$.

If we can show why these 3 quantities agree for the various models, we will have gone at least as far as anticipated in establishing connections among the models.

The integrated cross section for E1 absorption is model-independent, if we limit ourselves to ordinary, velocity-independent forces between the nu-

cleons. The integrated cross section is increased appreciably by two-body Majorana exchange forces. This increase in $\sigma_{\text{int}}$ is understood semi-quantitatively in a shell model as due to the velocity dependence of the shell model potential [22]). But the exchange force increase in $\sigma_{\text{int}}$ is only poorly understood in the various collective models [23]). Since the purpose of this paper is to compare different existing models we must compare with collective models in which the exchange-force increase in $\sigma_{\text{int}}$ does not occur, and therefore we use the analogous shell models for a velocity-independent shell model potential. We do not expect good agreement with experiment for $\sigma_{\text{int}}$ for any of the models considered in this paper, and we find as a trivial result that all models considered give identical values $\sigma_{\text{int}} = 0.015A$ MeV-barn.

We wish to emphasise that this model-independent character of $\sigma_{\text{int}}$ is characteristic *only* of E1 absorption. Its mathematical origin is that the integrated cross section is proportional to the double commutator $[[H, \boldsymbol{\mathcal{E}} \cdot \mathbf{r}], \boldsymbol{\mathcal{E}} \cdot \mathbf{r}]$ of the Hamiltonian $H$ of the system with the interaction term $\boldsymbol{\mathcal{E}} \cdot \mathbf{r}$ with the electromagnetic field. If we use the kinetic energy term in the Hamiltonian, and the E1 interaction with the electromagnetic field, this double commutator $[[p_z^2, z], z]$ is a constant. (An ordinary potential energy gives zero contribution to the double commutator.) Any normalised wave functions give us the same expectation value for the double commutator, and therefore the same $\sigma_{\text{int}}$ for E1 absorption. But the interaction term for any other multipole operator does not give a constant double commutator with the Hamiltonian, and therefore $\sigma_{\text{int}}$ for other multipoles is model-dependent. Also, for E1 interactions, every other moment of the absorption curve is model sensitive: e.g. $\sigma_0 = \int (\sigma/W)\mathrm{d}W$ is proportional to the ground state expectation value of the squared dipole moment, and thus involves the size of the system, and also the detailed shape of the wave functions.

The purpose of this paper is to calculate the resonance energy for collective and shell models, and thus to show the relations among the models. We shall actually calculate not the resonance energy $E_{\text{m}}$, but the mean energy

$$W_{\text{M}} = (\sigma_{\text{int}}/\sigma_{-2})^{\frac{1}{2}}. \tag{1}$$

Here the denominator $\sigma_{-2} = \int \sigma W^{-2}\mathrm{d}W$ is proportional to the nuclear polarisability. Since both collective and shell models have narrow resonances, equality of the $W_{\text{M}}$ values for two models shows that the $E_{\text{m}}$ values are very nearly equal.

We shall not calculate in this paper the resonance widths $\Gamma$ for collective and shell models. The intrinsic width is usually introduced phenomenologically into the model, by introducing a viscosity into the collective model or an opacity into the shell model potential. The collective model calculation [24]) of the viscosity and the shell model calculations [25]) of the opacity seem too crude to encourage a search for meaningful relations between the widths

calculated with the different models. We shall, however, discuss in section 3 the splitting of the giant resonance for derformed nuclei, which appears experimentally as an increased resonance width for these nuclei.

We have argued in earlier papers that certain photonuclear reactions would be sensitive to the respective validity of the collective or shell models used in their calculation: Levinger and Bethe [26]) claimed that the cross section for elastic photon scattering would be much less for a many-level calculation (e.g. square well shell model) than for the single excited level of a collective model. However, this argument was concerned with the photon scattering which we might denote as a "compound-elastic" process [27]). That is, the photon is absorbed, and later re-emitted in competition with other processes for decay of the excited system. Almost all of the photon scattering in the giant resonance region actually is "shape-elastic", i.e. its cross section is determined by the photon absorption cross section [28]). The imaginary part of the forward scattering amplitude is proportional to the absorption cross section at that energy, by the optical theorem. The real part of the forward scattering amplitude is given as a dispersion integral of the absorption cross section for all energies. Measurements of photon elastic scattering, then, are another way of measuring the absorption cross section, but are no more sensitive to the nuclear model than is the absorption cross section discussed above. More recently [2]) we argued that the observed emission of fast nucleons in numbers far greater than predicted by the statistical model demonstrated that the state reached by photon absorption was largely a bona fide shell model state. Wilkinson [13]) estimated the cross section $\sigma_d$ for emission of fast nucleons as $\sigma_d = \sigma\Gamma_p/2W'$, and showed that experimental results were in order of magnitude agreement with this formula. (Here $\Gamma_p$ is the escape width for the fast nucleon in question, and $W'$ is the imaginary part of the optical potential.) Brown and Levinger [29]) have derived a similar formula for $\sigma_d$ from the Kapur-Peierls dispersion formalism. The very large numbers of compound states have their shell-model-like parts (proportional to their strength functions) selected out, when we measure $\sigma_d$ in which the final state is a shell model state. The strength functions of the many compound states combine to give a value for $\sigma_d$ *as if* there were a single shell model level in a complex potential. The argument is illustrated in fig. 1. Each cross shows the position of a compound level reached by photon absorption, and decaying by the emission of a fast nucleon. The abscissa is the real part of the energy, while the small ordinate is the negative imaginary part of the energy, corresponding to the lifetime of the compound state. The inverse distance from a cross to a given point B on the real axis is proportional to the amplitude for direct emission due to that particular compound state. If the incident photon has a high energy, illustrated by point A, the many crosses combine to give the same amplitude

as the circle at S. This shell model state in a complex optical potential has an energy with real part $E_m$, and imaginary part corresponding to the imaginary part $W'$ of the complex optical potential. Near point B (i.e. in the region of the giant dipole resonance) $\sigma_d$ is hard to calculate; but $\bar{\sigma}_d$ averaged over an interval at least as large as $W'$ is about the same as the cross section at B', where again the crosses combine to give the effect of the circle at S. (The above qualitative arguments are made more precise [29]), so that the accuracy of the approximation becomes clear.).

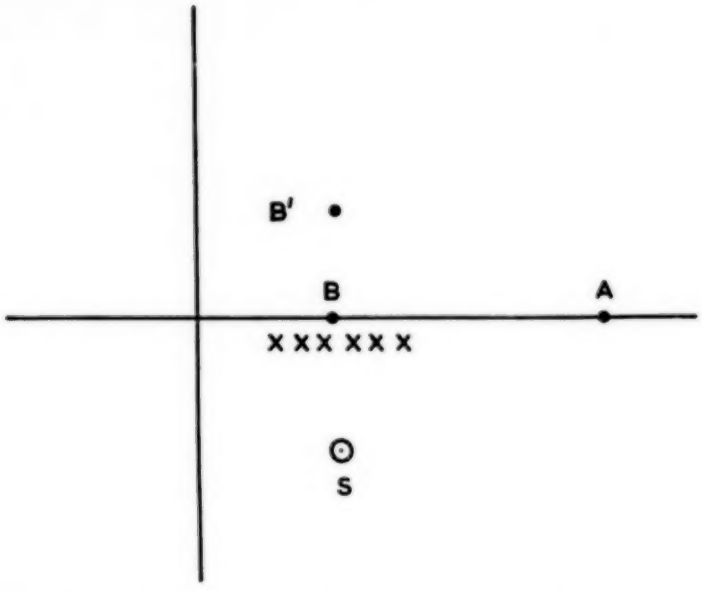


Fig. 1. Compound levels are indicated by crosses in the complex energy plane (Kapur-Peierls formalism). At photon energy $A$, the compound levels combine to give a cross section for direct emission about equal to that of the shell model state S in a complex potential.

We have now learned that neither measurements of elastic scattering of photons nor measurements of the direct emission of fast nucleons can show whether the shell model or the collective model is more nearly valid for calculations of the process of photon absorption. We shall return in section 4 to the problem of the relative merits of the two models.

Brink [30]) has shown a detailed relation between the collective model of 2 rigid spheres and the harmonic oscillator shell model. The wave functions for the degenerate excited states of this shell model can be combined to give precisely the wave function for the collective oscillation of 2 rigid spheres. This detailed agreement is of great interest for the idealised models, but its meaning is less clear as soon as damping is included in the models. Also, the two idealised models disagree in two respects:

i) the ground state nuclear density distribution is different for the two models;

ii) if we follow the simplifications made by Goldhaber and Teller [3]), then the collective model gives $E_m$ proportional to $A^{-\frac{1}{3}}$, while the shell model gives $E_m$ approximately proportional [11]) to $A^{-\frac{1}{6}}$.

Brueckner, Eden and Francis [31]) and other have provided the framework for combination of a shell model for infinite nuclear matter with a sub-unit model. Dąbrowski [32]) has introduced two-body dynamical correlations into a shell model of a finite nucleus. Dąbrowski's work may permit quantitative calculations for a model combining shell model and sub-unit properties.

## 3. Relation between Two-Fluid Model and Shell Model

We shall show that Migdal's mean energy (1) has the same value for the two-fluid collective model, and the shell model of two ideal completely degenerate Fermi gases. Since two Fermi gases are an example of two fluids, this result is almost trivial, and in fact was stated earlier without proof [33]). We give a detailed proof here, since we also wish to extend the correspondence between the shell and collective models to obtain agreement for the splitting of the resonance for deformed nuclei. We shall also discuss qualitatively the effect of the nuclear surface and the small effects of the Coulomb energy of the protonic fluid or Fermi gas, the effect of nuclear compressibility and the effect of the nuclear dielectric constant.

Migdal [34, 33]) calculated the change in the protonic and neutronic fluid densities ($\rho_p$ and $\rho_n$) in nuclear matter for an external static, spatially, constant electric field $\mathscr{E}$ along the $z$ axis. He found

$$\eta = \rho_p - \rho_n = (e\mathscr{E}\rho/4k)z. \tag{2}$$

Here $k$ is the coefficient of the symmetry energy term $(N-Z)^2/A$ in the Weizsäcker formula. The symmetry energy is assumed divided uniformly throughout nuclear matter as a symmetry energy density $k\eta^2/\rho$ and the volume integral of the symmetry energy density and energy in the external field $\mathscr{E}$ are minimised, giving the result above. (We have neglected the Coulomb energy of the protonic fluid and assumed $\rho = \rho_p + \rho_n$ = constant.) From this value of $\eta$ for nuclear matter, we find the polarisability for a sphere of radius $R$, and also $\sigma_{-2}$, and obtain

$$W_M = (40NZ\hbar^2 k/A^2 MR^2)^{\frac{1}{2}}. \tag{3}$$

Steinwedel and Jensen [4]) independently calculated the resonance energy $E_m$ in the two-fluid collective model and obtained essentially this value.

In a shell model the nuclear symmetry energy can be interpreted as due to the change in nuclear kinetic energy as $(N-Z)$ is varied, keeping the density constant. The increase of kinetic energy in the Fermi gas shell model agrees with the Weizsäcker formula, provided the Fermi energy $E_F = 3k$. (See e.g. Bethe and Bacher [35]), eqs. (165B) and (158B).) The value $E_F = 35$ MeV

from the nuclear density, and [36]) $k = 23$ MeV are in disagreement with the desired relation. Since in this paper we are not concerned with agreement with experiment, we need not use the numerical values for $E_F$ and $k$ given above; we merely stipulate that the relation $E_F = 3k$ holds, and proceed to use $k$ in Migdal's classical calculation and $E_F$ in the shell model calculation below. (We note, parenthetically, that the problem of making $E_F = 3k$ and the problem of making $\sigma_{int} > 0.015A$ MeV · barn are not unrelated. Both problems are solved semi-quantitatively by consideration of the velocity-dependence of the shell model potential.)

If a constant electric field $\mathscr{E}$ is present, the proton and neutron densities will vary with coordinate $z$ to keep the energy $E_F$ of the Fermi surface independent of $z$, as shown in fig. 2. Note that we use proton and neutron

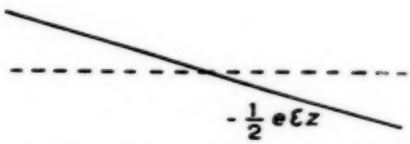


Fig. 2. Energy of protonic Fermi gas in electric field: the bottom of the Fermi sea slopes downwards to the right while the surface remains level.

"dipole effective charges" of $\frac{1}{2}e$ and $-\frac{1}{2}e$ respectively, since we are concerned with displacements relative to the nuclear centre of mass. The energy of the protonic Fermi surface for a linear variation of protonic density is (using $E_F = 3k$ and $\rho_p = \bar{\rho}_p + \frac{1}{2}\eta$)

$$3k\bar{\rho}_p^{-\frac{2}{3}}(\bar{\rho}_p + \tfrac{1}{2}\eta)^{\frac{2}{3}} - \tfrac{1}{2}e\mathscr{E}z = \text{constant}. \tag{4}$$

Setting the terms linear in $z$ equal to zero we have

$$\eta = (e\mathscr{E}/2k)\bar{\rho}_p z = (e\mathscr{E}\rho/4k)z. \tag{5}$$

This value for the rate of change of protonic density in nuclear matter is in exact agreement with Migdal's classical result (2). It must be, since our present treatment of degenerate Fermi gases is just one scheme of dividing the nuclear symmetry energy uniformly throughout the nucleus, and then adjusting the value of $\eta$ in an external electric field so as to minimise the nuclear energy. This Fermi gas treatment then gives Migdal's value of the polarizability, $W_M$, and $\sigma_{-2}$, and thus establishes the agreement of Fermi gas and collective model calculations of the energy $E_m$ of the giant dipole resonance.

The collective and shell models used above make the same approximation

of neglecting surface effects. In each treatment we find the linear change in $\eta = \rho_p - \rho_n$ for infinite nuclear matter. The nuclear surface enters only at the very end of the problem, when we integrate the dipole moment density $\frac{1}{2}e\eta z$ over the nuclear volume to find the total dipole moment produced by the external field, and the nuclear polarizability.

For a large nucleus this Fermi gas model might be expected to be a good approximation to the finite square well model. However, these two models give results differing appreciably in calculations [15]) of the value of the mean square dipole moment, and the corresponding bremsstrahlung weighted cross section $\sigma_b$. Nevertheless, our Fermi gas calculation of $\sigma_{-2}$ agrees rather closely with finite square well calculations [12,15]) of this quantity for copper and tantalum. (The numerical values are found for a shell model with nuclear radius parameter † $r_0 = 1.5\ f$ and corresponding values of $E_F$ and of $k$.) For copper the finite square well shell model and Fermi gas model give $\sigma_{-2} = 14.2$ and 12.6 mb/MeV respectively, while for tantalum the shell model and Fermi gas model give $\sigma_{-2} = 84$ and 72 mb/MeV respectively. Thus the Fermi gas model is low for the $\sigma_{-2}$ calculation by only 13 % for these two examples, and this difference gives only a $6\frac{1}{2}$ % difference between the shell and Fermi gas calculations of $W_M = (\sigma_{int}/\sigma_{-2})^{\frac{1}{2}}$. The Fermi gas model is a good approximation to the finite square well shell model for the $\sigma_{-2}$ calculation, but not for the $\sigma_b$ calculation, for the following reason. The principal approximation in the Fermi gas model consists in replacing a sum over discrete values of proton and neutron wave numbers by an integral over a continuous distribution of wave numbers. This replacement leads to small errors (if many terms are present in the sum) if we are summing a slowly varying function, but may lead to appreciable errors if we are summing a rapidly varying function. In the $\sigma_{-2}$ calculation we are summing over the nucleon's kinetic energy, to find the position of the Fermi surface. The kinetic energy varies smoothly and not very rapidly with wave number, so the Fermi gas approximation is reasonably good for a large nucleus. In one part of the $\sigma_b$ calculation [15]), we sum the values of the single particle squared dipole matrix element. The squared dipole matrix element oscillates rapidly with the particle wave numbers involved. Further the sum over discrete values (which are chosen to join the inside to outside wave functions) selects just the wave numbers giving a maximum value for the squared dipole matrix element, while the integral over the Fermi gas distribution gives a much lower and unreliable value.

Also, the value of $E_m$ in the simple harmonic oscillator shell model agrees fairly well with that in the finite square well shell model. (The agreement is shown [11]) by explicit calculation and is made plausible by reference to the uncertainty principle.) Thus the three approximate shell

† $f = 10^{-13}$ cm.

models treated here (Fermi gas, finite square well and simple harmonic oscillator) give very similar values of $E_m$; and this value agrees with the value of $E_m$ in the two-fluid collective model.

It is easy to extend the calculation of polarizability in the two-fluid or Fermi gases models to the case of deformed ellipsoidal nuclei. We merely take $\eta$ from eq. (2) and for this problem find the total polarization produced by integrating over the ellipsoidal volume. (We here assume that nuclear matter is isotropic, so that $\eta$ has the same value irrespective of the direction of the external field.) Let $R_1$ be the length of the major (principal) semi-axis, and $R_2$ the length of a minor semi-axis. If the electric field is directed along $z$ (the principal axis) the total polarization produced is

$$\int \tfrac{1}{2} e\eta z \mathrm{d}^3\tau = (e^2\mathscr{E}\rho/8k)\int z^2 \mathrm{d}^3\tau. \tag{6}$$

The polarizability, and hence $\sigma_{-2}$, for this direction of the electric field, is then proportional to the mean square value of $z$:

$$(\sigma_{-2})_z = a\overline{z^2} = aR_1^2/5. \tag{7}$$

If the electric field is along the $x$ (or $y$) axis, we find

$$(\sigma_{-2})_x = a\overline{x^2} = aR_2^2/5. \tag{8}$$

The proportionality constant is identical in (7) and (8). The different values of $\sigma_{-2}$ are used together with identical values for $\sigma_{\mathrm{int}}$ giving a mean energy inversely proportional to the length of the appropriate axis of the ellipsoid:

$$(W_M)_z = b/R_1, \qquad (W_M)_x = b/R_2. \tag{9}$$

The splitting $\Delta E$ of the giant resonance is expressed by Okamoto [7]) in terms of the energy $E_m$ of the resonance for a spherical nucleus of the same volume $E_m = a/R_0$ with $R_0^3 = R_1R_2^2$. The relative splitting from (9)

$$\Delta E/E_m = R_0(1/R_2 - 1/R_1) = \varepsilon(1-\varepsilon/3). \tag{10}$$

In the last equation we have introduced the eccentricity, defined as

$$\varepsilon = (R_1 - R_2)/R_0. \tag{11}$$

We have neglected terms in $\varepsilon^3$ in the last expression in (10). Our (10) is almost the same as Okamoto's result $\Delta E/E_0 = \varepsilon(1-\varepsilon)$. Further, (9) is almost the same as Danos's [8])

$$E_2/E_1 = 0.911\ R_1/R_2 + 0.089,$$

where the resonance energy $E_2 \approx (W_M)_x$ and $E_1 \approx (W_M)_z$. Recently Soga and Fujita [14]) have calculated the splitting for an ellipsoidal shell model, and obtain results similar to Okamoto's or ours. Since $\eta$ has the same value for the two-fluid and Fermi gas models, we see that collective and shell models should give very nearly the same value for the splitting $\Delta E$.

Here, as in the Okamoto-Danos collective treatment of photon absorption by deformed nuclei, we have implicitly assumed that the nuclear principal axis has some definite orientation. Hence the eccentricity $\varepsilon$ is taken corresponding to the intrinsic quadrupole moment $Q_0$ and (10) is applied even to nuclei of spin 0 or $\frac{1}{2}$, which cannot be polarized. Danos [8]) justifies this classical approximation of a definite orientation of the principal axis by the argument that the quantal fluctuations in the principal axis orientation occur at a much lower frequency $\omega_t$ than the resonance frequency $\omega_m = E_m/\hbar$. Hence in photon absorption the nucleus acts as if it has a fixed orientation. We make an analogous argument here: we have in fact been considering the nuclear polarizability for an external electric field of frequency $\omega$, where $\omega_t \ll \omega \ll \omega_m$. At frequency $\omega$ we can consider the principal axis as having a fixed orientation, but $\omega$ is small enough that $\eta$ will have very nearly the the same value as at zero frequency.

Also, see Baldin [37]) for a general treatment of effects due to the tensor character of the polarizability of an anisotropic nucleus.

There are several small corrections to the calculation of the polarizability of a spherical nucleus due to: i) dielectric constant of nuclear matter, ii) changes in the density $\rho = \rho_p + \rho_n$; iii) surface effects; iv) Coulomb energy of the protonic fluid.

The first effect is less than a 10 % correction for all nuclei [34]), since the polarization density is small.

The condition that the nuclear density $\rho$ remains constant for the displacement of the two fluids occurs naturally if we neglect the Coulomb energy of the protonic fluid, and correspondingly consider a self-conjugate nucleus. If we use effective charges $\frac{1}{2}e$ for each proton and $-\frac{1}{2}e$ for each neutron, the nuclear energy $E$ is

$$E = \int (k\eta^2/\rho - \tfrac{1}{2}e\mathcal{E}z\eta)\mathrm{d}^3r. \tag{12}$$

Minimising $E$ by taking a variation $\delta\eta$ we have

$$\int (2k\eta/\rho - \tfrac{1}{2}e\mathcal{E}z)\delta\eta\mathrm{d}^3r = 0. \tag{13}$$

We again obtain Migdal's result for $\eta$ given in (2): In fact all we have done is to repeat Migdal's calculation, introducing effective charges and neglecting the Coulomb energy. With our use of effective charges it is clear that the condition $\rho$ = constant is *not* a constraint imposed by assuming that nuclear matter is incompressible. On the contrary, $\rho$ does not appear at all in (12) or (13) except in the innocuous form of the denominator in $k\eta^2/\rho$, and therefore changes in the density $\rho$ will not be caused by the external electric field. (However, see Migdal, and below, for discussion of the small Coulomb effects.)

Measurements of the nuclear charge distribution show that the nuclear surface is a layer of some $3f$ thickness in which the density $\rho$ gradually decreases from its central value to zero. Effects of this diffuse surface can be included in the calculation above by inserting in (12), (13) and (2) the variation of $k/\rho$ with $\rho$, and hence with $z$. The dependence of $k$ on $\rho$ is not certain at present. If $k$ is proportional to $\rho$ we obtain $\eta$ proportional to $z$, as in Migdal's treatment. (The constraint $|\eta| \leqq \rho$ demands that (2) holds only out to the edge of the diffuse boundary of the nucleus.) We again find the polarizability proportional to the mean square value of $z$ as used in (7). If $k/\rho$ decreases rapidly with decreasing $\rho$ then $\eta$ increases rapidly in the diffuse boundary region. In this case we would obtain a large contribution to the polarizability from the surface region — the two-fluid model would be similar to the rigid spheres model of Goldhaber and Teller [3]) in which the polarization occurred only at the nuclear surface. However, we cannot obtain precisely the rigid sphere model unless we assume an *arbitrary* constraint on $\eta$. Thus the two-fluid model seems to us much more reasonable than the rigid spheres model. Effects in the interior of the nucleus should occur as in the two-fluid model, and effects in a diffuse boundary region can in principle also be included in the two-fluid model.

The Coulomb energy density of the protonic fluid modifies the calculation of $\eta$ in two ways. First, the Coulomb energy tends to keep the proton density isotropic, but increasing slightly towards the edge of the nucleus [34]). This tendency towards a slightly smaller value of $\eta$ gives a smaller polarizability and smaller $\sigma_{-2}$, and therefore a slightly larger $W_M$. This small increase in $W_M$ due to Coulomb effects was also found by Danos [5]). Second, the Coulomb energy adds a term to the nuclear energy that depends on the product $\eta\rho$.

The solution for $\eta$ now depends on the change in the value of $\rho$ which could be found by consideration of the nuclear compressibility. If we consider the dynamics of the two-fluid motion including both Coulomb and compressibility effects, as done by Araújo [6]), we find that in the absence of the Coulomb energy density there are two uncoupled oscillations possible: ordinary sound involving changes of $\rho$ and "second sound" involving changes in $\eta$. Only second sound is excited in electric dipole absorption. The Coulomb energy density couples the two oscillations, thus increasing the difference between the eigenfrequencies of the coupled system. Both effects of the Coulomb energy density are small, and will not be considered further here.

## 4. Discussion

In section 2 we have discussed various unsuccessful methods of determining whether the nuclear photoeffect can be better interpreted as a collective or a shell model effect. In section 3 we showed that collective and shell models

give the same value for the resonance energy $E_m$. In the case of well separated resonances, which was not treated above, any given compound nucleus level has a definite wave function, and by suitable experiments one can determine how closely this wave function corresponds to the wave function of one or another shell model, and how closely it corresponds to a collective model wave function, or to both. On the other hand, for the case discussed in this paper of overlapping compound nucleus levels, we are no longer able to study the wave function of a given level. Instead we must discuss the problem in terms of a distribution of strength functions, as used by Lane, Thomas and Wigner [21]) in discussing the success of the optical model of nucleon scattering. The scattering cross section, averaged over a small energy interval that contains many compound states, is proportional to the average of the strength function of some given shell model state. (The shell model strength function of a given compound state is the square of the overlap integral between the compound state wave function and the shell model wave function.)

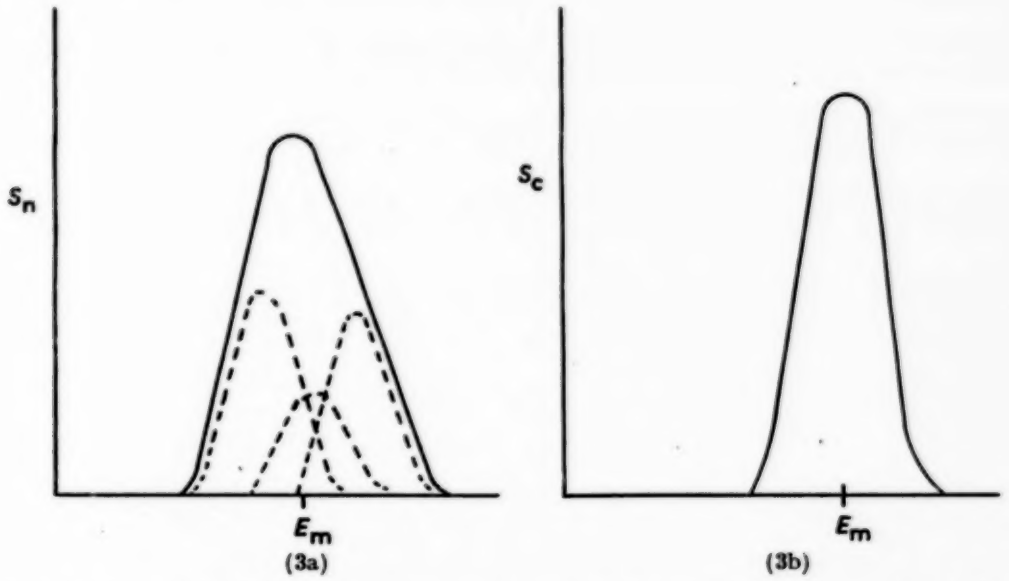


Fig. 3. Strength function distributions. In 3a the dotted curves show schematically $f_{0n}S_n$, where $S_n$ is the shell model strength function for shell model state $n$, and $f_{0n}$ is the shell model oscillator strength for transitions from the ground state. The solid curve shows the sum of the dotted curves and is proportional to the cross section for photon absorption. Fig. 3b shows the collective model strength function distribution. The collective model strength function is defined as the square of the overlap integral of the collective model wave function for the excited state with the compound nucleus wave function.

Experiments on the cross section for photon absorption can be analysed in terms of shell model strength functions for the different shell model states that may be excited. A schematic example of that analysis is shown in fig. 3a.

Each shell model strength function $S_n$ is assumed to have a symmetrical distribution peaked at the energy $E_n$ of the shell model state. The $n$'th state is weighted by the shell model oscillator strength $f_{0n}$ for transitions from the ground state to that state. The cross section $\sigma(W)$ is proportional to $\sum_n f_{0n}S_n$. This type of analysis was done by Rand [38]). However, we have reinterpreted his 'natural width of the shell model excited state' in terms of a distribution $S_n$ of strength functions. Further, in terms of the present lack of detailed theoretical or experimental knowledge concerning $S_n$, we do not specify that $S_n$ should have the same width for different states $n$.

As an alternative, the cross section for photon absorption can be analysed in terms of the collective model strength functions $S_c$, defined as the square of the overlap integral of the compound state wave function with the wave function for a collective excitation. $S_c$ will, presumably, have a symmetrical shape similar to that of one of the shell model strength function distributions, and is so shown in fig. 3b.

We now have a notation in which we can discuss the question whether the shell model or the collective model is better for the interpretation of photonuclear reactions. Neither model is exact but the better model has the narrower distribution for its strength function. At present the relevant strength function distributions are only poorly known, since the shell model $S_n$'s needed for photon absorption are principally for states of high orbital angular momenta for the excited particle [13]), whereas the analysis of nucleon scattering gives principally the strength function distribution for shell model states of low angular momenta. Further experiments on nucleon scattering could, in principle, give experimental values of the width of the strength function distributions for states in which the excited particle has a high angular momentum. These widths, combined with the energy spread of the shell model states would give the width of the $\sum_n f_{0n}S_n$ curve of fig. 3a. If this calculated width were appreciably larger than the experimental width of the photon absorption cross section for spherical nuclei, that would show that the shell model was not a good model for calculation of photon absorption. The smaller experimental width of the photon absorption curve would be interpreted in terms of the "pulling together" of the shell model states, and their strength function distributions, by collective effects. In this eventuality we would conclude that the collective model better represented the compound states reached by photon absorption. Until these experimental data are available, we are unable to show whether the shell or collective model is a better approximation to the very many compound states reached in the giant dipole resonance.

We are very grateful to Professor R. E. Peierls and to many other colleagues at the Universities of Birmingham, Oxford and Manchester, and at

the Institute of Theoretical Physics (Copenhagen) and at A.E.R.E., Harwell for helpful discussions of these problems.

## References

1) J. S. Levinger, Ann. Rev. Nucl. Sci **4** (1954) 13
2) J. S. Levinger, Rev. Mexicana de Fis. **5** (1956) 177
3) M. Goldhaber and E. Teller, Phys. Rev. **74** (1948) 1046
4) H. Steinwedel and J. H. D. Jensen, Z.f. Naturforsch. **5a** (1950); Z.f. Naturforsch. **5a** (1950) 413
5) M. Danos, Ann. Phys. **10** (1952) 265
6) J. M. Araújo, Nuovo Cimento **12** (1954) 780
7) K. Okamoto, Phys. Rev. **110** (1958) 143
8) M. Danos, Nuclear Physics **5** (1958) 23
9) M. Ferentz, M. Gell-Mann and D. Pines, Phys. Rev. **92** (1953) 836
10) S. S. Wu, Ph. D. Dissertation, University of Illinois (1951) (unpublished)
11) J. S. Levinger, Phys. Rev. **97** (1955) 122
12) J. L. Burkhardt, Phys. Rev. **91** (1953) 420
13) D. H. Wilkinson, Physica **22** (1956) 1039
14) M. Soga and J. Fujita, Nuovo Cimento **6** (1957) 1494
15) J. S. Levinger and D. C. Kent, Phys. Rev. **95** (1954) 418
16) Y. K. Khokhlov, Zh. Expt. The. Fis. **23** (1952) 241
17) J. S. Levinger, Phys. Rev. **84** (1951) 43
18) K. Dedrick, Phys. Rev. **100** (1955) 58
19) K. Gottfried, Nuclear Physics **5** (1958) 557
20) P. Kapur and R. E. Peierls, Proc. Roy. Soc. A **166** (1938) 277
21) A. M. Lane, R. G. Thomas and E. P. Wigner, Phys. Rev. **98** (1955) 693
22) J. S. Levinger, N. Austern and P. Morrison, Nuclear Physics **3** (1957) 456
23) J. Fujita, Prog. Theor. Phys. **14** (1955) 400
24) K. Wildermuth and H. Wittern, Z. f. Naturforsch. **12a** (1957) 39
25) A. M. Lane and C. F. Wandel, Phys. Rev. **98** (1955) 1524
26) J. S. Levinger and H. A. Bethe, Phys. Rev. **78** (1950) 115
27) H. Feshbach, C. E. Porter and V. F. Weisskopf, Phys. Rev. **96** (1954) 448
28) E. G. Fuller and E. Hayward, Phys. Rev. **101** (1956) 692
29) G. E. Brown and J. S. Levinger, Proc. Phys. Soc. **71** (1958) 733
30) D. Brink, Nuclear Physics **4** (1957) 213
31) K. A. Brueckner, R. J. Eden and N. C. Francis, Phys. Rev. **98** (1955) 1445
32) J. Dąbrowski, Proc. Phys. Soc. **71** (1958) 658
33) J. S. Levinger, Phys. Rev. **107** (1957) 554
34) A. Migdal, J. Phys. U.S.S.R. **8** (1944) 331
35) H. A. Bethe and R. F. Bacher, Revs. Mod. Phys. **8** (1936) 82
36) A. E. S. Green, Phys. Rev. **95** (1954) 1006
37) A. M. Baldin, Moscow Conference on Nuclear Physics (1957)
38) S. Rand, Phys. Rev. **107** (1957) 208

7.A:8.B *Nuclear Physics* 8 (1958) 444—460; © *North-Holland Publishing Co., Amsterdam*
Not to be reproduced by photoprint or microfilm without written permission from the publisher

# BOUND STATES AND SCATTERING OF BARYONS IN CONTACT INTERACTION

I. V. POLUBARINOV
*Joint Institute of Nuclear Research, Laboratory of Theoretical Physics, Dubna, USSR*

Received 4 April 1958

**Abstract:** The possibility of treating $\pi$ and K mesons as bound states in the four-baryon interaction theory is considered. The cross section for baryon-baryon scattering is derived within the framework of this theory in the chain approximation. The validity of the first approximation of perturbation theory for the cross section is discussed.

## 1. Introduction

Four-fermion interactions are apparently characteristic of a large number of phenomena encountered in elementary particle physics. These interactions determine $\beta$ decay of neutrons, $\mu$ meson decay and possibly $\mu$ and $\beta$ decays of hyperons, etc. The question arises as to how large is the number of fermions between which four-fermion interactions exist. Thus, for example, does a direct four-fermion interaction (contact interaction) exist between nucleons and in general baryons (nucleons, hyperons), or between electrons, etc., and, if so, how can they manifest themselves? What facts are inconsistent, or under what conditions would they be inconsistent, with the assumption of the existence of such forces?

We shall consider from this viewpoint the possibility of contact interaction between baryons. Interaction between baryons is usually treated as an interaction occurring via a third field (meson, electromagnetic). However, in the present status of the theory, one cannot exclude the possibility of an interaction specified by the interaction Lagrangian

$$\mathscr{L}(x) = \tfrac{1}{4}g[\bar{\psi}(x),\ O_{\mathrm{T}}\psi(x)][\bar{\varphi}(x),\ O_{\mathrm{T}}\varphi(x)] \qquad (1)$$

where $g$ is the coupling constant and $\psi(x)$ and $\varphi(x)$ are operators of the two Dirac fields of the baryons (e.g., of the proton and neutron).

Contact interaction is especially interesting in connection with the problem of classification of elementary particles. In the classification proposed by M. A. Markov [1]) † one of the important features was the

† A similar classification has been proposed in Japan by S. Sakata [2]).

assumption that baryons and antibaryons can combine to form bosons. This assumption can be understood either in a very broad sense or in a more restricted one as in the hypothesis of Fermi and Yang [3]). According to this hypothesis, the nuclear forces are not explained by $\pi$ mesons but the $\pi$ mesons themselves are considered to be products of some peculiar (contact) nuclear forces of the type (1), and, in fact, as bound nucleon-anti-nucleon states. In this sense K mesons can also be envisaged as nucleon-anti $\Lambda$ hyperon bound states [1]).

As Fermi and Yang [3]) have pointed out, in order that along with the $\pi$-meson as a bound nucleon-antinucleon state, no bound nucleon-nucleon systems exist which are as strongly bound as the $\pi$-meson system, only vector and tensor couplings should be suitable. All other types of coupling will yield identical mass defects for the nucleon-nucleon and nucleon-anti-nucleon bound states. However, the possibility remains of using linear combinations of vector or tensor coupling and of other types of coupling.

For the investigation of bound states it seems natural to adopt an equation of the Bethe-Salpeter type. Unfortunately, even in the lowest (chain) approximation for contact interaction this equation contains a divergence which can be excluded only by resorting to a cut-off procedure. Bound states have been studied from the point of view of a Bethe-Salpeter equation of this type by H. Katsumori [4]) and Z. Maki [5]). However, the first of these authors considered only bound states of particles with equal masses and some errors were made, in particular in the most interesting case of those considered, namely, in the case of vector coupling †. As we shall see in section 3, Katsumori's conclusion that vector coupling does not yield any advantages over scalar or pseudoscalar coupling is incorrect. Z. Maki [5]) considered an interaction which could be represented as a combination of all 5 types of interaction (1). This interaction was taken in a charge-independent form. The results obtained by Z. Maki are close to those derived by us and presented in section 3.

Our aim is to investigate (within the limits of the Bethe-Salpeter equation) the two main types of interaction in (1), viz., vector and tensor coupling. Not only bound states but scattering as well will be considered.

It should be mentioned that the field operator equations under consideration differ from the Heisenberg equations in that they contain a mass term (see ref.[6]) in which all preceding papers are listed). The boson wave function equations turn out to be similar to the corresponding Heisenberg equations; but we shall apply the usual "linear" quantization procedure (as was done in ref.[4]) and [5])) in which the free equations are considered to be meaningful.

† For example, the graphs corresponding to our fig. 1(a) are not correct.

## 2. Solution of Initial Equation

We shall consider our problem with the help of the Bethe-Salpeter equation † in the lowest (chain) approximation ††

$$\chi(12) = \chi^0(12) + \int \tfrac{1}{2} S_F(13) \tfrac{1}{2} S_F(24) G(34; 56) \chi(56) dx_3 \dots dx_6. \quad (2)$$

Here $\chi(12)$ is the Bethe-Salpeter wave function for a two-particle system. The function $\chi^0(12)$ vanishes in the bound state problem and in the scattering problem refers to the state of the system for $t_{1,2} = -\infty$, when the interaction is turned off.[9]) In the lowest approximation the $S_F(12)$ are simply free propagation functions. In the chain approximation the first term in the expansion of $G$ (34; 56) in $g$ is accepted as the interaction operator. In order to remove the divergence in the equation we replace the product of the three $\delta$-functions by a nonlocal form-factor $\delta(35)\delta(34)\delta(56) \to \mathscr{F}(34; 56)$, that is, we put

$$G(34; 56) = igO_T^1 O_T^2 \mathscr{F}(34; 56) \quad (3)$$

where the superscripts 1 and 2 in $O_T$ signify that these matrices refer to the first and second fields respectively (this notation will be employed in the following exposition). For $\mathscr{F}$ (34; 56) we accept the Kristensen-Möller form factor [10]) previously used in ref.[4])

$$\mathscr{F}(34; 56) = (2\pi)^{-12} \int G(\Pi^2) G(\Pi_1^2) \exp\{i[\alpha P(x_3 - x_5) + \beta P(x_4 - x_6) + p(x_3 - x_4) + q(x_5 - x_6)]\} d^4P d^4p d^4q$$

where

$$\Pi^2 = p^2 - (pP)^2 P^{-2}, \qquad \Pi_1^2 = q^2 - (qP)^2 P^{-2},$$

$G(\Pi^2)$ equals unity for $\Pi^2 \leqq q^2$ and is zero for $\Pi^2 > q^2$, $\alpha$ is an arbitrary quantity, and $\beta = 1 - \alpha$.

As shown by Nishijima [9]) the matrix elements of the $S$-matrix can be expressed through the Bethe-Salpeter wave functions in the following manner:

$$S_{ba} = \delta_{ba} + \int \bar{\chi}_b^0(12) G(12; 34) \chi_a(34) dx_1 dx_2 dx_3 dx_4 \quad (4)$$

where $\chi_b^0(12)$ is the wave function of the final state of the system. According to Nishijima the normalization condition in the lowest approximation can be written in the form †††

$$\int d\sigma_\mu \langle a | j_\mu^1(x) | a \rangle \approx i \int d\sigma_\mu \bar{\chi}_a(x, 2) \gamma_\mu^1 \tfrac{1}{2} S_F^1(x, 3) G(32; 54) \chi_a(54) dx_2 \dots dx_5 = 1. \quad (5)$$

† This equation can be derived in various ways. In ref.[7]) it was obtained specially for contact interaction by the Schwinger method [8]).

†† The numerical arguments include a 4-coordinate and spinor index; if the argument is encountered twice summation over the spinor index is implied.

††† This condition evidently signifies that there is one particle from field 1 ($j_\mu^1(x) = \frac{1}{2} i[\bar{\psi}(x). \gamma_\mu \psi(x)]$ is the current operator of the first field).

If the solution of eq. (2) be sought in the form

$$\chi(12) = \exp(iPX)\chi(x) \tag{6}$$

($P$ is the four-momentum of the system; $X = \alpha x_1 + \beta x_2$, $x = x_1 - x_2$) and $\chi^0(1, 2)$ be represented in a similar form, we obtain

$$\chi(x) = \chi^0(x) - \frac{ig}{(2\pi)^4}\int G(\Pi^2) S_F^1(\alpha P + p, m_1) S_F^2(\beta P - p, m_2) \exp(ipx) \mathrm{d}p O_T^1 O_T^2 \chi \tag{7}$$

where

$$S_F(p, m) = (i\gamma p + m)^{-1}, \qquad \chi = (2\pi)^{-4}\int G(\Pi^2) \exp(ipx)\chi(x)\mathrm{d}p\mathrm{d}x. \tag{8}$$

Hence for $\chi$ we obtain the equation †

$$\chi - g\{A - BM^{-2}(\gamma^1 P)(\gamma^2 P) + \tfrac{1}{3}C[(\gamma^1\gamma^2) + M^{-2}(\gamma^1 P)(\gamma^2 P)] - iDM^{-1}(\gamma^1 P) - iEM^{-1}(\gamma^2 P)\} O_T^1 O_T^2 \chi = \chi^0 \tag{9}$$

where $\chi_0$ is expression (8) for $\chi_0(x)$, and $M = \sqrt{-P_\mu^2}$ is the mass of the two-particle system. The expressions for the coefficients $A$, $B$, $C$, $D$ and $E$ are presented in appendix 1.

With the aid of (4), (6) and (7) we obtain the following expression for the matrix elements of the $S$ operator:

$$S_{ba} = \delta_{ba} + (2\pi)^4 ig\bar{\chi}_b^0 O_T^1 O_T^2 \chi_a \delta(P_b - P_a) \tag{10}$$

where $P_a$ and $P_b$ are the 4-momenta of the initial and final states. It is interesting to note that in accord with the general theory of the $S$ matrix these matrix elements have poles for those values of $M < m_1 + m_2$, which are the mass levels of the bound states. $\chi_a$ possesses such poles because, since it is a solution of the inhomogeneous equation (9), it is inversely proportional to the determinant of (9). On the other hand vanishing of this determinant is a condition of solubility of the homogeneous equation and yields the mass levels of the bound system.

With the aid of (5), (6) and (7) the following expression is obtained for the bound state normalization constant (in the c.m.s. in which $\mathbf{P} = 0$):

$$N^2 = Vg^2\bar{\psi}\{A' + B'\gamma_4^1\gamma_4^2 + \tfrac{1}{3}C'\gamma^1{}_k\gamma_k{}^2 + D'\gamma_4^1 + E'\gamma_4^2\}\psi \tag{11}$$

where

$$\psi = O_T^1 O_T^2 \chi, \qquad \bar{\psi} = \bar{\chi} O_T^1 O_T^2$$

(as above the first index $\chi$ refers to the first field and the second one to the second field). The primes in (11) denote derivatives with respect to $M$ ††.

† See appendix 1

†† Expression (11) can be easily obtained by using formula (A1) in appendix 1 and the relation

$$i\frac{\mathrm{d}}{\mathrm{d}p_\mu} S_F(p, m) = S_F(p, m)\gamma_\mu S_F(p, m).$$

Considering $\chi$ as a $4\times4$ matrix (the first index refers to the first field and the second to the second field) and representing it by the expansion

$$\chi = \sum_{i=1}^{16} a_i \gamma_i C \tag{12}$$

where the expansion coefficients are $a_i = 4^{-1}\,\mathrm{tr}\,[(\gamma_i C)^{-1}\chi]$ we transform equation (9) to a set of equations for $a_i$. An expansion in $\gamma_i C$ (and not $\gamma_i$) is convenient in that these matrices possess the transformation properties

$$S^1 S^2 \gamma_i C = S\gamma_i C\tilde{S} = S\gamma_i S^{-1} C = \tilde{a}_{ij}\gamma_j C$$

TABLE 1

| No. | Type $\chi$† | Spin | Space parity | Number of solutions | |
|---|---|---|---|---|---|
| | | | | In vector theory | In tensor theory |
| 1 | $[I+a(\gamma P)]C$ | 0 | even | 2 | 1 |
| 2 | $[I+b(\gamma P)]\gamma_5 C$ | 0 | odd | 2 | 1 |
| 3 | $[\gamma_\mu+M^{-2}(\gamma P)P_\mu+c\sigma_{\mu\nu}P_\nu]C$ | 1 | odd | 4 †† | 4 †† |
| 4 | $[\gamma_\mu+M^{-2}(\gamma P)P_\mu+d\sigma_{\mu\nu}P_\nu]\gamma_5 C$ | 1 | even | 4 †† | 4 †† |
| 5 | $\sigma_{\mu\nu}C$ | 1 | even, odd | 6 ††† | 0 |
| 6 | $\gamma_\mu C$ | 1,0 | odd, even | 0 | 4 †† |
| 7 | $\gamma_\mu\gamma_5 C$ | 1,0 | even, odd | 0 | 4 †† |

† Expression for coefficients $a$, $b$, $c$, $d$ are given in appendix 3. The spinor space-reflection operator is chosen in the form $i\gamma_4$. One has $\sigma_{\mu\nu} = i(\gamma_\mu\gamma_\nu - \delta_{\mu\nu})$.

†† $\mu = 1, 2, 3, 4$.

††† $\mu, \nu = 1, 2, 3, 4$, $\mu < \nu$.

($S^i$ and $||a_{ij}||$ are (Dirac) spinor and tensor transformation matrices). After solving the inhomogeneous set of equations (scattering) for $a_i$ we express the $a_i$ through coefficients $a_i^0$ of expansion (12) for $\chi^0$

$$a_i = \sum_{j=1}^{16} A_{ij} a_j^0$$

so that $\chi$ will have the form †

$$\chi = \sum_{i=1}^{16}\sum_{j=1}^{16} A_{ij} a_j^0 \gamma_i C. \tag{13}$$

The solutions of homogeneous eq. (9) obtained by solving the homogeneous set of equations for $a_i$ are presented in table 1. The $g^{-1}$ are obtained as eigenvalues by solving the homogeneous equation ††. This yields the relation

† The coefficients $A_{ij}$ for tensor and vector coupling in the c.m.s. ($\mathbf{P} = 0$) are presented in appendix 2.

†† They are given in appendix 3.

between $g$ and $M$. Such relations are plotted in fig. 1 and 2 for $k = m_N$ ($m_N$ is the nucleon mass). The masses of bound systems can be found from

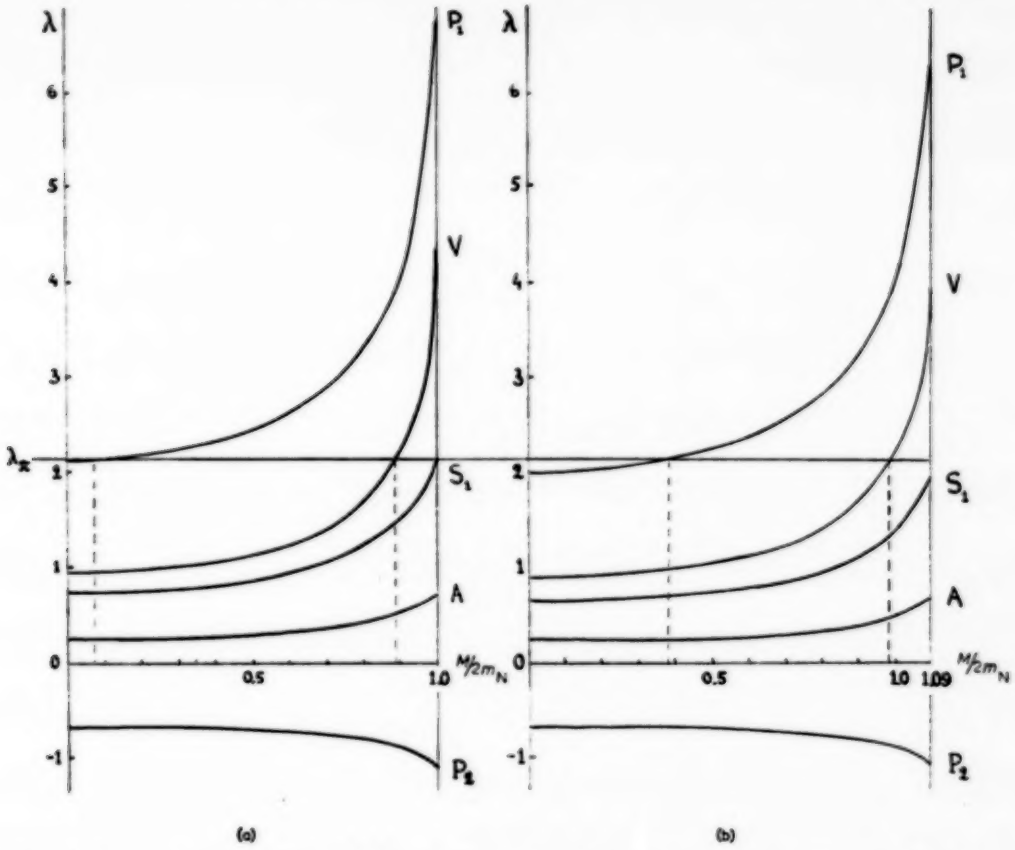


Fig. 1. Vector theory. $\lambda = 2(2\pi)^2 m_N^{-2} g^{-1}$ as a function of $M/2m_N$ for $k = m_N$ and (a) $m_1 = m_2 = m_N$ and (b) $m_1 = m_N$, $m_2 = m_A$. For $S_2$, $\lambda = 0$ in case (a) and in case (b) $\lambda$ closely approaches the abscissa axis. $\lambda_\pi$ is the value of $\lambda$ for which the mass of the pseudoscalar bound system $P_1$ with $m_1 = m_2 = m_N$ equals the experimental value of the $\pi$ meson mass. The dotted lines intersect the abscissa axis at points corresponding to the masses of the bound states at $\lambda = \lambda_\pi$.

the graphs by prescribing the couple constant $g$. For the last three types of solutions in table 1 one has $g^{-1} = 0$ and thus these solutions apparently do not have any physical meaning.

## 3. Bound States

The space parity and spin of $\chi$ presented in table 1 completely determine the space parity and spin of the final solutions (6). It should be noted that a linear dependence, $P_\mu \chi_\mu = 0$ exists between the solutions of types 3 and 4 in table 1. They therefore refer to spin 1 only. Hence for a finite $g$ only scalar, pseudoscalar, vector or pseudovector solutions can exist (in figs. 1 and 2 the corresponding functions $g^{-1}(M)$ are denoted by S, P, V and A).

One may attempt to identify the pseudoscalar states for $m_1 = m_2 = m_N$ with the $\pi$ meson by suitably choosing the coupling constant so that $M$

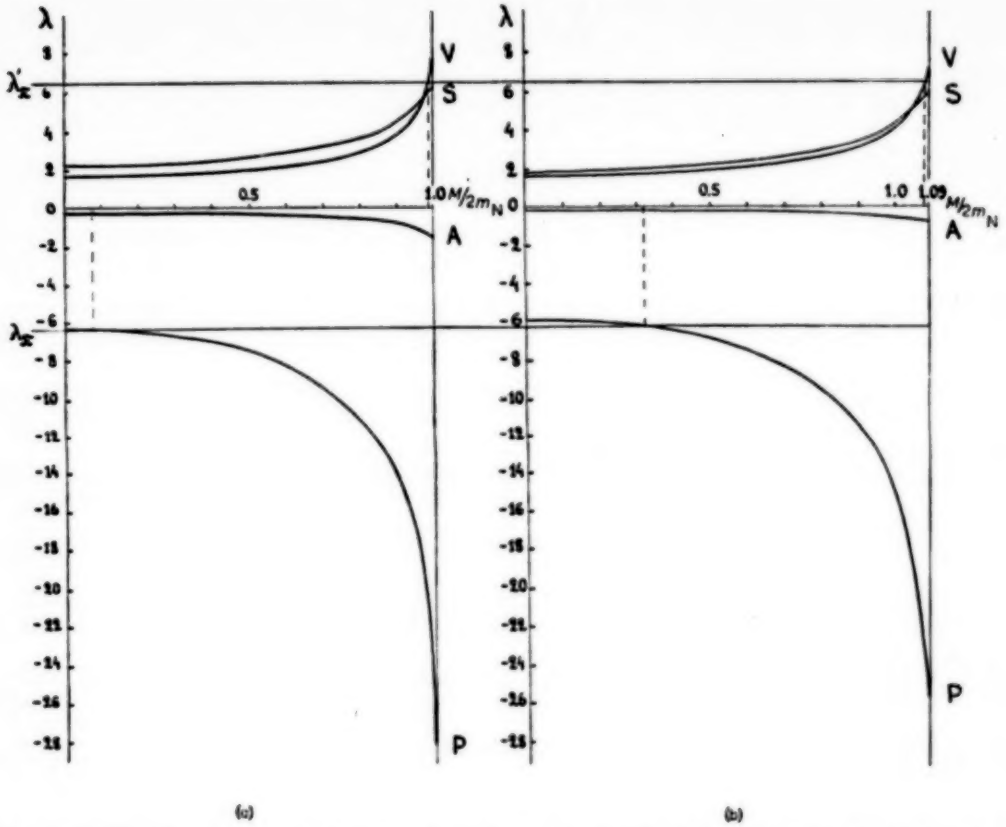


Fig. 2. Tensor theory. $\lambda = 2(2\pi)^2 m_N^{-2} g^{-1}$ as a function of $M/2m_N$ for $k = m_N$ and (a) $m_1 = m_2 = m_N$; (b) $m_1 = m_N$, $m_2 = m_\Lambda$. $\lambda_\pi$ is the value of $\lambda$ for which the mass of a psendoscalar system (P) with $m_1 = m_2 = m_N$ is equal to the experimental $\pi$-meson mass. $\lambda'_\pi = -\lambda_\pi$. The dotted lines intersect the abscissa axis at points corresponding to the masses of the bound states at $\lambda = \lambda_\pi$ and $\lambda'_\pi$.

equals the experimental $\pi$ meson mass. This can be done graphically; for example, for $k = m_N$ from graphs 1a and 2a. Other possible states for the same $g$ will also be states of particle-antiparticle systems. On the other hand for $g' = -g$ in vector or tensor coupling we obtain states of a particle-particle system. Results of identifying pseudoscalar states with $\pi$ mesons are presented in table 2 (S, P, V are respectively scalar, pseudoscalar and vector states).

Two types of pseudoscalar states ($P_1$ and $P_2$) are possible for vector coupling but from table 2 it can be seen that if $P_2$ is identified with the $\pi$ meson no bound states appear in the ($N\bar{\Lambda}$) system if $g \approx 10^{-49}$ erg · cm$^3$. According to table 2 for those values of the coupling constant for which a complex $\pi$ meson exists either no bound nucleon-nucleon system exists in general or (as in tensor theory for $k = m_N$) a bound state does exist, but its

mass strongly differs from that of the $\pi$ meson. The latter state is a vector state and the small mass defect may indicate that it is related in some way

TABLE 2
Masses of bound states in vector and tensor theories

| Theory | $k$ | $g_{\bar{n}-p}$ erg · cm³ | $m_1 = m_2 = m_N$ | | | $m_1 = m_N$, $m_2 = m_\Lambda$ | |
|---|---|---|---|---|---|---|---|
| | | | Nucleon-antinucleon ($\tilde{n}p$) or ($n\tilde{p}$) | | nucleon-nucleon (np) | ($N\tilde{\Lambda}$) ($\tilde{N}\Lambda$) | ($N\Lambda$) |
| | | | States identified with $\pi$-meson | Other states | | | |
| Vector | $m_N$ | $5.1 \times 10^{-43}$ | $P_1$ ($M = 273m_e$) | V ($M = 3300m_e$) | – | $P_1$ ($M = 1400m_e$) V ($M = 3600m_e$) | – |
| | $10^3 m_N$ | $2.8 \times 10^{-40}$ | $P_1$ ($M = 273m_e$) | – | – | $P_1$ ($M = 1300m_e$) | – |
| | $m_N$ | $-1.6 \times 10^{-43}$ | $P_2$ ($M = 273m_e$) | – | – | $P_2$ ($M = 980m_e$) | $S_1$ ($M = 1650m_e$) |
| | $10^6 m_N$ | $-1.2 \times 10^{-40}$ | $P_2$ ($M = 273m_e$) | – | – | – | – |
| Tensor | $m_N$ | $-1.7 \times 10^{-43}$ | P ($M = 273m_e$) | – | V ($M = 3600m_e$) | P ($M = 1200m_e$) | V ($M = 4000m_e$) |
| | $10^3 m_N$ | $-0.92 \times 10^{-40}$ | P ($M = 273\, m_e$) | – | – | P ($M = 1300m_e$) | – |

to the deuteron. However, the possibility exists that a more rigorous approach may reveal that the deuteron does not exist in the chain approximation (within the framework of our qualitative study a state of this type will not exist even in tensor theory for $k = 10^3 m_N$); however, if the theory is correct higher approximations should lead to this state.

Bound ($N\tilde{\Lambda}$) states appearing simultaneously with a $\pi$ meson may be interpreted as K mesons [1]). It is, of course, not surprising that the K meson mass ($\approx$ 1000—1300 $m_e$) does not quantitatively agree with the experimental value as our treatment is of a qualitative nature. However, it may be noted that substitution of $\tilde{\Lambda}$ for $\tilde{N}$ in a bound state leads to an increase of mass. From table 2 it can be seen that in the vector theory, when $g \approx 10^{-49}$ erg · cm³, identification of state $P_2$ with the $\pi$-meson does not lead to the K meson.

Finally it should be emphasized that (see table 2) along with the $\pi$ meson there are very few other bound states which can simultaneously exist, especially for $g \approx 10^{-49}$ erg · cm³. The effective $\pi$ meson-nucleon coupling constant can be estimated with the help of the normalized wave function for the

pseudoscalar pñ ($\pi$ meson) bound state. This can be performed in the same way as was done by Fermi and Yang [3]) by comparing the matrix element of the Lagrangian of interaction (1) for the virtual process $p \to n+\pi$ with the matrix element of the conventional meson theory. The effective pseudoscalar ($f$) and pseudovector ($\eta$) coupling constants between $\pi$ mesons and nucleons in the vector (V) or tensor (T) theories are presented in table 3 and seem to be reasonable. ($f^2/\hbar c \approx 10$ for $g \approx 10^{-49}$ erg · cm$^3$.) Only values for the $P_1$ state are presented in the table for vector theory. As far as the $P_2$ state is concerned (it was already mentioned above that this state, when $g \approx 10^{-49}$ erg · cm$^3$, is not sufficient to yield a unified description of $\pi$ and K mesons) we can only note that it yields $f/\eta \ll 1$ which is also not consistent with the experimental facts.

TABLE 3

Effective $\pi$ meson-nucleon coupling constants

| $k$ | $g_{\bar{n}-p}$ (erg · cm$^3$) | $\frac{f^2_{V,T}}{\hbar c}$ | $\frac{\eta_V^2}{\hbar c}$ | $\frac{\eta_T^2}{\hbar c}$ |
|---|---|---|---|---|
| $m_\pi$ | $g_V = 5\times10^{-43}$<br>$g_T = -2\times10^{-43}$ | 230 | 1.2 | 0 |
| $10^3\, m_\pi$ | $g_V = 3\times10^{-49}$<br>$g_T = -1\times10^{-49}$ | 6.3 | $\approx 10^{-12}$ | 0 |

## 4. Scattering

Suppose that in formula (10) we accept as states a and b those states which possess definite momenta and definite projections of the spin of the two particles (i.e., $\chi_a^0$ (12) and $\chi_b^0$ (12) are taken in the form of products of Dirac plane waves). If we then change over to the cross section, with the help of (13) average over the initial spin states and then sum over the final spin states, we obtain the following expression for the differential cross section in the c.m.s. ($\mathbf{P} = 0$)

$$\frac{d\sigma}{d\Omega} = \frac{g^2 G(p^2)}{2^{10}(2\pi)^2(\varepsilon_1+\varepsilon_2)^2} \sum_{i,j,i',j'=1}^{16} A_{ij} A^*_{i'j'} \cdot \tag{14}$$

$$\mathrm{tr}\,[(i\gamma p_1 - m_1)\beta\gamma_{j'}\beta(i\gamma p_2 + m_2)\gamma_j]\,\mathrm{tr}\,[(i\gamma p_3 - m_1)O_T\gamma_i O_T(i\gamma p_4 + m_2)O_{T'}\beta\gamma_{i'}\beta O_{T'}]$$

where $p_1$ and $p_2$ are the 4-momenta of the incident particles and $p_3$ and $p_4$ are the 4-momenta of the scattered particles; $\varepsilon_i = \sqrt{p^2+m_i^2}\,(i = 1, 2)$; $p$ is the momentum in the c.m.s. Evaluation of the sum in (14) leads to the following cross sections in vector (V) and tensor (T) theories ($\hbar = c = 1$):

$$\frac{d\sigma_V}{d\Omega} = \frac{g^2 G(p^2)}{16(2\pi)^2(\varepsilon_1+\varepsilon_2)^2}$$
$$\times\{|A_{04,04}(\varepsilon_1-\varepsilon_2)^2-4A_{00,04}(m_1+m_2)(\varepsilon_1-\varepsilon_2)$$
$$-2A_{00,00}(m_1+m_2)^2|^2\frac{p^4}{(\varepsilon_1\varepsilon_2-p^2+m_1m_2)^2}$$
$$+|A_{45,45}(\varepsilon_1-\varepsilon_2)^2+4iA_{05,45}(m_1-m_2)(\varepsilon_1-\varepsilon_2)$$
$$-2A_{05,05}(m_1-m_2)^2|^2\frac{p^4}{(\varepsilon_1\varepsilon_2-p^2-m_1m_2)^2}$$
$$+|A_{01,01}|^2(3\varepsilon_1\varepsilon_2-p^2+3m_1m_2)(\varepsilon_1\varepsilon_2+p^2+m_1m_2)$$
$$+|A_{15,15}|^2(3\varepsilon_1\varepsilon_2-p^2-3m_1m_2)(\varepsilon_1\varepsilon_2+p^2-m_1m_2)$$
$$-2\,\mathrm{Re}\,\{[A_{04,04}(\varepsilon_1-\varepsilon_2)^2-4A_{00,04}(m_1+m_2)(\varepsilon_1-\varepsilon_2)$$
$$-2A_{00,00}(m_1+m_2)^2]A^*_{01,01}\}p^2\cos\theta$$
$$-2\,\mathrm{Re}\,\{[A_{45,45}(\varepsilon_1-\varepsilon_2)^2+4iA_{05,45}(m_1-m_2)(\varepsilon_1-\varepsilon_2)$$
$$-2A_{05,05}(m_1-m_2)^2]A^*_{15,15}\}p^2\cos\theta$$
$$+4\,\mathrm{Re}\,(A_{01,01}A^*_{15,15})(\varepsilon_1+\varepsilon_2)^2p^2\cos\theta$$
$$+4(|A_{01,01}|^2+|A_{15,15}|^2)p^4\cos^2\theta\}, \tag{15}$$

$$\frac{d\sigma_T}{d\Omega} = \frac{g^2\,G(p^2)}{4(2\pi)^2(\varepsilon_1+\varepsilon_2)^2}$$
$$\times\{9|A_{00,00}|^2(\varepsilon_1\varepsilon_2+p^2-m_1m_2)^2+9|A_{05,05}|^2(\varepsilon_1\varepsilon_2+p^2+m_1m_2)^2$$
$$+|A_{23,23}|^2[4p^4-8p^2(\varepsilon_1\varepsilon_2+p^2-m_1m_2)+3(\varepsilon_1\varepsilon_2+p^2-m_1m_2)^2]$$
$$+|A_{14,14}|^2[4p^4-8p^2(\varepsilon_1\varepsilon_2+p^2+m_1m_2)+3(\varepsilon_1\varepsilon_2+p^2+m_1m_2)^2] \tag{16}$$
$$+2\,\mathrm{Re}\,[3(A_{14,14}A^*_{00,00}+A_{23,23}A^*_{05,05})(\varepsilon_1+\varepsilon_2)^2$$
$$-2A_{23,23}A^*_{14,14}(\varepsilon_1-\varepsilon_2)^2]p^2\cos\theta$$
$$+4(|A_{23,23}|^2+|A_{14,14}|^2)p^4\cos^2\theta\}.$$

If one puts $A_{ij}=\delta_{ij}$ and $G(p^2)=1$ in formulas (15) and (16) these will change into formulas of the first approximation in perturbation theory †.

$$\frac{d\sigma_V}{d\Omega} = \frac{g^2}{2(2\pi)^2(\varepsilon_1+\varepsilon_2)^2}\{2p^4+2p^2\varepsilon_1\varepsilon_2+m_1^2m_2^2+\varepsilon_1^2\varepsilon_2^2$$
$$+(2\varepsilon_1\varepsilon_2+m_1^2+m_2^2)p^2\cos\theta+p^4\cos^2\theta\}, \tag{17}$$

$$\frac{d\sigma_T}{d\Omega} = \frac{2g^2}{(2\pi)^2(\varepsilon_1+\varepsilon_2)^2}\{2p^4+4p^2\varepsilon_1\varepsilon_2+3\varepsilon_1^2\varepsilon_2^2+3m_1^2m_2^2$$
$$+(4\varepsilon_1\varepsilon_2+\varepsilon_1^2+\varepsilon_2^2)p^2\cos\theta+p^4\cos^2\theta\}. \tag{18}$$

† The transformation can be performed in formula (14) with aid of the orthogonality relation

$$\sum_{i=1}^{16}(\gamma_i)_{\mu\tau}(\gamma_i)_{\rho\sigma}=4\delta_{\mu\sigma}\delta_{\rho\tau}.$$

Consider now the cross sections for elastic scattering of neutrons and antineutrons on protons ($m_1 = m_2$) for $k = m_N$ and $10^3 m_N$, the coupling

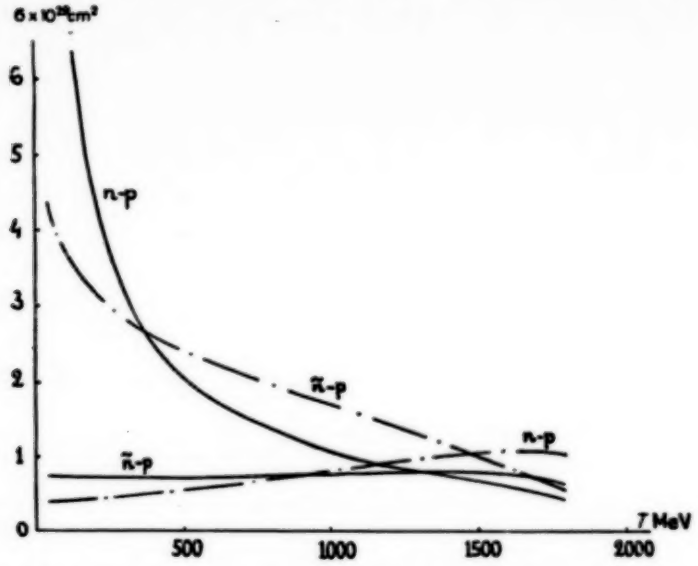


Fig. 3. Energy dependence in laboratory system of total elastic scattering cross sections for neutrons and antineutrons on protons for $k = m_N$
—·—·— vector theory
——— tensor theory.

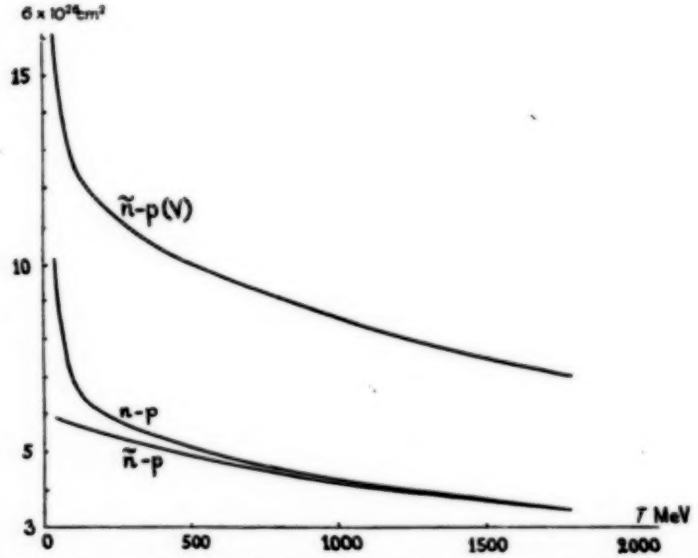


Fig. 4. Energy dependence in laboratory system of total elastic scattering cross sections for antineutrons on protons in vector theory (V) and for neutrons and antineutrons on protons in tensor theory; $k = 10^3 m_N \cdot \sigma_{n-p}$ in vector theory is of the order of $10^{-30}$ cm².

constants being assumed to be of a magnitude sufficient for the existence of a complex meson †. Only the pseudoscalar state $P_1$ will be considered in the

† See table 2.

vector theory. The total elastic scattering cross sections obtained in this way, $\sigma_{np}$ and $\sigma_{\bar{n}p}$ are presented in figs. 3 and 4. These cross sections possess the following peculiarities.

1) Cross sections $\sigma_{np}$ and $\sigma_{\bar{n}p}$ differ quite significantly, especially for $k = 10^3\, m_N$ in vector theory, whereas they are identical in the first approximation in perturbation theory.

2) For $k = m_N (g \approx 10^{-43}$ erg $\cdot$ cm$^3)$ the cross sections are about the same order of magnitude as those derived in the first approximation in perturbation theory (for the same value of $g$). However, already for $k = 10^3\, m_N$ $(g \approx 10^{-49}$ erg $\cdot$ cm$^3)$ cross sections $\sigma^V_{\bar{n}p}$, $\sigma^T_{np}$ and $\sigma^T_{\bar{n}p}$ turn out to be larger by 8—9 orders of magnitude than those obtained in the first approximation in perturbation theory for the same coupling constant ($\sigma^V_{np}$ is of the same order of magnitude as the cross section obtained in the first approximation in perturbation theory).

3) In the first approximation in perturbation theory the cross sections rapidly increase with energy whereas in the ladder approximation only $\sigma^V_{np}$ (for $k = 10^3\, m_N$) increases at the same rate. From figs. 3 and 4 it can be seen that the other cross sections either decrease or only slowly increase. The weak energy dependence of the cross sections at high energies is noteworthy.

4) For both values of $k$ the coefficients $a$, $b$ and $c$ in all differential cross sections, $\sigma(\theta) = a + b\cos\theta + c\cos^2\theta$ greatly differ from those which the perturbation theory yields. In particular, for $k = 10^3\, m_N$ cross sections $\sigma^V_{\bar{n}p}(\theta)$, $\sigma^T_{np}(\theta)$ and $\sigma^T_{\bar{n}p}(\theta)$ become practically isotropic.

If the theory of contact interaction of baryons is correct and all nucleon interactions can be reduced to contact interactions, perturbation theory should be inapplicable to it † due to the great difference between the cross sections $\sigma_{np}$ which it yields and the experimental values (e.g., in respect to the energy dependence). The result obtained above does not contradict this assumption as the cross sections in the higher chain approximation considerably differ (in order of magnitude and in respect to the energy and angular dependences) from the first approximation in perturbation theory.

All of these results, however, depend on a special choice of constants $k$ and $g$, which ensure the existence of a complex $\pi$ meson; for a prescribed $k$ a definite choice of $g$ must be made and vice versa.

Consider now the case of arbitrary values of $g$ and $k$. The coefficients $A_{i;i}$ in formulas (15) and (16) have the form†† $[1 - g a_i(k)]^{-1}$ and equal unity in the first approximation in perturbation theory which is thus valid only if all

† By this we mean that the result obtained in the first approximation in perturbation theory strongly differs from the exact value.

†† Some of coefficients $A_{i;i}$ in vector theory and all the $A_{i;j}$ with $i \neq j$ are of a somewhat different form (see appendix 2).

$|ga_i| < 1$, that is, when all lengths $l_i = |a_i(k)|^{-\frac{1}{2}}$ are larger than a characteristic length $l = \sqrt{|g|}$ related to the coupling constant $g$. The condition for existence of a bound state is $1-ga_i(k) = 0$, that is, one of the lengths $l_i$ should equal the characteristic length $l$. Hence for the same values of $g$ and $k$ one finds that in scattering $|ga_i(k)| \approx 1$ (a strict equality does not apply here as the $a_i$ are functions of the mass of the system). It is thus clear that perturbation theory is invalid for those values of $g$ and $k$ for which bound states exist. For $k/m_{1,2} \gg 1$ one has $l_i \approx 2\pi/k$ in tensor theory and in vector theory $l_i \approx 2\pi/k$ or $4\pi/|m_1 \pm m_2|\sqrt{\ln (k^2/m_1 m_2)}$. Hence for sufficiently small values of $g$, for example, $g \approx 10^{-49}$ erg · cm$^3$ ($l \approx 10^{-16}$ cm) the condition of applicability of perturbation theory can be written in the form $|g|k^2 \ll 1$. In vector theory (for $g > 0$) and in tensor theory bound states are possible for $(2\pi)^{-2}|g|k^2 \approx 1$. If $g < 0$ bound states are possible in vector theory only if

$$(4\pi)^{-2}|g|(m_1 \pm m_2)^2 \ln (k^2/m_1 m_2) \approx 1$$

(the pseudoscalar state $P_2$ in vector theory is of this type).

## 5. Conclusions

1) Assuming the existence of contact interaction one finds that in the chain approximation $\pi$ and K mesons can qualitatively be described as nucleon-antinucleon and nucleon-anti $\Lambda$ hyperon bound states respectively, in agreement with the classification of M. A. Markov [1]) and S. Sakata [2]).

2) This result is not inconsistent with the fact that only relatively weak bound states nucleon-nucleon (deuteron) exist in reality.

3) For $g \approx 10^{-49}$ erg · cm$^3$ the only bound state that appears besides the $\pi$ meson is the K meson.

4) Even in the present qualitative treatment the meson-nucleon pseudoscalar coupling constant for $g \approx 10^{-49}$ erg · cm$^3$ turns out to be of a reasonable magnitude from the experimental point of view ($\approx 10$).

5) Bound states are possible in the chain approximation only if (assuming $k/cm_{1,2} \gg 1$ and $g$ to be small) the length $l_k = h/k$, which is related to the cut-off momentum $k$, is of the order of magnitude of the characteristic length related to the coupling constant, i.e., $l = \sqrt{|g|/\hbar c}$; perturbation theory is valid only if $l_k \gg l$.

6) Connected with this is the fact that for the same values of $g$ and $k$ for which bound states (and in particular the complex $\pi$ meson) exist, the elastic scattering cross sections turn out to greatly differ from those obtained in the first approximation in perturbation theory.

7) The cross sections for scattering of neutrons and antineutrons on protons are not inconsistent with the experimental data.

8) In principle the levels of mass $M_n$ of the bound systems can be derived as poles in the $S$ matrix.

For reasons stated in the paper the results obtained here must be regarded as of a qualitative nature.

In conclusion the author takes the opportunity to express his appreciation to Professor M. A. Markov under whose guidance this work was carried out. Thanks are also extended to R. A. Asanov for numerous discussions and to the workers of the Computation Department of the Laboratory of Theoretical Physics of the Joint Institute of Nuclear Research for performing the numerical calculations.

## Appendix 1

By using the substitution of the integration variables

$$\mathbf{p} = \mathbf{p}' - \boldsymbol{\beta}\{-\mathbf{p}' \cdot \boldsymbol{\beta}\beta^{-2}(\gamma-1) + \gamma p'_0\}, \qquad p_0 = \gamma\{p'_0 - \boldsymbol{\beta} \cdot \mathbf{p}'\},$$
$$\boldsymbol{\beta} = -\mathbf{P}/P_0, \qquad \gamma = (1-\beta^2)^{-\frac{1}{2}},$$

the integral in (7) for $x = 0$ can be transformed to

$$\begin{aligned} &-i(2\pi)^{-4}\int S_F{}^1(\alpha P + p, m_1) S_F{}^2(\beta P - p, m_2) G(\Pi^2) \mathrm{d}^4 p \\ &= A - BM^{-2}(\gamma^1 P)(\gamma^2 P) + \tfrac{1}{3}C[\gamma_\mu{}^1 \gamma_\mu{}^2 + M^{-2}(\gamma^1 P)(\gamma^2 P)] \\ &\quad -iDM^{-1}(\gamma^1 P) - iEM^{-1}(\gamma^2 P). \end{aligned} \tag{A1}$$

The coefficients involved here are related by the equation

$$\begin{aligned} A &= m_1 M^{-1} D + m_2 M^{-1} E \\ B &= C + m_2 M^{-1} D + m_1 M^{-1} E \end{aligned} \tag{A2}$$
$$E \equiv E(m_1, m_2) = D(m_2, m_1), \qquad D(m_1, m_2) \equiv D.$$

After performing the integration over $p'$ the following expressions are obtained for coefficients $C$ and $D$:

$$\begin{aligned} C = [2(2\pi)^2 M]^{-1}\{&\tfrac{1}{4}a_4 k\sqrt{k^2+m_1{}^2} + \tfrac{1}{4}a_5 k\sqrt{k^2+m_2{}^2} \\ &- a_1 a_4 (W^2 + \tfrac{1}{2}m_1{}^2) - a_2 a_5 (W^2 + \tfrac{1}{2}m_2{}^2) + 2W^2 a_3\}, \end{aligned}$$

$$\begin{aligned} D = m_2 [2(2\pi)^2 M]^{-1}\{&\tfrac{1}{2}k(\sqrt{k^2+m_1{}^2} - \sqrt{k^2+m_2{}^2}) \\ &- 2(W^2 - \tfrac{1}{2}m_1{}^2)(a_1 - a_2) + M^2 a_2 - a_4 a_3\}, \end{aligned}$$

where

$$a_r = \tfrac{1}{2}\ln\frac{k+\sqrt{k^2+m_r{}^2}}{m_r} \qquad (r = 1, 2);$$

$$a_3 = \begin{cases} -W_1 \operatorname{ar\,th}(W_1 x) & 0 < M < |m_1 - m_2| \\ W \operatorname{arc\,tg}(Wx) & |m_1 - m_2| < M < m_1 + m_2 \\ -\frac{1}{2} W_1 \left[ \ln \left| \dfrac{1+W_1 x}{1-W_1 x} \right| + i\pi \right] & M > m_1 + m_2, \end{cases}$$

$$x = 2kM(m_1+m_2)[(m_1+m_2)^2 - M^2]^{-1}[m_1\sqrt{k^2+m_2^2} + m_2\sqrt{k^2+m_1^2}]^{-1};$$

$$a_{4,5} = M^{-1}(M^2 \pm m_1^2 \mp m_2^2),$$

$$W^2 = -W_1^2 = (2M)^{-2}[(m_1+m_2)^2 - M^2][M^2 - (m_1-m_2)^2].$$

The remaining coefficients can be obtained with the aid of (A2).

## Appendix 2

Non-vanishing coefficients $A_{i;j}$ of scattering states (for $\mathbf{P} = 0$). $k, m, n = 1, 2, 3$; $\mu, \nu = 1, 2, 3, 4$.

VECTOR THEORY

$$A_{00,00} = [1-2g(A-B+C)]D_1^{-1}, \qquad A_{00,04} = 2g(D-E)D_1^{-1}$$

$$A_{04,00} = -4g(D-E)D_1^{-1}, \qquad A_{04,04} = [1+4g(A-B-C)]D_1^{-1}$$

$$A_{0k,0k} = [1-2g(A+B+\tfrac{1}{3}C)]^{-1}$$

$$A_{k4,0k} = 2ig(D+E)[1-2g(A+B+\tfrac{1}{3}C)]^{-1}, \qquad A_{\mu\nu,\mu\nu} = 1 \ (\mu \neq \nu)$$

$$A_{mn,k5} = -2g(D-E)[1+2g(A-B-\tfrac{1}{3}C)]^{-1}\varepsilon_{mnk}$$

$$A_{k5,k5} = [1+2g(A-B-\tfrac{1}{3}C)]^{-1}$$

$$A_{45,45} = [1-4g(A+B+C)]D_2^{-1}, \qquad A_{45,05} = -4ig(D+E)D_2^{-1}$$

$$A_{05,45} = -2ig(D+E)D_2^{-1}, \qquad A_{05,05} = [1+2g(A+B-C)]D_2^{-1}$$

$$D_1 = [1-2g(A-B+C)][1+4g(A-B-C)]+8g^2(D-E)^2$$

$$D_2 = [1+2g(A+B-C)][1-4g(A+B+C)]+8g^2(D+E)^2.$$

TENSOR THEORY

$$A_{00,00} = [1+12g(A-B-C)]^{-1}$$

$$A_{04,00} = -12g(D-E)[1+12g(A-B-C)]^{-1}, \qquad A_{0\mu,0\mu} = 1$$

$$A_{0k,k4} = -4ig(D+E)[1-4g(A+B-\tfrac{1}{3}C)]^{-1}$$

$$A_{k4,k4} = [1-4g(A+B-\tfrac{1}{3}C)]^{-1}, \quad A_{mn,mn} = [1-4g(A-B+\tfrac{1}{3}C)]^{-1} \ (m \neq n)$$

$$A_{k5,mn} = 4g(D-E)[1-4g(A-B+\tfrac{1}{3}C)]^{-1}\varepsilon_{mnk}$$

$$A_{45,05} = 12ig(D+E)[1+12g(A+B+C)]^{-1}, \qquad A_{\mu5,\mu5} = 1$$

$$A_{05,05} = [1+12g(A+B+C)]^{-1}.$$

## Appendix 3

Functions $g^{-1} = f(k, M, m_1, m_2)$ and coefficients entering $\chi$ for the bound states in table 1

| Theory | Type of solution in table 1 | $g^{-1}$ | Coefficients $a$, $b$, $c$, $d$ |
|---|---|---|---|
| Vector | 1 | $g^{-1}_{1,2} = -(A-B-3C) \pm \sqrt{-8(D-E)^2+9(A-B-\frac{1}{3}C)^2}$ | $a = 4i(D-E)M^{-1}[g^{-1}_{1,2}-2(A-B+C)]^{-1}$ |
| | 2 | $g^{-1}_{1,2} = A+B+3C \pm \sqrt{-8(D+E)^2+9(A+B+\frac{1}{3}C)^2}$ | $b = -4i(D+E)M^{-1}[g^{-1}_{1,2}+2(A+B-C)]^{-1}$ |
| | 3 | $g^{-1} = 2(A+B+\frac{1}{3}C)$ | $c = 2g(D+E)M^{-1}$ |
| | 4 | $g^{-1} = -2(A-B-\frac{1}{3}C)$ | $d = -2g(D-E)M^{-1}$ |
| Tensor | 1 | $g^{-1} = -12(A-B-C)$ | $a = 12ig(D-E)M^{-1}$ |
| | 2 | $g^{-1} = -12(A+B+C)$ | $b = 12ig(D+E)M^{-1}$ |
| | 3 | $g^{-1} = 4(A+B-\frac{1}{3}C)$ | $c = [4g(D+E)M]^{-1}$ |
| | 4 | $g^{-1} = 4(A-B+\frac{1}{3}C)$ | $d = [4g(D-E)M]^{-1}$ |

## References

1) M. A. Markov, On the Classification of Elementary Particles (Acad. of Sci. USSR, Moscow 1955); M. A. Markov, Report at the VI Rochester Conference (1956)
2) S. Sakata, Progr. Theor. Phys. **16** (1956) 686
3) E. Fermi and C. N. Yang, Phys. Rev. **76** (1949) 1739
4) H. Katsumori, Progr. Theor. Phys. **11** (1954) 505
5) Ziro Maki, Progr. Theor. Phys. **16** (1956) 667
6) W. Heisenberg, Revs. Mod. Phys. **29** (1957) 269
7) I. V. Polubarinov, Report on Equations in Functional Derivatives for One- and Two-Particle Green's Functions for Contact Interaction of Dirac Fields (Lab. Theor. Phys. Joint Institute of Nuclear Research, 1956)
8) J. Schwinger, Proc. Nat. Acad. Sci. **37** (1951) 452, 455
9) K. Nishijima, Prog. Theor. Phys. **10** (1953) 549; **12** (1954) 279; **13** (1955) 305
10) P. Kristensen and G. Möller, Mat. Fys. Medd. Dan. Vid. Selsk **27** (1952) no. 7

8.B *Nuclear Physics* 8 (1958) 461—467; © *North-Holland Publishing Co., Amsterdam*
Not to be reproduced by photoprint or microfilm without written permission from the publisher

# ON THE ELEMENTARY PARTICLES AND THEIR STRONG INTERACTIONS

W. KRÓLIKOWSKI
*Institute of Theoretical Physics, University of Warsaw*
and
*Institute of Nuclear Research, Polish Academy of Sciences, Warsaw*

Received 25 July 1958

**Abstract:** In this paper a local theory of elementary particles is proposed. Types of fermions following from this theory seem to cover exactly the list of experimental baryons and leptons. The general expressions for the charge and strangeness operators are given. Some preliminary propositions are made for the form of strong interactions.

## 1. Introduction

This paper contains some theoretical propositions concerning elementary particles and their strong interactions †. The author imagines the elementary particles, e.g. hyperons, as *sui generis* compound systems but devoided of space-time extent. The transition from the conception of ordinary compound systems to the proposed conception of elementary particles has an analogy with the well known transition from rotators to spinning particles. In both transitions the space-time degrees of freedom are replaced by new "algebraic" degrees of freedom, which are connected with the spin of elementary particles in the second case and with their strangeness in the first case. The proposed theory differs from several compound theories due to Goldhaber [1]) and others just by carrying out the above transition.

## 2. Baryons

In the usual field theory, there are some operators, e.g. $\partial/\partial x_\mu$, $\gamma_\mu$, $\tau_i$, which act on the field operators (acting on the state vector). We introduce here new operators $\xi_\alpha (\alpha = 1, 2)$ acting on the field operators and satisfying the well known anticommutation relations

$$\{\xi_\alpha, \xi_\beta^*\} = \delta_{\alpha\beta}, \quad \{\xi_\alpha, \xi_\beta\} = 0 \quad (\alpha = 1, 2, \beta = 1, 2), \tag{1}$$

where $\alpha$ is *ex definitione* the isospin index. The asterisk denotes the hermitian

† The results of this paper were reported in the form of preprint, Institute of Nuclear Research, Polish Academy of Sciences, Report No. 17/VII (March, 1958).

conjugation. In the ordinary representation of $\tau_i = (\tau_{i,\alpha\beta})$ $(i = 1, 2, 3)$,

$$\tau_1 = \begin{pmatrix} 0 & 1 \\ 1 & 0 \end{pmatrix}, \qquad \tau_2 = \begin{pmatrix} 0 & -i \\ i & 0 \end{pmatrix}, \qquad \tau_3 = \begin{pmatrix} 1 & 0 \\ 0 & -1 \end{pmatrix}, \tag{2}$$

the index $\alpha = 1, 2$ corresponds to the eigenvalues of $\tau_3 = +1, -1$. There are *a priori* two possibilities: either the index $\alpha = 1, 2$, of $\xi_\alpha$ corresponds to charges $+e$, 0 or to charges 0, $-e$. We assume the second possibility. Then the charge connected with the index $\alpha$ of $\xi_\alpha$ has the form

$$\tfrac{1}{2}e(\tau_3 - 1). \tag{3}$$

The $\xi_\alpha$ and $\xi_\alpha^*$ are, of course, some annihilation and creation operators obeying Fermi-Dirac statistics (Pauli principle), but they act on the field operators and not on the state vector. For the sake of convenience we shall call the objects respectively annihilated and created by $\xi_\alpha$ and $\xi_\alpha^*$ the "strange parts" of elementary particles. These strange parts have charges 0 or $-e$.

In the representation in which the operators

$$n_\alpha = \xi_\alpha^* \xi_\alpha \quad (\alpha = 1, 2) \tag{4}$$

are diagonal, we have

$$\begin{aligned} n_1 &= (n_{1n_1n_2,\, n'_1n'_2}) = \begin{pmatrix} 0 & 0 \\ 0 & 1 \end{pmatrix} \times \begin{pmatrix} 1 & 0 \\ 0 & 1 \end{pmatrix}, \\ n_2 &= (n_{2n_1n_2,\, n'_1n'_2}) = \begin{pmatrix} 1 & 0 \\ 0 & 1 \end{pmatrix} \times \begin{pmatrix} 0 & 0 \\ 0 & 1 \end{pmatrix} \end{aligned} \tag{5}$$

and

$$\begin{aligned} \xi_1 &= (\xi_{1n_1n_2,\, n'_1n'_2}) = \begin{pmatrix} 0 & 1 \\ 0 & 0 \end{pmatrix} \times \begin{pmatrix} 1 & 0 \\ 0 & 1 \end{pmatrix}, \\ \xi_2 &= (\xi_{2n_1n_2,\, n'_1n'_2}) = \begin{pmatrix} 1 & 0 \\ 0 & -1 \end{pmatrix} \times \begin{pmatrix} 0 & 1 \\ 0 & 0 \end{pmatrix}. \end{aligned} \tag{6}$$

Now, we consider a field operator $B(x)$, which will be later identified with the field of all baryons. We take into account the local character of the field, i.e. we assume that the field components $B(x)$ in any representation satisfy ordinary local commutation relations. In the representation in which $n_\alpha (\alpha = 1, 2)$ given by (4) are diagonal, we obtain

$$B(x) = (B_{\alpha n_1 n_2}(x)), \tag{7}$$

where $\alpha = 1, 2$ is *ex definitione* the isospin index corresponding to the charges $+e$, 0. Thus, the charge connected with the index $\alpha$ has the form

$$\tfrac{1}{2}e(\tau_3 + 1). \tag{8}$$

The ordinary spin index is here suppressed. For the sake of convenience we shall call the object connected with the index $\alpha$ of $B_{\alpha n_1 n_2}(x)$ the "fundamental

part" of the B particles. This fundamental part has the charge $+e$ or 0. The indices $n_1 = 0,1$ and $n_2 = 0,1$ of $B_{\alpha n_1 n_2}(x)$ describe the numbers of strange parts of B particles, having charges 0 and $-e$ respectively.

Formula (7) represents the field $B(x)$ in the "occupation number representation". Going over to the "Fock representation" we obtain

$$B(x) = (B_{\alpha\alpha_1\ldots\alpha_n}(x)) = \begin{pmatrix} B_\alpha(x) \\ B_{\alpha\alpha_1}(x) \\ B_{\alpha\alpha_1\alpha_2}(x) \end{pmatrix}, \tag{9}$$

where

$$n = n_1 + n_2 \tag{10}$$

and

$$B_{\alpha\alpha_1\ldots\alpha_n}(x) = \frac{1}{\sqrt{n!}} B_{\alpha n_1 n_2}(x). \tag{11}$$

The total charge of the field $B(x)$ may be written in the form

$$\begin{aligned} Q^{\mathrm{B}} &= e\int \mathrm{d}_3 x B^*[\tfrac{1}{2}(\tau_3+1)+\tfrac{1}{2}\xi_\alpha^*(\tau_{3\alpha\beta}-\delta_{\alpha\beta})\xi_\beta]B \\ &= e(T_3^{\mathrm{B}}+\tfrac{1}{2}N^{\mathrm{B}}-\tfrac{1}{2}S^{\mathrm{B}}), \end{aligned} \tag{12}$$

where $T_3^{\mathrm{B}}$ is the 3rd component of the total isospin of the field $B(x)$,

$$\mathbf{T}^{\mathrm{B}} = \tfrac{1}{2}\int \mathrm{d}_3 x B^*(\boldsymbol{\tau}+\xi_\alpha^*\,\boldsymbol{\tau}_{\alpha\beta}\,\xi_\beta)B, \tag{13}$$

$N^{\mathrm{B}}$ is the total number of B particles (minus B antiparticles),

$$N^{\mathrm{B}} = \int \mathrm{d}_3 x B^* B, \tag{14}$$

and

$$S^{\mathrm{B}} = \int \mathrm{d}_3 x B^* \xi_\alpha^* \xi_\alpha B = \int \mathrm{d}_3 x B^* (\sum_\alpha n_\alpha) B \tag{15}$$

is the operator which we shall call the total strangeness of the field $B(x)$. This operator will turn out to be identical with the experimental strangeness of baryons.

In the representation (9), only the component $B_\alpha$ has a well defined total isospin. In order to obtain all components with determined total isospin we carry out the vector addition of isospins of the fundamental and strange parts of B particles. In this calculation we make use of the antisymmetry of the components (9) with respect to isospin indices of strange parts,

$$B_{\alpha\alpha_1\alpha_2} = -B_{\alpha\alpha_2\alpha_1} \tag{16}$$

(Fermi-Dirac statistics). Then the component corresponding to $S^{\mathrm{B}} = 2$ and $T^{\mathrm{B}} = \frac{3}{2}$ does not exist, because it is given by a combination symmetrical in the indices $\alpha_1$ and $\alpha_2$. The components corresponding to $S^{\mathrm{B}} \geqq 3$, of course, do not exist either (cf. (9)). We propose to identify the components, obtained

by this addition, with the bare fields of experimental baryons. The results are given in table 1.

TABLE 1

| Component and its symbol | $S^B$ | $T^B$ | $T_3^B$ | $Q^B$ | Identification |
|---|---|---|---|---|---|
| $B_\alpha = N_\alpha = \begin{cases} p \\ n \end{cases}$ | 0 | $\frac{1}{2}$ | $\pm\frac{1}{2}$ | $+e$<br>0 | proton<br>neutron |
| $\frac{1}{\sqrt{2}}(B_{12}-B_{21}) = i\Lambda^0$ | 1 | 0 | 0 | 0 | $\Lambda^0$ hyperon |
| $B_{11} = \Sigma^+$ | 1 | 1 | +1 | $+e$ | $\Sigma^+$ |
| $\frac{1}{\sqrt{2}}(B_{12}+B_{21}) = \Sigma^0$ | 1 | 1 | 0 | 0 | $\Sigma^0$ hyperons |
| $B_{22} = \Sigma^-$ | 1 | 1 | −1 | $-e$ | $\Sigma^-$ |
| $\frac{1}{\sqrt{2}}(B_{\alpha 21}-B_{\alpha 12}) = \sqrt{2}B_{\alpha 21} = i\Xi_\alpha = \begin{cases} \Xi^0 \\ \Xi^- \end{cases}$ | 2 | $\frac{1}{2}$ | $\pm\frac{1}{2}$ | 0<br>$-e$ | $\Xi^0$<br>$\Xi^-$ hyperons |
| does not exist<br>do not exist | 2<br>$\geqq 3$ | $\frac{1}{2}$ | | | |

We can see from table 1 that our theory seems to cover exactly the list of actually known baryons and to explain their experimental strangeness and charge multiplicity. The discovery of further baryons would mean, from our point of view, that their strange parts do not obey the Pauli principle.

We note that the isoscalar field $\Lambda^0$ and the isopseudovector field $\boldsymbol{\Sigma}$ may be written down as follows:

$$i\Lambda^0 = \frac{1}{i\sqrt{2}} C_{\alpha\beta} B_{\beta\alpha}, \quad \boldsymbol{\Sigma} = (\Sigma_i) = \frac{1}{\sqrt{2}} (C\boldsymbol{\tau})_{\alpha\beta} B_{\beta\alpha}, \tag{17}$$

where

$$C = \begin{pmatrix} 0 & i \\ -i & 0 \end{pmatrix} = -\tau_2 \tag{18}$$

and

$$\Sigma_1 = -\frac{1}{i\sqrt{2}}(\Sigma^+ - \Sigma^-), \quad \Sigma_2 = -\frac{1}{\sqrt{2}}(\Sigma^+ + \Sigma^-), \quad \Sigma_3 = \frac{1}{i}\Sigma^0. \tag{19}$$

## 3. Strong Interactions

In this section we propose some forms of strong interaction Hamiltonians for the baryon field $B(x)$, the K-meson field $K(x) = (K_\alpha(x))$,

$$K_\alpha(x) = \begin{cases} K^+(x) \\ K^0(x) \end{cases} \tag{20}$$

(being, according to d'Espagnat and Prentki [2]), an isospinor of the first

kind), and the $\pi$-meson field $\boldsymbol{\pi}(x) = (\pi_i(x))$ (being an isopseudovector); $\bar{B}(x)\xi_\alpha B(x)$ is assumed to be an isospinor of the second kind. These propositions should be regarded as tentative:

$$\mathscr{H}^{B\pi} = ig_0^{\pi}\bar{B}\gamma_5(\boldsymbol{\tau}+\xi_\alpha^*\boldsymbol{\tau}_{\alpha\beta}\xi_\beta)B\cdot\boldsymbol{\pi} \tag{21}$$

and

$$\mathscr{H}^{BK} = ig_0^{K}\bar{B}\gamma_5\xi_\alpha B(CK)_\alpha + \text{h.c.} \tag{22}$$

or the second interaction without $i\gamma_5$. Here $C$ is given by (18).

Using the results of the former section we obtain explicitly

$$\mathscr{H}^{B\pi} = ig_0^{\pi}(\bar{N}\gamma_5\boldsymbol{\tau}N+2i\bar{\boldsymbol{\Sigma}}\gamma_5\times\boldsymbol{\Sigma}+\bar{\Xi}\gamma_5\boldsymbol{\tau}\Xi)\cdot\boldsymbol{\pi}, \tag{23}$$

where $N(x) = (N_\alpha(x))$ is the nucleon field (isospinor of the first kind), $\boldsymbol{\Sigma}(x) = (\Sigma_i(x))$ the field of $\Sigma$ hyperons (isopseudovector) and $\Xi(x) = (\Xi_\alpha(x))$ the field of $\Xi$ hyperons (isospinor of the second kind).

We can see from (23) that the coupling $\bar{\Lambda}^0\boldsymbol{\Sigma}\cdot\boldsymbol{\pi}$ does not appear in the interaction (21).

In a similar way we get

$$\mathscr{H}^{BK} = \frac{ig_0^{K}}{\sqrt{2}}(\bar{N}\gamma_5\Lambda^0+\bar{N}\gamma_5\boldsymbol{\tau}\cdot\boldsymbol{\Sigma}+\bar{\Lambda}^0\gamma_5\Xi C-\bar{\Sigma}\gamma_5\Xi C\cdot\boldsymbol{\tau})K+\text{h.c.} \tag{24}$$

or without $i\gamma_5$.

The interaction (22) has the property that without the renormalization of the coupling constant $g_0^{K}$ it does not give charge exchange scattering of K-mesons, because this process would require a virtual emission of particle $B_{12} = (\Sigma^0+i\Lambda^0)/\sqrt{2}$ and an absorption of particle $B_{21} = (\Sigma^0-i\Lambda^0)/\sqrt{2}$ (or of their antiparticles), which are mutually orthogonal. The renormalization of $g_0^{K}$ caused by the interaction $\mathscr{H}^{B\pi}$ spoils the combinations $(\Sigma^0\pm i\Lambda^0)/\sqrt{2}$ and leads to charge exchange scattering of K-mesons. The rate of this process (which is of higher order in $g_0^{\pi}$) should be, however, smaller than that of the direct scattering.

The Hamiltonians

$$H^{B\pi} = \int \mathrm{d}_3 x\,\mathscr{H}^{B\pi}, \qquad H^{BK} = \int \mathrm{d}_3 x\,\mathscr{H}^{BK} \tag{25}$$

correspond in the fixed source theory to the following forms:

$$H^{B\pi} = \frac{f_0^{\pi}}{\mu^{\pi}}\sigma_i(\boldsymbol{\tau}+\xi_\alpha^*\boldsymbol{\tau}_{\alpha\beta}\xi_\beta)\cdot\int \mathrm{d}_3 x\rho^{\pi}\,\partial_i\boldsymbol{\pi} \tag{26}$$

and

$$H^{BK} = \frac{f_0^{K}}{\mu^{K}}\sigma_i\xi_\alpha\int \mathrm{d}_3 x\rho^{K}\partial_i(CK)_\alpha + \text{h.c.} \tag{27}$$

or the second form without $\sigma_i\partial_i/\mu^{K}$. In the fixed source theory the operators $\sigma_i$, $\tau_j$, $\xi_\alpha$ act, of course, on the state vector.

## 4. Leptons

It would be interesting to extend our theory to leptons. Let us introduce a field operator $L(x)$ and assume that 1) the fundamental part of L particles has the charge 0 or $-e$ (instead of $+e$ or 0 as in the case of baryons), and 2) the fundamental part and the strange parts of L particles obey *all together* the Fermi-Dirac statistics (Pauli principle). (The fundamental part and the strange parts have here the same charge possibilities: 0 or $-e$.) Then the field operator $L(x)$ has in the "Fock representation" the form

$$L(x) = \begin{pmatrix} L_\alpha(x) \\ L_{\alpha\alpha_1}(x) \end{pmatrix}. \tag{28}$$

The ordinary spinor index is here, of course, suppressed.

The total charge of the field $L(x)$ is given by

$$Q^{\mathrm{L}} = e\int \mathrm{d}_3 x L^*[\tfrac{1}{2}(\tau_3 - 1) + \tfrac{1}{2}\xi_\alpha^*(\tau_{3\alpha\beta} - \delta_{\alpha\beta})\xi_\beta]L = e(T_3{}^{\mathrm{L}} - \tfrac{1}{2}N^{\mathrm{L}} - \tfrac{1}{2}S^{\mathrm{L}}), \tag{29}$$

where $T_3{}^{\mathrm{L}}$ is the 3rd component of the total isospin of the field $L(x)$,

$$\mathbf{T}^{\mathrm{L}} = \tfrac{1}{2}\int \mathrm{d}_3 x L^*(\boldsymbol{\tau} + \xi_\alpha^* \boldsymbol{\tau}_{\alpha\beta}\xi_\beta)L, \tag{30}$$

the operator

$$N^{\mathrm{L}} = \int \mathrm{d}_3 x L^* L \tag{31}$$

is the total number of L particles (minus L antiparticles) and we shall call the operator

$$S^{\mathrm{L}} = \int \mathrm{d}_3 x L^* \xi_\alpha^* \xi_\alpha L = \int \mathrm{d}_3 x L^* (\sum_\alpha n_\alpha) L \tag{32}$$

the total strangeness of the field $L(x)$.

Carrying out as above, the vector addition of isospins we get the results listed in table 2.

TABLE 2

| Component and its symbol | $S^{\mathrm{L}}$ | $T^{\mathrm{L}}$ | $T_3{}^{\mathrm{L}}$ | $Q^{\mathrm{L}}$ | Identification |
|---|---|---|---|---|---|
| $\mathrm{L}_\alpha = \mathrm{e}_\alpha = \begin{cases} \nu \\ \mathrm{e}^- \end{cases}$ | 0 | $\frac{1}{2}$ | $\pm\frac{1}{2}$ | 0<br>$-e$ | neutrino<br>electron |
| $\frac{1}{\sqrt{2}}(\mathrm{L}_{12} - \mathrm{L}_{21}) = \sqrt{2}\mathrm{L}_{12} = \mu^-$ | 1 | 0 | 0 | $-e$ | $\mu^-$-meson |
| does not exist<br>do not exist | 1<br>$\geqq 2$ | 1 | | | |

Table 2 seems to cover exactly the list of presently known leptons and explain their experimental charge multiplicity.

## 5. Mesons

We might try to apply the above idea about fermions (baryons and leptons) also to K and $\pi$-mesons. We should introduce the field

$$M(x) = \begin{pmatrix} M_{\alpha}(x) \\ M_{\alpha\alpha_1}(x) \\ M_{\alpha\alpha_1\alpha_2}(x) \end{pmatrix}, \tag{33}$$

where the index of the fundamental part $\alpha = 1, 2$ would correspond to charges $+e$, 0, and the indices of the strange parts $\alpha_1 = 1, 2$ and $\alpha_2 = 1, 2$ would correspond to charges 0, $-e$. Then

$$Q^{M} = e(T_3{}^{M} - \tfrac{1}{2}S^{M}), \quad \text{where} \quad S^{M} = \int \mathrm{d}_3 x M^* \overleftrightarrow{\partial_4} (\xi_\alpha{}^* \xi_\alpha - 1) M. \tag{34}$$

By similar consideration as in the case of fermions, we should get the results listed in table 3.

TABLE 3

| Component and its symbol | $S^{M}$ | $T^{M}$ | $T_3{}^{M}$ | $Q^{M}$ | Identification |
|---|---|---|---|---|---|
| $M_\alpha = K_\alpha = \begin{cases} K^+ \\ K^0 \end{cases}$ | $-1$ | $\frac{1}{2}$ | $\pm\frac{1}{2}$ | $+e$<br>0 | $K^+$<br>$K^0$ } mesons |
| $M_{11} = \pi^+$ | 0 | 1 | $+1$ | $+e$ | $\pi^+$ |
| $\frac{1}{\sqrt{2}}(M_{12}+M_{21}) = \pi^0$ | 0 | 1 | 0 | 0 | $\pi^0$ } mesons |
| $M_{22} = \pi^-$ | 0 | 1 | $-1$ | $-e$ | $\pi^-$ |
| $\frac{1}{\sqrt{2}}(M_{12}-M_{21}) = \pi_0{}^0$ | 0 | 0 | 0 | 0 | a new neutral meson $\pi_0{}^0$ |
| $\frac{1}{\sqrt{2}}(M_{\alpha 21}-M_{\alpha 12}) = \sqrt{2}M_{\alpha 21} = ?$ | 1 | $\frac{1}{2}$ | $\pm\frac{1}{2}$ | 0<br>$-e$ | two new mesons (?) |
| does not exist<br>do not exist | 1<br>$\geq 3$ | $\frac{3}{2}$ | | | |

Table 3 contains a new hypothetical neutral meson † $\pi_0{}^0$ having $S^{M} = 0$ and $T^{M} = 0$, and two new mesons having $S^{M} = 1$ and $T^{M} = \frac{1}{2}$. If the meson $\pi_0{}^0$ is not found experimentally this could be understood, from the point of view of table 3, as an indication that the meson $\pi_0{}^0$ would be eliminated by means of an additional condition, as the scalar photon is eliminated in electrodynamics by means of the Lorentz condition.

The author is indebted to Dr. J. Prentki (CERN-Geneva) and to Dr. J. Plebański and Dr. J. Werle (Warsaw) for many valuable discussions.

† The existence of this meson was recently suggested by A. Baldin (Birmingham preprint) in connection with strong pion interactions.

## References

1) M. Goldhaber, Phys. Rev. **92** (1953) 1279; **101** (1956) 444
2) B. d'Espagnat and J. Prentki, Phys. Rev. **99** (1955) 328; Nuclear Physics **1** (1955)3

1.D.1:
1.E.2

*Nuclear Physics* **8** (1958) 468—483; © *North-Holland Publishing Co., Amsterdam*
Not to be reproduced by photoprint or microfilm without written permission from the publisher

# COULOMB ENERGIES OF MIRROR NUCLEI †

I. UNNA ††

*Hebrew University, Jerusalem, Israel*

Received 23 May 1958

**Abstract:** Coulomb energies of mirror nuclei ($A \leqq 45$) are calculated using the harmonic oscillator shell model. Correct isobaric spin wave functions have been used. Nevertheless, the results obtained are very close to those of Carlson and Talmi [1]) who used wave functions of the protons alone. Some formulae of more general interest, obtained during the calculations, are also included.

## 1. Introduction and Summary of the Results

Carlson and Talmi [1]), in their calculations of Coulomb energies of mirror nuclei, assumed, for simplicity, that the presence of the neutrons in the unfilled shell does not affect the coupling of the protons in this shell. In other words, they assumed that the proton seniority [2]) is a good quantum number. According to their approximation the protons in the ground state are coupled to $J = 0$(or $J = j$) for an even (or odd) proton number. The aim of this work is to examine the change in the theoretical values of Coulomb energies when the coupling between neutrons and protons is taken into account. The neutron-proton forces prevent the proton seniority and angular momentum from being good quantum numbers. The ground state of the nucleus is no longer the state of maximum pairing of protons.

In this work we assume that particles of both kinds are coupled together to form a state with a definite total isobaric spin $T$ and lowest seniority [3]) †††. This state will then be a linear combination of states with different proton seniorities (and angular momenta). The expectation value of the Coulomb energy will be a weighted mean of the contributions from these different states. In other words, the neutron-proton forces cause the weakening of the coupling of the protons to spin zero (or $j$) and the result is a decrease in the Coulomb energy. We shall use, like Carlson and Talmi [1]), the $jj$-coupling shell model and take the one-particle wave functions to be the stationary states of an isotropic harmonic oscillator potential, $V(r) = \frac{1}{2}m\omega^2 r^2 \equiv \frac{1}{2}\hbar\omega\nu r^2$.

† Presented as a M. Sc. Thesis to the Hebrew University, Jerusalem.

†† Now at the Weizmann Institute of Science, Rehovoth, Israel.

††† A single seniority number is not defined for particles of both kinds, except for the lowest seniority.

The only experimental information on Coulomb energies is the difference within a pair of mirror nuclei [4] †. The values of these differences will be denoted, as in ref. [1], by $\Delta(A)$. The theoretical values of the same turn out to be proportional to the parameter $e^2(\nu/\pi)^{\frac{1}{2}}$ with a proportionality factor $\xi(A)$ depending only upon the mass number $A$. In the experimental data, and especially in the first shells, the effect of proton pairing is very prominent. $\Delta(A)$ is not a smooth function of $A$ but a function which attains larger values for $A = 4k+1$ ($k$ is an integer) due to the pairing of the protons. The energy parameter as calculated from experimental data is given by $e^2(\nu/\pi)^{\frac{1}{2}} = \Delta(A)/\xi(A)$. The values obtained for this parameter in ref. [1] are approximately constant ††. Our calculations do not change appreciably the results of ref.[1]), which justifies the approximation of that work. Nevertheless, our results indicate, as expected, a weaker pairing effect. Thus, our results as well as the approximate results of ref.[1]) are not quite sufficient for explaining the pairing effect actually observed, if a constant potential well is used.

It is easy to see the nature of the approximation of ref.[1]) in the configuration of two protons and one neutron. In this case the eigenfunction can be written as follows:

$$\psi(j^3, T=\tfrac{1}{2}, J=j, M_T=-\tfrac{1}{2}) = \alpha_0\varphi(j^2(0),\ j, J=j) + \alpha_2\varphi(j^2(2),\ j, J=j) + \ldots + \alpha_{2j-1}\varphi(j^2(2j-1),\ j, J=j). \quad (1)$$

In the $\varphi$'s the protons are first coupled to form an even $J_1$ and the neutron is then coupled to this $J_1$ to form the state of total $J = j$. According to the approximation of ref.[1]) the two protons are coupled to $J = 0$. This amounts to using the values

$$\alpha_0^2 = 1, \qquad \alpha_J^2 = 0 \qquad (J = 2, 4, \ldots, 2j-1). \quad (2)$$

On the other hand we find the correct result to be

$$\alpha_0^2 = \frac{2(2j+2)}{3(2j+1)}, \qquad \alpha_J^2 = \frac{2(2J+1)}{3(2j+1)(2j+2)} \quad (J = 2,\ 4, \ldots, 2j-1), \quad (3)$$

which means that even for large values of $j$, $\alpha_0^2 > \frac{2}{3}$. In detail:

$$\begin{aligned} &\text{for } j=\tfrac{3}{2}: \alpha_0^2 = \tfrac{5}{6}, \quad \alpha_2^2 = \tfrac{1}{6}; \\ &\text{for } j=\tfrac{5}{2}: \alpha_0^2 = \tfrac{49}{63}, \quad \alpha_2^2 = \tfrac{5}{63}, \quad \alpha_4^2 = \tfrac{9}{63}; \\ &\text{for } j=\tfrac{7}{2}: \alpha_0^2 = \tfrac{81}{108}, \quad \alpha_2^2 = \tfrac{5}{108}, \quad \alpha_4^2 = \tfrac{9}{108}, \quad \alpha_6^2 = \tfrac{13}{108}. \end{aligned} \quad (4)$$

The energy according to ref. [1]) is the Coulomb energy $V(0)$ of two protons coupled to $J = 0$. The correct energy calculated with the coefficients (4) is $V(0) - [(2j+1)/3(2j+2)](V(0) - F^0)$ (where $F^0$ is a Slater integral). Since the Coulomb force is not a short range force $(V(0) - F^0)$ is only a small

† See also ref. [1]) for references to experimental work.

†† See also ref.[5]) where the use of a constant energy parameter gives good results for the calculated binding energies of light nuclei.

fraction of $V(0)$. Thus, the difference between the two energy values is very small. We see that the approximation made in ref.[1]) was fairly good.

An interesting outcome of the calculations is that for a given number of protons the Coulomb energy is independent of the number of neutrons (i.e. the energy of a nucleus with $\frac{1}{2}(A+1)$ protons and $\frac{1}{2}(A-1)$ neutrons equals that of a nucleus with $\frac{1}{2}(A+1)$ protons and $\frac{1}{2}(A+3)$ neutrons). This can apparently be explained by the fact that the two added neutrons are coupled to $J = 0$, as both nuclei, the one of the configuration $j^n$ and the one of the configuration $j^{n+2}$, are in the state of lowest seniority, so that these added neutrons do not change the coupling of the protons.

In the energy difference of a pair of mirror nuclei a term appears due to the interaction of a single proton with the closed shells, in addition to the difference of the energies of the unfilled shell (see table 5). This interaction is of course equal in both methods. As the number of filled shells grows, the part of the energy difference due to interactions within the unfilled shell becomes less important. Thus, even a large theoretical correction in the term due to the unfilled shell will only result in a small correction of the value of the total energy difference.

The numerical results, as seen in tables 2, 3, 6, confirm the various assertions mentioned above. We see that even for energy differences within the unfilled shell our correction amounts to less than 6 per cent. For the total energy differences the correction does not exceed 1 per cent. This shows that the method of ref.[1]) was a very good approximation.

Some identities and other results of more general interest were obtained and are presented in the appendix. These include

a) closed formulae for fractional parentage coefficients (in short f.p.c.) of 3 nucleons,

b) a closed formula for the expectation values of the operator $Q$ which measures the amount of coupling to $J = 0$ pairs,

c) the expression of two-particle f.p.c. in terms of one-particle f.p.c.,

d) relations between the f.p.c. of two complementary configurations,

e) formulae for expressions of the form

$$\sum_{\beta' T' J'} |(j^{n-2}(\beta' T' J')j^2(TJ)|\} j^n \beta'' T'' J'')|^2$$

for mirror nuclei in the state of lowest seniority, which can be used for calculating charge independent interactions of such nuclei.

## 2. Method of Calculation

The Coulomb energy of the nucleus is given by the expectation value of the operator

$$G = \sum_{i<j}^{n} g_{ij} = \tfrac{1}{4} \sum_{i<j}^{n} \frac{e^2}{r_{ij}} (1-\tau_{\zeta_i})(1-\tau_{\zeta_j}) \tag{5}$$

where $e$ is the electronic charge, $r_{ij}$ — the distance between nucleons $i$ and $j$. $\tau_{\zeta_i}$ is the operator whose eigenvalue is $-1$ when the nucleon $i$ is a proton and 1 when it is a neutron. Using two-particle f.p.c. [2]) (i.e. the coefficients by which a wave function of $n$ equivalent particles † is expressed in terms of the wave functions of $n-2$ and 2 equivalent particles, see appendix, eq. (A20)) we can write the expectation value of $G$ as a linear combination of the expectation values of $g_{ij}$ (ref.[2]), eq. (33a)):

$$\begin{aligned}
&(j^n \beta'' T'' M_T'' J''|G|j^n \beta'' T'' M_T'' J'') \\
&\quad = \tfrac{1}{2} n(n-1) \sum_{\beta' T' J' T M_T J} (j^2 T M_T J|g_{ij}|j^2 T M_T J) \\
&\quad \times |(j^{n-2}(\beta' T' M'_T J') j^2 (T M_T J) J''\}\, j^n \beta'' T'' M_T'' J'')|^2 \qquad (6) \\
&\quad = \tfrac{1}{2} n(n-1) \sum_{T M_T J} (j^2 T M_T J|g_{ij}|j^2 T M_T J) \\
&\quad \cdot \sum_{\beta' T' J'} |(j^{n-2}(\beta' T' M'_T J') j^2 (T M_T J) J''\}\, j^n \beta'' T'' M_T'' J'')|^2
\end{aligned}$$

where $\beta'$ and $\beta''$ are additional quantum numbers necessary to define the states. Obviously, the diagonal matrix element $(j^2 T M_T J|g_{ij}|j^2 T M_T J)$ is different from zero only in a state of two protons which is defined by $T = 1$ $M_T = -1$ ($J$ even). The Coulomb energies in these states, $(j^2 J|(e^2/r_{ij})|j^2 J)$, like energies due to any ordinary force can be calculated by well known methods [6]). These energies in the cases of interest to us are given in table 1 ††).

TABLE 1

Coulomb energies of $j^2$ proton configurations in terms of Slater integrals

| $j$ | $J$ | Coulomb energy |
|---|---|---|
| $\frac{1}{2}$ | 0 | $F^0$ |
| $\frac{3}{2}$ | 0 | $F^0+\frac{5}{25}F^2$ |
| | 2 | $F^0-\frac{3}{25}F^2$ |
| $\frac{5}{2}$ | 0 | $F^0+\frac{10.4}{175}F^2+\frac{6}{63}F^4$ |
| | 2 | $F^0+\frac{4}{175}F^2-\frac{3}{63}F^4$ |
| | 4 | $F^0-\frac{5.4}{175}F^2-\frac{1}{63}F^4$ |
| $\frac{7}{2}$ | 0 | $F^0+\frac{15}{63}F^2+\frac{9}{77}F^4+\frac{75}{1287}F^6$ |
| | 2 | $F^0+\frac{7}{63}F^2-\frac{3}{77}F^4-\frac{25}{1287}F^6$ |
| | 4 | $F^0-\frac{5}{63}F^2+\frac{1}{77}F^4-\frac{25}{1287}F^6$ |
| | 6 | $F^0-\frac{5}{63}F^2-\frac{3}{77}F^4-\frac{25/13}{1287}F^6$ |

† Equivalent particles are particles with the same $nlj$ quantum numbers.

†† A more complete table is given in ref. [7]).

They are given in terms of the Slater integrals, $F^k$, for the Coulomb potential and can be expressed as linear combinationing of Talmi integrals [8]) $I_p$. (Using a formula from ref. [8]), p. 539, we get for the Coulomb potential

$$I_p = 2\frac{(2p)!!}{(2p+1)!!}e^2\left(\frac{\nu}{\pi}\right)^{\frac{1}{2}} \tag{7}$$

where $\nu \equiv m\omega/\hbar$ and $V = \frac{1}{2}m\omega^2 r^2$ is the central potential which determines the one particle wave functions.)

Since in (6) the $(j^2 TM_T J|g_{ij}|j^2 TM_T J)$ depend on $M_T$, we have to calculate sums of squares of f.p.c. still dependent upon the $M_T$'s if we want to use eq. (6). For these sums we shall use the notations

$$Y_J{}^n(M_T, M_T'') \equiv \sum_{\beta' T' J'} |(j^{n-2}(\beta' T' M'_T J')j^2(TM_T J), J'' = j|\}j^n, \\ T'' = \tfrac{1}{2}, v'' = 1, t'' = \tfrac{1}{2}, J'' = j, M_T'')|^2. \tag{8}$$

We are interested only in the ground state of mirror nuclei characterized by

$$j^n,\ T'' = \tfrac{1}{2},\ v'' = 1,\ t'' = \tfrac{1}{2},\ J'' = j \qquad (n \text{ odd})\ \dagger.$$

Expressions, similar to the $Y_J{}^n(M_T M_T'')$, which are independent of the $M_T$'s, will be used for calculating the $Y_J{}^n(M_T M_T'')$. Such expressions will also be used for calculating the sums of the Coulomb energies of each mirror pair. For these expressions we shall use the following notations:

$$X_J{}^n \equiv \sum_{\beta' T' J'} |(j^{n-2}(\beta' T' J')j^2(TJ)j|\}j^n \tfrac{1}{2}1\tfrac{1}{2}j \mp \tfrac{1}{2})|^2. \tag{9}$$

For an even $J$ this sum splits into two terms corresponding to $T' = \frac{3}{2}$ and $T' = \frac{1}{2}$:

$$X_{J\frac{3}{2}}^n \equiv \sum_{\beta' J'} |(j^{n-2}(\beta' \tfrac{3}{2} J')j^2(1J)j|\}j^n \tfrac{1}{2}1\tfrac{1}{2}j \mp \tfrac{1}{2})|^2, \tag{10a}$$

$$X_{J\frac{1}{2}}^n \equiv \sum_{\beta' J'} |(j^{n-2}(\beta' \tfrac{1}{2} J')j^2(1J)j|\}j^n \tfrac{1}{2}1\tfrac{1}{2}j \mp \tfrac{1}{2})|^2. \tag{10b}$$

The expressions $X_J{}^n$ are calculated in the appendix. Their values are found to be

$$X_0{}^n = \frac{4j+7-n}{2n(2j+1)}$$

$$X_J{}^n = \frac{[(6j+5)n-14j-17](2J+1)}{2n(2j+1)(2j-1)(2j+2)} \qquad (0 < J \text{ even}) \tag{11}$$

$$X_J{}^n = \frac{(n+3)(2J+1)}{2n(2j+1)(2j+2)} \qquad (J \text{ odd}).$$

The coefficients $(j^{n-2}(\beta' T' M'_T J')j^2(TM_T J)J''|\}j^n \beta'' T'' M_T'' J'')$ which

† See ref.[2]) (there $s$ is used instead of $v$). It can be shown that the new quantum number $t_0$ ("additional isobaric spin"), which was recently introduced by Racah [9]), is well defined for this state. Its value is 0 for $\frac{1}{2}(n-1)$ even and 1 for $\frac{1}{2}(n-1)$ odd.

appear in the $Y_J^n(M_T M_T'')$ (eq. (8)) are products of the corresponding f.p.c. and Clebsch-Gordan coefficients:

$$(j^{n-2}(\beta' T' M'_T J')j^2(TM_T J)J''|\}j^n\beta'' T'' M_T'' J'') = (j^{n-2}(\beta' T' J')j^2(TJ)J''|\}j^n\beta'' T'' J'')(T' M'_T TM_T|T' TT'' M_T''). \quad (12)$$

Now the $Y$'s can be expressed in terms of the $X$'s. For even $J$ we get from (8), (10), (12)

$$Y_J^n(M_T M_T'') = |(1M_T \tfrac{3}{2}M'_T|1\tfrac{3}{2}\tfrac{1}{2}M_T'')|^2 X_{J\frac{1}{2}}^n + |(1M_T \tfrac{1}{2}M'_T|1\tfrac{1}{2}\tfrac{1}{2}M_T'')|^2 X_{J\frac{1}{2}}^n \quad (J \text{ even}). \quad (13)$$

Substituting the values of the Clebsch-Gordan coefficients (see ref. [6]), p. 76) into (13) we have

$$Y_J^n(\mp 1, \mp\tfrac{1}{2}) = \tfrac{1}{6}X_{J\frac{1}{2}}^n + \tfrac{2}{3}X_{J\frac{3}{2}}^n \quad (14a)$$

$$Y_J^n(0, \mp\tfrac{1}{2}) = \tfrac{1}{3}X_{J\frac{1}{2}}^n + \tfrac{1}{3}X_{J\frac{3}{2}}^n = \tfrac{1}{3}X_J^n \quad (14b)$$

$$Y_J^n(\pm 1, \mp\tfrac{1}{2}) = \tfrac{1}{2}X_{J\frac{1}{2}}^n \qquad (J \text{ even}) \quad (14c)$$

$$Y_J^n(0, \mp\tfrac{1}{2}) = X_J^n \qquad (J \text{ odd}). \quad (15)$$

Rewriting eq. (6) for the ground state of the configuration $j^n$ of a mirror nucleus, using the notation (8) we get

$$(j^n \tfrac{1}{2}1\tfrac{1}{2}j \mp \tfrac{1}{2}|G|j^n \tfrac{1}{2}1\tfrac{1}{2}j \mp \tfrac{1}{2}) = \tfrac{1}{2}n(n-1)\sum_{J=0,2,\cdots 2j-1} Y_J^n(-1, \mp\tfrac{1}{2})\left(j^2 J\left|\frac{e^2}{r_{ij}}\right|j^2 J\right). \quad (16)$$

The Coulomb energies can now be calculated by straight-forward calculations of the $Y_J^n(-1, \mp\frac{1}{2})$. For this purpose the f.p.c. appearing in (10) must be calculated and then the $Y_J^n(-1, \mp\frac{1}{2})$ are calculated using (10) and (14). But since such calculations are rather involved, we shall proceed using a different method wherever possible. We first calculate the sums of the energies of each pair of mirror nuclei. Indeed, these sums are the expectation values of the charge symmetric part of the Coulomb energy operator (5). From (14a) and (14c) we get

$$Y_J^n(-1, -\tfrac{1}{2}) + Y_J^n(-1, +\tfrac{1}{2}) = \tfrac{2}{3}X_J^n. \quad (17)$$

Combining (16) and (17) we get for the sum of the energies of a pair of mirror nuclei

$$(j^n \tfrac{1}{2}1\tfrac{1}{2}j - \tfrac{1}{2}|G|j^n \tfrac{1}{2}1\tfrac{1}{2}j - \tfrac{1}{2}) + (j^n \tfrac{1}{2}1\tfrac{1}{2}j + \tfrac{1}{2}|G|j^n \tfrac{1}{2}1\tfrac{1}{2}j + \tfrac{1}{2}) = \tfrac{1}{3}n(n-1)\sum_{J=0,2,\cdots,2j-1} X_J^n\left(j^2 J\left|\frac{e^2}{r_{ij}}\right|j^2 J\right). \quad (18)$$

These sums are thus immediately calculated by substituting the values of the $X_J^n$ from (11) (and using table 1).

We have now to separate the sums (18) into their components for the two

members of the mirror pair. For most cases this is easily done. For the configuration with one proton and two neutrons the Coulomb energy is of course zero. Thus, for $n = 3$ the sum is separated. For the configuration with $2j$ protons (i.e. one hole in the proton $j$-shell) the energy equals that calculated in ref.[1]). Since according to both methods the protons couple to $J = j$. Thus, the separation for the cases $n = 4j-1$, $n = 4j+1$ is also accomplished. It remains to calculate the separate energies in the cases $(\frac{5}{2})^5$ and $(\frac{5}{2})^7$. Subsitituting the value of $Y_J{}^n(-1, +\frac{1}{2})$ from (14c) into (16) we get

$$(j^n \tfrac{1}{2}1\tfrac{1}{2}j+\tfrac{1}{2}|G|j^n \tfrac{1}{2}1\tfrac{1}{2}j+\tfrac{1}{2}) = \tfrac{1}{4}n(n-1) \sum_{J=0,2,\cdots,2j-1} X^n_{J\frac{1}{2}} \left(j^2 J \left| \frac{e^2}{r_{ij}} \right| j^2 J\right). \qquad (19)$$

Thus for calculating the Coulomb energy of 2 protons and 3 neutrons in the $j = \frac{5}{2}$ shell we have to know $X^5_{0\frac{1}{2}}$, $X^5_{2\frac{1}{2}}$, $X^5_{4\frac{1}{2}}$. We calculate $X^5_{0\frac{1}{2}}$ and $X^5_{2\frac{1}{2}}$ using their definitions (10a). The necessary f.p.c. we calculate directly from tables of one-particle f.p.c. for $n = 4$ [7]) and $n = 5$ [10]), using eq. (A20)†. From $X^5_{0\frac{1}{2}}$ and $X^5_{2\frac{1}{2}}$ the coefficient $X^5_{4\frac{1}{2}}$ was calculated by (14c) and (A31d). Thus the case $(\frac{5}{2})^5$ is also completely solved. The energy for the configuration with 2 protons and 3 neutrons, just calculated, equals that of the configuration with 2 protons and 1 neutron. We deduce from this that the energy of the configuration with 4 protons and 3 neutrons (i.e. 2 holes in the $\frac{5}{2}$ proton shell and 3 holes in the $\frac{5}{2}$ neutron shell) equals that of the configuration with 4 protons and 5 neutrons (i.e. 2 proton holes and 1 neutron hole) which has already been calculated. The case $(\frac{5}{2})^7$ is therefore also solved ††.

In tables 2 and 3 the energies as calculated here and in ref. [1]), respectively, are represented. They are given in terms of the Slater integrals $F^k$. The values of these integrals in units of $e^2(\nu/\pi)^{\frac{1}{2}}$, the energy parameter, are tabulated in table 4. In table 5 the interaction of a single $nlj$-proton with the closed shells is tabulated for the various $nlj$ (this also is given in units of $e^2(\nu/\pi)^{\frac{1}{2}}$). To calculate the total Coulomb energy difference between the two mirror nuclei such a term must be added. In table 6 the numerical values of the energy differences are tabulated. For comparison the corresponding values calculated in ref.[1]) are also given together with percentages of our correction. In the last columns the numerical values of the energy parameter as calculated from experimental data ††† are tabulated.

The author would like to thank Prof. G. Racah for his invaluable guidance, to Prof. A. de-Shalit, who suggested this work, and to Prof. I. Talmi for many helpful discussions.

† The results were checked by calculating also $X^5_{0\frac{1}{2}}$ in the same way and using (11).

†† Detailed calculation of the energy for the configuration of 3 protons and 4 neutrons in the same way as before would be very difficult since full tables of the necessary f.p.c. are not yet calculated.

††† The experimental data given in ref.[4]) are used for these calculations.

TABLE 2

Calculated Coulomb energies

| $nl_j^k$ Configuration | $Z=\frac{1}{2}(A+1)$ $(M_T''=-\frac{1}{2})$ | $Z=\frac{1}{2}(A-1)$ $(M_T''=+\frac{1}{2})$ | Energy Differences in $e^2\left(\frac{\nu}{\pi}\right)^{\frac{1}{2}}$ units |
|---|---|---|---|
| $0s_{\frac{1}{2}}^3$ | $F^0$ | 0 | 2.000 |
| $0p_{\frac{3}{2}}$ | 0 | 0 | 0.000 |
| $0p_{\frac{3}{2}}^3$ | $F^0+\frac{11}{15}\left(\frac{1}{5}F^2\right)$ | 0 | 1.622 |
| $0p_{\frac{3}{2}}^5$ | $3F^0-\frac{15}{15}\left(\frac{1}{5}F^2\right)$ | $F^0+\frac{11}{15}\left(\frac{1}{5}F^2\right)$ | 2.711 |
| $0p_{\frac{3}{2}}^7$ | $6F^0-\frac{30}{15}\left(\frac{1}{5}F^2\right)$ | $3F^0-\frac{15}{15}\left(\frac{1}{5}F^2\right)$ | 4.333 |
| $0p_{\frac{1}{2}}$ | 0 | 0 | 0.000 |
| $0p_{\frac{1}{2}}^3$ | $F^0$ | 0 | 1.500 |
| $0d_{\frac{5}{2}}$ | 0 | 0 | 0.000 |
| $0d_{\frac{5}{2}}^3$ | $F^0+\frac{5}{7}\left(\frac{8}{35}F^2+\frac{2}{21}F^4\right)$ | 0 | 1.418 |
| $0d_{\frac{5}{2}}^5$ | $3F^0-\frac{1}{7}\left(\frac{8}{35}F^2+\frac{2}{21}F^4\right)$ | $F^0+\frac{5}{7}\left(\frac{8}{35}F^2+\frac{2}{21}F^4\right)$ | 2.325 |
| $0d_{\frac{5}{2}}^7$ | $6F^0-\frac{2}{7}\left(\frac{8}{35}F^2+\frac{2}{21}F^4\right)$ | $3F^0-\frac{1}{7}\left(\frac{8}{35}F^2+\frac{2}{21}F^4\right)$ | 3.743 |
| $0d_{\frac{5}{2}}^9$ | $10F^0-\frac{14}{7}\left(\frac{8}{35}F^2+\frac{2}{21}F^4\right)$ | $6F^0-\frac{2}{7}\left(\frac{8}{35}F^2+\frac{2}{21}F^4\right)$ | 4.651 |
| $0d_{\frac{5}{2}}^{11}$ | $15F^0-\frac{21}{7}\left(\frac{8}{35}F^2+\frac{2}{21}F^4\right)$ | $10F^0-\frac{14}{7}\left(\frac{8}{35}F^2+\frac{2}{21}F^4\right)$ | 6.068 |
| $1s_{\frac{1}{2}}$ | 0 | 0 | 0.000 |
| $1s_{\frac{1}{2}}^3$ | $F^0$ | 0 | 1.364 |
| $0d_{\frac{3}{2}}$ | 0 | 0 | 0.000 |
| $0d_{\frac{3}{2}}^3$ | $F^0+\frac{11}{15}\left(\frac{1}{5}F^2\right)$ | 0 | 1.370 |
| $0d_{\frac{3}{2}}^5$ | $3F^0-\frac{15}{15}\left(\frac{1}{5}F^2\right)$ | $F^0+\frac{11}{15}\left(\frac{1}{5}F^2\right)$ | 2.253 |
| $0d_{\frac{3}{2}}^7$ | $6F^0-\frac{30}{15}\left(\frac{1}{5}F^2\right)$ | $3F^0-\frac{15}{15}\left(\frac{1}{5}F^2\right)$ | 3.623 |
| $0f_{\frac{7}{2}}$ | 0 | 0 | 0.000 |
| $0f_{\frac{7}{2}}^3$ | $F^0+\frac{19}{27}\left(\frac{5}{21}F^2+\frac{9}{77}F^4+\frac{25}{429}F^6\right)$ | 0 | 1.282 |

TABLE 3

Coulomb energies calculated by Carlson and Talmi [1])

| $nl_j^k$ Configuration | $Z=\frac{1}{2}(A+1)$ $\left(M_T''=-\frac{1}{2}\right)$ | $Z=\frac{1}{2}(A-1)$ $\left(M_T''=+\frac{1}{2}\right)$ | Energy differences in $e^2(\nu/\pi)^{\frac{1}{2}}$ units | Percent deviation from our calculated values |
|---|---|---|---|---|
| $0s_{\frac{1}{2}}^3$ | $F^0$ | 0 | 2.000 | |
| $0p_{\frac{1}{2}}$ | 0 | 0 | 0.000 | |
| $0p_{\frac{3}{2}}^3$ | $F^0+\frac{15}{15}\left(\frac{1}{5}F^2\right)$ | 0 | 1.667 | −2.7 |
| $0p_{\frac{3}{2}}^5$ | $3F^0-\frac{15}{15}\left(\frac{1}{5}F^2\right)$ | $F^0+\frac{15}{15}\left(\frac{1}{5}F^2\right)$ | 2.667 | +1.6 |
| $0p_{\frac{3}{2}}^7$ | $6F^0-\frac{30}{15}\left(\frac{1}{5}F^2\right)$ | $3F^0-\frac{15}{15}\left(\frac{1}{5}F^2\right)$ | 4.333 | |
| $0p_{\frac{1}{2}}$ | 0 | 0 | 0.000 | |
| $0p_{\frac{1}{2}}^3$ | $F^0$ | 0 | 1.500 | |
| $0d_{\frac{5}{2}}$ | 0 | 0 | 0.000 | |
| $0d_{\frac{5}{2}}^3$ | $F^0+\frac{7}{7}\left(\frac{8}{35}F^2+\frac{2}{21}F^4\right)$ | 0 | 1.482 | −4.4 |
| $0d_{\frac{5}{2}}^5$ | $3F^0$ | $F^0+\frac{7}{7}\left(\frac{8}{35}F^2+\frac{2}{21}F^4\right)$ | 2.293 | +1.4 |
| $0d_{\frac{5}{2}}^7$ | $6F^0$ | $3F^0$ | 3.775 | −0.8 |
| $0d_{\frac{5}{2}}^9$ | $10F^0-\frac{14}{7}\left(\frac{8}{35}F^2+\frac{2}{21}F^4\right)$ | $6F^0$ | 4.587 | +1.4 |
| $0d_{\frac{5}{2}}^{11}$ | $15F^0-\frac{21}{7}\left(\frac{8}{35}F^2+\frac{2}{21}F^4\right)$ | $10F^0-\frac{14}{7}\left(\frac{8}{35}F^2+\frac{2}{21}F^4\right)$ | 6.068 | |
| $1s_{\frac{1}{2}}$ | 0 | 0 | 0.000 | |
| $1s_{\frac{1}{2}}^3$ | $F^0$ | 0 | 1.364 | |
| $0d_{\frac{3}{2}}$ | 0 | 0 | 0.000 | |
| $0d_{\frac{3}{2}}^3$ | $F^0+\frac{15}{15}\left(\frac{1}{5}F^2\right)$ | 0 | 1.410 | −2.8 |
| $0d_{\frac{3}{2}}^5$ | $3F^0-\frac{15}{15}\left(\frac{1}{5}F^2\right)$ | $F^0+\frac{15}{15}\left(\frac{1}{5}F^2\right)$ | 2.213 | +1.8 |
| $0d_{\frac{3}{2}}^7$ | $6F^0-\frac{30}{15}\left(\frac{1}{5}F^2\right)$ | $3F^0-\frac{15}{15}\left(\frac{1}{5}F^2\right)$ | 3.623 | |
| $0f_{\frac{7}{2}}$ | 0 | 0 | 0.000 | |
| $0f_{\frac{7}{2}}^3$ | $F^0+\frac{27}{27}\left(\frac{5}{21}F^2+\frac{9}{77}F^4+\frac{25}{429}F^6\right)$ | 0 | 1.356 | −5.6 |

TABLE 4

Values of Slater integrals, $F^k(nl^2)$, for Coulomb energies, in $e^2(\nu/\pi)^{\frac{1}{2}}$ units

| $nl^2$ | $F^0$ | $F^2$ | $F^4$ | $F^6$ |
|---|---|---|---|---|
| $0s^2$ | 2 | | | |
| $1s^2$ | $\frac{131}{96}$ | | | |
| $0p^2$ | $\frac{9}{6}$ | $\frac{5}{6}$ | | |
| $0d^2$ | $\frac{151}{120}$ | $\frac{91}{120}$ | $\frac{63}{120}$ | |
| $0f^2$ | $\frac{1241}{1120}$ | $\frac{789}{1120}$ | $\frac{561}{1120}$ | $\frac{429}{1120}$ |

TABLE 5

The interaction of a single $nl_j$ proton with lower closed shells in $e^2(\nu/\pi)^{\frac{1}{3}}$ units

| $0s_{\frac{1}{2}}$ | $0p_{\frac{3}{2}}$ | $0p_{\frac{1}{2}}$ | $0d_{\frac{5}{2}}$ | $1s_{\frac{1}{2}}$ | $0d_{\frac{3}{2}}$ | $0f_{\frac{7}{2}}$ |
|---|---|---|---|---|---|---|
| 0.000 | 3.000 | 8.667 | 10.450 | 18.113 | 20.198 | 22.985 |

TABLE 6

Coulomb energy differences, experimental in MeV and theoretical in $e^2(\nu/\pi)^{\frac{1}{3}}$ units

| Mass Number $A$ | Configuration $nl_j^k$ | Experimental Coulomb-energy differences | Calculated Coulomb energy differences | Energy differences calculated in ref.[1]) | Percent deviations of ref.[1]) results from ours | $e^2(\nu/\pi)^{\frac{1}{3}}$ (keV) | $e^2(\nu/\pi)^{\frac{1}{3}}$ (keV) from ref.[1]) |
|---|---|---|---|---|---|---|---|
| 3 | $0s_{\frac{1}{2}}^3$ | [a]) 0.764±0.001 | 2.000 | 2.000 | | 381.9 | 381.9 |
| 5 | $0p_{\frac{3}{2}}$ | 0.8 ±0.3 | 3.000 | 3.000 | | 270 | 270 |
| 7 | $p_{\frac{3}{2}}^3$ | 1.646±0.002 | 4.622 | 4.667 | −1.0 % | 356.2 | 352.6 |
| 9 | $p_{\frac{3}{2}}^5$ | [b]) 1.852±0.002 | 5.711 | 5.667 | +0.8 % | 324.1 | 326.8 |
| 11 | $p_{\frac{3}{2}}^7$ | 2.763±0.003 | 7.333 | 7.333 | | 376.8 | 376.8 |
| 13 | $0p_{\frac{1}{2}}$ | 3.006±0.005 | 8.667 | 8.667 | | 346.8 | 346.8 |
| 15 | $p_{\frac{1}{2}}^3$ | 3.539±0.006 | 10.167 | 10.167 | | 348.1 | 348.1 |
| 17 | $0d_{\frac{5}{2}}$ | 3.550±0.006 | 10.450 | 10.450 | | 339.6 | 339.6 |
| 19 | $d_{\frac{5}{2}}^3$ | 4.027±0.008 | 11.868 | 11.932 | −0.5 % | 339.3 | 337.6 |
| 21 | $d_{\frac{5}{2}}^5$ | 4.30 ±0.03 | 12.775 | 12.743 | +0.2 % | 337 | 338 |
| 23 | $d_{\frac{5}{2}}^7$ | 4.841±0.010 | 14.193 | 14.225 | −0.2 % | 341.1 | 340.4 |
| 25 | $d_{\frac{5}{2}}^9$ | 5.084±0.025 | 15.101 | 15.037 | +0.4 % | 337 | 338 |
| 27 | $d_{\frac{5}{2}}^{11}$ | 5.584±0.010 | 16.518 | 16.518 | | 338.1 | 338.1 |
| 29 | $1s_{\frac{1}{2}}$ | 5.749±0.010 | 18.113 | 18.113 | | 317.4 | 317.4 |
| 31 | $s_{\frac{1}{2}}^3$ | 6.22 ±0.06 | 19.477 | 19.477 | | 320 | 320 |
| 33 | $0d_{\frac{3}{2}}$ | 6.0 ±0.2 | 20.198 | 20.198 | | 297 | 297 |
| 35 | $d_{\frac{3}{2}}^3$ | 6.75 ±0.04 | 21.568 | 21.608 | −0.2 % | 313 | 312 |
| 37 | $d_{\frac{3}{2}}^5$ | [c]) 6.83 ±0.28 | 22.451 | 22.411 | +0.2 % | 304 | 305 |
| 39 | $d_{\frac{3}{2}}^7$ | 7.38 ±0.08 | 23.821 | 23.821 | | 310 | 310 |
| 41 | $0f_{\frac{7}{2}}$ | 6.74 ±0.05 | 22.985 | 22.985 | | 293 | 293 |
| 43 | $f_{\frac{7}{2}}^3$ | | 24.267 | 24.341 | −0.3 % | | |

[a]) ref. [4]) all the data, except $A = 9$ and $A = 37$, have been taken from this reference.
[b]) ref. [1]).
[c]) ref. [19]).

## Appendix

### A.1. CALCULATION OF F.P.C. FOR 3 EQUIVALENT PARTICLES

In this calculation we follow closely the method of Schwartz and de Shalit [11]).

An antisymmetric function for 3 equivalent particles can be written as

$$\psi(j^3\, TJM_T M_J) = N \sum_{\mathrm{P}} (-1)^{\mathrm{P}}\, \mathrm{P}\psi(j^2(T_0J_0)jTJ) \quad (T_0+J_0 \text{ odd}). \tag{A1}$$

P denotes a permutation of the particles, $(-1)^{\mathrm{P}}$ is 1 for even permutation and $(-1)$ for odd permutation. Since $\psi(j^2(T_0J_0)jTJ)$ is already antisymmetric with respect to the first two particles, the sum extends only over three terms instead of six. According to Racah [2]) an antisymmetric function can also be written as

$$\psi(j^3TJM_TM_J) = \sum_{T''J''} (j^2(T''J''T)jTJ|\}\, j^3TJ)\psi(j^2(T''J'')jTJ). \tag{A2}$$

Here, also, $\psi(j^2(T''J'')jTJ)$ is antisymmetric with respect to the first two particles. Now, equating (A1) and (A2) and using Racah's recoupling coefficients [12]) we get

$$\begin{aligned}(j^2(T'J')jTJ|\}j^3TJ) = {} & C(T_0J_0)[\delta(T'T_0)\delta(J'J_0)(\tfrac{1}{2}\tfrac{1}{2}T_0)(\tfrac{1}{2}TT_0)(jjJ_0)(jJJ_0) \\ & -(1-(-1)^{T'+J'})(2T_0+1)^{\frac{1}{2}}(2T'+1)^{\frac{1}{2}}(2J_0+1)^{\frac{1}{2}}(2J'+1)^{\frac{1}{2}} \\ & \begin{Bmatrix}\tfrac{1}{2}\tfrac{1}{2}T'\\ \tfrac{1}{2}TT_0\end{Bmatrix}\begin{Bmatrix}j\ j\ J'\\ j\ J\ J_0\end{Bmatrix}\left(\frac{1-(-1)^{T_0+J_0}}{2}\right)\end{aligned} \tag{A3}$$

where

$$(abc) = \begin{cases} 0 & \text{if } a,b,c \text{ cannot form a triangle} \\ 1 & \text{if } a,b,c \text{ can form a triangle}\end{cases} \tag{A3}$$

and

$$\begin{Bmatrix}abe\\ dcf\end{Bmatrix} = (-1)^{a+b+c+d}W(abcd;ef) \tag{A5}$$

is Wigner's form of Racah coefficient. $C(T_0J_0)$ is a normalization coefficient which depends on the parameters $T_0J_0$ and is decided (but for the sign) by the normalization condition

$$\sum_{T''J''} |(j^2(T''J'')jTJ|\}\, j^3TJ)|^2 = 1. \tag{A6}$$

Using the identities [13])

$$\begin{aligned}\sum_{J'} \begin{Bmatrix}j\ j\ J'\\ j\ J\ J_0\end{Bmatrix}^2 (2J'+1)(2J_0+1) &= (jjJ_0)(jJJ_0) \\ \sum_{J'} \begin{Bmatrix}j\ j\ J'\\ j\ J\ J_0\end{Bmatrix}^2 (2J'+1)(2J_0+1)(-1)^{J'} &= \begin{Bmatrix}j\ j\ J_0\\ j\ J\ J_0\end{Bmatrix}(2J_0+1)\end{aligned} \tag{A7}$$

and the analogous identities for the $\tau$'s, we get

$$C(T_0J_0) = \pm\Big[3(\tfrac{1}{2}\tfrac{1}{2}T_0)(\tfrac{1}{2}TT_0)(jjJ_0)(jJJ_0) - 6(2T_0+1)(2J_0+1)\begin{Bmatrix}\tfrac{1}{2}\tfrac{1}{2}T_0\\ \tfrac{1}{2}TT_0\end{Bmatrix}\begin{Bmatrix}j\ j\ J_0\\ j\ J\ J_0\end{Bmatrix}\Big]^{-\frac{1}{2}}. \quad \text{(A8)}$$

We shall now show that by choosing the parameters $T_0$, $J_0$ to be 1, 0 respectively we obtain the f.p.c. for the state of lowest seniority.

It can be shown [14]) that

$$Q([\lambda](\sigma)) = \tfrac{1}{2}\{(g[\lambda]-ng[1])-(g(\sigma)-ng(1))\} \quad \text{(A9)}$$

where $Q([\lambda](\sigma))$ is an eigenvalue of the operator $Q$ defined by [15])

$$Q = \sum_{i<j}^{n} q_{ij} \quad \text{(A10)}$$

and $q_{ij}$ is defined by

$$(j^2JM|q_{ij}|j^2JM) = (2j+1)\delta(J, 0); \quad \text{(A11)}$$

$g[\lambda]$ is the eigenvalue of Casimir's operator [16]) for the unitary group $U(2j+1)$ belonging to the state $j^n[\lambda]$ ($[\lambda]$ is the partition of $n$). $g(\sigma)$ is the eigenvalue of Casimir's operator for the symplectic group $\mathrm{Sp}(2j+1)$ belonging to the state $j^n[\lambda](\sigma)$. ($(\sigma)$ is the partition of the seniority $-v$. An equivalent characterization of this state can be given by $j^nTvt$ where $t$ is the reduced isobaric spin [3])). It can also be shown that

$$g[\lambda] = ng[1]-\tfrac{1}{2}n(n-1)+\tfrac{3}{2}n-2T(T+1) \quad \text{(A12)}$$

$$g(\sigma) = vg(\sigma)-\tfrac{1}{2}v(v-1)+\tfrac{3}{2}v-2t(t+1). \quad \text{(A13)}$$

Inserting these equations and the value of $g(1)-(2j+2)$ — into (A9) yields †

$$Q([\lambda](\sigma)) \equiv (j^nTvtJ|Q|j^nTvtJ) = \tfrac{1}{4}(n-v)(4j+8-n-v)-T(T+1)+t(t+1). \quad \text{(A14)}$$

Now, using the identities [17])

$$\begin{Bmatrix}j\ j\ J'\\ j\ j\ 0\end{Bmatrix} = (-1)^{2j-J'}\frac{1}{2j+1} \quad \text{(A15a)}$$

$$\begin{Bmatrix}j\ j\ J'\\ j\ j\ 1\end{Bmatrix} = (-1)^{2j-J'-1}\frac{2j(j+1)-J'(J'+1)}{2j(j+1)(2j+1)} \quad \text{(A15b)}$$

and inserting $T_0 = 1$, $J_0 = 0$, $T = \frac{1}{2}$††, $J = j$ into (A3) and (A8) we get

† Comparing (A14) with eq. (14) of ref.[11]) shows that the equation there is a special case of ours for $T = \frac{1}{2}n$, $t = \frac{1}{2}v$.

†† The case $T = \frac{3}{2}$ is also proved in the same way but since this is the case for 3 nucleons of the same kind, it is treated in ref.[11]).

$$(j^2(T'J')jT=\tfrac{1}{2}J=j|\}j^3T=\tfrac{1}{2}J=j)=\begin{cases}\left(\dfrac{2j+2}{3(2j+1)}\right)^{\frac{1}{2}} & (T',J')=(1,0)\\ \left(\dfrac{2J'+1}{3(2j+1)(2j+2)}\right)^{\frac{1}{2}} & (T',J')=(1,\ \text{even number}>0)\\ -\left(\dfrac{2J'+1}{(2j+1)(2j+2)}\right)^{\frac{1}{2}} & (T',J')=(0,\ \text{odd number}).\end{cases} \tag{A16}$$

For any operator

$$G=\sum_{i<j}^{n} g_{ij}, \tag{A17}$$

where $g_{ij}$ operates symmetrically on the particles $i$ and $j$, we have [2])

$$(j^nTvtJ|G|j^nTvtJ)=\tfrac{1}{2}n(n-1)\sum_{\substack{T'v't'J'\\T''J''}}(j^2T''J''|g_{ij}|j^2T''J'')\times|(j^{n-2}(T'v't'J')j^2(T''J'')TJ|\}j^nTvtJ)|^2. \tag{A18}$$

Setting $Q$ for $G$ and using (A11), (A14), (A16) we get

$$\tfrac{1}{4}(3-v)(4j+5-v)-\tfrac{3}{4}+t(t+1)=2j+2, \tag{A19}$$

the only solution of which is $v=1$, $t=\frac{1}{2}$ (remembering that $t$ can only be $\frac{1}{2}$ or $\frac{3}{2}$ and $v$ is an integer which cannot be greater than $2j+1$). Thus, our assertion is proved.

We now summarize some useful, easily obtainable, identities.

Two-particle f.p.c. can be expressed in terms of one-particle f.p.c.:

$$\begin{aligned}&(j^{n-2}(\beta'T'J')j^2(T''J'')J|\}j^n\beta TJ)\\&\quad=-\sum_{\beta_1T_1J_1}(2T''+1)^{\frac{1}{2}}(2T_1+1)^{\frac{1}{2}}(2J''+1)^{\frac{1}{2}}(2J_1+1)^{\frac{1}{2}}\\&\quad\times(-1)^{T+J+T'+J'}\begin{Bmatrix}\frac{1}{2}&\frac{1}{2}&T''\\T'&T&T_1\end{Bmatrix}\begin{Bmatrix}j&j&J''\\J'&J&J_1\end{Bmatrix}\\&\quad\cdot(j^{n-2}(\beta'T'J')jJ_1|\}j^{n-1}\beta_1T_1J_1)(j^{n-1}(\beta_1T_1J_1)jJ|\}j^n\beta TJ).\end{aligned} \tag{A20}$$

The f.p.c. of a given configuration can be expressed in terms of the f.p.c. of the complementary configuration:

$$\begin{aligned}&(j^{4j+1-n}(\beta'T'J')jJ|\}j^{4j+2-n}\beta TJ)\\&=(-1)^{T-T'+J+J'-j-\frac{1}{2}}\left[\frac{(n+1)(2T'+1)(2J'+1)}{(4j+2-n)(2T+1)(2J+1)}\right]^{\frac{1}{2}}(j^n(\beta TJ)jJ'|\}j^{n+1}\beta'T'J')\end{aligned} \tag{A21}$$

$$\begin{aligned}&(j^{4j-n}(\beta'T'J')j^2(T''J'')J|\}j^{4j+2-n}\beta TJ)\\&=-\left[\frac{(n+2)(n+1)(2T'+1)(2J'+1)}{(4j+1-n)(4j+2-n)(2T+1)(2J+1)}\right]^{\frac{1}{2}}(j^n(\beta TJ)j^2(T''J'')J'|\}j^{n+2}\beta'T'J').\end{aligned} \tag{A22}$$

Analogously to ref.[2]) eq. (20) we have here the orthogonality relation

$$\sum_{\beta' T' J'} (2T'+1)(2J'+1)(j^{n-1}(\beta'' T'' J'')jJ'|\}j^n\beta' T' J')(j^n\beta' T' J'\{|j^{n-1}(\beta T J)jJ') = [(4j+3-n)/n](2T+1)(2J+1)\delta(\beta,\beta'')\delta(T,T''). \quad \text{(A23)}$$

Matrix elements of an operator of type G for the filled shell are

$$D \equiv (j^{4j+2}00|G|j^{4j+2}00) = \sum_J [2+(-1)^J](2J+1)(j^2 TJ|g_{ij}|j^2 TJ). \quad \text{(A24)}$$

A.2. CALCULATIONS OF THE $X_J^n$

Using eq. (9), we obtain from (A18)

$$(j^n,\ T''=\tfrac{1}{2},\ v''=1,\ t''=\tfrac{1}{2},\ J''=j|G|j^n,\ T''=\tfrac{1}{2},\ v''=1,\ t''=\tfrac{1}{2},\ J''=j) = \tfrac{1}{2}n(n-1)\sum_{TJ}(j^2 TJ|g_{ij}|j^2 TJ)X_J^n. \quad \text{(A25)}$$

Equation (A25) may be used for calculating the $X_J^n$. This is done by choosing $g_{ij}$ (and $G$) to be an operator for which the eigenvalues appearing in (A25) are already known (or can be calculated without the use of (A25)). We take

$$g_{ij} = (2k+1)(\mathbf{u}_i^{(k)} \cdot \mathbf{u}_j^{(k)})$$

where $\mathbf{u}_i^{(k)}$ is a tensorial operator of degree $k$ which is defined by

$$(j||\mathbf{u}^{(k)}||j') = \delta(j,j'). \quad \text{(A26)}$$

From (A25) we get

$$(j^n \tfrac{1}{2}1\tfrac{1}{2}j|\sum_{i<j}^{n}(2k+1)(\mathbf{u}_i^{(k)} \cdot \mathbf{u}_j^{(k)})|j^n \tfrac{1}{2}1\tfrac{1}{2}j) = \tfrac{1}{2}n(n-1)\sum_{TJ}(j^2 TJ|(2k+1)(\mathbf{u}_i^{(k)} \cdot \mathbf{u}_j^{(k)})|j^2 TJ)X_J^n. \quad \text{(A27)}$$

From ref.[12]) eq. (38) and (A26) we have

$$(j^2 TJ|(2k+1)(\mathbf{u}_i^{(k)} \cdot \mathbf{u}_j^{(k)})|j^2 TJ) = (-1)^{2j-J}(2k+1)W(jjjj;Jk). \quad \text{(A28)}$$

Thus (A27) turns into

$$(j^n \tfrac{1}{2}1\tfrac{1}{2}j|\sum_{i<j}^{n}(2k+1)(\mathbf{u}_i^{(k)} \cdot \mathbf{u}_j^{(k)})|j^n \tfrac{1}{2}1\tfrac{1}{2}j) = \tfrac{1}{2}n(n-1)\sum_{J}(-1)^{2j-J}(2k+1)W(jjjj;Jk)X_J^n. \quad \text{(A29)}$$

The left hand side of this equation is calculated by a method of Racah [18]). Now, multiplying both sides of (A29) by $W(jjjj;J'k)$ and summing over $k$ (with the help of ref.[12]) eqs. (40), (42), ref. [18]) eqs. (28a), (28b) and (A15a)) we get

$$\frac{(-1)^{2j-J}X_J^n}{2J+1} = \frac{1}{4n(2j+1)}\left\{\frac{[(6j+5)n-14j-17][(-1)^{2j-J}-1+2\delta(J,0)]}{(2j-1)(2j+2)} + \frac{(n+3)[(-1)^{2j-J}+1]}{(2j+2)} - 2(4j+7-n)\delta(J,0)\right\}, \quad \text{(A30)}$$

which is the general form of (11).
The substitution $g_{ij} = (1 \mp \tau_{\zeta i})(1 \mp \tau_{\zeta j})/4$ into eq. (6) and using eq. (8) (calculating only for the ground state) yields

$$\text{a)} \quad \sum_{J=1,3,\cdots,2j} Y_J{}^n(0, \mp\tfrac{1}{2}) = \frac{n+3}{4n}$$

$$\text{b)} \quad \sum_{J=0,2,\cdots,2j-1} Y_J{}^n(\mp 1, \mp\tfrac{1}{2}) = \frac{n+1}{4n} \qquad \text{(A31)}$$

$$\text{c)} \quad \sum_{J=0,2,\cdots,2j-1} Y_J{}^n(0, \mp\tfrac{1}{2}) = \frac{n-1}{4n}$$

$$\text{d)} \quad \sum_{J=0,2,\cdots,2j-1} Y_J{}^n(\pm 1, \mp 1) = \frac{n-3}{4n}.$$

The eqs. (11) and (A31) can be checked by substituting in (6) for $g_{ij}$ the operators $1_{ij}$, $(\boldsymbol{\tau}_i \cdot \boldsymbol{\tau}_j)$ ($\boldsymbol{\tau}_i$ is the isobaric spin of the particle $i$), $q_{ij}$, $(\mathbf{j}_i \cdot \mathbf{j}_j)$.

Using Racah's results in ref.[12]) § 6 and taking into account the method of calculating the $X_J{}^n$ one can obtain

$$\tfrac{1}{2}(4j+2-n)(4j+1-n)X_J^{4j+2-n} = \tfrac{1}{2}n(n-1)X_J{}^n + \frac{4j+2-2n}{4j+2}[(2+(-1)^J)(2J+1)]. \qquad \text{(A32)}$$

For $n = 3$, $X^3_{Jt} = 0$ as may be seen from the defining eq. (10). Therefore $X^3_{Jt} = X_J{}^3$ and (14) together with (11) (or (A16) which is the same for $n = 3$) gives

$$\text{a)} \quad Y_0{}^3(\mp 1, \mp\tfrac{1}{2}) = \tfrac{1}{3}\left[\frac{2(2j+2)}{3(2j+1)}\right]$$

$$\text{b)} \quad Y_J{}^3(\mp 1, \mp\tfrac{1}{2}) = \tfrac{1}{3}\left[\frac{2(2J+1)}{3(2j+1)(2j+2)}\right] \quad (J = 2, 4, \ldots, 2j-1) \qquad \text{(A33)}$$

$$\text{c)} \quad Y_J{}^3(\pm 1, \mp\tfrac{1}{2}) = 0 \qquad (J = 0, 2, \ldots, 2j-1).$$

## References


1) B. C. Carlson and I. Talmi, Phys. Rev. **96** (1954) 436
2) G. Racah, Phys. Rev. **63** (1943) 367
3) B. H. Flowers, Proc. Roy. Soc. A **212** (1952) 248
4) O. Kofoed-Hansen, Nuclear Physics **2** (1956/57) 441
5) I. Talmi and R. Thieberger, Phys. Rev. **103** (1956) 718
6) E. U. Condon and G. H. Shortley, The Theory of Atomic Spectra (Cambridge University Press, Cambridge, 1953) p. 257 *et seq.*
7) B. H. Flowers, Proc. Roy. Soc. A **214** (1952) 515
8) R. Thieberger, Nuclear Physics **2** (1956/57) 533
9) G. Racah, Proc. Rehovoth Conference (North-Holland Publ. Co., 1958)
10) G. Racah and S. Goldstein (unpublished)
11) C. Schwartz and A. de-Shalit, Phys. Rev. **94** (1954) 1257

12) G. Racah, Phys. Rev. **62** (1942) 438
13) Ref.[12]) eqs. (42), (43)
14) Ref.[7]) p. 521 *et seq.*
15) G. Racah and I. Talmi, Physica **18** (1952) 1097; see also ref.[2]) § 6
16) G. Racah, Group Theory and Spectroscopy (Institute for advanced Study, Princeton, 1951)
17) Biedenharn, Tables of Racah Coefficients (U.S.A.E.C., 1952)
18) G. Racah, L. Farkas Memorial Volume (Research Council of Israel, Jerusalem, 1952)
19) P. C. Sood and A. E. S. Green, Nuclear Physics **5** (1958) 274

2.E:2.L *Nuclear Physics* **8** (1958) 484—492; © *North-Holland Publishing Co., Amsterdam*
Not to be reproduced by photoprint or microfilm without written permission from the publisher

# HIGH ENERGY SCATTERING OF DEUTERONS BY COMPLEX NUCLEI

SHIGUEO WATANABE

*Palmer Physical Laboratory, Princeton University, New Jersey* †

Received 23 June 1958

**Abstract:** An effective deuteron-nucleus potential consisting of an optical well plus a spin-orbit interaction was derived, starting from a Saxon potential plus a spin-orbit term for the interaction between each nucleon in the deuteron and the nucleus. The WKB method was used to calculate the angular distribution and the polarization of 94 MeV deuterons by carbon. The result of this calculation using well parameters which fit the scattering data of 40 MeV protons by carbon, is in good agreement with the measured values of the differential cross section. The predicted polarization shows a maximum of about 30 percent, but its sign is constant and does not oscillate as the experimental one does.

## 1. Introduction

The differential cross sections and the polarization of deuterons scattered elastically by carbon, aluminium, copper, lithium and beryllium have been measured by Baldwin *et al.*[1]). The theoretical explanation on the basis of the Born approximation has been attempted by Baldwin [1]) and Cheishvili [2]). Baldwin obtained a differential cross section which at small angles is larger than the experimental one and smaller at large angles. The maximum polarization he gets is much smaller than that of the measured one. Cheishvili considered a complex square well plus a spin-orbit interaction, $V_0\rho(r) + V_1/r(\mathrm{d}\rho/\mathrm{d}r)\mathbf{l}\cdot\mathbf{s}$ between the nucleons in the deuteron and the target nucleus, with $V_0\rho(r) = -(28+i16)$ MeV for $r < R_n$ and zero for $r > R_n$, where $R_n$ is the nucleon-nucleus interaction radius, and $V_1 = 9\times10^{-26}$ MeV · cm². The differential cross section for the incident polarized deuterons of 167 MeV scattered by carbon at 20° is three times smaller than the measured one. This differential cross section, according to Cheishvili, may be written $I(\theta,\varphi) = (p+q\cos\varphi+r\cos 2\varphi)\times10^{-27}$ cm²/steradian. For 156 MeV deuterons scattered by carbon, Cheishvili obtained the following results: the ratio $p/q$ agrees with the experimental values for angles greater than 16°, but not for smaller angles; furthermore the $r$ values came out incorrectly.

In a recent paper [3]) Stapp made an attempt to take into account the contribution of the deuteron D-state and the simultaneous scattering of

† Fellow of the National Research Council of Brazil, and on Leave from the University of São Paulo, Brazil.

both nucleons of the deuterons by the target nuclei. Both effects should enhance the differential cross section at large angles, the first effect through the sticking factor, which is the dominating factor in the large angle scattering, according to the impulse approximation which was used by Stapp; the second effect reduces the breaking up of the deuteron at large angles due to high momentum transfer, thus enhancing the elastic cross section. However the D-state contribution was found insufficient to yield a differential cross section of the order of magnitude of the measured one. The inclusion of the simultaneous scattering produces a result which agrees well with the measured values for angles smaller than 16°, but for angles larger than 16°, the theoretical differential cross section is higher [4]). A large deuteron polarization will not be obtained from Stapp's formulae if the nucleon amplitudes are consistent with the observed small nucleon polarizations [4]).

## 2. Effective Deuteron-Nucleus Potential

We assume that the Hamiltonian may be written

$$H = T_1+T_2+V_{12}(r_{12})+V_1(r_1)+V_2(r_2). \tag{1}$$

The indices 1 and 2 indicate the neutron and the proton in the deuteron, $T$ is the kinetic energy operator, $r_{12} = |\mathbf{r}_1-\mathbf{r}_2|$, $V_{12}(r_{12})$ is the interaction between the nucleons of the deuteron, and the $V_i$'s are the interaction of the neutron and the proton with the target nucleus. Using now the centre of mass and relative coordinates of the deuteron, the Schrödinger equation may be written

$$\left\{-\frac{\hbar^2}{2M}\nabla_R^2-\frac{\hbar^2}{2\mu}\nabla_r^2+V_{12}(r)+V_1(\tfrac{1}{2}|\mathbf{R}+\mathbf{r}|)+V_2(\tfrac{1}{2}|\mathbf{R}-\mathbf{r}|)\right\}\psi(\mathbf{R},\mathbf{r}) = E\psi(\mathbf{R},\mathbf{r}) \tag{2}$$

where

$$\mathbf{R} = \tfrac{1}{2}(\mathbf{r}_1+\mathbf{r}_2), \quad \mathbf{r} = \mathbf{r}_1-\mathbf{r}_2, \quad M = 2m, \quad \mu = \tfrac{1}{2}m,$$

$m$ denoting the nucleon mass. Denoting by $\chi(r)$ the deuteron wave function, we have

$$\{-(\hbar^2/2\mu)\nabla_r^2+V_{12}(r)\}\chi(r) = \varepsilon_d\chi(r). \tag{3}$$

The solution $\psi(\mathbf{R},\mathbf{r})$ of eq. (2) may be written

$$\psi(\mathbf{R},\mathbf{r}) = \chi(r)\phi(\mathbf{R})+F(\mathbf{R},\mathbf{r}). \tag{4}$$

We now multiply eq. (2) by $\chi(r)$ and integrate with respect to $\mathbf{r}$; we get

$$\{-(\hbar^2/2M)\nabla_R^2+V(R)-(E-\varepsilon_d)\}\phi(\mathbf{R})+g(\mathbf{R}) = 0 \tag{5}$$

where

$$V(R) = \int d\mathbf{r}\chi(\mathbf{r})[V_1(\tfrac{1}{2}|\mathbf{R}+\mathbf{r}|)+V_2(\tfrac{1}{2}|\mathbf{R}-\mathbf{r}|)]\chi(r) \tag{6}$$

and

$$g(\mathbf{R}) = \int d\mathbf{r}\chi(r)[V_1(\tfrac{1}{2}|\mathbf{R}+\mathbf{r}|)+V_2(\tfrac{1}{2}|\mathbf{R}-\mathbf{r}|)]F(\mathbf{R},\mathbf{r}). \tag{7}$$

The inhomogeneous term $g(\mathbf{R})$ in (5) given by (7) contains the dissociation of the deuteron and the distortion of the deuteron wave function. The effect of such processes will be approximated by adding an imaginary potential in the homogeneous part of eq. (5) and dropping $g(\mathbf{R})$. As we shall see later, the contribution of $g(\mathbf{R})$ is actually very small. Since we are interested in the polarization of the deuterons, we assume

$$V_i(r_i) = (v+iw)\rho(r_i)+V_{LS}(\hbar/m_\pi c)^2\frac{1}{r_i}\frac{d\rho(r_i)}{dr_i}\mathbf{l}_i\cdot\mathbf{s}_i. \tag{8}$$

Setting $\chi(r) = Nf(r)/r$, and noting that

$$1)\ \sum_{i=1}^{2} Y(r_i)\mathbf{l}_i\cdot\mathbf{s}_i = \tfrac{1}{2}(\mathbf{L}+\mathbf{l})\cdot\sum_{i=1}^{2} Y(r_i)\mathbf{s}_i+[\mathbf{s}_1Y(r_1)-\mathbf{s}_2Y(r_2)] \times[-\mathbf{R}\times\nabla_r+\tfrac{1}{4}\mathbf{r}\times\nabla_R] \tag{9}$$

where $\mathbf{L} = \mathbf{R}\times\nabla_R$, $\mathbf{l} = \mathbf{r}\times\nabla_r$;

$$2)\ \int d\mathbf{r}\chi(r)[\mathbf{s}_1Y(r_1)-\mathbf{s}_2Y(r_2)][\mathbf{R}\times\nabla_r]\chi(r) = 0; \tag{10}$$

3) since we assume a pure S-state for the deuteron ground state, $\mathbf{l}$ operated on $\chi(r)$ yields zero;

eq. (6) becomes

$$V(R) = 4\pi N^2[2(v+iw)\mathscr{V}(R)+\tfrac{1}{2}V_{LS}(\hbar/m_\pi c)^2\mathbf{L}\cdot(\mathbf{s}_1+\mathbf{s}_2)U_{LS}(R)] \tag{11}$$

where

$$\mathscr{V}(R) = \int d\mathbf{r}[\chi(r)]^2\rho(r_1).$$

Using the relations

$$d\mathbf{r} = 2d\mathbf{r}_1 = -2r_1^2dr_1d(\cos\theta)d\varphi$$

and

$$-d(\cos\theta) = rdr/4r_1R$$

where $\theta$ is the angle between $\mathbf{R}$ and $\mathbf{r}_1$, we get

$$\mathscr{V}(R) = R^{-1}\int_0^\infty r_1dr_1\rho(r_1)\int_{2|R-r_1|}^{2(R+r_1)} dr\frac{f^2(r)}{r}. \tag{12}$$

In a similar way we get

$$U_{LS}(R) = -R^{-2}\left\{\mathscr{V}(R)+R\int_0^\infty dr_1\rho(r_1)\left[\left(\frac{1}{R-r_1}-\frac{1}{R}\right)f^2(|2R-2r_1|) + \left(\frac{1}{R+r_1}-\frac{1}{R}\right)f^2(2R+2r_1)\right]\right\}. \tag{13}$$

If we set $k^2 = (2M/\hbar^2)(E-\varepsilon_d) = (2M/\hbar^2)E_d$, we get

$$\{\nabla_R^2-(2M/\hbar^2)4\pi N^2[2(v+iw)\mathscr{V}(R) -\tfrac{1}{2}V_{LS}(\hbar/m_\pi c)^2\mathbf{L}\cdot(\mathbf{s}_1+\mathbf{s}_2)U_{LS}(R)]+k^2\}\phi(\mathbf{R})=0. \quad (14)$$

We have thus derived an effective deuteron-nucleus potential which consists of a complex central potential plus a spin-orbit interaction the well parameters of which are dependent on those of the nucleon-nucleus potential. The solution $\phi(\mathbf{R})$ of this equation contains neither the dissociation of the deuteron nor the distortion of the deuteron wave function, but does include the simultaneous scattering of both nucleons of the deuteron by the nucleus.

Let us now use the Hulthén wave function for the ground state of the deuteron

$$f(r)=e^{-\alpha r}-e^{-\beta r} \quad (15)$$

with $\alpha^{-1}=4.31\times10^{-13}$ cm, $\beta=6\alpha$, and $4\pi N^2=2\alpha\beta(\alpha+\beta)/(\beta-\alpha)^2$. $\mathscr{V}(R)$ and $U_{LS}(R)$ were obtained by numerical integration of eqs. (12) and (13), and they are shown in fig. 1. We have taken Saxon's potential

$$\rho(r_1)=[1+\exp\left((r_1-R_n)/a\right)]^{-1} \quad (16)$$

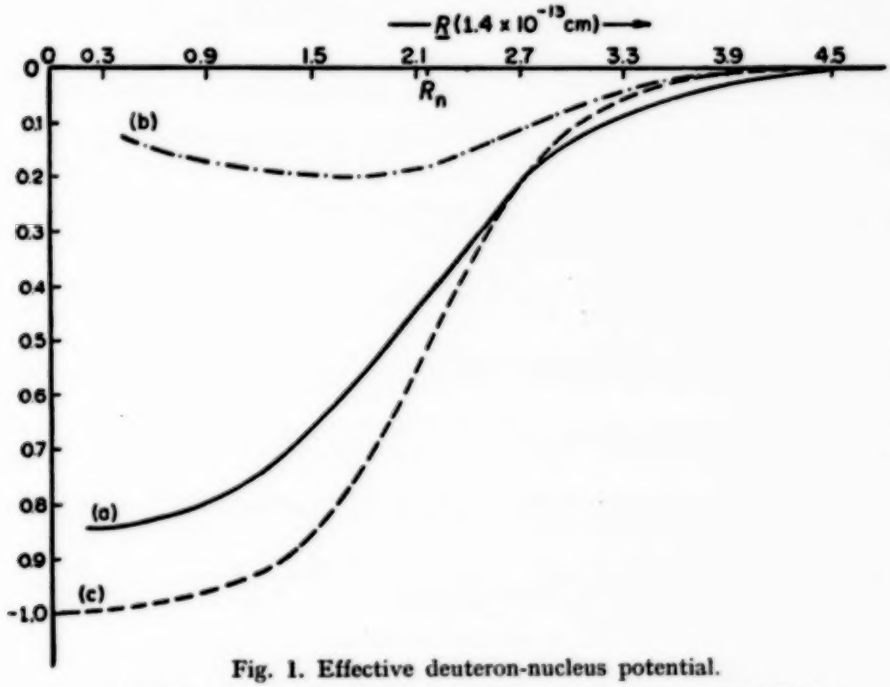


Fig. 1. Effective deuteron-nucleus potential.
(a) $\mathscr{V}(R)$, (b) $U_{LS}(R)$, (c) $\rho(r_1)=[1+\exp((r_1-R_n)/a)]^{-1}$.

where $R_n=1.33A^{\frac{1}{3}}\times10^{-13}$ cm is the nucleon-nucleus interaction radius, and $a$ is the surface diffuseness parameter. We have used [5]) $a=0.55\times10^{-13}$ cm.

The resulting potential has a very long tail: its effect extends to a distance of $R\approx R_n\times2.5$, and as a consequence, in the partial waves analysis we have to consider contributions of about 20 partial waves. Such a long tail is essentially due to the fact that the deuteron is an extended structure.

## 3. WKB Calculation

We have used the WKB method to calculate the phase shifts. The phase shift is given by [6])

$$\delta_L{}^{aJ} = \int_{R'_0}^{\infty} [k^2-(2M/\hbar^2)V(R)-L(L+1)/R^2]^{\frac{1}{2}}\,\mathrm{d}R - \int_{R''_0}^{\infty} [k^2-L(L+1)/R^2]^{\frac{1}{2}}\,\mathrm{d}R$$

where $R'_0$ and $R''_0$ are the respective zeros of the integrands. For $V(R) < E_d$ the above expression can be reduced to

$$\delta_L{}^{aJ} = \frac{k}{2E_d}\int_{R_0}^{\infty} [-2(v+iw)\mathscr{V}(R)-\alpha_J U_{LS}(R)(V_{LS}/2)(\hbar/m_\pi c)^2 \times [k^2(R^2-R_0^2)]^{-\frac{1}{2}} R\,\mathrm{d}R, \tag{17}$$

$(kR_0)^2 = L(L+1)$, and $\alpha_J = L$, $-1$, $-(L+1)$, respectively, for $J = L+1$, $J = L$, $J = L-1$.

We computed the angular distribution and the polarization of 94 MeV deuterons scattered by carbon, using the formulae † derived by the author [7]). Since each nucleon in the deuteron has half the deuteron energy, the well parameters $v$, $w$ and $V_{LS}$ must be those corresponding to scattering of nucleons of about 45 MeV. Melkanoff *et al.*[5]) in their analysis of the elastic scattering of 17 and 31.5 MeV protons by several nuclei, found the following average values of the parameters of the optical well:

| $E$(MeV) | $v$(MeV) | $w$(MeV) | $r_0(10^{-13}$ cm) | $a(10^{-13}$ cm) |
|---|---|---|---|---|
| 17 | −47 | − 8.5 | 1.33 | 0.49 |
| 31.5 | −35 | −15.5 | 1.33 | 0.53 |

In particular for the carbon nucleus they found for 31.5 MeV protons $v = -44$ MeV, $w = -11$ MeV, $r_0 = 1.28\times10^{-13}$ cm and $a = 0.5\times10^{-13}$ cm. Glassgold and Kellog [8]) analysed 40 and 95 MeV protons scattering by carbon, aluminium and lead, and got as average values of the well parameters, the following numbers:

1) for 40 MeV protons, $v = -36\pm4$ MeV, $w = -15\pm5$ MeV, $r_0 = 1.3\times10^{-13}$ cm;

2) for 95 MeV protons, $v = -26\pm2$ MeV, $w = -10\pm5$ MeV, $r_0 = 1.3\times10^{-13}$ cm.

In the analysis of these groups the spin-orbit potential was not included.

Fernbach, Heckrotte and Lepore [9]) calculated the angular distribution and the polarization of 290 MeV neutrons in an elastic scattering by carbon,

† There is an error in these formulae. The term $\frac{1}{2}(BD^*-B^*D)\sin\theta$ in formula (30) and the term $i[(C+A)D^*-(C+A)^*D]\sin\theta$ in (33) of ref. [7]) must be omitted. The contribution of these terms to the angular distribution and the polarization is anyway negligible.

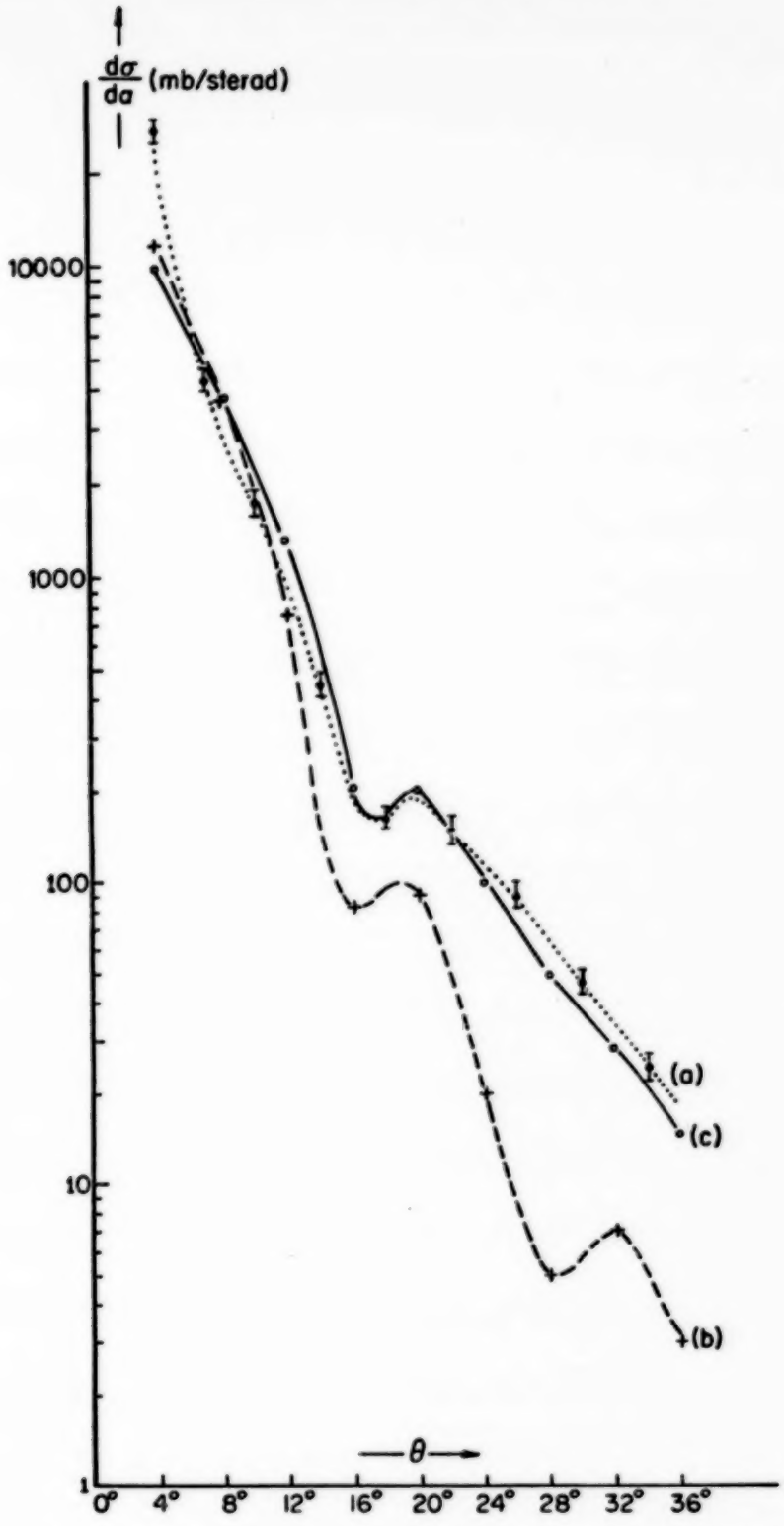


Fig. 2. Angular distribution of 94 MeV deuteron from $C^{12}$ (d,d)$C^{12}$
(a) Experiment (b) $v = -31.33$ MeV, $w = -62.66$ MeV, $V_{LS} = 2.55$ MeV
(c) $v = -40$ MeV, $w = -20$ MeV, $V_{LS} = 2.55$ MeV

including a spin-orbit potential of the form

$$V_{LS}(\hbar/m_\pi c)^2(1/r)(\mathrm{d}\rho/\mathrm{d}r)\mathbf{l}\cdot\mathbf{s}. \tag{18}$$

Three different shapes of the potential were used, namely, square, parabolic, and Gaussian well; however no definite conclusion can be drawn from their analysis. The well parameters used were as follows:

| | square | parabolic | Gauss. A | Gauss. B |
|---|---|---|---|---|
| $-v$(MeV) | 0 | 18 | 0 | 53 |
| $-w$(MeV) | 18 | 30 | 89 | 76 |
| $V_{LS}$(MeV) | 2.55 | 2.55 | 5.1 | 10 |
| $r_0(10^{-13}$ cm) | 1.4 | 1.6 | | |

Recently Bjorklund and Fernbach [10]) analysed the differential cross section of 4.1; 7 and 14 MeV neutrons scattered by magnesium, calcium, cadmium and bismuth, including the spin-orbit potential (18). Their best fit to the neutron scattering experimental data was obtained using the parameters:

| $E$(MeV) | $v$(MeV) | $w$(MeV) | $V_{LS}$(MeV) | $a(10^{-13}$ cm) | $r_0(10^{-13}$ cm) |
|---|---|---|---|---|---|
| 4.1 | −50 | − 7 | 9.5 | 0.65 | 1.25 |
| 7 | −45.5 | −9.5 | 8.6 | 0.65 | 1.25 |
| 14 | −44 | −11 | 8.3 | 0.65 | 1.25 |

Hafner [11]), from the analysis of 220 MeV polarized protons gets $R_n = 2.4\times10^{-13}$ cm, $a = 0.1\times10^{-13}$ cm, $v = -10$ MeV, $W = -25$ MeV and $V_{LS} = 5.056$ MeV.

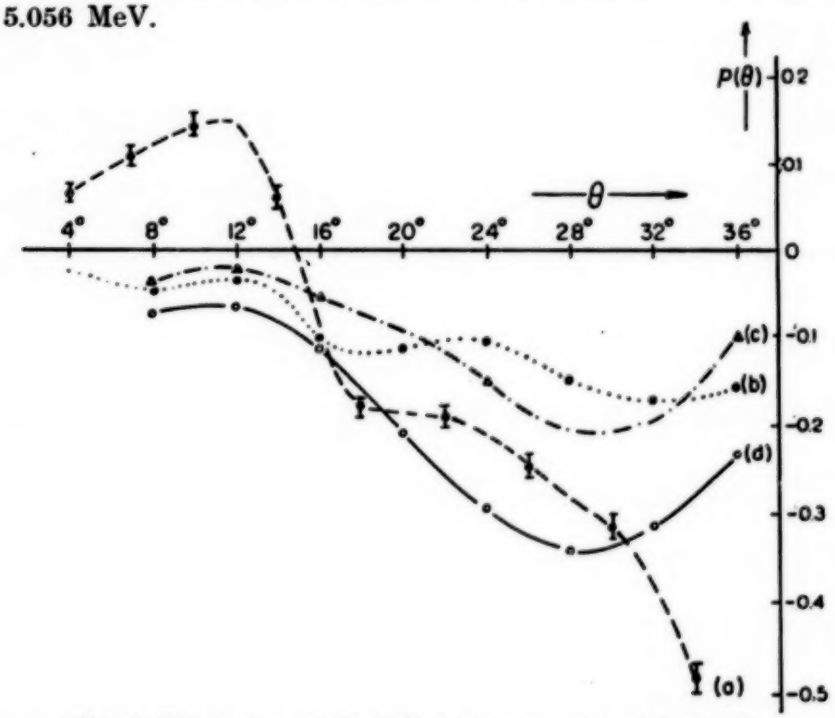


Fig. 3. Polarization of 94 MeV deuterons scattered from $C^{12}$.
(a) Experimental (b) $v+iw = -(32.33+i62.66)$ MeV, $V_{LS} = 2.55$ MeV
(c) $v+iw = -(40+i20)$ MeV, $V_{LS} = 2.55$ MeV (d) $v+iw = -(40+i20)$ MeV, $V_{LS} = 8$ MeV.

In the present work we used fixed values of $r_0$ and $a$ : $r_0 = 1.33 \times 10^{-13}$ cm and $a = 0.55 \times 10^{-13}$ cm. However $v$, $w$ and $V_{LS}$ were varied; we tried two sets of values of $v$ and $w$, namely, $v+iw = -(31.33+i\ 62.66)$ MeV and $v+iw = -(40+i\ 20)$ MeV; and two values of $V_{LS}$ : 2.55 MeV and 8 MeV. The angular distribution was calculated using, 1) $v+iw = -(31.33+i\ 62.66)$ MeV and $V_{LS} = 2.55$ MeV (curve b, fig. 2); 2) $v+iw = -(40+i\ 20)$ MeV and $V_{LS} = 2.55$ MeV (curve c, fig. 2). The polarization was obtained using, 1) $v+iw = (31.33+i\ 62.66)$ MeV and $V_{LS} = 2.55$ MeV; (curve b, fig. 3); 2) $v+iw = -(40+i\ 20)$ MeV and $V_{LS} = 2.55$ MeV (curve b, fig. 3); 3) $v+iw = -(40+i\ 20)$ MeV and $V_{LS} = 8$ MeV (curve c, fig. 3) In both figs. 2 and 3, the curve a represents the experimental results.

## 4. Conclusions

As we see in fig. 2, the predicted angular distribution for $v+iw = -(40+i\ 20)$ MeV agrees very well with the measured one. As mentioned in section 2 one might expect a large imaginary part in order to represent the neglected effects of deuteron dissociation. The value of 20 MeV however is not large compared to the imaginary parts found in fitting nucleon nucleus scattering discussed earlier. If one tries to fit the deuteron elastic cross section with larger values of the imaginary part then the large angle predictions are much smaller than the observed results. To the extent that one can approximate the effects of deuteron dissociation by an imaginary well parameter one can conclude that such effects are negligible for the experiment discussed here. The differential cross section shows a discrepancy at 4°; since at such small angles the Coulomb scattering becomes very large, we can blame this discrepancy on the neglect of the Coulomb effect. The number of maxima and minima increases with increasing $|w|$. The change of $V_{LS}$ from 2.55 to 8 MeV yields a very small variation in the differential cross section (less than one percent) at small angles. Let us now examine the polarization effect (here we are considering the vector polarization). Its magnitude depends on the value of $V_{LS}$ but varies very little with $v$ and $w$ (compare the curves b, c and d in fig. 3). The polarization increases with increasing $V_{LS}$: it is roughly three times as great for $V_{LS} = 8$ MeV as for $V_{LS} = 2.55$ MeV. The maximum polarization obtained for $V_{LS} = 8$ MeV is greater than 0.30 which is not far from that found experimentally. A comparison of the curves b, c and d in fig. 3 shows that the shape of the polarization curve is almost independent of $V_{LS}$, but varies with $v$ and $w$.

Although quantitatively the result is reasonable, the predicted polarization does not show any oscillation similar to the experimental one. We do not yet know the cause of this discrepancy.

We calculated the tensor component of the polarization which contributes

to the right-left asymmetry $e$ as defined in ref. [1]). Its values are listed below ($P$ stands for the vector polarization):

| $\theta$ | $P$ | tensor | $\lvert\text{tensor}/P\rvert$ |
|---|---|---|---|
| 8° | −0.0713 | 0.0013 | 0.018 |
| 12° | −0.0604 | 0.0010 | 0.017 |
| 16° | −0.1159 | −0.0054 | 0.047 |
| 24° | −0.2925 | −0.0052 | 0.018 |
| 36° | −0.2346 | −0.0089 | 0.038 |

As we see from this table, the tensor component is very small compared to the polarization $P$, therefore it cannot explain the discrepancy between the theoretical and experimental asymmetry $e$. Now the phase shifts given by the WKB method are good if their values are larger than 0.5 radian [12]). Since the phase shifts due to the spin-orbit potential are very small (in our case less than 0.1 radian), and the polarization is very much dependent on these phase shifts, it might happen that the incorrect polarization, or rather the asymmetry $e$ we obtained is due to this feature of the WKB method. It is interesting to note that the tensor component presents the correct oscillation of the measured $e$-value.

We also are intending to extend the calculation of the angular distribution and the polarization of deuterons to different energies and different nuclei. The polarization data, at the present moment are available only at energies between 94 and 167 MeV [1]), but the angular distributions of the elastically scattered deuterons were measured also at lower energies.

We would like to thank Prof. Carl A. Levinson, Prof. J. S. Blair and Dr. J. Sawicki for many valuable discussions and comments.

## References

1) J. Baldwin, O. Chamberlain, E. Segré, R. Tripp, C. Wiegand and T. Ypsilantis, Phys. Rev. **103** (1956) 1502
2) O. D. Cheishvili, J. Expt. Theoret. Phys. (U.S.S.R.) **32** (1957) 1240
3) H. Stapp, Phys. Rev. **107** (1957) 607
4) H. Stapp, private communication
5) M. A. Melkanoff, J. S. Nodvik, D. S. Saxon and D. Woods, Phys. Rev. **106** (1957) 793
6) K. M. Gatha and R. J. Ridell, Phys. Rev. **86** (1952) 1035; see also Mott and Massey, The theory of Atomic Collisions, 2nd edition, p. 127
7) S. Watanabe, Rev. Mex. de Fisica **6** (1957) 59
8) A. E. Glassgold and P. J. Kellogg, Phys. Rev. **109** (1958) 1291
9) S. Fernbach, W. Heckrotte and J. V. Lepore, Phys. Rev. (1955) 1059
10) F. Bjorklund and S. Fernbach, Phys. Rev. **109** (1958) 1295
11) E. M. Hafner, Phys. Rev., to be published
12) Morse and Feshbach, Methods of Theoretical Physics, p. 1102

1.D.2 *Nuclear Physics* 8 (1958) 493—594; © *North-Holland Publishing Co., Amsterdam*
Not to be reproduced by photoprint or microfilm without written permission from the publisher

# ÜBER DIE KREISELEIGENSCHAFTEN DES ATOMKERNS

LOTHAR MEICHSNER
*Max-Planck-Institut für Physik, Göttingen* †

Eingegangen am 4. August 1957, 28. August 1957
und 5. Februar 1958

**Abstract:** The motion of nucleons in a non-spherical potential is considered. Without changing the dynamical variables of the nucleons, the Hamiltonian and the magnetic moment operator are put into such a form as to contain collective rotations about axes perpendicular to a body-fixed axis. The transformation yields operators for the tensor $\Theta$ of the reciprocal moment of inertia, for a vector $\mathbf{W}$ connecting the collective and the individual motions of the nucleons, and for the gyromagnetic tensor $G$. These quantities are calculated. A set of so-called approximate basis functions describing an independent motion of the nucleons with respect to a rotating system of co-ordinates and being in accordance with the symmetry properties of the problem is established. Matrix elements of the Hamiltonian and of the nuclear moment operators are calculated. The errors resulting from the occurrence of redundant degrees of freedom are eliminated by the formalism. A typical feature is the appearance of the so-called "Zwangsenergie". The transformation formalism and the approximate basis functions are used to calculate the ground state of $Sc^{45}$. An orthonormal set of single particle functions containing a deformation parameter and a spin-orbit decoupling factor is established. The ground state function is a linear combination of five approximate basis functions. The function corresponding to the lowest energy clearly predominates. A comparison with the undeformed shell model shows that the calculated energy is too high. This fact seems to be due essentially to the oscillator potential, which does not hold in this region of nucleon numbers. The calculated magnetic moment is in good agreement with the experimental value. The results are discussed, and some other consequences of the formalism are mentioned. A sketch on rotational states is added and also a discussion of some other papers.

## INHALTSVERZEICHNIS

TEIL I:

**1. Einleitung** . . . . . 496
1.1. SCHALENMODELL MIT DEFORMIERBAREM POTENTIAL . . . 496
1.2. ZIEL UND EINTEILUNG DER ARBEIT . . . . . 497
**2. Das deformierte Potential** . . . . . 497
2.1. ÄQUIPOTENTIALFLÄCHEN . . . . . 497
2.2. FORMMOMENTE . . . . . 498
2.3. POTENTIAL . . . . . 499
2.4. SELBSTPOLARISATIONSKONSTANTE DER ELEKTRONENHÜLLE 500

† Jetzt am Max-Planck-Institut für Chemie in Mainz.

**3. Der Einachsenaspekt** . . . . . 501
3.1. FORDERUNGEN AN DAS ORTHONORMALSYSTEM . . . . . 501
3.2. ENERGETISCHER HINWEIS AUF EIN KREISELARTIGES VERHALTEN DES KERNS . . . . . 502
3.3. DIE AUSGEZEICHNETE ACHSE N . . . . . 502
3.4. ZERLEGUNG DES HAMILTONOPERATORS . . . . . 503
3.5. DIE INNEREN IMPULSE $\mathbf{p}_{\nu i}$ . . . . . 504
3.6. BEDEUTUNG DES IMPULSAUFTEILUNGSTENSORS $\Lambda_\nu$ . . . . 505
3.7. ANDERE FORM VON $\mathbf{p}_{\nu i}$ . . . . . 506
3.8. MIT N VERTAUSCHBARER OPERATOR DER KINETISCHEN ENERGIE . . . . . 506
3.9. MIT N VERTAUSCHBARES SPIN-BAHN-GLIED . . . . . 506
3.10. HAMILTONOPERATOR IM EINACHSENASPEKT . . . . . 507
3.11. OPERATOR DES MAGNETISCHEN MOMENTES IM EINACHSENASPEKT . . . . . 508
3.12. NÄHERUNGSWERT FÜR DEN GYROMAGNETISCHEN TENSOR $G$ 508
3.13. ANDERE MÖGLICHKEIT DES EINACHSENASPEKTES . . . . 509
3.14. BEMERKUNG ÜBER ANDERE ASPEKTE . . . . . 509
3.15. ASPEKTIERUNG UND NUKLEONENWECHSELWIRKUNG . . . 511

**4. Bedeutung von $\Theta$ und W** . . . . . 511
4.1. VERGLEICH DES REZIPROKEN TRÄGHEITSTENSORS MIT DEM DES KREISELS . . . . . 511
4.2. DIE TAUMELBEDINGUNG . . . . . 512
4.3. BEDEUTUNG DER GLIEDER VON W . . . . . 513
4.4. NOTWENDIGKEIT DER GLIEDER $\mathbf{W} \cdot \mathbf{J}$ UND $-\frac{1}{2}\Theta \cdot \cdot \mathbf{J}^2$ IN $\mathcal{H}_1$ 514

TEIL II:

**5. Berechnung von $\Lambda_\nu$ und davon abgeleiteter Größen** . . . . 515
5.1. IMPULSAUFTEILUNGSTENSOR $\Lambda_\nu$ . . . . . 515
5.2. REZIPROKER TRÄGHEITSTENSOR $\Theta$ . . . . . 516
5.3. WINKELGESCHWINDIGKEIT W . . . . . 516
5.4. GYROMAGNETISCHER TENSOR $G$ . . . . . 517

**6. Allgemeines zum Orthonormalsystem** . . . . . 517
6.1. LAGEKOORDINATEN . . . . . 517
6.2. ORTHONORMALSYSTEM ZU $\mathcal{H}_1$ . . . . . 518
6.3. ORTHONORMALSYSTEM ZU $\mathcal{H}$ . . . . . 520
6.4. DIE NULLSTELLE IM NENNER VON $\Theta$ . . . . . 521

**7. Approximative Basisfunktionen** . . . . . 523
7.1. FESTSETZUNGEN . . . . . 523
7.2. VERMEIDUNG DES AUFSTELLENS FALSCHER ZUSTÄNDE . . 523

7.3. SYSTEMKORREKTUR . . . . . 524
7.4. KLASSIFIKATION DER ZUSTÄNDE . . . . . 526
7.5. ZUSAMMENFASSUNG . . . . . 528

**8. Matrixelemente** . . . . . 529
8.1. SYMMETRIEBEZIEHUNGEN . . . . . 529
8.2. ZWANGSOPERATOR UND URSPRUNGSOPERATOR . . . . . 529
8.3. MITTELENERGIE UND SCHWANKUNGSENERGIE . . . . . 530
8.4. ROTATIONSOPERATOR . . . . . 532
8.5. ROTATIONSAUSTAUSCHOPERATOR; SONDERFALL $\Omega = \frac{1}{2}$ . . 533
8.6. TAUMELBEDINGUNG . . . . . 533
8.7. ELEKTRISCHES QUADRUPOLMOMENT . . . . . 534
8.8. INNERES MAGNETISCHES DIPOLMOMENT . . . . . 535
8.9. ÄUSSERES MAGNETISCHES DIPOLMOMENT . . . . . 535

TEIL III:

**9. Aufstellung des Orthonormalsystems** . . . . . 537
9.1. VORBEMERKUNGEN . . . . . 537
9.2. NUKLEONENEIGENFUNKTIONEN FÜR $\zeta = 0$ . . . . . 537
9.3. DEFORMIERTE FUNKTIONEN OHNE SPIN . . . . . 539
9.4. DEFORMIERTE FUNKTIONEN MIT SPIN, ABKOPPLUNGSGRAD 541
9.5. SCHREIBWEISE DER ZUSTÄNDE . . . . . 542

**10. Aufsuchen der approximativen Basisfunktion niedrigster Energie** . . . . . 542
10.1. POTENTIELLER UND KINETISCHER ANTEIL DER MITTELENERGIE, BEDEUTUNG VON $\langle \Gamma'_0 \rangle_{\varepsilon=0}$ . . . . . 542
10.2. SPIN-BAHN-ANTEIL DER MITTELENERGIE, ABKOPPLUNGSGRAD, FESTLEGUNG VON $\hbar\omega$ . . . . . 545
10.3. SCHWANKUNGSENERGIE . . . . . 548
10.4. MATRIXELEMENTE DES REZIPROKEN TRÄGHEITSTENSORS . 548
10.5. ZWANGSENERGIE, ZERLEGUNG UND ERSTES GLIED, BEDEUTUNG VON $\langle \Gamma'_0 \rangle_{\varepsilon=0}$ UND $\langle J'_p J'_q + J'_q J'_p \rangle_{\varepsilon=0}$ . . . . . 551
10.6. ZWEITES GLIED DER ZWANGSENERGIE . . . . . 552
10.7. GESAMTE ZWANGSENERGIE . . . . . 554
10.8. ROTATIONSENERGIE . . . . . 555
10.9. ROTATIONSAUSTAUSCHENERGIE . . . . . 555
10.10. APPROXIMATIVE BASISFUNKTION NIEDRIGSTER ENERGIE . . 555

**11. Der Grundzustand als Linearkombination** . . . . . 557
11.1. ZUSÄTZLICHE APPROXIMATIVE BASISFUNKTIONEN MIT $\Omega = J$ 557
11.2. APPROXIMATIVE BASISFUNKTIONEN MIT $\Omega = J-1$ . . . . 558
11.3. ZUSTANDSKOEFFIZIENTEN UND ENERGIE . . . . . 559

11.4. EINE BERICHTIGUNG . . . . . 561
11.5. ELEKTRISCHES QUADRUPOLMOMENT . . . . . 561
11.6. MAGNETISCHES DIPOLMOMENT . . . . . 563
11.7. UNSCHÄRFE DER AUSGEZEICHNETEN ACHSE . . . . . 565
11.8. BESPRECHUNG . . . . . 566

**12. Ergänzungen** . . . . . 567
12.1. ROTATIONSSPEKTREN . . . . . 567
12.2. ANDERE ARBEITEN . . . . . 579

**Mathematischer Anhang** . . . . . 582

## 1. Einleitung

### 1.1. SCHALENMODELL MIT DEFORMIERBAREM POTENTIAL

Beim Schalenmodell [1-6,38]) ist die exakte Wechselwirkungsenergie jedes Nukleons mit den übrigen ersetzt durch ein Potential $V_0(r)$, wo $r$ der Abstand des Nukleons vom Schwerpunkt ist. Es wird eine starke Spin-Bahn-Kopplung angenommen. Für jedes Nukleon gilt der Hamiltonoperator

$$\mathscr{H} = \frac{1}{2M}|\mathbf{p}|^2 + V_0(r) + \frac{\lambda}{M^2c^2}\mathbf{s}\cdot\mathbf{p}\times \operatorname{grad} V_0(r), \tag{1.1}$$

$M$ Mittelwert der Masse beider Nukleonensorten,
$\mathbf{p}$ Impulsoperator,
$\mathbf{s}$ Spinoperator,
$\lambda$ Spin-Bahn-Kopplungskonstante,
$c$ Lichtgeschwindigkeit.

Bei geeigneter Wahl von $V_0(r)$ ergeben sich die ausgezeichneten Nukleonenzahlen. Die Besetzung der Zustände und die Drehimpulse werden durch aus den Kernkräften zu erschließende Zusatzannahmen über die Paarungsenergie geregelt. Die Drehimpulse decken sich nicht in allen Fällen mit den experimentellen Werten, und die Übereinstimmung bei den Kernmomenten ist mangelhaft.

Die Tatsachse, daß die experimentellen Werte der elektrischen Momente größer sind als die des Modells, deutet auf eine Abweichung des Potentials von der Kugelform. Die elektrischen Momente entstehen nicht durch eine von der Kugelsymmetrie abweichende Auffüllung der mit dem Potential vorgegebenen kugelsymmetrischen Grundform, sondern diese selbst besitzt schon eine geringere Symmetrie. Ein von der Kugelform abweichendes Potential eröffnet daher die Aussicht, ohne ins einzelne gehende Annahmen über die Kernkräfte doch deren wesentliche Züge zu erfassen und so eine Verbesserung des Modells zu erreichen.

Das Potential ist durch die Lagen der Nukleonen völlig festgelegt. Für unabhängige Größen, die Lage und Gestalt der Äquipotentialflächen beschreiben, wie Eulersche Winkel und Oberflächenvariable, ist kein Raum. Wegen der Drehungsinvarianz des Hamiltonoperators stehen die Äquipotentialflächen nicht im Raum fest. Da sie dem Kern die Form aufprägen, teilt sich ihre Bewegung dem Kern mit, so daß sich den individuellen Bewegungen möglicherweise eine Rotation des ganzen Kerns überlagert, und diese veränderte Bewegungsform müßte sich in den magnetischen Momenten äußern.

### 1.2. ZIEL UND EINTEILUNG DER ARBEIT

Es soll ein von der Kugelform abweichendes Potential aufgestellt und der Hamiltonoperator so umgeformt werden, daß die zu erwartende Rotationsbewegung in der gleichen Weise hervortritt wie die Schwerpunktbewegung bei ihrer Abtrennung. Ein zur Darstellung der Eigenzustände des umgeformten Hamiltonoperators geeignetes Orthonormalsystem soll angegeben und als Beispiel der Grundzustand eines Kerns berechnet werden.

Im *ersten Teil* der Arbeit wird das deformierte Potential aufgestellt und der Hamiltonoperator umgeformt. Es werden nur kollektive Rotationen senkrecht zu einer mit dem Kern fest verbundenen Achse betrachtet. Der Operator des magnetischen Momentes wird ebenfalls umgeformt.

Der *zweite Teil* bereitet die Anwendung des Formalismus vor. Die im ersten Teil auftretenden kinematischen Größen werden als Funktionen der dynamischen Variablen der Nukleonen berechnet. Nach Aufstellung eines Orthonormalsystems werden die benötigten Matrixelemente ermittelt.

Im *dritten Teil* wird der Grundzustand des Kerns † (21, 24) berechnet. Die einzelnen Energieglieder werden untersucht und die Kernmomente ermittelt.

## 2. Das deformierte Potential

### 2.1. ÄQUIPOTENTIALFLÄCHEN

Wir beschränken uns auf kleine Deformationen, und berücksichtigen in der Darstellung der deformierten Gebilde nur die Kugelflächenfunktionen zweiter Ordnung $Y_m^2$, für die wir der Einfachheit halber $Y_m$ schreiben. Formeln für die Kugelflächenfunktionen sind im Anhang B zusammengestellt.

Gegeben sei ein Potential $V = V_0(r)$. Die Umkehrung dieser Funktion sei $r = r_0(V)$. Für die deformierten Äquipotentialflächen setzen wir an

$$r = r_0(V)\{1+\sum_m \varepsilon_m(V)Y_m(\vartheta,\varphi)-\tfrac{1}{5}\kappa(V)\sum_m|\varepsilon_m(V)|^2\}. \qquad (2.1)$$

Die $\varepsilon_m(V)$ beschreiben die Abweichung von der Kugelform und $\kappa(V)$ eine möglicherweise mit der Verformung eintretende Volumenänderung; $\kappa(V) = 1$

† Einen aus $Z$ Protonen und $N$ Neutronen bestehenden Kern bezeichnen wir mit $(Z, N)$.

ergibt Konstanz, $\kappa(V) > 1$ Verkleinerung und $\kappa(V) < 1$ Vergrößerung des Volumens. Sind die $\varepsilon_m$ und $\kappa$ von $V$ unabhängig, so nennen wir die Verformung homogen. Die Realität von (2.1) verlangt unter Berücksichtigung der in (B7) angegebenen Normierung der Kugelflächenfunktionen

$$\varepsilon_0 = \text{reell}, \qquad \varepsilon_{-1} = -\varepsilon_{+1}^*, \qquad \varepsilon_{-2} = \varepsilon_{+2}^* \tag{2.2}$$

und die Drehungsinvarianz, daß sich die $\varepsilon_m$ kontragredient zu den $Y_m$, nach (B19) also wie die $Y_m^*$, transformieren. Das durch (2.1) beschriebene Gebilde besitzt wie ein Ellipsoid in drei zueinander senkrechten Richtungen stationäre Werte von $r$, doch ist sein Volumen etwas größer als bei dem Ellipsoid mit den gleichen Hauptachsen.

### 2.2. FORMMOMENTE

Ein Maß für die Abweichung des Kerns von der Kugelform sind die Formmomente †

$$\Gamma_m = \sum_\nu r_\nu^2 Y_m^*(\vartheta_\nu, \varphi_\nu). \tag{2.3}$$

Sie haben aber die Dimension eines Längenquadrates und sind abhängig vom Kernvolumen und von der Nukleonenzahl, denn bei Multiplikation der Radiusvektoren der Nukleonen mit einer Zahl $C$ nehmen sie den Faktor $C^2$ an, und bei Erhöhung der Nukleonenzahl von $A$ auf $A'$ vervielfachen sie sich etwa mit $A'/A$, wenn die neu hinzutretenden Nukleonen räumlich in der gleichen Weise verteilt werden wie die bereits vorhandenen. Die mit der zusätzlichen Größe

$$\Gamma = \sum_\nu r_\nu^2 \tag{2.4}$$

gebildeten reduzierten Formmomente

$$\gamma_m = \frac{\Gamma_m}{\Gamma} \tag{2.5}$$

sind dagegen dimensionslos und unabhängig vom Kernvolumen und von der Nukleonenzahl. Sie erscheinen daher zur Beschreibung der Kernform geeigneter als die $\Gamma_m$. Um ihre Bedeutung zu veranschaulichen, nehmen wir an, es seien $A$ Nukleonen kontinuierlich und gleichmäßig innerhalb des Gebildes

$$r = R_0\{1 + \sum_m \eta_m Y_m(\vartheta, \varphi) - \tfrac{1}{5}\sum_m |\eta_m|^2\}, \tag{2.6}$$

wo $R_0$ und die $\eta_m$ vorgegebene Größen sind, verteilt. An die Stelle von (2.3) und (2.4) treten dann

$$\begin{aligned} \Gamma_m &= \int \rho r^2 Y_m^*(\vartheta, \varphi)\,\mathrm{d}\tau \\ \Gamma &= \int \rho r^2\,\mathrm{d}\tau, \end{aligned} \tag{2.7}$$

† Mit griechischen Buchstaben indizierte Summen erstrecken sich über alle Nukleonen.

und $\rho$, die Nukleonenzahl in der Volumeneinheit, ist gegeben durch

$$\rho = \frac{3A}{4\pi R_0^3}, \tag{2.8}$$

denn das Gebilde (2.6) hat nach den Erläuterungen über $\kappa$ in (2.1) das gleiche Volumen wie eine Kugel vom Radius $R_0$. Bei Beschränkung auf Glieder zweiter Ordnung in den $\eta_m$ wird dann

$$\begin{aligned} \Gamma_m &= \tfrac{3}{5} A R_0^2 \eta_m \\ \Gamma &= \tfrac{3}{5} A R_0^2 (1 + \sum_m |\eta_m|^2). \end{aligned} \tag{2.9}$$

Mit (2.5) ergibt sich bei Fortlassen von Gliedern dritter und höherer Ordnung die wichtige Beziehung

$$\gamma_m = \eta_m. \tag{2.10}$$

Sie zeigt, wie die $\eta_m$ zu wählen sind, wenn man eine Kernkonfiguration mit den Momenten $\gamma_m$ durch eine kontinuierliche und gleichmäßige Nukleonenverteilung ersetzen will.

### 2.3. POTENTIAL

Um die Verformungen von Kern und Äquipotentialflächen miteinander zu verknüpfen, setzen wir an

$$\varepsilon_m(V) = k(V)\gamma_m. \tag{2.11}$$

In der Wahl der Funktionen $k(V)$ und $\kappa(V)$ besteht eine große Freiheit. Am einfachsten ist es, $k(V) = \text{const} = \zeta$ und $\kappa = 1$ zu setzen. Diese Art der Verformung nennen wir homogen isochor. Das zugehörige Potential ist nach (2.1)

$$V(r, \vartheta, \varphi) = V_0\left(\frac{r}{1+\zeta \sum_m \gamma_m Y_m(\vartheta, \varphi) - \frac{1}{5}\zeta^2 \sum_m |\gamma_m|^2}\right). \tag{2.12}$$

Bei Entwicklung dieses Ausdrucks bis zu Gliedern zweiten Grades in den $\gamma_m$ treten Produkte $Y_m Y_n$ auf, die sich nach Anhang B durch die $Y_m^4$, $Y_m^2$ und Konstante ausdrücken lassen. Läßt man darin die Glieder mit den $Y_m^4$ und den $Y_m^2$ fort, so ergibt sich

$$V = V_0(r) - \zeta V_1(r) \sum_m \gamma_m Y_m(\vartheta, \varphi) + \tfrac{1}{2}\zeta^2 V_2(r) \sum_m |\gamma_m|^2, \tag{2.13}$$

$$V_1(r) = r V_0'(r), \tag{2.14}$$

$$V_2(r) = \tfrac{1}{5}\{r^2 V_0''(r) + 4 r V_0'(r)\} \sum_m |\gamma_m|^2. \tag{2.15}$$

Die Begründung für das Fortlassen der genannten Glieder tritt weiter unten zutage. Es wird sich zeigen, daß in der aus (2.13) durch Summation über alle Nukleonen folgenden potentiellen Energie des Kerns die Glieder mit $\zeta$ und $\zeta^2$ von gleicher Größenordnung, und zwar vom zweiten Grad in den $\gamma_m$ sind, während die fortgelassenen Glieder einen Beitrag dritten Grades liefern würden. Deren Vernachlässigung ist aber nicht nur durch diese Tatsache

gerechtfertigt, sondern auch durch den Ansatz (2.11) bedingt, denn nähme man dort rechts Glieder zweiten Grades in den $\gamma_m$ hinzu, so entstünde ein weiteres Glied dritten Grades in der gesamten potentiellen Energie.

Ein Potential von der Form (2.13) ergibt sich auch bei gewissen Verallgemeinerungen in der Wahl von $k(V)$ und $\kappa(V)$. Die dann entstehenden Formeln für $V_1(r)$ und $V_2(r)$ enthalten (2.14) und (2.15) als Sonderfall. Es besteht aber kein Grund, von dem einfachen Fall der homogenen isochoren Deformation abzugehen. Wir führen daher die entsprechenden Rechnungen nicht an.

Die in (2.13) enthaltenene Konstante $\zeta$ ist ein Maß für die allgemeine Verformung der Äquipotentialflächen bei gegebener Verformung des Kerns. Es zeigt sich, daß der Kern in einem von $\zeta$ abhängigen Ausmaß verformt wird. $\zeta$ mißt daher auch das Vermögen des Kerns, ohne Wirken kernfremder Einflüsse eine von der Kugelform abweichende Gestalt anzunehmen. Wir nennen $\zeta$ Selbstpolarisationskonstante und ein Potential von der Form (2.13) Selbstpolarisationspotential †.

### 2.4. SELBSTPOLARISATIONSKONSTANTE DER ELEKTRONENHÜLLE

Naheliegend ist die Frage, warum die Selbstpolarisationskonstante bei der Elektronenhülle keine Bedeutung hat. Das Potential eines Elektrons setzt

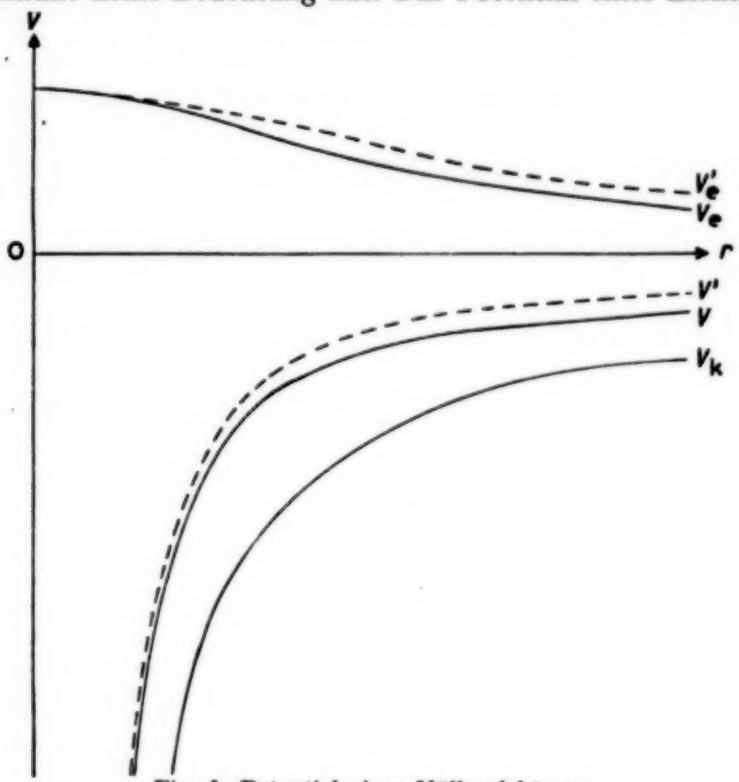


Fig. 1. Potential eines Hüllenelektrons.

† Bei der im Sommer 1951 erfolgten Aufstellung des Selbstpolarisationspotentials wurde $\gamma_m = \Sigma_\nu g(r_\nu) Y_m^*(\vartheta_\nu, \varphi_\nu)$ gesetzt, wobei über $g(r)$ noch verfügt werden konnte.

sich, wie in Fig. 1 dargestellt, aus dem vom Kern herrührenden negativen Anteil $V_k$ und dem positiven Beitrag $V_e$ der übrigen Elektronen zusammen. Bei Verformung der Elektronenhülle verformen sich die Äquipotentialflächen von $V_e$ im gleichen Sinn. Für eine Raumrichtung, in der die Punkte gegebener Elektronendichte nach außen rücken, geht $V_e$ in $V'_e$ und $V$ in $V'$ über; die Punkte mit gegebenem $V$ rücken daher nach innen. Die Selbstpolarisationskonstante ist negativ und drückt so die Tendenz zur Aufrechterhaltung der Kugelform aus.

## 3. Der Einachsenaspekt

### 3.1. FORDERUNGEN AN DAS ORTHONORMALSYSTEM

Ausgangspunkt zur Berechnung der Zustände ist der Hamiltonoperator

$$\mathscr{H}=\sum_\nu \left\{\frac{1}{2M}|\mathbf{p}_\nu|^2+V_\nu+\frac{\lambda}{M^2c^2}\mathbf{s}_\nu\cdot\mathbf{p}_\nu\times\operatorname{grad}_\nu V_\nu\right\}. \tag{3.1}$$

$V_\nu$ ist das durch (2.13) gegebene Selbstpolarisationspotential für das $\nu$-te Nukleon. $\mathscr{H}$ kommutiert mit allen Drehungen und mit der Spiegelung am Nullpunkt. Als dynamische Variable kommen nur die $\mathbf{r}_\nu$, $\mathbf{p}_\nu$, $\mathbf{s}_\nu$ vor.

Im Vordergrund des Interesses steht der Grundzustand. Ihn durch das Orthogonalsystem für $\zeta = 0$ auszudrücken, etwa in der Weise, daß man Slaterdeterminanten mit gleicher $z$-Komponente $M$ des Gesamtdrehimpulses und gleicher Parität $w$ zu einem Zustand mit scharfem Gesamtdrehimpuls $J$ überlagert und die Anteilkoeffizienten durch Aufsuchen des Energieminimums bestimmt, ist mühsam und das Ergebnis nicht durchsichtig. Es wird nur eine Verbesserung des Zustandes, aber keine Verbesserung des Modells selbst erreicht. Hierzu ist die Aufstellung eines Orthonormalsystems erforderlich, in dem die entscheidenden Konfigurationen besser geordnet sind. Das ist anscheinend bei einem Orthonormalsystem der Fall, das die wegen der Abweichung des Potentials von der Kugelform zu erwartende Veränderung der Nukleonenbewegung zum Ausdruck bringt.

Käme es nur darauf an, die gegenüber $\zeta = 0$ eintretende Energieänderung zu berechnen, so könnte man die von $\zeta$ abhängigen Glieder in (3.1) als kleine Störung $\mathscr{H}'$ auffassen. Zu der Energie $E_0$ des Grundzustandes $\Psi_0$ für $\zeta = 0$ träte dann der mit diesem Zustand gebildete Erwartungswert $\mathscr{H}'_{00}$. Die so bestimmte Energie

$$E_{kr} = E_0+\mathscr{H}'_{00} \tag{3.2}$$

bezeichnen wir als kritische Energie. Kennzeichen jedes verbesserten Grundzustandes ist, daß für seine Energie

$$E < E_{kr} \tag{3.3}$$

gelten muß.

### 3.2. ENERGETISCHER HINWEIS AUF EIN KREISELARTIGES VERHALTEN DES KERNS

Bei Vernachlässigung des Spin-Bahn-Gliedes ist nach (3.1) und (2.13)

$$\mathscr{H}' = -\zeta \sum_\nu \sum_m V_1(r_\nu) Y_m(\vartheta_\nu, \varphi_\nu) \gamma_m + \tfrac{1}{2}\zeta^2 \sum_\nu V_2(r_\nu) \sum_m |\gamma_m|^2. \tag{3.4}$$

Für den einfachen Fall des homogen isochor deformierten Oszillatorpotentials

$$V_0(r) = \tfrac{1}{2}M\omega^2 r^2, \quad V_1(r) = M\omega^2 r^2, \quad V_2(r) = M\omega^2 r^2, \tag{3.5}$$

wo $V_1$ und $V_2$ aus (2.14) und (2.15) folgen, ergibt sich unter Beachtung von (2.5) und (2.6)

$$\mathscr{H}' = -\tfrac{1}{2}\zeta(2-\zeta) M\omega^2 \Gamma \sum_m |\gamma_m|^2. \tag{3.6}$$

Für den vornehmlich in Betracht kommenden Fall $\zeta = 1$ wird also $\mathscr{H}'_{00} < 0$. Das negative Vorzeichen ist sicher nicht auf das Oszillatorpotential beschränkt, wie das Hinzufügen eines Gliedes mit $r^4$ in $V_0(r)$ zeigt. Auch im allgemeinen Fall sind $\sum_\nu V_1(r_\nu) Y_m(\vartheta_\nu, \varphi_\nu)$ und $\Gamma_m^*$ einander ungefähr proportional, also gilt

$$\mathscr{H}'_{00} \propto -\sum_m (|\gamma_m|^2)_{00}. \tag{3.7}$$

Das negative Vorzeichen von $\mathscr{H}'_{00}$ läßt vermuten, daß ein der Bedingung (3.3) genügender Zustand sich durch ein vergrößertes $\langle \sum_m |\gamma_m|^2 \rangle$ auszeichnet. Ein solches tritt aber dann auf, wenn die Schwankungen der $\gamma_m$ nicht lediglich durch die voneinander unabhängige Bewegung der Nukleonen, sondern auch durch eine Kollektivbewegung hervorgerufen werden. Als solche sind Schwingungen und Rotationen denkbar. Der einfachste Fall einer kollektiven Rotation liegt vor, wenn der Kern im Mittel die Form eines verlängerten oder eines verkürzten Rotationsellipsoides besitzt und um eine zur Figurenachse senkrechte Achse rotiert. Dann sind erstens höhere elektrische Quadrupolmomente als bei $\zeta = 0$ zu erwarten, und zweitens sollte, da eine der drei Hauptachsen ausgezeichnet ist, eine Kopplung der Nukleonenbewegung an die ausgezeichnete Achse eintreten, die sich in einer Veränderung des magnetischen Momentes bemerkbar machen müßte. Daher soll dieses kreiselartige Verhalten des Kerns untersucht werden.

### 3.3. DIE AUSGEZEICHNETE ACHSE N

Zur Festlegung der ausgezeichneten Achse, die durch den Einheitsvektor **N** gekennzeichnet sei, führen wir ein Koordinatensystem $\Sigma'$ mit den Eulerschen Winkeln † $\Theta$, $\Phi$, $\Psi$ ein, dessen $z'$-Achse mit **N** zusammenfällt, während wir für die anderen Achsen keine Festsetzung treffen. Das dem Kern zugeordnete ellipsoidähnliche Gebilde

† Zur Definition der Eulerschen Winkel siehe Fig. 7 in Anhang A.

$$r = R_0\{1+\sum_m \gamma_m Y_m(\vartheta,\varphi)-\tfrac{1}{5}\sum_m |\gamma_m|^2\}, \tag{3.8}$$

wo $R_0$ irgendein Radius, etwa der Kernradius, ist, liefert nach Transformation auf $\Sigma'$ genau dann eine Hauptachse mit der Richtung $\vartheta' = 0$, wenn $\gamma'_{\pm 1}$ und folglich auch $\Gamma'_{\pm 1}$ verschwinden. Nach (B20) und (B23) ist aber

$$\begin{aligned}\Gamma'_{\pm 1} = \pm e^{\pm i\Psi}\Big\{&\sqrt{6}\sin\frac{\Theta}{2}\cos\frac{\Theta}{2}\left(1-2\sin^2\frac{\Theta}{2}\right)\Gamma_0\\ &\pm e^{\pm i\Phi}\cos^2\frac{\Theta}{2}\left(1-4\sin^2\frac{\Theta}{2}\right)\Gamma_{\pm 1}\mp e^{\mp i\Phi}\sin^2\frac{\Theta}{2}\left(1-4\cos^2\frac{\Theta}{2}\right)\Gamma_{\mp 1}\\ &-2\sin\frac{\Theta}{2}\cos\frac{\Theta}{2}\left(e^{\pm 2i\Phi}\cos^2\frac{\Theta}{2}\Gamma_{\pm 2}-e^{\mp 2i\Phi}\sin^2\frac{\Theta}{2}\Gamma_{\mp 2}\right)\Big\}.\end{aligned} \tag{3.9}$$

Nullsetzen der rechten Seite dieser Gleichung liefert $\Theta$ und $\Phi$, und es ist

$$\mathbf{N} = (\sin\Theta\cos\Phi, \sin\Theta\sin\Phi, \cos\Theta). \tag{3.10}$$

$\Psi$ bleibt unbestimmt. Da $\Theta$ und $\Phi$ von den $\Gamma_m$ und diese von den $\mathbf{r}_\nu$ abhängen, ist $\mathbf{N}$ durch die $\mathbf{r}_\nu$ völlig bestimmt. Allerdings ist die Lösung von (3.9) sechsdeutig, denn sie liefert die Richtungen der drei Hauptachsen und deren Gegenrichtungen. Diese Mehrdeutigkeit verschwindet aber, wenn die in den folgenden Rechnungen ermittelten kinematischen Größen auf $\Sigma'$ transformiert werden. Zwar hängen deren Zahlwerte für eine gegebene Konfiguration davon ab, in welche der möglichen Richtungen man die $z'$-Achse legt, aber ihre Abhängigkeit von den gestrichenen Koordinaten, auf die es allein ankommt, ist in jedem System die gleiche. Diese Tatsache bedeutet, daß man für eine gegebene Konfiguration zwar die drei Hauptachsen bestimmen, aber nicht angeben kann, welche die kinematisch ausgezeichnete ist. Die kinematische Auszeichnung einer Achse ist anscheinend dann sinnvoll, wenn diese nicht springt, das heißt, wenn sie bei einer gegebenen kleinen Verschiebung der Nukleonen ihre Richtung nicht unverhältnismäßig stark ändert. Dazu ist erforderlich, daß die Schwankungen der Kernform kleiner sind als die über die Zeit gemittelte Verformung. Die elektrischen Kernmomente deuten darauf hin, daß diese Bedingung für eine Achse erfüllt ist, geben aber keinen Hinweis, daß sie für alle drei Achsen gilt. Es ist daher zweckmäßig, nur die Bewegung einer einzigen Achse und nicht die des ganzen Achsensystems zu verfolgen.

### 3.4. ZERLEGUNG DES HAMILTONOPERATORS

Um die Bewegung von $\mathbf{N}$ verfolgen zu können, müssen wir diese Größe im Hamiltonoperator auszeichnen. Zu diesem Zweck trennen wir von $\mathscr{H}$ ein mit $\mathbf{N}$ vertauschbares Glied $\mathscr{H}_1$ ab, dessen Zustände folglich scharfe Werte von $\mathbf{N}$ haben können. Die Bewegung von $\mathbf{N}$ wird dann durch den Rest $\mathscr{H}-\mathscr{H}_1$ geregelt. Da an $\mathscr{H}$ keine Stelle zu erkennen ist, an welcher der

trennende Schnitt zu führen ist, bilden wir $\mathscr{H}_1$ durch Addition eines die Vertauschbarkeit erzeugenden Zusatzgliedes zu $\mathscr{H}$. Da die Nichtvertauschbarkeit von $\mathscr{H}$ mit $\mathbf{N}$ lediglich durch die $\mathbf{p}_\nu$ bewirkt wird, läßt sich das so aufgebaute $\mathscr{H}_1$ derart bilden, daß man die $\mathbf{p}_\nu$ durch Addition von Zusatzgliedern zu mit $\mathbf{N}$ vertauschbaren Impulsen $\mathbf{p}_{\nu 1}$ abändert und diese anstelle der $\mathbf{p}_\nu$ einsetzt.

### 3.5. DIE INNEREN IMPULSE $\mathbf{p}_{\nu i}$

Um ein kreiselartiges Verhalten des Kerns ausdrücken zu können, verlangen wir, daß in dem zerlegten $\mathscr{H}$ der Term †)

$$\tfrac{1}{2}\Theta \cdot\cdot \mathbf{J}^2 \quad \text{oder} \quad \tfrac{1}{2}\Theta \cdot\cdot \mathbf{L}^2, \quad \Theta = \Theta(\mathbf{r}_1, \ldots, \mathbf{r}_A)$$

$\mathbf{J}$ Gesamtdrehimpuls-Operator des Kerns,

$\mathbf{L}$ Bahndrehimpuls-Operator des Kerns,

auftritt, wo $\Theta$ ein noch aufzufindender symmetrischer Tensor ist. Die Wahl von $\mathbf{J}$ oder $\mathbf{L}$ hängt davon ab, ob entweder $\mathbf{N}$ oder eine raumfeste Richtung Bezugsachse für den Spin sein soll, und dieses wiederum richtet sich nach der Stärke der Kopplung zwischen Spin und Bahn. Die Existenz der ausgezeichneten Nukleonenzahlen beruht auf einer starken Spin-Bahn-Kopplung. Wenn die Kerne deformiert sind und in das Schema der ausgezeichneten Zahlen eingeordnet werden können, muß diese Kopplung auch im deformierten Zustand noch stark genug sein. Daher ist $\mathbf{N}$ als Bezugsachse und das Kreiselglied mit $\mathbf{J}$ angebracht. Dessen Existenz führt auf den Ansatz ††

$$\begin{aligned}\mathbf{p}_{\nu 1} &= \mathbf{p}_\nu + \tfrac{1}{2}(\Lambda_\nu \cdot \mathbf{J} + \mathbf{J} \cdot \tilde{\Lambda}_\nu) \\ &= \mathbf{p}_\nu + \Lambda_\nu \cdot \mathbf{J} + \tfrac{1}{2}(\mathbf{J} \cdot \tilde{\Lambda}_\nu - \Lambda_\nu \cdot \mathbf{J}), \quad \Lambda_\nu = \Lambda_\nu(\mathbf{r}_1, \ldots, \mathbf{r}_A),\end{aligned} \tag{3.11}$$

wo $\Lambda_\nu$ zu bestimmen ist. $\mathbf{p}_{\nu 1}$ ist hermitisch, denn wenn $\Lambda_\nu$ nur von den Lagekoordinaten abhängt, sind $\Lambda_\nu \cdot \mathbf{J}$ und $\mathbf{J} \cdot \tilde{\Lambda}_\nu$ zueinander adjungiert. $\Lambda_\nu$ führt den axialen Vektor $\mathbf{J}$ in einen polaren über, daher muß sich das linke Indicestripel von $\Lambda_\nu$ wie ein polarer und das rechte wie ein axialer Vektor transformieren; $\Lambda_\nu$ ändert dann bei Spiegelungen am Nullpunkt das Vorzeichen. Da nach den Vertauschungsrelationen

$$\mathbf{J} \cdot \tilde{\Lambda}_\nu - \Lambda_\nu \cdot \mathbf{J} = \mathbf{L} \cdot \tilde{\Lambda}_\nu - \Lambda_\nu \cdot \mathbf{L} = -i\hbar \sum_\lambda \mathbf{r}_\lambda \times \nabla_\lambda \cdot \tilde{\Lambda}_\nu \tag{3.12}$$

nur von den Lagekoordinaten abhängt, also gewiß mit $\mathbf{N}$ vertauschbar ist, lautet die Bestimmungsgleichung für $\Lambda_\nu$ †††

† Wir benutzen die Gibbssche Bezeichnungsweise für Vektoren und Tensoren [7, 8]). $\mathbf{ab}$ Tensor mit der $kl$-Komponente $a_k b_l$, $|\mathbf{a}|^2 = \mathbf{a} \cdot \mathbf{a}$, $\mathbf{a}^2$ Tensor mit der $kl$-Komponente $a_k a_l$, $\Theta \cdot\cdot \mathbf{J}^2 = \sum_k \sum_l \Theta_{kl} J_l J_k$.

†† Der zu einem Tensor $T$ transponierte wird mit $\tilde{T}$ bezeichnet.

††† $[\mathbf{a}, \mathbf{b}]$ ist der Tensor mit der $kl$-Komponente $a_k b_l - b_l a_k$ [8]).

$$[\mathbf{p}_\nu, \mathbf{N}]+[\Lambda_\nu \cdot \mathbf{J}, \mathbf{N}] = [\mathbf{p}_\nu, \mathbf{N}]+\Lambda_\nu \cdot [\mathbf{J}, \mathbf{N}] = 0. \tag{3.13}$$

Nach den Vertauschungsrelationen gilt aber für irgendeinen Vektoroperator $\mathbf{A}(\mathbf{r}_1, \ldots, \mathbf{r}_A)$

$$[\mathbf{p}_\nu, \mathbf{A}] = -i\hbar\nabla_\nu \mathbf{A}, \tag{3.14}$$

$$[\mathbf{J}, \mathbf{A}] = [\mathbf{L}, \mathbf{A}] = -i\hbar \sum_\lambda \mathbf{r}_\lambda \times \nabla_\lambda \mathbf{A}, \tag{3.15}$$

und für die letzte Gleichung kann man, da $\mathbf{A}(\mathbf{r}_1, \ldots \mathbf{r}_A)$ mit den Nukleonen fest verbunden ist, schreiben †

$$[\mathbf{J}, \mathbf{A}] = [\mathbf{L}, \mathbf{A}] = -i\hbar \begin{pmatrix} 0 & -A_3 & A_2 \\ A_3 & 0 & -A_1 \\ -A_2 & A_1 & 0 \end{pmatrix} = -i\hbar\delta \times \mathbf{A} = -i\hbar \mathbf{A} \times \delta. \tag{3.16}$$

Dann wird aus (3.13) nach vektorieller Multiplikation von rechts mit $\mathbf{N}$

$$(\nabla_\nu \mathbf{N}) \times \mathbf{N} + \Lambda_\nu \cdot \mathbf{N}^2 - \Lambda_\nu = 0. \tag{3.17}$$

Diese Gleichung hat bei Beschränkung auf den einfachen Fall $\Lambda_\nu \cdot \mathbf{N} = 0$ die Lösung

$$\Lambda_\nu = (\nabla_\nu \mathbf{N}) \times \mathbf{N}. \tag{3.18}$$

### 3.6. BEDEUTUNG DES IMPULSAUFTEILUNGSTENSORS $\Lambda_\nu$

Verschiebt man in irgendeiner Konfiguration das Nukleon mit der Lage $\mathbf{r}_\nu$ um $\mathrm{d}\mathbf{r}_\nu$, so ändert sich $\mathbf{N}$ um

$$\mathrm{d}_\nu \mathbf{N} = \mathrm{d}\mathbf{r}_\nu \cdot \nabla_\nu \mathbf{N}. \tag{3.19}$$

Diese Änderung läßt sich durch eine Drehung $\mathrm{d}\mathbf{D}$ sämtlicher Nukleonen als starrer Körper rückgängig machen. Um $\mathrm{d}\mathbf{D}$ aufzufinden, bemerken wir, daß sich das mit den Nukleonen fest verbundene $\mathbf{N}$ dabei um

$$\mathrm{d}'\mathbf{N} = \mathrm{d}\mathbf{D} \times \mathbf{N} \tag{3.20}$$

ändert. Nullsetzen der Summe der rechten Seiten von (3.19) und (3.20) und vektorielle Multiplikation von rechts mit $\mathbf{N}$ ergibt

$$\mathrm{d}\mathbf{r}_\nu \cdot (\nabla_\nu \mathbf{N}) \times \mathbf{N} + \mathrm{d}\mathbf{D} \cdot \mathbf{N}^2 - \mathrm{d}\mathbf{D} = 0. \tag{3.21}$$

Diese Gleichung wird gelöst durch den zu $\mathbf{N}$ senkrechten Vektor

$$\mathrm{d}\mathbf{D} = \mathrm{d}\mathbf{r}_\nu \cdot (\nabla_\nu \mathbf{N}) \times \mathbf{N}, \tag{3.22}$$

zu dem eine zu $\mathbf{N}$ parallele willkürliche Drehung addiert werden kann. Aus (3.22) erkennen wir durch Vergleich mit (3.18), daß $\Lambda_\nu$ diejenige zu $\mathbf{N}$ senkrechte Drehung liefert, welche die durch Verschiebung des Nukleons der Lage $\mathbf{r}_\nu$ eintretende Änderung von $\mathbf{N}$ rückgängig macht.

† Siehe [8]); $\delta$ ist die dort mit $\mathfrak{J}$ bezeichnete Einheitsdyade.

### 3.7. ANDERE FORM VON $\mathbf{p}_{\nu i}$

Zur Berechnung von (3.12) ermittelt man für einen beliebigen Tensoroperator $T(\mathbf{r}_1, \ldots, \mathbf{r}_A)$ die $[L_k, T_{lm}]$. Da sich die Komponenten von $T$ bei Drehungen sämtlicher Nukleonen wie die aus den beliebigen Vektoroperatoren $\mathbf{A}(\mathbf{r}_1, \ldots, \mathbf{r}_A)$ und $\mathbf{B}(\mathbf{r}_1, \ldots, \mathbf{r}_A)$ gebildeten Tensors $\mathbf{AB}$ transformieren, lassen sich die gesuchten Kommutatoren nach der Regel der Produktdifferentiation auf die $[L_k, A_i]$ in (3.16) zurückführen. Unter Einführung des Vektors

$$T^\times = (T_{23}-T_{32},\ T_{31}-T_{13},\ T_{12}-T_{21}),\quad \tilde{T}^\times = -T^\times, \tag{3.23}$$

bei dem das Kreuz an die dem Vektorprodukt entsprechende Koeffizientenanordnung erinnern soll, ergibt sich dann

$$\mathbf{L}\cdot T-\tilde{T}\cdot\mathbf{L} = -i\hbar T^\times = i\hbar\tilde{T}^\times. \tag{3.24}$$

Bei Anwendung dieser Gleichung auf $\Lambda_\nu$ kann man für $\mathbf{p}_{\nu 1}$ nach (3.11) endgültig schreiben

$$\mathbf{p}_{\nu 1} = \mathbf{p}_\nu+\tfrac{1}{2}(\Lambda_\nu\cdot\mathbf{J}+\mathbf{J}\cdot\tilde{\Lambda}_\nu) = \mathbf{p}_\nu+\Lambda_\nu\cdot\mathbf{J}+\tfrac{1}{2}i\hbar\Lambda_\nu^\times. \tag{3.25}$$

### 3.8. MIT N VERTAUSCHBARER OPERATOR DER KINETISCHEN ENERGIE

Zur besseren Ordnung ziehen wir in $|\mathbf{p}_{\nu 1}|^2$ den Operator $\mathbf{J}$ nach rechts durch. Dabei ist zu bedenken, daß (3.15) auch bei Ersatz von $\mathbf{A}(\mathbf{r}_1, \ldots, \mathbf{r}_A)$ durch $\mathbf{p}_\nu$ gilt. Es ergibt sich

$$|\mathbf{p}_{\nu 1}|^2 = |\mathbf{p}_\nu|^2+(\mathbf{p}_\nu\cdot\Lambda_\nu+\tilde{\Lambda}_\nu\cdot\mathbf{p}_\nu)\cdot\mathbf{J}+(\tilde{\Lambda}_\nu\cdot\Lambda_\nu)\cdot\cdot\,\mathbf{J}^2 +\tfrac{1}{2}\hbar^2\nabla_\nu\cdot\Lambda_\nu^\times+\tfrac{1}{4}\hbar^2|\Lambda_\nu^\times|^2. \tag{3.26}$$

Dieser Ausdruck ist hermitisch und mit $\mathbf{N}$ vertauschbar. Da die beiden letzten Glieder die gleichen Eigenschaften haben, treffen sie auch für den Rest zu, und es genügt zur Bildung des mit $\mathbf{N}$ vertauschbaren Operators der kinetischen Energie die Substitution

$$|\mathbf{p}_\nu|^2 \to |\mathbf{p}_\nu|^2+(\mathbf{p}_\nu\cdot\Lambda_\nu+\tilde{\Lambda}_\nu\cdot\mathbf{p}_\nu+2\tilde{\Lambda}_\nu\cdot\Lambda_\nu\cdot\mathbf{J})\cdot\mathbf{J}-(\tilde{\Lambda}_\nu\cdot\Lambda_\nu)\cdot\cdot\,\mathbf{J}^2. \tag{3.27}$$

In dieser Zusammenfassung ist die runde Klammer im zweiten Glied ein mit $\mathbf{N}$ vertauschbarer hermitischer Operator.

### 3.9. MIT N VERTAUSCHBARES SPIN-BAHN-GLIED

Die Substitution

$$\mathbf{s}_\nu\cdot\mathbf{p}_\nu\times\operatorname{grad}_\nu V_\nu = \operatorname{grad}_\nu V_\nu\times\mathbf{s}_\nu\cdot\mathbf{p}_\nu \to \tfrac{1}{2}\{\operatorname{grad}_\nu V_\nu\times\mathbf{s}_\nu\cdot\mathbf{p}_{\nu 1}+\mathbf{p}_{\nu 1}\cdot\operatorname{grad}_\nu V_\nu\times\mathbf{s}_\nu\} \tag{3.28}$$

ergibt einen mit $\mathbf{N}$ vertauschbaren hermitischen Operator. Setzt man $\mathbf{p}_{\nu 1}$ in der durch die zweite Zeile von (3.25) gegebenen Form ein und drückt $\Lambda_\nu\cdot\mathbf{J}$ in (3.28) in dem Glied, wo $\mathbf{p}_{\nu 1}$ links steht, entsprechend zu (3.24) durch

$$\Lambda_\nu\cdot\mathbf{J} = \mathbf{J}\cdot\tilde{\Lambda}_\nu-i\hbar\Lambda_\nu^\times \tag{3.29}$$

aus, so fällt $\Lambda_\nu^\times$ heraus, und es wird

$$\tfrac{1}{2}\{\mathrm{grad}_\nu V_\nu \times \mathbf{s}_\nu \cdot \mathbf{p}_{\nu 1} + \mathbf{p}_{\nu 1} \cdot \mathrm{grad}_\nu V_\nu \times \mathbf{s}_\nu\}$$
$$= \mathrm{grad}_\nu V_\nu \times \mathbf{s}_\nu \cdot \mathbf{p}_\nu + \tfrac{1}{2}\{\mathrm{grad}_\nu V_\nu \times \mathbf{s}_\nu \cdot \Lambda_\nu \cdot \mathbf{J} + \mathbf{J} \cdot (\mathrm{grad}_\nu V_\nu \times \mathbf{s}_\nu \cdot \Lambda_\nu)\}. \quad (3.30)$$

Die beiden Glieder in der geschweiften Klammer sind aber einander gleich, denn die $\mathbf{s}_\nu$ transformieren sich bei Drehungen, die den Spinraum mit umfassen, wie $\mathbf{A}(\mathbf{r}_1, \ldots, \mathbf{r}_A)$ in (3.16) und folglich transformiert sich der Vektor $\mathrm{grad}_\nu V_\nu \times \mathbf{s}_\nu \cdot \Lambda_\nu$ ebenfalls wie $\mathbf{A}(\mathbf{r}_1, \ldots, \mathbf{r}_A)$. Dann verschwindet die Spur des Tensors $[\mathbf{J}, \mathrm{grad}_\nu V_\nu \times \mathbf{s}_\nu \cdot \Lambda_\nu]$, und aus (3.28) wird

$$\mathbf{s}_\nu \cdot \mathbf{p}_\nu \times \mathrm{grad}_\nu V_\nu \to \mathbf{s}_\nu \cdot \mathbf{p}_\nu \, \mathrm{grad}_\nu V_\nu + \mathrm{grad}_\nu V_\nu \times \mathbf{s}_\nu \cdot \Lambda_\nu \cdot \mathbf{J}. \quad (3.31)$$

### 3.10. HAMILTONOPERATOR IM EINACHSENASPEKT

Mit (3.26) und (3.30) ergibt sich unter Einführung der Abkürzungen

$$\Theta = \frac{1}{M} \sum_\nu \tilde{\Lambda}_\nu \cdot \Lambda_\nu \quad (3.32)$$

und

$$\mathbf{W} = \frac{1}{M} \sum_\nu \left\{ \tilde{\Lambda}_\nu \cdot \Lambda_\nu \cdot \mathbf{J} + \tfrac{1}{2}(\mathbf{p}_\nu \cdot \Lambda_\nu + \tilde{\Lambda}_\nu \cdot \mathbf{p}_\nu) + \frac{\lambda}{M^2 c^2} \mathrm{grad}_\nu V_\nu \times \mathbf{s}_\nu \cdot \Lambda_\nu \right\} \quad (3.33)$$

für die gesuchte Zerlegung des Hamiltonoperators †

$$\mathscr{H} = \mathscr{H}_\mathrm{a} + \mathscr{H}_\mathrm{1a} + \mathscr{H}_1, \quad (3.34)$$

$$\mathscr{H}_1 = \sum_\nu \left\{ \frac{1}{2M} |\mathbf{p}_\nu|^2 + V_\nu + \frac{\lambda}{M^2 c^2} \mathbf{s}_\nu \cdot \mathbf{p}_\nu \times \mathrm{grad}_\nu V_\nu \right\} + \mathbf{W} \cdot \mathbf{J} - \tfrac{1}{2} \Theta \cdot\cdot \mathbf{J}^2, \quad (3.35)$$

$$\mathscr{H}_\mathrm{a} = \tfrac{1}{2} \Theta \cdot\cdot \mathbf{J}^2, \quad (3.36)$$

$$\mathscr{H}_\mathrm{1a} = -\mathbf{W} \cdot \mathbf{J}. \quad (3.37)$$

$\mathscr{H}_1$ kommutiert mit $\mathbf{N}$ und beschreibt daher eine Bewegung der Nukleonen, die $\mathbf{N}$ nicht ändert. $\mathscr{H}_\mathrm{a}$ bewirkt eine Bewegung des ganzen Kerns wie ein Kreisel mit dem reziproken Trägheitstensor $\Theta$. $\mathbf{W}$ kommutiert mit $\mathbf{N}$. Da es die Impulse enthält, beschreibt es eine Bewegung der Nukleonen bei festem $\mathbf{N}$, die in $\mathscr{H}_\mathrm{1a}$ mit der Kollektivbewegung in Wechselwirkung tritt und eine Abweichung von dem Verhalten als starrer Körper zur Folge hat.

Durch die Abtrennung von $\mathscr{H}_1$ haben wir ohne Wechsel der Variablen eine Auszeichnung von $\mathbf{N}(\mathbf{r}_1, \ldots, \mathbf{r}_A)$ erreicht und die Möglichkeit zur Aufstellung von Zuständen geschaffen, die explizit von $\mathbf{N}$ abhängen. Es ist ein anderer Aspekt des Hamiltonoperators †† entstanden, der als Ein-

† Es ist $\mathbf{W} \cdot \mathbf{J} = \mathbf{J} \cdot \mathbf{W}$ und $\Theta \cdot\cdot \mathbf{J}^2 = \mathbf{J} \cdot \Theta \cdot \mathbf{J} = \mathbf{J}^2 \cdot\cdot \Theta$.

†† Die Gleichungen (3.32) ... (3.37) wurden im Januar 1952 aufgestellt. Sie sind das Ergebnis der im Dezember 1950 vorgetragenen Ansicht, zur Gewinnung eines reziproken Trägheitstensors müsse der kinetische Anteil im Hamiltonoperator ohne Einführung zusätzlicher Variabler so umgeformt werden, daß ein Glied mit $\mathbf{J}^2$ auftritt. Im Oktober 1951 wurden die entsprechenden Gleichungen in Differentialoperatoren angegeben, die Glieder der Zerlegung von $\mathscr{H}$ waren aber nicht hermitisch.

achsenaspekt oder partieller Rotationsaspekt bezeichnet werden kann, da er nur Rotationen um eine zu **N** senkrechte Achse herausstellt.

### 3.11. OPERATOR DES MAGNETISCHEN MOMENTES IM EINACHSENASPEKT

Jeder von den Impulsen abhängige Operator läßt sich durch Abtrennen eines mit **N** vertauschbaren Gliedes zerlegen. Wir zeigen das für den Operator des magnetischen Momentes

$$\mathcal{M} = \frac{\mu_K}{\hbar}(\mathbf{L}^P + g^P \mathbf{S}^P + g^N \mathbf{S}^N), \tag{3.38}$$

$\mu_K = \dfrac{e\hbar}{2M^P c}$ Kernmagneton,

$M^P$ Protonmasse,

$\mathbf{L}^P$ Bahndrehimpuls-Operator aller Protonen,

$\mathbf{S}^P$, $\mathbf{S}^N$ Spinoperator aller Protonen bzw. Neutronen,

$$\tfrac{1}{2}g^P = 2.7935, \quad \tfrac{1}{2}g^N = -1.9135.$$

Mit **N** vertauschbare hermitische Bahndrehimpulse $\mathbf{l}_{\nu 1}$ erhält man mit (3.25) unter Anwendung von (3.29) durch

$$\mathbf{l}_{\nu 1} = \tfrac{1}{2}(\mathbf{r}_\nu \times \mathbf{p}_{\nu 1} + \mathbf{p}_{\nu 1} \times \mathbf{r}_\nu) = \mathbf{l}_\nu + \mathbf{r}_\nu \times \Lambda_\nu \cdot \mathbf{J} + \tfrac{1}{2} i\hbar (\mathbf{r}_\nu \times \Lambda_\nu)^\times. \tag{3.39}$$

Summation über alle Protonen ergibt einen mit **N** vertauschbaren hermitischen Bahndrehimpuls $\mathbf{L}_1^P$ und sein Einsetzen in (3.38) den mit **N** vertauschbaren hermitischen Teil $\mathcal{M}_1$ von $\mathcal{M}$. Mit der Abkürzung

$$G = -\sum_{(P)} \mathbf{r} \times \Lambda_\nu \tag{3.40}$$

wird die gesuchte Zerlegung

$$\mathcal{M} = \mathcal{M}_a + \mathcal{M}_1 \tag{3.41}$$

$$\mathcal{M}_1 = \frac{\mu_K}{\hbar}\{\mathbf{L}^P + g^P \mathbf{S}^P + g^N \mathbf{S}^N - \tfrac{1}{2}(G \cdot \mathbf{J} + \mathbf{J} \cdot \tilde{G})\}, \tag{3.42}$$

$$\mathcal{M}_a = \frac{\mu_K}{\hbar}\tfrac{1}{2}(G \cdot \mathbf{J} + \mathbf{J} \cdot \tilde{G}). \tag{3.43}$$

### 3.12. NÄHERUNGSWERT FÜR DEN GYROMAGNETISCHEN TENSOR $G$

Der Tensor $G$ hat für infinitesimale Drehungen aller Protonen die gleiche Bedeutung wie $\Lambda_\nu$ für infinitesimale Verschiebungen des Nukleons mit der Lage $\mathbf{r}_\nu$: er liefert diejenige Drehung aller Nukleonen, welche die von der ersten Bewegung herrührende Änderung von **N** rückgängig macht. Wenn der Protonenanteil des Kerns im Mittel gleich stark deformiert ist wie der Neutronenanteil, so ist die durch Drehung der Protonen bewirkte Drehung von **N** im Mittel $(Z/A)$-mal so groß wie bei Drehung aller Nukleonen, also ist

$$G \approx -\frac{Z}{A}\sum_\nu \mathbf{r}_\nu \times \Lambda_\nu. \tag{3.44}$$

Daraus findet man mit (3.18), (3.15), (3.16)

$$G \approx \frac{Z}{A}(\delta - \mathbf{N}^2) \tag{3.45}$$

und

$$G\cdot\mathbf{J} \approx \frac{Z}{A}\mathbf{J}_\perp, \qquad \mathbf{J}\cdot\tilde{G} \approx \frac{Z}{A}\mathbf{J}_\perp, \tag{3.46}$$

wenn $\mathbf{J}_\perp$ der zu $\mathbf{N}$ senkrechte Teil von $\mathbf{J}$ ist. Weiter unten wird $G$ exakt berechnet werden.

### 3.13. ANDERE MÖGLICHKEIT DES EINACHSENASPEKTES

Die Verwendung des Kreiselgliedes mit $\mathbf{L}$ bedingt Ersatz von $\mathbf{J}$ durch $\mathbf{L}$ in (3.11) und (3.25) und führt auf eine Zerlegung von $\mathscr{H}$, die sich bis auf das Spin-Bahn-Glied nur durch den Ersatz von $\mathbf{J}$ durch $\mathbf{L}$ in (3.33) ... (3.37) unterscheidet. Für das Spin-Bahn-Glied ergibt die Substitution (3.28) und die an die Stelle von (3.29) tretende Gleichung

$$\Lambda_\nu\cdot\mathbf{L} = \mathbf{L}\cdot\tilde{\Lambda}_\nu - i\hbar\Lambda_\nu^\times \tag{3.47}$$

anstelle von (3.30)

$$\begin{aligned}&\tfrac{1}{2}\{\mathrm{grad}_\nu V_\nu\times\mathbf{s}_\nu\cdot\mathbf{p}_{\nu 1}+\mathbf{p}_{\nu 1}\cdot\mathrm{grad}_\nu V_\nu\times\mathbf{s}_\nu\}\\ &=\mathrm{grad}_\nu V_\nu\times\mathbf{s}_\nu\cdot\mathbf{p}_\nu+\tfrac{1}{2}\{\mathrm{grad}_\nu V_\nu\times\mathbf{s}_\nu\cdot\Lambda_\nu\cdot\mathbf{L}+\mathbf{L}\cdot(\mathrm{grad}_\nu V_\nu\times\mathbf{s}_\nu\cdot\Lambda_\nu)\}.\end{aligned} \tag{3.48}$$

Diese Gleichung unterscheidet sich von (3.30) äußerlich durch den Ersatz von $\mathbf{J}$ durch $\mathbf{L}$. Aber der Faktor von $\mathbf{L}$ transformiert sich nicht nach (3.16) da $\mathbf{L}$ auf die $\mathbf{s}_\nu$ nicht wirkt. Daher wird jetzt

$$\begin{aligned}&\tfrac{1}{2}\{\mathrm{grad}_\nu V_\nu\times\mathbf{s}_\nu\cdot\mathbf{p}_{\nu 1}+\mathbf{p}_{\nu 1}\cdot\mathrm{grad}_\nu V_\nu\times\mathbf{s}_\nu\}\\ &\quad=\mathrm{grad}_\nu V_\nu\times\mathbf{s}_\nu\cdot\mathbf{p}_\nu-\tfrac{1}{2}\mathbf{s}_\nu\cdot\{\mathrm{grad}_\nu V_\nu\times\Lambda_\nu\cdot\mathbf{L}+\mathbf{L}\cdot(\mathrm{grad}_\nu V_\nu+\Lambda_\nu)\tilde{}\}\\ &\quad=\mathrm{grad}_\nu V_\nu\times\mathbf{s}_\nu\cdot\mathbf{p}_\nu-\mathbf{s}_\nu\cdot\{\mathrm{grad}_\nu V_\nu\times\Lambda_\nu\cdot\mathbf{L}+\tfrac{1}{2}i\hbar(\mathrm{grad}_\nu V_\nu\times\Lambda_\nu)^\times\},\end{aligned} \tag{3.49}$$

denn der tensorielle Faktor von $\mathbf{L}$ befolgt (3.24). In der Substitution (3.31) ist also beim Übergang von $\mathbf{J}$ auf $\mathbf{L}$ das zweite Glied nach (3.48) oder (3.49) zu ersetzen. Der Ersatz von $\mathbf{J}$ durch $\mathbf{L}$ in (3.33) ... (3.37) ohne Abänderung des Spin-Bahn-Gliedes zerstörte zwar nicht die Vertauschbarkeit von $\mathscr{H}_1$ mit $\mathbf{N}$, aber die Hermitizität.

### 3.14. BEMERKUNG ÜBER ANDERE ASPEKTE

Die Aufstellung eines mit allen drei Hauptachsen vertauschbaren $\mathscr{H}_1$ ergibt einen Dreiachsen- oder vollständigen Rotationsaspekt. Die Gleichung (3.17) muß dann für alle drei $\mathbf{N}$ erfüllt sein. Für jedes $\mathbf{N}$ lautet die allgemeine Lösung

$$\Lambda_\nu = (\nabla_\nu \mathbf{N}_r)\times\mathbf{N}_r + \mathbf{a}_r\mathbf{N}_r, \qquad r \text{ Index der Hauptachse.} \tag{3.50}$$

Die Vektoren $\mathbf{a}_r$ werden bestimmt durch Gleichsetzen der drei Lösungen und ergeben

$$\Lambda_\nu = \tfrac{1}{2}\sum_r (\nabla_\nu \mathbf{N}_r)\times\mathbf{N}_r. \tag{3.51}$$

Für den Dreiachsenaspekt gelten dann ebenfalls die Gleichungen (3.32) ... (3.37), beziehungsweise die für das Kreiselglied mit $\mathbf{L}$; es ist nur (3.18) durch (3.51) zu ersetzen. Die Benutzung des Dreiachsen-Rotationsaspektes wäre dann angebracht, wenn Grund zu der Annahme bestünde, der Kern habe im Mittel die Form eines dreiachsigen Ellipsoides und bewege sich kreiselähnlich.

Die Aufgabe, ein mit allen $\gamma_m$ vertauschbares $\mathscr{H}_1$ zu finden, führt anscheinend auf ein $\mathbf{p}_{\nu 1}$, in dem anstelle von $\mathbf{J}$ oder $\mathbf{L}$ Operatoren auftreten, die eine homogene Deformation des Kerns verursachen. Diese Deformationsimpulse lassen sich aus dem allgemeinen hermitischen Tensoroperator

$$\omega_{kl} = \tfrac{1}{2}(x_k p_l + p_l x_k) \tag{3.52}$$

gewinnen durch Zerlegen in einen symmetrischen Teil

$$\begin{aligned}\sigma_{kl} &= \tfrac{1}{4}(x_k p_l + p_l x_k + x_l p_k + p_k x_l)\\ &= \tfrac{1}{2}(x_k p_l + x_l p_k - i\hbar\delta_{kl})\end{aligned} \tag{3.53}$$

und einen antisymmetrischen

$$\begin{aligned}\alpha_{kl} &= \tfrac{1}{4}(x_k p_l + p_l x_k - x_l p_k - p_k x_l)\\ &= \tfrac{1}{2}(x_k p_l - x_l p_k)\end{aligned} \tag{3.54}$$

und weiteres Zerlegen von $\sigma_{kl}$ in einen Tensor mit verschwindender Spur

$$\begin{aligned}\pi_{kl} &= \tfrac{1}{2}\{x_k p_l + x_l p_k - i\hbar\delta_{kl} - \tfrac{1}{3}\delta_{kl}\sum_r (2x_r p_r - i\hbar\delta_{rr})\}\\ &= \tfrac{1}{2}(x_k p_l + x_l p_k) - \tfrac{1}{3}\delta_{kl}\sum_r x_r p_r\end{aligned} \tag{3.55}$$

und den Rest

$$\kappa_{kl} = \delta_{kl}(\tfrac{1}{3}\sum_r x_r p_r - \tfrac{1}{2}i\hbar). \tag{3.56}$$

Da die $\pi_{kl}$ bis auf den Faktor $i\hbar$ die Operatoren infinitesimaler homogener isochorer Deformationen sind, stellen die

$$\Pi_{kl} = \sum_\nu \pi_{\nu kl} \tag{3.57}$$

anscheinend die geeigneten Deformationsimpulse dar, die im Ansatz für $\mathbf{p}_{\nu 1}$, verknüpft mit einem Tensor dritter Stufe, auftreten. Die so entstehende Zerlegung von $\mathscr{H}$ ist der Form- oder Schwingungsaspekt. Es sind auch Kombinationen zwischen Schwingungs- und Rotationsaspekt möglich, zum Beispiel eine solche, die Rotationen senkrecht zu einer Achse und Schwingungen parallel und senkrecht dazu herausstellt. Der Schwingungsaspekt oder

ein Rotations-Schwingungsaspekt wird notwendig, wenn die Frage entschieden werden soll, ob der Kern im Grundzustand schwingt, das heißt, ob die Schwankungen der $\gamma_m$ hauptsächlich durch eine Kollektivbewegung und nicht hauptsächlich durch eine voneinander unabhängige Bewegung der Nukleonen hervorgerufen werden.

### 3.15. ASPEKTIERUNG UND NUKLEONENWECHSELWIRKUNG

Die Aspektierung des Hamiltonoperators ist nicht an das Selbstpolarisationspotential gebunden. Sie läßt sich für jede Nukleonenwechselwirkung durchführen, die in einfacher Weise von den Impulsen abhängt. Das Selbstpolarisationspotential führte auf den Einachsenaspekt, weil die Größen $\Gamma''_{\pm 1}$, durch deren Nullsetzen **N** gefunden wird, im Potential selbst auftreten.

## 4. Bedeutung von $\Theta$ und W

### 4.1. VERGLEICH DES REZIPROKEN TRÄGHEITSTENSORS MIT DEM DES KREISELS

Der durch (3.32) gegebene reziproke Trägheitstensor lautet bei Darstellung in Komponenten des gestrichenen Systems wegen $\Lambda_\nu \cdot \mathbf{N} = 0$

$$\Theta = \begin{pmatrix} \Theta'_{11} & \Theta'_{12} & 0 \\ \Theta'_{12} & \Theta'_{22} & 0 \\ 0 & 0 & 0 \end{pmatrix}. \tag{4.1}$$

Er unterscheidet sich von dem eines Kreisels durch das Fehlen des dritten Hauptmomentes. Diese Eigentümlichkeit läßt sich durch Vergleich mit einem Kreisel [9–18]) völlig klären. Sind $A$, $B$, $C$ dessen reziproke Haupträgheitsmomente und $\Theta$, $\Phi$, $\Psi$ die Eulerschen Winkel eines Koordinatensystems $\Sigma'$, bei dem die dritte Achse mit der dritten Hauptträgheitsachse zusammenfällt und die erste Achse mit der ersten Hauptträgheitsachse den festen Winkel $\varphi$ bildet, so lautet der Hamiltonoperator

$$\mathscr{H} = \frac{A+B}{4}(J'^2_1+J'^2_2)+\frac{C}{2}J'^2_3 + \frac{A-B}{4}\{(J'^2_1-J'^2_2)\cos 2\varphi+(J'_1J'_2+J'_2J'_1)\sin 2\varphi\}. \tag{4.2}$$

Das Auftreten von $\varphi$ ermöglicht Abtrennung eines Gliedes $\mathscr{H}_1$ von $\mathscr{H}$, das nur Drehungen um die dritte Achse von $\Sigma'$ bei konstanten Eulerschen Winkeln enthält; $\varphi$ ist dann veränderlich. Zu diesem Zweck führen wir den Drehimpuls $J'_{31}$ ein, der mit den Eulerschen Winkeln kommutiert. Dann ist

$$\mathscr{H} = \mathscr{H}_3+\mathscr{H}'+\mathscr{H}_1, \tag{4.3}$$

$$\mathscr{H}_1 = \tfrac{1}{2}C J'^2_{3i}, \tag{4.4}$$

$$\mathscr{H}' = \tfrac{1}{2}C(J'^2_3 - J'^2_{3i}), \tag{4.5}$$

$$\mathscr{H}_a = \tfrac{1}{4}(A+B)(J'^2_1+J'^2_2) + \tfrac{1}{4}(A-B)\{(J'^2_1-J'^2_2)\cos 2\psi + (J'_1J'_2+J'_2J'_1)\sin 2\psi\}. \tag{4.6}$$

Da das gestrichene System nicht mit Masse belegt ist, darf kein Unterschied zwischen Drehungen des Kreisels bei konstantem $\psi$ in solchen bei konstantem $\Psi$ bestehen. Die Zustände $\mathscr{D}$ des Kreisels müssen daher die Bedingung

$$(J'_3 - J'_{3i})\mathscr{D} = 0 \tag{4.7}$$

erfüllen. Die Existenz scharfer Werte für $J'_3 - J'_{3i}$ verlangt aber

$$[\mathscr{H}, J'_3 - J'_{3i}] = 0, \tag{4.8}$$

und man kann sich mit Hilfe der Vertauschungsrelationen †

$$[J'_1, J'_2] = -i\hbar J'_3 \quad \text{und zyklisch Vertauschte} \tag{4.9}$$

überzeugen, daß jene Bedingung erfüllt ist, wobei beachtet werden muß, daß $J'_1, J'_2, J'_3$ den Winkel $\psi$ unverändert lassen und mit $J'_{3i}$ kommutieren. $\mathscr{H}'$ kann daher fortgelassen werden. In (3.36) kommen aber wegen (4.1) nur Glieder mit den gleichen $J'_k$ vor wie in (4.6). Das $\mathscr{H}_a$ des Kerns kann daher aufgefaßt werden als Hamiltonoperator eines Kreisels, von dem Drehungen um die dritte Achse abgetrennt worden sind. An die Stelle dieser Drehungen ist die durch (3.35) beschriebene Nukleonenbewegung getreten, und außerdem ist noch ein Glied $\mathscr{H}_{1a}$ vorhanden, das Abweichungen von dem Verhalten als starrer Körper zum Ausdruck bringt.

### 4.2. DIE TAUMELBEDINGUNG

Für den Kreisel erhält man die Differentialdarstellung der Komponenten von **J** durch Multiplikation von (C2) und (C3) mit $i\hbar$. Darüber hinaus gilt wegen der dem Operator $J'_{3i}$ zugeschriebenen Eigenschaften

$$J'_{3i} = -i\hbar\frac{\partial}{\partial\psi}. \tag{4.10}$$

Die Differentialdarstellungen liefern Vertauschungsrelationen der Drehimpulskomponenten mit den Eulerschen Winkeln. Mit diesen Beziehungen läßt sich zeigen, daß die Gleichung

$$[P, \Psi] + \tfrac{1}{2}\{\cos\Theta\,[P, \Phi] + [P, \Phi]\cos\Theta\} \tag{4.11}$$

erfüllt ist, wenn für $P$ einer der Operatoren $J'_1, J'_2, J'^2_2, J'^2_2, J'_1J'_2+J'_2J'_1$ eingesetzt wird. Sie gilt dann ebenfalls für das durch (4.6) gegebene $\mathscr{H}_a$ und, da sie für das durch (4.4) bestimmte $\mathscr{H}_1$ definitionsgemäß erfüllt ist, auch für $\mathscr{H}_a+\mathscr{H}_1$, also für den Operator, der die richtigen Zustände des Kreisels

† Siehe Anhang C.

liefert. Schreibt man die mit $\mathscr{H}_a+\mathscr{H}_1$ gebildeten Kommutatoren als zeitliche Änderungen, so ist also

$$\dot{\Psi}+\tfrac{1}{2}(\cos\Theta\,\dot{\Phi}+\dot{\Phi}\cos\Theta)=0. \tag{4.12}$$

Außerdem ergibt sich

$$\dot{\psi}=CJ'_{31}. \tag{4.13}$$

Die Beziehung (4.12) ist das quantenmechanische Analogon zur klassischen anholonomen Nebenbedingung

$$d\Psi+\cos\Theta d\Phi=0 \tag{4.14}$$

und besagt, daß sich $\Sigma'$ ohne Drehung um die dritte Achse bewegt. Wir bezeichnen dieses Verhalten als Taumelbewegung und nennen (4.12) Taumelbedingung. Bildet man dagegen die zeitlichen Ableitungen mit dem Operator $\mathscr{H}_a+\mathscr{H}'+\mathscr{H}_1$ der ebenfalls die richtigen Zustände des Kreisels liefert, so ergibt sich anstelle von (4.12) und (4.13)

$$\dot{\Psi}+\tfrac{1}{2}(\cos\Theta\,\dot{\Phi}+\dot{\Phi}\cos\Theta)=CJ'_3, \tag{4.15}$$

$$\dot{\psi}=0. \tag{4.16}$$

Das gestrichene System bleibt jetzt mit dem Kreisel verbunden.

Die Taumelbedingung gilt auch für den aspektierten Hamiltonoperator (3.32) ... (3.37), denn $\mathscr{H}_1$, $\Theta$, $\mathbf{W}$ kommutieren mit $\mathbf{N}$, also mit $\Theta$ und $\Phi$, aber auch mit $\Psi$, weil dieser Winkel von den Nukleonenlagen unabhängig ist, und in $\mathscr{H}_a$ und $\mathscr{H}_{1a}$ treten nur solche Kombinationen der Komponenten von $\mathbf{J}$ auf, für die (4.11) gilt.

### 4.3. BEDEUTUNG DER GLIEDER VON W

Die Beiträge der in $\mathscr{H}_1$ enthaltenen Terme

$$\sum_\nu \frac{1}{2M}|\mathbf{p}_\nu|^2, \qquad \frac{\lambda}{M^2c^2}\sum_\nu \mathbf{s}_\nu\cdot\mathbf{p}_\nu\times\operatorname{grad}_\nu V_\nu, \qquad \tfrac{1}{2}\Theta\cdot\cdot\,\mathbf{J}^2$$

zu dem (verschwindenden) Operator der zeitlichen Ableitung von $\mathbf{N}$ lassen sich unter Anwendung der Vertauschungsrelationen mit Hilfe dreier Winkelgeschwindigkeiten wie folgt ausdrücken:

$$\begin{gathered}\frac{i}{\hbar}\sum_\nu\frac{1}{2M}[|\mathbf{p}_\nu|^2,\,\mathbf{N}]=\tfrac{1}{2}(\mathbf{W}_T\times\mathbf{N}-\mathbf{N}\times\mathbf{W}_T)\\ \mathbf{W}_T=-\frac{1}{2M}\sum_\nu(\mathbf{p}_\nu\cdot\Lambda_\nu+\tilde{\Lambda}_\nu\cdot\mathbf{p}_\nu),\end{gathered} \tag{4.17}$$

$$\begin{gathered}\frac{i}{\hbar}\frac{\lambda}{M^2c^2}\sum_\nu[\mathbf{s}_\nu\cdot\mathbf{p}_\nu\times\operatorname{grad}_\nu V_\nu,\,\mathbf{N}]=\mathbf{W}_S\times\mathbf{N}=-\mathbf{N}\times\mathbf{W}_S\\ \mathbf{W}_S=\frac{\lambda}{M^2c^2}\sum_\nu\mathbf{s}_\nu\times\operatorname{grad}_\nu V_\nu\cdot\Lambda_\nu,\end{gathered} \tag{4.18}$$

$$\frac{i}{\hbar}[\tfrac{1}{2}\Theta\cdot\cdot\mathbf{J}^2,\mathbf{N}]=\tfrac{1}{2}(\mathbf{W}_K\times\mathbf{N}-\mathbf{N}\times\mathbf{W}_K)$$
$$\mathbf{W}_K=\Theta\cdot\mathbf{J}=\mathbf{J}\cdot\Theta. \tag{4.19}$$

Alle drei Winkelgeschwindigkeiten stehen auf **N** senkrecht. $\mathbf{W}_S$ kommutiert außerdem mit **N**. Dagegen ist

$$[\mathbf{W}_T,\mathbf{N}]=[\mathbf{W}_K,\mathbf{N}]=-i\hbar\Theta\times\mathbf{N}. \tag{4.20}$$

Durch Vergleich von (3.33) mit (4.17) ... (4.19) erkennt man

$$\mathbf{W}=\mathbf{W}_K-\mathbf{W}_T-\mathbf{W}_S, \tag{4.21}$$

wie es sein muß, damit das Glied $\mathbf{W}\cdot\mathbf{J}$ in $\mathscr{H}_1$ den Beitrag der anderen Terme zu $[\mathscr{H}_1,\mathbf{N}]$ aufhebt. **W** steht senkrecht auf **N** und ist mit **N** vertauschbar.

Die durch **W** beschriebene Bewegungsform des Kerns wird nach Berechnung der Komponenten von **N** untersucht werden.

### 4.4. NOTWENDIGKEIT DER GLIEDER $\mathbf{W}\cdot\mathbf{J}$ UND $-\frac{1}{2}\Theta\cdot\cdot\mathbf{J}^2$ IN $\mathscr{H}_1$

Es ist nicht möglich, aus $\mathscr{H}$ nur durch Subtrahieren eines Kreiselgliedes $\frac{1}{2}\Theta\cdot\cdot\mathbf{J}^2$ mit irgendeinem $\Theta(\mathbf{r}_1,\ldots,\mathbf{r}_A)$ einen mit **N** vertauschbaren Operator zu gewinnen, denn dann müßte $\mathbf{W}_K-\mathbf{W}_T-\mathbf{W}_S$ identisch verschwinden. Diese drei Winkelgeschwindigkeiten sind aber verschiedene Funktionen der dynamischen Variablen. Das ist die quantenmechanische Formulierung folgenden Sachverhaltes: Rotiert der Kern als starrer Körper, so ist $\mathrm{d}\mathbf{N}/\mathrm{d}t$ durch die Winkelgeschwindigkeit der Rotation bestimmt, die man aus **J** und $\Theta$ errechnen kann. Bewegt sich der Kern bei gleichem **J** und $\Theta$ in einer anderen Weise, so ergibt sich auch ein anderes $\mathrm{d}\mathbf{N}/\mathrm{d}t$. Es ist zum Beispeil möglich, daß sich trotz einem endlichen **J** die $\gamma_m$ und damit **N** nicht ändern. Die Kenntnis von **J** und $\Theta$ genügt also nicht zur Berechnung von $\mathrm{d}\mathbf{N}/\mathrm{d}t$; in einem Koordinatensystem, in dem die aus **J** und $\Theta$ berechnete Winkelgeschwindigkeit verschwindet, braucht $\mathrm{d}\mathbf{N}/\mathrm{d}t$ nicht zu verschwinden.

Es ist aber auch nicht möglich, $\mathscr{H}$ durch Hinzufügen von $-(\mathbf{W}_T+\mathbf{W}_S)\cdot\mathbf{J}$ mit **N** vertauschbar zu machen. Zum Beweis bemerken wir, daß dieser Ausdruck hermitisch ist, denn man kann zeigen, daß (3.16) auch bei Ersatz von $\mathbf{A}(\mathbf{r}_2,\ldots,\mathbf{r}_A)$ durch $\mathbf{W}_T$ oder $\mathbf{W}_S$ gilt. Nun ist aber nach (4.17) und (4.18)

$$i\hbar\left[\sum_\nu\left\{\frac{1}{2M}|\mathbf{p}_\nu|^2+\frac{\lambda}{M^2c^2}\mathbf{s}_\nu\cdot\mathbf{p}_\nu\times\operatorname{grad}_\nu V_\nu\right\}-(\mathbf{W}_T+\mathbf{W}_S)\cdot\mathbf{J},\mathbf{N}\right]$$
$$=\tfrac{1}{2}\{(\mathbf{W}_T+\mathbf{W}_S)\times\mathbf{N}-\mathbf{N}\times(\mathbf{W}_T+\mathbf{W}_S)\}-(\mathbf{W}_T+\mathbf{W}_S)\times\mathbf{N}, \tag{4.22}$$

und dieser Ausdruck verschwindet nicht, denn aus (4.20) folgt

$$\mathbf{W}_T\times\mathbf{N}\neq-\mathbf{N}\times\mathbf{W}_T. \tag{4.23}$$

## 5. Berechnung von $\Lambda_\nu$ und davon abgeleiteter Größen

### 5.1. IMPULSAUFTEILUNGSTENSOR $\Lambda_\nu$

Bei der Zerlegung des Hamiltonoperators und des Operators des magnetischen Momentes steht der Impulsaufteilungstensor (3.18) an entscheidender Stelle. Seine Kenntnis ermöglicht die Berechnung des reziproken Trägheitstensors $\Theta$, der Winkelgeschwindigkeit $\mathbf{W}$ und des gyromagnetischen Tensors $G$. Die Abhängigkeit dieser Größen von den dynamischen Variablen der Nukleonen soll jetzt ermittelt werden. Von $\mathbf{W}$ ist außerdem die kinematische Bedeutung zu klären; bis jetzt wurde nur festgestellt, daß dieser Operator die kollektive Rotation des Kerns mit der individuellen Nukleonenbewegung bei festem $\mathbf{N}$ verknüpft und sich aus drei Winkelgeschwindigkeiten zusammensetzt.

Die auf das durch $\Gamma''_{\pm 1} = 0$ ausgezeichnete drehbare System $\Sigma'$ bezogenen Komponenten des in $\Lambda_\nu$ enthaltenen Tensors $\nabla_\nu \mathbf{N}$ sind die gleichen wie in einem festen System, das für die betrachtete Konfiguration gerade mit $\Sigma'$ übereinstimmt, nämlich

$$(\nabla_\nu \mathbf{N})'_{kl} = \frac{\partial N'_l}{\partial x'_{\nu k}} = \frac{\partial N'_l}{\partial \Gamma''_{+1}} \frac{\partial \Gamma''_{+1}}{\partial x'_{\nu k}} + \frac{\partial N'_l}{\partial \Gamma''_{-1}} \frac{\partial \Gamma''_{-1}}{\partial x'_{\nu k}}. \tag{5.1}$$

Die Ableitungen sind bei festgehaltenem Koordinatensystem zu bilden. Zu ihrer Berechnung betrachten wir eine benachbarte Konfiguration, die, bezogen auf das System der Ausgangskonfiguration, die Momente $\Gamma''_m + \mathrm{d}\Gamma''_m$ und die Eulerschen Winkel $\mathrm{d}\Theta'$, $\Phi'$, $\Psi'$ haben möge. Nach Voraussetzung ist $\Gamma''_{\pm 1} = 0$, und die Taumelbedingung verlangt $\Psi' = -\Phi$. Die benötigten Beziehungen zwischen $\mathrm{d}N'_{1,2}$ und $\mathrm{d}\Gamma''_{\pm 1}$ ergeben sich aus

$$\mathrm{d}N'_1 \pm i\,\mathrm{d}N'_2 = \mathrm{e}^{\pm i\Phi'}\,\mathrm{d}\Theta' \tag{5.2}$$

und (3.9). Nullsetzen der linken Seiten liefert $\Theta$, $\Phi$ in Abhängigkeit von den $\Gamma_m$. Ersetzt man in dieser Gleichung die ungestrichenen Größen durch die gestrichenen und bildet das totale Differential an der Stelle $\Theta' = 0$, so wird

$$\mathrm{d}\Gamma''_{\pm 1} = \pm(\Gamma''_{\pm 2}\mathrm{e}^{\pm i\Phi'} - \sqrt{\tfrac{3}{2}}\,\Gamma''_0 \mathrm{e}^{\mp i\Phi'})\mathrm{d}\Theta' \tag{5.3}$$

und folglich

$$\frac{\partial N'_1}{\partial \Gamma''_{\pm 1}} = \mp \frac{\sqrt{\frac{3}{2}}\,\Gamma''_0 + \Gamma''_{\mp 2}}{3\Gamma''^2_0 - 2|\Gamma''_2|^2}, \qquad \frac{\partial N'_2}{\partial \Gamma''_{\pm 1}} = -i\frac{\sqrt{\frac{3}{2}}\,\Gamma''_0 - \Gamma''_{\mp 2}}{3\Gamma''^2_0 - 2|\Gamma''_2|^2}. \tag{5.4}$$

Entnimmt man $\partial\Gamma''_{\pm 1}/\partial x'_{\nu k}$ aus

$$\Gamma''_{\pm 1} = \sum_\lambda r_\lambda^2 Y^*_{\pm 1}(\vartheta_\lambda, \varphi_\lambda) = \sqrt{\tfrac{3}{2}} \sum_\lambda (\mp x'_\lambda + i y'_\lambda) z'_\lambda, \tag{5.5}$$

so lauten die gesuchten Komponenten von $\Lambda_\nu$

$$
\begin{aligned}
\Lambda'_{\nu 11} &= \sqrt{\frac{3}{2}}\,\frac{i(\Gamma'_{+2}-\Gamma'_{-2})z'_\nu}{3\Gamma'^2_0-2|\Gamma'_2|^2}\\
\Lambda'_{\nu 21} &= \sqrt{\frac{3}{2}}\,\frac{(\sqrt{6}\Gamma'_0-\Gamma'_{+2}-\Gamma'_{-2})z'_\nu}{3\Gamma'^2_0-2|\Gamma'_2|^2}\\
\Lambda'_{\nu 31} &= \sqrt{\frac{3}{2}}\,\frac{i(\Gamma'_{+2}-\Gamma'_{-2})x'_\nu+(\sqrt{6}\,\Gamma'_0-\Gamma'_{+2}-\Gamma'_{-2})y'_\nu}{3\Gamma'^2_0-2|\Gamma'_2|^2}\\
\Lambda'_{\nu 12} &= -\sqrt{\frac{3}{2}}\,\frac{(\sqrt{6}\,\Gamma'_0+\Gamma'_{+2}+\Gamma'_{-2})z'_\nu}{3\Gamma'^2_0-2|\Gamma'_2|^2}\\
\Lambda'_{\nu 22} &= -\sqrt{\frac{3}{2}}\,\frac{i(\Gamma'_{+2}-\Gamma'_{-2})z'_\nu}{3\Gamma'^2_0-2|\Gamma'_2|^2}\\
\Lambda'_{\nu 32} &= -\sqrt{\frac{3}{2}}\,\frac{(\sqrt{6}\,\Gamma'_0+\Gamma'_{+2}+\Gamma'_{-2})x'_\nu+i(\Gamma'_{+2}-\Gamma'_{-2})y'_\nu}{3\Gamma'^2_0-2|\Gamma'_2|^2}\\
\Lambda_{\nu 13} &= \Lambda_{\nu 23} = \Lambda_{\nu 33} = 0.
\end{aligned}
\tag{5.6}
$$

### 5.2. REZIPROKER TRÄGHEITSTENSOR $\Theta$

Aus (3.32) ergibt sich mit (5.6) bei Benutzung der in Anhang A erläuterten $p$- und $q$-Komponenten

$$
\begin{aligned}
\Theta'_{pq} = \Theta'_{qp} &= \Theta'_{11}+\Theta'_{22} = \frac{4}{3M}\,\frac{\Gamma'^2_0(\Gamma+\frac{1}{2}\Gamma'_0)+\frac{2}{3}|\Gamma'_2|^2(\Gamma+\frac{7}{2}\Gamma'_0)}{(\Gamma'^2_0-\frac{2}{3}|\Gamma'_2|^2)^2}\\
\left.\begin{matrix}\Theta'_{pp}\\ \Theta'_{qq}\end{matrix}\right\} &= \Theta'_{11}-\Theta'_{22}\pm 2i\Theta'_{12} = -\frac{8\sqrt{6}}{9M}\,\frac{\Gamma'_0(\Gamma+\frac{5}{4}\Gamma'_0)+\frac{1}{2}|\Gamma'_2|^2}{(\Gamma'^2_0-\frac{2}{3}|\Gamma'_2|^2)^2}\,\Gamma'_{\mp 2}.
\end{aligned}
\tag{5.7}
$$

### 5.3. WINKELGESCHWINDIGKEIT W

Nach (4.17) ... (4.19) läßt sich $\mathbf{W}$ in die drei Anteile $\mathbf{W}_T$, $\mathbf{W}_S$, $\mathbf{W}_K$ zerlegen. $\mathbf{W}_T$ kann mit Hilfe der durch (3.55) und (3.57) erklärten Deformationsimpulse wie folgt geschrieben werden:

$$
\begin{aligned}
W'_{Tp} = +\frac{i}{M}\Big\{&(\Pi'_{p3}\Gamma'_0+\sqrt{\tfrac{2}{3}}\,\Pi'_{q3}\Gamma'_{-2})\,\frac{1}{\Gamma'^2_0-\frac{2}{3}|\Gamma'_2|^2}\\
&+\frac{1}{\Gamma'^2_0-\frac{2}{3}|\Gamma'_2|^2}\,(\Gamma'_0\Pi'_{p3}+\sqrt{\tfrac{2}{3}}\,\Gamma'_{-2}\Pi'_{q3})\Big\}\\
W'_{Tq} = -\frac{i}{M}\Big\{&(\Pi'_{q3}\Gamma'_0+\sqrt{\tfrac{2}{3}}\,\Pi'_{p3}\Gamma'_{+2})\,\frac{1}{\Gamma'^2_0-\frac{2}{3}|\Gamma'_2|^2}\\
&+\frac{1}{\Gamma'^2_0-\frac{2}{3}|\Gamma'_2|^2}\,(\Gamma'_0\Pi'_{q3}+\sqrt{\tfrac{2}{3}}\,\Gamma'_{+2}\Pi'_{p3})\Big\}.
\end{aligned}
\tag{5.8}
$$

$\Pi'_{13}$ und $\Pi'_{23}$ beschreiben bis auf den Faktor $i\hbar$ infinitesimale homogene

isochore Deformationen, deren Richtungen mit der $z'$-Achse den Winkel $\pi/4$ bilden und die **N** ändern. Das in $\mathbf{W}_K$ enthaltene **J** beschreibt dagegen Rotationen des Kerns als starrer Körper, die **N** ebenfalls ändern. Die in **W** enthaltene Differenz $\mathbf{W}_K - \mathbf{W}_T$ beschreibt daher wegen ihrer Vertauschbarkeit mit **N** eine Überlagerung beider Bewegungsformen, die **N** konstant läßt, oder, anders ausgedrückt, sie beschreibt eine im ausgezeichneten System erfolgende Rotation der Nukleonen als nichtstarrer Körper. Die Anwesenheit von $\mathbf{W}_S$ in **W** ändert daran nichts, da $\mathbf{W}_S$ die Impulse nicht enthält. Die durch **W** und **J** beschriebenen Bewegungen lassen sich durch die Prägungen „Es rotiert *im* Kern" und „*Der* Kern rotiert" schlagwortartig kennzeichnen. Sie stehen durch das Glied $\mathscr{H}_{1a}$ in Wechselwirkung; dieses werde daher als Rotationsaustauschoperator bezeichnet. Die Bedeutung von **W** ist jetzt völlig klargestellt.

Schwingungen parallel und senkrecht zu **N** stehen wegen Fehlens der zugehörigen Deformationsimpulse in **W** nicht in Wechselwirkung mit der Rotation des Kerns als starrer Körper. Schwankungen in der Kernform wirken sich nur über die reziproken Trägheitsmomente auf die Rotation aus, die Bewegungsform dieser Schwankungen ist daher gleichgültig.

### 5.4. GYROMAGNETISCHER TENSOR $G$

Unter Einführung der Formmomente des Protonenteils des Kerns

$$\Gamma_m^{\mathrm{P}} = \sum_{(\mathrm{P})} r_\nu^2 Y_m(\vartheta_\nu, \varphi_\nu) \tag{5.9}$$

ergibt (3.40) mit (5.6)

$$G'_{pq} = 2\frac{\Gamma'_0\Gamma_0^{\mathrm{P}'} - \frac{2}{3}\Gamma'_{+2}\Gamma_{-2}^{\mathrm{P}'}}{\Gamma_0'^2 - \frac{2}{3}|\Gamma'_2|^2} \qquad G'_{qp} = 2\frac{\Gamma'_0\Gamma_0^{\mathrm{P}'} - \frac{2}{3}\Gamma'_{-2}\Gamma_{+2}^{\mathrm{P}'}}{\Gamma_0'^2 - \frac{2}{3}|\Gamma'_2|^2}$$

$$G'_{pp} = \sqrt{\frac{2}{3}}\frac{\Gamma'_0\Gamma_{-2}^{\mathrm{P}'} - \Gamma'_{-2}\Gamma_0^{\mathrm{P}'}}{\Gamma_0'^2 - \frac{2}{3}|\Gamma'_2|^2} \qquad G'_{qq} = \sqrt{\frac{2}{3}}\frac{\Gamma'_0\Gamma_{+2}^{\mathrm{P}'} - \Gamma'_{+2}\Gamma_0^{\mathrm{P}'}}{\Gamma_0'^2 - \frac{2}{3}|\Gamma'_2|^2} \tag{5.10}$$

$$G'_{3p} = -\sqrt{\frac{2}{3}}\frac{\Gamma'_0\Gamma_{-1}^{\mathrm{P}'} + \sqrt{\frac{2}{3}}\Gamma'_{-2}\Gamma_{+1}^{\mathrm{P}'}}{\Gamma_0'^2 - \frac{2}{3}|\Gamma'_2|^2} \qquad G'_{3q} = \sqrt{\frac{2}{3}}\frac{\Gamma'_0\Gamma_{+1}^{\mathrm{P}'} + \sqrt{\frac{2}{3}}\Gamma'_{+2}\Gamma_{-1}^{\mathrm{P}'}}{\Gamma_0'^2 - \frac{2}{3}|\Gamma'_2|^2}.$$

## 6. Allgemeines zum Orthonormalsystem

### 6.1. LAGEKOORDINATEN

$\mathscr{H}_1$ beschreibt eine Bewegung der Nukleonen bei festem **N** und hängt über die $\Lambda_\nu$ von **N** ab. **N** ist aber bestimmt als eine der Hauptachsenrichtungen des dem Kern zugeordneten ellipsoidähnlichen Gebildes (3.8). Diese Richtungen sind völlig bestimmt, wenn alle drei Hauptachsen voneinander verschieden sind; bei Axialsymmetrie des Gebildes (3.8) ist nur eine Richtung völlig bestimmt, und bei Kugelsymmetrie ist die Lage der Hauptachsen

völlig unbestimmt. Die in den $\Lambda_\nu$ enthaltenen Ausdrücke $\partial N'_1/\partial \Gamma''_{\pm 1}$, $\partial N'_2/\partial \Gamma''_{\pm 1}$ existieren nur, wenn für **N** eine völlig bestimmte Hauptachsenrichtung eingesetzt wird. Ersetzt man ein derartiges **N** durch $-\mathbf{N}$, so bleiben die $\Lambda_\nu$ und damit $\mathscr{H}_1$ invariant, Ersatz des **N** durch eine dazu senkrechte Richtung verändert im allgemeinen die $\Lambda_\nu$, denn $d\mathbf{r}_\nu \cdot \Lambda_\nu$ gibt die Drehung senkrecht zu **N** an, welche die Änderung von **N** infolge Verschiebung des $\nu$-ten Nukleons um $d\mathbf{r}_\nu$ rückgängig macht, und die zu **N** senkrechten Hauptachsen werden durch diese Drehung im allgemeinen nicht in ihre ursprüngliche Lage gebracht. $\mathscr{H}_1$ und folglich auch $\mathscr{H}_3$ und $\mathscr{H}_{13}$ sind daher im allgemeinen dreideutige Funktionen der $\mathbf{r}_\nu$, und jedes $\mathscr{H}_1$ kommutiert nur mit dem zugehörigen **N** und dessen Gegenrichtung. Die Mehrdeutigkeit verschwindet bei Bezug der dynamischen Variablen auf ein Koordinatensystem $\Sigma'$, in dem **N** eine fest vorgegebene Richtung, etwa die der $z'$-Achse, hat. Für jedes mögliche **N** gibt es dann ein $\Sigma'$, das bis auf willkürliche Drehungen um das betreffende **N** festgelegt ist, aber die Abhängigkeit von den auf $\Sigma'$ bezogenen Komponenten der dynamischen Variablen ist für alle **N** die gleiche; die verschiedenen $\Sigma'$ sind also ununterscheidbar. Wir setzen fest, daß die Aussage, ein Operator befinde sich im Einachsenaspekt, einschließt, daß die dynamischen Variablen auf ein Koordinatensystem $\Sigma'$ bezogen sind, in dem **N** eine fest vorgegebene Richtung hat, und wählen hierfür die $z'$-Achse. Die Lagekonfigurationen des Kerns werden dann beschrieben durch $3A$ Relativkoordinaten und 3 Eulersche Winkel. Die ersteren sind den beiden Bedingungen

$$N'_{1,2} = 0 \quad \text{oder} \quad \Gamma''_{\pm 1} = 0 \tag{6.1}$$

und die letzteren der Taumelbedingung unterworfen. Es gibt also $3A+1$ unabhängige Lagekoordinaten, aber $3A$ unabhängige Differentiale.

### 6.2. ORTHONORMALSYSTEM ZU $\mathscr{H}_1$

$\mathscr{H}_1$ ist invariant gegen die Drehung $Z'_\alpha$ aller Nukleonen um den beliebigen Winkel $\alpha$ um die $z'$-Achse, gegen die Spiegelung $S_0$ am Nullpunkt und gegen die Drehung um den Winkel $\pi$ um irgendeine zur $z'$-Richtung senkrechte Achse. Jede solche Umklappung läßt sich zusammensetzen aus Drehungen um die $z'$-Achse und der Umklappung $U'_2$ um die $y'$-Achse und $U'_2$ wiederum aus der Spiegelung $S'_2$ an der $x'z'$-Ebene und aus $S_0$ nach

$$U'_2 = S'_2 S_0 = S_0 S'_2. \tag{6.2}$$

$\mathscr{H}_1$ ist also auch invariant gegen $S'_2$.

Da $\mathscr{H}_1$, **N**, $Z'_\alpha$, $S_0$ ein System vertauschbarer Variabler bilden, gibt es Zustände $[\Phi]^{wE_1}_{\Omega}$, die für $J'_3$, $S_0$, $\mathscr{H}_1$ die Eigenwerte $\hbar\Omega$, $w = \pm 1$, $E_1$ haben und die Bedingung $\Gamma''_{\pm 1} = 0$ erfüllen, was durch die eckigen Klammern am Zustandssymbol gekennzeichnet sei. $S'_2$ kommutiert zwar mit $\mathscr{H}_1$, **N**, $S_0$, aber nicht mit $Z'_\alpha$, denn es ist

$$S'_2 Z'_\alpha = Z'_{-\alpha} S'_2. \tag{6.3}$$

Aus dieser Gleichung folgt

$$S'_2 J'_3 = -J'_3 S'_2 \tag{6.4}$$

und daraus die Vertauschbarkeit von $S'_2$ mit $J'^2_3$. Es ist also auch möglich, Zustände mit scharfen Werten für $J'^2_3$, $S_0$, $S'_2$, $\mathscr{H}_1$ und $\Gamma''_{\pm 1} = 0$ anzugeben.

Zustände, die der Bedingung $\Gamma''_{\pm 1} = 0$ genügen, hängen in verwickelter Weise von den Lagekoordinaten ab. Wir werden daher die $[\Phi]^{wE_1}_\Omega$ durch Zustände approximieren, in denen sich die Nukleonen unabhängig voneinander bewegen und **N** angenähert mit der $z'$-Achse zusammenfällt. Zunächst ermitteln wir die Symmetrieeigenschaften des exakten Orthonormalsystems.

Die Vertauschbarkeit von $\mathscr{H}_1$ und $S'_2$ hat, wie in der Theorie der zweiatomigen Moleküle [19]) gezeigt wird, die Existenz zweier Zustände mit entgegengesetzt gleichem $\Omega$ für gleiches $w$, $E_1$ zur Folge. Die Zustände transformieren sich bei $S'_2$ bis auf Zahlfaktoren ineinander, die so gewählt werden können, daß

$$S'_2 [\Phi]^{wE_1}_\Omega = [\Phi]^{wE_1}_{-\Omega}, \qquad \Omega > 0, \tag{6.5}$$

gilt. Daraus folgt die Umkehrung

$$S'_2 [\Phi]^{wE_1}_{-\Omega} = f[\Phi]^{wE_1}_\Omega, \qquad \Omega > 0, \tag{6.6}$$

wo $f$ ein Zahlfaktor vom Betrag 1 ist. Bei seiner Berechnung macht sich die Zweideutigkeit des Spins bemerkbar, denn nach (6.2) ist

$$S'_2 = S_0 U'_2 = U'_2 S_0, \tag{6.7}$$

und die Umklappung einer Spinfunktion um $+\pi$ hat das entgegengesetzte Vorzeichen wie die um $-\pi$. Wir unterscheiden daher zwischen Rechts- und Linksumklappungen $U'^+_2$ und $U'^-_2$ und nach (6.7) ebenso zwischen Rechts- und Linksspiegelungen $S'^+_2$ und $S'^-_2$. Verabredet man, daß (6.5) für $S'^+_2$ gilt, so folgt daraus durch Multiplikation mit $S'^-_2$

$$S'^-_2 S'^+_2 [\Phi]^{wE_1}_\Omega = [\Phi]^{wE_1}_\Omega = S'^-_2 [\Phi]^{wE_1}_{-\Omega}, \qquad \Omega > 0. \tag{6.8}$$

Bei Kernen mit ungerader Nukleonenzahl ändert sich das Vorzeichen, wenn man $S'^+_2$ durch $S'^-_2$ ersetzt und umgekehrt, bei Kernen mit gerader Nukleonenzahl nicht. Da $\Omega$ bei ersteren halbzahlig, bei letzteren ganzzahlig ist, gilt für alle Kerne

$$S'^\pm_2 [\Phi]^{wE_1}_\Omega = (-1)^{|\Omega| \mp \Omega} [\Phi]^{wE_1}_{-\Omega}, \qquad \Omega \neq 0. \tag{6.9}$$

Bei $\Omega = 0$ sind die Zustände $[\Phi]^{wE_1}_{0^+}$ und $[\Phi]^{wE_1}_{0^-}$ möglich, die durch

$$S'_2 [\Phi]^{wE_1}_{0^\pm} = \pm [\Phi]^{wE_1}_{0^\pm} \tag{6.10}$$

gekennzeichnet sind, wobei wegen der Geradzahligkeit der Nukleonenzahl

zwischen Rechts- und Linksspiegelungen nicht unterschieden zu werden braucht.

### 6.3. ORTHONORMALSYSTEM ZU $\mathscr{H}$

Da die Kreiseleigenfunktionen † $\mathscr{D}^J_{MK}$ ein vollständiges Orthonormalsystem für den Konfigurationsraum der Eulerschen Winkel bilden, bauen sich die Zustände des Kerns auf aus Gliedern $\mathscr{D}^J_{MK}[\Phi]^{wE_1}_{\Omega}$. Die Zustände müssen bei gegebenen Nukleonenlagen unabhängig von der Wahl des gestrichenen Systems sein. Unterwirft man dieses der Drehung $Z'_\alpha$, so bedeutet das Drehung der $\mathscr{D}^J_{MK}$ um $Z'_\alpha$ im festen und Drehung der $[\Phi]^{wE_1}_{\Omega}$ um $Z'_{-\alpha}$ im gestrichenen System, und $\mathscr{D}^J_{MK}[\Phi]^{wE_1}_{\Omega}$ geht über in

$$(Z'_\alpha \mathscr{D}^J_{MK})(Z'_{-\alpha}[\Phi]^{wE_1}_{\Omega}) = \mathrm{e}^{-i(K-\Omega)\alpha}\mathscr{D}^J_{MK}[\Phi]^{wE_1}_{\Omega}. \tag{6.11}$$

Die Unabhängigkeit von der Wahl des gestrichenen Systems verlangt $K = \Omega$. Diese Bedingung entspricht der für den Kreisel geltenden Gleichung (4.7). Unterwirft man $\Sigma'$ einer solchen Änderung, daß die dadurch in $\Sigma'$ bestimmte Raumtransformation $\mathscr{H}_1$ invariant läßt, so werden gewisse $[\Phi]^{wE_1}_{\Omega}$ ineinander transformiert, und die Unabhängigkeit der Zustände von $\Sigma'$ verlangt, daß alle durch eine derartige Transformation auseinander hervorgehenden $[\Phi]^{wE_1}_{\Omega}$ im Zustand des Kerns vorkommen. Eine derartige Transformation ist $U'_2$. Um $U'^{\pm}_2\mathscr{D}^J_{M\Omega}$ zu finden, bedenken wir, daß unter der Drehung $D\mathscr{D}^J_{M\Omega}$ der Funktion $\mathscr{D}^J_{M\Omega}$ folgendes verstanden wird: $D$ bedeute eine Drehung von $\Sigma'$ um eine bestimmte Achse um einen bestimmten Winkel, und $\Theta$, $\Phi$, $\Psi$ mögen dabei in $D\Theta$, $D\Phi$, $D\Psi$ übergehen. Dann soll $\mathscr{D}^J_{M\Omega}$ in eine Funktion $D\mathscr{D}^J_{M\Omega}$ übergehen, die durch

$$D\mathscr{D}^J_{M\Omega}(D\Theta, D\Phi, D\Psi) = \mathscr{D}^J_{M\Omega}(\Theta, \Phi, \Psi) \tag{6.12}$$

definiert wird. Also ist

$$D\mathscr{D}^J_{M\Omega}(\Theta, \Phi, \Psi) = \mathscr{D}^J_{M\Omega}(D^{-1}\Theta, D^{-1}\Phi, D^{-1}\Psi). \tag{6.13}$$

Angewandt auf $U'^{\pm}_2$, bedeutet das

$$U'^{\pm}_2\mathscr{D}^J_{M\Omega}(\Theta, \Phi, \Psi) = \mathscr{D}^J_{M\Omega}(U'^{\mp}_2\Theta, U'^{\mp}_2\Phi, U'^{\mp}_2\Psi). \tag{6.14}$$

Aus Fig. 7 in Anhang A ist zu ersehen, daß die Eulerschen Winkel des umgeklappten Systems

$$\Theta' = \pi - \Theta, \quad \Phi' = \Phi + \pi = \Phi - \pi, \quad \Psi' = \pi - \Psi = -\pi - \Psi \tag{6.15}$$

sind. Bei halbzahligem $J$ ist es nicht gleichgültig, welchen der beiden Werte für $\Phi'$ und $\Psi'$ man einsetzt. Um hier Klarheit zu erzielen, denken wir uns die Umklappung stetig ausgeführt. Dann ergibt sich

† Formeln für die Kreiseleigenfunktionen sind in Anhang C zusammengestellt.

$$\Theta < \frac{\pi}{2},\ 0 < \Psi < \pi: \qquad U_2'^{\pm}\Theta = \pi - \Theta,\quad U_2'^{\pm}\Theta = \Theta \pm \pi,\quad U_2'^{\pm}\Psi = \pi - \Psi;$$
$$\Theta > \frac{\pi}{2},\ \pi < \Psi < 2\pi: \tag{6.16}$$
$$\Theta < \frac{\pi}{2},\ \pi < \Psi < 2\pi: \qquad U_2'^{\pm}\Theta = \pi - \Theta,\quad U_2'^{\pm}\Phi = \Phi \pm \pi,\quad U_2'^{\pm}\Psi = -\pi - \Psi.$$
$$\Theta > \frac{\pi}{2},\ 0 < \Psi < \pi:$$

Die noch unerledigten Fälle $\Psi = 0, \pi$ und $\Theta = \pi/2$ lassen sich als Grenzfälle der betrachteten ansehen. Es ergeben sich dann verschiedene Werte, je nachdem, von welcher Seite man sich nähert. Einsetzen von (6.16) in (6.14) ergibt für alle Fälle, also auch für die erwähnten Grenzfälle,

$$U_2'^{\pm}\mathfrak{D}^J_{M\Omega} = (-1)^{J\pm\Omega}\mathfrak{D}^J_{M,-\Omega}. \tag{6.17}$$

Hieraus wird mit (6.7) und (6.9)

$$(U_2'^{\pm}\mathfrak{D}^J_{M\Omega})(U_2'^{\mp}[\Phi]^{wE_1}_{\Omega}) = w(-1)^{J+|\Omega|-2\Omega}\mathfrak{D}^J_{M,-\Omega}[\Phi]^{wE_1}_{-\Omega},\quad \Omega \neq 0, \tag{6.18}$$

und der Zustand

$$\Psi^{JwE_1}_{M\Omega} = \frac{1}{\sqrt{2}}\{\mathfrak{D}^J_{M\Omega}[\Phi]^{wE_1}_{\Omega} + w(-1)^{J-\Omega}\mathfrak{D}^J_{M,-\Omega}[\Phi]^{wE_1}_{-\Omega}\},\quad \Omega > 0, \tag{6.19}$$

geht bei einer Umklappung von $\Sigma'$ in sich über. Für $\Omega = 0$ ergibt sich aus (6.7), (6.10), (6.17), wobei zwischen $U_2'^{+}$ und $U_2'^{-}$ nicht unterschieden zu werden braucht,

$$(U'_2\mathfrak{D}^J_{M0})(U'_2[\Phi]^{wE_1}_{0^{\pm}}) = \pm w(-1)^J\mathfrak{D}^J_{M0}[\Phi]^{wE_1}_{0^{\pm}}, \tag{6.20}$$

und unveränderlich gegen Umklappungen von $\Sigma'$ ist

$$\Psi^{JwE_1}_{M0} = \mathfrak{D}^J_{M0}[\Phi]^{wE_1}_{0^{\pm}},\quad w(-1)^J = \pm 1. \tag{6.21}$$

Das Verhalten von $[\Phi]^{wE_1}_{0^{\pm}}$ gegen $S_0$ und $S'_2$ bestimmt hier die möglichen Gesamtdrehimpulse.

### 6.4. DIE NULLSTELLE IM NENNER VON $\Theta$

Angenommen, die Zustände $[\Phi]^{wE_1}_{\Omega}$ liegen vor. Die zur Berechnung von $\langle\mathscr{H}_{\mathfrak{a}}\rangle$ erforderlichen Matrixelemente der Komponenten von $\Theta$ lassen sich nur dann bilden, wenn die $[\Phi]^{wE_1}_{\Omega}$ bei Annäherung an die Nullstelle des Nenners von (5.7) hinreichend stark verschwinden. Das Gleiche gilt anscheinend für die Matrixelemente der Komponenten von $\mathbf{W}$ in $\langle\mathscr{H}_{1\mathfrak{a}}\rangle$. Ob die Zustände das erforderliche Verhalten zeigen, ist zweifelhaft. Die Aspektierung ist aber sinnlos, wenn sich nicht für alle drei Bestandteile $\langle\mathscr{H}_{\mathfrak{a}}\rangle$, $\langle\mathscr{H}_{1\mathfrak{a}}\rangle$, $\langle\mathscr{H}_{1}\rangle$ endliche Werte ergeben. Die Konfigurationen mit kleinem Nenner sind wegen der Bedeutung von $\Lambda$, solche, bei denen eine

kleine Verschiebung eines Nukleons genügt, um eine große Änderung von **N** und damit eine große kompensierende Drehung aller Nukleonen in $\Sigma'$ herbeizuführen. Wenn der Kern im Mittel stark deformiert ist, sind derartige Konfigurationen selten und können fortgelassen werden. Zu diesem Zweck haben wir die $[\Phi]$, die wegen der vorausgesetzten Seltenheit der Konfigurationen in der Umgebung der Nullstelle dort kleine Beträge haben, so abzuändern, daß sie bei Annäherung an diese Stelle hinreichend stark verschwinden. Die Matrixelemente der singularitätenfreien Operatoren ändern sich dann praktisch nicht, und die von $\Theta$ hängen praktisch nicht von der Art der Abänderung der $[\Phi]$ ab, denn in dem Integral

$$\int \Theta'_{kl}[\Phi]_1^*[\Phi]_2 \mathrm{d}\tau',$$

das sich über den Konfigurationsraum der durch $\Gamma'_{\pm 1}=0$ eingeschränkten Relativkoordinaten erstreckt, nimmt der Betrag des Integranden bei Annäherung an die Nullstelle von $\Gamma'^2_0 > |\Gamma'_2|^2$ aus zunächst ab wegen des Absinkens der Beträge der $[\Phi]$ infolge der Seltenheit der Konfigurationen und steigt dann wegen des sich durchsetzenden Einflusses des Nenners wieder an. Bei den abgeänderten $[\Phi]$ steigt der Betrag des Integranden nicht wieder an, sondern verschwindet bei Erreichen der Nullstelle. Wenn die Konfigurationen in der Umgebung der Nullstelle selten sind, setzt der Einfluß der Abänderung der $[\Phi]$ erst dort ein, wo der Betrag des Integranden schon klein und der Verlauf der Extrapolation auf Null daher unwesentlich ist.

Andererseits ist für einen im Mittel genügend stark deformierten Kern für die weitaus häufigsten Konfigurationen $|\Gamma'_2|^2 \ll \Gamma'^0_0$, und man erhält dann für (5.7) bei Entwicklung bis zu Gliedern zweiter Ordnung in $\Gamma'_{\pm 2}/\Gamma'_0$

$$\Theta'_{pq} = \frac{4}{3M}\,\frac{\Gamma+\frac{1}{2}\Gamma'_0+2\,\dfrac{|\Gamma'_2|^2}{\Gamma'^2_0}\,(\Gamma+\frac{3}{2}\Gamma'_0)}{\Gamma'^2_0} \tag{6.22}$$

$$\left.\begin{matrix}\Theta'_{pp}\\ \Theta'_{qq}\end{matrix}\right\} = -\frac{8\sqrt{6}}{9M}\,\frac{\Gamma+\frac{5}{4}\Gamma'_0}{\Gamma'^2_0}\,\frac{\Gamma'_{\mp 2}}{\Gamma'_0}.$$

Bei einem gegebenen Zustand $[\Phi]_D^{wE_1}$ mit dem Erwartungswert $\langle\Gamma'_0\rangle$ ist dann ebenso für die weitaus häufigsten Konfigurationen

$$\frac{\Gamma'^2_0-\langle\Gamma'_0\rangle^2}{\langle\Gamma'_0\rangle^2} \ll 1, \quad \frac{|\Gamma'_2|^2}{\langle\Gamma'_0\rangle^2} \ll 1$$

und daher bei entsprechender Entwicklung von (6.22)

$$\Theta'_{pq} = \frac{4}{3M\langle\Gamma'_0\rangle^2}\left\{\Gamma+\tfrac{1}{2}\Gamma'_0-\frac{\Gamma'^2_0-\langle\Gamma'_0\rangle^2}{\langle\Gamma'_0\rangle^2}\,(\Gamma+\tfrac{1}{2}\Gamma'_0)+2\,\frac{|\Gamma'_2|^2}{\langle\Gamma'_0\rangle^2}\,(\Gamma+\tfrac{3}{2}\Gamma'_0)\right\}, \tag{6.23}$$

und der damit gebildete Erwartungswert $\langle\Theta'_{pq}\rangle$ wird auch dann endlich,

wenn die $[\Phi]$ nicht abgeändert sind. Formt man alle zu bildenden Matrixelemente der Komponenten von $\Theta$ und die anderer Operatoren, bei denen die gleichen Schwierigkeiten auftreten, in entsprechender Weise um, so brauchen die $[\Phi]$ nicht abgeändert zu werden. Damit ergibt sich folgendes: Die Aspektierung ist, streng genommen, nur anwendbar, wenn $\langle \mathscr{H}_a \rangle$, $\langle \mathscr{H}_{1a} \rangle$, $\langle \mathscr{H}_1 \rangle$ endlich sind. Aber auch wenn das nicht zutrifft, läßt sich die Anwendbarkeit der Aspektierung erzielen durch Verzicht auf gewisse als selten vorausgesetzte Konfigurationen oder durch Verzicht auf deren strenge Erfassung, wobei die Stelle, an welcher der Verzicht beginnt, nicht wesentlich ist.

## 7. Approximative Basisfunktionen

### 7.1. FESTSETZUNGEN

Wir untersuchen jetzt die Folgen, die eintreten, wenn die $[\Phi]$ in den Basisfunktionen ersetzt werden durch Zustände $\Phi$, die voneinander unabhängige Bewegungen der Nukleonen beschreiben und die Bedingung $\Gamma''_{\pm 1} = 0$ angenähert erfüllen. Man erhält die $\Phi$ durch Deformation in Richtung der $z'$-Achse der auf das gestrichenen System bezogenen Slaterdeterminanten des Hamiltonoperators mit Kugelpotential. Wir setzen voraus, daß die Deformation invariant gegen $Z'_z$, $S_0$, $S'_z$ ist. Die deformierten Slaterdeterminanten haben dann scharfe Quantenzahlen $\Omega$, $w$ und befolgen nach entsprechender Normierung die Bedingungen (6.9) oder (6.10). Wir bezeichnen sie mit $\Phi^{wr}_{\Omega}$, wo $r$ ein Ordnungsindex für die Zustände mit gleichem $\Omega$, $w$ ist. An die Stelle der exakten Basisfunktionen (6.19) und (6.21) treten jetzt die approximativen Basisfunktionen

$$\Psi^{Jwr}_{M\Omega} = \frac{1}{\sqrt{2}} \{ \mathscr{D}^J_{M\Omega} \Phi^{wr}_{\Omega} + w(-1)^{J-\Omega} \mathscr{D}^J_{M,-\Omega} \Phi^{wr}_{-\Omega} \}, \tag{7.1}$$

$$\Psi^{Jwr}_{M0} = \mathscr{D}^J_{M0} \Phi^{wr}_{0\pm}, \quad w(-1)^J = \pm 1. \tag{7.2}$$

### 7.2. VERMEIDUNG DES AUFSTELLENS FALSCHER ZUSTÄNDE

Die $\Phi$ können als Überlagerungen von Zuständen $[\Phi]$ mit verschiedenem $\mathbf{N}$ angesehen werden, wobei die Verteilungsfunktion von $\mathbf{N}$ für die $z'$-Achse ein Maximum hat und mit wachsendem Winkelabstand von der $z'$-Achse umso steiler auf kleine Werte abfällt, je stärker die Deformation ist. Sie beschreiben mit der Nukleonenbewegung auch eine Bewegung von $\mathbf{N}$, enthalten mehr Freiheitsgrade als die $[\Phi]$ und bilden folglich eine größere Mannigfaltigkeit. Der Gefahr, falsche Zustände aufzustellen, kann man in folgender Weise begegnen. Angenommen, der Grundzustand sei bekannt; er habe die Quantenzahlen $J$, $w$. Die angeregten Zustände mit dem gleichen $J$, $w$ müssen zum Grundzustand und zueinander orthogonal sein. Da die $\Phi$

mit der Nukleonenbewegung auch eine Bewegung von **N** beschreiben, lassen sich Linearkombinationen der $\Phi$ bilden, die sich voneinander nur in der Bewegung von **N** unterscheiden, bei denen aber die Bewegung der Nukleonen relativ zu **N** die gleiche ist. Derartige Zustände sind als identisch zu betrachten, da sie nur verschiedene Approximationen des gleichen exakten Sachverhaltes sind. Es lassen sich nur Zustände mit der gleichen Bewegung von **N** miteinander vergleichen. Die Orthogonalität zwischen Grundzustand und angeregten Zuständen vom gleichen $J$, $w$ und die der letztgenannten Zustände untereinander darf nur von der Bewegung der Nukleonen relativ zu **N** herrühren. Das Gleiche gilt anscheinend für die Zustände mit anderen $J$, $w$ als beim Grundzustand: Beim Aufstellen des energetisch tiefsten Zustandes für gegebenes $J$, $w$ braucht man die Bewegung von **N** nicht zu beachten, die höheren Zustände vom gleichen $J$, $w$ müssen aber so konstruiert werden, daß die Orthogonalität nur von der Bewegung der Nukleonen relativ zu **N** herrührt.

Wie die verschärfte Orthogonalitätsbedingung zu formulieren ist, soll hier nicht überlegt werden, da wir uns nur dem Grundzustand widmen wollen. Hat dieser die einfachste Gestalt, indem er im wesentlichen aus einer einzigen approximativen Basisfunktion besteht, so wird die verschärfte Orthogonalitätsbedingung das Auftreten mehrerer approximativer Basisfunktionen in den angeregten Zuständen zur Folge haben, so daß deren Aufbau mit steigender Energie immer weniger einfach wird; die zu hohe Mannigfaltigkeit des Systems der approximativen Basisfunktionen ist nicht einfach durch Streichen bestimmter Funktionen zu beheben. Die Zahl der praktisch berechenbaren angeregten Zustände ist daher begrenzt.

### 7.3. SYSTEMKORREKTUR

Die oben berechneten Komponenten von $\Theta$, **W**, $G$ gelten nur unter der Voraussetzung, daß **N** mit der $z'$-Achse zusammenfällt. Um sie im Bezugssystem der $\Phi^{wr}_{\Omega}$ zu erhalten, das wir weiterhin mit $\Sigma'$ bezeichnen wollen und dessen Eulersche Winkel $\Theta$, $\Phi$, $\Psi$ seien, führen wir das Koordinatensystem $\Sigma^0$ ein, dessen dritte Achse mit **N** zusammenfällt. Die Eulerschen Winkel von $\Sigma'$ gegen $\Sigma^0$ seien $\vartheta^\circ$, $\varphi^\circ$, $\psi^\circ$, die von $\Sigma^0$ gegen $\Sigma'$ $\vartheta'$, $\varphi'$, $\psi'$. Dann ist nach (A6) $\vartheta' = \vartheta^\circ$, $\varphi' = \pi - \psi^\circ$, $\psi' = \pi - \varphi^\circ$. Zunächst rechnen wir die Komponenten von $\Theta$, **W**, $G$ nach den Transformationsformeln (A9) und (A10) für Vektoren und Tensoren von $\Sigma^0$ auf $\Sigma'$ um und erhalten sie als Funktionen der $\Gamma_m^0$ und von $\vartheta'$, $\varphi'$, $\psi'$. Die Transformationsformeln (B20) und (B23) für die Kugelflächenfunktionen liefern die $\Gamma_m^0$ als Funktionen der $\Gamma''_m$ und von $\vartheta'$, $\varphi'$, $\psi'$. Da sich $\vartheta'$, $\varphi'$, $\psi'$ ebenfalls durch die $\Gamma''_m$ ausdrücken lassen, ergeben sich so die Komponenten von $\Theta$, **W**, $G$ als Funktionen der $\Gamma''_m$. Wir nehmen $\Gamma''_{\pm 1}/\Gamma''_0$, $\Gamma''_{\pm 2}/\Gamma''_0$, $\vartheta'$ als klein an und entwickeln bis zu Größen zweiter Ordnung. Für das willkürlich wählbare $\psi'$ setzen wir $\psi' = -\varphi'$

fest. Mit (5.7) und (5.8) ergibt sich dann

$$\begin{aligned}
\Theta'_{pq} &= \frac{4}{3M\Gamma'^2_0}\left\{\Gamma+\tfrac{1}{2}\Gamma'_0+2\frac{|\Gamma'_2|^2}{\Gamma'^2_0}(\Gamma+\tfrac{3}{2}\Gamma'_0)-\tfrac{7}{3}\frac{|\Gamma'_1|^2}{\Gamma'^2_0}(\Gamma+\tfrac{3}{7}\Gamma'_0)\right\}\\
\left.\begin{matrix}\Theta'_{pp}\\ \Theta'_{qq}\end{matrix}\right\} &= -\frac{8\sqrt{6}}{9M\Gamma'^2_0}\left\{(\Gamma+\tfrac{5}{4}\Gamma'_0)\frac{\Gamma'_{\mp 2}}{\Gamma'_0}+\frac{1}{\sqrt{24}}(\Gamma+\tfrac{1}{2}\Gamma'_0)\frac{\Gamma'^2_{\mp 1}}{\Gamma'^2_0}\right\}\\
\left.\begin{matrix}\Theta'_{p3}\\ \Theta'_{q3}\end{matrix}\right\} &= \pm\frac{2\sqrt{6}}{9M\Gamma'^2_0}\left\{(\Gamma+\tfrac{1}{2}\Gamma'_0)\frac{\Gamma'_{\mp 1}}{\Gamma'_0}+\sqrt{\tfrac{2}{3}}(\Gamma+2\Gamma'_0)\frac{\Gamma'_{\pm 1}}{\Gamma'_0}\frac{\Gamma'_{\mp 2}}{\Gamma'_0}\right\}\\
\Theta'_{33} &= \frac{4}{9M\Gamma'^2_0}(\Gamma+\tfrac{1}{2}\Gamma'_0)\frac{|\Gamma'_1|^2}{\Gamma'^2_0},
\end{aligned} \tag{7.3}$$

$$\begin{aligned}
W'_{Tp} = \frac{i}{M}\Big\{\Big[&\Pi'_{p3}\left(1+\frac{2}{3}\frac{|\Gamma'_2|^2}{\Gamma'^2_0}-\frac{4}{3}\frac{|\Gamma'_1|^2}{\Gamma'^2_0}\right)+\Pi_{q3}\left(\sqrt{\frac{2}{3}}\frac{\Gamma'_{-2}}{\Gamma'_0}+\frac{1}{3}\frac{\Gamma'^2_{-1}}{\Gamma'^2_0}\right)\\
&+(\Pi'_{33}-\tfrac{1}{2}\Pi'_{pq})\left(\sqrt{\frac{2}{3}}\frac{\Gamma'_{-1}}{\Gamma'_0}-\frac{4}{3}\frac{\Gamma'_{-2}}{\Gamma'_0}\frac{\Gamma'_{+1}}{\Gamma'_0}\right)\\
&+\Pi'_{pp}\left(\frac{1}{\sqrt{6}}\frac{\Gamma'_{+1}}{\Gamma'_0}-\frac{1}{3}\frac{\Gamma'_{+2}}{\Gamma'_0}\frac{\Gamma'_{-1}}{\Gamma'_0}\right)-\tfrac{1}{3}\Pi'_{qq}\frac{\Gamma'_{-2}}{\Gamma'_0}\frac{\Gamma'_{-1}}{\Gamma'_0}\Big]\frac{1}{\Gamma'_0}\\
&+\frac{1}{\Gamma'_0}\Big[\left(1+\frac{2}{3}\frac{|\Gamma'_2|^2}{\Gamma'^2_0}-\frac{4}{3}\frac{|\Gamma'_1|^2}{\Gamma'^2_0}\right)\Pi'_{p3}+\left(\sqrt{\frac{2}{3}}\frac{\Gamma'_{-2}}{\Gamma'_0}+\frac{1}{3}\frac{\Gamma'^2_{-1}}{\Gamma'^2_0}\right)\Pi'_{q3}\\
&+\left(\sqrt{\frac{2}{3}}\frac{\Gamma'_{-1}}{\Gamma'_0}-\frac{4}{3}\frac{\Gamma'_{-2}}{\Gamma'_0}\frac{\Gamma'_{+1}}{\Gamma'_0}\right)(\Pi'_{33}-\tfrac{1}{2}\Pi'_{pq})\\
&+\left(\frac{1}{\sqrt{6}}\frac{\Gamma'_{+1}}{\Gamma'_0}-\frac{1}{3}\frac{\Gamma'_{+2}}{\Gamma'_0}\frac{\Gamma'_{-1}}{\Gamma'_0}\right)-\frac{1}{3}\frac{\Gamma'_{-2}}{\Gamma'_0}\frac{\Gamma'_{-1}}{\Gamma'_0}\Pi'_{qq}\Big]\Big\}.
\end{aligned} \tag{7.4}$$

Daraus $W'_{Tq}$ durch Ändern des Vorzeichens, Vertauschen von $p$ mit $q$ und von $\Gamma'_{+1}$ mit $-\Gamma'_{-1}$.

$$\begin{aligned}
W'_{T3} = \frac{i}{2M}\Big\{&\Big[\sqrt{\frac{2}{3}}\left(\Pi'_{p3}\frac{\Gamma'_{+1}}{\Gamma'_0}+\Pi'_{q3}\frac{\Gamma'_{-1}}{\Gamma'_0}\right)+\frac{1}{3}\left(\Pi'_{pp}\frac{\Gamma'^2_{-1}}{\Gamma'^2_0}+\Pi'_{qq}\frac{\Gamma'^2_{+1}}{\Gamma'^2_0}\right)\Big]\frac{1}{\Gamma'_0}\\
&+\frac{1}{\Gamma'_0}\Big[\sqrt{\frac{2}{3}}\left(\frac{\Gamma'_{+1}}{\Gamma'_0}\Pi'_{p3}+\frac{\Gamma'_{-1}}{\Gamma'_0}\Pi'_{q3}\right)+\frac{1}{3}\left(\frac{\Gamma'^2_{-1}}{\Gamma'^2_0}\Pi'_{pp}+\frac{\Gamma'^2_{+1}}{\Gamma'^2_0}\Pi'_{qq}\right)\Big]\Big\}.
\end{aligned}$$

Da sich nach (4.17) und (4.18) $\mathbf{W}_S$ aus $\mathbf{W}_T$ mittels Ersatz von $\mathbf{p}_\nu$ durch $-(\lambda/Mc^2)\mathbf{s}_\nu\times\operatorname{grad}_\nu V_\nu$ ergibt, sind auch die Komponenten von $\mathbf{W}_S$ in $\Sigma'$ bekannt. Beim gyromagnetischen Tensor ist zu beachten, daß die $\Gamma_m^{P'}$ wegen $\Gamma_{\pm 1}^{P0}\neq 0$ nicht in der gleichen Weise von den $\Gamma_m^{P0}$ abhängen wie die $\Gamma'_m$ von den $\Gamma_m^0$. Dieser Unterschied wirkt sich aber erst in den Gliedern zweiter Ordnung aus. Der Einfachheit halber entwickeln wir nur bis zu Gliedern

erster Ordnung und erhalten

$$
\begin{aligned}
G'_{pq} &= G'_{qp} = 2\frac{\Gamma_0^{P'}}{\Gamma'_0} \\
\left.\begin{matrix} G'_{pp} \\ G'_{qq} \end{matrix}\right\} &= \sqrt{\frac{2}{3}}\,\frac{\Gamma_{\mp 2}^{P'}}{\Gamma'_0} \\
\left.\begin{matrix} G'_{p3} \\ G'_{q3} \end{matrix}\right\} &= \pm\sqrt{\frac{2}{3}}\,\frac{\Gamma'_{\mp 1}}{\Gamma'_0}\,\frac{\Gamma_0^{P'}}{\Gamma'_0} \\
&= \pm\sqrt{\frac{2}{3}}\left(\frac{\Gamma'_{\mp 1}}{\Gamma'_0}\,\frac{\Gamma_0^{P'}}{\Gamma'_0} - \frac{\Gamma_{\mp 1}^{P'}}{\Gamma'_0}\right) \\
G'_{33} &= 0.
\end{aligned}
\tag{7.5}
$$

### 7.4. KLASSIFIKATION DER ZUSTÄNDE

Die Zustände des Hamiltonoperators mit Kugelpotential bilden ein vollständiges Orthonormalsystem. Jeder Zustand des Hamiltonoperators im Einachsenaspekt, dargestellt durch eine Linearkombination von approximativen Basisfunktionen, muß sich daher einem Zustand des Hamiltonoperators mit Kugelpotential zuordnen lassen. Damit entsteht die Möglichkeit, sich beim Aufstellen von Zuständen des aspektierten Hamiltonoperators von denen des einfachen Schalenmodells leiten zu lassen. Hierfür soll eine Regel aufgestellt werden.

Der Kern wird durch die ausgezeichneten Nukleonenzahlen folgendermaßen in Schalen eingeteilt:

1. Schale: $s_{\frac{1}{2}}$;
2. „ : $p_{\frac{3}{2}}$, $p_{\frac{1}{2}}$;
3. „ : $d_{\frac{5}{2}}$, $d_{\frac{3}{2}}$, $s_{\frac{1}{2}}$;
4. „ : $f_{\frac{7}{2}}$;
5. „ : $f_{\frac{5}{2}}$, $p_{\frac{3}{2}}$, $p_{\frac{1}{2}}$, $g_{\frac{9}{2}}$;
6. „ : $g_{\frac{7}{2}}$, $d_{\frac{5}{2}}$, $d_{\frac{3}{2}}$, $s_{\frac{1}{2}}$, $h_{\frac{11}{2}}$;
7. „ : $h_{\frac{9}{2}}$, $f_{\frac{7}{2}}$, $f_{\frac{5}{2}}$, $p_{\frac{3}{2}}$, $p_{\frac{1}{2}}$, $i_{\frac{13}{2}}$.

Die Gesamtheit der zu einem spektroskopischen Symbol gehörigen Zustände nennen wir Unterschale und bezeichnen sie durch das spektroskopische Symbol mit vorangesetzter Schalennummer; falls notwendig, schreiben wir das Zeichen der Nukleonensorte davor, Beispiel $N3d_{\frac{5}{2}}$. Einen bestimmten Zustand der Unterschale kennzeichnen wir durch Anfügen seines $|m|$ und dessen Vorzeichen an das Zeichen der Unterschale, Beispiel $P4f_{\frac{7}{2}}\frac{5}{2}+$. Bei gegebener Besetzung der Unterschalen sind im allgemeinen verschiedene $J$ möglich, und ein bestimmtes $J$ kann mehrmals vorkommen. Wir nennen die

TABELLE 1

Die bei Berücksichtigung des Ausschließungsprinzips möglichen Gesamtdrehimpulse der Teilchen einer Unterschale

| $j$ | $z_j$ | $J_j$ |
|---|---|---|
| $\frac{1}{2}$ | 1 | $\frac{1}{2}$ |
| | 2 | 0 |
| $\frac{3}{2}$ | 1, 3 | $\frac{3}{2}$ |
| | 2 | 2, 0 |
| | 4 | 0 |
| $\frac{5}{2}$ | 1, 5 | $\frac{5}{2}$ |
| | 2, 4 | 4, 2, 0 |
| | 3 | $\frac{9}{2}$, $\frac{5}{2}$, $\frac{3}{2}$ |
| | 6 | 0 |
| $\frac{7}{2}$ | 1, 7 | $\frac{7}{2}$ |
| | 2, 6 | 6, 4, 2, 0 |
| | 3, 5 | $\frac{15}{2}$, $\frac{11}{2}$, $\frac{9}{2}$, $\frac{7}{2}$, $\frac{5}{2}$, $\frac{3}{2}$ |
| | 4 | 8, 6, 5, $4^2$, $2^2$, 0 |
| | 8 | 0 |
| $\frac{9}{2}$ | 1, 9 | $\frac{9}{2}$ |
| | 2, 8 | 8, 6, 4, 2, 0 |
| | 3, 7 | $\frac{21}{2}$, $\frac{17}{2}$, $\frac{15}{2}$, $\frac{13}{2}$, $\frac{11}{2}$, $\frac{9^2}{2}$, $\frac{7}{2}$, $\frac{5}{2}$, $\frac{3}{2}$ |
| | 4, 6 | 12, 10, 9, $8^2$, 7, $6^2$, 5, $4^2$, 3, $2^2$, $0^2$ |
| | 5 | $\frac{25}{2}$, $\frac{21}{2}$, $\frac{19}{2}$, $\frac{17^2}{2}$, $\frac{15^2}{2}$, $\frac{13^2}{2}$, $\frac{11^2}{2}$, $\frac{9^2}{2}$, $\frac{7^2}{2}$, $\frac{5^2}{2}$, $\frac{3}{2}$, $\frac{1}{2}$ |
| | 10 | 0 |
| $\frac{11}{2}$ | 1, 11 | $\frac{11}{2}$ |
| | 2, 10 | 10, 8, 6, 4, 2, 0 |
| | 3, 9 | $\frac{27}{2}$, $\frac{23}{2}$, $\frac{21}{2}$, $\frac{19}{2}$, $\frac{17}{2}$, $\frac{15^2}{2}$, $\frac{13}{2}$, $\frac{11^2}{2}$, $\frac{9^2}{2}$, $\frac{7}{2}$, $\frac{5}{2}$, $\frac{3}{2}$ |
| | 4, 8 | 16, 14, 13, $12^2$, 11, $10^3$, $9^2$, $8^4$, $7^2$, $6^4$, $5^2$, $4^4$, 3, $2^3$, $0^2$ |
| | 5, 7 | $\frac{35}{2}$, $\frac{31}{2}$, $\frac{29}{2}$, $\frac{27^2}{2}$, $\frac{25^2}{2}$, $\frac{23^3}{2}$, $\frac{21^3}{2}$, $\frac{19^4}{2}$, $\frac{17^4}{2}$, $\frac{15^5}{2}$, $\frac{13^4}{2}$, $\frac{11^5}{2}$, $\frac{9^4}{2}$, $\frac{7^4}{2}$, $\frac{5^2}{2}$, $\frac{3^4}{2}$ |
| | 6 | 18, 16, 15, $14^2$, $13^2$, $12^4$, $11^2$, $10^5$, $9^4$, $8^5$, $7^4$, $6^7$, $5^3$, $4^5$, $3^2$, $2^4$, 0 |
| | 12 | 0 |

$j$ Drehimpuls der Unterschale, $z_j$ Zahl der Teilchen in der Unterschale, $J_j$ Gesamtdrehimpuls der Unterschale. Hochgestellte Indices geben die Häufigkeit an. Der Index 1 ist fortgelassen.

Gesamtheit aller bei gegebener Besetzung möglichen $J$, jedes entsprechend oft gezählt, das Besetzungsmultiplett. Zur Ermittlung der möglichen $J$ dient Tab. 1, deren Aufstellung folgendermaßen vollzogen wurde: Alle mit dem Ausschließungsprinzip verträglichen Verteilungen der Nukleonen auf die Zustände der Unterschale wurden aufgesucht und die zugehörigen Drehimpulsquantenzahlen $M_j$ der $z$-Komponente notiert. Mit dem maximalen Wert $M_{j1}$ beginnend, wurden $2M_j+1$ durch $M_{j1}-k$, $0 \leqq k \leqq 2M_{j1}$, bestimmte $M_j$ gestrichen und $M_{j1}$ als mögliches $J_j$ angemerkt. Mit dem jetzt vorhandenen Maximalwert $M_{j2}$ wurde das Gleiche wiederholt und so bis zum Verbrauch aller fortgefahren. Bei dem Kern (21,24) befinden sich im Grundzustand ein Proton und vier Neutronen in $4f_{\frac{7}{2}}$. Für das Proton ist $J_{\frac{7}{2}} = \frac{7}{2}$, während für die vier Neutronen nach Tab. 1 die Werte $J_{\frac{7}{2}} = 8, 6, 5, 4^2, 2^2, 0$ möglich sind. Dann ist das Besetzungsmultiplett

$$J = \tfrac{23}{2},\ \tfrac{21}{2},\ \tfrac{19^2}{2},\ \tfrac{17^3}{2},\ \tfrac{15^5}{2},\ \tfrac{13^6}{2},\ \tfrac{11^7}{2},\ \tfrac{9^7}{2},\ \tfrac{7^6}{2},\ \tfrac{5^6}{2},\ \tfrac{3^5}{2},\ \tfrac{1^2}{2}.$$

Es hat die Vielfachheit 50. Das Beispiel zeigt, daß die Zahl der möglichen $J$ im allgemeinen groß ist.

Beim Aufstellen der Zustände kann man dann wie folgt verfahren. Da jedem $J$ eines bestimmten Besetzungsmultipletts eine Linearkombination der $\Psi^{Jwr}_{M\Omega}$ entspricht, nimmt man in die Linearkombination des zu bildenden Zustandes zunächst nur solche $\Psi^{Jwr}_{M\Omega}$ auf, deren $\Phi^{wr}_{\Omega}$ durch den erwähnten Deformationsprozeß aus den Slaterdeterminanten des zugehörigen Besetzungsmultipletts hervorgehen; falls notwendig, fügt man dann noch Zustände $\Psi^{Jwr}_{M\Omega}$ aus anderen Besetzungsmultipletts hinzu. Auf die Erfüllung der verschärften Orthogonalitätsbedingung ist dabei zu achten.

### 7.5. ZUSAMMENFASSUNG

Von den approximativen Basisfunktionen ausgehend, läßt sich das Erreichte folgendermaßen zusammenfassen. Wegen des einfachen Aufbaus der approximativen Basisfunktionen ist es wünschenswert, sie zur Beschreibung eines sich kreiselartig verhaltenden Kerns zu verwenden. Das ist zunächst nicht möglich, da sie drei überzählige Freiheitsgrade enthalten. Das Hindernis läßt sich aber beseitigen, indem man den Größen $\Gamma''_{\pm 1}$ oder, was dasselbe bedeutet, dem durch $\Gamma''_{\pm 1}$ im Verein mit $\Gamma''_0$ und $\Gamma''_{\pm 2}$ relativ zu $\Sigma'$ festgelegten $\mathbf{N}$ die Eigenschaft dynamischer Variabler abspricht und $\mathbf{N}$ zu einem Unschärfeparameter in $\Sigma'$ erklärt. Die $\Phi^{wr}_{\Omega}$ lassen sich dann ansehen als Annäherung an einen Idealfall, bei dem $\mathbf{N}$ mit der $z'$-Achse zusammenfällt. So entsteht Raum zur Einführung zweier weiterer unabhängiger Variabler. Zur Durchführung dieser Auffassung mußten wir alle Operatoren zerlegen; auf die $\Phi^{wr}_{\Omega}$ dürfen nur mit $\mathbf{N}$ vertauschbare Operatoren wirken. Als mit $\mathbf{N}$ vertauschbaren Teil von $\mathscr{H}$ fanden wir den inneren Hamiltonoperator $\mathscr{H}_1$, den Rest $\mathscr{H}-\mathscr{H}_1$ teilten wir in den Rotationsoperator $\mathscr{H}_a$

und den Rotationsaustauschoperator $\mathscr{H}_{1a}$ auf und stellten fest, daß die durch $\mathscr{H}_a+\mathscr{H}_{1a}$ geregelte Bewegung von $\Sigma'$ der Taumelbedingung genügt. Es gibt daher $3A+1$ unabhängige Lagekoordinaten, aber nur $3A$ unabhängige Differentiale. Nicht beseitigen läßt sich die zu hohe Mannigfaltigkeit des Systems der approximativen Basisfunktionen, mit Hilfe der verschärften Orthogonalitätsbedingung läßt sich jedoch die Aufstellung falscher Zustände vermeiden.

## 8. Matrixelemente

### 8.1. SYMMETRIEBEZIEHUNGEN

Die Berechnung von Kernzuständen erfordert Bildung der Matrixelemente von $\mathscr{H}$ und der Momentoperatoren mit den approximativen Basisfunktionen (7.1) und (7.2). Hierfür stellen wir einige Symmetriebeziehungen bereit, die es gestatten, Glieder in den Matrixelementen auf andere zurückzuführen. Die Symmetriebeziehungen (6.9) und (6.10) müssen auch für die $\Phi^{wr}_{\Omega}$ gelten. Ist $O_i$ irgendein Operator, der nicht auf die Eulerschen Winkel wirkt — notwendig und hinreichend hierfür ist seine Vertauschbarkeit mit $\mathbf{N}$ —, so folgt wegen der Unitarität von $S'^{\pm}_2$

$$(\Phi^{wr}_{\Omega}, O_i\Phi^{w'r'}_{\Omega'}) = (S'^{\pm}_2\Phi^{wr}_{\Omega}, S'^{\pm}_2 O_i S'^{\mp}_2 S'^{\pm}_2\Phi^{\Omega'}_{w'r'})$$
$$= (-1)^{|\Omega|\mp\Omega+|\Omega'|\mp\Omega'}(\Phi^{wr}_{-\Omega}, S'^{\pm}_2 O_i S'^{\mp}_2\Phi^{w'r'}_{-\Omega'}); \quad \Omega, \Omega' \neq 0; \quad (8.1)$$

und ebenso

$$(\Phi^{wr}_{\Omega}, O_i\Phi^{w'r'}_{0\pm}) = \pm(-1)^{|\Omega|\mp\Omega}(\Phi^{wr}_{-\Omega}, S'^{\pm}_2 O_i S'^{\mp}_2\Phi^{w'r'}_{0\pm}), \quad (8.2)$$

$$(\Phi^{wr}_{0\pm}, O_i\Phi^{w'r'}_{0\pm}) = (\Phi^{wr}_{0\pm}, S'^{\pm}_2 O_i S'^{\mp}_2\Phi^{w'r'}_{0\pm}). \quad (8.3)$$

Für irgendeinen nur auf die Eulerschen Winkel wirkenden Operator $O_a$ ergibt sich mit (6.17) wegen der Unitarität von $U'^{\pm}_2$

$$(\mathscr{D}^J_{M\Omega}, O_a\mathscr{D}^J_{M\Omega'}) = (U'^{\pm}_2\mathscr{D}^J_{M\Omega}, U'^{\pm}_2 O_a U'^{\mp}_2 U'^{\pm}_2\mathscr{D}^J_{M\Omega'})$$
$$= (-1)^{2J\pm\Omega\pm\Omega'}(\mathscr{D}^J_{M,-\Omega}, U'^{\pm}_2 O_a U'^{\mp}_2\mathscr{D}^J_{M,-\Omega}). \quad (8.4)$$

### 8.2. ZWANGSOPERATOR UND URSPRUNGSOPERATOR

Das Glied $\mathbf{W}\cdot\mathbf{J}-\frac{1}{2}\Theta\cdot\cdot\mathbf{J}^2$ führt den ursprünglichen Hamiltonoperator, der mit der Nukleonenbewegung zugleich eine Bewegung von $\mathbf{N}$ beschreibt, in den Operator $\mathscr{H}_1$ über, der ein gegebenes $\mathbf{N}$ für alle Zeiten konstant läßt. Daher ist $-\mathbf{W}\cdot\mathbf{J}+\frac{1}{2}\Theta\cdot\cdot\mathbf{J}^2$ der Operator der mit der Bewegung von $\mathbf{N}$ verbundenen Energie, oder, wie man auch sagen kann,

$$\mathscr{H}_z = \mathbf{W}\cdot\mathbf{J}-\tfrac{1}{2}\Theta\cdot\cdot\mathbf{J}^2 \quad (8.5)$$

ist der Operator der Energie, die zur Unterdrückung der Bewegung von $\mathbf{N}$ erforderlich ist. Wir bezeichnen ihn als Zwangsoperator und das mit irgendeinem $\Psi^{Jwr}_{M\Omega}$ oder einer Überlagerung derartiger Zustände gebildete $E_z =$

$\langle \mathcal{H}_2 \rangle$ als Zwangsenergie. $\mathcal{H}_1 - \mathcal{H}_2$ nennen wir Ursprungsoperator und das wie $\langle \mathcal{H}_2 \rangle$ zu bildende $\langle \mathcal{H}_1 - \mathcal{H}_2 \rangle$ Ursprungsenergie. Die Aufteilung von $\mathcal{H}_1$ in $\mathcal{H}_1 - \mathcal{H}_2$ und $\mathcal{H}_2$ setzt als notwendig voraus, daß $\mathcal{H}_1$ auf einen Zustand mit kontinuierlicher Verteilung von **N** angewandt wird, denn die in $\mathcal{H}_1 - \mathcal{H}_2$ und $\mathcal{H}_2$ enthaltenen infinitesimalen Verschiebungen der Nukleonen sind Grenzübergänge aus kleinen Verschiebungen, bei denen **N** nicht konstant bleibt, und eine von den Nukleonenkoordinaten abhängige Zustandsfunktion $[\Phi]$ ändert sich bei jeder noch so kleinen Nukleonenverschiebung, die zugleich **N** ändert, unstetig auf den Wert Null, die Ausdrücke $(\mathcal{H}_1 - \mathcal{H}_2)[\Phi]$ und $\mathcal{H}_2[\Phi]$ existieren daher nicht. Bei einem Zustand $\Phi$ mit kontinuierlicher Verteilung von **N** können $(\mathcal{H}_1 - \mathcal{H}_2)\Phi$, $\mathcal{H}_2\Phi$ und damit $(\Phi, [\mathcal{H}_1 - \mathcal{H}_2]\Phi)$, $(\Phi, \mathcal{H}_2\Phi)$ existieren, doch wachsen die letzten beiden Ausdrücke über alle Grenzen, wenn die Unschärfe immer kleiner wird. Bildet man jedoch erst $(\Phi, \mathcal{H}_1\Phi)$ und geht dann zur Grenze verschwindender Unschärfe von **N** über, so bleibt dieser Ausdruck endlich, weil $\mathcal{H}_2$ die divergenzerzeugenden Terme im Ursprungsoperator abzieht, denn $\mathcal{H}_1$ enthält die Impulse nur in Form der $\mathbf{p}_{\nu 1}$, die infinitesimalen Verschiebungen erfolgen bei festem **N**, so daß dessen Unschärfegrad keine Rolle spielt.

Der Zwangsoperator ist maßgebend für die Symmetrie von $\mathcal{H}_1$, denn er ist nur invariant gegen Drehungen um die $z'$-Achse, während der Ursprungsoperator invariant gegen beliebige Drehungen ist. Die Darstellung der Nukleonenzustände in $\Sigma'$ durch Zustände, die nur eine scharfe Komponente des Gesamtdrehimpulses in $z'$-Richtung, aber keinen scharfen Gesamtdrehimpuls selbst haben, wird daher erst durch die Anwesenheit von $\mathcal{H}_2$ wohlbegründet.

Die Zwangsenergie ist charakteristisch für die Deutung von **N** als Unschärfeparameter in $\Sigma'$, zu der wir wegen des Vorhandenseins überzähliger Freiheitsgrade veranlaßt wurden. Bei Systemen, die sich ebenfalls kreiselartig verhalten, aber frei von überzähligen Freiheitsgraden sind, wie zum Beispiel zweiatomige Moleküle, tritt eine Zwangsenergie nicht auf.

### 8.3. MITTELENERGIE UND SCHWANKUNGSENERGIE

Von den mit irgendeinem $\Psi^{Jwr}_{M\Omega}$ oder einer Linearkombination dieser Zustände gebildeten $\langle \gamma'_m \rangle$ verschwinden die mit $m = \pm 1, \pm 2$. Zerlegt man $V_\nu$ in den Anteil

$$\bar{V}_\nu = V_0(r_\nu) - \zeta V_1(r_\nu)\langle \gamma'_0 \rangle Y_0(\vartheta'_\nu, \varphi'_\nu) + \tfrac{1}{2}\zeta^2 V_2(r_\nu)\langle \gamma'_0 \rangle^2 \tag{8.6}$$

und den Rest $V_\nu - \bar{V}_\nu$, so entsteht eine Aufteilung der Ursprungsenergie in die Mittelenergie

$$E_{\mathrm{m}} = \left\langle \sum_\nu \left\{ \frac{1}{2M} |\mathbf{p}_\nu|^2 + \bar{V}_\nu + \frac{\lambda}{M^2 c^2} \mathbf{s}_\nu \cdot \mathbf{p}_\nu \times \mathrm{grad}_\nu \bar{V}_\nu \right\} \right\rangle \tag{8.7}$$

und die Schwankungsenergie

$$E_s = \left\langle \sum_\nu \left\{ V_\nu - \bar{V}_\nu + \frac{\lambda}{M^2c^2} \mathbf{s}_\nu \cdot \mathbf{p}_\nu \times \mathrm{grad}_\nu (V_\nu - \bar{V}_\nu) \right\} \right\rangle . \tag{8.8}$$

Für das homogem isochor deformierte Oszillatorpotential findet man auf die gleiche Weise, die zu (3.6) führte, bei Vernachlässigung des Spin-Bahn-Gliedes

$$E_s = -\tfrac{1}{2}\zeta(2-\zeta) M\omega^2 \langle \Gamma \sum_m (|\gamma'_m|^2 - \delta_{m0}\langle \gamma'_0 \rangle^2) \rangle . \tag{8.9}$$

Das Vorzeichen von $E_s$ ist also negativ. Wir zeigen, daß das auch für ein allgemeineres $V_\nu$ gilt, und schreiben dazu (8.8) nach (2.13) in der Form

$$E_s = -\zeta \Big\langle \sum_m \{\gamma'_m - \delta_{m0}\langle \gamma'_0 \rangle\} \{ \sum_\nu V_1(r_\nu) Y_m(\vartheta'_\nu, \varphi'_\nu) - \delta_{m0} \langle \sum_m V_1(r_\nu) Y_0(\vartheta'_\nu, \varphi'_\nu) \rangle \} \Big\rangle$$
$$+ \tfrac{1}{2}\zeta^2 \Big\langle \sum_\nu V_2(r_\nu) \sum_m (|\gamma'_m|^2 - \delta_{m0}\langle \gamma'_0 \rangle^2) \Big\rangle . \tag{8.10}$$

Die Größen $\sum_\nu V_1(r_\nu) Y_m(\vartheta'_\nu, \varphi'_\nu)$ und $\dot{\Gamma}''_m$ werden im wesentlichen einander proportional sein, denn sie unterscheiden sich nur in der Abhängigkeit von den $r_\nu$. Setzt man daher

$$\sum_\nu V_1(r_\nu) Y_m(\vartheta'_\nu, \varphi'_\nu) = C_1 \dot{\Gamma}''_m , \tag{8.11}$$

wo $C_1$ eine positive Konstante ist, so wird das erste Glied in (8.10)

$$\zeta C_1 \Big\langle \sum_m \{\gamma'_m - \delta_{m0}\langle \gamma'_0 \rangle\} \{ \dot{\Gamma}''_m - \delta_{m0}\langle \Gamma''_0 \rangle \} \Big\rangle$$
$$= -\zeta C_1 \Big\langle \sum_m \{\gamma'_m \dot{\Gamma}''_m - \delta_{m0}\langle \gamma'_0 \rangle \langle \Gamma''_0 \rangle \} \Big\rangle , \tag{8.12}$$

und darin kann man in guter Näherung setzen

$$\Big\langle \sum_m \{\gamma_m' \dot{\Gamma}''_m - \delta_{m0}\langle \gamma'_0 \rangle \langle \Gamma''_0 \rangle \} \Big\rangle = \langle \Gamma \rangle \Big\langle \sum_m \{|\gamma'_m|^2 - \delta_{m0}\langle \gamma'_0 \rangle^2\} \Big\rangle , \tag{8.13}$$

denn erstens wird bei den meisten Konfigurationen bei nicht zu kleiner Nukleonenzahl der Augenblickswert von $\Gamma$ nicht wesentlich von $\langle \Gamma \rangle$ abweichen, und zweitens sind keine starken Korrelationen zwischen dem in $\Gamma$ zum Ausdruck kommenden Kernvolumen und der Kernform zu erwarten. Entsprechend kann man im zweiten Glied von (8.10) schreiben

$$\Big\langle \sum_\nu V_2(r_\nu) \sum_m \{|\gamma'_m|^2 - \delta_{m0}\langle \gamma'_0 \rangle^2\} \Big\rangle = \Big\langle \sum_\nu V_2(r_\nu) \Big\rangle \Big\langle \sum_\nu \{|\gamma'_m|^2 - \delta_{m0}\langle \gamma'_0 \rangle^2\} \Big\rangle$$
$$= C_2 \Big\langle \sum_\nu \{|\gamma'_m|^2 - \delta_{m0}\langle \gamma'_0 \rangle^2\} \Big\rangle . \tag{8.14}$$

Mit (8.11) ... (8.14) wird dann aus (8.10)

$$E_s = -\{\zeta C_1 - \tfrac{1}{2}\zeta^2 C_2\} \Big\langle \sum_m \{|\gamma'_m|^2 - \delta_{m0}\langle \gamma'_0 \rangle^2\} \Big\rangle . \tag{8.15}$$

Behandelt man das durch (3.4) gegebene $\mathscr{H}'$ in der gleichen Weise, so ergibt

sich anstelle von (3.7) die ausführlichere Formel

$$\mathscr{H}'_{00} = -(\zeta C_1 - \tfrac{1}{2}\zeta^2 C_2)(\sum_m |\gamma'_m|^2)_{00}. \tag{8.16}$$

In der gleichen Weise, wie wir damals auf $\mathscr{H}'_{00} < 0$ für $\zeta \approx 1$ schlossen, finden wir hier $E_s < 0$ für $\zeta \approx 1$. Die Schwankungsenergie ist also die negative Energie einer gegen die Ruhelage $\langle \gamma'_0 \rangle$ verspannten Oberfläche. Ein kinetischer Anteil tritt in $E_s$ nicht auf; die mit den Schwankungen der Kernform verknüpfte kinetische Energie ist implizit in dem kinetischen Glied von $\mathscr{H}_1$ enthalten.

Es ist allerdings ungewiß, ob die Schwankungen der Kernform durch voneinander unabhängige Bewegungen der Nukleonen oder durch kollektive Schwingungen hervorgerufen werden. Zur Entscheidung dieser Frage müßte man, wie früher erwähnt wurde, einen Rotations-Schwingungsaspekt aufstellen, der erlaubt, außer den Eulerschen Winkeln noch $\gamma'_0$ und $\gamma'_{\pm 2}$ als unabhängige Variable einzuführen und in dem dann auch Deformationsimpulse auftreten. Die Existenz von kollektiven Schwingungen hängt davon ab, ob der Rotations-Schwingungsaspekt einen energetisch niedrigeren Grundzustand liefert als der Einachsenaspekt oder nicht. Diese Frage soll hier nicht untersucht werden, da wir uns im Rahmen des Einachsenaspektes halten wollen.

### 8.4. ROTATIONSOPERATOR

Nach (3.26) und (A5) ist

$$\begin{aligned}\mathscr{H}_s = {} & \tfrac{1}{8}\{\Theta'_{pq}(J'_pJ'_q+J'_qJ'_p)+\Theta'_{pp}J'^2_q+\Theta'_{qq}J'^2_p\} \\ & +\tfrac{1}{4}\{\Theta'_{p3}(J'_qJ'_3+J'_3J'_q)+\Theta'_{q3}(J'_pJ'_3+J'_3J'_p)\}+\tfrac{1}{2}\Theta'_{33}J'^2_3.\end{aligned} \tag{8.17}$$

Fiele **N** in die $z'$-Richtung, so wäre bei Symmetrie des Kreisels nur $\Theta'_{pq}$ von Null verschieden. Abweichungen von der Symmetrie ergeben nichtverschwindendes $\Theta'_{pp}$ und $\Theta'_{qq}$. Fällt **N** nicht mehr in die $z'$-Richtung, so werden auch $\Theta'_{p3}$, $\Theta'_{q3}$, $\Theta'_{33}$ von Null verschieden, und in $\Theta'_{pq}$, $\Theta'_{pp}$, $\Theta'_{qq}$ treten Zusatzglieder auf. Die nicht identisch verschwindenden Matrixelemente von $\mathscr{H}_s$ sind

$$\begin{aligned}(\Psi^{Jwr}_{M\Omega}, \mathscr{H}_s \Psi^{Jws}_{M\Omega}) = {} & \frac{\hbar^2}{4}(\Phi^{wr}_{\Omega}, \Theta'_{pq}\Phi^{ws}_{\Omega})\{J(J+1)-\Omega^2\}+\frac{\hbar^2}{4}(\Phi^{wr}_{\Omega}, \Theta'_{33}\Phi^{ws}_{\Omega})\Omega^2 \\ & -\delta_{\Omega 1}\frac{\hbar^2}{8}w(-1)^J(\Phi^{wr}_{+1}, \Theta'_{pp}\Phi^{ws}_{-1})J(J+1) \quad \text{für alle } \Omega,\end{aligned} \tag{8.18}$$

$$\begin{aligned}(\Psi^{Jwr}_{M\Omega}, \mathscr{H}_s \Psi^{Jws}_{M\Omega-1}) = {} & \frac{\hbar^2}{4}(\Phi^{wr}_{\Omega}, \Theta'_{p3}\Phi^{ws}_{\Omega-1})(2\Omega-1)\sqrt{(J+\Omega)(J-\Omega+1)} \\ & +\delta_{\Omega 1}\frac{\hbar^2}{8}w(-1)^{J-\frac{1}{2}}(\Phi^{wr}_{\frac{1}{2}}, \Theta'_{pp}\Phi^{ws}_{-\frac{1}{2}})(J+\tfrac{1}{2})\sqrt{(J-\tfrac{1}{2})(J+\tfrac{3}{2})}, \quad \Omega \geqq \tfrac{3}{2},\end{aligned} \tag{8.19}$$

$$(\Psi^{Jwr}_{M1}, \mathscr{H}_{a}\Psi^{Jws}_{M0^{\pm}}) = \frac{\hbar^2}{2\sqrt{2}}(\Phi^{wr}_{1}, \Theta'_{p3}\Phi^{ws}_{0^{\pm}})\sqrt{J(J+1)}, \tag{8.20}$$

$$(\Psi^{Jwr}_{M\Omega}, \mathscr{H}_{a}\Psi^{Jws}_{M\Omega-2}) = \frac{\hbar^2}{8}(\Phi^{wr}_{\Omega}, \Theta'_{pp}\Phi^{ws}_{\Omega-2})\sqrt{(J+\Omega)(J-\Omega+1)(J+\Omega-1)(J-\Omega+2)}, \quad \Omega \geqq \tfrac{5}{2}, \tag{8.21}$$

$$(\Psi^{Jwr}_{M2}, \mathscr{H}_{a}\Psi^{Jws}_{M0^{\pm}}) = \frac{\hbar^2}{4\sqrt{2}}(\Phi^{wr}_{2}, \Theta'_{pp}\Phi^{ws}_{0^{\pm}})\sqrt{J(J-1)(J+1)(J+2)}. \tag{8.22}$$

Das zusätzliche Auftreten von $\Theta'_{pp}$ in (8.18) bei $\Omega = 1$ und in (8.19) bei $\Omega = \frac{3}{2}$ ist praktisch bedeutungslos, da sich bei genügend starker Deformation in $z'$-Richtung die Diagonalelemente von $\Theta'_{pq}$ als groß gegen die Nichtdiagonalelemente und die Matrixelemente der anderen Komponenten von $\Theta$ erweisen.

### 8.5. ROTATIONSAUSTAUSCHOPERATOR; SONDERFALL $\Omega = \frac{1}{2}$

Nach (3.37) und (A3)

$$\mathscr{H}_{1a} = -\tfrac{1}{2}(W'_{p}J'_{q}+W'_{q}J'_{p})-W'_{3}J'_{3}, \tag{8.23}$$

wobei $W'_3$ bei Zusammenfallen von N mit der $z'$-Achse verschwände. Die nicht identisch verschwindenden Matrixelemente sind

$$(\Psi^{Jwr}_{M\Omega}, \mathscr{H}_{1a}\Psi^{Jws}_{M\Omega}) = -\hbar(\Phi^{wr}_{\Omega}, W'_{3}\Phi^{ws}_{\Omega})\Omega - \delta_{\Omega\frac{1}{2}}\frac{\hbar}{2}w(-1)^{J-\frac{1}{2}}(\Phi^{wr}_{\frac{1}{2}}, W'_{p}\Phi^{ws}_{-\frac{1}{2}})(J+\tfrac{1}{2}) \quad \text{für alle } \Omega, \tag{8.24}$$

$$(\Psi^{Jwr}_{M\Omega}, \mathscr{H}_{1a}\Psi^{Jws}_{M\Omega-1}) = -\frac{\hbar}{2}(\Phi^{wr}_{\Omega}, W'_{p}\Phi^{ws}_{\Omega-1})\sqrt{(J+\Omega)(J-\Omega+1)}, \quad \Omega \geqq \tfrac{3}{2}, \tag{8.25}$$

$$(\Psi^{Jwr}_{M1}, \mathscr{H}_{1a}\Psi^{Jws}_{M0^{\pm}}) = -\frac{\hbar}{\sqrt{2}}(\Phi^{wr}_{1}, W'_{p}\Phi^{ws}_{0^{\pm}})\sqrt{J(J+1)}. \tag{8.26}$$

Das in (8.24) bei $\Omega = \frac{1}{2}$ auftretende Glied mit $W'_p$ kann wesentlich größer sein als das mit $W'_3$ und daher einen entscheidenden Beitrag zur Gesamtenergie liefern. Der Fall $\Omega = \frac{1}{2}$ ist daher ausgezeichnet. Die von ihm verursachten Besonderheiten wirken sich auf den Kerndrehimpuls und die Kernmomente aus.

### 8.6. TAUMELBEDINGUNG

Die infolge der Systemkorrektur auftretenden Zusatzglieder in $\mathscr{H}_a$ und $\mathscr{H}_{1a}$ setzen die Taumelbedingung außer Kraft. Anstelle von (4.12) ergibt sich jetzt

$$\dot{\Psi}+\tfrac{1}{2}(\cos\Theta\,\dot{\Phi} + \dot{\Phi}\cos\Theta) = \tfrac{1}{2}(\Theta'_{p3}J'_{q}+\Theta'_{q3}J'_{p})+\Theta'_{33}J'_{3}-W'_{3}. \tag{8.27}$$

Mit Hilfe der Symmetriebeziehungen läßt sich aber zeigen, daß alle Matrix-

elemente von (8.27) verschwinden. Die Taumelbedingung ist daher für beliebige Zustände im Mittel erfüllt.

### 8.7. ELEKTRISCHES QUADRUPOLMOMENT

Das elektrische Quadrupolmoment $q$ ist der Erwartungswert von $2\Gamma_0^{\mathrm{P}}$, gebildet über einen Eigenzustand mit $M = J$. Nach (B20) und (B23) ist

$$\Gamma_0 = \sum_m Y_{-m}(\Theta, \Psi)\Gamma'_m, \tag{8.28}$$

und als nicht identisch verschwindende Matrixelemente für gegebenes $J$ und $M = J$ ergeben sich

$$\begin{aligned}(\Psi_{J\Omega}^{Jwr}, 2\Gamma_0^{\mathrm{P}}\Psi_{J\Omega}^{Jws}) &= \frac{1}{2}\,\frac{3\Omega^2 - J(J+1)}{(J+1)(J+\frac{3}{2})}\,(\Phi_\Omega^{wr}, 2\Gamma_0^{\mathrm{P}'}\Phi_\Omega^{ws}) \\ &\quad -\delta_{\Omega 1}w(-1)^J\sqrt{\frac{3}{8}}\,\frac{J}{J+\frac{3}{2}}\,(\Phi_{+1}^{wr}, 2\Gamma_{-2}^{\mathrm{P}'}\Phi_{-1}^{ws}) \quad \text{für alle } \Omega,\end{aligned} \tag{8.29}$$

$$\begin{aligned}(\Psi_{J\Omega}^{Jwr}, 2\Gamma_0^{\mathrm{P}}\Psi_{J\Omega-1}^{Jws}) &= \sqrt{\frac{3}{2}}\,\frac{(\Omega-\frac{1}{2})\sqrt{(J+\Omega)(J-\Omega+1)}}{(J+1)(J+\frac{3}{2})}\,(\Phi_\Omega^{wr}, 2\Gamma_{+1}^{\mathrm{P}'}\Phi_{\Omega-1}^{ws}) \\ &\quad +\delta_{\Omega\frac{1}{2}}w(-1)^{J-\frac{1}{2}}\sqrt{\frac{3}{8}}\,\frac{J+\frac{1}{2}}{J+1}\sqrt{\frac{J-\frac{1}{2}}{J+\frac{3}{2}}}\,(\Phi_{+\frac{1}{2}}^{wr}, 2\Gamma_{-2}^{\mathrm{P}'}\Phi_{-\frac{1}{2}}^{ws}), \quad \Omega \geqq \tfrac{3}{2},\end{aligned} \tag{8.30}$$

$$(\Psi_{J1}^{Jwr}, 2\Gamma_0^{\mathrm{P}}\Psi_{J0^\pm}^{Jws}) = \frac{\sqrt{3}}{2}\,\frac{1}{J+\frac{3}{2}}\sqrt{\frac{J}{J+1}}\,(\Phi_{+1}^{wr}, 2\Gamma_{-1}^{\mathrm{P}'}\Phi_{0^\pm}^{ws}), \tag{8.31}$$

$$\begin{aligned}&(\Psi_{J\Omega}^{Jwr}, 2\Gamma_0^{\mathrm{P}}\Psi_{J\Omega-2}^{Jws}) \\ &= \sqrt{\frac{3}{8}}\,\frac{\sqrt{(J+\Omega)(J+\Omega-1)(J-\Omega+1)(J-\Omega+2)}}{(J+1)(J+\frac{3}{2})}\,(\Phi_\Omega^{wr}, 2\Gamma_{-2}^{\mathrm{P}'}\Phi_{\Omega-2}^{ws}), \quad \Omega \geqq \tfrac{5}{2},\end{aligned} \tag{8.32}$$

$$(\Psi_{J2}^{Jwr}, 2\Gamma_0^{\mathrm{P}}\Psi_{J0^\pm}^{Jws}) = \frac{\sqrt{3}}{2}\,\frac{1}{J+\frac{3}{2}}\sqrt{\frac{J(J-1)(J+2)}{J+1}}\,(\Phi_{+2}^{wr}, 2\Gamma_{-2}^{\mathrm{P}'}\Phi_{0^\pm}^{ws}). \tag{8.33}$$

Der Erwartungswert $q'$ von $2\Gamma_0^{\mathrm{P}'}$ kann als relatives elektrisches Quadrupolmoment bezeichnet werden, und $q$ wäre dann zur Unterscheidung absolutes elektrisches Quadrupolmoment zu nennen. Die Matrixelemente von $2\Gamma_0^{\mathrm{P}'}$ sind

$$(\Psi_{J\Omega}^{Jwr}, 2\Gamma_0^{\mathrm{P}'}\Psi_{J\Omega}^{Jws}) = (\Phi_\Omega^{wr}, 2\Gamma_0^{\mathrm{P}'}\Phi_\Omega^{ws}). \tag{8.34}$$

Das für einen Zustand $\Psi_{J\Omega}^{Jwr}$, $\Omega \neq 1$, gebildete $q$ ist daher nach (8.29) das Produkt aus $q'$ und einem von $J$ und $\Omega$ abhängigen Faktor, der über die Lagen des Kerns mittelt. Diese Verknüpfung zwischen $q$ und $q'$ gilt auch für den allgemeineren Zustand

$$\Psi_{J\Omega}^{Jw} = \sum_r C_r\Psi_{J\Omega}^{Jwr}, \qquad \sum_r |C_r|^2 = 1. \tag{8.35}$$

### 8.8. INNERES MAGNETISCHES DIPOLMOMENT

Das magnetische Dipolmoment ist der Erwartungswert des in (3.38) angegebenen Operators $\mathcal{M}_3$, gebildet über einen Eigenzustand mit $M = J$. Wir führen die Berechnung für die beiden Teile, in die sich $\mathcal{M}_3$ nach (3.41) ... (3.43) zerlegen läßt, getrennt durch.

$\mathcal{M}_{13}$ gibt den Teil des magnetischen Momentes, der von der Bewegung der Nukleonen bei festgehaltenem Koordinatensystem $\Sigma'$, gemittelt über dessen Lagen, herrührt. Wir bezeichnen es als inneres Moment. Auf $\Sigma'$ bezogen, ist

$$\mathcal{M}_{13} = -\tfrac{1}{2}\sin\Theta(e^{+i\Psi}\mathcal{M}'_{1p}+e^{-i\Psi}\mathcal{M}'_{1q})+\cos\Theta\mathcal{M}'_{13}, \tag{8.36}$$

und die nicht identisch verschwindenden Matrixelemente für gegebenes $J$ und $M = \Omega$ sind

$$\begin{aligned}(\Psi^{Jwr}_{J\Omega}, \mathcal{M}_{13}\Psi^{Jws}_{J\Omega}) &= \frac{\Omega}{J+1}(\Phi^{Jwr}_{\Omega}, \mathcal{M}'_{13}\Phi^{Jws}_{\Omega}) \\ &+ \delta_{\Omega\frac{1}{2}}\tfrac{1}{2}w(-1)^{J-\frac{1}{2}}\frac{J+\frac{1}{2}}{J+1}(\Phi^{wr}_{+\frac{1}{2}}, \mathcal{M}'_{1p}\Phi^{ws}_{-\frac{1}{2}}), \quad \text{für alle } \Omega,\end{aligned} \tag{8.37}$$

$$(\Psi^{Jwr}_{J\Omega}, \mathcal{M}_{13}\Psi^{Jws}_{J\Omega-1}) = \frac{1}{2}\frac{\sqrt{(J+\Omega)(J-\Omega+1)}}{J+1}(\Phi^{wr}_{\Omega}, \mathcal{M}'_{1p}\Phi^{ws}_{\Omega-1}), \quad \Omega \geqq \tfrac{3}{2}, \tag{8.38}$$

$$(\Psi^{Jwr}_{J1}, \mathcal{M}_{13}\Psi^{Jws}_{J0^{\pm}}) = \frac{1}{\sqrt{2}}\sqrt{\frac{J}{J+1}}(\Phi^{wr}_{1}, \mathcal{M}'_{1p}\Phi^{ws}_{0^{\pm}}). \tag{8.39}$$

Entsprechend zum elektrischen Quadrupolmoment könnte man den Erwartungswert von $\mathcal{M}'_{13}$ als relatives inneres magnetisches Dipolmoment bezeichnen. Aus Symmetriegründen verschwinden aber alle über die $\Psi^{Jwr}_{J\Omega}$ gebildeten Matrixelemente von $\mathcal{M}'_{13}$. Daher ist es trotz dem gleichen Aufbau der Gleichungen (8.37) und (8.29) nicht möglich, das innere magnetische Moment in einem Zustand $\Psi^{Jwr}_{J\Omega}$ oder in dem allgemeineren Zustand (8.35) als Produkt eines relativen magnetischen Momentes mit einem von $J$ und $\Omega$ abhängigen Faktor zu deuten. Die in den genannten Zuständen enthaltenen Teile entgegengesetzten Vorzeichens von $\Omega$ haben Matrixelemente von $\mathcal{M}'_{13}$ mit entgegengesetzten Vorzeichen. Da sich auch der von $J$ und $\Omega$ abhängige Faktor für beide Teile im Vorzeichen unterscheidet, ergibt sich ein endlicher Erwartungswert von $\mathcal{M}_{13}$.

### 8.9. ÄUSSERES MAGNETISCHES DIPOLMOMENT

$\mathcal{M}_{a3}$ gibt den Teil des magnetischen Dipolmomentes, der durch die Rotation des ganzen Kerns als starrer Körper entsteht. Wir bezeichnen ihn als äußeres Moment. Im Gegensatz zu $\mathcal{M}_{13}$ wirken hier die Komponenten von $\mathbf{J}$ auf die $\mathcal{D}^{J}_{M\Omega}$. Beim Darstellen von $\mathcal{M}_{a3}$ in Komponenten von $\Sigma'$ ist auf die

Wahrung der Hermitizität zu achten. Das gelingt sicher, wenn man $\mathcal{M}_{a3}$ zunächst in Komponenten des festen Systems anschreibt und die Komponenten von $\mathbf{J}$ und von $G$ einzeln auf $\Sigma'$ transformiert. Die Darstellung von $\mathcal{M}_{a3}$ in Komponenten von $\Sigma'$ wird aber auch richtig bei Benutzung der hermitisierten Transformationsformel (A9)

$$\mathcal{M}_{a3} = \tfrac{1}{2}\{-\tfrac{1}{2}\sin\Theta(e^{+i\Psi}\mathcal{M}'_{ap}+e^{-i\Psi}\mathcal{M}'_{aq})+\cos\Theta\mathcal{M}'_{a3} \\ -\tfrac{1}{2}(\mathcal{M}'_{ap}e^{+i\Psi}+\mathcal{M}'_{aq}e^{-i\Psi})\sin\Theta+\mathcal{M}'_{a3}\cos\Theta\}. \quad (8.40)$$

Bei $\mathcal{M}_a$ ist es im Gegensatz zu $\mathbf{J}$ und $\mathcal{M}_1$ nämlich nicht gleichgültig, auf welcher Seite die Transformationskoeffizienten stehen. Dieser Unterschied ergibt sich aus der Unsymmetrie von $G$. Das Ergebnis der Transformation ist

$$\begin{aligned}\mathcal{M}_{a3} = \frac{\mu_K}{\hbar}\,\tfrac{1}{2}\{&[-\tfrac{1}{4}(G'_{pq}e^{+i\Psi}+G'_{qq}e^{-i\Psi})\sin\Theta+\tfrac{1}{2}G'_{3q}\cos\Theta]J'_p\\ &+[-\tfrac{1}{4}(G'_{pp}e^{+i\Psi}+G'_{qp}e^{-i\Psi})\sin\Theta+\tfrac{1}{2}G'_{3p}\cos\Theta]J'_q\\ &+[-\tfrac{1}{2}(G'_{p3}e^{+i\Psi}+G'_{q3}e^{-i\Psi})\sin\Theta+G'_{33}\cos\Theta]J'_3\\ &+J'_p[-\tfrac{1}{4}\sin\Theta(e^{+i\Psi}G'_{pq}+e^{-i\Psi}G'_{qq})+\tfrac{1}{2}\cos\Theta G'_{3q}]\\ &+J'_q[-\tfrac{1}{4}\sin\Theta(e^{+i\Psi}G'_{pp}+e^{-i\Psi}G'_{qp})+\tfrac{1}{2}\cos\Theta G'_{3q}]\\ &+J'_3[-\tfrac{1}{2}\sin\Theta(e^{+i\Psi}G'_{p3}+e^{-i\Psi}G'_{q3})+\cos\Theta G'_{33}]\}.\end{aligned} \quad (8.41)$$

Die nicht identisch verschwindenden Matrixelemente von $\mathcal{M}_{a3}$ für gegebenes $J$ und $M = J$ sind

$$(\Psi^{Jwr}_{J\Omega}, \mathcal{M}_{a3}\Psi^{Jws}_{J\Omega}) = \mu_K\left\{\frac{1}{4}\,\frac{J(J+1)-\Omega^2}{J+1}\,(\Phi^{wr}_{\Omega}, [G'_{pq}+G'_{qp}]\Phi^{ws}_{\Omega})\right. \\ \left. +\frac{\Omega^2}{J+1}\,(\Phi^{wr}_{\Omega}, G'_{33}\Phi^{ws}_{\Omega})-\delta_{\Omega 1}\tfrac{1}{4}w(-1)^J J(\Phi^{wr}_{+1}, G'_{pp}\Phi^{ws}_{-1})\right\} \text{ für alle } \Omega, \quad (8.42)$$

$$(\Psi^{Jwr}_{J\Omega}, \mathcal{M}_{a3}\Psi^{Jws}_{J\Omega-1}) = \mu_K\left\{\tfrac{1}{2}\sqrt{(J+\Omega)(J-\Omega+1)}\,(\Omega-\tfrac{1}{2})(\Phi^{wr}_{\Omega}, [G'_{p3}+G'_{3p}]\Phi^{ws}_{\Omega-1})\right. \\ \left. +\delta_{\Omega\frac{1}{2}}\tfrac{1}{4}w(-1)^{J-1}\frac{J+\frac{1}{2}}{J+1}\sqrt{(J-\tfrac{1}{2})(J+\tfrac{3}{2})}\,(\Phi^{wr}_{+\frac{1}{2}}, G'_{pp}\Phi^{ws}_{-\frac{1}{2}})\right\}, \quad \Omega \geqq \tfrac{3}{2}, \quad (8.43)$$

$$(\Psi^{Jwr}_{J1}, \mathcal{M}_{a3}\Psi^{Jws}_{J0^{\pm}}) = \frac{\mu_K}{2\sqrt{2}}\sqrt{\frac{J}{J+1}}\,(\Phi^{wr}_{+1}, [G'_{p3}+G'_{3p}]\Phi^{ws}_{0^{\pm}}), \quad (8.44)$$

$$(\Psi^{Jwr}_{J\Omega}, \mathcal{M}_{a3}\Psi^{Jws}_{J\Omega-2}) \\ = \frac{\mu_K}{4}\,\frac{\sqrt{(J+\Omega)(J+\Omega-1)(J-\Omega+1)(J-\Omega+2)}}{J+1}\,(\Phi^{wr}_{\Omega}, G'_{pp}\Phi^{ws}_{\Omega-2}), \quad \Omega \geqq \tfrac{5}{2}, \quad (9.45)$$

$$(\Psi^{Jwr}_{J\Omega}, \mathcal{M}_{a3}\Psi^{Jws}_{J0^{\pm}}) = \frac{\mu_K}{2\sqrt{2}}\sqrt{\frac{J(J-1)(J+2)}{J+1}}\,(\Phi^{wr}_{+2}, G'_{pp}\Phi^{ws}_{0^{\pm}}). \quad (8.46)$$

Weiter gilt

$$(\Psi^{Jwr}_{J\Omega}, [G'_{pq}+G'_{qp}]\Psi^{Jws}_{J\Omega}) = (\Phi^{wr}_{\Omega}, [G'_{pq}+G'_{qp}]\Phi^{ws}_{\Omega}). \tag{8.47}$$

Diese Beziehung gestattet es, das für einen Zustand $\Psi^{Jwr}_{J\Omega}$ oder den allgemeineren Zustand (8.35) gebildete $\langle \mathcal{M}_{a3} \rangle$ als Produkt des zu diesem Zustand gehörigen gyromagnetischen Faktors $\frac{1}{4}\langle G'_{pq}+G'_{qp}\rangle$ mit einem von $J$ und $\Omega$ abhängigen Faktor aufzufassen.

## 9. Aufstellung des Orthonormalsystems

### 9.1. VORBEMERKUNGEN

Wir wenden uns jetzt der Berechnung von Kernzuständen zu und behandeln als Beispiel den Kern (21,24). Bei undeformiertem Potential befinden sich ein Proton und vier Neutronen in $4f_{\frac{7}{2}}$. Diese Unterschale bildet eine eigene Schale, ist also von den benachbarten Unterschalen energetisch merklich abgesetzt. Daher ist auch bei deformiertem Potential und dem dadurch bedingten kinematischen Verhalten des Kerns die gleiche Besetzung zu erwarten. Wir möchten wissen, aus welchen $\Psi^{Jwr}_{M\Omega}$ sich der Grundzustand zusammensetzt, wie groß die einzelnen Energieglieder und die Kernmomente sind und ob das Kriterium (3.3) erfüllt ist.

Der Einfachheit halber rechnen wir mit dem Oszillatorpotential, obwohl das wirkliche Potential davon abweicht, denn sonst wäre $4f_{\frac{7}{2}}$ keine selbständige Schale. Das Verfahren zur Aufstellung des Orthonormalsystems wählen wir dagegen so, daß es auch für ein allgemeineres Potential anwendbar ist.

### 9.2. NUKLEONENEIGENFUNKTIONEN FÜR $\zeta = 0$

Die in den approximativen Basisfunktionen (7.1) und (7.2) auftretenden Zustände $\Phi^{wr}_{\Omega}$ und $\Phi^{wr}_{0\pm}$ sind, wie am Anfang von 7. erwähnt wurde, Slaterdeterminanten aus Nukleoneneigenfunktionen. Zur Aufstellung eines geeigneten Systems derartiger Funktionen gehen wir aus von dem Operator

$$\mathcal{H} = \frac{1}{2M}|\mathbf{p}|^2+V_0(r)+\frac{\lambda}{M^2c^2}\mathbf{s}\cdot\mathbf{p}\times\operatorname{grad}V_0(r). \tag{9.1}$$

Er beschreibt nach 1. das Verhalten des einzelnen Nukleons im undeformiertem Potential. Wir setzen $\lambda = 0$ und interessieren uns zunächst für die spinlosen Eigenfunktionen. Sie haben mit (B11) die Form

$$f^{nl}_{m_l}(r, \vartheta, \varphi) = R^{nl}(r)X^{l}_{m_l}(\vartheta, \varphi), \tag{9.2}$$

$l$ Quantenzahl des Bahndrehimpulses,
$m_l$ Quantenzahl für dessen $z$-Komponente,
$n$ Ordnungsindex.

Im Sonderfall des Oszillatorpotentials

$$V = \tfrac{1}{2}M\omega^2 r^2 = \tfrac{1}{2}M\omega^2(x^2+y^2+z^2) \tag{9.3}$$

gilt

$$R^{nl}(r) = \sqrt{\frac{2\kappa^3\left(\frac{n-l}{2}\right)!}{\Gamma\left(\frac{n+l+3}{2}\right)}}\, e^{-\frac{\kappa^2 r^2}{2}} \kappa^l r^l L_{\frac{n-l}{2}}^{l+\frac{1}{2}}(\kappa^2 r^2), \quad \kappa = \sqrt{\frac{M\omega}{\hbar}}, \tag{9.4}$$

$L$ Laguerresches Polynom [20]), $n$ ganz oder Null,
$l \leqq n$, $(n-l)/2$ ganz oder Null.

Auf Grund der Orthogonalitätsrelationen und der Rekursionsformeln [20]) für die Laguerreschen Polynome gilt

$$\int_0^\infty R^{nl} R^{pl} r^2 \mathrm{d}r = \delta_{np}, \tag{9.5}$$

$$\kappa^2 r^2 R^{nl} = (n+\tfrac{3}{2})R^{nl} - \tfrac{1}{2}\sqrt{(n-l+2)(n+l+3)}R^{n+2,l} - \tfrac{1}{2}\sqrt{(n-l)(n+l+1)}R^{n-2,l}, \tag{9.6}$$

$$r\frac{\mathrm{d}R^{nl}}{\mathrm{d}r} = -\tfrac{3}{2}R^{nl} - \tfrac{1}{2}\sqrt{(n-l+2)(n+l+3)}R^{n+2,l} - \tfrac{1}{2}\sqrt{(n-l)(n+l+1)}R^{n-2,l}. \tag{9.7}$$

Beim Oszillatorpotential lassen sich die spinlosen Eigenfunktionen aber auch durch die Eigenfunktionen

$$\chi_n(x) = \sqrt{\frac{\kappa}{2^n n!\sqrt{\pi}}}\, e^{-\frac{\kappa^2 x^2}{2}} H_n(\kappa x), \quad \kappa = \sqrt{\frac{M\omega}{\hbar}}, \tag{9.8}$$

des eindimensionalen Oszillators ausdrücken, wo $H_n(\kappa x)$ das durch

$$H_n(x) = (-1)^n e^{x^2}\frac{\mathrm{d}}{\mathrm{d}x^n} e^{-x^2} \tag{9.9}$$

definierte Hermitesche Polynom [20]) ist. Es bestehen die Beziehungen

$$\int_{+\infty}^{-\infty} \chi_n \chi_p \mathrm{d}x = \delta_{np}, \tag{9.10}$$

$$\kappa x \chi_n = \sqrt{\frac{n+1}{2}}\,\chi_{n+1} + \sqrt{\frac{n}{2}}\,\chi_{n-1}, \tag{9.11}$$

$$\frac{\mathrm{d}\chi_n}{\mathrm{d}\kappa x} = -\sqrt{\frac{n+1}{2}}\,\chi_{n+1} + \sqrt{\frac{n}{2}}\,\chi_{n-1}. \tag{9.12}$$

Die spinlosen Eigenfunktionen von (9.1) sind dann

$$\chi_{n_1 n_2 n_3}(x, y, z) = \chi_{n_1}(x)\chi_{n_2}(y)\chi_{n_3}(z). \tag{9.13}$$

Der Vergleich der $f_{m_l}^{nl}$ mit den $\chi_{n_1 n_2 n_3}$ ergibt

$$f_0^{00} = \chi_{000}, \tag{9.14}$$

$$\begin{aligned} f_{\pm 1}^{11} &= -\frac{1}{\sqrt{2}}(\pm\chi_{100}+i\chi_{010}) \\ f_0^{11} &= \chi_{001}, \end{aligned} \tag{9.15}$$

$$\begin{aligned} f_{\pm 2}^{22} &= \tfrac{1}{2}(\chi_{200}-\chi_{020})\pm\frac{i}{\sqrt{2}}\chi_{110} \\ f_{\pm 1}^{22} &= -\frac{1}{\sqrt{2}}(\pm\chi_{101}+i\chi_{011}) \\ f_0^{22} &= \sqrt{\tfrac{2}{3}}\chi_{002}-\frac{1}{\sqrt{6}}(\chi_{200}+\chi_{020}), \end{aligned} \tag{9.16}$$

$$f_0^{20} = -\frac{1}{\sqrt{3}}(\chi_{200}+\chi_{020}+\chi_{002}), \tag{9.17}$$

$$\begin{aligned} f_{\pm 3}^{33} &= \mp\left(\frac{1}{\sqrt{8}}\chi_{300}-\sqrt{\tfrac{3}{8}}\chi_{120}\right)-i\left(\frac{1}{\sqrt{8}}\chi_{030}-\sqrt{\tfrac{3}{8}}\chi_{210}\right) \\ f_{\pm 2}^{33} &= \tfrac{1}{2}(\chi_{201}-\chi_{021})\pm\frac{i}{\sqrt{2}}\chi_{111} \\ f_{\pm 1}^{33} &= \mp\left(\sqrt{\tfrac{2}{5}}\chi_{102}-\sqrt{\tfrac{3}{40}}\chi_{300}-\frac{1}{\sqrt{40}}\chi_{120}\right)-i\left(\sqrt{\tfrac{2}{5}}\chi_{012}-\sqrt{\tfrac{3}{40}}\chi_{300}-\frac{1}{\sqrt{40}}\chi_{210}\right) \\ f_0^{33} &= \sqrt{\tfrac{2}{5}}\chi_{003}-\sqrt{\tfrac{3}{10}}(\chi_{201}+\chi_{021}), \end{aligned} \tag{9.18}$$

$$\begin{aligned} f_{\pm 1}^{31} &= \pm\left\{\sqrt{\tfrac{3}{10}}\chi_{300}+\frac{1}{\sqrt{10}}(\chi_{120}+\chi_{102})\right\}+i\left\{\sqrt{\tfrac{3}{10}}\chi_{030}+\frac{1}{\sqrt{10}}(\chi_{210}+\chi_{012})\right\} \\ f_0^{31} &= -\frac{1}{\sqrt{5}}(\chi_{201}+\chi_{021})-\sqrt{\tfrac{3}{5}}\chi_{003}. \end{aligned} \tag{9.19}$$

### 9.3. DEFORMIERTE FUNKTIONEN OHNE SPIN

Wir deformieren das Oszillatorpotential in $z'$-Richtung derart, daß eine enge Beziehung zu dem aus (9.3) nach (2.13) ... (2.15) abzuleitenden Selbstpolarisationspotential

$$V = \tfrac{1}{2}M\omega^2 r^2\{1-2\zeta\sum_m \gamma_m Y_m(\vartheta,\varphi)+\zeta^2\sum_m|\gamma_m|^2\} \tag{9.20}$$

besteht. In diesem ersetzen wir $\gamma'_0$ durch einen Deformationsparameter $2\varepsilon$ und lassen $\gamma'_{\pm 1}$ und $\gamma'_{\pm 2}$ fort, oder, was dasselbe ist, wir ersetzen in dem Mittelpotential (8.6) $\zeta\langle\gamma'_0\rangle$ durch $2\varepsilon$. Das entstehende Potential

$$\begin{aligned} V_\varepsilon &= \tfrac{1}{2}M\omega^2 r^2\{1-4\varepsilon Y_0(\vartheta,\varphi)+4\varepsilon^2\} \\ &= \tfrac{1}{2}M\omega^2 r^2\{(1+2\varepsilon+4\varepsilon^2)(x'^2+y'^2)+(1-2\varepsilon)^2 z'^2\} \\ &= \tfrac{1}{2}M\{\omega_1^2(x'^2+y'^2)+\omega_3^2 z'^2\}. \end{aligned} \tag{9.21}$$

bezeichnen wir als Parameterpotential. Einsetzen von $V_\varepsilon$ anstelle von $V_0$ in (9.1) ergibt für $\lambda = 0$ Eigenfunktionen $\bar{\chi}_{n_1 n_2 n_3}(x', y', z')$, die sich von den $\chi_{n_1 n_2 n_3}(x, y, z)$ in (9.13), abgesehen vom Koordinatensystem, dadurch unterscheiden, daß das in (9.4) und (9.8) angegebene $\kappa$ für $x'$ und $y'$ durch

$$\kappa_1 = \sqrt{\frac{M\omega_1}{\hbar}} = \kappa(1+\tfrac{1}{2}\varepsilon+\tfrac{5}{3}\varepsilon^2) \tag{9.22}$$

und für $z'$ durch

$$\kappa_3 = \sqrt{\frac{M\omega_3}{\hbar}} = \kappa(1-\varepsilon+\tfrac{1}{2}\varepsilon^2) \tag{9.23}$$

zu ersetzen ist. Da aus (9.22) und (9.23) bei Entwicklung bis zu Gliedern mit $\varepsilon^2$

$$\kappa_1^2\kappa_3 = 1 \tag{9.24}$$

folgt, ist der Ersatz, wie (9.8) zeigt, nur dort vorzunehmen, wo $\kappa$ in der Verbindung $\kappa x$, $\kappa y$, $\kappa z$ auftritt. Dann ist aber nach (9.22) und (9.23)

$$\bar{\chi}_{n_1 n_2 n_3}(x', y', z') = \chi_{n_1 n_2 n_3}(x'[1+\tfrac{1}{2}\varepsilon+\tfrac{5}{8}\varepsilon^2],\ y'[1+\tfrac{1}{2}\varepsilon+\tfrac{5}{8}\varepsilon^2],\ z'[1-\varepsilon+\tfrac{1}{2}\varepsilon^2]), \tag{9.25}$$

und die Entwicklung dieses Ausdrucks ergibt

$$\bar{\chi}_{n_1 n_2 n_3}(x', y', z') = \{1-\varepsilon D+\tfrac{1}{2}\varepsilon^2(D^2-2D)\}\chi_{n_1 n_2 n_3}(x', y', z') \tag{9.26}$$

mit der Abkürzung

$$D = z'\frac{\partial}{\partial z'} - \frac{1}{2}\left(x'\frac{\partial}{\partial x'} + y'\frac{\partial}{\partial y'}\right). \tag{9.27}$$

Für das Parameterpotential kann man entsprechend schreiben

$$V_\varepsilon = \{1-2\varepsilon D+2\varepsilon^2(D^2-D)\}\,\tfrac{1}{2}M\omega^2 r^2. \tag{9.28}$$

Die Eigenfunktionen deformieren sich also in erster Näherung halb so stark wie die Äquipotentialflächen. Um $\varepsilon$ als Deformationsparameter der Eigenfunktionen bezeichnen zu können, haben wir von vornherein den Deformationsparameter des Potentials gleich $2\varepsilon$ gesetzt.

Ersetzt man in den $f^{nl}_{m_l}$ die $\chi_{n_1 n_2 n_3}$ durch die $\bar{\chi}_{n_1 n_2 n_3}$, so entstehen deformierte Funktionen $\bar{f}^{nl}_{m_l}$ mit scharfen Bahndrehimpulskomponenten in $z'$-Richtung, während der Drehimpuls selbst unscharf wird; $l$ ist daher keine Quantenzahl mehr, sondern nur noch Ordnungsindex. Sind $\bar{f}$, $\bar{g}$ zwei beliebige Funktionen, die durch den Deformationsprozeß (9.26) aus $f$, $g$ hervorgehen, und ist $P$ irgendein Operator, so findet man unter Beachtung der Antihermitizität von $D$

$$(\bar{f}, P\bar{g}) = (f, Pg)+\varepsilon(f, [D, P]g)+\tfrac{1}{2}\varepsilon^2\{(f, [D, [D, P]]g)+2(f, [D, P]g)\}. \tag{9.29}$$

Diese Gleichung zeigt, daß Orthogonalität und Normierung bei der Deformation erhalten bleiben, und gestattet, die Matrixelemente der deformierten Funktionen auf die der undeformierten zurückzuführen. Sie ermöglicht die Anwendung des Deformationsverfahrens auf die $f^{nl}_{m_l}$ beliebiger $V_0(r)$: man ordnet nach (9.26) jedem $f^{nl}_{m_l}$ ein $\bar{f}^{nl}_{m_l}$ zu und berechnet die Matrixelemente

nach (9.29); die Frage nach dem Hamiltonoperator, der die $\bar{f}^{nl}_{m_l}$ als Eigenfunktionen liefert, interessiert nicht.

### 9.4. DEFORMIERTE FUNKTIONEN MIT SPIN, ABKOPPLUNGSGRAD

Im Fall des undeformierten Potentials lassen sich die spinlosen Eigenfunktionen (9.2) mit den Spinfunktionen $\alpha$, $\beta$ zu Funktionen

$$\psi^{njl}_m = c^{jl}_{mm-\frac{1}{2}} f^{nl}_{m-\frac{1}{2}} \alpha + c^{jl}_{mm+\frac{1}{2}} f^{nl}_{m+\frac{1}{2}} \beta, \tag{9.30}$$

$j$ Quantenzahl des Gesamtdrehimpulses,
$m$ Quantenzahl für dessen $z$-Komponente,

vereinigen. Die $c$ sind gruppentheoretisch festgelegt und in (B16) angegeben. In entsprechender Weise vereinigen wir die $\bar{f}^{nl}_{m_l}$ mit den jetzt auf $\Sigma'$ zu beziehenden Spinfunktionen $\alpha$, $\beta$ zu Funktionen

$$\varphi^{njl}_m = b^{jl}_{mm-\frac{1}{2}} \bar{f}^{nl}_{m-\frac{1}{2}} \alpha + b^{jl}_{mm+\frac{1}{2}} \bar{f}^{nl}_{m+\frac{1}{2}} \beta, \tag{9.31}$$

wo $j$ und $l$ keine Quantenzahlen mehr sind. Die $b$ beschreiben die Kopplung zwischen Spin und Bahn und brauchen mit den $c$ in (B16) nicht übereinzustimmen. Wir verlangen nur die Gültigkeit der Beziehungen

$$b^{l\pm\frac{1}{2},l}_{-m,-m-\frac{1}{2}} = \pm b^{l\pm\frac{1}{2},l}_{m,m+\frac{1}{2}}, \quad b^{l\pm\frac{1}{2},l}_{-m,-m+\frac{1}{2}} = \pm b^{l\pm\frac{1}{2},l}_{m,m-\frac{1}{2}}, \tag{9.32}$$

$$b^{l-\frac{1}{2},l}_{m,m-\frac{1}{2}} = b^{l+\frac{1}{2},l}_{m,m+\frac{1}{2}}, \qquad b^{l-\frac{1}{2},l}_{m,m+\frac{1}{2}} = -b^{l+\frac{1}{2},l}_{m,m-\frac{1}{2}} \tag{9.33}$$

und die Erfüllung der Normierungsbedingung

$$(b^{l\pm\frac{1}{2},l}_{m,m-\frac{1}{2}})^2 + (b^{l\pm\frac{1}{2},l}_{m,m+\frac{1}{2}})^2 = 1. \tag{9.34}$$

(9.32) wahrt die Symmetrie zwischen $\varphi^{njl}_m$ und $\varphi^{njl}_{-m}$ und (9.33) die Orthogonalität zwischen $\varphi^{n,l+\frac{1}{2},l}_m$ und $\varphi^{n,l-\frac{1}{2},l}_m$. Wir vereinheitlichen die $b$ aller $\varphi^{njl}_m$ durch Einführung des Abkopplungsgrades $\tau$ mit der Festsetzung

$$\frac{b^{l+\frac{1}{2},l}_{m,m+\frac{1}{2}}}{b^{l+\frac{1}{2},l}_{m,m-\frac{1}{2}}} = \frac{c^{l+\frac{1}{2},l}_{m,m+\frac{1}{2}}}{c^{l+\frac{1}{2},l}_{m,m-\frac{1}{2}}} \frac{1-\tau}{1+\tau}, \quad m > 0. \tag{9.35}$$

Die anderen $b$ folgen aus (9.32) und (9.33).

In einem Zustand $\varphi^{njl}_m$ mit $j = l+\frac{1}{2}$ wächst nach diesen Festsetzungen bei einer Zunahme von $\tau$ derjenige Anteil, bei dem die $z'$-Komponenten von Bahndrehimpuls und Spin das gleiche Vorzeichen haben, bei einem Zustand mit $j = l-\frac{1}{2}$ fällt er. Das ist das gleiche Verhalten, wie es die Eigenfunktionen des Hamiltonoperators

$$\mathcal{H} = \frac{1}{2M} |\mathbf{p}|^2 + V_\varepsilon + \frac{\lambda}{M^2c^2} \mathbf{s} \cdot \mathbf{p} \times \operatorname{grad} V_\varepsilon \tag{9.36}$$

mit dem Potential

$$V_\varepsilon = V_0(r) - 2\varepsilon V_1(r) Y_0(\vartheta', \varphi') + 2\varepsilon^2 V_2(r) \tag{9.37}$$

mit $V_1(r)$ und $V_2(r)$ nach (2.14) und (2.15) bei zunehmendem $\varepsilon$ zeigen. Da $\varepsilon > 0$ ein gedehntes und $\varepsilon < 0$ ein abgeplattetes Potentialellipsoid und andererseits $\langle \gamma'_0 \rangle > 0$ einen gedehnten und $\langle \gamma'_0 \rangle < 0$ einen abgeplatte-

ten Kern bedeuten, ist zu erwarten, daß $\tau$ das gleiche Vorzeichen hat wie $\langle\gamma'_0\rangle$.

Aus den $\varphi_m^{nlj}$ werden die in 7. erklärten Determinanten $\Phi_\Omega^{wr}$ und die approximativen Basisfunktionen $\Psi_{M\Omega}^{Jwr}$ gebildet. Sie enthalten die beiden Parameter $\varepsilon$ und $\tau$, die nach dem Ritzschen Verfahren zu bestimmen sind. Damit ist das Orthonormalsystem aufgestellt. Die Berechnung der erforderlichen Matrixelemente mit approximativen Basisfunktionen erfolgt nach Anhang D in Verbindung mit Formeln aus Anhang B und C sowie den Relationen (9.5) ... (9.7) und (9.10) ... (9.12).

### 9.5. SCHREIBWEISE DER ZUSTÄNDE

Um mit möglichst wenigen Indices auszukommen, schreiben wir für die Zustände von $4f_{\frac{7}{2}}$, für die $n = 3, j = \frac{7}{2}, l = 3$ ist, unter Beachtung von (9.32)

$$\begin{aligned}
4f_{\frac{7}{2}}\tfrac{7}{2}^{\pm} &= f^{33}_{\pm 3}\,{}^{\alpha}_{\beta} \\
4f_{\frac{7}{2}}\tfrac{5}{2}^{\pm} &= a_1 f^{33}_{\pm 2}\,{}^{\alpha}_{\beta} + a_2 f^{33}_{\pm 3}\,{}^{\beta}_{\alpha} \\
4f_{\frac{7}{2}}\tfrac{3}{2}^{\pm} &= b_1 f^{33}_{\pm 1}\,{}^{\alpha}_{\beta} + b_2 f^{33}_{\pm 2}\,{}^{\beta}_{\alpha} \\
4f_{\frac{7}{2}}\tfrac{1}{2}^{\pm} &= c_1 f^{33}_{0}\,{}^{\alpha}_{\beta} + c_2 f^{33}_{\pm 1}\,{}^{\beta}_{\alpha}\,.
\end{aligned} \tag{9.38}$$

Die mit den $\varphi_m^{nlj}$ zu bildenden Determinantenfunktionen sind völlig bestimm durch die Besetzung und durch die Angabe von $\varepsilon$ und $\tau$. Die für die Besetzung benutzte Schreibweise erläutern wir an dem Beispiel $P4f_{\frac{7}{2}}\tfrac{7}{2}^{\pm}N4f_{\frac{7}{2}}\tfrac{7}{2}^{2}\tfrac{5}{2}^{2}$. Das heißt, im Protonenteil ist von der Unterschale $4f_{\frac{7}{2}}$ ein Zustand des Paares $|m| = \frac{7}{2}$ besetzt, und zwar entweder $m = +\frac{7}{2}$ oder $m = -\frac{7}{2}$, im Neutronenteil sind in der Unterschale $4f_{\frac{7}{2}}$ die beiden Zustandspaare $|m| = \frac{7}{2}$ und $|m| = \frac{5}{2}$ voll besetzt. Die nicht angeführten drei ersten Schalen sind voll besetzt. In diesem Zustand ist $\Omega = \pm\frac{7}{2}$ und $w = -1$. Die für die Darstellung des Grundzustandes benötigten Determinanten bezeichnen wir nicht durch die Angabe dreier Zahlen $\Omega$, $w$, $r$, sondern halten sie durch einen einzigen Index auseinander.

## 10. Aufsuchen der approximativen Basisfunktion niedrigster Energie

### 10.1. POTENTIELLER UND KINETISCHER ANTEIL DER MITTELENERGIE, BEDEUTUNG VON $\langle\Gamma''_0\rangle_{\varepsilon=0}$

Für gegebenes $\Phi_\Omega^{wr}$ ist der potentielle Anteil der Mittelenergie nach (8.6), (8.7), (2.3) ... (2.5), wenn man erlaubterweise

$$\langle\gamma'_0\rangle = \frac{\langle\Gamma''_0\rangle}{\langle\Gamma\rangle} \tag{10.1}$$

setzt,

$$E_m^{pot} = \tfrac{1}{2}M\omega^2\langle\Gamma\rangle\{1-\zeta(2-\zeta)\langle\gamma'_0\rangle^2\}. \tag{10.2}$$

Dieser Ausdruck hat ein Minimum bei $\zeta = 1$ und geht bei Ersatz von $\zeta$ durch $2-\zeta$ in sich über. Mit (9.29) ergibt sich weiter

$$\langle\Gamma\rangle = \langle\Gamma\rangle_{\varepsilon=0}+2\varepsilon\langle\Gamma'_0\rangle_{\varepsilon=0}+\varepsilon^2\{\langle\Gamma\rangle_{\varepsilon=0}+3\langle\Gamma'_0\rangle_{\varepsilon=0}\}, \tag{10.3}$$

$$\langle\Gamma'_0\rangle = \langle\Gamma'_0\rangle_{\varepsilon=0}+\varepsilon\{\langle\Gamma\rangle_{\varepsilon=0}+\langle\Gamma'_0\rangle_{\varepsilon=0}\}+\tfrac{1}{2}\varepsilon^2\{3\langle\Gamma\rangle_{\varepsilon=0}+5\langle\Gamma'_0\rangle_{\varepsilon=0}\}. \tag{10.4}$$

Bildet man mit diesen beiden Formeln $\langle\gamma'_0\rangle$ nach (10.1) bis zum Glied mit $\varepsilon^2$ und beschränkt sich im Koeffizienten von $\varepsilon$ auf Glieder höchstens zweiten und im Koeffizienten von $\varepsilon^2$ auf Glieder höchstens ersten Grades in $\langle\gamma'_0\rangle_{\varepsilon=0}$, so wird, wenn man noch anstelle von $\zeta$ die Größe

$$\xi = 1-\zeta \tag{10.5}$$

einführt, der endgültige Wert

$$E_m^{pot} = \tfrac{1}{2}M\omega^2\langle\Gamma\rangle_{\varepsilon=0}\{1-(1-\xi^2)\langle\gamma'_0\rangle^2_{\varepsilon=0}+2\varepsilon[\xi^2\langle\gamma'_0\rangle_{\varepsilon=0}-(1-\xi^2)\langle\gamma'_0\rangle^2_{\varepsilon=0}] \\ +\varepsilon^2[\xi^2-(2-5\xi^2)\langle\gamma'_0\rangle_{\varepsilon=0}]\}. \tag{10.6}$$

Zur Berechnung des kinetischen Anteils der Mittelenergie für gegebenes $\Phi_D^{wr}$ führen wir die Größen

$$Q = \sum_\nu |\mathfrak{p}_\nu|^2, \quad Q'_0 = \sum_\nu \{p'^2_{\nu 3}-\tfrac{1}{2}(p'^2_{\nu 1}+p'^2_{\nu 2})\} \tag{10.7}$$

ein, die aus $\Gamma$ und $\Gamma''_0$ durch Ersatz der Lagekoordinaten durch die Impulse hervorgehen. Nach (9.29) ist dann

$$\langle Q\rangle = \langle Q\rangle_{\varepsilon=0}-2\varepsilon\langle Q'_0\rangle_{\varepsilon=0}+\varepsilon^2\{\langle Q\rangle_{\varepsilon=0}-\langle Q'_0\rangle_{\varepsilon=0}\}. \tag{10.8}$$

Es läßt sich aber zeigen, daß für jede aus Eigenfunktionen zum Oszillatorpotential gebildete Slaterdeterminante die Beziehungen

$$\frac{1}{2M}\langle Q\rangle_{\varepsilon=0} = \frac{M\omega^2}{2}\langle\Gamma\rangle_{\varepsilon=0}, \quad \frac{1}{2M}\langle Q'_0\rangle_{\varepsilon=0} = \frac{M\omega^2}{2}\langle\Gamma'_0\rangle_{\varepsilon=0} \tag{10.9}$$

bestehen. Dann ist nach (10.7) ... (10.9)

$$E_m^{kin} = \tfrac{1}{2}M\omega^2\{\langle\Gamma\rangle_{\varepsilon=0}-2\varepsilon\langle\Gamma'_0\rangle_{\varepsilon=0}+\varepsilon^2(\langle\Gamma\rangle_{\varepsilon=0}-\langle\Gamma''_0\rangle_{\varepsilon=0})\}. \tag{10.10}$$

Für $\zeta = 0$, $\varepsilon = 0$ ist bei der zugrundegelegten Besetzung

$$E_m^{pot} = E_m^{kin} = \tfrac{1}{2}M\omega^2\langle\Gamma\rangle_{\varepsilon=0} = \tfrac{285}{4}\hbar\omega. \tag{10.11}$$

Die für $\zeta \neq 0$, $\varepsilon \neq 0$ eintretenden Energieänderungen $\Delta E_m^{pot}$ und $\Delta E_m^{kin}$ schreiben wir in der Form

$$\frac{\Delta E_m^{pot}}{\tfrac{1}{2}M\omega^2\langle\Gamma\rangle_{\varepsilon=0}} = -(1-\xi^2)\langle\gamma'_0\rangle^2_{\varepsilon=0}+2\varepsilon[\xi^2\langle\gamma'_0\rangle_{\varepsilon=0}-(1-\xi^2)\langle\gamma'_0\rangle^2_{\varepsilon=0}] \\ +\varepsilon^2[\xi^2-(2-5\xi^2)\langle\gamma'_0\rangle_{\varepsilon=0}], \tag{10.12}$$

$$\frac{\Delta E_m^{kin}}{\frac{1}{2}M\omega^2\langle\Gamma\rangle_{\varepsilon=0}} = -2\varepsilon\langle\gamma'_0\rangle_{\varepsilon=0}+\varepsilon^2[1-\langle\gamma'_0\rangle_{\varepsilon=0}]. \tag{10.13}$$

Beide Ausdrücke sind als Funktionen von $\varepsilon$ Parabeln. Die zweite geht durch den Nullpunkt und hat bei

$$\varepsilon = \frac{\langle\gamma'_0\rangle_{\varepsilon=0}}{1-\langle\gamma'_0\rangle_{\varepsilon=0}} \tag{10.14}$$

ein Minimum mit dem Wert

$$\left(\frac{\Delta E_m^{kin}}{\frac{1}{2}M\omega^2\langle\Gamma\rangle_{\varepsilon=0}}\right)_{min} = -\frac{\langle\gamma'_0\rangle^2_{\varepsilon=0}}{1-\langle\gamma'_0\rangle_{\varepsilon=0}}. \tag{10.15}$$

Die erste Parabel schneidet die Ordinatenachse bei $\xi^2 < 1$ unterhalb des Nullpunktes und verläuft für den vornehmlich in Betracht kommenden Fall $\xi \approx 0$ wegen der Kleinheit von $|\langle\gamma'_0\rangle_{\varepsilon=0}|$ viel flacher als die erste. Der Verlauf von $\Delta E_m^{pot}+\Delta E_m^{kin}$ in Abhängigkeit von $\varepsilon$ wird daher bei $\xi \approx 0$ im wesentlichen durch $\Delta E_m^{kin}$ bestimmt.

Damit die Energie bei der Deformation abnimmt, müssen die Vorzeichen von $|\langle\gamma'_0\rangle_{\varepsilon=0}|$ und $\varepsilon$ übereinstimmen; der Kern muß sich so deformieren, daß die bei $\varepsilon = 0$ vorhandene Abweichung von der Kugelform vergrößert wird. Eine möglichst starke Energieabnahme bei der Deformation verlangt ein möglichst hohes $|\langle\gamma'_0\rangle_{\varepsilon=0}|$. Wir setzen voraus, für jede Unterschale sei die Anzahl der besetzten Zustände gegeben, und fragen, welche Zustände in jeder Unterschale zur Erzielung eines möglichst hohen $|\langle\gamma'_0\rangle_{\varepsilon=0}|$ besetzt werden müssen. Hierzu genügt es wegen (10.1), das höchste $|\langle\Gamma'_0\rangle_{\varepsilon=0}|$ zu suchen, da $\langle\Gamma\rangle_{\varepsilon=0}$ sich bei Umbesetzung innerhalb der Unterschalen nicht ändert. Da die gesuchte Besetzung im allgemeinen von $\tau$ abhängen wird, ist die vollständige Beantwortung der gestellten Frage zu verwickelt. Wir beschränken uns daher auf das größte $|\langle\Gamma'_0\rangle_{\varepsilon=0}|$ für $\tau = 0$ und überlegen anschließend, wie $\tau$ abzuändern ist, damit $|\langle\Gamma'_0\rangle_{\varepsilon=0}|$ noch größer wird. Das so gefundene $|\langle\Gamma'_0\rangle_{\varepsilon=0}|$ ist dann sicher das größte für eine gewisse Umgebung von $\tau = 0$. Für $\varepsilon = 0$, $\tau = 0$ werden die $\varphi_m^{njl}$ mit den $\psi_m^{njl}$ identisch, und jeder Zustand leistet zu $\langle\Gamma'_0\rangle_{\varepsilon=0}$ nach (9.6) und (B17) den Beitrag

$$(\psi_m^{njl}, r^2Y_0\psi_m^{njl}) = \frac{\hbar}{M\omega}(n+\tfrac{3}{2})\tfrac{1}{4}\left[1-\frac{3m^2}{j(j+1)}\right]. \tag{10.16}$$

Die über die besetzten $m$ gebildete Summe der Ausdrücke

$$P_m{}^j = \tfrac{1}{4}\left[1-\frac{3m^2}{j(j+1)}\right] \tag{10.17}$$

verschwindet bei vollbesetzter Unterschale. Ist $z_j$ die Anzahl der besetzten Zustände der betrachteten Unterschale, so ist der Betrag der Summe am größten, wenn bei $z_j < j+\frac{1}{2}$ die Zustände mit den größten, bei $z_j > j+\frac{1}{2}$ die

mit den kleinsten $|m|$ besetzt sind. Im ersten Fall ist die Summe positiv, im zweiten negativ. Bei $z_j = j+\frac{1}{2}$ ist der Betrag der Summe für beide Besetzungsfälle gleich, die Vorzeichen sind jedoch verschieden. Für den Kern (21, 24) ist $|\langle \Gamma'_0 \rangle_{\varepsilon=0}|$ bei der angenommenen Besetzung am größten für den Zustand

$$\Phi_1 = \mathrm{P4f}_{\frac{7}{2}}\tfrac{7}{2}{+}\mathrm{N4f}_{\frac{7}{2}}\tfrac{5}{2}^2\tfrac{7}{2}^2 \tag{10.18}$$

und dem damit durch (6.9) verknüpften Zustand vom entgegengesetzten $\Omega$, den wir aber nicht anzugeben brauchen. Bei beliebigem $\tau$ setzt sich $\langle \Gamma'_0 \rangle_{\varepsilon=0}$ aus Gliedern

$$(f^{nl}_{m_l}, r^2 Y_0 f^{nl}_{m_l}) = \frac{\hbar}{M\omega}(n+\tfrac{3}{2})\frac{l(l+1)-3m_l^2}{(2l+3)(2l-1)} \tag{10.19}$$

zusammen. Maßgebend für den Anteil einer Unterschale zu $\langle \Gamma'_0 \rangle_{\varepsilon=0}$ sind dann die Ausdrücke

$$P^l_{m_l} = \frac{l(l+1)-3m_l^2}{(2l+3)(2l-1)}. \tag{10.20}$$

Jedes $P^l_{m_l}$ wird mit dem Gewicht, mit dem $f^{nl}_{m_l}$ in den besetzten Zuständen der Unterschale auftritt, multipliziert, dann wird über $m_l$ summiert. Bei vollbesetzter Unterschale verschwindet die Summe nur für $\tau = 0$, die Summe über beide Unterschalen, die aus dem gleichen $l$ durch verschiedene Spin-Bahn-Kopplung hervorgehen, verschwindet dagegen für beliebiges $\tau$.

Für den Zustand $\Phi_1$ ist

$$\begin{aligned}
\langle \Gamma \rangle &= \frac{\hbar}{M\omega}\left\{\frac{285}{2} - (15-6a_1^2)\varepsilon + (360+9a_1^2)\varepsilon^2\right\} \\
\langle \Gamma'_0 \rangle &= \frac{\hbar}{M\omega}\left\{-\tfrac{15}{2} + 3a_1^2 + (135+3a_1^2)\varepsilon + (195+\tfrac{15}{2}a_1^2)\varepsilon^2\right\} \qquad (10.21)\\
\langle \gamma'_0 \rangle_{\varepsilon=0} &= -0.0346 \quad \text{für} \quad \tau = 0 \\
&= -0.0526 \quad \text{für} \quad \tau = -1.
\end{aligned}$$

Das damit berechnete $\Delta E^{\mathrm{pot}}_{\mathrm{m}} + \Delta E^{\mathrm{kin}}_{\mathrm{m}}$ ist in Fig. 2 dargestellt.

Der Vergleich von (10.17) und (10.20) zeigt, daß der Fall $l = 1$ ausgezeichnet ist. Es gilt nämlich

$$|P^j_{\frac{1}{2}}| < |P^j_j| \quad \text{für} \quad j \geqq \tfrac{5}{2}, \quad |P^{\frac{1}{2}}_{\frac{1}{2}}| = |P^{\frac{3}{2}}_{\frac{1}{2}}|, \tag{10.22}$$

dagegen

$$|P^l_0| < |P^l_l| \quad \text{für} \quad l \geqq 3, \quad |P^2_0| = |P^2_2|, \quad |P^1_0| > |P^1_1|. \tag{10.23}$$

### 10.2. SPIN-BAHN-ANTEIL DER MITTELENERGIE, ABKOPPLUNGSGRAD, FESTLEGUNG VON $\hbar\omega$

Wir gehen aus von dem durch (8.6) allgemein bestimmten Mittelpotential und setzen zur Abkürzung

$$\mathbf{v} = \mathbf{p} \times \mathrm{grad}\, \bar{V}. \tag{10.24}$$

Der mit irgendeinem $\varphi_m^{nlj}$ gebildete Erwartungswert des Spin-Bahn-Gliedes wird dann, da die $b$ reell sind,

$$\frac{\lambda}{M^2c^2}\langle \mathbf{s}\cdot\mathbf{p}\times\operatorname{grad}\bar{V}\rangle = \frac{\lambda\hbar}{2M^2c^2}\{2b^{jl}_{mm-\frac{1}{2}}b^{jl}_{mm+\frac{1}{2}}\operatorname{Re}(\bar{f}^{nl}_{m-\frac{1}{2}}, v'_q\bar{f}^{nl}_{m+\frac{1}{2}}) + (b^{jl}_{mm-\frac{1}{2}})^2(\bar{f}^{nl}_{m-\frac{1}{2}}, v'_3\bar{f}^{nl}_{m-\frac{1}{2}}) - (b^{jl}_{mm+\frac{1}{2}})^2(\bar{f}^{nl}_{m+\frac{1}{2}}, v'_3\bar{f}^{nl}_{m+\frac{1}{2}}). \tag{10.25}$$

In $\mathbf{v}$ wird das $\bar{V}$ des Oszillatorpotentials eingesetzt und folgender Ausdruck gebildet:

$$\begin{aligned} v'_q\bar{\chi}_{n_1n_2n_3} = {} & M\omega^2\hbar\{\sqrt{n_1(n_3+1)}\,\bar{\chi}_{n_1-1n_2n_3+1} - i\sqrt{n_2(n_3+1)}\,\bar{\chi}_{n_1n_2-1n_3+1} \\ & -\sqrt{n_3(n_1+1)}\,\bar{\chi}_{n_1+1n_2n_3-1} + i\sqrt{n_3(n_2+1)}\,\bar{\chi}_{n_1n_2+1n_3-1}\} \\ & \cdot\{1-\tfrac{1}{2}\zeta\langle\gamma'_0\rangle+\zeta^2\langle\gamma'_0\rangle^2-\tfrac{9}{4}\varepsilon\zeta\langle\gamma'_0\rangle+\tfrac{9}{8}\varepsilon^2\} \\ & +M\omega^2\hbar\{\sqrt{n_1n_2}\,\bar{\chi}_{n_1-1n_2n_3-1} - i\sqrt{n_2n_3}\,\bar{\chi}_{n_1n_2-1n_3-1} \\ & -\sqrt{(n_1+1)(n_3+1)}\,\bar{\chi}_{n_1+1n_2n_3+1} + i\sqrt{(n_2+1)(n_3+1)}\,\bar{\chi}_{n_1n_2+1n_3+1}\} \\ & \cdot\{-\tfrac{3}{2}\zeta\langle\gamma'_0\rangle+\tfrac{3}{2}\varepsilon-\tfrac{3}{4}\varepsilon\zeta\langle\gamma'_0\rangle+\tfrac{1}{2}\varepsilon^2\}. \end{aligned} \tag{10.26}$$

Da bei der Deformation die Anteile der $\bar{\chi}_{n_1n_2n_3}$ in den $\bar{f}^{nl}_{m_l}$ sich nicht ändern, ist

$$\begin{aligned} & (\bar{f}^{nl}_{m-\frac{1}{2}}, v'_q\bar{f}^{nl}_{m+\frac{1}{2}}) \\ & \quad = \{1-\tfrac{1}{2}\zeta\langle\gamma'_0\rangle+\zeta^2\langle\gamma'_0\rangle^2-\tfrac{9}{4}\varepsilon\zeta\langle\gamma'_0\rangle+\tfrac{9}{8}\varepsilon^2\}(f^{nl}_{m-\frac{1}{2}}, v'_qf^{nl}_{m+\frac{1}{2}})_{\zeta=0} \end{aligned} \tag{10.27}$$

und darin für $\varepsilon = 0$, $\zeta = 0$

$$v'_qf^{nl}_{m_l} = -M\omega^2l'_qf^{nl}_{m_l} = -M\omega^2\hbar\sqrt{(l+m_l)(l-m_l+1)}\,f^{nl}_{m_l-1}. \tag{10.28}$$

Weiter ist

$$v'_3 = -M\omega^2l'_3\{1+\zeta\langle\gamma'_0\rangle+\zeta^2\langle\gamma'_0\rangle^2\}. \tag{10.29}$$

Drückt man die $b$ nach (9.35) durch die $c$ und $\tau$ aus und setzt für die $c$ die Werte (B16) ein, so ergibt sich bei Entwicklung bis zu $\varepsilon$ und $\zeta\langle\gamma'_0\rangle$ für $j = l+\frac{1}{2}$

$$\begin{aligned} \frac{\lambda}{M^2c^2}\langle \mathbf{s}\cdot\mathbf{p}\times\operatorname{grad}\bar{V}\rangle = {} & -\frac{\lambda\hbar^2\omega^2}{2Mc^2}\Bigg\{j-\tfrac{1}{2}-2\tau^2\frac{j^2-m^2}{j(1+\tau^2)+2|m|\tau} \\ & +\frac{\tfrac{1}{2}[3m^2-j(j+1)]+2\tau|m|(j-\tfrac{1}{2})+\tfrac{1}{2}\tau^2[m^2+j(j-1)]}{j(1+\tau^2)+2\tau|m|}\zeta(\langle\gamma'_0\rangle_{\varepsilon=0}+\varepsilon)\Bigg\} \end{aligned} \tag{10.30}$$

und für $j = l-\frac{1}{2}$

$$\begin{aligned} \frac{\lambda}{M^2c^2}\langle \mathbf{s}\cdot\mathbf{p}\times\operatorname{grad}\bar{V}\rangle = {} & +\frac{\lambda\hbar^2\omega^2}{2Mc^2}\Bigg\{j+\tfrac{3}{2}-2\tau^2\frac{(j+1)^2-m^2}{(j+1)(1+\tau^2)+2|m|\tau} \\ & +\frac{\tfrac{1}{2}[3m^2-j(j+1)]+2\tau|m|(j+\tfrac{3}{2})+\tfrac{1}{2}\tau^2[m^2+(j+1)(j+2)]}{(j+1)(1+\tau^2)+2\tau|m|}\zeta(\langle\gamma'_0\rangle_{\varepsilon=0}+\varepsilon)\Bigg\}. \end{aligned} \tag{10.31}$$

Das gesamte Spin-Bahn-Glied $E_m^{SB}$ der Mittelenergie für gegebenes $\Phi_\Omega^{\varkappa\tau}$ folgt aus (10.30) durch Summation über die besetzten Zustände von $4f_{\frac{7}{2}}$;

die ersten drei Schalen leisten keinen Beitrag. Damit die gegenüber $\tau = 0$, $\zeta = 0$ eintretende Änderung $\Delta E_m^{SB}$ möglichst klein wird, muß $\tau \approx 0$ sein. Trifft das nicht zu, so müssen möglichst die Zustände mit den höchsten $|m|$ besetzt sein, da das Glied mit $\tau^2$ in (10.30) mit steigendem $|m|$ abnimmt. Das steht bei höchstens bis zur Hälfte besetzten Unterschalen mit der Forderung nach möglichst kleinem $\Delta E_m^{pot} + \Delta E_m^{kin}$ in Einklang und ist bei $\Phi_1$ erfüllt. Im Gegensatz zu $\Delta E_m^{SB}$ verlangt $\Delta E_m^{pot} + \Delta E_m^{kin}$ $\tau = -1$ für $\Phi_1$. Das Minimum der gesamten Mittelenergie liegt daher bei $-1 < \tau < 0$.

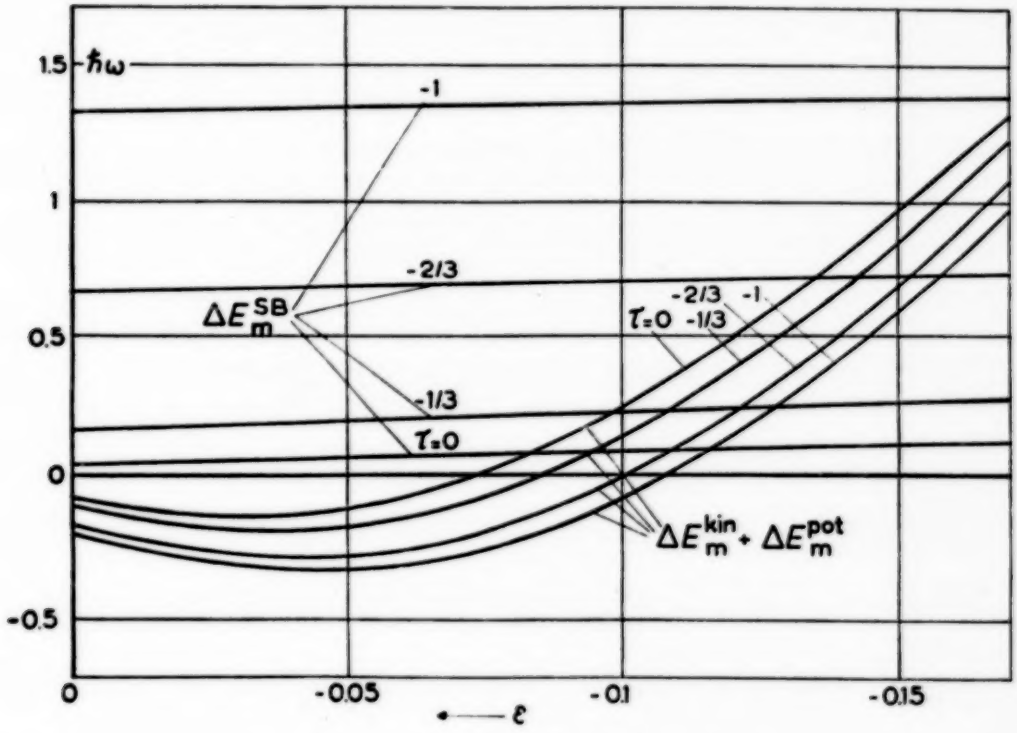


Fig. 2. Mittelenergie im Zustand $\Phi_1$ für $\zeta = 1$.

Der Vergleich der Spin-Bahn-Kopplungsenergie mit den anderen Energietermen erfordert Festlegung eines Wertes für $\lambda\hbar\omega/Mc^2$. Wir setzen $\lambda = 20$ und bestimmen $\hbar\omega$ aus dem Kernradius, für den wir

$$R_0 = 1.3 \times 10^{-13} A^{\frac{1}{3}} \text{ cm} = 6.18\, A^{\frac{1}{3}} \frac{\hbar}{M\omega} \tag{10.32}$$

annehmen. Definiert man $R_0$ durch

$$R_0 = \sqrt{\frac{5}{3}\frac{1}{A}\langle \Gamma \rangle}, \tag{10.33}$$

so wird mit dem aus (10.21) für $\varepsilon = 0$ zu entnehmenden $\langle \Gamma \rangle$

$$\hbar\omega = 10.9\,\mathrm{TME}, \tag{10.34}$$

und bei Zugrundelegung dieses Wertes ergibt sich

$$\lambda \frac{\hbar\omega}{Mc^2} = 0.218. \tag{10.35}$$

Das damit für $\zeta = 1$ berechnete $\Delta E_{\mathrm{m}}^{\mathrm{SB}}$ ist in Fig. 2 dargestellt. Man sieht, daß der Einfluß der Verformung unbedeutend ist. Das wichtigste Glied in (10.30) und (10.31) ist daher das mit $\tau^2$. Es hat für die beiden Kopplungsfälle entgegengesetztes Vorzeichen, und sein Betrag nimmt mit steigendem $|m|$ ab. Das gesamte $\Delta E_{\mathrm{m}}$ ist in Fig. 6 aufgezeichnet.

### 10.3. SCHWANKUNGSENERGIE

In (8.9) kann man mit der gleichen Begründung, die auf (8.13) führte, setzen

$$E_{\mathrm{s}} = -\tfrac{1}{2}(1-\xi^2)\,\frac{M\omega^2}{\langle\Gamma\rangle}\sum_m \{\langle|\Gamma''_m|^2\rangle - \delta_{m0}\langle\Gamma''_0\rangle^2\}. \tag{10.36}$$

Die Vernachlässigung des Spin-Bahn-Anteils ist gestattet, weil hierzu nur die fünf Nukleonen in $4f_{\frac{7}{2}}$ beitragen und dieser Anteil den kleinen Faktor $\lambda\hbar\omega/Mc^2$ trägt; die Berechtigung zum Fortlassen folgt auch aus der in Fig. 2 zum Ausdruck kommenden schwachen Abhängigkeit gegen Verformungen.

Die Glieder in der Summe von (10.36) hängen nur wenig von der Art der Besetzung von $4f_{\frac{7}{2}}$ ab, da der Hauptanteil zu ihnen von den vollbesetzten ersten drei Schalen herrührt. Die Abhängigkeit vom Zustand ist bei der Mittelenergie und vor allem bei der noch zu besprechenden Zwangsenergie viel größer, so daß $E_{\mathrm{s}}$ beim Aufsuchen des tiefsten Zustandes keine entscheidende Bedeutung hat.

Für den Zustand $\Phi_1$ ist

$$\begin{aligned}
\langle\Gamma''^2_0\rangle - \langle\Gamma''_0\rangle^2 &= \left(\frac{\hbar}{M\omega}\right)^2 \{\tfrac{135}{2} + 6a_1^2 - \tfrac{9}{2}a_1^4 + (120 + 18a_1^2 - 9a_1^4)\varepsilon \\
&\qquad + (510 + 51a_1^2 - 27a_1^4)\varepsilon^2\} \\
\langle|\Gamma''_1|^2\rangle &= \left(\frac{\hbar}{M\omega}\right)^2 75(1+\varepsilon+\tfrac{3}{2}\varepsilon^2) \\
\langle|\Gamma''_2|^2\rangle &= \left(\frac{\hbar}{M\omega}\right)^2 (\tfrac{345}{4} - 3a_1^2)(1-2\varepsilon).
\end{aligned} \tag{10.37}$$

Die einzelnen Glieder zeigen eine Abhängigkeit von $\varepsilon$, doch hebt sich diese in der Summe nahezu heraus, wie das in Fig. 6 aufgezeichnete $E_{\mathrm{s}}$ zeigt.

### 10.4. MATRIXELEMENTE DES REZIPROKEN TRÄGHEITSTENSORS

Zur Berechnung von $\langle\Theta'_{pq}\rangle$ für gegebenes $\Phi_\Omega^{wr}$ setzen wir in (7.3) in dem Ausdruck für $\Theta'_{pq}$ vor der geschweiften Klammer

$$\frac{1}{\Gamma_0'^2} = \frac{1}{\langle\Gamma'_0\rangle^2}\left\{1-2\frac{\Gamma'_0-\langle\Gamma'_0\rangle}{\langle\Gamma'_0\rangle}+3\left(\frac{\Gamma'_0-\langle\Gamma'_0\rangle}{\langle\Gamma'_0\rangle}\right)^2\right\} \tag{10.38}$$

und beschränken uns auf Glieder erster Ordnung in den Schwankungsgrößen $(|\Gamma'_m|^2-\delta_{m0}\langle\Gamma'_0\rangle^2)/\langle\Gamma'_0\rangle^2$; diese Verabredung verlangt bei den in der geschweiften Klammer von $\Theta'_{pq}$ in (7.3) stehenden $|\Gamma'_2|^2/\Gamma_0'^2$ und $|\Gamma'_1|^2/\Gamma_0'^2$ Ersatz von $\Gamma'_0$ durch $\langle\Gamma'_0\rangle$. Wegen der Kleinheit von $\langle\Gamma'_0\rangle$ gegen $\langle\Gamma\rangle$ vernachlässigen wir auch die Produkte von $\langle\Gamma'_0\rangle$ mit den Schwankungsgrößen, ausgenommen das stärker ins Gewicht fallende $\Gamma'_0|\Gamma'_2|^2/\langle\Gamma'_0\rangle^2$. Bei Ersatz der Erwartungswerte der Produkte von $\Gamma$ oder $\Gamma'_0$ mit den Schwankungsgrößen durch die Produkte der Erwartungswerte ergibt sich dann

$$\langle\Theta'_{pq}\rangle = \frac{4}{3M\langle\Gamma'_0\rangle^2}\left\{\langle\Gamma\rangle\left(1+3\frac{\langle\Gamma_0'^2\rangle-\langle\Gamma'_0\rangle^2}{\langle\Gamma'_0\rangle^2}-\frac{7}{3}\frac{\langle|\Gamma'_1|^2\rangle}{\langle\Gamma'_0\rangle^2}+2\frac{\langle|\Gamma'_2|^2\rangle}{\langle\Gamma'_0\rangle^2}\right)\right.$$
$$\left.+\tfrac{1}{2}\langle\Gamma'_0\rangle\left(1+6\frac{\langle|\Gamma'_2|^2\rangle}{\langle\Gamma'_0\rangle^2}\right)\right\} \tag{10.39}$$

und in der gleichen Weise

$$\langle\Theta'_{33}\rangle = \frac{4}{9M\langle\Gamma'_0\rangle^2}\langle\Gamma\rangle\frac{\langle|\Gamma'_1|^2\rangle}{\langle\Gamma'_0\rangle^2}. \tag{10.40}$$

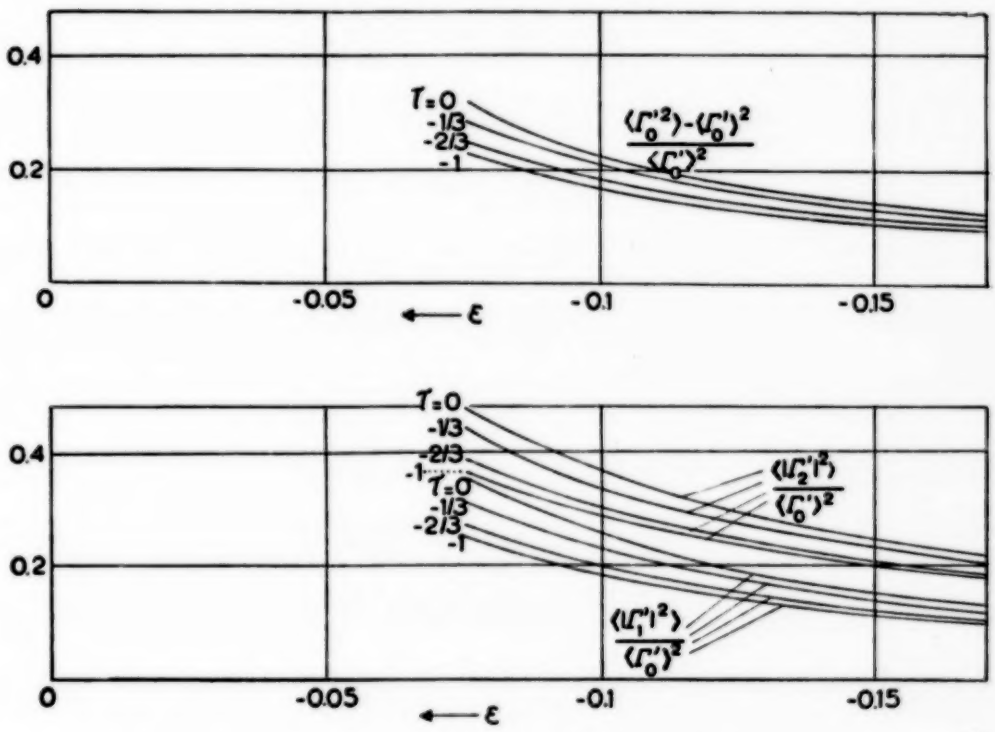


Fig. 3. Schwankungsgrößen im Zustand $\Phi_1$.

Die errechneten Ausdrücke für $\langle \Theta'_{pq} \rangle$ und $\langle \Theta'_{33} \rangle$ verlangen Kleinheit der Schwankungsgrößen, also genügend großes $|\langle \Gamma'_0 \rangle|$ und daher nicht zu kleines $|\varepsilon|$. Der Ausdruck für $\langle \Theta'_{33} \rangle$ ist ungenauer, aber auch wesentlich kleiner als der für $\langle \Theta'_{pq} \rangle$. Die Schwankungsgrößen sind in Fig. 3, die reziproken Trägheitsmomente in Fig. 4 dargestellt.

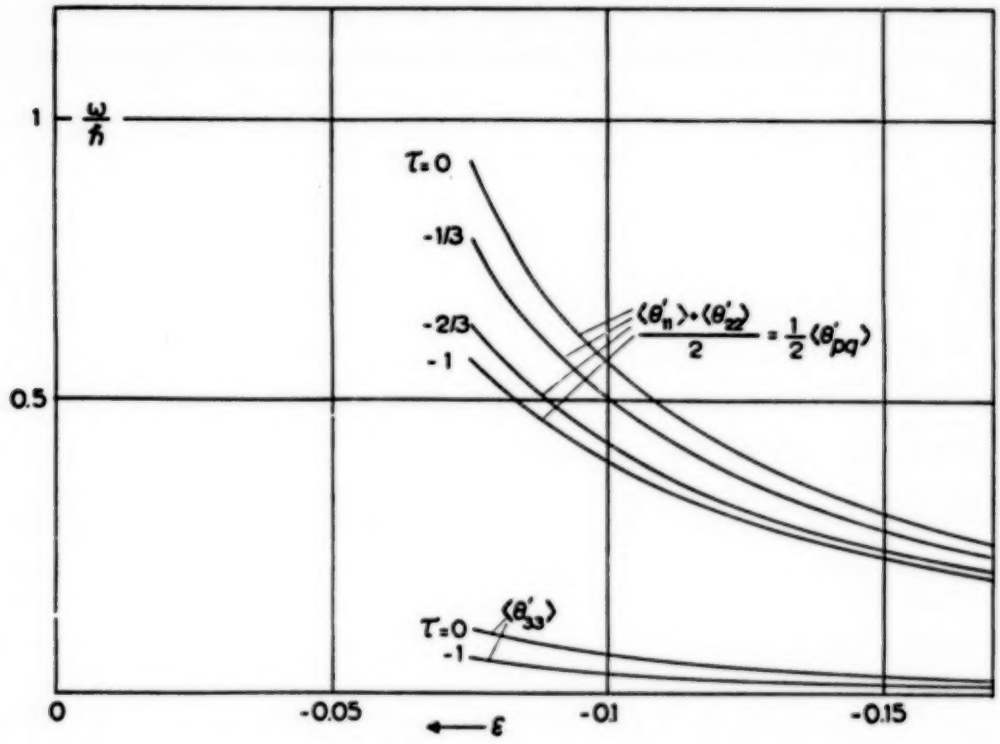


Fig. 4. Reziproke Trägheitsmomente im Zustand $\Phi_1$.

Die Nichtdiagonalelemente von $\Theta'_{pq}$ sind klein gegen die Diagonalelemente, wie man auf Grund allgemeiner Überlegungen und Abschätzungen folgern kann. Daß auch die Matrixelemente der anderen Komponenten klein sind, ist aus dem Fehlen von Gliedern nullten Grades in $\Gamma'_{\pm 1}/\Gamma'_0$, $\Gamma'_{\pm 2}/\Gamma'_0$ in (7.3) zu schließen und wird durch Rechnungen bestätigt. Es erweist sich als konsequent, in allen Ausdrücken, die $\Theta$ enthalten, nur die Diagonalelemente von $\Theta'_{pq}$ und $\Theta'_{33}$ zu berücksichtigen.

Die Zahlwerte von $\langle \Theta'_{pq} \rangle$ sind etwa die gleichen wie bei der wirbelfreien Strömung einer inkompressibelen Flüssigkeit [21, 22]). Daraus darf aber nicht auf zu große Termabstände bei den Rotationsspektren geschlossen werden, denn $\mathscr{H}_{1a}$ ergibt in zweiter störungstheoretischer Näherung einen negativen Beitrag, der nach (8.26) proportional zu $J/(J+1)$ ist †.

† Siehe 12.

### 10.5. ZWANGSENERGIE, ZERLEGUNG UND ERSTES GLIED, BEDEUTUNG VON $\langle \Gamma'_0 \rangle_{\varepsilon=0}$ UND $\langle J'_\varrho J'_\sigma + J'_\sigma J'_\varrho \rangle_{\varepsilon=0}$

Den Zwangsoperator (8.5) kann man nach (4.21) und (4.19) schreiben

$$\mathscr{H} = \tfrac{1}{2}\Theta \cdot\cdot \mathbf{J}^2 - \mathbf{W}_T \cdot \mathbf{J} - \mathbf{W}_S \cdot \mathbf{J}. \tag{10.41}$$

Die Zwangsenergie wird dadurch in drei Teile zerlegt. Im ersten berücksichtigen wir nur die Produkte der Erwartungswerte der Komponenten von $\Theta$ und $\mathbf{J}^2$, setzen also mit (A5) für gegebenes $\Phi_\Omega^{wr}$

$$\tfrac{1}{2}\langle \Theta \cdot\cdot \mathbf{J}^2 \rangle = \tfrac{1}{8}\langle \Theta'_{\varrho\sigma} \rangle \langle J'_\varrho J'_\sigma + J'_\sigma J'_\varrho \rangle + \tfrac{1}{2}\langle \Theta'_{33} \rangle \langle J'^2_3 \rangle. \tag{10.42}$$

Zur Rechtfertigung der begangenen Vernachlässigungen bemerken wir, daß in der Entwicklung

$$\langle \Theta_{\varrho\sigma}(J'_\varrho J'_\sigma + J'_\sigma J'_\varrho) \rangle = \sum_k (\Phi_1, \Theta'_{\varrho\sigma}\Phi_k)(\Phi_k, [J'_\varrho J'_\sigma + J'_\sigma J'_\varrho]\Phi_1) \tag{10.43}$$

die Glieder mit $k \neq 1$ klein gegen die mit $k = 1$ sind und daß diese Kleinheit, wie Abschätzungen zeigen, anscheinend nicht durch die hohe Zahl der Summanden aufgehoben wird. Das Fortlassen der Glieder mit $\Theta'_{\varrho\varrho}$, $\Theta'_{\sigma\sigma}$, $\Theta'_{\varrho 3}$, $\Theta'_{\sigma 3}$ ergibt, groben Rechnungen zufolge, keinen nennenswerten Fehler. Es erscheint nicht folgerichtig, das verhältnismäßig kleine Glied mit $\langle \Theta'_{33} \rangle$ zu berücksichtigen. Dieses kommt aber außerdem in $E_a$ und, versehen mit dem Faktor $-2$, in $E_{1a}$ vor; hebt sich also in der Gesamtenergie heraus und beeinflußt nur deren Aufteilung in $E_1$, $E_a$, $E_{1a}$. Da sein Fortlassen merkliche Fehler in $E_a$ und $E_{1a}$ verursachen würde, wird es in allen drei Energietermen berücksichtigt.

Das in (10.42) auftretende $\langle J'_\varrho J'_\sigma + J'_\sigma J'_\varrho \rangle$ besteht aus zwei Gliedern. Das erste, $\langle J'_\varrho J'_\sigma + J'_\sigma J'_\varrho \rangle_{\varepsilon=0}$, hängt stark von der Verteilung der Nukleonen auf die Zustände der teilbesetzten Unterschalen und im allgemeinen auch von $\tau$ ab. Das zweite Glied ist proportional zu $\varepsilon^2$ und ändert sich nicht wesentlich, weil der Hauptanteil von den ersten drei Schalen herrührt. Es bringt zum Ausdruck, daß die Nukleonen bei Deformation des Kerns stärker auf einen gewissen Winkelbereich lokalisiert werden, so daß die entsprechenden Drehimpulsquadrate zunehmen. Für den Zustand $\Phi_1$ ist

$$\langle J'_\varrho J'_\sigma + J'_\sigma J'_\varrho \rangle = \hbar^2\{31 + (180 + 36a_1^2)\varepsilon^2\}. \tag{10.44}$$

Ein möglichst kleiner Wert von (10.42) verlangt ein möglichst kleines $\langle \Theta'_{\varrho\sigma} \rangle$; das erfordert nach (10.39) und (10.4) ein möglichst großes $|\langle \Gamma''_0 \rangle_{\varepsilon=0}|$ und führt ebenfalls auf $\Phi_1$. Beim Aufsuchen der Zustandsdeterminante mit dem niedrigsten $\langle J'_\varrho J'_\sigma + J'_\sigma J'_\varrho \rangle_{\varepsilon=0}$ beschränken wir uns auf $\tau = 0$; der so aufgefundene Zustand ist dann sicher auch in einer gewissen Umgebung von $\tau = 0$ der mit dem kleinsten $\langle J'_\varrho J'_\sigma + J'_\sigma J'_\varrho \rangle_{\varepsilon=0}$. Unter Benutzung von (D14) ergibt sich

$$\langle J'_\nu J'_\varrho + J'_\varrho J'_\nu \rangle_{\substack{\varepsilon=0 \\ \tau=0}} = 2\hbar^2 \Big\{ \sum_m [j(j+1) - m^2] - \sum_m \sum_{m'} (j-m)(j+m+1)\delta_{mm'-1} \Big\}. \quad (10.45)$$

Die Summe erstreckt sich über die besetzten Zustände $m$ und $m'$ der teilbesetzten Unterschalen. Der Zustand $\Phi_1$ zeichnet sich dadurch aus, daß (10.45) für ihn ein relatives Minimum hat. Damit meinen wir, daß bei Verschiebung eines Nukleons oder einiger weniger Nukleonen auf benachbarte Plätze der Wert von (10.45) zunimmt. Das ist stets der Fall, wenn die Nukleonen entweder auf die höchsten oder die niedrigsten $|m|$ zusammengedrängt sind. Der Wert $31\hbar^2$ von (10.45) für $\Phi_1$ ist aber nicht der niedrigste, den eine Zustandsdeterminante der gegebenen Unterschalenbesetzung haben kann. Dieser liegt vielmehr bei $\mathrm{P4f}_{\frac{7}{2}}{}^{\frac{7}{2}\pm}\mathrm{N4f}_{\frac{7}{2}}{}^{\frac{7}{2}+\frac{5}{2}+\frac{3}{2}+\frac{1}{2}+}$ und beträgt $23\ \hbar^2$. Aber für diesen Zustand ist auch $|\langle \Gamma''_0 \rangle_{\varepsilon=0}|$ kleiner als bei $\Phi_1$, $\langle \Theta'_{\nu\varrho} \rangle$ also größer, und die Rechnung zeigt, daß bei $-1 \leqq \tau \leqq 0$ für alle in Betracht kommenden $\varepsilon$ der Ausdruck $\langle \Theta'_{\nu\varrho} \rangle \langle J'_\nu J'_\varrho + J'_\varrho J'_\nu \rangle$ größer ist als bei $\Phi_1$. Außerdem ist die Mittelenergie größer. Das Gleiche ist der Fall für $\mathrm{P4f}_{\frac{7}{2}}{}^{\pm}\mathrm{N4f}_{\frac{7}{2}}{}^{\frac{7}{2}\frac{5}{2}+\frac{3}{2}+}$. Andererseites ist $31\ \hbar^2$ nicht der niedrigste Wert, den $\langle J'_\nu J'_\varrho + J'_\varrho J'_\nu \rangle_{\varepsilon=0}$ für einen Zustand mit $\Omega = \frac{7}{2}$ annehmen kann, sondern $7\hbar^2$. Zustände mit diesem Wert sind aber Linearkombinationen von Determinanten, deren innere Energien wegen der verschiedenen $\langle \Gamma''_0 \rangle_{\varepsilon=0}$ und $\langle J'_\nu J'_\varrho + J'_\varrho J'_\nu \rangle_{\varepsilon=0}$ wesentlich voneinander abweichen.

Die Forderung nach einem möglichst großen $|\langle \Gamma''_0 \rangle_{\varepsilon=0}|$ und einem möglichst kleinen $\langle J'_\nu J'_\varrho + J'_\varrho J'_\nu \rangle_{\varepsilon=0}$ führt also auf verschiedene Zustandsdeterminanten, aber der Einfluß von $|\langle \Gamma''_0 \rangle_{\varepsilon=0}|$ überwiegt.

### 10.6. ZWEITES GLIED DER ZWANGSENERGIE

Der mit dem Parameterpotential gebildete Hamiltonoperator

$$\mathscr{H} = \sum_\nu \left\{ \frac{1}{2M} |\mathbf{p}_\nu|^2 + V_\varepsilon(r_\nu, \vartheta_\nu) \right\} \quad (10.46)$$

gestattet eine Umformung des zu berechnenden Gliedes. In $\mathbf{W}_\mathrm{T}$ vernachlässigen wir Schwankungen der Formmomente, gehen also nach (7.4) aus von

$$\begin{aligned} W'_{\mathrm{T}\nu} &= \frac{i}{M} \left( \Pi'_{\nu 3} \frac{1}{\Gamma''_0} + \frac{1}{\Gamma''_0} \Pi'_{\nu 3} \right) \\ W'_{\mathrm{T}\varrho} &= -\frac{i}{M} \left( \Pi'_{\varrho 3} \frac{1}{\Gamma''_0} + \frac{1}{\Gamma''_0} \Pi'_{\varrho 3} \right) \\ W'_{\mathrm{T}3} &= 0 \end{aligned} \quad (10.47)$$

und ersetzen $\Gamma''_0$ durch das $\langle \Gamma''_0 \rangle$ des Zustandes $\Phi_\Omega^{\mathrm{wr}}$, für das $\langle \mathbf{W}_\mathrm{T} \cdot \mathbf{J} \rangle$ zu bilden ist. Dann sind nur noch $\langle \Pi'_{\nu 3} J'_\varrho \rangle$ und $\langle \Pi'_{\varrho 3} J'_\nu \rangle$ zu berechnen. Für

die durch (3.55) und (3.57) festgelegten Deformationsimpulse ergeben die elementaren Vertauschungsrelationen

$$\frac{1}{M}\Pi'_{p3}=\frac{i}{\hbar}\frac{1}{\sqrt{6}}[\mathscr{H}_\varepsilon, \Gamma'_{-1}]. \tag{10.48}$$

Dann wird

$$\frac{1}{M}\langle\Pi'_{p3}J'_q\rangle=\frac{i}{\hbar}\frac{1}{\sqrt{6}}\langle[\mathscr{H}_\varepsilon, \Gamma'_{-1}J'_q]+\Gamma'_{-1}[J'_q, \mathscr{H}_\varepsilon]\rangle, \tag{10.49}$$

und mit (B2) folgt unter Beachtung, daß dort **I** der Operator der infinitesimalen Drehungen des Einzelnukleons ist,

$$[J'_q, \mathscr{H}_\varepsilon]=-2\hbar\sqrt{6}\,M\omega^2\varepsilon\Gamma^*_{-1}. \tag{10.50}$$

Nach Ausführung der gleichen Rechnung für $\langle\Pi'_{q3}J'_p\rangle$ ergibt sich

$$\frac{1}{M}\{\langle\Pi'_{p3}J'_q\rangle-\langle\Pi'_{q3}J'_p\rangle\}$$
$$=i\left\{\frac{1}{\hbar\sqrt{6}}\langle[\mathscr{H}_\varepsilon, \Gamma'_{-1}J'_q+\Gamma'_{+1}J'_p]\rangle-4M\omega^2\varepsilon\langle|\Gamma'_1|^2\rangle\right\}. \tag{10.51}$$

Das Ergebnis läßt sich unter Benutzung der aus (B2) herzuleitenden Beziehung

$$[J'_p, \Gamma'_{+1}]=-\hbar\sqrt{6}\,\Gamma'_0 \tag{10.52}$$

etwas klarer fassen. Danach kann in (10.51) $\Gamma'_{+1}J'_p$ durch $J'_p\Gamma'_{+1}$ unter Hinzufügen von $[\mathscr{H}_\varepsilon, \Gamma'_0]$ unter die geschweifte Klammer ersetzt werden. Das letzte Glied ist aber wegen des verabredeten Ersatzes von $\Gamma'_0$ durch $\langle\Gamma'_0\rangle$ fortzulassen. Der entstandene Operator ist antihermitisch und läßt deswegen die Hermitizität des Kommutators dieses Operators mit $\mathscr{H}_\varepsilon$ erkennen.

Die Determinanten $\Phi^{wr}_\Omega$ sind Überlagerungen von Eigenfunktionen des Operators $\mathscr{H}_\varepsilon$, weil jede Nukleoneneinzelfunktion (9.31) die Summe zweier Eigenfunktionen mit verschiedenen Eigenwerten des in (10.46) enthaltenen Einzeloperators ist. Zur Berechnung des ersten Gliedes auf der rechten Seite von (10.51) ist $\Phi^{wr}_\Omega$ als Summe von Eigenfunktionen von $\mathscr{H}_\varepsilon$ darzustellen. Die Diagonalelemente fallen heraus, und die Nichtdiagonalelemente sind klein gegen das zweite Glied, also kann man schreiben

$$\langle\mathbf{W}_T\cdot\mathbf{J}\rangle=4M\omega^2\varepsilon\frac{\langle|\Gamma'_1|^2\rangle}{\langle\Gamma'_0\rangle}. \tag{10.53}$$

Die Berücksichtigung weiterer Glieder in $\mathbf{W}_T$ führt auf Glieder höherer Ordnung in $\Gamma'_{\pm1}/\Gamma'_0$ und $\Gamma'_{\pm2}/\Gamma'_0$. Ihr Fortlassen steht in Einklang damit, daß bei den reziproken Trägheitsmomenten auch nur Glieder höchstens zweiter Ordnung berücksichtigt wurden.

Da $\mathbf{W}_T\cdot\mathbf{J}$ nach (10.41) in $\mathscr{H}_z$ mit dem negativen Vorzeichen versehen ist,

muß der wegen des gleichen Vorzeichens von $\varepsilon$ und $\langle \Gamma'_0 \rangle$ positive Ausdruck (10.53) zur Erzielung eines möglichst kleinen $E_z$ möglichst groß, $|\langle \Gamma'_0 \rangle_{\varepsilon=0}|$ also möglichst klein sein, während $\Delta E_m$ und das erste Glied in (10.41) ein möglichst großes $|\langle \Gamma'_0 \rangle_{\varepsilon=0}|$ verlangen.

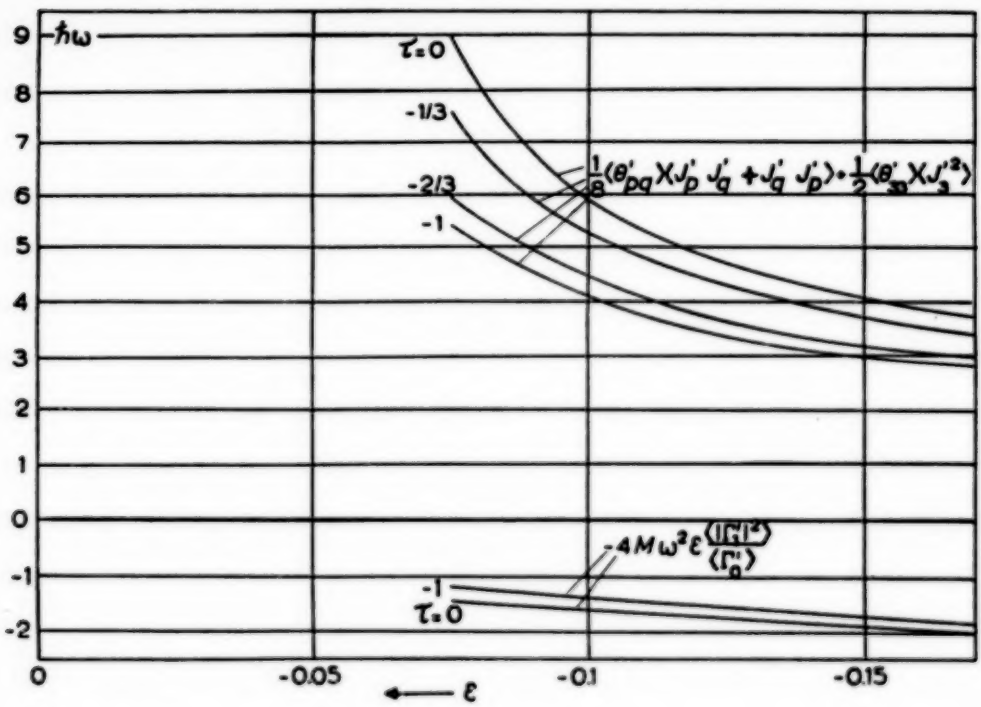


Fig. 5. Zwangsenergie im Zustand $\Phi_1$.

### 10.7. GESAMTE ZWANGSENERGIE

Da das letzte Glied in (10.41) sich als vernachlässigbar erweist, ergibt sich mit (10.42) und (10.53)

$$E_z = \tfrac{1}{8}\langle\Theta'_{pq}\rangle\langle J'_p J'_q + J'_q J'_p\rangle + \tfrac{1}{2}\langle\Theta'_{33}\rangle\langle J'^2_3\rangle - 4M\omega^2\varepsilon\frac{\langle|\Gamma'_1|^2\rangle}{\langle\Gamma'_0\rangle}. \quad (10.54)$$

In Fig. 5 sind für $\Phi_1$ die Summe aus den beiden ersten Gliedern und das letzte Glied einzeln dargestellt. Da die ersten beiden Glieder größer sind als das letzte und außerdem $\langle \Gamma'_0 \rangle$ in den ersten beiden quadratisch, im letzte nur linear vorkommt, wird das Verhalten von $E_z$ in Abhängigkeit von $\langle \Gamma'_0 \rangle$ durch die ersten beiden Glieder bestimmt. Ein möglichst kleines $E_z$ verlangt dann ein möglichst großes $|\langle \Gamma'_0 \rangle_{\varepsilon=0}|$ und ein möglichst kleines $\langle J'_p J'_q + J'_q J'_p \rangle_{\varepsilon=0}$.

### 10.8. ROTATIONSENERGIE

Nach (8.18) gilt für gegebenes $\Psi^{Jwr}_{M\Omega}$

$$E_a = \frac{\hbar^2}{4}\langle\Theta'_{pq}\rangle\{J(J+1)-\Omega^2\}+\frac{\hbar^2}{2}\langle\Theta'_{33}\rangle\Omega^2. \tag{10.55}$$

Ein möglichst kleines $E_a$ verlangt nach (10.39) und (10.40) ein möglichst großes $|\langle\Gamma'_0\rangle_{\varepsilon=0}|$ und wegen der aus Fig. 4 zu erkennenden Größenverhältnisse von $\langle\Theta'_{pq}\rangle$ und $\langle\Theta'_{33}\rangle$ außerdem $\Omega = J$.

### 10.9. ROTATIONSAUSTAUSCHENERGIE

Sie ist durch (8.24) gegeben. Wie in der Zwangsenergie vernachlässigen wir $\mathbf{W}_S$, entnehmen $\mathbf{W}_T$ aus (10.47), das dann ebenfalls fortfällt, und lassen in dem durch (4.19) gegebenen und nach (A4) zu berechnenden $\mathbf{W}_K$ die Glieder mit $\Theta'_{3p}$ und $\Theta'_{3q}$ fort. Dann ist für gegebenes $\Psi^{Jwr}_{M\Omega}$

$$E_{1a} = -\hbar^2\langle\Theta'_{33}\rangle\Omega^2. \tag{10.56}$$

Aus (10.54) ... (10.56) erkennt man, daß die Glieder mit $\langle\Theta'_{33}\rangle$ sich in der Gesamtenergie fortheben, was schon früher bemerkt wurde. Die bei (10.56) fortgelassenen Komponenten von $E_{1a}$ verursachen einen Fehler von etwa 30 %. Diese Ungenauigkeit von $E_{1a}$ wird aber relativ kleiner, wenn der Grundzustand aus mehreren approximativen Basisfunktionen aufgebaut wird, weil dann $|E_{1a}|$ größer ist.

### 10.10. APPROXIMATIVE BASISFUNKTION NIEDRIGSTER ENERGIE

Nach den vorangegangenen Rechnungen ist $\Phi_1$ die Determinantenfunktion mit dem niedrigsten

$$\Delta E_1 = \Delta E_m + E_S + E_a. \tag{10.57}$$

Für $\Phi_1$ ist $\Omega = \frac{7}{2}$. Es lassen sich daher aus $\Phi_1$ und der mit $\Phi_1$ durch (6.9) verknüpften Determinantenfunktion approximative Basisfunktionen $\Psi^{Jwr}_{M\Omega}$ mit $\Omega = \frac{7}{2}$ und $J \geqq \frac{7}{2}$ bilden. Die mit $J = \frac{7}{2}$ hat das niedrigste $E_a$ und daher auch das niedrigste

$$\begin{aligned}\Delta E &= \Delta E_1 + E_a + E_{1a}\\ &= \Delta E_1 - \frac{\hbar^2}{2}\langle\Theta'_{33}\rangle\Omega^2 + \frac{\hbar^2}{4}\langle\Theta'_{pq}\rangle\{J(J+1)-\Omega^2\}.\end{aligned} \tag{10.58}$$

Wir bezeichnen sie mit $\Psi_1$. Nach Fig. 6 liegt das Minimum von $\Delta E$ bei $\varepsilon \approx -0.145$, $\tau \approx -\frac{2}{3}$ und beträgt etwa 1.7 $\hbar\omega$. Es ist nachzuprüfen, ob $\Psi_1$ das $\Psi^{Jwr}_{M\Omega}$ mit der niedrigsten Energie überhaupt ist. Hierzu brauchen wir nur den Fall $\Omega = J$ zu betrachten. Jedes bei der gegebenen Unterschalenbesetzung mögliche $\Psi^{Jwr}_{M\Omega}$ mit $J \neq \frac{7}{2}$ ist auf einem $\Phi^{wr}_{\Omega}$ aufgebaut, dessen $|\langle\Gamma'_0\rangle_{\varepsilon=0}|$ kleiner ist als bei $\Phi_1$. Folglich sind das erste Glied rechts in (10.58) und

$\langle \Theta'_{pq} \rangle$ größer als bei $\Psi_1$. Für $J > \frac{7}{2}$ ist außerdem $J(J+1)-\Omega^2 = J$ größer, so daß $\Delta E$ sicher größer ist als bei $\Psi_1$. Für $J < \frac{7}{2}$ ist $J(J+1)-\Omega^2 = J$

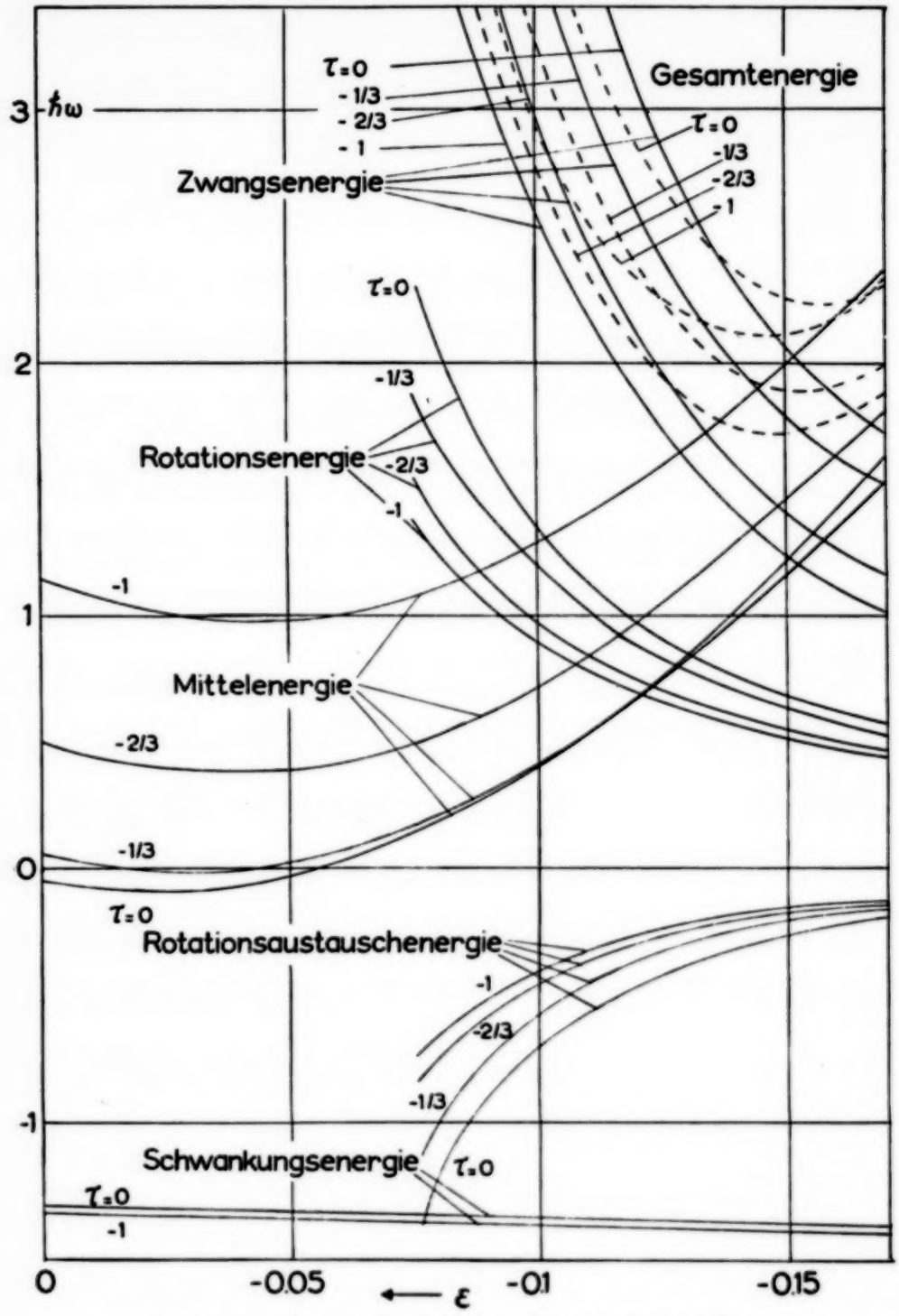


Fig. 6. Einzelenergien und Gesamtenergie im Zustand $\Psi_1$.

kleiner als bei $\Psi_1$; das zweite Glied rechts in (10.58) könnte dann vielleicht kleiner sein als bei $\Psi_1$ und womöglich die Vergrößerung des ersten übertreffen. Die Rechnung zeigt aber, daß das nicht zutrifft; das $\Psi^{Jwr}_{M\Omega}$ mit dem niedrigsten $\Delta E$ hat also den experimentellen Wert $J = \frac{7}{2}$. Eine derartige Übereinstimmung ist nicht für alle Kerne zu erwarten. Es wird beispielsweise vorkommen, daß ein $\Psi^{Jwr}_{M\Omega}$ mit $J = \Omega$ zwar das niedrigste $\Delta E_1$ und auch das richtige $J$, aber nicht das niedrigste $\Delta E$ hat und daß erst die auf dem genannten $\Psi^{Jwr}_{M\Omega}$ aufgebaute Linearkombination die mit dem niedrigsten $\Delta E$ ist.

## 11. Der Grundzustand als Linearkombination

### 11.1. ZUSÄTZLICHE APPROXIMATIVE BASISFUNKTIONEN MIT $\Omega = J$

Wir fragen jetzt, welche $\Psi^{Jwr}_{M\Omega}$ mit $\Omega = J = \frac{7}{2}$ zu $\Psi_1$ hinzuzufügen sind, um eine Verbesserung des Grundzustandes zu erreichen. Hierzu betrachten wir das vom Zwangsoperator herrührende Matrixelement

$$(\Phi_k, \Theta'_{pq}[J'_pJ'_q+J'_qJ'_p]\Phi_l)=\sum_s(\Phi_k, \Theta'_{pq}\Phi_s)(\Phi_s, [J'_pJ'_q+J'_qJ'_p]\Phi_l). \quad (11.1)$$

Wegen der Kleinheit der Nichtdiagonalelemente von $\Theta'_{pq}$ gegen die Diagonalelemente ist es besonders groß für solche Paare $\Phi_k$, $\Phi_l$, für die $(\Phi_k, [J'_pJ'_q+J'_qJ'_p]\Phi_l)$ groß, das heißt, mit $(\Phi_k, [J'_pJ'_q+J'_qJ'_p]\Phi_k)$ und $(\Phi_l, [J'_pJ'_q+J'_qJ'_p]\Phi_l)$ vergleichbar ist. Wir setzen dann näherungsweise

$$(\Phi_k, \Theta'_{pq}[J'_pJ'_q+J'_qJ'_p]\Phi_l) = (\Phi_k, \Theta'_{pq}\Phi_k)(\Phi_k, [J'_pJ'_q+J'_qJ'_p]\Phi_l). \quad (11.2)$$

In der gleichen Weise ergibt sich

$$(\Phi_k, [J'_pJ'_q+J'_qJ'_p]\Theta'_{pq}\Phi_l) = (\Phi_l, \Theta'_{pq}\Phi_l)(\Phi_k, [J'_pJ'_q+J'_qJ'_p]\Phi_l). \quad (11.3)$$

Wenn aber $(\Phi_k, [J'_pJ'_q+J'_qJ'_p)]\Phi_l)$ groß ist, so sind, wie man nachprüfen kann, die entsprechenden Matrixelemente aller Teiloperatoren in $\mathcal{H}$, die nur auf die inneren Zustände wirken, klein gegen die rechten Seiten von (11.2) und (11.3). Bildet man mit $\Phi_k$ und $\Phi_l$, die nach den Voraussetzungen gleiches $\Omega$ und $w$ haben, zwei Zustände $\Psi^{Jwr}_{M\Omega}$ mit gleichem $J$ und $M$, die wir sinngemäß mit $\Psi_k$ und $\Psi_l$ bezeichnen, so gilt dann näherungsweise für die Nichtdiagonalelemente von $\mathcal{H}$

$$\mathcal{H}_{kl} = \tfrac{1}{16}\{(\Phi_k, \Theta'_{pq}\Phi_k)+(\Phi_l, \Theta'_p\Phi_l)\}(\Phi_k, [J'_pJ'_q+J'_qJ'_p]\Phi_l), k\neq l. \quad (11.4)$$

Der Wert von $\mathcal{H}_{kl}$ wird also wesentlich nur durch den Zwangsoperator und davon wesentlich nur durch das Glied mit $\Theta'_{pq}$ bestimmt.

Von den zu $\Psi_1$ hinzuzufügenden $\Psi_k$ verlangen wir nun, daß sie zu $\Psi_1$ energetisch benachbart sind und daß $(\Phi_1, [J'_pJ'_q+J'_qJ'_p]\Phi_k)$ groß ist. Für $\varepsilon = 0$ und $\tau = 0$ gibt es nach den in Anhang D angegebenen Formeln für die Matrixelemente von Determinantenfunktionen überhaupt nur zwei $\Phi_k$ mit endlichem $(\Phi_1, [J'_pJ'_q+J'_qJ'_p]\Phi_k)$, nämlich

$$\Phi_2 = \mathrm{P4f}_{\frac{7}{2}}\tfrac{7}{2}+\mathrm{N4f}_{\frac{7}{2}}\tfrac{7}{2}\tfrac{3}{2}, \tag{11.5}$$

$$\Phi_3 = \mathrm{P4f}_{\frac{7}{2}}\tfrac{5}{2}+\mathrm{N4f}_{\frac{7}{2}}\tfrac{7}{2}\tfrac{5}{2}+\tfrac{3}{2}-. \tag{11.6}$$

Man gelangt zu ihnen durch Verschiebung zweier Nukleonen innerhalb $4f_{\frac{7}{2}}$ auf benachbarte Plätze derart, daß $m$ bei dem einen Einzelzustand um 1 erhöht, bei dem anderen um 1 erniedrigt wird. Ist $\varepsilon \neq 0$, aber weiter $\tau = 0$, so ergeben sich auch endliche Matrixelemente zwischen $\Phi_1$ und Zuständen $\Phi_k$ mit anderen Unterschalenbesetzungen, doch sind ihre Werte von der Größenordnung $\varepsilon$ oder $\varepsilon^2$ und die damit gebildeten $\Psi_k$ von $\Psi_1$ energetisch weiter entfernt. Bei größerem $|\tau|$ gelangt man dagegen zu Zuständen $\Phi_k$ mit großem $(\Phi_1, [J'_pJ'_q+J'_qJ'_p]\Phi_k)$ auch durch Verschieben von Nukleonen aus $4f_{\frac{7}{2}}$ nach $5f_{\frac{7}{2}}$, beispielsweise durch Verschieben der Neutronen von $4f_{\frac{7}{2}}\frac{5}{2}^2$ nach $5f_{\frac{7}{2}}\frac{3}{2}^2$. Auch sind dann Verschiebungen eines einzelnen Nukleons ohne Änderung von $m$ möglich, nämlich von $4f_{\frac{7}{2}}\frac{5}{2}^{\pm}$ nach $5f_{\frac{7}{2}}\frac{5}{2}^{\pm}$. Die Berücksichtigung dieser Zustände würde aber die Zahl der $\Psi_k$ in der Linearkombination sehr erhöhen. Es ist daher zweckmäßig, nur Zustände der gleichen Unterschalenbesetzung wie $\Psi_1$ heranzuziehen und erst dann, wenn sich diese als durchaus ungenügend erweisen, andere Zustände aufzunehmen. Diese Regelung steht im Einklang mit dem Aufsuchen des größten $|\langle \Gamma'_0 \rangle_{\varepsilon=0}|$ und des kleinsten $\langle J'_pJ'_q+J'_qJ'_p \rangle_{\varepsilon=0}$ in 10.: wir nehmen zunächst $\tau = 0$ an und lassen in der so gefundenen Linearkombination $\tau \neq 0$ zu. Dieses Vorgehen ist berechtigt, wenn $|\tau|$ nicht zu groß ausfällt.

### 11.2. APPROXIMATIVE BASISFUNKTIONEN MIT $\Omega = J-1$

Für die zu $\Psi_1$ hinzutretenden Zustände $\Psi^{Jwr}_{M\Omega}$ mit $\Omega = J-1 = \frac{5}{2}$ sind $\mathscr{H}_{1a}$ und die Glieder mit $\Theta'_{p3}$ und $\Theta'_{q3}$ in $\mathscr{H}_a$ maßgebend. Das in den Matrixelementen von $\mathscr{H}_{1a}$ nach (8.25) auftretende $(\Phi_k, W'_p\Phi_l)$ ist nach (4.21) und (4.19) besonders groß, wenn $(\Phi_k, J'_p\Phi_l)$ groß ist, und zwar gilt dann näherungsweise wegen der Kleinheit der Nichtdiagonalelemente von $\Theta'_{pq}$ gegen die Diagonalelemente und der Vernachlässigbarkeit von $\mathbf{W_T}$ und $\mathbf{W_S}$

$$(\Phi_k, W'_p\Phi_l) = \tfrac{1}{4}\{(\Phi_k, \Theta'_{pq}\Phi_k)+(\Phi_l, \Theta'_{pq}\Phi_l)\}(\Phi_k, J'_p\Phi_l). \tag{11.7}$$

Bildet man aus den beiden Zuständen $\Phi_k$ und $\Phi_l$, für die $(\Phi_k, J'_p\Phi_l)$ groß sein soll und für die wegen des Nichtverschwindens dieses Matrixelementes $\Omega_l = \Omega_k-1$ sein muß, zwei mit $\Psi_k$ und $\Psi_l$ bezeichnete Zustände $\Psi^{Jwr}_{M\Omega}$ mit gleichem $J$, $M$, $w$, so gilt daher annähernd für die Nichtdiagonalelemente von $\mathscr{H}$

$$\mathscr{H}_{kl} = -\frac{\hbar}{8}\sqrt{(J+\Omega_k)(J-\Omega_k+1)}\{(\Phi_k, \Theta'_{pq}\Phi_k)+(\Phi_l, \Theta'_{pq}\Phi_l)\}(\Phi_k, J'_p\Phi_l), \quad k \neq l, \tag{11.8}$$

denn der Beitrag von $\mathscr{H}_a$ ist wegen der Kleinheit der Matrixelemente von

$\Theta'_{33}$ zu den Diagonalelementen von $\Theta'_{pq}$ vernachlässigbar. Der Wert von $\mathscr{H}_{kl}$ wird also im wesentlichen nur durch $\mathscr{H}_{1a}$ und davon wesentlich nur durch das Glied mit $\Theta'_{pq}$ bestimmt.

In die Linearkombinationen für den Grundzustand nehmen wir solche $\Psi_k$ auf, die zu $\Psi_1$ energetisch benachbart sind und für die $(\Phi_1, J'_p\Phi_k)$ groß ist. Zu derartigen Zuständen gelangt man durch Verschieben eines Nukleons innerhalb $4f_{\frac{7}{2}}$ auf einen Nachbarzustand mit einem um 1 erniedrigten $m$, nämlich

$$\Phi_4 = \mathrm{P}4f_{\frac{7}{2}}\tfrac{5}{2}+\mathrm{N}4f_{\frac{7}{2}}\tfrac{7}{2}\tfrac{5}{2}, \tag{11.9}$$

$$\Phi_5 = \mathrm{P}4f_{\frac{7}{2}}\tfrac{7}{2}+\mathrm{N}4f_{\frac{7}{2}}\tfrac{7}{2}\tfrac{5}{2}-\tfrac{3}{2}+. \tag{11.10}$$

Für $\varepsilon = 0$, $\tau = 0$ sind diese Zustände die einzigen mit nichtverschwindendem $(\Phi_1, J'_p\Phi_k)$; für $\varepsilon \neq 0$, $\tau = 0$ sind sie die einzigen mit großem $(\Phi_1, J'_p\Phi_k)$. Für größeres $|\tau|$ gelangt man dagegen zu Zuständen mit großem $(\Phi_1, J'_p\Phi_k)$ auch durch Verschieben eines Nukleons aus $4f_{\frac{7}{2}}$ nach $5f_{\frac{7}{2}}$. Diese werden aus dem vorhin angegebenem Grund nicht berücksichtigt.

Die Glieder mit $\Theta'_{pp}$ und $\Theta'_{qq}$ in $\mathscr{H}_a$ führen auf Zustände $\Psi^{Jwr}_{M\Omega}$ mit $\Omega = J-2 = \frac{3}{2}$. Sie sind nach (8.21) wegen der Kleinheit der Matrixelemente von $\Theta'_{pp}$ gegen die Diagonalelemente von $\Theta'_{pq}$ zu vernachlässigen.

### 11.3. ZUSTANDSKOEFFIZIENTEN UND ENERGIE

Der Grundzustand hat jetzt die Gestalt

$$\Psi = \sum_k C_k\Psi_k, \quad \sum_k |C_k|^2 = 1. \tag{11.11}$$

Die $\Psi_k$ sind die mit den in (10.18) (11.5), (11.6), (11.9), (11.10) angegebenen Zuständen $\Phi_1 \ldots \Phi_5$ zu bildenden approximativen Basisfunktionen. Gesucht sind $\varepsilon$, $\tau$ und die $C_k$. Die $\mathscr{H}_{kl}$ sind nach (11.4) oder (11.5) zu errechnen. Sie sind reell; $\mathscr{H}_{12}$, $\mathscr{H}_{13}$, $\mathscr{H}_{23}$, $\mathscr{H}_{45}$ sind vom Typ (11.4) und positiv, $\mathscr{H}_{14}$, $\mathscr{H}_{15}$, $\mathscr{H}_{25}$, $\mathscr{H}_{34}$ vom Typ (11.8) und negativ, $\mathscr{H}_{24}$ und $\mathscr{H}_{35}$ verschwinden. Die $C_k$ sind dann ebenfalls reell. Zum Auffinden der gesuchten Größen wurden für $\varepsilon = -0.1$, $-0.125$, $-0.15$ und $\tau = 0$, $-\frac{1}{3}$, $-\frac{2}{3}$, $-1$ die $\mathscr{H}_{kl}$ und die Gesamtenergie berechnet. Für jedes $\tau$ wurde das Energieminimum und das zugehörige $\varepsilon$ bestimmt unter Approximation des Energieverlaufs zwischen den angegebenen $\varepsilon$ durch eine Parabel. Die Energieminima und ihre Lagen $\varepsilon$ wurden durch eine Gleichung dritten Grades als Funktion von $\tau$ dargestellt und das $\tau$ mit der niedrigsten Energie und das zugehörige $\varepsilon$ aufgesucht. Für die so bestimmten Werte $\varepsilon$, $\tau$ wurden erneut die $\mathscr{H}_{kl}$ und damit die $C_k$ berechnet. Mit dem nun bekannten $\varepsilon$, $\tau$ und den $C_k$ wurden $\Delta E_m$, $E_s$, $E_z$, $\Delta E_1$, $E_a$, $E_{1a}$, $\Delta E$ bestimmt. Die Lösung des Säkularproblems

$$\sum_l (\mathscr{H}_{kl}-\delta_{kl}E)C_l = 0 \tag{11.12}$$

wurde durch schrittweise Näherungen gewonnen. Es ergeben sich die Werte

$$\begin{array}{llllll} \varepsilon = -0.136 & C_1 = 0.937 & \Delta E_m = 0.90\,\hbar\omega & E_s = 0.78\,\hbar\omega & & \\ \tau = -0.308 & C_2 = -0.211 & E_s = -1.41\,\hbar\omega & E_{ls} = -0.91\,\hbar\omega & & \\ & C_3 = -0.143 & E_z = 1.44\,\hbar\omega & \Delta E = -0.80\,\hbar\omega & & (11.13) \\ & C_4 = 0.128 & \Delta E_1 = 0.93\,\hbar\omega & & & \\ & C_5 = 0.203 & & & & \end{array}$$

Wir erinnern, daß bei der Aufteilung in Mittel- und in Schwankungsenergie

$$\langle \Gamma'_0 \rangle = \sum_k \sum_l C_k C_l (\Phi_k, \Gamma'_0 \Phi_l) \tag{11.14}$$

zu setzen ist, wobei allerdings die Nichtdiagonalelemente von $\Gamma'_0$ verschwinden. Wegen des Überwiegens von $\Psi_1$ in $\Psi$ ergibt sich aber fast das Gleiche, wenn man die Aufteilung für jeden Zustand getrennt vornimmt und die gleichen Anteile addiert. Aus dem gleichen Grund kann im Spin-Bahn-Glied $\langle \Gamma'_0 \rangle$ durch $(\Phi_1, \Gamma'_0 \Phi_1)$ ersetzt werden.

Typisch am Aufbau des Zustandes $\Psi$ ist das klare Überwiegen von $\Psi_1$. Wir bezeichnen daher $\Psi_1$ als Dominante, die übrigen $\Psi_k$ als Satelliten und teilen sie ihrer Herkunft nach ein in die Zwangssatelliten $\Psi_2$, $\Psi_3$ und die Rotationsaustauschsatelliten $\Psi_4$, $\Psi_5$. Da die Satelliten nicht nur eine Abnahme von $E_z$ und $E_{ls}$, sondern auch für abnehmendes $|\varepsilon|$ ein schwächeres Ansteigen von $E_z$ und ein stärkeres Abfallen von $E_{ls}$ verursachen, liegt das Minimum der Gesamtenergie jetzt bei einem kleineren $|\varepsilon|$, und infolge der Zunahme der Beträge von $\mathcal{H}_{12}$, $\mathcal{H}_{13}$, $\mathcal{H}_{14}$, $\mathcal{H}_{15}$ für fallendes $|\tau|$ ist dieses ebenfalls kleiner. Vergleicht man das errechnete $\Delta E_m$, $E_s$, $E_z$, $E_s$, $E_{ls}$ mit den entsprechenden Energiewerten der Dominanten bei demselben $\varepsilon$, $\tau$, so zeigt sich eine Abnahme von $E_z$ und $E_{ls}$ und eine leichte Zunahme von $E_s$, hervorgerufen von den Rotationsaustauschsatelliten wegen des wesentlich größeren $J(J+1)-\Omega^2$; $\Delta E_m$ und $E_s$ bleiben praktisch ungeändert.

Der errechnete Grundzustand verletzt das Kriterium (3.3). Dieses läßt sich nämlich nach Abzug von $E_0$ auf die Form

$$\Delta E < \mathcal{H}'_{00} \tag{11.15}$$

bringen; am Anfang von 3. wurde festgestellt, daß $\mathcal{H}'_{00} < 0$ ist, und nach (11.13) ist $\Delta E > 0$. Also sollte der sich für $\zeta = 0$ ergebende Grundzustand $\Psi_0$, bei dem keine Kollektivbewegung besteht, besser sein als $\Psi$. Das mit $\Psi_0$ zu bildende $\mathcal{H}'_{00}$ ist nach den Ausführungen über die Schwankungsenergie etwa gleich dem für $\Psi$ errechneten $E_s$. Damit $\Psi$ der bessere Grundzustand ist, müßte $\Delta E$ um mindestens 2.2 $\hbar\omega$ niedriger liegen. Das sind etwa 3 % der kinetischen Energie im Zustand $\Psi_0$.

Das Ergebnis, $\Psi_0$ sei besser als $\Psi$, steht im Gegensatz zu den am Anfang von 3. ausgesprochenen Erwartungen. Sollte der noch zu führende Vergleich mit der Erfahrung hingegen $\Psi$ als den besseren Grundzustand erweisen, so muß festgestellt werden, ob der Formalismus unbrauchbar ist oder ob nur

die bei der Rechnung gemachten Annahmen fehlerhaft sind. Abschätzungen zeigen, daß bei einer Verbesserung von $V_0(r)$ die in (11.13) unbefriedigend hohe Zwangsenergie wesentlich sinkt. Dann ist vielleicht bei richtiger Wahl von $V_0(r)$ das Kriterium (11.15) erfüllt. Aber möglicherweise ist die Energiedifferenz zwischen $\Psi$ und $\Psi_0$ so klein, daß sie bei den begangenen Vernachlässigungen nicht erfaßt wird. Wir verfolgen die Frage später weiter.

### 11.4. EINE BERICHTIGUNG

$V_\nu$ ist die potentielle Energie zwischen dem $\nu$-ten Nukleon und allen anderen. Das in $\mathscr{H}$ auftretende $\sum_\nu V_\nu$ ist folglich die doppelte gesamte potentielle Energie und $\langle\mathscr{H}\rangle$ daher nicht gleich der Gesamtenergie. Wir müssen nachprüfen, ob deswegen Fehler bei der Berechnung des Grundzustandes entstanden sind. Das Aufsuchen der stationären Zustände bedeutet Lösung des Eigenwertproblems für $\mathscr{H}$, das wir näherungsweise durch Bestimmung von $\varepsilon$, $\tau$ und der $C_k$ erledigt haben. Auch das Kriterium (11.15) bezieht sich auf $\mathscr{H}$ und nicht auf die Energie. $\langle\mathscr{H}\rangle$ wurde in einzelne Glieder aufgeteilt, die wir kritiklos als Energie bezeichnet haben. Beim Schalenmodell mit undeformiertem Potential erhält man die Energie richtig, wenn man für den Grundzustand und für die angeregten Zustände von $\langle\mathscr{H}\rangle$ das für den Grundzustand gebildete $\frac{1}{2}\langle\sum_\nu V_\nu\rangle$ abzieht. Bei deformierbarem Potential zerfällt der potentielle Anteil von $\langle\mathscr{H}\rangle$ in den schon bei $\zeta = 0$, $\varepsilon = 0$ vorhandenen deformationsunabhängigen Anteil und den Zusatz infolge $\zeta \neq 0$, $\varepsilon \neq 0$. Es ist zunächst nicht klar, ob zur Ermittlung der potentiellen Energie für alle Zustände bei beiden Anteilen der halbe Erwartungswert des Grundzustandes abzuziehen ist. Für den deformationsunabhängigen Anteil ist es sicher richtig, aber unwichtig, da wir uns nur für die Energiedifferenzen der Zustände und für die Aufteilung der Energie in den einzelnen Zuständen interessieren. Der Schwankungsanteil $E_s$ ändert sich nur unbedeutend mit der Besetzung, und der potentielle Anteil von $\Delta E_m$ ist klein gegen die anderen Energieterme. Daraus folgt, daß der Zustand mit dem niedrigsten $\langle\mathscr{H}\rangle$ auch der mit der niedrigsten Energie ist. Die Bezeichnung der Terme $\Delta E_m$ und $E_s$ als Energien ist dagegen nicht richtig. Den Deformationsanteil der Mittelenergie erhält man aus $\Delta E_m$ durch Abziehen des halben potentiellen Anteils, und die Energie infolge Schwankungen der Kernform ist nicht $E_s$, sondern $\frac{1}{2}E_s$.

### 11.5. ELEKTRISCHES QUADRUPOLMOMENT

Die Berechnung erfolgt mit den allgemeinen Formeln von 8. Die durch (9.38) erklärten Koeffizienten $a_1, a_2, b_1, b_2$ sind nach (9.35)

$$\begin{aligned} a_1 &= 0.792 \quad a_2 = 0.610 \\ b_1 &= 0.642 \quad b_2 = 0.766. \end{aligned} \tag{11.16}$$

Für die Größen

$$q'_{kl} = (\Phi_k, 2\Gamma_0^{P'}\Phi_l) \tag{11.17}$$

ergeben sich dann die Zahlwerte

$$\begin{aligned} q'_{11} = q'_{22} = q'_{55} &= -16.70\,\frac{\hbar}{M\omega} \\ q'_{33} = q'_{44} &= -15.00\,\frac{\hbar}{M\omega} \\ q'_{14} &= \phantom{-}1.12\,\frac{\hbar}{M\omega} \\ q_{kl} &= \phantom{-}0 \quad \text{sonst.} \end{aligned} \tag{11.18}$$

Die $q'_{kk}$ sind die relativen Quadrupolmomente der betreffenden $\Psi_k$. Das relative Quadrupolmoment des gesamten Zustandes ist

$$q' = \sum_k \sum_l C_k C_l (\Psi_k, 2\Gamma_0^{P'}\Psi_l) = \sum_k C_k^2 q'_{kk} = 16.55\,\frac{\hbar}{M\omega}. \tag{11.19}$$

Für die Ausdrücke

$$q_{kl} = (\Psi_k, 2\Gamma_0^{P}\Psi_l), \tag{11.20}$$

von denen die $q_{kk}$ die absoluten Quadrupolmomente der betreffenden $\Psi_k$ sind, ergibt sich

$$\begin{aligned} q_{11} = q_{22} &= -7.79\,\frac{\hbar}{M\omega} \qquad q_{33} = -7.00\,\frac{\hbar}{M\omega} \\ q_{44} &= -1.00\,\frac{\hbar}{M\omega} \qquad q_{55} = -1.11\,\frac{\hbar}{M\omega} \\ q_{14} &= -0.48\,\frac{\hbar}{M\omega}. \end{aligned} \tag{11.21}$$

Das gesamte Quadrupolmoment

$$q = \sum_k \sum_l C_k C_l q_{kl} \tag{11.22}$$

zerlegen wir in den für $C_1 = 1$ allein vorhandenen Dominantenanteil und den Rest. Dessen Glieder sind

$$\begin{aligned} (C_1^2 - 1) q_{11} &= +0.95\,\frac{\hbar}{M\omega} \\ C_2^2 q_{22} &= -0.35\,\frac{\hbar}{M\omega} \\ C_3^2 q_{33} &= -0.14\,\frac{\hbar}{M\omega} \\ C_4^2 q_{44} &= -0.02\,\frac{\hbar}{M\omega} \\ C_5^2 q_{55} &= -0.05\,\frac{\hbar}{M\omega} \\ 2C_1 C_4 q_{14} &= -0.12\,\frac{\hbar}{M\omega} \\ \hline \text{Summe} &= +0.27\,\frac{\hbar}{M\omega}. \end{aligned} \tag{11.23}$$

Dann ist

$$\begin{aligned} q &= -7.52\,\frac{\hbar}{M\omega} \\ &= -7.52\left(\frac{\hbar}{Mc}\right)^2\frac{Mc^2}{\hbar\omega} \\ &= -7.52\times(0.210\times10^{-13}\text{ cm})^2\frac{Mc^2}{\hbar\omega} \\ &= -3.32\,\frac{Mc^2\times10^{-3}}{\hbar\omega}\times10^{-24}\text{ cm}^2. \end{aligned} \tag{11.24}$$

$q$ ist nur um etwa 3.5 % von $q_{11}$ verschieden. Bei einem nicht deformierten Kern ist, wenn sich die vier Neutronen in $4f_{\frac{7}{2}}$ zum Drehimpuls Null zusammensetzen,

$$q_{\varepsilon=0} = \langle 4f_{\frac{7}{2}}\tfrac{7}{2}^{\pm}|2r^2Y_0|4f_{\frac{7}{2}}\tfrac{7}{2}^{\pm}\rangle_{\varepsilon=0} = -3\,\frac{\hbar}{M\omega}\,. \tag{11.25}$$

Setzen sich die fünf Nukleonen in $4f_{\frac{7}{2}}$ auf eine allgemeinere Art zu $J=\frac{7}{2}$ zusammen, so ist $|q_{\varepsilon=0}|$ kleiner, weil dann das Proton, auf das feste System bezogen, nicht nur im Zustand $4f_{\frac{7}{2}}\frac{7}{2}^{\pm}$ ist. Daher ist nach (11.19), (11.24), (11.25)

$$|q'| \geqq 5.6|q_{\varepsilon=0}|, \quad |q| \geqq 2.5|q_{\varepsilon=0}|. \tag{11.26}$$

Der experimentelle Wert von $q$ ist zwar nicht bekannt, doch fügt sich das mit $\hbar\omega = 10.9$ TME aus (11.24) folgende $q = -0.30\times10^{-24}$ cm² gut in die Werte der anderen Kerne [23, 24, 25]) ein.

### 11.6. MAGNETISCHES DIPOLMOMENT

Ausgangspunkt sind die allgemeinen Formeln von 8. Wie bei $\Theta$ sind im Fall genügender Deformation in $z'$-Richtung die Diagonalelemente von $G'_{pq}$ und $G'_{qp}$ groß gegen die Nichtdiagonalelemente und die Matrixelemente der übrigen Komponenten von $G$. Wir berücksichtigen nur die ersteren, vernachlässigen also die Schwankungen der Kernform, und haben dann nach (7.5) zu setzen

$$(\Phi^{wr}_{\Omega}, G'_{pq}\Phi^{wr}_{\Omega}) = \frac{(\Phi^{wr}_{\Omega}, 2\Gamma_0{}^{p'}\Phi^{wr}_{\Omega})}{(\Phi^{wr}_{\Omega}, 2\Gamma''_0\Phi^{wr}_{\Omega})}\,. \tag{11.27}$$

In dieser Näherung fällt bei (8.37) in dem Matrixelement mit $\mathcal{M}'_{13}$, wie (3.42) und (A4) zeigen, der gyromagnetische Tensor überhaupt heraus. In den Matrixelementen mit $\mathcal{M}'_{1p}$ in (8.38) und (8.39) ist wie in dem entsprechenden Fall (11.4) zu setzen

$$\begin{aligned} &(\Phi^{wr}_{\Omega}, [G\cdot\mathbf{J}+\mathbf{J}\cdot G]'_p\Phi^{ws}_{\Omega-1}) \\ &\qquad = \{(\Phi^{wr}_{\Omega}, G'_{pq}\Phi^{wr}_{\Omega}) + (\Phi^{ws}_{\Omega-1}, G'_{pq}\Phi^{ws}_{\Omega-1})\}(\Phi^{wr}_{\Omega}, J'_p\Phi^{ws}_{\Omega-1}), \end{aligned} \tag{11.28}$$

und von den in (8.42) ... (8.46) angegebenen Matrixelementen mit $\mathcal{M}_{s3}$ ist nur das erste für $s = r$ von Null verschieden. Bei Rückkehr zur Bezeichnung der Funktionen mit einem Index gelten also mit der Abkürzung

$$\eta_{kl} = \frac{1}{2}\left\{\frac{(\Phi_k, \Gamma_0^{P'}\Phi_k)}{(\Phi_k, \Gamma'_0\Phi_k)} + \frac{(\Phi_l, \Gamma_0^{P'}\Phi_l)}{(\Phi_l, \Gamma'_0\Phi_l)}\right\} \tag{11.29}$$

die Formeln

$$(\Phi_k, \mathcal{M}'_{13}\Phi_l) = \frac{\mu_K}{\hbar}(\Phi_k, [L_3^{P'} + g^P S_3^{\,l} + g^N S_3^{N'}]\Phi_l), \quad \Omega_l = \Omega_k, \tag{11.30}$$

$$\begin{aligned}(\Phi_k, \mathcal{M}'_{1p}\Phi_l) = \frac{\mu_K}{\hbar}(\Phi_k, [&(1-\eta_{kl})L_p^{P'} + (g^P - \eta_{kl})S_p^{P'} \\ &-\eta_{kl}L_p^{N'} + (g^N - \eta_{kl})S_i^{N'}]\Phi_l), \quad \Omega_l = \Omega_k - 1,\end{aligned} \tag{11.31}$$

$$(\Psi_k, \mathcal{M}_{a3}\Psi_k) = \mu_K \eta_{kk}\frac{J(J+1)-\Omega^2}{J+1} \quad \text{für alle } \Omega. \tag{11.32}$$

Die Ausdrücke (11.30) und (11.31) können nach Anhang D nur dann von Null verschieden sein, wenn $\Phi_k$ und $\Phi_l$ sich bei $k \neq l$ in nur einer Einzelfunktion unterscheiden. Dann kommt entweder nur der Protonenteil oder nur der Neutronenteil des Operators zur Geltung.

Für den Kern (21,24) ergibt

$$\begin{aligned}&\eta_{11} = 0.407 \quad \eta_{14} = 0.394 \quad \eta_{15} = 0.416\\ &\eta_{22} = 0.443 \quad\quad\quad\quad \eta_{25} = 0.434\\ &\eta_{33} = 0.378 \quad \eta_{34} = 0.380\\ &\eta_{44} = 0.382\\ &\eta_{55} = 0.425.\end{aligned} \tag{11.33}$$

Bei Benutzung des Näherungswertes (3.45) für $G$ träte an die Stelle aller $\eta_{kl}$ der Wert $Z/A = 0.467$. Mit den Abkürzungen

$$\begin{aligned}\mu_{kl} &= \mu_{1kl} + \mu_{akl}\\ \mu_{1kl} = \frac{1}{\mu_K}(\Psi_k, \mathcal{M}_{13}\Psi_l), &\quad \mu_{akl} = \frac{1}{\mu_K}(\Psi_k, \mathcal{M}_{a3}\Psi_l)\end{aligned} \tag{11.34}$$

wird das gesamte magnetische Moment

$$\mu = \sum_k \sum_l C_k C_l \mu_{kl}. \tag{11.35}$$

Es ergeben sich die Zahlwerte

$$\begin{aligned}&\mu_{111} = 4.51 \quad \mu_{a11} = 0.32 \quad \mu_{14} = \quad 1.29 \quad \mu_{15} = -1.10\\ &\mu_{122} = 4.51 \quad \mu_{a22} = 0.34 \quad\quad\quad\quad \mu_{25} = -1.12\\ &\mu_{133} = 2.66 \quad \mu_{a33} = 0.29 \quad \mu_{34} = -1.06\\ &\mu_{144} = 1.72 \quad \mu_{a44} = 0.80\\ &\mu_{155} = 3.04 \quad \mu_{a55} = 0.90.\end{aligned} \tag{11.36}$$

Wir zerlegen $\mu$ in die folgenden drei Teile:

| I | II | III | |
|---|---|---|---|
| $\mu_{11} = 4.82$ | $2C_4\mu_{14} = +0.33$ | $(C_1^2-1)\mu_{11} = -0.59$ | |
| | $2C_5\mu_{15} = -0.45$ | $2(C_1-1)C_4\mu_{14} = -0.02$ | |
| | Summe $= -0.12$ | $2(C_1-1)C_5\mu_{15} = 0.03$ | |
| | | $C_2^2\mu_{22} = 0.22$ | |
| | | $C_3^2\mu_{33} = 0.06$ | (11.37) |
| | | $C_4^2\mu_{44} = 0.04$ | |
| | | $C_5^2\mu_{55} = 0.16$ | |
| | | $2C_2C_5\mu_{25} = 0.10$ | |
| | | $2C_3C_4\mu_{34} = 0.04$ | |
| | | Summe $= 0.04.$ | |

Typisch für den dritten Teil ist, daß er kleiner ausfällt als die Einzelglieder des zweiten und daß er nur wenig zu $\mu$ beiträgt. $\mu$ wird also im wesentlichen durch den ersten und den zweiten Teil festgelegt. Der Gesamtwert

$$\mu = 4.74 \tag{11.38}$$

liegt etwa 0.3 % unter dem experimentellen Wert [23, 24, 25]) $4.7556 \pm 0.0010$.

### 11.7. UNSCHÄRFE DER AUSGEZEICHNETEN ACHSE

Für den Winkel $\vartheta'$ zwischen **N** und der $z'$-Achse ergeben die bei der Systemkorrektur angestellten Rechnungen bei kleinem $\vartheta'$

$$\vartheta'^2 = \frac{2}{3}\frac{|\Gamma'_1|^2}{\Gamma'^2_0}. \tag{11.39}$$

Daher ist der für gegebenes $\Phi^{wr}_{\Omega}$ gebildete Erwartungswert dieser Größe, für den wir näherungsweise

$$\langle\vartheta'^2\rangle = \frac{2}{3}\frac{\langle|\Gamma'_1|^2\rangle}{\langle\Gamma'_0\rangle^2} \tag{11.40}$$

schreiben können, ein Maß für die Unschärfe von **N**. Um seine Bedeutung zu erkennen, bedenken wir, daß die Oberfläche der Kugelkappe der Einheitskugel gegeben ist durch

$$\begin{aligned} f(\vartheta') &= 2\pi(1-\cos\vartheta') \\ &= \pi\vartheta'^2 \qquad \text{für kleine } \vartheta'. \end{aligned} \tag{11.41}$$

Wäre **N** gleichmäßig auf $0 \leqq \vartheta' \leqq \vartheta'_0$, $\vartheta'_0 \leqq \pi/2$, verteilt, so gälte

$$\left\langle \frac{f(\vartheta')}{\pi} \right\rangle = \int_{\varphi'=0}^{2\pi}\int_{\vartheta'=0}^{\vartheta'_0} 2(1-\cos\vartheta')\frac{\sin\vartheta'\,d\vartheta'\,d\varphi'}{2\pi(1-\cos\vartheta'_0)} = 1-\cos\vartheta'_0. \tag{11.42}$$

Dabei wurde berücksichtigt, daß wegen der Vertauschbarkeit von **N** mit

$-\mathbf{N}$ nur Werte $0 \leqq \vartheta' \leqq \pi/2$ betrachtet zu werden brauchen. Im Fall gleichmäßiger Verteilung über die halbe Einheitskugel ist $\langle f(\vartheta')/\pi \rangle = 1$. Verdichten sich die Lagen von **N** nach der $z'$-Achse hin, so ist $\langle f(\vartheta')/\pi \rangle < 1$, und bei Zusammenfallen von **N** mit der $z'$-Achse wird $\langle f(\vartheta')/\pi \rangle = 0$. Folglich ist $\langle f(\vartheta')/\pi \rangle$ ein absolutes Maß für die Unschärfe von **N**. Es läßt sich nach (11.42) deuten als Anteil der halben Einheitskugel, auf den **N** verteilt ist. Bei kleinem $\vartheta'$ kann aber $f(\vartheta')/\pi$ nach (11.41) durch $\vartheta'^2$ ersetzt werden. Also ist $\langle \vartheta'^2 \rangle$, wenn es klein ausfällt, ein absolutes Maß für die Unschärfe von **N**. Für die einzelnen Zustände ist

$$\begin{array}{rccccc} & \Psi_1 & \Psi_2 & \Psi_3 & \Psi_4 & \Psi_5 \\ \langle \vartheta'^2 \rangle = & 0.10 & 0.13 & 0.12 & 0.12 & 0.12. \end{array} \tag{11.43}$$

Für den Gesamtzustand ergibt sich, da die Nichtdiagonalelemente vernachlässigt werden können

$$\langle \vartheta'^2 \rangle = 0.10. \tag{11.44}$$

### 11.8. BESPRECHUNG

Die gute Übereinstimmung zwischen dem berechneten und dem gemessenen Wert für $\mu$ zeigt zwar, daß $\Psi$ der richtige Grundzustand sein kann, schließt aber $\Psi_0$ nicht aus, da wir dessen $\mu$ nicht kennen. Der experimentelle Wert für $q$ ist nicht bekannt. Wäre aber $\Psi_0$ der bessere Grundzustand, so müßte $q$ nach (11.26) erheblich kleiner sein als der für $\Psi$ berechnete Wert. Der Kern (21,24) bildete dann eine Annahme von der Regel, daß die Quadrupolmomente bedeutend größer sind, als wenn sie nur von einem Proton herrührten. Das ist unwahrscheinlich.

Eine Betrachtung der Kerne bis zu $A \approx 60$ weist auf die Brauchbarkeit des Formalismus. Es ist nämlich möglich, die Grundzustände so aus approximativen Basisfunktionen des für den betreffenden Kern gemessenen $J$ aufzubauen, daß sich die richtigen Werte für $\mu$ ergeben und daß Einklang oder zumindest kein Widerspruch mit energetischen Erörterungen besteht. Die Grundzustände bauen sich im allgemeinen aus einer Dominante und einigen Satelliten auf, doch ist die Unterschalenbesetzung nicht immer die mit der tiefsten Energie für $\zeta = 0$, weil die Forderung nach einem möglichst großen $|\langle \Gamma''_0 \rangle_{\epsilon=0}|$ teilbesetzte Unterschalen begünstigt. Als Ausnahmen erweisen sich (23,28), (19,22), (8,9). Die ersten besitzen zwei Dominanten. Der letzte Kern zeigt keine kollektive Rotation; der für $\zeta = 0$ berechnete Grundzustand ist hier der bessere.

Der Grundzustand von (23,28) läßt auch verstehen, daß für *gg*-Kerne $J = 0$ ist. Bestände er nur aus einer Dominante, so zeigt die Untersuchung, daß dann $J = \frac{5}{2}$ sein muß, während der richtige Wert $J = \frac{7}{2}$ eine Doppeldominante erfordert. Die entsprechende Erscheinung bei *gg*-Kernen, daß anstelle eines monodominanten Grundzustandes mit $J = 0$ ein bidominanter

mit $J = 1$ auftritt, ist aber nicht möglich, weil die eine zur Bildung der Doppeldominanten erforderliche Basisfunktion aus Symmetriegründen nicht existiert.

Die Zwangsenergie zeigt, daß die Dehnung des Kerns in Richtung der ausgezeichneten Achse im allgemeinen energetisch günstiger ist als die Abplattung. Zum Beweis betrachten wir das im Nenner von $\langle \Theta'_{pq} \rangle$ auftretende $\langle \Gamma'_0 \rangle$ in (10.4). Da $\varepsilon$ das gleiche Vorzeichen hat wie $\langle \Gamma'_0 \rangle_{\varepsilon=0}$ und da $|\langle \Gamma'_0 \rangle_{\varepsilon=0}| \ll \langle \Gamma \rangle_{\varepsilon=0}$ ist, haben die beiden ersten Glieder das gleiche Vorzeichen. Ist dieses negativ, so schwächt das stets positive dritte Glied die ersten beiden, wirkt also im Sinn einer Vergrößerung von $\langle \Theta'_{pq} \rangle$ und damit der Zwangsenergie; im anderen Fall tritt das Gegenteil ein. Dieser Einfluß vermag sich bei kleinem $|\varepsilon|$ gegenüber den anderen Energietermen nicht durchzusetzen, wird aber bei größerem $|\varepsilon|$ entscheidend. Zum Beispiel ist für den Kern (9,10) im Grundzustand $\varepsilon < 0$ unmöglich. Es wird daher verständlich, daß hohe Quadrupolmomente niemals das negative Vorzeichen haben.

Zusammenfassend ergibt sich, daß der Formalismus brauchbar ist, doch machen die bei seiner Anwendung getroffenen Vernachlässigungen den angestrebten Existenzbeweis eines kreiselartigen Verhaltens vielleicht unmöglich, und das Kriterium (11.15) ist nur für gröbere Vergleiche nützlich. Kennzeichnend ist das starke Überwiegen einer approximativen Basisfunktion in der Linearkombination des Grundzustandes. Sie allein gibt schon einen besseren Wert für das magnetische Moment als das Schalenmodell mit undeformiertem Potential. Die Anzahl der Funktionen in der Linearkombination ist bedeutend kleiner als die Nukleonenzahl. Die mühevolle Aufgabe, eine erhebliche Anzahl von Zustandsdeterminanten zu einer Funktion mit scharfem Gesamtdrehimpuls zusammenzusetzen, wird vermieden. Der gestellte Vorsatz, das Modell zu verbessern durch Verwendung von Funktionen, die eine kollektive Rotation des Kerns zum Ausdruck bringen, ohne sich über die Frage der überzähligen Freiheitsgrade einfach hinwegzusetzen, kann als gelungen angesehen werden.

## 12. Ergänzungen

### 12.1. ROTATIONSSPEKTREN

Der Einfachheit halber betrachten wir zunächst einen Kern mit $J = 0$ im Grundzustand und fragen nach der Struktur des tiefsten Zustandes für $J = 2$. Der Grundzustand bestehe aus einer Dominante und einigen Zwangssatelliten; alle diese Funktionen sind vom Typ (7.2). Wir schreiben sie vereinfachend

$$\Psi_k^0 = \mathfrak{D}_{00}^0 \Phi_k = \frac{1}{\sqrt{8\pi}} \Phi_k. \tag{12.1}$$

Die Indices $k = 0, 1, 2, \ldots$ numerieren die inneren Zustände, $k = 0$ sei die Dominante.

Im tiefsten Zustand für $J = 2$ sind approximative Basisfunktionen mit $\Omega = 0, 1, 2$ enthalten. Bei großem $\langle \Theta'_{pq} \rangle$ ist für eine möglichst kleine Gesamtenergie die Rotationsenergie entscheidend. Sie ist nach (8.18) am niedrigsten für $\Omega = J$. Also kommen in dem Zustand überwiegend approximative Basisfunktionen mit $\Omega = 2$ vor. Deren innere Zustände sind aber sicher von $\Phi_0$ verschieden. Bei kleinem $\langle \Theta'_{pq} \rangle$ dagegen ist die innere Energie für eine möglichst kleine Gesamtenergie entscheidend. Da $\Phi_0$ die Zustandsdeterminante mit dem kleinsten $\langle \mathscr{H}_1 \rangle$ ist, besteht der Zustand im wesentlichen aus der auf $\Phi_0$ aufgebauten approximativen Basisfunktion mit $J = 2$. Dazu kommen Zwangssatelliten mit den gleichen $\Phi_k$ wie im Grundzustand und, vermittelt durch $\mathscr{H}_{1a}$, einige Rotationsaustauschsatelliten mit $\Omega = 1$. Zustände mit $\Omega = 2$ brauchen nicht berücksichtigt zu werden, da sie klein von zweiter Ordnung sind. Also sind die approximativen Basisfunktionen des tiefsten Zustandes für $J = 2$ nach (7.2) und (7.1)

$$\begin{aligned} \Psi_k^J &= \mathscr{D}^J_{M0} \Phi_k \\ \Psi_l^J &= \frac{1}{\sqrt{2}} \{ \mathscr{D}^J_{M1} \Phi_l + \ldots \end{aligned} \tag{12.2}$$

wobei der Index $l = 1, 2, \ldots$ die inneren Zustände mit $\Omega = 1$ numeriert.

Bei Vernachlässigung der Satelliten und der durch die Rotation bedingten leichten Änderung von $\varepsilon$ und $\tau$ träte zur Energie des Grundzustandes nach (8.18) im tiefsten Zustand mit $J = 2$ die Rotationsenergie

$$E_a = \frac{\hbar^2}{4} \langle 0 | \Theta'_{pq} | 0 \rangle J(J+1), \quad \langle 0 | \Theta'_{pq} | 0 \rangle \equiv (\Phi_0, \Theta'_{pq} \Phi_0). \tag{12.3}$$

Zur Energieberechnung mit Berücksichtigung der Satelliten nehmen wir deren Anteil als so klein an, daß die Störungsrechnung angewendet werden kann. Alle hierzu benötigten Matrixelemente sind reell. Dann ist im Grundzustand

$$\begin{aligned} E^0 &= \langle 0 | \mathscr{H}_1 | 0 \rangle - \sum_k{}' \frac{\langle k | \mathscr{H}_1 | 0 \rangle^2}{E^0_k - E^0_0} \\ E^0_k &\equiv (\Psi^0_k, \mathscr{H} \Psi^0_k) = \langle k | \mathscr{H}_1 | k \rangle \end{aligned} \tag{12.4}$$

und im tiefsten Zustand mit $J = 2$, wenn wir das kleine Glied mit $\Theta'_{33}$, das sich in der Gesamtenergie forthebt, überall weglassen, mit (8.18) und (8.24)

$$E^J = \langle 0|\mathscr{H}_1|0\rangle - \sum_k{}' \frac{\langle k|\mathscr{H}_1|0\rangle^2}{E_k^J - E_0^J} + \frac{\hbar^2}{4}\left\{\langle 0|\Theta'_{pq}|0\rangle - 2\sum_l{}' \frac{\langle l|W'_p|0\rangle^2}{E_l^J - E_0^J}\right\} J(J+1),$$

$$E_k^J \equiv (\Psi_k^J, \mathscr{H}\Psi_k^J) = \langle k|\mathscr{H}_1|k\rangle + \frac{\hbar^2}{4}\langle k|\Theta'_{pq}|k\rangle J(J+1) \tag{12.5}$$

$$E_l^J \equiv (\Psi_l^J, \mathscr{H}\Psi_l^J) = \langle l|\mathscr{H}_1|l\rangle + \frac{\hbar^2}{4}\langle l|\Theta'_{pq}|l\rangle\{J(J+1)-1\}.$$

Vernachlässigt man die kleinen Unterschiede in den Matrixelementen für $\Theta'_{pq}$, so wird $E_k^J - E_0^J \doteq E_k^0 - E_0^0$ und $E_l^J - E_0^J$ unabhängig von $J$. Dann ist $E^J - E^0$ dem Glied mit $J(J+1)$ gleich und die in der geschweiften Klammer stehende Größe das effektive reziproke Trägheitsmoment.

Bei genügend kleinem $\langle 0|\Theta'_{pq}|0\rangle$ haben auch die tiefsten Zustände mit höherem geraden $J$ fast die gleiche innere Struktur wie der Grundzustand. Sie bauen sich dann ebenfalls aus den in (12.2) angegebenen Zuständen auf; Zustände mit $\Omega > 1$ sind klein von höherer Ordnung und daher zu vernachlässigen.

Wir betrachten jetzt einen Kern mit $J = J_0 \neq 0, \frac{1}{2}$ im Grundzustand und fragen nach dem tiefsten Zuständen für $J > J_0$. Der Grundzustand soll wie beim Kern (21, 24) aus einer Dominanten mit $\Omega = J_0$, einigen Zwangssatelliten mit $\Omega = J_0$ und aus einigen Rotationsaustauschsatelliten mit $\Omega = J_0 - 1$ bestehen. Die approximativen Basisfunktionen des Grundzustandes seien

$$\Psi_k^{J_0} = \frac{1}{\sqrt{2}}\{\mathscr{D}^{J_0}_{MJ_0}\Phi_k + \dots$$
$$\Psi_j^{J_0} = \frac{1}{\sqrt{2}}\{\mathscr{D}^{J_0}_{MJ_0-1}\Phi_j + \dots. \tag{12.6}$$

$k = 0, 1, 2, \dots$ numeriert die inneren Zustände mit $\Omega = J_0$, $j = 1, 2, \dots$ die mit $\Omega = J_0 - 1$, $k = 0$ bedeute die Dominante. In den tiefsten Zuständen mit $J > J_0$ sind die gleichen inneren Zustände $\Phi_k$ und $\Phi_j$ enthalten, hierzu treten kleine Beimengungen von Zuständen mit $\Omega = J_0 + 1$, Zustände mit $\Omega > J_0 + 1$ sind klein von höherer Ordnung. Die approximativen Basisfunktionen sind

$$\Psi_k^J = \frac{1}{\sqrt{2}}\{\mathscr{D}^J_{MJ_0}\Phi_k + \dots$$
$$\Psi_j^J = \frac{1}{\sqrt{2}}\{\mathscr{D}^J_{MJ_0-1}\Phi_j + \dots \tag{12.7}$$
$$\Psi_l^J = \frac{1}{\sqrt{2}}\{\mathscr{D}^J_{MJ_0+1}\Phi_l + \dots$$

$l = 1, 2, \ldots$ numeriert die Zustände mit $\Omega = J_0+1$. Die Energie ist im Grundzustand

$$E^{J_0} = \langle 0|\mathscr{H}_1|0\rangle - \sum_k{}' \frac{\langle k|\mathscr{H}_1|0\rangle^2}{E_k^{J_0} - E_0^{J_0}} + \frac{\hbar^2}{4}\left\{\langle 0|\Theta'_{pq}|0\rangle - \sum_j \frac{\langle 0|W'_p|j\rangle^2}{E_j^{J_0} - E_0^{J_0}}\right\} J_0 \tag{12.8}$$

und in den Rotationszuständen

$$\begin{aligned} E^J = {} & \langle 0|\mathscr{H}_1|0\rangle - \sum_k{}' \frac{\langle k|\mathscr{H}_1|0\rangle^2}{E_k^J - E_0^J} + \frac{\hbar^2}{4}\langle 0|\Theta'_{pq}|0\rangle\{J(J+1) - J_0^2\} \\ & - \frac{\hbar^2}{4}\sum_j \frac{\langle 0|W'_p|j\rangle^2}{E_j^J - E_0^J}(J+J_0)(J-J_0+1) \\ & - \frac{\hbar^2}{4}\sum_l \frac{\langle l|W'_p|0\rangle^2}{E_l^J - E_0^J}(J-J_0)(J+J_0+1). \end{aligned} \tag{12.9}$$

Vernachlässigt man wieder die Unterschiede in den Matrixelementen von $\Theta'_{pq}$, so wird

$$\begin{aligned} E^J - E^{J_0} = {} & \frac{\hbar^2}{4}\left\{\langle 0|\Theta'_{pq}|0\rangle \right. \\ & \left. - \sum_j \frac{\langle 0|W'_p|j\rangle^2}{E_j^{J_0} - E_0^{J_0}} - \sum_l \frac{\langle l|W'_p|0\rangle^2}{E_l^{J_0} - E_l^{J_0}}\right\}\{J(J+1) - J_0(J_0+1)\}. \end{aligned} \tag{12.10}$$

Bei $J_0 = \frac{1}{2}$ macht sich das anomale Glied in (8.24) bemerkbar. Im Grundzustand besteht der Kern nur aus Zuständen mit $\Omega = \frac{1}{2}$; die approximativen Basisfunktionen seien

$$\Psi_k^{\frac{1}{2}} = \frac{1}{\sqrt{2}}\{\mathscr{D}^{\frac{1}{2}}_{M\frac{1}{2}}\Phi_k + w\mathscr{D}^{\frac{1}{2}}_{M,-\frac{1}{2}}\Phi_{\bar{k}}\}. \tag{12.11}$$

Die $\Phi_{\bar{k}}$ sind die in (7.1) mit dem Index $-\Omega$ versehenen Zustände. Die Rotationszustände bestehen aus den Funktionen

$$\begin{aligned} \Psi_k^J &= \frac{1}{\sqrt{2}}\{\mathscr{D}^J_{M\frac{1}{2}}\Phi_k + w(-1)^{J-\frac{1}{2}}\mathscr{D}^J_{M,-\frac{1}{2}}\Phi_{\bar{k}}\} \\ \Psi_l^J &= \frac{1}{\sqrt{2}}\{\mathscr{D}^J_{M\frac{1}{2}}\Phi_l + \ldots. \end{aligned} \tag{12.12}$$

Die Energien sind

$$\begin{aligned} E^{\frac{1}{2}} = {} & \langle 0|\mathscr{H}_1|0\rangle + \frac{\hbar^2}{4}\langle 0|\Theta'_{pq}|0\rangle\tfrac{1}{2} - \frac{\hbar}{2}w\langle 0|W'_p|\bar{0}\rangle \\ & - \sum_k \frac{\left\{\langle 0|\mathscr{H}_1|k\rangle - \frac{\hbar}{2}w\langle 0|W'_p|\bar{k}\rangle\right\}^2}{E_k^{\frac{1}{2}} - E_0^{\frac{1}{2}}}, \end{aligned} \tag{12.13}$$

$$E^J=\langle 0|\mathscr{H}_1|0\rangle+\frac{\hbar^2}{4}\langle 0|\Theta'_{pq}|0\rangle\{J(J+1)-\tfrac{1}{4}\}-\frac{\hbar}{2}w(-1)^{J-\frac{1}{2}}\langle 0|W'_p|\bar{0}\rangle(J+\tfrac{1}{2})$$
$$-\sum_k{}'\frac{\left\{\langle 0|\mathscr{H}_1|k\rangle-\frac{\hbar}{2}w(-1)^{J-\frac{1}{2}}\langle 0|W'_p|\bar{k}\rangle(J+\tfrac{1}{2})\right\}^2}{E_k^J-E_0^J} \tag{12.14}$$
$$-\frac{\hbar^2}{4}\sum_l\frac{\langle l|W'_p|0\rangle^2}{E_l^J-E_0^J}(J+\tfrac{3}{2})(J-\tfrac{1}{2}).$$

Dann ist

$$E^J-E^{\frac{1}{2}}=\frac{\hbar^2}{4}\left\{\langle 0|\Theta'_{pq}|0\rangle-\sum_k{}'\frac{\langle 0|W'_p|k\rangle^2}{E_k^{\frac{1}{2}}-E_0^{\frac{1}{2}}}-\sum_l\frac{\langle l|W'_p|0\rangle^2}{E_l^J-E_0^J}\right\}\{J(J+1)-\tfrac{3}{4}\}$$
$$-\frac{\hbar}{2}w\left\{\langle 0|W'_p|\bar{0}\rangle-2\sum_k{}'\frac{\langle 0|\mathscr{H}_1|k\rangle\langle 0|W'_p|\bar{k}\rangle}{E_k^{\frac{1}{2}}-E_0^{\frac{1}{2}}}\right\}\{(-1)^{J-\frac{1}{2}}(J+\tfrac{1}{2})-1\}. \tag{12.15}$$

Wir gelangten zu den Rotationsspektren durch die Frage nach den tiefsten Zuständen. Es ist aber grundsätzlich nicht notwendig, daß die Rotationszustände die tiefsten Zustände der betreffenden $J$ sind. Unsere Art des Vorgehens erleichterte nur den Existenzbeweis.

Ob die Störungsrechnung anwendbar ist, kann bezweifelt werden, denn beim Kern (21,24) ist sie auch nicht brauchbar. Nun kommt es aber offensichtlich nur auf die Kleinheit des Anteils der Rotationsaustauschsatelliten an, damit sie Energieabstände $\approx J(J+1)$ sind, wenn wir den Fall $J_0=0$ betrachten. Der Anteil dieser Satelliten ist dann nach (8.25) $\approx\sqrt{J(J+1)}$; der Operator $\mathscr{H}_{1a}$ liefert daher einen Energieanteil $\approx J(J+1)$. Die Kleinheit des Anteils der Rotationsaustauschsatelliten ist aber bei den Kernen mit Rotationsspektren zu erwarten, denn diese Kerne haben mehrere nicht vollbesetzte Unterschalen, und bei *gg*-Kernen ist die Zahl der Rotationsaustauschsatelliten gleich der Zahl der teilbesetzten Unterschalen, die Zahl der Zwangssatelliten dagegen gleich deren Quadrat. Der den Satelliten zustehende Anteil in der Zustandsfunktion wird also in überwiegendem Maß von den Zwangssatelliten beansprucht.

Ein Rotationsspektrum hat stets endlich viele Niveaus, weil der Anteil der als klein oder vernachlässigbar angenommenen infolge der Rotation hinzutretenden Basisfunktionen mit steigendem $J$ wächst, so daß der Kern bei genügend hohem $J$ eine vom Grundzustand merklich verschiedene innere Struktur besitzt und die Abhängigkeit der Energie von $J$ geändert wird.

$\Theta$ läßt sich mit W auf Grund der Vertauschungsrelationen (C4) zu dem effektiven reziproken Trägheitstensor $\overline{\Theta}$ zusammenfassen mit den Komponenten

$$\overline{\Theta}'_{kk} = \Theta'_{kk}$$

$$\overline{\Theta}'_{12} = \Theta'_{12} - \frac{i}{\hbar} W'_3, \quad \text{entspr. } \overline{\Theta}'_{23}, \overline{\Theta}'_{31}, \tag{12.16}$$

$$\overline{\Theta}'_{21} = \Theta'_{12} + \frac{i}{\hbar} W'_3, \quad \text{entspr. } \overline{\Theta}'_{32}, \overline{\Theta}'_{13}.$$

Dann ist

$$\mathscr{H}_a + \mathscr{H}_{1a} = \tfrac{1}{2} \sum_k \sum_l \overline{\Theta}'_{kl} J'_k J'_l. \tag{12.17}$$

Der reziproke Trägheitstensor eines starren Körpers ist symmetrisch, hängt nur von der Massenverteilung ab und gibt die mit der Rotation verknüpfte Energie. Unser Tensor $\Theta$ hat mit ihm die ersten beiden Eigenschaften gemeinsam, liefert aber nur denjenigen mit der Rotation des kernfesten Koordinatensystems verknüpften Energieanteil, der von der Relativbewegung der Nukleonen nicht abhängt und den wir wegen seiner Gleichheit mit dem entsprechenden Ausdruck des starren Körpers als Rotationsenergie bezeichnet haben. $\overline{\Theta}$ gibt dagegen die Abstände der Gesamtenergie in den Rotationsspektren, enthält aber die Impulse und ist nicht symmetrisch; die letzte Eigenschaft regelt den Anteil der Rotationsaustauschsatelliten und bewirkt dadurch kleine Unterschiede der inneren Struktur in den verschiedenen Rotationszuständen. Daß die Eigenschaften des reziproken Trägheitstensors für den starren Körper hier auf zwei Tensoren verteilt sind, kann als typisch für die nichtstarren Eigenschaften des Kerns angesehen werden.

Die Energiedifferenzen der Rotationszustände verteilen sich auf die drei Anteile $E_a$, $E_{1a}$, $E_1$. Deren Größe hängt von der Art der Verknüpfung des drehbaren Systems mit dem Kern ab. Verschwände **W**, so würde $\Theta = \overline{\Theta}$, es träten keine Rotationsaustauschsatelliten auf und die Energien der Rotationszustände ergäben sich als Erwartungswerte; dieser Fall ist daher ausgezeichnet. Das Aufsuchen eines mit dem Kern verknüpften Koordinatensystems, das $\mathbf{W} = 0$ zur Folge hat, wäre sinnvoll, wenn es in übersichtlicher Weise von den dynamischen Variablen der Nukleonen abhinge und der Formalismus nicht verwickelter würde. Augenscheinlich ist aber das Gegenteil der Fall. Solange die ausgezeichnete Achse **N** nur von den Lagen abhängt, verschwindet **W** nach dem am Ende von 4. Gesagten nicht. Also müßte **N** außerdem die Spins oder die Impulse enthalten. Da für das Bestehen einer kollektiven Rotation die Existenz des Spins anscheinend nicht entscheidend ist, wird man die Impulse in **N** aufnehmen müssen. Dann kommutiert **N** nicht mehr mit der potentiellen Energie, und man kann mit Sicherheit schließen, daß **N** in verwickelter Weise von den dynamischen Variablen der Nukleonen abhängt, denn es enthält implizit die gesamte Kerndynamik. Diese verwickelte Abhängigkeit überträgt sich auf alle

Größen, wie $\Theta$ und $G$. Die Vereinfachung durch den Wegfall von **W** wird erkauft durch erhebliche Schwierigkeiten an anderen Stellen. Es ist einfacher und natürlicher, **N** mit Hilfe der Massenmomente zweiter Ordnung zu definieren und die Bewegung des so bestimmten Koordinatensystems zu untersuchen. Bei den Rotationsspektren kommt es darauf an, ihre Existenz nachzuweisen und die Berechnung der Energie zu ermöglichen. Die Forderung daß die Energiedifferenzen Erwartungswerte sind, ist übertrieben.

Es bleibt die Frage, ob sich durch eine geeignete Wahl der Abhängigkeit der Achse **N** von den Nukleonenlagen eine Verkleinerung des Einflusses von $\mathscr{H}_{1a}$ erreichen läßt. Hierzu müßte man die Abhängigkeit der Formmomente von den $r_\nu$ ändern †. Es zeigt sich aber, daß dadurch nichts Nennenswertes erreicht wird, die Formmomente werden beim Rechnen unbequemer, und ihre Verwandtschaft mit den elektrischen Quadrupolmomenten geht verloren.

### 12.2. ANDERE ARBEITEN

Während wir im Hamiltonoperator kollektive Rotationen durch eine bestimmte Umgruppierung der abstrakten Nukleonenoperatoren in Erscheinung treten ließen und erst dann zur Differentialdarstellung der Operatoren übergingen, stellt Nataf [26]) eine allgemeine Zustandsfunktion, die von den Lagekoordinaten der Nukleonen in bezug auf ein festes System abhängt, und die zugehörige Schrödingersche Differentialgleichung an den Anfang. Er trennt zunächst die Schwerpunktbewegung ab, was wir der Einfachheit halber unterließen, führt sechs Formmomente ein, die unseren $\Gamma_m$ entsprechen, und bestimmt ein gestrichenes Koordinatensystem, in dem drei der Formmomente verschwinden. Es gibt dann drei Schwerpunktkoordinaten, drei Eulersche Winkel, drei Formmomente und $3A$ auf das gestrichene System bezogene Nukleonenkoordinaten, die neun Nebenbedingungen unterworfen sind. Anschließend wird die Schrödingersche Differentialgleichung auf die neuen Koordinaten transformiert. Die Lösungen der Differentialgleichung brauchen die Nebenbedingungen nicht zu erfüllen, Eulersche Winkel und Formmomente können zunächst als unabhängig Variable betrachtet werden. Die zur Bildung der Matrixelemente erforderliche Integration erstreckt Nataf dagegen nur auf den durch die Nebenbedingungen eingeschränkten Teil des Konfigurationsraumes. Dieses Verfahren zur Behandlung überzähliger Freiheitsgrade ist zwar korrekt, aber für die Anwendung zu umständlich; es macht den Vorteil des Schalenmodells, die Bewegung der Nukleonen als unabhängig voneinander ansehen zu können, zunichte. Nataf richtet sein Interesse nun ausschließlich auf die kollektive Rotation und vernachlässigt hierzu die Änderungen der drei noch verbliebenen Formmomente. Dann wäre es grundsätzlich einfacher

† Siehe Fußnote auf S. 500.

gewesen, diese gar nicht erst aufzunehmen; dem Verfasser kommt es aber darauf an, das kollektive Modell von A. Bohr [21, 22, 27, 29, 30]) zu untersuchen, das die Nukleonenkoordinaten und sechs Oberflächenvariable enthält. Der gewonnene Ausdruck für die kinetische Energie

$$T = \sum_{i=1}^{A} \frac{p_i'^2}{2m} + \hbar^2 \sum_{\kappa} \left\{ \frac{(I_\kappa - J_\kappa)^2}{2\mathcal{J}_\kappa} + \frac{N'_\kappa (I_\kappa - J_\kappa)}{\mathcal{J}_\kappa} + \frac{1}{2\mathcal{J}_\kappa} P'_\kappa \right\} \quad (12.18)$$

gestattet einen Vergleich mit unserem aspektierten Hamiltonoperator. Bezieht man diesen auf ein Koordinatensystem, das gerade mit sämtlichen Hauptachsen des Kernellipsoides zusammenfällt, so ergibt sich ein Ausdruck, den man aus (12.18) durch Streichen der Terme $\kappa = 3$ und der $P'_\kappa$ erhält. Die Terme mit $\kappa = 3$ treten bei Nataf auf, weil er kollektive Rotationen um alle drei Achsen behandelt, die Anwesenheit der $P'_\kappa$ erscheint dagegen vom Standpunkt unserer Theorie aus merkwürdig, da diese Operatoren mit allen Hauptachsenrichtungen kommutieren.

Was Nataf an dem Energieausdruck (12.18) stört, sind die Glieder $N'_\kappa I_\kappa / \mathcal{J}_\kappa$; er befürchtet, daß sie den gewohnten Bau der Rotationsspektren zerstören. Er zeigt, daß sie klein sind gegen die Glieder mit $I_\kappa J_\kappa$, die er nicht als störend empfindet, doch erfüllte bei ihrem Fortlassen der Hamiltonoperator die zur fehlerfreien Anwendung der Methode der überzähligen Variablen notwendigen Kommutierungsforderungen nicht mehr. Nataf kommt so zum Schluß, daß die dynamischen Variablen der Kernoberfläche nicht als Funktionen der Nukleonenlagen allein betrachtet werden können; andererseits entstünden Komplikationen, wenn sie auch die Impulse enthielten. Einen Ausweg aus diesen Schwierigkeiten sieht er in den Arbeiten von Inglis [31]) sowie von Peierls und Yoccoz [32, 33]). Wir fanden dagegen bei den Rotationsspektren, daß jeder Operator von der Form $\mathbf{W} \cdot \mathbf{J}$, wo $\mathbf{W}$ irgendein mit $\mathbf{N}$ vertauschbarer Vektor ist, bei genügender Kleinheit einen Beitrag zur Energie liefert, welcher die gleiche Abhängigkeit von den Gesamtdrehimpulsen hat wie $\mathscr{H}_a$; die Notwendigkeit, gewisse Teile in $\mathscr{H}_{1a}$ zu beseitigen, ergab sich nicht.

Villars [34]) verwendet bei seiner Behandlung der kollektiven Rotation $3A$ unabhängige Lagekoordinaten, nämlich drei Schwerpunktkoordinaten, die drei Eulerschen Winkel eines mit dem Kern verbundenen Koordinatensystems und $3A-6$ innere Variable, welche die Lage der Nukleonen relativ zum drehbaren System angeben. Die zu den Eulerschen Winkeln gehörigen Impulse sind lineare Funktionen der Drehimpulskomponenten, also gibt die kanonische Form der kinetischen Energie deren Abhängigkeit vom Drehimpuls und damit den reziproken Trägheitstensor. Die diesen bestimmenden Größen $M_{1\alpha,AB}$ entsprechen unseren für den Dreiachsenaspekt abgeleiteten Impulsaufteilungstensor $\Lambda_\nu$ in (3.51). Für das Auftreten von Rotationsspektren ist nach Villars notwendig, daß erstens die im Gesamtdrehimpuls

linearen Glieder als kleine Störung betrachtet werden können und zweitens die Abweichung des reziproken Trägheitstensors von einem geeignet gewählten Mittelwert klein ist. Die letzte Bedingung entspricht unserer bereits bei der Berechnung des Kerns (21,24) aufgestellten Forderung nach Kleinheit der Schwankungsgrößen.

Der Wert der Komponenten des reziproken Trägheitstensors hängt davon ab, wie das drehbare System mit dem Kern verbunden ist. Villars stellt hierzu Molekül und Atomkern gegenüber. Beim Molekül kann man, da die Kerne um Gleichgewichtslagen schwingen, das drehbare System so wählen, daß die bei uns mit **W** bezeichnete Größe so klein wie möglich wird. Das führt auf den reziproken Trägheitstensor des starren Körpers. Beim Atomkern dagegen erstreckt sich die Wellenfunktion jedes Nukleons über den ganzen Kern. Hier bestimmt Villars das drehbare System durch das Nullsetzen dreier Massenmomente zweiter Ordnung. In diese nimmt er Gewichtsfaktoren $w(i)$ auf, die er zunächst gleich 1 setzt. Dann ist das drehbare System in der gleichen Weise festgelegt wie bei uns im Fall des Dreiachsenaspektes, und die reziproken Trägheitsmomente sind die gleichen wie bei Nataf.

Das Rechnen mit Zustandsfunktionen, die von den inneren Variablen abhängen, ist zu verwickelt. Villars umgeht diese Schwierigkeit durch Bildung eines unsymmetrischen Hamiltonoperators. Der Kern wird in einen Rumpf und in eine Anzahl „Valenz"-Nukleonen eingeteilt. Diese werden durch unabhängige Lage- und Impulskoordinaten beschrieben, und die kinetische Energie des Rumpfes wird auf die kanonische Form gebracht. Über den Rumpf denkt sich Villars mit Hilfe geeigneter Funktionen, die drei Oberflächenvariable enthalten, gemittelt. Um den Hamiltonoperator auf die von A. Bohr angegebene Form [28]) bringen zu können, muß er die Annahme machen, daß die von ihm eingeführten inneren Drehimpulse für den Rumpf verschwinden. Ob diese Bedingung tatsächlich erfüllt ist, steht, wie er erwähnt, nicht fest, aber ihre Befriedigung liefert ein dynamisches Argument zur Bestimmung der $w(i)$. Hierzu sei bemerkt, daß die Einteilung des Kerns in Rumpf und Valenznukleonen im allgemeinen nicht von vornherein feststeht, oft bieten sich verschiedene Möglichkeiten für die Besetzung der Unterschalen an, von denen die richtige durch Energievergleich gefunden werden muß. Villars zeigt schließlich unter Weglassen des Spins, daß sich aus dem gewonnenen unsymmetrischen Hamiltonoperator die gleichen effektiven Trägheitsmomente ergeben wie bei Inglis [31]), wenn der Gesamtdrehimpuls als klassischer Vektor aufgefaßt wird.

Wir stellen bei dieser Gelegenheit einige Formeln zusammen, die für die Betrachtungsweise von Inglis [31]) nützlich sind.

Ein Koordinatensystem $\Sigma$ rotiere mit der vorgegebenen Winkelgeschwin-

digkeit $\omega$. Dann lautet der auf $\Sigma$ bezogenen Hamiltonoperator eines spinlosen Teilchens

$$\mathscr{H} = \frac{1}{2M}|\mathbf{p}|^2 - \boldsymbol{\omega}\cdot\mathbf{l} + V, \quad \mathbf{l} = \mathbf{r}\times\mathbf{p}. \tag{12.19}$$

Er ist nicht mit dem Energieoperator $\mathscr{E}$ identisch, vielmehr gilt

$$\mathscr{E} = \frac{1}{2M}|\mathbf{p}|^2 + V. \tag{12.20}$$

Wir leiten zunächst die entsprechenden klassischen Formeln ab. Alle relativen Zeitdifferentiationen werden mit einem Punkt bezeichnet. Dann ist

$$\mathbf{v}_{\mathrm{rel}} = \dot{\mathbf{r}}, \quad \mathbf{v}_{\mathrm{abs}} = \dot{\mathbf{r}} + \boldsymbol{\omega}\times\mathbf{r}, \tag{12.21}$$

und als richtige Lagrangefunktion erweist sich

$$L = T_{\mathrm{abs}} - V, \tag{12.22}$$

wobei $\mathrm{d}/\mathrm{d}t\ \partial L/\partial\dot{\mathbf{r}}$ als relative zeitliche Änderung zu nehmen, also nur auf die Koordinaten und nicht auf die Basisvektoren zu erstrecken ist. Dann ergibt sich mit dem Impuls

$$\mathbf{p} \equiv \frac{\partial L}{\partial \dot{\mathbf{r}}} = M(\dot{\mathbf{r}} + \boldsymbol{\omega}\times\mathbf{r}) \tag{12.23}$$

die Hamiltonfunktion

$$H = \frac{1}{2M}|\mathbf{p}|^2 - \boldsymbol{\omega}\cdot\mathbf{l} + V, \tag{12.24}$$

jedoch für die Energie mit (12.21) und (12.23)

$$E_{\mathrm{abs}} \equiv \frac{M}{2}|\mathbf{v}_{\mathrm{abs}}|^2 + V = \frac{1}{2M}|\mathbf{p}|^2 + V. \tag{12.25}$$

Die Aufteilung von $\mathbf{v}_{\mathrm{abs}}$ nach (12.21) legt eine entsprechende Zerlegung

$$E_{\mathrm{abs}} = E_{\mathrm{a}} + E_{\mathrm{ia}} + E_{\mathrm{i}} \tag{12.26}$$

nahe:

$$\begin{aligned} E_{\mathrm{i}} &\equiv \frac{M}{2}|\mathbf{v}_{\mathrm{rel}}|^2 + V = \frac{1}{2M}|\mathbf{p}|^2 - \boldsymbol{\omega}\cdot\mathbf{l} + \frac{M}{2}|\boldsymbol{\omega}\times\mathbf{r}|^2 \\ E_{\mathrm{a}} &\equiv \frac{M}{2}|\boldsymbol{\omega}\times\mathbf{r}|^2 \\ E_{\mathrm{ia}} &\equiv M\mathbf{v}_{\mathrm{rel}}\cdot\boldsymbol{\omega}\times\mathbf{r} = \boldsymbol{\omega}\cdot\mathbf{l} + M|\boldsymbol{\omega}\times\mathbf{r}|^2. \end{aligned} \tag{12.27}$$

Keine der Energien ist mit $H$ identisch. $\mathscr{H}$ folgt aus $H$ durch Umdeuten von $\mathbf{p}$ und $\mathbf{r}$ als Operatoren, die den elementaren Vertauschungsrelationen genügen. Um zu beweisen, daß (12.25) ... (12.27) auch quantenmechanisch gelten, bilden wir

$$\dot{\mathbf{r}} \equiv \frac{i}{\hbar}[\mathscr{H}, \mathbf{r}] = \frac{1}{M}\mathbf{p} - \boldsymbol{\omega} \times \mathbf{r} \tag{12.28}$$

und erkennen, daß $\dot{\mathbf{r}}$ der Operator der Relativgeschwindigkeit ist, denn die elementaren Vertauschungsrelationen, aus denen (12.28) folgt, wirken nur auf die Komponenten der Vektoren und nicht auf die Koordinatenachsen. Der Operator der Absolutgeschwindigkeit folgt aus (12.28) durch Addition der Fahrzeuggeschwindigkeit $\boldsymbol{\omega} \times \mathbf{r}$. Dann gelten die Gleichungen (12.21) und (12.23) und folglich (12.25) ... (12.27) auch für die Operatoren.

Die andere Möglichkeit zur Ableitung von (12.19) hat als Ausgangspunkt die Schrödingergleichung für ein festes Koordinatensystem

$$\left(\mathscr{H} + \frac{\hbar}{i}\frac{\partial}{\partial t}\right)\psi = 0, \quad \mathscr{H} = \frac{1}{2M}|\mathbf{p}|^2 + V. \tag{12.29}$$

Übergang auf das rotierende System $\Sigma$ bedeutet Einführung von Funktionen, deren Raumkoordinaten auf $\Sigma$ zu beziehen sind. Dann ist die bei konstanten Absolutkoordinaten zu nehmende Zeitableitung in (12.29) durch die Zeitableitung bei konstanten Relativkoordinaten zu ersetzen. So entsteht gerade das Glied $-\boldsymbol{\omega} \cdot \mathbf{l}$. Diese Ableitung läßt sofort erkennen, daß der neue Hamiltonoperator nicht mit dem Energieoperator identisch ist.

Bei mehreren Teilchen lauten die Operatoren

$$\mathscr{H} = \sum_\nu \frac{1}{2M}|\mathbf{p}_\nu|^2 - \boldsymbol{\omega} \cdot \mathbf{L} + V, \tag{12.30}$$

$$\mathscr{E} = \sum_\nu \frac{1}{2M}|\mathbf{p}_\nu|^2 + V \tag{12.31}$$

$$\begin{aligned} \mathscr{E}_1 &= \sum_\nu \frac{1}{2M}|\mathbf{p}_\nu|^2 - \boldsymbol{\omega} \cdot (\mathbf{L} - \boldsymbol{\omega} \cdot \mathscr{J}) - \tfrac{1}{2}\omega^2 \cdot\cdot \mathscr{J} + V \\ \mathscr{E}_2 &= \tfrac{1}{2}\omega^2 \cdot\cdot \mathscr{J} \\ \mathscr{E}_{12} &= \boldsymbol{\omega} \cdot (\mathbf{L} - \boldsymbol{\omega} \cdot \mathscr{J}), \end{aligned} \tag{12.32}$$

$$\mathscr{J} = M \sum_\nu \{|\mathbf{r}_\nu|^2 \delta - \mathbf{r}_\nu^2\}. \tag{12.33}$$

Die Glieder in (12.32) sind auf die gleiche Form gebracht wie der aspektierte Hamiltonoperator (3.34) ... (3.37). An die Stelle von $\mathbf{J}$ ist $\boldsymbol{\omega}$ und an die Stelle des reziproken Trägheitstensors der Trägheitstensor, und zwar der des starren Körpers, getreten; $\mathbf{W}$ ist ersetzt durch den relativen elementaren Bahndrehimpuls $\mathbf{L} - \boldsymbol{\omega} \cdot \mathscr{J}$. Wir nehmen mit Inglis an, daß sich die Nukleonen in einem mit der Winkelgeschwindigkeit rotierenden Ellipsoidpotential bewegen. Das Aufsuchen der im System $\Sigma$ stationären Lösungen bedeutet Lösung des Eigenwertproblems für $\mathscr{H}$. Der niedrigste Eigenwert $H$ von $\mathscr{H}$, dessen Kenntnis grundsätzlich nicht nötig ist, da $\mathscr{H}$ mit keinem der Energieoperatoren übereinstimmt, lautet in zweiter Näherung nach Inglis

$$H = E_0 - \tfrac{1}{2}\omega^2 \mathcal{J}_{ett}. \tag{12.34}$$

Nachdem die Eigenfunktionen störungsmäßig bestimmt sind, bildet man mit diesen die Erwartungswerte der Energieoperatoren und erhält

$$\langle \mathcal{E} \rangle = E_0 + \tfrac{1}{2}\omega^2 \mathcal{J}_{ett}, \tag{12.35}$$

$$\langle \mathcal{E}_1 \rangle = E_0 + \tfrac{1}{2}\omega^2 \{\langle \mathcal{J}_{xx} \rangle - \mathcal{J}_{ett}\}$$

$$\langle \mathcal{E}_a \rangle = \tfrac{1}{2}\omega^2 \langle \mathcal{J}_{xx} \rangle \tag{12.36}$$

$$\langle \mathcal{E}_{ia} \rangle = -\omega^2 \{\langle \mathcal{J}_{xx} \rangle - \mathcal{J}_{ett}\}.$$

Man sieht, daß $H$ und $\langle \mathcal{E}_1 \rangle$ nicht gleich sind, wie es von Inglis angegeben und von Villars übernommen wurde.

Eine ganz andere Methode zur Bestimmung der Rotationsniveaus stammt von Peierls und Yoccoz [23, 33]). Betrachtet wird ein *gg*-Kern. Die Nukleonen sollen sich in einem Ellipsoidpotential mit Symmetrie um die $z$-Achse bewegen. $\Phi(\mathbf{x})$, wo $\mathbf{x}$ die Gesamtheit der Lagekoordinaten bedeutet, sei der Zustand mit dem tiefsten Erwartungswert des exakten Hamiltonoperatores $\mathcal{H}$. Es kann als Hartree-Fock-Lösung zu $\mathcal{H}$ angenommen werden. Zustände mit verschiedenen Richtungen der ausgezeichneten Achse werden überlagert:

$$\Psi = \int \sin\vartheta \mathrm{d}\vartheta \mathrm{d}\varphi \chi(\vartheta, \varphi) \Phi(R_{\vartheta\varphi}\mathbf{x}). \dagger \tag{12.37}$$

$R_{\vartheta\varphi}$ ist der Operator, der die $z$-Achse in die Richtung $\vartheta$, $\varphi$ dreht. Da $\Phi$ axialsymmetrisch ist, erübrigt sich die Einführung eines weiteren Winkels. $\chi(\vartheta, \varphi)$ wird bestimmt durch die Forderung

$$E_0 \equiv \frac{(\Psi, \mathcal{H}\Psi)}{(\Psi, \Psi)} = \text{Minimum}. \tag{12.38}$$

Das ergibt

$$\chi(\vartheta, \varphi) = \text{const} \cdot Y_{lm}(\vartheta, \varphi), \tag{12.39}$$

und die Energie erscheint in der Form

$$E_{lm} = \frac{\int (\Phi(R_{\vartheta\varphi}\mathbf{x}), \mathcal{H}\Phi(R_{\vartheta'\varphi'}\mathbf{x})) Y^*_{lm}(\vartheta, \varphi) Y_{lm}(\vartheta', \varphi') \mathrm{d}\omega \mathrm{d}\omega'}{\int (\Phi(R_{\vartheta\varphi}\mathbf{x}), \Phi(R_{\vartheta'\varphi'}\mathbf{x})) Y^*_{lm}(\vartheta, \varphi) Y_{lm}(\vartheta', \varphi') \mathrm{d}\omega \mathrm{d}\omega'}. \tag{12.40}$$

Bei genügend starker Deformation wird

$$E_{lm} = \frac{H_0}{N_0} + \tfrac{1}{2} l(l+1) \left[\frac{N_2 H_0}{N_0^2} - \frac{H_2}{N_0}\right], \tag{12.41}$$

wo $H_0$, $H_2$, $N_0$, $N_2$ Konstanten sind.

Die Methode ist die Übertragung des folgenden für die Translation gültigen Sachverhaltes auf die Rotation. Will man die Zustände eines Kerns näherungsweise mit Hilfe eines im Koordinatenursprung befindlichen kugel-

† Der Faktor $\sin\vartheta$ ist in der zitierten Arbeit versehentlich fortgelassen.

symmetrischen Potentialtopfes beschreiben, so verstößt man gegen die Symmetrie, denn der Hamiltonoperator ist invariant gegen Translationen. Die Symmetrie läßt sich wiederherstellen durch Überlagerung von Zuständen mit allen möglichen Lagen des Potentialtopfes, die Bestimmung der Überlagerungsfunktion erfolgt nach dem Variationsprinzip. Die Verwendung eines von der Kugelform abweichenden Potentials wird von Peierls und Yoccoz damit begründet, daß nach Rainwater [35]) ein Ellipsoidpotential im allgemeinen einen niedrigeren Wert für

$$E_0 = \frac{(\Phi, \mathcal{H}\Phi)}{(\Phi, \Phi)} \tag{12.42}$$

ergibt. Nun interessieren Rainwater aber die Eigenwerte zu einem Hamiltonoperator $\mathcal{H}_0$ mit Ellipsoidpotential in Abhängigkeit von dessen Deformationsgrad, während Peierls und Yoccoz hier die Erwartungswerte eines exakten Hamiltonoperators $\mathcal{H}$, gebildet mit Eigenfunktionen von $\mathcal{H}_0$, betrachten. Die Erniedrigung der Energie hat aber dann folgende Gründe. Es seien $\Psi_k$ $(k = 0, 1, 2, \ldots)$ die Eigenfunktionen eines Hamiltonoperators mit Kugelpotential. Jedes $\Psi_k$ habe Drehimpulsquantenzahlen $J, M$; $\Psi_0$ sei die Funktion mit dem niedrigsten $(\Psi_k, \mathcal{H}\ \Psi_k)$. Der Grundzustand kann durch Ansetzen einer Linearkombination

$$\Psi'_0 = \sum_k \Psi_k c_{k0} \tag{12.43}$$

verbessert werden. Andererseits können die bei deformiertem Potential sich ergebenden Zustände $\Phi_k$ nach dem Orthogonalsystem der $\Psi_k$ entwickelt werden. Für den Zustand $\Phi_0$ mit dem niedrigsten $(\Phi_k, \mathcal{H}\Phi_k)$ gilt dann

$$\Phi_0 = \sum_k \Psi_k b_{k0}(\varepsilon), \tag{12.44}$$

wo $\varepsilon$ der Deformationsgrad des Potentials ist. $\Phi_0$ enthält sicher einen wesentlichen Anteil von $\Psi_0$. Die $\Psi_k$ in $\Phi_0$ lassen sich danach unterscheiden, ob sie auch in $\Psi'_0$ vorkommen oder nicht. Die ersten verbessern bei geeignet gewähltem $\varepsilon$ den Grundzustand, die anderen verschlechtern ihn und erzeugen besonders eine Unschärfe des Drehimpulses, die wegen der Rotationssymmetrie von $\mathcal{H}$ gar nicht aufzutreten braucht und daher unerwünscht ist. Die Verbesserung des Grundzustandes durch Deformation des Potentials besteht also lediglich darin, daß zu $\Psi_0$ unter anderen solche Funktionen hinzutreten, die auch in dem korrekten Ausdruck enthalten sind; der beste Wert von $\varepsilon$ ist derjenige, bei dem der verbessernde Einfluß dieser Funktionen die Verschlechterung durch die anderen am meisten überwiegt. Die von Peierls und Yoccoz an den Anfang gestellte Funktion $\Phi(\mathbf{x})$ ist ein derart verbesserter Grundzustand. Die Integration mit $Y_{lm}$ nach (12.37) und (12.39) erfaßt die verschiedenen Drehimpulse, die das unerwünschte Nebenprodukt

der Verbesserung des Grundzustandes sind. Beweis: $\Phi(\mathbf{x})$ läßt sich nach den einzelnen Drehimpulsen $L$ entwickeln, es ist also

$$\Phi(\mathbf{x}) = \sum_L c^L \Psi_0{}^L(\mathbf{x}). \tag{12.45}$$

Das in (12.37) auftretende $\Phi(R_{\vartheta\varphi}\mathbf{x})$ geht durch eine Drehung $D$ aus $\Phi(\mathbf{x})$ hervor, und es gilt entsprechend zu (B18)

$$D\Phi(\mathbf{x}) = \sum_L \sum_M c^L \Psi_M{}^L(\mathbf{x}) a^L_{M0}(D). \tag{12.46}$$

Nach (C6) und (C7) ist aber †

$$a^L_{M0}(D) = \sqrt{\frac{4\pi}{2L+1}}\, \mathring{Y}_{LM}(\vartheta, \varphi), \tag{12.47}$$

wenn $\vartheta, \varphi$ die zwei wesentlichen Eulerschen Winkel der Drehung sind. Dann wird aber

$$\int \mathrm{d}\omega Y_{lm}(\vartheta, \varphi) D\Phi(\mathbf{x}) = \sqrt{\frac{4\pi}{2l+1}}\, c^l \Psi_m{}^l(\mathbf{x}), \quad \text{q. e. d.}. \tag{12.48}$$

Die Energie dieser Anteile ist durch (12.41) gegeben; sie hängt nicht von der Stärke der Anteile, sondern nur von der Struktur von $\Phi(\mathbf{x})$ ab.

Offenbar muß man in $\Phi(\mathbf{x})$ mehr erblicken können als einen mangelhaft verbesserten Grundzustand. Das ist tatsächlich möglich, wenn man die von Peierls und Yoccoz betrachteten Verhältnisse bei der Translation auf die Rotation überträgt. Es wird dort die Funktion $\Phi(\mathbf{x}_1, \ldots \mathbf{x}_A)$ eingeführt, welche die Bewegung der Nukleonen in einem Kugelpotential mit dem Zentrum im Koordinatenursprung beschreibt. Was man kennen möchte, ist die Nukleonenbewegung bei festem Schwerpunkt. $\Phi$ enthält dagegen Schwerpunktbewegungen, die von Elliot und Skyrme [36]) untersucht worden sind. Die Bedeutung der von Peierls und Yoccoz gebildeten Funktion

$$\Psi(\mathbf{x}_1, \ldots, \mathbf{x}_A) = \frac{1}{\sqrt{2\pi}^3} \int \mathrm{e}^{\mathrm{i}\mathbf{k}\cdot\mathbf{r}} \Phi(\mathbf{x}_1 - \mathbf{r}, \ldots, \mathbf{x}_A - \mathbf{r}) \mathrm{d}^3\mathbf{r}, \tag{12.49}$$

mit der sie die Energie berechnen und für nicht zu große $\mathbf{k}$ einen Ausdruck von der Form

$$E = E_0 + \frac{\hbar^2 k^2}{2A_{\mathrm{eff}} M} \tag{12.50}$$

erhalten, erkennt man durch Einführung von Schwerpunkt- und Relativkoordinaten und Fourierzerlegung der Schwerpunktbewegung:

$$\Phi(\mathbf{x}_1, \ldots, \mathbf{x}_A) = (2\pi)^{-\frac{3}{2}} \int \mathrm{e}^{\mathrm{i}\mathbf{k}\cdot\mathbf{x}} F(\mathbf{x}'_1, \ldots, \mathbf{x}'_A, \mathbf{k}) \mathrm{d}^3\mathbf{k}. \tag{12.51}$$

† Zwecks Übereinstimmung mit Peierls und Yoccoz bezeichnen wir hier die auf 1 normierten Kugelflächenfunktionen mit $Y_{lm}(\vartheta, \varphi)$.

Dann ist nämlich

$$\Psi(\mathbf{x}_1, \ldots, \mathbf{x}_A) = e^{i\mathbf{k}\cdot\mathbf{x}} F(\mathbf{x}'_1, \ldots, \mathbf{x}'_A, \mathbf{k}). \tag{12.52}$$

Das zweite Glied in (12.50) gibt nicht nur die Translationsenergie, sondern auch die Abhängigkeit der inneren Energie der Fourierkomponenten von $\mathbf{k}$. Nach Peierls und Yoccoz ist $A_{\text{eff}} \approx A$, also sind die $F$ fast gleich. Die kennzeichnende Eigenschaft von $\Phi(\mathbf{x}_1, \ldots, \mathbf{x}_A)$ ist, daß es näherungsweise aus den Translationszuständen des Kerns bei gleichem inneren Zustand besteht.

Bei der Übertragung auf Rotationen muß man dem Ellipsoidpotential die Eigenschaft zuschreiben, daß die von ihm beschriebenen Nukleonenbewegung mit mehr Freiheitsgraden erfolgt, als man ursprünglich wünscht. Die Rotation des Kerns läßt sich so darstellen, daß man die Bewegung einer mit dem Kern verbundenen Achse $\mathbf{N}$ verfolgt und die Nukleonenbewegung relativ zu $\mathbf{N}$ untersucht. Wir führen das schon benutzte Ellipsoidpotential mit Symmetrie um die $z$-Achse ein und betrachten den Zustand $\Phi(\mathbf{x})$ mit dem Drehimpuls Null um die Potentialachse, der zu (12.37) führte. Sodann führen wir ein Koordinatensystem $\Sigma'$ ein, dessen $z'$-Achse mit $\mathbf{N}$ zusammenfällt. Man gewinnt es in folgender Weise. Zunächst wird ein Koordinatensystem mit den beliebigen Eulerschen Winkeln $\Theta$, $\Phi$, $\Psi$ aufgestellt und das nach (12.45) zerlegte $\Phi(\mathbf{x})$ darauf bezogen. Das gibt nach Anhang B

$$\Phi(\mathbf{x}) = \sum_L \sum_\Omega c^L \Psi_\Omega{}^L(\mathbf{x}') \mathring{a}^L_{0\Omega}(T), \tag{12.53}$$

wenn $T$ die Raumdrehung mit den genannten Eulerschen Winkeln ist. Diese werden jetzt wie in 3. so gewählt, daß $I'_{\pm 1} = 0$ wird. Dadurch verlieren die $\Psi_\Omega{}^L(\mathbf{x}')$ ihre scharfen Drehimpulse, und die auf $\Sigma'$ bezogenen Lagekoordinaten $\mathbf{x}'$ werden zwei Nebenbedingungen unterworfen; um das zum Ausdruck zu bringen, schreiben wir $\Phi^{(L)}_\Omega[\mathbf{x}']$ anstelle von $\Psi_\Omega{}^L(\mathbf{x}')$. Wir können jetzt die Eulerschen Winkel und die $\mathbf{x}'$ als neue Variable wählen. Unter Berücksichtigung von (C6) wird dann

$$\Phi(\mathbf{x}) = \sum_L \sum_\Omega \frac{2\pi}{\sqrt{L+\frac{1}{2}}} \Phi^{(L)}_\Omega[\mathbf{x}'] \mathring{\mathcal{D}}^L_{0\Omega}(\Theta, \Phi, \Psi). \tag{12.54}$$

Dreht man die Achse des Potentialellipsoides in die Richtung $\vartheta$, $\varphi$, so wird, wenn $D$ die Drehung mit den Eulerschen Winkeln $\vartheta$, $\varphi$, $\psi$ ist,

$$D\Phi(\mathbf{x}) = \sum_L \sum_\Omega \sum_M \frac{2\pi}{\sqrt{L+\frac{1}{2}}} c^L \Phi^{(L)}_\Omega[\mathbf{x}'] \mathring{\mathcal{D}}^L_{M\Omega}(\Theta, \Phi, \Psi) a^L_{M0}(D) \tag{12.55}$$

und mit (C6) und (C7)

$$D\Phi(\mathbf{x}) = \sum_L \sum_\Omega \sum_M \frac{\sqrt{8\pi^3}}{L+\frac{1}{2}} c^L \Phi^{(L)}_\Omega[\mathbf{x}'] \mathring{\mathcal{D}}^L_{M\Omega}(\Theta, \Phi, \Psi) \mathring{Y}_{LM}(\vartheta, \varphi). \tag{12.56}$$

Der zu $\vartheta$, $\varphi$ hinzugefügte willkürliche Winkel $\psi$ tritt also nicht auf. Die Funktionen, deren Energien Peierls und Yoccoz berechnen, sind dann nach (12.37) und (12.39)

$$\int D\Phi(\mathbf{x})Y_{lm}(\vartheta,\varphi)\mathrm{d}\omega=\frac{\sqrt{8\pi^3}}{l+\frac{1}{2}}c^l\sum_{\Omega}\Phi^{(l)}_{\Omega}[\mathbf{x}']\mathscr{D}^l_{M\Omega}(\Theta,\Phi,\Psi). \quad (12.57)$$

Das sind aber, in unserer Sprache ausgedrückt, exakte Basisfunktionen. Das Verfahren erzeugt also für jedes $l$ eine bestimmte Linearkombination exakter Basisfunktionen, deren innere Struktur und Anteile in der Linearkombination summarisch durch das Variationsprinzip festgelegt sind. Der Ersatz der exakten durch approximative Basisfunktionen wird vermieden, weil die in (12.57) angegebene Darstellung in Wirklichkeit nicht aufgesucht wird. Allerdings dürfte das Berechnen der Matrixelemente von $\mathscr{H}$ über Funktionen $\Phi$ mit verschiedener Orientierung des Potentialellipsoides ziemlich schwierig sein. Es bleibt die Frage, ob die summarisch durch das Variationsprinzip gegebenen Zustände (12.57) die gleichen sind, wie man sie bei voneinander unabhängigen Anteilen der Zustände erhielte. Als unbefriedigend könnte empfunden werden, daß die Existenz einer kollektiven Rotation als Folge der Verwendung von Näherungsfunktionen für die Kernzustände erscheint.

Der Verfasser dankt den Herren R. Hagedorn, A. Bohr und K. W. Ford für das der Arbeit entgegengebrachte Interesse. Das Urteil dieser Personen war entscheidend für die Anerkennung der schon sehr früh begonnenen und infolge ungewöhnlich widriger Umstände erst gegen Ende 1956 abgeschlossenen Arbeit. Daß sie nicht völlig zum Erliegen kam, ist Herrn Professor von Weizsäcker zu danken, der den Verfasser unterstützte, obwohl die Arbeit gar nicht bei ihm angefertigt wurde. Der 12. Abschnitt wurde jetzt auf freundliche Anregung von Herrn Professor L. Rosenfeld hinzugefügt.

## Mathematischer Anhang

### A. VEKTOREN UND TENSOREN

*p- und q-Komponenten.* Anstelle der Komponenten $a_1$, $a_2$, $a_3$ des Vektors $\mathbf{a}$ benutzt man bisweilen vorteilhafter [19]) die Komponenten $a_p$, $a_q$, $a_3$ mit der Festsetzung

$$a_p=a_1+ia_2, \quad a_q=a_1-ia_2 \quad (A1)$$

und bei einem Tensor zweiter Stufe die Komponenten $T_{pp}$, $T_{pq}$, $T_{qp}$, $T_{qq}$, $T_{p3}$, $T_{q3}$, $T_{3p}$, $T_{3q}$, $T_{33}$:

$$
\begin{aligned}
T_{pp} &= T_{11}+iT_{21}+i(T_{12}+iT_{22}) = T_{11}-T_{22}+i(T_{12}+T_{21})\\
T_{pq} &= T_{11}+iT_{21}-i(T_{12}+iT_{22}) = T_{11}+T_{22}-i(T_{12}-T_{21})\\
T_{qp} &= T_{11}-iT_{21}+i(T_{12}-iT_{22}) = T_{11}+T_{22}+i(T_{12}-T_{21})\\
T_{qq} &= T_{11}-iT_{21}-i(T_{12}-iT_{22}) = T_{11}-T_{22}-i(T_{12}+T_{21})\\
T_{p3} &= T_{13}+iT_{23}\\
T_{q3} &= T_{13}-iT_{23}\\
T_{3p} &= T_{31}+iT_{32}\\
T_{3q} &= T_{31}-iT_{32}.
\end{aligned}
\tag{A2}
$$

Die Bedingungen für Symmetrie oder Antisymmetrie lauten dann $T_{kl} = \pm T_{lk}$, und die Komponenten des zu $T$ transponierten Tensors $\tilde{T}$ sind gegeben durch $\tilde{T}_{kl} = T_{lk}$; in beiden Fällen ist $k, l = p, q, 3$. Für die Skalarprodukte gilt

$$\mathbf{a}\cdot\mathbf{b} = \tfrac{1}{2}(a_p b_q + a_q b_p) + a_3 b_3, \tag{A3}$$

$$
\begin{aligned}
(\mathbf{a}\cdot T)_k &= \tfrac{1}{2}(a_p T_{qk} + a_q T_{pk}) + a_3 T_{3k}\\
(T\cdot\mathbf{a})_k &= \tfrac{1}{2}(T_{kp} a_q + T_{kq} a_p) + T_{k3} a_3
\end{aligned}
\qquad k = p, q, 3, \tag{A4}
$$

$$
\begin{aligned}
T\cdot\cdot S = \tfrac{1}{4}&(T_{pp}S_{qq}+T_{pq}S_{pq}+T_{qp}S_{qp}+T_{qq}S_{pp})\\
&+\tfrac{1}{2}(T_{p3}S_{3q}+T_{q3}S_{3p}+T_{3p}S_{q3}+T_{3q}S_{p3})+T_{33}S_{33}.
\end{aligned}
\tag{A5}
$$

*Eulersche Winkel; Koordinatentransformationen.* Gegeben seien die gegeneinander verdrehten Koordinatensysteme $\Sigma$ und $\Sigma'$. Die Lage von $\Sigma'$ relativ zu $\Sigma$ wird durch die in Fig. 7 erklärten Eulerschen Winkel $\Theta$, $\Phi$, $\Psi$ bestimmt.

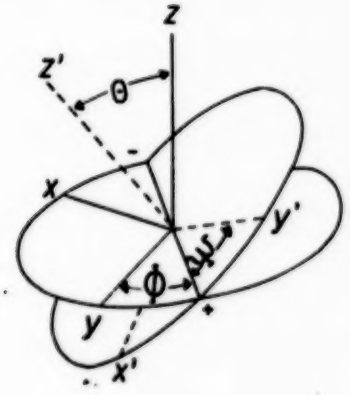


Fig. 7. Eulersche Winkel. $\pm$ positive bzw. negative Richtung der Knotenlinie.

Die Eulerschen Winkel $\Theta'$, $\Phi'$, $\Psi'$ von $\Sigma$ relativ zu $\Sigma'$ sind dann

$$\Theta' = \Theta, \quad \Phi' = \pi - \Psi, \quad \Psi' = \pi - \Phi. \tag{A6}$$

Die Komponenten eines Vektors $\mathbf{v}$ in den beiden Systemen seien mitein-

ander verknüpft durch

$$v'_k = \sum_l c_{kl} v_l. \tag{A7}$$

Die Transformationskoeffizienten lauten dann

$$\begin{aligned}
c_{11} &= \cos\Theta\cos\Phi\cos\Psi - \sin\Phi\sin\Psi \\
c_{12} &= \cos\Theta\sin\Phi\cos\Psi + \cos\Phi\sin\Psi \\
c_{13} &= -\sin\Theta\cos\Psi \\
c_{21} &= -\cos\Theta\cos\Phi\sin\Psi - \sin\Phi\cos\Psi \\
c_{22} &= -\cos\Theta\sin\Phi\sin\Psi + \cos\Phi\cos\Psi \\
c_{23} &= \sin\Theta\sin\Psi \\
c_{31} &= \sin\Theta\cos\Phi \\
c_{32} &= \sin\Theta\sin\Phi \\
c_{33} &= \cos\Theta.
\end{aligned} \tag{A8}$$

Dann lauten die Transformationsformeln für die durch (A1) und (A2) bestimmten Komponenten

$$\begin{aligned}
v'_{p,q} &= \{\tfrac{1}{2}v_p(\cos\Theta\pm1)e^{-i\Phi} + \tfrac{1}{2}v_q(\cos\Theta\mp1)e^{+i\Phi} + v_3\sin\Theta\}e^{\mp i\Psi} \\
v'_3 &= \tfrac{1}{2}(v_p e^{-i\Phi} + v_q e^{+i\Phi})\sin\Theta + v_3\cos\Theta,
\end{aligned} \tag{A9}$$

$$\left.\begin{matrix} T'_{pp} \\ T'_{qq} \end{matrix}\right\} = \{\tfrac{1}{4}T_{pp}(\cos\Theta\pm1)^2e^{+2i\Psi} - \tfrac{1}{4}(T_{pq}+T_{qp})\sin^2\Theta + \tfrac{1}{4}T_{qq}(\cos\Theta\mp1)e^{-2i\Psi}$$
$$+\tfrac{1}{2}(T_{p3}+T_{3p})\sin\Theta(\cos\Theta\pm1)e^{+i\Psi} + \tfrac{1}{2}(T_{q3}+T_{3q})\sin\Theta(\cos\Theta\mp1)e^{-i\Psi}$$
$$+T_{33}\sin^2\Theta\}e^{\pm2i\Phi}$$

$$\left.\begin{matrix} T'_{pq} \\ T'_{qp} \end{matrix}\right\} = -\tfrac{1}{4}(T_{pp}e^{+i\Psi} + T_{qq}e^{-i\Psi})\sin^2\Theta + \tfrac{1}{4}T_{pq}(1\pm\cos\Theta)^2 + \tfrac{1}{4}T_{qp}(1\mp\cos\Theta)^2$$
$$+\tfrac{1}{2}[T_{p3}(\cos\Theta\pm1)+T_{3p}(\cos\Theta\mp1)]\sin\Theta e^{+i\Psi}$$
$$+\tfrac{1}{2}[T_{q3}(\cos\Theta\mp1)+T_{3q}(\cos\Theta\pm1)]\sin\Theta e^{-i\Psi} + T_{33}\sin^2\Theta$$

$$\left.\begin{matrix} T'_{p3} \\ T'_{q3} \end{matrix}\right\} = \{-\tfrac{1}{4}[(T_{pp}e^{+2i\Psi}+T_{pq})(\cos\Theta\pm1)+(T_{qq}e^{-2i\Psi}+T_{qp})(\cos\Theta\mp1)]\sin\Theta$$
$$+\tfrac{1}{2}[T_{p3}(\cos\Theta\pm1)e^{+i\Psi}+T_{q3}(\cos\Theta\mp1)e^{-i\Psi}]\cos\Theta$$
$$-\tfrac{1}{2}(T_{3p}e^{+i\Psi}+T_{3q}e^{-i\Psi})\sin^2\Theta + T_{33}\sin\Theta\cos\Theta\}e^{\pm i\Phi} \tag{A10}$$

$$\left.\begin{matrix} T'_{3p} \\ T'_{3q} \end{matrix}\right\} = \{-\tfrac{1}{4}[(T_{pp}e^{+2i\Psi}+T_{qp})(\cos\Theta\pm1)+(T_{qq}e^{-2i\Psi}+T_{pq})(\cos\Theta\mp1)]\sin\Theta$$
$$+\tfrac{1}{2}[T_{3p}(\cos\Theta\pm1)e^{+i\Psi}+T_{3q}(\cos\Theta\mp1)e^{-i\Psi}]\cos\Theta$$
$$-\tfrac{1}{2}(T_{p3}e^{+i\Psi}+T_{q3}e^{-i\Psi})\sin^2\Theta + T_{33}\sin\Theta\cos\Theta\}e^{\pm i\Phi}$$

$$T'_{33} = \tfrac{1}{4}[T_{pp}e^{+2i\Psi}+T_{pq}+T_{qp}+T_{qq}e^{-2i\Psi}]\sin^2\Theta$$
$$-\tfrac{1}{2}[(T_{p3}+T_{3p})e^{+i\Psi}+(T_{q3}+T_{3q})e^{-i\Psi}]\sin\Theta\cos\Theta + T_{33}\cos^2\Theta.$$

## B. KUGELFLÄCHENFUNKTIONEN

*Definitionen und Formeln.* Die Kugelflächenfunktionen $Y_m^l(\vartheta, \varphi)$, $l$ und $m$ ganz, $l \geqq 0$, $-l \leqq m \leqq +l$, sind so normiert, daß sie sich in der Normaldarstellung der Drehungsgruppe [19]) befinden. Ist **I** der Operator der infinitesimalen Drehungen — er wird in Polarkoordinaten durch

$$\begin{aligned} I_{p,q} &= e^{\pm i\varphi}\left(\operatorname{ctg}\vartheta\frac{\partial}{\partial\varphi} \mp i\frac{\partial}{\partial\vartheta}\right) \\ I_3 &= -\frac{\partial}{\partial\varphi} \end{aligned} \tag{B1}$$

dargestellt — , so gilt

$$\begin{aligned} I_{p,q}Y_m^l &= -i\sqrt{(l\mp m)(l\pm m+1)}\,Y_{m\pm1}^l \\ I_3 Y_m^l &= -imY_m^l. \end{aligned} \tag{B2}$$

Verlangt man noch unter Benutzung der Definitionen [20])

$$P_l^m(\cos\vartheta) = (-1)^m(1-\cos^2\vartheta)^{\frac{m}{2}}\frac{\mathrm{d}^m}{\mathrm{d}\cos^m\vartheta}P_l(\cos\vartheta), \quad m \geqq 0, \tag{B3}$$

$$P_l(\cos\vartheta) = \frac{1}{2^l l!}\frac{\mathrm{d}^l}{\mathrm{d}\cos^l\vartheta}(\cos^2\vartheta-1)^l \tag{B4}$$

die Erfüllung der Beziehung

$$Y_0^l(\vartheta,\varphi) = P_l(\cos\vartheta), \tag{B5}$$

so sind die $Y_m^l$ völlig bestimmt und lauten

$$Y_m^l(\vartheta,\varphi) = (-1)^{\frac{|m|-m}{2}}\sqrt{\frac{(l-|m|)!}{(l+|m|)!}}\,P_l^{|m|}(\cos\vartheta)e^{im\varphi}. \tag{B6}$$

Dann gilt

$$\int_0^{2\pi}\mathrm{d}\varphi\int_0^{\pi}\mathrm{d}\vartheta\sin\vartheta\dot{Y}_m^l Y_{m'}^{l'} = \frac{4\pi}{2l+1}\delta_{ll'}\delta_{mm'}, \tag{B7}$$

$$\sum_m |Y_m^l|^2 = 1. \tag{B8}$$

Die $Y_m^2$, bei denen im Text der obere Index fortgelassen ist, lauten

$$\begin{aligned} Y_0^2(\vartheta,\varphi) &= \tfrac{1}{2}(3\cos^2\vartheta-1) \\ Y_{\pm1}^2(\vartheta,\varphi) &= \mp\sqrt{\tfrac{3}{2}}\sin\vartheta\cos\vartheta\,e^{\pm i\varphi} \\ Y_{\pm2}^2(\vartheta,\varphi) &= \sqrt{\tfrac{3}{8}}\sin^2\vartheta e^{\pm 2i\varphi}. \end{aligned} \tag{B9}$$

Die Produkte $Y_m^2 Y_{m'}^2$ lassen sich folgendermaßen durch die $Y_{m+m'}^4$, $Y_{m+m'}^2$, $Y_{m+m'}^0$ ausdrücken:

$$
\begin{aligned}
Y^2_{\pm2}Y^2_{\pm2} &= \sqrt{\tfrac{18}{35}}\,Y^4_{\pm4}\\
Y^2_{\pm2}Y^2_{\pm1} &= \sqrt{\tfrac{9}{35}}\,Y^4_{\pm3}\\
Y^2_{\pm2}Y_0{}^2 &= \sqrt{\tfrac{27}{245}}\,Y^4_{\pm2}-\tfrac{2}{7}\,Y^2_{\pm2}\\
Y^2_{\pm2}Y^2_{\mp1} &= \sqrt{\tfrac{9}{245}}\,Y^4_{\pm1}-\sqrt{\tfrac{6}{49}}\,Y^2_{\pm1}\\
Y^2_{\pm2}Y^2_{\mp2} &= \tfrac{3}{35}\,Y_0{}^4-\tfrac{2}{7}\,Y_0{}^2+\tfrac{1}{5}\\
Y^2_{\pm1}Y^2_{\pm1} &= \sqrt{\tfrac{72}{245}}\,Y^4_{\pm2}-\sqrt{\tfrac{6}{49}}\,Y^2_{\pm2}\\
Y^2_{\pm1}Y_0{}^2 &= \sqrt{\tfrac{54}{245}}\,Y^4_{\pm1}+\tfrac{1}{7}\,Y^2_{\pm1}\\
Y^2_{\pm1}Y^2_{\mp1} &= \tfrac{12}{35}\,Y_0{}^4-\tfrac{1}{7}\,Y_0{}^2-\tfrac{1}{5}\\
Y_0{}^2Y_0{}^2 &= \tfrac{18}{35}\,Y_0{}^4+\tfrac{2}{7}\,Y_0{}^2+\tfrac{1}{5}.
\end{aligned}
\tag{B10}
$$

Aus den $Y_m{}^l$ lassen sich auf 1 normierte Kugelflächenfunktionen

$$
X_m{}^l(\vartheta,\varphi)=\sqrt{\frac{2l+1}{4\pi}}\,Y_m{}^l(\vartheta,\varphi) \tag{B11}
$$

bilden. Für sie gelten folgende Beziehungen:

$$
\begin{aligned}
Y_0{}^2X_m{}^l &= \frac{3}{2}\,\frac{1}{2l+3}\sqrt{\frac{[(l+2)^2-m^2][(l+1)^2-m^2]}{(2l+5)(2l+1)}}\,X_m{}^{l+2}\\
&-\frac{l(l+1)-3m^2}{(2l+3)(2l-1)}\,X_m{}^l+\frac{3}{2}\,\frac{1}{2l-1}\sqrt{\frac{[l^2-m^2][(l-1)^2-m^2]}{(2l+1)(2l-3)}}\,X_m{}^{l-2},
\end{aligned}
\tag{B12}
$$

$$
\begin{aligned}
Y^2_{\pm1}X_m{}^l &= \sqrt{\frac{3}{2}}\,\frac{\sqrt{(l+1)^2-m^2}}{2l+3}\sqrt{\frac{(l\pm m+2)(l\pm m+3)}{(2l+5)(2l+1)}}\,X^{l+2}_{m\pm1}\\
&\pm\sqrt{\frac{3}{2}}\,\frac{2m\pm1}{(2l+3)(2l-1)}\sqrt{(l\mp m)(l\pm m+1)}\,X^l_{m\pm1}\\
&-\sqrt{\frac{3}{2}}\,\frac{\sqrt{l^2-m^2}}{2l-1}\sqrt{\frac{(l\mp m-1)(l\mp m-2)}{(2l+1)(2l-3)}}\,X^{l-2}_{m\pm1},
\end{aligned}
\tag{B13}
$$

$$
\begin{aligned}
Y^2_{\pm2}X_m{}^l &= \sqrt{\frac{3}{8}}\,\frac{1}{2l+3}\sqrt{\frac{(l\pm m+1)(l\pm m+2)(l\pm m+3)(l\pm m+4)}{(2l+5)(2l+1)}}\,X^{l+2}_{m\pm2}\\
&-\sqrt{\frac{3}{8}}\,\frac{2}{(2l+3)(2l-1)}\sqrt{(l\pm m+1)(l\pm m-1)(l\mp m)(l\mp m-1)}\,X^l_{m\pm2}\\
&+\sqrt{\frac{3}{8}}\,\frac{1}{2l-1}\sqrt{\frac{(l\mp m)(l\mp m-1)(l\mp m-2)(l\mp m-3)}{(2l+1)(2l-3)}}\,X^{l-2}_{m\pm2}.
\end{aligned}
\tag{B14}
$$

*Spin-Winkel-Funktionen.* Die aus den $X_m^l$ und den Spinfunktionen $\alpha$, $\beta$ gebildeten Funktionen mit den Quantenzahlen $j = l \pm \frac{1}{2}$ lauten, wenn $m$ jetzt die Quantenzahl des Gesamtdrehimpulses in Richtung der $z$-Achse ist,

$$Z_m^{jl} = c^{jl}_{mm-\frac{1}{2}} X^l_{m-\frac{1}{2}} \alpha + c^{jl}_{mm+\frac{1}{2}} X^l_{m+\frac{1}{2}} \beta, \tag{B15}$$

$$\begin{aligned} c^{l+\frac{1}{2}l}_{mm-\frac{1}{2}} &= -c^{l-\frac{1}{2}l}_{mm+\frac{1}{2}} = \sqrt{\frac{l+m+\frac{1}{2}}{2l+1}} \\ c^{l+\frac{1}{2}l}_{mm+\frac{1}{2}} &= \quad c^{l-\frac{1}{2}l}_{mm-\frac{1}{2}} = \sqrt{\frac{l-m+\frac{1}{2}}{2l+1}}. \end{aligned} \tag{B16}$$

Wichtig ist die aus (B12) folgende Beziehung

$$\begin{aligned} Y_0^2 Z_m^{j\,j\mp 1} = {} & \frac{3}{8}\sqrt{1-\frac{m^2}{(j+1)^2}}\sqrt{1-\frac{m^2}{(j+2)^2}}\, Z_m^{j+2\;j\mp 1+2} \\ & + \frac{3}{4}\frac{m}{j(j+2)}\sqrt{1-\frac{m^2}{(j+1)^2}}\, Z^{j+1\;j\mp 1+1} \\ & + \frac{1}{4}\left[1-\frac{3m^2}{j(j+1)}\right] Z_m^{j\;j\mp 1} \\ & + \frac{3}{4}\frac{m}{j^2-1}\sqrt{1-\frac{m^2}{j^2}}\, Z_m^{j-1\;j\mp 1-1} \\ & + \frac{3}{8}\sqrt{1-\frac{m^2}{j^2}}\sqrt{1-\frac{m^2}{(j-1)^2}}\, Z_m^{j-2\;j\mp 1-2}. \end{aligned} \tag{B17}$$

Entsprechende Gleichungen folgen aus (B13) und (B14).

*Transformation auf ein gedrehtes Koordinatensystem; gruppentheoretische Drehungskoeffizienten.* Die Kugelflächenfunktionen vom gleichen $l$ bilden eine Darstellung der Drehungsgruppe [19]). Bei der Raumdrehung $D$ geht daher $Y_m^l(\vartheta, \varphi)$ über in die Funktion

$$DY_m^l(\vartheta, \varphi) = \sum_n Y_n^l(\vartheta, \varphi) a^l_{nm}(D). \tag{B18}$$

Die Matrix der $a^l_{nm}(D)$ ist unitär. Das bedeutet

$$a^l_{nm}(D^{-1}) = \bar{a}^l_{mn}(D). \tag{B19}$$

Ist $D$ die Raumdrehung, die in Fig. 7 $\Sigma$ in $\Sigma'$ überführt, so ist $DY_m^l(\vartheta, \varphi)$ gerade das auf $\Sigma'$ zu beziehende $Y_m^l(\vartheta', \varphi')$. Sind $\vartheta$, $\varphi$ und $\vartheta'$, $\varphi'$ die Koordinaten des gleichen Punktes in $\Sigma$ und $\Sigma'$, so gilt also

$$Y_m^l(\vartheta', \varphi') = \sum_n Y_n^l(\vartheta, \varphi) a_{nm}(D). \tag{B20}$$

Die gruppentheoretischen Drehungskoeffizienten lauten, wenn sich die Funktionen der Darstellung gegenüber infinitesimalen Drehungen nach (B2) verhalten, mit $\Theta$, $\Phi$, $\Psi$ als Eulerschen Winkeln der Raumdrehung

$$a^l_{nm}(D) = C^l_{nm} e^{-i(n\Phi+m\Psi)} \sin^{2\sigma}\frac{\Theta}{2}\cos^{2\tau}\frac{\Theta}{2} G_{l-\sigma+\tau}\left(1+2\sigma+2\tau,\ 1+2\sigma,\ \sin^2\frac{\Theta}{2}\right)$$

$$2\sigma = |n-m|, \quad 2\tau = |n+m|;$$

$$C^l_{nm} = \begin{cases} (-1)^{n-m}\sqrt{\binom{l+n}{l+m}\binom{l-m}{l-n}}, & n \geqq m \\ \sqrt{\binom{l+m}{l+n}\binom{l-n}{l-m}}, & n \leqq m. \end{cases} \tag{B21}$$

Die $G$ sind Jacobische Polynome und können definiert werden durch [37])

$$G_n(\alpha, \gamma, x) = \frac{(\gamma-1)!}{(\gamma-1+n)!}\frac{\frac{\mathrm{d}}{\mathrm{d}x^n}[x^{\gamma-1+n}(1-x)^{\alpha-\gamma+n}]}{x^{\gamma-1}(1-x)^{\alpha-\gamma}}. \tag{B22}$$

Für $l = 2$ ist

$$\begin{aligned}
a^2_{\pm2,\pm2}(D) &= e^{\mp2i(\Phi+\Psi)}\cos^4\frac{\Theta}{2} \\
a^2_{\pm2,\pm1}(D) &= \mp2e^{\mp i(2\Phi+\Psi)}\sin\frac{\Theta}{2}\cos^3\frac{\Theta}{2} \\
a^2_{\pm2,0}(D) &= \sqrt{6}\, e^{\mp2i\Phi}\sin^2\frac{\Theta}{2}\cos^2\frac{\Theta}{2} = \dot{Y}^2_{\pm2}(\Theta, \Phi) \\
a^2_{\pm2,\mp1}(D) &= \mp2e^{\mp i(2\Phi-\Psi)}\sin^3\frac{\Theta}{2}\cos\frac{\Theta}{2} \\
a^2_{\pm2,\mp2}(D) &= e^{\mp2i(\Phi-\Psi)}\sin^4\frac{\Theta}{2} \\
a^2_{\pm1,\pm2}(D) &= \pm2e^{\mp i(\Phi+2\Psi)}\sin\frac{\Theta}{2}\cos^3\frac{\Theta}{2} \\
a^2_{\pm1,\pm1}(D) &= e^{\mp i(\Phi+\Psi)}\cos^2\frac{\Theta}{2}\left(1-4\sin^2\frac{\Theta}{2}\right) \\
a^2_{\pm1,0}(D) &= \mp\sqrt{6}\, e^{\mp i\Phi}\sin\frac{\Theta}{2}\cos\frac{\Theta}{2} = \dot{Y}^2_{\pm1}(\Theta, \Phi) \\
a^2_{\pm1,\mp1}(D) &= -e^{\mp i(\Phi-\Psi)}\sin^2\frac{\Theta}{2}\left(1-4\cos^2\frac{\Theta}{2}\right)
\end{aligned} \tag{B23}$$

$$a^2_{\pm 1,\mp 2}(D) = \mp 2 e^{\mp i(\Phi - 2\Psi)} \sin^3 \frac{\Theta}{2} \cos \frac{\Theta}{2}$$

$$a^2_{0,\pm 2}(D) = \sqrt{6}\, e^{\mp 2i\Psi} \sin^2 \frac{\Theta}{2} \cos^2 \frac{\Theta}{2} \qquad = Y^2_{\mp 2}(\Theta, \Psi)$$

$$a^2_{0,\pm 1}(D) = \pm \sqrt{6}\, e^{\mp i\Psi} \sin \frac{\Theta}{2} \cos \frac{\Theta}{2} \left(1 - 2 \sin^2 \frac{\Theta}{2}\right) = Y^2_{\mp 1}(\Theta, \Psi)$$

$$a^2_{00}(D) = 1 - 6 \sin^2 \frac{\Theta}{2} + 6 \sin^4 \frac{\Theta}{2} \qquad = Y_0{}^2(\Theta, \Psi) = \mathring{Y}_0{}^2(\Theta, \Phi).$$

### C. KREISELEIGENFUNKTIONEN

*Definitionen und Formeln.* Gegeben seien die Koordinatensysteme $\Sigma$ und $\Sigma'$ der Fig. 7. Die Kreiseleigenfunktionen $\mathfrak{D}^J_{M\Omega}(\Theta, \Phi, \Psi)$ beschreiben das Verhalten des drehbaren Systems und sind bestimmt durch

$$\begin{aligned} \{|\mathbf{I}|^2 + J(J+1)\}\mathfrak{D}^J_{M\Omega} &\equiv 0 \\ \{I_3 + iM\}\mathfrak{D}^J_{M\Omega} &\equiv 0 \\ \{I'_3 + i\Omega\}\mathfrak{D}^J_{M\Omega} &\equiv 0. \end{aligned} \tag{C1}$$

$\mathbf{I}$ ist der Operator der infinitesimalen Drehungen des drehbaren Systems. Die Differentialdarstellungen seiner Komponenten lauten

$$\begin{aligned} I_{p,q} &= e^{\pm i\Phi} \left\{ \operatorname{ctg} \Theta \frac{\partial}{\partial \Phi} - \frac{1}{\sin \Theta} \frac{\partial}{\partial \Psi} \mp i \frac{\partial}{\partial \Theta} \right\} \\ I_3 &= -\frac{\partial}{\partial \Phi}, \end{aligned} \tag{C2}$$

$$\begin{aligned} I'_{p,q} &= e^{\mp i\Psi} \left\{ \frac{1}{\sin \Theta} \frac{\partial}{\partial \Phi} - \operatorname{ctg} \Theta \frac{\partial}{\partial \Psi} \pm i \frac{\partial}{\partial \Theta} \right\} \\ I'_3 &= -\frac{\partial}{\partial \Psi}. \end{aligned} \tag{C3}$$

Es gelten die Vertauschungsrelationen

$$[I_1, I_2] = I_3 \qquad \text{und zyklisch Vertauschte,} \tag{C4}$$

$$[I'_1, I'_2] = -I'_3 \quad \text{und zyklisch Vertauschte.} \tag{C5}$$

Die Verschiedenheit der Vorzeichen in (C4) und (C5) kommt daher, daß bei zwei aufeinanderfolgenden Drehungen um gegebene Achsen in $\Sigma'$ die räumliche Lage der zweiten Drehachse durch die erste Drehung verändert wird.

Die Kreiseleigenfunktionen sind mit den gruppentheoretischen Drehungs-

koeffizienten verknüpft durch

$$\mathfrak{D}^J_{M\Omega}(\Theta, \Phi, \Psi) = \frac{\sqrt{J+\frac{1}{2}}}{2\pi} \mathring{a}^J_{M\Omega}(D), \tag{C6}$$

wenn $D$ die Raumdrehung mit den Eulerschen Winkeln $\Theta$, $\Phi$, $\Psi$ ist. Speziell für $\Omega = 0$ gilt

$$\mathfrak{D}^J_{M0}(\Theta, \Phi, \Psi) = \frac{1}{\sqrt{2\pi}} X_M{}^J(\Theta, \Phi). \tag{C7}$$

Die $\mathfrak{D}^J_{M\Omega}$ befinden sich in der Normaldarstellung der Drehungsgruppe. Entsprechend zu (B2) gilt

$$\begin{aligned} I_{p,q}\mathfrak{D}^J_{M\Omega} &= -i\sqrt{(J\mp M)(J\pm M+1)}\,\mathfrak{D}^J_{M\pm1,\Omega} \\ I_3\mathfrak{D}^J_{M\Omega} &= -iM\mathfrak{D}^J_{M\Omega}. \end{aligned} \tag{C8}$$

Dagegen ergibt sich mit (C2)

$$\begin{aligned} I'_{p,q}\mathfrak{D}^J_{M\Omega} &= -i\sqrt{(J\pm\Omega)(J\mp\Omega+1)}\,\mathfrak{D}^J_{M\Omega\mp1} \\ I'_3\mathfrak{D}^J_{M\Omega} &= -i\Omega\mathfrak{D}^J_{M\Omega}. \end{aligned} \tag{C9}$$

Die Normierungsgleichung lautet

$$(\mathfrak{D}^J_{M\Omega}, \mathfrak{D}^{J'}_{M'\Omega'}) = \int_0^{2\pi} d\Psi \int_0^{2\pi} d\Phi \int_0^{\pi} d\Theta \sin\Theta \mathring{\mathfrak{D}}^J_{M\Omega}\mathfrak{D}^{J'}_{M'\Omega'} = \delta_{JJ'}\delta_{MM'}\delta_{\Omega\Omega'}. \tag{C10}$$

Die Drehimpulsoperatoren sind die mit $i\hbar$ multiplizierten Operatoren der infinitesimalen Drehungen. Werden die $\mathfrak{D}^J_{M\Omega}$ zur Beschreibung eines quantenmechanischen Systems benutzt, dessen Bestandteile Bahndrehimpuls und Spin besitzen, so ist auseinanderzuhalten, ob die Bezugsachse für den Spin in der $z$- oder in der $z'$-Richtung liegt. Im zweiten Fall wird bei einer Änderung der Eulerschen Winkel zugleich das Bezugssystem für den Spin gedreht, und es gilt, wenn $\mathbf{J}$ der Gesamtdrehimpuls-Operator ist,

$$\mathbf{J} = i\hbar\mathbf{I}. \tag{C11}$$

Für den ersten Fall ist dagegen mit $\mathbf{L}$ als Bahndrehimpuls-Operator

$$\mathbf{L} = i\hbar\mathbf{I} \tag{C12}$$

Die Quantenzahlen von $\mathfrak{D}^J_{M\Omega}$ beziehen sich dann auf den Bahndrehimpuls. Man ersetzt sie in diesem Fall durch für den Bahndrehimpuls übliche Zeichen, etwa $L$, $M_L$, $\Lambda$.

Die $\mathfrak{D}^J_{M\Omega}$ sind Eigenfunktionen des symmetrischen Kreisels. Dessen Hamiltonoperator ist nach (4.2)

$$\mathscr{H} = \frac{A}{2}|\mathbf{J}|^2 + \frac{C-A}{2} J'^2_3, \tag{C13}$$

und die Energieeigenwerte sind nach (C5)

$$E_\Omega^J = \hbar^2\left\{\frac{A}{2}J(J+1)+\frac{C-A}{2}\Omega^2\right\}. \tag{C14}$$

*Matrixelemente*

$$(\mathfrak{D}^J_{J\Omega}, \sin\Theta e^{\pm i\Psi} I'_{\nu,\varrho}\mathfrak{D}^J_{J\Omega}) = -i\frac{\Omega(\Omega\mp1)-J(J+1)}{J+1}, \tag{C15}$$

$$(\mathfrak{D}^J_{J\Omega}, \cos\Theta\,\mathfrak{D}^J_{J\Omega}) = \frac{\Omega}{J+1}, \tag{C16}$$

$$(\mathfrak{D}^J_{J\Omega\pm1}, \cos\Theta\, e^{\pm i\Psi}\mathfrak{D}^J_{J\Omega}) = -\frac{\sqrt{(J\mp\Omega)(J\pm\Omega+1)}}{J+1}, \tag{C17}$$

$$(\mathfrak{D}^J_{J\Omega}, Y_0^2(\Theta,\Phi)\mathfrak{D}^J_{J\Omega}) = \frac{1}{2}\frac{3\Omega^2-J(J+1)}{(J+1)(J+\frac{3}{2})}, \tag{C18}$$

$$(\mathfrak{D}^J_{J\Omega\pm1}, Y^2_{\pm1}(\Theta,\Phi)\mathfrak{D}^J_{J\Omega}) = \pm\sqrt{\frac{3}{2}}\frac{\sqrt{(J\mp\Omega)(J\pm\Omega+1)}(\Omega\pm\frac{1}{2})}{(J+1)(J+\frac{3}{2})}, \tag{C19}$$

$$(\mathfrak{D}^J_{J\Omega\pm2}, Y^2_{\pm2}(\Theta,\Phi)\mathfrak{D}^J_{J\Omega}) = \sqrt{\frac{3}{8}}\frac{\sqrt{(J\mp\Omega)(J\pm\Omega+1)(J\mp\Omega-1)(J\pm\Omega+2)}}{(J+1)(J+\frac{3}{2})} \tag{C20}$$

## D. MATRIXELEMENTE VON OPERATORSUMMEN MIT SLATERDETERMINANTEN

*Eine einzige Determinante.* $\Phi$ sei eine Slaterdeterminante, bestehend aus den Einzelzuständen $\varphi_k$, $1 \leqq k \leqq Z$, und $\alpha$ ein Operator, der nur von den Koordinaten eines Teilchens abhängt. Sollen $\varphi_k$ und $\alpha$ sich auf das $\nu$-te Teichen beziehen, so schreiben wir $\varphi_k(\nu)$ und $\alpha(\nu)$. Der Operator

$$A = \sum_\nu \alpha(\nu) \tag{D1}$$

hat dann den Erwartungswert

$$\langle A\rangle = (\Phi, A\Phi) = \sum_\nu a_{kk}, \quad a_{kk} = (\varphi_k, \alpha\varphi_k). \tag{D2}$$

$\Psi$ sei eine andere Slaterdeterminante, die sich von $\Phi$ nur in einem Einzelzustand unterscheidet, und zwar nehmen wir $\psi_1 \neq \varphi_1$, $\psi_k = \varphi_k$ für $k \neq 1$ an. Dann ist

$$(\Phi, A\Psi) = (\varphi_1, \alpha\psi_1). \tag{D3}$$

Für Slaterdeterminanten, die sich in mehr als einem Einzelzustand unterscheiden, verschwinden die Matrixelemente von (D1).

$\beta$ sei ein Operator, der ebenfalls nur von den Koordinaten eines Teilchens abhängt. Für den Operator

$$AB = \sum_{\mu} \alpha(\mu) \sum_{\nu} \beta(\nu) \tag{D4}$$

ergibt sich

$$\langle AB\rangle = (\Phi, AB\Phi) = \sum_{k} (\alpha\beta)_{kk} + \sum_{k} \sum_{l} (\alpha_{kk}\beta_{ll} - \alpha_{kl}\beta_{lk}), \tag{D5}$$

$$\langle AB\rangle - \langle A\rangle\langle B\rangle = \sum_{k} (\alpha\beta)_{kk} - \sum_{k} \sum_{l} \alpha_{kl}\beta_{lk}, \tag{D6}$$

$$(\Phi, AB\Psi) = (\varphi_1, \alpha\beta\psi_1) + \sum_{k} \{(\varphi_1, \alpha\psi_1)\beta_{kk} - \alpha_{1k}(\varphi_k, \beta\psi_1) + \alpha_{kk}(\varphi_1, \beta\psi_1) - (\varphi_k, \alpha\psi_1)\beta_{1k}\}. \tag{D7}$$

$X$ sei eine Slaterdeterminante, die sich von $\Phi$ in zwei Einzelzuständen unterscheidet; es sei $\chi_1 \neq \varphi_1$, $\chi_2 \neq \varphi_2$, $\chi_k = \varphi_k$ für $k \neq 1, 2$. Dann ist

$$(\Phi, ABX) = (\varphi_1, \alpha\chi_1)(\varphi_2, \beta\chi_2) - (\varphi_1, \alpha\chi_2)(\varphi_2, \beta\chi_1) + (\varphi_2, \alpha\chi_2)(\varphi_1, \beta\chi_1) - (\varphi_2, \alpha\chi_1)(\varphi_1, \beta\chi_2). \tag{D8}$$

Für Slaterdeterminanten, die sich in mehr als zwei Einzelzuständen unterscheiden, verschwinden die Matrixelemente von (D4).

*Produkt von Protonen- und Neutronendeterminanten.* Es seien $\Phi^{\mathrm{P}}$ und $\Phi^{\mathrm{N}}$ Slaterdeterminanten für die Protonen und Neutronen und $\varphi_k^{\mathrm{P}}$, $\varphi_k^{\mathrm{N}}$, $\alpha^{\mathrm{P}}$, $\alpha^{\mathrm{N}}$ die zugehörigen Einzeleigenfunktionen und -operatoren. Die Nukleonen jeder Sorte seien getrennt numeriert, ebenso die zugehörigen Einzelzustände. Der mit

$$\bar{\Phi} = \Phi^{\mathrm{P}}\Phi^{\mathrm{N}} \tag{D9}$$

gebildete Erwartungswert des Operators

$$A = A^{\mathrm{P}} + A^{\mathrm{N}}, \quad A^{\mathrm{P,N}} = \sum_{\nu} \alpha^{\mathrm{P,N}}(\nu), \tag{D10}$$

ist dann nach (D2)

$$\langle A\rangle = (\bar{\Phi}, A\bar{\Phi}) = (\Phi^{\mathrm{P}}, A^{\mathrm{P}}\Phi^{\mathrm{P}}) + (\Phi^{\mathrm{N}}, A^{\mathrm{N}}\Phi^{\mathrm{N}}) = \sum_{\nu} \alpha_{kk}^{\mathrm{P}} + \sum_{\nu} \alpha_{kk}^{\mathrm{N}}. \tag{D11}$$

Das Produkt $\overline{\Psi}$ von Slaterdeterminanten der beiden Nukleonensorten soll sich von $\bar{\Phi}$ in einem Einzelzustand unterscheiden. Das gibt die beiden Möglichkeiten

$$\overline{\Psi} = \Psi^{\mathrm{P}}\Phi^{\mathrm{N}}, \quad \Phi^{\mathrm{P}}\Psi^{\mathrm{N}}. \tag{D12}$$

Für die erste ist nach (D3)

$$(\bar{\Phi}, A\overline{\Psi}) = (\Psi^{\mathrm{P}}, A^{\mathrm{P}}\Phi^{\mathrm{P}}) = (\varphi_1^{\mathrm{P}}, \alpha\psi_1^{\mathrm{P}}), \tag{D13}$$

und die zweite folgt daraus durch Ersatz von P durch N.

Für den Operator $AB$, bei dem $B$ in der gleichen Weise bestimmt ist wie $A$ in (D10), ergibt sich mit (D5), (D2), (D11)

$$\begin{aligned}\langle AB\rangle &= (\bar{\Phi}, AB\bar{\Phi})\\ &= (\Phi^{\mathrm{P}}, A^{\mathrm{P}}B^{\mathrm{P}}\Phi^{\mathrm{P}})+(\Phi^{\mathrm{P}}, A^{\mathrm{P}}\Phi^{\mathrm{P}})(\Phi^{\mathrm{N}}, B^{\mathrm{N}}\Phi^{\mathrm{N}})\\ &+(\Phi^{\mathrm{P}}, B^{\mathrm{P}}\Phi^{\mathrm{P}})(\Phi^{\mathrm{N}}, A^{\mathrm{N}}\Phi^{\mathrm{N}})+(\Phi^{\mathrm{N}}, A^{\mathrm{N}}B^{\mathrm{N}}\Phi^{\mathrm{N}})\\ &= \sum_k (\alpha^{\mathrm{P}}\beta^{\mathrm{P}})_{kk}+\sum_k\sum_l(\alpha^{\mathrm{P}}_{kk}\beta^{\mathrm{P}}_{ll}-\alpha^{\mathrm{P}}_{kl}\beta^{\mathrm{P}}_{lk})+\sum_k\alpha^{\mathrm{P}}_{kk}\sum_l\beta^{\mathrm{N}}_{ll}\\ &+\sum_k\alpha^{\mathrm{N}}_{kk}\sum_l\beta^{\mathrm{P}}_{ll}+\sum_k(\alpha^{\mathrm{N}}\beta^{\mathrm{N}})_{kk}+\sum_k\sum_l(\alpha^{\mathrm{N}}_{kk}\beta^{\mathrm{N}}_{ll}-\alpha^{\mathrm{N}}_{kl}\beta^{\mathrm{N}}_{lk}),\end{aligned} \tag{D14}$$

$$\langle AB\rangle-\langle A\rangle\langle B\rangle=\sum_k(\alpha^{\mathrm{P}}\beta^{\mathrm{P}})_{kk}-\sum_k\sum_l\alpha^{\mathrm{P}}_{kl}\beta^{\mathrm{P}}_{lk}+\sum_k(\alpha^{\mathrm{N}}\beta^{\mathrm{N}})_{kk}-\sum_k\sum_l\alpha^{\mathrm{N}}_{kl}\beta^{\mathrm{M}}_{lk} \tag{D15}$$

und für den ersten Fall in (D12)

$$\begin{aligned}&(\bar{\Phi}, AB\bar{\Psi})\\ &= (\Phi^{\mathrm{P}}, A^{\mathrm{P}}B^{\mathrm{P}}\Psi^{\mathrm{P}})+(\Phi^{\mathrm{P}}, A^{\mathrm{P}}\Psi^{\mathrm{P}})(\Phi^{\mathrm{N}}, B^{\mathrm{N}}\Phi^{\mathrm{N}})+(\Phi^{\mathrm{P}}, B^{\mathrm{P}}\Psi^{\mathrm{P}})(\Phi^{\mathrm{N}}, A^{\mathrm{N}}\Phi^{\mathrm{N}})\\ &= (\varphi_1{}^{\mathrm{P}}, \alpha^{\mathrm{P}}\beta^{\mathrm{P}}\psi_1{}^{\mathrm{P}})+\sum_k\{(\varphi_1{}^{\mathrm{P}}, \alpha^{\mathrm{P}}\psi_1{}^{\mathrm{P}})\beta^{\mathrm{P}}_{kk}-\alpha^{\mathrm{P}}_{1k}(\varphi_k{}^{\mathrm{P}}, \beta^{\mathrm{P}}\psi_1{}^{\mathrm{P}})\\ &+\alpha^{\mathrm{P}}_{kk}(\varphi_1{}^{\mathrm{P}}, \beta^{\mathrm{P}}\psi_1{}^{\mathrm{P}})-(\varphi_k{}^{\mathrm{P}}, \alpha^{\mathrm{P}}\psi_1{}^{\mathrm{P}})\beta^{\mathrm{P}}_{1k}\}\\ &+(\varphi_1{}^{\mathrm{P}}, \alpha^{\mathrm{P}}\psi_1{}^{\mathrm{P}})\sum_k\beta^{\mathrm{N}}_{kk}+(\varphi^{\mathrm{P}}{}_1, \beta^{\mathrm{P}}\psi_1{}^{\mathrm{P}})\sum_k\alpha^{\mathrm{N}}_{kk}.\end{aligned} \tag{D16}$$

Der zweite Fall von (D12) ergibt sich hieraus durch Vertauschen von P und N.

Das Produkt $\bar{X}$ von Slaterdeterminanten der beiden Nukleonensorten soll sich von $\bar{\Phi}$ in zwei Einzelzuständen unterscheiden. Dann sind die drei Fälle

$$\bar{X} = X^{\mathrm{P}}\Phi^{\mathrm{N}},\quad \Psi^{\mathrm{P}}\Psi^{\mathrm{N}},\quad \Phi^{\mathrm{P}}X^{\mathrm{N}} \tag{D17}$$

möglich. Für den ersten ist nach (D8)

$$\begin{aligned}(\bar{\Phi}, AB\bar{X}) &= (\Phi^{\mathrm{P}}, A^{\mathrm{P}}B^{\mathrm{P}}X^{\mathrm{P}})\\ &= (\varphi_1{}^{\mathrm{P}}, \alpha^{\mathrm{P}}\chi_1{}^{\mathrm{P}})(\varphi_2{}^{\mathrm{P}}, \beta^{\mathrm{P}}\chi_2{}^{\mathrm{P}})-(\varphi_1{}^{\mathrm{P}}, \alpha^{\mathrm{P}}\chi_2{}^{\mathrm{P}})(\varphi_2{}^{\mathrm{P}}, \beta^{\mathrm{P}}\chi_1{}^{\mathrm{P}})\\ &+(\varphi_2{}^{\mathrm{P}}, \alpha^{\mathrm{P}}\chi_2{}^{\mathrm{P}})(\varphi_1{}^{\mathrm{P}}, \beta^{\mathrm{P}}\chi_1{}^{\mathrm{P}})-(\varphi_2{}^{\mathrm{P}}, \alpha^{\mathrm{P}}\chi_1{}^{\mathrm{P}})(\varphi_1{}^{\mathrm{P}}, \beta^{\mathrm{P}}\chi_2{}^{\mathrm{P}}).\end{aligned} \tag{D18}$$

Daraus geht der dritte Fall durch Vertauschen von P und N hervor. Für den zweiten Fall ist nach (D3)

$$\begin{aligned}(\bar{\Phi}, AB\bar{X}) &= (\Phi^{\mathrm{P}}, A^{\mathrm{P}}\Psi^{\mathrm{P}})(\Phi^{\mathrm{N}}, B^{\mathrm{N}}\Psi^{\mathrm{N}})+(\Phi^{\mathrm{P}}, B^{\mathrm{P}}\Psi^{\mathrm{P}})(\Phi^{\mathrm{N}}, A^{\mathrm{N}}\Psi^{\mathrm{N}})\\ &= (\varphi_1{}^{\mathrm{P}}, \alpha^{\mathrm{P}}\psi_1{}^{\mathrm{P}})(\varphi_1{}^{\mathrm{N}}, \beta^{\mathrm{N}}\psi_1{}^{\mathrm{N}})+(\varphi_1{}^{\mathrm{P}}, \beta^{\mathrm{P}}\psi_1{}^{\mathrm{P}})(\varphi_1{}^{\mathrm{N}}, \alpha^{\mathrm{N}}\psi_1{}^{\mathrm{N}}).\end{aligned} \tag{D19}$$

## Literatur


1) E. Feenberg und K. C. Hammack, Phys. Rev. **75** (1949) 1877
2) E. Feenberg, Phys. Rev. **76** (1949) 1275; **77** (1950) 771
3) E. Feenberg, Shell Theory of the Nucleus (Princeton University Press, 1955)
4) M. Goeppert-Mayer, Phys. Rev. **74** (1948) 235; **75** (1949) 1969
5) O. Haxel, J. H. D. Jensen und H. E. Suess, Naturwiss. **35** (1948) 376
6) H. E. Suess, O. Haxel und J.H.D. Jensen, Naturwiss. **36** (1949) 153
7) M. Lagally, Vorlesungen über Vektor-Rechnung (Akad. Verl. Ges., Leipzig, 1934)
8) E. U. Condon und G. H. Shortley, The Theory of Atomic Spectra (University Press, Cambridge, 1953)
9) H. B. G. Casimir, Phys. Z. **59** (1930) 623
10) O. Klein, Phys. Z. **58** (1929) 730
11) H. A. Kramers und G. P. Ittmann, Z. Phys. **53** (1924) 553; **58** (1929) 217; **60** (1930) 663
12) R. de L. Kronig und J. J. Rabi, Phys. Z. **29** (1927) 262
13) R. de L. Kronig, Band Spectra and Molecular Structure (University Press, Cambridge, 1930)
14) C. Manneback, Phys. Z. **28** (1927) 72
15) H. Rademacher und F. Reiche, Z. Phys. **41** (1927) 453
16) F. Reiche, Z. Phys. **39** (1926) 444
17) S. C. Wang, Phys. Rev. **34** (1929) 243
18) E. E. Witmer, Proc. Nat. Acad. **13** (1927) 60
19) B. L. van der Waerden, Die gruppentheoretische Methode in der Quantenmechanik (J. Springer, Berlin, 1932)
20) W. Magnus, F. Oberhettinger, Formeln und Sätze für die speziellen Funktionen der mathematischen Physik, 2. Aufl. (Springer, Berlin, Göttingen, Heidelberg, 1948)
21) A. Bohr. Rotational States of Atomic Nuclei (Ejnar Munksgaard Forlag, København, 1954)
22) A. Bohr und B. Mottelson, Moments of Inertia of Rotating Nuclei, Mat. Fys. Medd. Dan. Vid. Selsk. **30** (1955) no. 1
23) F. Klinkenberg, Revs. Mod. Phys. **24** (1953) 63
24) J. E. Mack, Revs. Mod. Phys. **22** (1950) 64
25) N. F. Ramsay, Nuclear Moments (John Wiley & Sons, New York, Chapman and Hall, London, 1953)
26) R. S. Nataf, Nuclear Physics **2** (1956/57) 497
27) A. Bohr, Phys. Rev. **81** (1951) 134 und 331
28) A. Bohr, Mat. Fys. Medd. Dan. Vid. Selsk. **26** (1952) no. 14
29) A. Bohr and B. Mottelson Mat. Fys. Medd. Dan. Vid. Selsk. **27** (1953) no. 16
30) S. G. Nilsson, Binding States of Individual Nucleons in Strongly Deformed Nuclei, Mat. Fys. Medd. Dan. Vid. Selsk. **29** (1955) no. 16
31) D. R. Inglis, Phys. Rev. **96** (1954) 1059
32) R. E. Peierls and J. Yoccoz, Proc. Phys. Soc. A **70**, 381
33) J. Yoccoz, Proc. Phys. Soc. A **70**, 388, 553
34) F. Villars, Nuclear Physics **3** (1957) 240
35) J. Rainwater, Phys. Rev. **79** (1950) 432
36) J. P. Elliot und T. H. R. Skyrme, Proc. Roy. Soc. A **232** (1955) 561
37) E. C. Kemble, The Fundamental Principles of Quantum Mechanics, 1st Edition, 4th Impression (McGraw-Hill Book Company, New York and London, 1937)
38) J. H. D. Jensen, H. E. Suess und O. Haxel, Naturwiss. **36** (1948) 156

8.B *Nuclear Physics* 8 (1958) 595—601; © *North-Holland Publishing Co., Amsterdam*
Not to be reproduced by photoprint or microfilm without written permission from the publisher

# ON GENERALIZED FOLDY-WOUTHUYSEN TRANSFORMATIONS

D. L. PURSEY †

*Universitetets Institut for Teoretisk Fysik, Copenhagen*

Received 26 June 1958

**Abstract:** The Foldy-Wouthuysen transformation is generalized in one direction to yield a non-relativistic approximation procedure for an arbitrary number of interacting Dirac particles, and in another direction to give an extreme relativistic approximation for a single particle in an external field. The application of the formalism to high energy scattering is briefly sketched. Ambiguities in the procedure are discussed, and are shown to be equivalent, within the validity of the approximation, to unitary transformations of the approximate theory.

## 1. Introduction

This paper discusses three problems concerning the approximate decoupling of the Dirac equation by means of successive unitary transformations (generalized Foldy-Wouthuysen transformations), namely the non-relativistic approximation for an arbitrarily large number of Dirac particles, the extreme relativistic approximation for a single particle, and the essential uniqueness of the approximation method.

## 2. Non-Relativistic Approximation for Many Particles

The most satisfying procedure for the approximate decoupling of the equations for the 'large' and 'small' components of the Dirac equation, in order to obtain an approximate two-component non-relativistic equation, is that due to Foldy and Wouthuysen [1]). This method defines a sequence of unitary transformations which make the coupling terms of arbitrarily high order in the inverse of the particle mass. The non-relativistic approximation is obtained by dropping all terms of the same or higher order in the inverse mass as the coupling terms, and by retaining only that one of the two uncoupled two-component equations so obtained which corresponds to a positive rest energy.

Chraplyvy [2,3]) solved the corresponding problem for two particles. In this case, it is important to realize that one need only uncouple four components (corresponding to both rest energies positive) from the remaining twelve, and it is unnecessary to decouple these twelve. Chraplyvy [3]) found that the sequence of unitary transformations which performs the decoupling

† Permanent address: Tait Institute of Mathematical Physics, University of Edinburgh, Scotland.

is not unique. Indeed it will be seen later that there is still greater ambiguity than was considered by Chraplyvy, and there is even an ambiguity in the single particle case.

For a system of $n$ interacting Dirac particles, the Hamiltonian can be written

$$H = \sum_{j=1}^{n} \beta_j m_j + \mathcal{E} + \sum_{j=1}^{n} \mathcal{O}_j + \sum_{k=1}^{n} \sum_{j=1}^{k-1} \mathcal{O}_{jk} + \ldots, \tag{1}$$

where $\beta_j$ is the Dirac $\beta$ matrix for the $j$th particle, which has mass $m_j$, and $\mathcal{E}$, $\mathcal{O}_j$, $\mathcal{O}_{jk}, \ldots$, are defined by the commutation properties

$$\begin{aligned} &[\beta_j, \mathcal{E}] = 0, \text{ all } j, \\ &\{\beta_j, \mathcal{O}_{kl\ldots}\} = 0 \text{ if } j \text{ is one of } k, l, \ldots, \\ &[\beta_j, \mathcal{O}_{kl\ldots}] = 0 \text{ if } j \text{ is not one of } k, l \ldots. \end{aligned} \tag{2}$$

Here $[\ldots, \ldots]$ and $\{\ldots, \ldots\}$ denote respectively commutators and anticommutators.

It is convenient to define the projection operators

$$P_j = \tfrac{1}{2}(1+\beta_j) \tag{3}$$

and

$$P = \prod_{j=1}^{n} P_j. \tag{4}$$

If an operator commutes with $\beta_j$ then it is called even with respect to $P_j$; if it anticommutes with $\beta_j$, then it is odd with respect to $P_j$.

The expansion parameters to be used are the inverse masses, which are all presumed to be of the same order of magnitude. The components of the wave function for which all the rest energies are positive are defined by the eigenvalue $+1$ of $P$. We wish therefore to decouple these components from the rest. As a first step, we wish to find a unitary transformation

$$H \to H' \equiv e^S H e^{-S} = H + [S, H] + \ldots \tag{5}$$

of the Hamiltonian so that the terms in $H'$ which are odd with respect to $P$ are of one order higher in the inverse masses than the corresponding terms in $H$.

It is easily seen that

$$\mathcal{O}_{jkl\ldots} + \tfrac{1}{2}[[P_j P_k P_l \ldots, \mathcal{O}_{jkl\ldots}], \beta_j]$$

is even with respect to $P_j P_k P_l \ldots$ and therefore also with respect to $P$, and is symmetric in all the indices $j, k, l \ldots$. It follows that a particular solution for $S$ is

$$\begin{aligned} S = &\sum_{j=1}^{n} \frac{1}{2m_j} [P_j, \mathcal{O}_j] + \sum_{k=1}^{n} \sum_{j=1}^{k-1} \frac{1}{2(m_j+m_k)} [P_j P_k, \mathcal{O}_{jk}] \\ &+ \sum_{l=1}^{n} \sum_{k=1}^{l-1} \sum_{j=1}^{k-1} \frac{1}{2(m_j+m_k+m_l)} [P_j P_k P_l, \mathcal{O}_{jkl}] + \ldots. \end{aligned} \tag{6}$$

The terms odd with respect to $P$ can now be made of arbitrarily high order in the inverse masses by iteration. To obtain a non-relativistic approximation, it remains only to drop all terms in the Hamiltonian of order equal to or higher than the terms odd with respect to $P$, and to multiply by $P$ in order to project out that part which corresponds to all the rest energies positive.

The solution (6) is not unique: the most general operator $S$ which satisfies the conditions of the problem is obtained from (6) by adding any operator whose even part with respect to $P$ is at least of first order and whose odd part is at least of second order in the inverse masses. This ambiguity exists even in the single particle case. All the ambiguities discussed by Chraplyvy [3]) are included as special cases. Further discussion of the ambiguities is postponed till section 5.

## 3. Relativistic Limit for a Single Particle

The non-relativistic theory obtained by successive unitary transformations was an expansion in inverse powers of the particle mass. If a similar approach could be developed to generate an expansion in inverse powers of the momentum or of the momentum together with some other parts of the Hamiltonian, this could be used as the basis of an extreme relativistic approximation, which might be valuable for the discussion of high energy scattering. Indeed we shall see that the approach of Yennie, Ravenhall and Wilson [4]) and of Brenner, Brown and Elton [5]) to the scattering of fast electrons by nuclei is essentially the zero order approximation in such a theory.

To carry out this programme, it is necessary to consider a more general version of the Foldy-Wouthuysen procedure which is analogous to regarding the mass as an operator rather than a $c$-number. We consider the Hamiltonian

$$H = \gamma\lambda + \mathscr{E} + \mathscr{O}, \tag{7}$$

where $\gamma$ is an operator whose eigenvalues are $\pm 1$, and which has the following commutation properties:

$$[\gamma, \lambda] = [\gamma, \mathscr{E}] = \{\gamma, \mathscr{O}\} = 0. \tag{8}$$

The state-vectors $|\lambda'\rangle$ are a complete set of simultaneous eigenvectors of $\gamma$ and $\lambda$, such that

$$\lambda|\lambda'\rangle = \lambda'|\lambda'\rangle. \tag{9}$$

If

$$H' \equiv e^S H e^{-S} = H + [S, H] + \ldots, \tag{10}$$

where

$$S = \gamma \sum_{\lambda', \lambda''} \frac{|\lambda'\rangle\langle\lambda'|\mathscr{O}|\lambda''\rangle\langle\lambda''|}{\lambda' + \lambda''}, \tag{11}$$

then the terms in $H'$ odd with respect to $P = \frac{1}{2}(1+\gamma)$ are of one order higher in the inverse eigenvalues of $\lambda$ than the corresponding terms of $H$. By iteration, these odd terms can be made of arbitrary high order in the inverse eigenvalues of $\lambda$. Provided we are concerned only with eigenstates of the total Hamiltonian for which $(\lambda'+\lambda'')^{-1}\langle\lambda'|\mathcal{O}|\lambda''\rangle\langle\lambda''|E\rangle$ is sufficiently small, we can get an approximate theory by dropping all terms of higher than some chosen order in the inverse eigenvalues, and reduce the dimension of the problem by using the diagonal character of the approximate Hamiltonian with respect to $\gamma$. Particular care must be taken in discussing the validity of the procedure if the eigenvalues of $\lambda$ have not all the same sign, for then there may be a cancellation in some of the denominators of (11).

$H'$ defined by (10) will have corrections to $\mathscr{E}$ of first and higher orders in the inverse eigenvalues of $\lambda$. The first order correction is

$$\tfrac{1}{2}\gamma \sum_{\lambda',\lambda'',\lambda'''} \left(\frac{1}{\lambda'+\lambda''}+\frac{1}{\lambda''+\lambda'''}\right) |\lambda'\rangle\langle\lambda'|\mathcal{O}|\lambda''\rangle\langle\lambda''|\mathcal{O}|\lambda'''\rangle\langle\lambda'''|, \tag{12}$$

which corresponds to the term $(1/2m)\beta\mathcal{O}^2$ in the usual Foldy-Wouthuysen theory. It is obvious from (12) that the additional corrections to $\mathscr{E}$ obtained by iteration will be of at least third order, so that the transformation with $S$ given by (11) already gives $\mathscr{E}$ correct to second order.

## 4. Application to High Energy Scattering

As an example, we consider the scattering of an electron by an electrostatic field, such as that of a nucleus. The Hamiltonian has the form

$$H = \beta m+\boldsymbol{\alpha}\cdot\mathbf{p}+\varphi(\mathbf{r}). \tag{13}$$

The choice of $\gamma = \boldsymbol{\alpha}\cdot\mathbf{p}/p$, $\lambda = p$ which at first suggests itself is not convenient, because $\varphi$ will be comparable in importance to $\boldsymbol{\alpha}\cdot\mathbf{p}$ near the nucleus except for extremely high energies. We therefore take

$$\gamma\lambda = \boldsymbol{\alpha}\cdot\mathbf{p}+\varphi. \tag{14}$$

The mathematical discussion of the problem will be simplified if the factorization of (14) is chosen so that the mass term is wholly odd. This suggests that we take

$$\gamma = \gamma_5, \qquad \lambda = \boldsymbol{\sigma}\cdot\mathbf{p}+\gamma_5\varphi. \tag{15}$$

Unfortunately, the eigenvalues of $\lambda$ can have either sign, so that the denominators in (11) and (12) may be small even though the eigenvalues are themselves large. However, provided $\varphi$ is bounded everywhere, and tends to zero sufficiently rapidly outside a finite region, as is true for the potential due to a finite nucleus screened by its atomic electrons, it is easy to show that the matrix elements $\langle\lambda'|\beta|\lambda''\rangle$ are of order $(\lambda'-\lambda'')^{-1}$, so that all terms in (11) are in fact of the same order in the inverse eigenvalues. The sums in

(11) and (12) should here be interpreted as principal value integrals. There are still questions, which we shall not discuss, concerning the convergence of these expressions.

The zero-order approximation is obtained by dropping the mass term entirely, as in ref. [4,5]). The next lowest correction to the Hamiltonian is given by (12) with $\mathcal{O} = \beta m$, and is therefore proportional to $m^2$. It follows that the mass corrections to the scattering phase-shifts and therefore to the differential cross-section are of order $m^2$ rather than $m$. For the cross-section, this is a well-known result [5,6]).

Elton [7]) has investigated the mass corrections in detail, and found that although the correction to the cross-section is of order $m^2$, the corrections to the phase shifts are of order $m$. The contradiction with the present result is only apparent, and its resolution illumines the underlying reason for the cross-section result. Elton's partial wave analysis is the usual one in terms of simultaneous eigenstates of angular momentum and parity. The partial wave analysis used implicitly here is quite different from this, and indeed is in terms of states for which parity is not a good quantum number. In effect, we have found an operator of the form $\gamma_5 + O(m)$, which has eigenvalues $\pm 1$, and which up to first order in $m$ commutes with the Hamiltonian (though not with the parity operator), and by means of a unitary transformation we have mapped this operator onto $\gamma_5$ which we have then taken diagonal. In this way, we have a partial wave analysis in terms of simultaneous eigenstates of this operator ($\Gamma$, say) and the total angular momentum, and in this analysis the phase shifts have no terms linear in $m$. However, when the eigenstates of parity are expressed as linear combinations of those of $\Gamma$, the coefficients contain terms of first order in $m$, so that in the parity-angular momentum analysis the phase shifts will have terms of first order in $m$ as well as second order terms.

The approach outlined here is the natural extension to the case of non-vanishing mass of the approach used by Yennie, Ravenhall and Wilson [4]). It bears the same relationship to the Cini-Touschek [8]) transformation for a free particle as does the usual sequence of Foldy-Wouthuysen transformations for a particle in an external field to the exact transformation for a free particle.

## 5. Essential Uniqueness of Procedure

In section 2 it was shown that there is great ambiguity in the definition of the successive unitary transformations in the Foldy-Wouthuysen procedure, and it is not *a priori* obvious that the different non-relativistic approximations are equivalent. In this section we shall show that any two approximate Hamiltonians, each valid to order $n$ in the expansion parameters, can be transformed one into the other (apart from terms of order greater than $n$ in

the expansion parameters) by a unitary transformation which operates separately in the subspaces corresponding to positive and negative rest energies. This means that within the validity of the approximation the ambiguities in the transformations can cause at most a unitary transformation of the approximate theory, so that the approximation procedure is essentially unique.

The result will be proved in detail for the single particle case; the extension to the many particle case is straightforward. Ambiguities in the relativistic limit described in section 3 may be treated analogously.

We consider the Hamiltonian

$$H = \beta m + \mathcal{E} + \mathcal{O}, \tag{16}$$

and two unitary transforms of $H$,

$$H' = e^{S'} H e^{-S'}$$

and (17)

$$H'' = e^{S''} H e^{-S''},$$

such that both $H'$ and $H''$ are even with respect to $P = \frac{1}{2}(1+\beta)$ up to order $n$ in $1/m$. Then certainly there exists an anti-hermitian operator $\alpha$ so that

$$H'' = e^{\alpha} H' e^{-\alpha}. \tag{18}$$

Since both $S'$ and $S''$ are of at least first order in $1/m$, so is $\alpha$. We consider $\alpha$ to be expanded in inverse powers of $m$, and wish to show that $\alpha$ is even with respect to $P$ up to order $n+1$.

The leading term in $H'$, regarded as a power series in $1/m$, is $\beta m$. The first two terms in $H''$ are therefore

$$\beta m + H'_0 + m[\alpha_1, \beta], \tag{19}$$

where $H'_0$ is the zero order part of $H'$ and $\alpha_1$ the first order part of $\alpha$. Since this by hypothesis must be even, $[\alpha_1, \beta]$ must be even, and this is possible only if $\alpha_1$ itself is even. The next term in $H''$ is

$$H''_1 = H'_1 + [\alpha_1, H'_0] + m[\alpha_2, \beta], \tag{20}$$

and since this is even and we have already shown $\alpha_1$ to be even, it follows that $\alpha_2$ is also even. Step by step procedure in this manner shows that $\alpha$ is even up to order $n+1$.

It follows that $H''$, up to order $n$ in $1/m$, is just a unitary transform of $H'$ by a unitary operator which, up to order $n+1$ in $1/m$, operates separately in the subspace of Hilbert space defined by $P = 1$, so that the two approximate Hamiltonians define non-relativistic theories which are equivalent within their common range of validity.

I wish to thank Dr. K. Johnson for a number of valuable discussions. It is a pleasure to thank Professor Niels Bohr for hospitality at Universitetets Institut for Teoretisk Fysik, Copenhagen, and also to acknowledge financial support from the Ford Foundation.

## References

1) L. L. Foldy and S. Wouthuysen, Phys. Rev. **78** (1950) 29
2) Z. V. Chraplyvy, Phys. Rev. **91** (1953) 388
3) Z. V. Chraplyvy, Phys. Rev. **92** (1953) 1310
4) D. R. Yennie, D. G. Ravenhall and R. N. Wilson, Phys. Rev. **95** (1954) 500
5) S. Brenner, G. E. Brown and L. R. B. Elton, Phil. Mag. **45** (1954) 524
6) L. K. Acheson, Phys. Rev. **82** (1951) 488
7) L. R. B. Elton, Proc. Phys. Soc. A **68** (1955) 741
8) M. Cini and B. Touschek, Nuovo Cimento **7** (1958) 422

1.B *Nuclear Physics* 8 (1958) 602—606; © *North-Holland Publishing Co., Amsterdam*
Not to be reproduced by photoprint or microfilm without written permission from the publisher

# REPULSIVE CORE FORCES IN THE TRITON

J. M. BLATT and G. DERRICK

*The F.B.S. Falkiner Nuclear Research and Adolph Basser Computing Laboratories, School of Physics, University of Sydney* †

Received 3 July 1958

**Abstract:** A variational calculation is made for $H^3$ with repulsive core forces fitted to two-body data. The binding energy so found increases with increasing core radius.

## 1. Introduction

Considerable information about the forces operating between two nucleons has been gained from the experimental data on the ground state of the deuteron, on neutron-proton scattering, and on proton-proton scattering[1,2,3]). It is interesting to investigate the consequences of this force law between two nuclear particles for three body nuclei.

The present paper deals with one limited phase of this investigation, namely, the discussion of the effect of 'repulsive core' forces within the main, attractive, interaction. For this purpose, we have ignored other complications in the problem (primarily the spin-orbit coupling introduced by the tensor force and by a possible $\mathbf{L} \cdot \mathbf{S}$ force). From studies of the two-body data, it seems very likely that the nuclear force becomes highly repulsive when two nucleons approach each other closely, to distances of the order $5 \times 10^{-14}$ cm or less. It is conventional to idealize this situation by an 'infinite repulsive core' in the nuclear potential, i.e., the central force is assumed to become repulsive and infinitely large for inter-nucleon distances $r$ less than or equal to some 'core radius' $r_0$. The wave function of a many-body nucleus is required to vanish whenever any two nucleons approach each other more closely than $r = r_0$.

To the extent that a repulsive core restricts the amount of configuration space available to the wave function, we expect an increase in kinetic energy and hence a decreased amount of binding energy in the triton. However, in order to give a reasonable fit to the low-energy two-body data, the introduction of a repulsive core implies a change in the force law outside the core as well: the central force outside the core becomes deeper and narrower [4]). This effect results in an increase of the binding energy in the triton. Thus two opposing effects are at work.

† Also supported by the Nuclear Research Foundation within the University of Sydney.

## 2. Variation Method and Trial Function Used

The wave equation can be written as

$$(T+\lambda V)\phi = E\phi \tag{1}$$

where $T$ is the kinetic energy operator, $\lambda V$ the potential energy operator, $\phi$ is the wave function, and $E$ is the energy of the triton. $\lambda$ is a multiplicative 'strength constant' for the potential. Since the actual energy of the triton is known experimentally, we can rewrite (1) as an eigenvalue problem for the strength constant $\lambda$ required to give the observed triton energy, i.e.

$$(T-E)\phi = -\lambda V\phi. \tag{2}$$

From (2) we can derive a variational expression which gives an upper bound for the lowest eigenvalue $\lambda$, namely

$$\lambda \leqq \frac{(\psi, (T-E)\psi)}{(\psi, -V\psi)}. \tag{3}$$

Here $\psi$ is any trial function; the operator $-V$ is usually positive; for $\psi = \phi$, the equality sign holds.

We have used central forces for the potential, i.e.,

$$V = V_c(r_{12})+V_c(r_{23})+V_c(r_{31}) \tag{4}$$

where $r_{ij}$ is the distance between nucleons $i$ and $j$, and $V_c$ is the average of the central force potentials in the triplet-even and singlet-even states of the two-body system:

$$V_c(r) = \tfrac{1}{2}[V_c(\text{sing-even})+V_c(\text{trip-even})]. \tag{5}$$

The reason for this choice is explained in ref. [5]).

With central forces only, the ground state of the triton is a pure $^2S_{\frac{1}{2}}$ state; its wave function depends on three coordinates only, which may be chosen as the three interparticle distances $r_{ij}$. In the presence of the repulsive core, this is the most appropriate choice of coordinates. Our trial function has the following form:

$$\psi = u(r_{12})u(r_{23})u(r_{31}) \tag{6}$$

where $u(r)$ vanishes at the core radius, $r = r_0$, and is otherwise at our disposal. Although it would be possible to determine the 'best' function $u(r)$ in (6), the resulting equation is an integral equation of awkward type, and we felt that we could get a sufficient approximation to $\lambda$ by choosing $u(r)$ from among a certain set of functions, namely the set of functions satisfying the differential equation

$$\frac{d^2}{dr^2}u(r)+\frac{2}{r}\frac{d}{dr}u(r) = [\gamma^2+\mu V_c(r)]u(r). \tag{7}$$

This equation arises in the 'equivalent two-body approximation' which has often been used for the triton [6,7]). Since it is known that this approximation leads to surprisingly accurate results for the triton energy, we believe that a trial wave function constructed along these lines should be a reasonable approximation to the 'best' trial wave function of type (6). The parameter $\gamma$ in (7) is a free parameter, and we evaluate (3) with various choices for $\gamma$, until we find that value of $\gamma$ which gives the lowest upper bound for $\lambda$ in (3). The eigenvalue $\mu$ is chosen so that $u(r)$ decreases exponentially for large $r$.

We have performed a check on the accuracy of our choice of trial wave function by making one calculation with the more elaborate trial wave function:

$$\psi = u(r_{12})u(r_{23})u(r_{31}) + C\,[u(r_{12})u(r_{23})v(r_{31}) + \text{permutations}] \qquad (8)$$

where $C$ is an adjustable parameter, and $v(r)$ is a solution of the differential equation (7) with one node at finite $r$, and a correspondingly different value of $\mu$. The resulting upper bound on $\lambda$, from (3), was only 0.2 percent lower than the value obtained with the trial function (6).

As a second check, we have computed $\lambda$ for potentials with which very elaborate variational calculations have been carried out by Rarita and Present [8]) and by Svartholm [9]). With the trial function (6), (7), our value of $\lambda$ was 1.1 percent higher (i.e. not as good as) the value of Rarita and Present for the same potential; using a potential investigated by Svartholm (Gaussian well) our value of $\lambda$ differed from his by only 0.4 percent, ours being the better.

## 3. Results

In table 1 we give the value of $\lambda$ obtained by our variational calculation

TABLE 1

| Well shape | Well depth $s$ | Force strength $\lambda$ | | | |
|---|---|---|---|---|---|
| | | $r_0 = 0$ | $r_0 = 0.22$ | $r_0 = 0.43$ | $r_0 = 0.65 \times 10^{-13}$cm |
| Exponential | 0.3 | — | 1.90 | 1.81 | 1.76 |
| | 0.6 | 1.52 | 1.47 | 1.44 | 1.42 |
| | 0.9 | 1.23 | 1.21 | 1.20 | 1.20 |
| | 1.0 | 1.16 | 1.15 | 1.14 | 1.14 |
| Yukawa | 0.6 | — | 1.45 | 1.41 | 1.38 |
| | 0.9 | 1.18 | 1.18 | 1.17 | 1.15 |
| | 1.0 | 1.11 | 1.12 | 1.11 | 1.09 |

This table contains values of $\lambda$ for various core radii $r_0$ and triplet central force well depths $s$. $\lambda = 1$ means that, within the accuracy of our variational calculation, the central forces in the $^1S$ and $^3S$ states alone suffice to give the observed binding energy of the triton. A value of $\lambda$ in excess of 1 means that additional binding forces (e.g. the tensor force) are necessary to yield the observed binding energy of the triton; and the excess of $\lambda$ over 1 is an indication of the necessary strength of such additional binding forces.

for various choices of the nuclear force. In all cases the well shape and the core radius $r_0$ were the same for singlet and triplet wells. The well depth and range of the singlet force were adjusted to fit the scattering length and effective range in the $^1$S state of the two-body system; the triplet (central) well depth and range were taken from the tables of ref. [4]); for each triplet central well used, there exists a tensor potential of the same well shape, such that the binding energy of the deuteron, the quadrupole moment of the deuteron, and the $^3S+^3D$ $\alpha$-wave scattering length can all be fitted.

If our value of $\lambda$ for any entry in this table had turned out to be *less* than unity, the corresponding potential would be automatically excluded, since the tensor force (which we have ignored) must necessarily add to the binding of the triton, and with $\lambda < 1$, the actual central force ($\lambda = 1$) gives already too much binding for the triton. However, all values of $\lambda$ in table 1 exceed unity; thus none of these potentials are excluded by our present calculation.

It will be seen that on the whole the force strength $\lambda$ decreases with increasing core radius $r_0$ for a given triplet central well depth. This means that for the actual potential $V(\lambda = 1)$ the binding energy *increases* with increasing $r_0$. Though the change in $\lambda$ with $r_0$ is small there is a much greater proportionate change in the binding energy since the potential and kinetic energies are each many times larger in magnitude than their difference.

It should be pointed out that the opposite result is obtained if the tensor force in the triplet-even states is disregarded completely, and the triplet even central force is adjusted to fit the binding energy of the deuteron and the triplet scattering length. (Such a force necessarily gives zero for the quadrupole moment of the deuteron.) Such a calculation has been carried out by Kikuta *et al.*[10]) using analytic methods and a trial wave function of the same form, (6) as ours. We find good agreement between their results † and our machine results. Our results for $\lambda$ are given in table 2.

TABLE 2

| $r_0$ in $10^{-13}$ cm | $\lambda$ |
|---|---|
| 0 | 0.96 |
| 0.2 | 0.99 |
| 0.4 | 1.02 |
| 0.6 | 1.03 |

Values of $\lambda$ for alternative (unrealistic) assumptions about the central force in the triplet-even states: the tensor force is ignored and the triplet-even central force is determined so as to fit the binding energy of the deuteron and the triplet scattering length.

We see that this time $\lambda$ *increases* with increasing core radius: furthermore, for very small core radii ($r_0 = 0$ and $r_0 = 0.2\times 10^{-13}$ cm), $\lambda$ is less than unity,

† The coefficient of $C^1(x)$ in the second line of the expression for $K^{11}(x)$ on page 232 of ref. [16]) should be $(D^2-14D/x-8/x^2)$.

indicating that the potential is unacceptable. This is of course the well-known result that a central force of zero core radius which binds the deuteron properly gives too much binding for the triton. We do not attribute much significance to the results of table 2, since the nuclear force law used there is quite unrealistic; we use table 2 merely to point out that the results of table 1 depend on the existence of the tensor force and the quadrupole moment of the deuteron, even though this dependence is entirely implicit.

We are grateful to the staff of the Adolph Basser Computing Laboratories for the excellent facilities afforded us, and in particular for the use of the electronic computor SILLIAC. One of us (G. D.) would also like to thank the Australian Atomic Energy Commission for a Post Graduate Research-Studentship which has enabled him to carry out this work.

## References

1) Gammel, Christian and Thaler, Phys. Rev. **105** (1957) 311; **107** (1957) 291
2) Gammel, Christian and Thaler, Phys. Rev. **107** (1957) 1337
3) Signell and Marshak, Phys. Rev. **106** (1957) 832
4) Biedenharn, Blatt and Kalos, Nuclear Physics **6** (1958) 359
5) J. M. Blatt and V. F. Weisskopf, Theoretical Nuclear Physics (John Wiley & Sons, New York, 1952) Ch. 5
6) E. P. Wigner, Phys. Rev. **43** (1933) 252
7) E. Feenberg, Phys. Rev. **47** (1935) 850
8) Rarita and Present, Phys. Rev. **51** (1937) 788
9) Svartholm, Thesis, Lund (1945)
10) T. Kikuta, M. Morita and M. Yamada, Prog. Theor. Phys. **15** (1956) 222

1.E.1 *Nuclear Physics* **8** (1958) 607—012; © *North-Holland Publishing Co., Amsterdam*
Not to be reproduced by photoprint or microfilm without written permission from the publisher

# $\beta$—$\gamma$ COINCIDENCE SPECTROMETRIC INVESTIGATION OF THE DECAY-SCHEME OF $Nd^{147}$

D. BERÉNYI
*Institute of Nuclear Research of the Hungarian Academy of Sciences, Debrecen*

Received 5 July 1958

**Abstract:** We carried out beta-gamma ray coincidence investigations by means of a magnetic spectrometer and a NaI(Tl) scintillation gamma-ray spectrometer incorporated into the former one in order to determine the number and maximum energy of partial beta-ray spectra at the decay of $Nd^{147}$. We found the following beta-ray groups of end point energy: 815±10, 529±25, 365±15, and 215±15 keV.

## 1. Introduction

The decay of $Nd^{147}$ has been investigated by a number of authors, yet its decay scheme cannot be considered as thoroughly clarified even today. Generally two beta-ray groups are distinguished in the earlier investigations [1–4]), although Kondaiah suggests the existence of a possible third group on the basis of gamma-ray spectrum analysis.

The beta-ray spectrum and at the same time the internal conversion spectrum of neodymium-147 were last examined by Emmerich and Kurbatov [5,6]). Their measurements were supplemented also by coincidence absorption measurements to determine the decay scheme. On the other hand, level schemes were established through careful analyses of internal conversion lines by Rutledge, Cork and Burson [7]) and of the gamma spectrum by Hans, Saraf and Mandeville [8,9]). The values for the maximum energy of partial spectra obtained by the afore-mentioned investigations are represented in the corresponding columns of table 1.

Until recently, coincidence beta-ray spectrometric measurements have not been made for the neodymium-147 isotope. We report on measurements of this kind in the following to contribute to the clarification of the $Nd^{147}$ decay scheme.

## 2. Experimental Details

In our measurements, a magnetic spectrometer of the toroid-sector type was employed. For the detection of $\beta$-rays, an anthracene crystal scintillation counter was made available inside the instrument [10,11]).

We combined a coincidence spectrometer out of the above beta-ray spectrometer, an NaI(Tl) crystal scintillation $\gamma$-ray spectrometer and a coincidence-circuit [12,13]). The diameter of the cylindrical NaI(Tl) crystal was 35.5 mm, and its height 22 mm. The multipliers both in the anthracene detector and scintillation spectrometer were of the RCA 5819 type. The resolving time of the coincidence circuit was $\approx 1.5 \times 10^{-7}$ sec.

Our $Nd^{147}$ isotope was supplied by Harwell in the form of $NdCl_3$. It was carrier-free but containing organic break-down material from ion exchange resin in a concentration of about 1—2 mg/ml. The source was prepared by drop method with a backing of $\approx 1$ mg/cm$^2$ mylar foil. In order to prevent charging of the backing, it had been previously coated with vacuum evaporation of aluminium together with the plexi source holder. The thickness of the source was $\approx 1$ mg/cm$^2$. No covering foil was used.

In order to check the radioactive purity of the shipped $Nd^{147}$, we carefully observed the decay of a sample for over a month. For the half-life we obtained the value reported in litterature [14]) within the limit of error. Thus, the presence of radioactive contamination could not be detected.

## 3. Results and Discussion

Considering that in our measurements we intended to find also groups of low intensity, it was advisable not to use the differential discriminator in the $\gamma$-channel, but only the integral one.

At one series of measurements the $\gamma$-discriminator was set so that only the detection of $\gamma$-rays with a quantum energy exceeding 91 keV might be possible. That is to say, according to measurements referred to in the introduction, the $\beta$-ray group of the highest intensity and, at the same time, of the highest energy is in coincidence with the $\gamma$-radiation of 91 keV. With this discrimination it can be expected that the internal groups may be observed more distinctly. In fig. 1, the Fermi-Kurie analysis of the coincidence spectrum obtained under the above circumstances can be seen. Each single value of measurement is the result of measurements of $10 \times 10$ minute duration.

In the second series of measurements, on the other hand, we proceeded with such a setting of the discriminator to obtain the $\beta$—$\gamma$ coincidence counting rate for all $\gamma$-rays from the decay of $Nd^{147}$. The Fermi-Kurie analysis of measurement values obtained in this manner is shown in fig. 2. The values in this plot were obtained as a result of a series of three ten-minute measurements.

Two partial spectra are well distinguishable in fig. 1, and three in fig. 2. In the coincidence studies, the spectrum of lower end-point energy somewhat above 200 keV that were expected on the basis of the $\gamma$-spectrum investiga-

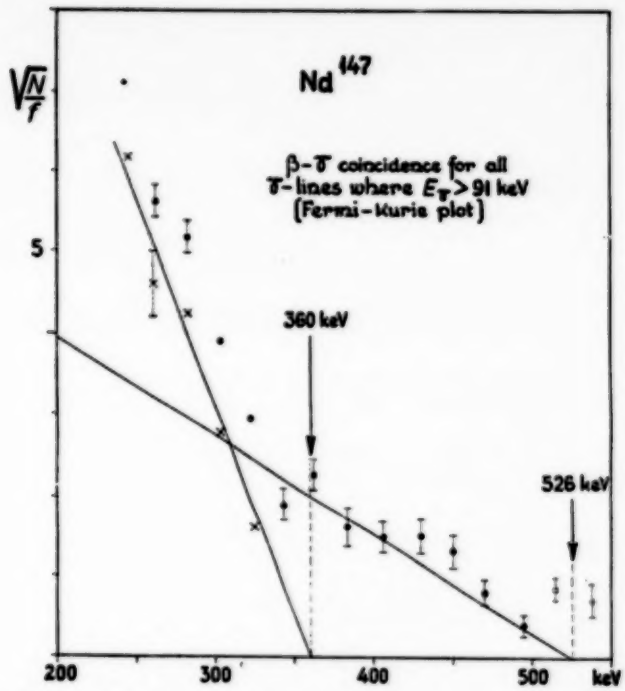


Fig. 1. The Fermi-Kurie plot of the $\beta-\gamma$ coincidence spectrum at which the coincidence was measured only for the $\gamma$-rays of energy $E_\gamma > 91$ keV.

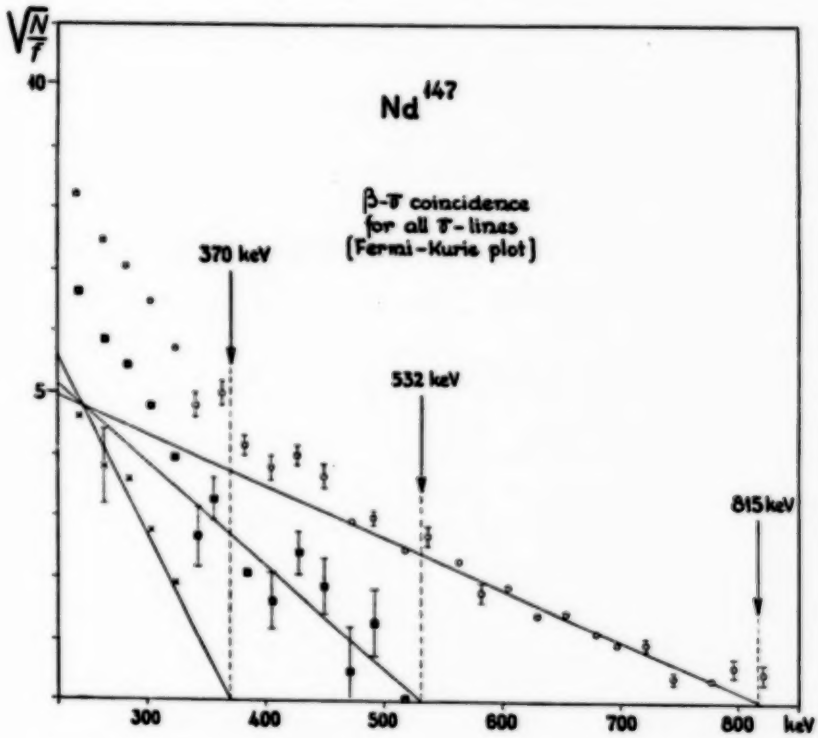


Fig. 2. The Fermi-Kurie plot of the $\beta-\gamma$ coincidence spectrum when every $\gamma$-line took part in the coincidence.

tions of Mandeville and co-workers, could not be found. The reason for this failure was that because of the long series of measurements, the discriminator had to be set in the $\beta$-channel in such a way that it made the counting of lower energies impossible in our experimental conditions. Nevertheless we measured the $\beta$-spectrum itself — without making coincidence measurements — at a setting of the discriminator favourable for lower energies. The Fermi-Kurie diagram of the measured $\beta$-spectrum is represented in fig. 3. Here the partial spectrum of 215 keV end point energy is well distinguishable. The group distinctly observable at the coincidence spectra, with an end point energy not much higher than 500 keV, was not discernible here at all. By this measurement, however — as it can be seen also in fig. 3 —

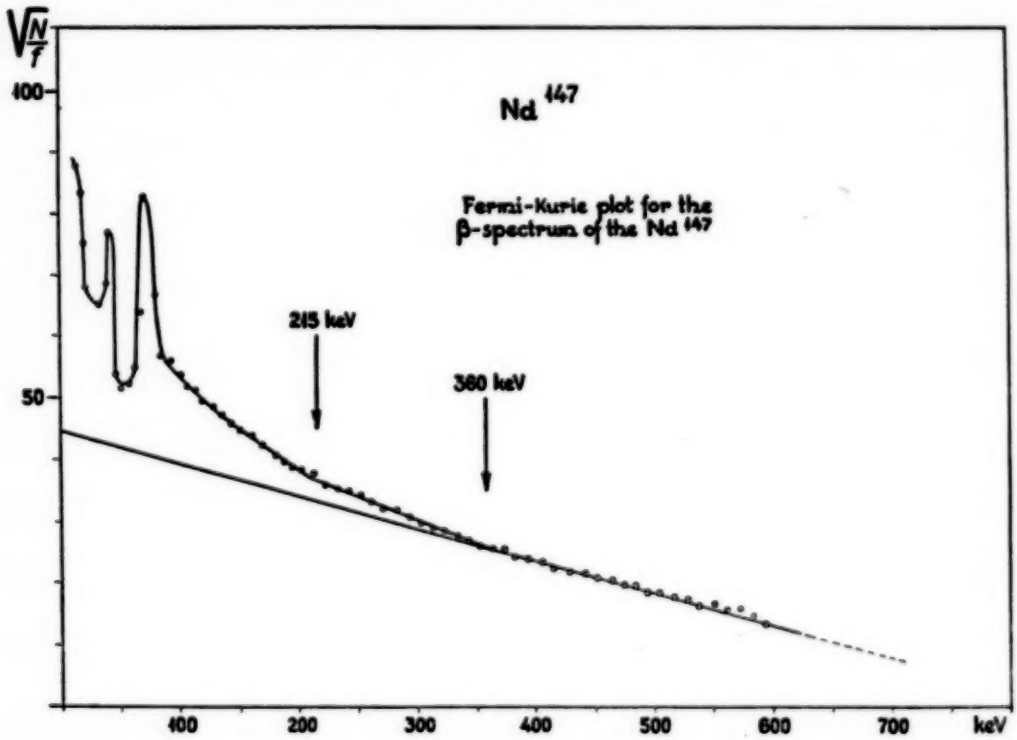


Fig. 3. The Fermi-Kurie plot for the part of lower energy of the $\beta$-spectrum.

the maximum energy of the group with the highest end point energy could not be well evaluated.

The reported errors of measured values are the results of estimation. The least exactitude we could reach in giving the maximum energy value of the group with an energy not much higher than 500 keV end point energy. Taking a mean value from the analyses of the two coincidence spectra (cf. figs. 1 and 2), the end point energy of this group is $529 \pm 25$ keV. Although as it can be seen in figs. 1 and 2 the errors of the single measuring data are rather considerable, on the ground of the plots, the supposition might not be

too daring that in the case of this group we are confronted with a transition uniquely forbidden in the first order, the plot of which can be straightened out by an $a_1$ factor [15]), that is $\Delta I = 2$, $\Delta\pi = -1$. This hypothesis seems to be supported also by the log $ft$ values (cf. ref. [6,7,8])) published up to now regarding this transition. All these values are within the 7.3—10.1 region characteristic of the transition uniquely forbidden in the first order [16]).

No intensity data were derived from these measurements.

In the course of our studies, we received an unclassified report that several Canadian authors [17]) also carried out $\beta$—$\gamma$ coincidence spectrometric measurements for the decay scheme of $Nd^{147}$. Their results together with ours and those of some other authors mentioned before have been summed up in table 1.

TABLE 1

The end point energy of the partial spectra of $Nd^{147}$ according to the measurements of several authors

| Kondaiah [3,4]) (1951) | Emmerich *et al.* [5,6]) (1951) | Rutledge *et al.*[7]) (1952) | Hans *et al.*[8,9]) (1955) | Ewan *et al.*[17]) (1956) | Our data (1958) |
|---|---|---|---|---|---|
| | | | 227 ≈ 2 % | 214±15 | 215±15 |
| 350±8 32 % | 380±30 25 % | 384 | 395 20 % | 368±10 | 365±15 |
| ?470 3 % | | ?518 | 516 ≈ 3 % | | 529±25 |
| | 600±30 15 % | 598 | | | |
| | | ?643 | | | |
| 780±8 65 % | 825±15 60 % | 825 | 835 75 % | 818±7 | 815±10 |
| $\beta$-spectrum, internal conversion measurements | $\beta$-spectrum, internal conversion and abs. coincidence measurements | internal conversion measurements | $\gamma$-scintillation spectrometer measurements | $\beta$—$\gamma$ coincidence spectrometric measurements | $\beta$—$\gamma$ coincidence spectrometric measurements |

All energies in keV.

The estimates of error relating to the individual groups as well as the relative intensity data are represented in the table only where they were also given in the original paper. The table was arranged so that data referring to probably identical groups should be in the same line. We indicated under each column the type of measurement applied in obtaining the recorded results.

I should like to take advantage of this opportunity to express my deep gratitude to Prof. A. Szalay for the continuous interest he has shown in my work, and for his valuable help. I am also greatly indebted to Prof. O. B.

Nielsen (Copenhagen) for having called my attention to the problem.

Thanks are due to my colleagues T. Schárbert and G. Máthé for their help in the solution of electronic problems, as well as to Cs. Ujhelyi for the careful preparation of the sources.

## References

1) C. E. Mandeville, Phys. Rev. **78** (1950) 319
2) C. E. Mandeville and E. Shapiro, Phys. Rev. **79** (1950) 391
3) E. Kondaiah, Phys. Rev. **81** (1951) 1056
4) E. Kondaiah, Ark. för Fys. **4** (1952) 81
5) W. S. Emmerich and J. D. Kurbatov, Phys. Rev. **81** (1951) 1062
6) W. S. Emmerich and J. D. Kurbatov, Phys. Rev. **83** (1951) 40
7) W. C. Rutledge, J. M. Cork and S. B. Burson, Phys. Rev. **86** (1952) 775
8) H. S. Hans, B. Saraf and C. E. Mandeville, Phys. Rev. **97** (1955) 1267
9) H. S. Hans, B. Saraf and C. E. Mandeville, Phys. Rev. **98** (1955) 1173
10) A. Szalay and D. Berényi, Bull. of the Academy of Sci. USSR. Phys. Ser. **22** (1958)
11) A. Szalay and D. Berényi, Acta Physica Hungarica, to be published
12) D. Berényi, Thesis (Debrecen, 1958) (unpublished)
13) D. Berényi, Acta Universitatis Debreceniensis de L. Kossuth n., to be published
14) J. M. Hollander, I. Perlman and G. T. Seaborg, Revs. Mod. Phys. **25** (1953) 469
15) C. S. Wu, Beta- and Gamma-ray Spectroscopy, Editor Kai Siegbahn (North Holland Publ. Co., 1955) Ch. XI
16) E. J. Konopinski and L. M. Langer, Ann. Rev. Nuc. Sci. **2** (1953) 261
17) G. T. Ewan, M. A. Clark and J. W. Knowles, AECL, PR-P-30, p. 12

3.C *Nuclear Physics* **8** (1958) 613—620; © *North-Holland Publishing Co., Amsterdam*

Not to be reproduced by photoprint or microfilm without written permission from the publisher

# BREMSSTRAHLUNG FROM MULTIPLE SCATTERING

J. S. BELL

*Atomic Energy Research Establishment, Harwell, Didcot, Berks.*

Received 11 July 1958

**Abstract:** It has been predicted, by largely classical arguments, that destructive interference of the radiation from many collisions greatly reduces the rate of energy loss by very high energy electrons undergoing multiple scattering. It is observed that this is incompatible with a standard formula in classical theory, and the discrepancy is traced to an inadequate account of the high frequency part of the radiation spectrum. It is concluded that any real effect of this kind is of essentially quantal origin.

## 1. Introduction

It has been claimed by Landau and Pomerančuk (see the review article of Feinberg and Pomerančuk [1])), and in more detail by Migdal [2]), that at sufficiently high energies electrons become penetrating particles. It is argued, largely on the basis of classical theory, that the expected increase of bremsstrahlung with energy is actually changed to a decrease when interference of the radiations from many deflections is considered. However, this conflicts with the standard classical formula [3]) for the energy radiated by an electron moving in an electric field,

$$\frac{2e^4}{3m^2}\int \frac{\mathbf{E}^2-(\mathbf{E}\cdot\mathbf{v})^2}{1-v^2}\,\mathrm{d}t$$

(we take $c = 1$) where $\mathbf{v}$ is the velocity of, and $\mathbf{E}$ the electric field on, the electron at time $t$. The integrand is positive definite ($v = |\mathbf{v}| < 1$) so that energies radiated during different intervals simply add; as far as the total radiated energy is concerned there can be no question in a strictly classical theory of destructive interference. To discover the origin of the discrepancy the work of Migdal has been re-examined. It is found that a more careful treatment of the upper end of the spectrum is needed, and that then interference effects there *enhance* the radiation in just such a way as to cancel in the integrated effect the reduction at lower frequencies. However, the compensating enhancement is in a region where classical theory is quite wrong, so that as an essentially quantum effect the increase of penetrating power found by the above authors may indeed exist.

Note that we are not here concerned with the effect of the polarizability of the medium, as discussed by Ter-Mikaeljan [1]), which is important only for extremely low frequency radiation.

## 2. Migdal's Result

We first rederive Migdal's result in such a way that the necessary modifications are readily incorporated. His starting point is the following expression for the energy radiated by a single electron into the frequency range $d\omega$ and unit of solid angle $d\hat{\mathbf{k}}$:

$$dI = \left(\frac{e}{2\pi}\right)^2 \omega^2 d\omega\, d\hat{\mathbf{k}} \left| \int_{-\infty}^{\infty} dt\, \hat{\mathbf{k}} \times \mathbf{v} e^{-i\omega t + i\mathbf{k}\cdot\mathbf{r}} \right|^2 \tag{1}$$

where $\mathbf{r}$ and $\mathbf{v}$ are position and velocity at time $t$ and $\mathbf{k}$ is related to the unit vector $\hat{\mathbf{k}}$ by $\mathbf{k} = \omega\hat{\mathbf{k}}$. We shall start instead with

$$dI = \left(\frac{e}{2\pi}\right)^2 d\omega\, d\hat{\mathbf{k}} \left| \int_{-\infty}^{\infty} dt\, e^{-i\omega t + i\mathbf{k}\cdot\mathbf{r}} \frac{d}{dt} \frac{\hat{\mathbf{k}} \times \mathbf{v}}{1 - \hat{\mathbf{k}} \cdot \mathbf{v}} \right|^2, \tag{2}$$

which is obtained from (1) by partial integration, ignoring a contribution from $t = -\infty$ on the ground that we are not interested in radiation emitted while the electron was initially accelerated. The use of (2) forces us to be rather more explicit than Migdal in describing the path, which we assume to be a series of straight sections with sharp bends due to collisions. Denoting by $\boldsymbol{\delta}_i$ the change in $\hat{\mathbf{k}} \times \mathbf{v}(1 - \hat{\mathbf{k}} \cdot \mathbf{v})^{-1}$ at the $i$th collision, (2) becomes

$$\left(\frac{2\pi}{e}\right)^2 \frac{dI}{d\omega} = d\hat{\mathbf{k}} \left[ \boldsymbol{\delta}_i \cdot \boldsymbol{\delta}_i + 2\,\mathrm{Re} \sum_{j>i} \boldsymbol{\delta}_i \cdot \boldsymbol{\delta}_j e^{-i\omega(t_j - t_i) + i\mathbf{k}\cdot(\mathbf{r}_j - \mathbf{r}_i)} \right]. \tag{3}$$

The terms involving a particular collision $i$ are

$$d\hat{\mathbf{k}} \left[ \boldsymbol{\delta}_i^2 + 2\,\mathrm{Re} \sum_{j>i} \boldsymbol{\delta}_i \cdot \boldsymbol{\delta}_j e^{-i\omega(t_j - t_i) + i\mathbf{k}\cdot(\mathbf{r}_j - \mathbf{r}_i)} \right] \tag{4}$$

where the second term is the interference effect. To find the energy radiated on average in the range $d\omega$ by a single collision, (4) must be averaged over all possible collisions $i$, all possible subsequent collisions $j$, and integrated over $\hat{\mathbf{k}}$. At the final stage the integrand can depend only on the angle between $\mathbf{k}$ and the velocity $\mathbf{u}' = \mathbf{u}'v$ before the collision $i$; so instead of integrating over $\hat{\mathbf{k}}$ we can equivalently integrate over $\hat{\mathbf{u}}'$. The resulting expression is

$$\begin{aligned} &\int d\hat{\mathbf{u}}'\, d\hat{\mathbf{u}}\, P(\hat{\mathbf{u}}' \to \hat{\mathbf{u}}) \left[ \{\boldsymbol{\delta}(\mathbf{u}', \mathbf{u})\}^2 \right. \\ &\left. + 2\,\mathrm{Re} \int_0^{\infty} dt \int d\mathbf{r}\, d\hat{\mathbf{v}}\, d\hat{\mathbf{v}}'\, e^{-i\omega t + i\mathbf{k}\cdot\mathbf{r}}\, \boldsymbol{\delta}(\mathbf{u}', \mathbf{u}) \cdot \boldsymbol{\delta}(\hat{\mathbf{v}}, \hat{\mathbf{v}}') P(\mathbf{v} \to \mathbf{v}') n v \sigma W \right] \end{aligned} \tag{5}$$

where $P(\hat{\mathbf{u}}' \to \hat{\mathbf{u}})$ is the probability that in a collision with initial direction $\hat{\mathbf{u}}'$ the final direction is $\hat{\mathbf{u}}$,

$$\boldsymbol{\delta}(\mathbf{u}', \mathbf{u}) = \frac{\hat{\mathbf{k}} \times \mathbf{u}}{1 - \hat{\mathbf{k}} \cdot \mathbf{u}} - \frac{\hat{\mathbf{k}} \times \mathbf{u}'}{1 - \hat{\mathbf{k}} \cdot \mathbf{u}'}, \tag{6}$$

$n$ is the number of atoms per unit volume and $\sigma$ the scattering cross section, and $W(\hat{\mathbf{u}}, \mathbf{r}, \hat{\mathbf{v}}, t)$ is the probability that a particle with velocity $\hat{\mathbf{u}}v$ at some instant is after a time $t$ found displaced by distance $\mathbf{r}$ and with velocity $\hat{\mathbf{v}}v$.

Note that the magnitude of the velocity, $v$, is treated as constant; this is permissible because the important contributions to the integral in (5) are expected to be for $|\mathbf{r}|$ small compared with the radiation length $L$. The important values of $|\mathbf{r}|$ are presumably of the order of the length required for the root mean square angle of multiple scattering to equal the angle $(1-v^2)^{\frac{1}{2}} = m/E$ characteristic of high energy bremsstrahlung. This latter length is in fact [4])

$$(m/E_s)^2 L \approx L/1600.$$

We now make the simplifying assumption, implicit also in the work of Migdal, that typical angles of single scattering are small compared with $m/E$. The quantities $\boldsymbol{\delta}$ can then be evaluated as power series in the relevant velocity changes. To lowest order in $\overline{\theta^2}$, the mean square angle of scattering in a single collision, one finds

$$\begin{aligned}
&\int \mathrm{d}\hat{\mathbf{u}}'\,\mathrm{d}\hat{\mathbf{u}}\,P(\hat{\mathbf{u}}'\to\hat{\mathbf{u}})\{\boldsymbol{\delta}(\mathbf{u}',\mathbf{u})\}^2 = \frac{8\pi}{3}\left(\frac{E}{m}\right)^2\overline{\theta^2}\\
&\int \mathrm{d}\hat{\mathbf{u}}'\,P(\hat{\mathbf{u}}'\to\hat{\mathbf{u}})\boldsymbol{\delta}(\mathbf{u}',\mathbf{u}) = \tfrac{1}{2}\left(\frac{m}{E}\right)^2\overline{\theta^2}\,\frac{\hat{\mathbf{k}}\times\mathbf{u}}{(1-\hat{\mathbf{k}}\cdot\mathbf{u})^3} \qquad (7)\\
&\int \mathrm{d}\hat{\mathbf{v}}'\,P(\hat{\mathbf{v}}\to\hat{\mathbf{v}}')\boldsymbol{\delta}(\mathbf{v},\mathbf{v}') = -\tfrac{1}{2}\left(\frac{m}{E}\right)^2\overline{\theta^2}\,\frac{\hat{\mathbf{k}}\times\mathbf{v}}{(1-\hat{\mathbf{k}}\cdot\mathbf{v})^3}
\end{aligned}$$

where the approximation $2(1-v) \approx (1-v^2) = (m/E)^2$ has been used as sufficient for $E \gg m$. The average energy radiated per collision is then, ignoring interference,

$$\frac{2e^2}{6\pi}\left(\frac{E}{m}\right)^2\overline{\theta^2} \qquad (8)$$

and interference causes a correction factor

$$\begin{aligned}
\Phi = 1 - \frac{3nv\sigma}{16\pi}\left(\frac{m}{E}\right)^6\overline{\theta^2}\,\mathrm{Re}\int \mathrm{d}t\,\mathrm{d}\mathbf{r}\,\mathrm{d}\hat{\mathbf{u}}\,\mathrm{d}\hat{\mathbf{v}}\,\mathrm{e}^{-i\omega t+i\mathbf{k}\cdot\mathbf{r}}\\
\times\frac{\hat{\mathbf{k}}\times\mathbf{u}}{(1-\hat{\mathbf{k}}\cdot\mathbf{u})^3}\cdot\frac{\hat{\mathbf{k}}\times\mathbf{v}}{(1-\hat{\mathbf{k}}\cdot\mathbf{v})^3}W.
\end{aligned} \qquad (9)$$

The expression (8) gives a classical approximation to the Bethe-Heitler formula which should be accurate at low frequencies. Actually it is too large by a factor of about 2. The error is in our assumption that single scattering angles are small compared with $m/E$. The largest deflection $\theta_{\max}$, controlled by finite nuclear size, even for lead is about 60 $m/E$; that the error in (8) is only a factor two is because $\theta_{\max}$ occurs only as the argument of a logarithm. While strictly our considerations apply only to hypothetical atoms with very large nuclei, it is probable that the results are at least qualitatively relevant to the real case.

For $E \gg m$, the angles of scattering and radiation are very small, so that the vectors

$$\boldsymbol{\xi} = \hat{\mathbf{u}} - \hat{\mathbf{k}}, \quad \boldsymbol{\eta} = \hat{\mathbf{v}} - \hat{\mathbf{k}} \tag{10}$$

are essentially confined to a plane perpendicular to $\hat{\mathbf{k}}$, and $\mathrm{d}\boldsymbol{\xi}$ and $\mathrm{d}\boldsymbol{\eta}$ will denote elements of area in this plane. For $\gamma = (m/E)^2 \ll 1$ one finds

$$(1-\hat{\mathbf{k}}\cdot\hat{\mathbf{u}}) = \tfrac{1}{2}(\gamma+\xi^2), \quad (1-\hat{\mathbf{k}}\cdot\mathbf{v}) = \tfrac{1}{2}(\gamma+\eta^2), \quad (\hat{\mathbf{k}}\times\mathbf{u})\cdot(\hat{\mathbf{k}}\times\mathbf{v}) = \boldsymbol{\xi}\cdot\boldsymbol{\eta} \tag{11}$$

so that with

$$q = \tfrac{1}{4} n v \sigma \overline{\theta^2}, \tag{12}$$

we have

$$\Phi = 1 - \mathrm{Re}\,\frac{48}{\pi} q\gamma^3 \int \mathrm{d}t\,\mathrm{d}\mathbf{r}\,\mathrm{d}\boldsymbol{\xi}\,\mathrm{d}\boldsymbol{\eta}\,\mathrm{e}^{-i\omega t + i\mathbf{k}\cdot\mathbf{r}} \frac{\boldsymbol{\xi}\cdot\boldsymbol{\eta}}{(\gamma+\xi^2)^3(\gamma+\eta^2)^3} W(\boldsymbol{\xi}, \mathbf{r}, \boldsymbol{\eta}, t). \tag{13}$$

To determine $W$ we have the initial condition

$$W(\boldsymbol{\xi}, \mathbf{r}, \boldsymbol{\eta}, 0) = \delta(\mathbf{r})\delta(\boldsymbol{\xi}-\boldsymbol{\eta}) \tag{14}$$

and the Boltzmann equation

$$\frac{\partial W}{\partial t} + \mathbf{v}\cdot\frac{\partial}{\partial \mathbf{r}} W = nv\sigma \int \mathrm{d}\boldsymbol{\eta}\, P(\boldsymbol{\eta}' \to \boldsymbol{\eta})\{W(\boldsymbol{\eta}') - W(\boldsymbol{\eta})\}. \tag{15}$$

However, with the assumption that angles of single scattering are small compared with $m/E$, the latter can be replaced, following Migdal, by the Fokker-Planck equation

$$\frac{\partial W}{\partial t} + \mathbf{v}\cdot\frac{\partial}{\partial \mathbf{r}} W = q\left(\frac{\partial}{\partial \boldsymbol{\eta}}\right)^2 W \tag{16}$$

where $(\partial/\partial\boldsymbol{\eta})^2$ is the two-dimensional Laplacian.

Now the quantity

$$\int \mathrm{d}t\,\mathrm{d}\mathbf{r}\,\mathrm{d}\boldsymbol{\xi}\,\mathrm{e}^{-i\omega t + i\mathbf{k}\cdot\mathbf{r}}\, W \boldsymbol{\xi}(\gamma+\xi^2)^{-3} \tag{17}$$

can depend on $\hat{\mathbf{k}}$ only through $\boldsymbol{\eta}$, and so must have the form

$$\boldsymbol{\eta} H(\eta^2, \omega). \tag{18}$$

Then

$$\Phi = 1 - \mathrm{Re}\,\frac{48}{\pi} q\gamma^3 \int \mathrm{d}\boldsymbol{\eta}\,\eta^2(\gamma+\eta^2)^{-3} H, \tag{19}$$

and from (16),

$$i\omega(1-\hat{\mathbf{k}}\cdot\mathbf{v})H - (\gamma+\eta^2)^{-3} = 4q\{\mathrm{d}^2/\mathrm{d}(\eta^2)^2\}\eta^2 H. \tag{20}$$

With

$$z = \eta^2/\gamma, \quad G = 8q\gamma^2 z H, \quad s^2 = \omega\gamma^2/64q, \tag{21}$$

(19) and (20) become

$$\Phi = 1 - \operatorname{Re} 6 \int_0^\infty \mathrm{d}z (1+z)^{-3} G, \tag{22}$$

$$i(1+z)G = \frac{z}{8s^2}\left\{\frac{\mathrm{d}^2 G}{\mathrm{d}z^2} + \frac{2}{(1+z)^3}\right\}. \tag{23}$$

The required solution of (23) is that regular at infinity (so that (22) converge) and zero at the origin (assuming $H$ to be finite there). By a couple of partial integrations

$$\Phi = 1 + \operatorname{Re} 3 \int \mathrm{d}z \frac{z}{1+z} \frac{\mathrm{d}^2 G}{\mathrm{d}z^2} \tag{24}$$

$$= 24\, s^2 \operatorname{Re} \int \mathrm{d}z F \tag{25}$$

where the second derivative has been calculated from (23), and

$$-iF = G - z(1+z)^{-1}. \tag{26}$$

From (23),

$$z \frac{\mathrm{d}^2 F}{\mathrm{d}z^2} - 8s^2 i(1+z)F = -8s^2 z. \tag{27}$$

Migdal's equations (7) and (8) are obtained from (25) and (27) by trivial multiplicative changes of variables and the addition of an imaginary constant to the unknown function. Following Migdal, solution of (27) by Laplace transformation yields

$$\Phi = -\operatorname{Re} 6s(1+i) \int_0^\infty \mathrm{d}x \left\{\frac{1}{\sinh^2 x} - \frac{1}{x^2}\right\} \mathrm{e}^{-2s(1+i)x}. \tag{28}$$

By partial integration and the change of variable $2x \to x$, this can be shown equivalent to Migdal's formula (11); also by partial integration one finds the slightly simpler form

$$\Phi = \operatorname{Re} 24 s^2 i \int \mathrm{d}x \{\coth x - x^{-1}\} \mathrm{e}^{-2s(1+i)x} \tag{29}$$

or finally

$$\Phi = 24 s^2 \int_0^\infty \mathrm{d}x \, \mathrm{e}^{-2sx} (\sin 2sx)(\coth x - x^{-1}). \tag{30}$$

For small and large $s$,

$$\begin{aligned} \Phi &= 6s + \ldots \\ \Phi &= 1 - \frac{1}{84 s^4} + \ldots \end{aligned} \tag{31}$$

Instead of $\frac{1}{84}$, Migdal quotes $\frac{48}{7}$.

The quantity

$$\int_0^\infty \mathrm{d}\omega (1-\Phi) = \frac{128 q}{\gamma^2} \int_0^\infty \mathrm{d}s (1-\Phi) s \tag{32}$$

measures the overall reduction in radiated energy. From (29), after partial integrations to remove the factor $s^3$, one finds

$$s\Phi = s - \mathrm{Re}\,\tfrac{3}{4}i(i+1)\int \mathrm{d}x\,\mathrm{e}^{-2s(1+i)x}\,\frac{\mathrm{d}^3}{\mathrm{d}x^3}\left(\coth x - \frac{1}{x}\right). \tag{33}$$

Using this in (32), performance of the $s$ integral first and taking the real part leads to a $\delta$-function at $x = 0$. The result is

$$\int_0^\infty \mathrm{d}\omega(1-\Phi) = 8\pi q/5\gamma^2. \tag{34}$$

We have to explain why this is not zero.

## 3. Correlation Effect

Returning to the expression (4), note that the $\omega$ dependence is entirely in the exponent, and the expression can be integrated over $\omega$ using

$$\mathrm{Re}\int_0^\infty \mathrm{d}\omega\,\mathrm{e}^{-i\omega t + i\mathbf{k}\cdot\mathbf{r}} = \frac{\pi\delta(t)}{1-\hat{\mathbf{k}}\cdot\mathbf{u}}.$$

The interference term integrates to zero, for the $\delta$-function could contribute only if $t_j - t_i$ were zero, which would imply coincident atoms. However, in (5) subsequent collisions were tacitly allowed to be indefinitely close to the original; this then is the origin of the spurious effect. We will now incorporate in the analysis a minimum time $\tau$ between collisions, which is that required by the electron to pass between the centres of two atoms at their distance of closest approach. Strictly, perhaps, we should at the same time remove the idealization of infinitely sharp deflections, which would result in the $\omega$ integral of the first term in (4) being finite; but for simplicity this will not be done. In (5) we change the origin of $t$ and $\mathbf{r}$ to the point $(\tau, \mathbf{u}\tau)$ at which the first subsequent collision could occur, so introducing a factor

$$\mathrm{e}^{-i\omega\tau(1+\hat{\mathbf{k}}\cdot\mathbf{u})} \tag{35}$$

into the integrand. After the minimum time it will be supposed that collisions; (when the average is taken over a suitable ensemble of atomic configurations) again occur at random — this amounts to using for the two-atom correlation function that appropriate to a low density gas of hard spheres. The function $W$ is then precisely as before, and the correlation effect is entirely represented by the factor (35). Proceeding as before, the expression (13) for the correction factor is found to be augmented by a term

$$\Delta\Phi = \mathrm{Re}\,\frac{48}{\pi}q\gamma^3\{\mathrm{e}^{-\frac{1}{2}i\omega\tau(\gamma+\xi^2)} - 1\}\int \mathrm{d}t\,\mathrm{d}\mathbf{r}\,\mathrm{d}\boldsymbol{\xi}\,\mathrm{d}\boldsymbol{\eta}\,\mathrm{e}^{-i\omega t + i\mathbf{k}\cdot\mathbf{r}}\,\frac{\boldsymbol{\xi}\cdot\boldsymbol{\eta}}{(\gamma+\xi^2)^3(\gamma+\eta^2)^3}\,W. \tag{36}$$

At high frequencies the important values of $t$ in the integrand of (36) are presumably those up to and of the order of

$$\{\omega(1-v)\}^{-1} \approx (2\omega\gamma)^{-1}.$$

The typical angle of multiple scattering produced over such an interval, divided by $m/E$, is of order

$$(n\overline{v\theta^2}/2\omega\gamma^2)^{\frac{1}{2}} = (2q/\omega\gamma^2)^{\frac{1}{2}} = (32s^2)^{-\frac{1}{2}}. \tag{37}$$

So with $32s^2 \gg 1$, the multiple scattering can be ignored and an adequate approximation to $W$ is

$$\delta(\mathbf{r}-\mathbf{u}t)\delta(\boldsymbol{\xi}-\boldsymbol{\eta})$$

which yields

$$\Delta\Phi = \frac{48}{\pi} q\gamma^3 \tau \int \mathrm{d}\boldsymbol{\xi}\, \frac{\xi^2}{(\gamma+\xi^2)^6} \frac{\sin\{\frac{1}{2}(\gamma+\xi^2)\omega\tau\}}{\frac{1}{2}(\gamma+\xi^2)\omega\tau}. \tag{38}$$

As a function of $\omega$ this is positive and roughly constant until $\gamma\omega\tau$ is comparable with unity, and then falls off.

It is more difficult to determine $\Delta\Phi$ for small $\omega$, except at $\omega = 0$, where (36) gives $\Delta\Phi = 0$. However, the condition $32s^2 \gg 1$, using standard multiple scattering expressions [4]) may also be written

$$\tfrac{1}{2}\gamma\omega\tau \gg (\tau/L)(E_s/m)^2 \approx 1600\tau/L. \tag{39}$$

In air and lead respectively the right hand side is of order $10^{-9}$ and $10^{-4}$. Thus (38) will be valid over all but a very small fraction of the range $\gamma\omega\tau \lesssim 1$. We may use it therefore to compute the integral of $\Delta\Phi$ over $\omega$, with the result

$$\int \Delta\Phi\, \mathrm{d}\omega = 8\pi q/5\gamma^2. \tag{40}$$

This just cancels (34) as expected; the exact form of $\Delta\Phi$ must give the same result. In the limit $\tau \to 0$ the correction factor for all $\omega$ approaches (30); but the small residual enhancement extends to continually higher frequencies in such a way as to keep the limit of the integral different from the integral of the limit of the integrand.

## 4. Conclusion

It has been found that the reduction in radiation at low frequencies is compensated for by enhancement at very high frequencies. But it must be admitted that the enhancement is mainly in a frequency range where classical theory is quite wrong. Frequencies of order $(\tau\gamma)^{-1}$ correspond to photon energies $\hbar\omega$ such that

$$\hbar\omega/E = (\hbar/m\tau)(E/m) \approx 10^{-3}\, E/m.$$

At the energies for which interference effects become of interest ($E/m \approx 10^{11}$ in air, $10^{6}$ in lead) such photons are energetically impossible. So it may be that in the quantum theory [5]) there is no important analogue of our compensating effect, but this should be investigated.

## References

1) Feinberg and Pomerančuk, Suppl. to Nuovo Cimento **3** (1956) 652
2) A. B. Migdal, Dokl. Akad. Nauk SSSR, **96** (1954) 49
3) Landau and Lifshitz, The Classical Theory of Fields (Addison-Wesley Press, 1951) p. 212
4) Rossi and Greisen, Revs. Mod. Phys. **13** (1941) 240
5) A. B. Migdal, J.E.T.P. **5** (1957) 527

1.B:2.I *Nuclear Physics* **8** (1958) 621—636; © *North-Holland Publishing Co., Amsterdam*
Not to be reproduced by photoprint or microfilm without written permission from the publisher

# POLARIZATION PHENOMENA IN NEUTRON-PROTON RADIATIVE CAPTURE

W. CZYŻ

*Institute for Theoretical Physics, University of Copenhagen* †

and

J. SAWICKI

*Palmer Physical Laboratory, Princeton University* ††

Received 7 July 1958

**Abstract:** An analysis of the polarization phenomena in the neutron-proton radiative capture and the photodisintegration of the deuteron is given. The usefulness of some polarization experiments is indicated.

## 1. Introduction

The present paper contains an analysis of polarization effects occurring in the photodisintegration of deuterium and radiative neutron-proton capture. Previously obtained results concerning the polarization of nucleons in the photodisintegration of deuterium have been published in two recent papers [1, 2]).

All calculations presented below are performed for the radiative capture reaction; a mathematical formalism suitable for this purpose has been constructed. We obtain several formulas in which the angular distributions and polarizations of emitted $\gamma$-rays are expressed in terms of the radial integrals of the multipole moments and phase shifts of the neutron-proton scattering problem. These formulas contain, beside several new results, all the main ones of refs.[1, 2]). The angular distribution of nucleons from photodisintegration of deuterium (incident $\gamma$-rays unpolarized) is the same as the angular distribution of $\gamma$-rays from the radiative capture of unpolarized neutrons by unpolarized protons (detailed balance theorem). Similarly, polarization of the neutrons from photodisintegration of deuterium (incident $\gamma$-rays unpolarized) is equal to the left-right asymmetry in angular distribution of emitted $\gamma$-rays from radiative capture of polarized neutrons by unpolarized protons (Blin-Stoyle's theorem, see ref.[3])).

As mentioned before, in refs.[1, 2]) polarization experiments may give an additional check on the sets of phase shifts obtained from neutron-proton

† On leave from the Institute of Nuclear Research of the Polish Academy of Sciences.

†† This work was supported in part by the U.S. Atomic Energy Commission and the Higgins Scientific Trust Fund.

scattering analyses and on the phenomenological neutron-proton potential.

Recently, de Swart and Marshak have employed the differential cross section, which gives two relations between the various integrals, to check the Singell-Marshak nucleon-nucleon forces. The success of their work has encouraged us to work out various further relations that can be obtained from polarization experiments.

Special attention is paid to two aspects of the problem. The first concerns the role of M1 transitions in the $P(\vartheta)$ function describing reactions with polarized nucleons (see, e.g., eq. (11)). M1 transitions interfere here with E1 and play therefore a considerable part. Recent theoretical analysis of the photodisintegration of deuterium [4]) shows that, in the medium energy range, E1 transition matrix elements are well reproduced by the matrix elements of the static dipole electric moment with wave functions corresponding to the phenomenological two-nucleon potential as proposed by Singell and Marshak [6]) (the Siegert theorem is valid) †.

This indicates that E1 transition integrals in low and medium energy ranges are rather well known. Therefore, measurements of the nucleon polarization from the D($\gamma$, n)p reaction ($\gamma$ unpolarized) or equivalent measurements of the left-right asymmetry in the angular distribution of $\gamma$-rays from n(p, $\gamma$)D reaction with polarized neutrons can give information about M1 transitions which at present are much less known than E1 ones.

The second point to be emphasized is the role of the $^3D_1$ component in the ground state of the deuteron. For low energies (incident photon beam of few MeV), the contribution of the $^3D_1$ state to the polarization of the outgoing nucleons from the D($\gamma$, n)p reaction is considerable (about 15 %). For the n(p, $\gamma$)D reaction in the same energy range, the polarization of the outgoing deuterons is entirely due to the presence of a $^3D_1$ component in the deuteron ground state and, if corresponding measurements were performed, one would obtain information about the percentage of the $^3D_1$ component in the deuteron ground state. These two examples show that the polarizations in the low energy limit are much more sensitive to the presence of the $^3D_1$ component in the deuteron ground state than in the differential total photodisintegration and cross sections.

## 2. Notation

$D(\mu)$ Deuteron spin function: $\mu$-projection of the spin of the deuteron on the $z$-axis. We have $\sum D^*(\mu)D(\mu') = \delta_{\mu\mu'}$ (summation over spin variables).

$\mathcal{E}_{e,m}(L, M)$ Electric field of $L$, $M$-pole electric and magnetic radiation defined as in ref.[9]), table 1.

† The influence of retardation effects for energies of the order of 100 MeV has been investigated in ref.[5]).

$\sigma$ The $z$-component of the total spin of the neutron-proton system.

$a_{e,m}(L, M)$ Amplitude defined as in ref.[7]), Chapter XII.

$\psi_1^{\sigma}$, $\psi_t^{\mu}$ The neutron-proton initial and final states.

$J$, $M_J$ The total angular momentum of the neutron-proton system, and its $z$-component.

$Y_{l,m}(\vartheta, \varphi)$ The spherical harmonics defined as in ref.[7]).

$\mathcal{Y}^{M_J}_{J,l,s}(\vartheta, \varphi)$ The total angular momentum eigenfunction defined as in ref.[7]), Appendix A.

$v_J$ The radial eigenfunction of the uncoupled ($l = J$) state of the neutron-proton system in the continuum.

$u_J^{\alpha,\beta}$, $w_J^{\alpha,\beta}$ The radial eigenfunctions of the coupled ($l = J-1, l = J+1$) states of the neutron-proton system in the continuum.

$\varepsilon_J$ The mixture parameter defined as in ref.[8]).

$\delta_{J0}$, $\delta_{J\alpha}$, $\delta_{J\beta}$ The phase shifts defined as in ref.[8]). This notation is used only in formula (3).

$\alpha$, $\beta$ The standard spin $\frac{1}{2}$ functions (see, e.g., ref.[8]), Appendix A).

$\chi_{1,0,-1}$ The triplet spin functions.

$\chi_0^0$ The singlet spin function.

$\mathbf{k}_0$ The wave vector of the outgoing photon.

$\mathbf{k}$ The wave vector of the incident neutron.

$\mathbf{n}$ The unit vector perpendicular to the reaction plane,

$$\mathbf{n} = \frac{\mathbf{k} \times \mathbf{k}_0}{|\mathbf{k} \times \mathbf{k}_0|}.$$

$u, w$ The deuteron ground state radial eigenfunctions (of the $^3S_1$ and $^3D_1$ states, respectively).

$u_S$ The $^1S_0$-state radial eigenfunction.

$\eta_0$ The $^3P_0$ state phase shift.

$\eta_1$ The $^3P_1$ state phase shift.

$\eta_{2\alpha}$, $\eta_{2\beta}$ The $^3P_2 + ^3F_2$ states phase shifts (see ref.[8])).

$\delta_S$ The $^1S_0$ state phase shift.

$\gamma = \left(\frac{M\varepsilon_d}{\hbar^2}\right)^{\frac{1}{2}}$ The parameter of the deuteron ground state wave function ($\lim_{r\to\infty} u = \text{const} \cdot e^{-\gamma r}$).

$M$ The nucleon mass.

$\alpha$ $\alpha = \frac{\hbar}{Mc}(\mu_p - \mu_n)$,

$\mu_p$ and $\mu_n$ are the proton and neutron magnetic moments, respectively.

$\tilde{\sigma}(\vartheta)$ The angular distribution of $\gamma$-rays from the radiative capture of unpolarized neutrons by unpolarized protons (see eq. (6)).

$F(\vartheta)$ The angular distribution of $\gamma$-rays from the radiative capture of polarized neutrons by unpolarized protons (see eq. (8)).

$\mathbf{P}_{\text{inc}}$ The vector of polarization of the incident neutron beam.

$P(\vartheta)$ The polarization of the outgoing neutrons from the D ($\gamma$, n) p reaction with unpolarized $\gamma$-rays. This function was calculated in refs.[1]) and [2]).

$\Pi(\vartheta)$ The polarization of the outgoing $\gamma$-rays from the radiative capture of unpolarized neutrons by unpolarized protons.

$F_L^M(\vartheta)$ The angular distribution of the $(L, M)$ multipole radiation $F_L^M(\vartheta) = 4\pi^2 r^2 \mathscr{E}(L, M)\mathscr{E}^*(L, M)$.

$W(\vartheta, \xi)$ The probability of finding a $\gamma$-quantum in the direction $\vartheta$ with polarization vector $\xi$ (see ref.[9])).

$\xi$ The polarization vector of the $\gamma$-quantum. We describe the polarization of $\gamma$-quanta, exactly as Tolhoek and Cox do, by means of Stokes parameters $\xi_1\ \xi_2\ \xi_3$: $\xi = \xi_1\chi_{\|} + \xi_2\chi_{\perp} + \xi_3\chi_c$, where $\chi_{\|}$ determines the state of linear polarization when the electric vector lies in the plane $\mathbf{k}_0$ and $\mathbf{k}$. Here $\pm\chi_{\perp}$ give the states of linear polarization rotated through $\frac{1}{4}\pi$ compared with $\chi_{\|}$. Besides, $+\chi_c$, $-\chi_c$ give left and right circular polarized radiation, respectively. For details, see ref.[9]).

$\xi_{0L}^M$ The polarization vector of the $(L, M)$ multipole. For details, see ref.[9]).

$f(\vartheta, \Phi)$ The angular distribution of nucleons from the photodisintegration reaction by linearly polarized photons.

Definition of the radial integrals involved in tables 1 and 2:

$$L_0 = \int_0^\infty (\gamma r) v_0 (u - 2^{\frac{1}{2}} w)\,\mathrm{d}r, \qquad L_1 = \int_0^\infty (\gamma) v_1 (u + 2^{-\frac{1}{2}} w)\,\mathrm{d}r$$

$$J_\alpha = \tfrac{1}{3}(-\sqrt{\tfrac{3}{2}}\cos\varepsilon_2 + \sin\varepsilon_2)(L_2^\alpha + L_1^\alpha\sqrt{\tfrac{3}{2}})$$

$$J_\beta = \tfrac{1}{3}(\sqrt{\tfrac{3}{2}}\sin\varepsilon_2 + \cos\varepsilon_2)(L_2^\beta + L_1^\beta\sqrt{\tfrac{3}{2}})$$

$$Z_\alpha = \tfrac{1}{3}(-\sqrt{\tfrac{2}{3}}\cos\varepsilon_2 - \sin\varepsilon_2)(L_2^\alpha + L_1^\alpha\sqrt{\tfrac{3}{2}})$$

$$Z_\beta = \tfrac{1}{3}(\sqrt{\tfrac{2}{3}}\sin\varepsilon_2 - \cos\varepsilon_2)(L_2^\beta + L_1^\beta\sqrt{\tfrac{3}{2}})$$

$$L_2^{\alpha,\beta} = \int_0^\infty (\gamma r) u_2^{\alpha,\beta}\left(u - \frac{1}{5\sqrt{2}}\,w\right)\mathrm{d}r, \qquad L_1^{\alpha,\beta} = \frac{3\sqrt{2}}{5}\int_0^\infty (\gamma r) w_2^{\alpha,\beta}\, w\,\mathrm{d}r$$

$$M_S = \gamma \int_0^\infty u_S u\,\mathrm{d}r.$$

## 3. Mathematical Description of the Emitted $\gamma$-rays

The emitted electromagnetic field will be described by the mathematical scheme given by Blatt and Weisskopf [7]) and adapted to our purposes. Our starting point is the construction of the electric field of $\gamma$-rays produced in n—p radiative capture

$$\mathbf{E}^{\sigma} = \sum_{L,M} D[\mu(\sigma, M)] a_{\mathrm{e}}{}^{\sigma}(L, M) \boldsymbol{\mathcal{E}}_{\mathrm{e}}(L, M) + \sum_{L,M} D[\mu(\sigma, M)] a_{\mathrm{m}}{}^{\sigma}(L, M) \boldsymbol{\mathcal{E}}_{\mathrm{m}}(L, M). \tag{1}$$

Eq. (1) represents the electric field produced by an initial state of the neutron-proton system with $z$-projection of the total spin equal to $\sigma$. The recoil effect after $\gamma$-ray emission is neglected, therefore $D(\mu)$ are just deuteron spin functions. We shall work in the frame of reference shown in fig. 1.

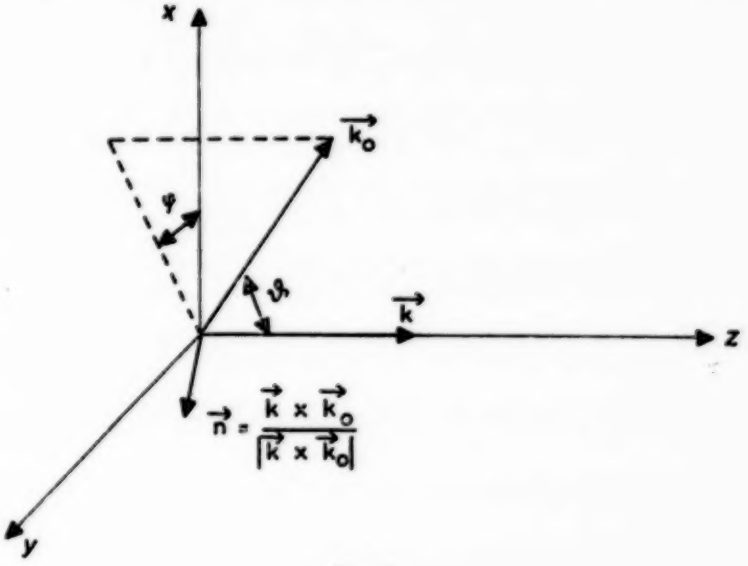


Fig. 1

Therefore, $\sigma$ is the $z$-component of the total angular momentum of the incident beam. Using conservation of angular momentum, we can find a relation between $\mu$, $M$, $\sigma$. Here, $\mu+M$ represents the $z$-component of the total angular momentum in the final state ($\gamma$-ray + deuteron); therefore,

$$\mu+M = \sigma. \tag{2}$$

This is the reason why in eq. (1) $\mu$ is written as a function of $M$ and $\sigma$.

All calculations are performed in the C.M. system. For calculation of the $a^{\sigma}_{\mathrm{e,m}}(L, M)$ amplitudes we shall use the following initial and final neutron-proton system wave functions: $\psi_1{}^{\sigma}$ is asymptotically a plane wave plus a *divergent* spherical wave. It can be shown by a procedure similar to that used in appendix 1 of ref.[1]) that the general form of $\psi_1{}^{\sigma}$ is

$$\psi_1^{\sigma} = \sum_J \Big\{ e^{i(\frac{1}{2}\pi J + \delta_{J0})} C_{J,1}(J, \sigma; 0, \sigma) Y^*_{J,0}(0, 0) \mathscr{Y}^{\sigma}_{J,J,1}(\vartheta', \varphi') \frac{v_J(r)}{r}$$
$$+ (\cos \varepsilon_J e^{i[\frac{1}{2}\pi(J-1)+\delta_{J\alpha}]} C_{J-1,1}(J, \sigma; 0, \sigma) Y^*_{J-1,0}(0, 0)$$
$$+ \sin \varepsilon_J e^{i[\frac{1}{2}\pi(J+1)+\delta_{J\alpha}]} C_{J+1,1}(J, \sigma; 0, \sigma) Y^*_{J+1,0}(0, 0))$$
$$\times \left( \frac{u_J^{\alpha}(r)}{r} \mathscr{Y}^{\sigma}_{J,J-1,1}(\vartheta', \varphi') + \frac{w_J^{\alpha}(r)}{r} \mathscr{Y}^{\sigma}_{J,J+1,1}(\vartheta', \varphi') \right) \qquad (3)$$
$$+ (-\sin \varepsilon_J e^{i[\frac{1}{2}\pi(J-1)+\delta_{J\beta}]} C_{J-1,1}(J, \sigma; 0, \sigma) Y^*_{J-1,0}(0, 0)$$
$$+ \cos \varepsilon_J e^{i[\frac{1}{2}\pi(J+1)+\delta_{J\beta}]} C_{J+1,1}(J, \sigma; 0, \sigma) Y^*_{J+1,0}(0, 0))$$
$$\times \left( \frac{u_J^{\beta}(r)}{r} \mathscr{Y}^{\sigma}_{J,J-1,1}(\vartheta', \varphi') + \frac{w_J^{\beta}(r)}{r} \mathscr{Y}^{\sigma}_{J,J+1,1}(\vartheta', \varphi') \right) \Big\}.$$

The above function is constructed for triplet spin states of a neutron-proton system and is sufficiently general to describe the influence of spin-orbit plus tensor forces. For singlet spin states of a neutron-proton system, there is neither spin-orbit nor tensor coupling present and the construction of $\psi_1^{\sigma}$ is trivial. We shall write the final state wave function in the form

$$\psi_1^{\mu} = \frac{u(r)}{r} \mathscr{Y}^{\mu}_{1,0,1} + \frac{w(r)}{r} \mathscr{Y}^{\mu}_{1,2,1}. \qquad (4)$$

Now, using (3) and (4), we can perform all angular integrations in the $a^{\sigma}_{e,m}(L, M)$ matrix elements and express them as functions of phase shifts and radial integrals.

Having calculated all the $a^{\sigma}_{e,m}(L, M)$ important in the chosen energy range, we can get from expansion (1) all information about the electromagnetic radiation and deuterons emitted after the capture reaction. E.g., we can calculate the angular distribution of $\gamma$-rays after capture of unpolarized or polarized particles, polarization of $\gamma$-rays after capture of unpolarized or polarized particles, polarization of deuterons created in capture reaction, etc.

In the following applications we shall use mainly E1 and M1 transitions. We therefore give the tables of $a_e^{\sigma}(1, M)$ and $a_m^{\sigma}(1, M)$ only. In $a_e^{\sigma}(1, M)$ we take into account all possible E1 transitions from $^3P_0$, $^3P_1$, $^3P_2+^3F_2$ continuum states to the $^3S_1+^3D_1$ ground state. In $a_m^{\sigma}(1, M)$ we take into account only the most important M1 transitions $^1S_0 \rightarrow {}^3S_1+{}^3D_1$.

## 4. Angular Distribution of $\gamma$-rays. Neutrons and Protons are Unpolarized

The angular distribution can be obtained from formula (1) by evaluating the following expression:

TABLE 1

$a_e{}^{\sigma}(1, M) \times k_0{}^{-2} e^{-1}(-i)$

| $M$ \ $\sigma$ | 1 | 0 | −1 |
|---|---|---|---|
| 1 | $\mu = 0$<br>$\frac{1}{2}\left(e^{i\eta_1}\frac{1}{\sqrt{6}}L_1 + e^{i\eta_{2\alpha}}J_\alpha + e^{i\eta_{2\beta}}J_\beta\right)$ | $\mu = -1$<br>$\frac{1}{2}(e^{i\eta_0}\frac{1}{3}\sqrt{\frac{2}{3}}L_0 + e^{i\eta_{2\alpha}}Z_\alpha + e^{i\eta_{2\beta}}Z_\beta)$ | |
| 0 | $\mu = 1$<br>$\frac{1}{2}\left(-e^{i\eta_1}\frac{1}{\sqrt{6}}L_1 + e^{i\eta_{2\alpha}}J_\alpha + e^{i\eta_{2\beta}}J_\beta\right)$ | $\mu = 0$<br>$\frac{1}{2}(-e^{i\eta_0}\frac{1}{3}\sqrt{\frac{2}{3}}L_0 + e^{i\eta_{2\alpha}}Z_\alpha + e^{i\eta_{2\beta}}Z_\beta)$ | $\mu = -1$<br>$\frac{1}{2}\left(-e^{i\eta_1}\frac{1}{\sqrt{6}}L_1 + e^{i\eta_{2\alpha}}J_\alpha + e^{i\eta_{2\beta}}J_\beta\right)$ |
| −1 | | $\mu = 1$<br>$\frac{1}{2}(e^{i\eta_0}\frac{1}{3}\sqrt{\frac{2}{3}}L_0 + e^{i\eta_{2\alpha}}Z_\alpha + e^{i\eta_{2\beta}}Z_\beta)$ | $\mu = 0$<br>$\frac{1}{2}\left(e^{i\eta_1}\frac{1}{\sqrt{6}}L_1 + e^{i\eta_{2\alpha}}J_\alpha + e^{i\eta_{2\beta}}J_\beta\right)$ |

TABLE 2

$a_m{}^{\sigma}(1, M) \times k_0{}^{-2} e^{-1}$

| $M$ \ $\sigma$ | 0 |
|---|---|
| 1 | $\mu = -1$<br>$\frac{1}{\sqrt{6}}\frac{\hbar}{Mc}(\mu_n - \mu_p)M_S e^{i\delta_S}$ |
| 0 | $\mu = 0$<br>$\frac{1}{\sqrt{6}}\frac{\hbar}{Mc}(\mu_n - \mu_p)M_S e^{i\delta_S}$ |
| −1 | $\mu = 1$<br>$\frac{1}{\sqrt{6}}\frac{\hbar}{Mc}(\mu_n - \mu_p)M_S e^{i\delta_S}$ |

$$\{\mathrm{S}\, r^2 \mathbf{E}^{\sigma} \cdot \mathbf{E}^{\sigma *}\}_{\mathrm{av}}, \tag{5}$$

where $\mathrm{S}$ represents the summation over spin variables and $\{\ldots\}_{\mathrm{av}}$ the averaging over 4 possible values of $\sigma$ (three triplet values, one singlet value). All cross terms vanish because of the orthogonality of the $D(\mu)$ functions and incoherence of all initial states labelled by $\sigma$ (nucleons are unpolarized!). In the E1+M1 approximation (see preceding section) we get the following expression for the angular distribution of $\gamma$-rays:

$$\tilde{\sigma}(\vartheta) = \alpha^2 M_{\mathrm{S}}{}^2 + \tfrac{3}{2} p_1 + \tfrac{3}{4}(p_0 - p_1) \sin^2 \vartheta_1 \tag{6}$$

where

$$\alpha = \frac{\hbar}{Mc}(\mu_{\mathrm{p}} - \mu_{\mathrm{n}}), \qquad \tfrac{1}{4} p_0 = k_0^{-6} e^{-2} \sum_{\sigma} |a_{\mathrm{e}}{}^{\sigma}(1, 0)|^2,$$
$$\tfrac{1}{4} p_1 = k_0^{-6} e^{-2} \sum_{\sigma} |a_{\mathrm{e}}{}^{\sigma}(1, 1)|^2 = k_0^{-6} e^{-2} \sum_{\sigma} |a_{\mathrm{e}}{}^{\sigma}(1, -1)|^2.$$

If we want properly normalized differential cross-sections we have to multiply $\tilde{\sigma}(\vartheta)$ by the factor $B(k)$ defined in ref.[4]). From table 1 of the preceding section we can easily get explicit expressions for $p_1$ and $p_0$:

$$\begin{aligned} p_1 = {} & \tfrac{1}{6} L_1{}^2 + J_x{}^2 + J_y{}^2 + \frac{2}{\sqrt{6}} L_1 J_x \cos(\eta_1 - \eta_{2x}) + \frac{2}{\sqrt{6}} L_1 J_y \cos(\eta_1 - \eta_{2y}) \\ & + 2 J_x J_y \cos(\eta_{2x} - \eta_{2y}) + \tfrac{2}{27} L_0{}^2 + Z_x{}^2 + Z_y{}^2 + \tfrac{2}{3}\sqrt{\tfrac{2}{3}} L_0 Z_x \cos(\eta_0 - \eta_{2x}) \\ & + \tfrac{2}{3}\sqrt{\tfrac{2}{3}} L_0 Z_y \cos(\eta_0 - \eta_{2y}) + 2 Z_x Z_y \cos(\eta_{2x} - \eta_{2y}) \end{aligned} \tag{7a}$$

$$\begin{aligned} p_0 = {} & \tfrac{1}{3} L_1{}^2 + 2 J_x{}^2 + 2 J_y{}^2 - \frac{4}{\sqrt{6}} L_1 J_x \cos(\eta_1 - \eta_{2x}) - \frac{4}{\sqrt{6}} L_1 J_y \cos(\eta_1 - \eta_{2y}) \\ & + 4 J_x J_y \cos(\eta_{2x} - \eta_{2y}) + \tfrac{2}{27} L_0{}^2 + 4 Z_x{}^2 + 4 Z_y{}^2 \\ & - \tfrac{4}{3}\sqrt{\tfrac{2}{3}} L_0 Z_x \cos(\eta_0 - \eta_{2x}) - \tfrac{4}{3}\sqrt{\tfrac{2}{3}} L_0 Z_y \cos(\eta_0 - \eta_{2y}) \\ & + 8 Z_x Z_y \cos(\eta_{2x} - \eta_{2y}). \end{aligned} \tag{7b}$$

It should be noted that eq. (6) represents also (detailed balance theorem) the angular distribution of nucleons from the photodisintegration of deuterium. Formula (6) takes into account the tensor coupling between ${}^3\mathrm{P}_2$ and ${}^3\mathrm{F}_2$ states and, to the best of our knowledge, has not been published so far.

## 5. Angular Distribution of $\gamma$-rays. Polarized Neutrons Impinging on Unpolarized Protons

First of all let us remark that, according to the Blin-Stoyle result (see ref.[3])), the angular distribution we are looking for is given by the formula

$$F(\vartheta) = \tilde{\sigma}(\vartheta)[1 + \mathbf{n} \cdot \mathbf{P}_{\mathrm{inc}} P(\vartheta)]. \tag{8}$$

The function $P(\vartheta)$ was calculated in ref.[1]) and ref.[2]). Therefore, using eq. (6)

of the preceding section, we can immediately get the result. We prefer, however, to present some points of the calculation for two reasons. Firstly, in ref.[1,2]), $P(\vartheta)$ was calculated without taking into account the ${}^3P_2+{}^3F_2$ tensor coupling, and now, using table 1, we are able to do so. Secondly, we want to present an alternative scheme of practical calculation of the $P(\vartheta)$ function.

We can use, of course, formula (5). Only the averaging process must be different now. First, let us write down the spin function of two nucleons having directions of spin fixed in space. The spinor pointing $(\theta, \phi)$ direction in space is described by the superposition

$$a\alpha+b\beta, \quad a = \cos \tfrac{1}{2}\theta \, e^{\frac{1}{2}i\phi}, \quad b = \sin \tfrac{1}{2}\theta \, e^{\frac{1}{2}i\phi}. \tag{9}$$

Suppose now that the neutron and proton spin functions are $a_1\alpha(1)+b_1\beta(1)$, and $a_2\alpha(2)+b_2\beta(2)$, respectively. The total spin function is therefore

$$[a_1\alpha(1)+b_1\beta(1)][a_2\alpha(2)+b_2\beta(2)]$$
$$= a_1a_2\chi_1+b_1b_2\chi_{-1}+a_1b_2\frac{1}{\sqrt{2}}(\chi_0{}^0+\chi_0)+b_1a_2\frac{1}{\sqrt{2}}(\chi_0-\chi_0{}^0). \tag{10}$$

We want to have the neutron polarized (say along the $x$-axis) and the proton unpolarized. The spin function for the neutron is a *superposition* $(1/\sqrt{2})\alpha(1)+(1/\sqrt{2})\beta(1)$ (according to (9)); for the proton we have, instead, a *mixture* of $\alpha(2)$ and $\beta(2)$ spin functions. Therefore, we put $a_1 = 1/\sqrt{2}$, $b_1 = 1/\sqrt{2}$, and $a_2 = 1$, $b_2 = 0$ or $a_2 = 0$, $b_2 = 1$. Now, we calculate the angular distribution for two $\psi_1$ in which the plane wave part of the asymptotic form is multiplied by the spin functions $\frac{1}{2}(\sqrt{2}\,\chi_1+\chi_0-\chi_0{}^0)$ and $\frac{1}{2}(\sqrt{2}\,\chi_{-1}+\chi_0+\chi_0{}^0)$ and then average over them. In these calculations, interference terms occur because of *coherent* contributions of the different spin functions (in the preceding example different spin functions gave *incoherent* contributions). This is a typical example of how to deal with polarized nucleons in the radiative capture scheme. The generalization to the case of two polarized nucleons is straightforward (one uses the spin function (10) without any averaging). The above calculations are sketched for the case of a totally polarized incident neutron beam ($|\mathbf{P}_{\text{inc}}| = 1$ in formula (8)). Generalization to $|\mathbf{P}_{\text{inc}}| < 1$ is immediate.

The averaging process described gives formula (8) with $\mathbf{P}_{\text{inc}} = \mathbf{e}_x$, where $\mathbf{e}_x$ is a unit vector of the $x$-axis (see fig. 1). The function $P(\vartheta)$ represents the left-right asymmetry of the $\gamma$-rays in the reaction plane. In the $yz$-plane the asymmetry reaches a maximum, in the $xz$ plane the asymmetry vanishes. We can easily separate the $P(\vartheta)$ function from the angular distribution and obtain in the E1+M1 approximation

$$P(\vartheta) = (\tilde{\sigma})^{-1}(c \sin 2\vartheta+\alpha d \sin \vartheta), \tag{11}$$

where

$$c = -\{\tfrac{3}{4}\sqrt{\tfrac{3}{2}}L_1[Z_\alpha \sin(\eta_1-\eta_{2\alpha})+Z_\beta \sin(\eta_1-\eta_{2\beta})]$$
$$+\tfrac{1}{2}\sqrt{\tfrac{2}{3}}L_0[J_\alpha \sin(\eta_0-\eta_{2\alpha})+J_\beta \sin(\eta_0-\eta_{2\beta})]+\tfrac{3}{4}(J_\alpha Z_\beta - J_\beta Z_\alpha)\sin(\eta_{2\alpha}-\eta_{2\beta}),$$
$$d = -M_S L_1 \sin(\eta_1-\delta_S).$$

If we decouple the $^3P_2$ and $^3F_2$ states, the above formula is in complete agreement with the analogous formulas in refs.[1]) and [2]).

Now we want to obtain the low energy limit of $P(\vartheta)$ which would give us a formula valid for energies of few MeV above the reaction threshold. For low energies, we have

$$\eta_0 = \eta_1 = \eta_2 = \eta_t = 0 \text{ and } L_0 = L-\sqrt{2}\,W, \quad L_1 = L+\frac{1}{\sqrt{2}}W,$$
$$L_2^{\alpha} = L-\frac{1}{5\sqrt{2}}W, \quad L_2^{\beta} = 0, \quad L_t^{\alpha,\beta} = 0,$$
$$L = \int_0^\infty (\gamma r)vu\,\mathrm{d}r, \quad W = \int_0^\infty (\gamma r)vw\,\mathrm{d}r,$$

where $v(r)$ is the radial part of the continuum P-state wave function (no splitting of the $^3P_J$ states).

The final result for $P(\vartheta)$ is

$$P(\vartheta) = \frac{\alpha M_S(L+\frac{1}{\sqrt{2}}W)\sin\delta_S \sin\vartheta}{\alpha^2 M_S{}^2+\frac{9}{25}W^2+(\frac{3}{2}L^2+\frac{3}{50}W^2)\sin^2\vartheta}. \tag{12}$$

This formula shows that for low energy radiative capture (or photodisintegration) the $^3D_1$ state in the ground state of deuteron plays a more important role in $P(\vartheta)$ than in the angular distribution (the angular distribution is given by the denominator of $P(\vartheta)$). If we accept a reasonable value $W/L \approx 0.22$ (see, e.g., ref.[11])) we get the result that the polarization is about 15 % larger if we take into account the $^3D_1$ state in the ground state of the deuteron. The above discussion indicates that it is necessary to introduce a rather important modification into the low-energy polarization formula presented in ref.[10]), in which the presence of a $^3D_1$ state in the ground state was neglected.

## 6. Polarization of Outgoing $\gamma$-rays. Incident Neutrons and Protons Unpolarized

In this section extensive use is made of the results of Tolhoek and Cox's paper (see ref. [9])), keeping an almost identical notation for quantities describing the polarization of light.

Let us confine ourselves for the moment to E1 transitions. For the $(1, M)$ multipole the probability of finding a $\gamma$-quantum in the direction $\vartheta$ with a polarization vector $\xi$ is $F_1{}^M(\vartheta)\frac{1}{2}(1+\xi\cdot\xi_{01}^M)$. On the other hand (for radiative

capture of unpolarized nucleons), the probability of finding the $(1, M)$ multipole in our radiation is $p(1, \pm 1) = p_1$, $p(1, 0) = p_0$. $p_1$ and $p_0$ are defined in eq. (6) Therefore,

$$W(\vartheta, \xi) = \sum_M p(1, M) F_1^M(\vartheta) \tfrac{1}{2}(1 + \xi \cdot \xi_{01}^M) = \tilde{\sigma}(\vartheta) \tfrac{1}{2}(1 + \Pi_{\xi_0} \cdot \xi);$$

$\Pi_{\xi_0}$ is the function we are looking for. Since $\tilde{\sigma}(\vartheta) = \sum_M p(1, M) F_1^M(\vartheta)$, we get

$$\Pi(\vartheta)\xi_0 = \frac{\sum_M p(1, M) F_1^M(\vartheta) \xi_{01}^M}{\sum_M p(1, M) F_1^M(\vartheta)}. \tag{13}$$

Using the expressions for $F_1^M$ and $\xi_{01}^M$ tabulated in ref.[9]), we get finally

$$\Pi(\vartheta)\xi_0 = \frac{\frac{3}{4}(p_0 - p_1) \sin^2 \vartheta}{\frac{3}{2} p_1 + \frac{3}{4}(p_0 - p_1) \sin^2 \vartheta} \chi_{\|}. \tag{14}$$

We can generalize the above result immediately to the case of E1+M1 transitions. For M1 transitions the $p(1, M)$ coefficients are all equal and the contribution to the numerator of the expression (14) is zero (see corresponding table in ref.[9])). Therefore, the only contribution from M1 transitions is to the denominator, and finally we obtain

$$\Pi(\vartheta)\xi_0 = \frac{\frac{3}{4}(p_0 - p_1) \sin^2 \vartheta}{\alpha^2 M_S^2 + \frac{3}{2} p_1 + \frac{3}{4}(p_0 - p_1) \sin^2 \vartheta} \chi_{\|}. \tag{15}$$

We can now make a few general comments. The polarization given by (15) is linear. One should expect this because of a general theorem proved by Simon (ref.[12])): circularly polarized light cannot result from a nuclear reaction initiated by unpolarized particles.

In the E1+M1 approximation we can get $\Pi(\vartheta)$ immediately from the angular distribution $\tilde{\sigma}(\vartheta)$: *we obtain the numerator of* $\Pi(\vartheta)$ *from* $\tilde{\sigma}(\vartheta)$ (*denominator of* $\Pi(\vartheta)$) *by dropping the isotropic term.* From $\tilde{\sigma}(\vartheta)$ given by experiment we can now describe the behaviour of $\Pi(\vartheta)$ for a wide range of energies (provided the E1+M1 approximation is accurate enough):

(a) *Very low energies.* Incident neutron energy below 0.4 MeV in lab. system: the M1 transition dominates. There is no polarization.

(b) *Low energies.* Energy of the incident neutrons a few MeV: the $\sin^2 \vartheta$ term predominates, because the magnetic transition is already small and spin-orbit and tensor splittings are still small. The maximum polarization is almost 100 %.

(c) *Medium energies.* Energy of the incident neutron from a few to 200 MeV: the isotropic term increases with increasing energy because of the strong spin-orbit splitting. The maximum polarization decreases with energy rather slowly. Table 3 gives some illustration of the behaviour of

$\Pi(\vartheta)$ in the medium energy range. $\Pi(\vartheta = \frac{1}{2}\pi)$ tabulated in table 3 is approximately equal to the maximum polarization.

TABLE 3

| Energy of the incident neutrons in the laboratory system (MeV) | 40.8 | 102.2 | 155.6 |
|---|---|---|---|
| Corresponding photon energy (MeV) | 22.4 | 53.5 | 80 |
| $\tilde{\sigma}(\vartheta)$ from experiment | $4.8+47\sin^2\vartheta$ | $5.1+9.5\sin^2\vartheta$ | $4.5+3.9\sin^2\vartheta$ |
| $\Pi(\vartheta = \frac{1}{2}\pi) \approx \Pi_{\max}$ | 0.91 | 0.65 | 0.46 |

The statement that one can get polarization $\Pi(\vartheta)$ from the angular distribution $\tilde{\sigma}(\vartheta)$ is not generally true. For instance, if we take into account all possible E2 transitions, our statement breaks down. Nevertheless, one can show that, if we neglect the spin-orbit and tensor splitting in the continuum D-state and take into account from all E2 transitions only the D → S one, then our statement still holds. The D → S transition is dominant. It is also quite possible that splitting is much smaller for even states than for odd ones. Therefore, it is to be hoped that, from the experimental angular distribution $a+b(1+c\cos\vartheta)\sin^2\vartheta$, one can construct approximately the function $\Pi(\vartheta)$ as follows:

$$\Pi(\vartheta) = \frac{b(1+c\cos\vartheta)\sin^2\vartheta}{a+b(1+c\cos\vartheta)\sin^2\vartheta}. \tag{16}$$

In any case, E2 transitions do not play a very important role and eq. (16) gives us probably quite a good approximation for $\Pi(\vartheta)$.

It may be worthwhile to mention that one can measure the $\Pi(\vartheta)$ function in the reaction of photodisintegration of the deuteron by linearly polarized $\gamma$-rays. This can be seen from the detailed balance theorem. Let us consider the photodisintegration process where the linear polarization of the incident photon is given by the unit vector **e** (see fig. 2). $\Phi$ is the angle between the **e** and the vector **n** perpendicular to the reaction plane. It is always possible to represent $H'$ (the interaction of the nucleons with the radiation field) in the form

$$H' = H'_{\perp}\cos\Phi + H'_{\parallel}\sin\Phi,$$

since **e** is involved in $H'$ as a component of the scalar product. This decomposition was performed in special cases, for instance, in refs.[1]) and [2]). The reaction amplitude of the photodisintegration process is therefore

$$\langle \mathrm{f}|H'|\mathrm{i}\rangle = \langle \mathrm{f}|H'_{\perp}|\mathrm{i}\rangle\cos\Phi + \langle \mathrm{f}|H'_{\parallel}|\mathrm{i}\rangle\sin\Phi.$$

We denote

$$\langle \mathrm{f}|H'_{\perp}|\mathrm{i}\rangle = c_2, \quad \langle \mathrm{f}|H'_{\parallel}|\mathrm{i}\rangle = c_1.$$

Here $|c_1|^2$ and $|c_2|^2$ give the probabilities of the emission of a nucleon (in the direction given by the angle $\vartheta$) by a photon polarized in the $(\mathbf{k}_0, \mathbf{k})$-plane (the reaction plane) and $(\mathbf{k}_0, \mathbf{n})$-plane, respectively. Because of the hermiti-

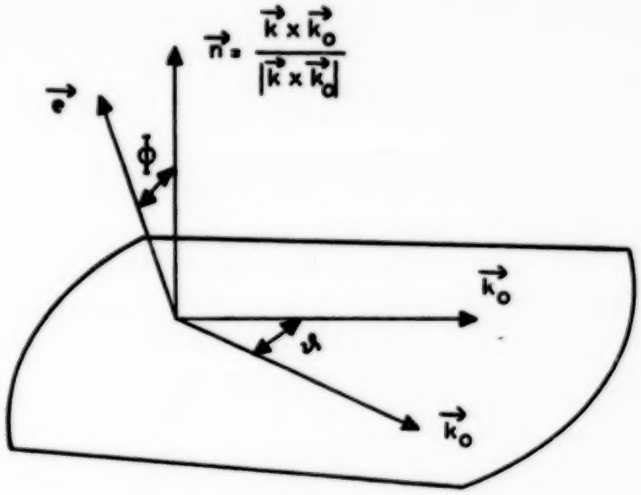


Fig. 2

city of the $H_{\parallel}$ and $H_{\perp}$, $|c_1|^2$ and $|c_2|^2$ give also the probabilities of the emission of a photon (from the capture reaction) polarized in the $(\mathbf{k}_0, \mathbf{k})$-plane and the $(\mathbf{k}_0, \mathbf{n})$-plane, respectively. In the language of the mathematical formulation of § 3, $|c_1|^2$ and $|c_2|^2$ represent the squares of the absolute values of the two perpendicular components of the electric field emitted from the capture reaction.

Let us now calculate the angular distribution of the nucleons from the photodisintegration reaction with linearly polarized photons. After some simple algebra we obtain

$$\{|\langle \mathrm{f}|H'|\mathrm{i}\rangle|^2\}_{\mathrm{av}} = \tfrac{1}{2}\{|c_1|^2+|c_2|^2\}_{\mathrm{av}}\left[1-\frac{\{|c_1|^2-|c_2|^2\}_{\mathrm{av}}}{\{|c_1|^2+|c_2|^2\}_{\mathrm{av}}}\cos 2\Phi+\frac{\{2\,\mathrm{Re}(c_1 c_2^*)\}_{\mathrm{av}}}{\{|c_1|^2+|c_2|^2\}_{\mathrm{av}}}\sin 2\Phi\right]$$

where, as usual, $\{\ldots\}_{\mathrm{av}}$ means the averaging over the initial states and the summation over the final states. Now, let us remark that the expression $\{|c_1|^2-|c_2|^2\}_{\mathrm{av}}/\{|c_1|^2+|c_2|^2\}_{\mathrm{av}}$ is equal to our $\Pi(\vartheta)$ function because the above expression is, by definition, equal to $\xi_1 = \Pi(\vartheta)$ (see ref.[9])). On the other hand, we know from our previous calculations of the radiative capture process that

$$\{2\ \mathrm{Re}\ (c_1 c_2^*)\}_{\mathrm{av}}/\{|c_1|^2+|c_2|^2\}_{\mathrm{av}} = \xi_2 = 0$$

and that $\frac{1}{2}\{|c_1|^2+|c_2|^2\}_{\mathrm{av}} = \tilde{\sigma}(\vartheta)$ (the angular distribution). Therefore, we get

$$\{|\langle \mathrm{f}|H'|\mathrm{i}\rangle|^2\}_{\mathrm{av}} = f(\vartheta, \Phi) = \tilde{\sigma}(\vartheta)[1-\Pi(\vartheta)\cos 2\Phi]. \tag{17}$$

We can reinterpret the angle $\Phi$ and say that (17) represents the angular distribution of the nucleons from the reaction of photodisintegration by linearly polarized photons, $\Phi$ being the azimuthal angle of the emerging nucleon. Therefore, we can measure $\Pi(\vartheta)$ by measuring the following asymmetry in the angular distribution of the emerging nucleons:

$$\Pi(\vartheta) = \frac{f(\vartheta, \frac{1}{2}\pi) - f(\vartheta, 0)}{f(\vartheta, \frac{1}{2}\pi) + f(\vartheta, 0)}. \tag{18}$$

In the case of a partially polarized incident photon beam we have, of course,

$$f(\vartheta, \Phi) = \tilde{\sigma}(\vartheta)[1 - \Pi_{\text{inc}}\Pi(\vartheta)\cos 2\Phi]. \tag{19}$$

The above consideration shows that the measurement of the polarization of the outgoing photons from the radiative capture reaction with unpolarized nucleons gives us exactly the same information as the measurement of the azimuthal asymmetry of the outgoing nucleons from the photodisintegration by linearly polarized photons.

## 7. Polarization of Deuterons. Incident Neutrons and Protons Unpolarized

The investigation of the polarization of deuterons emerging from the radiative capture reaction seems to be beyond the existing experimental possibilities. Therefore we sketch only one characteristic example.

We shall neglect the recoil of deuterons coming from $\gamma$-ray emission. In this approximation, in the laboratory system all deuterons move in the same direction as the incident neutrons. We calculate $\{T_{J,M}\}_{\text{av}}$, the tensor describing the polarization of deuterons defined as in ref.[13]). It turns out that only the $T_{2,0}$ component gives a non-zero contribution. We use the same definition of the magnitude of polarization as Lakin does in ref.[13]):

$$P_{\text{D}} = (\tfrac{1}{2}\sum_{JM}{}' |\{T_{J,M}\}_{\text{av}}|^2)^{\frac{1}{2}}. \tag{20}$$

For central neutron-proton forces with no spin-orbit splitting, this polarization is zero. $P_{\text{D}}$ is different from zero if spin-orbit or tensor forces are present. We give the expression for $P_{\text{D}}$ in the low energy limit (incident neutrons of several MeV). In this energy region, we can use the same kind of approximation as in deriving formula (12). Only the M1 transition can be neglected because there are no interference terms of E1 and M1 transitions. The result is

$$\{T_{2,0}\}_{\text{av}} = \frac{\sqrt{2}(\frac{4}{5}\sqrt{2}LW - \frac{7}{25}W^2)}{2L^2 + \frac{20}{25}W^2} \approx \frac{4}{5}\frac{W}{L}. \tag{21}$$

Therefore, according to (13),

$$P_D = \frac{1}{\sqrt{2}} \frac{4}{5} \left| \frac{W}{L} \right| \approx 0.12, \tag{22}$$

if we use once more the $W/L$ ratio estimate from ref.[11]). We see therefore that the polarization of deuterons in the low energy region is entirely due to the presence of a $^3D_1$ component in the deuteron ground state.

## 8. Conclusion

It seems to us that, in polarization effects in radiative capture and deuteron photodisintegration reactions, there are some points worth experimental exploration.

(a) From measurements of the function $P(\vartheta)$ in the low energy region (see formula (12)), information about the $^3D_1$ state in the ground state of the deuteron can be obtained. The integrals $L$ and $M_S$ are rather well known for low energies and the $W$ integral can be extracted from the measured $P(\vartheta)$.

(b) In the energy region where $^3P_J$ states phase shifts begin to play some role, the function $P(\vartheta)$ exhibits a characteristic change in comparison to the low energy (a few MeV) behaviour. Namely, from eqs. (11) and (12), it follows that $P(\vartheta)$ which is symmetric with respect to the direction $\vartheta = \frac{1}{2}\pi$ for low energies (see eq. (12)) becomes asymmetric when phase shifts start to play some role (see eq. (11)). Therefore, measurements of the asymmetry of the $P(\vartheta)$ function with respect to the $\vartheta = \frac{1}{2}\pi$ direction give information about the tensor plus spin-orbit splittings of the $^3P_J$ states.

(c) Medium energy measurements can supply us with information about M1 transitions which are rather badly known in this energy range. For instance, $P(\vartheta)$ for $\vartheta = \frac{1}{2}\pi$ is due entirely to M1—E1 interference; the $^3P_J$ splitting gives zero contribution at that angle.

One of us (W.C.) is grateful to Professors Niels Bohr and Aage Bohr for the hospitality granted him at the Institute for Theoretical Physics, University of Copenhagen, and thanks the Polish Atomic Energy Commission for a fellowship. He wishes to acknowledge several discussions with Dr. G. E. Brown; the other author (J. S.) had helpful discussions with Dr. J. S. Blair.

## References

1) W. Czyż and J. Sawicki, Nuovo Cimento **5** (1957) 45
2) W. Czyż and J. Sawicki, Phys. Rev. **110** (1958) 900
3) R. J. Blin-Stoyle, Proc. Phys. Soc. A **65** (1952) 452
4) J. J. de Swart and R. E. Marshak, Phys. Rev. **111** (1958) 272
5) A. F. Nicholson and G. E. Brown, to be published
6) P. S. Singell and R. E. Marshak, Phys. Rev. **109** (1958) 1229
7) J. M. Blatt and V. Weisskopf, Theoretical Nuclear Physics (1952)

8) J. M. Blatt and L. C. Biedenharn, Phys. Rev. **86** (1952) 399
9) H. A. Tolhoek and J. A. M. Cox, Physica **19** (1953) 101
10) L. N. Rosenzweig, Physica **22** (1956) 1182
11) Handbuch der Physik **39** (1957) 75
12) A. Simon, Phys. Rev. **92** (1953) 1050
13) W. Lakin, Phys. Rev. **98** (1955) 139

7.C *Nuclear Physics* 8 (1958) 637—649; © *North-Holland Publishing Co., Amsterdam*
Not to be reproduced by photoprint or microfilm without written permission from the publisher

# INVESTIGATION OF THE REACTION $p+p \rightarrow d+\pi^+$ WITH POLARIZED PROTONS OF HIGH ENERGY

Yu. K. AKIMOV, O. V. SAVCHENKO and L. M. SOROKO
*Joint Institute of Nuclear Research, Laboratory of Nuclear Problems, Dubna, USSR*

Received 28 March 1958

**Abstract:** The angular dependence of the asymmetry in the emission of $\pi^+$-mesons in the reaction $p+p \rightarrow \pi^+ + d$ was measured on a polarized proton beam at energies 536, 616 and 654 MeV. Direct proof of the existence of the d-state of the mesons in the reaction $p+p \rightarrow \pi^+ + d$ has been obtained. The results of the experiment are in agreement with the assumption that the amplitudes of the s- and d-transitions are considerably less than the amplitude of the transition $^1D_2 \rightarrow (^3S_1, p)_2$. The limiting values of some partial cross sections have been estimated.

## 1. Introduction

Measurements of the total cross section of the reaction

$$p+p \rightarrow \pi^+ + d \qquad (1)$$

at proton energies ranging from 460 MeV to 660 MeV [1]), as well as the data for higher energies obtained from experiments on the inverse reaction $\pi^+ + d \rightarrow p+p$ at $\pi^+$-meson energies of 174—307 MeV [2]) have led to the conclusion that these two mutually inverse reactions bear a resonance character due to the strong interaction between the $\pi^+$-meson and the proton in the p-state with a total moment $J = \frac{3}{2}$.

The angular distributions of the $\pi^+$-mesons in reaction (1) at proton energies of 460—660 MeV has been explained on the assumption that the $\pi^+$-meson is emitted primarily in the p-state [1]). However, these experiments alone do not allow us to draw definite conclusions regarding the relation between the various amplitudes; in particular, the problem of the intensity of the transitions in reaction (1) accompanied by the emission of a $\pi^+$-meson in the d-state evades solution.

More complete information on the relation between the amplitudes of the various transitions can be obtained from observations on different polarization effects. Reaction (1) was studied on a polarized proton beam at 314 MeV energy [3]), at which the observed asymmetry was due to interference between the s- and p-states. Similar experiments have also been performed at 415 MeV [4]). The values of the asymmetry obtained in the latter case at two different angles were interpreted by the authors [4]) simply as a possible indication of the existence of the d-wave effect.

It is known that the scattering of a $\pi^+$-meson on a proton in the d-state is a highly improbable event at an energy of the $\pi^+$-meson of $\approx$ 150 MeV becoming appreciable only at $\approx$ 300 MeV [5]), where $\delta_{33} \approx 10°$ and $\delta_{35} \approx -10°$. In some papers, as for example in ref.[6]), the preliminary data on the role of the d-wave in the scattering of the $\pi^+$-meson on protons are considered as sufficient ground to neglect the d-state of the $\pi$-meson and to analyze both the differential cross section and the polarization effects in reaction (1) on the basis of the s- and p-states alone.

However, the well known analogy between the resonance properties of reaction (1) and the resonance in meson-nucleon scattering, although true in its general outlines, may in reality differ essentially in the details. This difference may be due to the participation of a second nucleon in reaction (1). In the phenomenological theory of the formation of $\pi^{\pm,0}$-mesons in (p—p)-collisions [7]) it is shown that in the reactions $p+p \to \pi^+ + n + p$ and $p+p \to \pi^0 + p + p$ at 400—900 MeV proton energies there is a sufficiently great probability of observing the mechanism of P-wave scattering in the intermediate meson-nucleon resonance system in the $^2P_{\frac{3}{2}}$-state relative to the second nucleon. The probability of P-wave scattering in reaction (1) proved to be extremely small. The result of this event in reaction (1) would be the emission of a $\pi^+$-meson in the d-state and also in the s-state. Thus, the additional moment of momentum carried off by the second nucleon, which is not associated with the $\pi$-meson, can lead to the appearance of the d-state of the $\pi^+$-meson in reaction (1) in the absence of such a state in the intermediate meson-nucleon system.

In the present investigation we obtained direct proofs of the existence of the d-state of the $\pi^+$-meson in reaction (1) at proton energies 536, 616 and 654 MeV. From the results obtained, as well as on the basis of ref.[4]), we can conclude that the d-state effect becomes observable starting from an energy $E_p \approx 400$ MeV. The data obtained on the polarized beam are not sufficient for determining all the elements of the $S$-matrix of reaction (1). In order to solve this problem measurements must be made on other polarization effects in addition. However, if we make several assumptions regarding the relation between the transition amplitudes of reaction (1), then on the basis of our experimental results we can indicate the minimum values of the emission probabilities for $\pi$-mesons in the s- and d-states.

## 2. Experimental Procedure

The experiments were performed on a polarized proton beam obtained by scattering on carbon nuclei the unpolarized beam of 673 MeV protons extracted from the synchrocyclotron. The polarized protons, scattered "right" at an angle of 6° 20′ to the direction of the primary beam (fig. 1), were directed by two collimators on to the centre of a deflecting magnet with poles 100 cm in

diameter. Between the pole pieces of this magnet, in a 13-cm gap, specially shaped shims [8]), set up along the path of the beam, created an inhomogeneous magnetic field equivalent to the field of a system of two quadrupole lenses. The computed value of the focal length of the lenses was 2.5 metres. Such a method of focusing made it possible to treble the intensity of the beam of polarized protons at the point where the hydrogen target was set up.

A concrete wall 4 metres thick and lead blocks set up along the path of the primary beam beyond the carbon target and between the yoke and the magnet poles shielded the measuring apparatus from the background created by the primary beam and the scattered particles. To increase the unpolarized beam density at the carbon target we utilized focusing quadruple lenses of 40 mm aperture. At optimal values of the current in the windings of these lenses the density of the polarized beam increased 1.7 times.

The experimental set-up consisted of a liquid hydrogen target [9]), recording scintillation counters, a single counter for determining the profile of the beam in the course of the measurements, and an ionization chamber set up beyond the hydrogen target.

The target and the counters were adjusted relative to the axis of the 4-metre collimator. The position of this axis was fixed by means of a polyamide filament 0.2 mm in diameter. The container for the liquid hydrogen target was aligned with the axial line of the target with an accuracy of $\pm 0.3$ mm and was fixed in place with stopscrews. The alignment of the target and the collimator was checked immediately before each run with an accuracy up to several fractions of a millimeter. Misalignment of the target was corrected if it exceeded 0.4—0.5 mm.

The absence of asymmetry in the apparatus was proved in experiments on an unpolarized proton beam by recording the reactions $p+p \to \pi^+ + d$ with the other experimental conditions unchanged. The value of asymmetry at the angle $\theta_{lab} = 20°$, the most unfavourable angle as regards the appearance of latent asymmetry, was equal to $\varepsilon_0 = -(2.4 \pm 1.9)$ %. In addition to these control experiments we measured the asymmetry in elastic (p—p) scattering on the polarized proton beam at an angle $\theta_{lab} = 41°$, which corresponds to $\varepsilon_{pp}\, 41° = 0$. The measured value of the asymmetry proved equal to $\varepsilon_{pp}\, 41° = -(0.5 \pm 0.9)$ %.

Both the control measurements and the main experiments were carried out at values of the field of the deflecting magnet corresponding to maximum intensity of the polarized beam. In order to exclude the effect of drift in the value of the angle of deflection of the protons provision was made for controlling the position and profile of the polarized proton beam in the process of measurement. This was effected by means of a movable scintillation counter set up beyond the hydrogen target (fig. 1). The counter consisted of a narrow crystal of tolan (diphenylacetylene) $1 \times 40 \times 40$ mm in di-

mensions set up with its narrow end facing the beam. The current from the photomultiplier tube of this counter was recorded with an EPPV-51 potentiometer. The position of the centre of the beam was determined with an accuracy up to $\approx 1$ mm from the curve on the ribbon with calibration marks. This corresponded to a relative drift of the value of the current in the magnet winding of $\approx 0.5\,\%$, or to a misalignment of the beam and the collimator of $\approx 0.05°$.

The degree of polarization of the proton beam was determined in the usual manner by means of double scattering on carbon nuclei at an angle of 6°20′ and proved equal to $P_1 = (44 \pm 2.4)\,\%$. As a check on the quantity

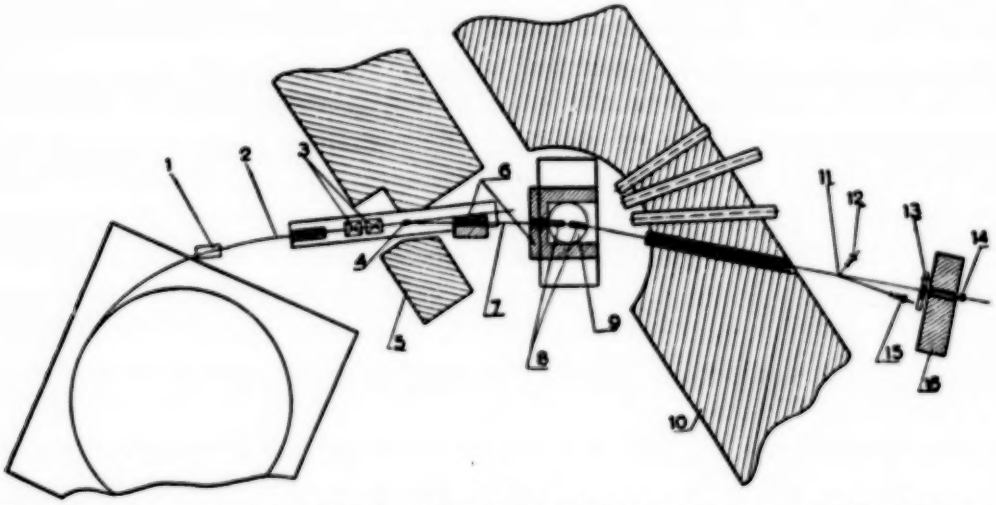


Fig. 1. The apparatus: 1. Deflecting slates. 2. Unpolarized proton beam. 3. Magnetic quadrupole lens 40 mm. 4. Carbon scattering. 5. Concrete shield. 6. Lead shield. 7. Polarized proton beam. 8. Focusing shims. 9. Deflecting magnet. 10. Protective wall. 11. Liquid hydrogen target. 12. Meson telescope. 13. Movable counter. 14. Ionization chamber. 15. Deuteron telescope. 16. Concrete shield.

$P_1$ we measured the asymmetry $\varepsilon$ of elastic p—p scattering at a laboratory angle of 30°; the value of this asymmetry was determined in ref.[10]) on a $(58 \pm 3)\,\%$ polarized beam. For our beam we obtained $\varepsilon_{pp}(30°) = (11.9 \pm 0.6)\,\%$, whereas the value of the asymmetry computed for $P_1 = 44\,\%$ [10]) should equal $\varepsilon = 12\,\%$.

The energy of the polarized beam and the spread in energy were determined by measuring the range curves with a telescope of several scintillation counters, the last of which was connected in anticoincidence with the others. Fig. 2 shows two range curves: curve 1 on the unpolarized proton beam with energy $E_p = 670$ MeV and spread in energy $\Delta E = \pm 5$ MeV, curve 2 on the polarized beam with mean energy $E_p = 616$ MeV and spread in energy $\Delta E = \pm 7$ MeV. In computing the energy of the protons from the dimensions of the filter we utilized the computed values of the correction coefficient for the effect of multiple scattering of the protons in copper [11]).

The remaining characteristics of the polarized beam for the three energies used are given in table 1. The secondary particles from the reaction $p+p \rightarrow \pi^+ + d$ were registered by two conjugate telescopes of scintillation counters in coincidence. The radiotechnical circuit was sufficiently stable due to the coincidence arrangement of the telescopes [12]) with negative values of the selection coefficients. The three-counter telescope recorded $\pi^+$-mesons.

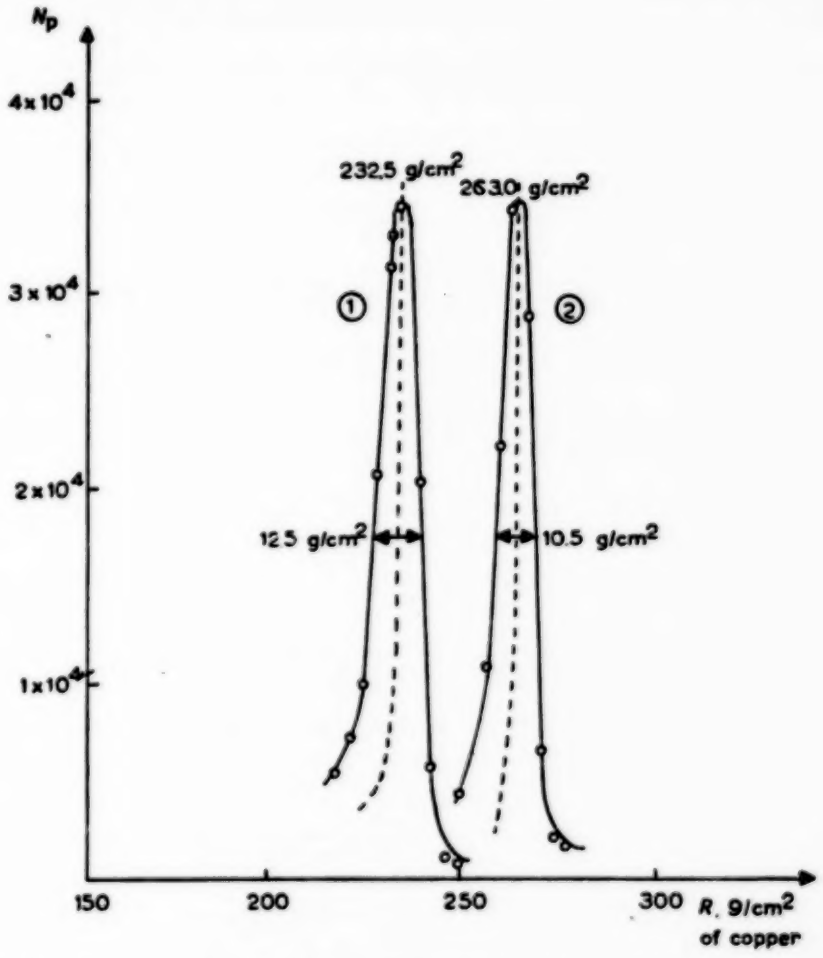


Fig. 2. 1. Polarized proton beam. $E_p = 616$ MeV. 2. Unpolarized proton beam. $E_p = 670$ MeV.

TABLE 1

| Energy of the polarized beam (MeV) | 536 | 616 | 654 |
|---|---|---|---|
| Intensity (protons/cm² · sec) | $0.9 \times 10^5$ | $5.5 \times 10^5$ | $2.8 \times 10^5$ |
| Thickness of carbon scatterer (g/cm²) | 22.9 | 22.9 | 7.3 |
| Thickness of carbon absorber in the path of the incident beam (g/cm²) | 34.2 | not utilized | |

The deuteron telescope consisted of five counters. The first three counters were connected in coincidence, the last two in anti-coincidence with the first three. Between the second and third counters an absorbing copper filter was set up, the thickness of which corresponded to the minimum range of the deuterons from reaction (1) at the conjugate angle. The interval of ranges was determined by the filter set up between counters 3 and 4. With such an arrangement of filters the telescope recorded deuterons of a definite energy, while the counting efficiency for the reactions $p+p \to \pi^+ + n + p$ and $p+p \to \pi^0 + p + p$ was considerably reduced. The contributions of these reactions and chance coincidences between the telescopes were measured with the thickness of the filter placed between counters 2 and 3 increased to such a value that reaction (1) was not recorded. The background did not exceed 10 % of the reaction $p+p \to \pi^+ + d$ under investigation. The angular resolution of the telescope at an angle $\theta_\pi^{\text{lab}} = 20°$ ($\theta_\pi^{\text{c-of-m}} = 35°$) comprised $\pm 1.9°$ ($\pm 3°$ in c–of–m), and at an angle $\theta_\pi^{\text{lab}} = 96° \pm 2.5°$ ($\theta_\pi^{\text{c-of-m}} = 130° \pm 2°$).

## 3. Discussion of Results

As is well known [4]), the differential cross section of the reaction $p+p \to \pi^+ + d$ on a polarized proton beam has the form

$$k^2 \frac{d\sigma(\theta, \varphi)}{d\Omega} = (\gamma_0 + \gamma_2 \cos^2\theta + \gamma_4 \cos^4\theta) + P \sin\theta \cos\varphi (\lambda_0 + \lambda_1 \cos\theta + \lambda_2 \cos^2\theta + \lambda_3 \cos^3\theta), \quad (2)$$

where $P$ is the degree of polarization of the beam, and the coefficients $\gamma$ and $\lambda$ [13]) are determined by the elements of the $S$-matrix of the reaction (1). In our case the emission of a $\pi^+$-meson "to the right" corresponds to an azimuthal angle $\varphi = \pi$, while the polarization vector $P$ is directed "down" [14,15]).

In the experiments described we measured the asymmetry in "right versus left" scattering $\varepsilon = (R-L)/(R+L)$ at angles of emission of the $\pi^+$-meson ranging from 35° to 130°.

The results of measurement of $\varepsilon$ at three energies are given in fig. 3. In analysing the experimental data we introduced the quantity

$$A = \frac{\varepsilon}{P \sin\theta} \frac{4\pi}{\sigma_{\text{total}}} \left(\frac{d\sigma}{d\Omega}\right)_{\text{unpol}} \quad (3)$$

where $P$ is the degree of polarization.

The normalization factor $\sigma/4\pi$ is convenient in the analysis of the magnitude of asymmetry of the reaction (1) in a wide range of energies.

The differential cross section $(d\sigma/d\Omega)_{unpol}$ on the unpolarized proton beam, and the total cross sections $\sigma_{total}$ for the reaction $p+p \to \pi^+ + d$,

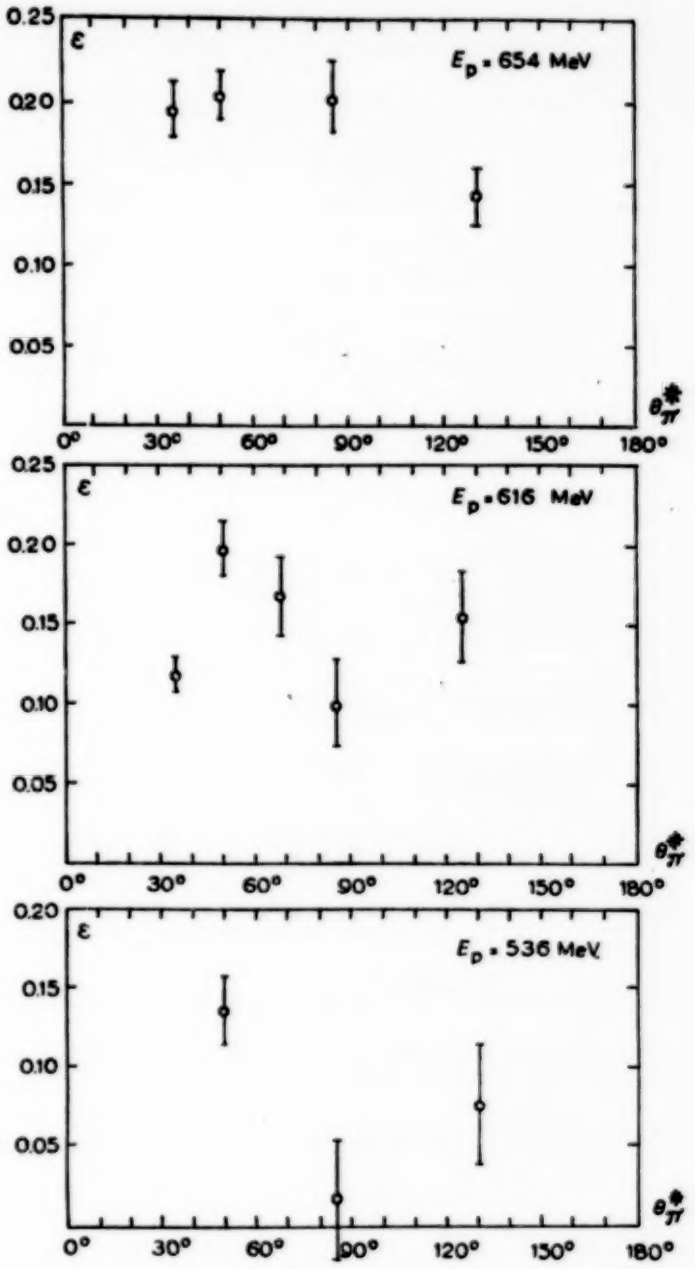


Fig. 3. Measured values of the asymmetry $\varepsilon$ in the reaction $p+p \to d+\pi^+$.

the values of which were utilized to compute $A$, were obtained by averaging the results of the papers [1, 2, 16]) and were as follows:

1) $E_p = 654$ MeV: $\frac{d\sigma}{d\Omega} \approx 0.27 + \cos^2\theta$; $\sigma_{total} = 3.1 \times 10^{-27}$ cm$^2$

2) $E_p = 616$ MeV: $\frac{d\sigma}{d\Omega} \approx 0.22 + \cos^2\theta$; $\sigma_{total} = 3.14 \times 10^{-27}$ cm$^2$

3) $E_p = 536$ MeV: $\frac{d\sigma}{d\Omega} \approx 0.24 + \cos^2\theta$; $\sigma_{total} = 2.42 \times 10^{-27}$ cm$^2$.

In fig. 4 are given the centre-of-mass values of the magnitude $A$ as a function of $\theta_\pi$ for proton energies of 654, 616 and 536 MeV. In the absence of d-transitions $A$ should be constant for a given value of the energy. The fact that a strong angular dependence of $A(\theta_\pi)$ was discovered in the experiment, as

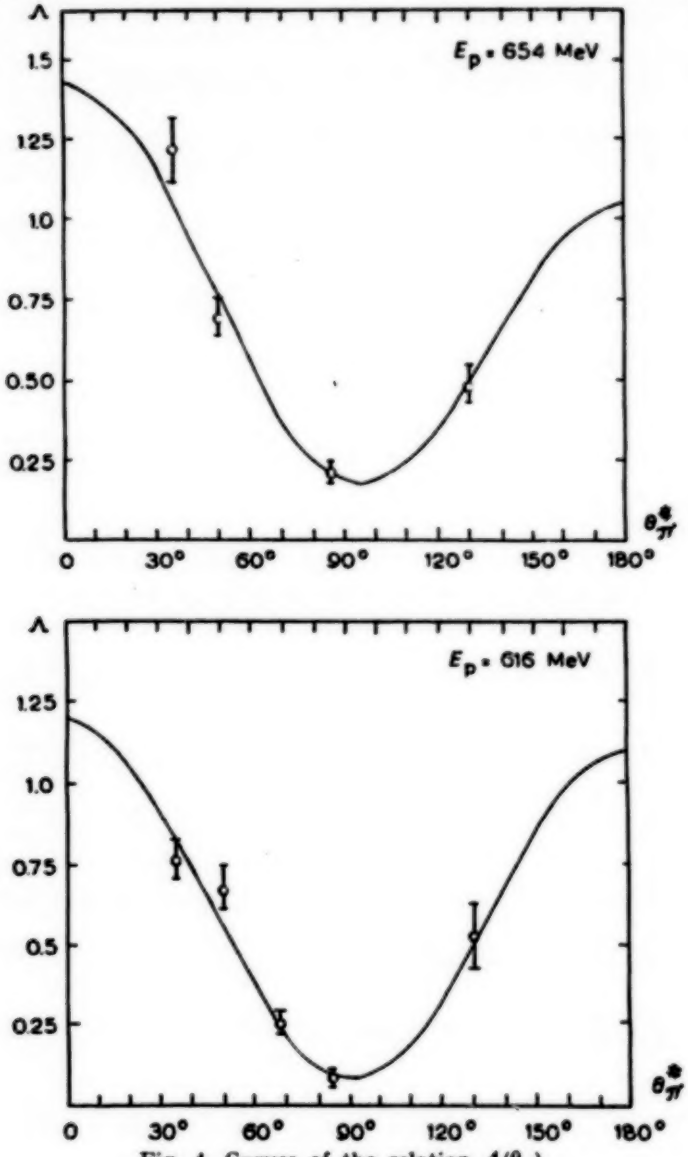


Fig. 4. Curves of the relation $A(\theta_\pi)$.

can be seen from the graphs, is direct proof of the existence of d-states of the $\pi^+$-meson in reaction (1) at all three energies. The experimental values of $A(\theta_\pi)$ were approximated by the expressions

$$A = \frac{1}{(\gamma_0+\frac{1}{3}\gamma_2)}(\lambda_0+\lambda_1\cos\theta+\lambda_2\cos^2\theta)$$

by the method of orthogonal polynomials [17]). The following values of the coefficients $\lambda_i$ and the errors were obtained:

TABLE 2

| $E_p$ (MeV) | $\frac{\lambda_0}{\gamma_0+\frac{1}{3}\gamma_2}$ | $\frac{\lambda_1}{\gamma_0+\frac{1}{3}\gamma_2}$ | $\frac{\lambda_2}{\gamma_0+\frac{1}{3}\gamma_2}$ | $\frac{\delta\lambda_0\,\delta\lambda_1}{(\gamma_0+\frac{1}{3}\gamma_2)^2}$ | $\frac{\delta\lambda_0\,\delta\lambda_2}{(\gamma_0+\frac{1}{3}\gamma_2)^2}$ | $\frac{\delta\lambda_1\,\delta\lambda_2}{(\gamma_0+\frac{1}{3}\gamma_2)^2}$ |
|---|---|---|---|---|---|---|
| 654 | 0.18 ±0.03 | 0.20±0.06 | 1.05±0.10 | $-2.2\times10^{-4}$ | $-14.0\times10^{-4}$ | $-15.0\times10^{-4}$ |
| 616 | 0.09 ±0.03 | 0.05±0.08 | 1.06±0.11 | $-7\times10^{-4}$ | $-5.5\times10^{-4}$ | $-6\times10^{-4}$ |
| 536 | −0.003±0.04 | 0.15±0.12 | 0.87±0.20 | $-1.1\times10^{-3}$ | $-3.4\times10^{-3}$ | $-7.7\times10^{-3}$ |

We did not succeed in deriving reliable values of the coefficient $\lambda_3$ from our experimental data. In order to determine this coefficient it was necessary to

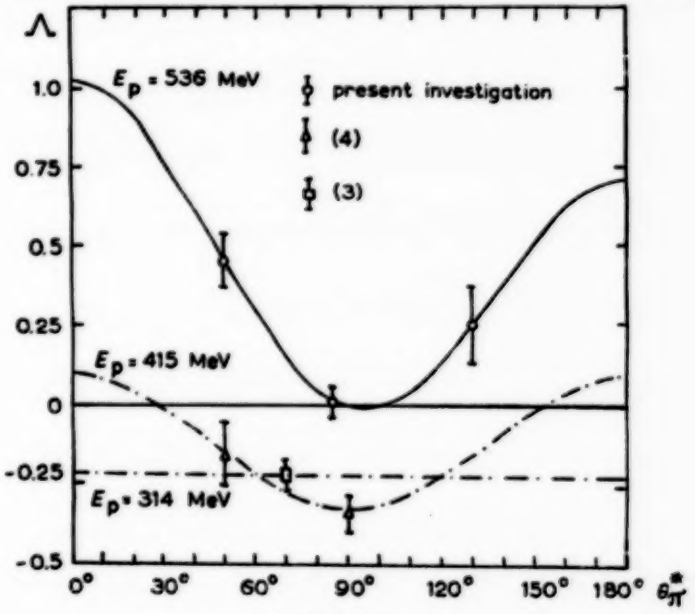


Fig. 4a.

perform extremely difficult measurements of the asymmetry at angles $\theta_\pi$ close to 0° and 180°, where the asymmetry effect disappears due to the dependence $\approx \sin\theta_\pi$. The coefficients are determined with the smallest error when only three terms of the series expansion are taken, hence the expansion can be cut off on the term $\approx \cos^2\theta_\pi$. The problem of the real values of the coefficient $\lambda_3$ must be considered in conjunction with the problem of determining the coefficient $\gamma_4$ in the angular distribution on the unpolarized beam, since both these coefficients are given by expressions which are

quadratic in the amplitudes of the d-transitions, and these, as is shown below, are sufficiently small.

The variation of energy dependence of $A(\theta_\pi)$ discovered in the present investigation can also be revealed in the region of smaller energies, if we utilize the results of experiments performed at 415 [4]) and 314 MeV [3]).

In our designations the results of the latter two investigations may be represented in the following table.

TABLE 3

| $E_p$ (MeV) | $\frac{\lambda_0}{\gamma_0+\frac{1}{3}\gamma_2}$ | $\frac{\lambda_2}{\gamma_0+\frac{1}{3}\gamma_2}$ | $\frac{\delta\lambda_0\,\delta\lambda_2}{(\gamma_0+\frac{1}{3}\gamma_2)^2}$ |
|---|---|---|---|
| 415 | $-0.34\pm0.05$ | $0.43\pm0.28$ | $-6.2\times10^{-3}$ |
| 314 | $-0.22\pm0.03$ | – | – |

As appears from fig. 4a, at a proton energy $E_p \approx 500$ MeV a change in the sign of the asymmetry is observed. The values of the coefficients

$$\frac{\lambda_0}{(\gamma_0+\frac{1}{3}\gamma_2)}, \quad \frac{\lambda_1}{(\gamma_0+\frac{1}{3}\gamma_2)}, \quad \frac{\lambda_2}{(\gamma_0+\frac{1}{3}\gamma_2)}$$

are given in fig. 5 as functions of the momentum of the $\pi$-meson in $m_\pi c$ units in the centre-of-mass system. At zero energy only the S-state of the meson is possible, and all the coefficients $\lambda_i$ should disappear. At small values of the momentum of the $\pi^+$-meson the coefficient $\lambda_0/(\gamma_0+\frac{1}{3}\gamma_2)$, being negative, increases with the momentum to an extremal value, then falls off to zero at $E_p \approx 530$ MeV, after which it again increases, but this time with positive values. At small $\eta$ the variation of $\lambda_0/(\gamma_0+\frac{1}{3}\gamma_2)$ is related to the increase in the effective amplitude of the P-wave relative to the s-amplitude. At large values of $\eta$(p—d)-interference is superposed upon the (s—p)-interference. The effects of these two interferences are probably comparable, starting from the energy $E_p \approx 400$ MeV at which the coefficient $\lambda_2/(\gamma_0+\frac{1}{3}\gamma_2)$, due to interference between the p- and d-states alone, becomes appreciable. The coefficient $\lambda_1/(\gamma_0+\frac{1}{3}\gamma_2)$ related to the effects of (s—d)- and (d—d)-interference proved to be very small, and it was with difficulty that we succeeded in detecting it in our experiments.

All these effects can be explained simultaneously, if we assume that at $E_p \approx 600$ MeV the amplitude of the transition $^1D_2 \to {}^3S_1\, p_2$ considerably exceeds the values of the s- and d-amplitudes. In this case only the (s—p)- and (p—d)-interferences will be observable, whereas the (s—d)- and (d—d)-interferences will correspond to second order effects.

The experiments performed on the polarized proton beam, while providing important additional information on reaction (1), does not permit of determining the values of all the elements of the $S$-matrix for this reaction. However, in view of the smallness of the s- and d-amplitudes, an estimate

may be made of several partial cross sections. It is necessary in this connection to take into consideration that the d-transitions in reaction (1) are connected with the change in the orbital moment of the system of two nucleons before and after the reaction, and also with the change in parity.

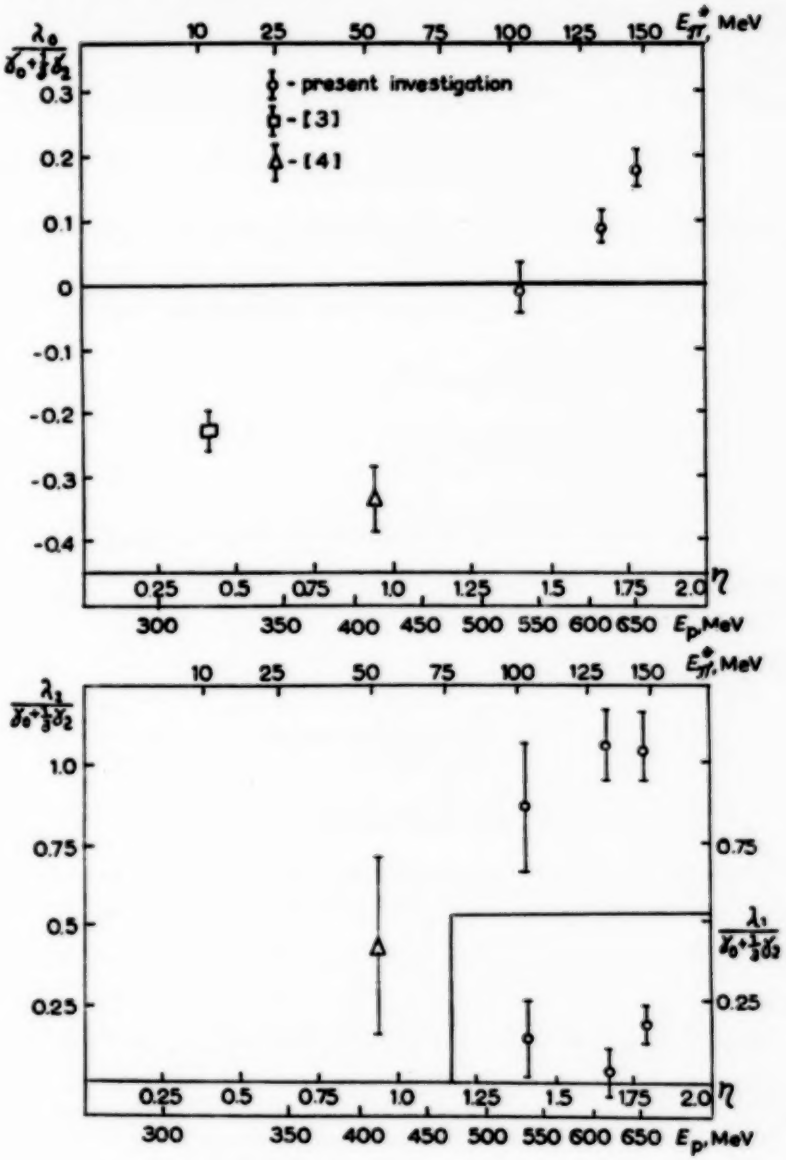


Fig. 5. Measured values of the coefficients

$$\frac{\lambda_0}{\gamma_0+\frac{1}{3}\gamma_2};\quad \frac{\lambda_1}{\gamma_0+\frac{1}{3}\gamma_2};\quad \frac{\lambda_2}{\gamma_0+\frac{1}{3}\gamma_2}$$

as functions of the momentum of the π-meson.

This circumstance leads to a very small probability of the d-transitions. The transition $^3F_2 \to (^3S_1 d)_2$ and $^3F_3 \to (^3S_1 d)_3$, connected with the change in

the orbital moment of the system of two nucleons, $\Delta l = 3$, should be especially difficult. In view of this we may put the amplitudes of these transitions equal to zero, and thus obtain for the limiting estimates of the partial cross sections the values:

$$\sigma(^1S_0 \to {}^3S_1 p_0) \geqq 10^{-3} \cdot \sigma_t(pp \to d\pi^+);$$
$$\sigma(s+d) \geqq 5.4 \times 10^{-2} \cdot \sigma_t(pp \to d\pi^+);$$
$$\sigma(^1D_2 \to {}^3S_1 p_2) \leqq 0.945 \cdot \sigma_t(pp \to d\pi^+).$$

## 4. Conclusions

1. Measurements of the asymmetry in the differential cross section of the reaction $p+p \to d+\pi^+$ on a polarized proton beam at energies 536, 616 and 654 MeV show that $\pi^+$-mesons in the d-state are emitted.

2. An analysis of the results of the present experiment, as well as those of other investigations [3,4]), shows that the effect of the d-state of the $\pi^+$-meson in the experiments on the polarized beam becomes observable starting from a proton energy of $E_p \approx 400$ MeV.

3. The results obtained are in agreement with the assumption that the amplitudes of the transitions accompanied by the emission of a $\pi^+$-meson in the s- and d-states are small compared with the amplitude of the transition $^1D_2 \to (^3S_1 p)_2$ throughout the entire energy range investigated.

4. Assuming that transitions from the initial $^3F_2$- and $^3F_3$-states can be neglected, we obtain the following limiting values:

$$\sigma(^1S_0 \to {}^3S_1 p_0) \geqq 10^{-3} \cdot \sigma_t(pp \to d\pi^+);$$
$$\sigma(s+d) \geqq 5.4 \times 10^{-2} \cdot \sigma_t(pp \to d\pi^+)$$
$$\sigma(^1D_2 \to {}^3S_1 p_2) \leqq 0.945 \cdot \sigma_t(pp \to d\pi^+).$$

5. The phenomenological theory of the production of $\pi$-mesons in (p—p)-collisions, put forward by S. Mandelstam [7]), is in agreement with the estimates obtained.

In conclusion the authors wish to thank M. G. Meshcheryakov, B. S. Neganov and L. I. Lapidus for discussion of the investigation, as well as N. P. Klepikov and S. N. Sokolov for help in the treatment of the experimental data.

## References

1) M. G. Meshcheryakov and B. S. Neganov, Doklady AN SSSR **100** (1955) 677
2) B. S. Neganov and L. B. Parfenov, JETP **34** (1958) 767
3) F. S. Crawford Jr. and M. L. Stevenson, Phys. Rev. **95** (1954) 1112
4) T. H. Fields, F. G. Fox, F. A. Kane, R. A. Stallwood and R. B. Sutton, Phys. Rev. **96** (1954) 812
5) A. I. Mukhin, E. B. Ozerov, B. M. Pontecorvo, E. L. Grigoriev and A. N. Mitin, Report at CERN Symposium (1956)

6) F. Mandl and T. Regge, Phys. Rev. **99** (1955) 1478
7) S. Mandelstam, Proc. Roy. Soc. A **244** (1958) 491
8) V. I. Danilov and O. V. Savchenko, Method of Focusing Charged Particles from Accelerators (Joint Institute of Nuclear Research, 1958)
9) A. Bogomolov, V. Vovchenko, L. Soroko and I. Shtirin, A Liquid Hydrogen and Liquid Deuterium Target (Joint Institute of Nuclear Research, 1958)
10) M. G. Meshcheryakov, S. B. Nurushev and G. D. Stoletov, JETP **33** (1957) 37
11) V. P. Zrelov (private communication, 1957)
12) Yu. K. Akimov, Pribory i Tekhnika Eksperimenta **1** (1957) 95
13) L. M. Soroko, Polarization Effects in the Reaction $p+p \to \pi^+ + d$ with a Consideration of the s-, p- and d-states of the $\pi$-meson (Joint Institute of Nuclear Research, 1958)
14) L. Marshall and J. Marschall, Phys. Rev. **98** (1955) 1398
15) H. Bradner and W. Isbell, Phys. Rev. **108** (1957) 463
16) V. P. Dželepow, V. S. Kiselev, K. O. Oganesyan and V. B. Flyagin, JETP (1958) (in print)
17) N. P. Klepikov and S. N. Sokolov, Treatment of Experimental Data by the Method of Maximum Verisimilitude (Joint Institute of Nuclear Research, 1958)

2.1 *Nuclear Physics* 8 (1958) 650—660; © *North-Holland Publishing Co., Amsterdam*
Not to be reproduced by photoprint or microfilm without written permission from the publisher

# ($\gamma$, p) REACTIONS IN $Na^{23}$, $K^{39}$, $I^{127}$ AND $Cs^{133}$

L. KESZTHELYI and J. ERÖ
*Central Research Institute for Physics,*
*Department of Atomic Physics, Budapest* †

Received 27 July 1958

**Abstract:** Proton spectra of $K^{39}(\gamma, p)A^{38}$, $Na^{23}(\gamma, p)Ne^{22}$, $I^{127}(\gamma, p)Te^{126}$ and $Cs^{133}(\gamma, p)Xe^{132}$ reactions have been investigated by irradiating KI(Tl), NaI(Tl) and CsI(Tl) crystals by Li(p, $\gamma$) gamma rays, and the corresponding cross sections have been determined. Electron background was reduced by placing a guard crystal in front of the target crystal. Approximate cross sections are $15\pm5.8$ mb for $K^{39}(\gamma, p)$; $3.6\pm1.5$ mb for $Na^{23}(\gamma, p)$ and $1.5\pm0.6$ mb for $I^{127}(\gamma, p)$ and $Cs^{133}(\gamma, p)$ reactions at 17.6 MeV $\gamma$-energy. The proton spectrum of $K^{39}(\gamma, p)$ reaction shows peaks at 6.1, 9.2 and 11 MeV corresponding to the 5, 2.15 and 0 MeV levels of $A^{38}$. The $I^{127}(\gamma, p)$ and $Cs^{133}(\gamma, p)$ spectra are inconsistent with the statistical theory owing to the effect of direct interaction.

## 1. Introduction

The study of ($\gamma$, p) reactions is a very useful method to obtain information as to the real nature of the nuclear photoeffect. As is well known, the proton emission shows very sensitively whether the interaction between the $\gamma$-quantum and the nucleus leads to the ordinary compound nucleus or some kind of direct interaction takes place [1]). In this respect the investigation of the energy spectra of emitted protons may give some useful data. Most of the measurements in this field were performed up till now by bremsstrahlung $\gamma$-rays and consequently reaction products show a large spread in energy. The use of bremsstrahlung is prompted by the fact that monochromatic $\gamma$-rays can only be obtained by nuclear reactions providing low intensity sources. In this case, however, the use of an energy sensitive $4\pi$-detector has proved fairly successful. Measurements of this kind were carried out previously [2]) by means of proportional counters filled with the gas to be investigated: thus, the target itself serves as a detector. In our measurements the target was a scintillating crystal mounted on a photomultiplier and in this way we also obtained an energy-sensitive target-detector system. By this arrangement it is possible to investigate nuclei which are components of scintillating crystals i.e. Na, K, Cs, I, Li etc. In a recent work the same scintillation method was used by Ophel *et al.*[3]) for measuring the energy spectrum of protons in the $Na^{23}(\gamma, p)Ne^{22}$ reaction.

† Lecture delivered at the Nuclear Physics Symposium of the Eötvös Lóránd Physical Society at Mátraháza (Hungary) on the 3rd December, 1957.

## 2. Experimental Method

KI(Tl), NaI(Tl) and CsI(Tl) crystals were irradiated by Li(p, $\gamma$) gamma rays from the 800 keV Cockroft-Walton generator of the KFKI. High energy $\gamma$-rays interact with the material of the crystal and its surroundings by (1) electron photoeffect, (2) Compton effect, (3) pair production, (4) nuclear photoeffect. Effects (1) to (3) release high energy electrons travelling mainly in the direction of the incident $\gamma$-rays owing to the high $\gamma$-energy (the mean solid angle of electrons $\approx m_0c^2/h\nu$). The cross section for producing these electrons is about 10 barns.

By effect (4) neutral as well as charged particles are released. If the crystal is not too large, most of the neutral particles (neutrons and inelastically scattered $\gamma$-rays) leave the crystal without interaction. The charged particles are mainly protons, the emission of deuterons and $\alpha$-particles being highly improbable. The cross section for ($\gamma$, p) reactions is of the order of millibarns, i.e. $10^{-3}$—$10^{-4}$ times smaller than that for electron production. The high electron background can be eliminated by using crystals of a thickness equal to the range of protons. For 11 MeV protons, that is for the maximum energy at a binding energy of 6.5 MeV which may be considered as typical, the proton range in the crystal is about 300 mg/cm$^2$. Thus, if we use a thin crystal of that thickness, the protons transfer their full energy, whereas the average energy loss of high energy electrons is only 400 keV for the same thickness.

Irradiating the crystal by a $\gamma$-ray perpendicular to the crystal face, the electrons originated in the surroundings and in the crystal will traverse it perpendicularly undergoing the small loss of energy mentioned above. A small fraction of these electrons, however, will be scattered at a large angle and as they move parallel to the face, the energy transfer may amount to several MeV. To eliminate the effect of electrons produced in the surrounding material, a guard crystal was placed in front of the measuring one viewed by another multiplier and the pulses of this crystal were connected in anti-coincidence to those of the target crystal.

## 3. Experimental Arrangement

The target crystal was placed at a distance of about 4 cm from the target spot of the generator (fig. 1). It was covered by an Al foil of 4 mg/cm$^2$ thickness, to shut out light, and when using NaI to keep off water vapour. The anticoincidence crystal was a thin NaI crystal.

In fig. 2 the block diagram of the arrangement is shown. Pulses coming from the two multipliers are transmitted to the anticoincidence set driving the single sweep. Pulses of the target crystal pass through a stretcher to the vertical deflector of an oscilloscope. Each pulse was photographed by means of a camera and the photographs were projected for counting.

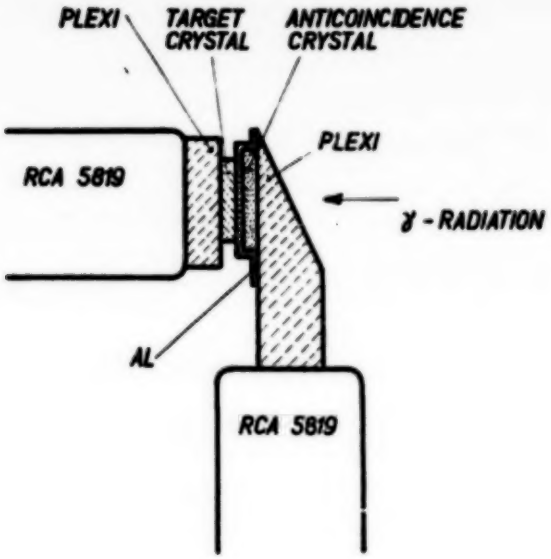


Fig. 1. Experimental arrangement of target and anticoincidence crystals.

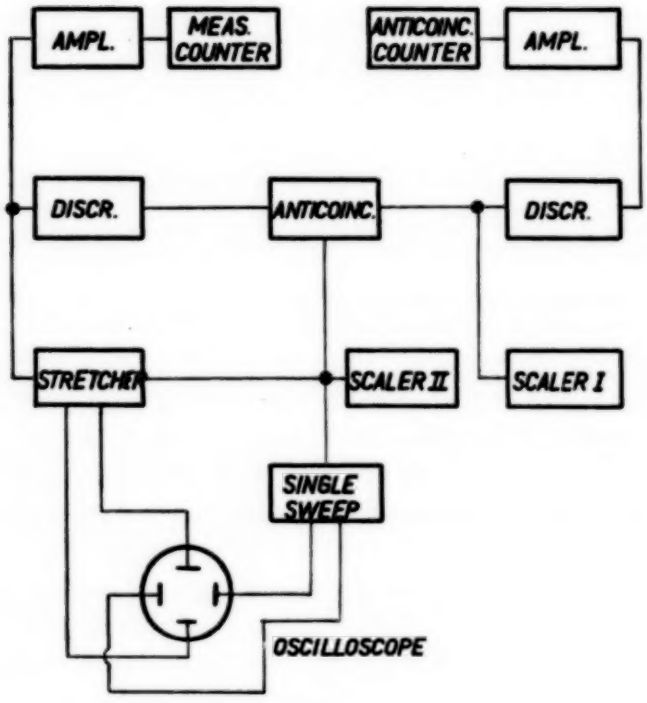


Fig. 2. Block diagram of electronic instruments.

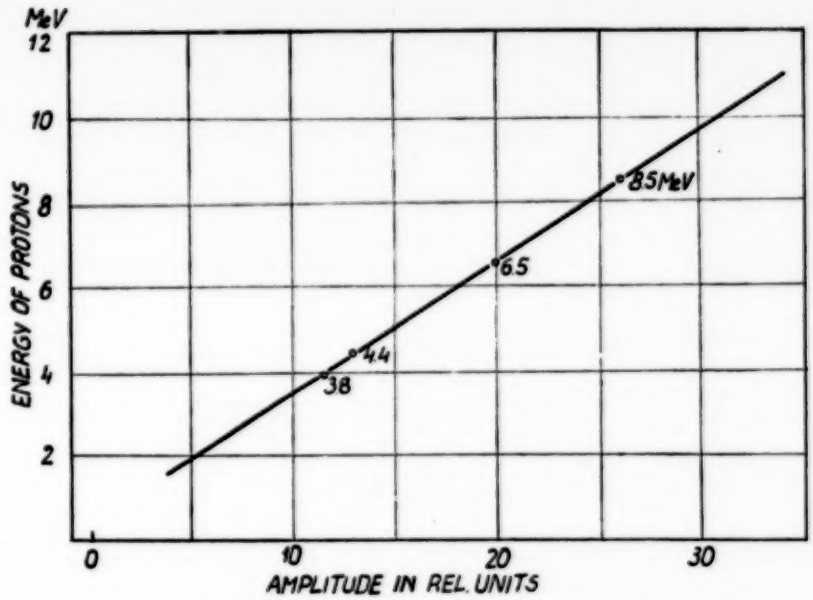


Fig. 3. Calibration of CsI target-crystal by means of $B^{10}$(d, p) $B^{11}$ protons.

Counters were calibrated by the $B^{10}$(d, p)$B^{11}$ reaction. Protons arriving from a 1 mg/cm² thick boron target at 90° to the deuteron beam traverse a 5 mg/cm² Al foil to reach the target crystal. Calibration curve of CsI crystal is shown in fig. 3. Similar linear relationships were obtained with KI and NaI crystals, respectively.

## 4. Measurements

### 4.1. ELECTRON BACKGROUND

In a previous paper [4]) it has been mentioned that although the major fraction of electrons producing pulses in the target crystal were passing through the anticoincidence crystal, a certain amount of them was produced in the target crystal itself. To effect a correction for these electrons, we assumed the electron spectrum to fall exponentially. This assumption was found to be strongly supported by the fact that all spectra did fall exponentially at energies where electron pulses predominated. This exponential character until the appearance of protons (scale 400 in the figure) is clearly shown in fig. 4. The spectrum taken with 200 mg/cm² plastic phosphor (fig. 5.) shows no deviation from the exponential law even at high energies for the maximum energy of photoprotons is only 1.6 MeV with $C^{12}$.

### 4.2. PROTON SPECTRA

In figs. 6, 7 and 8 measured spectra for NaI, KI and CsI crystals are shown. At the low energy end we have to make corrections for electrons and this was

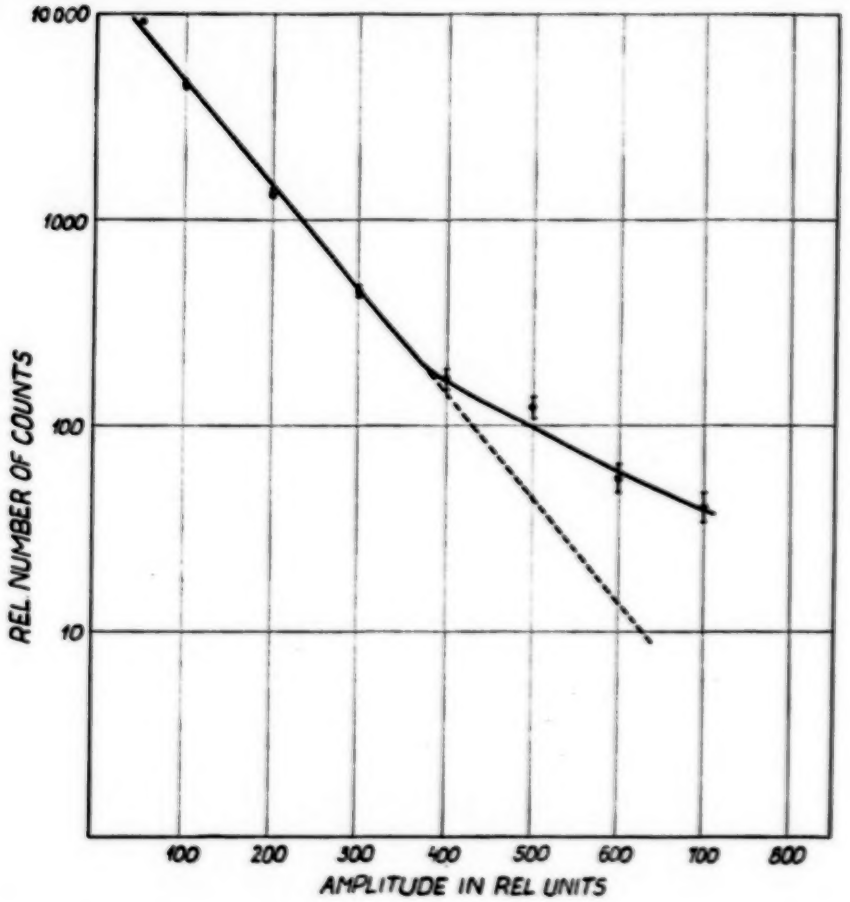


Fig. 4. Low energy end of the pulse-spectrum in KI crystal showing an exponential fall until the appearance of proton pulses.

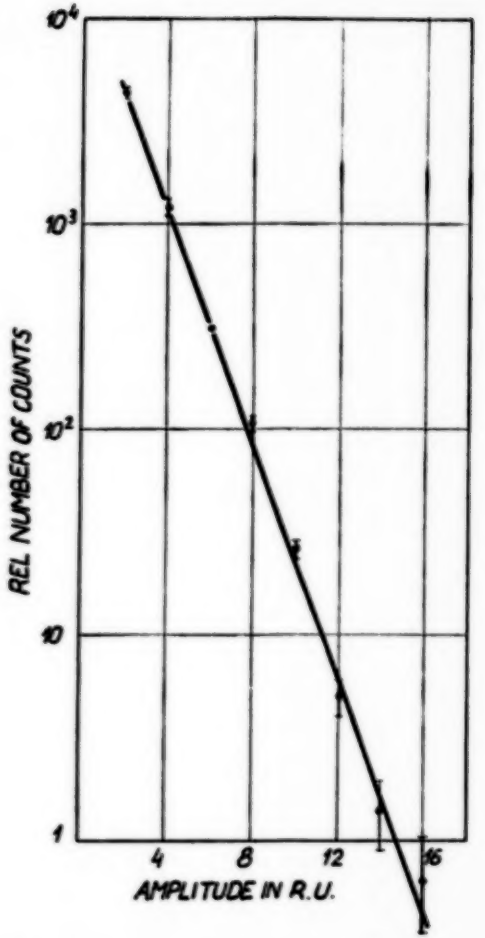


Fig. 5. Pulse spectrum in plastic phosphor. There is no deviation from the exponential law within limits of error.

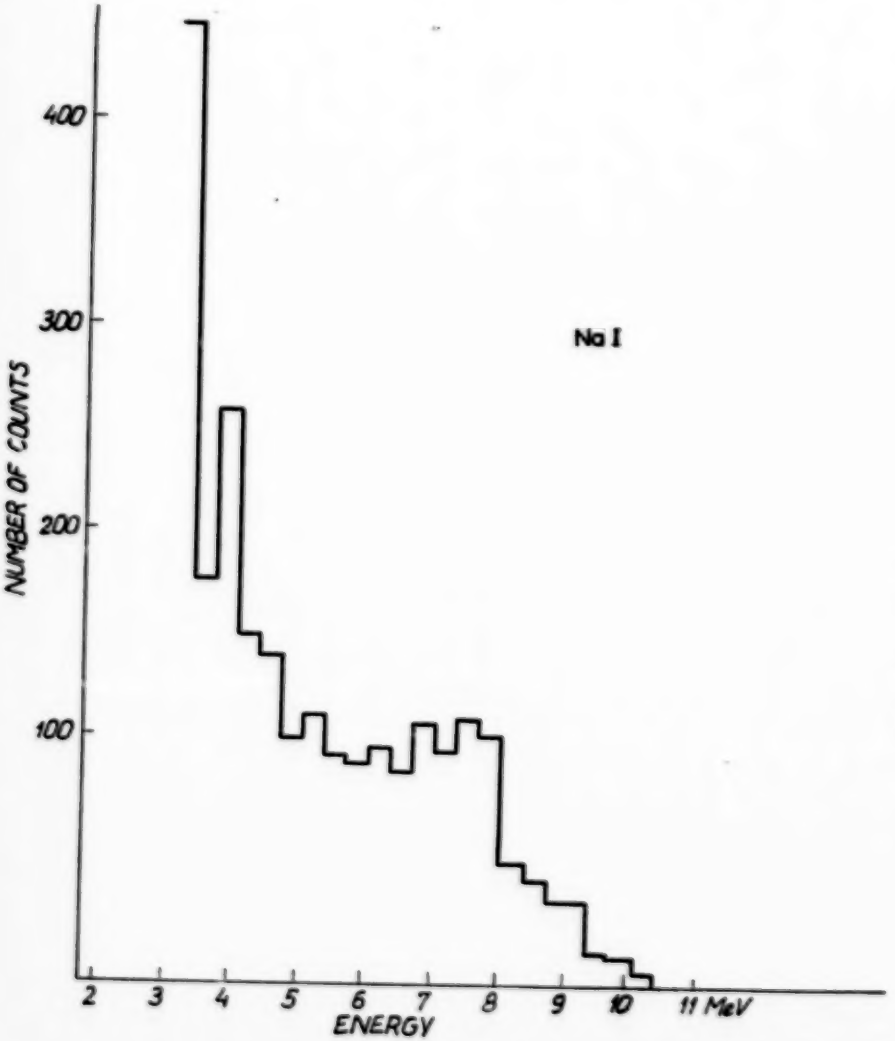


Fig. 6. Pulse spectrum of NaI crystal.

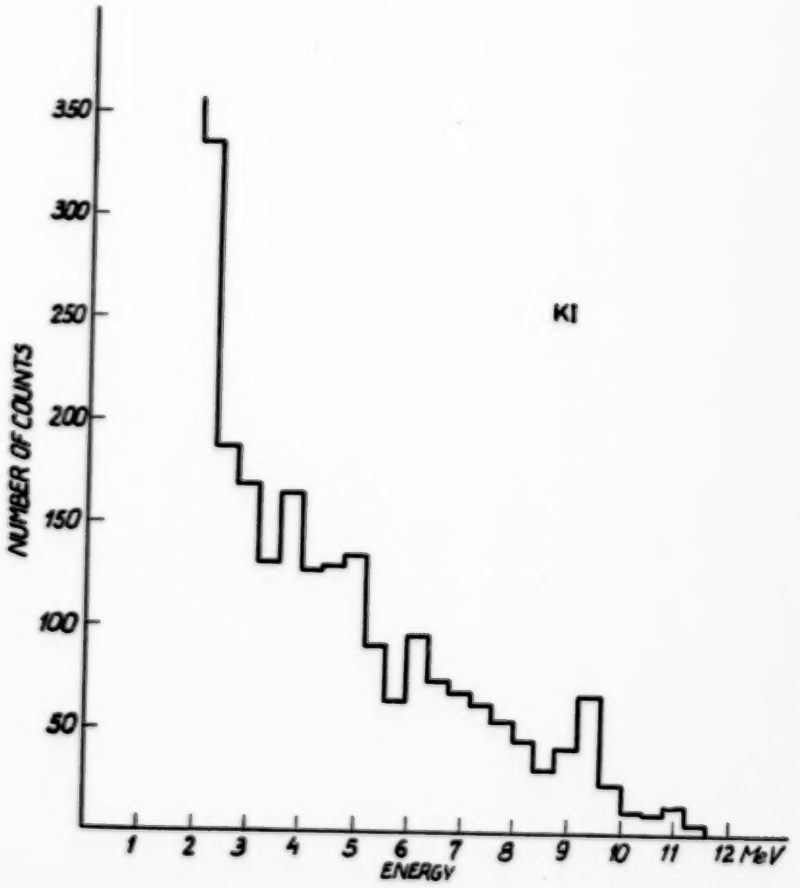


Fig. 7. Pulse spectrum of KI crystal.

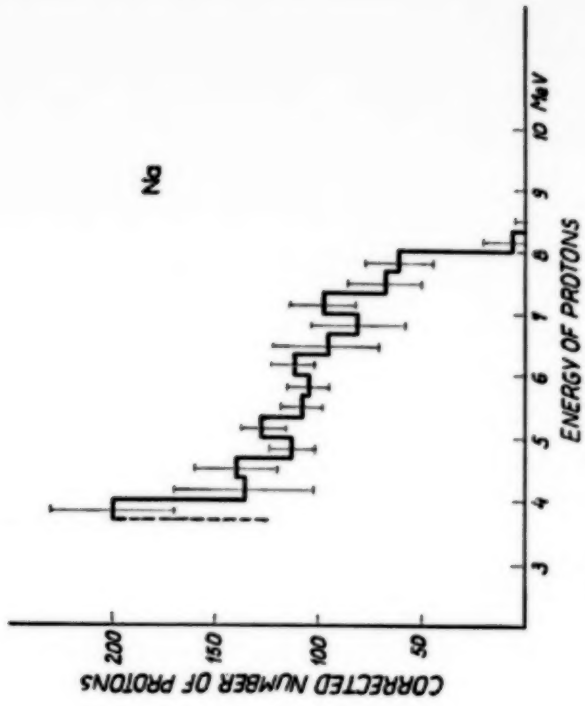


Fig. 9. Energy spectrum of protons from Na nuclei.

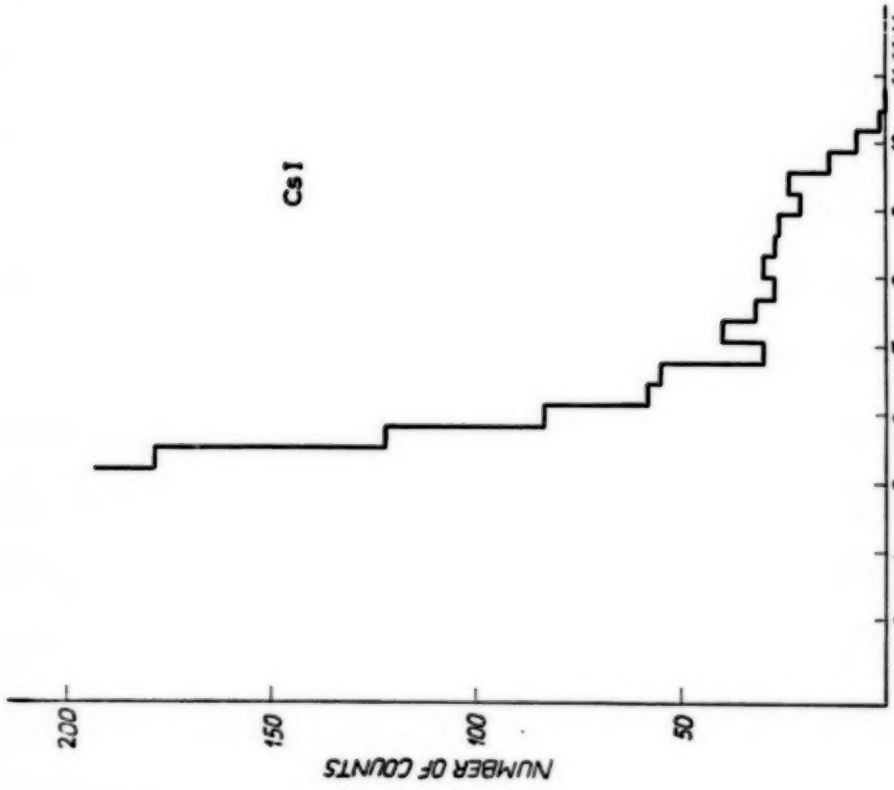


Fig. 8. Pulse spectrum of CsI crystal.

done by assuming the exponential fall mentioned above. The proton spectrum thus obtained is a complex one, each crystal consisting of two kinds of nuclei. First of all, we have assumed the cross sections and proton spectra of $Cs^{133}$ and $I^{127}$ to be almost the same, both being heavy nuclei with nearly the

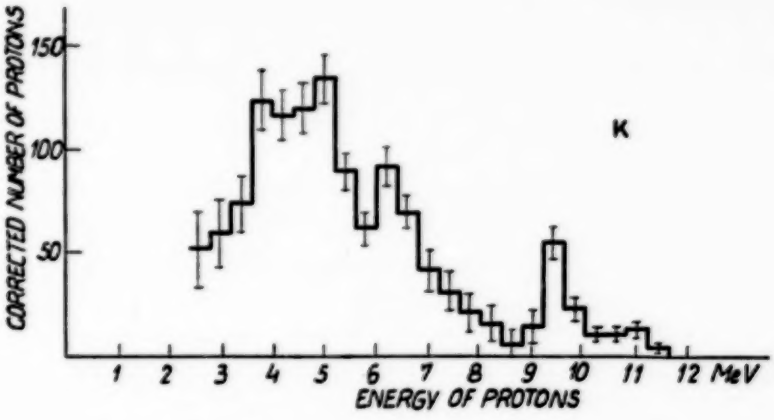


Fig. 10. Energy spectrum of protons from K nuclei.

same mass numbers and the same threshold energies. This specrum is to be seen in fig. 11. Upon suitable normalization it has been subtracted from the KI and NaI spectra to obtain the proton spectrum of $Na^{23}$ and $K^{39}$ shown in figs. 9 and 10, respectively.

## 5. Discussion

### 5.1. CROSS SECTIONS

Integrating the spectra, we obtained information about the cross sections for various ($\gamma$, p) reactions. The cross section is given in ref. [5]) as

$$\sigma_p = \sigma_e \frac{N_p}{N_e}$$

where $N_p$ and $N_e$ are the total number of photoprotons and electrons, respectively, produced in the target crystal by a given irradiation, and $\sigma_e$ is the cross section for producing electrons.

To determine $N_e$ we have also counted the pulses of the anticoincidence crystal, as their number is proportional to $N_e$. The proportionality factor was determined by taking an integral spectrum of the target crystal and extrapolating it to zero pulse height [5]). The accuracy of this procedure was about 30 %.

The value of $\sigma_e$ has been calculated from theoretical data [5]). The number of photoprotons $N_p$ cannot be considered simply as the integrated value of

proton spectra, for a small amount of pulses is produced by (n, p) and (n, $\alpha$) reactions. Neutrons are produced partly by the Li(d, n) reactions initiated by deuterons of our unanalysed proton beam, partly by ($\alpha$, n) reactions due to the $\alpha$'s of the $Li^7$(p, $\alpha$) $He^4$ reaction. The latter effect can be neglected as the maximum energy of these neutrons is only 2.3 MeV. The number of $\alpha$'s and protons due to Li(d, n) neutrons $N_{\alpha p}$, determined from the yield of the reaction [6]) and the (n, p) and (n, $\alpha$) cross sections [7,8]), was found to be less than 10 % of the photoprotons except for $Na^{23}$ where 30 % was obtained. If $N'_p$ is the number of pulses in the spectra of figs. 8, 9 and 10, then the number of photoprotons is $N_p = N'_p - N_{\alpha p}$.

The cross section $\sigma(\gamma, p)$ determined from (1) is an averaged value for 14.3 and 17.6 MeV $\gamma$-rays of the Li(p, $\gamma$) radiation having an intensity ratio 1 : 2 [9]). From the shape of the giant resonance of heavy and light elements it is probable [10]) that $\sigma(14.3) \approx \sigma(17.6)$ for Cs and I while $\sigma(14.3) \ll \sigma(17.6)$ for Na and K. Thus $\sigma(17.6)$ is equal to the average $\sigma(\gamma, p)$ determined above for Cs and I and is 1.5 times higher for Na and K. These data are listed in table 1.

TABLE 1

| Nucleus | $N_e$ | $\sigma_e$ (b) | $N'_p$ | $N_{\alpha p}$ | $\sigma(\gamma, p)$ (mb) | $\sigma(17.6)$ (mb) |
|---|---|---|---|---|---|---|
| $_{11}Na^{23}$ | $4.2 \times 10^6$ | 10.7 | $1176 \pm 96$ | 240 | $2.4 \pm 1.1$ | $3.6 \pm 1.5$ |
| $_{19}K^{39}$ | $3.8 \times 10^6$ | 11.8 | $3578 \pm 98$ | 230 | $10 \pm 3.5$ | $15 \pm 5.8$ |
| $_{53}I^{127}$ | $1.7 \times 10^6$ | 20.8 | $130 \pm 10$ | 10 | $1.5 \pm 0.6$ | $1.5 \pm 0.6$ |
| $_{55}Cs^{133}$ | $1.7 \times 10^6$ | 20.8 | $130 \pm 10$ | 10 | $1.5 \pm 0.6$ | $1.5 \pm 0.6$ |

5.2. ENERGY SPECTRA

The high (n, p) and (n, $\alpha$) background as well as the poor resolution power of our NaI crystal made it impossible to obtain an evaluable proton spectrum for $Na^{23}$.

In the spectrum of $K^{39}(\gamma, p)Al^{28}$ reaction a well defined level structure was found. This can be seen in fig. 10. Three groups can be distinguished, at $6.1 \pm 0.3$, $9.2 \pm 0.3$ and $11 \pm 0.3$ MeV. The 11 MeV group is obviously due to transitions to the ground state of $A^{38}$, the binding energy of protons in $K^{39}$ being 6.5 MeV. Two excited levels of $A^{38}$ are well known [11]), one at 2.15 MeV, the other at 3.75 MeV. The 9.2 MeV group corresponds to a transition to the 2.15 level. No transition, however, has been found to the 3.75 MeV level. Recently Towle *et al.*[12]) by investigating the $Cl^{37}$(p, $\gamma$)$A^{38}$ reaction, have concluded to the existence of the 5 MeV level of $A^{38}$. This result is supported by our measurements concerning the 6.1 MeV group. The 4.8 MeV group, not well resolved in our spectrum, corresponds probably to a transition to the 6.7 MeV level of $A^{38}$ also mentioned by Towle *et al.* The relative intensities of

our 6.1, 9.2 and 11 MeV groups are 10 : 5 : 1. These intensity data are not corrected for protons escaping from the crystal as the angular distribution of protons is unknown and the correction is very sensitive to it.

We have assumed the energy spectra of $I^{127}(\gamma, p)\,Te^{126}$ and $Cs^{133}(\gamma, p)Xe^{132}$ to be identical. According to the statistical model [13]) the spectrum is given as

$$P(\varepsilon) = \varepsilon \cdot \sigma_{cp}(\varepsilon) \cdot \omega(\varepsilon_{max} - \varepsilon). \tag{2}$$

For $\sigma_{cp}$ we used the value given in ref.[13]). The maximum energy of protons for above reactions is $\varepsilon_{max} = 11$ MeV and the level density was obtained according to ref.[14]) as

$$\omega(\varepsilon) \propto \exp\,[b^2(\varepsilon_{max} - \varepsilon)]^{\frac{1}{2}} \tag{3}$$

with $b^2 = 55$. This spectrum is plotted in fig. 11, having been normalized to give an integrated cross section of 0.15 mb obtained from the ratio $\sigma(\gamma,p)/\sigma(\gamma, n) = 1.2 \times 10^{-3}$ calculated on the basis of the statistical theory. $\sigma(\gamma, n)$ is known to be 125 mb [5]).

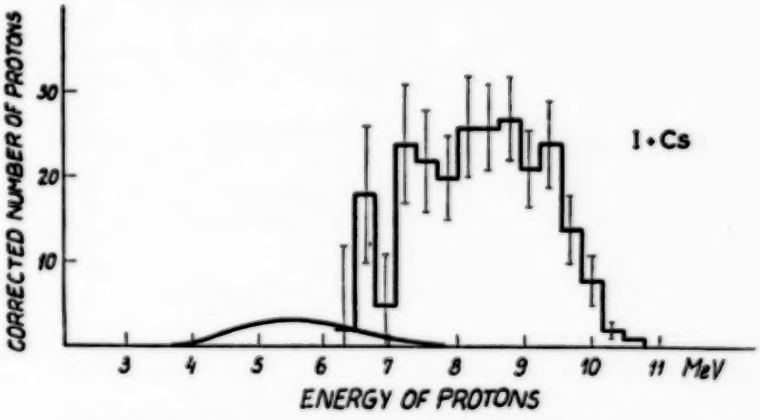


Fig. 11. Energy spectrum of protons from Cs+I nuclei.

The experimental spectrum is far from agreeing with that based upon the statistical theory. The number of protons as well as their energy are much higher than expected, thus indicating a pronounced effect of direct interaction. According to Wilkinson's theory of direct resonance mechanism [1]) for elements with $Z = 53-55$, the ratio of proton emission to total absorption is 0.8 % for bremsstrahlung of 23 MeV maximum energy. Assuming the same energy dependence for $\gamma$-absorption as for $(\gamma, p)$ reaction, the same ratio is obtained for monoenergetic radiation. Knowing that the cross-section of $\gamma$-ray absorption $\sigma_{abs}$ is equal to 150mb [5]), by our measurement we obtain $\sigma(\gamma, p)/\sigma_{abs} = 1 \pm 0.4$ % which is in agreement with Wilkinson's data.

## References

1) D. H. Wilkinson, Physica **22** (1956) 1039
2) D. H. Wilkinson and J. H. Carver, Phys. Rev. **83** (1951) 466 L
3) T. R. Ophel and I. F. Wright, Proc. Phys. Soc. A **71** (1958) 389
4) J. Erő and L. Keszthelyi, KFKI Reports **5** (1957) 428 (in Hungarian)
5) J. Erő and L. Keszthelyi, Nuclear Physics **2** (1956) 371
6) Landolt-Börnstein, Zahlenwerte und Funktionen 5. Teil (Springer, Berlin, Gottingen, Heidelberg, 1952)
7) E. B. Paul and R. L. Clarke, Can. J. Phys. **31** (1953) 267
8) H. Wäffler, Helv. Phys. Acta **23** (1950) 239
9) B. C. McDaniel and R. L. Walker, Phys. Rev. **74** (1948) 315
10) R. Montalbetti, L. Katz and J. Goldemberg, Phys. Rev. **91** (1953) 659; R. Nathans and J. Halpern, Phys. Rev. **93** (1954) 437
11) P. M. Endt and C. M. Braams, Revs. Mod. Phys. **29** (1957) 683
12) J. H. Towle, R. Berenbaum and J. A. Matthews, Proc. Phys. Soc. A **70** (1957) 84
13) J. M. Blatt and V. F. Weisskopf, Theoretical Nuclear Physics (Wiley, New-York, 1952)
14) P. C. Gugelot, Phys. Rev. **81** (1951) 51

8.B *Nuclear Physics* **8** (1958) 661—674; © *North-Holland Publishing Co., Amsterdam*
Not to be reproduced by photoprint or microfilm without written permission from the publisher

# A UNIFIED THEORY OF THE FERMI INTERACTION

TOSHIYUKI TOYODA
CERN, *Geneva* †

Received 30 June 1958

**Abstract:** A method developed by Infeld and van der Waerden for generalizing the free Dirac field equation into the scheme of general relativity is used to unify the interaction types by adding some new hypotheses but still remaining in the usual Minkowski space. An explanation for a modified Pauli-Gürsey transformation is given in relation with the coupling types. Neither conventional isospinspace nor strangeness quantum number are used, but only the usual three dimensional spin space is necessary. The results seem to be similar to those of the Feynman—Gell-Mann theory, except for a few points. A comparison with their theory is made.

## 1. Introduction

Since Lee and Yang [1]) discovered that there exist parity non-conserving interactions in weak interactions many hypotheses [2–8]) have been proposed for a more or less fundamental principle by which parity violation and lepton-number conservation may be understood in some organic way. On the other hand, since Gell-Mann [9]) and Nishijima [10]) successfully introduced the new quantum number to describe the selection rule of strange particles in a phenomenological way, many attempts [11–21]) have been made to interpret the strangeness quantum number. Among these the concept of two kinds of iso spinors †† introduced by d'Espagnat and Prentki [11]) seems to be hopeful, because the violation of isoparity in the weak decay of strange particles suggests that a close relation between the two kinds of phenomena may be obtained from the same point of view.

Already in 1933 Infeld and van der Waerden [22]) ††† investigated the mathematical structure of the relativistic wave equation of electrons in great detail and gave a general relativistic extension of the Dirac equation, using the concept of gauge invariance invented by Weyl [23]). Assuming a general spin space at each world point, Infeld and van der Waerden constructed the theory to be covariant with respect to the coordinate transformation and the parallel displacement. Although it seems very interesting

† On leave of absence from Rikkyo University, Tokyo, Japan, at CERN, Geneva, on a Ford Foundation Fellowship.

†† Although the concept of isoparity had been previously used by Pais [24]), it was not successful due to his unsuitable classification of elementary particles.

††† In Bergmann's paper of ref.[22]) the role of parity and time reversal is examined.

that their results involve a non-linear term in the Klein-Gordon-like equation in the present paper we shall be particularly interested in the neutral vector field which is automatically introduced by their fundamental postulates, and which is simply identified by them as the "electromagnetic field in the sense of Weyl's principle of gauge invariance".

We would like to point out that any spinor field must be coupled with this vector field in order to maintain the covariance of the formalism, but that the relevant coupling constant may be different for different fields. Therefore, if there exist more than two fields, there will be some change of transformation property of each field, as a result of the coupling of the fundamental vector field with the other fields. A general expression for the Fermi interaction which is invariant with respect to the generalized transformation will be derived below and its physical interpretation will be given.

## 2. Mathematical Formulation

Following Infeld and van der Waerden's treatment [22]), let us assume a spin space † at each world point $x^k$ and describe the spin quantities by a set of two complex quantities $\psi^\lambda$, where latin indices $k$'s run from 1 to 4, and greek indices $\lambda$'s run from 1 to 2. For the sake of simplicity we shall confine ourselves to the usual flat Minkowski space; the metric tensor $g_{ik}$ is then

$$g_{11} = g_{22} = g_{33} = -g_{44} = -1. \tag{1}$$

Since we want to extend the usual transformations then as is shown below, the metric tensor of the spin space can no longer be taken as constant with respect to variations of $x^k$. This may be made plausible by considering the connection of the metric tensor of the spin space with the fundamental vector field mentioned above.

We shall define a generalized transformation of $\psi^\lambda$ by a two-by-two matrix whose determinant is not unity but $e^{i\vartheta}$:

$$\psi^{\lambda'} = \Lambda_\rho{}^\lambda \psi^\rho, \qquad \psi^{\dot\lambda'} = \Lambda_{\dot\rho}{}^{\dot\lambda} \psi^{\dot\rho}, \qquad \Delta = \det |\Lambda_\rho{}^\lambda| = e^{i\vartheta}, \tag{2}$$

where $\vartheta$ is an arbitrary real function of $x^k$ and the usual notational convention is used. As is well known, the metric tensor can be defined in the following way:

$$\begin{aligned} &\gamma_{\lambda\mu} = -\gamma_{\mu\lambda}, \\ &\psi_\lambda = \psi^\mu \gamma_{\mu\lambda}, \quad \psi^\lambda = \gamma^{\lambda\mu} \psi_\mu, \\ &\psi_{\dot\lambda} = \psi^{\dot\mu} \gamma_{\dot\mu\dot\lambda}, \quad \psi^{\dot\lambda} = \gamma^{\dot\lambda\dot\mu} \psi_{\dot\mu}. \end{aligned} \tag{3}$$

The transformation formula for $\gamma_{\lambda\mu}$ is easily obtained as

† This spin space is entirely different from Pais' [24]) "$\omega$-space" which is independent of the Minkowski space. On the contrary, our spin space is intimately related with the Minkowski space through its transformation property, as will be shown below.

$$\gamma'_{12} = \frac{1}{\Delta}\gamma_{12} = e^{-i\vartheta}\gamma_{12},$$
$$\gamma^{12'} = -\Delta\gamma^{12} = -e^{i\vartheta}\gamma^{12}. \tag{4}$$

Concerning the connection operators between a general world vector $a^k$ and a spin tensor $\psi_{\dot{\lambda}\mu}$, a mixing tensor $\sigma^{k\dot{\lambda}\mu}$ can be derived, satisfying the following commutation relations:

$$a^k = \sigma^{k\dot{\lambda}\mu}\psi_{\dot{\lambda}\mu},$$
$$\sigma^{l\dot{\lambda}\mu}\sigma^k_{\dot{\lambda}\sigma} + \sigma^{k\dot{\lambda}\mu}\sigma^l_{\dot{\lambda}\sigma} = g^{kl}\delta_\sigma{}^\mu, \tag{5}$$
$$\sigma^{l\dot{\rho}\mu}\sigma^k_{\dot{\lambda}\mu} + \sigma^{k\dot{\rho}\mu}\sigma^l_{\dot{\lambda}\mu} = g^{kl}\delta_{\dot{\lambda}}{}^{\dot{\rho}},$$

where $\delta_\sigma{}^\mu$ and $\delta_{\dot{\lambda}}{}^{\dot{\rho}}$ are Kronecker's deltas. Normalizing the volume tensor in the spin space, i.e. putting $\gamma_{12}\gamma_{\dot{1}\dot{2}} = 1$, we may write down explicitly the metric tensor $\gamma_{\lambda\mu}$ as

$$\gamma_{\lambda\mu} = \begin{pmatrix} 0 & e^{\frac{1}{2}i\varphi} \\ -e^{\frac{1}{2}i\varphi} & 0 \end{pmatrix}, \tag{6}$$

where $\varphi$ is an arbitrary function of the world point $x^k$.

As was clearly demonstrated above, the generalization (2) is completely compatible with Lorentz covariance. However, since we like to make the smallest possible modification of the usual theory, we shall restrict our generalization (2) to the rather limited transformation

$$\Lambda_\rho{}^\lambda = {}_0\Lambda_\rho{}^\lambda e^{\frac{1}{2}i\vartheta},$$
$$\det|{}_0\Lambda_\rho{}^\lambda| = 1, \tag{2'}$$

where $\vartheta$ is still an arbitrary function of $x^k$, but ${}_0\Lambda_\rho{}^\lambda$ are now parameters independent of $x^k$. Then our generalized transformation is reduced to the product of a well known gauge transformation [23]) and the proper Lorentz transformation. Consequently, in so far as we are concerned with a single free field, we have no room to add something new to the usual theory. However, as we shall discuss later, the metric tensor in spin space, $\gamma_{\lambda\mu}$, may be taken to be connected with a neutral vector field $\Phi^k$ which most generally is a mixture of vector and axial vector fields and subject to the gauge transformation. Therefore it seems to us rather plausible to assume that each spinor field couples with this new field with a different magnitude of the coupling constant. The difference of the coupling magnitudes will be able to explain many conservation laws in the case of an interacting system of more than two fields. We shall denote the vector field by $B$ for the sake of convenience. This new field may have some analogy with the gravitational field in the general relativity, in the sense that both of them are intimately related with the corresponding metric tensor in each space.

Let us consider a system of two fields, $a$ and $b$ which are described by the

four-component spinors

$$\Psi_a = \begin{pmatrix} \psi^1(a) \\ \psi^2(a) \\ \chi_{\dot{1}}(a) \\ \chi_{\dot{2}}(a) \end{pmatrix}, \qquad \Psi_b = \begin{pmatrix} \psi^1(b) \\ \psi^2(b) \\ \chi_{\dot{1}}(b) \\ \chi_{\dot{2}}(b) \end{pmatrix}. \tag{7}$$

In general, these two fields are coupled to each other through the $B$ field. Therefore, the metric of the spin space for the case where there exist two fields $a$ and $b$ which are coupled to each other can be different from that for an isolated field. Before discussing the general case, we shall consider a very special case, viz., in the limit where the field $b$ is coupled extremely weakly with the $B$ field we may make the following hypothesis:

(I) The metric of the spin space is determined only by the existence of the field $a$, so that the transformation of $\Psi_a$ is just the same as for the isolated case, i.e.

$$\begin{aligned} \psi^\lambda(a) &\to e^{\frac{1}{2}i\theta}\psi^\lambda(a), \\ \gamma_{12}(a) &\to e^{-i\theta}\gamma_{12}(a). \end{aligned} \tag{8}$$

On the other hand the metric $\gamma_{12}$ appropriate to the transformation of $\Psi_b$ is only influenced by the coupling of $B$ with the field $a$ because of our assumption of very weak coupling of $b$ with $B$, i.e.

$$\begin{aligned} \psi^\lambda(b) &\to e^{\frac{1}{2}i\theta}\psi^\lambda(b), \\ \gamma_{12}(b) &\to \gamma_{12}(b). \end{aligned} \tag{9}$$

Thus any physical quantity of the system should be invariant under the transformation (8) and (9). The neutrino field is the best example of the field $b$.

If we rewrite the transformations (8) and (9) using the familiar notation for the $\gamma$-matrices †, we obtain Touschek's transformation [5])

† Although our final results do not depend on the representation of the $\gamma$-matrices, it is useful to note that van der Waerden's representation (7) is associated with the following representation for the $\gamma$-matrices:

$$\gamma^1 = \begin{pmatrix} 0 & -\sigma^1 \\ \sigma^1 & 0 \end{pmatrix}, \quad \gamma^2 = \begin{pmatrix} 0 & -\sigma^2 \\ \sigma^2 & 0 \end{pmatrix}, \quad \gamma^3 = \begin{pmatrix} 0 & -\sigma^3 \\ \sigma^3 & 0 \end{pmatrix}, \quad \gamma^4 = \begin{pmatrix} 0 & I \\ I & 0 \end{pmatrix}$$

$$\sigma^1 = \begin{pmatrix} 0 & 1 \\ 1 & 0 \end{pmatrix}, \qquad \sigma^2 = \begin{pmatrix} 0 & -i \\ i & 0 \end{pmatrix}, \qquad \sigma^3 = \begin{pmatrix} 1 & 0 \\ 0 & -1 \end{pmatrix}, \qquad I = \begin{pmatrix} 1 & 0 \\ 0 & 1 \end{pmatrix}.$$

With the usual definition of $\gamma_5$ this is given in this representation by

$$\gamma_5 = \gamma^1\gamma^2\gamma^3\gamma^4 = i\begin{pmatrix} I & 0 \\ 0 & -I \end{pmatrix}.$$

However, with our choice of metric in the Minkowski space we shall define

$$\gamma_5 = -i\gamma^1\gamma^2\gamma^3\gamma^4 = \begin{pmatrix} I & 0 \\ 0 & -I \end{pmatrix}.$$

Such a definition does not change the usual important relations

$$\gamma_5\gamma^k + \gamma^k\gamma_5 = 0$$

except that now $\gamma_5^2 = 1$.

$$\Psi'_a = e^{\frac{1}{2}i\vartheta}\Psi_a, \tag{8'}$$

$$\Psi'_b = e^{\frac{1}{2}i\gamma_5\vartheta}\Psi_b. \tag{9'}$$

Assuming the non-derivative couplings, then, as is well known, the only coupling type which is invariant with respect to (8′) and (9′) is uniquely given by

$$\overline{\Psi}_a(1+\gamma_5)\Psi_b. \tag{10}$$

In the general case of a system of two fields, it is not easy to find the transformation law of the system, because the metric of the spin space depends on both fields. Such a situation has some analogy with the two-body problem in general relativity [25]). Fortunately, our antisymmetric spin metric depends on only one real function instead of the dependence of the Riemannian metric on ten functions as in general relativity.

This encourages us to make the second hypothesis: (II) When the field $a$ undergoes the transformation (2′), the metric of the spin space is not subject to the full transformation (4), which would occur in the absence of the other field $b$, but is only subject to the somewhat less general transformation

$$\begin{aligned} &\psi^\lambda(a) \to e^{\frac{1}{2}i\vartheta}\psi^\lambda(a), \\ &\gamma_{12}(a) \to e^{-i\varepsilon_1\vartheta}\gamma_{12}(a), \\ &0 < \varepsilon_1 < 1. \end{aligned} \tag{11}$$

Similarly, the transformation of the field $b$ is given by

$$\begin{aligned} &\psi^\lambda(b) \to e^{\frac{1}{2}i\vartheta}\psi^\lambda(b), \\ &\gamma_{12}(b) \to e^{-i\varepsilon_2\vartheta}\gamma_{12}(b), \\ &0 < \varepsilon_2 < 1. \end{aligned} \tag{12}$$

We now postulate that any physical quantity of the system should be invariant under the transformations (11) and (12).

With Riemannian geometry transformations such as (11) or (12) may be too simple. However, in order to obtain the more realistic transformation law we need more information about the coupling between each spinor field and the $B$ field. For the moment we do not have this information and so we choose a simple form for the transformation such as the above.

The transformation given by (11) and (12) can be expressed as

$$\Psi'_a = \exp\left[\{i\varepsilon_1 + i(1-\varepsilon_1)\gamma_5\}\tfrac{1}{2}\vartheta\right]\Psi_a, \tag{11'}$$

$$\Psi'_b = \exp\left[\{i\varepsilon_2 + i(1-\varepsilon_2)\gamma_5\}\tfrac{1}{2}\vartheta\right]\Psi_b. \tag{12'}$$

For the existence of couplings invariant under the transformations (11′), (12′) the choice of $\varepsilon_1$ and $\varepsilon_2$ must be limited to $\varepsilon_1 = 1$ or $\varepsilon_2 = 1$. It is interesting that the only possible invariant coupling form coincides either with the previous case (10) or with

$$\overline{\Psi}_a(1-\gamma_5)\Psi_b.$$

Therefore we shall make the next step, namely, to consider Fermi type interactions. In the case of the system of four spinors, the transformation of each field may be expressed as follows:

$$\Psi'_i = \exp\left[\{i\varepsilon_i + i(1-\varepsilon_i)\gamma_5\}\tfrac{1}{2}\vartheta\right]\Psi_i. \tag{13}$$

This expression can be derived by making use of hypothesis (II) applied to the case of four spinors. If we postulate that Fermi type interactions are to be invariant under the above transformation, then the only possible kinds of interaction are the following three kinds:

$$\overline{\Psi}_1(A+B\gamma_5)\gamma^k\Psi_2\,\overline{\Psi}_3(A'+B'\gamma_5)\gamma^k\Psi_4, \tag{14}$$

$$\overline{\Psi}_1(A+B\gamma_5)\gamma^k\Psi_2\,\overline{\Psi}_3(1-\gamma_5)\gamma^k\Psi_4, \tag{15}$$

$$\overline{\Psi}_1(1-\gamma_5)\gamma^k\Psi_2\,\overline{\Psi}_3(1-\gamma_5)\gamma^k\Psi_4, \tag{16}$$

where $A$, $B$, $A'$ and $B'$ are arbitrary constants. The differences among these three types of interaction come from the different transformation properties of the four spinor fields relative to each other. Namely for each of the interaction types (14)—(16) the following conditions must be satisfied (see appendix):

$$\varepsilon_1 = \varepsilon_2, \quad \text{and} \quad \varepsilon_3 = \varepsilon_4, \tag{14'}$$

$$\varepsilon_1 = \varepsilon_2, \ \varepsilon_3 \text{ and } \varepsilon_4 \text{ can have different values,} \tag{15'}$$

$$\varepsilon_1, \ \varepsilon_2, \ \varepsilon_3 \text{ and } \varepsilon_4 \text{ can have different values.} \tag{16'}$$

The condition (14') is very strong and we shall discuss later in detail the case when it is satisfied. The coupling (16) is identical with that of Feynmann and Gell-Mann [26] and corresponds to the V—A combination in the two-component neutrino theory. However, in the case of (15) we have freedom in the choice of the mixing ratio of V—A and V+A in the sense of the two-component neutrino theory, but this freedom is gained at the expense of the rather strong condition (15').

In the present paper we are concerned with local and non-derivative couplings. However, in order to see how our metric spin space works, it may be worth while to review some equations [22] concerning the covariant derivative. To define a covariant derivative of a spinor we need the so-called affine tensor $\Gamma^\alpha_{\rho k}$:

$$\psi^\alpha_{|k} = \partial_k\psi^\alpha + \Gamma^\alpha_{\rho k}\psi^\rho. \tag{17}$$

In order to determine $\Gamma^\alpha_{\rho k}$ two postulates are essential:

(i) $\psi^\alpha_{|k}$ must be covariant under Lorentz transformations,

(ii) a volume element of spinor space must be invariant under a parallel displacement in the Minkowski space (local conservation law) †.

† Recently a lucid physical proof that the second kind of gauge transformation is necessary and sufficient for the local conservation law has been given by Ferretti [27].

Since we confine ourselves to the usual Minkowski space, an explicit representation can be given for $\Gamma^{\alpha}_{\rho k}$:

$$\Gamma^{\alpha}_{\rho k} = \tfrac{1}{2} i g \Phi_k \delta_\rho{}^\alpha, \tag{18}$$

where $\Phi_k$ is an arbitrary real function of $x^k$, $g$ an arbitrary constant and $\delta_\rho{}^\alpha$ Kronecker's delta. If there is only one spinor field, $\Phi_k$ is a world vector and is subject to the second kind gauge transformation

$$\Phi_k \to \Phi_k - \frac{1}{g} \partial_k \vartheta. \tag{19}$$

Then $\Phi_k$ could be interpreted as the electro-magnetic four potential. However, it should be stressed that this *neutral* vector field which must be associated with any spinor field need not satisfy the Maxwell equation. In fact, if we borrow Stueckelberg's method [28]) which enables us to treat a general vector field similarly to the electromagnetic field, the interaction between spinor fields and a vector field which has a finite rest mass can be handled by a formalism which is completely analogous to that developed for quantum electrodynamics. A possibility is then to assume an extremely large rest mass for this neutral vector field so that the region of non-locality associated with this is very small. It might be possible to identify this neutral boson field with that proposed by Lee and Yang [29]) for the explanation of a possible non-locality in $\mu$-e decay.

In the case of interacting spinor fields, corresponding to the transformation (13), $\Phi_k$ should undergo the transformation

$$\Phi_k \to \Phi_k - \{\varepsilon + (1-\varepsilon)\gamma_5\} \partial_k \vartheta. \tag{20}$$

Then $\Phi_k$ no longer has a definite space parity.

The idea of such a gauge field was used by Yang and Mills [30]) in a rather arbitrary way to explain the selection rules in strange particle processes. Therefore, following Yang and Mills, we have referred to our spin metric field as the $B$ field. In the present paper we do not intend to discuss the explicit behaviour of the $B$ field but shall be content to consider only its effects on the form of the interaction between spinor fields.

As is well known, the usual four-component Dirac equation is not invariant with respect to a transformation involving $\gamma_5$ except for the case of vanishing mass. In particular it is not invariant with respect to

$$\Psi' = e^{i\gamma_5 \alpha} \Psi \qquad (\alpha : \text{parameter}). \tag{21}$$

However, as Gürsey [1]) has shown recently, if we introduce an additional four-component spinor which transforms differently than $\Psi$, according to

$$\hat{\Psi}' = e^{-i\gamma_5 \alpha} \hat{\Psi}, \tag{22}$$

then we can construct the equation ($\hbar = c = 1$)

$$\begin{pmatrix} \gamma^k\partial_k & im\gamma_5 \\ -im\gamma_5 & \gamma^k\partial_k \end{pmatrix}\begin{pmatrix} \Psi \\ \hat{\Psi} \end{pmatrix} = 0, \tag{23}$$

which is invariant if $\Psi$, $\hat{\Psi}$ transform according to (21) and (22) respectively. We may slightly rewrite this equation in the following form:

$$(\Gamma^k\partial_k + im)\begin{pmatrix} \Psi \\ \hat{\Psi} \end{pmatrix} = 0, \tag{24}$$

where

$$\Gamma^k = \begin{pmatrix} 0 & -\gamma_5\gamma^k \\ \gamma_5\gamma^k & 0 \end{pmatrix}, \tag{25}$$

and satisfy the commutation rules

$$\Gamma^k\Gamma^l + \Gamma^l\Gamma^k = 2g^{kl}. \tag{26}$$

It is then quite evident that eq. (24) is a Dirac equation in an eight-component spinor representation. Such an eight-component representation is of course reducible † but not trivial. This is because this change of representation is necessary in order that the Dirac equation is invariant with respect to the transformation (21), (22) and because it can now also have another important property: eq. (24) is invariant with respect to Pauli's transformation (I) [33])

$$\begin{aligned} \Psi' &= a\Psi + b\gamma_5\Psi^c, \quad & \Psi^{c'} &= a^*\Psi^c - b^*\gamma_5\Psi, \\ \hat{\Psi}' &= a\hat{\Psi} + b\gamma_5\hat{\Psi}^c, \quad & \hat{\Psi}^{c'} &= a^*\hat{\Psi}^c - b^*\gamma_5\hat{\Psi}. \end{aligned} \tag{27}$$

Since this group of transformations is isomorphic to the unimodular group and also maintains the invariance of the generalized Dirac equation (24), we may interpret this group as the usual isospin group. Therefore to a solution of eq. (24) we can attribute an isospin quantum number and an isospin parity, but not a definite space parity.

It is rather straightforward to apply the above discussion to our theory when $\alpha$ is not a real parameter but a real function such as $\frac{1}{2}(1-\varepsilon)\vartheta$ where $\vartheta$ is a function of $x^k$: if we replace $\partial_k$ in eq. (23) by $\partial_{1k}$ and $\hat{\partial}_{1k}$ so that now

$$\begin{pmatrix} \gamma^k\partial_{1k} & im\gamma_5 \\ -im\gamma_5 & \gamma^k\hat{\partial}_{1k} \end{pmatrix}\begin{pmatrix} \Psi \\ \hat{\Psi} \end{pmatrix} = 0, \tag{28}$$

this equation is covariant with respect to our generalized transformation if $\partial_{1k}$ and $\hat{\partial}_{1k}$ transform according to

$$\begin{aligned} \partial_{1k} &\to \partial_{1k} - \tfrac{1}{2}i\{\varepsilon + (1-\varepsilon)\gamma_5\}\partial_k\vartheta, \\ \hat{\partial}_{1k} &\to \hat{\partial}_{1k} - \tfrac{1}{2}i\{\varepsilon - (1-\varepsilon)\gamma_5\}\partial_k\vartheta. \end{aligned} \tag{29}$$

† An irreducible representation of the $\Gamma^k$ by eight-by-eight matrices has been considered by Biedenharn [32]), by extending the Lorentz group to include time reversal in $c$-number theory. The author is grateful to Dr. J. Serpe for drawing his attention to Biedenharn's paper.

However, we now lose the invariance with respect to Pauli's transformation (I) even in the case where $a$ and $b$ are not functions but only parameters. In other words, only in a certain approximation, which we may call "non-electric approximation", i.e. only when

$$\partial_{1k} = \hat{\partial}_{1k} = \partial_k, \tag{30}$$

can we define the isospin and isoparity.

As we have emphasized repeatedly, our generalization causes some difference only in the case of interacting spinor system. For an isolated spinor field, $\varepsilon = 1$ and the difference of transformation properties between $\Psi$ and $\hat{\Psi}$ disappears. In fact, if we substitute $\gamma_5\Psi = \hat{\Psi}$ in eq. (24), this becomes identical with the conventional four-component Dirac equation.

We shall now construct several invariant interaction forms by making use of $\Psi$ as well as $\hat{\Psi}$.

Defining $\alpha$ and $\bar{\alpha}$ by

$$\alpha = \tfrac{1}{2}(1+\gamma_5), \qquad \bar{\alpha} = \tfrac{1}{2}(1-\gamma_5) \tag{31}$$

and noting the following simple relations:

$$\begin{aligned} &\alpha^2 = \alpha, && \bar{\alpha}^2 = \bar{\alpha}, \quad \alpha\bar{\alpha} = 0, \\ &\alpha e^{i\gamma_5 u} = \alpha e^{iu}, && \bar{\alpha} e^{i\gamma_5 u} = \bar{\alpha} e^{-iu}, \end{aligned} \tag{32}$$

we can readily write down the invariants in the case of $\varepsilon_1 = \varepsilon_2 = \varepsilon_3 = \varepsilon_4$. These are

$$\begin{aligned} I_1 &= \overline{\Psi}_1\alpha\Psi_2\overline{\Psi}_3\bar{\alpha}\Psi_4, & I'_1 &= \overline{\Psi}_1\bar{\alpha}\Psi_2\overline{\Psi}_3\alpha\Psi_4, \\ I_2 &= \overline{\Psi}_1\alpha\Psi_2\overline{\hat{\Psi}}_3\alpha\hat{\Psi}_4, & I'_2 &= \overline{\Psi}_1\bar{\alpha}\Psi_2\overline{\hat{\Psi}}_3\bar{\alpha}\hat{\Psi}_4, \\ I_3 &= \overline{\hat{\Psi}}_1\alpha\hat{\Psi}_2\overline{\Psi}_3\alpha\Psi_4, & I'_3 &= \overline{\hat{\Psi}}_1\bar{\alpha}\hat{\Psi}_2\overline{\Psi}_3\bar{\alpha}\Psi_4, \\ I_4 &= \overline{\hat{\Psi}}_1\alpha\hat{\Psi}_2\overline{\hat{\Psi}}_3\bar{\alpha}\hat{\Psi}_4, & I'_4 &= \overline{\hat{\Psi}}_1\bar{\alpha}\hat{\Psi}_2\overline{\hat{\Psi}}_3\alpha\hat{\Psi}_4, \end{aligned} \tag{33}$$

$$\begin{aligned} K_1 &= \overline{\Psi}_1\hat{\Psi}_2\overline{\Psi}_3\hat{\Psi}_4, & K_2 &= \overline{\Psi}_1\hat{\Psi}_2\overline{\hat{\Psi}}_3\Psi_4, \\ K_3 &= \overline{\hat{\Psi}}_1\Psi_2\overline{\Psi}_3\hat{\Psi}_4, & K_4 &= \overline{\hat{\Psi}}_1\Psi_2\overline{\hat{\Psi}}_3\Psi_4, \end{aligned} \tag{34}$$

where $\overline{\Psi}_i$ and $\overline{\hat{\Psi}}_i$ are defined in the usual manner:

$$\overline{\Psi}_i = \Psi_i^\dagger\gamma^4, \qquad \overline{\hat{\Psi}}_i = \hat{\Psi}_i^\dagger\gamma^4.$$

Each of the above types in (33) and (34) is invariant with respect to our generalized transformation (13), but not invariant with respect to Pauli's first group (27). However, if we take suitable linear combinations of these types, we can construct quantities which are also invariant under the transformation (27). In order to see such transformation properties in a more familiar way, it is convenient to rewrite these linear combinations using Gürsey's transformation

$$\begin{aligned}\Psi_i &= \alpha\psi_{ai}+i\tilde{\alpha}\psi^c_{bi},\\ \hat{\Psi}_i &= \tilde{\alpha}\psi_{ai}-i\alpha\psi^c_{bi}.\end{aligned} \tag{35}$$

Then we obtain the following familiar expressions:

$$\begin{aligned}I_1-I_2+I'_4-I'_3 &= \bar{\psi}^c_{b1}\psi_{a2}\bar{\psi}_{a3}\psi^c_{b4},\\ I_1+I_2-I'_4-I'_3 &= \bar{\psi}^c_{b1}\gamma_5\psi_{a2}\bar{\psi}_{a3}\gamma_5\bar{\psi}^c_{b4},\\ I_4-I_3+I'_1-I'_2 &= \bar{\psi}_{a1}\psi^c_{b2}\bar{\psi}^c_{b3}\psi_{a4},\\ I_4-I_3-I'_1-I'_2 &= \bar{\psi}_{a1}\gamma_5\psi^c_{b2}\bar{\psi}^c_{b3}\gamma_5\psi_{a4},\end{aligned} \tag{36}$$

$$\begin{aligned}K_1+K_2+K_3+K_4 &= (\bar{\psi}_{a1}\psi_{a2}-\bar{\psi}^c_{b1}\psi^c_{b2})(\bar{\psi}_{a3}\psi_{a4}-\bar{\psi}^c_{b3}\psi^c_{b4}),\\ K_1-K_2+K_3-K_4 &= (\bar{\psi}_{a1}\gamma_5\psi_{a2}+\bar{\psi}^c_{b1}\gamma_5\psi^c_{b2})(\bar{\psi}_{a3}\gamma_5\psi_{a4}+\bar{\psi}^c_{b3}\gamma_5\psi^c_{b4}).\end{aligned} \tag{37}$$

If, for example, we make the identifications

$$\psi_a = p, \quad \psi_b{}^c = n,$$

it may be seen directly that the following combination is charge independent:

$$\begin{aligned}&\bar{\psi}_{a1}\psi^c_{b2}\psi^c_{b3}\bar{\psi}_{a4}+\bar{\psi}^c_{b1}\psi_{a2}\bar{\psi}_{a3}\psi^c_{b4}+\tfrac{1}{2}(\bar{\psi}_{a1}\psi_{a2}-\bar{\psi}^c_{b1}\psi^c_{b2})(\bar{\psi}_{a3}\psi_{a4}-\bar{\psi}^c_{b3}\psi^c_{b4})\\ &\quad = (\bar{p}n)(\bar{n}p)+(\bar{n}p)(\bar{p}n)+\frac{1}{\sqrt{2}}(\bar{p}p-\bar{n}n)\frac{1}{\sqrt{2}}(\bar{p}p-\bar{n}n).\end{aligned} \tag{38}$$

Furthermore, it is quite obvious that (38) conserves the space parity.

On the other hand, if $\varepsilon_1 = \varepsilon_2 \neq \varepsilon_3 = \varepsilon_4$, we cannot construct a charge independent coupling such as (38) now only the last term of (38), corresponding to the third component of an isovector, is a possible interaction. Thus, in the case of $\varepsilon_1 = \varepsilon_2 \approx \varepsilon_3 = \varepsilon_4$ we may have the charge independent coupling in the first approximation and the $\tau_3$-interaction in the second approximation [34,35]).

## 3. Discussion

As has been emphasized in the preceding section, our generalized transformation, under which the physical description must be invariant, only affects systems of two or more coupled spinor fields, but does not in any way modify the properties of a single isolated Dirac field. In the case of two or more fields there is a modification of the transformation properties of each field. This modification enables us to classify various types of interactions, which have previously been proposed, phenomenologically, and to associate each of the types with a corresponding conservation law.

One of the essential points of our generalization is to postulate affine covariance as well as Lorentz covariance. The former necessarily introduces a neutral vector field associated with any spinor field. Although this vector field has been interpreted as the electromagnetic field by Infeld and van der

Waerden, we would like to consider that this field consists of two kinds of fields, i.e. the electromagnetic field and the $B$ field. The difficulty due to the finite rest mass of the $B$ field can be avoided by Stueckelberg's formalism, so that these two fields can be treated in completely the same way. Assuming that any complex spinor field couples with the electromagnetic field with the same coupling constant as usual, we readily obtain the charge conservation law. It is evident that invariance under our generalized transformation will guarantee the invariance under the special transformation which leads to charge conservation.

Since we are interested in the interacting fields, we may classify Fermion fields into two categories according to the magnitude of $\varepsilon_i$ appearing in their transformation function:

$$\text{(i) lepton for } \varepsilon_i \ll 1, \tag{39}$$

$$\text{(ii) baryon for } \varepsilon_i \approx 1. \tag{40}$$

If a baryon pair appears in the interacting fields, a baryonic current vector which satisfies the continuity equation can be defined. This is possible because the interaction between baryon fields and the $B$ field is a vector coupling and direct couplings between baryon fields are also invariant with respect to the generalized transformation (13).

Rewriting the transformation (13) for $\psi_a$ and $\psi_b{}^c$, this becomes

$$\begin{aligned} \psi_a &\to e^{\frac{1}{2}i(\epsilon\theta+\frac{1}{2}i(1-\epsilon)\theta}\psi_a, \\ \psi_b{}^c &\to e^{\frac{1}{2}i(\epsilon\theta-\frac{1}{2}i(1-\epsilon)\theta}\psi_b{}^c. \end{aligned} \tag{41}$$

As we have mentioned at the beginning of the preceding section, the case $\varepsilon = 0$ may be interpreted as that of a neutrino field. Therefore it seems plausible to interpret $\psi_a$ and $\psi_b{}^c$ as having the same baryonic charge but opposite leptonic charge.

Such an idea was first proposed by Touschek [5]) and later investigated extensively by Konuma [36]) in connection with the conservation of lepton number.

Let us now discuss briefly the correspondence between our interaction forms and previously proposed Fermi interactions. The most typical weak interactions, e.g. $\mu$-e decay, belong to the type

$$\overline{\Psi}_1(1-\gamma_5)\gamma^k\Psi_2\,\overline{\Psi}_3(1-\gamma_5)\gamma^k\Psi_4, \tag{42}$$

because $\mu$, e and $\nu$ may all have different values of $\epsilon$ although all of these are nearly zero. This is exactly the same situation as that of Feynman and Gell-Mann, who have investigated this case quantitatively. However, it should be noticed that if four fermions all have different $\varepsilon$ our theory limits the possible interactions to only this type. Another possible example is

$$\Lambda^0 \to \mathrm{p}+\mathrm{e}+\bar{\nu}. \tag{43}$$

The usual $\beta$-decay interaction involves a nucleon pair, and this is of the following type:

$$\overline{\Psi}_1(A+B\gamma_5)\gamma^k\Psi_2\,\overline{\Psi}_3(1-\gamma_5)\gamma^k\Psi_4 \tag{44}$$

where the ratio $A/B$ can be chosen arbitrarily. Thus it is possible to have any degree of mixing of the alternative couplings V−A, V+A (in the case of two-component neutrino theory). On the contrary, in Feynman and Gell-Mann's theory it seems that one can only choose one of these alternatives, because their hypothesis for construction of the Fermi interactions requires one to replace $\Psi$ by either one of the projected components $\frac{1}{2}(1\pm\gamma_5)\Psi$. Therefore, if the experiments on the angular distribution of electrons from polarized neutrons do not agree with one of the alternatives predicted by Feynman and Gell-Mann, this would seem favourable for our theory.

Finally, keeping in mind a spinor model in which all bosons may be regarded as composite systems of fermions, except the electromagnetic field and the $B$ field, we shall consider interactions of Fermi interaction type.

In the case of interacting fields it is necessary to introduce the eight-component spinor representation of the Dirac equation in order to describe each spinor field in a covariant way. Within this expanded framework the concept of isospin appears naturally in association with a particular interaction type. In fact, in the case of $\varepsilon_1=\varepsilon_2=\varepsilon_3=\varepsilon_4$ we have charge-independent interactions

$$\bar{\psi}_{a1}\psi^c_{b2}\bar{\psi}^c_{b3}\psi_{a4}+\bar{\psi}^c_{b1}\psi_{a2}\bar{\psi}_{a3}\psi^c_{b4}+\tfrac{1}{2}(\bar{\psi}_{a1}\psi_{a2}-\bar{\psi}^c_{b1}\psi^c_{b2})(\bar{\psi}_{a3}\psi_{a4}-\bar{\psi}^c_{b3}\psi^c_{b4}), \tag{45}$$

or

$$\bar{\psi}_{a1}\gamma_5\psi^c_{b2}\bar{\psi}^c_{b3}\gamma_5\psi_{a4}+\bar{\psi}^c_{b1}\gamma_5\psi_{a2}\bar{\psi}_{a3}\gamma_5\psi^c_{b4}+\tfrac{1}{2}(\bar{\psi}_{a1}\gamma_5\psi_{a2}+\bar{\psi}^c_{b1}\gamma_5\psi^c_{b2})(\bar{\psi}_{a3}\gamma_5\psi_{a4}+\bar{\psi}^c_{b3}\gamma_5\psi^c_{b4}). \tag{46}$$

If we take into account the possibility of introducing two kinds of isospinor [11]) the strangeness (corresponding to the isoparity) is obviously conserved in both the above cases, as well as the space parity. Therefore it seems plausible to take the above two interaction forms as typical of strong interactions. Furthermore it is interesting that the case $\varepsilon_1=\varepsilon_2\neq\varepsilon_3=\varepsilon_4$ gives us only the last term ($\tau_3$ part) in the above two interactions (45), (46). Therefore, if $\varepsilon_1=\varepsilon_2\approx\varepsilon_3=\varepsilon_4$, we have the strong interaction (45) or (46) in the first approximation and $\tau_3$-interactions in the second approximation. This corresponds to the modification of Gell-Mann—Nishijima's selection rule proposed by Takeda [34]) and also by d'Espagnat, Prentki and Salam [35]).

The modification of the spin metric associated with interacting fields has some analogy to the modification of the Riemannian metric associated with the interaction of two or more bodies in general relativity. Another analogy might be with the modification of the interaction between two charged particles due to their presence in a polarizable medium and the association of this modification with the state of polarization of the medium.

In the present paper we have tried to unify all known conservation laws by use of a generalized transformation group, which is associated with the transformation of the metric in the *usual* spin space. The author would like to express his sincere thanks to Professor B. Ferretti for valuable discussions and Professor L. Rosenfeld for the kind interest. He wishes to thank Professor C. J. Bakker for the hospitality extended to him at CERN.

## Appendix

For calculations which include $\gamma_5$ the following identities are useful:

$$(1+\gamma_5)e^{i\gamma_5 u} = (1+\gamma_5)e^{iu}, \qquad (1-\gamma_5)e^{i\gamma_5 u} = (1-\gamma_5)e^{-iu},$$

where $u$ is real and $\exp\{i\gamma_5 u) = \cos u + i\gamma_5 \sin u$. If we transform two four-component spinors as

$$\Psi_1 \to e^{iu_1+i\gamma_5 v_1}\Psi_1, \qquad \Psi_2 \to e^{iu_2+i\gamma_5 v_2}\Psi_2,$$

the coupling

$$I = \overline{\Psi}_1(A+B\gamma_5)\gamma^k\Psi_2$$

is transformed in the following way:

$$\begin{aligned} I' &= \overline{\Psi}_1 e^{-iu_1+i\gamma_5 v_1}\left(\tfrac{1}{2}(A+B)(1+\gamma_5)+\tfrac{1}{2}(A-B)(1-\gamma_5)\right)e^{iu_2-i\gamma_5 v_2}\gamma^k\Psi_2 \\ &= \overline{\Psi}_1 e^{-i(u_1-u_2-v_1+v_2)}\tfrac{1}{2}(A+B)(1+\gamma_5)\gamma^k\Psi_2 \\ &+ \overline{\Psi}_1 e^{-i(u_1-u_2+v_1-v_2)}\tfrac{1}{2}(A-B)(1-\gamma_5)\gamma^k\Psi_2. \end{aligned}$$

Therefore $I$ is invariant for the following two cases:

(i) $A$, $B$ are arbitrary, but $u_1 = u_2$, $v_1 = v_2$,

(ii) $A = -B$, but $u_1+v_1 = u_2+v_2$.

The case of $u_1-v_1 = (u_2-v_2)$ is omitted because in our theory it is included in (i).

*Note added in proof:* Recently Tanikawa and Watanabe have proposed an intermediary chiral boson field to derive the Fermi interaction. The author is grateful to Professor S. Watanabe for sending him the preprint and also for interesting discussions on the relation between their theory and ours.

## References

1) T. D. Lee and C. N. Yang, Phys. Rev. **104** (1956) 254
2) A. Salam, Nuovo Cimento **5** (1957) 299
3) L. Landau, Nuclear Physics **3** (1957) 127
4) T. D. Lee and C. N. Yang, Phys. Rev. **105** (1957) 1671
5) F. Touschek, Nuovo Cimento **5** (1957) 1281
6) K. Nishijima, Nuovo Cimento **5** (1957) 1349
7) E. J. Schremp, Phys. Rev. **108** (1957) 1076

8) H. Umezawa and A. Visconti, Nuclear Physics **4** (1957) 224
9) M. Gell-Mann, Phys. Rev. **92** (1953) 833
10) T. Nakano and K. Nishijima, Prog. Theor. Phys. **10** (1953) 581; **12** (1954) 107; **13** (1955) 285
11) B. d'Espagnat and J. Prentki, Nuclear Physics **1** (1956) 33
12) A. Salam and J. C. Polkinghorne, Nuovo Cimento **2** (1955) 685
13) R. G. Sachs, Phys. Rev. **99** (1955) 1573
14) J. Schwinger, Phys. Rev. **104** (1956) 1164
15) M. Goldhaber, Phys. Rev. **101** (1956) 433
16) M. A. Marcov, Uspekhi Fiz. Nauk **51** (1953) 317
17) S. Sakata, Prog. Theor. Phys. **16** (1956) 686
18) H. Yukawa, Prog. Theor. Phys. **16** (1956) 688
19) J. Rayski, Nuovo Cimento **10** (1951) 1729; **12** (1951) 815
20) J. Tiomno, Nuovo Cimento **6** (1957) 69
21) N. Dallaporta, Nuovo Cimento **7** (1957) 200
22) L. Infeld and B. L. van der Waerden, Sitzungsberichte der Preussischen Akad. der Wiss. (1933) 380; reviewed in W. L. Bade and H. Jehle, Revs. Mod. Phys. **25** (1953) 714; also in P. G. Bergmann, Phys. Rev. **107** (1957) 624
23) H. Weyl, Sitzungsberichte der Königlich Preussischen Akademie der Wissenschaften **26** (1918) 465; see Nachtrag von Weyl, Selecta Hermann Weyl (Birkhäuser Verlag, Basel und Stuttgart, 1956)
24) A. Pais, Physica **19** (1953) 869
25) See for review L. Infeld, Revs. Mod. Phys. **29** (1957) 398
26) R. P. Feynman and M. Gell-Mann, Phys. Rev. **109** (1958) 193;
J. J. Sakurai, Nuovo Cimento **7** (1958) 649;
E. C. G. Sudarshan and R. E. Marshak, Padua-Venice International Conference on Mesons and Recently Discovered Particles (1957); Phys. Rev. **109** (1958) 1860;
S. B. Freiman and H. W. Wyld, Jr., Phys. Rev. **106** (1957) 1320
27) B. Ferretti, Nuovo Cimento **6** (1957) 997
28) E. C. G. Stueckelberg, Helv. Phys. Acta **11** (1938) 225, 299
29) T. D. Lee and C. N. Yang, Phys. Rev. **108** (1957) 1611
30) C. N. Yang and R. L. Mills, Phys. Rev. **96** (1954) 191
31) F. Gürsey, Nuovo Cimento **7** (1958) 411
32) L. Biedenharn, Phys. Rev. **82** (1951) 100
33) W. Pauli, Nuovo Cimento **6** (1957) 204
34) G. Takeda, Prog. Theor. Phys. **19** (1958) 631
35) B. d'Espagnat, J. Prentki and A. Salam, Nuclear Physics **5** (1958) 447
36) M. Konuma, Nuclear Physics **5** (1958) 504

8.B *Nuclear Physics* 8 (1958) 675—691; © *North-Holland Publishing Co., Amsterdam*
Not to be reproduced by photoprint or microfilm without written permission from the publisher

# ON THE GROUP STRUCTURE OF ELEMENTARY PARTICLES

FEZA GÜRSEY

*Radiation Laboratory, University of California, Berkeley, California* †

Received 7 July 1958

**Abstract:** An attempt is made to account for the group structure of elementary particles by assuming that they are obtained by combining a limited number of basic fields. It is shown that if the basic fields are all taken to be fermions, one needs three fields to account for the continuous group structure only, but four fields are necessary if distinct operations for C and P are to be incorporated in the scheme. On the other hand, a model with half the number of independent field components can describe the group structure correctly if both bosons and fermions are taken as basic fields, their common feature in this case being that they are all strange fields. Difficulties inherent in such schemes are discussed.

## 1. Introduction

Not much can be expected from a formal scheme for elementary particles which evades the fundamental problem of interaction, as no quantitative conclusions regarding masses, lifetimes and coupling constants can be drawn from the model. However, even a qualitative and descriptive scheme may be useful if it accounts for the group structure of particles and throws light on some remarkable mathematical facts and empirically observed rules, such as the seemingly limited number of particles, the possible connection between strangeness and parity [1]), a satisfactory explanation of the form of weak interactions [2]), the curious isomorphism between the gauge group of a massless neutral Dirac particle and the group of strong interactions [3]), the absence of a neutral particle other than the neutrino associated with the $\mu$ meson, the possible four-dimensional Euclidean symmetry of the baryon-pion interactions and partial breakdown of this symmetry in K-meson interactions [4]). One should also try to give an answer to the problem of determining the nature and the number of fundamental fields, if, following Heisenberg [5]), Goldhaber [6]), and Sakata [7]), all particles are regarded as having a compound structure.

This paper is devoted to the discussion of some examples of spinor and mixed (fermion + boson) models with a simple (non-degenerate) vacuum. It is found that, with three fundamental spinor fields (2 lepton fields and

† On leave from the University of Istanbul, Turkey, and at Brookhaven National Laboratory, Upton, N. Y. for a portion of this work. Work performed under the auspices of the U.S. Atomic Energy Commission and the International Cooperation Administration.

1 baryon field), one may account for the group structure of the particles as far as the continuous gauge groups are concerned. One discontinuous group — for instance, CP — can also be incorporated. However, the model fails to explain the discontinuous group structure which must comprise two distinct reflection operations, C and P, that are presumably conserved in strong and electromagnetic interactions. In order to incorporate the latter feature in the scheme one needs four four-spinor fields. But then, one meets with the difficulty of unobserved new particles and a greater arbitrariness in the formulation of the interaction problem. The large number of basic fields required seems to be a fundamental difficulty associated with such fermion models.

Because of the poor success of the spinor approach, we have also investigated a mixed model in which boson fields as well as fermion fields are taken to be basic from the start. This line seems to be more promising. Indeed, three fundamental fields — namely, a 2-component isosinglet fermion field $\lambda$; two boson fields, $k_1$ and $k_2$ (forming an isodoublet complex boson field $k$); and an isosinglet baryon four-spinor field $\Lambda$ — suffice to account both for the continuous and for the discontinuous group structure of elementary particles. The assumption is that the fundamental fields $\lambda$, $k$ and $\Lambda$, which all together have eight components, are not observable by themselves but give rise to compound states that represent "elementary" particles. We note that these fields are strange in the sense that they have a spin difference of $\frac{1}{2}$ in ordinary and isobaric spin spaces.

In all the schemes under consideration that are based on the idea of extending strangeness and isobaric spin to leptons, the status of the $\mu$ meson is ill defined, since the problem of finding a natural place for it has no easy solution.

Before discussion of a few simple schemes a remark is necessary about the fairly generally accepted two-component nature of the neutrino. Let us introduce a basic leptonic isodoublet which we may tentatively identify with a four-component electron $\varepsilon$ and a four-component neutrino $\nu$. We may assume that the mass of the electron vanishes in the limit of electromagnetic forces being neglected. In this limit, the concept of isospin should be applicable and the electron-neutrino system should emerge as an isodoublet. One objection to this conception of the leptonic field $(\varepsilon, \nu)$ might be the two-component nature of the neutrino. The way in which such a reduction of the available states of the neutrino affects the scheme is a matter for separate discussion (section 2, scheme A′). However, it is worth noting that the neutrino is not the only particle that behaves like a two-component field in weak interactions. Had our experience with electrons been limited to those produced in decays only, we might be tempted to ascribe a two-component nature to the electron too. The reason this cannot be done is that the missing

states of the electron are actually produced in electromagnetic interactions that do not affect the neutrino. In any compound-particle scheme comprising the electron and the neutrino among its building units, neutrinos could be produced not only in weak interactions, but also perhaps in very energetic collisions of strongly interacting particles. The nature of neutrinos produced under such conditions might be very different from that of decay neutrinos.

## 2. Schemes with three Spinor Fields (A and A'). Continuous Groups

As fundamental fields we take $\varepsilon$, $\nu$ and a neutral isosinglet baryon field $\Lambda$. All three are anticommuting four-spinor fields. We use the notation

$$\psi_{\mathrm{L}} = \tfrac{1}{2}(1+\gamma_5)\psi, \qquad \psi_{\mathrm{R}} = \tfrac{1}{2}(1-\gamma_5)\psi \tag{1}$$

for any four-spinor $\psi$, $\gamma_5$ being taken diagonal, so that $\psi_{\mathrm{L}}$ and $\psi_{\mathrm{R}}$ are essentially two-component spinors. To study the groups involved it is also useful to introduce the $2\times 2$ matrices $F$ and $G$ defined by

$$F = (\nu_{\mathrm{L}}, \varepsilon_{\mathrm{L}}), \qquad G = (-i\sigma_2\varepsilon_{\mathrm{R}}^*, i\sigma_2\nu_{\mathrm{R}}^*), \tag{2}$$

where the symbols in the brackets stand for the columns associated with the two-component spinors (1). Under a Lorentz transformation, $F$ and $G$ transform in the same way, both being multiplied to the left by a unimodular $2\times 2$ matrix $L$ (see ref.[3])). Let us also introduce the notation

$$\bar{F} = \sigma_2 F^{\mathrm{T}} \sigma_2 \tag{3}$$

for the adjoint matrix, so that $\bar{F}F$ would be equal to the determinant of $F$ in $C$-number theory. Now we form the Lorentz invariant matrix

$$\theta = \bar{F}G. \tag{4}$$

The elements of this matrix are products of the operators $\varepsilon$ and $\nu$ at the same point. Strictly speaking, such products are not defined in conventional field theory. As shown by Zimmermann [8]), to describe a compound state of the fields $\psi$ and $\phi$ one should start from the time-ordered product $T(\psi[x], \phi[x'])$ and use a limiting process to define the product operator at the point corresponding to the centre of mass. However, this procedure does not alter the symmetry properties of the product function, and in the following we shall use products of operators to represent compound states.

Two Lorentz-invariant, commuting rotation groups (which combine in a four-dimensional Euclidean rotation group) may now be defined:

$$F \to FR, \qquad G \to G \tag{5-I}$$

$$F \to F, \qquad G \to GQ \tag{5-II}$$

where

$$R = \exp i\boldsymbol{\sigma}\cdot\mathbf{t} \qquad \text{and} \qquad Q = \exp i\boldsymbol{\sigma}\cdot\mathbf{u} \tag{6}$$

are two unitary, unimodular $2\times 2$ matrices, $\mathbf{t}$ and $\mathbf{u}$ are real vectors, and the $\sigma$'s denote the Pauli matrices. Under the four-dimensional rotation, $\theta$ obeys the law

$$\theta \to \bar{R}\theta Q, \tag{7}$$

so that $\mathrm{Tr}\,\theta\bar{\theta}$ is invariant. We also obtain

$$\bar{\theta} \to \bar{Q}\bar{\theta}R \tag{8}$$

and

$$\theta^\dagger \to \bar{Q}\theta^\dagger R. \tag{8'}$$

The elements of the matrix $\theta$ represent four spin-zero boson fields, namely

$$\theta^0 = \varepsilon_R{}^\dagger\varepsilon_L, \qquad \theta^+ = \varepsilon_R{}^\dagger\nu_L, \qquad \theta^- = \nu_R{}^\dagger\varepsilon_L, \qquad \bar{\theta}^0 = \nu_R{}^\dagger\nu_L, \tag{9}$$

so that one has

$$\theta = \begin{pmatrix} \theta^0 & -\theta^- \\ -\theta^+ & \bar{\theta}^0 \end{pmatrix} \tag{10}$$

and

$$\bar{\theta} = \begin{pmatrix} \overline{\theta^0} & \theta^- \\ \theta^+ & \theta^0 \end{pmatrix}. \tag{11}$$

If the rotation group (5-I) is regarded as generating the isospin group to which it is isomorphic, then $\theta^0$, $\theta^+$ on one hand and $\overline{\theta^0}$, $\theta^-$ on the other behave like isospinor bosons. A transformation isomorphic to the hypercharge (or isofermion) gauge group introduced by D'Espagnat and Prentki [9]) is obtained by considering the subgroup of (5-II) corresponding to $u_1 = u_2 = 0$, $u_3 = u$. Under this group we have

$$\theta \to \theta \exp i\sigma_3 u \tag{12}$$

or

$$\begin{gathered} \theta^0 \to \theta^0 e^{iu}, \quad \theta^+ \to \theta^+ e^{iu}, \quad \overline{\theta^0} \to \overline{\theta^0} e^{-iu}, \\ (\theta^0)^* \to (\theta^0)^* e^{-iu}, \quad (\overline{\theta^0})^* \to (\overline{\theta^0})^* e^{iu}, \quad \theta^- \to \theta^- e^{-iu}. \end{gathered} \tag{13}$$

We see that as far as continuous groups are concerned, the operators $(\theta^0, \theta^+)$ behave like the K-meson field $(K^0, K^+)$. The full rotation group (5-II) mixes states of opposite hypercharge and hence is a representation of the global-symmetry group considered by Gell-Mann and Schwinger [4]). It is seen to be the three-dimensional generalization of the hypercharge transformation.

Since $\theta$ and $\bar{\theta}^\dagger$ transform in the same way under the full group (5), we may construct the isovector boson field $\boldsymbol{\phi}$ in such a way that we have

$$\boldsymbol{\sigma}\cdot\boldsymbol{\phi} = \tfrac{1}{2}(\theta\theta^\dagger - \bar{\theta}^\dagger\bar{\theta}) = \theta\theta^\dagger - \tfrac{1}{2}\,\mathrm{Tr}\,\theta\theta^\dagger. \tag{14}$$

It transforms as

$$\boldsymbol{\sigma}\cdot\boldsymbol{\phi} \to \bar{R}(\boldsymbol{\sigma}\cdot\boldsymbol{\phi})R \tag{15}$$

under the isospin group (5-I), but is invariant under (5-II), and in particular under the hypercharge group. Hence, as far as continuous groups are concerned $\boldsymbol{\phi}$ behaves like the pion field $\boldsymbol{\pi}$.

We note that an isoscalar boson field $\phi^0$ can also be defined by

$$\phi^0 = \tfrac{1}{2}\,\mathrm{Tr}\,\theta\theta^+. \tag{16}$$

We now combine the field $\theta$ with the four-spinor field $\Lambda$ to introduce baryons in the scheme. The baryon gauge transformation is given by

$$\Lambda \to e^{ib}\Lambda. \tag{17}$$

For the isofermion baryons N(nucleon) and $\Xi$(cascade particle) we can write

$$\begin{pmatrix} \Xi_L^0 & \Xi_L^- \\ p_L & n_L \end{pmatrix} = \Lambda_L\theta = \begin{pmatrix} \Lambda_L\theta^0 & \Lambda_L\theta^- \\ \Lambda_L\theta^+ & \Lambda_L\theta^0 \end{pmatrix} \tag{18}$$

and

$$\begin{pmatrix} \Xi_R^0 & \Xi_R^- \\ p_R & n_R \end{pmatrix} = \Lambda_R\theta^\dagger = \begin{pmatrix} \Lambda_R\theta^{0*} & -\Lambda_R\theta^{+*} \\ -\Lambda_R\theta^{-*} & \Lambda_R\theta^{0*} \end{pmatrix}. \tag{19}$$

The $\Lambda^0$ and the $\Sigma$ (isoboson) baryons may be defined as

$$\Lambda^0 = \Lambda \tag{20}$$

or

$$\Lambda^0 = \Lambda\phi^0 \tag{20'}$$

and

$$\Sigma_n = \Lambda\phi_n, \quad (n = 1, 2, 3) \tag{21}$$

where $\phi^0$ and $\phi_n$ are defined by eqs. (14) and (16). It may be verified that the operators introduced above all have the correct transformation properties under Lorentz transformations, isobaric spin, charge, and hypercharge transformations.

Another continuous group, the leptonic charge group may be introduced in two different ways:

$$G_l: \quad \varepsilon \to e^{il}\varepsilon, \quad \nu \to e^{il}\nu, \quad \Lambda \to \Lambda, \tag{22}$$

$$G_{l'}: \quad \varepsilon_L \to e^{il'}\varepsilon_L, \quad \nu_L \to e^{il'}\nu_L, \quad \Lambda \to \Lambda \tag{23}$$

$$\varepsilon_R \to \varepsilon_R, \quad \nu_R \to \nu_R.$$

The group $G_l$ is general and can help to formulate lepton conservation with any type of weak interaction. But if it is true that all leptonic weak interactions are of the (V—A) type, then only left-handed electrons and neutrinos enter such interactions and it is sufficient to consider the group $G_{l'}$ (eq. (23)) as defining the leptonic charge. Since the $\mu^-$ meson must have the same leptonic charge as the electron (evidence from the value of the Michel parameter in $\mu$ decay), then we could define the muon operator as

$$\mu = \varepsilon\phi^0. \tag{24}$$

But, as discussed in the final section, there is no simple way of incorporating the muon into such schemes without running into additional difficulties.

Although the operators $\theta$ and $\phi$ behave like the K and $\pi$ meson respectively, this identification would not be satisfactory from a dynamical standpoint, since these bosons must include the operator $\Lambda$ because of their strong interactions with baryons. Therefore we introduce the bosons through the definitions

$$\begin{pmatrix} K^0 \\ K^+ \end{pmatrix} = \bar{\Lambda}\Lambda \begin{pmatrix} \theta^0 \\ \theta^+ \end{pmatrix}, \tag{25}$$

$$\pi = \bar{\Lambda}\Lambda\phi, \tag{26}$$

where $\bar{\Lambda}$ denotes the usual adjoint four-spinor

$$\bar{\Lambda} = \Lambda^\dagger\gamma_0. \tag{27}$$

The scheme just described will be referred to as scheme A.

We obtain a modified version of scheme A by imposing the Majorana condition on the neutrino. Since there is a one-to-one correspondence between a Majorana neutrino and a two-component neutrino [10]), this is equivalent to reducing the number of the independent components of the basic field by two. The scheme thus obtained (scheme A′) involves then 10 components instead of 12. We have

$$\nu = \nu^c = \gamma_2\nu^* \tag{28}$$

or

$$\nu_L = -\sigma_2\nu_R{}^*, \qquad \nu_R = \sigma_2\nu_L{}^*. \tag{28′}$$

Hence $\nu_L$ only need be considered. The available continuous groups are reduced. Group (5-I), which gave rise to isorotations, still survives, but the group of global symmetry (5-II) is lost. The leptonic charge group (22) can no longer be defined but (23) is still valid. For the isofermion boson operator $\theta$ we now have

$$\theta^0 = \varepsilon_R{}^\dagger\varepsilon_L, \qquad \theta^+ = \varepsilon_R{}^\dagger\nu_L, \tag{29}$$

so that the leptonic number $l'$ can now be used to define hypercharge. We take $u = l'$. The conservation of leptonic charge and the conservation of strangeness (which follows from the conservation of the hypercharge) become identical. In mesonic decays of hyperons there are no leptons involved, but the leptonic charge changes by one. In leptonic decays, leptons are conserved as well as strangeness. A consequence would be to allow $\beta$ decay only within a charge multiplet. The $\beta$ decay of the $\Lambda^0$, for example, is forbidden. This is an example of a model in which strangeness and parity are not necessarily conserved simultaneously. It is interesting to note the resemblance of this model to the one proposed by Konuma, Nakamura and Umezawa [11]) in which the "neutrino charge" is identified with strangeness.

## 3. Schemes A and A′. Difficulties Associated with the Discontinuous Group Structure

We first consider scheme A. Let us introduce the parity operation for the four-component neutrino-electron system:

$$P_l: \quad \varepsilon_L \to \varepsilon_R, \quad \nu_L \to \nu_R, \tag{30}$$

and the parity operation for the baryon field,

$$P_b: \quad \Lambda_L \to \Lambda_R. \tag{31}$$

From eqs. (9) and (10) we see that under $P_l$ the boson matrix $\theta$ transforms in the following way:

$$P_l: \quad \theta \to -\theta^\dagger. \tag{32}$$

Further, eqs. (5) and (8′) show that the roles of the transformation (5-I) and (5-II) are exchanged under $P_l$. In particular the hypercharge and the third component of the isobaric spin are also exchanged. Therefore, at this stage we note that parity-conserving interactions that are invariant under the isorotations around the third axis must also be invariant under hypercharge transformations. In other words, strangeness and the third component of the isobaric spin must be conserved simultaneously in order to be compatible with parity conservation in this model. The groups (5-I) and (5-II) do not commute separately with parity. However, the group obtained by taking $R = Q = B$ in eq. (7) does commute with parity. Under this group we have

$$(\nu_L, \varepsilon_L) \to (\nu_L, \varepsilon_L)B, \quad (\nu_R, \varepsilon_R) \to (\nu_R, \varepsilon_R)B \tag{33}$$

and

$$\theta \to \bar{B}\theta B,$$

so that the right and the left fields behave in a symmetrical way. The leptonic group $G_l(22)$ also commutes with the parity operation, so that the charge gauge group which is a product of $G_l$ with a subgroup of (33) also commutes with parity. This means that the electromagnetic interaction of the electron, which is charge gauge invariant, is also invariant under parity, as it should be. Leptonic decays for which the group $G_{l'}$ is valid destroy the parity invariance.

We now turn to the question of parity conservation in strong interactions. To do this, we note that the boson fields $\theta$ are not parity eigenstates. From the definition (9) and the law (32) we have explicitly

$$P_l: \begin{array}{ll} \theta^0 \to (\theta^0)^*, & \theta^+ \to -(\theta^-)^*, \\ \theta^- \to -(\theta^+)^*, & \overline{\theta^0} \to -(\overline{\theta^0})^*. \end{array} \tag{34}$$

Now, according to eq. (14) the explicit expressions for the components of the isovector field $\phi$ are

$$\begin{aligned}\phi_3 &= \tfrac{1}{2}[\theta^0\theta^{0*}-\overline{\theta^0}(\overline{\theta^0})^*+\theta^-(\theta^-)^*-\theta^+(\theta^+)^*],\\ \phi^- &= \phi_1-i\phi_2 = -\theta^0(\theta^+)^*-\theta^-(\overline{\theta^0})^*,\\ \phi^+ &= \phi_1+i\phi_2 = -\theta^+(\theta^0)^*-\overline{\theta^0}(\theta^-)^*,\end{aligned} \tag{35}$$

which are seen not to be parity eigenstates. The expression

$$\boldsymbol{\sigma}\cdot\boldsymbol{\phi}' = \tfrac{1}{4}(\theta\theta^\dagger+\theta^\dagger\theta-\bar\theta^\dagger\bar\theta-\bar\theta\bar\theta^\dagger) \tag{36}$$

would be a parity eigenstate, but no isobaric spin vector. nor even strangeness eigenstate. It would only be a vector for the transformations (33) under which $\theta$ transforms like a vector. It follows that an interaction term involving the field $\boldsymbol{\phi}$ and the baryons cannot be invariant under isorotations and parity at the same time. This is because the only rotation groups available (5-I and II) that can serve to define the isogroup and the hypercharge group do not commute with parity, and the only rotation group that commutes with parity, namely (33), cannot be used to define a boson that is an isospinor. On the other hand the operation CP is

$$\text{CP:}\quad \begin{aligned}&\nu_L\to\sigma_2\nu_L^*, \quad \varepsilon_L\to\sigma_2\varepsilon_L^*, \quad \Lambda_L\to\sigma_2\Lambda_L^*,\\ &\nu_R\to-\sigma_2\nu_R^*, \quad \varepsilon_R\to-\sigma_2\nu_R^*, \quad \Lambda_R\to-\sigma_2\Lambda_R^*,\end{aligned} \tag{37}$$

or, using the matrices $F$ and $G$ defined by (2) and the definition (3), we have

$$F\to\sigma_2F^*=\bar F^\dagger\sigma_2, \quad G\to-\sigma_2G^*=-\bar G^\dagger\sigma_2,$$

so that from (4) we obtain

$$\bar FG\to\sigma_2F^\dagger\bar G^\dagger\sigma_2=(\bar FG)^*$$

or

$$\text{CP:}\quad \theta\to\theta^*. \tag{38}$$

Then CP corresponds to the operation of complex conjugation for the field $\theta$. It also switches the sign of the hypercharge. The field $\boldsymbol{\phi}$ now is an eigenstate of CP. The transformation

$$\theta\to\bar\theta^\dagger, \tag{39}$$

which is induced by CP followed by a special four-dimensional rotation (7) defined by

$$F\to i\sigma_2F, \qquad G\to i\sigma_2G, \tag{40}$$

commutes with the full four-dimensional group (7). Hence if strong interactions have global symmetry, invariance under (39) will imply invariance under CP. It is then possible to introduce CP invariance in the strong interactions, unlike separate C and P invariance.

Since scheme A′ is a special case of scheme A, the same difficulties also arise in this case in addition to new difficulties resulting from the lower symmetry of the model with respect to P. This need not be discussed here.

We note that it is possible to define an operation that transforms right-handed baryons into left-handed ones, namely

$$\mathrm{P}': \quad \varepsilon \to \nu^c, \quad \nu \to \varepsilon^c, \quad \Lambda_L \to \Lambda_R. \tag{41}$$

Under this operation we have

$$\theta^+ \to -(\theta^-)^*, \quad \theta^0 \to \overline{\theta^0}^*. \tag{42}$$

We can therefore have simultaneous conservation of strangeness, $P'$, and isobaric spin (since $P'$ commutes with the isospin as defined in this model). We may be tempted to call $P'$ the parity operation, since it is the parity operation for the baryons. But as far as leptons are concerned it is the $G$ conjugation [12]) and it cannot be regarded as parity since it is not conserved in electromagnetic interactions.

We have shown that the scheme A, which accounts for the transformation properties of particles under continuous groups, leaves no freedom for the definition of a parity operation distinct from CP, which would be conserved both in strong and in electromagnetic interactions.

## 4. Schemes with four Four-Spinor Fields (B and C)

### 4.1. SCHEME B

We start with scheme B, in which the fundamental fields are $\varepsilon$, $\nu$, $\Lambda$, and an isosinglet neutral lepton field $\rho$, all four-spinor fields. Since separation into left-handed and right-handed fields plays no special role in the definition of continuous groups in this model, we use the usual four-spinor formalism instead of $2\times 2$ matrices, the bar denoting the adjoint four-spinor in the sense of the definition in (27).

We now redefine the isofermion boson field $\theta$ as

$$\theta^0 = \bar{\nu}\rho = \nu_R^\dagger \rho_L + \nu_L^\dagger \rho_L, \qquad \theta^+ = \bar{\varepsilon}\rho = \varepsilon_R^\dagger \rho_L + \varepsilon_L^\dagger \rho_R. \tag{43}$$

The parity operation now is

$$P: \quad \varepsilon \to \gamma_0 \varepsilon, \quad \nu \to \gamma_0 \nu, \quad \rho \to \gamma_0 \rho, \quad \Lambda \to \gamma_0 \Lambda, \tag{44}$$

and leaves $\theta$ invariant. Thus $\theta$ is a scalar field. We could equally well define a pseudoscalar $\theta$ by replacing $\rho$ by $\gamma_5\rho$.

We introduce the isovector boson field $\boldsymbol{\phi}$ and the isoscalar $\phi^0$ by

$$\phi^0 + \boldsymbol{\sigma}\cdot\boldsymbol{\phi} = \begin{pmatrix} \theta^0 \\ \theta^+ \end{pmatrix} (\theta^{0*}\theta^-), \tag{45}$$

where $\theta^- = (\theta^+)^*$.

We now keep the definitions (20′) and (21) so that we have

$$\Lambda^0 = \Lambda\phi^0, \quad \boldsymbol{\Sigma} = \Lambda\boldsymbol{\phi}, \tag{46}$$

and redefine the baryons N and $\Xi$ as follows:

$$\begin{aligned} \mathrm{p} &= \Lambda\theta^+, \quad \Xi^0 = \Lambda\theta^{0*}, \\ \mathrm{n} &= \Lambda\theta^0, \quad \Xi^- = \Lambda\theta^-. \end{aligned} \tag{47}$$

The K (scalar for instance) and $\pi$ (pseudoscalar) mesons may be defined as

$$K^0 = \bar{\Lambda}\Lambda\theta^0, \quad K^+ = \bar{\Lambda}\Lambda\theta^+, \tag{48}$$

$$\pi = i\bar{\Lambda}\gamma_5\Lambda\phi. \tag{49}$$

The continuous groups are

$$(\nu, \varepsilon) \to (\nu, \varepsilon)e^{\alpha \mathbf{I}\cdot\sigma}, \quad \Lambda \to e^{ib}\Lambda, \quad \rho \to e^{iu}\rho, \tag{50}$$

where $(\nu, \varepsilon)$ means the $4\times 2$ matrix the columns of which are the four-spinors $\nu$ and $\varepsilon$. The vector $\mathbf{I}$ stands for the parameters of the isospin group and $b$ and $u$ are respectively the parameters corresponding to the baryon number and the hypercharge. The lepton gauge group can still be introduced by (22) or (23), assuming $\rho$ invariant under this transformation. For the muon we can still take the provisional definition (24).

The discontinuous groups are $P$, given by (44), and the charge-conjugation operator

$$C: \quad \varepsilon \to \varepsilon^c, \quad \nu \to \nu^c, \quad \rho \to \rho^c, \quad \Lambda \to \Lambda^c. \tag{51}$$

The Racah parity is a special case of the hypercharge gauge group and is given by

$$P_R: \quad \rho \to i\rho, \quad \varepsilon \to \varepsilon, \quad \nu \to \nu, \quad \Lambda \to \Lambda. \tag{52}$$

This scheme leads to the same results as the conventional theory of elementary particles, giving no deeper relationship between strangeness and parity. However, it does give a basis to the isomorphism between the Pauli group and the isogroup of strongly interacting particles. Indeed, in the non-electromagnetic approximation, the equations for the free electron and the neutrino are

$$\gamma_\mu \partial_\mu \nu = 0, \quad \gamma_\mu \partial_\mu \varepsilon = 0. \tag{53}$$

Now, the four-spinors

$$\chi = \begin{pmatrix} \nu_L \\ i\sigma_2 \varepsilon_L^* \end{pmatrix} \quad \text{and} \quad \zeta = \begin{pmatrix} -i\sigma_2 \varepsilon_R^* \\ \nu_R \end{pmatrix} \tag{54}$$

transform in the same way as $\nu$ and $\varepsilon$ under Lorentz transformations and satisfy the same zero-mass Dirac equation

$$\gamma_\mu \partial_\mu \chi = 0, \quad \gamma_\mu \partial_\mu \zeta = 0. \tag{55}$$

These equations are invariant under the simultaneous Pauli transformations [13])

$$\chi \to a\chi + b\gamma_5 \chi^c, \quad \zeta \to a\zeta + b\gamma_5 \zeta^c (|a|^2 + |b|^2 = 1). \tag{56}$$

But this transformation is equivalent to the isogroup in eq. (50) which, according to the model, induces the isobaric rotations of strongly interacting particles. Therefore, in this model there is still a strong connection between the Pauli invariance of zero-mass spinor fields and the isobaric spin invariance of baryons and mesons. The introduction of the $\rho$ field to provide the

hypercharge group is, on the other hand, an unsatisfactory feature of the scheme. For the muon we now have another possibility, namely

$$\mu^- = \rho\theta^-, \tag{57}$$

which of course does not exclude a neutral muon defined by

$$\mu^0 = \rho\theta^{0*}. \tag{58}$$

In this scheme C and P can be conserved simultaneously with isospin and strangeness, although this is not a necessary consequence of the scheme.

### 4.2. SCHEME C

Before leaving the spinor schemes we note briefly a more symmetrical-looking scheme with four four-spinors, which runs into difficulty with the conservation of parity in interactions involving strange particles. The fundamental fields are $\varepsilon$, $\nu$, p, n, and the definitions of scheme A are kept for the $\theta$ field. The baryon and the hypercharge transformations are now defined as

$$G_b: \quad (\nu, \varepsilon) \to (\nu, \varepsilon), \qquad (\mathrm{p}, \mathrm{n}) \to e^{ib}(\mathrm{p}, \mathrm{n}), \tag{59}$$

$$G_u: \quad (\nu_L, \varepsilon_L) \to (\nu_L, \varepsilon_L), \quad (\nu_R, \varepsilon_R) \to e^{-iu}(\nu_R, \varepsilon_R) \tag{60}$$
$$(\mathrm{p}, \mathrm{n}) \to e^{iu}(\mathrm{p}, \mathrm{n}).$$

Therefore under $G_u$ we have

$$G_u: \ \theta^0 \to \theta^0 e^{iu}, \quad \theta^+ \to \theta^+ e^{iu}. \tag{61}$$

The hyperons may now be defined as in the Goldhaber model,

$$\begin{aligned}
\Lambda^0 &= \frac{1}{\sqrt{2}}(\mathrm{p}\theta^- - \mathrm{n}\theta^{0*}) && \text{(isosinglet)},\\
\Sigma^0 &= \frac{1}{\sqrt{2}}(\mathrm{p}\theta^- + \mathrm{n}\theta^{0*}) &&\\
\Sigma^+ &= \mathrm{p}\theta^{0*} && \text{(isotriplet)},\\
\Sigma^- &= \mathrm{n}\theta^- &&\\
\Xi^0 &= \Lambda^0\theta^{0*} &&\\
\Xi^- &= \Lambda^0\theta^- && \text{(isodoublet)}.
\end{aligned} \tag{62}$$

The mesons are defined as

$$\pi^+ = i\bar{\mathrm{n}}\gamma_5\mathrm{p}, \quad \pi^- = i\bar{\mathrm{p}}\gamma_5\mathrm{n}, \quad \pi^0 = \frac{i}{\sqrt{2}}(\bar{\mathrm{p}}\gamma_5\mathrm{p} - \bar{\mathrm{n}}\gamma_5\mathrm{n}), \tag{63}$$

$$\mathrm{K}^+ = \bar{\Lambda}^0\mathrm{p}, \quad \mathrm{K}^0 = \bar{\Lambda}^0\mathrm{n}. \tag{64}$$

It can now be shown that the parity difficulties associated with scheme A are now limited to interactions involving strange particles. In this scheme, C and P would be conserved in electromagnetic and pionic strong interactions, but would be violated by the K-meson interactions.

## 5. A Model with Mixed Fermion and Boson Fields (Scheme D)

We have seen that in a pure spinor model at least four four-spinor fields are required in order to give the continuous gauge groups as well as C and P separately, so that the basic field has 16 components. Moreover, because of the different nature of the fields involved, there is a great arbitrariness in formulating the interaction Lagrangian in terms of the basic field. Therefore it is desirable to have a model with a smaller number of fundamental fields at the price of sacrificing their common spinor character. Such an example is now given.

### 5.1. SCHEME D (THREE TWO-SPINOR, TWO SCALAR FIELDS)

The basic fields are taken to be

$$\lambda = \begin{pmatrix} \lambda_1 \\ \lambda_2 \end{pmatrix}, \quad \Lambda_L = \begin{pmatrix} \Lambda_1 \\ \Lambda_2 \end{pmatrix}, \quad \Lambda_R = \begin{pmatrix} \Lambda_3 \\ \Lambda_4 \end{pmatrix}, \quad k = \begin{pmatrix} k_1 \\ k_2 \end{pmatrix}. \tag{65}$$

Here $\lambda$, $\Lambda_L$, and $\Lambda_R$ are two-spinors, whereas the components of $k$ are scalars, one being neutral and the other positively charged. We further assume that $\lambda$, $\Lambda_L$, and $\Lambda_R$ are scalar in isobaric spin space while $k$ is an isobaric spinor. We shall often combine $\Lambda_L$ and $\Lambda_R$ into the four-spinor

$$\Lambda = \begin{pmatrix} \Lambda_L \\ \Lambda_R \end{pmatrix} \tag{66}$$

and use the four-spinor notation. We note that each basic field is chosen to have different spins in the ordinary and isobaric spin spaces, so that in a sense they are all strange fields. All together we now have eight components — that is, half the number of components in model B.

For four-spinor fields we use the notations (1), (27), and (66). For two-spinor fields $\xi$ we define

$$\hat{\xi} = i\sigma_2 \xi^*, \tag{67}$$

where the star denotes complex conjugation as usual. If $\xi$ is a two-spinor of the first kind, then $\hat{\xi}$ is a two-spinor of the second kind (see ref. [8])). Further, as in (59) if $\psi$ and $\phi$ are two four-spinors, by the notation $(\psi, \phi)$ we mean the $4\times 2$ matrix the columns of which are respectively the four-spinors $\psi$ and $\phi$, so that we have

$$(\psi, \phi) = \begin{pmatrix} \psi_L & \phi_L \\ \psi_R & \phi_R \end{pmatrix} = \begin{pmatrix} \psi_1 & \phi_1 \\ \psi_2 & \phi_2 \\ \psi_3 & \phi_3 \\ \psi_4 & \phi_4 \end{pmatrix}. \tag{68}$$

Similarly, $(\xi, \eta)$ is $2\times 2$ matrix, the columns of which are the two-spinors $\xi$ and $\eta$ as in (2).

We now propose the view that the basic fields cannot be observed by themselves owing to their strong interactions, and that they tend to form compound states which correspond to elementary particles. Considering provisionally the muon as the charged member of a doublet, and choosing a scalar $K$, we define the scheme by the following operators:

$$\begin{aligned}
&\text{(a)}\ (\nu_L, \varepsilon_L) = \lambda k^\dagger, && (\nu_R, \varepsilon_R) = \hat{\lambda} k^\dagger,\\
&\text{(b)}\ (\mathrm{p}, \mathrm{n}) = \Lambda k^\dagger, && (\Xi^0, \Xi^-) = \Lambda \hat{k}^\dagger,\\
&\text{(c)}\ \Lambda^0 = \Lambda k^\dagger k, && \Sigma = \Lambda k^\dagger \sigma k,\\
&\text{(d)}\ \pi = \bar{\Lambda} \gamma_5 \Lambda k^\dagger \sigma k, && \mathrm{K} = \bar{\Lambda} \Lambda k,\\
&\text{(e)}\ (\mu_L^-, \mu_L^0) = \lambda k^\dagger k k^\dagger, && (\mu_R^-, \mu_R^0) = \hat{\lambda} k^\dagger k k^\dagger.
\end{aligned} \tag{69}$$

The continuous groups are given by

$G_L$ (proper Lorentz group):

$$\lambda \to L\lambda, \quad \Lambda_L \to L\Lambda_L, \quad \hat{\Lambda}_R \to L\hat{\Lambda}_R, \quad k \to k, \tag{70}$$

where $L$ is a unimodular $2\times 2$ matrix.

$G_b$(baryon group):

$$\Lambda \to e^{ib}\Lambda, \quad \lambda \to \lambda, \quad k \to K. \tag{71}$$

$G_I$(isospin group):

$$k \to Rk, \quad \lambda \to \lambda, \quad \Lambda \to \Lambda, \tag{72}$$

where $R$ is unitary and unimodular as in (6) so that it has the form

$$R = \exp(i\sigma \cdot \mathbf{I}).$$

$G_u$(hypercharge group):

$$k \to e^{-iu}k, \quad \lambda \to \lambda, \quad \Lambda \to \Lambda. \tag{73}$$

$G_w$($\gamma_5$ group for leptons):

$$\lambda \to e^{iw}\lambda, \quad \Lambda \to \Lambda, \quad k \to k. \tag{74}$$

$G_a$($\gamma_5$ group for baryons):

$$\Lambda \to e^{i\gamma_5 a}\Lambda, \quad \lambda \to \lambda, \quad k \to k. \tag{75}$$

These are the continuous groups available. The charge gauge group is a combination of $G_u$ and $G_{I_3}$, so that we have

$G_q$(charge group):

$$k \to e^{\frac{1}{2}i(1+\sigma_3)q}k, \quad \lambda \to \lambda, \quad \Lambda \to \Lambda. \tag{76}$$

We shall expect $G_L, G_b, G_q$ to be always valid. Strong interactions are assumed to have additional invariance under $G_I$ and $G_u$. The groups $G_w$ and $G_a$ are expected to play a role in weak interactions only.

We now consider the discontinuous groups.

P(parity):

$$\lambda \to \hat{\lambda}, \quad \Lambda \to \gamma_0\Lambda, \quad k \to k. \tag{77}$$

C(charge conjugation):

$$\lambda \to \lambda, \quad \Lambda \to \Lambda^c, \quad k \to k^*. \tag{78}$$

By combining these and by using $R_{(2)}$ defined as a special isorotation of 180° around the second axis, we can also define

$$\text{CP:} \qquad \lambda \to \hat{\lambda}, \quad \Lambda \to \gamma_0 \Lambda^c, \quad k \to k^*, \tag{79}$$

$$\text{G}(= \text{C} \times \text{R}_{(2)}): \qquad \lambda \to \lambda, \quad \Lambda \to \Lambda^c, \quad k \to \hat{k}, \tag{80}$$

$$\text{GP:} \qquad \lambda \to \hat{\lambda}, \quad \Lambda \to \gamma_0 \Lambda^c, \quad k \to \hat{k}. \tag{81}$$

To C and P we may add another reflection operation $\mathscr{M}$ (mirror operation):

$$\lambda \to \lambda, \quad \Lambda \to \Lambda, \quad k \to \hat{k}. \tag{82}$$

Strong and electromagnetic interactions are presumed to conserve C and P separately, while CP remains valid for weak interactions. The mirror operation $\mathscr{M}$, which changes leptons into antileptons, K mesons into anti K's and exchanges the nucleon and the cascade particles, while not affecting the remaining particles, is not known to play an important part in the formulation of interactions, although it may be related to global symmetry.

Finally we note the following discontinuous groups, which are special cases of the continuous groups:

$P_R$(Racah's parity) is a special case of $G_u$:

$$\lambda \to \lambda, \quad \Lambda \to \Lambda, \quad k \to -ik. \tag{83}$$

$\mathscr{R}_m$(mass reversal) is a special case of $G_w$ and $G_u$:

$$\lambda \to i\lambda, \quad \Lambda \to i\gamma_5 \Lambda, \quad k \to k. \tag{84}$$

Their product is

$$P_R \mathscr{R}_m: \qquad \lambda \to i\lambda, \quad \Lambda \to i\gamma_5 \Lambda, \quad k \to -ik. \tag{85}$$

$P_R$ is expected to be conserved in strong interactions [14]) and $\mathscr{R}_m$ in weak interactions [15]).

If both $G_w$ and $G_a$ are assumed to be valid in weak interactions we obtain the same weak interactions as in the Feynman-Gell Mann scheme [2]), provided the neutral leptons $\lambda$, $\nu_L$, and $\mu_L^0$ are regarded as physically undistinguishable. This is also equivalent to postulating invariance under (84). However, if both the Racah parity and the mass reversal are assumed to be conserved in Fermi interactions, then, as in scheme A, we would observe $\beta$ decay only within a charge multiplet. This seems to be supported by recent experiments.

## 6. Concluding Remarks

From the preceding discussion it appears that if one insists on a pure spinor model, then a 16-component basic field (scheme B) seems to be necessary in order to account for separate conservation of C and P in

strong and electromagnetic interactions. However, three spinor fields would be sufficient in a scheme in which the only reflection operation would be CP (scheme A). Scheme B necessitates the introduction of a field $\rho$ whose only role is to save parity conservation besides introducing the hypercharge into the scheme. A 16-component spinor model which tries to do away with such an extra field and attempts to derive strangeness from symmetry properties of the basic isodoublets (scheme C) is also confronted with the difficulty of conserving parity in strong interactions involving strange particles. If we relax the requirement of a spinor model and take the view that a basic field with a minimum number of components compatible with the observed group structure of elementary particles has more chance of corresponding to nature, then, the highly economical but less symmetrical scheme D with eight components should be preferred. But the mixed model, unlike the spinor models, does not relate isospin rotations to the Pauli invariance of zero-mass Dirac fields. Both strangeness and isospin are introduced as basic concepts and no attempt is made to connect them with the group properties of spinor fields.

Some of the difficulties inherent in the schemes under discussion can be noted.

### 6.1. OCCURRENCE OF NEW PARTICLES

The baryons and spin-zero mesons seem to form a fairly closed system (except for the possibility of an isoscalar pion). But as no such closure property is apparent for leptons and spin-one particles, any scheme that purports to unify elementary particles by a group theoretical classification is bound to offer the possibility of defining new particles that will give a more symmetrical structure to the scheme. One is then forced to explain away the extra particles by assuming that they have very short life-times owing to the nature of the fundamental interactions.

### 6.2. THE $\mu$ MESON

If the isobaric-spin concept is extended to the leptons, as it is in all such schemes, then, there are three possibilities for the muon. It may be a charged singlet, the charged component of an isodoublet, or the charged component of an isotriplet. None of these assumptions is satisfactory. In the first case, if one admits the possibility of charged isosinglets, then there is no reason to eliminate baryons that have the same property. In the second and third cases we are forced to admit a neutral muon ($\mu^0$) into the scheme. The only other way out is to regard the muon as a heavy electron. Then we are confronted with the problem of the large mass of the muon. Further, $\beta$ decay is predicted both for the $\pi$ and K mesons.

### 6.3. THE PHOTON

The photon is a massless, neutral, spin-one particle. Again if one constructs such a particle operator from spinor operators, one is led to consider also charged spin-one particles (Schwinger's Z particles), for which there is no experimental evidence. Another problem is to explain why electromagnetic interactions necessarily destroy full isospin invariance.

### 6.4. PARITY AND STRANGENESS

Many authors have envisaged the possibility of a connection between strangeness and parity which seem to be conserved or violated simultaneously wherever strangeness is defined; although mathematically the two quantum numbers are unrelated. If one were to extend the notion of strangeness to leptons, it would be attractive to do it in such a way as to have strangeness violated in all, including leptonic, decays. Such a common selection rule for all weak interactions would help to understand their universal character (common A—V structure, approximately equal coupling constants). None of the schemes surveyed above gives such a selection rule. The non-conservation of C and P seems to be the only feature common to all weak interactions. To take an example, in scheme D strangeness is conserved in the $\beta$ decay of nucleons, but not conserved in the mesonic decay of hyperons, while in both cases parity is violated. Therefore the scheme makes a sharp distinction between leptonic and non-leptonic decays, giving no connection between strangeness and parity. Such a connection is also absent in scheme B, whereas a strong connection of the wrong kind appears in schemes A and C.

### 6.5. RELATIVE PARITIES OF DIFFERENT FIELDS

Within an ambiguity due to superselection rules [16]) the relative parities of fields can be defined. For instance, the relative parity of the pion and the nucleon system is odd. Experiments are under way to determine the relative parity of the nucleon and the ($\Lambda^0$, K) system. In the above schemes there is freedom to change the relative parity of the particles, which should be determined in a unique way in a successful theory of elementary particles.

This discussion leads to the inevitable conclusion that no satisfactory scheme for elementary particles has been discovered yet.

In conclusion I would like to express my deepest gratitude to Prof. W. Pauli for advice and criticism. I am indebted to Dr. Henry P. Stapp for the formulation of the present form of Model B and to Dr. Sidney A. Bludman for stimulating discussions. My thanks are due to Dr. David L. Judd for hospitality at the Radiation Laboratory, where this work was carried out.

## References


1) A. Pais, Proc. 7th An. Rochester Conf. **9** (1957) 36; M. Gell-Mann and A. H. Rosenfeld, Ann. Rev. Nuclear Sci. **7** (1957) 422
2) R. P. Feynman and M. Gell-Mann, Phys. Rev. **109** (1958) 193; E. C. G. Sudarshan and R. E. Marshak, Phys. Rev. **109** (1958) 1860
3) F. Gürsey, Nuovo Cimento **7** (1958) 411
4) M. Gell-Mann, Phys. Rev. **106** (1957) 1296; J. Schwinger, Ann. of Phys. **2** (1957) 407; A. Pais, Phys. Rev. **110** (1958) 574
5) W. Heisenberg, Revs. Mod. Phys. **29** (1957) 269
6) M. Goldhaber, Phys. Rev. **92** (1953) 127; and **101** (1956) 433
7) S. Sakata, Progr. Theor. Phys. **16** (1956) 686
8) W. Zimmermann, Nuovo Cimento (to be published)
9) B. D. Espagnat and J. Prentki, Nuclear Physics **1** (1956) 33
10) K. M. Case, Phys. Rev. **107** (1957) 307; B. Touschek, Nuovo Cimento **5** (1957) 1281
11) M. Konuma, S. Nakamura and H. Umezawa, Nuclear Physics **6** (1958) 282
12) T. D. Lee and C. N. Yang, Nuovo Cimento **3** (1956) 749
13) W. Pauli, Nuovo Cimento **6** (1957) 204
14) G. Racah, Nuclear Physics **1** (1956) 302
15) J. Sakurai, Nuovo Cimento **7** (1958) 649
16) G. C. Wick, A. S. Wightman and E. P. Wigner, Phys. Rev. **88** (1952) 101

# AUTHOR INDEX


ABOU HADID, L., *see* EL NADI

ABRAHAM, G. and C. S. WARKE, $F^{19}$ in the unified model . . . . 69

AKIMOV, YU. K., O. V. SAVCHENKO and L. M. SOROKO, Investigation of the reaction $p+p \rightarrow d+\pi^+$ with polarized protons of high energy . . . . . 637

ARMBRUSTER, R., *see* GORODETZKY

BEARD, G. B. and W. H. KELLY, The use of a samarium loaded liquid scintillator for the determination of the half-life of $Sm^{147}$ . . . . 207

BELL, J. S., Bremsstrahlung from multiple scattering . . . . . 613

BERÉNYI, D., $\beta-\gamma$ coincidence spectrometric investigation of the decay scheme of $Nd^{147}$ . . . . . 607

BERNARDINI, M., P. BROVETTO and S. FERRONI, Scattering of polarized electrons by a Coulomb field . . . . . 294

BLATT, J. M. and G. DERRICK, Repulsive core forces in the triton . . 602

BLATT, J. M., *see* DERRICK

BLOCH, CLAUDE et JULES HOROWITZ, Sur la détermination des premiers états d'un système de fermions dans le cas dégénéré . . . 91

BOZÓKI, G., E. FENYVES and ÉVA GOMBOSI, On the angular distribution of shower particles generated in high-energy nuclear interactions . . . . . 199

BROVETTO, P., *see* BERNARDINI

CHEVALLIER, P., *see* GORODETZKY

COWLAND, W. S., On Schwinger's theory of the muon . . . . . 397

CZYŻ, W. and J. SAWICKI, Polarization phenomena in neutron-proton radiative capture . . . . . 621

DANIEL, H., Die Formen der $\beta$-Spektren von $Na^{22}$, $Na^{24}$ und $P^{32}$ . . . 191

DAVYDOV, A. S. and G. F. FILIPPOV, Rotational states in even atomic nuclei . . . . . 237

DELVES, L. M., Effective range expansion of the scattering matrix . . 358

DERRICK, G. and J. M. BLATT, Classification of triton wave functions 310

DERRICK, G., *see* BLATT

DE WAARD, H., *see* SIEKMAN

DIAMOND, R. M. and J. M. HOLLANDER, Neutron-deficient iridium isotopes . . . . . 143

DŽELEPOW, B. S., N. N. ZHUKOVSKY, S. A. SHESTOPALOVA and I. F. UCHEVATKIN, Gamma-ray spectrum of radium in equilibrium with its decay products . . . . . 250

EL BEDEWI, F. A. and S. TADROS, Magnetic analysis of the reaction $V^{51}$ (d, p) $V^{52}$ . . . . . 71
EL BEDEWI, F. A. and S. TADROS, Low energy levels in cobalt 60 . . 79
EL NADI, M. and L. ABOU HADID, The (d, t) reactions and the internal structure of the triton . . . . . 51
ERICSON, TORLEIF, Level density of degenerate Fermi systems . . . 265
ERICSON, T. and V. STRUTINSKI, On angular distributions in compound nucleus processes . . . . . 284
ERÖ, J., *see* KESZTHELYI
FELDMAN, GORDON and THOMAS FULTON, Determination of the relative $\Sigma-\Lambda$ parity . . . . . 106
FENYVES, E., *see* BOZÓKI
FERRONI, S., *see* BERNARDINI
FILIPPOV, G. F., *see* DAVYDOV
FINDLER, N. V., Nuclear binding energies on the statistical model . 338
FINK, R. W., *see* NURMIA
FULTON, THOMAS, *see* FELDMAN
GALLMANN, A., *see* GORODETZKY
GAUVIN, J. N. L., Magnetic moments of highly deformed nuclei . . 213
GOMBOSI, ÉVA, *see* BOZÓKI
GORODETZKY, S., P. CHEVALLIER, R. ARMBRUSTER, G. SUTTER et A. GALLMANN, Corrélation angulaire des paires de conversion interne provenant des niveaux 6.09 MeV du carbone 14 et 5.69 MeV de l'azote 14 . . . . . 412
GÜRSEY, FEZA, On the group structure of elementary particles . . . 675
HODGSON, P. E., Proton-alpha reactions in light and heavy nuclei . . 1
HOLLANDER, J. M., *see* DIAMOND
HOROWITZ, JULES, *see* BLOCH
INGLIS, D. R., Nuclear moments of inertia and effective nucleon mass . . . . . 125
KASCHLUHN, FRANK, Impulse approximation and dispersion relations for pion-deuteron scattering . . . . . 303
KELLY, W. H., *see* BEARD
KESZTHELYI, L. and J. ERÖ, ($\gamma$, p) reactions in $Na^{23}$, $K^{39}$, $I^{127}$ and $Cs^{133}$ 650
KRÓLIKOWSKI, W., On the elementary particles and their strong interactions . . . . . 461
LAURIKAINEN, K. V., Phenomenological two-nucleon potentials and the deuteron . . . . . 210
LAURIKAINEN, K. V. and SEIJA LYYTIKÄINEN, A variational procedure for hard core potentials . . . . . 416
LEITE LOPES, J., A model of the universal Fermi interaction . . . . 234
LEVINGER, J. S., Relations among different models of the nuclear

photoeffect . . . . . 428
LICHTENBERG, D. B., Application of the Serber potential to low energy hyperon-nucleon scattering . . . . . 13
LIPKIN, H. J., On the connection between degeneracy and rotational states in the nuclear shell model. . . . . 421
LOGUNOV, A. A. and A. N. TAVKHELIDZE, Some problems encountered in the theory of the dispersion relations . . . . . 374
LOVAS, I., Polarization of elastically scattered gamma-rays . . . . . 155
LUKYANOV, A. V., YU. V. ORLOV and V. V. TUROVTSEV, Optical model of the interaction between intermediate energy neutrons and nuclei . . . . . 325
LYYTIKÄINEN, SEIJA, *see* LAURIKAINEN
MEICHSNER, LOTHAR, Über die Kreiseleigenschaften des Atomkerns . 493
MITTELSTAEDT, P., Zur phänomenologischen Theorie der Kernmaterie 171
MONTAGUE, J. H., *see* PAUL
MOSHINSKY, MARCOS, Short range forces and nuclear shell theory . . 19
MURDOCH, H. S., The absolute density distribution of cosmic-ray air showers at low densities. . . . . 157
NING HU, On the interaction of strange particles . . . . . 85
NURMIA, M. J. and R. W. FINK, Cross-sections for (n, p) and (n, $\alpha$) reactions of magnesium with 14.8 MeV neutrons; a new isotope $Na^{26}$ 139
ORLOV, YU. V., *see* LUKYANOV
PAUL, E. B. and J. H. MONTAGUE, The levels of $Na^{23}$ on the unified model . . . . . 61
POLUBARINOV, I. V., Bound states and scattering of baryons in contact interaction . . . . . 444
PURSEY, D. L., On generalized Foldy-Wouthuysen transformations . 595
SATCHLER, G. R., Time reversal and polarized nuclear reactions . . . 65
SAVCHENKO, O. V., *see* AKIMOV
SAWICKI, J., *see* CZYŻ
SHESTOPALOVA, S. A., *see* DŽELEPOW
SIEKMAN, J. G. and H. DE WAARD, Lifetime measurements of the first excited states of $Tl^{208}$ and $Ra^{224}$. . . . . 402
SKARSVÅG, KRISTIAN, Proton-proton scattering with unpolarized beam and target . . . . . 55
SOROKO, L. M., *see* AKIMOV
SQUIRES, E. J., The use of an effective three-body potential in the nucleus . . . . . 41
STRATHDEE, J. and Y. TAKAHASHI, On the self-stress of composite particles . . . . . 113
STRUTINSKI, V., *see* ERICSON
SUTTER, G., *see* GORODETZKY

TADROS, S., *see* EL BEDEWI
TAKAHASHI, Y., *see* STRATHDEE
TAVKHELIDZE, A. N., *see* LOGUNOV
TOYODA, TOSHIYUKI, A unified theory of the Fermi interaction . . . 661
TUROVTSEV, V. V., *see* LUKYANOV
UCHEVATKIN, I. F., *see* DŽELEPOW
UNNA, I., Coulomb energies of mirror nuclei . . . . . 468
WARKE, C. S., *see* ABRAHAM
WATANABE, SHIGUEO, High energy scattering of deuterons by complex nuclei . . . . . 484
ZHUKOVSKY, N. N., *see* DŽELEPOW

# SUBJECT INDEX

## 1. Nuclear Structure

### 1.B *Two- and three-body problems*

The (d, t) reactions and the internal structure of the triton, M. El Nadi and L. Abou Hadid . . . . . 51
Phenomenological two-nucleon potentials and the deuteron, K. V. Laurikainen . . . . . 210
Classification of triton wave functions, G. Derrick and J. M. Blatt . . . 310
A variational procedure for hard core potentials, K. V. Laurikainen and Seija Lyytikäinen . . . . . 416
Repulsive core forces in the triton, J. M. Blatt and G. Derrick . . . . . 602
Polarization phenomena in neutron-proton radiative capture, W. Czyż and J. Sawicki . . . . . 621

### 1.C *Many-particle systems*

The use of an effective three-body potential in the nucleus, E. J. Squires . 41
Sur la détermination des premiers états d'un système de fermions dans le cas dégénéré, Claude Bloch et Jules Horowitz . . . . . 91
Zur phänomenologischen Theorie der Kernmaterie, P. Mittelstaedt . . . 171
Level density of degenerate Fermi systems, Torleif Ericson . . . . . 265
Nuclear binding energies on the statistical model, N. V. Findler . . . . . 338

### 1.D *Nuclear models*

#### 1.D.1 *Shell model*

Short range forces and nuclear shell theory, Marcos Moshinsky . . 19
Coulomb energies of mirror nuclei, I. Unna . . . . . 468

#### 1.D.2 *Collective model*

The levels of $Na^{23}$ on the unified model, E. B. Paul and J. H. Montague. . . . . 61
$F^{19}$ in the unified model, G. Abraham and C. S. Warke. . . . . 69
Nuclear moments of inertia and effective nucleon mass, D. R. Inglis 125
Magnetic moments of highly deformed nuclei, J. N. L. Gauvin . . 213
Rotational states in even atomic nuclei, A. S. Davydov and G. F. Filippov . . . . . 237
On the connection between degeneracy and rotational states in the nuclear shell model, H. J. Lipkin. . . . . 421
Über die Kreiseleigenschaften des Atomkerns, Lothar Meichsner . 493

#### 1.D.3 *Other models*

Proton-alpha reactions in light and heavy nuclei, P. E. Hodgson . 1

### 1.E *Properties of nuclei*

#### 1.E.1 *Energy levels*

Magnetic analysis of the reaction $V^{51}$ (d, p) $V^{52}$, F. A. El Bedewi and S. Tadros. . . . . 71

Low energy levels in cobalt 60, F. A. El Bedewi and S. Tadros . . 79
Neutron-deficient iridium isotopes, R. M. Diamond and J. M. Hollander . . . . . 143
Level density of degenerate Fermi systems, Torleif Ericson . . . 265
Corrélation angulaire des paires de conversion interne provenant des niveaux 6.09 MeV du carbone 14 et 5.69 MeV de l'azote 14, S. Gorodetzky, P. Chevallier, R. Armbruster, G. Sutter et A. Gallmann . . . . . 412
$\beta-\gamma$ coincidence spectrometric investigation of the decay-scheme of $Nd^{147}$, D. Berényi . . . . . 607

1.E.2 *Binding energies; masses*

Zur phänomenologischen Theorie der Kernmaterie, P. Mittelstaedt 171
Nuclear binding energies on the statistical model, N. V. Findler . 338
Coulomb energies of mirror nuclei, I. Unna . . . . . 468

1.E.3 *Electric and magnetic moments*

Magnetic moments of highly deformed nuclei, J. N. L. Gauvin . . 213

1.E.4 *Transition probabilities; Cross sections*

Lifetime measurements of the first excited states of $Tl^{208}$ and $Ra^{224}$, J. G. Siekman and H. de Waard . . . . . 402

## 2. Nuclear Reactions

### 2.A *General properties*

2.A.1 *Cross-sections, energy relations*

Cross-sections for (n, p) and (n, $\alpha$) reactions of magnesium with 14.8 MeV neutrons; a new isotope $Na^{26}$, M. J. Nurmia and R. W. Fink . . . . . 139

### 2.B *Angular distributions; Correlations; Polarization*

Time reversal and polarized nuclear reactions, G. R. Satchler . . . . . 65
On angular distributions in compound nucleus processes, T. Ericson and V. Strutinski . . . . . 284

### 2.C *Resonance reactions; R-matrix theory*

Effective range expansion of the scattering matrix, L. M. Delves . . . . 358

### 2.D *Statistical model*

Level density of degenerate Fermi systems, Torleif Ericson . . . . . 265

### 2.E *Optical model*

On angular distributions in compound nucleus processes, T. Ericson and V. Strutinski . . . . . 284
Optical model of the interaction between intermediate energy neutrons and nuclei, A. V. Lukyanov, Yu. V. Orlov and V. V. Turovtsev . . . . . 325
High energy scattering of deuterons by complex nuclei, Shigueo Watanabe 484

### 2.F *Direct interaction (other than stripping)*

Proton-alpha reactions in light and heavy nuclei, P. E. Hodgson . . . 1

### 2.G *Stripping and pick-up*

The (d, t) reactions and the internal structure of the triton, M. El Nadi and L. Abou Hadid . . . . . 51

Magnetic analysis of the reaction $V^{51}$ (d, p) $V^{52}$, F. A. El Bedewi and S. Tadros . . . . . 71
Low energy levels in cobalt 60, F. A. El Bedewi and S. Tadros . . . . . 79

### 2.I *Photonuclear processes*

Relations among different models of the nuclear photoeffect, J. S. Levinger 428
Polarization phenomena in neutron-proton radiative capture, W. Czyż and J. Sawicki . . . . . 621
($\gamma$, p) reactions in $Na^{23}$, $K^{39}$, $I^{127}$ and $Cs^{133}$, L. Keszthelyi and J. Erö . . . 650

### 2.L *Scattering processes (except two-nucleon system and meson scattering)*

Proton-proton scattering with unpolarized beam and target, Kristian Skarsvåg . . . . . 55
Scattering of polarized electrons by a Coulomb field, M. Bernardini, P. Brovetto and S. Ferroni . . . . . 294
High energy scattering of deuterons by complex nuclei, Shigueo Watanabe 484

## 3. Electromagnetic Radiation

### 3.A *Gamma radiation*

Gamma-ray spectrum of radium in equilibrium with its decay products, B. S. Dželepow, N. N. Zhukovsky, S. A. Shestopalova and I. F. Uchevatkin . . . . . 250

### 3.B *Internal conversion*

Corrélation angulaire des paires de conversion interne provenant des niveaux 6.09 MeV du carbone 14 et 5.69 MeV de l'azote 14, S. Gorodetzky, P. Chevallier, R. Armbruster, G. Sutter et A. Gallmann . . . . . 412

### 3.C *Extranuclear effects*

Bremsstrahlung from multiple scattering, J. S. Bell . . . . . 613

## 4. Beta Decay; Parity

### 4.E *Analysis of data*

Die Formen der $\beta$-Spektren von $Na^{22}$, $Na^{24}$ und $P^{32}$, H. Daniel . . . . . 191

## 6. Methods and Instruments

### 6.A *Experimental*

The use of a samarium loaded liquid scintillator for the determination of the half-life of $Sm^{147}$, G. B. Beard and W. H. Kelly . . . . . 207

### 6.B *Theoretical*

A variational procedure for hard core potentials, K. V. Laurikainen and Seija Lyytikäinen . . . . . 416

### 6.D *Tables and computational aids*

Short range forces and nuclear shell theory, Marcos Moshinsky . . . . . 19

## 7. Quantum Field Theory

### 7.A *General*

On the self-stress of composite particles, J. Strathdee and Y. Takahashi . 113
Some problems encountered in the theory of the dispersion relations, A. A. Logunov and A. N. Tavkhelidze . . . . . 374
Bound states and scattering of baryons in contact interaction, I. V. Polubarinov . . . . . 444

### 7.B *Quantum Electrodynamics*

Polarization of elastically scattered gamma-rays, I. Lovas . . . . . 155

### 7.C *π-meson field (scattering and nuclear forces)*

Impulse approximation and dispersion relations for pion-deuteron scattering, Frank Kaschluhn . . . . . 303
Investigation of the reaction $p+p \to d+\pi^+$ with polarized protons of high energy, Yu. K. Akimov, O. V. Savchenko and L. M. Soroko . . . . 367

## 8. Elementary Particles

### 8.B *Theory; interactions, transformation properties*

Application of the Serber potential to low energy hyperon-nucleon scattering, D. B. Lichtenberg . . . . . 13
On the interaction of strange particles, Ning Hu . . . . . 85
Determination of the relative $\Sigma-\Lambda$ parity, Gordon Feldman and Thomas Fulton . . . . . 106
A model of the universal Fermi interaction, J. Leite Lopes . . . . . 234
Scattering of polarized electrons by a Coulomb field, M. Bernardini, P. Brovetto and S. Ferroni . . . . . 294
On Schwinger's theory of the muon, W. S. Cowland . . . . . 397
Bound states and scattering of baryons in contact interaction, I. V. Polubarinov . . . . . 444
On the elementary particles and their strong interactions, W. Królikowski 461
On generalized Foldy-Wouthuysen transformations, D. L. Pursey . . . 595
A unified theory of the Fermi interaction, Toshiyuki Toyoda . . . . . 661
On the group structure of elementary particles, Feza Gürsey . . . . . 675

### 8.C *Fundamental theory of matter*

On the self-stress of composite particles, J. Strathdee and Y. Takahashi. . 113

## 9. Cosmic Radiation

### 9.A *General*

The absolute density distribution of cosmic-ray air showers at low densities, H. S. Murdoch . . . . . 157
On the angular distribution of shower particles generated in high-energy nuclear interactions, G. Bozóki, E. Fenyves and Éva Gombosi . . . . 199

## 10. News Items

### 10.A *News items*

Symposium on nuclear fuel cycles . . . . . 396

## 10.D *Book reviews*

DUNGEY, J. W., Cosmic electrodynamics (L.R.) . . . . . 394
FLÜGGE, S. and E. CREUTZ, editors, Handbuch der Physik-Encyclopedia of Physics, vol. 45 (L.R.) . . . . . 394
FRENKEL, J. I., Prinzipien der Theorie der Atomkerne (A. Herzenberg) 395
GALANIN, A. D., The theory of thermal-neutron nuclear reactors (K. T. Spinney) . . . . . 124
MAGNER, T. F., Manual of scientific Russian (L.R.) . . . . . 395
MASSIGNON, D., Mécanique statistique des fluides (P. T. Landsberg). . . 124
PRICE, W. J., Nuclear radiation Detection (O. Nathan) . . . . . 395

## 10.E *Errata*

L. R. B. ELTON, Nuclear Physics **5** (1958) 173 . . . . . 396